Brain Educational Course

STROKE BIOMARKER DISCOVERY: MODEL SAMPLES AND PROTEOMICS STRATEGIES

J.-C. Sanchez, N. Turck

Human Protein Sciences, Geneva University, Geneva, Switzerland

Vascular cerebral accident, or stroke, is a leading cause of death and disability in industrialized countries. An early diagnostic blood marker of stroke would allow immediate therapeutic interventions and hence reduce the extent of brain damage and risk of death. However, the discovery of novel diagnostic markers is limited by the difference in the protein copy numbers in body fluids such as plasma. Up to 12 orders of magnitude can be encounter when comparing the most abundance plasma protein (albumin) and a single protein copy released in the plasma by a cell. The separation of these proteins in amounts sufficient for quantitative evaluation is an important issue in proteome studies and presents a real challenge for the development of new diagnostic tools. This wide dynamic range can be overcome by the use of appropriate models and experimental designs that can simplify the protein complex mixtures. Here, we will report the use of post-mortem cerebrospinal fluid and cerebral extracelullar microdialysis fluid as models of stroke brain damage events as well as their proteomics evaluation for the discovery of potential early markers of stroke. The validation of proteins found differentially expressed in model samples by proteomics strategies will be shown in the blood of stroke patients to demonstrate the value of this concept as a first step toward the discovery of blood markers of stroke.

STROKE BIOMARKER DISCOVERY: GENOMICS

F.R. Sharp, G.C. Jickling, B.S. Stamova, B.P. Ander, X. Zhan, D. Liu

Neurology, University of California at Davis, Davis, CA, USA

This presentation will review the basics of choosing different approaches for developing biomarkers. The advantages of studying cell based RNA and proteins from blood versus plasma or serum microRNA and proteins will be reviewed. Since our work has focused on cellular mRNA and miRNA as well as plasma miRNA the remainder of the presentation will focus on these genomics approaches.

Our initial animal work using different brain injury models laid the foundation for our subsequent human studies. Several different brain injury models were chosen, including ischemic stroke, intracerebral hemorrhage, status epilepticus, hypoxia and hypoglycemia. One day later RNA was isolated from blood and processed on whole genome microarrays. The rationale for using whole genome approaches is to survey all known genes, and then choose those that are the best biomarkers for each type of injury. Several general principles arose from the studies. First, no single gene could distinguish ischemic stroke from controls or other types of brain injury. Second, a panel of genes was necessary to distinguish each type of injury from each other and from controls. Lastly, the fold changes were small so that technical rigor was essential in obtaining reliable, repeatable results.

We have now extended these results to humans with stroke and Transient Ischemic Attacks (TIAs). An important decision in our early studies was to use specific vacutainer tubes that lyse cells when the blood is drawn and immediately stabilize the RNA. This is important since isolating cells after blood is drawn WILL change gene expression of those cells, and potentially affect some proteins. After drawing blood into these tubes (PAXgene and others) the RNA is stable for weeks to years when kept frozen. Using these tubes we have shown specific RNA profiles for (1) ischemic stroke compared to controls and myocardial infarction (2) different causes of stroke including large vessel, cardioembolic and lacunar stroke (3) transient ischemic attacks and (4) and used these profiles to predict the cause of stroke in patients with cryptogenic stroke and to differentiate transient neurological events due to ischemic causes from those with non-ischemic causes. Preliminary studies have also been performed examing microRNA derived from whole blood and from plasma. These studies are of particular interest since they have identified dozens of miRNA that likely regulate mRNA expression in blood following stroke.

Technical issues related to processing arrays and analyzing the data will be discussed. Issues related to design of experiments and

studies will be examined, and in particular the need to build in a test set and validation set of samples within any given study. The diffculties in translating these studies to diagnositic testing will be discussed, along with the reasons for limited successes seen in other fields. Clinical variables important in designing biomarker studies will be outlined, and importance of defining the cohort to be studied will be emphasized. Finally, the wealth of biological information that will be gained in the basic science of the immunology of human stroke wil highlighted including need for cell specific studies.

TRANSLATIONAL SCIENCE AT THE NEUROVASCULAR INTERFACE: CHALLENGES OF IN VITRO TO IN VIVO BIOLOGY

A. Prat

Neuroscience, Université de Montréal, Montreal, QC, Canada

The Blood Brain Barrier (BBB) protects the central nervous system by regulating molecular and cellular exchanges between the brain and the blood. The BBB is made of a network of tightly adherent endothelial cells (ECs) surrounded by astrocytic processes and pericytes which provide factors that contribute to BBB maintenance. Several proteomic based-profiling of human and animal BBB endothelial cells have revealed the presence of unique regulatory proteins involved in BBB physiology and trans-endothelial leukocyte migration, including proteins involved in cellular adhesion, cell structure, BBB development, immunity and defense, transport and trafficking and signal transduction. Recent work, using animal models of MS and spinal cord contusion, as well as human in vitro, in situ and ex vivo analyses revealed that these new BBB candidate proteins, including the adhesion molecules, as well as some specific brain morphogen are involved in the regulation of immune cell trafficking across vascular structures of the CNS. This presentation will provide a short overview of the progresses that were made over the last 5 years to identify novel pathways that are involved in the selective recruitment of specific immune cells to the CNS and in the process of CNS immune quiescence. These molecules are currently seen as the basis for the development of future therapies to treat neuroinflammatory disorders and represent good examples of bench-to-bedside translational Neuroscience.

QUANTIFICATION OF BLOOD BRAIN BARRIER PERMEABILITY IN HUMANS WITH CONTRAST-ENHANCED MRI: A NOVEL TOOL TO STUDY VASCULAR DISEASES

G.A. Rosenberg

Neurology, University of New Mexico School of Medicine, Albuqueruqe, NM, USA

A basal lamina, astrocyte foot processes, and pericytes surround the cerebral capillary, which forms the first interface between the systemic circulation and the brain tissues; this complex series of interfaces is collectively referred to as the neurovascular unit. Normally, there are intact tight junctions formed by a group of proteins that create a epithelial like layer, preventing the movement of most molecules between the blood and the brain. We identified a family of proteolytic enzymes that regulate the permeability of the bood-brain barrier (BBB). This family is the matrix metalloproteinases (MMPs) and they are important in central nervous system development, injury, and repair. In early studies, we showed that the gelatinases (MMP-2 and MMP-9) disrupted the blood-brain barrier after intracerebral injection. During an injury, the MMPs are expressed and contribute to the vasogenic edema that complicates brain injury including acute stroke. More recently, we found that MMP-2 initiates the opening of the blood-brain barrier shortly after reperfusion in stroke by attacking the basal lamina and tight junction proteins in cerebral vessels. Besides acute ischemia MMPs are involved in neuroinflammation in multiple sclerosis, cerebral infections, Alzheimer's disease, and vascular dementia. MRI is an excellent tool to study the permeability of the BBB. Injection of a contrast agent, such as Gd-DTPA, can be visualized as it leaks across the capillary. Using a one-compartment analysis originally developed for autoradiography it is possible to measure transport from blood-to-brain. Our group has used the Patlak Plot method to quantify subtle changes in the BBB in patients with vascular cognitive impairment. Dementia is a major concern and there is increasing evidence that both Alzheimer's disease and vascular dementia are affected by neuroinflammation through the action of the MMPs. Our group has demonstrated that MMPs disrupt the blood-brain barrier in patients with vascular cognitive impairment of the small vessel type. We have identified MMPs in the CSF and brain tissue of patients with Binswanger's disease who have extensive white matter disease. Using dynamic contrast-enhanced MRI with Gadolinium to quantify the

permeability of the BBB, we have found a persistent disruption of the BBB that may be involved in the growth of the white matter lesions. These studies in humans could inform clinical trials of agents that block the inflammatory response.

BRAIN VASCULAR GENOMICS: METHODS FOR QUANTITATION, ANALYSIS AND INTERPRETATION

L.R. Drewes

Biomedical Sciences, University of Minnesota, Duluth, MN, USA

The Human Genome Project ushered in new technologies for increasing the speed and lowering the cost DNA sequencing. As advanced technologies (next generation sequencing) for accurate and reliable analysis have emerged, so have the applications to diverse species, disease tissues, individual patients and even small samples such as brain vascular endothelial cells. It is now possible to determine the cellular transcriptome with digital quantitation in order to characterize at a molecular level gene expression profiles at different disease or developmental stages. New challenges exist as well for quantitation and statistically reliable comparisons. This presentation will focus on the state-of-the-art technologies, some considerations for data collection and analysis, and potential future applications for advancing the characterization of the neurovascular unit/blood-brain barrier (NVU/BBB).

ADVANCES IN FUNCTIONAL AND STRUCTURAL MRI OF THE BRAIN

C.C.-C. Yen, A.C. Silva

NINDS, National Institutes of Health, Bethesda, MD, USA

Magnetic resonance imaging (MRI) is an *in vivo* imaging modality that produces excellent soft tissue contrast. A major application of MRI is in studies of the brain, in which a wide range of metrics such as the volume and location of structures, patterns of folding in the cortex and cortical thickness can be used to characterize neuroanatomy. We believe that MRI has a crucial role in improving our knowledge of both anatomical and functional organization of the cortex. We have been using anatomical and functional MRI to study neuroanatomy and neurovascular coupling in the brains of conscious, awake common marmosets (Callithrix jacchus), a small New World non-human primate with a brain size equivalent to the relative brain size of humans that is becoming increasingly useful in the research setting. The marmoset's relatively large brain shares many aspects of neural anatomy found in more commonly studied primates, including a large and well-developed cerebral cortex and cerebellum. Our group has developed MRI techniques to visualize the rich myeloarchitecture of the marmoset cortex (Figure 1), producing high-resolution anatomical maps of six major cortical areas with high myelination that correspond to the major sensory areas of the brain. In addition, diffusion-tensor imaging and T2*-weighted imaging complement the structural information that can be obtained from the brain. These data provide anatomical landmarks for studying functional brain activation in response to visual, somatosensory (Figure 2) and auditory stimulation. The ability to visualize such features opens up new avenues in morphological and functional studies that require longitudinal follow up of the changes in size and location of these areas during development or in response to plasticity induced reorganization due to learning or injury, as well as for guiding and confirming the location of functional measurements.

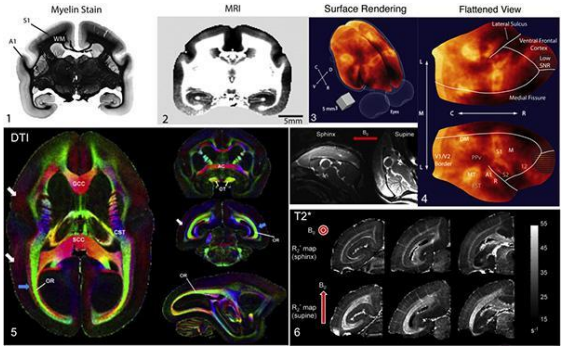

Figure 1:

(1) Coronal myelin-stained histological section of a marmoset brain. White matter (WM), primary somatosensory (S1) and auditory (A2) cortices are indicated.

(2) Corresponding T1-weighted MRI acquired in vivo. Notice the increased contrast throughout the cortex.

(3) 3D map of the myeloarchitecture in a 3-year old female marmoset.

(4) Flattened view of the cortex.

(5) Diffusion-tensor Imaging.

(6) T2*-weighted MRI. V1/V2 = primary/secondary visual areas, DM = dorsomedial area, MT = middle temporal area, A1/R = primary/rostral auditory areas, S1/S2 = primary/secondary somatosensory cortex, M = motor cortex including primary and premotor areas and the frontal eye fields.

Cortical features are labeled in gray: PPv = ventral posterior parietal cortex, FST = fundus of the superior temporal area, 12 = area 12. C = caudal, R = rostral, V = ventral, D = dorsal.

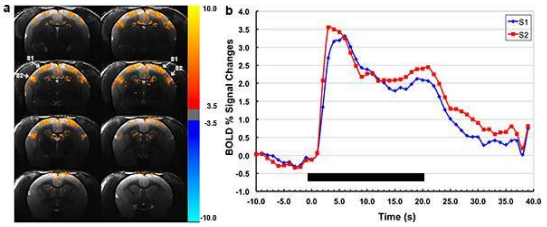

Figure 2:

(a) High-resolution BOLD fMRI activation maps and corresponding time courses obtained from a conscious awake marmoset in response to somatosensory stimulation, showing robust, bilateral BOLD activation in primary (S1) and secondary (S2) somatosensory cortices.

(b) Corresponding functional time-courses.

Acknowledgements: This Research was funded by the Intramural Research Program of the NIH, NINDS.

OPTICAL IMAGING OF NEUROVASCULAR FUNCTION

D. Boas

Radiology, Massachusetts General Hospital, Harvard Medical School, Charlestown, MA, USA

In vivo optical imaging of cerebral blood flow (CBF) and metabolism did not exist 50 years ago. While point optical fluorescence and absorption measurements of cellular metabolism and hemoglobin concentrations had already been introduced by then, point blood flow measurements appeared only 40 years ago. The advent of digital cameras has significantly advanced two- dimensional optical imaging of neuronal, metabolic, vascular, and hemodynamic signals. More recently, advanced laser sources have enabled a variety of novel three-dimensional high-spatial-resolution imaging approaches. Combined, as we discuss here, these methods are permitting a multifaceted investigation of the local regulation of CBF and metabolism with unprecedented spatial and temporal resolution. Through multimodal combination of these optical techniques with genetic methods of encoding optical reporter and actuator proteins, the future is bright for solving the mysteries of neurometabolic and neurovascular coupling and translating them to clinical utility.

Note that this abstract is copied from our review paper in recent JCBFM special issue.

Devor, A. *et al.* Frontiers in optical imaging of cerebral blood flow and metabolism. *J Cereb Blood Flow Metab* (2012).doi:10.1038/jcbfm.2011.195

CHRONIC CEREBRAL HYPOPERFUSION AS A PUTATIVE MODEL FOR VASCULAR DEMENTIA

H. Tomimoto

Neurology, Mie University Graduate School of Medicine, Tsu, Japan

Subcortical ischemic vascular dementia (SIVD), a most prevalent form of vascular dementia, is strongly related to hypertensive small vessel disease. Hypertension induces arteriolosclerotic changes, and consequently, chronic cerebral hypoperfusion. Similarly, in strongly hypertensive rats (SHR), hypertension induces arteriolar changes and cerebral hypoperfusion, being followed by small vessel occlusion and white matter lesions. SHR is ideal for simulating SIVD, however, mild degree and late emergence of white matter lesions are not suitable for pharmacological studies. Therefore, we initially designed a putative model which simulates chronic cerebral hypoperfusion by modulating blood flow.

There are several models of chronic cerebral hypoperfusion in gerbils, rats, mice and more recently monkeys. Here, we focus on rat and mouse model which we developed in the past two decades. We first raised a rat model by ligating the bilateral common carotid arteries. A variety of strains was screened and found Wistar rat to be the best with highest survival

rates and reproducibility of white matter lesions. Rats maintain CBF at 40-50% of the baseline level because their brain has a well-developed post. communicating artery (Pcom) and is perfused from the vertebrobasilar arteries even after occlusion of the common carotid arteries. Microglia are activated at 3 days and astroglia at 7 days. White matter lesions become explicit after 14 days in the optic chiasm and corpus callosum etc. Unfortunately, this model has a drawback such as compromised visual system which may hamper exact estimation in cognitive tests and limited applicability in genetic studies.

To circumvent these drawbacks, we further designed a mouse model by bilateral common carotid artery stenosis (BCAS). Mouse has a poorly-developed Pcom and does not survive after bilateral occlusion of the common carotid arteries. Among various strains we selected C57Bl6 because the Pcom is thin, and subsequently applied microcoils with various internal diameters. Using a microcoil with 0.18 mm internal diameter, the mice exhibited selective damages in the cerebral white matter but not in the gray matter. The CBF was decreased to approximately 70-80% of the baseline. Blood flow velocity was markedly decreased and rolling, adhesion and extravasation of leukocytes from the microvessels were observed by two-photon laser microscopy. In the white matter, microglia were activated at 7 days and astroglia at 14 days, and emergence of white matter lesions was delayed until 30 days. Notably, the blood brain barrier is damaged at 3 days probably because of an increased activity of matrix metalloproteinase (MMPs). The damage in the visual system was mild and showed no optic nerve atrophy because blood flow in the ophthalmic artery was maintained.

This BCAS model has advantages over the rat model in terms of cognitive and genetic investigations. Working memory deficit is found after 30 days with an additional emergence of reference memory deficit and hippocampal atrophy after 9 months survival. The presentation also includes examples of experiments using these models, which may provide a new way in the field of vascular cognitive impairment and neurodegenerative diseases.

BrainPET Educational Course

TRANSLATIONAL PET TRACER DEVELOPMENT

J. Passchier

Radiochemical Sciences, Imanova Ltd, London, UK

PET tracer development and subsequent translation to clinical application is a long and arduous journey with many dangers along the way. Many considerations need to be taken into account right from the start such as which target to select, what buy in there will be from the field, what chemistry to implement to facilitate application, what level of toxicology/dosimetry is required to support clinical use and what preclinical experiments are required to support clinical translation. What does the latter mean anyway? This presentation aims to review the steps that need to be taken as well as new ways of working that could be considered to successfully deliver a new CNS PET tracer as a clinical tool. In addition, a number of pitfalls that should and can be avoided will be highlighted and addressed.

QUANTITATIVE ANALYSIS OF NEURORECEPTOR STUDIES

H. Ito

Molecular Imaging Center, National Institute of Radiological Sciences, Chiba, Japan

There are several functions of neurotransmission in synapse. The endogenous neurotransmitter is synthesized in presynaptic neuron and released into synaptic cleft. The released neurotransmitter binds to the neuroreceptors in postsynaptic membrane and then signalings are caused. The released neurotransmitter is removed from synaptic cleft through the neurotransporters in presynaptic membrane. A neuroreceptor is a protein molecule in the cell membrane of neuron. For transmembrane neuroreceptors, there are two kinds of receptors, the metabotropic receptors including the G protein-coupled receptors and the ionotropic receptors. The receptors of dopaminergic and serotonergic neurotransmission system are categorized as the G protein-coupled receptors. A neurotransporter is a membrane

protein in presynaptic neuron. Both pre- and postsynaptic functions can be estimated by positron emission tomography (PET) with various radiotracers. The binding potential relative to the concentration of nondisplaceable radiotracer in brain (BP_{ND}), corresponding to the ratio of the density of neuroreceptors or neurotransporters available to bind radiotracer *in vivo* (B_{avail}) to the dissociation constant of the radiotracer (K_D), can be measured by PET with various radiotracers [1]. PET measures the total radioactivity in brain regions, and therefore the differentiation of specific binding from the background of nondisplaceable binding is a fundamental problem in quantitative analyses of PET data. A true equilibrium condition can be obtained only by continuous intravenous infusion of radiotracer [2]. Equilibrium condition after bolus injection of radiotracer can practically be defined as peak equilibrium at the transient moment when the specific binding is maximal [2, 3]. For equilibrium condition, BP_{ND} is expressed as the ratio of radiotracer concentration of specific binding to nondisplaceable binding estimated using a reference region. Kinetic analysis, which is based on the assumption that radiotracer binding can be described by the standard two-tissue compartment model, allows the differentiation of the specific binding from the background of nondisplaceable binding using arterial input function, and therefore revealing BP_{ND} [3]. For radiotracers with no ideal reference region, BP_{ND} can be calculated only by kinetic analysis. Distribution volumes can also be estimated by several graphic plot analyses, as well as by kinetic analysis. Graphic plot analyses can be used to distinguish graphically whether radiotracers show reversible or irreversible binding. A graphic plot analysis recently developed can also be used to distinguish graphically whether the radiotracer binding includes specific binding or not. To avoid the measurement of arterial input function, several quantitative approaches based on the use of a reference region have been developed. Both the simplified reference tissue model and multilinear reference tissue model methods were widely used to calculate BP_{ND} without the arterial input function. For each radiotracer and each purpose of PET study, an adequate quantification method should be employed.

References:

[1] Innis RB, et al. J Cereb Blood Flow Metab 2007; 27: 1533-1539.

[2] Ito H, et al. J Cereb Blood Flow Metab 1998; 18: 941-950.

[3] Farde L, et al. J Cereb Blood Flow Metab 1989; 9: 696-708.

QUANTIFICATION ACROSS SPECIES

R.N. Gunn[1,2]

[1]Imperial College London, [2]Imanova Ltd, London, UK

Determination of normo- and patho-physiology, the discovery of diagnostics and the development of therapies in man often build on translational neuroscience studies across a range species. Common translational pathways include a component of the mouse, rat, pig, and primate species progression prior to studies in man. Biological differences and technological limitations in lower species can impact on their ability to accurately predict outcomes in man. Thus, these factors need to be considered carefully in order to accurately select an optimal translational pathway ensuring that chosen experiments provide value. Relevant biological factors include differences in genotype, expression of transporters, affinity of the molecule for its target of interest, kinetics and the existence of preclinical models of disease. Technical limitations relate to differences in the volume of brain structures, mass-dose effects as a result of limitations in specific activity, requirements for anaesthesia and the ability to derive arterial input function data from reduced blood volumes. The challenges of quantification across species and the selection of an optimal translational pathway are discussed in relation to relevant examples from PET neuroimaging studies.

NONINVASIVE INPUT FUNCTION

M. Naganawa

Yale PET Center, Diagnostic Radiology, Yale University School of Medicine, New Haven, CT, USA

Quantitative brain PET studies typically require an arterial input function for kinetic modeling. In general, arterial blood sampling is considered to be the gold standard procedure to obtain this input function. However, its usage introduces several concerns. Invasive

arterial blood sampling often discourages volunteers from participating in experiments. Preparing for blood sampling (weighting tubes) and counting the blood samples in the tubes are laborious work, and a frequent access to subject's artery introduces additional radiation exposure to personnel. In addition to these drawbacks, performing arterial cannulation requires much more skill than venous blood sampling, and may fail in a non-negligible number of studies. For small animal imaging (rats/mice), the total volume of blood that can be drawn is limited and blood sampling may affect the physiological process. Therefore, it is desirable to develop a method that eliminates or alleviates the arterial blood sampling.

In the past decade, alternative methods have been proposed and addressed in a huge number of articles. The non-invasive input function estimation consists of two points: 1) estimating the shape and 2) estimating the scale of the input function. Shape estimation methods fall into 4 categories: 1) population-based approach that creates a template input function by normalizing individual input functions measured from a population of subjects, 2) carotid ROI placement approach which requires carotid identification and correction for partial volume effect and spill-in, 3) factor analysis approach which does not use any anatomical information, and 4) simultaneous estimation approach that estimates kinetic parameters of more than one region and a set of parameters of a common input function over the regions. Compared with variety of shape estimation methods, there are a few ways of scaling the input function. Usually, one or more arterial (or venous) blood samples are taken for scaling. Sampling-free approaches are also proposed. However, a trade-off exists between the accuracy of estimation and the number of samples available for the estimation.

There are many challenges to accurately estimate the input function noninvasively. One of the challenges is that a whole blood activity curve is estimated in most methods. Depending on the types of tracers or subject conditions, the plasma and whole blood curves are different in shape and scale. In receptor binding study, radiometabolites in the plasma make the estimation more difficult.

In this presentation, the measurement of the input function is briefly introduced, and we will discuss the advantage and challenging issues of the proposed methods. We will also briefly discuss other challenges in noninvasive input function estimation.

NOVEL METHODOLOGY FOR SIMULTANEOUS ASSESSMENT OF $CMRO_2$ AND CBF - CHALLENGES TOWARDS "ON-DEMAND" EXAMINATION USING $^{15}O_2$ AND PET

H. Iida

Department of Investigative Radiology, National Cardiovascular Center-Research Institute, Suita, Japan

Use of ^{15}O-labeledoxygen ($^{15}O_2$) and PET has a unique feature, and is capable of providing absolute quantitation of cerebral metabolic rate of oxygen ($CMRO_2$) and oxygen extraction fraction (OEF) in regional cerebral tissue in man. Despite the importance of those functional parametric images in characterizing the pathological status of several diseases, usage of $^{15}O_2$ has been limited, because of complex logistics of the examination. This paper is intended to summarize the previous problems and/or limitations of the ^{15}O-PET technique, and also to overview the recent progress how they could be overcome. Our preliminary system towards the "on-demand" operation, for ultra-rapid assessment of $CMRO_2$/CBF from single PET scanning will also be introduced.

The discussion will include following topics

1. Methodological backgrounds

ž This includes the kinetic model for $^{15}O_2$, and typical examination procedures. Possible error factors will also be discussed.

2. Recent improvement in the kinetic model ž This includes a novel formulation for simultaneous $CMRO_2$, CBF and OEF determination from a single PET scanning, and also how to compensate metabolized water. Improvement of the blood volume correction method in diseased conditions will also be discussed.

3. Improved quantitative accuracy in recent 3D PET ž This includes the importance of physical accuracy of PET, such as improved counting rate performance, and adequate scatter correction for high radioactivity in the trachea and facemask.

4. United system development

ž This includes ^{15}O-dedicated small cyclotron, operated with fully automated system for radio-synthesis and supply of ^{15}O-labeled gases to patients. There are also several peripheral devices which need to be united.

5. Validation and application

TWO COMPLEXITIES OF BRAIN IMAGING: GENOTYPE AND PERIPHERAL DISTRIBUTION

R.B. Innis

National Institute of Mental Health, Bethesda, MD, USA

Second-generation radioligands for translocator protein (TSPO), an inflammation marker, are confounded by the co-dominant rs6971 polymorphism that affects binding affinity. The resulting three groups are homozygous for high affinity state (HH), homozygous for low affinity state (LL), or heterozygous (HL). We tested if in vitro binding to lymphocytes distinguished TSPO genotypes and if genotype could affect clinical studies using the TSPO radioligand [^{11}C]PBR28. In vitro binding to lymphocytes and [^{11}C]PBR28 brain imaging was performed in 27 human subjects with known TSPO genotype. Specific [^{3}H]PBR28 was measured in prefrontal cortex of 45 schizophrenia patients and 47 healthy controls. Lymphocyte binding to PBR28 predicted genotype in all subjects. Brain uptake was ~40% higher in HH than HL subjects. Specific [^{3}H]PBR28 binding in LL controls was negligible, while HH controls had ~80% higher binding than HL controls. After excluding LL subjects, specific binding was 16% greater in schizophrenia patients than controls. This difference was insignificant by itself ($p = 0.085$), but was significant after correcting for TSPO genotype ($p = 0.011$). Our results show TSPO genotype influences PBR28 binding in vitro and in vivo. Correcting for this genotype increased statistical power in our postmortem study and is recommended for in vivo PET studies.

DRUG DEVELOPMENT IN NEUROPSYCHIATRIC DISORDERS: FROM BENCH TO BED

T. Suhara

Molecular Neuroimaging Program, National Institute of Radiological Science, Chiba, Japan

Positron emission tomography (PET) techniques have enabled the visualization of target molecules of various psychotropic drugs, such as receptors and transporters in the living human brain. The concept of occupancy has been used as a reliable index for therapeutic drug monitoring at specific binding sites. Previous PET studies on antipsychotics have suggested that 70%-80% of central dopamine D_2 receptor occupancy provides the desired therapeutic effects without any extrapyramidal symptom. Regarding the antidepressant therapy, serotonin transporter occupancy is also used as one of the indices for the evaluation of antidepressants such as selective serotonin reuptake inhibitors. Clinical doses of clomipramine and fluvoxamine occupied about 80% of serotonin transporter, and dose escalation would have minimal effect on serotonin transporter blockade. Norepinephrine transporter (NET) is another target of antidepressants. The mean NET occupancies by nortriptyline doses were 16.4 % at 10 mg, 33.2 % at 25 mg, and 41.1% at 75 mg, respectively. The application of PET method on drug evaluation can provide us useful information about the characteristics of psychotropics, including an optimal clinical dose and the kinetic profile at the sites of action as well as their ability to penetrate into the brain. However, in psychiatric disorders, reliable diagnostic biomarkers are still awaited. Nonetheless, in the case of Alzheimer disease (AD), distinctive pathological changes such as deposition of β-amyloid (Aβ) and tau protein have been identified. Several amyloid ligands, such as [^{11}C]PIB and [^{11}C]BF227, have been developed for imaging Aβ deposition. On the other hand, tau pathology is considered to be closely related with neural dysfunction in AD and non-AD tauopathy, and could accordingly be an important target for both therapeutic intervention and diagnostic imaging. [^{11}C]PBB3 has been recently developed as a tau imaging PET ligand, and showed high affinity and selectivity for tau deposits in our preclinical studies. [^{11}C]PBB3-PET demonstrated high accumulation in the medial

temporal cortex of all AD patients, in which binding of [^{11}C]PIB was minimal. Distribution of [^{11}C]PBB3 accumulation observed in AD patients extended to the entire limbic system and subsequently to the neocortex as a function of the disease severity.

HUMAN HYBRID PET/MR IMAGING

H. Herzog

Forschungszentrum Juelich GmbH, Jülich, Germany

A new hybrid imaging technology combining positron emission tomography (PET) and magnetic resonance imaging (MRI) is emerging presently. The motivation towards this bimodal imaging tool has been driven by the fact that the complementary capabilities of PET and MRI when combined in one instrument deliver a considerable added value in comparison to their separate use at different dates and locations. To allow for truly simultaneous PET/MRI imaging a new type of MR-compatible PET detectors had to be developed. First experimental PET/MRI scanners for studying small animals with different design strategies were realized by several research groups. After the introduction of the Siemens 3TMR-BrainPET as the first industrial prototype of integrated MR-PET scanners for human brain studies - one of them at the Forschungszentrum Juelich - two types of PET/MRI scanners for whole-body studies are now commercially available. Whereas the Biograph mMR scanner offered by Siemens integrates the PET detector within the MR scanner, the Ingenuity TF PET/MR available from Philips consists of a PET scanner and an MR scanner linked by a common patient bed.

In this presentation, the technological challenges and different concepts of present instrumentation for human hybrid PET/MR imaging will be discussed shortly. While the primary clinical use of PET/MRI is expected to be in the field of oncology as in the case of PET/CT, this lecture - given at BrainPET 2013 - will focus on brain applications. The performance characteristics of the PET components installed in the different PET/MRI scanners will be summarized. Our own experiences with first studies done with the 3TMRBrainPET operated at the Forschungszentrum Juelich will be presented. The advantages of time saving in patient management and optimal spatial overlay of anatomic and functional information offered by PET/MRI with regard to the simultaneous observation of physiological and metabolic processes will be demonstrated. In brain tumour patients simultaneous multiparametric MR-BrainPET confirmed the feasibility of versatile MR imaging during dynamic PET. Until now functional brain activation (observed by fMRI) and interaction of receptor ligands during special activation tasks or pharmacological intervention (measured by PET) could not be explored in humans simultaneously. Using integrated PET/MRI such studies become possible for basic investigations as well as for clinical research and applications.

MOLECULAR STROKE

J. Hatazawa

Nuclear Medicine and Tracer Kinetics, Osaka University Graduate School of Medicine, Suita, Japan

Molecular, cellular, and tissue pathology after cerebral ischemia has been extensively studied over the last decades in experimental animals and in patients. In clinical setting, the imaging technology of Positron Emission Tomography (PET), Single Photon Emission Computed Tomography (SPECT), X-ray Computed Tomography (CT), and Magnetic Resonance Imaging (MR) visualized the ischemic penumbra, a tissue at risk for cerebral infarction. Recently, further development of imaging modalities for small animals combined with new biological probes made it possible to study molecular basis of ischemic penumbra. Here, I review the important clinical works regarding cerebral energy failure following acute embolic occlusion of carotid/cerebral arteries by ^{15}O-PET and Diffusion-Perfusion MR. I also provide a testable hypothesis that astrocytic TCA (Tricarboxylic acid) cycle activity has a critical role for protection of cerebral tissue damages induced by acute ischemia.

In patients with acute embolic occlusion of carotid/cerebral arteries, the initial 3-day infarct volume expansion was associated with disturbed $CMRO_2$ but not with cytotoxic edema (defined as “Metabolic penumbra”) as early as 6 hours of onset (Shimosegawa E, et al. Ann Neurol 2005).

The next question was a role of astrocytes in ischemic brain and how astrocytes relate to

the expansion of infarct volume. Acetate is preferentially taken up and metabolized by astrocytes. We demonstrated that ^{14}C-acetate is a sensitive marker of TCA cycle activity in astrocytes (Hosoi R, et al. 2004 JCBFM). After short-term ischemia, ^{14}C-acetate uptake in the brain was reduced but not immediately recovered after reperfusion (Hosoi R, et al. JSCD, 2007). Astrocytic metabolic dysfunction caused cerebral infarction even after short-term ischemia in rats (Hosoi R, et al. Ann Nucl Med, 2006). These findings indicated that recovery of astrocytic TCA cycle activity is a key issue to protect infarct volume expansion.

It is well known that the astrocytic TCA cycle is coupled with glutamate-glutamine cycle. Extracellular glutamate concentration was increased after astrocytic TCA cycle inhibition by fluoro-citrate (Largo P, et al. J Neurosci, 1996; Rodriguez Diaz, et al., Glia, 2005). These studies indicated that astrocytic TCA cycle dysfunction during ischemia and initial reperfusion period may induce an elevation of extracellular glutamate concentration. Hirose et al. revealed in rat brain that astrocytic TCA cycle inhibition induced enhanced glucose consumption, which was protected by pretreatment of NMDA receptor antagonists (Neuroscience Letters, 2007).

The hypothesis that astrocytic TCA cycle dysfunction may occur in ischemic or metabolic penumbra is now testable by the PET with ^{11}C-acetate.

Brain Symposium

ASTROCYTIC AQUAPORIN 4 ROLES IN NEUROIMAGING SIGNALS: DWI AND DTI

J. Badaut[1,2]

[1]Dpt of Pediatrics, [2]Dpt of Physiology, Loma Linda University, Loma Linda, CA, USA

The non-invasive neuroimaging using magnetic resonance imaging (MRI) is widely used for functional brain mapping as well as a biomarker for daily clinical diagnosis and prognostic. Cellular localization of changes in water mobility observed with diffusion weighted imaging (DWI) or in diffusion tensor imaging (DTI) are critical for the interpretation of the images in normal and pathological brains. Aquaporin 4 (AQP4), a water channel, is located in astrocyte processes in contact of blood vessels and neuronal synapses. Thus, interpretation of the neuroimaging signal changes depends on an understanding of water movement at cellular level in brain. However, the cellular and molecular mechanisms that underlie such signal changes in ADC and DTI are still in progress. Using siRNA targeting AQP4 (siAQP4) injection *in vivo* induces a decrease of ADC values, extracted from DWI, without major tissue structural changes and water content. Similarly, the DTI signals are changed in the cortex with a decrease of the axial diffusibility and increase of the relative anisotropy. Interestingly, siAQP4 injection also decreases the level of connexin 43, and then possibly changes the connectivity with less functional gap junctions in the astrocyte. Therefore, the decreases of astrocytic water channel and the changes in the astrocyte connectivity are possibly contributing to neuroimaging signals for the DWI and DTI. A better understanding of the astrocyte network physiology is critical for the interpretation of the neuroimaging changes in pathophysiological conditions.

Financial support: NIH R01HD061946 Swiss Science Foundation (FN 31003A-122166)

CELLULAR, VASCULAR AND FUNCTIONAL DEVELOPMENT OF THE BRAIN

E. Hillman, M. Kozberg, A. McCaslin, B. Chen, M. Bouchard, L. Grosberg

Biomedical Engineering and Radiology, Columbia University, New York, NY, USA

Introduction: The brain exhibits tightly coupled increases in cortical blood flow in response to specific stimuli. These blood flow changes are the basis of the BOLD signal detected in fMRI. However, the cellular mechanisms controlling these blood flow changes, and even the underlying purpose of modulating blood flow, are not well understood.

Aims of study: One current hypothesis is that astrocytes play a critical role in coupling neuronal activity to blood flow increases, while the involvement of direct neuronal signaling, interneurons and endothelial cells have also been explored. We hypothesized that if astrocytes were the primary drivers of blood flow changes, that their physical distribution and connectivity with each other, and with blood vessels, would need to be consistent with the vascular dynamics observed during functional hyperemia.

Materials and methods: Our studies used in-vivo two-photon microscopy and high-speed multispectral optical intrinsic signal imaging (MS-OISI) in rats and mice. Astrocytes were labeled with SR101.

Results: In initial studies, we found that astrocytes are intimately associated with blood vessels within the cortex, with almost all directly contacting a diving artery, capillary or ascending vein. Astrocyte processes were found to ensheath all sub-pial vessels, potentially forming a conduit of sheathing capable of long-range signaling. However, we also confirmed that no astrocyte processes extend above the glia limitans, despite the strong dilations of pial arterioles observed during functional hemodynamic responses to stimulation [1, 2]. Based on earlier reports of abnormal, typically inverted, fMRI responses in human infants and children, we decided to explore whether the neonatal brain could provide further insights into neurovascular mechanisms. Using MS-OISI, we characterized the developmental evolution of the hemodynamic response at the vascular level [3]. We confirmed that P12-P13 rats show almost no 'positive BOLD' blood flow increase in response to stimulation, in fact we observed strong, bilateral decreases in blood flow, with corresponding constriction of pial arteries. With increasing age, we observed the gradual establishment of a positive, localized hemodynamic response to stimulation, which reached a fully positive response around P23. Only by adulthood did the response include the dilation of large pial arteries. We also found that strong stimuli in the neonatal rat induced large systemic blood pressure increases which, owing to immature autoregulation, produced strong, highly misleading bilateral positive cortical hemodynamic responses.

Conclusions: We interpret our neonatal results as revealing the gradual development of neurovascular control in the brain. Using in-vivo two-photon microscopy, we are now exploring the neuronal, astrocytic and vascular changes that accompany the gradual development of localized, mature functional hyperemia to isolate the role of each in the generation of functional hyperemia. One consistent finding between both our initial astrocyte, and developmental studies is a need for a mediator other than astrocytes to invoke rapid dilation of pial arteries, a mechanism that appears to mature by with developmental age.

1. McCaslin, A.F.H., et al, J Cereb Blood Flow Metab, 2011. **31**: p. 795-806.

2. Chen, B.R., et al, Neuroimage, 2011. **54**(2): p. 1021-1030.

3. Kozberg, M.G., et al, PNAS, 2013.

CELLULAR AND MOLECULAR MR IMAGING IN NEUROLOGICAL DISEASES

R.M. Dijkhuizen[1], N.R. Sibson[2]

[1]Biomedical MR Imaging & Spectroscopy Group, Image Sciences Institute, University Medical Center Utrecht, Utrecht, The Netherlands, [2]Gray Institute for Radiation Oncology & Biology, University of Oxford, Oxford, UK

Primary goals of what is now termed 'molecular imaging' are the visualisation of pathological processes at the (sub)cellular level, often long before disease symptoms become clinically apparent, and the direct monitoring of effects of targeted therapeutic interventions. Both PET and SPECT have been used in this way for many years, but with limited spatial resolution. In recent years the concept of molecular MRI has evolved and we now have the ability to gain information not only on the upregulation of specific molecules associated with pathology, but also on alterations to neuronal pathways and recruitment of specific cell populations, including stem cells, to disease areas.

The potential of MRI to detect events at cellular and molecular levels has become imminent by current advancements in contrast agent design and synthesis. Molecular and cellular MRI typically employ (super)paramagnetic nano- or microparticles with or without conjugated ligand. Cellular labeling and molecular targeting with tailored contrast agents enable direct detection of cells and biomarkers, which can be applied for noninvasive measurement of migration of cells, e.g. leukocytes, and expression of molecular markers, e.g. cell adhesion molecules. An alternative approach makes use of paramagnetic manganese (Mn^{2+}) as a calcium analogue that can enter neurons through Ca^{2+}-channels. Manganese-enhanced MRI has been successfully used for in vivo studies on cytoarchitecture and activity in the brain and retina.

Cellular and molecular MR imaging are cutting-edge translational areas in current MRI research, involving preclinical and clinical studies on neural tissue structure and function, neuroinflammatory processes, and neurorestorative therapies. The invited speakers in this symposium will cover all aspects of this exciting field, from molecular mechanisms to applications in animal models and human patients.

TRACKING STEM CELLS IN VIVO USING MRI

J. Bulte

Johns Hopkins University, Baltimore, MD, USA

Translational cellular imaging is expected to play a key role in evaluating the outcome of regenerative medicine clinical trials using stem cells. In order to facilitate and implement the translation of novel stem cell therapies into the clinic, one needs to be able to monitor the cellular biodistribution non-invasively following administration. Among the different clinically used cellular imaging techniques, 111-In oxine scintigraphy is the only FDA-approved method and has been primarily for imaging of infection and inflammation. Cellular magnetic resonance (MR) imaging, with its superior spatial resolution and excellent soft tissue anatomical detail, is emerging as the technique of choice to monitor in real-time image-guided cell delivery, immediate engraftment, and short-term homing. Up until now, 7 clinical MRI cell tracking studies have been published, all using superparamagnetic iron oxide nanoparticles or SPIOs in an off-label fashion. SPIOs are clinically approved and create strong local magnetic field disturbances that spoil the MR signal leading to hypo- or hyperintense contrast. A major setback is that the particles that were being used have been taken off the market, as their primary, FDA-approved indication (liver imaging of Kupffer cells) did not live up to its promise. However, several companies have started manufacturing novel particles, which possibly can also be used for magnetic particle imaging (MPI). There are also other MRI techniques based on reporter genes, e.g. ferritin, lysin-rich protein, supercharged GFP, and thymidine kinase. These offer the advantage that it is possible to determine cell survival and differentiation of stem cells, when the reporter is placed under a specific promotor. Finally, fluorine (19F) MRI is gaining attention for MRI cell tracking, with the first clinical trials expected to begin in 2013.

MOLECULAR MRI IN NEUROLOGICAL DISEASE

N. Sibson

Department of Oncology, University of Oxford, Oxford, UK

The primary goal of what is now termed *molecular imaging* is the visualisation pathological processes at the cellular level, often long before disease symptoms become clinically apparent. The ability to do this confers two major benefits: earlier diagnosis of disease and targeting of individual therapy. Both PET and SPECT have been used in this way for many years, but with limited spatial resolution. In recent years the idea of molecular MRI has evolved, with the advantage of considerably greater spatial resolution than either of the radioisotope-based methods. Typically, diagnostic MRI has relied on the effects of pathology on the water molecules in the tissue, and as a consequence has provided indirect and, frequently, rather non-specific information on the underlying processes. With the advent of molecular MRI we now have the ability to gain information on the expression, upregulation or downregulation, of specific molecules associated with pathology. Using this approach we have shown that we can detect specific adhesion molecules expressed on the vascular endothelium using ligand-targeted MRI contrast agents early in the progression of experimental brain disease. Moreover, we are able to do this at a time when the presence of pathology is undetectable by either existing imaging methods or clinical scoring. In this talk I will discuss the various novel targeted contrast agents that we have been developing in Oxford and our *in vivo* work in experimental models of multiple sclerosis, stroke and brain cancer. I hope, thereby, to demonstrate the potential of molecular MRI for sensitive detection of neurological disease.

MAGNETIC RESONANCE IMAGING OF MACROPHAGE BRAIN INFILTRATION AND OF MOLECULAR BLOOD BRAIN BARRIER ALTERATIONS IN EXPERIMENTAL AND CLINICAL MULTIPLE SCLEROSIS

K.G. Petry

Neuroinflammation, Imaging and Therapy of Multiple Sclerosis, INSERM U 1049, University Bordeaux Segalen, Bordeaux, France

In Multiple Sclerosis (MS), myelin and axonal degeneration is caused by a proinflammatory autoimmune response involving molecular and cellular activity of the blood brain barrier (BBB). With the aim to characterize these active modulations, we have developed strategies by using in vivo Magnetic Resonance Imaging (MRI) to define the cellular and molecular events of the neuroinflammation process at the BBB in MS and experimental neuroinflammation models. These tools allow to monitor various events of active BBB alterations for which we analysed the cellular and molecular basis:

1) the macrophage activity in comparison to BBB leakage in acute MS lesions and their follow-up,

2) the involvement of water transporter AQUP4 in inflammatory oedema formation and resolution, and

3) the molecular alterations of the endothelial cells by a series of newly defined peptide ligands.

I will present the in vivo selection strategy to generate the peptide ligands and the tool developments of molecular biology and bioinformatics to determine peptide ligands binding specifically to the molecular alterations at the inflamed BBB in the experimental MS rat model. I will show the in vivo application to target with peptides linked to nanocargos such molecular alterations during neuroinflammation that was monitored in vivo by MRI. I will further discuss and present some preliminary data to transfer the developed tools and in vivo markers that we have characterized in MS towards other brain pathologies (like tumour, but also neurodegeneration, trauma, infection) involving nervous tissue remodelling and cellular activation, in particular of endothelial cells and activation of proinflammatory and immunomodulating cell phenotypes.

CEREBRAL BLOOD FLOW IN MOUSE MODELS OF AD

A.J. Kiliaan, D. Jansen, V. Zerbi

Anatomy, Donders Institute for Brain, Cognition, and Behavior Radboud University Nijmegen Medical Centre, Nijmegen, The Netherlands

Although food has classically been perceived as provider of energy and building material to the body, its ability to prevent and protect against diseases is starting to be recognized. Already 30 y ago pioneering studies on Greenland Eskimos indicated that intake of n-3 long chain polyunsaturated fatty acids (n-3 LCPUFA) from fish has protective effects against cardiovascular diseases. Also the Mediterranean diet containing n-3 LCPUFA as important component has been shown in several prospective world-wide studies to be inversely associated with cardiovascular disease (CVD) and to be a strong protective factor against hypertension, obesity, and Alzheimer disease. The important role of diets and healthy lifestyle as preventative of vascular diseases is therefore widely accepted. Dietary lipids, which originally were thought to affect the brain through their effects on cardiovascular physiology, are also starting to be recognized for their direct actions on the brain like on synaptic function and plasticity and cognitive processes. The other way around, diets that are high in saturated fat are becoming notorious for reducing molecular substrates that support cognitive processing and increasing the risk of neurological dysfunction in both humans and animals. Also several other dietary components have been recognized for their effects on cognitive abilities. Dietary factors can affect multiple brain processes by regulating neurotransmitter pathways, synaptic transmission, membrane fluidity and signal-transduction pathways. Based on previously published data, and also on our new preliminary data in mice models for Alzheimer, treatment with dietary supplementation comprising the nutritional precursors and cofactors for membrane synthesis, viz. DHA, eicosapentaenoic acid (EPA), UMP, choline, phospholipids, folic acid, vitamins B6, B12, C, E, and selenium promotes neuroprotection by decreasing inflammation, restoring cerebral blood flow and volume, and inhibiting neurodegeneration, enhancing neural plasticity by increasing neurogenesis. In this talk the capacity of nutrients to affect brain function and structure in both mice and men will be reviewed.

VASCULAR PATHOLOGY IN ALZHEIMER´S DISEASE

D.R. Thal

University of Ulm, Ulm, Germany

Objectives: To clarify associations between Alzheimer´s disease (AD) and cerebral amyloid angiopathy (CAA), small vessel disease (SVD), atherosclerosis in the vessels of the circle of Willis, brain infarction and hemorrhage.

Methods: Brains from autopsy cases with AD and non-demented controls as well as cases with preclinical AD pathology were neuropathologically studied for AD pathology, CAA, SVD, atherosclerosis in the circle of Willis, brain infarction and hemorrhage. Additionally, sections from the basal ganglia of selected human autopsy cases were studied immunohistochemically for the distribution of the amyloid β-protein (Aβ), apolipoprotein E (apoE), and immunoglobulin G (IgG) in the vessels, perivascular spaces and in brain parenchyma.

Results: CAA was strongly associated with AD. Cases with capillary CAA were, thereby, most frequently carriers of the APOE ε4 allele. The severity of atherosclerosis in the circle of Willis as well as of SVD was not associated with AD. Likewise the prevalence of brain infarction and hemorrhage did not vary significantly between AD and control cases, whereas brain infarction but not hemorrhage was more prevalent in cases with vascular dementia than in AD and controls. Cases with microinfarcts in the CA1-subiculum regions in cases categorized as vascular dementia were usually associated with low - intermediate levels of AD pathology.The immunohistochemical analysis revealed that vessels of the basal ganglia with SVD exhibit vessel wall lesions that accumulate plasma proteins such as apoE and IgG. These proteins were also found in the perviascular space indicating a defect of the blood-brain barrier (BBB) at the arterial (precapillary) level. These changes were frequently observed in AD cases. Here, perivascular astrocytes near such SVD-affected vessels contained apoE and Aβ.

Conclusions: These results show that CAA is strongly associated with AD whereas only a trend was observed for an associated between AD and SVD. SVD, however, can cause defects of the BBB at the precapillary level. The influx of plasma proteins into the perivascular space and brain parenchyma may impair the apoE-related clearance of Aβ into the perivascular space. Moreover, vascular lesions such as infarcts and microinfarcts, especially in strategic regions, may further aggravate impairment of brain function initiated by even mild to moderate AD-related lesions, and may, thereby, lower the threshold for the development of cognitive symptoms.

IMPAIRED CEREBRAL AUTOREGULATION AND VASOMOTOR REACTIVITY IN SPORADIC ALZHEIMER'S DISEASE

J.A.H.R. Claassen

Geriatric Medicine, Radboud Alzheimer Center, Donders Institute, Radboud University Medical Center, Nijmegen, The Netherlands

Background: Understanding the relationship between vascular disease and AD will enhance our insight into this disease and pave the way for novel therapeutic research. Cerebrovascular dysfunction, expressed as impaired cerebral autoregulation and cerebral vasomotor reactivity, has been observed in transgenic mouse models for AD. Translation to human AD is limited and conficting however.

Objective: To investigate if impaired cerebral autoregulation and cerebral vasomotor reactivity, found in animal models for AD, are present in human sporadic AD.

Methods: In 12 patients with mild to moderate AD (age 75 ± 4 yr) and 24 controls matched for age and history of hypertension, we measured blood pressure (Finapres) and cerebral blood flow-velocity (transcranial Doppler). Cerebral autoregulation was assessed during changes in blood pressure induced by single and repeated sit-stand maneuvers. Cerebral vasomotor reactivity was assessed during hyperventilation and inhalation of 5 % carbon dioxide.

Results: During single sit-stands, controls had a 4% (SD 8) decrease in cerebrovascular resistance during a reduction in blood pressure, and an 8 % (SD 11) increase during a rise in blood pressure, indicating normal cerebral autoregulation. These changes were not seen in AD (p=0.04). During repeated sit-stands, blood pressure fluctuated by 20 % of baseline. This led to larger fluctuations in

cerebral blood flow in AD (27 (6) %) than in controls (22 (6) %, $p < 0.05$). Cerebral vasomotor reactivity to hypercapnia was reduced in AD (42.7 % increase in CBFV, versus 79.5 % in controls, $p = 0.03$).

Conclusion: Observations of impaired cerebrovascular function (impaired autoregulation and vasoreactivity) in transgenic mouse models for AD were confirmed in patients with sporadic AD.

COMORBIDITIES AND STROKE: FROM THE BEDSIDE TO THE BENCH

M.A. Moro[1], M. Castellanos[2], D.W. Howells[3], X. Wang[4], S.M. Allan[5], J.D. Huber[6]

[1]Universidad Complutense de Madrid, Madrid, [2]Hospital Dr. Josep Trueta, Girona, Spain, [3]Melbourne Brain Centre, Melbourne, VIC, Australia, [4]Massachusetts General Hospital and Harvard Medical School, Charlestown, MA, USA, [5]University of Manchester, Manchester, UK, [6]West Virginia University, Virginia, VA, USA

Ischemic stroke is the third leading cause of death in industrialized countries and the most frequent cause of adult disability worldwide. Moreover, its incidence is increasing in developing countries, a reason for which it has been identified by the WHO as a major public health problem. Despite advances in the understanding of the pathophysiology of cerebral ischemia, therapeutic options remain limited. At present thrombolytic therapy is the only licensed treatment and for various reasons this will never become widely available, best estimates being that 10-15% patients might benefit. Continued failure to translate successful preclinical stroke findings to patient benefit has been explained by a number of factors. One such factor is the failure to adequately consider clinically relevant comorbidities in experimental models of stroke. These comorbidities, including hypertension, diabetes, infection, as well as age, may change the response to cerebral ischemia and therefore affect the efficacy of potential stroke treatments. It is extremely important therefore to determine underlying mechanisms by which comorbidity contributes to the onset of stroke and subsequent outcome, such that better preclinical trials of potential therapies can be conducted.

Pre-existing hypertension, highly prevalent among stroke patients, is associated to early and late death and dependency. Specifically, Dr. Howells will focus on the impact of pre-existing hypertension on the efficacy of candidate stroke drugs and on the need to use different experimental models for their assessment. Dr. Wang's lecture will focus on diabetes, another important comorbidity. His talk will detail the relative contribution of preexisting diabetes and post-stroke hyperglycemia on hemorhagic transformation after tPA thrombolytic therapy. Infection is not only a common post-stroke complication post-stroke; also, increasing clinical evidence suggests a link between preceding acute infection and stroke onset. Prof. Allan will discuss the mechanisms by which acute inflammatory challenges or bacterial infections lead to a worsening of stroke outcome in experimental stroke models. Finally, we cannot forget the high prevalence of stroke among the aged population. Dr. Huber will focus on the role of aging in the effect of stroke therapeutics and will detail his work using specific drugs that may be beneficial for aged stroke patients.

HYPERTENSION AND STROKE

D. Howells, V. O'Collins

Stroke Division, Florey Institute of Neuroscience and Mental Health, Melbourne, VIC, Australia

High blood pressure affects approximately 26% of the adult population and is a well-recognised modifiable risk factor for stroke. Pre-existing hypertension is present in more than 50% of patients and 80% of stroke patients have SBP >140 mmHg during the acute phase of stroke. Early and late death and dependency are increased by hypertension and the efficacy of antihypertensive medications in preventing vascular events is well established.

During drug development it is important to know whether candidate stroke drugs retain efficacy in the face of hypertension.

At least 20 models of hypertension ranging from surgical ligation of arteries supplying a kidney, through pharmacological or genetic manipulation of vascular reactivity to selective breeding of hypertensive rabbits and rats have been reported. Broadly all that have been studied exacerbate ischemic injury caused by thread occlusion of the middle cerebral artery

and are prone to spontaneous haemorrhagic stroke.

When data were pooled from 3,288 acute ischemic stroke experiments (47,899 animals) testing the effect of therapies on infarct size (published 1978 - 2010), it was found that only the genetically induced strain of Spontaneous Hypertensive Rat and its variants (e.g. the Stroke Prone Spontaneous Hypertensive Rat) had been used. Of the 502 therapies tested in acute experimental stroke and included in the dataset, 474 had been tested in normotensive animals, 86 had been tested in hypertensive animals and 58 had been tested in both. Overall, hypertension was associated with lower treatment efficacy. Of the 58 tested in both, 12 therapies were less effective in hypertensive animals compared to normotensive animals (TNF-alpha, isoflurane, albumin, exercise, pentobarbital, halothane, dizocilpine, tPA, nicardipine, aminoguanidine, Ac-YVAD.cmk and NXY-059) and six therapies were more effective (hypothermia, citicholine, L-Name, isradipine, SB-221420-A and L-arginine).

Within the basic science testing of acute stroke therapies, 10% of studies had been undertaken in hypertensive animals - substantially less than the estimated prevalence of hypertension in the stroke population. To the extent that acute stroke therapies have been tested in hypertensive animals, the testing has been undertaken predominantly in the genetically hypertensive rat (SHR). Hypertension has a significant effect on the efficacy of candidate stroke drugs: standard basic science testing regimes may overestimate the efficacy which could be reasonably expected in hypertensive patient groups.

The strength of basic science evidence demonstrating the effect of hypertension on acute stroke therapies would be stronger if validated in models other than the SHR.

IMPROVING TPA THROMBOLYTIC THERAPY OF ISCHEMIC STROKE WITH DIABETES MELLITUS AND POST-STROKE HYPERGLYCEMIA

X. Fan, M.-M. Ning, E.H. Lo, **X. Wang**

Departments of Neurology and Radiology, Massachusetts General Hospital and Harvard Medical School, Charlestown, MA, USA

Background: Post-stroke hyperglycemia is presented in all preexisting diabetes mellitus (about 30% of ischemic stroke) and 50% of non-diabetic ischemic stroke patients. Hyperglycemia itself and hyperglycemia/diabetes-associated inflammatory cerebrovascular damage are considered of major contributors to the increased risk of hemorrhagic transformation and worse functional outcomes after tPA thrombolytic therapy. Thus we performed two sets of experiments investigating the effects of early insulin glycemic control plus tPA combination or the effects of anti-inflammatory agent minocycline plus tPA combination in acute brain tissue outcomes of focal embolic stroke in type I diabetic rats.

Method: Type I diabetes of male Wistar rats (diabetes for 6 weeks, 14 weeks old) were subjected to embolic focal stroke. In the first set of experiments, all rats were treated with insulin or saline control at 1 hour followed by tPA or saline at 1.5 hours after stroke. Infarction, hemispheric swelling, hemorrhagic volume, perfusion defects and mortality were examined and compared at 24 hours after stroke. Total plasma plasminogen activator inhibitor-1 (PAI-1) antigen and activity levels were measured at before stroke, and at 1.5, 3 and 6 hours after stroke. In the second set of experiments, stroke animals were divided into three treatment groups: (1) saline at 1.5 hours after stroke; (2) tPA alone at 1.5 hours after stroke; (3) combined minocycline (IV) at 1 hour plus tPA at 1.5 hours, and second treatment of minocycline (IP) at 12 hours after stroke. Acute brain tissue damage was assessed at 24 hours after stroke. Inflammatory biomarkers interleukin 1β (IL-1β) and matrix metalloproteinase 2 and 9 (MMP-2/-9) were examined in plasma. Neutrophil infiltration, microglia activation, MMP activity and tight junction protein claudin-5 degradation were examined in peri-infarct brain sections.

Results: In the first set of experiments, early insulin glycemic control alone or tPA alone had no significant effects in brain infarction reduction. However, insulin combined with tPA significantly reduced brain infarction, hemispheric swelling and tPA-mediated intracerebral hemorrhage. In addition, the combination also significantly decreased plasma PAI-1 antigen level at 6 hours, and PAI-1 activity at 1.5 and 6 hours after stroke, as well improved plasma perfusion at 24 hours after stroke. Results from the second set of experiments showed that compared to saline or tPA alone treatments, minocycline plus tPA

combination significantly reduced brain infarction, hemispheric swelling and intracerebral hemorrhage at 24 hours after stroke. The combination also significantly suppressed the elevated plasma levels of MMP-9 and IL-1β up to 24 hours after stroke. At 16 hours after stroke, neutrophil infiltration, microglia activation, MMP-9 activity and tight junction protein claudin-5 degradation in the peri-infarct brain tissues were also significantly attenuated by minocycline plus tPA combination.

Conclusions: Combination of early insulin glycemic control with tPA may be beneficial in lowering blood glucose and diminishing reperfusion defeat that result in reductions of brain tissue damage and hemorrhagic transformation. Combination of minocycline plus tPA may be beneficial in ameliorating systematic and neurovascular inflammation that leads to decreased infarction, brain swelling and hemorrhage for ischemic stroke with diabetes mellitus or post-stroke hyperglycemia.

PRECEDING INFECTION AND ITS EFFECT ON STROKE OUTCOME

Á. Dénes[1,2], J. Pradillo[1], B. McColl[3], C. Drake[1], K.N. Murray[1], P. Warn[4], B. Nieswandt[5], N.J. Rothwell[1], **S. Allan**[1]

[1]Faculty of Life Sciences, University of Manchester, Manchester, UK, [2]Laboratory of Molecular Neuroendocrinology, Institute of Experimental Medicine, Budapest, Hungary, [3]Neurobiology Division, The Roslin Institute, University of Edinburgh, Edinburgh, [4]Manchester Academic Health Science Centre, National Institute for Health Research Translational Research Facility in Respiratory Medicine, University of Manchester, Manchester, UK, [5]University Hospital and Rudolf Virchow Center for Experimental Biomedicine, University of Würzburg, Würzburg, Germany

A number of risk factors for stroke have been identified, yet these are rarely considered in experimental studies. Infection has long been recognised as a serious complication post-stroke and major contributor to mortality, and increasing clinical evidence also suggests a strong link between preceding acute infection and stroke onset. Respiratory and urinary tract infections in particular appear to show the strongest association. Experimental evidence is lacking in this area and our recent studies have set out to establish possible mechanisms underlying the effects of infection pre-stroke. Using rodent models of focal ischaemia we find that an acute inflammatory challenge immediately before stroke can worsen outcome, via interleukin-1 and neutrophil dependent mechanisms. Furthermore infection with Streptococcus pneumonia, a more clinically relevant challenge, also worsens stroke outcome, in both young and old atherosclerotic animals, via interleukin-1 and platelet dependent mechanisms. No spontaneous stroke is observed in co-morbid animals when exposed to pulmonary infection. These observations highlight an important role of preceding infection in determining outcome post-stroke.

NEUROPLASTICITY-PROMOTING THERAPIES

R.M. Dijkhuizen[1], **M. Chopp**[2,3]

[1]Biomedical MR Imaging & Spectroscopy Group, Image Sciences Institute, University Medical Center Utrecht, Utrecht, The Netherlands, [2]Department of Neurology, Henry Ford Hospital, Detroit, [3]Department of Physics, Oakland University, Rochester, MI, USA

There is increasing evidence of the adult brain's capacity to remodel after injury, which opens up exciting opportunities for plasticity-enhancing therapies to improve functional recovery. Therapies that promote neurorepair and -regeneration - including neurogenesis, synaptic plasticity and angiogenesis - provide promising strategies to overcome functional deficits associated with neurological disorders. An effective therapeutic approach to stimulate recovery may be particularly valuable for patients after acute cerebrovascular injury, e.g. stroke, in which the treatment time-window for neuroprotection is limited.

Brain plasticity after injury involves a complex pattern of molecular and cellular events that leads to dynamic reorganization of neuronal circuitries. Early phenomena, such as induction of growth-promoting genes, modulation of excitatory and inhibitory signaling, and recruitment of inflammatory cells, are followed by gradual structural remodeling of neuronal connections. Ultimately, the formation of reorganized neural networks can significantly contribute to recovery of function after brain damage.

Although new concepts of brain reorganization

are progressively being assessed, it remains essentially unknown to what level specific plasticity processes contribute to neurological improvement, and to what degree brain adaptations can be manipulated to promote functional recovery. Various therapeutic approaches to stimulate brain plasticity have been suggested, including physical rehabilitation, administration of growth-promoting drugs and stem cells, modulation of inflammatory processes, and non-invasive brain stimulation. However, these interventions may also disrupt intrinsic networks or induce other adverse effects, which stresses the importance of thorough preclinical assessment before these promising plasticity-enhancing strategies are translated to the clinic.

The scientific symposium 'Neuroplasticity-promoting therapies' will inform on recent developments of various neurorestorative strategies from experimental studies to clinical applications. The invited speakers will discuss advantages and prospects as well as limitations and risks of different therapeutic approaches in cerebrovascular and neurodegenerative disorders.

NEUROTHERAPEUTICS IN BRAIN REPAIR: EXCITATORY SIGNALING, GROWTH FACTORS AND PLASTICITY AGENTS

S.T. Carmichael

David Geffen School of Medicine at UCLA, Los Angeles, CA, USA

The current principles of recovery from stroke involve physical medicine. Occupational, physical and speech therapy utilize activity-dependent and task-focused behavioral therapies that lead to the limited recovery in this disease. However, the targeted pharmacological approaches so characteristic of molecular medicine have not been available in neurorehabilitation. Recent basic science studies support novel therapeutics for neural repair in stroke. These include activation of molecular memory programs, selective growth factor stimulation, induction of brain growth-promoting cellular programs, blockade of growth inhibitors induced by stroke and targeted delivery of cell therapies. When combined with physical rehabilitation these may stimulate greater recovery in stroke.

INTRODUCTION TO THE SYMPOSIUM „IMPROVING QUALITY AND PREDICTIVENESS OF TRANSLATIONAL BRAIN RESEARCH: STATE-OF-THE-ART METHODS AND FUTURE PERSPECTIVES"

J. Boltze[1,2]

[1]*Department of Cell Therapy, Fraunhofer Institut for Cell Therapy and Immunology, Leipzig, Germany,* [2]*Massachusetts General Hospital and Harvard Medical School, Boston, MA, USA*

Improving the predictive power and quality of preclinical stroke research is mandatory in order to ensure maximum safety and best chances for success in subsequent clinical investigations. Given the setbacks during the development of neuroprotective therapies for ischemic stroke in the large decades, novel strategies and a thorough assessment of the animal models and techniques we use is mandatory.

This short introductory note will introduce the basic idea and aims of session, some of the most interesting concepts to be discussed as well as the contributing speakers.

IS THERE SOMETHING WRONG HOW WE PRODUCE STROKE IN RODENTS?

J. Jolkkonen

Institute of Clinical Medicine - Neurology, University of Eastern Finland, Kuopio, Finland

Experimental models are indispensable in understanding the pathology and brain repair in stroke on which development of new therapies is based. Producing cerebral ischemia is in principal straightforward. Next I will refer to the transient MCAO model (filament), which is perhaps the most common stroke model. Although craniectomy is not needed, yet the model is invasive and complicated by high variability in lesion size and location, hemorrhage and high mortality, which are difficult to overcome even in skillful hands.

Anesthesia used during ischemia operation varies a lot between laboratories, but usually gas anesthesia and isoflurane is used. However, isoflurane is neuroprotective (compared to halothane), it is vasodilative and it causes damage to the blood-brain barrier. Another variable possibly affecting results is postoperative care of the animals, including the administration of painkillers, which should

be used to lessen suffering from the operation. Also an inherited complication in the MCAO model are difficulties in swallowing and drinking leading to severe loss of body weight, which bias all food rewarded behavioral tests at acute phase.

The methods used to measure tissue damage (e.g., TTC staining) may also contribute to translational failure. The stained tissue may seem to be viable, but in fact it is not functional as shown by fMRI. Thus, sensitive behavioral tests could be used as an additional and often more reliable measure of neuroprotection. In addition, one overlooked difference between rodents and humans is the secondary pathology in the thalamus (e.g., accumulation of β-amyloid and calcium), which further exacerbate the inflammation and neuronal damage and is likely to affect the long-term outcome in rodents.

Maybe there is not that much wrong in our stroke models, but the procedures how we induce stroke and how we assess outcome need adjusting. Most of the issues raised here could be overcome if the stroke community put forces together to establish common standard operating procedures. This should result in more reliable and consistent data and hopefully prevent translational failures in future.

Lipsanen A, Jolkkonen J. Experimental approaches to study functional recovery following cerebral ischemia. Cell Mol Life Sci 68: 3007-17, 2011

MODELLING COMORBIDITIES IN EXPERIMENTAL STROKE: MECHANISMS AND CONFOUNDERS

A. Denes[1,2]

[1]*Faculty of Life Sciences, University of Manchester, Manchester, UK,* [2]*Institute of Experimental Medicine, Hungarian Academy of Sciences, Budapest, Hungary*

Mechanisms of brain injury are still improperly understood and despite considerable research in the field, a widely effective treatment is not available for stroke. A role for inflammation in ischaemic injury is increasingly recognised, and inflammation is also an important contributor to the main risk factors for stroke, including atherosclerosis, diabetes, obesity and hypertension. A greater understanding of inflammatory mechanisms in brain injury could therefore provide new therapeutic approaches for the treatment of stroke, which is a primary public interest.

A common link in major risk factors for stroke is acute or chronic inflammation, which has not been considered in animal models until recently. This is likely to have contributed to the failure of clinical trials in stroke to date. Animal models of comorbidities (such as infection, diabetes, hypertension or obesity) in stroke show worse neurological outcome, increased infarct size, blood-brain barrier injury, and pronounced expression of inflammatory cytokines in both the periphery and the brain. Blocking key inflammatory mediators, such as interleukin-1, is protective against brain injury in these models. Systemic inflammatory mechanisms and bi-directional interactions between the periphery and the brain also contribute to stroke outcome even in the absence of comorbidities. Moreover, neuro-immune effects of anaesthesia and surgical stress are inherent confounders in all current models of cerebral ischaemia.

Thus, the development of appropriate animal models, with special respect to comorbidities in stroke (and other brain diseases), is essential to facilitate understanding of systemic inflammatory mechanisms that have profound impact on brain injury and recovery. Targeting of key inflammatory processes is likely to be beneficial in prevention and treatment of brain disorders.

NEUROFUNCTIONAL ASSESSMENTS IN RODENT MODELS OF STROKE

G. Metz

Canadian Centre for Behavioural Neuroscience, University of Lethbridge, Lethbridge, AB, Canada

Objectives: Stroke frequently affects the ability to perform skilled movements with the upper limbs. Thus, a main focus of stroke rehabilitation programs is the development of skill in extremity function. Skilled movements are characterized by a complex sequence of movement components. In rats and mice, skilled movements can be observed in eating specialty food items or when navigating across a difficult territory. Tests of skilled limb movements in rodents are sensitive to even subtle motor deficits and therapeutic success in pre-clinical studies of stroke. Skilled limb movements have the advantage that they

produce a variety of measures that reflect behavioural and neuronal plasticity.

Methods:

Skilled Reaching Tasks. The majority of skilled movement tests focus on the analysis of forelimb use, such as grasping and retrieving pieces of food. The sequence of components comprising skilled reaching movements in rodents is relatively fixed. Thus, rats and mice possess limited ability to modify movement components to adapt to a changing context. Consequently, even a discrete lesion can permanently compromise reaching movement performance. In addition, physiological conditions such as stress, strain, sex and aging affect both reaching success and qualitative movement performance.

End point measures, such as success rates, can be assessed daily, while at the same time performance can be video recorded for frame-by-frame analysis. Recent studies have shown that skilled reaching movements are useful tools for distinguishing between genuine functional recovery and compensation. Through practice animals with an ischemic lesion might show considerable improvement in reaching success, however, qualitative analysis of reaching movements might still reveal permanent deficits. Thus, rodents are able to develop successful alternative movement strategies to overcome primary motor deficits. Descriptive movement analysis represents an important method to distinguish compensatory behaviour from permanent motor deficits.

Skilled Walking Tasks. When navigating across difficult territory, rats and mice use skilled fore- and hind limb movements to adapt their gait pattern. In the ladder rung walking task, the spacing between the rungs of a ladder can be varied to prevent learning of rung locations in repeated test sessions. Measures include fore- and hind limb placing, stepping, and inter-limb co-ordination. This task is useful for assessing loss and recovery of function due to brain or spinal cord injury, the effectiveness of treatment therapies, as well as compensatory processes through which animals adapt to nervous system injury.

Conclusions: Skilled movement tasks provide reliable and high-resolution test strategies for studies of functional recovery. The combination of quantitative and qualitative measures in skilled movement tasks elaborates recovery versus compensation, thus providing insights into underlying structural changes of regeneration and plasticity. Notably, skilled reaching movements in rodents are homologous to humans as demonstrated by comparative studies. Reaching movement abnormalities detected in rodent models of stroke show similarities to human patients. Thus, skilled movement tasks represent valid tools in the assessment of stroke rehabilitation and therapeutic effectiveness.

THE CONCEPT OF INTERNATIONAL, MULTICENTER, RANDOMIZED AND CONTROLLED 'PHASE III' PRECLINICAL TRIALS - EXPECTED IMPACT ON STROKE RESEARCH

M. Macleod

Department of Neuroscience, Centre for Clinical Brain Sciences, University of Edinburgh, Edinburgh, UK

Although large numbers of novel treatment strategies for diseases such as stroke are developed in laboratories each year and are shown beneficial in animal models, very few ultimately prove effective in patients. Reasons for this translational failure include limited validity, poor generalisability, and inadequate sample size of many animal studies. At present, no systematic or evidence-based criteria inform the decision to venture from preclinical testing into clinical development. We propose that preclinical research should learn from the experience of clinical trialists by seeking firmer evidence to inform the process of translation.

Animal experiments testing the efficacy of potential treatments are central to drug development. The outputs from these preclinical studies need to be reliable and valid in order to improve human health. Systematic analyses of preclinical data used to justify clinical trials have revealed substantial overestimates of treatment effects because of compromised internal and external validity. In addition, animal studies are in general too small to detect reliably the effects they purport to observe; and groups may use models which are highly sensitive to the phenomena being studied at the expense of the generalisability of their conclusions. Adequate sample size, and hence statistical power, is fundamental to the usefulness of preclinical research findings. Sample size calculations based on published data for effect size and variance suggest that

experiments should be substantially larger than reported in the literature. Indeed, the typical focal ischaemia study is powered at only 30%. Animals with co-morbidities prevalent in stroke patients (e.g. diabetes, hypertension) show smaller treatment effects, and this has important clinical implications.

Most animal studies are therefore underpowered to detect potentially important treatment effects under tightly defined conditions in healthy young animals, let alone to detect smaller but nonetheless potentially important effects in less tightly controlled conditions in older animals with relevant comorbidities. It is therefore likely that for many stroke drugs tested in animals, true biological efficacy in those models is substantially lower than that suggested by the published literature, and in some cases agent itself may be inert.

The impact of selection bias (eliminated by randomisation), of performance bias (eliminated by blinded conduct of the experiment) and of measurement bias (eliminated by blinded outcome assessment) are widely recognised in clinical trials. This has resulted in clear standards for good clinical practice in clinical trials, and to the development of ethical, regulatory, funding, reporting and methodological standards to ensure the validity of conclusions drawn from clinical studies. At present clear standards such as these do not exist for most preclinical research, and the reporting of measures to avoid bias is uncommon.

Multi-centre animal studies (www.multi-part.org) offer an opportunity to address these issues of internal and external validity and of the feasibility of adequately powered studies; I will outline some of the advantages of this approach, together with some of the challenges which must be addressed if it is to succeed.

SYMPOSIUM OVERVIEW: DISEASE OF THE BLOOD-BRAIN BARRIER

W.A. Banks[1], S. Dohgu[2]

[1]*University of Washington, Seattle, WA, USA,*
[2]*Fukuoka University, Fukuoka, Japan*

The blood-brain barrier (BBB) and neurovascular unit (NVU) function as regulatory interfaces between the peripheral tissues and central nervous system. Their dysfunction results in significant disease, with dysfunction arising either from them as a primary site or because they are the target of developed disease processes. This symposium considers four cases in which the BBB and the NVU are intimately involved in disease processes. Case one will consider how LRP-1, a brain-to-blood transporter that rids the brain of amyloid beta peptide and whose dysfunction is thought to promote the progression of Alzheimer's disease, becomes impaired in the face of inflammation. Case two will consider how the pericyte, the latest cell to be added to the NVU pantheon, is critical to maintaining BBB integrity in the face of the oxidative insult which occurs in diabetes mellitus and will consider the mechanisms by which diabetes leads to pericyte loss and, hence, to BBB disruption. Case three will examine the mechanisms by which cell-free HIV-1 crosses the BBB, how inflammation promotes such entry, and will highlight the newly discovered receptor which the virus co-opts to cross the BBB. Case four will consider the mechanisms by which the BBB transport of leptin, a protein produced by adipose tissue which crosses the BBB to inform the brain of the status of caloric reserves, is impaired in obesity and how impairing BBB transport of leptin leads to a positive feedback loop leading to further gains in body weight.

DYSFUNCTIONAL TRANSPORT OF LEPTIN: IS OBESITY A DISEASE OF THE BBB?

W.A. Banks

University of Washington, Seattle, WA, USA

Leptin is a 16 KDa protein secreted into the blood by adipose tissue. Blood levels of leptin correlate with adiposity so that the more obese an individual is, the higher is the individual's blood leptin level. In the brain, leptin induces a cascade of events that result in a decrease in appetite and an increase in thermogenesis. Together, these actions would result in a decrease in adiposity, in turn resulting in reduced levels of leptin in the blood. Thus, leptin participates in a negative feedback loop between brain and fat tissue that in theory should regulate adiposity. The current epidemic of obesity illustrates that this system becomes impaired; one cause of this impairment results from the ways in which leptin interacts with the BBB. Circulating leptin accesses its CNS receptors after being transported across the BBB by a saturable

mechanism. Although leptin deficiency results in obesity, the majority of obese humans have a resistance to leptin rather than a deficiency. The leptin transporter becomes increasingly saturated as blood levels rise, with the first signs of saturation occurring at blood levels that correspond to ideal body weight. Thus, one basis for leptin resistance is the saturation of the BBB leptin transporter. The BBB leptin transporter is regulated by a host of circulating factors with the most studied being epinephrine, which increases the transport rate, and triglycerides, which decrease it. We speculate that triglycerides, which are elevated in starvation as well as in obesity, evolved as a signal to the brain of starvation, impairing leptin transport across the BBB and so reducing its anorectic signal to the brain. Supporting this is the finding that triglycerides increase ghrelin transport, a hormone secreted by the stomach that induces hunger and is often considered the orexigenic counterpart to leptin's anorectic actions. Thus, the characteristics of the BBB transport of feeding hormones have been shaped by evolutionary pressures to not only respond to daily caloric needs, but to adapt to life-threatening events such as starvation.

INFLAMMATION INHIBITS EFFLUX OF AMYLOID BETA PEPTIDE: IMPLICATIONS FOR ALZHEIMER'S DISEASE

M. Erickson[1,2], P. Hartvigson[2], K. Hansen[2], W. Banks[1,3]

[1]GRECC, VA Medical Center, [2]University of Washington, [3]Internal Medicine, University of Washington, Seattle, WA, USA

Introduction and objectives: The amyloid cascade hypothesis of Alzheimer's disease (AD) states that accumulation of the amyloid beta peptide (Aβ) in the brain is the primary cause of disease pathogenesis. In idiopathic AD, Aβ accumulation is thought to occur due to defective clearance. Two Aβ transporters at the blood-brain barrier (BBB), the low-density lipoprotein receptor-related protein (LRP-1) and p-glycoprotein (Pgp), facilitate clearance of Aβ from the brain and become impaired in AD. An additional route of Aβ clearance is bulk flow of cerebrospinal fluid, which is also impaired in AD. The mechanisms leading to these impairments are, however, unclear. Because inflammation in the CNS and periphery is also implicated in AD, our objectives were to determine whether inflammation causes impaired clearance of Aβ from the brain, and mechanisms by which impaired clearance occurs.

Methods: LPS was administered by intraperitoneal injection to induce systemic inflammation in CD-1 mice. In some studies, the antioxidant N-acetylcysteine was pre-administered to limit oxidative stress. To evaluate effects of these treatments on CNS clearance of Aβ, 125I-Aβ was injected into the lateral ventricle and its disappearance from brain was measured over time. Peripheral clearance was evaluated by measuring liver and kidney uptake of 125I-Aβ injected in the jugular vein. To assay function of LRP-1 and Pgp at the BBB independently, CNS efflux or uptake of 125I-alpha2-macroglobulin or 3H-verapamil respectively was measured. Protein markers of oxidative stress and cytokines were measured in brain and serum using dot blots and bead-based multiplex assays. Microvascular expression of LRP-1 and Pgp was quantified by Western blot.

Results: Our results show that systemic inflammation inhibits Aβ transport across the BBB, bulk flow of cerebrospinal fluid, and systemic clearance of Aβ by the liver and kidneys. We also found that the antioxidant N-acetylcysteine protects against LPS-induced impairment of Aβ transport across the BBB.

Conclusions: These findings support that systemic inflammation contributes to AD pathogenesis by promoting Aβ accumulation in the brain, and highlight a novel mechanism by which N-acetylcysteine could protect against AD.

DISRUPTION OF THE BBB IN DIABETES: PROTECTION BY PERICYTES AND THE ROLE OF MITOCHONDRIAL CARBONIC ANHYDRASES

G.N. Shah[1], W. Banks[2], T.O. Price[1]

[1]Internal Medicine, St. Louis University, St. Louis, MO, [2]Internal Medicine, University of Washington, Seattle, WA, USA

Both types of diabetes cause damage to the microvasculature of the brain leading to the disruption of blood-brain barrier (BBB). The BBB acts both to prevent the unrestricted leakage of plasma proteins into the brain and as a regulatory interface between brain and blood. Disruption and other dysfunctions can both lead to impaired brain function. Though made of specially modified endothelial cells

pericytes in close vicinity of the endothelial cells maintain the viability and integrity of BBB. Pericytes make the first line of defense against hyperglycemia-induced disruption of the BBB. Pericytes show increase percent of apoptotic cells when cultured in high glucose media. Our recently published data show a loss in pericyte/endothelial cell ratio due to a loss in cerebral pericyte numbers in streptozotocin-diabetic mice.

An increasing body of evidence implicates mitochondrial oxidative stress as a mechanism for hyperglycemia-induced pericyte loss and disruption of BBB. In diabetes, oxidative stress is caused by overproduction of reactive oxygen species during mitochondrial oxidative metabolism of glucose. Briefly, glucose is converted to pyruvate in the cytoplasm. The pyruvate enters the mitochondria where it combines with bicarbonate (HCO_3^-) to form oxaloacetate, the key intermediate in Krebs cycle. Oxaloacetate combines with acetyl-CoA to form citric acid which enters the Krebs cycle to generate electron donors, FADH2 and NADH. In electron transport chain reactions, these electron donors produce ATP, and ROS are produced as a normal byproduct. In DM, hyperglycemia shuttles more glucose to the Krebs cycle, in insulin-independent tissues such as the brain, thus increasing the rate of production of electron donors ($FADH_2$ and NADH). These electron donors generate a proton gradient across the inner mitochondrial membrane during electron transport reactions. When the electrochemical potential difference across the inner mitochondrial membrane generated by the proton gradient is high, the lifetime of superoxide-generating electron-transport intermediates is prolonged. There seems to be a threshold above which superoxide production is markedly increased, thus causing oxidative stress. In diabetes, hyperglycemia stimulates a marked increase in production of reactive oxygen species leading to oxidative stress and target organ damage.

HCO_3^- is imperative for the generation of oxaloacetate and must be produced inside the mitochondria as mitochondrial membranes are impermeant to HCO_3^-. Carbonic anhydrases generate HCO_3^- by reversible hydration of CO_2 in a simple yet vital reaction: (CO2 + H2O $HCO3^-$ + H^+). Only two of the 16 known isozymes of carbonic anhydrases are found in the mitochondria. They are designated as mitochondrial carbonic anhydrases and are essential for the generation of HCO_3^- in the mitochondria needed for carboxylation of pyruvate to oxaloacetate, regulation of oxidative metabolism of glucose, and oxidative stress. We showed a decrease in hyperglycemia-induced oxidative stress and pericyte loss in diabetic mouse brain upon pharmacological inhibition of mitochondrial carbonic anhydrases. Thus, making mitochondrial carbonic anhydrases a new therapeutic target for oxidative stress related illnesses of the brain.

Carbonic anhydrase inhibitors have a long history of safe clinical use and can be immediately evaluated for this new indication in translational research.

TRANSPORT OF HIV-1 ACROSS THE BBB: KEY ROLE OF THE MANNOSE-6-PHOSPHATE RECEPTOR

S. Dohgu

Pharmaceutical Care and Health Sciences, Fukuoka University, Fukuoka, Japan

Introduction: HIV-1 circulates both as free virus and within immune cells, with the level of free virus being predictive of clinical course. Both forms of HIV-1 cross the blood-brain barrier (BBB) and much progress has been made in understanding the mechanisms by which infected immune cells cross the blood-brain barrier BBB. How HIV-1 as free virus crosses the BBB is less clear as brain endothelial cells are CD4 and galactosylceramide negative. Here, we found that HIV-1 can use the mannose-6 phosphate receptor (M6PR) to cross the BBB.

Materials and methods: Brain uptake of HIV-1 was determined by the brain perfusion method. We isolated brain microvascular endothelial cells from 8 weeks old CD-1 mice. We made in vitro BBB models with the primary culture of mouse brain endothelial cells using Costar Transwell inserts.

Results: Brain perfusion studies showed that HIV-1 crossed the BBB of all brain regions consistent with the uniform distribution of M6PR. Ultrastructural studies showed HIV-1 crossed by a transcytotic pathway consistent with transport by M6PR. Uptake of HIV-1 into brain endothelial cells was saturable. An in vitro model of the BBB was used to show that transport of HIV-1 was inhibited by mannose, mannan, and mannose-6 phosphate and that enzymatic removal of high mannose oligosaccharide residues from HIV-1 reduced

transport. Wheatgerm agglutinin and protamine sulfate, substances known to greatly increase transcytosis of HIV-1 across the BBB in vivo, were shown to be active in the in vitro model and to act through a mannose-dependent mechanism. Transport was also cAMP and calcium-dependent, the latter suggesting that the cation-dependent member of the M6PR family mediates HIV-1 transport across the BBB.

Conclusion: We conclude that M6PR is an important receptor used by HIV-1 to cross the BBB.

BRAIN FUNCTIONAL CONNECTIVITY FROM BENCH TO BEDSIDE

W. Lin, **Y.-Y.I. Shih**

Biomedical Research Imaging Center, University of North Carolina at Chapel Hill, Chapel Hill, NC, USA

Most of our knowledge regarding brain functions stem from stimulus- or task-evoked studies where an “input” is given attempting to active specific regions of the brain responding to this “input.” However, brain signaling is massively parallel. Yet, task-evoked studies mostly measure activations of specific neuroanatomical pathways instead of dynamic interactions between brain areas. In addition, a “physically” resting condition does not translate to a resting brain. In fact, accumulating evidence has suggested that neural signals are temporally synchronized in functionally connected regions. Spontaneous neural activities can thus be used to resolve brain functional wiring. This design, compared with traditional task-evoked neuroscience studies, is largely unbiased and can also be used to study the working brains. Recent developments in brain imaging technologies have greatly improved the spatiotemporal representation of neural network coherence and advanced our understanding of brain functional connectivity in normal and pathological conditions. This symposium aims to provide the latest updates on translational brain connectivity studies from preclinical animal models to human applications through the utilization of different imaging modalities, including optical imaging, MRI and MEG. *Dr. Joseph Culver* from Washington University in St. Louis will introduce functional connectivity in animal brain using optical imaging, followed by *Dr. Christopher Pawela* from Medical College of Wisconsin to address functional connectivity in animal brain using MRI, *Dr. Fa-Hsuan Lin* from National Taiwan University to illustrate functional connectivity in human brain using MEG, and, finally, *Dr. Randy Buckner* from Harvard University to cover functional connectivity in human brain using MRI. Resolving brain functional networks with these cutting-edge imaging techniques should open new avenues toward a better understanding of brain functions and could complement our knowledge obtained from goal-directed neuroscience studies over the past century.

FUNCTIONAL CONNECTIVITY IN ANIMAL BRAIN USING FCMRI

C. Pawela

Plastic Surgery, Medical College of Wisconsin, Milwaukee, WI, USA

Introduction: Resting State Functional Connectivity Magnetic Resonance Imaging (fcMRI) is becoming a widely used research methodology. Controlled manipulations are possible in animal models that are not possible in human subjects. Animal models of disease can also provide insights into important clinical relevant questions. The number of fcMRI studies in animal models is rapidly expanding. However, there are many specific challenges when performing small animal fcMRI experiments.

Objective: In this presentation, the state of the art in fcMRI methodology will be discussed in the context of small animal imaging. Several resting state brain networks in rats will be described. Two applications of fcMRI to animal imaging will be shown; imaging genetics and peripheral nerve injury.

Results: Data will be presented demonstrating how changes in fcMRI networks between different strains of rats can be used as phenotypic markers in imaging genetic studies. We will show how structural and functional brain differences may be responsible for these variations in network connectivity. Further studies will be presented showing how brain plasticity induced by peripheral nerve injury can modify brain network connectivity. The limitations of the fcMRI methodology will also be detailed.

Conclusions: FCMRI can be an effective tool in researching functional brain changes in small animal models. However, caution must be applied when using the methodology. This

presentation will detail two different applications of fcMRI in small animal models that have clinical relevance to human disease and injury.

FUNCTIONAL CONNECTIVITY OF HUMAN BRAIN USING MAGNETOENCEPHALOGRAPHY

F.-H. Lin

National Taiwan University, Taipei, Taiwan R.O.C.

Magnetoencephalography (MEG) measures the weak extra-cranial magnetic fields elicited by spatiotemporally coherent post-synaptic neuronal currents using highly sensitive detectors inside a magnetically shielded room. Different from functional magnetic resonance imaging (fMRI) using blood oxygen level dependent (BOLD) contrast, MEG is directly sensitive to neuronal activity and has millisecond temporal resolution. Thus MEG allows us to study brain electrophysiology noninvasively not only with a high temporal resolution, but also at different frequency bands.

In this presentation, after a brief introduction about MEG, I will present a few studies of using MEG to study the functional connectivity of human brain to help us better understand how brain areas are orchestrated spatiotemoporally and spectrally to complete the sensory processing, tasks, and at the resting condition. Challenges and opportunities of using MEG to study functional connectivity will also be discussed.

SELECTIVE NEURONAL LOSS IN CHRONIC OBSTRUCTIVE DISEASE OF THE MAJOR CEREBRAL ARTERIES: A PET STUDY

H. Yamauchi

Division of PET Imaging, Shiga Medical Center Research Institute, Moriyama, Japan

Background: In patients with atherosclerotic internal carotid artery (ICA) or middle cerebral artery (MCA) occlusive disease, hemodynamic cerebral ischemia may cause not only cerebral infarction but also minor tissue damage in the cerebral cortex that is not detectable as infarction on CT or MRI. Imaging of the central type benzodiazepine receptors (BZRs), which are expressed by most cortical neurons, has made it possible to visualize the neuronal alterations induced by ischemia in vivo in humans. Recognizing selective neuronal damage is important for understanding the pathophysiology of hemodynamic cerebral ischemia in atherosclerotic major cerebral artery disease.

Observations: Chronic hemodynamic compromise causes selective neuronal damage. Using PET and ^{11}C-Flumazenil, we showed that selective neuronal damage demonstrated as a decrease in BZR in the normal-appearing cerebral cortex was associated with increased oxygen extraction fraction (OEF) (misery perfusion) in patients with atherosclerotic ICA or MCA occlusive disease in the chronic stage. Follow-up examinations of the patients without ischemic episode showed that a decrease of BZR was associated with an increase of OEF (hemodynamic deterioration).

Hemodynamic mechanism was also supported by the correlation of cortical neuronal damage with low-flow infarcts. In ICA or MCA occlusive disease, selective neuronal damage demonstrated as decreased cortical BZR was associated with the presence of borderzone infarcts, suggesting that hemodynamic ischemia leading to borderzone infarcts may cause selective neuronal damage beyond the regions of infarcts in the chronic stage.

Selective neuronal damage has considerable impact on the functional outcomes of patients with ICA or MCA disease. Cortical neuronal damage demonstrated as decreased BZR was associated with a decrease in cortical oxygen metabolism, suggesting that the decreased BZR is accompanied by cortical dysfunction. Furthermore, a decrease in BZRs in the non-infarcted cerebral cortex was associated with executive dysfunction. Imaging of BZRs is useful as an objective measure of cognitive impairments.

Conclusion: In atherosclerotic major cerebral artery disease, chronic hemodynamic cerebral ischemia causes selective neuronal damage demonstrated as decreased BZRs. Therapeutic strategies for preventing neuronal damage, including vascular reconstruction surgery and neuro-protective agents, is needed, especially when hemodynamic measurements detect chronic hemodynamic compromise.

References:

1. Yamauchi H, Kudoh T, Kishibe Y, Iwasaki J,Kagawa S. (2005) Selective neuronal damage and borderzone infarction in carotid artery occlusive disease: a 11C-flumazenil PET study. *J Nucl Med* 46:1973-1979.

2. Yamauchi H, Kudoh T, Kishibe Y, Iwasaki J,Kagawa S. (2007) Selective neuronal damage and chronic hemodynamic cerebral ischemia. *Ann Neurol* 61: 454-465.

3. Yamauchi H, Nishii R, Higashi T, Kagawa S, Fukuyama H. (2009) Hemodynamic compromise as a cause of internal border-zone infarction and cortical neuronal damage in atherosclerotic middle cerebral artery disease. *Stroke* 40: 3730-3735.

4. Yamauchi H, Nishii R, Higashi T, Kagawa S, Fukuyama H. (2011) Silent cortical neuronal damage in atherosclerotic disease of the major cerebral arteries. *J Cereb Blood Flow Metab* 31:953-961

5. Yamauchi H, Nishii R, Higashi T, Kagawa S, Fukuyama H. (2011) Selective neuronal damage and Wisconsin Card Sorting Test performance in atherosclerotic occlusive disease of the major cerebral artery. *J Neuro Neurosurg Psychiatry* 82:150-156.

STRIATAL SELECTIVE NEURONAL LOSS AND SPECTACULAR SHRINKING DEFICIT IN RODENTS AND MAN: MRI, BEHAVIOR AND HISTOPATHOLOGY

M. Fujioka

Neuroscience Unit, Emergency and Critical Care Medical CTR, Nara Medical University, Kashihara, Japan

We review a specific MRI change in the brains of humans and/or rats subjected to a transient ischemic stress. Transient global brain ischemia produces symmetrical lesions of hyperintensity on T1-weighted MRI localized in the bilateral striatum, thalami, and/or substantia nigra in a delayed fashion. Susceptibility weighted imaging study in cardiac arrest survivors indicated that the ischemic delayed T1-hyperintensity unlikely represents microbleeds. Further, brief focal ischemia leading to temporary neurological deficits (ex. spectacular shrinking deficit) also induces the delayed hyperintensity on T1-weighted MRI in the striatum of humans and rats. Therefore, to clarify the significance of this MRI modification, namely, delayed-onset and slowly-progressive T1-hyperintensity after brief cerebral ischemia, we investigated the changes in the dorsolateral striatum of rats from 4 hours through 16 weeks after a 15-minute period of middle cerebral artery occlusion, for MRI changes, Mn concentration, neuronal number, reactivities of astrocytes and microglia/macrophages, mitochondrial Mn-superoxide dismutase (Mn-SOD), glutamine synthetase (GS), and amyloid precursor protein. The cognitive and behavioral studies were performed in patients and rats and compared with striatal T1 hyperintensity to show whether alteration in brain function correlated with MRI and histological changes. This early study suggests that (1) the delayed hyperintensity on T1-weighted MRI after mild ischemia may involve tissue Mn accumulation accompanied by Mn-SOD and GS induction in reactive astrocytes, (2) the MRI changes correspond to striatal neurodegeneration with a chronic inflammatory response and signs of oxidative stress, and (3) the subjects with these MRI changes are at risk for showing a late impairment of brain function even though the transient ischemia is followed by total neurological recovery. Interestingly, this type of delayed T1-hyperintensity of neurodegeneration also appears in the human brains after severe hypoglycemic coma. These data suggest that a transient tissue energy failure may give rise to a common pathogenic pathway of neurodegeneration resulting in the delayed T1-hyperintensity on MRI.

In conclusion, brief cerebral ischemia can trigger slowly-progressive MRI change of T1-hyperintensity and histological neurodegeneration leading to cognitive dysfunction even if the ischemia produces no infarcts.

SELECTIVE NEURONAL LOSS: BASIC AND EXPERIMENTAL ASPECTS IN RODENT TEMPORARY MCA OCCLUSION MODELS

M. Endres[1,2], K. Gertz[1,2], G. Kronenberg[2,3]

[1]Neurology, [2]Center for Stroke Research Berlin, [3]Psychiatry, Charite-Universitaetsmedizin, Berlin, Germany

We have extensively characterized a model of mild brain ischemia in the mouse. Following 30 min transient filamentous occlusion of the middle cerebral artery followed by reperfusion, selective neuronal cell death evolves in a delayed fashion over time in the lateral

striatum. Dying neurons show early markers of apoptosis such as activation of caspase-3 at 9-12 hrs and also become TUNEL positive at 48-72 hrs after stroke onset. Also, there is evidence of abortive cell-cycle re-entry. In contrast, however, electron microscopic imaging fails to demonstrate *bona fide* apoptotic morphology. As demonstrated by immunocytochemistry neuronal cell death in the striatum affects almost exclusively GABAergic medium spiny neurons (type I and type II both in the patch and matrix component) and to a much lesser degree also parvalbuminergic interneurons, while cholinergic, GABAergic and somatostatin-containing interneurons are resistant to ischemic cell death.

In addition, there is strong reactive gliosis with morphologic changes and proliferation of GFAP- and nestin-positive cells. Interestingly, these cells also change their eletrophysiologic properties ("astron-like"). However, they do not differentiate into a neuronal phenotype. In addition, there is profound activation, proliferation and invasion of monocytic inflammatory cells (both brain-derived microglia and bone-marrow derived monocytes which remain in the ischemic lesion even at late time points). At present, the contribution of reactive astrocytes and activated microglia to the delayed maturation of the primary ischemic lesion is not entirely clear. Also, there is delayed angiogenesis which consists both of an in-situ response and the invasion of bone-marrow derived presumed endothelial progenitor cells. Angiogenesis can be augmented by a number of therapeutic strategies and is associated with increased density of perfused microvessels, increased absolute blood flow levels, and improved sensory-motor scores.

In addition to the primary ischemic lesion in the striatum there is remote neuronal cell death in a number of brain regions including cortex, hippocampus, hypothalamus, thalamus, and midbrain. Cell death in the ipsilateral midbrain is confined to dopaminergic neurons in the substantia nigra pars compacta and the ventral tegmental area and is delayed to 10-14 days after ischemia onset. We have demonstrated that this exofocal dopaminergic degeneration is followed by an increase of dynorphin mRNA expression in the nucleus accumbens and the development of a depressive-like phenotype with anxiety, despair, and anhedonia. Chronic antidepressant treatment initiated as late as 7 days after brain ischemia reversed the behavioral phenotype, prevented degeneration of dopaminergic midbrain neurons, and attenuated lesion maturation and striatal atrophy at 4 months. Prevention of exofocal remote dopaminergic cell death in the midbrain may emerge as a novel target for neuroprotection by antidepressants.

IMMUNE RESPONSES IN SYNAPSE FUNCTION AND BRAIN DAMAGE

H. Wake[1], H. Hagberg[2], **D. Sun**[3]

[1]National Ins of Basic Biology, Okazaki, Japan, [2]Imperial College London, London, UK, [3]Neurology, Univ. of Pittsburgh, Pittsburgh, PA, USA

Inflammation is increasingly recognized as being of both physiological and pathological importance in the central nervous system (CNS). Microglia functions in pruning neuronal processes and strengthening synapse formation in the developing brain. Post-ischemic inflammation mediated by both resident and circulating immune cells is involved in the evolution of the injury as well as the repair. Microglia are likely the primary immunecompetent cells in the immature CNS. Depending on the stimulus, molecular context, and timing during the perinatal period, these cells will acquire a variety of phenotypes which are critical to both the short- and long-term consequences of inflammation and brain development including synpase function. Mast cells are gaining increasing attention as important players in the central immune response to acute and chronic injury, and may play an important role in both the immature brain and adult brain. This symposium will present a synthesis of the current state of the field in the understanding of the unique aspects of the inflammatory response for neurologic and neuropsychiatric disease in both children and adults.

SYSTEMIC INFLAMMATION IN THE NEONATE ALTERS BRAIN DEVELOPMENT

P. Gressens

Inserm U 676, Paris, France

Introduction: Perinatal inflammation is a major risk factor for neurological deficits in preterm infants. Several experimental studies have shown that systemic inflammation can alter the programming of the developing brain.

However, these studies do not offer detailed pathophysiological mechanisms and they rely on relatively severe infectious or inflammatory stimuli that, most likely, do not reflect the levels of systemic inflammation observed in many human preterm infants.

Objective: In this context, we have aimed to test the hypothesis that moderate systemic inflammation is sufficient to alter white matter development.

Methods: Accordingly we developed a mouse model where newborn mice received twice-daily intraperitoneal injections of IL-1b over five days and were studied for myelination, oligodendrogenesis, behavior and with MRI.

Results: Mice exposed to IL-1b had a long lasting myelination defect that was characterized by an increased number of non-myelinated axons. They also displayed a reduction of the diameter of the myelinated axons. In addition, IL-1b induced a significant reduction of the density of myelinating oligodendrocytes accompanied by an increased density of oligodendrocyte progenitors, suggesting a partial blockade in the oligodendrocyte maturation process. Accordingly, IL-1b disrupted the coordinated expression of several transcription factors known to control oligodendrocyte maturation. These cellular and molecular abnormalities were correlated with a reduced white matter fractional anisotropy on diffusion tensor imaging and with memory deficits.

Conclusions: This original model shows that moderate perinatal systemic inflammation alters the developmental programs of the white matter. This insult induces a long lasting myelination deficit accompanied by cognitive defects and MRI abnormalities, further supporting the clinical relevance of the present data.

ROLE OF MAST CELLS IN HYPOXIC-ISCHEMIC INJURY TO THE IMMATURE BRAIN

S. Vannucci

Pediatrics/Newborn Medicine, Weill Cornell Medical College, New York, NY, USA

Perinatal hypoxic-ischemic (HI) brain damage is a major cause of acute mortality and chronic neurologic morbidity in infants and children. The mechanisms leading to brain damage following HI are complex and relate to the developmental state of the brain and the severity of the insult. Inflammation plays an important role in the pathogenesis of damage and represents an important target for therapeutic intervention. The majority of studies focus on microglial activation as mediating this inflammatory cascade. However, recent studies suggest that another immune cell, the mast cell, may play a central role as well.

Mast cells are hematopoietic immune cells located throughout the body, largely in association with blood vessels. Mast cells are numerous in the pia and brain of neonatal rats and can rapidly initiate inflammation due to the presence of pre-formed inflammatory mediators, such as TNF-a. Mast cell activation has been shown to contribute to edema and BBB breakdown following experimental stroke in adult rodents. Studies from our laboratory have shown extensive mast cell migration and activation to be very early events following HI in the neonatal rat and mast cell stabilization with sodium chromoglycate confers longterm neuroprotection. Thus, it appears that mast cells are early responding cells to HI in the neonatal brain and represent a novel target for neuroprotection.

This work is supported by a grant from the Fondation LeDcuq

POST-STROKE INFLAMMATION AND LONG-TERM OUTCOMES

Y. Xu

Neurology, The Affiliated Drum Tower Hospital of Nanjing University Medical School, Nanjing, China

Objectives: Ischemic stroke can induce not only cerebral immuno-inflammation, but also system immuno- inflammation which including immediate activation and later inhibition of the peripheral immune system. Both they may contribute to a worse outcome. The aims of this study are from bench to clinic to show:

1) Inhibiting inflammatory mediators protect against brain injury.

2) Modulating post-stroke system immune response and exerts a neuroprotective effect in experimental stroke and patients.

3) Possible mechanisms.

Methods: Mice were subjected to MCAO and then sacrificed at indicated time point. The brains were stained with TTC to detect the infarction volume. Apoptotic cells were determined by TUNEL stain and TUNEL positive cells were counted by Image-Pro Plus 6.0. Western blot and Q-PCR were involved to detect the protein level or mRNA level of mouse tissue respectively. CD4+/CD8+ ratio and CD4+CD25+FOXP3+T cells in the blood and spleens of mice were determined by flow cytometry.

210 acute ischemic stroke patients were enrolled in this study (this study was approved by the ethics committee of the Affiliated Drum Tower Hospital of Nanjing University). The patients treated with Aspirin with or without Human urinary kallidinogenase (HUK) , follow up 12 months. ELISA was involved to measure the level of inflammatory cytokines in the serum of mice or human beings. National institute health stroke scale (NIHSS) score and the modified Rankin Scale (mRS) were used to determine patients outcome. Brain edema and brain reperfusion of stroke patients were calculated by MRI Diffusion Weighted Imaging (DWI) and Perfusion-Weighted Imaging (PWI) images.

Results:

Part 1: **Inhibiting** inflammatory mediators protect against brain injury In experimental stroke mice HUK reduced infracted size, apoptotic cells and alleviated ischemic-induced neurologic deficit. HUK suppressed mRNA and protein level of inflammatory mediators including IL-1, TNF-α, MCP-1, ELAM-1, iNOS and COX-2 6h 24h, 48h after stroke. HUK inhibited the NF-κB pathway and activated the MAPK/ERK pathway in this neuroprotection. In patient study, stroke patients receiving HUK demonstrated smaller penumbra volume and edema volume and high brain perfusion determined by MRI DWI and PWI image. At the same time, HUK decreased the 1L-1 and TNF in stroke patient serum by ELISA. Correlation analysis showed that a linear correlation was found between the serum level of 1L-1 ,TNF and NIHSS, mRS, brain perfusion.

Part 2: Modulating post-stroke system immune response and exerts a neuroprotective effect in experimental stroke

Cocaine- and amphetamine-regulated transcript CART reduced blood CD4+/CD8+ ratio and pro-inflammatory cytokine expression in MCAO mice at 24 h, while upregulated spleen CD4+/CD8+ ratio and enhanced anti-inflammatory cytokines expressions in MCAO mice at 96 h. CART-treated mice demonstrated elevated serum catecholamins (CAs) at 6 and 24 h, whereas reduced serum levels of CAs and blood Treg cells at 96 h. CART reduced post-stroke infarct volume and improved neurological functions in the injured mouse brain.

Conclusion: Inflammatory mediators as well as immune cells play critical and complicated roles in the pathogenesis of ischemic stroke. Drugs modulating cerebral immuno-inflammation may benefit clinical stroke patients in the future.

RESTING MICROGLIA DIRECTLY MONITOR SYNAPSES IN VIVO AND DETERMINE THE FATE OF ISCHEMIC TERMINALS

H. Wake[1], J. Nabekura[2]

[1]Division of Brain Circuits, National Institute for Basic Biology, NINS, [2]Division of Homeostatic Development, National Institute for Physiological Sciences, NINS, Okazaki, Japan

Brain function depends critically on the interactions amongst the underlying components that comprise neural circuits. This includes coordinated activity in pre-synaptic and postsynaptic neuronal elements, but also in the non-neuronal elements such as glial cells. Microglia are glial cells in the central nervous system that have well-known roles in neuronal immune function, responding to infections and brain injury and influencing the progress of neurodegenerative disorders. However microglia also are surveyors of the healthy brain, continuously extending and retracting their processes and making contacts with pre- and postsynaptic elements of neural circuits, a process that clearly consumes considerable energy. Pruning of synapses during development and in response to injury has also been documented, and we propose that this extensive surveillance of the brain parenchyma in adult healthy brain results in similar “fine-tuning” of neural circuits. A reasonable extension is that a dysfunction of such a homeostatic role of microglia could be a primary cause of neuronal disease. Indeed, neuronal functions including cognition, personality and information processing are affected by immune status. In this presentation, we focus on these interactions

between microglia and synapses in the physiological brain and the possible implications these interactions may have in the fine tuning of neural circuits that is so important for physiological brain function.

VASCULAR PATHOLOGY FOLLOWING SUBARACHNOID HEMORRHAGE: NOVEL ASPECTS AND THERAPEUTIC APPROACHES

N. Plesnila

Institute for Stroke and Dementia Research, University of Munich Medical Center, Munich, Germany

Subarachnoid hemorrhage (SAH) is the subtype of stroke with the highest mortality and morbidity. SAH is in most cases caused by rupture of an arterial aneurysm with subsequent bleeding into the subarachnoid space, the space which hosts the large cerebral vessels before they enter the brain parenchyma. Most SAH patients die within the first few days after the initial bleeding, however, the reason for this early mortality remained unclear for many years. Only recently it has been appreciated that an early reduction of cerebral blood flow (CBF) is an important feature of the events finally resulting in early brain injury (EBI) following SAH.

The current presentation aims to discuss the mechanisms responsible for early ischemia and EBI after SAH and to present novel findings on how the cerebral microcirculation is involved in this process. Based on this deepened understanding of the pathophysiology of SAH and the emerging role of microvascular dysfunction for EBI, novel therapeutic concepts for the treatment of post-hemorrhagic ischemia with a specific emphasis on inhaled nitric oxide (iNO) are presented and discussed.

TRANSGENIC MOUSE MODELS OF CEREBRAL AMYLOID ANGIOPATHY: ARTERIOLAR VS CAPILLARY AMYLOID ACCUMULATION

W.E. Van Nostrand

Neurosurgery & Medicine, Stony Brook University, Stony Brook, NY, USA

Cerebral amyloid angiopathy (CAA), a condition that is characterized by the accumulation of fibrillar amyloid ß-protein (Aß) in blood vessels of the brain, is commonly found in patients with Alzheimer's disease (AD) and related disorders. Additionally, familial forms of CAA exist that result from specific mutations in the Aß peptide. Patients with familial forms of CAA develop early-onset and severe vascular amyloid accumulation that is typically associated with recurrent, and often fatal, intracerebral hemorrhage. There are two prominent forms of CAA known as CAA-type 1 and CAA-type 2. In CAA-type 2 the amyloid deposition occurs within the vessel wall of the brain arterioles and small arteries and generally does not promote surrounding neuroinflammation. Accumulation of fibrillar amyloid in CAA-type 2 has been shown to cause degeneration and loss of smooth muscle cells in affected larger cerebral vessels and cause hemorrhage. On the other hand, CAA type-1 involves amyloid deposition along the brain capillaries. In contrast to CAA type-2, microvascular CAA type-1 involves penetrance of the fibrillar amyloid deposits into the surrounding parenchyma that promotes a localized, robust neuroinflammatory response characterized by strong astrogliosis and perivascular microglial activation. Furthermore, CAA type-1 microvascular Aß deposition and its accompanying neuroinflammatory response is more often correlated with cognitive impairment in individuals afflicted with AD and CAA disorders.

Transgenic mice, which robustly express human AßPP in brain, produce abundant levels of normal human Aß peptides, and develop cerebral amyloid deposits, have been a significant advancement for the study of the pathogenic effects of brain Aß accumulation *in vivo*. The common pathology observed in most of these particular transgenic mouse lines includes regional and age-dependent accumulation of parenchymal fibrillar amyloid plaques and varying degrees of larger vessel CAA type-2. These mouse models with CAA type-2 can exhibit vascular smooth muscle cell degeneration and evidence of cerebral microhemorrhage thus recapitulating the features of this condition that are observed in afflicted humans.

To generate a more specific cerebral vascular amyloid model, the Tg-SwDI mouse was developed to express familial “Dutch/Iowa” CAA mutant human Aß in brain. Tg-SwDI mice develop early-onset and progressive accumulation of microvascular CAA type-1 in the absence of parenchymal fibrillar Aß plaque deposits. In this model the penetrance of

microvascular fibrillar amyloid into the adjacent brain parenchyma promotes disruption of the neurovascular unit and a localized robust neuroinflammatory response characterized by pericyte degeneration, astrogliosis, and microglial activation, which is intimately linked to behavioral impairment in Tg-SwDI mice. Thus, this mouse model of CAA type-1 supports the strong relationship between capillary amyloid, neurovascular inflammation, and dementia in humans and offers a viable therapeutic target for vascular amyloid-mediated cognitive impairment.

SYMPOSIUM: NOVEL OPTICAL TECHNIQUES TO ELUCIDATE CEREBROVASCULAR FUNCTION AND DISEASE

C. Schaffer[1], D. Boas[2]

[1]Biomedical Engineering, Cornell University, Ithaca, NY, [2]Martinos Center, Dept. of Radiology, Massachusetts General Hospital, Charlestown, MA, USA

In the last two years, several new and very powerful optical approaches have been applied to the study of cerebrovascular regulation and stroke. Optogenetics allows select classes of neurons to be activated, providing a powerful strategy to unravel the mechanisms of neurovascular coupling and a deeper insight into functional MRI. Oxygen-sensitive indicators that can be imaged using nonlinear microscopy enable the study of oxygenation changes in blood vessels and brain tissue during activation and after stroke. This symposium will feature leading researchers who both develop these cutting-edge methods and use them to study brain function and disease.

DECIPHERING NEURONAL CIRCUITRY CONTROLLING LOCAL BLOOD FLOW IN CEREBRAL CORTEX OF RODENTS WITH OPTOGENETICS AND CHRONIC FUNCTIONAL ULTRASOUND IMAGING

J. Rossier, A. Urban

Centre de Psychiatrie et Neurosciences, INSERM U894, Paris, France

Although it is know since more than a century that neuronal activity is coupled to blood supply regulation, the underlying neuronal pathways remain to be identified. In the brain, neuronal activation triggers a local increase of cerebral blood flow (CBF) that is controlled by the neurogliovascular unit composed of terminals of neurons, astrocytes and blood vessel muscles. It is generally accepted that the regulation is adjusted to local metabolic demand by local circuits. Today experimental data led us to realize that the regulatory mechanisms are more complex. Indeed, how to explain that a stimulus of the whisker pad in rodents is associated with local increase in the corresponding barrel field but also with decreases in the surrounding deeper area and in the opposite barrel field?

By combining both *in vitro* studies in acute slice and *in vivo* imaging by chronic functional ultrasound imaging in anesthetized rats, we demonstrated that neurovascular coupling is a process through which neuronal activity leads to increases of local CBF in the activated area but also to decreases in other brain regions. In order to explain these observations, we propose that a neuronal system within the brain is devoted to the control of local brain blood flow. Our optogenetic experiments revealed that neurons expressing the calcium binding protein parvalbumin could control local blood flow. We demonstrated that channel rhodopsin-based photostimulation of these cells give rise to an effective contraction of penetrating arterioles. These results therefore support the neurogenic hypothesis of a complex distributed nervous system controlling the CBF.

HIGH RESOLUTION IMAGING OF OXYGEN TENSION AND BLOOD FLOW AFTER MICROVASCULAR OCCLUSION

A.K. Dunn

Biomedical Engineering, University of Texas at Austin, Austin, TX, USA

During ischemic stroke, oxygen delivery in interrupted to a region of the brain resulting in a complex cascade of hemodynamic and cellular events that ultimately leads to cell death and tissue damage. Although recent advances in high resolution in vivo imaging have enabled some aspects of this cascade to be visualized dynamically, the detailed changes in blood flow and oxygenation during stroke remain only partially understood. This talk will describe recent developments in optical imaging techniques for high resolution imaging of cortical hemodynamics and their application to animal models of stroke. Multi-

exposure laser speckle imaging (MESI) is extension to traditional laser speckle contrast imaging that enables quantitative imaging of blood flow over periods of weeks to months. MESI allows detailed analysis of vascular remodeling following stroke. In addition, we will describe the use of two-photon phosphorescence lifetime microscopy for determination of oxygen levels in single, subsurface blood vessels with three-dimensional micron scale resolution. We have found a significant longitudinal gradient in oxygen tension within the first few hundred microns of penetrating arterioles in mouse cortex. Following occlusion of single arterioles, the downstream alterations in oxygen tension are significantly affected by the locations of branches from the penetrating arterioles. Together, multi-exposure laser speckle imaging and two photon phosphorescence lifetime microscopy enable detailed investigation of hemodynamic alterations in the cortex during stroke.

NOVEL DRUGS FROM NATURAL PRODUCTS OR TRADITIONAL MEDICINE FOR CNS DISEASES

P. Wong

Pharmacology, National University of Singapore, Singapore, Singapore

Natural products from herbs, animals or even human, have long been used by people to treat diseases or to improve general health. Despite its long history, traditional Chinese medicine (TCM) is still widely used today and plays a very important role in healthcare in China. Its importance is also increasing in Western societies as more westerners turn to herbal remedies. Compared to Western medicine, TCM places greater emphasis on overall well-being of a person and many of its applications have been proven to be clinically useful. Most remedies of TCM are composed of a combination of many plants with the aim of maximizing their therapeutic effects and easing adverse effects. This led to a significant problem in investigating these remedies in research as they are complex mixtures, and to much effort in standardizing preparation as well as extracting single active compounds. For example, huperzine A, a sesquiterpene alkaloid compound extracted from firmoss Huperzia serrata, is an acetylcholinesterase inhibitor and NMDA receptor antagonist found to be effective in improving cognition and memory in Alzheimer's disease (AD) patients. It is now available as a dietary supplement for memory support. However, TCM products generally lack solid scientific evidence for clinical efficacy.In this symposium, we attempt to cover a spectrum of activities from basic to translational research. Firstly, Prof. YH Suh of Seoul National University will present his work on potential TCM drugs for AD and Parkinson's disease; in particular, dehydroevodiamine hydrochloride (DHED), which is extracted from Evodia rutaecarpa Bentham, as a potential therapeutic candidate for AD. Secondly, Prof. YZ Zhu of Fudan University will speak on leonurine (SCM198), extracted from *Herba leonuri*, which has neuroprotective effects against stroke in animal studies. Prof. C Chen of the National University of Singapore will present clinical trials done on a marketed TCM-based product called NeuroAiD for the treatment of stroke and dementia. Last but not least, Dr Y Qiu of GSK will speak on the development of innovative TCM products with better defined clinical efficacy and safety from an industry perspective.

POTENTIAL DRUGS FROM NATURAL PRODUCTS FOR AD AND PD

Y.-H. Suh

Korea Brain Research Institute, Daegu, Republic of Korea

Several lines of evidence suggest that some neurotoxicity in Alzheimer's disease (AD) is due to proteolytic fragment of amyloid precursor protein (APP) such as Ab and APP-CTs.

Among 29 plants treated *Evodia rutaecarpa* Bentham showed a strong inhibitory effect on acetylcholinesterase in vitro and an antiamnesic effect in vivo.

By sequential fractionation of *Evodia rutaecarpa* Bentham the active component was finally identified as dehydroevodiamine hydrochloride(DHED).

We found that DHED (*Evodia rutaecarpa* Bentham) had anticholinesterase effect and its beneficial effects on neuronal death and damage in various animal models. We recently confirmed neuroprotective effects of DHED *in vitro* and *in vivo* AD models. DHED might attenuate neuronal damages and cognitive dysfunction caused by toxic metabolites of APP such as Aβ and CT105 through multi-

neuroprotective mechanisms antagonizing oxidative stress and NMDA receptor. Thus, DHED might be one of the potential therapeutic candidates for AD. We have complete the phase 1 clinical study. In addition, We have synthesized and investigated several derivatives of DHED to increase solubility and efficacy.

We have screened and isolated an active constituent from Indigenous herb Indigofera tinctoria Linn(I. tinctoria, Fabaceae) in experimental models of PD. I. tinctoria, is an annual herb found throughout India and other parts of Asia.

The herb is widely used for several years in the traditional Indian and Chinese system of Medicine for the treatment of epilepsy, nervous disorders, bronchitis, liver ailments, sores, ulcers and hemorrhoids.

To evaluate the in vitro protective activities the butanol sub-fraction, SF-6 was assessed using human neuroblastoma SH-SY5Y cells against α-synuclein-, 6-hydroxydopamine(6-OHDA)-, and H_2O_2- induced cytotoxicity using WST-1 cell viability assay.

The butanol sub-fraction, SF-6 attenuated the α-synuclein-induced cytotoxicity in SH-SY5Y cells and scaven ged directly hydroxyl free radical as estimated using the ESR spectroscopy.

The single compound methylparaben (MP) was isolated form sub-fraction SF-6.

In-vivo studies of methylparaben were evaluated against 6-OHDA-lesioned neuronal damage by stereotaxically injecting 6-OHDA unilaterally into the substantia nigra.

The single compound MP isolated from butanol sub-fraction (SF-6) showed significant and potent neuroprotective effects in both in vitro and in vivo evaluations.

Considering the results obtained our in vitro and in vivo findings suggest the possibility of MP to show neruoprotection in experimental models of PD via the antioxidant properties and therefore can further be developed as potential agent for treating neurodegenerative processes seen in PD.

LEONURINE (SCM-198), A NOVEL COMPOUND FROM CHINESE HERB FOR PREVENTION AND ACUTE TREATMENT IN THE ANIMAL MODEL OF ISCHEMIC STROKE

Y.Z. Zhu

Dept of Pharmacology, School of Pharmacy, Fudan University, Shanghai, China

Stroke especially ischemic stroke is a key factor for causing high mortality in Asian populations. Many therapeutic approaches have been investigated to solve this problem though it remains a main issue for treating stroke. Recently, we found a unique single compound Leonurine (named also as SCM-198, J CVP 2009, Atherosclerosis 2012a and Atherosclerosis 2012b) extracted from Chinese herb—herba leonuri could prevent (Stroke 2010) and treat ischemic stroke (to be submitted). Middle cerebral artery occlusion (MCAO) was used and the animals were pretreated with orally for 7 days and the surgery was done. SCM-198 pretreatment reduced infarct volume, improved neurological deficit in stroke groups, increased activities of antioxidant enzymes superoxide dismutase and glutathione peroxidase, and decreased levels from the lipid peroxidation marker malondialdehyde. SCM-198 further inhibited mitochondrial reactive oxygen species production and adenosine triphosphate biosynthesis. In the acute treatment group, rats were treated by i.v. with SCM-198 15mg/kg at 0.5h, 1h and 2h after surgery and continued for 7 days. PET/CT and the neurological deficit score showed a significant amelioration in the treated group compared to vehicle group. TTC staining after 3 days' treatment showed a reduced infarct volume. Results in immunohistochemical staining, Iba-1 immunoreactivity in hippocampal CA1 region were markedly decreased in the treated groups. Further, a significant better maintenance of neuronal structure in hippocampal CA1 region and fewer activated microglia in the treated groups (especially in the 0.5h group) was observed than the vehicle group. SCM-198 could go through BBB rapidly with $T_{1/2}$ of 25.4mins analyzed by microdialysis. Our results demonstrated that SCM-198 not only served as a prophylactic agent for ischemic stroke but also a potential drug candidate for acute treatment of stroke.

CLINICAL TRIALS OF TCM-BASED DRUGS FOR STROKE AND DEMENTIA

C. Chen

Pharmacology, National University of Singapore, Singapore, Singapore

Background and aims: Stroke is a major cause of death and disability: not only due to motor deficits but also to cognitive impairment and dementia. TCM have been utilized for the treatment of stroke and dementia but meta-analyses have shown that the evidence base is scanty, hence the need for more well designed scientific studies and clinical trials.

NeuroAiD™ has recently been shown to restore neurological and cellular function in animal models of stroke by processes involved in repair (Heurteaux, 2010). Previous clinical studies performed in China have shown that NeuroAiD™ increases stroke patients' recovery in terms of neurological disability and functional outcome [Chen et al, 2009] and thus may be beneficial as part of a post-stroke rehabilitation programme. In the CHIMES study, we seek to test the hypothesis that NeuroAiD™ is superior to placebo in reducing neurological deficit and improving functional outcome after acute ischemic stroke in patients with cerebral infarction with intermediate range of severity ($6 \leq$ NIHSS ≤ 14). The NEURITES study aims to investigate the effects and tolerability of NeuroAiD™ in patients with vascular cognitive impairment not dementia (VCIND).

Methods: Details of the study protocols have been published [Venketasubramanian et al, 2009; Chen et al, in press].

Results: CHIMES recruited its target of 1100 patients by June 2012. It involved sites in the Philippines, Singapore, Thailand, Sri Lanka, Hong Kong and Malaysia. Safety data for additional laboratory tests was conducted only in Singapore sites at the request of the Singapore regulators. These results were analysed with the investigators and steering committee remaining blinded to the treatment allocation [Young et al, 2010] and showed no safety concerns. Baseline data on demographics, clinical characteristics and drop-out rates will be reported. NEURITES will begin recruitment in 2013.

Conclusions: CHIMES is the largest trial investigating the efficacy of a Traditional Chinese Medication on stroke recovery, performed in compliance with international guidelines and using Western clinical trial standards. NEURITES will provide important information on the use of TCM in dementia associated with cerebrovascular disease.

DEVELOPMENT OF INNOVATIVE TCM PRODUCT

Y. Qiu

GSK R&D China, Shanghai, China

Traditional Chinese Medicine (TCM) has been widely practiced for thousands of years in China. It is based on ancient Chinese philosophy and views diseases as a disharmony between Yin and Yang and the five elements of the universe (metal, wood, water, fire and earth). Recent years, TCM has evolved to modern formulations and plays even more important role in health care system in China. However, current TCM products are mainly derived from ancient recipes and sold based on traditional belief and subjective experience. There is a general lack of objective and modern scientific evidence for their efficacies. In addition, product qualities are not well controlled and variable. The advancement of modern technology and the experience of western drug development provide the unique opportunity to develop innovative TCM products with demonstrated clinical efficacy and safety as well as quality assurance. The current trends in understanding potential underline mechanism of TCM using system biology, developing mixture with quality consistency, and demonstration of clinical efficacy will be discussed.

BrainPET Symposium

IMAGING OF SIGNAL TRANSDUCTION CASCADE IN ALZHEIMER´S DISEASE

M. Higuchi, M. Maruyama, H. Shimada, B. Ji, J. Maeda, M. Ono, M.-R. Zhang, T. Suhara

Molecular Imaging Center, National Institute of Radiological Sciences, Chiba, Japan

Objectives and methods: Alzheimer's disease (AD) is neuropathologically characterized by deposition of amyloid beta peptide (Aβ) and tau fibrils, and this dual fibrillogenesis is supposed to trigger chain reactions of key molecular and cellular processes, including neuroinflammation, disrupted intraneuronal calcium homeostasis,

synaptic abnormalities and eventual neuronal death. Meanwhile, mechanistic links between Aβ/tau amyloidosis and downstream processes in the cascade are largely unknown.

We aimed at visualizing accumulation of Aβ and tau aggregates and activation of deleterious microglia expressing 18-kDa translocator protein in living brains with the aid of PET and specific radioligands.

Results:

1) Aβ amyloidosis and microgliosis

By comparative PET/autoradiographic assay with [^{11}C]Pittsburgh Compound-B ([^{11}C]PIB) and immunohistochemistry of human and amyloid precursor protein (APP) transgenic mouse brains, we identified an N-terminally truncated and pyroglutamated Aβ (AβN3pE) as a major constituent of binding sites for plaque PET tracers. In the interim, a number of works by independent research groups have recently supported crucial roles of this Aβ species in neurodegenerative changes characteristic of AD. Distinct regulation of AβN3pE deposition by protective and deleterious microglia was also demonstrated by implantation of two different microglial clones expressing TSPO at low and high levels into APP transgenic mouse brains. Subsequent biochemical comparison of these two clones indicated the significance of a proinflammatory chemokine, CCL2, in detrimental microgliosis promoting Aβ pathogenesis. Notably, generation of AβN3pE and stabilization of CCL2 are catalyzed by the same enzyme, glutaminyl cyclase (QC), suggesting parallel enhancement of amyloidosis and microgliosis by QC. In addition, TSPO was found to augment release of CCL2 from microglia. Hence, reciprocal links among QC, CCL2 and TSPO could be therapeutic targets for modifying the amyloid cascade in AD, and changes in these molecules would be monitored by PET.

2) Tau accumulation, microgliosis and neuronal loss

We also developed a new class of radioligands permitting PET imaging of tau lesions. Intense PET signals were intimately associated with abundance of fibrillar tau inclusions in tau transgenic mice, while marked hippocampal atrophy in this animal model preceded formation of PET-positive tau inclusions. Detailed biochemical and histological analyses of tau transgenics indicated neurotoxicity of soluble phospho-tau species. The accumulation of this soluble tau was accelerated by autophagic impairments, resulting in aggravation of TSPO-positive microgliosis and subsequent neuronal loss. We then applied one of these tau radioligands to an exploratory clinical PET study, and observed a progressive increase of the radioligand binding in the transition from normal aging to AD, which resembled advance of Braak stages of tau pathology and was in sharp contrast to [^{11}C]PIB-PET data. Moreover, accumulation of the tau radioligand in the medial temporal region was inversely correlated with volume of this area, implicating insoluble tau aggregates in neuronal loss by a mechanism somewhat distinct from neurotoxicity induced by soluble tau in transgenic mice.

Conclusions: PET imaging of amyloid-triggered signaling cascade in animal models and humans potentially facilitate clarification of molecular culprits pivotally implicated in the neurodegenerative pathogenesis of AD, providing significant insights into therapeutic strategies against this disease.

TRANSLATIONAL AB AND TAU IMAGING IN ALZHEIMER'S DISEASE

V.L. Villemagne[1,2,3]

[1]Nuclear Medicine and Center for PET, Austin Health, [2]Mental Health Research Institute, [3]Medicine, University of Melbourne, Melbourne, VIC, Australia

β-amyloid (Aβ) and tau are the neuropathological hallmarks of Alzheimer's disease (AD). Positron emission tomography (PET) radiotracers for the in vivo assessment of Aβ burden have transformed the evaluation of AD pathology, extending our insight into Aβ deposition in aging and AD by providing highly accurate, reliable, and reproducible quantitative statements of regional and global Aβ burden in the brain, essential for therapeutic trial recruitment and for the evaluation of anti-Aβ therapies. While this progress has already resulted in the approval of an Aβ radiotracer for clinical use, it is only in recent years that there has been significant progress in the development of tau imaging tracers.

In general, useful neuroimaging probes must meet a number of key general properties: they

should be non-toxic lipophilic molecules of low molecular weight that cross the blood brain barrier, with rapid clearance from blood and preferably are not metabolized, whilst reversibly binding to AD pathology in a specific and selective fashion. After initial high throughput screening of compound libraries or structure-activity relationship studies, further characterization requires in vitro saturation and/or competition studies assessing affinity and selectivity of the binding using either synthetic fibrils or brain homogenates. Ex vivo or small animal PET studies are used to evaluate the biodistribution and brain uptake of candidate neuroimaging tracers. Furthering tracer characterization, testing its ability to detect pathology in vivo, involves studies in transgenic mice models of the disease. After the preclinical examination confirms the candidate fulfils ligand criteria for PET studies, microdose toxicity and receptor panel analysis are performed, and human PET studies, assessing tracer safety and its ability to distinguish control from pathological cases, are started.

As new treatment strategies to prevent or slow disease progression through early-intervention are being developed and implemented, there is an urgent need for early disease recognition, which is reflected in the necessity of developing sensitive and specific biomarkers as adjuncts to clinical and neuropsychological tests. Antecedent, diagnostic and prognostic biomarkers include the examination of disease specific traits such as Aβ, tau or α-synuclein in blood and cerebrospinal fluid, as well as the application of neuroimaging techniques such as PET for the characterization and quantification of metabolic and neurochemical alterations that lead to neurodegeneration and cognitive impairment. Because the molecular changes occur well before the phenotypical manifestation of the disease, a change in the diagnostic paradigm is needed, where diagnosis moves away from the identification of signs and symptoms of neuronal failure to the early and non-invasive detection of a particular trait or traits underlying the pathological process, that will also allow evaluation of efficacy and monitoring of the molecular effects of disease-modifying therapies. Furthermore, given the complexity and sometimes overlapping characteristics of these disorders, it is unlikely that a single biomarker will be able to provide the diagnostic certainty required, especially for the identification of at-risk individuals before the development of the typical phenotype. Consequently, a multimodality approach for the accurate and early diagnosis, monitoring disease progression, and better treatment follow-up of AD is warranted.

Niels Lassen Award

CALORIC RESTRICTION ENHANCES OXIDATIVE BRAIN METABOLISM IN HEALTHY AGING DETECTED BY $^{1}H[^{13}C]$ MRS

A.-L. Lin[1], D. Coman[2], L. Jiang[2], D. Rothman[2], F. Hyder[2]

[1]Research Imaging Institute, University of Texas Health Science Center at San Antonio, San Antonio, TX, [2]Magnetic Resonance Research Center, Yale University, New Haven, CT, USA

Objectives: Caloric restriction (CR) is the most studied anti-aging manipulation and has been shown to increase the lifespan of a broad range of species. Rats treated with CR also showed enhanced memory (1). Here we used in vivo proton observed carbon edit (POCE) or $^{1}H[^{13}C]$ MRS to characterize the effect of CR on the rates of neuronal TCA cycle flux ($V_{TCA,N}$), total glutamatergic neurotransmission from the glutamate and glutamine cycle flux ($V_{cyc(tot)}$), and lactate concentration in aged rats.

Methods: Male control and CR F344BNF1 rats at 24 month of age (N= 6) were anesthetized with alpha chloralose. In vivo $^{1}H[^{13}C]$ NMR study was performed on a Varian 11.7T MR system. The POCE spectra were obtained from a localized volume (8x4x 6 mm^3) that covered cortex and hippocampus. [1,6-^{13}C] labeled glucose was continuously infused via the femoral vein of the rat for 2-hour and POCE spectra were acquired simultaneously. Six blood samples were taken from a femoral artery during the 2-hour scan to determine the [1,6-^{13}C] labeled glucose level. The concentrations of the metabolites (including lactate) were also determined in the brain extracts at the end point of the labeled isotope infusions. Data were analyzed with the CWave program for mathematical modeling to determine $V_{TCA,N}$ and $V_{cyc(tot)}$. T-test was used to determine the difference of the measured indices between the control and CR rats.

Results: Aged CR rats had significantly higher $V_{TCA,N}$ ($P < 0.0001$) and $V_{cyc(tot)}$ ($P < 0.001$), but lower lactate concentration, relative to

controls. Our results demonstrated that $V_{TCA,N}$ and $V_{cyc(tot)}$ has a ~ 2:1 ratio, similar to literature value for a variety of other conditions examined, from awake to different anesthetized states (2). We also found that aged CR rats had similar $V_{TCA,N}$ (~ 0.4 µmol/g/min) and $V_{cyc(tot)}$ (~ 0.22 µmol/g/min) relative to those of the younger control rats as reported in literature (3).

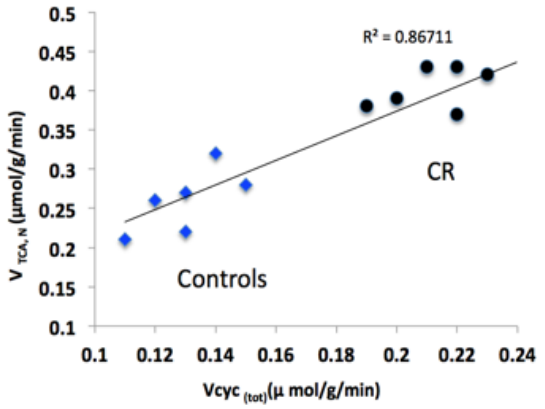

[Figure 1]

Conclusions: We demonstrated that CR enhanced brain mitochondrial functions, including increased $V_{TCA,N}$ and $V_{cyc(tot)}$, and decreased lactate concentration. The results suggest that preserved or increased cerebral oxidative metabolism with age may play a key role in maintaining brain function. Further, we observed that aged CR rats had enhanced neuronal metabolism and that was similar to young ones, suggesting that CR may delay brain age-related metabolic reduction in rodents. As brain function plays a crucial role in lifespan determination (4), CR could be an important intervention in extending healthspan of the brain and thus lifespan. Future studies are needed to identify the cellular mechanism of CR-induced enhancement of brain function in healthy aging and in neurodegenerative disorders.

References:

(1) Carter et al., J Gerontol A Biol Sci Med Sci. 64A: 850 (2009);

(2) Hyder et al., J, Cereb Blood Flow & Metab. 26:865 (2006);

(3) Ennis et al., Neurochem Res. 36:1962 (2011);

(4) Mattson et al., Ageing Res Rev 1:155 (2002).

REGULATORY T CELLS LIMIT ISCHEMIC BRAIN INFLAMMATION AND NEUROVASCULAR DISRUPTION *VIA* SUPPRESSION OF PERIPHERAL MATRIX METALLOPEPTIDASE-9

P. Li[1,2], Y. Gan[1,2], B. Sun[3], F. Zhang[1,2], Y. Gao[1], W. Liang[1], J. Chen[1,2], X. Hu[1,2]

[1]Anesthesiology Department of Huashan Hospital, State Key Laboratory of Medical Neurobiology and Institute of Brain Sciences, Fudan University, Shanghai, China, [2]Center of Cerebrovascular Disease Research, University of Pittsburgh School of Medicine, Pittsburgh, PA, USA, [3]Department of Neurology and Key Laboratory of Cerebral Microcirculation, University of Shandong, Affiliated Hospital of Taishan Medical College, Taian, China

Objectives: Ischemic stroke elicits a profound inflammatory response involving both innate and adaptive immunity. The reciprocal interaction between the immune system and the ischemic brain helps determine stroke pathology and represents a promising target for stroke treatment (*1*). Recent evidence suggests that peripheral regulatory T cells (Tregs), an innate immuno-modulator, might be an endogenous protective mechanism that counterbalances cerebral inflammation following ischemic stroke (*2*). However, the therapeutic potential of Treg adoptive therapy in stroke has not been evaluated and the underlying mechanism for Treg-afforded neuroprotection is still poorly understood.

Methods: Cerebral ischemia was induced by middle cerebral artery occlusion (MCAO) for 60 minutes in mice or 120 minutes in rats. Tregs were isolated from donor animals by CD4 and CD25 double selection and systemically transferred to ischemic recipients at 2, 6 or 24 hours after MCAO. Brain infarction and neurological performance was assessed up to 28 days post-stroke. The mechanisms of Treg-afforded neuroprotection were investigated using cell-specific depletion, gene knockout mice, bone marrow chimeras and *in vitro* Treg-neutrophil co-cultures.

Results: Using both mouse and rat models of transient focal cerebral ischemia, we demonstrate that adoptively transferred Tregs markedly reduced brain damage and improved

long-term neurological outcomes with a wide temporal window of efficacy (24h). Maximal protection occurred upon early Treg transfer with a 2h delay after MCAO, which resulted in approximately 50% reduction of infarct volume. The protective effects of Tregs were associated with decreased cerebral inflammation and reduced infiltration of peripheral inflammatory cells into the lesioned brain. Treg treatment also attenuated blood-brain barrier (BBB) disruption as early as 1 day after ischemia, as manifested by reduced extravasation of plasma-derived IgG and exogenous tracers, preserved continuity of tight junction protein ZO-1 and protected ultrastructure of tight junctions by electron microscopy. Surprisingly, using Tregs with the CD45.1 congenic marker or cell tracker labeling, we noticed that exogenous Tregs exerted early neuroprotection without penetrating into the brain parenchyma. Rather, Tregs suppressed peripheral neutrophil-derived matrix metallopeptidase-9 (MMP-9), thereby preventing proteolytic damage of the BBB. Treg-afforded neuroprotection after MCAO was abolished by

1) gene knockout of MMP-9,

2) transplantation of bone marrow from MMP-9 knockout mice into irradiated wide type mice, or

3) depletion of neutrophils with anti-Gr1 antibody. *In vitro* studies using Treg-neutrophil co-cultures further confirmed that Tregs suppressed neutrophil-derived MMP-9 in a cell-cell contact dependent manner. In additions to its potent central neuroprotection, Treg treatment was shown to ameliorate post-stroke lymphopenia, suggesting an additional beneficial effect on systemic immune status.

Conclusions: Our study demonstrates that Treg adoptive therapy is a novel and potent cell-based therapy targeting post-stroke inflammatory dysregulation and neurovascular disruption.

NF-KB PATHWAY CONTRIBUTES TO THE BRAIN REPAIR INDUCED BY HEMATOPOIETIC GROWTH FACTORS IN CHRONIC STROKE

L. Cui[1], N.S. Duchamp[2], B.J. Dakota[2], X. Ren[1], H. Hu[1], L.-R. Zhao[3]

[1]Neurology, [2]School of Medicine, [3]Neurology, Cellular Biology and Anatomy, Louisiana State University Health Sciences Center, Shreveport, LA, USA

Objectives: Stroke is a leading cause of adult permanent disability worldwide. The phase of chronic stroke usually starts 3-6 months after stroke onset. Currently no pharmaceutical therapy is available for the treatment of chronic stroke. Stem cell factor (SCF) and granulocyte-colony stimulating factor (G-CSF) are the essential members of hematopoietic growth factor family, and play a key role in the regulation of blood cell production. Recent findings suggest that SCF and G-CSF may be also involved in neuronal plasticity in the central nervous system. In our early study, we have demonstrated that SCF in combination with G-CSF (SCF+G-CSF) improves functional outcome when administered in the chronic phase of stroke in animal models. However, the mechanism by which SCF+G-CSF repairs the brain in chronic stroke remains poorly understood. Recently, we have revealed that NF-kB pathway is required for SCF+G-CSF-induced enhancement of neurite outgrowth in primary cortical neurons. In this study, we determined whether NF-kB pathway contributes to brain repair induced by SCF+G-CSF in chronic stroke.

Methods: Focal cerebral ischemia was induced by permanent occlusion of the right common carotid artery and middle cerebral artery in 4-month-old male mice. At 3.5 months post-ischemia, SCF and G-CSF were subcutaneously administered for 7 days. NF-kB inhibitor, BAY 11-7085, was infused into the contralateral ventricle with a 7-day-infusion osmotic pump 1 hour before SCF+G-CSF treatment. At week 8 after treatment, biotinylated dextran amine (10,000 MW) was stereotaxically injected into the contralateral cortex to detect the axonal sprouting. Functional restoration was examined using the Rotarod test 2 and 6 weeks after treatment. Axonal sprouting, synapses and vascular formation were determined at the end of the experiment.

Results: SCF+G-CSF significantly improved functional outcome in chronic stroke mice. The axonal sprouting in the peri-infarct area which was projected from both of the contralesional and ipsilesional cortex was significantly increased by SCF+G-CSF treatment. Moreover, the functional post-synaptic element and the blood vessel density in the cortex adjacent to the infarct cavities were also increase by SCF+G-CSF treatment. Remarkably, the effects of SCF+G-CSF on functional restoration, neuronal network remodeling and cerebrovascular regeneration in the brain of chronic stroke were blocked by the NF-kB inhibitor.

Conclusions: These results suggested that SCF+G-CSF treatment improves functional restoration in chronic stroke though rewiring neural networks and regenerating new blood vessels, and that NF-kB pathway is critically involved in SCF+G-CSF-induced brain repair in chronic stroke. This study provides new insights into the contribution of hematopoietic growth factors in brain repair and helps in developing a new pharmaceutical therapy for treatment of chronic stroke.

This study was supported by The National Institutes of Health, National Institute of Neurological Disorders and Stroke (NINDS), R01 NS060911 to L.R.Z.

SEROTONIN 2A RECEPTOR AGONIST BINDING IN THE HUMAN BRAIN: FIRST EVALUATION OF [^{11}C]CIMBI-36

A. Ettrup[1], S. da Cunha-Bang[1], B. McMahon[1], A. Dyssegaard[1], S. Lehel[2], M. Hansen[3], A.O. Baandrup[4], K. Møller[5], C. Svarer[1], J.L. Kristensen[3], N. Gillings[2], G.M. Knudsen[1]

[1]Neurobiology Research Unit and Center for Integrated Molecular Brain Imaging (CIMBI), [2]PET- and Cyclotron Unit, Copenhagen University Hospital, Rigshospitalet, [3]Department of Drug Design and Pharmacology, Faculty of Health and Medical Sciences, University of Copenhagen, [4]Department of Radiology, [5]Intensive Care Unit, Copenhagen University Hospital, Rigshospitalet, Copenhagen, Denmark

Introduction: [^{11}C]Cimbi-36 was recently developed as an agonist radioligand for brain imaging of serotonin 2A receptors (5-HT$_{2A}$) with positron emission tomography (PET)[1]. This may be used to quantify the functional and high-affinity state of 5-HT$_{2A}$ receptors, and it may have the potential to quantify changes in cerebral serotonin levels in vivo. For the first time, we here evaluate [^{11}C]Cimbi-36 binding in the human brain.

Methods: Six healthy volunteers (mean age 26.2 years, 3 males) were included in the study, and each study participant was scanned twice for 2 hours after [^{11}C]Cimbi-36 bolus injection (n=12; injected activity: 443±136 MBq; injected cold Cimbi-36 dose: 0.45±0.28 µg) in a high resolution research tomography (HRRT) PET scanner. Arterial blood samples were obtained from a catheter in the radial artery, and input measurements including radiometabolite analyses with radio-HPLC were obtained in all the participants. Five subjects received a per oral (p.o.) blocking dose of ketanserin (Ketansin®, 10 mg or 20 mg) before the second [^{11}C]Cimbi-36 PET scan. To quantify 5-HT$_{2A}$ receptor binding, BP_{ND} was calculated using the simplified reference tissue model (SRTM) with cerebellar grey matter as a reference region and distribution volumes (V_T) derived from 2-tissue compartment modelling were used for occupancy plotting.

Results: [^{11}C]Cimbi-36 showed high uptake in the human brain, and the radioligand distribution was in accordance with the expected 5-HT$_{2A}$ receptor pattern in humans. Time-activity curves indicated that [^{11}C]Cimbi-36 possess relatively slow kinetics in the human brain. At baseline, the [^{11}C]Cimbi-36 SRTM BP_{ND} in the neocortex was 1.24±0.19 indicating adequate signal-to-noise ratios for quantifying 5-HT$_{2A}$ receptor binding in cortical areas of the human brain. Pre-treatment with ketanserin had a pronounced effect on the brain uptake and time-activity curves of [^{11}C]Cimbi-36, and the cortical binding was particularly affected by the ketanserin pre-treatment suggesting 5-HT$_{2A}$ receptor selectivity of [^{11}C]Cimbi-36. Occupancy plots with 2TC V_T at baseline and after blockade showed that the ketanserin pre-treatment lead to an average receptor occupancy of 86±4% (following 20 mg Ketansin, n=3) and 70±9% (following 10 mg Ketensin, n=2). No effect of ketanserin pre-treatment was observed on the [^{11}C]Cimbi-36 V_T in cerebellum.

Conclusions: The novel receptor agonist PET radioligand, [^{11}C]Cimbi-36, successfully labelled 5-HT$_{2A}$ receptors in the human brain. This enables studies on 5-HT$_{2A}$ receptor agonist binding in larger population or patient samples including investigations of the

sensitivity of cerebral [^{11}C]Cimbi-36 binding to changes in endogenous levels of serotonin in the human brain.

Reference:

[1] Ettrup A, et al. (2011) Eur J Nucl Med Mol Imaging. 2011;38(4):681-693.

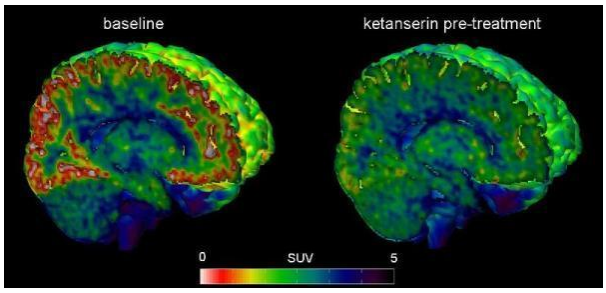

Figure 1: Representative PET images of cerebral [^{11}C]Cimbi-36 binding in the human brain at baseline and after ketanserin pre-treatment. PET images show radioligand uptake from 40-120 min and scaled to standardized uptake values (SUV in g/ml), and images are superimposed on a MRI template of the brain.

Oral Sessions

NEURAL BASIS OF THE ASSOCIATION BETWEEN REMITTED GERIATRIC DEPRESSION AND APOE E4 ALLELE: RESTING-STATE FMRI STUDY

H. Shu[1,2], Y. Yuan[1], C. Xie[1], F. Bai[1], J. You[3], L. Li[4], S. Li[2], Z. Zhang[1]

[1]Department of Neuropsychiatry, Affiliated Zhongda Hospital and Institute of Neuropsychiatry of Southeast University, Nanjing, China, [2]Department of Biophysics, Medical College of Wisconsin, Milwaukee, WI, USA, [3]Department of Psychiatry, Nanjing Brain Hospital Affiliated to Nanjing Medical University, Nanjing, [4]Mental Health Institute, Second Xiangya Hospital of Central South University, Changsha, China

Objectives: To detect the influence of remitted geriatric depression (RGD) and APOE ε4 allele with their interaction on hippocampal functional connectivity (HFC) networks.

Methods: 31 RGD and 29 normal control (NC) subjects were recruited and were further divided into four subgroups according to their APOE genotypes（for NC group: 7 APOE4+ and 22 APOE4- subjects; for RGD group: 11 APOE4+ and 20 APOE4- subjects）. Each subject completed neuropsychological tests and underwent MRI scan (General Electric 1.5T). Hippocampal seed-based functional connectivity approach was employed and 2×2 factorial analysis of variance was used to test the main effects and interactive effects of RGD and APOE ε4 allele on HFC networks. Additionally, multivariate regression analysis was used to identify the behavioral significance of these altered HFC networks.

Results:

1. The main effect of RGD on bilateral HFC networks mainly located in frontal-occipital regions. Specifically, frontal regions demonstrated decreased positive or enhanced negative HFC, whereas occipital lobe showed enhanced positive or decreased negative HFC in RGD patients relative to non-RGD subjects.

2. The main effects of APOE ε4 allele were mostly seen in bilateral insula, bilateral dorsolateral prefrontal cortex (DLPFC), and regions within the default mode network (DMN). Particularly, APOE ε4 allele carriers showed increased positive HFC in bilateral insula and decreased positive or enhanced negative HFC in bilateral DLPFC and regions within DMN compared with APOE ε4 non-carriers.

3. The interactive effects of RGD and APOE ε4 allele were found in right IOG, bilateral somatomotor area and dorsal ACC (dACC) that connected to left hippocampus. Specifically, the two factors showed inverse interaction on the left hippocampus connected to bilateral dACC, while synergistic contribution was found in the other regions.

4. For RGD patients, the decreased negative left HFC network in right cuneus was negatively correlated with visuospatial scores, and the increased and decreased HFC network in right lingual gyrus and left somatomotor area was respectively negatively and positively correlated with episodic memory scores . On the other hand, for APOE ε4 allele carriers, the decreased positive right HFC network in the left ACC and left DLPFC are both positively correlated with working memory scores.

Conclusions: Not only the factors of RGD and APOE ε4 allele could affect HFC network distinctively, but the two factors could also

exert interactive effects on the left HFC network, especially for dACC, the key region of the interaction between cognitive and emotional processing, was significantly disrupted. Therefore, we suggest that such disconnection may imply cognitive deterioration for RGD patients with APOEε4 allele over time[1-2]. Conclusively, our findings indicated the neural substrate of the association between RGD and APOE ε4 allele, which may contribute to monitor the cognitive decline as well as it conversion to AD in high-risk group.

Reference: 1. Wang L, et al. Am J Geriatr Psychiatry. 2012; 20, 653-663; 2. Mosconi L, et al. Neurology. 2004; 63, 2332-2340.

DIFFERENTIAL EFFECTS OF CHRONIC ORAL METHYLPHENIDATE TREATMENT IN ADOLESCENT AND ADULT RAT BRAIN

K. van der Marel[1], A. Klomp[2], G.F. Meerhoff[3], P.J. Lucassen[3], J.R. Homberg[4], L. Reneman[2], R.M. Dijkhuizen[1]

[1]Biomedical MR Imaging and Spectroscopy Group, Image Sciences Institute, University Medical Center Utrecht, Utrecht, [2]Department of Radiology, Academic Medical Center, [3]Swammerdam Institute for Life Sciences, Center for Neuroscience, University of Amsterdam, Amsterdam, [4]Department of Cognitive Neuroscience, Centre for Neuroscience, Donders Institute for Brain, Cognition and Behaviour, Radboud University Nijmegen Medical Centre, Nijmegen, The Netherlands

Objectives: Methylphenidate is a widely prescribed psychostimulant for treatment of attention deficit hyperactivity disorder (ADHD) in children and adolescents, but its effects on the developing brain remain elusive[1]. Patient studies have suggested that psychostimulant medication normalizes ADHD-related deficits in white matter volume, anterior cingulate cortex volume, caudate nuclei shapes, and cortical thinning[2-5]. As retrospective patient studies are hampered by the heterogeneity of the population sample with mixed treatment histories, our aim was to measure the effects of chronic stimulant treatment on the brain in a well-controlled experimental setting.

Methods: Male Wistar rats (*n*=64, 16/group) were treated with vehicle or 5 mg/kg oral methylphenidate HCl dissolved in saline, daily for 21 days starting from post-natal day 25 (adolescent) or 65±4 (adult), followed by a 1-week washout period.

In vivo MRI (4.7T) was performed while animals were anesthetized (propofol) and mechanically ventilated. Functional connectivity (FC) was measured under resting conditions with resting-state fMRI (rs-fMRI; 1000 images; 10min), and activation responses following a dopaminergic challenge with pharmacological MRI (phMRI; 675 images; 45min; *n*=13/group received 1 mg/kg D-amphetamine i.v. after 10min).

Post mortem MRI (9.4T) was performed (*n*=12/group) to obtain high-resolution anatomical images for analysis of brain volumes and cortical thickness, and diffusion tensor imaging was performed (2×60 diffusion-weighted images) to assess white matter fractional anisotropy (FA).

Additionally, CNPase immunohistochemistry was used (*n*=7-8/group) to quantify myelin content.

Results: Rs-fMRI identified three networks (Figure1A) and the average FC within each network was calculated (Figure1B):

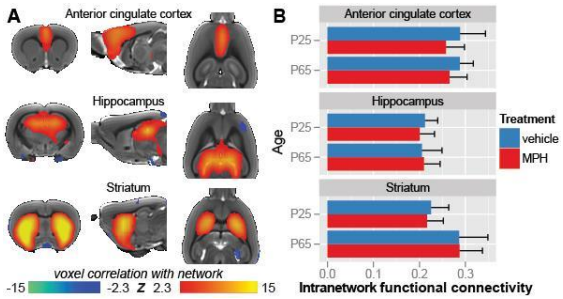

[Three rs-fMRI-based networks and their average FC]

Many age-related differences were found, including cortical thinning (from 1.52±0.50mm to 1.49±0.48mm in controls), white matter growth (+0.19%-0.49% relative volume), and in the striata increased phMRI responses (*t*=3.16, *p*=0.003) and rs-fMRI FC (*t*=4.06, *p*=0.001).

Methylphenidate reduced body weight development by $0.4 \cdot 10^{-3}$kg/day (*p*=0.045), but did not result in significantly different weights after 1-week washout (*F*=1.81, *p*=0.18). Methylphenidate reduced anterior cingulate cortical network strength in both adolescents and adults as measured from rs-fMRI (*t*=-2.03,

p< 0.05). In contrast to clinical observations from ADHD patient studies, methylphenidate did not increase white matter tissue volume or cortical thickness in rat.

Methylphenidate differentially affected adolescents and adults on measures of FA in the corpus callosum (adolescents=+9.2%, adults=-0.3%), volume of the striatum (adolescents=-1.6%, adults=+2.8%; p=0.02), and myelination in the striatum (adolescents=-9.7%, adults=+3.1%; p=0.03). However, we did not observe treatment effects on striatal functional activity.

Conclusions: Our study indicates that methylphenidate has small effects on brain structure and function in healthy rats. The observation of sustained striatal activation responses, however, corroborates studies in healthy animals that showed no negative behavioral effects of long-term methylphenidate treatment. Nevertheless, we found age-dependent treatment effects in the striatum. This is of relevance for children that are being treated with stimulants, without suffering from ADHD[6]. Our findings thus stress the importance of ensuring a proper diagnosis of ADHD and a well-considered associated treatment.

References:

[1]Andersen and Navalta, *Int.J.Dev.Neurosci.* **22**(2004);

[2]Castellanos et al., *JAMA* **288**(2002);

[3]Semrud-Clikeman et al., *Neurology* **67**(2006);

[4]Sobel et al., *Am.J.Psychiatry* **167**(2010);

[5]Shaw et al., *Arch.Gen.Psychiatry* **66**(2009);

[6]Lakhan and Kirchgessner, *Brain.Behav.* **2**(2012).

IMAGING AMYLOID BETA DEPOSITION FOLLOWING TRAUMATIC BRAIN INJURY WITH [^{11}C]PIB PET: A CROSS SECTIONAL STUDY

D.K. Menon[1], Y.T. Hong[2], T. Veenith[1], D. Dewar[3], J.G. Outtrim[1], V. Mani[4], C. Williams[4], S. Pimlott[3], P.J. Hutchinson[4], A. Tavares[3], C.A. Mathis[5], W.E. Klunk[6], F.I. Aigbirhio[4], **J.P. Coles**[1], J.-C. Baron[7], J.D. Pickard[4], W. Stewart[3], T.D. Fryer[4]

[1]Division of Anaesthesia, [2]Wolfson Brain Imaging Centre, University of Cambridge, Cambridge, [3]University of Glasgow and Southern General Hospital, Glasgow, [4]University of Cambridge, Cambridge, UK, [5]University of Pittsburgh, [6]University of Pittsburgh School of Medicine, Pittsburgh, PA, USA, [7]INSERM U 894, Université Paris Descartes, Sorbonne Paris Cité, Paris, France

Background: Several studies report that patients dying within weeks of traumatic brain injury (TBI) show β-amyloid (Aβ) aggregates in the brain. These are seen not just in elderly, but also in young patients. Although amyloid deposits are not common in subjects who survive for several months to years after TBI, recent data suggest that amyloid deposits may reappear in patients who die several decades after TBI. Full understanding of the extent and consequences of amyloid deposition in TBI have been limited by our inability to serially monitor the process in living subjects.

Methods: We used positron emission tomography (PET) with Pittsburgh compound B ([^{11}C]PIB]) to map amyloid deposition in 16 patients (33 [21-50] y), between 1 and 361 days following moderate/severe TBI, and compared these with data obtained from 11 healthy, age-matched controls (median [range] age 35 [24-60] y). [^{11}C]PIB binding was quantified using distribution volume ratio (DVR) in regions of interest (ROIs) which included all of cortical grey matter, striatal grey matter, thalamic grey matter and white matter. Partial volume effects were minimised by application of the Lucy-Richardson algorithm. In order to confirm the biological substrate for our PET findings, we also undertook in vitro [^{3}H]PIB autoradiography and immunocytochemistry for Aβ and β-amyloid precursor protein in brain tissue obtained from a neurotrauma archive, in separate cohorts of 16 patients aged 46 [21-70] who died between

3 hours and 56 days post-TBI, and 7 controls aged 61 [29-71] who died of other causes.

Findings: When compared to controls, patients following TBI showed significant increases in [^{11}C]PIB DVR in cortical grey matter and striatal ROIs ($p = 0.006$ and 0.003, respectively), but not in thalamic or white matter ROIs. Temporal changes in [^{11}C]PIB DVR over time after TBI suggested that binding in the cortical grey matter and white matter rapidly increased in the first few weeks following TBI, and then returned to normal levels. These increases in [^{11}C]PIB binding in TBI could not be accounted for by a range of methodological confounders. Autoradiography showed robust and specific [^{3}H]PIB binding in cortical grey matter, where it correlated, on a regional basis, with amyloid deposition demonstrated by immunocytochemistry. Both Aβ and β-APP were also clearly demonstrated in white matter, but significant [^{3}H]PIB binding could not be demonstrated in these areas.

Interpretation: These data document the fact that early [^{11}C]PIB PET is feasible in critically ill patients within days post-TBI. The temporal patterns of PIB binding that we demonstrate using PET conform to previous post-mortem data in TBI. While we were able to show correspondence between cortical [^{3}H]PIB binding and amyloid deposition in TBI in cortical grey matter, we were unable to show [^{3}H]PIB binding in white matter. These data provide guidance on optimal timing of [^{11}C]PIB PET imaging in TBI. [^{11}C]PIB PET could be valuable in imaging the temporal dynamics and clinical correlates of amyloid deposition following TBI.

SIMULTANEOUS SMALL ANIMAL PET/MR IMAGING YIELDS NOVEL INSIGHTS INTO MULTIPLE LEVELS OF BRAIN FUNCTION

H.F. Wehrl[1], M. Hossain[1], C.-C. Liu[1], I. Bezrukov[1,2], K. Lankes[3], G. Reischl[1], B.J. Pichler[1]

[1]Department of Preclinical Imaging and Radiopharmacy, University of Tuebingen, [2]Max Planck Institute for Intelligent Systems, Tuebingen, [3]Bruker BioSpin MRI, Ettlingen, Germany

Objectives: Brain function depends on a complex interplay of energy metabolism and hemodynamics, and can be assessed on multiple metabolic and time scales. Here we present a small animal PET/MR system constructed by our group that allows to simultaneously acquire PET and MR data. We study brain function in rats observing isochronously slower changes in CMR_{Glc} by [^{18}F]FDG-PET and faster changes in $CMRO_2$ and CBF by BOLD-fMRI. Additionally, neuronal networks were investigated using both, dynamic PET and fMRI data to reveal information about functional connectivity.

Methods: The PET-insert uses 16 circularly arranged detector cassettes, with each consisting of three Lutetium oxyorthosilicate blocks read out by avalanche photodiodes. The PET-insert is installed inside a 7 T small animal MR system (Fig. 1 a-c). Resolution and sensitivity of the PET were assessed as well as MR parameters such as SNR and fMRI stability. For the simultaneous study of brain function we used 8 Lewis rats (356-456g). The left whisker pad of the animals was electrically stimulated while 37 MBq of [^{18}F]FDG were administered simultaneous to the BOLD-fMRI (TR=2000ms, TE=18ms, voxel size=0.5x0.5x1.0mm³) acquisition. Statistical parametric mapping of simultaneously acquired PET and fMRI data was performed. In addition dynamic PET and fMRI data was used for an independent component analysis.

Results: Spatial resolution of the PET-insert was 1.4mm using an OS-EM (4 sub, 16 iter) algorithm. PET sensitivity was 3.2±0.2% at the center of FOV, and did not change significantly when a MR sequence was applied. MR SNR showed only for a turbo-spinecho sequence a slight drop of 2.1% ($P=5x10^{-5}$), but remained stable for flash and gradient-echo sequences. Relevant fMRI parameters such as signal drift or RMS stability were not significantly altered by the presence of the PET-insert. Whisker stimulation yielded strong PET ($P=3x10^{-6}$) and fMRI ($P=4x10^{-16}$) activation in the contralateral barrel field (S1BF). CMR_{Glc} increased in this area by 11±7% (resting whole brain CMRGlc 28 µmol/min/100g [1]), BOLD signal change was 0.5±0.7%. Areas such as the insula or amygdala showed strong significant changes in CMR_{Glc} (19±9% and 32±14%) but no corresponding BOLD signal change (Fig. 1 d). Functional connectivity using dynamic PET data identified seven glucose metabolic networks, whereas the fMRI technique, based on CBF and CMR_{O2} proportional signals, yielded nine networks (Fig. 1 e,f).

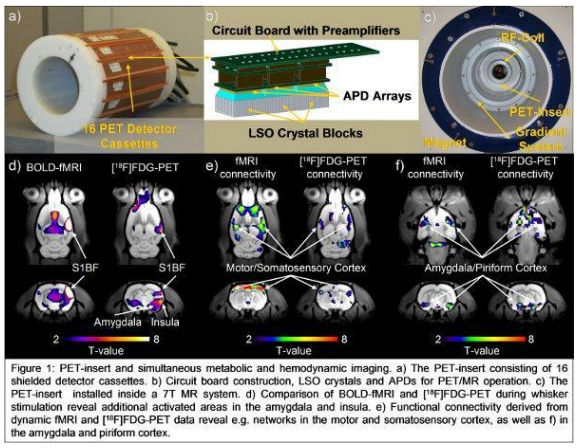

Figure 1: PET-insert and simultaneous metabolic and hemodynamic imaging. a) The PET-insert consisting of 16 shielded detector cassettes. b) Circuit board construction, LSO crystals and APDs for PET/MR operation. c) The PET-insert installed inside a 7T MR system. d) Comparison of BOLD-fMRI and [^{18}F]FDG-PET during whisker stimulation reveal additional activated areas in the amygdala and insula. e) Functional connectivity derived from dynamic fMRI and [^{18}F]FDG-PET data reveal e.g. networks in the motor and somatosensory cortex, as well as f) in the amygdala and piriform cortex.

[Figure 1]

Conclusions: PET/MR allows to study brain function on different metabolic and temporal scales. Our CMR_{Glc}/BOLD comparison suggests that in some areas of the brain BOLD changes might be too small or too slow to be picked up, whereas CMR_{Glc} changes can be identified by PET. This hints towards complex metabolic-hemodynamic coupling and uncoupling mechanism. The novel approach of metabolic neuronal network mapping, using dynamic PET data shows some similarities, in respect to discoverd networks, to fMRI functional connectivity. Further studies, utilizing PET/MR, will focus on the complimentarity with fMRI connectivity.

References: [1]: Shimoji, K.*, et al. J Nucl Med* **45**, 665-672 (2004)

DEEP BRAIN STIMULATION AT THE SUBTHALAMIC NUCLEUS AND THE INTERNAL GLOBUS PALLIDUS PRODUCES FMRI RESPONSE IN THE MOTOR CORTEX

H.-Y. Lai, J.R. Younce, Y.-C.J. Kao, Y.-Y.I. Shih

Experimental Neuroimaging Laboraory, Department of Neurology and Biomedical Research Imaging Center, University of North Carolina, Chapel Hill, NC, USA

Objectives: Deep brain stimulation (DBS) is used to treat several neurological disorders, including Parkinson's disease (PD), although its mechanism is still incompletely understood [1,2]. DBS combined with fMRI is capable of visualizing regional neural activity *in vivo*, enabling to study a specific neuroanatomical pathway/connectivity of the response to DBS in various brain regions and to determine the optimal treatment policy according to the treatment outcome. The goal of this study was to characterize fMRI response to DBS at the internal globus pallidus (GPi) and subthalamic nucleus (STN), the targets used clinically for treatment of PD. We hypothesized that DBS would produce frequency-dependent fMRI-visible responses in the motor cortex.

Methods: Sprague-Dawley rats were stereotactically implanted with platinum electrodes unilaterally in either the STN (n=6) or GPi (n=5) [4]. After at least 24 hours, rats under 1.25-1.75% isoflurane anesthesia were imaged using a Bruker 9.4T system with a 4-shot gradient-echo EPI sequence and stimulated with a bipolar square-wave current of 1 mA at 9 frequencies between 10 and 310 Hz.

Results: BOLD response to DBS at both the STN and GPi in the ipsilateral motor cortex was positive (**Fig. A**), and peaked at 100 Hz (**Fig. B**). GPi DBS produced diffuse negative BOLD response in the contralateral hemisphere, peaking at 40 Hz (**Fig. B**). DBS produced significant responses in frequencies known to be therapeutic for PD, while no response was observed at 10 Hz, which is known to exacerbate symptoms [5, 6], suggesting a possible relationship to the therapeutic effect of DBS. Several hypothetical mechanisms for the ipsilateral response exist, including (a) direct inhibition of the STN and GPi output leading to increased thalamic activity [3] and (b) antidromic conduction to motor cortex [6]. The negative BOLD observed with GPi DBS may be related to (a) inhibition via corticocortical projection neurons [7] or (b) collateral stimulation of the nearby internal capsule.

Conclusion: This study demonstrated that DBS at both STN and GPi produced a positive BOLD response centered in the ipsilateral motor cortex, indicating increased activity of motor cortical circuits. This response was frequency-dependent in a manner which suggests a possible relationship to the therapeutic mechanism of DBS for PD. Use of DBS fMRI in the setting of hemiparkinsonian animals may further permit examination of the effect of DBS on parkinsonian pathophysiology *in vivo*.

References:

[1] Kringelbach et al, Eur J Neurosci. 2010, 32:1070.

[2] DeLong et al, Ann. N.Y. Acad Sci. 2012, 1265-1.

[3] Albin et al, Trends Neurosci. 1989, 12:366.

[4] Paxinos and Watson, The Rat Brain in Stereotaxic Coordinates, 2005.

[5] Birdno and Grill, Neurotherapeutics. 2008, 5:14.

[6] Gradinaru et al, Science, 2009, 324:354.

[7] Logothetis et al, Nat Neurosci. 2010, 13:1283.

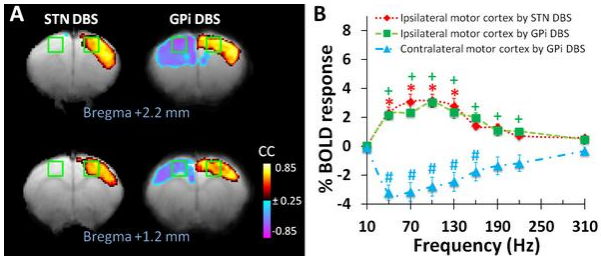

Figure (A) Group-averaged BOLD activation maps of STN DBS (n = 6) and GPi DBS (n = 5). Green boxes indicate 8x8 voxel ROIs centered in motor cortex. **(B)** BOLD frequency-tuning curves. Error bars are SEM. *, + and # indicate significant difference from 10 Hz.

METABOLIC BRAIN NETWORK IN RBD PATIENTS BASED ON 18F-FDG PET IMAGING

C. Zuo[1], Y. Ma[2], J. Ge[1], S. Peng[2], H. Yu[3], J. Wang[3], P. Wu[1], D. Eidelberg[2]

[1]PET Center, Huashan Hospital, Fudan University, Shanghai, China, [2]Center for Neurosciences, The Feinstein Institute for Medical Research, Manhasset, NY, USA, [3]Department of Neurology, Huashan Hospital, Fudan University, Shanghai, China

Background and aims: Rapid-eye-movement sleep behavior disorder (RBD) has a strong association with neurodegenerative diseases particularly Parkinson Disease (PD). Over the past 10 years, it has been reported in many cases that RBD precedes the development of PD. In this study with FDG PET, we assessed PD-specific network expression in RBD patients based on the use of an abnormal spatial covariance pattern in PD patients (PDRP). To explore possible brain network connections between RBD and PD patients, we also derived a RBD-related covariance pattern (RBDRP).

Materials and methods: We studied 10 clinically confirmed RBD patients (age 62.1±6.8 years) and 10 healthy volunteers (age 53.6±12.5 years) with metabolic imaging on a Siemens Biograph 64 PET/CT. The expression of PDRP was quantified in each subject with respect to a PDRP pattern generated from 33 PD patients and 33 normal controls scanned at our PET Center. Furthermore, RBDRP was identified from the combined sample of 10 RBD and 10 healthy controls by using the multivariate network modeling approach based on principal component analysis.

Results: PDRP scores were elevated (p< 0.01;Fig 1A) in the RBD patients compared with the healthy controls, but lower than those of the PD patients in PDRP validation scans. We also found that RBD was associated with a specific metabolic brain network. This RBDRP (selected from the first principal component accounting for 21.2% subject x voxel variance; Fig 1B) was characterized by relative metabolic increases in the premotor cortex, putamen, thalamus and cerebellum along with relative metabolic decreases in the occipital cortex. In addition, the expression of RBDRP in individual subjects significantly discriminated the RBD patients from the healthy controls (p< 0.0001; Fig 1C).

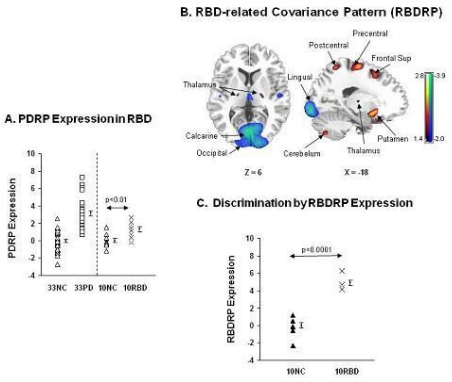

[Fig.1: Metabolic Network Analyses in RBD patients.]

Conclusions: The elevation of PDRP in RBD patients indicates that our RBD patients may be at prodromal stages of Parkinson disease. The establishment of RBDRP shows the

existence of a distinct pattern of relative regional metabolic activity in patients with RBD. These results suggest that RBDRP can serve as a quantifiable imaging marker of RBD and can be used as a tool to identify preclinical brain changes in RBD patients at high risk for developing PD.

THE DUAL ROLE OF BRAIN GLYCOGEN: THE GOOD AND THE BAD

J. Duran, I. Saez, J.J. Guinovart

Molecular Medicine, Institute for Research in Biomedicine, Barcelona, Spain

Introduction: The role of glycogen in the brain has been traditionally associated to the preservation of neuronal function during energetically challenging states such as hypoxia, hypoglycemia, ischemia or seizures. Nevertheless, glycogenolysis also occurs in euglycemia during an increase in neuronal activity, indicating that brain glycogen also has a role in supporting neuronal function in non-pathological conditions. According to this, several reports have stated the importance of glycogenolysis for memory processing.

Brain glycogen is almost exclusively restricted to astrocytes. However, in some pathological conditions, aberrant glycogen accumulation can be found in neurons. Lafora Disease (LD) and Adult Polyglucosan Body Disease (APGB) are the most striking examples of the consequences of glycogen accumulation in neurons.

Objectives: Our aim is to investigate both the physiological role of glycogen in the brain and the pathological consequences of the over-accumulation of glycogen in neurons.

Design: To investigate the physiological role of brain glycogen, we generated a brain-specific Glycogen Synthase (GS) knockout mouse and studied the functional consequences of the lack of glycogen in the brain.

Conversely, we generated the following mouse models to study the deleterious effect of glycogen in neurons: first, a knockout of Malin, a negative regulator of GS the loss of which stands on the basis of Lafora disease (LD); second, a mouse model in which we overexpressed a superactive form of GS (saGS) specifically in neurons.

Results and conclusions: We analyzed the learning abilities and the electrophysiological properties of the synapses in the brain-specific GS knockout animals. These mice showed a significant deficiency in the acquisition of an associative learning task and in the concomitant activity-dependent changes in hippocampal synaptic strength. Long-term potentiation (LTP) evoked in the hippocampal CA3-CA1 synapse was also decreased in GS knockout mice. These results unequivocally demonstrate a key role of brain glycogen in the proper acquisition of new motor and cognitive abilities and in the underlying changes in synaptic strength.

Malin knockout mice presented glycogen accumulations in several brain areas, as do patients of LD. This phenomenon was accompanied by a progressive neuronal loss and neurophysiological alterations. In accordance, the neuron-specific overexpression of saGS and the consequent accumulation of glycogen also caused a progressive neurodegeneration. These results illustrate the need for a strict control of GS in neurons.

References:

Impairment in long-term memory formation and learning-dependent synaptic plasticity in mice lacking Glycogen Synthase in the brain

Jordi Duran, Isabel Saez, Agnès Gruart, Joan J. Guinovart, José M. Delgado-García

J Cereb Blood Flow Metab. 2012 Dec Accepted.

Neurodegeneration and functional impairments associated with glycogen synthase accumulation in a mouse model of Lafora disease.

Valles-Ortega J, Garcia-Rocha M, Bosch C, Saez I, Pujadas L, Serafin A, Cañas X, Soriano E, Delgado-García JM, Gruart A, Guinovart JJ.

EMBO Mol Med. 2011 Nov;3(11):667-81. doi: 10.1002/emmm.201100174.

Deleterious effects of neuronal accumulation of glycogen in flies and mice.

Duran J, Tevy MF, Garcia-Rocha M, Calbó J, Milán M, Guinovart JJ.

EMBO Mol Med. 2012 Aug;4(8):719-29. doi: 10.1002/emmm.201200241.

ENERGY REQUIREMENTS DURING SPREADING DEPOLARISATION - MULTIMODAL MEASUREMENT AND KINETIC MODELLING

D. Feuerstein[1], H. Backes[1], M. Gramer[1], M. Takagaki[1,2], T. Kumagai[1,2], R. Graf[1]

[1]Max Planck Institute for Neurological Research, Cologne, Germany, [2]Osaka University Graduate School of Medicine, Osaka, Japan

Introduction: Spreading depolarisation (SD) is a slowly propagating wave of tissue depolarisation that could be closely linked to secondary deterioration of brain injury patients [1,2]. It is hypothesised that progressive worsening of the lesion would be due to the hemodynamic and metabolic disturbances caused by the SDs [3,4]. We have here investigated these events by simultaneously measuring:

· cerebral blood flow with laser speckle flowmetry (LSF)

· glucose utilization with ^{18}F-flurodeoxyglucose (FDG) positron emission tomography (PET)

· glucose and lactate concentrations in the extracellular space with rapid-sampling microdialysis (rsMD) [4]

These data were then integrated into a kinetic model of brain metabolism that accounted for the neuronal and astrocytic rates of glucose transport, glycolysis, mitochondrial oxidative metabolism, lactate production and use, glycogen breakdown and synthesis.

Methods: LSF was continuously acquired in anesthetised Wistar rats through thinned skull. A microdialysis probe was implanted via a small craniotomy and the dialysate was analysed for glucose and lactate concentrations every minute by rsMD. After recovery from implantation and baseline measurement, FDG was injected. At 20 minutes post-injection, SDs were elicited either by needle prick (single SD) or KCl infusion (multiple SDs). The hemodynamic and metabolic responses to SDs were observed for 70 minutes.

Results: SD waves were detected by LSF as propagating hyperemic waves. The metabolic response to one single SD wave was biphasic: 1) within 5 minutes, glucose dropped by 20%, lactate increased by 60% and FDG uptake rose above control, 2) during the next 65 minutes, extracellular glucose concentration remained below baseline, lactate fully recovered and FDG uptake gradually declined to normal values. This response could be modelled by a transient surge for ATP followed by a prolonged reduced energy demand. During phase 1, glycogen is rapidly broken down and glucose is fully catabolised via glycolysis and mitochondrial oxidative metabolism. ATP levels are quickly restored to normal. During phase 2, cells are repolarised and glycogen stores are partially re-filled.

Following multiple SD waves, we observed a sustained increase in energy demand, with an ever-decreasing extracellular glucose, a prolonged elevated lactate level, and an up to 40% increase in FDG uptake compared to control. This indicates a prolonged period of high energy demand that might lead to irreversible depolarisation of brain cells.

Conclusions: We suggest that the energy requirements to recover from a single SD wave are largely fulfilled in physiological conditions, notably thanks to the quick breakdown of astrocytic glycogen. However frequent SDs could lead to an energy crisis that endangers tissue viability even in a well-perfused brain.

References:

1. Dohmen *et al.*, *Annals of Neurology*, 2008, 63:6: 720-728.

2. Hartings *et al.*, *Lancet Neurology*, 2011, 10:12:1058-64.

3. Dreier *et al.*, *Brain*, 2009, 132:7:1866-81.

4. Feuerstein *et al.*, *JCBFM*, 2010, 30:7: 1343-1355.

PEROXYNITRITE AND POLY(ADP-RIBOSE) POLYMERASE ARE RESPONSIBLE FOR THE NEUROVASCULAR DYSFUNCTION INDUCED BY BETA-AMYLOID

L. Park, G. Wang, P. Zhou, H. Girouard, J. Anrather, C. Iadecola

Brain and Mind Research Institute, Weill Cornell Medical College, New York, NY, USA

Introduction: Amyloid-beta (Ab) impairs vital regulatory mechanisms of the cerebral microcirculation, thereby making the brain susceptible to injury (1). The cerebrovascular dysregulation requires CD36, a putative Ab receptor, and reactive oxygen species (ROS) generated by NADPH oxidase (2,3). However, the downstream mechanisms by which Ab-induced ROS alter cerebral blood vessels remain unclear. We tested the hypothesis that the ROS superoxide reacts with nitric oxide (NO) to form peroxynitrite, which, in turn, impairs cerebrovascular regulation by activating poly(ADP-ribose) polymerase (PARP).

Methods: Cerebral blood flow (CBF) was monitored by laser-Doppler flowmetry in the neocortex of anesthetized mice (n=5/group) equipped with a cranial window. ROS production was assessed in situ by hydroethidine (HE) fluoromicrography, and peroxynitrite formation by 3-nitrotyrosine (3-NT) immunoreactivity.

Results: In wild-type (WT) mice, neocortical superfusion of Ab_{1-40} (5 µM) attenuated the CBF increase evoked by whisker stimulation (WS) (vehicle: 24±2%; Ab_{1-40}: 17±2%; p< 0.05; mean±SE) or by topical application of the endothelium-dependent vasodilator acetylcholine (ACh) (vehicle: 25±2%; Ab_{1-40}: 15±2%; p< 0.05). Ab_{1-40} superfusion increased neocortical ROS production (+43%; p< 0.05) and induced immunoreactivity for the peroxynitrite marker 3-nitrotyrosine (3-NT) (+255%; p< 0.05) (Figure A). ROS production was not affected by the peroxynitrite scavenger uric acid (UA, 100 µM) or the PARP inhibitor PJ-34 (3 µM), whereas 3-NT immunoreactivity was reduced by UA and not PJ-34, attesting to the specificity of UA as a peroxynitrite scavenger (Figure B,C). Cerebrovascular dysregulation and 3-NT immunoreactivity were attenuated by the NO synthase inhibitor L-NNA, the ROS scavenger MnTBAP, and by UA. In PARP1-null mice, Ab_{1-40} superfusion did not alter CBF responses to WS (vehicle: 24±2%; Ab: 24±1%; p>0.05) and ACh (vehicle: 18±2%; Ab_{1-40}: 22±3%; p>0.05). Furthermore, neocortical superfusion with PJ-34 prevented the cerebrovascular alterations induced by exogenous Ab_{1-40} and rescued the neurovascular dysfunctions in mice overexpressing the amyloid precursor protein (Tg2576) (WS: vehicle, 14±1%; PJ-34, 25±1%; p< 0.05; ACh: vehicle, 13±1%; PJ-34, 22±2%; p< 0.05).

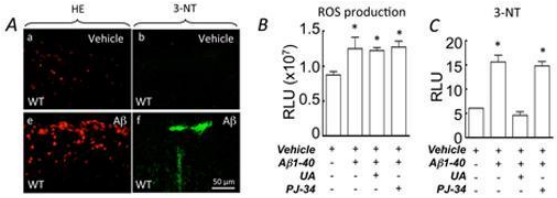

[Figure]

Conclusions: These findings are consistent with the hypothesis that peroxynitrite induces activation of PARP1, which, in turn, mediates the deleterious cerebrovascular effects of Ab_{1-40}. Therefore, counteracting peroxynitrite or PARP1 may have therapeutic value to forestall the deleterious cerebrovascular effects of Ab.

References:

1. Iadecola, Acta Neuropathol, 120:287, 2010.

2. Park et al., PNAS, 105:1347, 2008.

3. Park et al., PNAS, 108:5063, 2011.

REDUCED RESPONSE IN CORTICAL PENETRATING ARTERY BUT SUSTAINED RESPONSE IN CORTICAL SURFACE ARTERY TO WHISKER STIMULATION IN CHRONIC HYPOXIA MICE

I. Kanno[1], Y. Sekiguchi[2], H. Takuwa[1], K. Masamoto[1,3], H. Kawaguchi[1], J. Taniguchi[1], Y. Tomita[4], R. Sudo[2], K. Tanishita[2], Y. Itoh[4], N. Suzuki[4], H. Ito[1]

[1]Molecular Imaging Center, National Institute of Radiological Sciences, Chiba, [2]Faculty of Science and Technology, Keio University, Yokohama, [3]Center for Frontier Science and Engineering, University of Electro-Communications, Chofu, [4]Department of Neurology, Keio University School of Medicine, Tokyo, Japan

Introduction: We reported massive parenchymal vasodilation in chronic hypoxia mice using a two-photon laser scan microscopy (2P) (1), and reduced neurovascular coupling (NVC) responses but sustained CO2 responses using a laser Doppler flowmetry (LDF) (2,3). We here measure diameter changes of cortical surface and penetrating arteries of somatosensory cortex triggered by a single whisker vibration using 2P in the chronic hypoxia mice.

Aims: The present study aims to elucidate whether two cortical vascular systems, surface and penetrating arteries, are identical or different in response to somatosensory neuronal stimulation in chronic hypoxia mice.

Methods: We used Tie2-GFP transgenic mice (N=6, 7-11 weeks) of which vascular endothelium had GFP for measuring cortical surface vessels. We used intraperitoneal Sulforhodamine 101 for labeling blood plasma for measuring cortical penetrating vessels. All mice were fixed by chronic closed cranial window over the somatosensory cortex one week before experiment (4). Before (day 0) and on days 7, 14 and 21 after chronic keeping in the 8-9% O2 chamber, dynamic spatiotemporal images of cortical arteries to single whisker vibration (10Hz, 5sec) were measured in awake condition. We used confocal microscopy for cortical surface arteries and 2P for cortical penetrating arteries at 100, 200, 300 and 400 μm depths. We analyzed images to assess dynamic changes of diameter of each cortical artery (5). CBF responses at the somatosensory cortex were also assessed using LDF in the same mice.

Results: Diameters of cortical surface arteries increased to whisker stimulation by approximately 10% throughout hypoxia duration lengths. On the other hand, diameters of cortical penetrating arteries revealed to decrease as prolonged hypoxia duration, i.e. d0 (15%), d7 (10%), d14 (9-7%） and d21 (7-5%). The LDF responses were also reduced along hypoxia duration, i.e. d0（20%）, d7（15%）, d14（9-12%） and d21（5-9%）.

Discussion: The results suggest that our previous observation of the reduced NVC response by LDF in chronic hypoxia resulted from a reduced response in diameter change of cortical penetrating arteries. Combining with anothor previous observation by LDF, i.e. sustained response to CO2 in chronic hypoxia mice, it is suggested that the cortical penetrating artery in chronic hypoxia revealed reduced response only to NVC but not to CO2 during chronic hypoxia.

Conclusion: Chronic hypoxia induced reduction in NVC response only in cortical penetrating artery but not in cortical surface artery. This discrepancy between two cortical vascular systems suggests different role in supplying blood flow to brain tissues. Different response to NVC and CO2 in the cortical penetrating arteries implies essential part of NVC response.

References:

(1) Yoshihara K, et al. 357-63, Adv Exp Med Biol 765: 2013.

(2) Kanno I, et al. 507.19, SFN, Washington DC, 2011.

(3) Takuwa H, et al, JCBFM (in press) 2013.

(4) Tomita Y, et al. 858-867, JCBFM 25: 2005.

(5) Sekiguchi Y, et al. Adv Exp Med Biol (in press) 2013.

ARTERIAL FUNCTION CHANGES IN SUB-CORTEX AFTER FOCAL CEREBRAL ISCHEMIA IN LIVING RAT

X. Lin[1], P. Miao[1,2], Y. Guan[1], F. Yuan[1], Y. Tang[1], X. He[1], G. Tang[1], Y. Wang[1], G.-Y. Yang[1]

[1]Neuroscience and Neuroengineering Research Center, Med-X Research Institute and School of Biomedical Engineering, Shanghai Jiao Tong University, [2]School of Communication and Information Engineering, Shanghai University, Shanghai, China

Objectives: Functional changes of arterial network after focal cerebral ischemia are vital to the repair and rewire of the brain.[1] Traditional imaging methods cannot probe sub-cortex arterial vascular network which supplies injured tissue in striatum.[2, 3] The aim of this study is to develop a functional synchrotron radiation X-ray microangiography (fSRA) for studying the sub-cortex arterial function changes after transient middle cerebral artery occlusion (tMCAO) in living animals.

Methods: Adult Sprague-Dawley rats (n=30) were divided into six groups: five tMCAO groups which suffered 90 minutes occlusion following 1, 3, 7, 14 and 28 days reperfusion and one sham group. Lesion volume was detected by MRI (T2-weighted). SRA image sequence was recorded and processed by fSRA to extract blood flow velocity (BFV) and vascular elasticity (VE) information of arteries by surface fitting technique. The fSRA was validated by Laser Speckle Imaging (LSI) in estimating the property of vascular network in brain surface.

Results: MRI showed that tissue hyperintense which indicated brain edema was increased from day 1, peaked at day 3, and recovered from day 7 after tMCAO ($p< 0.05$). Liquid hyperintense which indicated tissue liquefaction was obvious at day 28 after tMCAO ($p< 0.05$). fSRA showed that BFV in both brain surface and sub-cortex arteries decreased from day 1 to day 3 comparing to the sham ($p< 0.05$) and recovered to the baseline following 28 day of tMCAO. VE changed in a similar way. We found that blood flow (BF) supply was preferentially to middle cerebral artery (MCA) region and then anterior cerebral artery (ACA) area in normal rat, while BF supply was preferentially to ACA area during the acute phase (day 1 to day 3). Interestingly, the BF supply was returning to MCA region preference after day 7 ($p< 0.05$). The results suggested that arterial BFV and VE were weakened and BF pattern was changed due to edema in sub-cortex during acute phase, while recovered during the sub-acute phase of ischemia although tissue liquefaction occurred. LSI showed that the brain surface arterial diameter expansion was significantly reduced after 1 day of tMCAO comparing to the sham ($p< 0.05$) when performed lower limb electrical stimulation, which indicated that the VE was reduced, suggesting the validity of fSRA.

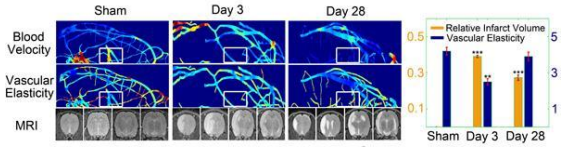

[Figure 1]

Figure 1. In-vivo imaging of rat's sub-cortex changes after tMCAO using fSRA and MRI.

Conclusions: MRI and fSRA provided a novel multi-modality technique for investigation of vasculature functions in sub-cortex. Our studies demonstrated that brain edema could cause changes in BF pattern and vasculature elasticity in sub-cortex, suggesting that ischemia induced edema is the main factor to cause vascular function changes in sub-cortex.

References:

1. Harb R, Whiteus C, Freitas C, Grutzendler J*. J Cereb Blood Flow Metab* 2012 Oct 24. doi: 10.1038.

2. Guan Y, Wang Y, Yuan F, Lu H, Ren Y, Xiao T, *et al. Stroke* 2012; 43: 888-891.

3. Yuan F, Tang Y, Lin X, Xi Y, Guan Y, Xiao T, *et al. J Neurotrauma* 2012; 29: 1499-1505.

A1R-MEDIATED SPREADING DEPRESSION IS MODULATED BY METABOLIC STATUS

B.E. Lindquist, C.W. Shuttleworth

Department of Neurosciences, University of New Mexico School of Medicine, Albuquerque, NM, USA

Introduction: Spreading depression is the reduction of synaptic activity observed in the wake of large spreading depolarizations (SD) of brain tissue. We recently described a role for adenosine A1 receptor (A1R) activation in mediating the bulk of synaptic depression following SD in brain slices (Lindquist and Shuttleworth, 2012). It is not known whether such adenosine accumulation is related to metabolic status, or whether adenosine accumulates to a functionally significant level following SD in normally perfused brain tissue.

Objectives: We investigated the role of metabolic supply in SD-induced adenosine accumulation and A1R activation *in vitro* and *in vivo*.

Methods: We prepared acute brain slices from C57Bl/6 mice, varying slice thickness (250, 350 or 450µm) to manipulate the efficacy of substrate delivery in the absence of vascular perfusion. SD was induced in the hippocampal CA1 region by microinjection of KCl, and confirmed by DC potential shifts and optical signals. We also monitored evoked field excitatory postsynaptic potentials (EPSPs), and measured adenosine concentration via an electrochemical probe. To evaluate responses in well perfused brain tissue, we induced SD in the cortex of anesthetized C57Bl/6 mice, and assessed spontaneous electrocorticographic activity (ECoG), DC potential, and evoked transcallosal EPSPs.

Results: Brain slice thickness significantly affected recovery from SD in an adenosine dependent manner. DC shift duration increased from 16.0±1.3s in thin slices (250µm) to 38.4±3.6s in standard slices (350µm) and 45.8±7.0s in thick slices (450µm) (ANOVA $p< 0.0001$, n=11,14,9 respectively). Following SD, estimated peak adenosine concentrations measured at the slice surface increased with slice thickness (6.1±0.7 vs. 50.6±9.2 vs. 91.3±13.0µM, thin vs. standard vs. thick slices, ANOVA $p< 0.001$, n=5,5). A1R-dependent EPSP depression also increased with slice thickness (200.0±49.0 vs. 864.4±151.5s, thin vs. standard $p< 0.01$, n=7,7). Oxidative metabolism was likely impaired in thick slices, as resting NADH autofluorescence was significantly elevated compared with thin slices (n=5,5). Reducing the buffer glucose concentration from 10 to 0.5mM tended to prolong EPSP depression following SD. In otherwise healthy perfused brain, adenosine effects were not significant following SD. In vivo, DC duration averaged 49.1±4.0s, and transcallosal EPSPs were depressed for 125.8±13.5s; ECoG was depressed for 381.7±40.1s (n=12). Neither EPSPs nor ECoG recovered faster in animals treated with A1R antagonist DPCPX (10mg/kg) as compared with vehicle controls ($p=0.67$, 0.46, respectively, n=6,6).

Conclusions: Limiting metabolic supply (by increasing diffusion distance or otherwise reducing substrate availability) appears to increase adenosine accumulation and A1R-mediated synaptic depression after SD. Despite long-lasting ECoG suppression following SD in the healthy brain, transcallosal potentials recovered rapidly and there was little evidence of adenosine accumulation in vivo, likely due to adequate metabolic supply via intact neurovascular coupling. Adenosine may have an important role in SD occurring in the context of hypoxia, hypoglycemia, or reduced perfusion pressure. Thick brain slices are a useful model for injury depolarizations.

References:

1. Lindquist, B.E. & Shuttleworth, C.W. Adenosine receptor activation is responsible for prolonged depression of synaptic transmission after spreading depolarization in brain slices. *Neuroscience* **223** (2012) 365-376.

Grant support: This research was supported by NIH grants NS051288 & NS078805.

ANTI-AMNESIC EFFECT OF COCAINE- AND AMPHETAMINE REGULATED TRANSCRIPT (CART) THROUGH SYNAPTIC PROTECTION IN APP/PS1MICE

J. Jin, K. Yin, L. Qian, X. Zhu, **Y. Xu**

Department of Neurology, Affiliated Drum Tower Hospital of Nanjing University Medical School, Nanjing, China

Objectives: Alzheimers disease (AD) is characterized by cognitive impairment and progressive memory loss due to accumulation of senile plaques, neurofibrillary tangles and loss of synapses and neurons. Synaptic deficiency in AD is associated with reduced mRNA expression of several immediate early genes (IEGs) and A-induced mitochondrial dysfunction. Our previous work indicated that the cocaine- and amphetamine-regulated transcript (CART) peptide had neuroprotective

effects following stroke. The aims of this study are:

1) to determine the expression patterns of CART in APP/PS1 transgenic mouse brains;

2) to investigate the effects of CART on synaptic impairment induced by Aβ;

3) to explore the mechanism underlying of CART on Aβ-induced synaptic toxicity.

Methods: The expression patterns of CART and Aβ in WT, APP/PS1 mice and AD patients were determined by immunostaining. APP/PS1 transgenic mice (10 months old, n=30/group) were injected with CART or vehicle (2.5ug/kg, intra-vena caudalis). The blood-to-brain unidirectional influx of 131I-CART was tested by radioactive labeling procedure. Learning and memory impairment was tested by Morris water maze, and the induction of synaptic plasticity was assessed electrophysiologically. The structure and number of synapses were determined by transmission electron microscope (TEM) and western blot in vivo. The expression of synaptic-related proteins, mitochondrial fission and fusion proteins were measured by real time PCR or western blot, and the expression of IEGs were determined by a reporter gene assay. Mitochondrial depolarization and reactive oxygen species (ROS) production were measured by fluorescence Microscopy and FACS analysis. The levels of 4-HNE, 3-NT, and ATP were measured by the ELISA. Statistical analyses were performed using ANOVA and post hoc Fisher's PLSD tests, with $P< 0.05$ considered statistically significant.

Results: In non-AD controls, CART was mainly distributed in cell body and neuritis in hypothalamus and cortex. In APP/PS1 mice, CART was observed in amyloid plaques and neuritis, especially in pyriform cortex. Similar to APP/PS1 mice, AD patients had CART immunoreactive in amyloid plaques, cells, and processes. The uptake of CART by the brain was high in thalamus, cortex, and hippocampus. CART administration significantly protected against learning and memory impairments in APP/PS1 mice ($P< 0.05$, n=30/group), and partially improved LTP induction and synaptic efficiency. CART treatment induced several IEGs, including Nur77, Arc and Homer1a, and regulated the expression of Nur77 by increasing promoter activity. CART could suppress Aβ induced intracellular ROS production and attenuated mitochondrial potentials reduction. Furthermore, mitochondrial functions were significantly improved in CART-treated animals compared to vehicle treatment.

Conclusion: Our findings suggest that CART distributes in amyloid plaques and neuritis. CART significantly improves synaptic plasticity in AD models. The improvement in synaptic plasticity is also associated with the upregulation of IEGs expression and the reversion of mitochondrial dysfunction. Thus, CART and its downstream mechanism of action may serve as novel therapeutic targets for AD.

ALTERED BLOOD THIAMINE METABOLISM AS A BIOMARKER FOR ALZHEIMER'S DISEASE

X. Pan, G. Fei, J. Lu, C. Zhong

Zhongshan Hospital & State Key Laboratory of Medical Neurobiology & Institute of Brain Science, Fudan University, Shanghai, China

Background: Reduced cerebral glucose metabolism is an invariant feature in Alzheimer's disease (AD). A key coenzyme of glucose metabolism and the active form of thiamine, thiamine diphosphate (TDP), has been shown to be significantly reduced in AD. Altered blood thiamine metabolism may represent a useful biomarker for AD diagnosis.

Methods: Control subjects with normal cognition (n=500) and patients with AD (n=108) and vascular dementia (n=53) were recruited. Blood TDP, thiamine monophosphate and thiamine levels were measured using high performance liquid chromatography.

Results: Blood TDP levels in AD patients were significantly reduced as compared with those of control subjects (83.55±2.93 vs. 118.60±1.12 nmol/L, $P< 0.001$), whereas blood thiamine monophosphate and thiamine levels were significantly elevated (5.26±0.48 vs. 3.59±0.09 nmol/L, $P< 0.001$ and 4.10±0.41 vs. 3.41±0.11 nmol/L, $P< 0.05$). Blood TDP level exhibited significantly diagnostic value, with an area under receiver operating characteristic curve (AUC) of 0.862, a sensitivity of 80.40% and a specificity of 77.78%. The (10000/TDP)*age*T^(1/6.4)/TMP^0.0001 ratio exhibited an even higher diagnostic value, with AUC of 0.901, a sensitivity of 88.20% and a

specificity of 80.00% when the cut-off point was 9242. Nearly 70% of vascular dementia patients could be differentiated from AD patients according to this cut-off point. The (10000/TDP)*age*T^(1/6.4)/TMP^0.0001 ratio exhibited an excellent diagnostic power in AD patients with APOE ε4 alleles, with AUC of 0.905, a sensitivity of 91.00% and a specificity of 81.63%. The disease severity of AD patients evaluated by MMSE, CDR and ADL scores didn't correlate with blood TDP levels.

Conclusion: Altered functional status of blood thiamine metabolism can serve as an ideal biomarker for AD diagnosis, that is reliable, non-invasive, simple to perform and inexpensive.

CHRONIC RAPAMYCIN RESTORES BRAIN VASCULAR INTEGRITY THROUGH ENOS ACTIVATION IN MICE MODELING ALZHEIMER'S DISEASE

A.-L. Lin[1], W. Zheng[2], J. Halloran[3], R. Burbank[3], S. Hussong[3], Y.-Y. Shih[4], E. Muir[1], A. Richardson[3], P. Fox[1], V. Galvan[3]

[1]Research Imaging Institute, [2]Cellular and Stuctural Biology, [3]Barshop Institute for Longevity and Aging Studies, University of Texas Health Science Center at San Antonio, San Antonio, TX, [4]University of North Carolina, Chapel Hill, NC, USA

Objectives: Vascular pathology is a major feature of Alzheimer's disease (AD) and other dementias. Cerebral microbleeds and macroscopic hemorrhage are frequently consequences of cerebral amyloid angiopathy (CAA), which arises from the deposition of amyloid-ß peptide (Aß) in blood vessels. Rapamycin, a drug originally used to keep the immune system from attacking transplanted organs, has been recently found having significant effects on increased lifespan and delayed aging in mice (1). We recently showed that treatment of mice modeling AD with rapamycin halts the progression of AD-like memory deficits and reduces Aß accumulation in mice (2). The purpose of the present study was to use multi-metric methods (e.g., imaging and biochemistry) to investigate the effect of rapamycin on hemodynamic and vascular functions in brains of the AD transgenic mice.

Methods: AD transgenic mice (Tg; hAPP (J20)) and age-matched controls (NTg) (F:M = 4:4 for each group) were used in the study. Separate groups of Tg mice were fed with rapamycin, starting at 7 months of age (earliest detectable cognitive deficits). Cerebral blood flow was measured using MRI-based arterial spin labeling techniques. Vascular density was measured using MR angiography and MION contrast agent. We used optical imaging and the nitric oxide (NO) indicator dye DAF-FM to observe NO derived from blood vessels. Aß plaques and microhemorrhages were determined by western blot and immunohistochemistry. Statistical analyses were performed using one-way ANOVA followed by Tukey's post-hoc test. Evaluation of differences between two groups was evaluated using Student's t test. Values of $P < 0.05$ were considered significant.

Results: Rapamycin was found to activate endothelial nitric oxide synthase (eNOS) in vascular endothelium. Accordingly, we found that rapamycin-treated AD mice had significantly increased CBF (26 ± 4%) and vascular density (20 ± 5%) compared to Tg controls. They also showed reduced CAA (-18 ± 4%) and Aß plaques (-24 ± 6%). However, the Aß production was not found different between treated and non-treated animals. The results indicate that rapamycin can restore vascular function by activate eNOS pathway, increase blood flow, increase Aß clearance rate and thus preserve vascular integrity in mice modeling Alzheimer's disease.

Conclusions: We demonstrate that chronic rapamycin treatment after disease onset negated brain vascular breakdown through activation of eNOS in vascular endothelium, reduced CAA and microhemorrhages, decreased amyloid burden, and improved cognitive function in symptomatic AD mice. Our data suggest that chronic rapamycin ameliorated established AD-like cognitive histopathological deficits by preserving brain vascular integrity and function through eNOS activation. Rapamycin, an FDA-approved drug already used in the clinic, may have promise as a therapy for AD and possibly for vascular dementia.

References:

(1) Harrison et al., Nature, 460:392, 2009;

(2) Spilman et al PLoS One, 5:e9979. 2010.

CORTICAL AND SUBCORTICAL NEURAL AND FMRI RESPONSES IN AN ALZHEIMER´S DISEASE RAT MODEL

B.G. Sanganahalli[1], P. Herman[1], K. Behar[1], H. Blumenfeld[2], D.L. Rothman[1,3], **F. Hyder**[1,3]

[1]Diagnostic Radiology, [2]Neurology, [3]Biomedical Engineering, Yale University, New Haven, CT, USA

Introduction: Alzheimer's disease (AD) is a neurodegenerative disease categorized by progressive loss of memory and other cognitive functions. AD is characterized by increased levels of amyloid β peptide (Aβ) plaques and neurofibrillary tangles in the brain that are associated with neuronal damage [1] and vascular toxicity [2-3].

Objectives: Based on the hypothesis that amyloid plaques found throughout the cerebral cortex can affect every cortical functions and presumably not affect subcortical function in the AD brain, we investigated alterations of functional responses in an AD rat model. High-field fMRI and multi-unit activity (MUA) measurements were applied to characterize brain functions from cortical and subcortical regions in a non-transgenic rat model of AD comparing to age matched healthy control group of rats.

Materials and methods:

Animal preparation*:* Experiments conducted on artificially ventilated (70% N_2O / 30% O_2) adult male Long Evans (250-350 g; Charles River, Wilmington, MA) and Alzheimer's rats (250-350g; Taconic Farms Inc, NY). We used Samaritan Alzheimer´s Rat Model from Taconic Farms (surgery model # FAB) (*www.taconic.com; surgery model# FAB*).During the animal preparation 2% isoflurane was used for induction. Intraperitoneal line was inserted for administration of α-chloralose (46±4 mg/kg/hr) and D-tubocurarine chloride (1 mg/kg/hr).

Forepaw stimuli (2mA, 0.3 ms, 3Hz): Stimulation was achieved by insertion of thin needle copper electrodes under the skin of the forepaw.

fMRI (n=10): All fMRI data were obtained on a modified 11.7T Varian horizontal-bore spectrometer using a ^{1}H surface coil (Ø = 1.4 cm). The images were acquired with gradient echo EPI sequence (TR/TE = 1000/15).

Neural activity measurements (n=10): Tungsten microelectrodes (FHC Inc, Bowdoinham, ME) were inserted up to layer 4 for $S1_{FL}$ and the thalamic nuclei (VPL) with stereotaxic manipulators (Kopf). Neural (multi unit activity: MUA) data from $S1_{FL}$ and VPL regions were normalized to the initial peak response during forepaw stimulation. All signals were then digitized (>20 kHz) with a µ-1401 interface using Spike2 software (CED, Cambridge, UK).

Results and discussion: Electrical stimulation of the forepaw (2mA, 3Hz, 0.3 ms) led to evoked BOLD and neural (MUA) responses in the contralateral somatosensory cortex ($S1_{FL}$) and the thalamus (VPL). In AD brain we noted more than 50% smaller BOLD activation patterns in $S1_{FL}$ and moreover, the dynamics of MUA was significantly attenuated. However evoked BOLD and MUA responses in VPL were unaltered in AD rats. These results suggest that cortical energy metabolism in Alzheimer's rats is significantly reduced, presumably due to increased levels of Aβ plaques and neurofibrillary tangles, as compared with the normal control rats. In future studies, application of calibrated fMRI to extract cerebral metabolic rate of oxygen consumption (CMR_{O2}) can help to better understand the relationship between neural activity, cerebral blood flow and metabolic changes in normal and disease states. These studies may have implications for understanding altered brain function in human Alzheimer's disease.

References:

[1] Hardy and Selkoe (2002) Science **297**:353-356.

[2] Iadecola, (2004) Nature reviews Neuroscience **5**:347-360.

[3]. Huang and Mucke, (2012) Cell **148**:1204-1222

Acknowledgements: Supported by NIH (R01 MH-067528, P30 NS-52519).

CALORIC RESTRICTION ALTERS FLOW-METABOLISM COUPLING IN HEALTHY AGING: A COMBINED PET AND MRI STUDY

A.-L. Lin[1], D. Coman[2], L. Jiang[2], P. Fox[1], A. Richardson[3], D. Rothman[2], F. Hyder[2]

[1]Research Imaging Institute, University of Texas Health Science Center at San Antonio, San Antonio, TX, [2]Magnetic Resonance Research Center, Yale University, New Haven, CT, [3]Barshop Institute for Longevity and Aging Studies, University of Texas Health Science Center at San Antonio, San Antonio, TX, USA

Objectives: Since the 1930s, caloric restriction (CR) has been repeatedly shown to increase the lifespan of a broad range of species (1). CR also demonstrated positive effects on brain funciton, e.g., rats treated with CR showed enhanced memory (2). Nontheless, the CR effects on brain metabolism and hemodynamics remain unexplored. Here we used PET and MRI to characterize the effect of CR on cerebral metabolic and vascular coupling in aged rats.

Methods: Male control and CR F344BNF1 rats at 24 month of age (N = 6) were anesthetized with alpha chloralose. Cererbral metabolic rate of glucose (CMR_{Glc}) was measured using ^{18}FDG PET (Focus 220 MicroPET). 0.5 mCi ^{18}FDG was injected through the tail vein. Emission data was acquired for 20 min after 40 min of injection. CMR_{Glc} was determined using the mean standardized uptake value (SUV_{mean}) equation. Cerebral blood flow (CBF) was acquired using MRI arterial spin labeling (ASL) techniqu at a horizontal 7T Bruker Biospec system. ASL image was analyzed with Matlab and STIMULATE software. T-test was used to determine the difference of the measured indices between the control and CR rats.

Results: Aged CR rats had lower CMR_{Glc}, (-28 ± 6%, $p < 0.01$) but significant higher CBF (32 ± 9%, $p < 0.001$), compared to the controls. In another study (see abstract by Lin A et al A-551-0015-00454), we found that aged CR rats had significant higher rates of neuronal glucose oxidation (TCA cycle flux) and total glutamatergic neurotransmission from the glutamate and glutamine cycle flux, and lower lactate concentration. These results suggest that healthy aging CR rats had enhanced mitochondrial function in the brain (e.g., higher oxidative metabolism and lower lactate), and that basal CBF was coupled with oxidative metabolism, rather than glucose metabolism.

Conclusions: It is well known that basal glucose/oxygen metabolism and CBF are tightly coupled under normal conditions. However, CR alters this fundamental flow-metabolism coupling relationship. Our results suggest that preserved coupling between CBF and CMR_{Glc} (and presumably oxidative metabolism) may play a key role in maintating brain function and healthspan. Although glucose utilization is lower in CR rats, the neuronal activity is higher, suggesting that CR rat's brain may use alternative fuel substrate, such as ketone bodies, to meet the energy demand (3). As ketone bodies are known to be neuroprotective, the shift in the metabolic pathway (from glucose to ketone bodies) may be another contributing factor for extended healthspan and lifespan of the CR rats. Future calorie restricted studies on the interplay between metabolic-vascular coupling with neuronal activity may have profound implications on retarding aging and age-related neurodegenerative disorders.

References:

(1) McCay et al., J Nutrition 10:63-79 (1935);

(2) Carter et al., J Gerontol A Biol Sci Med Sci. 64A: 850 (2009);

(3) Maalouf et al., Brain Res Rev 293-315 (2009).

THE PATTERN OF METABOLIC HETEROGENEITY IN THE HIPPOCAMPUS BY 3T MULTI-VOXEL PROTON SPECTROSCOPY IN ALZHEIMER´S DISEASE

F. Chen[1], B. Zhang[1], M. Li[1], X. Zhang[1], H. Wang[1], Y. Xu[2], B. Zhu[1]

[1]Department of Radiology, The Affiliated Drum Tower Hospital of Nanjing University Medical School, [2]Department of Neurology, Nanjing Brain Hospital of Nanjing Medical University, Nanjing, China

Objectives: We explore the metabolic changes in the head, body and tail of hippocampal in Alzheimer´s disease (AD) compared with normal control. We also investigate the distribution rules of metabolites

concentration among different parts of the hippocampus for more accurate clinical diagnosis of AD.

Table 3 The statistical results of hippocampal head, body and tail metabolites concentration distribution in AD group. StatisticRHPRHP-A RHP-MRHP-A RHP-PRHP-M RHP-PLHPLHP-A LHP-MLHP-A LHP-PLHP-M LHP-P NAA/CrF1.749 1.566 p0.1800.3250.4131.0000.2150.1870.7290.097 MI/CrF1.060 1.566 p0.3510.1780.8240.2600.2150.1330.9770.126 MI/NAAF1.653 1.294 p0.1970.0880.1790.7100.2790.1600.9590.175 Note: AD represents probable AD. RHP represents whole right hippocampal. RHP-A represents right hippocampal head. RHP-M represents right hippocampal body. RHP-P represents right hippocampal tail. LHP represents whole left hippocampal. LHP-A represents left hippocampal head. LHP-M represents left hippocampal body. LHP-P represents left hippocampal tail. Table 2 The statistical results of hippocampal head, body and tail metabolites concentration distribution in CN group. StaRHPRHP-A RHP-MRHP-A RHP-PRHP-M RHP-PLHPLHP-A LHP-MLHP-A LHP-PLHP-M LHP-P NAA/CrF15.882 10.280 p< 0.001< 0.001< 0.0010.575< 0.001< 0.001< 0.0010.713 MI/CrF2.404 1.725 p0.0960.4360.0330.1710.1840.1200.1040.941 MI/NAAF9.583 11.478 p< 0.0010.004< 0.0010.197< 0.001< 0.001< 0.0010.916 Note: Sta means Statistic method. CN represents cognition normal control. RHP represents whole right hippocampal. RHP-A represents right hippocampal head. RHP-M represents right hippocampal body. RHP-P represents right hippocampal tail. LHP represents whole left hippocampal. LHP-A represents left hippocampal head. LHP-M represents left hippocampal body. LHP-P represents left hippocampal tail.

Methods: Thirty patients with AD and 30 cognitively normal person (CN) were scanned by a 3.0 T magnetic resonance (MR) by Multivoxel proton spectroscopy (Achieva, Philips Medical Systems, Netherlands). The 8channels-HEAD coil was employed. The data was processed by commercially available postprocessing workstation (Extended Workspace (EWS), Philips Medical Systems, Netherlands). The hippocampus was divided equally into three parts (head, body and tail). N-acetylaspartate (NAA)/creatine (Cr), myoinositol (MI)/Cr and MI/NAA ratio were calculated separately from each part. We compared with each metabolites concentration data of AD and CN groups and analyzed the anteroposterior metabolic profile in hippocampus.

Result: The mean value of NAA/Cr is decreased and that of MI/Cr, MI/NAA are elevated in the bilateral hippocampi and hippocampal body and tail in AD group ($p < 0.01$). MI/NAA in the head of left hippocampus is also increased statistically ($p < 0.01$). Fig.1 shows NAA/Cr in the bilateral hippocampi from head to tail have the gradually rising trend ($p < 0.01$) and MI/NAA gradually declines in CN group ($p < 0.01$). MI/Cr in CN group and each metabolite concentration in AD group have no anteroposterior metabolic heterogeneity in bilateral hippocampil. (Fig.1). All detail data are recorded in Table 1-3.

	NAA/Cr	NAA/Cr	MI/Cr	MI/Cr	MI/NAA	MI/NAA
Groups	AD	CN	AD	CN	AD	CN
RHP	1.99±0.36**	2.61±0.44	0.91±0.40*	0.63±0.24	0.46±0.19**	0.25±0.09
RHP-A	2.09±0.54	2.12±0.34	0.79±0.27	0.65±0.21	0.39±0.12	0.31±0.10
RHP-M	1.92±0.28**	2.65±0.47	0.88±0.33**	0.61±0.23	0.46±0.13**	0.24±0.10
RHP-P	1.92±0.37**	2.71±0.50	0.80±0.23**	0.54±0.16	0.44±0.20**	0.21±0.18
LHP	1.98±0.37**	2.50±0.37	0.82±0.21**	0.61±0.15	0.41±0.12**	0.25±0.07
LHP-A	2.06±0.52	2.02±0.54	0.80±0.21*	0.66±0.17	0.42±0.16	0.35±0.14
LHP-M	1.89±0.32**	2.46±0.32	0.89±0.29**	0.59±0.17	0.48±0.14**	0.24±0.08
LHP-P	2.10±0.61*	2.50±0.49	0.79±0.22**	0.59±0.18	0.42±0.19**	0.24±0.09

[Table 1 Metabolites ratios in AD and CN groups.]

	Statistic	RHP	RHP-ARH	RHP-ARH	RHP-	LHP	LHP-ALH	LHP-ALH	LHP-M

			P-M	P-P	MRHP-P		P-M	P-P	LHP-P
NAA/Cr	F	15.882				10.280			
	p	<0.001	<0.001	<0.001	0.575	<0.001	<0.001	<0.001	0.713
MI/Cr	F	2.404				1.725			
	p	0.096	0.436	0.033	0.171	0.184	0.120	0.104	0.941
MI/NAA	F	9.583				11.478			
	p	<0.001	0.004	<0.001	0.197	<0.001	<0.001	<0.001	0.916

[Table 2 The statistical results in CN group.]

	Statistic	RHP	RHP-ARHP-M	RHP-ARHP-P	RHP-MRHP-P	LHP	LHP-ALHP-M	LHP-ALHP-P	LHP-MLHP-P
NAA/Cr	F	1.749				1.566			
	p	0.180	0.325	0.413	1.000	0.215	0.187	0.729	0.097
MI/Cr	F	1.060				1.566			
	p	0.351	0.178	0.824	0.260	0.215	0.133	0.977	0.126
MI/NAA	F	1.653				1.294			
	p	0.197	0.088	0.179	0.710	0.279	0.160	0.959	0.175

[Table 3 The statistical results in AD group.]

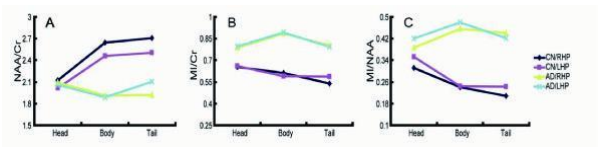

[Fig.1]

Conclusion: The anteroposterior metabolic heterogeneity is dismissed in AD, which might be helpful on the early clinical diagnosis of AD.

CONSTRAINT-INDUCED MOVEMENT THERAPY ENHANCES AXONAL REGENERATION BY OVERCOMING THE INTRINSIC GROWTH INHIBITORY SIGNALS IN STROKE RATS

C. Zhao, S. Zhao, H. Qu, C. Song, S. Wang

Neurology, The First Hospital of China Medical University, Shenyang, China

Objectives: To confirm the hypothesis that constraint-induced movement therapy (CIMT) could enhance axonal regeneration by overcoming the intrinsic growth inhibitory signals leading eventually to improved behavioral performance in stroke rats.

Methods: Male Wistar rats (200-250g) were divided into a sham-operated group, an ischemic group and an ischemic group treated with CIMT (n=12 per group). Focal cerebral ischemia was induced by intracortical and intrastriatal injection of endothelin-1 [1]. Three weeks of CIMT beginning at post-stroke day 7 was performed by fitting a plaster cast around the unimpaired upper limb of rats [2]. Biotinylated dextran amine (BDA) was injected into the sensorimotor cortex on postoperative day 14 to trace intact CST fibers and their growth toward the contralateral denervated spinal gray matter at the cervical spinal cord. Behavioral recovery was analyzed 4 weeks after ischemia by the beam walking test and the water maze test. The BDA-positive axons and the expressions of axonal inhibitors including Nogo-A, Nogo receptor (NgR), Rho-A and Rho-associated kinase (ROCK) in the infarct cortex as well as the expressions of synaptic markers including GAP-43, synaptophysin, vGlut1 and PSD-95 in the the ventral horn of denervated spinal were measured by immunofluorescence staining and Western blots. BDA-postive axons and their colocalization with the synaptic markers were detected by confocal microscope. The number and length of BDA positive axons and the positive cells of axonal inhibitors as well as the integrated density pixels of synaptic markers were measured by NIH Image J software.

Results: Infarct volumes were not different between groups after stroke. The number and sum length of the midline-crossing axons of the intact corticospinal to the denervated cervical spinal cord were increased significantly after ischemia and further increased by CIMT. The expressions of Nogo-A/NgR and RhoA/ROCK in the infarct cortex which were increased in respond to focal stroke were decreased significantly by CIMT. The expressions of the GAP-43, synaptophysin, vGlut1 and PSD-95 which were decreased after ischemia were elevated significantly by CIMT and these synaptic markers were colocalized with BDA positive axons. Motor funtion assessed by the beam-walking test and the spatial learning and memory functions assessed by the Morris water maze test which were impaired after focal ischemia were improved significantly by CIMT.

Conclusions: CIMT promoted poststroke axonal regeneration and synaptic plasticity at least partially by overcoming the intrinsic growth inhibitory signaling to improved behavioral outcome after ischemia stroke in adult rats.

References:

1. Windle V, Szymanska A, Granter-Button S, et al. An analysis of four different methods of producing focal cerebral ischemia with endothelin-1 in the rat. Exp Neurol 2006;201:324-34.

2. Muller HD, Hanumanthiah KM, Diederich K, Schwab S, Schabitz W-R, Sommer C. Brain-derived neurotrophic factor but not forced arm use improves long-term outcome after photothrombotic stroke and transiently upregulates binding densities of excitatory glutamate receptors in the rat brain. Stroke 2008;39:1012-21.

DELAYED TREATMENT WITH SCF AND G-CSF IN CHRONIC STROKE PROMOTES SYNAPTOGENESIS IN THE PERI-INFARCT AREA THROUGH NF-κB PATHWAY

L. Cui[1], L.-R. Zhao[2]

[1]Neurology, Louisiana State University Health Sciences Center, [2]Neurology/Cellular Biology and Anatormy, LSUHSC-S, Shreveport, LA, USA

Objective: Stroke, a leading cause of adult permanent disability, is a critical medical condition with lack of effective treatment. Chronic stroke is the phase beyond 3 months after stroke onset. We have demonstrated that the combination of two hematopoietic growth factors, stem cell factor (SCF) and granulocyte-colony stimulating factor (G-CSF) (SCF+G-CSF), induces stable and long-term functional improvement with enhancement of neuronal activity in the lesion side brain in an animal model of chronic stroke. It remains unclear, however, how SCF+G-CSF repairs the brain during chronic stroke. Recently, we have revealed that SCF+G-CSF treatment in chronic stroke enhances neuronal network remodeling in the cortex adjacent to the infarct cavities and that SCF+G-CSF promotes neurite outgrowth through the regulation of NF-κB pathway. The aim of this study, therefore, was to determine whether SCF+G-CSF rebuilds up synaptic networks in the peri-infarct cortex through NF-κB pathway.

Methods: Cortical brain ischemia was produced in transgenic mice expressing yellow fluorescent proteins in the layer V pyramidal neurons (Thy-1-YFPH). Seven-day injection of SCF+G-CSF was initiated 7 months after induction of cortical brain ischemia. NF-κB inhibitor (Bay 11-7082) or saline was infused into the contralateral ventricle for 7 days with an osmotic minipump 1 h before SCF+G-CSF treatment. The apical dendrites of layer V pyramidal neurons in the peri-infarct cortex were scanned before treatment, two and six weeks after treatment in the same animals with a multi-photon microscope. After completing brain live imaging at 6 weeks post-treatment, functional postsynaptic element was detected with an anti-PSD-95 antibody through immunohistochemistry.

Results: Before treatment, the mushroom dendritic spines were significantly reduced in both stroke groups (vehicle control and SCF+G-CSF) as compared to the intact controls, whereas there was no difference between the two stroke groups. However, 2 and 6 weeks after treatment, mushroom spines were significantly increased by SCF+G-CSF when compared to the vehicle controls, and the SCF+G-CSF-induced increase in mushroom spines was significantly blocked by NF-κB inhibitor. In addition, the size of spine heads was also increased by SCF+G-CSF, and the effects of SCF+G-CSF in enlarging the size of spine heads were prevented by intracerebral infusion of NF-κB inhibitor. Furthermore, PSD-95 positive puncta was

significantly increased in the peri-infarct cortex by SCF+G-CSF treatment, whereas the SCF+G-CSF-induced increase of PSD-95 positive puncta was significantly blocked by NF-kB inhibitor.

Conclusions: Systemic administration of SCF+G-CSF in a much-delayed time during chronic stroke can stimulate surviving neurons to generate new and functioning synaptic connections with other neurons. NF-κB signaling is required for SCF+G-CS-induced neuronal network remodeling in the pre-infarct cortex. This study provides supportive evidence for the therapeutic role of SCF+G-CSF in chronic stroke.

This study was supported by The National Institutes of Health, National Institute of Neurological Disorders and Stroke (NINDS), R01 NS060911 to L.R.Z.

THE CONSEQUENCES OF EXPERIMENTAL HEMISPHERECTOMY ON WHITE MATTER INTEGRITY AND FUNCTIONAL CONNECTIVITY IN THE REMAINING HEMISPHERE

W.M. Otte[1], K. van der Marel[1], M.P. van Meer[1], K.P. Braun[2], R.M. Dijkhuizen[1]

[1]Biomedical MR Imaging and Spectroscopy Group, Image Sciences Institute, [2]Pediatric Neurology, Rudolf Magnus Institute of Neuroscience, University Medical Center Utrecht, Utrecht, The Netherlands

Introduction: Following hemispherectomy—the surgical removal or disconnection of one hemisphere—there is often remarkable recovery of cognitive and motor functions[1]. This reflects the plastic capacities of the remaining hemisphere which is assumed to involve large-scale structural and functional adaptations. A better understanding of these adaptations may guide development of postoperative rehabilitation strategies that enhance recovery after hemispheric lesioning.

Methods: We assessed the effect of anatomical hemispherectomy on brain structure and function in the remaining cerebral hemisphere in a rat model[3]. With MRI we mapped changes in structural white matter integrity and functional connectivity in hemispherectomized (n=8) and control rats (n=12). Functional behavioral testing involved calculation of a composite sensorimotor performance score[2]. Diffusion tensor imaging (DTI) and resting state fMRI (rs-fMRI) were acquired 7 and 49 days following surgery (DTI: spin-echo; TR/TE=3500/26 ms; 25 0.5mm slices; voxels 0.5×0.5×0.5 mm^3; 50 directions with b=1250 s/mm^2; Δ/δ=11/6 ms. Rs-fMRI: gradient-echo; TR/TE=500/19 ms; 10 min acquisition at 1% isoflurane) (4.7T MR system). DTI was used to calculate volume, fractional anisotropy and mean, axial and radial diffusivity for the contralateral cerebral peduncle. Rs-fMRI images were motion-corrected, spatially smoothed, band-pass filtered between 0.01 and 0.1 Hz, and nonlinearly matched with an atlas for functional connectivity (FC) analysis. Time series were extracted for 15 contralateral sensorimotor regions to calculate pair-wise FCs (correlation coefficient). Intraregional signal coherence and interregional FC were also calculated[4]. Functional network characteristics included segregation (measured as clustering coefficient) and integration (measured as shortest path length)[4].

Results: Successful hemispherectomy caused significant sensorimotor deficits in young adult rats after which animals recovered within 2 weeks. Important changes during this recovery period included increased axial diffusivity in the contralateral cerebral peduncle. (Figure, top)

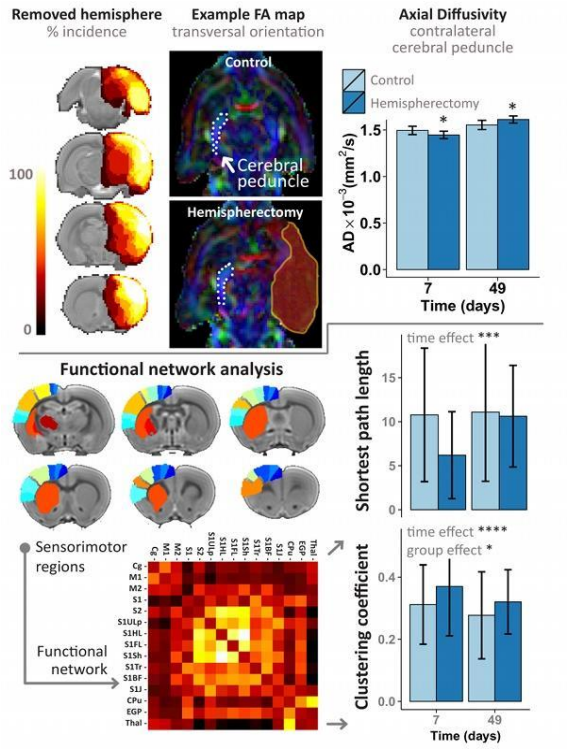

[Figure]

FC was enhanced in the contralateral hemisphere, with higher segregation in the contralateral sensorimotor network (Figure, bottom) contributed by particularly the motor cortex and thalamus. Specifically, in the remaining hemisphere the motor cortex exhibited increased FC with the caudate-putamen complex (CPu) and primary somatosensory cortex (S1), which was most pronounced 7 days after hemispherectomy. Intraregional signal coherence was significantly elevated in S1 in the hemispherectomy group. In the same rats interregional FCs were significantly elevated between motor cortex and CPu.

Conclusions: Our study sheds new light on patterns of change in sensorimotor function in relation to changes in white matter and FC in the contralateral brain after hemispherectomy. Sensorimotor recovery after experimental hemispherectomy paralleled with increases in intraregional signal coherence and interregional FC in the contralateral hemisphere, as well as with an overall enhanced sensorimotor network segregation. These changes may be reflective of (early) compensatory mechanisms, such as recruitment or strengthening of latent but existing pathways in contralateral cortical and subcortical sensorimotor areas, but may also relate to structural neuronal plasticity after hemispherectomy.

References:

[1]Samargia and Kimberley, *Pediatr Phys Ther* 4(2009)

[2]van der Zijden et al, *J Cereb Blood Flow Metab* 28(2008)

[3]Machado *et al*, *Epilepsia* 4(2003)

[4]van Meer *et al*, *J Neurosci* 32(2012)

DYNAMIC IMAGING OF MESENCHYMAL STEM CELL TRACKING TO CEREBRAL INFARCTION WITH MULTI FUNCTIONAL PROBE

Y. Tang[1], B. Cai[1], X. Lin[1], J. Wang[1], L. Xiong[1], Y. Wang[1], C. Zhang[1], G.-Y. Yang[1,2]

[1]Neuroscience and Neuroengineering Research Center, Med-X Research Institute and School of Biomedical Engineering, [2]Department of Neurology, Ruijin Hospital, School of Medicine, Shanghai Jiao Tong University, Shanghai, China

Objectives: Transplantation of mesenchymal stem cell (MSC) after stroke has been shown to improve functional recovery.[1] However, the migration, distribution and survival of grafted MSCs in ischemic brain are still unclear. In this study, we investigated the effects of administrative approach on transplanted MSC migration and distribution in living rats after cerebral ischemia. We further assessed the correlation between cell grafting site and therapeutic efficiency.

Methods: MSCs were incubated with ^{125}Iodine labeled fluorescent -super paramagnetic iron oxide nanoparticles (^{125}I-SPIO). Cytotoxicity and labeling efficiency were examined in these MSCs. ^{125}I-SPIO labeled MCSs (1×10^6) were transplanted into ischemic rats via intravenous (IV), intracerebral (IC) or intra-artery (IA) following one day of transient middle cerebral artery occlusion (tMCAO). In vivo MR and microSPECT/CT imaging were performed to quantify track the transplanted MSCs from 1 day to 14 days after ischemia. Histological analysis and behavioral tests were performed following14 days of tMCAO.

Results: Flow cytometry analysis demonstrated that 75% MSCs were labeled by ^{125}I-SPIO. Cytotoxicity and differentiation assay showed that ^{125}I-SPIO did not affect MSC survival and differentiation in vitro. microSPECT/CT imaging showed that 4% MSCs migrated to the lesion site 1 day after IC and 10% MSCs accumulated in the border zone of the lesion from 3 to 14 days after tMCAO. 90% MSCs migrated and accumulated into the lung from 1 to13 days after IV transplantation while no MSCs could be detected in the brain. Interestingly, both IV and IC transplantation of MSC improved neurobehavior recovery compared to the PBS group ($p< 0.05$), although did not reduce

infarct volume 14 days after tMCAO. High mortality (6/7) due to micro-occlusions after IA transplantation poses a serious concern for using this route of administration.

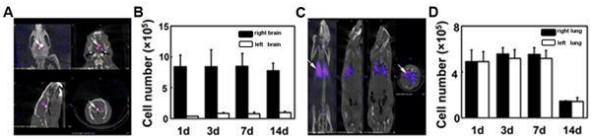

Figure 1. MicroSPECT/CT image of rats after IC (**A**) or IV (**C**) injection of ^{125}I-SPIO labeled MSCs (arrows) 14 days after tMCAO. Bar graph showed the number of MSCs in brain (**B**) quantified from (A) and lung (**D**) quantified from (C) following 1, 3, 7 and 14 day after tMCAO.

Conclusions: We demonstrated that MSC transplantation via IV or IC improved neurobehavior recovery 7 and 14 days after tMCAO although few MSCs targeted to the brain through IV injection, suggesting that the number of MSCs in the brain is not correlated with its therapeutic effect.

Reference:

1. Parr AM, Tator CH, and Keating A. Bone marrow-derived mesenchymal stromal cells for the repair of central nervous system injury. Bone Marrow Transplant 2007; 40: 609-419.

BDNF MET ALLELE IS ASSOCIATED WITH ENHANCED MOTOR FUNCTION THROUGH THE CONTRALATERAL STRIATAL PLASTICITY FOLLOWING STROKE

L. Qin[1], D. Jing[2], F. Lee[2], R. Ratan[1], **S. Cho**[1]

[1]Neurology/Neuroscience, Weill Cornell Medical College at Burke Med Res Inst, White Plains, [2]Psychiatry and Pharmacology, Weill Cornell Medical College, New York, NY, USA

Objectives: Stroke induces structural plasticity and behavioral adaptation. BDNF plays a key role in CNS repair and plasticity. Single nucleotide polymorphism (SNP) in prodomain of Bdnf (*val66met*) occurs with high frequency in humans. Several disadvantages, including anxiety-related behavior and cognitive impairment, have been associated with individuals carrying the SNP. However, the high rate of SNP occurrence raises the intriguing possibility of a selective advantage, such as motor function, to carrying the allele. This study investigates the effect of BDNF SNP on motor function following stroke and the underlying events for the restorative processes.

Methods: Adult male $BDNF^{+/+}$ (WT) and $BDNF^{Met/Met}$ (M/M) mice were subjected to proximal middle cerebral artery occlusion. Motor and gait functions were assessed by rotarod and Catwalk during acute and recovery phases up to 6m. Sub-regional volume in the brain was determined at 6m post ischemia. Detailed neuronal morphology and the expression of excitatory and inhibitory synaptic markers were also assessed.

Results: Despite a greater acute motor impairment as we previously reported (Qin et al., 2011), M/M mice displayed enhanced rotarod performance at 2 weeks and during the long term stroke recovery phase until 6m. Similarly, gait analyses revealed that M/M mice exhibited enhanced gaits (i.e. faster and longer stride) than WT mice during recovery. The enhancement was prominent in the ipsilesional right hind limb that is controlled by the contralateral hemisphere. Sub-regional volume analyses at 6m showed that the contralateral striatum volume was significantly increased in M/M mice (WT vs M/M, 6.8 ± 0.1 vs, 7.7 ± 0.2 % of contralateral hemisphere, $p<$ 0.05, n=8/group). The volume increase was associated with higher degree of dendritic arbor (FIgure 1A) of medium spiny neurons in this region as indicated by fractal dimension, a statistical index of complexity of pattern (Figure 1B). We determined the expression of excitatory (VGluT1/T2) and inhibitory synaptic markers (VGAT) in the contralateral striatum to assess synaptic plasticity. M/M mice displayed increased expression of VGluT1 and VGluT2 protein in the contralateral striatum (WT vs M/M, VGLUT1, 265±18 vs 339 ± 23mm^2, *$p<$ 0.05; VGLUT2, 215 ± 13 vs 292 ± 13, $p<$ 0.01). There was no difference in the expression of VGAT between the genotypes, suggesting a shift of synaptic balance to excitation in this region.

Conclusions: The findings indicate that BDNF SNP have a selective advantage in promoting motor recovery through a synaptic balance shift to excitation in the contralateral striatum. The study suggests clinical importance as the structural, molecular, and functional findings may provide a means to predict the course of stroke recovery based on an individual's SNP.

Reference: Qin L, Kim E, Ratan R, Lee FS, Cho S. J Neurosci. 2011, 31(2):775-83.

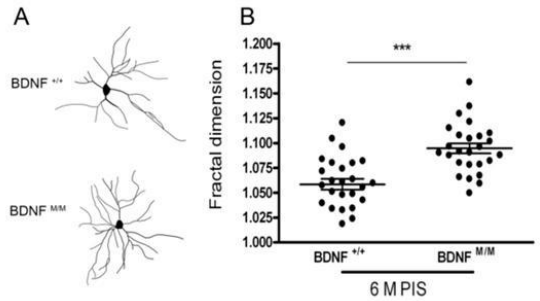

[Figure 1]

BRAIN COOLING BY INTRA-VENTRICULAR CATHETERS WITH BIRDS: A 7T SHEEP STUDY

D. Coman[1], Y. Huang[1], J.W. Simmons[2], J.A. Goodrich[3], B. McHugh[4], J.A. Elefteriades[5], D.L. Rothman[1,6], **F. Hyder**[1,6]

[1]Diagnostic Radiology, Yale University School of Medicine, New Haven, [2]Coolspine LLC, Woodbury, [3]Comparative Medicine, [4]Neurosurgery, [5]Cardiothoracic Surgery, [6]Biomedical Engineering, Yale University School of Medicine, New Haven, CT, USA

Introduction: Selective brain hypothermia can help alleviate damage caused by brain trauma, cardiac arrest and stroke, among other conditions **[1,2]**. Towards this translational goal a cerebrospinal fluid (CSF)-based cooling platform for selective brain hypothermia was developed **[3]**. This novel system uses cool saline circulating in a closed loop through a catheter with an expandable balloon placed in the lateral ventricles to induce cooling in neighboring brain tissue. Temperature distributions in the whole brain are needed to understand the cooling efficiency of the device prior its translation to humans. Temperature mapping by a novel chemical shift imaging (CSI) technique, which utilizes a lanthanide macrocyclic probe extremely sensitive to temperature (TmDOTMA) was employed. The method, termed ***B***iosensor ***I***maging of ***R***edundant ***D***eviation in ***S***hifts (BIRDS), is based on detection of ^{1}H signals from TmDOTMA**[4,5]**. Using BIRDS the time dependence of absolute temperature distribution during the cooling process was obtained.

Methods: Two adult male sheep (30kg) were sedated with acepromazine (0.5mg/kg,intramuscular) and valium (0.5mg/kg,intravenous), followed by ketamine (2.2-2.75mg/kg,intravenous), and then intubated. Burr holes were made bilaterally 1.5cm anterior and lateral to the posterior fontanelle. The cooling catheters were placed via the burr holes in both ventricles. These catheters were also used to inject $TmDOTMA^-$ (7mg/kg) directly into ventricles at 1ml/h. A water-heating blanket was used to maintain normothermic body temperature(38^0C). 25x25x25 3D CSI datasets **(Fig.1A)** were obtained on a Varian 7.0T/68cm spectrometer using a ^{1}H resonator/surface RF probe. The temperature maps **(Fig.1B,1C)** were calculated from the chemical shift of $TmDOTMA^-$ methyl group**[5].**

Results: The brain average temperature before cooling was 38.0 ± 0.4^0C. First, we circulated ice-cold saline via the left catheter and we observed selective cooling of left hemisphere to 33.6 ± 0.8^0C**(Fig. 1D)**, while the average temperature in the right hemisphere was decreased to 37.7 ± 0.9^0C **(Fig.1E)**. However, when we started circulation of ice-cold saline through both catheters, we observed an increase in the temperature of the left hemisphere to 34.9 ± 0.2^0C **(Fig.1D)** and a decrease in the right hemisphere to 35.3 ± 0.4^0C **(Fig.1E).** Increasing the flow rate from 35ml/min to 42ml/min resulted in a decrease in temperature to 32.3 ± 0.2^0C and 33.5 ± 0.3^0C in left and right hemispheres, respectively **(Fig.1D,1E)**. 10 minutes after cooling was stopped, a temperature of 37.8 ± 0.2^0C and 38.1 ± 0.5^0C was measured in the left and right hemispheres, respectively **(Fig.1D,1E)**.

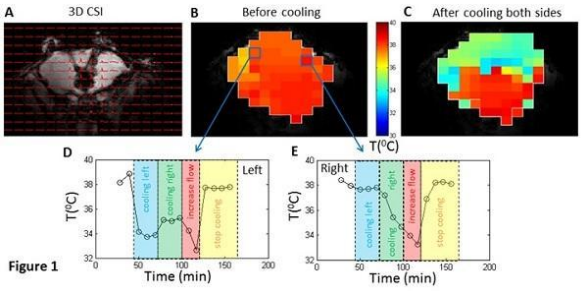

[Figure 1]

Conclusions: Detection of TmDOTMA was obtained for the first time in sheep brain by simultaneous delivery directly in each ventricle. Selective cooling of each hemisphere was observed within 10 minutes of cooling. A fast recovery to physiological

brain temperature was observed within 10 minutes after cooling was stopped. In summary, we demonstrate that absolute changes and dynamics of brain temperatures in sheep during selective intra-ventricular CSF cooling can be measured by BIRDS with TmDOTMA. These measurements have a direct impact on designing selective brain hypothermia procedures in humans during brain trauma, cardiac arrest or stroke.

References:

[1] Holzer M. (2008)*Eur.J.Anaesthesiol.Suppl.* 42:31-38;

[2] Christian E et.al.(2008)*Neurosurg.Focus* 25:E9;

[3] Moomiaie RM, et.al.(2007)*J.Cardiovasc.Surg.(Torino)* 48:103-108;

[4] Coman D, et.al.(2009)*NMR.Biomed.* 22:229-239;

[5] Coman D, et.al.(2009)*NMR.Biomed.* 23:277-285.

Acknowledgements: Supported in part by P30-NS052519 and NSF-0923928.

DOCOSAHEXAENOIC ACID COMPLEXED TO ALBUMIN AS A PROMISING NEUROPROTECTANT IN BRAIN ISCHEMIA: NEW EXPERIMENTAL EVIDENCE

L. Belayev[1], L. Khoutorova[2], A. Obenaus[3], T.N. Eady[2], N.G. Bazan[2]

[1]Neuroscience and Neurosurgery, Louisiana State University, [2]Neuroscience, Louisiana State University Health Sciences Center, New Orleans, LA, [3]Pediatrics, Loma Linda University, Loma Linda, CA, USA

Introduction: Docosahexaenoic acid complexed to albumin (DHA-Alb) is highly neuroprotective after temporary middle cerebral artery occlusion (MCAo), but whether a similar effect occurs in permanent MCAo and older rats is unknown. We used magnetic resonance imaging (MRI) in conjunction with behavior and immunohistopathology to expand our understanding of this novel therapeutic approach.

Methods: Two protocols were employed.

In series 1, male young Sprague-Dawley (SD) rats (270-330g) underwent permanent MCAo. Neurological status was evaluated on days 1, 2 and 3 after MCAo; a grading scale of 0-12 was employed (normal score=0, maximal deficit=12). Six groups we studied: DHA (5mg/kg), Alb (0.63 or 1.25g/kg), DHA-Alb (5mg/kg+0.63g/kg or 5mg/kg+1.25g/kg) or saline were administered i.v. at 3 h after onset of stroke (n=8-10 per group). *Ex vivo* imaging of the brains and histopathology were conducted on day 3.

In series 2, male aged (18-months old) SD rats received 2 h MCAo by poly-L-lysine-coated intraluminal suture. The neurological status was evaluated during MCAo and on days 1, 2, 3 and 7 after MCAo. DHA (5mg/kg), Alb (0.63g/kg), DHA-Alb (5mg/kg+0.63g/kg) or saline were administered i.v. at 3 h after onset of stroke (n=8-10 per group). *Ex vivo* imaging of the brains and immunohistochemistry were conducted on day 7.

Results: The physiological variables were entirely comparable between groups. *In the permanent MCAo study,* saline- and Alb-treated rats developed severe neurological deficit and were not different from one another. In contrast, rats treated with low and moderate doses of DHA-Alb showed improved neurological score compared to Alb on days 2 and 3. Total, cortical and subcortical lesion volumes computed from T2WI images were reduced by a moderate dose of DHA-Alb by 25%, 22%, 34%, respectively, compared to the corresponding Alb group. The total corrected infarct, cortical and subcortical infarct volumes were reduced by lower (by 36-40%) and moderate doses (by 34-42%) of DHA-Alb compared to the Alb group. *In the temporary MCAo study of aged animals,* DHA-Alb treatment improved the neurological score compared to vehicle rats by 33% (day 1), 39% (day 2), 41% (day 3) and 45% (day 7). Total and cortical lesion volumes computed from T2WI images were reduced by DHA-Alb treatment by 62% and 69%, respectively, compared to the Alb group. Histological assessment showed that DHA-Alb treatment also reduced total infarct volume (by 62%) and cortical infarct was virtually eliminated compared to the Alb group. In addition, DHA-Alb treatment decreased ED-1-activated microglia/microphages and increased NeuN and GFAP-positive cell count compared to the Alb group.

Conclusions: DHA-Alb therapy is highly

neuroprotective in permanent MCAo and also in temporary MCAo in middle-aged rats. This treatment might provide the basis for future therapeutics for patients suffering from ischemic stroke.

This study was supported by R01 NS065786 (LB)

TREADMILL PRE-TRAINING AMELIORATES BRAIN EDEMA IN CEREBRAL ISCHEMIA VIA DOWNREGULATION OF AQP4—A MRI STUDY OF RAT

X. Wang[1], Z. He[1], X. Yang[1], Z. Wu[1], M. Li[1], Z. Guo[1], J. Guo[2], **J. Jia**[1]

[1]Rehabilitation, Huashan Hospital, Fudan University, [2]Insutitute of Neurobiology, Fudan University, Shanghai, China

Treadmill pre-training has been proved to ameliorate ischemia-reperfusion injury, yet its role on ischemic brain edema remain covered.

In present study, rats were randomly divided into 3 groups: Sham group, Treadmill pre-training (TT/Stroke) group and Stroke group. Animals in TT/Stroke group underwent two weeks of treadmill training, while animals in Stroke group and Sham group were allowed 2-week free movement. Middle cerebral artery occlusion (MCAO) was then performed in rats in Stroke group and TT/Stroke group. Rats in Sham group were performed the same surgical procedure without MCAO. Magnetic resonance imaging (MRI) was used to evaluate the impact of pre-training on dynamic process of cerebral edema after ischemia and reperfusion injury in vivo. Diffusion Weighted Magnetic Imaging (DWI) and T2 Weighted Resonance Imaging (T2WI) were used to detect the development of cerebral edema from 1 hour to 2 days after ischemia. Contrast agent injection and post-T1 Weighted Resonance Imaging (T1WI) was performed to detect the change of blood brain barrier (BBB) permeability at 7.5 hours and 2 days after ischemia. Simultaneously, brain water content measurement and Evans blue (EB) assay were performed to test the cerebral water content and BBB permeability 2 days after stroke. The expression of Aquaporin 4 (AQP4) was measured by Western Blot and immunofluorescence staining from 6 hours to 3 days after stroke, to explore the relationship between treadmill pre-training and brain edema. Neurological deficits were evaluated through Garcia scoring system at 2 days post injury.

T2WI values of the ipsilateral cortex and striatum increased while the relative apparent diffusion coefficient (rADC) decreased through MRI, which reflects a formation of cerebral edema. In cortex, the rADC of TT/Stroke group increased compared with Stroke group at 1 hours and 2.5 hours after stroke, while the T2 values from 7.5 hours to 2 days after stroke decreased as compared with Stroke group. In striatum, at 2.5 hours after stroke, TT/Stroke group had increased rADC compared with Stroke group. T2 values at 2.5 hours, 1 day, 2 days after stroke decreased compared with Stroke group. The brain water content of treadmill pre-training group decreased as compared with the Stroke group at 48 hours after reperfusion. On the ipsilateral brain, the semi-quantitative amount of contrast agent leakage of TT/Stroke group significantly decreased when comparing with Stroke group at 7.5 hours and 2 days after ischemia through MRI. The EB exudation in TT/Stroke group significantly increased when compared to Stroke group at 2 days after ischemia. Immunofluorescence staining of AQP4-positive cells significantly decreased in TT/stroke group in cortical region around ischemic lesions. Western blot results showed the expression of AQP4 after treadmill pre-training decreased at 1 hour, 2.5 hours,7.5 hours, 2 days after ischemia. Significant difference was also observed in items of 1. spontaneous activity; 3. outstretching while held by tail; and 5. response to vibrissae touch of the Garcia score after treadmill pre-training.

The result showed treadmill pre-training may reduce edema after cerebral ischemia via down-regulating the BBB damage and the expression of AQP4.

FEASIBILITY SAFETY AND EFFICACY OF REMOTE ISCHEMIC PRECONDITIONING FOR SYMPTOMATIC INTRACRANIAL ARTERIAL STENOSIS IN OCTOGENARIANS

R. Meng[1], J. Jia[1], G. Li[1], Y. Liu[1], F. Ling[1], J. Shi[1], Y. Duan[1], X. Wang[2], Y. Ding[3], E.H. Lo[4], X. Ji[1]

[1]Neurology Department and Cerebral Vascular Diseases Research Institute (China-America Institute of Neuroscience), Xuanwu Hospital, Capital Medical University, Beijing, China, [2]Departments of Neurology and Radiology, Massachusetts General Hospital, Harvard Medical School, Boston, MA, [3]Wayne State University School of Medicine, Detroit, MI, [4]Massachusetts General Hospital and Harvard Medical School, Boston, MA, USA

Background: Making a limb transiently ischemic induces ischemic tolerance in distant organs such as the heart. This study aims to evaluate the feasibility, safety and initial efficacy of using briefly repetitive bilateral limb ischemic preconditioning (BLIPC) to protect the brain in octogenarians with symptomatic intracranial arterial stenosis.

Methods: A total of 58 consecutive octogenarians with symptomatic intracranial arterial stenosis (diagnosed by imaging) were enrolled in this prospective and randomized study. The BLIPC group (n=30) underwent five cycles of 5 minutes bilateral upper limb ischemia-reperfusion, performed twice daily for 180 consecutive days, along with conventional medical treatment. Control subjects (n=28) underwent equivalent medical treatments only. Blood pressure, heart rate, local skin presentation and plasma myoglobin levels before and during the first 30 days after treatment were documented. Plasma levels of high sensitive C-reactive protein (hsCRP), interleukin-6 (IL-6), leukocyte count, fibrinogen, D-dimer, tissue plasminogen activator (TPA) and plasminogen activator inhibitor (PAI-1) in both groups were compared during the first 30 days of treatment. Finally, incidences of recurrent stroke and clinical outcomes of patients in both groups were compared over the 180-day treatment period.

Clinical Trial Registration-URL: www.clinicaltrials.gov, unique identifier: NCT01321749.

Findings: BLIPC had no adverse effects on blood pressure, heart rate, local skin integrity and plasma myoglobin, and did not increase symptomatic cerebral hemorrhage in octogenarians. BLIPC decreased plasma levels of hsCRP, IL-6, PAI-1, leukocyte count, platelet aggregation rate, and increased TPA. Incidences of recurrent stroke and TIA were significantly lower in the BLIPC group (6.7% and 23.3%) compared to controls (28.6% and 39.3%, P = 0.027 and 0.035 respectively).

Interpretation: BLIPC is a safe and feasible method to protect brain in octogenarians with symptomatic intracranial arterial stenosis. BLIPC may decrease the incidence of recurrent stroke and ameliorate biomarkers of inflammation and coagulation.

References:

1. Przyklenk K, Bauer B, Ovize M, Kloner RA, Whittaker P. Regional ischemic ´preconditioning´ protects remote virgin myocardium from subsequent sustained coronary occlusion. Circulation 1993;87:893-899.

2. Botker HE, Kharbanda R, Schmidt MR, Bottcher M, Kaltoft AK, Terkelsen CJ, et al. Remote ischaemic conditioning before hospital admission, as a complement to angioplasty, and effect on myocardial salvage in patients with acute myocardial infarction: a randomised trial. Lancet 2010;375:727-734.

3.Ran Meng, Karam Asmaro, Lu Meng, Chun Ma,; Yu Liu,; Chunjiang Xi, Guoqing Li, Canghong Ren; Yumin Luo,; Feng Ling, Jianping Jia,; Yang Hua, Xiaoying Wang,; Yuchuan Ding,; Eng H Lo, [2]; Xunming Ji, ' Bilateral Arm Ischemic Preconditioning Prevents Recurrent Stroke in Intracranial Arterial Stenosis. Neurology; 2012;79(18):1853-1861

A NOVEL APPROACH TO NEUROPROTECTION: INHIBITING 12/15-LIPOXYGENASE TO TREAT STROKE

H. Karatas[1], K. Yigitkanli[1], J.E. Jung[1], A. Pekcec[1], E.T. Mandeville[1], Y. Liu[1], J. Montaner[2], T.R. Holman[3], E.H. Lo[1], **K. van Leyen**[1]

[1]Neuroprotection Research Laboratory, Massachusetts General Hospital and Harvard Medical School, Charlestown, MA, USA, [2]Neurovascular Research Laboratory, Vall d'Hebron University Hospital Research Institute, Barcelona, Spain, [3]Chemistry, University of California Santa Cruz, Santa Cruz, CA, USA

Objectives: New approaches are necessary to develop novel therapeutics as treatment for ischemic stroke[1]. We and others have previously shown that 12/15-lipoxygenase (12/15-LOX) contributes to acute brain injury in mice subjected to experimental stroke[2-4]. We are now targeting 12/15-LOX with a small molecule inhibitor[5], with the aim of reducing oxidative stress-related injury to both vasculature and neurons. We here tested the neuroprotective effects of the novel 12/15-LOX inhibitor LOXBlock-1 in several models of focal ischemia.

Methods: Transient focal ischemia was induced by filament occlusion of the middle cerebral artery (MCAO), or by inducing thrombosis using iron chloride (distal MCAO)[6, 7]. Recombinant tPA was used with or without LOXBlock-1 to achieve thrombolysis. Intracerebral hemorrhage (ICH) was induced by injecting bacterial collagenase into the striatum. Hemorrhage was measured either photometrically or by DAB staining. 12-HETE was measured using an enzyme immunoassay kit. LOXBlock-1 was administered by intraperitoneal injection.

Results: 12/15-LOX and its product 12-HETE were increased in the ischemic hemisphere following transient focal ischemia in the filament model. LOXBlock-1 reduced both infarct size and 12-HETE levels in the brain, without increasing injury in the ICH model. LOXBlock-1 reduced tPA-associated hemorrhage in the distal MCAO model, and reduced infarct size both in the presence or absence of tPA.

Conclusions: LOXBlock-1 provides efficient neuroprotection in a variety of ischemic stroke models, including both transient and permanent focal ischemia. LOXBlock-1 shows promise as a neuroprotectant in clinically relevant scenarios, including both as a stand-alone first line treatment, and as an adjuvant to thrombolysis with tPA.

References:

[1] Moskowitz MA, Lo EH, Iadecola C. Neuron. 2010 Jul 29;67 (2):181-98.

[2] Khanna S, Roy S, Slivka A, et al. Stroke. 2005 Oct;36 (10):2258-64.

[3] van Leyen K, Kim HY, Lee SR, Jin G, Arai K, Lo EH. Stroke. 2006 Dec;37 (12):3014-8.

[4] Jin G, Arai K, Murata Y, et al. Stroke. 2008 Sep;39 (9):2538-43.

[5] van Leyen K, Arai K, Jin G, et al. J Neurosci Res. 2008 Mar;86 (4):904-9.

[6] Karatas H, Erdener SE, Gursoy-Ozdemir Y, et al. J Cereb Blood Flow Metab.

2011 Jun;31 (6):1452-60.

[7] Yigitkanli K, Pekcec A, Karatas H, et al. Ann Neurol, 2012; doi 10.1002/ana. 23734 In Press

HAMARTIN IS A NOVEL NEUROPROTECTIVE TARGET MEDIATING THE RESISTANCE OF CA3 HIPPOCAMPAL NEURONS TO GLOBAL ISCHEMIA BY INDUCING AUTOPHAGY

M. Papadakis[1], G. Hadley[1], M. Xilouri[2], M.M. McMenamin[3], M.J. Wood[3], K. Vekrellis[2], A.M. Buchan[1]

[1]Radcliffe Department of Clinical Medicine, University of Oxford, Oxford, UK, [2]Division of Basic Neurosciences, Biomedical Research Foundation of the Academy of Athens, Athens, Greece, [3]Department of Physiology, Anatomy and Genetics, University of Oxford, Oxford, UK

Objectives: The endogenous resistance of CA3 hippocampal neurons to global forebrain ischemia has unexplored potential to provide novel neuroprotective targets. Proteomic studies investigating the events induced in the CA3 area demonstrated that following ischemia, the expression of hamartin (the gene product of tuberous sclerosis complex 1

(TSC1)), was selectively induced[1]. Hippocampal primary neurons and CA3 neurons in which hamartin expression had been attenuated by TSC1 shRNA lentiviral vectors, showed increased vulnerability to oxygen glucose deprivation (OGD) and ischemia, respectively[1].

Hamartin induces autophagy by inhibiting the molecular target of rapamycin (mTOR)[2]. Autophagy degrades damaged organelles and protein aggregates by enclosing them inside autophagosomes and digesting them with hydrolases following fusion with lysosomes, the efficient completion of which is termed productive autophagy[3]. Our objective was to establish the neuroprotective capacity of hamartin by overexpression experiments and by delineating the involvement of autophagy in its molecular mechanism.

Methods: E-18 primary hippocampal neurons transduced with TSC1 shRNA, pEZ-Lv201 TSC1 (rat TSC1) or control lentiviral vectors were subjected to 3h OGD and 24h reperfusion. Cell survival was quantified by counting the number of intact nuclei[4]. Cell homogenates were analysed by immunoblotting and probed with anti-phospho-S6 Ribosomal Protein (p-S6RP), anti-LC3 and anti-p62 antibodies to assess mTOR activity, autophagosome formation and autophagic flux, respectively. Autophagy-dependent lysosomal proteolysis was measured with protein degradation assays[5]. Cell cultures were treated with the mTOR inhibitor, rapamycin (10nM) or the autophagy inhibitor, 3-Methyladenince (3MA; 10mm) 24h before OGD.

Results: S6RP phosphorylation was increased in TSC1 shRNA-treated primary hippocampal neurons compared to control shRNA-transduced neurons (p=0.0066). Pretreatment with rapamycin of TSC1 shRNA-transduced cultures exposed to OGD restored cell viability to levels of control shRNA-transduced cultures (p< 0.001).

Cultures transduced with rat TSC1 vectors showed 31±8.9% higher resistance to OGD compared to control-transduced neurons. Following OGD, transduction of hippocampal neurons with rat TSC1 upregulated LC3-II expression (p=0.036), suppressed p62 expression 1.8±0.2 fold (p=0.036) and increased autophagy-dependent lysosomal degradation 5.4±0.4 fold (p< 0.05) all compared to control-transduced cultures. 3MA abolished the protection to OGD conferred by rat TSC1, reducing surviving cells to 49.7±3.9% of untreated cultures overexpressing hamartin (p< 0.001)

Conclusions: Hamartin suppression in primary hippocampal neurons exacerbated injury following OGD by overactivating mTOR, which was reversed with rapamycin. The neuroprotective properties of hamartin were directly demonstrated by the increased resistance to OGD of hamartin-overexpressing neurons. This protection was abolished by inhibiting autophagy with 3MA. Hamartin overexpression significantly increased LC3-II and decreased p62 expression levels, indicating that autophagosme formation and autophagic flux were increased. In addition, autophagy-dependent lysosomal degradation was induced. Overall, hamartin is a novel neuroprotective target, increasing resistance to OGD by inducing productive autophagy via mTOR.

References:

1. Papadakis M. et al. (2011) abstract, XXVth International Symposium on Cerebral Blood Flow, Metabolism and Function, Barcelona, Spain.

2. Tee A.R. et al. (2002) Proc. Natl. Acad. Sci. U. S. A 99, 13571-13576.

3. Gabryel B. et al. (2012) Pharmacol. Rep. 64, 1-15.

4. Xilouri M. et al. (2009) PLoS. One. 4, e5515.

5. Jakobsson J. & Lundberg C. (2006) Mol. Ther. 13, 484-493.

REPETITIVE HYPOXIC PRECONDITIONING MODULATES ADAPTIVE IMMUNE MECHANISMS PRIOR TO STROKE

S.J. Ireland[1], M. Li[1], E. Shubel[1], V. Fontanier[1], J.D. Hankins[1], A.J.M. Meeuwissen[1], R. Zhang[1,2], J.M. Gidday[3], N.L. Monson[1], **A.M. Stowe**[1]

[1]Dept. of Neurology & Neurotherapeutics, UT Southwestern Medical Center, [2]Institute for Experimental and Environmental Medicine, Texas Health Presbyterian Hospital, Dallas, TX, [3]Dept. of Neurological Surgery, Washington University School of Medicine, St. Louis, MO, USA

Objectives: Repetitive hypoxic preconditioning (RHP) creates a naturally-protective, long-lasting anti-inflammatory phenotype that reduces neurovascular injury in murine stroke, despite only moderately reducing post-ischemic leukocyte diapedesis.[1] More recent data from our lab show that $CD19^+$ B cells move out of the peripheral circulation and into the ischemic cortex to represent one-third of total leukocytes in RHP-treated mice two days following reperfusion. This suggests a potential protective role for B cells selectively recruited into the ischemic hemisphere by RHP. As one brief exposure to systemic hypoxia significantly increases peripheral B cell representations,[2] we sought to determine if RHP induces sustained elevations in resident B cell populations prior to stroke onset, and, in addition, whether these B cells were phenotypically altered by RHP.

Methods: Adult male SW/ND4 mice were exposed to RHP (9 exposures over 2 wks; 8% or 11% O_2; 2 or 4 h duration, with 21% O_2 as control).[1] One and two weeks following RHP, leukocytes were isolated from peripheral blood and spleen, stained with antibodies, and profiled on a BD-FACS Aria flow cytometer (n=5-10/group). Student's t-test determined significance ($p< 0.05$). Additionally, sorted $CD19^+$ B cells were isolated from spleen at 2 wks after RHP by flow cytometry (n=5/group), analyzed on an Illumina MouseWG-6 V2 Bead Chip, and final gene pathways determined using Ingenuity Pathway Analysis (IPA).

Results: Two weeks after the final hypoxic exposure, but not one week, RHP increased peripheral, circulating leukocytes ($p=0.06$), with a significant increase in only B cell populations ($p< 0.05$). Levels of monocytes, CD4 and CD8 T cells, and neutrophils did not change. RHP also induced a non-significant increase in total B cells in the spleen. The overall gene expression profiles of B cells isolated from control mice show a distinct clustering, with unique differentiation from 4 out of 5 RHP-treated mice. RHP altered over 1,900 genes, including a 6,800-fold downregulation of HLA-DOB, selectively expressed in B cells and required for antigen presentation under the transcriptional regulation of the MHC class II transactivator,[3] which was also downregulated (-1.68-fold; $p=4.6E-06$). In fact, the canonical pathway with the greatest downregulation and second-highest significance was the antigen presentation pathway (13/29 genes; 85% downregulated; $p=3.5E-06$). Other biological functions significantly downregulated (z-scores >-2) include development and differentiation of lymphocytes, quantity of IgG, B and T cells, and the production of antibodies.

Conclusions: RHP reprograms B cells to exhibit an immunosuppressive phenotype even prior to stroke, as reflected by alterations in gene expression, antigen presentation, antibody production, and biological functions; this B cell phenotype may contribute to the cerebroprotection afforded by RHP. Studies to validate the role of B cells in minimizing injury and promoting CNS recovery, to analyze the temporal-spatial features of the B cell subset expression profile, and to determine whether B cells mediate an adaptive immunity to systemic hypoxia that protects from subsequent stroke in RHP-treated mice are underway.

References:

1. Stowe, A.M., et al., Ann Neurol, 2011. PMID:21437933

2. Stowe, A.M., et al., J Neuroinflammation, 2012. PMID:22340958

3. Nagarajan, U.M., et al., J Immunol, 2002. PMID:11823510

ROLE OF LYMPHATIC DRAINAGE FROM CNS IN THE DEVELOPMENT OF CEREBRAL VASOSPASM AND RELATED CEREBRAL ISCHEMIC INJURY FOLLOWING SUBARACHNOID HEMORRHAGE

B.-L. Sun[1], X. Wang[1], Z.-Y. Zhang[1], M.-F. Yang[1], D.-W. Li[1], H. Yuan[1], Y.-B. Zhang[1], X.-Y. Yang[1], X. Hu[1,2], F. Zhang[1,2]

[1]Key Lab of Cerebral Microcirculation in Universities of Shandong, Department of Neurology, Affiliated Hospital, Taishan Medical University, Taian, China, [2]Center of Cerebrovascular Disease Research, University of Pittsburgh School of Medicine, Pittsburgh, PA, USA

Objectives: Recent studies suggest that cerebral lymphatic drainage to extracranial lymph compartments may be a major route for cerebrospinal fluid (CSF) to circulate back to blood; therefore cerebral lymphatic drainage my play an important role in the removal of large molecular substances in the brain and CSF. Following subarachnoid hemorrhage (SAH), large amount of macromolecular

substances, such as cellular lysates, proteins and peptides, were accumulated in the subarachnoid space, CSF and brain tissues, which may contribute to pathogenesis of cerebral vasospasm and related cerebral ischemic injury. The present study was carried out to investigate 1) the effect of cerebral lymphatic drainage on the pharmacokinetics of CSF protein clearance, and 2) the possible role of cerebral lymphatic drainage in preventing cerebral vasospasm and related ischemic brain injury.

Methods: Cerebral lymphatic blockade (CLB) was accomplished by ligating the cervical lymphatic input and output tubes and removing bilateral shallow and deep lymphatic nodes in male adult Wistar rats. ^{125}I-labeled human albumin (100µg) was used as a macromolecular tracer and stereotypically injected into the intacerebral ventricle. Radioimmunoassay was used to detect plasml levels of ^{125}I-labeled albumin, and a concentration-time curve was subsequently established. Peak concentration (Cmax) of the albumin, time of maximal concentration (Tmax) and elimination rate constant (Ka) were calculated. SAH was induced by double cisternal injections of autologus arterial blood; in selected rats, CLB was performed one day prior to SAH. The diameter of basilar artery (BA) was measured 48 hours after SAH via a transclivus approach. The pathological alterations of BA were exanimated under light microscope, and immunofluorescent staining was performed to detect caspase-3 levels in brain sections.

Results: Cerebral lymphatic blockade decreased Cmax by 68.82%, delayed Tmax by 5.47 hours and decreased Ka by 43.24%, suggesting that a good proportion of macromolecular substances in CSF was removed by lymphatic drainage. In rats with SAH, a decrease in the diameters of BA occurred, accompanied by increased BA wall thickness and decreased BA cavity areas. Caspase-3 positive cells were also observed in the cortex. In SAH+CLB group, more severe vasospasm of BA was observed. Immunostaining and DAPI staining showed that the number of apoptotic cells also increased after CLB, indicating that CLB deteriorates SAH induced cerebral vasospasm and related cerebral ischemic injury.

ISCHEMIC PRECONDITIONING REGULATES MITOCHONDRIAL NAMPT VIA THE PROTEIN KINASE C EPSILON-AMPK PATHWAY IN CORTICAL CULTURES

K.C. Morris-Blanco, J.T. Neumann, M.A. Perez-Pinzon

Neurology, University of Miami Miller School of Medicine, Miami, FL, USA

Objectives: Protein kinase C epsilon (PKCε) and AMP-activated protein kinase (AMPK) have been previously implicated in ischemic preconditioning (IPC)[1,2], a paradigm where a brief ischemic insult protects the brain against subsequent lethal ischemia. AMPK enhances expression of nicotinamide phosphoribosyl transferase (Nampt)[3], the major biosynthetic pathway for NAD^+/NADH production. Nampt overexpression has been shown to protect the brain against ischemic injury in an AMPK-dependent manner[4]. However, whether mitochondrial-localized Nampt is regulated by IPC-mediated protective pathways is currently unknown. Therefore, we hypothesized that PKCε and AMPK may functionally cooperate to provide ischemic protection and may regulate mitochondrial pools of Nampt during IPC, or treatment with the IPC mimetic resveratrol.

Methods: Preconditioning was induced by exposing cortical glial-neuronal cultures to 1h of oxygen- glucose deprivation (IPC), resveratrol (25uM) (RPC), εPKC agonist ψεRACK (100nM) (εPC), or AMPK activator AICAR (0.5mM) (APC) with pharmacological inhibitors εV1-2 (εPKC antagonist) (100nM; or 250nM during IPC) or Compound C (CC) (AMPK inhibitor) (15uM). Forty-eight hours following preconditioning cultures were subjected to lethal oxygen-glucose deprivation (OGD). Neuronal cell death was analyzed using lactate dehydrogenase (LDH) assay 48h following lethal OGD. Western blot analysis was used to determine protein levels in whole cell lysates or mitochondrial fractions.

Results: We first examined whether AMPK and PKCε activity is integral for IPC and resveratrol-mediated protection against lethal ischemia. IPC and RPC reduced cell death following lethal OGD by 32.1±7.6% ($p < .001$, $n=6$) and 25.0±4.4% ($p < .001$, $n=6$), respectively, which was reversed with exposure to CC or εV1-2. The addition of CC during εPC, or εV1-2 during APC reversed

ischemic protection mediated by PKCε and AMPK activity (p< .01, n=7; p< .01, n=5, respectively) (Fig.1a), indicating PKCε and AMPK require each other for protection. We next determined whether PKCε and AMPK are involved in activating each other. Exposure to εV1-2 during IPC or RPC blocked increased AMPK^{Thr172} phosphorylation (p< .05, n=4; p< .05, n=6, respectively). Similarly, CC treatment during IPC or RPC, inhibited increased phospho-PKCε^{Ser729} (p< .01, n=6; p< .01, n=6, respectively) (Fig1b,c). Mitochondrial fractions isolated 48h following εPC or APC revealed significant increases in Nampt levels (p< .05, n=4; p< .05, n=4, respectively). IPC also induced mitochondrial Nampt which was blocked with the addition of CC (p< .05, n=4) or εV1-2 (p< .05, n=4) (Fig.2a,b)

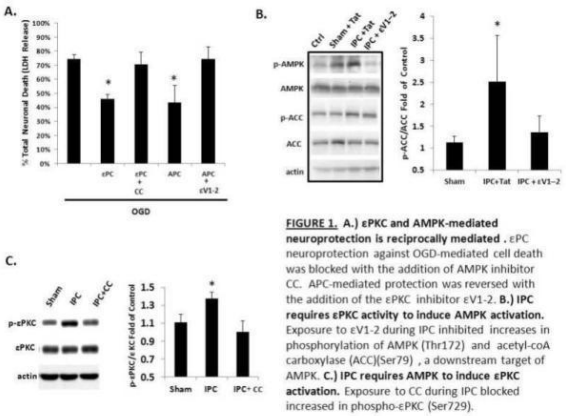

FIGURE 1. A.) εPKC and AMPK-mediated neuroprotection is reciprocally mediated . εPC neuroprotection against OGD-mediated cell death was blocked with the addition of AMPK inhibitor CC. APC-mediated protection was reversed with the addition of the εPKC inhibitor εV1-2. **B.) IPC requires εPKC activity to induce AMPK activation.** Exposure to εV1-2 during IPC inhibited increases in phosphorylation of AMPK (Thr172) and acetyl-coA carboxylase (ACC)(Ser79) , a downstream target of AMPK. **C.) IPC requires AMPK to induce εPKC activation.** Exposure to CC during IPC blocked increased in phospho-εPKC (Ser729).

[Figure 1]

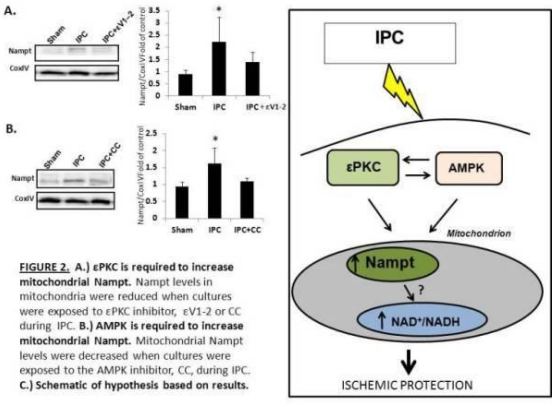

FIGURE 2. A.) εPKC is required to increase mitochondrial Nampt. Nampt levels in mitochondria were reduced when cultures were exposed to εPKC inhibitor, εV1-2 or CC during IPC. **B.) AMPK is required to increase mitochondrial Nampt.** Mitochondrial Nampt levels were decreased when cultures were exposed to the AMPK inhibitor, CC, during IPC. **C.) Schematic of hypothesis based on results.**

[Figure 2]

.

Conclusions: This study has revealed that PKCε and AMPK are both important mediators of IPC or resveratrol-mediated ischemic neuroprotection in cortical cultures. Our data indicate that PKCε and AMPK reciprocally mediate each other's activation and ability to provide ischemic neuroprotection. We further show that this PKCε-AMPK pathway regulates mitochondrial pools of Nampt, an important enzyme in the production of NAD^+/NADH (Fig.2c). These novel findings may shed light on how NAD^+/NADH is modulated during IPC.

References:

1. Raval et al. (2003). *J Neurosci*

2. Nishino et al. (2004). *Cardiovas Res*

3. Fulco et al. (2008). *Dev Cell*

4. Wang et al. (2011). *Ann Neurol*

Support: AHA(10PRE3050053), NIH(NS45676, NS054147, NS34773)

REST-DEPENDENT EPIGENETIC REMODELING PROMOTES THE *IN VIVO* DEVELOPMENTAL SWITCH IN SYNAPTIC NMDA RECEPTORS

A. Rodenas-Ruano, A.E. Chávez, P.E. Castillo, **R.S. Zukin**

Dominick P. Purpura Department of Neuroscience, Albert Einstein College of Medicine, New York, NY, USA

NMDA receptors (NMDARs) are critical to synaptogenesis, neural circuitry and higher cognitive functions. The precise subunit composition determines NMDAR functional properties. A hallmark feature of NMDARs is an early postnatal developmental switch from those containing primarily GluN2B to primarily GluN2A subunits. This is significant in that GluN2B expression can restrict synaptic incorporation of AMPARs, reduce the threshold for and enhance the magnitude of long-term potentiation (LTP), and promote hippocampal-dependent learning, plasticity-induced spine growth, and dendritic patterning critical to information processing. Although the switch in phenotype has been an area of intense interest for two decades, the mechanisms that trigger it and the link between experience and the switch are unclear. Here we show a new role for the transcriptional repressor element 1 silencing transcription factor (REST, also known as NRSF) in the developmental switch of synaptic NMDARs. REST is activated at a critical window of time early in postnatal development

and acts *via* epigenetic remodeling to repress *grin2b* expression and alter NMDAR properties at rat hippocampal synapses. RNAi-mediated knockdown of REST *in vivo* prevented the decline in GluN2B and developmental switch in NMDARs. A prevailing view has been that REST serves as a master regulator of neuronal gene expression in pluripotent stem cells and neural progenitors. To our knowledge, our study is the first demonstration that REST-dependent epigenetic modifications alter properties of a synaptic protein in differentiated neurons and that REST can regulate synaptic function. We further show that adverse early life experience in the form of maternal deprivation impairs REST activation, alters the epigenetic landscape at the *grin2b* promoter, and prevents acquisition of the mature NMDAR phenotype at hippocampal synapses. Thus, REST is essential for experience-dependent fine-tuning of genes involved in synaptic plasticity. Given the widespread localization of NMDARs in the CNS, REST dependent regulation of the NMDAR phenotype at synapses during normal and abnormal brain development is a powerful mechanism to modulate synaptic efficacy. These findings are relevant to our understanding of NMDAR function, as it pertains to memory formation, synaptic stabilization, brain development and cognitive information flow, and how its dysregulation can cause the neurodegeneration associated with stroke, epilepsy and Huntington´s disease.

MTOR PATHWAY IN THE NEUROPROTECTIVE MECHANISMS OF ISCHEMIC POSTCONDITIONING

P. Wang[1,2,3], R. Xie[1,4], X. Ji[2], H. Zhao[1]

[1]Neurosurgery, Stanford University, Palo Alto, CA, USA, [2]Neurosurgery, Xuanwu Hospital, Capital Medical University, Beijing, [3]Neurosurgery, Huashan Hospital (Jingan Branch), Fudan University, [4]Neurosurgery, Huashan Hospital, Fudan University, Shanghai, China

Introduction: In brain mTOR activity is required for neuron survival. Ischemic postconditioning, which refers to a series of temporary blood flow occlusions at the beginning period of reperfusion after stroke, protects against brain injury. We investigated how ischemic postconditioning promotes brain recovery by regulating the mTOR pathway from 1 to 3 weeks after stroke. We also measured neuronal markers GAP-43,PSD-95 and MAP-2, which are closely related with neuronal survival.

Method: We constructed lentiviral vectors containing the S6K and mTOR-shRNA genes. The GFP virus and scramble virus were used as a control respectively.

Focal ischemia was generated by permanent distal MCA occlusion combined with 30 min of transient bilateral CCA occlusion in male SD rats. Ischemic postconditioning was performed by 3 cycles of 30s reperfusion/10s occlusion of the bilateral CCA at the beginning of reperfusion. Rapamycin, an mTOR inhibitor, was injected into the cerebral ventricle one hour before stroke. The viral vectors were injected into the cortex 5 days before stroke onset. Brain injury sizes were evaluated 3 weeks after stroke. Behavioral tests, including home cage and vibrissa-elicited limb use tests, were examined at 1d, 2d, 3d, 1w, 2w and 3w after stroke.

Ischemic brains corresponding to the peri-infarct area were harvested at 1w and 3w after stroke onset. In S6K lentiviral vector injection experiments, brain tissue around the needle track were dissected at 1h, 5h, 24h, 1w and 3w after stroke onset. To investigate the effects of mTOR-shRNA on the protein expression of the mTOR pathway, brain tissue around the needle track were dissected at 1w and 3w after stroke.

Results:

1. Ischemic postcondtioning significantly decreased infarct size at 3 weeks after stroke injury ($p < 0.05$). The behavior performance of rats in home cage and vibrissa-elicited limb use tests were significantly better in ischemic postconditioning groups than rats in control stroke groups at 1 week and 2 weeks after stroke ($p < 0.05$). Rapamycin diminished these effects of ischemic postconditioning.

2. Main elements of mTOR pathway (total and phosphorylated mTOR, S6K and 4ebp-1) were significantly upregulated in ischemic postconditioning groups at 1 week after stroke ($p < 0.05$). Neuron markers, MAP-2, GAP-43 and PSD-95 also were significantly upregulated in ischemic postconditioning groups than in control stroke groups at 1 week after stroke ($p < 0.05$). Rapamycin diminished up-regulation of mTOR pathway and associated neuron marker molecules in postconditioning groups ($p < 0.05$). mTOR-shRNA also diminished the up-regulation of

mTOR pathway and associated molecules by ischemic postconditioning at 1 week after stroke ($p < 0.05$).

3. In S6K virus experiments total and phosphorylated S6K and 4ebp-1 were significantly up-regulated in S6K virus groups at 5h, 24h, 1w and 3w after stroke ($p < 0.05$). The expression of MAP-2, GAP-43 and PSD-95 also were significantly up-regulated in S6K virus groups at the same time points ($p < 0.05$).

Conclusion: Ischemic postconditioning improved the neural repair and behavior test results in the recovery period of stroke. The neuroprotective effects of postconditioning are associated with the up-regulation of proteins in the mTOR pathway and other neuronal synaptic and dendritic proteins.

EXPRESSION AND ROLE OF IQGAP1 IN THE BRAIN AFTER FOCAL ISCHEMIA

Y. Yagita, K. Kitagawa, N. Oyama, T. Yukami, A. Watanabe, T. Sasaki, H. Mochizuki

Neurology, Osaka University Graduate School of Medicine, Suita City, Japan

Objectives: Dysfunction of the endothelial adherence junction accelerates vascular permeability and aggravation of brain ischemic injury. VE-cadherin mediates the adherence junction between the endothelial cells. Adhesive ability of VE-cadherin is regulated by interaction with associated proteins. IQGAP1, a scaffold protein, can regulate cell-cell adhesion through binding to β-catenin and dissociation of cadherin-catenin system from the actin cytoskeleton. It is reported that vascular endothelial growth factor (VEGF) can induce IQGAP1 association with cadherin system. Because VEGF expression is induced after brain ischemia, IQGAP1 may be involved in regulation of endothelial adherence junction in the ischemic brain. The aim of this study is

(1) to elucidate the expression profile of VE-cadherin and IQGAP1 after cerebral ischemia,

(2) to assess the interaction between β-catenin and IQGAP1 and

(3) to evaluate the effect of VEGF on IQGAP1 expression.

Methods: Male Wistar rats were subjected to middle cerebral artery (MCA) occlusion with the use of a 4-0 nylon monofilament and reperfusion 80 min after induction of ischemia. Tissue injury was evaluated by immunohistochemistry. Double immunofluorescent staining with cell markers was performed to evaluate the localization of IQGAP1. Western blot was performed using primary antibody against IQGAP1, VE-cadherin, β-catenin and β-actin. Brain samples were taken from the MCA area at the each period after ischemia. The supernatant of the tissue homogenate was precipitated with antibody against IQGAP1 using protein A/G agarose. VEGF (10ng/μl) was chronically treated in the cerebral ventricle using osmotic minipump (1μl/hour).

Results: In the normal brain, IQGAP1 was mainly expressed in the endothelial cell and neuronal progenitor cell in the subventricular zone. In the present cerebral ischemia model, endothelia were preserved even in the MCA core in the cerebral cortex. Western blot analysis revealed that VE-cadherin expression was not significantly changed in the MCA core at the period of 6 and 24 hours after ischemia ($n=5$). IQGAP1 expression was increased ($n=5$, $P < 0.05$) and immunohistochemical analysis showed that it localized in the endothelial cells 24 hours after ischemia. Co-immunoprecipitation analysis revealed that IQGAP1 was more strongly associated with β-catenin 24 hours after ischemia than in the normal brain. Intracerebral ventricular injection of VEGF induced the IQGAP1 expression in the endothelia of brain small vessels.

Conclusions: These findings suggest that VE-cadherin-mediated cell-cell adhesive activity is decreased by interaction between IQGAP1 and β-catenin after cerebral ischemia. VEGF signal may regulate IQGAP1 activity in the brain small vessels. In order to estimate adhesive activity, it is necessary to assess interaction between VE-cadherin and IQGAP1. This system may be a therapeutic target in the acute brain ischemia.

ROLE OF TOLL-LIKE RECEPTORS IN THE REGULATION OF BRAIN ENDOTHELIAL FUNCTION

I. Krizbai, I. Wilhelm, A.E. Farkas, C. Fazakas, Á. Nyúl-Tóth, J. Haskó, J. Molnár, P. Nagyőszi

Institute of Biophysics, Biological Research Centre, Szeged, Hungary

Objectives: Cerebral endothelial cells - the principal components of the blood-brain barrier (BBB) - fulfill several important functions in the central nervous system (CNS). They form an active interface between the blood and the neuronal tissue and play a key role in the maintenance of the homeostasis of the CNS. The functional integrity of the blood-brain barrier may be affected by systemic inflammations caused by different pathogens. In this process Toll-like receptors (TLRs) play an important role. These receptors recognize a broad range of exogenous and endogenous molecules and initiate inflammatory reactions. Toll-like receptors are mainly distributed on cells of the immune system but there is also growing experimental evidence suggesting TLR expression on different non-immune type cells as well, like epithelial and endothelial cells. The goal of our study was to investigate the role of Toll-like receptors in the pathophysiology of the blood-brain barrier.

Methods: We have used an in vitro BBB model based on the culture of primary rat brain endothelial cells and the hCMEC/D3 human cerebral endothelial cell line.

Results: Our results showed that cells of a human brain endothelial cell line (hCMEC/D3) express TLR2, 3, 4 and 6, while primary rat brain endothelial cells express TLR2, 3 and 6 under basal conditions. The mRNA expression of all identified human endothelial Toll-like receptors was induced by oxidative stress caused by DMNQ, whereas TNF-alpha upregulated the expression of TLR2 and TLR3. Zymosan, a TLR2/6 agonist elevated the expression of these two receptors while having no effect on the expression of TLR3 and 4. Moreover, zymosan treatment increased the permeability of the endothelial cell cultures accompanied by a decrease in the expression of occludin and claudin-5 and loss of membrane staining of these two transmembrane components of the tight junctions. U0126, the ERK1/2 kinase inhibitor was able to prevent the changes of occludin caused by zymosan.

Conclusions: Our results are the first to identify the presence of Toll-like receptor 6 besides TLR2, 3 and 4 in cerebral endothelial cells. TLR2/6 activation causes tight junction disruption, mediated partly by ERK 1/2 kinases. Furthermore, TLRs can be upregulated by oxidative stress in cerebral endothelial cells, suggesting that oxidative stress may play a potentiating role in endothelial dysfunction caused by infections. Our results suggest a significant role of the cerebral endothelium in mediation of the CNS effects of different inflammatory processes.

TARGETING ORGANIC ANION TRANSPORTING POLYPEPTIDES TO TREAT PAIN AND HYPOXIA/REOXYGENATION STRESS

P.T. Ronaldson, L.M. Slosky, B.J. Thompson, T.P. Davis

Pharmacology, University of Arizona College of Medicine, Tucson, AZ, USA

Objectives: Limited drug penetration is an obstacle to effective treatment of CNS diseases (i.e., pain, hypoxia/reoxygenation (H/R) stress). Brain biochemical characteristics (i.e., tight junction complexes, expression of influx/efflux transporters) determine CNS drug permeation (Seelbach et al. 2007; Lochhead et al. 2011; Ronaldson et al. 2011); however, most studies have focussed on understanding mechanisms that prevent CNS drug accumulation. Recently, brain targets that directly facilitate drug delivery have been identified. One potential target is the organic anion transporting polypeptides (OATP in humans; Oatp in rodents) that facilitate drug uptake, including efficacious therapeutics for treatment of pain and/or H/R (i.e., opioid analgesic peptides, HMG CoA reductase inhibitors) (Ronaldson et al. 2011; Ronaldson & Davis, 2012). The objectives of this study were to investigate, *in vivo,* effects of i) peripheral inflammatory pain (PIP) and ii) H/R stress on Oatp-mediated drug transport at the BBB.

Methods: PIP was induced in female Sprague-Dawley rats (200-250 g) by subcutaneous injection of 3% λ-carrageenan into the plantar surface of the right hind paw. Control animals were injected with 0.9% saline instead of λ-carrageenan. To examine effects of H/R stress, female Sprague-Dawley rats (200-250 g) were subjected to normoxia (Nx 21% O2, 60 min), hypoxia (Hx, 6% O2, 60 min) or H/R (6% O2, 60 min followed by 21% O2, 10 min). Following treatment, animals were sacrificed and brain microvessels isolated. Protein expression of Oatp1a4 was determined using western blot analysis. Brain permeability to [^{3}H]taurocholate (1.0 µCi/ ml perfusate), [^{3}H]D-penicillamine(2,5)-enkephalin (DPDPE; 0.5 µCi/ ml perfusate), and [^{3}H]atorvastatin (1.0 µCi/ ml perfusate), three established Oatp1a4 substrates, were

assessed using *in situ* brain perfusion and capillary depletion.

Results: Following PIP and H/R, both Oatp1a4 protein expression and brain taurocholate accumulation were increased. Taurocholate uptake was reduced in the presence of Oatp1a4 inhibitors (100 µM estrone-3-sulfate, 100 µM fexofenadine), further suggesting involvement of Oatp1a4 in BBB taurocholate transport. Capillary depletion analysis showed a time-dependent increase in brain parenchyma associated taurocholate, implying that this Oatp1a4 substrate accumulated within CNS tissue and was not trapped within brain microvessels. Oatp1a4-mediated DPDPE uptake was enhanced during PIP while Oatp1a4-mediated atorvastatin uptake was increased during H/R, suggesting that Oatp1a4 can be targeted to optimize CNS drug delivery. During PIP and/or H/R, pharmacological inhibition of TGF-β/ALK5 signaling with the selective TGF-β/ALK5 inhibitor SB431542 increased Oatp1a4 functional expression, which implicates this pathway in regulation of Oatp1a4 at the BBB.

Conclusions: These data demonstrate that targeting an endogenous BBB transporter may be a viable approach for delivering drugs to the brain during PIP and/or H/R. Our study also identifies an endothelial intracellular signaling mechanism that can be targeted to control BBB Oatp1a4 functional expression for optimization of CNS drug delivery.

References:

1. Lochhead et al. (2011). *Am J Physiol Heart Circ Physiol.* **302**: H582-H593.
2. Ronaldson et al. (2011). *J Pharmacol Exp Ther.* **336**: 827-839.
3. Ronaldson & Davis (2012). *Pharmacol Rev.* **In press.**
4. Seelbach et al. (2007). *J Neurochem.* **102**: 1677-1690.

This work was supported by NIH grant R01-DA11271 to TPD and AHA grant 12BGIA-9850007 to PTR.

SPATIO-TEMPORAL DYNAMICS OF MORPHOLOGICAL CHANGES IN NEURO-GLIA-VASCULAR UNIT AFTER CEREBRAL ISCHEMIA MEASURED WITH TWO-PHOTON MICROSCOPY IN MOUSE CORTEX

K. Masamoto[1,2], T. Abe[3], H. Takuwa[2], H. Toriumi[3], Y. Tomita[3], M. Unekawa[3], Y. Itoh[3], H. Kawaguchi[2], H. Ito[2], N. Suzuki[3], I. Kanno[2]

[1]University of Electro-Communications, Tokyo, [2]National Institute of Radiological Sciences, Chiba, [3]Keio University School of Medicine, Tokyo, Japan

Objectives: It has become clear that neuro-glia-vascular unit (NGVU) has a crucial role in rescuing and repairing the central nervous system functions after events of cerebral ischemia. In the present study, spatio-temporally varying changes of NGVU following transient episodes of cerebral ischemia induced by middle cerebral artery occlusion (MCAO) were characterized with *in vivo* two-photon microscopy in the anesthetized mouse cortex.

Methods: Animal use and experimental protocols were approved by the Institutional Animal Care and Use Committee. A total of 12 male Tie2-GFP transgenic mice (21-31 g) in which vascular endothelium had expressed green fluorescent proteins (GFP) were used for the experiments. A week before the surgery of MCAO, a 3-4 mm diameter of closed cranial window with a custom-made attachment device for imaging stage was made over the left parietal region of the mouse head (Tomita et al., 2005). Under isoflurane anesthesia (1.5-2.0%) with maintaining the animal body temperature (37 ºC), a transient MCAO was performed with inserting surgical suture into the origin of MCA via external carotid artery, and occlusion was made for periods of 40 min with monitoring a reduction of cerebral blood flow (> 85% of pre-occlusion) by using laser-Doppler flowmetry. The animals were then recovered and housed into normal cage with a free access to food and water. On 1-15 days after MCAO, morphological changes of NGVU were repeatedly measured with two-photon microscopy. An excitation light was 900 nm (~2.0 W) and fluorescent signals of GFP originating from endothelium and astroglia labeled with sulforhodamine 101 were simultaneously imaged with band-path filter of 525/50 nm and 610/75 nm,

respectively, through a cranial window. An in-plane image resolution was 0.25-0.46 µm per pixel and the image consists of 1024 by 1024 pixels, and was acquired up to a depth of 0.6 mm from the cortical surface. The imaging experiment was repeatedly performed in the identical locations to track single cell morphological changes around the ischemic boundary (Masamoto et al., 2012).

Results: Near the side of MCA territory, a loss of both neurons and astroglias was remarkably observed one day after transient MCAO. In these regions, intraperitoneally-injected sulforhodamine leaked and non-specifically stained extravascular tissue, indicating a disruption of blood-brain-barrier (BBB), although the morphology of endothelium labeled with Tie2-GFP were relatively preserved. In the peripheral boundary of ischemia, a selective loss of astroglia was found four days after the MCAO, whereas there were no detectable changes of the morphology of neurons and microvasculature. Also, no leakage of suforhodamine was observed in these regions, which indicates that BBB was also preserved. Further, we observed extension deformity of activated astroglia around the peripheral regions, but newly-developed vasculatures were not detected up to 14 days after the MCAO.

Conclusion: A transient episode of ischemia directly interferes in both neurons and astroglias, but astroglia is more sensitive to a delayed interference located in the peripheral boundary.

References:

Tomita Y, Kubis N, Calando Y, et al. J Cereb Blood Flow Metab 25:858-867 (2005)

Masamoto K, Tomita Y, Toriumi H, et al. Neuroscience 212:190-200 (2012)

CRITICAL ROLE OF PROGRAM DEATH-LIGAND 1 SIGNALING IN REGULATORY T CELLS-AFFORDED PROTECTION AGAINST BLOOD-BRAIN BARRIER DAMAGE AFTER ISCHEMIA/REPERFUSION

P. Li[1], Y. Gan[1], Y. Gao[1], J. Chen[1,2], **X. Hu**[1,2]

[1]State Key Laboratory of Medical Neurobiology and Institute of Brain Sciences, Fudan University, Shanghai, China, [2]Department of Neurology, University of Pittsburgh, Pittsburgh, PA, USA

Objectives: Breakdown of the blood-brain barrier (BBB) is a significant contributing mechanism in ischemic brain injury. Neutrophil-derived metalloproteinase-9 (MMP-9) mediates BBB damage after transient focal cerebral ischemia and may represent a peripheral target for stroke treatment [1-2]. Our recent research revealed that adoptively transferred regulatory T cells (Tregs) could reduce acute ischemic brain injury by inhibiting neutrophil production of MMP-9 and protecting against BBB damage. However, the molecular mechanism underlying the functional interaction between Tregs and activated neutrophils after stroke is unknown. Program death-ligand 1 (PD-L1) is an important signaling molecule that expresses on cell surface and helps Tregs regulate targeting cells. Therefore, the goal of this study was to evaluate the role of PD-L1 in Treg-afforded neutrophil inhibition and neuroprotection in a murine stroke/reperfusion model.

Methods: *In vitro* experiments using a transwell system or a co-culture system allowing cell-to-cell contacts were employed to explore the involvement of PD-L1/PD-1 in Treg-neutrophil interactions. The focal ischemia/reperfusion mouse model was used to confirm the importance of PD-L1 in Treg-afforded neutrophil inhibition and neuroprotection. Tregs were isolated from donor animals by CD4/CD25 double selection and systemically transferred to ischemic recipients at 2h after 60 minutes middle cerebral artery occlusion (MCAO). Animals were sacrificed at 1 or 3 days of reperfusion. MMP-9 production, BBB permeability and brain infarct were compared between animals treated with PD-L1-competent or PD-L1-compromised Tregs.

Results: In vitro experiment using a transwell system suggested that Treg-afforded inhibition on neutrophil MMP-9 requires direct cell contact. The expression of PD-L1 was detected on Tregs. PD-L1 neutralizing antibody, but not the CTLA-4 or TGF-β neutralizing antibodies, abolished the inhibitory effect of Tregs on TNFα-induced MMP-9 production in co-cultured neutrophils. Tregs also failed to inhibit neutrophil-derived MMP-9 when neutrophils were pre-treated with PD-1 neutralizing antibody. In contrast, incubation with active PD-L1 protein directly inhibited MMP-9 production in neutrophil cultures following TNFa challenge. *In vivo* studies confirmed that the administration of Tregs isolated from PD-L1-deficient mice or wild-type Tregs pre-treated with the PD-L1 antibody

failed to inhibit MMP-9 production in the blood neutrophils in stroke animals and failed to mitigate the infiltration of MMP-9-producing neutrophils into stroke brain. Furthermore, BBB damage after MCAO, as manifested by increased extravasation of plasma IgG or exogenous tracers and disrupted continuity of tight junction protein ZO-1, was remarkably ameliorated in mice treated with PD-L1-competent Tregs but not in mice treated with PD-L1-deficient Tregs. As a result, PD-L1 disability abolished Treg-afforded brain protection and neurological improvement after MCAO.

Conclusions: PD-L1 plays a critical role in mediating the inhibitory effect of Tregs on neutrophil MMP-9 production and, consequently, Treg therapy-afforded neuroprotection against BBB disruption after ischemic brain injury.

References:

1. Gidday, J.M., et al. Leukocyte-derived matrix metalloproteinase-9 mediates blood-brain barrier breakdown and is proinflammatory after transient focal cerebral ischemia. American journal of physiology 289, H558-568 (2005).

2. Justicia, C., et al. Neutrophil infiltration increases matrix metalloproteinase-9 in the ischemic brain after occlusion/reperfusion of the middle cerebral artery in rats. J Cereb Blood Flow Metab 23, 1430-1440 (2003).

MULTI-MODAL BIOMARKERS FACILITATE DIAGNOSIS IN VASCULAR COGNITIVE IMPAIRMENT: IDENTIFICATION OF PATIENTS WITH SUBCORTICAL ISCHEMIC VASCULAR DISEASE

G.A. Rosenberg[1], J. Prestopnik[1], J. Thompson[1], A. Caprihan[2], B. Huisa[1], J.C. Adair[1]

[1]Neurology, University of New Mexico, [2]MIND Research Network, Albuquerque, NM, USA

Introduction: Treatment of vascular cognitive impairment (VCI) has proven difficult in multiple strokes and the microvascular form with progressive subcortical ischemic vascular disease (SIVD) is thought to be the optimal treatment target. However, diagnosis of SIVD is difficult in the early stages, and biomarkers are needed.

Objective: Extensive microvascular damage to the white matter as viewed on FLAIR MRI is associated with SIVD. We and others have shown that white matter damage is caused by matrix metalloproteinase (MMP)-mediated disruption of the BBB. We hypothesized that multi-modal biomarkers could identify the subgroup of VCI patients with SIVD, and we tested the hypothesis that clinical, neuropsychological, imaging and CSF findings can facilitate diagnosis of SIVD.

Patients: We studied 62 VCI patients with clinical, imaging, and CSF studies. Diagnoses were made after one to three years of follow-up; categories included multi-infarct (MI), mixed VCI and Alzheimer´s disease (MX), subcortical ischemic vascular disease (SIVD), or leukoaraiosis (LA) in those with white matter lesions but without a diagnosis.

Methods: We used MRI studies including proton magnetic resonance spectroscopy (^{1}H-MRS) to determine white matter ischemia and dynamic contrast-enhanced MRI (DCEMRI) to quantify BBB permeability with measurement of MMPs and albumin index in the CSF. A 10-point SIVD scale score (SIVDSS) was constructed from the results. A subgroup of 20 patients was studied twice over 1 to 2 years with repeat MRI lesion growth and BBB permeability measurements.

Results: Final clinical diagnosis of SIVD was made in 38/62 patients based on extensive white matter hyperintensities (WMHs), vascular risk factors, and executive dysfunction. Biomarkers used for the SIVDSS, but not for clinical diagnosis, included reduced N-acetylaspartate (NAA) on ^{1}H-MRS, reduced MMP-2 index and elevated albumin index in the CSF. SIVDSS scores were based on three axes: clinical, neuroimaging, and CSF. Only 1/15 patients with a SIVDSS of 3 or less had a final diagnosis of SIVD. Those with SIVDSS of 4 to 6 (N=31) were classified as SIVD (N=21), with the remainder MI or MX. A SIVDSS of 7 or greater was determined in 14 with all except one being classified as SIVD clinically. In the small cohort with repeat MRI studies, 14/16 showed WMH growth, and 6/16 showed an increase in the area of permeability. The six with growth of the permeability area had a diagnosis of SIVD, while only one of those with no growth had that diagnosis ($p < 0.05$; Chi-square).

Conclusion: We found that more patients had a clinical diagnosis of SIVD than those

selected by a combination of biomarkers. The combination of biomarkers identified SIVD patients with suspected protease-mediated inflammatory disruption of the BBB. Those patients with high SIVDSS represent a small subgroup of SIVD patients and the high score suggests that white matter damage is due to an inflammatory reaction. We propose that this group is more homogeneous than identified by clinical diagnosis, and that the multi-modal approach can be used to select patients for treatment trials.

PROGRESSION OF AXONAL DEGENERATION FOLLOWING NEONATAL CEREBRAL HYPOXIA-ISCHEMIA IN RATS DETECTED USING DIFFUSION TENSOR IMAGING AND HISTOLOGY

U.I. Tuor[1,2], M. Morgunov[1], M. Sule[1], M. Qiao[1], T. Foniok[3], A. Kirton[2]

[1]Physiology and Pharmacology, Hotchkiss Brain Institute, University of Calgary, [2]Clinical Neurosciences, [3]Experimental Imaging Centre, Faculty of Medicine, University of Calgary, Calgary, AB, Canada

Introduction: Cerebral hypoxia-ischemia (HI) in neonates is an important cause of perinatal brain injury. Standard magnetic resonance imaging (MRI) detects acute changes in the descending cortico-spinal tract (DCST) and have been found to correlate with motor outcome. We hypothesized that diffusion tensor imaging (DTI) would provide additional insights into the progression of acute microstructural changes in axons remote to cortex damaged by cerebral HI.

Objective: To determine axonal and cortical changes in diffusion tensor parameters and histology occurring from 2 hours to 7 days after a transient hypoxia+unilateral cerebral ischemia in neonatal rats.

Methods: Rats (P7) were exposed to either a sham surgery (control) or carotid artery ligation + transient hypoxia (8%O_2). Animals (n=6-8/group) were imaged using MRI to acquire DTI scans at various times following hypoxia (2hr, 1d, 2d and 7d post-HI). DTI measures were obtained within ipsilateral and contralateral regions of interest, including: parietal cortex, cerebral peduncle of the descending corticospinal tract and pons (latter two regions remote from HI). Brains were processed for immuno/staining with myelin basic protein antibody (MBP), neurofilament antibody, glial fibrillary acidic protein antibody (GFAP) for reactive astrocytes and ED1 antibody for activated microglia/macrophages.

Results: In the pons, the DTI parameters (fractional anisotropy (FA), mean diffusivity and eigenvalues) and the various histological stains were generally not affected by HI. In the ipsilateral ischemic cortex, DTI parameters had marked early changes ipsilaterally that recovered by 7d post-insult except for FA. In the cerebral peduncle, changes in DTI parameters were modest at 2hr (i.e. a decrease in FA, ADC and eigenvalues). These changes became pronounced at 1 and 2 days post HI with normalization by 7 days except for FA. White matter tractography of the DCST detected fewer fibres ipsilaterally in the DCST at 2hr to 2d post HI, although mean DTI values were similar to those in controls. Ipsilateral and contralateral MBP staining was similar. Cortical increases in staining for ED1 were observed at 2hr and 1w. GFAP staining was increased by 1 d post HI in cerebral cortex and by 2 d in cerebral peduncle. Neurofilament staining was reduced in cerebral peduncle at all times investigated.

Discussion: ADC changes are comparable to those reported previously using standard imaging sequences (T2 or ADC) and eigenvalue changes measured using DTI. In contrast to these DTI parameters that normalized or increased to above control values by 7d, FA ratios remained reduced at all times. The 'fibers' detected with tractography were also reduced at all time points examined, corresponding to reduced neurofilament staining. Acute (2hr-1d) DTI changes in cerebral peduncle were not associated with changes in staining for myelin, microglia/macrophages or reactive astrocytes.

Conclusion: Axonal changes in the cerebral peduncle of the DCST can be detected within hours following a unilateral HI injury using standard imaging and DTI. There is a pseudonormalization of MRI changes by 1 wk post-insult, except for FA which detects well axonal degenerative changes at acute and subacute time points.

(Supported by Heart and Stroke Fndn, Markin USRP and Alberta Innovates Health Solutions.)

RESTORATION OF DAMAGE AND MOTOR ACTIVITY AFTER NEONATAL HYPOXIA-ISCHEMIABY IMPLANTATION OF PERIPHERAL BLOOD MONONUCLEAR CELLS

Y.-X. Liu, X.-M. Guo, Z.-W. Zhang, **J.-H. Xue**, H.-T. Zhang, J.-F. Li

First Affiliated Hospital of Chinese PLA General Hospital, Beijing, China

Hypoxia-ischemia encephalopathy is one of the most popular diseases in current life. It is a frequent cause of disability and mortality with limited therapeutic options. To evaluate the effect of implantation of peripheral blood mononuclear cells (PB-MNCs) on ischemic brain, we collected peripheral blood mononuclear cells (PB-MNC) from hypoxia-ischemia encephalopathy patients after they were treated by human granulocyte-colony stimulating factor (G-CSF), and implanted these cells into postnatal day 10 rats after neonatal hypoxia-ischemia (HI) by tail-vein injection. Before implantation, cells were labed by fluorescent dye (CM-Dill). Then we observed the migration of transplanted cells by fluorescence microscope, the differentiation of cells by immuno-fluorescent staining, the function restoration of HI rats by suspending and tiltboard experiment and apoptosis rate of brain cell in HI rats by tunnel staining .The results showed that PB-MNC could survive in the brain of hosts and migrate into the damage area. Three weeks after transplantation, PB-MNC from patients could differentiate into glial cells and neurons. The HI rats that received PB-MNC showed a significant reduction in motor function impairment and in the number of apoptosis cells in the brain. In addition, there was no turmorigenesis in the rats which received cells during 6 weeks. For further understanding the mechanism of cell migration, the normal rats were also injected PB-MNC by tail-vein, then we found that PB-MNC mainly located in the brain of HI rats, but in the lungs and spleens of normal rats. Then the expression of stromal cell-derived factor-1 (SDF-1) in the brain of normal and HI rats were measured by real-time PCR, and more than 20-fold increase of SDF-1 was observed in the brain of HI rats which indicated that the migration of PB-MNC might be dictated by adaptive specific signals provided by the damaged and regenerating brain. Our results implied that PB-MNC may be a feasible candidate for HI therapy.

Supported by: Grant from the Ministry of Science and Technology of China (2011DFA30550).

TH17 LYMPHOCYTES ARE CRITICAL MEDIATORS OF PERIPHERAL INFLAMMATION-SENSITIZED HYPOXIC-ISCHEMIC BRAIN INJURY IN NEWBORNS

D. Yang[1], Y.-Y. Sun[1], J.B. Baumann[1], D.M. Lindquist[2], **C.-Y. Kuan**[1]

[1]Pediatrics, Emory University School of Medicine, [2]Radiology, Cincinnati Children's Hospital, Atlanta, GA, USA

Objectives: Intrauterine infection (chorioamnionitis) and the ensuing fetal inflammatory response increase brain vulnerability to secondary insults, such as hypoxia-ischemia (HI). Since the fetal inflammatory response initates outside the nervous system, likely there are peripheral mediators that induce greater microglia activation and brain damage in response to HI insults. We hypothesize that the blood-borne Th17 lymphocytes are critical mediators of inflammation-sensitized neonatal HI brain injury. If this hypothesis is correct, oral medication with FTY720 (Fingolimod), a sphiongosine-1-phosphate (S1P) pro-analogue, may provide brain protection in infection-sensitized HI injury without suppressing the entire immune system in neonates.

Methods: The cord blood mononuclear cells in late preterm (33-36 gestational age) infants with and without histological chorioamninonitis were used to assess the expression of IL-23 receptor, a Th17-cell marker. In preclinical studies, low-dose (0.3 mg/kg) Lipopolysaccharide (LPS) was injected intraperitoneally to 7-day-old rats at 4 h before the Rice-Vannucci model of unilateral HI to mimic the peripheral inflammation-sensitized brain injury in neonates. FTY720 (1.5 mg/g) or saline was administered after LPS/HI to compare the outcomes in NF-kB signaling, microglia activation, brain atrophy, and the white-matter development by diffusion tensor imaging (DTI) analysis.

Results: The transcripts for IL-23 receptor were elevated and the S1P receptor (S1PR)-1 mRNA was reduced in the blood mononuclear cells of chorioamnionitis (+) preterm infants and LPS/HI-injured rat pups at 4 h recovery.

This result suggested that combined infection/HI activates S1P signaling and attracts Th17 lymphocytes into the circulation quickly. In LPS/HI-injured rat pups, FTY720 markedly blocked NF-kB activity and microglia activation, correlated with significantly reduced brain tissue loss and white-matter damage at 7d recovery. Moreover, FTY720 blocks the infiltration of T-cells, especially Th17 cell, into the LPS/HI-injured brain with evidences ranging from immunostaining, quantitative RT-PCR, and fluorescence-activated cell sorting (FACS) of Th17 cells. Importantly, FTY720 failed to inhibit microglia activation directly in either in-vitro or in-vivo model, due to a high expression of S1PR2 isoform that does not respond to FTY720.

Conclusions: First, the blood-borne T-lymphocytes, or Th17 cells alone, have an essential role of "priming" microglia for more severe response to the secondary HI brain injury. Second, using agents like FTY720 to block the entry of Th17 cells may be a promising brain protection strategy in infection-sensitized HI without compromising the immune function of newborns.

OMEGA-3 POLYUNSATURATED FATTY ACIDS MARKEDLY ATTENUATE DAMAGE TO WHITE MATTER AND THE BLOOD-BRAIN-BARRIER IN NEONATAL HYPOXIC-ISCHEMIC BRAIN INJURY

H. Zhang[1], W. Zhang[2], J. Chen[2,3], Y. Gao[2], Q. Dong[1]

[1]Department of Neurology, Huashan Hospital, State Key Laboratory of Medical Neurobiology, Fudan University, [2]State Key Laboratory of Medical Neurobiology and Institute of Brain Science, Fudan University, Shanghai, China, [3]Department of Neurology and Center of Cerebrovascular Disease Research, University of Pittsburgh School of Medicine, Pittsburgh, PA, USA

Objectives: Neonatal hypoxic/ischemic (H/I) brain injury is a leading cause of morbidity and perinatal mortality. To date, there are limited effective strategies for the prevention and treatment of this condition. OMEGA-3 polyunsaturated fatty acids (n-3 PUFAs) are highly enriched in brain and are known to attenuate H/I-induced brain damage and neurological deficits. In the present study, we investigated the prophylactic effect of n-3 PUFAs against blood-brain-barrier (BBB) and white matter damage in a neonatal H/I model.

Methods: Female rats were treated with or without an n-3 PUFA-enriched diet from the second day of pregnancy until 14 days after parturition. Seven-day-old neonates were subjected to H/I and euthanized 1, 4, 24, 48, and 72 h later. BBB integrity (Evans blue extravasation and electron microscopy) and brain edema (wet and dry weights) were measured 48 h post-H/I. Expression of MMPs, occludin, tissue inhibitor of metalloproteinase-1 (TIMP-1), zonula occludens-1 (ZO-1), cadherin-10 (Western blots and gelatin zymography) were examined at 1, 4, 24, 48, 72 h post-H/I. The integrity of myelin sheaths and axons was assessed by electron microscopy and expression of myelin basic protein (MBP) and non-phosphorylated neurofilament (SMI32; immunostaining and Western blots).

Results: Our results show that n-3 PUFAs markedly prevent the loss of MBP in response to H/I injury, suggesting that the integrity of myelin sheaths and axons was preserved. n-3 PUFAs also significantly improved BBB integrity after H/I, robustly suppressed H/I-induced loss of occludin and TIMP-1 and decreased MMP-9 at 48 h post-H/I. n-3 PUFAs also attenuated MMP-9 and MMP-2 activity.

Conclusions: n-3 PUFAs prevent BBB disruption and white matter injury after H/I in neonates. This may contribute to the potent neuroprotection against neonatal H/I brain injury. Our results support the hypothesis that a diet high in fish products or fish oil capsules during pregnancy may improve neonatal brain health. Further investigations into n-3 PUFAs as a prophylactic or therapeutic agent against neonatal H/I brain injury are therefore warranted.

EVOKED CHANGES IN OXYGEN CONSUMPTION IN THE SOMATOSENSORY CORTEX OF PREMATURE NEONATES

N. Roche-Labarbe[1,2], A. Fenoglio[3], H. Radakrishnan[1], M. Kocienski-Filip[4], S.A. Carp[1], J. Dubb[1], D.A. Boas[1], P.E. Grant[3,4], M.A. Franceschini[1]

[1]AA Martinos Center for Biomedical Imaging, Massachusetts General Hospital, Boston, MA, USA, [2]PALM - UFR Psychologie, Université de Caen Basse-Normandie, Caen, France, [3]Fetal-Neonatal Neuroimaging & Developmental Science Center, Children's Hospital Boston, [4]Newborn Medicine, Brigham and Women's Hospital, Boston, MA, USA

The hemodynamic functional response is used as a reliable marker of neuronal activity in countless studies of brain function and cognition. In newborns and infants however, conflicting results have appeared in the literature concerning the typical response, and there is little information on brain metabolism and functional activation. Non-invasive measurement of all hemodynamic components and oxygen metabolism is critical for understanding neurovascular coupling in the developing brain.

To this aim we combined multiple near infrared spectroscopy (NIRS) techniques: we used diffuse correlation spectroscopy (DCS) to measure relative cerebral blood flow changes (rCBF), frequency domain near infrared spectroscopy (FDNIRS) to measure baseline hemoglobin oxygenation (SO_2), oxy- and deoxy-hemoglobin concentrations (HbO and HbR respectively) and cerebral blood volume (CBV), and continuous wave near infrared spectroscopy (CWNIRS) to measure relative hemoglobin concentration and oxygenation changes (rSO_2). By combining all these measures we estimated relative changes in the cerebral metabolic rate of oxygen ($rCMRO_2$) in the somatosensory cortex of 6 preterm neonates during passive tactile stimulation of the hand.

Our data shows in preterm neonates the typical pattern of hemodynamic response to sensory stimulation: an increase in rSO_2 and CBV. However, the “preterm” response however is slower (longer time to peak, see figure) compared with adults. We did not observe any inverted response pattern associated with stimulation. Blood flow starts increasing immediately after stimulus onset, and returns to baseline before blood volume. This is consistent with the model of pre-capillary arteriole active dilation driving the CBF response, with a subsequent CBV increase influenced by capillaries and veins dilating passively to accommodate the extra blood. The higher compliance of the veins relative to arterioles can explain the slower return to baseline of CBV with respect to CBF.

$rCMRO_2$ shows a biphasic pattern: an increase immediately after stimulus onset, followed by a significant post-stimulus undershoot due to blood flow returning faster to baseline than oxygenation. However, if we calculate $rCMRO_2$ taking into account the longer mean transit time through the venous compartment in preterm infants compared with adults ($\tau \geq 5s$), the undershoot disappears (see figure). We observed an evoked flow-metabolism ratio of $n=2.8$, consistent with numerous studies in animals and human adults.

We describe, for the first time, changes in local rCBF and $rCMRO_2$ during functional activation in preterm infants. The ability to measure these variables in addition to hemoglobin concentration changes is critical for understanding neurovascular coupling in the developing brain, and for using the coupling as a reliable functional imaging marker in neonates.

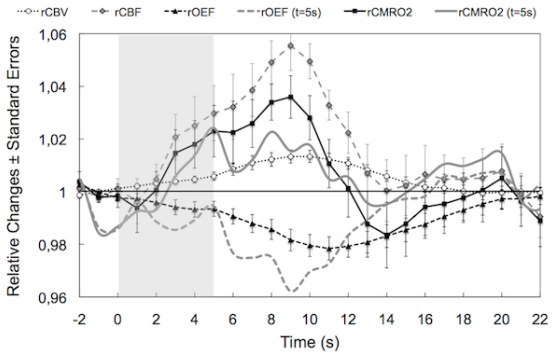

[rCMRO2_changes]

INTRAVENOUS IMMUNOGLOBULIN (IVIG) OFFERS NEUROPROTECTION AGAINST NEONATAL HYPOXIA/ISCHEMIA

B. Chen[1], M. Basta[2], C. Liu[2], B. Hu[2]

[1]Center for Shock, Trauma and Anesthesiology Research, University of Maryland, [2]Center for Shock, Trauma and Anesthesiology Research, Baltimore, MD, USA

Objectives: Mechanisms underlying delayed neuronal death after neonatal cerebral hypoxia/ischemia (HI) are not fully understood. In this study, we investigated whether Intravenous Immunoglobulin (IVIG) therapy protects immature neonatal brains from HI.

Methods: Postnatal 7 days pups were subjected to sham-operation or to a 2 h period of HI followed by 48 h of recovery. They were given slowly, at 1 h before and 30 min after HI, 0.30 ml of either vehicle (0.25 M glycine) or 2 g/kg of 10% human IVIG through the left common carotid artery. About 15 pups were treated either with vehicle, pre-ischemic IVIG, or post-ischemic IVIG, respectively. Brains were stained with TTC (2,3,5-triphenyltetrazolium chloride), and infart volumes were evaluated by NIH Image J software.

Results: Both pre- and post-ischemic IVIG treatment offers significant neuroprotection. The results demonstrated that human IVIG is effective in protecting neonatal brains from hypoxia/ischemia. The pattern of neuronal damage in neonates after HI is mainly distributed in radial columns parallel to the cerebral vessels and vertical to the surface. This contrasts to the predominant laminar pattern of neuronal death seen in mature brains after HI.

Conclusions: This study as well as previous publications suggest that IVIG's neuroprotective effects may be due to inhibition of the complement cascades. Therefore, IVIG may protect neonatal brain from HI by inhibiting complement overaction after HI. This study is supported by Baxter Grant (BRH).

TRPM2 CHANNELS ARE COINCIDENCE DETECTORS OF PARP-1 AND ANDROGEN RECEPTOR SIGNALING FOLLOWING EXPERIMENTAL STROKE IN MICE

T. Shimizu[1], N. Quillinan[1], R.J. Traystman[2], **P.S. Herson**[2]

[1]Anesthesiology, [2]Anesthesiology & Pharmacology, University of Colorado, Denver, Aurora, CO, USA

Objectives: Stroke is a sexually dimorphic disease that affects men more severely than women[1]. We recently demonstrated that pharmacological and genetic inhibition of TRPM2, a member of the transient receptor potential (TRP) channel superfamily, protects against cerebral ischemia in male mice, while having no effect in females[2]. In addition, TRPM2 channels are activated following oxidative stress by adenine dinucleotide phosphate ribose (ADPr) generated by poly(ADPr) polymerase (PARP)[3, 4]. In this study, we examined the role of PARP and male sex steroids in TRPM2 engagement following experimental stroke.

Methods: Transient focal ischemia was induced by 60 min of middle cerebral artery occlusion in male C57Bl/6 mice. To assess the efficacy of post-insult administration of the TRPM2 inhibitor clotrimazole (CTZ), intact mice were treated with either CTZ (30 mg/kg) or vehicle 1 hr after reperfusion. Mice were castrated (CAST) in order to remove sex steroids and either dihydrotestosterone (DHT) or vehicle was implanted. Then, animals were treated with either CTZ or vehicle 1 hr after reperfusion. The infarct sizes were evaluated in TRPM2-/- mice to confirm TRPM2 engagement and PARP-1 -/- mice treated with TRPM2 inhibitor. We further compared the PARP activity in intact male and female brain to that in ischemic brain. Data presented as mean±SEM.

Results: Animals treated with CTZ had significantly smaller infarcts compared to vehicle treated animals (46.2±3.1% (n=8) in vehicle vs. 32.5±3.6% (n=8; $P< 0.05$) in CTZ). Removal of sex steroids resulted in loss of protection by CTZ (44.6±3.1% (n=9) in vehicle treated CAST vs. 35.8±3.6% (n=11) in CTZ treated CAST). Androgen replacement with DHT (CAST+DHT) resulted in recovery of CTZ protection (40.4±2.3% (n=12) in vehicle vs. 31.5±2.8% (n=11; $P< 0.05$) in CTZ). We

observed smaller infarct size in TRPM2-/- mice compared to wild type (28.4±7.0 (n=5) vs. 49.0±1.2 (n=5); P< 0.05). We found significantly higher PARP activity in male penumbral tissues compared to male normal tissues (P< 0.05), while having no difference in females.

Conclusions: These data indicate that TRPM2 inhibition provides protection from ischemic stroke in male animals in an androgen-dependent and PARP-1 manner. Therefore, androgen status must be considered when considering inhibition of TRPM2 channels as a potential therapeutic strategy in men.

References:

1. Roger VL, Go AS, Lloyd-Jones DM, Benjamin EJ, Berry JD, Borden WB, et al. Heart disease and stroke statistics--2012 update: A report from the american heart association. *Circulation*. 2012;125:e2-e220

2. Jia J, Verma S, Nakayama S, Quillinan N, Grafe MR, Hurn PD, Herson PS. Sex differences in neuroprotection provided by inhibition of trpm2 channels following experimental stroke. *J.Cereb.Blood Flow Metab*. 2011

3. Fonfria E, Marshall IC, Benham CD, Boyfield I, Brown JD, Hill K, Hughes JP, Skaper SD, McNulty S. Trpm2 channel opening in response to oxidative stress is dependent on activation of poly(adp-ribose) polymerase. *Br.J.Pharmacol.* 2004;143:186-192

4. Miller BA. Inhibition of trpm2 function by parp inhibitors protects cells from oxidative stress-induced death. *British journal of pharmacology*. 2004;143:515-516

CONTRIBUTION OF PARTHANATOS TO CELL DEATH FROM HYPERGLYCEMIC ISCHEMIC STROKE

R.C. Koehler[1], J. Zhang[1], X. Li[1], Z.-J. Yang[1], H. Kwansa[1], Y.T. Kim[1], V.L. Dawson[2,3], T.M. Dawson[2,3]

[1]Department of Anesthesiology/Critical Care Medicine, [2]Institute for Cell Engineering, [3]Department of Neurology, Johns Hopkins University, Baltimore, MD, USA

Objectives: Hyperglycemia is known to augment neuronal injury during transient focal cerebral ischemia. The augmentation has been assumed to result from enhanced acidosis and reactive oxygen species (ROS) generation leading to classical necrosis. Parthanatos is a caspase-independent cell death pathway in which oxidative damage to DNA results in activation of poly(ADP-ribose) polymerase (PARP) and generation of poly(ADP-ribose) polymers (PAR) that trigger release of mitochondrial apoptosis-inducing factor (AIF). We investigated whether parthanatos also contributes to neuronal death in hyperglycemic transient middle cerebral artery occlusion (MCAO). Because hyperglycemia enhances cerebral ischemic acidosis, we also examined whether acidosis per sé is capable of augmenting parthanatos signaling in neurons.

Methods: Mice received an infusion of saline or dextrose (to increase blood glucose to approximately 400 mg/dL) before and during 45 min of MCAO produced by the filament technique. To assess ROS production in vivo, ethidium concentration was measured by HPLC in the ischemic hemisphere of mice that received an intravenous injection of hydroethidine. In other cohorts, Western blotting was used to quantify PAR at 1 hour of reperfusion and AIF in nuclear and mitochondrial fractions at 1 day of reperfusion. In primary neuronal culture, parthanatos was produced pharmacologically with a submaximal dose (25 μM) of the DNA alkylating agent, *N*-methyl-*N*'-nitro-*N*-nitrosoguanidine (MNNG), for 15 minutes. After MNNG washout, the neurons were exposed to media with a pH of 7.4 or 6.2 for 4 hours followed by a pH of 7.4.

Results: Hyperglycemia increased infarct volume from 19±3% to 36±2%% of hemisphere volume (±SE) in wild-type mice. Infarct volume in hyperglycemic PARP-1 null mice was reduced to 28±3%. Tissue ethidium concentration in the hyperglycemic hemisphere after reperfusion was three-fold greater than in the normoglycemic hemisphere. Compared to normoglycemic mice, hyperglycemic mice had a 43±18% greater amount of PAR and a 78±23% greater amount of AIF in the nuclear fraction. Exposure of neurons to media with pH 6.2 for 4 hours after washing out MNNG produced an increase in intracellular calcium. This increase was not seen with pH 7.4 media after MNNG washout or in acid-sensitive ion channel 1a (ASIC1a) null neurons with pH 6.2 media after

MNNG washout. Acidic pH exposure augmented the MNNG-induced increase in PAR, nuclear AIF, and cell death. This augmented cell death was blocked by inhibitors of PARP and ASIC1a but not by a caspase inhibitor.

Conclusions: The *in vivo* data show that hyperglycemia augments ischemia-induced ROS, PAR, and nuclear AIF and that infarct volume is reduced in hyperglycemic PARP-1 null mice. Collectively, these results are consistent with the concept that parthanatos contributes to the hyperglycemic augmentation of ischemic injury. The *in vitro* data demonstrate that acidosis is capable of amplifying neuronal parthanatos in the absence of ischemia and further support parthanatos as one of the mechanisms by which tissue acidosis associated with hyperglycemic ischemia augments cell death. Targeting parthanatos may be beneficial in diabetic stroke patients.

VISUALIZATION AND ANALYSIS OF SPATIO-TEMPORAL MOLECULAR CHANGES IN HIPPOCAMPUS AFTER TRANSIENT GLOBAL ISCHEMIA USING IMAGING MASS SPECTROMETRY

S. Miyawaki[1], T. Hayasaka[2], H. Imai[1], H. Ono[1], H. Horikawa[1], T. Ochi[1], A. Ito[1], H. Nakatomi[1], M. Setou[2], N. Saito[1]

[1]Department of Neurosurgery, The University of Tokyo, Bunkyo-ku, [2]Department of Cell Biology and Anatomy, Hamamatsu University School of Medicine, Hamamatsu, Japan

Background and aims: Ischemic vulnerability of brain, particularly neuron, remains to be elucidated. There is a limitation in conventional approaches focusing on particular genes or pathways to solve this mystery. In this study we tried to reveal comprehensive molecular dynamics change in rat hippocampus after transient global ischemia (delayed neuronal cell death) using imaging mass spectrometry (IMS). IMS is a novel molecular imaging method which enables us to visualize the molecule on the tissue section comprehensively.

Methods: A transient global cerebral ischemia (6 min) model was created using Sprague-Dawley rats (300-360 g males). Fresh frozen sections were obtained after euthanizing the rats on day 1, 2, 4, 7, 10, 14, and 21 (n = 3 for each) after transient global cerebral ischemia. For histopathological evaluation, Hematoxylin-Eosin staining and immunostaining for NeuN, GFAP and ED-1 were performed. IMS were also performed for molecular analysis. Phosholipids were targeted in this study.

Results: Evaluation and analysis of histopathological changes revealed several findings after transient global cerebral ischemia, including neuronal death in the CA1 domain, gliosis, and inflammation.

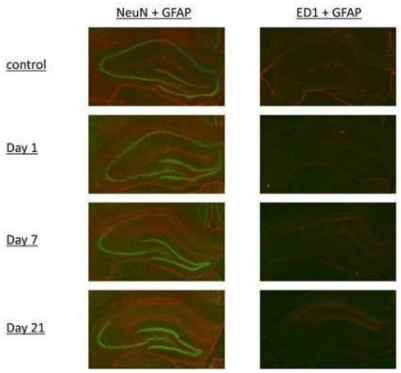

[figure1]

Molecular dynamic state changes of phospholipids analyzed by IMS revealed differences in anatomical distributions and serial changes in phosphatidylcholine (PC) and sphingomyelin (SM) according to the differences in constituent fatty acids. Analysis by IMS enabled us to visualize the molecular changes in various phase in the neuronal cell death. After day7, most of the pyramidal neuronal cells of CA1 domain of hippocampus were extinct and replaced by the inflammatory cells such as microglia, and gliotic astrocytes. In this phase, by IMS analysis, PC (16:0 18:1) increases in the CA1 domain. So this molecular change was supposed to correspond to the inflammatory change.

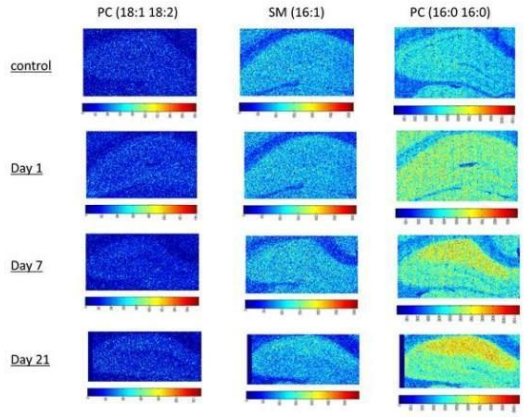

[figure2]

Immediately after transient ischemia, no obvious histological changes emerged. However, molecular change was detected in this phase by IMS analysis. It was found that PC, which contains polyunsaturated fatty acids such as arachidonic acid (20:4) and docosahexaenoic acid (22:6), was increased in the cell body layer of the hippocampus and dentate gyrus on day 1. These molecular changes are supposed to represent the initial change or the reaction of neuronal cells to ischemic stress.

Conclusion: We have demonstrated that IMS enables visualization and analysis of the dynamic state change of phospholipids in the various phases in the course of delayed neuronal death. We believe IMS would be a powerful tool in the analysis of ischemic vulnerability of the neuronal cell.

TRPM2 CHANNELS ARE COINCIDENCE DETECTORS OF PARP-1 AND ANDROGEN RECEPTOR SIGNALING FOLLOWING EXPERIMENTAL STROKE IN MICE

T. Shimizu[1], N. Quillinan[1], R.J. Traystman[2], P. Herson[2]

[1]Anesthesiology, [2]Anesthesiology & Pharmacology, University of Colorado Denver, Aurora, CO, USA

Objectives: Stroke is a sexually dimorphic disease that affects men more severely than women[1]. We recently demonstrated that pharmacological and genetic inhibition of TRPM2, a member of the transient receptor potential (TRP) channel superfamily, protects against cerebral ischemia in male mice, while having no effect in females[2]. In addition, TRPM2 channels are activated following oxidative stress by adenine dinucleotide phosphate ribose (ADPr) generated by poly(ADPr) polymerase (PARP)[3, 4]. In this study, we examined the role of PARP and male sex steroids in TRPM2 engagement following experimental stroke.

Methods: Transient focal ischemia was induced by 60 min of middle cerebral artery occlusion in male C57Bl/6 mice. To assess the efficacy of post-insult administration of the TRPM2 inhibitor clotrimazole (CTZ), intact mice were treated with either CTZ (30 mg/kg) or vehicle 1 hr after reperfusion. Mice were castrated (CAST) in order to remove sex steroids and either dihydrotestosterone (DHT) or vehicle was implanted. Then, animals were treated with either CTZ or vehicle 1 hr after reperfusion. The infarct sizes were evaluated in TRPM2-/- mice to confirm TRPM2 engagement and PARP-1 -/- mice treated with TRPM2 inhibitor. We further compared the PARP activity in intact male and female brain to that in ischemic brain. Data presented as mean±SEM.

Results: Animals treated with CTZ had significantly smaller infarcts compared to vehicle treated animals (46.2±3.1% (n=8) in vehicle vs. 32.5±3.6% (n=8; P< 0.05) in CTZ). Removal of sex steroids resulted in loss of protection by CTZ (44.6±3.1% (n=9) in vehicle treated CAST vs. 35.8±3.6% (n=11) in CTZ treated CAST). Androgen replacement with DHT (CAST+DHT) resulted in recovery of CTZ protection (40.4±2.3% (n=12) in vehicle vs. 31.5±2.8% (n=11; P< 0.05) in CTZ). We observed smaller infarct size in TRPM2-/- mice compared to wild type (28.4±7.0 (n=5) vs. 49.0±1.2 (n=5); P< 0.05). We found significantly higher PARP activity in male penumbral tissues compared to male normal tissues (P< 0.05), while having no difference in females.

Conclusions: These data indicate that TRPM2 inhibition provides protection from ischemic stroke in male animals in an androgen-dependent and PARP-1 manner. Therefore, androgen status must be considered when considering inhibition of TRPM2 channels as a potential therapeutic strategy in men.

References:

1. Roger VL, Go AS, Lloyd-Jones DM,

Benjamin EJ, Berry JD, Borden WB, et al. Heart disease and stroke statistics--2012 update: A report from the american heart association. *Circulation*. 2012;125:e2-e220

2. Jia J, Verma S, Nakayama S, Quillinan N, Grafe MR, Hurn PD, Herson PS. Sex differences in neuroprotection provided by inhibition of trpm2 channels following experimental stroke. *J.Cereb.Blood Flow Metab*. 2011

3. Fonfria E, Marshall IC, Benham CD, Boyfield I, Brown JD, Hill K, Hughes JP, Skaper SD, McNulty S. Trpm2 channel opening in response to oxidative stress is dependent on activation of poly(adp-ribose) polymerase. *Br.J.Pharmacol.* 2004;143:186-192

4. Miller BA. Inhibition of trpm2 function by parp inhibitors protects cells from oxidative stress-induced death. *British journal of pharmacology*. 2004;143:515-516

THE EFFECT OF MITOPHAGY IN TRANSIENT ISCHEMIC BRAIN IN RATS

Q. Li[1,2,3], T. Zhang[2], J.-X. Wang[4], G.-Y. Yang[5], X.-J. Sun[2]

[1]Department of Neurology, Shanghai Ninth People's Hospital, Shanghai Jiao Tong University School of Medicine, [2]Department of Neurology, Shanghai Sixth People's Hospital, Shanghai Jiao Tong University, Shanghai, China, [3]Anesthesiology and Critical Care Medicine, Johns Hopkins University, Baltimore, MD, USA, [4]Med-X Research Institute, Shanghai Jiao Tong University, Sshanghai, [5]Med-X Research Institute, Shanghai Jiao Tong University, Shanghai, China

Background and aims : Mitochondria provides energy to maintain normal cell functioning. Mitophagy is one of mitochondria functions, which can clear out injured mitochondria, ensure stability of mitochondria and promote cell survival in hostile environment. However, if mitophagy occurs during cerebral ischemia is unknown. The present study explored dynamic mitophagy, the effect of promoting mitophagy, and the molecular mechanisms of mitophagy during cerebral ischemia/reperfusion.

Methods: Adult male SD rats underwent 2h middle cerebral artery occlusion (MCAO) followed by 6 to 72h reperfusion. Dynamic changes of mitophagy were determined by LC3 immunostaining, Western blot analysis, and transmission electron microscope. To study the impact of mitophagy, we injected rapamycin, a mitophagy stimulator, into the left ventricle in rats underwent transient MCAO.To evaluate the effect of mitophagy, neuronal death and neurological deficits were determined. To explore the effect of mitophagy on mitochondria function,the number of mitochondria, the levels of MDA, ATP, and JC-1 were examined.To study the mechanism of mitophagy, mitochondrial Beclin-1 and p62 expression were also determined.

Results: We demonstrated that autophagy was mainly detected in mitochondria in the peri-focal area of ischemic cortex after ischemia/reperfusion. Mitophagy was increased at 6h ($p< 0.05$), peaked at 24h ($p< 0.05$), gradually reduced at 48h ($p< 0.05$), and returned to normal at 72h of transient MCAO. Pre-treatment with rapamycin greatly enhanced mitophagy, reduced infarct volume, and improved neurological outcomescompared to the control ($p< 0.05$). We found that the number of mitochondria and mtDNA copy, mitochondria ATPsynthesis level, andJC-1were increased($p< 0.05$), and MDA was reduced in rapamycin treated rats($p< 0.05$). We further demonstrated that rapamycin pre-treatment enhanced mitochondrial Beclin-1and p62 in mitochondria.

Conclusion: We demonstrated ischemia could induce mitophagy in brain cells. Rapamycin attenuated ischemic brain injury, which was via stimulating mitophagy that canreduce oxidative stress and improvemitochondria function. The mechanism of rapamycin promoting mitophagy was through increasing Beclin-1 and p62 expression.

TEMPORAL PROFILE OF THE MITOCHONDRIAL PROTEOME IN THE ISCHEMIC PENUMBRA

L. Meissner[1], G. Chen[2], T. Froehlich[3], U. Mamrak[1], M. Gonik[1], I. Johnston[4], G.J. Arnold[3], H. Zischka[5], **N. Plesnila**[1]

[1]Institute for Stroke and Dementia Research, University of Munich Medical School - Campus Großhadern, Munich, Germany, [2]Department of Physiology, Royal College of Surgeons in Ireland, Dublin, Ireland, [3]LAFUGA, Gene Center Munich, Munich, [4]Miltenyi Biotec, Bergisch-Gladbach, [5]Department of Toxicology, Helmholtz Center Munich, Munich, Germany

Objectives: Mitochondria play a prominent role in neuronal cell death after stroke. In the past several key players of the BLC-2 family such as Bid, Bax and Bak have been identified to associate with mitochondria in order to initiate mitochondrial cell death signalling and the release of pro-apoptotic executers like AIF and cytochrome C. Recently, mitochondrial dynamics have been associated with neuronal cell death. Bid and Bax were found to interact with Drp1, the regulator of mitochondrial fission[1,2] and inhibition of mitochondrial fission was neuroprotective following cerebral ischemia in vivo[3]. However the exact mechanisms how mitochondrial cell death signalling and mitochondrial dynamics interact in vivo to execute cell death are not clear.

Methods: A novel mouse specific immuno-magnetic bead isolation method was used to isolate mitochondria from the cortical penumbra of mice subjected to 60 min middle cerebral artery occlusion (MCAo). In order to identify proteins associated with mitochondria at different time points after stroke, mitochondria of ischemic and sham operated mice were isolated 1, 6, 12, and 24 h after MCAo. Proteomic profiles of these highly purified penumbral mitochondria were generated using a comparative iTRAQ-based LC-MS approach in order to obtain relative quantification of mitochondrial proteins between sham and MCAo animals. Immunohistochemical staining on paraffin sections was applied to confirm the proteomic results.

Results: The proteomic screen identified up to 600 proteins per mitochondrial fraction. Interestingly the most significant increase in protein levels over time was observed in proteins of the cytoskeletal mitochondrial transport machinery. Immunohistochemical staining revealed that this association of cytoskeletal proteins with mitochondria reflects the retraction of these organelles along the microtubules towards the nucleus during the time course of neuronal cell death after ischemia. This involvement of retrograde mitochondrial transport in ischemic neuronal cell death has so far only been demonstrated in vitro[4].

Conclusions: These findings suggest that retrograde mitochondrial transport is an important component of neuronal mitochondrial cell death signalling in the ischemic brain in vivo and may represent a novel target for neuroprotective strategies.

References:

1. *Grohm, J., Plesnila, N. & Culmsee, C. Bid mediates fission, membrane permeabilization and peri-nuclear accumulation of mitochondria as a prerequisite for oxidative neuronal cell death. Brain Behav Immun 24, 831-8 (2010)*
2. *Montessuit, S. et al. Membrane remodeling induced by the dynamin-related protein Drp1 stimulates Bax oligomerization. Cell 142, 889-901 (2010).*
3. *Grohm, J. et al. Inhibition of Drp1 provides neuroprotection in vitro and in vivo. Cell Death Differ (2012).*
4. *Landshamer, S. et al. Bid-induced release of AIF from mitochondria causes immediate neuronal cell death. Cell Death Diff (2008).*

VALIDATION OF THE ENTIRE NADPH OXIDASE FAMILY AS TARGETS FOR STROKE THERAPY

K.A. Radermacher[1], E. Göb[2], H. van Essen[1], J. Debets[1], P. Lijnen[1], P. Kleikers[1], S. Altenhöfer[1], R. Hermans[1], K. Wingler[1], C. Kleinschnitz[2], H.H. Schmidt[1]

[1]Pharmacology Department, Maastricht University, Maastricht, The Netherlands, [2]Neurologische Klinik, Universität Würzburg, Würzburg, Germany

Objectives: The enzyme family of NADPH oxidases has as sole function to produce reactive oxygen species (ROS). As oxidative stress is well known to be implicated in many neurodegenerative diseases, such as in stroke, we showed in our previous publication (*Kleinschnitz et al*.) that genetic deletion of the NADPH isoform NOX4 provided tremendous neuroprotection after ischemic stroke, as well as a pan-NOX inhibitor that was applied post stoke. As various cells express NOX4, we are now looking for the cell type that is responsible for detrimental ROS production by NOX4. In this study, we also investigate the role of other vascular NOX isoforms, namely NOX2 and NOX5. It has been generally agreed that the NOX1 subtype does not play a role in stroke disease.

Methods: To validate the NOX family as a target, two different cell-specific NOX4 knock-out mouse strains have been created, by deleting the NOX4 gene in endothelial (eNOX4 KO) or smooth muscle cells (sNOX4 KO). The global NOX2 KO is commercially available. As NOX5 is not expressed in mice, an endothelial NOX5 knock-in model (eNOX5 KI) has been created. Stroke surgery (middle cerebral artery occlusion) is performed on those animals and several parameters, such as infarct volume, neurological function or blood-brain-barrier disruption, are measured.

Results: Young male eNOX4 KO animals were protected from ischemic stoke injury with regard to infarct size, neurological scores, edema and survival. Also apoptosis, oxidative and nitrative stress was reduced 24h after stroke in those animals. This phenotype was neither observed in female or older mice, nor in a permanent stroke model. Preliminary experiments in sNOX4 KOs show that sNOX4 does not seem to play a role in cerebral ischemia-reperfusion. With regard to NOX2, all KO animals (male, female, young and adult) were slightly protected from stroke. In our NOX5 KI animals, a worse neurological outcome was only observed in the female cohort.

Conclusion: The neuroprotection previously observed in our global NOX4 KO mice was clearly confirmed in young eNOX4 KO mice, although to smaller extent (50% *versus* 75% reduction in infarct size). Endothelial NOX4 thus seems to be the major vascular player (compared to sNOX4). However, the higher neuroprotection that was achieved in global NOX4 KOs points also towards a contribution from the neuronal NOX4. NOX2 also seems to mediate neurological damage after stroke, however, only to a minor degree (infarcts reduced by 17%). Regarding the role of NOX5, female eNOX5 KI mice had larger infarcts, what could either be explained by a gender effect or also by a dose effect, as females were homozygous for NOX5 whereas males were hemizygous. To summarize the major outcomes of this study it can be said that several NOX isoforms are implicated in stroke pathology, however to different extents. Finally, NOX4 still seems to be the most promising target for neuroprotective stroke therapy.

Reference: *Kleinschnitz et al, PLoS Biol. 2010 Sep 21;8(9). pii: e1000479.*

INTRAVENTRICULAR ERYTHROCYTE LYSIS AND HYDROCEPHALUS

C. Gao[1,2], Y. Hua[1], R.F. Keep[1], **G. Xi**[1]

[1]Neurosurgery, University of Michigan, Ann Arbor, MI, USA, [2]Neurosurgery, Huashan Hospital, Fudan University, Shanghai, China

Objectives: Intraventricular hemorrhage (IVH) occurs in up to 50% of patients with primary intracerebral hemorrhage and 45% of patients with aneurysmal subarachnoid hemorrhage. Recent studies have found IVH is a predictor of poor outcome after intracerebral hemorrhage (1). Hydrocephalus develops in 55% patients with IVH. Our recent study showed that iron has a role in hydrocephalus development following IVH (2). This study investigated the role of erythrocyte lysis in hydrocephalus. The effect of deferoxamine (DFX), an iron chelator, on erythrocyte lysis-induced hydrocephalus and brain injury was also determined.

Methods: There were two parts in this study. First, male Sprague-Dawley rats received an injection of 30-µl of saline, packed or lysed erythrocytes into the right lateral ventricle. Rats were euthanized at 24 hours later after magnetic resonance imaging (MRI) and the brain were used for brain water content measurement, Western blotting, and immunohistochemistry. Second, rats received intraventricular injection of 30-µl of lysed erythrocytes mixed with DFX (5 mg) or saline and were euthanized 24 hours later for the brain water content determination and immunohistochemistry after MRI scans.

Results: Lysed erythrocytes resulted in

significant ventricular enlargement (67.9 ± 10.0 mm^3, n=15) compared with the saline control (15.4 ± 1.9 mm^3, n=15, p< 0.01) and packed erythrocytes (24.1 ± 6.2 mm^3, n=15, p< 0.01) at 24 hours. Intraventricular injection of lysed erythrocytes, but not packed RBCs caused significant brain edema formation, blood-brain barrier disruption and neuronal death (p< 0.01). Lysed erythrocytes also upregulated heme oxygenase-1, superoxide dismutase and ferritin levels in the periventricular area and in hippocampus. In our proof of concept experiments, co-injection of DFX with lysed erythrocytes resulted in smaller ventricular enlargement (47.8 ± 17.8 vs. 59.9 ± 15.7 mm^3 with saline co-injection, n=15, p< 0.05) and less neuronal death in the hippocampus (p< 0.05). There was a tendency for less brain edema in the DFX-treated group, but the results did not reach significance.

Conclusions: Intraventricular erythrocyte lysis causes hydrocephalus, blood-brain barrier disruption, brain edema, and neuronal death. The hydrocephalus induced by erythrocyte lysate can be reduced by DFX. These results suggest that erythrocyte lysis and iron are two potential therapeutic targets for hydrocephalus after IVH.

References:

1. Hanley DF. Intraventricular hemorrhage: severity factor and treatment target in spontaneous intracerebral hemorrhage. Stroke. 2009;40(4):1533-8.

2. Chen Z, Gao C, Hua Y, Keep RF, Muraszko K, Xi G. Role of iron in brain injury after intraventricular hemorrhage. Stroke. 2011;42(2):465-70.

ROLE OF IRON IN BRAIN LIPOCALIN 2 EXPRESSION AFTER INTRACEREBRAL HEMORRHAGE IN RATS

M. Dong[1,2], G. Xi[1], R.F. Keep[1], **Y. Hua**[1]

[1]Neurosurgery, University of Michigan, Ann Arbor, MI, USA, [2]Neurology, 1st Affiliated Hospital, Jilin University, Changchun, China

Objectives: Brain iron overload has a detrimental role in brain injury after intracerebral hemorrhage (ICH) (1, 2). Lipocalin 2 (LCN2), a siderophore-binding protein, is involved in cellular iron transport. The present study investigated the role of iron in brain LCN2 expression after ICH.

Methods: Male Sprague-Dawley rats had an intracaudate injection of autologous blood (100-µl) or iron (30-µl, 1 mM $FeCl_2$). Control rats received needle insertion or saline injection. Some ICH rats were treated with either vehicle or deferoxamine (100 mg/kg at 2 hours and then every 12 hours). Brain LCN2 expression was determined by Western blot analysis (and expressed as a ratio to β-actin) and immunohistochemistry. Real time PCR was also used to confirm brain LCN2 expression.

Results: LCN2 positive cells were found in the ipsilateral but not the contralateral basal ganglia after ICH. Western blotting showed that LCN2 protein levels in the ipsilateral basal ganglia were significantly increased at day 1, remained high at days 3 and 7, and then decreased markedly at day 14 after ICH.

Immunoreactivity of LCN2 was very weak in sham brain but increased significantly after ICH. LCN2 positive cells were astrocyte-like. By Western blot, the LCN2/β-actin ratio the ipsilateral basal ganglia was 71-fold higher than in contralateral basal ganglia (2.70 ± 0.46 vs. 0.04 ± 0.01, p< 0.001) and 84-fold higher than in sham animals (0.92 ± 0.14 vs. 0.01 ± 0.01, p< 0.001) at 3 days after ICH. Double-labeling showed that LCN2 immunoreactivity co-localized with glial fibrillary acid protein immunoreactivity after ICH. LCN2 immunoreactivity rarely co-localized with neuronal nuclear antigen in cortex.

Real time PCR was used to elucidate whether the increase in LCN2 after ICH was related to increased brain LCN2 mRNA expression. Expression in the ipsilateral basal ganglia increased 6.5-fold after ICH compared to contralateral (p< 0.05).

The effects of iron on brain LCN2 levels were also examined. LCN2 positive cells were found in the ipsilateral basal ganglia after injection of iron but not saline. Iron injection caused a 136-fold increase of LCN2 protein levels at day 3 (ratio of LCN2/β-actin: 1.77 ± 0.43 vs. 0.013 ± 0.004 in saline controls, p< 0.01). ICH-induced LCN2 expression was attenuated by the iron chelator, deferoxamine. Thus, deferoxamine reduced ICH-induced LCN2 upregulation at day 7 (p< 0.01).

Conclusions: Our findings indicate a role of iron in brain LCN2 upregulation after ICH. It also suggests that LCN2 may play an

important role in the handling of iron released from the hematoma during clot resolution.

References:

1. Keep RF, Hua Y, Xi G. Intracerebral haemorrhage: mechanisms of injury and therapeutic targets. Lancet Neurology. 2012;11(8):720-31.

2. Okauchi M, Hua Y, Keep RF, Morgenstern LB, Schallert T, Xi G. Deferoxamine treatment for intracerebral hemorrhage in aged rats: therapeutic time window and optimal duration. Stroke. 2010;41(2):375-82.

INHIBITION OF S100B/RAGE- RELATED PATHWAY PREVENTS SUBARACHNOID HEMORRHAGE (SAH)-ASSOCIATED NEUROINFLAMMATION AND NEUROLOGIC DYSFUNCTION IN RATS

D. Pelligrino, H. Xu, C. Paisansathan

Neuranesthesia Research, Univ. of Illinois at Chicago, Chicago, IL, USA

Objective: Multiple lines of evidence have indicated a dramatic elevation of S100B in both CSF and serum samples from subarachnoid hemorrhage (SAH) patients. However, the pathological role of this astrocyte-derived protein, if any, remains unclear. In a previous study, we found that:

(1) protein expression of both S100B, and its receptor, the receptor for advanced glycation end products (RAGE), is elevated in SAH rats;

(2) activation of RAGE-related pathway contributes to cerebral arteriolar dilating dysfunction.

Since RAGE activation is linked to the occurrence and exacerbation of inflammatory reactions, and neuroinflammation is a contributor to cerebrovascular dysfunction, we suspect that

(1) RAGE-S100B activation pathway is involved in post-SAH neuroinflammation; and

(2) preventing RAGE activation, using either S100B inhibitor (ONO-2506) or a RAGE decoy protein [soluble RAGE (sRAGE)], attenuates SAH-associated neuroinflammation, and recovers neurological function.

Methods: Rats were randomized into four groups:

(1) sham surgical controls,

(2) vehicle-treated SAH controls,

(3) ONO-2506-treated SAH rats, and

(4) sRAGE-treated SAH rats.

sRAGE solution were delivered intracerebroventicularly at 30 min following SAH via an osmotic pump. The SAH model involved suture perforation of the anterior cerebral artery. Neuroinflammation was quantified via recording adhesion and infiltration of Rhodamine-6G-labeled leukocytes through a closed cranial window. The window was implanted 24h post-SAH, followed by initiation of Rhodamine-6G iv infusion. Measurements of pial venular leukocyte adhesion (PVLA) were started right after the onset of Rhodamine-6G infusion. This was followed by a 2h period of leukocyte extravasation analysis. PVLA was expressed as the % of the pial venular area occupied by adherent Rhodamine-6G-labeled leukocytes within the venular margins. Neurobehavioral function, which included spontaneous activity, muscle tone, and neurologic reflex, was evaluated at 48 h post-SAH in all groups.

Results: Compared to the sham surgical group, a substantial increased PVLA was observed in vehicle-treated animals (10.8±2.2 % vs 2.7±0.1 % in sham), with a profound leukocyte extravascular infiltration revealed during the 2h extended observation period (infiltration index was 4.8±2.8%). No sign of infiltration was found in the sham surgical group. Both ONO-2506 and sRAGE treatments significantly decreased SAH-associated PVLA (5.5±0.2% with ONO-2506-treatment, and 5.5±0.3% with sRAGE-treatment), with complete elimination of leukocyte extravasation. Additionally, SAH was associated with a marked neurological deficit (11.6±0.9, compared to 20.5±0.5 in sham group), which was significantly restored by either ONO-2506 or sRAGE treatments (16.7±1.3 and 18.7 ±1.4 for ONO2506- and sRAGE-treated group, respectively).

Conclusion: Activation of the S100B/RAGE signaling pathway plays an important role in mediating neuroinflammation that contributes to neurological deficit following SAH. Blockade

of the S100B-RAGE interaction represents a promising clinical strategy for SAH treatment.

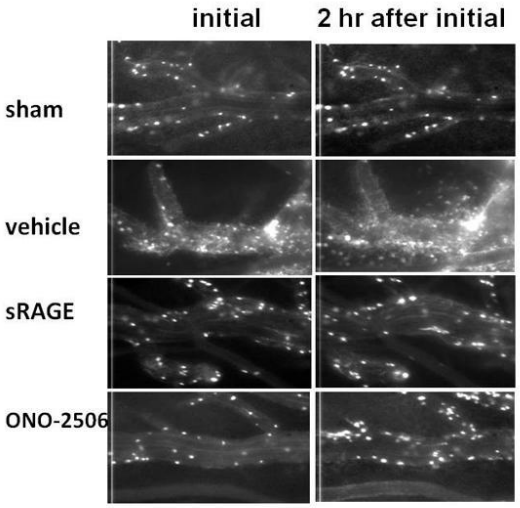

Fig. 1. Representative images captured at 24 h post-SAH (initial, left column) showing the effect of inhibition of S100B (via ONO-2506) or RAGE (via sRAGE) on SAH-associated pial venular leukocyte adhesion. The observation period was extended for an additional 2 hours (2hr after initial, right column) to evaluate the severity of SAH-induced leukocyte extravasation.

[Leukocyte adhesion]

EFFECTS OF CILOSTAZOL ON CEREBRAL VASOSPASM AFTER ANEURYSMAL SUBARACHNOID HEMORRHAGE: A MULTICENTER PROSPECTIVE, RANDOMIZED, OPEN-LABEL BLINDED END POINT TRIAL

H. Kinouchi, N. Senbokuya, Y. Nishiyama, K. Kanemaru, T. Yagi, H. Yoshioka, K. Hashimoto, T. Horikoshi

Department of Neurosurgery, University of Yamanashi, Chuo, Japan

Objectives: Cerebral vasospasm following aneurysmal subarachnoid hemorrhage (SAH) is a major cause of subsequent morbidity and mortality. Cilostazol, a selective inhibitor of phosphodiesterase 3, may attenuate cerebral vasospasm because of its antiplatelet and vasodilatory effects[1, 2]. A multicenter prospective randomized trial was conducted to investigate the effect of cilostazol on cerebral vasospasm.

Material and methods: Patients admitted with SAH caused by a ruptured anterior circulation aneurysm who were in Hunt and Kosnik Grades I to IV and were treated by clipping within 72 hours of SAH onset were enrolled at 7 neurosurgical sites in Japan. These patients were assigned to one of 2 groups: the usual therapy group (control group) or the add-on 100 mg cilostazol twice daily group (cilostazol group). The group assignments were done by a computer-generated randomization sequence. The primary study end point was the onset of symptomatic vasospasm. Secondary end points were the onset of angiographic vasospasm and new cerebral infarctions related to cerebral vasospasm, clinical outcome as assessed by the modified Rankin scale, and length of hospitalization. All end points were assessed for the intention-to-treat population.

Results: Between November 2009 and December 2010, 114 patients with SAH were treated by clipping within 72 hours from the onset of SAH and were screened. Five patients were excluded because no consent was given. Thus, 109 patients were randomly assigned to the cilostazol group (n = 54) or the control group (n = 55). Symptomatic vasospasm occurred in 13% (n = 7) of the cilostazol group and in 40% (n = 22) of the control group (p = 0.0021, Fisher exact test). The incidence of angiographic vasospasm was significantly lower in the cilostazol group than in the control group (50% vs 77%; p = 0.0055, Fisher exact test). Multiple logistic analyses demonstrated that nonuse of cilostazol is an independent factor for symptomatic and angiographic vasospasm. The incidence of new cerebral infarctions was also significantly lower in the cilostazol group than in the control group (11% vs 29%; p = 0.0304, Fisher exact test). Clinical outcomes at 1, 3, and 6 months after SAH in the cilostazol group were better than those in the control group, although a significant difference was not shown. There was also no significant difference in the length of hospitalization between the groups. No severe adverse event occurred during the study period.

Conclusion: Oral administration of cilostazol is effective in preventing cerebral vasospasm with a low risk of severe adverse events.

Reference:

1. Kambayashi J, Liu Y, Sun B, Shakur Y, Yoshitake M, Czerwiec F: Cilostazol as a unique antithrombotic agent. Curr Pharm Des 9: 2289-2302, 2003

2. Yamaguchi-Okada M, Nishizawa S, Mizutani A, Namba H: Multifaceted effects of selective inhibitor of phosphodiesterase III, cilostazol, for cerebral vasospasm after subarachnoid hemorrhage in a dog model. Cerebrovasc Dis 28: 135-142, 2009

ASPIRIN ATTENUATES INFLAMMATION IN THE WALL OF HUMAN CEREBRAL ANEURYSMS: PRELIMINARY RESULTS

D. Hasan

University of Iowa, Iowa City, IA, USA

Background: Inflammatory cells and molecules play a critical role in formation and rupture of cerebral aneurysms. Recently, an epidemiologic study reported that aspirin decreases the risk of aneurysm rupture. The goal of this study was to determine effects of aspirin on inflammatory cells and molecules in the wall of human cerebral aneurysms, using radiographic and histological techniques.

Methods: Ten prospectively enrolled patients harboring 11 unruptured intracranial aneurysms were randomized into *aspirin*-treated (81 mg daily) and untreated (control) *groups.* Aneurysms were imaged at baseline using ferumoxytol-enhanced MRI to estimate uptake by macrophages. After three months, all 10 patients were re-imaged before undergoing microsurgical clipping. Aneurysm tissues were collected for immunostaining with monoclonal antibodies for cyclooxygenase-1 (COX-1), cyclooxygenase-2 (COX-2), microsomal prostaglandin E2 synthase-1 (mPGES-1) and macrophages.

Results: A decrease in signal intensity on ferumoxytol-enhanced MRI was observed after three months of aspirin treatment. Expression of COX-2 (but not COX-1), mPGES-1, and macrophages was lower in the aspirin group than the control group.

Conclusion: These preliminary results provide radiographic and histological evidence that aspirin attenuates the inflammatory process in the wall of human cerebral aneurysms.

DETOXIFICATION OF HEMOGLOBIN IS NEUROPROTECTIVE AFTER INTRACEREBRAL HEMORRHAGE; PRE-CLINICAL STUDIES

X. Zhao, G.-H. Sun, S. Song, J. Zhang, R. Strong, J.C. Grotta, J. Aronowski

Neurology, University of Texas, Medical School at Houston, Houston, TX, USA

After intracerebral hemorrhage (ICH), a large amount of hemoglobin (Hb) is released into brain parenchyma due to intra-hematoma hemolysis, causing oxidative stress, delayed brain edema and secondary brain injury. Thus, it is critical to effectively detoxify the extracellular Hb around hematoma in order for reducing the hemolytic products-mediated cytotoxicity within the affected brain. We had reported that haptoglobin (Hp), an endogenous Hb-binding protein, could neutralize Hb and play cytoprotective role after ICH. Hp is normally produced in liver and secreted into bloodstream, and plays hemocytoprotective function by neutralizing the Hb resulting from the erythrocyte lysis. After ICH, we find that Hp can be synthesized in brain by oligodendrocytes, and that this synthesis can be further upregulated by sulforaphane (SF), an activator of the nuclear factor-erythroid 2 p45-related factor 2 (Nrf2). Our study indicated that the brain Hp produced by oligodendrocytes is biologically functional and it can effectively neutralize Hb and protect neurons and oligodendrocytes from hemolytic products mediated cytotoxicity. Although Hp could temporarily neutralize Hb by forming Hb-Hp complex, the final removal of Hb-Hp complexes from extracellular space is mediated by macrophages via the Hb scavenger receptor, CD163. CD163 is present on perivascular macrophages in brain, where its expression is regulated by numerous pro- and anti-inflammatory cytokines. Here, we find that $CD163^{+}$-macrophages are robustly increased in brain around hematoma after ICH and that treatment with an anti-inflammatory glucocorticoid, dexamethasone (DEX), can further increase CD163 expression. Interestingly, co-treatment of animals after ICH with SF (to upregulate Hp) and DEX (to stimulate the expression of CD163) was more robust in reduced brain edema, neuronal damage, and the neurological deficits than SF or DEX alone. We suggest that the effective Hb-detoxification after ICH is instrumental to prevent secondary brain injury after ICH. We

also propose that the approach based on SF and DEX combination has potential therapeutic relevance as management for ICH-mediated injury.

MULTIMODAL IMAGING OF MICROGLIAL ACTIVATION AND MATRIX-METALLOPROTEINASES AFTER EXPERIMENTAL STROKE

B. Zinnhardt[1], T. Viel[1], A. Vrachimis[1,2], A. Faust[1,2], L. Wachsmuth[3], S. Hermann[1], K. Kopka[2], C. Faber[3], F. Dollé[4], B. Tavititan[4], M. Schäfers[1,2], M.T. Kuhlmann[1], A.H. Jacobs[1,2,5]

[1]European Institute for Molecular Imaging (EIMI), [2]Department of Nuclear Medicine and Interdisciplinary Centre for Clinical Research (IZKF) of the University Medical Center, [3]Department Clinical Radiology of the University Medical Center, Westfälische Wilhelms-Universität (WWU), Münster, Germany, [4]CEA, Service Hospitalier Frédéric Joliot, Orsay, France, [5]Department of Geriatrics, Johanniter Hospital, Bonn, Germany

Introduction: Ischemic stroke is the most common neurological disorder and the second leading cause of death worldwide. In the cascade of molecular changes following acute cerebral ischemia, activation of the immune response and tissue factors are known to be key factors in promoting, on the one hand, the extent of tissue damage and, on the other hand, in serving tissue repair functions. Imaging approaches aiming at increasing the understanding of the temporal and spatial dynamics of the immune system and tissue factors shall improve our understanding of deciphering “bad” and “good” activation states.

Aim: To establish two new radiotracers for µPET imaging of microglial activation and matrix-metallo proteinases (MMPs) after cerebral ischemia in a mouse model of transient middle cerebral artery occlusion (MCAo) to reveal possible spatial interactions of these two histopathological hallmarks after ischemic stroke.

Methods: 53 mice were subjected to transient (30 min) MCAo. Success of surgery was verified intraoperatively via Laser Doppler and by ^{99m}Tc-hexamethylpropyleneamine oxime (HMPAO) µSPECT imaging one day post operation. Two weeks after surgery, surviving mice (n=10) were subjected to µPET imaging using the tracers [^{18}F]DPA-714 and [^{18}F]BR-351 for molecular imaging of microglial activation and MMP activation respectively. [^{18}F]DPA-714 µPET images were acquired 45-75 min post i.v. injection of 10 MBq [^{18}F]DPA-714. [^{18}F]BR-351 µPET images were acquired 95-110 min post i.v. injection of 10 MBq [^{18}F]BR-351. Lesion-to-background ratios (L/B) were calculated between the ischemic and the contralateral control hemisphere. T2-weighted µMRI was conducted for identification of stroke location and size and co-registration to µPET and µSPECT images. Immunohistochemistry is being performed in coronal sections employing antibodies for microglia (Iba-1) and MMP (anti-MMP-2/MMP-9).

Results: N=7 mice showed an infarction on T2-weighted µMRI in the right MCA territory. All mice reveal pronounced [^{18}F]DPA-714 tracer accumulation in and around the infarct region compared to the contralateral reference region (3,23± 2,22). Also, [^{18}F]BR-351 accumulation was observed in and around the infarct region (1,47± 0,97). In 6/7 mice [^{18}F]BR-351 tracer signal accumulation occurred partially in areas with increased DPA accumulation. The *in vivo* findings are currently quantified and being validated using immunohistochemical analysis for microglial- and MMP activation.

Conclusion: Radiotracer accumulation in and around the infarct zone indicates microglial and MMP activation in the infarcted region 2 weeks after transient MCAo. Immunohistochemical verification is ongoing. [^{18}F]DPA-714 and [^{18}F]BR-351 may serve as a potential marker combination to study neuroinflammatory reactions and tissue remodelling of the CNS *in vivo*.

The research leading to these results has received funding in part by a fellowship of the NRW Research School Cell Dynamics and Disease to B. Zinnhardt and the EU 7th Framework Programme (FP7/2007-2013) under grant agreement n° 278850 (INMiND).

IN VITRO AND *IN VIVO* EVIDENCE THAT MESENCHYMAL STEM CELLS DRIVE PROTECTIVE M2 MICROGLIA POLARIZATION

E.R. Zanier[1], L. Riganti[2], F. Pischiutta[1], E. Turola[2], S. Fumagalli[1], C. Perego[1], G. D'amico[3], D. Lecca[4], E. Biagi[3], M.P. Abbracchio[4], C. Verderio[2], M.G. De Simoni[1]

[1]Neuroscience, Mario Negri Institute, [2]CNR Institute of Neuroscience, [3]Pediatric Department, Laboratory for Cell Therapy 'Stefano Verri' University of Milano-Bicocca, San Gerardo Hospital, [4]Department of Pharmacological Sciences, University of Milano, Milan, Italy

Objectives: We have previously shown that microglia activation is associated with a protective phenotype after acute brain injury and that infused stem cells induce a microglial switch toward a nonphagocytic phenotype (1). Here we investigate if human mesenchymal stem cells (hMSC) can drive M2 microglial polarization.

Methods: Primary murine microglial cultures were exposed for 72h to:

1) TNF/INFγ for M1 classical activation;

2) hMSC;

3) TNF/INFγ followed 2h later by hMSC coculture.

Unexposed cultures served as controls. Co-cultures were then analyzed for marker expression of M1 (iNOS and COX2) and of M2 (CD206 and Ym1) by real time RT-PCR and immunohistochemistry. C57Bl/6 mice were subjected to sham or traumatic (TBI) brain injury. PBS or MSC (150,000/5ul) were infused intracerebroventricularly 24h later. Mice were sacrificed 72h or 7 days post-injury for real time RT-PCR or immunohistochemistry respectively.

Results: experiments on primary murine microglial cultures showed that

1) M1 classical activation induced an up-regulation of the pro-inflammatory genes iNOS compared to controls,

2) exposure to MSC decreased Cox2 and increased CD206 and Ym1 mRNA and protein expression compared to controls and to M1 classical activated cells, thus polarizing microglia towards M2 phenotype

3) MSC exposure after M1 classical stimulus was able to partially revert the M1 polarization as shown by the decrease of iNOS, Cox2 and increase of Ym1 and CD206 compared to controls and to M1 classical activated cells.

In vivo experiments showed that TBI induced a comparable increase in CD11b expression (a marker of microglia activation) in MSC treated (345%) and untreated (342%) mice. Notably MSC infusion in TBI mice induced a significant up-regulation of the microglia M2 markers Ym1 (200%) and Arginase1 (182%) compared to TBI-PBS mice, thus showing a protective microglial phenotypic switch. Furthermore quantification of coexpression changes of microglia after MSC transplantation by confocal microscopy, revealed a selective decrease of Ym1-CD68 double positive cells compared to TBI-PBS mice.

Conclusions: This study shows that, both *in vitro* and *in vivo*, MSC activate a M2 microglial phenotype. Furthermore *in vivo* data indicate a reduction in content of lysosomes in M2 polarized microglia in TBI MSC mice compared to controls suggesting an increase of the M2a subpopulation that is involved in growth stimulation and tissue repair (2).

References:

1. Zanier ER et al., Critical Care Medicine. 2011.

2. David S and Kroner A., Nature Review Neuroscience 2011

THE LINK BETWEEN STRESS RESPONSE, IMMUNOMODULATION AND INFECTIONS IN MICE AND MEN WITH CEREBROVASCULAR DISEASES

A. Liesz[1], E. Mracsko[1], J. Purrucker[1], P.P. Nawroth[2], H. Rüger[1], M. Möhlenbruch[3], W. Hacke[1], R. Veltkamp[1]

[1]Department of Neurology, [2]Department of Endocrinology, [3]Department of Neuroradiology, University Heidelberg, Heidelberg, Germany

Objectives: Infectious complications are the leading cause of mortality in the subacute phase after acute brain injury. Current concepts assume a stress-mediated immune suppression as the underlying cause of increased susceptibility to infections. However, this assumption was proposed only for ischemic stroke and the molecular mechanisms are unsufficiently investigated. We therefore performed a prospective study analyzing 184 patients with cerebrovascular diseases and additionally investigated the interaction between the sympathetic nervous system (SNS), the hypothalamic-pituitary-adrenal (HPA) axis and their impact on

leukocyte subpopulations in experimental stroke.

Methods: Blood samples of patients with TIA, stroke, ICH and controls were quantified for catecholamines and metabolites, ACTH, cortisol, differential blood cell counts, serum cytokines and infection markers at day 1, 2, 3, and 7 and at follow-up at 2-3 month. Clinical parameters and microbiological results were analyzed. Multivariate regression analyses were performed for determination of independent predictors of immune dysfunction or infections. Experimental brain ischemia was induced in mouse models of transient ischemia-reperfusion with varying MCA occlusion times. Stress and immune biomarkers were measured corresponding to the clinical study protocol at various time points after stroke. Adrenoreceptor (AR) and glucocorticoid-receptor (GCR) expression were investigated on different leukocyte subpopulations. Specific AR (α, β, β1, β2) and GCR-blockage as well as treatment paradigms (catecholamine and dexamethasone) were used to detect their impact on lymphocyte number and function.

Results: Increase of stress mediators (catecholamines, cortisol) was detected in blood and urine only of patients with large ischemic and hemorrhagic strokes but not after TIA and small lesions. A marked lymphocytopenia occurred after large strokes and after small and large ICH already within 24h and remained until 7d. Furthermore, immunemodulation in these patients was revealed by manifold increased production of key cytokines. The same patient groups had significantly increased clinical and laboratory infection markers and positive bacterial cultures. Intriguingly, despite the apparent association of stress mediator increase with immune dysfunction and infections, multivariate regression analysis in this large study population detected only clinical severity (NIHSS) and age as independent variables of lymphocytopenia. On the other side, lymphoctopenia and admission to ICU were the only early independent variables and had high predictive values for infections within the first week after brain lesion. Correspondingly, in experimental stroke models only large lesions induced immune-dysfunction. Also in experimental stroke, catecholamines did not affect lymphocyte numbers but their ability to produce IFN-γ - this effect was specifically mediated via β2-AR on lymphocytes. In contrast, treatment with a GCR-antagonist prevented lymphocytopenia by reduced splenic apoptosis in large experimental stroke but also increased catecholamine secretion and altered leukocyte-sensitivity to catecholamines.

Conclusions: This translational study demonstrates the importance of immune-dysfunction after acute severe cerebrovascular events in patients and experimental models and sets lymphocytes at the center of this complex phenomenon. We showed lymphocytopenia within 24h of onset to be a valuable predictive marker of subacute infections. Analyzing SNS and HPA axis interaction with lymphocytes in experimental stroke was able to detect the specific receptors and pathways involved.

INCIDENCE OF PLUGGED CAPILLARIES IN MOUSE MODELS OF AD CAN BE REDUCED BY ANTIBODIES TO LEUKOCYTE MARKERS

N. Nishimura[1], C.J. Kersbergen[1], I. Ivasyk[1], J.C. Cruz-Hernandez[1], J. Zhou[1], J.D. Beverly[1], G. Otte[1], P. Karlsson[1], E. Slack[1], T.P. Santisakultarm[1], C. Iadecola[2], C.B. Schaffer[1]

[1]Biomedical Engineering, Cornell University, Ithaca, [2]Neurology and Neuroscience, Weill Medical College of Cornell University, New York, NY, USA

Objectives: Alzheimer's disease (AD) is characterized by the aggregation of amyloid-beta which eventually accumulates into dense plaques scattered throughout the brain. Clinical research and experimental work suggest that cerebral blood flow is impaired in AD. In addition, chronically increased inflammation is observed in both AD patients and animal models of AD. We hypothesize that inflammation could contribute to the reductions in blood flow in AD by leukocyte plugging of capillaries.

Methods: We used in vivo two-photon excited fluorescence microscopy to examine cortical blood flow in mouse models of AD (B6.Cg-Tg(APPswe,PSEN1dE9)85Dbo/J) implanted with cranial windows. We label the blood vessels by intravenous injection of Texas red-conjugated dextran. To determine whether individual brain microvessels are stalled or flowing, we monitor the movement of non-fluorescent blood cells within the dye-labeled blood plasma. Additionally, methoxy-X04 is used to fluorescently label the amyloid plaques. Intravenous rhodamine-6G enables

the discrimination of red blood cells and leukocytes. Heart rate and saturation of peripheral oxygen were monitored during imaging using a pulse oximeter.

Results: In previous work, we found that in wild type littermates of the Alzheimer mice, the fraction of capillaries stalled in the cortex to be 0.3%, while in same-aged transgenic mice this fraction rises to 1.6%. We found that approximately two-thirds of the stalled vessels were plugged by leukocytes. The majority of plugged capillaries in both AD and wild type animals reperfuse with a ~2 minute half-life, but about 20% of the stalls in AD mice remain for an hour or more. We also find that some capillaries are plugged repeatedly (Fig. 1), indicating that these vessels may mark a "hotspot" of inflammation and leukocyte adhesion. In order to test the hypothesis that leukocytes drive the plugging of these vessels, we treated AD mice with intravenous injections of monoclonal antibodies against LFA-1 (4 mg/kg, clone M17/4). One to two days after injection, the mice were imaged and we found that the number of stalls was reduced by an average of 53% (standard deviation 43%, 4 mice) compared to before the injection. In animals injected with saline, the number of stalls was increased by 38% (2 mice) compared to before the injection.

Conclusions: These data suggest that modulating inflammation in Alzheimer's disease could decrease chronic leukocyte adhesion and capillary plugging. Because the progression of AD has been linked to vascular pathology and hypoperfusion, addressing blood flow in AD could provide an interesting target for manipulating the disease.

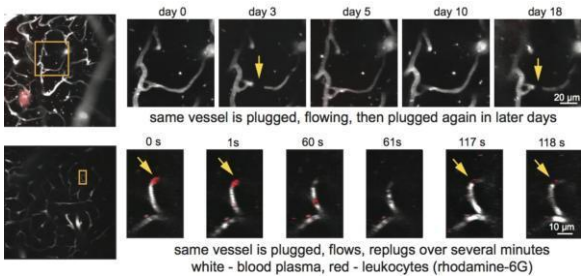

[Figure 1]

IDENTIFICATION OF INFLAMMATORY MARKERS TO DISTINGUISH LARGE - FROM SMALL VESSEL DISEASE IN PATIENTS WITH ACUTE ISCHEMIC STROKE

L. Zeng[1,2], Y. Wang[2], J. Liu[1], L. Wang[1], S. Weng[1], G.-Y. Yang[1,2]

[1]Department of Neurology, Ruijin Hospital, School of Medicine, [2]Neuroscience and Neuroengineering Research Center, Med-X Research Institute and School of Biomedical Engineering, Shanghai Jiao Tong University, Shanghai, China

Objectives: The early identification of non-cardioembolic stroke subtype is important for personalized treatment. In this study, we aim to determine plasma biomarkers for distinguishing cerebral large- from small vessel disease after stroke.

Methods: 99 patients with non-cardioembolic stroke were divided into large artery atherosclerosis (LAA) and small-artery occlusion (SAO) according to TOAST classification. A panel of plasma inflammatory markers including leukocyte, lymphocyte, CRP, fibrinogen, D-dimer, CD40L, IFN-γ, IL-1α, IL-1β, IL-6, IL-8, IL-17 and TNF-α were measured within 72 hours following cerebral ischemia. The relation of biomarkers with stroke subtype was further studied. All statistical data analysis was performed by SPSS 17.0 software.

Results: We found that only CRP were closely associated with stroke subtype ($p< 0.05$). Compared to SAO subgroup, the plasma levels of CRP was higher in LAA subgroup. The predictive efficiency of CRP more than 3.2 for LAA was 85.7% sensitivity. The influencing factor of CRP includes IL-6, lymphocyte, fibrinogen and D-dimer.

Conclusion: CRP can be served as a potential biomarker for the diagnosis of non-cardioembolic stroke subtype.

POST-ISCHEMIC ADMINISTRATION OF A POTENT PTEN INHIBITOR REDUCES SPONTANEOUS LUNG INFECTION FOLLOWING EXPERIMENTAL STROKE

J. Cheng[1], J. Jia[2], L. Mao[3], C. Dong[4], H. Liu[1], Y. Xiao[1], X. Zhou[5], X. Mao[3], Y. Guan[6]

[1]Institute of Neuroscience, Soochow University, [2]School of Pharmacy, Soochow University, Suzhou, [3]Department of Neurology, Changhai Hospital Affiliated to the Second Military Medical University, Shanghai, [4]Institute of Biology and Medical Science, Soochow University, [5]The Second Affiliated Hospital of Soochow University, Institute of Neuroscience, Soochow University, Suzhou, [6]Department of Neurology, Changhai Hospital Affiliated to the Second Military Medical University, Shanghai Institute for Stroke Prevention and Treatment, Shanghai, China

Post-stroke bacterial pneumonia is the most common complication following stroke, which not only increases mortalities but also exacerbates brain infarction (Harms et al., 2008; Meisel et al., 2004) .This study investigated the effects of bpv, a potent PTEN inhibitor, on stroke-induced lung bacterial infection. Adult male mice were subjected to 1 hour middle cerebral artery occlusion (MCAO). Bpv was administered daily, starting at 24 hours after MCAO. Compared to vehicle treatment, post-ischemic administration of bpv significantly reduced mortalities of MCAO mice from 3 to 7 days after MCAO, a period during which the major cause of mouse death following MCAO is reported to be lung bacterial infection (Prass et al., 2003). Consistently, bpv remarkably reduced lung bacterial loads and ameliorated lung tissue damage at 4 days after MCAO. PTEN deletion is reported to prevent mice from developing pneumonia and increase animal survival in the experimental pneumonia by acting on Akt activation to improve macrophage phagocytosis (Schabbauer et al., 2010). We found that cerebral ischemia significantly decreased local PTEN phosphorylation (inactivation) and reduced Akt activation (phosphorylation) in the lung at 4 days after MCAO. Bpv treatment increased PTEN phosphorylation (inactivation) and restored Akt activation in the lung following MCAO. Furthermore, bpv enhanced macrophage phagocytosis of bacteria in vitro. Therefore, our data indicate that post-ischemic administration of bpv reduced mortalities following experimental stroke via reducing lung bacterial infection. Furthermore, our data provided evidence, for the first time, suggesting that stroke-activated PTEN and subsequently impaired local Akt inactivation in the lung contribute to post-stroke spontaneous pneumonia. Restoration of lung Akt activation and subsequent enhancement of macrophage phagocytosis in part mediated bpv beneficial effects on post-stroke lung bacterial infection.

Harms, H., Prass, K., Meisel, C., Klehmet, J., Rogge, W., Drenckhahn, C., Gohler, J., Bereswill, S., Gobel, U., Wernecke, K.D., Wolf, T., Arnold, G., Halle, E., Volk, H.D., Dirnagl, U., Meisel, A., 2008. Preventive antibacterial therapy in acute ischemic stroke: a randomized controlled trial. PLoS One. 3**,** e2158.

Meisel, C., Prass, K., Braun, J., Victorov, I., Wolf, T., Megow, D., Halle, E., Volk, H.D., Dirnagl, U., Meisel, A., 2004. Preventive antibacterial treatment improves the general medical and neurological outcome in a mouse model of stroke. Stroke. 35**,** 2-6.

Prass, K., Meisel, C., Hoflich, C., Braun, J., Halle, E., Wolf, T., Ruscher, K., Victorov, I.V., Priller, J., Dirnagl, U., Volk, H.D., Meisel, A., 2003. Stroke-induced immunodeficiency promotes spontaneous bacterial infections and is mediated by sympathetic activation reversal by poststroke T helper cell type 1-like immunostimulation. J Exp Med. 198**,** 725-36.

Schabbauer, G., Matt, U., Gunzl, P., Warszawska, J., Furtner, T., Hainzl, E., Elbau, I., Mesteri, I., Doninger, B., Binder, B.R., Knapp, S., 2010. Myeloid PTEN promotes inflammation but impairs bactericidal activities during murine pneumococcal pneumonia. J Immunol. 185**,** 468-76.

THYMOSIN BETA 4 PROMOTES BRAIN AND SPINAL CORD REMODELING AND IMPROVES FUNCTIONAL RECOVERY IN RATS AFTER TRAUMATIC BRAIN INJURY

Y. Xiong[1], Y. Zhang[1], Y. Meng[1], Z.G. Zhang[2], A. Mahmood[1], M. Chopp[2,3]

[1]Neurosurgery, [2]Neurology, Henry Ford Health System, Detroit, [3]Physics, Oakland University, Rochester, MI, USA

Objectives: Despite improvements in the supportive and rehabilitative care of traumatic brain injury (TBI) patients, TBI leads to

mortality and disability. There are no pharmacological treatments for TBI. Our previous studies demonstrate that thymosin beta4 (Tβ4), a small multifunctional peptide, significantly improves functional recovery in animal models of stroke, experimental autoimmune encephalomyelitis and TBI. In this study, we investigated the mechanisms underlying the Tβ4 therapeutic effect after TBI in rats.

Methods: TBI was induced by using the controlled cortical impact (CCI) injury in adult male Wistar rats. CCI rats received intraperitoneal (ip) injection of either saline or Tβ4 (6 mg/kg, RegeneRx Biopharmaceuticals Inc, Bethesda, MD) starting at 24 hours post injury and then every third day for 2 weeks. The modified Morris water maze test was performed one month after TBI to evaluate spatial learning function. The modified neurological severity score (mNSS) test and footfault test were performed to measure sensorimotor function. Rats were sacrificed at 35 days after TBI (n=6-10/group). Immunostaining was performed for assay of angiogenesis and neurogenesis. Another set of rats was sacrificed at 2 days after TBI (n=3/group) for Western blot assay of angiopoietin 1(Ang1), Akt, cAMP responsive element-binding protein (CREB), p38 mitogen-activated protein kinase (p38MAPK), and extracellular signal regulated kinase (ERK) expression. An additional set of rats was injected with biotinylated dextran amine into the contralateral intact cortex before injury for anterograde labeling of the corticospinal track (CST) (n=3/goup). These rats were sacrificed at 35 days post injury. Their cervical and lumbar spinal cords were processed for measurement of midline-crossing axons.

Results: Tβ4 treatment initiated 24 hr post injury did not alter cortical lesion volume, but significantly improved spatial learning and sensorimotor functional recovery, and promoted angiogenesis and neurogenesis, as well as increased expression of Ang1, p-Akt, p-CREB, p-p38MAPK and decreased p-ERK in both the injured cortex and hippocampus compared to saline treatment ($p< 0.05$). Tβ4 administration significantly promoted axonal sprouting from the intact side into the denervated side in both of the cervical and lumbar enlargements in CCI rats after TBI compared to saline treatment ($p< 0.05$). The number of axons crossing at the cervical ($R^2=0.955$, $p< 0.001$) and lumbar ($R^2=0.8487$, $p< 0.001$) spinal cord was highly and inversely correlated to the incidence of forelimb and hindlimb footfaults examined at day 35 after TBI, respectively. The total number of axons crossing at both the cervical and lumbar spinal cord was highly and inversely correlated to the mNSS score assessed at day 35 after TBI ($R^2=0.862$, $p=0.007$). s These data imply that CST fibers originating from the contralesional intact cerebral hemisphere are capable of sprouting into the denervated spinal cord after TBI and Tβ4 treatment, which may at least partially contribute to functional recovery.

Conclusions: These data suggest that the therapeutic effects of Tβ4 may be mediated through activation of Ang1, p-Akt, p-CREB, p-p38MAPK and inhibition of p-ERK signaling pathways, which may subsequently induce neurorestoration including angiogenesis, neurogenesis, and axonal remodeling, thereby leading to improvement in functional recovery after TBI in rats.

CANNABINOID RECEPTOR DENSITY IS INCREASED IN A NEWBORN PIGLET BUT NOT AN ADULT RAT MODEL OF TRAUMATIC BRAIN INJURY

C. Donat[1], K. Gaber[2], F. Fischer[1], B. Walter[3], W. Deuther-Conrad[1], R. Bauer[4], J. Meixensberger[2], P. Brust[1]

[1]Department of Neuroradiopharmaceuticals, Institute of Radiopharmacy, Helmholtz-Zentrum Dresden-Rossendorf, Research Site Leipzig, [2]Department of Neurosurgery, University of Leipzig, Leipzig, [3]Heinrich Braun Hospital Zwickau, Zwickau, [4]Institute of Molecular Cell Biology & Center for Sepsis Control and Care (CSCC), Jena University Hospital, Jena, Germany

Objectives: Traumatic brain injury (TBI) is a leading cause of death and disability in the paediatric age group and also among adults, causing lifelong impairments and concomitant socioeconomic consequences. There is evidence from animal experiments and patient studies that cannabinoid signalling is involved in TBI, either by modulating neuroinflammation, as well as for neuroprotective pathways. However, almost no data exist on changes of cannabinoid receptors (CBR) after TBI. The present study was performed to investigate CBR in two different animal models of TBI. The identification of disease-related targets within the cannabinoid system is a precondition for potential molecular imaging of TBI patients with Positron-Emission-Tomography (PET),

e.g. for monitoring of a neuroprotective pharmacotherapy.

Methods: Thirteen female newborn piglets (post-TBI survival time: 6 h) underwent moderate fluid percussion (FP) injury (n = 7) or sham operation (n = 6) with an impact pressure of 3.8 ± 0.3 atmospheres. Furthermore, male Sprague-Dawley rats were randomized into three groups (post-TBI survival time: 6, 24, and 72 h), anaesthetized and subjected to sham injury/craniotomy (control, n = 3-5) or mild-to-moderate controlled cortical impact injury (CCI) (n = 5, 2 mm depth at 4 m/sec). From brains of both species, cryostat sections were cut (rat 12 µm, pig 20 µm) and density of CB1/2R ([^{3}H]CP-55,940) and CB1R ([^{3}H]SR141716A) was assessed with in vitro autoradiography. If appropriate, CB1- and CB2-specific ligands SR141716A and SR144528, respectively, were applied for receptor blockade.

Results: In the newborn piglet model, we found a statistically significant overall increase of [^{3}H]CP-55,940 binding in the brains of injured animals (15 of 24 investigated brain regions, including cerebral cortex, hippocampus, thalamus hypothalamus and midbrain; max: +140%, mean: +47%). No significant increases in [^{3}H]SR141716A binding were observed. In contrast, adult rats exhibited no statistically significant changes in CBR density, although some brain regions showed increases/decreases up to 30% of [^{3}H]CP-55,940 binding.

Conclusions: In conclusion, the expression density of CBR is significantly altered after experimental TBI in newborn piglets. Because CB1R show no significant alterations after injury, it is very likely, that the increases are of CB2R origin, probably due to activated microglia. This data therefore suggests an involvement of cannabinoid mechanisms in paediatric TBI.

In a mild-to-moderate adult rat model, no statistically significant changes in CBR density are found, which can either be attributed to species differences, e.g. brain morphology, or differences in the severity of the employed models.

The identification of the underlying mechanisms, supported for instance by molecular imaging with PET, could help to detect clinically relevant neuroreceptor changes after TBI and provide valuable insights which may prove helpful in the development of cannabinoid-based neuroprotectants.

CAVEOLIN EXPRESSIONS AND FUNCTIONS AFTER JUVENILE TRAUMATIC BRAIN INJURY

A.M. Fukuda[1], D.O. Ajao[1], D. Sorensen[2], **J. Badaut**[2]

[1]Physiology Department, [2]Pediatrics and Physiology Departments, Loma Linda University, Loma Linda, CA, USA

Introduction: Caveolins are structural proteins involved in caveolae formation. A subdomain within the caveolins called the caveolin-scaffolding-domain (CSD) function as a modulator of activities of several signaling molecules. Recently, a synthetic peptide mimicking the CSD has become available (cav-AP), and was shown to reproduce well-known CSD functions such as the inhibition of the Endothelial Nitric Oxide Synthase (eNOS). Three isoforms of caveolin (cav-1,2 and 3) are known to be present in the mammalian brain and are hypothesized to be involved in the blood-brain barrier (BBB) and cerebral blood flow (CBF) dysfunctions after brain injury. Traumatic brain injury (TBI) is one of the major causes of death and disability in children and adolescents, and results in a complex cascade of events including the disruption of the BBB and CBF changes. Studies in Cav-1 knockout mice suggested a beneficial role of this protein on the recovery of the neurovascular unit (NVU) after stroke.

Objective: We hypothesized that the increase of cav-1 is beneficial by facilitating the recovery of the NVU after juvenile-TBI (jTBI). We explored the changes of the caveolin expression and distribution after jTBI, which may contribute to the pathological changes within the NVU. We then tested whether injection of Cav-AP would result in improved BBB recovery and decreased edema translating into improved behavior.

Methods: The model of jTBI was controlled-cortical-impact on post-natal 17 day-old rats. The changes in the level of Cav-1, 2, 3, the BBB properties (IgG and claudin 5 staining), and in the level of eNOS were evaluated at 1,3,7 and 60 days (d) post-injury. The role of Cav-1 post-jTBI was evaluated using cav-AP i.p. injection at 3h post-jTBI. Outcomes were measured at 1 and 3d after jTBI using MRI (T2

to evaluate edema), behavior (rotarod), and BBB phenotype changes.

Results: BBB was disrupted at 1 and 3d after injury and went back to normal by 7d as observed via increased IgG extravasation. Cav-1 was increased in the endothelial cells and reactive astrocytes within the perilesional-cortex by 36% at 1d, 105% at 3d, 92% at 7d and 88% at 60d compared to the shams ($p< 0.05$,n=5 each group). In contrast, cav-2 expression, only present in the endothelium, was not modified over-time after injury. Cav-3 was increased in the border of the lesion in the reactive astrocytes at 1 and 3d after injury.

Cav-AP treatment prevented BBB disruption (decreased IgG extravasation), decreased edema (T2 values of cav-AP treated jTBI 67.22± 4.59ms vs non-treated jTBI 89.97 ± 4.59ms) and improved behavior functions as observed via the rotarod test (time spent on rotarod before falling off for Cav-AP was 30± 3s vs non-treated 19± 2s, n=4).

Conclusions: The increase of Cav-1 in the endothelium after jTBI may be contributing to the recovery of the disrupted BBB after injury through the CSD. This hypothesis was tested via the injection of the peptide mimicking the Cav-1 CSD (Cav-AP), which facilitated functional recovery associated with decreased BBB disruption and less edema. Thus, the Cav-AP may be a potential clinical tool to treat jTBI.

HISTONE DEACETYLASE INHIBITION PREVENTS WHITE MATTER LESIONS BY TITRATING MICROGLIA/MACROPHAGE POLARIZATION FOLLOWING EXPERIMENTAL TRAUMATIC BRAIN INJURY

G. Wang[1,2], X. Hu[1,2], Y. Guo[1], X. Jiang[1], H. Pu[1], L. Mao[1,2], A.K.-F. Liou[2], R.K. Leak[3], Y. Gao[1,2], J. Chen[1,2]

[1]State Key Laboratory of Medical Neurobiology and Institute of Brain Science, Fudan University, Shanghai, China, [2]Department of Neurology, University of Pittsburgh School of Medicine, [3]Division of Pharmaceutical Sciences, Mylan School of Pharmacy, Duquesne University, Pittsburgh, PA, USA

Objectives: Traumatic brain injury (TBI) is a major cause of death and disability in young adults. TBI results not only in grey matter damage but also severe white matter injury (WMI). This WMI correlates with the long-term deficits in motor and cognitive function in TBI patients (*Brain*. 2011, 134:449-63). Thus, the singular emphasis of most preclinical TBI studies on the protection of gray matter may explain the failure of experimental therapeutic agents in patients (*Trends Pharmacol Sci*. 2010, 31:596-604). We recently reported the potent neuroprotective effects of *Scriptaid*, a novel inhibitor of class I/II histone deacetylase, against TBI (*Neurotherapeutics*. 2012, [Epub ahead of print]). However, the effects of *Scriptaid* on long-term neurological functions and WMI following TBI remain elusive.

Methods: TBI was induced in C57/BL6 mice by a controlled cortical impact (CCI). *Scriptaid* was administered at 3.5 mg/kg 6 hours after injury. Motor deficits were determined using the rotarod, hang wire, cylinder, and foot fault tests. Animals were sacrificed up to 35 days post-TBI. WMI was evaluated by myelin-specific Luxol fast blue staining, immunohistochemical staining for myelin basic protein (MBP) and neurofilament SMI-32, and Western immunoblotting for MBP. Electron microscopy was used to detect myelinated and unmyelinated fiber damage in the corpus callosum. White matter inflammation after TBI was characterized by the quantification of pro-inflammatory cytokines. Reverse-transcriptase polymerase chain reaction and immunohistochemical staining for M1 and M2 markers were performed to characterize microglia/macrophage phenotypic changes in cerebral white matter. In vitro experiments using a conditioned medium transfer system were used to further elucidate the effect of *Scriptaid* on microglia/macrophage polarization and the effect of microglia/macrophage phenotype on the fate of injured oligodendrocytes.

Results: *Scriptaid* elicited robust white matter protection at 35 days after TBI, as demonstrated by reductions in abnormally dephosphorylated neurofilament proteins SMI-32, increases in MBP staining and luxol blue positive myelin as well as preserved myelination. *Scriptaid* also mitigated inflammatory responses elicited by CCI. Moreover, microglia/macrophages surrounding the brain lesions were shifted from the M1 phenotype to M2 by *Scriptaid*. In vitro experiments revealed that *Scriptaid* primes microglial polarization towards the protective M2 phenotype. As expected, M1 microglia-conditioned media exacerbated oxygen glucose deprivation (OGD)-induced oligodendrocytes death. In contrast, M2

microglia-conditioned media protected oligodendrocytes against OGD.

Conclusions: Our results indicate that *Scriptaid* improves long term neurological outcomes after TBI through potent protection of white matter. Furthermore, HDAC inhibitors may attenuate WMI by shifting the balance towards beneficial microglia/macrophage responses.

METABOLIC CHANGES IN TRAUMATIZED CULTURED HUMAN ASTROCYTES

S.M. Wolahan[1], I.B. Wanner[2], T.C. Glenn[1]

[1]Department of Neurosurgery, [2]Semel Institute for Neuroscience and Human Behavior, UCLA, Los Angeles, CA, USA

Objectives: The objective of this study is to determine astrocytic changes in metabolic function acutely after trauma in a newly developed human astrocyte mechanical injury culture model. Cerebral metabolic changes and dysfunction in response to traumatic brain injury (TBI) have been attributed to a neurometabolic cascade which plays a central role in severity and complications following TBI. We have evidence for injury-inflicted loss of key glycolytic enzymes due to leaking from transiently membrane porated cells that could contribute this metabolic dysfunction. We hypothesize that astrocytes initially respond to trauma by increasing glycolytic rates but are unable to sustain this response after enzymes leak from cells with damaged membranes, resulting in glycolytic depression.

Methods: Human primary cortical astrocytes were purified, expanded, and matured in vitro and grown on deformable membranes [1]. Defined pressure pulses abruptly deflect deformable culture bottoms and stretch the cells [2]. Transient mechanoporation was monitored by passive uptake of propidium iodine (PI) and dye-conjugated dextrans using time-lapse imaging. Conditioned medium was collected from injured and control cell cultures at 5 and 48 hours post-stretching. Released enzymes were identified using 2D gel electrophoresis and mass spectrometry [3] and confirmed by western blotting. Nuclear magnetic resonance (NMR) spectroscopy was used to measure metabolic concentrations in the medium.

Results: Mechanical trauma resulted in a transient loss in astrocyte membrane integrity shown by uptake of PI and various size dextran rhodamine tracers by injured cells. Compromised cells identified by PI uptake coincide with astrocytes that show morphological signs of cell injury, including beading and fragmentation. Lactate dehydrogenase along with several key glycolytic enzymes, including glyeraldehyde 3-phosphate dehydrogenase, aldolase C, alpha enolase, and phosphoglycerate kinase were released from traumatized astrocytes as shown by a larger than 1.8 fold fluid increase of the enzymes. Increased fluid enzyme levels were associated with a depletion of these enzymes from the injured cells, as demonstrated by reduced aldolase C immunofluorescence in PI-positive, injured astrocytes. We probed astrocyte metabolism by monitoring the fluid metabolite profile 48 hrs post-stretch in injured and control astrocytes and observed a significant decrease in pyruvate concentrations in mildly stretched astrocyte medium (0.1±0.02 v 0.2±0.02, p=0.03) resulting in a significantly higher lactate-pyruvate ratio (LPR) after stretch (59.2±5.5 v 46.8±5.0, p=0.04).

Conclusions: Our data show for the first time traumatic injury-induced metabolic changes in human astrocytes. Transient membrane permeability is associated with cellular enzyme release. Significantly decreased pyruvate levels suggest depressed glycolysis in injured compared to control cells. Low pyruvate translates to a significantly elevated LPR. LPR is used clinically to assess the metabolic state of cerebral tissue as an elevated LPR predicts tissue atrophy [4]. Future studies correlating enzymatic release to metabolic activity using stable isotope-labeled substrate metabolism monitored with ^{13}C NMR spectroscopy are planned.

References:

[1] Wanner, I.B. Methods Mol Biol. 2012: 814,189.

[2] Ellis, E.F., et. al. J Neurotrauma. 1995:12,325.

[3] Sondej, M., et. al. in Sample preparation in biological mass spectrometry. 2011:39,829-849.

[4] Marcoux, J., et. al. Crit Care Med. 2008:36,2871.

LONG-TERM EFFECTS OF MILD AND MODERATE-SEVERE BRAIN INJURY ON COGNITIVE FUNCTION AND LOCAL FUNCTIONAL CONNECTIVITY DENSITY

A. Livny-Ezer[1], M. Weiser[1], T. Kushnir[1], S. Harnof[1], D. Tomasi[2], C. Hoffmann[1], E. Fruchter[3], **A. Biegon**[4,5]

[1]Sheba Medical Center, Ramat Gan, Israel, [2]NIAA, Bethesda, MD, USA, [3]IDF Medical Corp, Ramat Gan, Israel, [4]Neurology, Stony Brook University, Stony Brook, [5]Biosciences, Brookhaven National Lab, Upton, NY, USA

Introduction: Traumatic brain injury (TBI) is a major cause of death and disability. Cognitive deficits, especially memory deficits, are extremely common in TBI survivors. Functional connectivity in the default mode network may also be altered due to TBI and contribute to cognitive deficits.

Aims: To assess the influence of injury severity determined by initial Glasgow Coma Scale (GCS) on cognitive deficits and patterns of brain activation during resting state condition in long-term TBI survivors compared to age and sex matched healthy controls.

Methods: Forty-seven TBI survivors and 35 age matched healthy controls were administered 3 cognitive tests: the similarities-R, which assesses verbal abstraction, arithmetic- R, which assesses mathematical reasoning and Raven's progressive matrices-R (RPM-R), which measures non-verbal abstract reasoning. All subjects had performed equivalent tests at age 17 as part of pre-military screening and results were obtained from the Israeli Defense Forces database. TBI survivors were tested a year or more after injury (Mean, SD=34.9, 16.6 months). Both pre and post-morbid scores were standardized based on population means and SD. A difference in z-scores between post and pre injury scores (post-pre injury) was calculated for each individual. The TBI group was stratified by initial Glasgow Coma Scale (GCS) scores to mild (mTBI, GCS=13-15, N=18) and moderate-severe (msTBI, GCS=3-12, N=29) injury groups and their post-pre injury scores were compared using a one way analysis of covariance controlling for significant differences in premorbid baseline scores. Post hoc analyses were then conducted to evaluate pairwise differences among adjusted means. Ten mTBI and 8 msTBI patients were additionally scanned during a resting-state condition of 5 min in which subjects were instructed to relax and close their eyes. These patients were compared to 40 healthy control subjects from the Cambridge research site of the "1000 Functional Connectomes" Project (http://www.nitrc.org/projects/fcon_1000/). Brain activations were assessed with functional magnetic resonance imaging (fMRI) using a 3T MRI system (HDxt, GE). The preprocessed image time series underwent functional connectivity density mapping (FCDM) to compute the strength of the local FCD (Tomasi and Volkow 2010, 2011).

Results: Significant (p=0.001) declines in RPM-R performance were observed in both mTBI (Mean, SE= -0.54, 0.22) and msTBI (Mean, SE= -0.80, 0.19) groups relative to controls (Mean, SE= 0.12, 0.16). For similarities-R the msTBI group had the greatest decline (Mean, SE= -0.051 0.14), significantly greater than controls (Mean, SE= -.016, 0.13) and mTBI (Mean, SE= .027, 0.17). No effect of TBI was found for the arithmetic-R. In addition, msTBI patients exhibited higher short range FCD in the cerebellum and lower short range FCD in frontal and parietal areas compared to healthy controls. mTBI was associated with similar decreases in FCD in cortical areas but no increase in cerebellum.

Conclusions: These results indicate that TBI has long-term effects on cognitive performance and the pattern of local FCD in resting-state condition; and these effects are modulated by injury severity.

References:

1. Tomasi, D. and N.D. Volkow, Neuroimage. 2011: **57**:908-17.

2. Tomasi, D. and N.D. Volkow,. Conf Proc IEEE Eng Med Biol Soc. **2010**:4274-7.

LAMINAR NEURAL ACTIVITY AND FLOW-METABOLISM COUPLINGS IN CEREBRAL CORTEX

P. Herman[1], B.G. Sanganahalli[1], D. Rothman[1,2], H. Blumenfeld[3,4], **F. Hyder**[1,2]

[1]Department of Diagnostic Radiology, [2]Biomedical Engineering, [3]Department of Neurobiology, [4]Department of Neurology, Yale University, New Haven, CT, USA

Introduction: Neuroanatomical variations across cortical lamina are well characterized [1,2,3,4]. However layer-specific variations of neurophysiologic, hemodynamic, and metabolic measurements are needed to

interpret high-resolution functional magnetic resonance imaging (fMRI) data. We examined the degree to which neurovascular and neurometabolic couplings vary across three transcortical segments (i.e., each ~600 µm thick) along the vertical axis of the rat's primary somatosensory cortex during forepaw stimulation [5]. We measured dynamic responses of blood oxygenation level-dependent (BOLD; gradient-echo) signal, blood volume (CBV; superparamagnetic iron oxide) and blood flow (CBF; arterial spin labeling and laser-Dopper flowmetry) as well as high impedance extracellular recordings of local field potential (LFP) and multi-unit activity (MUA).

Methods: ***Animal preparations:*** Anesthetized Sprague-Dawley rats were tracheotomized and artificially ventilated. Initial isoflurane anesthesia was switched to i.p. α-chloralose (80mg initial dose, then 40 mg/kg/hr) after the surgery. Electrical forepaw stimulations were applied (0.3ms, 3Hz, 2mA) for 30s duration. ***Neurophysiological measurements (n=32):*** Tiny burr holes above the contralateral forepaw somatosensory regions were drilled into rat sculls and high impedance tungsten microelectrodes together with micro laser-Doppler probes were inserted gradually into the cortex (0.3 mm, 1 mm, and 1.5 mm depths). MUA and LFP were extracted from the raw signal with band-pass (300-3000Hz), and low pass (< 150 Hz) filters, respectively. CBF data were calculated from LDF signals. ***fMRI measurements (n=24):*** All fMRI data (BOLD and CBV) were obtained on a modified 11.7T Varian horizontal-bore spectrometer using a 1H surface coil (Ø = 1.4 cm). The images were acquired with gradient echo EPI sequence (TR/TE = 1000/15) [4]. ***CMR_{O2} calculations:*** CMR_{O2} signals were derived from the BOLD, CBV and CBF signals using the calibrated fMRI equation (M=0.4) [6].

Results: Layer-specific BOLD, CBV, and CBF responses were combined to calculate changes in oxidative metabolism (CMR_{O2}) by calibrated fMRI at 11.7T. Both BOLD and CBV responses decreased from superficial to deep lamina (**Figure 1**). However BOLD and CBV responses were not well correlated with layer-specific neural measures; LFP responses were uniform throughout the cortex, whereas MUA responses were weakest superficially. In contrast CBF responses were quite consistently stable across lamina similar to LFP responses. However CMR_{O2} responses varied across lamina but in a correlated manner with MUA responses, both being significantly smaller in superficial lamina.

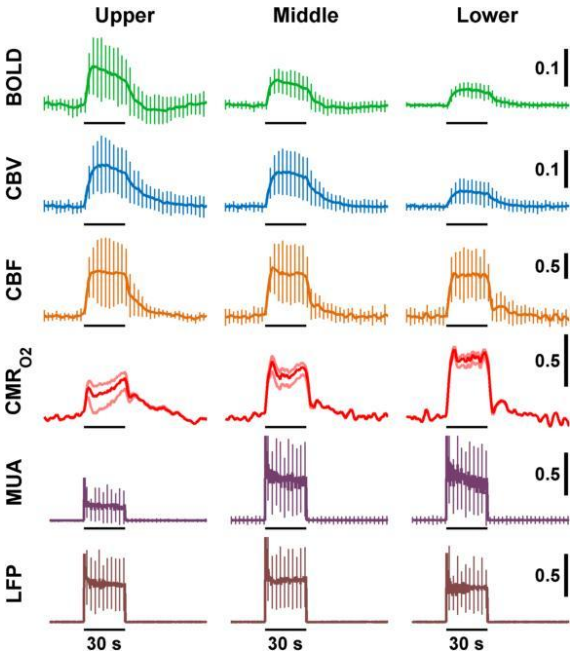

[Figure 1.]

Discussion: Overall these results reveal transcortical uncoupling of BOLD and CBV responses with either neural measure, whereas MUA and CMR_{O2} responses seem to be uncoupled from LFP and CBF responses in superficial layers. Therefore fMRI proxies for transcortical MUA-based and LFP-based neural measures could potentially be achieved with high-resolution CMR_{O2} and CBF mapping, respectively.

References:

[1] Lauritzen M, (2001) JCBFM 21:1367-1383

[2] Logothetis et al, (2001) Nature, 412:150-157

[3] Smith et al, (2002) PNAS, 99:10765-10770

[4] Sanganahalli et al, (2009) J Neurosci, 29:1707-1718

[5] Silva et al, (2002) PNAS 99:15182-15187

[6] Hyder et al, (2001) NMR in Biomed, 14:413-431

Acknowledgement: Supported by NIH (R01 MH-067528, P30 NS-52519).

HYPOGLYCEMIA ACTIVATION OF CEREBRAL BLOOD FLOW IS MEDIATED BY GLUT-2 GLUCOSE TRANSPORTER

H. Lei[1,2], F. Preitner[3,4], B. Thorens[3,4], R. Gruetter[1]

[1]University of Geneva, Geneva, [2]Ecole Polytechnique Fédérale de Lausanne, [3]Center for Integrative Genomics, University of Lausanne, [4]Mouse Metabolic Facility of the Cardiomet Center, University Hospital Lausanne, Lausanne, Switzerland

Introduction: Deletion of GLUT2 might influent hormonal responses upon hypoglycemia. We aimed to determine the effect of deleting GLUT2$^{-/-}$ on cerebral blood flow at euglycemia and upon hypoglycemia at 9.4T.

Methods:

Animals: Male GLUT2$^{-/-}$ mice with transgenic re-expression of GLUT1 in the pancreatic b cells (RIPGLUT1GLUT2$^{-/-}$), aged 16-20th weeks, were maintained under 1-2% isoflurane anesthesia. Breathing rate was controlled (>100bpm) in order to maintain $PaCO_2$ in the physiological range (35-45mmHg). Glycemia was measured from tail bleeds using glucometers (Bayer Breeze2), immediately before and after MR measurements, which lasted approximately 90 minutes in total. After an initial scan at basal (random fed) glycemia, a five-minute bolus and followed by a continuous rate at 0.1-0.2u/ml of insulin infusion was used (25.2±5.9UI/kg insulin in WT mice and 15.1±1.6UI/kg insulin in RIPGLUT1GLUT2$^{-/-}$ mice) to induce hypoglycemia in all mice. Once near-steady state hypoglycemia was established (glycemia < 2mM), animals were scanned again.

MR measurements: All MR measurements were performed in a horizontal 9.4T magnet (26cm-diameter bore). CBF was measured using a well-established continuous arterial spin labeling (CASL) technique in combination with a home-built actively-detuned system. Four segmented semi-adiabatic EPI sequence was adopted with a labeling module to implement the CASL sequence (3 consecutive 2mm-thick slices, 23×15mm^2, 128×64 data matrix). Cerebral blood flow (CBF) was assessed at euglycemia (random feed) and hypoglycemia.

Data analysis: CBF maps were calculated from 16 paired labeled and controlled images with a labeling efficiency 0.8. Significant difference was when $p< 0.05$.

Results and discussion: Random-fed glycemia under anesthesia was 10.1±1.4mM (mean±SDs, 8.6-12.4mM) in WT mice and 7.8±2.9mM (mean±SDs, 4.3-12.4mM) in RIPGLUT1GLUT2-/- mice. At euglycemia, CBF was globally higher in RIPGLUT1GLUT2$^{-/-}$ mice and significantly so in hippocampus (Figure 1, Table 1). During the insulin infusion, glycemia dropped to 1.6±0.2mM (mean±SDs, 1.2-2.3mM) in WT mice and 1.2±0.1mM (0.9-1.6mM) in knockout mice. In WT mice hypoglycemia elicited robust CBF changes (> 30% increase vs euglycemia). Strikingly, in RIPGLUT1GLUT2$^{-/-}$ this response was suppressed in all measured brain regions (Figure 2). In conclusion, the GLUT-2 glucose transporter plays a key role in the CBF response to hypoglycemia. This to our knowledge is the first report of a role for a glucose transporter in hypoglycemia-induced CBF increase.

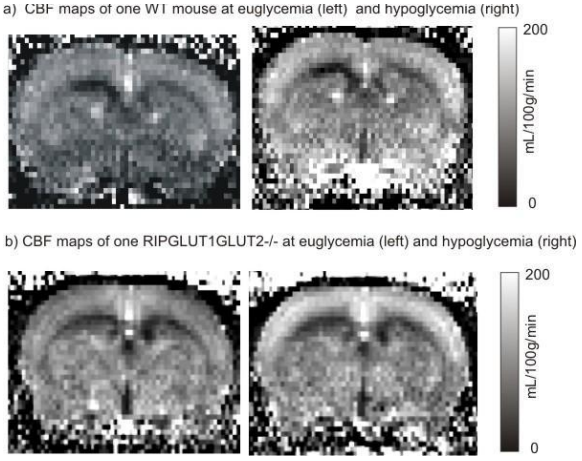

[Figure 1 Typical calculated CBF maps]

Region	WT(ml/100g/min)	KO (ml/100g/min)
hippocampus	111.7±14.0	122.4±7.4*
hypothalamus	91.3±9.9	99.0±16.1
cortex	119.7±15.6	123.9±11.9
brain	102.7±6.3	106.4±6.6

[Summary of CASL on regional blood flow]

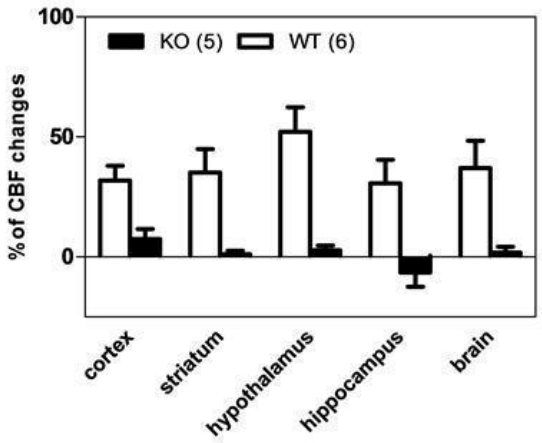

[Figure 2 Percent CBF changes upon hypoglycemia]

MODULATION OF CORTICAL PERFUSION AND SENSORY-EVOKED HEMODYNAMIC RESPONSES BY SELECTIVE OPTOGENETIC STIMULATION OF LOCUS COERULEUS NORADRENERGIC NEURONS

X. Toussay[1], M. Wyss[2], B. Weber[2], A. Adamantidis[3], E. Hamel[1]

[1]Montreal Neurological Institute, McGill University, Montreal, QC, Canada, [2]Institute of Pharmacology and Toxicology, Department of Nuclear Medicine, University of Zurich, University Hospital Zurich, Zurich, Switzerland, [3]Douglas Hospital Research Centre, Department of Psychiatry, McGill University, Montreal, QC, Canada

Background and objectives: Changes in hemodynamic signals are commonly used as surrogate markers to map changes in neural activity in functional brain imaging techniques. However, the exact mechanisms that govern neurovascular coupling are still only partially understood and, particularly, under conditions of altered cortical states (1-2). The locus coeruleus-noradrenergic (LC-NA) system is a potent modulator of cortical activity, promoting arousal, cortical neuronal activity (3) and enhancing synaptically-evoked neuronal excitation (4). Here, we investigated whether the optogenetic activation of LC-NA neurons modulates cortical cerebral blood flow (CBF) and the neurovascular coupling response to sensory stimulation.

Methods: Under isoflurane anesthesia, a Cre-recombinase-dependent channelrhodopsin-2 (ChR2-eYFP) adeno-associated virus (rAAV) was injected stereotaxically lateral to the LC (anteroposterior (AP): 5.45 mm; mediolateral (ML): ±1.28 mm; dorsoventral (DV): 3.65 mm) in dopamine β-hydroxylase (DBH)-Cre mice (3). After viral injection, optical fiber implants were placed slightly above the LC. Four weeks after surgery, mice were anesthetised (ketamine/xylazine), placed in a stereotaxic frame and prepared for optical LC-NA stimulation (blue light, 473 nm). In some experiments, sub-threshold LC photostimulations were designed to precede (< 10 sec) mechanical whisker stimulation (8-10Hz, 20s). Changes in CBF were measured in the parietal cortex with laser Doppler flowmetry. At the end of the experiment, ChR2-eYFP expression was verified in each animal brains.

Results: Successful transgene expression was confirmed by selective ChR2-eYFP expression in NA neurons throughout the entire LC by fluorescence (green) microscopy. Photostimulation (pulse width: 10-100 ms; frequency: 1-10Hz; and total duration: 5-10s) of the LC induced significant changes in cortical CBF. Maximal CBF increases (+32.4% at peak over baseline value, $p < 0.05$) were obtained with 100 ms light pulses delivered at 2Hz over 10s. Photostimulation at other wavelengths had no effect, thus excluding a non-specific light effect. Whisker stimulation elicited CBF increases in the contralateral somatosensory cortex (+19%, $p < 0.01$), a response significantly potentiated (+24.3%, $p < 0.05$) by ipsilateral LC-NA optogenetic stimulation. Blockade of α-adrenoceptors with the non-selective antagonist phentolamine (10 mg/kg, i.p.) significantly reduced the CBF responses to LC photostimulation and whisker stimulation, and prevented the LC-potentiating effects on the neurovascular coupling response to sensory stimulation.

Conclusions: These data show that selective optogenetic activation of homogenous NA neurons of the LC increases cortical perfusion in part through α-adrenoceptor activation, a neurovascular coupling response totally compatible with the role of the LC-NA system in enhancing arousal and cortical activity. Moreover, our findings show a facilitating modulatory role of the LC-NA system on the hemodynamic response to sensory

stimulation, consistent with previous effects of the LC on the activity of barrel field somatosensory neurons (5).

References:

1. Logothetis NK et al. (2001). *Nature* 412, 150-157. 2.

Lauritzen M and Gold L. (2003). *J. Neurosci.* 23, 3972-3980.

3. Carter ME et al. (2010) Nat Neurosci 13(12):1526-33.

4. Waterhouse BD et al., (1998) Brain Res 790:33-44.

5. Devilbiss DM and Waterhouse BD (2004) J Neurosci 24: 10773-10785.

Supported by the Canadian Institutes of Health Research (CIHR, grant MOP-84209, EH) and a McGill/ZNZ Pilot Project grant (EH, AA and BW).

GLUTATHIONE IS A KEY REGULATOR OF ASTROCYTE CONTRIBUTIONS TO NEUROVASCULAR COUPLING

C. Howarth[1,2], B.A. Sutherland[3], H.B. Choi[2], C. Martin[4], J. Pakan[2], G. Ellis-Davies[5], N. Sibson[1], A.M. Buchan[3], B. Macvicar[2]

[1]Department of Oncology, University of Oxford, Oxford, UK, [2]Department of Psychiatry, University of British Columbia, Vancouver, BC, Canada, [3]Radcliffe Department of Clinical Medicine, University of Oxford, Oxford, [4]Department of Psychology, University of Sheffield, Sheffield, UK, [5]Department of Neuroscience, Mt. Sinai School of Medicine, New York, NY, USA

Objectives: Neurovascular coupling and arteriole dilation are known to be mediated in part by increased astrocyte calcium (Ca^{2+}) which triggers phospholipase A2 activation, arachidonic acid (AA) formation and prostaglandin (PgE_2) synthesis[1-2]. As the type of PgE_2 synthase[3-4] expressed in astrocytes requires the cofactor glutathione (GSH), we investigated the effect of altering GSH levels in vitro on astrocyte $[Ca^{2+}]_i$-evoked PgE_2 release and vasodilation. In vivo, we investigated whether cerebral blood flow (CBF) responses to whisker pad stimulation and hypercapnia (10% CO_2) are attenuated when brain GSH levels are decreased.

Methods: Hippocampal slices from juvenile Sprague-Dawley rats were superfused with aCSF bubbled with 20% O_2, 5% CO_2, balanced N_2. Astrocytes were loaded with an IP_3-caged compound and/or the Ca^{2+}-indicator, rhod-2/AM. A two-photon laser-scanning microscope (Zeiss LSM510-Axioskop-2 fitted with a 40x-W/1.0 numerical aperture objective lens) coupled to a Chameleon ultra-tunable ultra-fast laser (~100fs pulses, 76MHz, Coherent) provided excitation of rhod-2 and was used to uncage IP_3. Arterioles were imaged by acquiring the transmitted laser light and using IR-DIC optics. Quantification of lumen diameter and Ca^{2+} changes were performed offline using ImageJ. PgE_2 release and tissue GSH levels were measured by biochemical assay. Immunohistochemistry was performed using antibodies against cPGES (Cayman chemical) and mPGES-1 (Agrisera) and markers for astrocytes (GFAP, Sigma) and neurons (MAP2, Chemicon). For in vivo experiments, male Wistar rats (250-370g) were used. 80mg/ml buthionine sulfoximine (BSO) or saline was infused into the right whisker barrel cortex. 24 hours post-injection, animals were anesthetized and laser Doppler flowmetry used to measure evoked blood flow responses to whisker pad stimulation and hypercapnia.

Results: The enzymes necessary for the production of PgE_2 (COX-1 and mPGES-1) are expressed in astrocytes. Furthermore, astrocyte $[Ca^{2+}]_i$-evoked vasodilation and PgE_2 release are blocked by the COX-1 inhibitor SC560, as is the CBF response to hypercapnia in vivo. Together these data suggest that PgE_2 is required for astrocyte-induced vasodilation.

In vitro, we demonstrate that PgE_2 efflux triggered by increased astrocytic $[Ca^{2+}]_i$ is decreased when tissue GSH levels are reduced by treatment with BSO. Astrocyte $[Ca^{2+}]_i$ transients evoke vasodilation in control slices, but induce only small constrictions in BSO-treated slices. In vivo, we found that the CBF increase evoked by whisker pad stimulation is attenuated when GSH levels are reduced. Furthermore, we demonstrate that astrocyte dependent PgE_2 synthesis is critical for the hypercapnia induced CBF increase and that decreased tissue GSH levels result in attenuation of the CBF response to hypercapnia.

Conclusions: Our data suggest that downstream of $[Ca^{2+}]_i$-evoked AA release in

astrocytes, the component of functional hyperaemia mediated by PgE_2 release from astrocytes requires GSH. Following stroke, when oxidative stress occurs and GSH levels decrease, the reduced vasodilatory effect of PgE_2 may underlie prolonged decrease of blood flow that contributes to neuronal damage.

References:

1 Zonta, M. *et al. Nat Neurosci* **6**, 43, (2003).

2 Gordon, G. R. *et al. Nature* **456**, 745, (2008).

3 Tanioka, T. *et al. J Biol Chem* **275**, 32775, (2000).

4 Jakobsson, P. J. *et al. Proc Natl Acad Sci U S A* **96**, 7220, (1999).

SEGMENTAL VARIATION IN CAPILLARY DIAMETER AND FLOW CORRELATE TO LOCALIZATION OF BRAIN PERICYTES

B. Gesslein[1], C. Hall[2], D. Attwell[2], M. Lauritzen[1]

[1]Department of Neuroscience and Pharmacology, University of Copenhagen, Copenhagen N, Denmark, [2]Department of Neuroscience, Physiology and Pharmacology, University College London, London, UK

Objectives: The dogma that cerebral blood flow is controlled solely by arterioles has been challenged with findings that pericytes can control capillary diameter and that damage to pericytes contributes to the long-lasting decrease in blood flow that occurs after stroke (*1, 2*). Pericytes contain several of the contractile proteins that have previously been found in smooth muscle cells and the contractility of cultured pericytes is well established (*3, 4*). In cerebellar slice preparations, noradrenaline resulted in constriction of capillaries by pericytes which was reversed by glutamate (*1*), suggesting a general capacity of capillaries to increase blood supply locally. However, a recent study on the behavior of brain pericytes in vivo suggested that pericytes do not dilate capillaries physiologically (*5*). Thus, the extent to which pericytes in capillaries are responsible for the blood flow increase induced by normal neural activity is still uncertain.

Methods: In the current project we applied two-photon microscopy to examine pericytes in the live, α-chloralose anaesthetized, mouse brain (n=12). To visualize the pericytes we used a transgenic mouse that expresses a red fluorescent protein in the pericytes under control of the NG2 promoter (Ng2 DsRed). Pericyte and capillary contraction/dilation were imaged upon increased activation of the cerebral cortex evoked by whisker pad stimulation (3Hz, 15s). Linescans were used to measure arteriole and capillary blood flow, after injection of FITC-dextran (*6*). Blood-pressure, blood-gases and CO_2 in the expired air was monitored during the experiment, to ensure that the animal was kept under physiological conditions.

Results: Vessel diameter in layer II-III of the whisker barrel cortex was measured at several locations in each FITC-dextran filled vessel and correlated with pericyte location. Somatosensory stimulation triggered a dilation and velocity increase in pre-capillary arterioles and capillaries, and changes in diameter were observed also in small (< 4 μm) capillaries. The frequency of responders (vessel segments with more than a 2% diameter change) was greater near pericyte cell bodies (n=154) than between pericytes (n=309; Shi square, p=0.004) for capillaries and ditto pre-capillaries (pericyte n=32; between-pericyte n=52; p=0.001). Furthermore the dilation was larger near pericytes than between pericytes both in capillaries (K-S p=0.0013) and pre-capillaries (K-S p=0.0016). Time to max velocity after stimulation onset was longer in pre-capillary arterioles (n=17) than capillaries (n=47, 28.0±4.2s vs. 19.5±1.8s; mean ± SD, students *t*-test p=0.0347).

Conclusions: We here provide evidence for segmental variation in capillary diameter and flow in response to somatosensory stimulation, which may suggest that pericytes on capillaries are involved in the mechanisms that underlie functional hyperaemia.

References:

1. C. M. Peppiatt, C. Howarth, P. Mobbs, D. Attwell, *Nature* 443, 700 (Oct, 2006).

2. M. Yemisci *et al.*, *Nat Med* 15, 1031 (Sep, 2009).

3. N. B. Hamilton, D. Attwell, C. N. Hall, *Front Neuroenergetics* 2, (2010).

4. D. Shepro, N. M. Morel, *FASEB J* 7, 1031 (Aug, 1993).

5. F. Fernandez-Klett, N. Offenhauser, U. Dirnagl, J. Priller, U. Lindauer, *Proc Natl Acad Sci U S A* 107, 22290 (Dec, 2010).

6. C. B. Schaffer *et al.*, *PLoS Biol* 4, e22 (Feb, 2006).

NEUROVASCULAR HETEROGENEITY IN MURINE CEREBRAL CAPILLARIES UNDER ELECTRICAL AND CHEMICAL STIMULATION

C. Cai, N.K. Iversen, E.G. Jimenez, L. Østergaard

Center of Functionally Integrative Neuroscience (CFIN), Department of Health, Aarhus University, Aarhus, Denmark

Introduction: *Neurovascular coupling* is a phenomenon that adjusts cerebral blood flow according to the metabolic needs of brain tissue [1]. It is central in our understanding of cerebral energy homeostasis and in the use of modern neuroimaging techniques to study brain function. Recent studies [2] suggest that not only cerebral blood flow, but also capillary transit time heterogeneity (CTTH) which originates from multifaceted blood flow variations in a highly interconnected capillary network, can determines oxygen availability. In this study, we used two-photon microscopy to measure the red blood cell (RBC) velocity and diameter changes in multi capillaries of mouse cerebral cortex. We also used electrophysiology to record the local field potentials, in order to monitor neuronal activities in response to stimulations.

Methods: Mice were anesthetized by Ketamine-xylazine. Vital signs were monitored all through the experiment. A femoral catheter was made to intravenously (i.v.) inject FITC-dextran, which stained the plasma. A cranial window was made over somatosensory cortex of the mice. RBCs in multi capillaries were visualized by using two-photon microscope. A glass pipette was guided by the microscope and inserted into the stimulated cortex region and local field potentials were recorded. Linescans were made by two-photon microscope to monitor the RBC velocities and diameter changes in multi capillaries and precapillary arteriole. Forepaw electrical stimulation (3 Hz, pulse duration of 0.2 ms, amplitude of 5-20 V) was applied; Acetazolamide (increase flow speed) and Phenylephrine (increase blood pressure) were injected i.v. to disturb the flow while monitoring flow and diameter changes in capillaries.

Results:

1. Flow heterogeneity was calculated as the standard deviation of multi capillaries flow in one capillary network, which can stand for CTTH. Flow heterogeneity was found to decrease and diameter of precapillary arteriole increased when applying forepaw stimulation. When injecting i.v. Acetazomamide, flow heterogeneity was decreased by 20%; on top of that, i.v. injection of Phenylephrine can lead to slight increase of flow heterogeneity, but still statistically significant lower than control.

2. Two types of capillaries can be classified - 'active' and 'passive'. Passive capillaries can passively change or even reverse the flow velocity according to the pressure change of the both ends, and therefore have larger flow heterogeneity with time; while active capillaries seemingly interact with nearby neurovascular unit and actively regulate blood flow.

Discussion: This study suggests a new dimension of neurovascular coupling - CTTH, which affects oxygen availability in capillary network. Stimulus which elicit neuron activities will decrease CTTH and increase oxygen availability. In terms of CTTH affecting oxygenation, 'active' capillaries should be used for calculating CTTH instead of 'passive' capillaries. Pericytes, contractile cells in the wall of capillaries, are thought to involve in the mechanism of CTTH.

Reference:

[1] Roy CS, Sherrington C. On the regulation of the blood-supply of the brain. The Journal of Physiology. 1890;11(1-2):85.

[2] Jespersen SN, Østergaard L. The Roles of Cerebral Blood Flow, Capillary Transit Time Heterogeneity and Oxygen Tension in Brain Oxygenation and Metabolism. J Cereb Blood Flow Metab. 2012; 32: 264-277.

PTEN MODULATES WHITE MATTER RECOVERY AFTER TRAUMATIC BRAIN INJURY

X. Jiang[1], G. Wang[1], H. Pu[1], S. Lu[1], W. Zhang[1], H. Gao[1], J. Chen[1,2], Y. Gao[1]

[1]State Key Laboratory of Medical Neurobiology and Institute of Brain Science, Fudan University, Shanghai, China, [2]Department of Neurology and Center of Cerebrovascular Disease Research, University of Pittsburgh School of Medicine, Pittsburgh, PA, USA

Objectives: Traumatic brain injury (TBI) is a major cause of mortality and disability in young adults and lacks an effective therapeutic strategy. Similar to ischemic injury, TBI injures both gray and white matter. Although white matter injury contributes to short and long term neurological deficits, studies of white matter injury or recovery after TBI are still limited. Phosphatase and tensin homolog deleted on chromosome 10 (PTEN), a potent regulator of the PI3K/Akt pathway, is known to attenuate injury from TBI (*1*). The present study therefore investigates the modulatory role of PTEN in white matter injury induced by TBI.

Methods: Heterozygous brain-specific $PTEN^{+/-}$ knockout (KO) mice were used in lieu of homozygous $PTEN^{-/-}$ KO mice in this study as the latter possess anatomical abnormalities in their brain and die within 2 weeks. Heterozygous brain-specific $PTEN^{+/-}$ KO mice were derived from heterozygous brain-specific hGFAP $Cre^{+/-}$ mice and homozygous PTEN $loxP^{+/+}$ mice. Age-matched mice were subjected to controlled cortical impact (CCI, velocity, 3.5 m/sec; duration, 150 msec; depth, 1.5mm) or sham surgery. At 7 days post-injury, motor deficits were measured by wire-hang, cylinder and foot-fault tests. Tissue volume loss in CCI mice was determined by summing the area of loss in serial, Nissl-stained coronal sections. White matter injury was measured by the differential intensity of immunofluorescent staining for matured oligodendrocytes with anti-myelin basic protein (MBP) and for loss of neurofilament integrity with anti-SMI32.

Results: Unlike homozygous brain-specific $PTEN^{-/-}$ KO mice, heterozygous brain-specific $PTEN^{+/-}$ KO mice exhibited no detectable physiological and behavioral changes. Nevertheless, endogenous PTEN levels were decreased by at least 60% with a concomitant increase in GFAP, as shown by Western blot analysis. At 7 days post-CCI, heterozygous $PTEN^{+/-}$ KO mice experienced significantly less tissue loss compared to age-matched controls. However, CCI elicited comparable motor asymmetry in heterozygous $PTEN^{+/-}$ KO mice and control mice as measured by cylinder and foot-fault tests. Superior performance of these mice in the wire-hanging test indicated enhanced myodynamia. With regard to white matter injury, heterozygous $PTEN^{+/-}$ KO mice retained significantly higher MBP staining, suggesting less damage to myelin sheaths and oligodendrocytes. Concomitantly, the intensity of SMI32 was lower in these mice, indicating greater preservation of neurofilament integrity.

Conclusions: Decreasing endogenous PTEN expression in heterozygous $PTEN^{+/-}$ KO mice increases myodynamia but has no impact on motor asymmetry. Moreover, these mice experience significantly less tissue loss and white matter injury from CCI. This is the first demonstration of the modulatory impact of PTEN on white matter. Our findings demonstrate that downregulation of PTEN may be a viable therapeutic approach to improve the recovery of white matter and help stroke victims.

References:

1. G. Wang *et al.*, Scriptaid, a novel histone deacetylase inhibitor, protects against traumatic brain injury via modulation of PTEN and AKT pathway. *Neurotherapeutics* Nov 7. 2012 [Epub ahead of print]

ROLE OF ASTROCYTIC ACTIVATION IN WHITE MATTER DISRUPTION AND COGNITIVE IMPAIRMENT IN A MOUSE MODEL OF VASCULAR DEMENTIA

F.J. Gerich, T. Schumacher, R. Saggu, C. Ulbrich, G.C. Petzold

DZNE, Bonn, Germany

Objectives: Subcortical vascular dementia (VaD) is the second most common form of dementia. It is characterized by a reduction of cerebral blood flow (CBF) predominantly in the white matter, as well as white matter disruption induced by diffuse demyelination and axonal loss, and progressive cognitive decline. Interestingly, inflammatory changes and strong activation of astrocytes (reactive astrocytosis) occur early in the disease course. However,

the signaling pathways underlying these cellular changes, as well as their contribution to cognitive impairment, have largely remained unknown[1].

Methods: Using the bilateral carotid artery stenosis (BCAS) model of VaD[2] in mice, we determined the contribution of the proinflammatory transcription factor NF-κB in activated astrocytes to disease progression. To this end, we used a mouse line expressing a dominant negative variant of the NF-κB inhibitor IκBα specifically in astrocytes (GFAP-IκBα-dn mice)[3]. These mice were subjected to BCAS, and compared to wildtype littermates subjected to BCAS as well as sham-operated mice. Changes in CBF were monitored by longitudinal Laser-Speckle measurements. White matter damage was quantified using magnetic resonance diffusion tensor imaging (DTI). Cognitive and motor function was assessed using a series of behavioral tests (Open Field, Novel Object Location, Y-Maze). In addition, neurodegenerative and inflammatory changes were determined using biochemical and immunohistochemical methods.

Results: BCAS resulted in a CBF reduction by ~30 % that was similar in all groups. We detected increased expression of the p65 subunit of NF-κB in wildtype mice after BCAS, indicating NF-κB activation. This increase was attenuated in GFAP-IκBα-dn mice after BCAS. DTI revealed prominent changes in axial and radial diffusivity, indicating axonal damage and demyelination, in wildtype mice subjected to BCAS, but these changes were attenuated in GFAP-IκBα-dn after BCAS. Accordingly, histological and biochemical markers of demyelination, axonal loss and inflammation were less pronounced in GFAP-IκBα-dn mice. Finally, preliminary data suggest that, while motor function remained unchanged in all groups, decline of spatial memory function after BCAS was ameliorated in GFAP-IκBα-dn mice compared to wildtype littermates.

Conclusions: Our data suggest that activation of NF-κB and downstream proinflammatory changes in astrocytes contribute to neurodegeneration and cognitive decline in VaD, and that pharmacological intervention of these inflammatory pathways may prove therapeutically beneficial.

References:

1. Petzold GC, Murthy VN (2011) Role of astrocytes in neurovascular coupling. *Neuron* 71: 782-797.

2. Shibata M et al. (2004) White matter lesions and glial activation in a novel mouse model of chronic cerebral hypoperfusion. *Stroke* 35: 2598-2603.

3. Brambilla R et al. (2005) Inhibition of astroglial nuclear factor kappaB reduces inflammation and improves functional recovery after spinal cord injury. *J Exp Med* 202: 145-156.

POST-ACUTE CXCL12 GENE THERAPY PROTECTS AGAINST CEREBRAL WHITE MATTER INJURY BY PROMOTING OLIGODENDROCYTE PROGENITOR CELL PROLIFERATION, MIGRATION AND REMYELINATION

Y. Li[1], J. Huang[1], X. He[1], Y. Tang[1], X. Lin[1], Y. Lyu[1], G. Tang[1], G.-Y. Yang[1,2], Y. Wang[1]

[1]Neuroscience and Neuroengineering Research Center, Med-X Research Institute and School of Biomedical Engineering, [2]Department of Neurology, Ruijin Hospital, School of Medicine, Shanghai Jiao Tong University, Shanghai, China

Objectives: Our previous study showed that inhibition of binding of chemotactic attractor CXCL12 with its receptor CXCR4 protects blood-brain barrier integrity and reduces inflammatory response during acute ischemia in mice.[1] CXCL12 was known to attract progenitor cells that might be beneficial for neurovascular regeneration. However, the detailed function of CXCL12 in post-acute ischemia remains unclear. In this study, we aim to investigate the effects of adeno-associated virus mediated CXCL12 (AAV-CXCL12) gene therapy on the proliferation and migration of oligodendrocyte progenitor cells and remyelination during the post-acute phase after ischemic stroke.

Methods: Thirty-six adult ICR male mice received sterotactical injection of AAV-CXCL12 into the perifocal area one week after middle cerebral artery occlusion (MCAO). Brain atrophic volume and neurobehavioral tests were examined to evaluate the outcomes following AAV-CXCL12 gene transfer. Oligodendrocyte progenitor cells (OPCs) proliferation and migration were semi-quantified by CD140a cell staining in subventricular zone (SVZ) and perifocal area.

Remyelization was evaluated by myelin-binding protein (MBP) cell staining in perifocal area. Inflammation response was determined by myeloperoxidase expression and activity assay.

Results: CXCL12 was expressed in perifocal area for at least four weeks after AAV-CXCL12 gene transfer. The CXCL12 gene treated group exhibited significantly reduced brain atrophic volume (20±15 vs. 5±4 (mm^3), n=6, p< 0.05) and improvement of neurological score (2.3±1.1 vs. 1.5±0.7, n=15, p< 0.05) and motor function (30±11 vs. 45±15 (s), n=7, p< 0.05) at five weeks after MCAO compared to control groups received AAV-GFP. Further study showed that OPCs proliferation (2.1 folds increase, p< 0.01, 3 weeks after MCAO; 1.5 folds increase, p< 0.05, 5 weeks after MCAO; Figure 1A), migration (1.5 folds increase, p< 0.05, 3 weeks after MCAO; 2.5 folds increase, p=0.01, 5 weeks after MCAO; Figure 1B) and remyelination (2.1 folds increase, p< 0.05, 5 weeks after MCAO) were improved in CXCL12 transduced mice compared to the control. In addition, AAV mediated delayed CXCL12 h gene expression in the recovery phase did not elicit focal inflammation response.

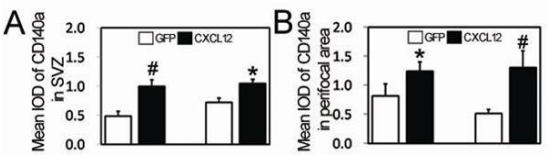

[Figure 1]

Figure 1. AAV mediated CXCL12 gene therapy promoted OPCs proliferation, migration and remyelination after MCAO in AAV-CXCL12 group. Bar graph showed semi-quantification of $CD140a^+$ cells in SVZ and perifocal area after 3 and 5 weeks of MCAO in AAV-GFP (□) and AAV-CXCL12 (■) transduced mice. n=3. *, p< 0.05; #, p< 0.01; AAV-CXCL12 vs. AAV-GFP (mean ± SD), IOD represents integral optical density.

Conclusions: Post-acute CXCL12 gene therapy is beneficial for white matter recovery without eliciting inflammatory response. Such recovery might be related to the proliferation and migration of oligodendrocyte progenitor cells mediated by CXCL12.

Reference:

1. Huang J, Li Y, Tang Y, Tang G, Yang GY, Wang Y. CXCR4 Antagonist AMD3100 Protects Blood-Brain Barrier Integrity and Reduces Inflammatory Response After Focal Ischemia in Mice. Stroke 2012.

A NEW RAT MODEL OF STRESS-INDUCED DEPRESSION ASSOCIATED WITH AGE-RELATED, SELECTIVE WHITE MATTER INJURY

H. Ono[1], H. Imai[1], S. Miyawaki[1], H. Horikawa[1], T. Ochi[1], A. Ito[1], S. Miyata[2], M. Kurachi[3], Y. Ishizaki[3], H. Yamagata[4], H. Nakatomi[1], M. Mikuni[2], N. Saito[1]

[1]Department of Neurosurgery, Graduate School of Medicine, The University of Tokyo, Tokyo, [2]Department of Psychiatry and Neuroscience, Gunma University Graduate School of Medicine, [3]Department of Molecular and Cellular Neurobiology, Gunma University Graduate School of Medicine, Gunma, [4]Division of Neuropsychiatry, Department of Neuroscience, Yamaguchi University School of Medicine, Yamaguchi, Japan

Background: Recently, late onset depression (LOD) is an important area of research given the growing elderly population in developed countries. The occurrence of white matter hyperintensities on T2-weighted magnetic resonance images is more frequent in patients with LOD, compared with early-onset depression. This fact indicates that deep white matter injuries (WMIs) may provoke some kind of vulnerability leading to depression with daily stress. In this study, we have developed a selective WMI rat model with restraint stress (RS) to evaluate stress vulnerability and depression related to WMI.

Methods: Sprague-Dawley rats (302-380g, total n=62) were used in this study. Selective WMI was induced under general anesthesia with bilateral endothelin-1 (0.5μg/μl) stereotaxically injected into the internal capsule. Sham animals received stereotaxic injections of phosphate buffered saline. 2 hours of RS was induced for 13 days. Animals were randomly assigned to 4 groups: WMI with RS (group 1, n=23); sham operation with RS (group2, n=17); WMI no RS (group3, n=11); sham operation, no RS (group 4, n=11). Two weeks after stereotaxic surgery , group 1 and 2 animals received 2 hours of RS a day, for 13 days. Body weight (BW) was recorded daily and the animals underwent a

forced swimming test (FST) on the day following the 13th RS day to evaluate depressive-like state. Serum corticosterone level was measured. Animals were euthanized after the FST, and brain sections analyzed with histology to confirm WMI in the internal capsule. Ladder test was conducted to analyze neurological status on the day before the first stress day.

Result: RS significantly suppressed weight gain in groups 1 and 2 compared with the non RS groups. Moreover the change in BW over time in group 1 was significantly different from group 2 (p=0.0013).

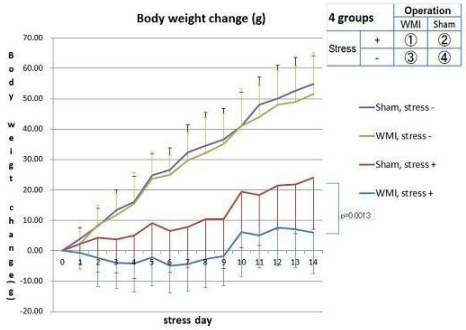

[Body weight change]

The immobility time on the FST for group 1 (mean 369.6 second) was longer than that of other groups (311.4, 283.7 and 259.9 second). Corticosterone levels were elevated at the 7th stress day and returned to basal levels at the 13th day in both RS groups. Histopathology confirmed selective damage within the internal capsule and the volume of the lesions were not significantly different between groups 1 and 3. Also neurological analysis showed no significant difference among 4 groups.

Consideration: We have investigated whether animals with selective WMI showed evidence of increased stress-induced depressive behavior. Accompanied with WMI, repeated RS induced a reduction in weight gain and prolongation of the immobility time in the FST. These results provide some preliminary evidence that WMI could influence stress vulnerability. One proposed etiology for LOD is the vascular depression hypothesis, where ischemic lesions in deep white matter disrupt projections to the frontal cortex. We have confirmed the connectivity of WMI with rostral frontal and caudate nucleus by using the retrograde tracer, Fluoro-gold. Although further study is needed, this study provides the first evidence that changes in the frontal cortex caused by WMI may have the potential to contribute to stress vulnerability.

SERUM AND CSF BIOMARKER LEVELS CORRELATE WITH BIOMECHANICAL RESPONSE AND AXONAL INJURY LEVELS IN CLOSED HEAD IMPACT TRAUMATIC BRAIN INJURY

L. Zhang, Y. Li, S. Kallakuri, J.M. Cavanaugh

Biomedical Engineering, Wayne State University, Detroit, MI, USA

Biomarkers have been studied in various TBI models and clinical settings in an effort to monitor the severity and progression of TBI. There is a lack of unified, biomechanically relevant injury models and direct correlation between tissue injury severity and levels of biomarkers. A head impact model was used to screen reliable biomarkers for various injury severities.

Anesthetized male Sprague-Dawley rats were subjected to TBI by a modified Marmarou impact acceleration device from 1.25, 1.75 and 2.25m heights (n=8/group, including controls). Linear and angular responses of the head were directly measured with two transducers affixed to the skull. Twenty-four hours post-trauma, CSF and blood were collected just before perfusion. CSF and serum levels of amyloid beta (Aβ) 1-42, neurofilament H (NF-H), glial fibrillary acid protein (GFAP) and interleukin (IL-6) were assessed by ELISA. Traumatic axonal injury (TAI) number accounted the total number of β-APP-reactive axonal swellings and retraction balls in the CC in each animal. Bivariate correlation was analyzed to correlate biomechanical parameters, with TAI number in CC and biomarker levels.

Compared to controls, significantly higher CSF and serum NF-H levels were observed in all impact groups, except 1.25m group in serum. CSF and serum NF-H levels at 2.25m were significantly higher than in other heights, and CSF and serum NF-H levels at 1.75 m were significantly higher than at 1.25m. In both CSF and serum, GFAP levels were significantly higher at 2.25m compared to other heights and controls. Though no significant difference in CSF and serum GFAP levels between 1.75m and 1.25m, these groups were significantly higher than controls. TBI rats also showed significantly higher levels of IL-6

versus control in both CSF and serum. However no significant difference was observed between TBI rats. Levels of Aβ were not significantly different between groups. Pearson's correlation analysis showed NF-H and GFAP levels in CSF had positive correlation with power ($p< 0.001$), average linear acceleration ($p< 0.01$) and surface righting ($p< 0.01$), which are strong predictors for TAI in our previous study. NF-H and GFAP levels in serum also showed good correlation with power, average and linear acceleration, and surface righting ($p< 0.01$). Both CSF and serum NF-H levels had good correlation with TAI number in CC ($r^2=0.607$, $r^2=0.600$, respectively). GFAP in CSF also showed good correlation with TAI number in CC ($r^2=0.622$), but no correlation was observed between serum GFAP and TAI number ($r^2=0.164$).

Correlations between the biomechanical parameters, biomarker levels, and TAI number in CC indicated that NF-H and GFAP in CSF and serum were reliable predictors for severe TBI in this model, whereas CSF NF-H was also a good indicator for mild TBI. GFAP in CSF and serum was a good indicator of mild/moderate TBI. Furthermore, the levels of NF-H and GFAP in CSF and serum had positive correlation with power and average linear acceleration, and CSF and serum NF-H, as well as CSF GFAP correlated well with quantified TAI in CC, suggesting they are directly related to the severity of the mechanical trauma to the brain.

CHARACTERIZATION OF WHITE MATTER INJURY BY DIFFUSION TENSOR MRI IN A RAT MODEL OF CHRONIC CEREBRAL HYPOPERFUSION

D.B. Back[1], B.-R. Choi[2], J.-S. Han[3], J.-H. Seo[1], W.J. Moon[4], B.R. Kim[5], J. Lee[5], H.Y. Kim[1]

[1]Neurology, [2]Neurology and Biological Sciences, [3]Biological Sciences, [4]Radiology, [5]Rehabilitation Medicine, Konkuk University, Seoul, Republic of Korea

Background: White matter lesions, resulting from chronic cerebral hypoperfusion, have been suggested as a culprit of cognitive impairments in patients with vascular dementia. Using diffusion tensor MRI (DTI), we investigated characteristics of white matter injury in a rat model of chronic cerebral hypoperfusion and possible attenuation of white matter injury by cilostazol, a potent antiplatelet agent working as a phophodiesterase 3 inhibitor.

Methods: In Wistar rats, chronic cerebral hypoperfusion was modeled by permanent occlusion of bilateral common carotid arteries. The experimental animals were divided into the cilostazol group (n=4) and the vehicle group (n=5). White matter injury was investigated by serial DTI at 1 week and 5 weeks after hypoperfusion. Parameters for white matter injury, including fractional anisotropy (FA), trace, axial diffusivity ($\lambda\parallel$), and radial diffusivity ($\lambda\perp$) were evaluated in the white matter of the cranial nerve, such as optic chiasm, or brain parenchymal white matter, such as corpus callosum and external capsule. Values of each parameter, compared to those of baseline, were evaluated by t-test and serial changes of two groups by paired t-test.

Results: Both experimental groups showed significantly reduced FA in the optic chiasm, compared to the baseline FA ($p< 0.05$). In the serial DTI study, vehicle group showed significant ongoing decrease of FA in the optic chiasm, compared to the cilostazol group ($p=0.034$). The vehicle group showed significant ongoing elevation of trace ($p=0.024$), $\lambda\parallel$ ($p=0.044$), and $\lambda\perp$($p=0.042$) values of the corpus callosum. Compared to the vehicle group, white matter injury was attenuated in the cilostazol group.

Conclusion: Characteristics of white matter injury resulting from chronic cerebral hypoperfusion may consist of demyelination and ongoing vasogenic edema with loss of tissue integrity. Cilostazol may have protective effect for the white matter injury by chronic cerebral hypoperfusion.

BrainPET Program

[^{11}C]CIMBI-36 BINDS 5-HT$_{2A}$ AND 5-HT$_{2C}$ RECEPTORS IN THE NON-HUMAN PRIMATE BRAIN - A COMPARISON STUDY WITH [^{11}C]MDL 100907

S.J. Finnema[1], V. Stepanov[1], A. Ettrup[2], R. Nakao[1], N. Amini[1], G.M. Knudsen[2], C. Halldin[1]

[1]Department of Clinical Neuroscience, Karolinska Institutet, Stockholm, Sweden, [2]Cimbi and Neurobiology Research Unit, Rigshospitalet and University of Copenhagen, Copenhagen, Denmark

Objectives: Agonist PET radioligands have potential for evaluation of the high affinity state of G protein-coupled receptors *in vivo*. Very recently the first agonist radioligands for the serotonin-2A (5-HT_{2A}) receptor have been reported [1] and we previously described the initial evaluation of [^{11}C]Cimbi-36 in non-human primates [2]. In the current study, we compared the regional receptor binding of the 5-HT_{2A} receptor agonist [^{11}C]Cimbi-36 and the 5-HT_{2A} receptor antagonist [^{11}C]MDL 100907. In addition, we evaluated the *in vivo* 5-HT_2 receptor subtype selectivity of [^{11}C]Cimbi-36 by performing blocking studies with the 5-HT_{2C} receptor selective antagonist SB 242084.

Methods: A total of 14 PET measurements were conducted in five rhesus monkeys on six experimental days. On each day, baseline PET measurements were obtained after an i.v. bolus injection of [^{11}C]Cimbi-36 and [^{11}C]MDL 100907. The two baseline PET measurements were conducted 2.5 hours apart and the order of radioligands was randomized. On two of the experimental days a third PET measurement was conducted, in which [^{11}C]Cimbi-36 was injected after pretreatment with SB 242084 (1.0 mg/kg, i.v.). PET measurements were performed for two hours and conducted in the HRRT PET system. Quantification of radioligand binding was performed using kinetic modeling with the simplified reference tissue model (SRTM). The outcome measure was the non-displaceable binding potential estimate (BP_{ND}), obtained using the cerebellar cortex as reference region. The relative BP_{ND} of [^{11}C]Cimbi-36 was defined as a percentage of [^{11}C]MDL 100907 BP_{ND} in the given regions.

Results: In general, [^{11}C]MDL 100907 provided higher BP_{ND} estimates than [^{11}C]Cimbi-36, e.g. 2.7±0.4 vs. 1.5±0.3 in neocortex. The mean relative BP_{ND} of [^{11}C]Cimbi-36 was consistently 50-60% across striatum and neocortex, but higher in several other brain regions, including hippocampus (116±26%), midbrain (112±57%), amygdala (86±23%) and thalamus (78±16%) (n=6). Administration of SB 242084 reduced [^{11}C]Cimbi-36 BP_{ND} estimates completely in the choroid plexus; partly in the midbrain (88 and 57%), hippocampus (45 and 69%) and amygdala (14 and 38%); but not in the neocortex (-1 and -2%) (n=2).

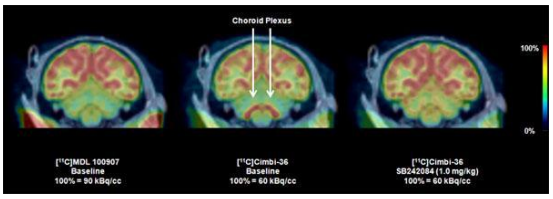

[Summation Images: 9-123 min]

Conclusions: The current study indicates that there are differences in the regional receptor binding of [^{11}C]Cimbi-36 and [^{11}C]MDL 100907. These regional difference are likely related to [^{11}C]Cimbi-36 binding to 5-HT_{2C} receptors. Thus [^{11}C]Cimbi-36 provides the unique opportunity for specific examination of 5-HT_{2A} receptors in the neocortex and of 5-HT_{2C} receptors in the choroid plexus.

References:

[1] Ettrup et al, 2011, Eur. J. Nucl. Med. Mol. Imaging, 681-693.

[2] Finnema et al, 2011, J. Nucl. Med, No 495.

CHARACTERIZATION OF [^{18}F]PF-05270430 AS A NOVEL PET RADIOTRACER TO IMAGE THE PHOSPHODIESTERASE-2A (PDE2A) BINDING SITES IN NON-HUMAN PRIMATES

N. Nabulsi[1], M. Naganawa[1], M. Skadden[2], L. Zhang[2], C. Helal[2], E.M. Beck[2], A. Villalobos[2], S.-F. Lin[1], S. Najafzadeh[1], D. Labaree[1], L. Chen[2], K. Zasadny[2], T. Bocan[2], R.N. Waterhouse[2], R.E. Carson[1], Y. Huang[1]

[1]PET Center, Department of Diagnostic Radiology, Yale University, New Haven, [2]Pfizer Inc., Groton, CT, USA

Objectives: Phosphodiesterase-2A (PDE2A) is a dual-substrate enzyme for both cyclic AMP and cyclic GMP, with the highest levels of expression in the limbic and basal ganglia brain circuitry. In preclinical studies, PDE2A inhibitors are found to enhance cognitive function, and thus are pursued as potential therapeutic agents for the treatment of cognitive impairment. PF-05270430 is a potent PDE2A inhibitor with excellent selectivity over other PDE subtypes. The purpose of this study was to evaluate the ability of the novel radiotracer [^{18}F]PF-05270430 to image and

quantify the PDE2A binding sites in non-human primates.

Methods: [^{18}F]PF-05270430 was synthesized via [^{18}F]fluorination of a tosylate precursor. Brain PET scans in rhesus monkeys were acquired on the Focus-220 for up to 180 min. Arterial blood samples were collected for measurement of radioactive metabolites and tracer free fraction in the plasma, and for generation of arterial input function for kinetic analysis. Regional time-activity curves (TACs) were measured in ten brain regions including striatum, neocortical regions, and cerebellum. TACs were analyzed with one- and two- tissue compartment models (1T and 2T) and the multilinear analysis method (MA1) to derive regional distribution volumes (V_T) and binding potentials (BP_{ND}, using the cerebellum as a reference region). The Simplified Reference Tissue Model (SRTM) was also evaluated for determination of regional BP_{ND}. Variability in model-derived binding parameters between test and retest scans was calculated as %diff=100×|retest-test|/(test+retest)×2.
Blocking studies with PDE2A inhibitors were conducted to assess in vivo binding specificity of the radiotracer.

Results: [^{18}F]PF-05270430 was prepared in >99% radiochemical purity and mean specific activity of 3.3 mCi/nmol (n = 8) at end of synthesis. The peripheral metabolism rate of [^{18}F]PF-05270430 was moderate. Plasma free fraction was 19 ± 3 % (n = 7). Tracer uptake in the brain was rapid, with peak levels at ~5 min after injection. The highest level of uptake was in the striatum, with intermediate levels in other regions and lowest level in the cerebellum. Model fitting selected the MA1 as the optimal model for derivation of regional V_T and BP_{ND}. SRTM was also suitable for calculation of regional BP_{ND} without the use of arterial input data. A scan duration of 120 min was sufficient to reliably quantify regional V_T and BP_{ND}. Test-retest variability in high-binding regions (putamen, caudate, and nucleus accumbens) was 4 ± 6%, 13 ± 6%, and 13 ± 7%, respectively, for V_T(MA1), BP_{ND}(MA1), and BP_{ND}(SRTM). Pretreatment with a structurally similar selective PDE2A inhibitor at a dose of 2.0 mg/kg (sc) reduced [^{18}F]PF-05270430 BP_{ND} by ~72%, while a reduction of ~48% was seen when unlabeled PF-05270430 (65 µg/kg, iv) was co-injected with [^{18}F]PF-05270430.

Conclusions: We characterized the binding specificity and imaging quality of the first selective PDE2A tracer in rhesus monkeys and demonstrated that [^{18}F]PF-05270430 can be used to reliably quantify PDE2A binding sites *in vivo***.** Based on its favorable imaging properties, this novel radiotracer has been advanced to further evaluation in humans.

A PET SCANNER WITH 0.6 MM RESOLUTION DESIGNED FOR NEUROIMAGING IN MICE

Y. Yang[1], J. Bec[1], J. Zhou[1], M. Zhang[1], M.S. Judenhofer[1], X. Bai[1], K. Di[1], Y. Wu[1], K.S. Shah[2], R. Farrell[2], J. Qi[1], **S.R. Cherry**[1]

[1]Department of Biomedical Engineering, UC Davis, Davis, CA, [2]Radiation Monitoring Devices Inc, Watertown, MA, USA

Objectives: To build and evaluate a prototype small-animal positron emission tomography (PET) scanner for imaging the mouse brain that approaches the resolution limits set by the physics of positron emission and annihilation.

Methods: The scanner consists of 16 dual-ended readout tapered scintillation detectors arranged in a ring of diameter 61 mm. The scintillator arrays consist of 14x14 lutetium oxyorthosilicate (LSO) elements, with a crystal size of 0.43x0.43 mm^2 at the front end and 0.80x0.43 mm^2 at the back end. The crystal elements are 13 mm long. The axial field of view is 7 mm and transaxial field of view is 40 mm. The arrays are read out by an 8x8 mm^2 and a 13x8 mm^2 position-sensitive avalanche photodiodes placed at opposite ends of the scintillator array to provide depth-of-interaction information. The intrinsic spatial resolution, sensitivity and reconstructed spatial resolution of the scanner were measured. First phantom and *in-vivo* mouse images were acquired.

Results: The sensitivity of the scanner at center of the field of view is 1.1% for a lower energy threshold of 100 keV and 0.6% for a lower energy threshold of 250 keV. The average detector intrinsic spatial resolution in the axial direction is 0.61 mm. The spatial resolution within a field of view that can accommodate the entire mouse brain is better than 0.6 mm using a ML-EM reconstruction algorithm of line/point sources. Sources were reconstructed in a warm background to ensure they were not artificially improved due to the non-negativity constraint in the ML-EM algorithm. Images of a micro hot-rod phantom showed that rods with diameter down to 0.5 mm can be resolved. First in vivo studies were obtained using ^{18}F-fluoride and confirmed that

0.6 mm resolution can be achieved in the mouse head in vivo.

Conclusions: A prototype preclinical PET scanner dedicated to mouse brain imaging with a spatial resolution less than 0.6 mm was developed. The performance of the scanner was measured and phantom and *in-vivo* studies performed. Brain imaging studies with ^{18}F-fluorodeoxyglucose as well as neuroreceptor ligands will be acquired. Future plans are to add more detector rings to extend the axial field of view of the scanner and increase sensitivity.

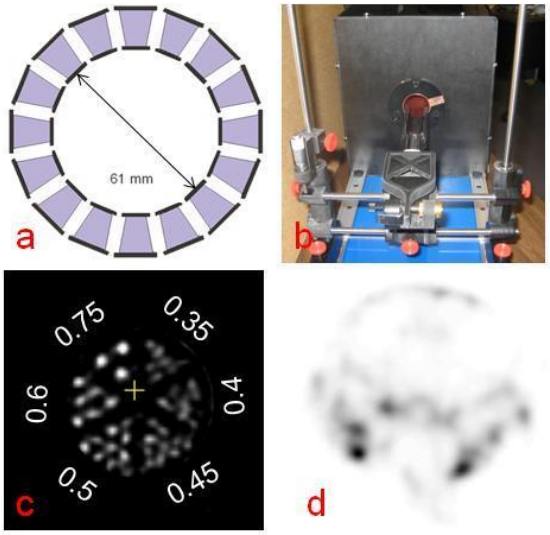

[Figure]

Figure:

(a) Schematic of the prototype scanner showing the 16 dual-ended tapered detectors;

(b) Photograph of completed scanner;

(c) Image of a micro hot rod phantom showing that 0.5 mm are resolved;

(d) Coronal section of juvenile mouse head showing the ability to image the 0.2-0.3 mm thick skull with 18F-fluoride.

BRAIN PET IMAGING OF FREELY MOVING RATS: SYSTEM DESIGN AND PILOT ANIMAL DATA

A. Kyme[1,2], R. Fulton[1,2,3,4], J. Eisenhuth[1], G. Angelis[1,2], W. Ryder[1,2], K. Popovic[1,2], V. Zhou[5], R. Bashar[1,2], S. Meikle[1,2]

[1]Faculty of Health Sciences, [2]Brain & Mind Research Institute, [3]School of Physics, University of Sydney, [4]Department of Medical Physics, Westmead Hospital, Sydney, NSW, [5]Faculty of Science, Engineering and Health, University of Central Queensland, Mackay, QLD, Australia

Objective: The objective of this work is to develop a PET imaging system for simultaneously measuring the brain function and behaviour of freely moving rats.

Introduction: Small animal positron emission tomography (PET) is a vital tool for non-invasive, longitudinal investigations in laboratory animals. In particular, brain PET has the potential to improve our understanding of the molecular origins of debilitating brain disorders such as dementia, depression and schizophrenia. In most imaging studies involving animals, anaesthesia is used to prevent motion which would otherwise result in corrupted images of the radiotracer biodistribution. However, anaesthetics are known to interfere with key biological processes [1]. Moreover, imaging unconscious animals precludes the study of brain function during learning tasks and complex behaviours. In this paper we describe a system under development that overcomes these limitations by enabling the brain of an awake, freely moving rat to be imaged while simultaneously studying its behaviour in response to environmental or drug stimuli.

Methods: The imaging system is based on a commercial small animal PET scanner (Siemens Focus 220) in conjunction with a robot-controlled observation chamber and optical motion tracking to provide the animal head pose in real time [2] (figure 1). Head pose measurements (obtained at 30 Hz with 0.2 mm r.m.s accuracy) from the tracking system serve two purposes: they are translated into robot manipulator movements aimed at maintaining the rat's head centrally in the PET field-of-view; and they are used within an event-by-event image reconstruction algorithm that corrects for motion. To validate the system, a rat was administered 60 MBq of ^{18}F-FDG and imaged for 20 minutes while awake and moving freely within the observation chamber. During this time the animal made numerous complete turns within the scanner. For comparison, the animal was then imaged (motionless) under anaesthesia.

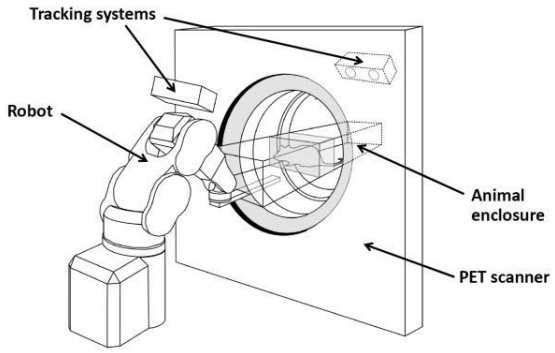

[Figure 1]

Results: Figure 2 shows orthogonal reconstructed slices of the brain of the freely moving animal with motion correction (left column) and the same animal motionless under anaesthesia (right column). The results are qualitatively comparable and indicate the feasibility of observing the brain and its internal structures when motion compensation is applied. We are currently working on methods to optimise the quantitative accuracy of brain PET measurements in awake animals, including corrections for photon attenuation and partial volume effect.

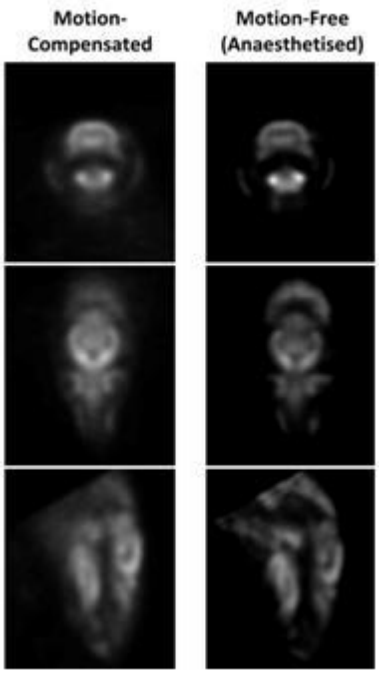

[Figure 2]

Conclusions: A system has been developed to simultaneously measure the brain function and behaviour of freely moving rats. Pilot data confirm the feasibility of the system for obtaining useful brain images. Further work is in progress to improve the quantitative accuracy of these images. We conclude that imaging the brain function of a freely moving animal with PET is feasible, making simultaneous studies of behaviour and brain function a realistic and exciting prospect.

References:

[1] Momosaki S et al., *Synapse*, 54: 207-213, 2004.

[2] Kyme A et al., *J R Soc Interface*, 9: 3094-3107, 2012.

COMPARISON BETWEEN BETA-MICROPROBE AND MICROPET IN INVESTIGATING RECEPTOR BINDING EXEMPLIFIED BY THE MGLUR5 TRACER [11C]ABP688

T. Wyckhuys[1], J. Verhaeghe[1], L. Wyffels[1,2], M. Schmidt[3], X. Langlois[3], S. Stroobants[1,2], S. Staelens[1]

[1]Molecular Imaging Center Antwerp, University of Antwerp, Wilrijk, [2]Nuclear Medicine, University Hospital Antwerp, Edegem, [3]Department of Neuroscience, Janssen Pharmaceutica NV, Beerse, Belgium

Objectives: Beta-microprobes are radiosensitive probes implanted stereotactically in anesthetized animals. They are used to record regional real-time kinetics of positron-emitters and are suggested as an alternative to microPET. The present study aims to compare the capacity of both microPET and beta-microprobes to measure binding of [11C]ABP688, an allosterically bound mGluR5 tracer. It has high affinity for various brain regions, including striatum. Due to low specific binding, the cerebellum is a suitable reference region for image analysis.

Methods: Three experiments were performed

i) rats (n=6) were anesthetised, positioned into the microPET Inveon scanner and injected with [11C]ABP688 (iv., < 3 nmol/kg) at initiation of a dynamic scan (1h). Images were normalized to a [11C]ABP688 rat brain template and time-activity curves (TAC) were extracted from a VOI-template containing striatum and cerebellum. Non-displaceable binding potential (BP_{ND}) and R1, the rate of

delivery of the tracer to the tissue were calculated using the simplified reference tissue model (SRTM) with the cerebellum as reference;

ii) rats (n=6) were anesthetised, implanted with two beta-microprobes: one in the striatum (stereotactic coordinates: AP +0.2, ML 3.0, DV -6.0) and one in the cerebellum (AP -11.8, ML 0.0, DV -3.5). Recording of radioactivity (1h) was started at the time of [11C]ABP688 injection. Both TACs, BP_{ND}s and R1 were determined similarly as in the microPET experiment;

iii) rats (n=6) were implanted with dummy beta-microprobes in an identical way as in the beta-microprobe experiment. Dummy probes were identically coated as the beta-microprobe and were secured to the skull with dental cement after implantation. Animals were then transferred to the microPET scanner, injected, scanned and analysed similar to the first experiment.

Results: Average BP_{ND} in the striatum for the microPET experiment was 2.49 +/- 0.13 closely resembling those observed in previous studies. The BP_{ND} for the beta-microprobe experiment was significantly ($p< 0.05$) lower i.e. 1.14 +/- 0.31 and suffered from higher variability. Further, microPET images of dummy-probe implanted animals revealed significantly lower BP_{ND} and R1 values at the side of implantation in comparison with the intact side (Fig.). BP_{ND} and R1 values are 2.51 +/- 0.12 and 0.72 +/- 0.07 at the intact site and 2.16 +/- 0.19 and 0.46 +/- 0.05 at the side of implantation respectively.

Figure: TACs for both microPET

(a) and beta-microprobe

(b) experiments, with larger variance for beta-microprobes in comparison with microPET. In

(c) the results of the dummy-probe implanted microPET scanned animals are indicated: significantly lower BP_{ND} and R1 in the striatum at the side of implantation in comparison with the intact side.

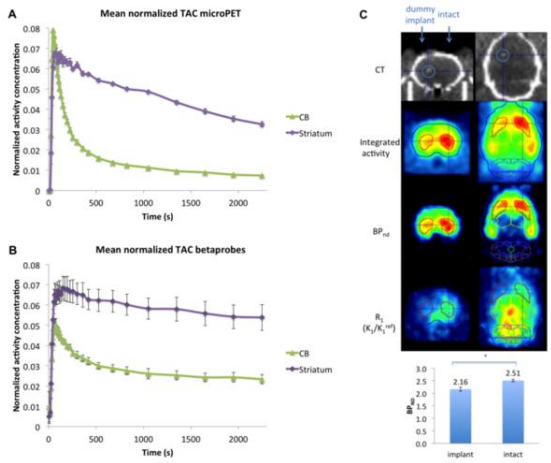

[Figure]

Conclusions: Implantation of beta-microprobes gives rise to a lower rate of delivery of the tracer to the tissue and significantly affects the BP_{ND} values. Further, high variability and the lack of intra-animal comparison in beta-microprobe experiments, contribute to the necessity of high animal numbers. This study thus reveals a number of disadvantages inherent to the use of beta-microprobes relative to microPET as a means to measure radioligand binding in the rat brain.

ACTIVATED ASTROCYTES OVEREXPRESS TSPO AND ARE DETECTED BY TSPO-RADIOLIGANDS

S. Lavisse[1], M. Guillermier[1], A.-S. Hérard[1], F. Petit[1], N. Van Camp[1], L. Ben Haim[1], V. Lebon[1], P. Remy[1,2], F. Dollé[3], T. Delzescaux[1], G. Bonvento[1], P. Hantraye[1], C. Escartin[1]

[1]MIRCen and CNRS URA 2210, Commissariat à Energie Atomique, Fontenay-aux-Roses, [2]Neurology, CHU Henri Mondor, AP-HP and UPE-C, Creteil, [3]SHFJ, Commissariat à Energie Atomique, Orsay, France

Under neuroinflammatory condition, it is widely considered that TSPO PET signal reveals reactive microglia. As astrocytes and microglia are both involved in neuroinflammatory processes but play very different roles, the objective is to determine *in vivo* whether reactive astrocytes can also overexpress TSPO and yield to a detectable TSPO PET signal.

We used a model of selective astrocyte

activation through lentiviral gene transfer of the cytokine ciliary neurotrophic factor (CNTF). Sprague-Dawley rats were injected with lenti-LacZ (control) and lenti-CNTF in the left and right striatum, respectively.

Rats were analyzed between 2 and 6 months after injection, as CNTF effects are stable for at least 6 months. Animals were scanned on a Concorde Focus 220 microPET using two recently-developed and on-site available TSPO-radioligands [^{18}F]DPA-714 and [^{11}C]SSR180575. TSPO selectivity of these radioligands was assessed through displacement and blocking studies with unlabelled PK11195.

T2-weighted MRI was performed on a 7-Tesla system to confirm the injection site and define anatomical regions of interest (ROI) in the striata through PET/MRI co-registration. The mean activity concentration values in the ROIs were calculated to obtain regional time activity curves.

One week after PET scan, rats were euthanized. Immunohistochemistry was performed on frozen sections with GFAP, ED1/CD68, IBA1 and Vimentin-targeted primary antibodies. Staining intensity on digitized sections was evaluated in the striatum on 6-8 slices per rat, using a computer based image analysis system. Double fluorescent immunostaining was also performed on free floating sections with primary antibodies directed against GFAP, CD11b, TSPO and Vimentin.

GFAP histological volume was reconstructed in 3D and co-registrated with the corresponding PET volume to compare GFAP and TSPO localization.

We confirmed that CNTF induced a strong activation of astrocytes with a significant increase in GFAP and vimentin immunoreactivity while minimal microglial activation was observed with only a small increase in IBA1 and ED1/CD68 staining (1.2-fold). TSPO immunoreactivity was increased in the striatum injected with lenti-CNTF, in an area that overlapped with the GFAP-positive area. Cells that overexpressed TSPO in this striatum were also strongly immunoreactive for GFAP. There was a minimal expression of TSPO in CD11b-positive microglia, that was not different from the one observed in the controlateral side.

Both [^{18}F]DPA-714 and [^{11}C]SSR180575 highlighted a significant increased binding in the lenti-CNTF-injected striatum, as compared with the contralateral side. Following pre-saturation with PK11195, the uptake of both radioligands was faster and higher than in the standard experiment and was followed by a rapid wash-out of radioactivity to the same low level for both sides. In the displacement studies, injection of PK11195 induced a fast decline in the binding of both [^{18}F]DPA-714 and [^{11}C]SSR180575 in the lenti-CNTF-injected striatum.

Volumes of [^{18}F]DPA-714 and [^{11}C]SSR180575 binding unambiguously coincided with the GFAP-positive reconstructed volume.

We showed that reactive astrocytes overexpress TSPO, yielding to a significant and selective binding of TSPO radioligands. Therefore, caution must be used to interpret TSPO PET imaging in animals or patients because reactive astrocytes can contribute to the signal in addition to reactive microglia.

CBF MEASURED BY 15O-WATER-PET AND ASL-MRI SIMULTANEOUSLY IN AN INTEGRATED 3TMR-BRAINPET

H. Herzog[1], K. Zhang[1], J. Mauler[1], C. Filss[1], E. Rota Kops[1], L. Tellmann[1], T. Fischer[2], B. Brocke[2], W. Sturm[3], A. Buck[4], N.J. Shah[1]

[1]Inst. of Neuroscience and Medicine - 4, Forschungszentrum Juelich GmbH, Juelich, [2]Dept. of Psychology, Technical University Dresden, Dresden, [3]Dept. of Neurology, RWTH Aachen University, Aachen, [4]Dept. Nuclear Medizine, ETH and University Zuerich, Zuerich, Germany

Introduction: Measurements of cerebral blood flow (CBF) using 15O-water-PET and ASL-MRI have been compared previously. Until now the two procedures were not performed simultaneously. Using a 3TMR-BrainPET, which integrates a BrainPET developed by Siemens as an insert in a Siemens 3T MAGNETOM MRI, we studied 15O-water-PET and ASL-MRI simultaneously. Here we report our first experiences.

Material and methods: Four healthy male volunteers (20 - 30 yrs) were studied in the 3TMR-BrainPET twice. At each study 555 MBq 15O-water were intravenously injected as a fast bolus four times with intervals of 15 min. At the time of injection the BrainPET listmode

acquisition was started for 3 min. During this period arterial blood was withdrawn from a radial artery and the time-activity curve (TAC) of whole blood was monitored with an MR-compatible bloodsampler (Swisstrace®). The BrainPET data were corrected and reconstructed into quantitative images. The optimum image resolution is 3mm before and 5 mm after filtering. Combining these images and the blood data corrected for delay and dispersion into the autographic 15O-water method quantitative CBF images became available. In two measurements blood could not be sampled. In this case an image derived input function (IDIF) was applied, which was defined with volumes-of-interest (VOIs) placed over the internal carotid arteries (CA) in an MPRAGE image and transferred to the PET images. The IDIF was corrected for partial volume effect and spillover utilizing other data sets of the same subject with both arterial blood and CA-TAC. Two minutes prior to each PET scan a pseudo-Continuous Arterial Spin Labeling (pCASL) sequence was started for 6 min. pCASL uses a 1.4s train of RF and gradient pulses to invert the magnetization of blood water flowing through the labeling plane. The labeling plane was selected on a time of flight angiography to ensure optimal orientation of the carotid and vertebral arteries. A delay of 1s between labeling and readout guaranteed blood perfusion of the majority of the voxels. The pre-saturation pulses are applied to the imaging region before labeling to avoid spin perturbation in imaging planes caused by the labeling train. Using readouts with single-shot 2DEPI, 100 measurements with 50 pairs of label-control volumes were obtained. Explicit sequence parameters were: α/TE/TR=90°/14/4150ms, dim: 64×64×26, Partial Fourier=6/8, voxel size: 3.4×3.4×5mm3. ASL-CBF was quantified using the ASLtbx in MATLAB.

Results: The visual comparison between PET-CBF- und ASL-CBF-images revealed a good agreement. The ASL-CBF-images presented minor artifacts at the outer cortical border. Evaluating a whole-brain VOI and averaging over all measurements (n=4x8=32) PET-CBF was 49.2±10.6 ml/100g/min and ASL-CBF 36.9±5.22 ml/100g/min. After normalizing all images in the MNI space and averaging all PET- and ASL-images, respectively, the white matter CBF at the level of the centrum semiovale was 25.8±2.3 ml/100g/min for PET and 18.8±5.8 ml/100g/min for ASL. The corresponding gray matter CBF was 59.5±7.6 ml/100g/min and 61.2±12.5 ml/100g/min.

Conclusion: The simultaneous MR-PET study of CBF with 15O-Wasser-PET and ASL-MRI allowed a first direct comparison of both methods in humans. The observed differences are to be examined in further subjects.

ROBUST VOI BASED ANALYSIS OF MGLUR5 IMAGING IN RAT BRAIN USING [^{11}C]ABP688

J. Verhaeghe[1], T. Wyckhuys[1], L. Wyffels[1,2], M. Schmidt[3], X. Langlois[3], S. Stroobants[1,2], S. Staelens[1]

[1]Molecular Imaging Center Antwerp, University of Antwerp, Wilrijk, [2]Nuclear Medicine, University Hospital Antwerp, Edegem, [3]Department of Neuroscience, Janssen Pharmaceutica NV, Beerse, Belgium

Objectives: Normalization is an important step in small-animal PET/CT imaging of the brain that maps the PET data from different subjects into a common stereotaxic space using a template image. Ideally a PET template mimics the uptake of the given tracer. In this study a PET template of [^{11}C]ABP688, a tracer for mGluR5, has been developed. Additionally, alternative CT and PET/CT templates were developed.

Methods: Rats (n=11) received two dynamic [^{11}C]ABP688 PET/CT scans (1h) in a test-retest protocol. Time summed PET, thresholded CT and a weighted sum of both images were used to create a PET, a CT and a PET/CT template respectively by iterative elastic registering and averaging these 22 brain scans. Additionally, a T2 weighted MRI and high count [^{11}C]ABP688 PET/CT scan of a single rat was performed. The aforementioned average PET, CT and PET/CT images were then co-registered to the high count PET/CT that was aligned with the MR. To form the final template, these images were then transformed to the stereotaxic space according to the normalization of the animal's MR to an existing MR image in the stereotaxic space. To evaluate if PET, CT or PET/CT normalization is preferred, each test-retest scan was normalized according to the three different templates. Non-displaceable binding potential (BP_{ND}) and ΔBP_{ND} (test-retest) of [^{11}C]ABP688 was calculated for five predefined regions (Figure). In an additional experiment (n=6), [^{11}C]ABP688 specific binding was completely blocked. After normalizing these images, the number of skull pixels that were erroneously

normalized into the cerebellum was counted to quantify the normalization procedure in this challenging case.

Results: For all tested regions, the mean ΔBP_{ND} was lowest for the PET based registration (Figure) indicating that normalization using this template is more robust, although these differences were not significant. The variability of ΔBP_{ND} was however always lower for the PET based method (Figure) (significant ($p< 0.05$) in frontal cortex and hippocampus). Also, the absolute BP_{ND} value from the CT based normalization was significantly different from the BP_{ND} value from PET and PET/CT based normalization. The largest difference in BP_{ND} between the PET and CT based method was 23% (frontal cortex). For the blocking experiment on the other hand, the number of skull pixels that were normalized into the cerebellum was largest for the PET based and lowest for the CT based normalization. Differences were significant.

Figure: The three templates, mean and coefficient of variation (COV) of ΔBP_{ND} for test-retest

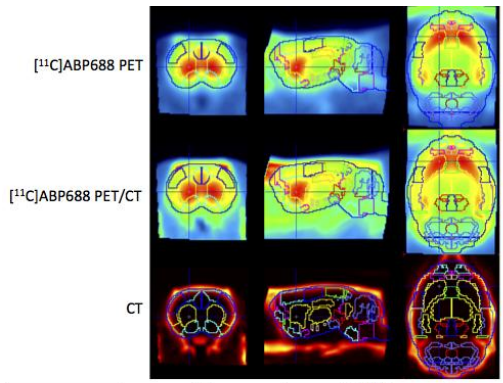

n=11	PET		PECT/CT		CT	
	mean ΔBP_{ND}	COV ΔBP_{ND}	mean ΔBP_{ND}	COV ΔBP_{ND}	mean ΔBP_{ND}	COV ΔBP_{ND}
Striatum	1.6%	13.2%	7.1%	17.2%	6.1%	22.6%
Frontal cortex	-0.3%	13.8%	-4.2%	30.1%	-4.4%	46.8%
Cortex	0.5%	10.0%	4.6%	20.0%	5.2%	31.1%
Hippocampus	0.5%	10.8%	7.7%	17.0%	8.0%	25.0%
Whole brain	1.3%	12.8%	6.9%	17.8%	7.4%	24.7%

[Figure 1]

Conclusions: Rat brain templates for [^{11}C]ABP688 imaging were developed. When specific binding was present the use of the PET template resulted in the best test-retest performance. The use of the CT template drastically increased test-retest variability. When no specific binding was present due to a blocking challenge a large number of skull pixels were normalized into brain regions when using the PET template, which could be remedied by using the CT template. In both the test-retest and blocking experiment, the results of the PET/CT template was ranked intermediate.

PHARMACOKINETIC MODEL BASED GROUPWISE IMAGE REGISTRATION OF 4D BRAIN PET DATA AND ITS IMPACT ON CLINICAL OCCUPANCY STUDIES WITH [^{11}C]-(+)-PHNO

J. Jiao[1,2], G.E. Searle[2], J.A. Schnabel[1], R.N. Gunn[1,2,3]

[1]Oxford University, Oxford, [2]Imanova Limited, [3]Imperial College, London, UK

Aims: Subject motion can introduce significant errors into measured PET emission data that are then propagated into inaccurate biological parameter estimates. We present a kinetic model based spatio-temporal image registration method for 4D brain PET data that registers all image frames together in a groupwise manner. The performance of the method is then assessed using realistic phantom and clinical data from an occupancy study with the D3 preferring PET radioligand [^{11}C]-(+)-PHNO and a D3 antagonist.

Methods: 8 healthy volunteers each received a high resolution T1 MRI scan and up to three [^{11}C]-(+)-PHNO PET scans (one at baseline and up to two further scans between 1.5 and 29 hours after administration of a single oral dose of 5 - 300 mg of GSK618334). Arterial blood was sampled for input function generation and venous blood for measurement of GSK618334 plasma concentration. For validation purposes, a motion-free 4D [^{11}C]-(+)-PHNO phantom was first developed, using data from one subject with negligible motion. Known rigid-body head motion was applied to the phantom data to generate a range of simulated datasets. A pharmacokinetic model based groupwise image registration motion correction algorithm (GIR method [1]) was applied to both simulated and measured data sets. D3 relevant ROIs were manually delineated as described previously and applied to dynamic data to generate time activity curves (TACs) [2]. A two-tissue compartment model (2TC) was applied to the realigned TAC data to derive BP_{ND} estimates. For the measured data, a competitive binding model accounting for 2-site binding and PHNO mass dose effects was used to model the relationship between [^{11}C]-(+)-PHNO BP_{ND} and the plasma concentration of GSK618334 [3].

We also compared GIR with a frame-by-frame registration method based on the normalised mutual information (FBF method).

Results: Simulation results in Fig1 (b) show that GIR provided more accurate estimates of occupancy. For measured data, the residual sum of squares from 2TC model fit was lowest with GIR (54.6±28.1% of the non-motion corrected values across all TACs, whereas FBF was 71.7±42.6%). In addition, 4.78% of FBF corrected TACs led to problems in convergence for the optimiser, whereas all TACs derived from GIR were fitted successfully. In the competitive binding analysis, the residual sum of squares was mostly lowest for GIR corrected data sets (FBF values in brackets) 60.3(73.8)%, 71.6(97.3)%, 63.5(52.8)%, 69.3(77.5)%, 93.1(108.2) % and 113.2(91.2) % of the non-motion corrected values for structures SN, GP, VST, CD, PU and TH.

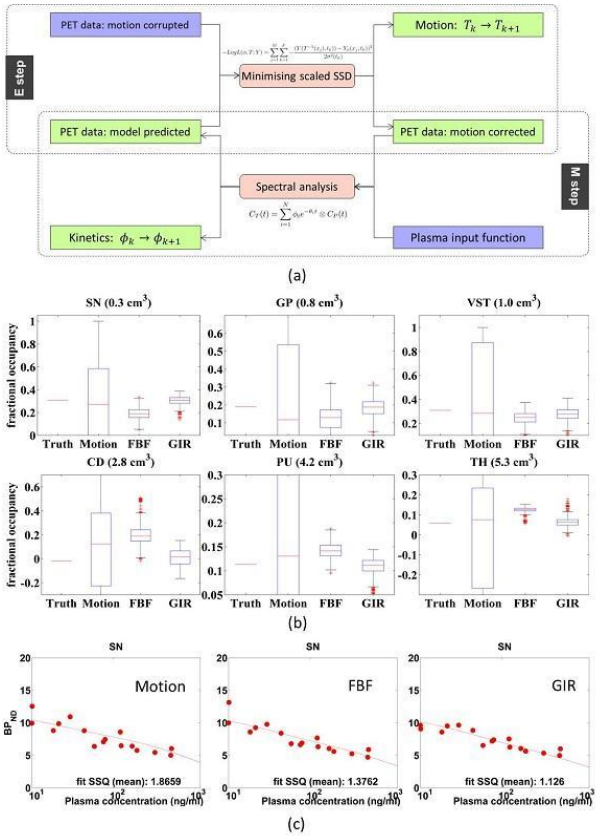

Fig 1 (a) GIR Algorithm (b) Simulation results for a dose of 25 mg: recovery of occupancy (c) Measured data: Competitive binding model fits.

Conclusions: Application of pharmacokinetic model based groupwise image registration significantly improves the accuracy of quantitative [^{11}C]-(+)-PHNO PET neuroimaging studies. This method is applicable to all dynamic brain PET imaging studies due to the incorporation of a generic kinetic model.

References:

[1] Jiao *et al*. LNCS 2012; 7570: 100-112.

[2] Tziortzi *et al*.Neuroimage 2011;54, 264-77.

[3] Searle *et al*. Mathematical modelling of [11C]-(+)-PHNO human competition studies. Neuroimage (in press)

IMPACT OF PARTIAL VOLUME CORRECTION AND BRAIN ATROPHY ON AMYLOID IMAGING QUANTIFICATION

Y. Su[1,2], T. Blazey[1], A.Z. Snyder[1,2,3], J.C. Morris[2,3], T.L.S. Benzinger[1,2,4]

[1]Radiology, [2]Knight Alzheimer's Disease Research Center, [3]Neurology, [4]Neurological Surgery, Washington University School of Medicine, St. Louis, MO, USA

Objectives: The goal of this study is to evaluate the impact of partial volume effects (PVE) and brain atrophy on amyloid imaging quantification in both cross sectional and longitudinal studies using simulation and clinical data.

Methods: MR images of six participants with low, medium and high cortical thicknesses were chosen from our Knight Alzheimer Disease Research Center (KADRC) cohort to use as the anatomical references for creating simulated images. Partial-volume-corrected regional time-activity curves (TAC) from five participants with different amyloid load were used as the functional references for the simulation. Simulated dynamic PET data was created for each combination of MR data and PET data. The simulated image was then smoothed to PET resolution. For three out of the six subjects, a second MR scan was also used to create additional simulations to evaluate the impact of atrophy on longitudinal studies. In the clinical study, 90 participants enrolled at KADRC with repeated imaging sessions were included. Each imaging session included a PiB PET and a T1-weighted magnetization-prepared rapid gradient echo (MPRAGE) sequence. FreeSurfer v5.1 (Martinos Center for Biomedical Imaging, Charlestown, Massachusetts, USA) was used to segment the T1-weighted MRI for each

participant. Regional quantification was performed using Logan graphical analysis. PVE corrections (PVC) were performed using both a two-component (PVC2C) approach and a regional-spread-function (RSF) technique.

Results: The simulation study demonstrated that in a cross-sectional analysis, without PVC, there was an underestimation of both regional and global BP_{nd}. For a particular amyloid load the estimated BP_{nd} positively correlated with cortical thickness. The slope of the linear relationship increased together with the amyloid load. Both PVC techniques were able to keep the estimated BP_{nd} unchanged with different cortical thicknesses. However, there is a differential underestimation of the actual BP_{nd} for the PVC2C method, with minimal underestimation at low amyloid load and large underestimation at high amyloid load. Similar patterns of PVE were observed in longitudinal simulation study and false decreases in BP_{nd} were observed without PVC. Both PVC techniques were able to reduce the impact of PVE, although the RSF technique was more stable. In the clinical study, the baseline BP_{nd} was highly correlated between the PVC and uncorrected results (r=0.982 for PVC2C and r=0.990 for RSF). Among the 42 participants whose baseline MCBP were greater than 1.06 in the longitudinal study, decreased global BP_{nd} was observed in 9 participants and decreased precuneus BP_{nd} was observed in 11 participants. When RSF PVC was performed, 4 of the 9 decreases in global BP_{nd} reversed, and 7 of the 11 decreases in precuneus BP_{nd} reversed. When PVC2C was performed, decreased global BP_{nd} was observed in 8 participants, and decreased precuneus BP_{nd} was observed in 8 participants.

Conclusions: The simulation and patient study demonstrate the importance of PVC in quantitative amyloid imaging studies. Both PVC2C and RSF techniques were able to reduce the impact of PVE in amyloid load quantification, while the RSF technique is more effective in reducing false decreases in BP_{nd} for longitudinal studies.

PERFORMANCE EVALUATION OF AN INTEGRATIVE SOFTWARE ENVIRONMENT FOR ANALYSIS OF MULTI-MODALITY NEUROIMAGING DATA IN PEDIATRIC EPILEPSY

O. Muzik[1], D. Pai[2], E. Asano[1], C. Juhasz[1], J. Hua[2]

[1]Pediatrics, [2]Computer Science, Wayne State University, Detroit, MI, USA

Objectives: The objective of this study was to quantitatively assess the spatial accuracy of a method that allows parcellation of the cortical surface in native space that yields finite cortical elements (FCEs) that are homotopic across subjects. These FCEs are subsequently used to integrate information obtained from PET, diffusion tensor imaging (DTI) and intracranial electrocorticography (ECoG) into a cohesive computational framework. The integration of complementing modalities is likely to improve our understanding of mechanisms involved in seizure propagation.

Methods: FCEs in native space were created using landmark-constrained conformal mapping. A set of 9 major cortical landmarks was manually defined in native space and mapped onto a sphere based on a conformal transformation. Landmarks were then aligned on the sphere and a recursive parcellation scheme was applied to create 512 finite surface elements that were subsequently transferred back into native space. The surface elements were subsequently extended 10mm inside the brain, thus creating 256 FCEs for each hemisphere that are homotopic across subjects. To assess the spatial accuracy of the FCEs, we compared our method to results derived using the Freesurfer software in 10 normal subjects with respect to the cortical parcellation of 5 cortical territories per hemisphere. Moreover, to demonstrate usefulness for integrative analysis in clinical epilepsy research, we applied this framework to 7 young children who underwent presurgical evaluation and compared the obtained functional/connectivity patterns against 12 age-matched normal children. All children underwent FDG PET and MR/DTI imaging, moreover ECoG was performed in children who underwent two-stage epilepsy surgery. Connectivity analysis using probabilistic fiber tracking was performed between areas of

ECoG defined seizure onset or PET defined abnormalities and the remaining cortex.

Results: The agreement between cortical parcellation performed using Freesurfer and our FCEs was higher than 80% for all anatomical territories, with highest agreement in the frontal/central area (92%) and lowest agreement in the parieto-occipital lobe (81%, see **Figure 1A**). No L/R differences were determined. Variance of FDG PET tracer distribution was highest in the temporal lobe (19%) and lowest in the frontal lobe (16%). Application of our method in children with epilepsy showed only few PET abnormalities within the EEG confirmed seizure onset area, however, PET abnormalities were frequently observed adjacent to this area in the temporal and parietal lobes. This result confirms the hypothesis that PET abnormalities represent functional barriers that disconnect adjacent brain regions from ictal involvement. Moreover, connectivity analysis showed that cortical areas representing PET abnormalities in the parieto-temporal lobe have unilaterally lower connectivity to the frontal lobe (see **Figure 1B**).

Conclusions: Using the developed software tool, quantitative results obtained from diverse imaging modalities can be merged into a single data structure. Application to clinical data suggests that functional PET abnormalities are frequently located in the borderzone to EEG-defined seizure onset regions. Moreover, in addition to decreased fractional anisotropy (FA), the cortical distribution pattern of fibers originating in the seizure onset zone or from the functional abnormality region differs from a normative pattern.

ADEQUACY OF KINETIC MODEL FOR ^{15}O-BASED $CMRO_2$ IN PET - CLEARANCE AFTER INTRA-CAROTID ^{15}O-RADIOACTIVITY BOLUS INJECTION ON MACACA FASCICULARRIS

H. Iida[1], N. Kudomi[2], S. Iguchi[1], T. Moriguchi[1], N. Teramoto[1], K. Koshino[1], T. Zeniya[1], A. Yamamoto[1], Y. Hori[1], J. Enmi[1], H. Kawashima[1]

[1]Department of Investigative Radiology, National Cardiovascular Center-Research Institute, Suita, [2]Department of Nuclear Medicine, Kagawa University, Faculty of Medicine, Takamatsu, Japan

Introduction: Regional cerebral metabolic rate of oxygen ($CMRO_2$) and oxygen extraction fraction (OEF) have been quantitatively assessed using ^{15}O-labeled oxygen ($^{15}O_2$) and PET both in experimental animals and human. A number of mathematical formulations have been proposed for several PET scanning protocols. There was a common assumption, in which the extracted $^{15}O_2$ from the capillary bed to the brain tissue is metabolised immediately to become labeled water ($H_2{}^{15}O$), so that backflux of $^{15}O_2$ from the brain is negligibly small. Encouraging results were shown in early 70's [1] but was suffered from a large level of background, due to the single photon detector design. Seki et al [2] recently claimed that the clearance after bolus administration of $^{15}O_2$-labeled Oxy-hemoglobin ($^{15}O_2$-Hb) into the carotid artery of rats differs from that after the bolus injection of $H_2{}^{15}O$, suggesting the limitation of the compartment model in $^{15}O_2$ PET, unless technical errors are present, attributed to the difficulty in small animal experiments. This study was aimed at evaluating whether or not the clearance of $^{15}O_2$ from brain is identical to that for $H_2{}^{15}O$. Adequacy of the assumption of instantaneous metabolism of $^{15}O_2$ to become $H_2{}^{15}O$ was then investigated.

Methods: Three sets of PET experiments were carried out on 2 monkeys of body weight 7.0-7.5 kg. Blood samples with $^{15}O_2$-Hb, and with C^{15}O-hemoglobin (C^{15}O-Hb), as well as $H_2{}^{15}O$-saline of approximately 20 MBq in 0.4 mL were injected into the carotid artery by slow bolus (< 3 sec), immediately after the initiation of PET scanning using an ECAT HR scanner in listmode. The $^{15}O_2$-Hb and C^{15}O-Hb were prepared using the previously presented artificial lung, by circulation the venous blood with the introduction of $^{15}O_2$ and C^{15}O gases. Dynamic images were reconstructed using FBP for 30x1 sec, 15x2 sec, 12x5 sec, and 18x10 sec, in total 5min. Five sets of ROIs were defined on reconstructed images in the middle-carotid artery territory of the injected hemisphere on different slice levels. Time-activity curves were fitted to a single exponential function, and then the clearance slopes were compared between $^{15}O_2$-Hb and $H_2{}^{15}O$.

Results: Typical coincidence counting rate of the whole PET gantry was approximately 35 kcps, 60 kcps and 30 kcps at peak, corresponding to the $^{15}O_2$-Hb, $H_2{}^{15}O$ and C^{15}O-Hb, respectively. Deadtime loss was < 5% at all scans. The clearance slopes were close to each other between $^{15}O_2$-Hb and

$H_2{}^{15}O$ (no significant difference), while much faster for $C^{15}O$-Hb.

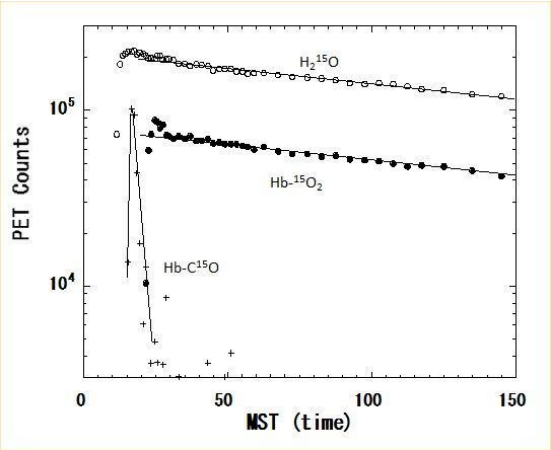

[Typical clearance after 15O2-Hb and H215O]

Conclusion: The clearance of ^{15}O radioactivity for $^{15}O_2$-Hb was identical to that for $H_2{}^{15}O$, suggesting that negligible amount of back diffusion of non-metabolized $^{15}O_2$ is a good approximation. Sophisticated mathematical approaches may further contribute to improve accuracy in the quantitative assessment of $CMRO_2$ in vivo.

References:

[1] Ter-Pogossian MM et al., JCI 1970

[2] Seki C et al., JCBFM, 2003

[3] Magata Y et al., JCBFM 2003

[4] Temma et al. JCBFM, 2006

[5] Temma et al., EJNMMI 2010

PET DEMONSTRATES FUNCTIONAL RECOVERY AFTER TRANSPLANTATION OF INDUCED PLURIPOTENT STEM CELLS IN A RAT MODEL OF CEREBRAL ISCHEMIC INJURY

F. Song[1], J. Wang[1], F. Han[2], G. Zhang[2], Q. Xi[1], J. Li[1], H. Jiang[1], J. Wang[1], G. Yu[1], M. Tian[1], H. Zhang[1]

[1]Department of Nuclear Medicine, Second Affiliated Hospital of Zhejiang University School of Medicine, [2]Institute of Pharmacology, Toxicology and Biochemical Pharmaceutics, Zhejiang University, Hangzhou, China

Aim: The purpose of this study was to evaluate the therapeutic efficacy of induced pluripotent stem cells (iPSCs) in a rat model of cerebral ischemia with use of fluorodeoxyglucose ^{18}F (^{18}F-FDG) micro-positron emission tomography (PET) imaging.

Methods: Middle cerebral artery occlusion was used to establish cerebral ischemia. Twenty-four rats were randomly assigned to one of three groups: iPSCs treatment, embryonic stem cells (ESCs) treatment, and phosphate-buffered saline (PBS) injection groups. After neurological function tests and ^{18}F-FDG microPET were performed, 1.0×10^6 suspended iPSCs or ESCs were injected stereotactically into the left lateral ventricle. The treatment response was evaluated weekly by ^{18}F-FDG PET scans and neurological function tests. Histological analyses and autoradiographic imaging were performed at 4 weeks after stem cell transplantation.

Results: Compared with the PBS injection group, higher ^{18}F-FDG accumulation in the ipsilateral cerebral infarction was observed in both the iPSCs and ESCs treatment groups during the 4-week period ($P < 0.05$). ^{18}F-FDG accumulation in the ipsilateral cerebral infarction increased steadily over time in the iPSCs treatment group. At 1 and 2 weeks after stem cell transplantation, significant recovery of glucose metabolism was found in the ESCs treatment group ($P < 0.05$), which then decreased gradually. The neurological score in both stem cell-treated groups was significantly lower than that in the PBS group, which indicated functional improvement. Immunohistochemical analysis demonstrated that transplanted stem

cells survived and migrated close to the ischemic region and most of the stem cells expressed protein markers for cells of interest.

Conclusion: ^{18}F-FDG microPET imaging demonstrated metabolic recovery after iPSCs and ESCs transplantation in the rat model of cerebral ischemia. iPSCs could be considered a potentially better therapeutic approach than ESCs and are worthy of further translational investigation.

HIERARCHICAL ORGANIZATION OF THE SEROTONERGIC SYSTEM: A MULTI-TRACER PET STUDY ON HEALTHY SUBJECTS

M. Savli[1], Y.-S. Ding[2], A. Neumeister[2], A. Bauer[3], D. Haeusler[4], W. Wadsak[4], M. Mitterhauer[4], R. Lanzenberger[1]

[1]Psychiatry and Psychotherapy, Medical University of Vienna, Vienna, Austria, [2]Radiology and Psychiatry, New York University School of Medicine, New York, NY, USA, [3]Institute of Neuroscience and Medicine (INM-2), Research Centre Jülich, Jülich, Germany, [4]Department of Nuclear Medicine, Medical University of Vienna, Vienna, Austria

Introduction: The serotonergic system is a highly diverse composition of various pre- and postsynaptic receptor subtypes and the serotonin transporter. Previous in vivo and postmortem studies revealed a rather distinct distribution pattern of these proteins throughout the human brain [1-2]. The cerebral cortex has often been subdivided into numerous areas characterized by structural, functional and cytoarchitectonic features [3] while protein-based organizations schemes are lacking. In the current study we propose a new organizational model of the brain based on protein distributions of the serotonergic system including the major inhibitory (5-HT_{1A} and 5-HT_{1B}), the major excitatory (5-HT_{2A}) receptors and the transporter (SERT) of healthy subjects.

Methods: Dynamic PET scans were performed in 95 healthy subjects (age=28.0±6.9 years; 59% males) divided into 4 groups using the selective radioligands [*carbonyl*-^{11}C]WAY100635 for 5-HT_{1A}, [^{18}F]altanserin for 5-HT_{2A}, [^{11}C]P943 for 5-HT_{1B} and [^{11}C]DASB for SERT. After motion correction and spatial normalization in SPM8 dynamic PET scans were quantified from radioactivity concentrations by a multi-linear reference tissue model (MRTM2; $5HT_{1A}$, 5-HT_{1B}, SERT; BP_{ND}) and a bolus/infusion approach ($5HT_{2A}$; BP_P) in PMOD 3.3. A standard template in MNI stereotactic space served for ROI delineation. The ROI template based on the macro-anatomical criteria according to AAL (automated anatomical labeling) including 52 regions [4]. Similarities between receptor distribution patterns were analyzed by means of a hierarchical cluster analysis using Euclidean distances in combination with the Ward-linkage method as implemented in R2.15.0. All values were z-transformed across areas prior to analysis in order to establish equal weight between the protein bindings.

Results: Receptor densities as represented by binding potentials were computed for all ROIs. Hierarchical cluster analysis of group-average BP values revealed two main protein-distinct clusters. The first exclusively comprised subcortical areas such as the raphe nuclei, thalamus, pallidum, caudate nucleus, putamen, midbrain, and striatum, whereas in the second the remaining cortical areas were aggregated. Of note is the strikingly pronounced dissimilarity between these two clusters given by the high distance. In the cortical cluster occipital, parietal and frontal ROIs displayed closer similarities than temporal ROIs. Basal ganglia ROIs showed shorter Euclidean distance than raphe nuclei in the subcortical cluster.

Discussion: We quantified in vivo PET data of 4 key proteins of the serotonergic system and subsequently used a data-driven approach to identify brain regions of similar features within the serotonergic system. Interestingly, spatially distant ROIs such as the subcortical areas were identified with close molecular similarity in contrast to cortical ROIs as given by the large Euclidean distance between these two clusters. The two clusters found were in accordance with the familiar classification of cortical und subcortical ROIs. Furthermore, temporal ROIs but also some frontal ROIs (ACC, Insula) exert a similar role as opposed to the remaining lobes. This result reflects an explicit hierarchical organization of the serotonergic system and emphasizes functions and interactions of the binding proteins beyond topologies.

References:

[1] Savli M et al. Neuroimage. 2012

[2] Varnäs K et al. Hum Brain Mapp. 2004

[3] Zilles, K., European Neuropsychopharmacology 2002

[4] Tzourio-Mazoyer N et al. Neuroimage 2002

QUANTIFYING THE SPECIFIC TSPO SIGNAL OF ^{11}C-PBR28 IN HEALTHY HUMANS: FROM IN VITRO TO IN VIVO

Q. Guo[1,2,3], D.R. Owen[3], N. Kalk[3], A. Colasanti[1,3], A.A. Weekes[1,3], P.M. Matthews[3,4], F.E. Turkheimer[2], E.A. Rabiner[1,2], R.N. Gunn[1,3]

[1]Imanova Centre for Imaging Sciences, [2]Institute of Psychiatry, King's College London, [3]Department of Brain Sciences, Imperial College London, [4]GlaxoSmithKline, London, UK

Objectives: Positron Emission Tomography (PET) is used to quantify active inflammatory processes by targeting the translocator protein (TSPO), which is up regulated in activated macrophages and microglia across various brain diseases. In vitro, human tissue samples have been shown to bind to 2nd generation TSPO radioligands, such as ^{11}C-PBR28, with either high affinity (HABs), low affinity (LABs) or a mixture of the two (MABs). The expression of these different binding sites in human is encoded by the rs6971 polymorphism in the TSPO gene[1], and it was predicted that the specific signal from PET ligands in vivo would vary accordingly. It was also predicted from in silico biomathematics that ^{11}C-PBR28 would have a high specific to nonspecific ratio and that there would be a significant specific TSPO signal in the healthy human brain[2]. Here we assess these predictions in vivo in humans with ^{11}C-PBR28 by evaluating the signal in different genetic groups at baseline, at follow-up three-months later and after blockade with a novel anxiolytic XBD173[3].

Methods: 18 healthy human subjects (10 HABs, 6 MABs and 2 LABs) were genotyped for the rs6971 polymorphism and underwent 90 min PET scans with arterial sampling following bolus injection of ^{11}C-PBR28. 10 (5 HABs, 3 MABs, and 2 LABs) were scanned twice 3 months apart, 6 (3 HABs and 3 MABs) were scanned at baseline only and 2 (HABs) were scanned at baseline and following pre-blockade with 90mg or 45mg of XBD173. A 2-tissue-compartment model described the data well and enabled estimation of the total volume of distribution (V_T) in the examined regions of interest (ROIs). The nondisplaceable volume of distribution (V_{ND}) was estimated using three different methods: i) by assuming no specific binding in the LABs, thus $V_{T\_HAB}=2V_{T\_MAB}-V_{ND}$; ii) by a plot relating the V_T of HABs and MABs, $V_{T\_HAB}- V_{T\_MAB} = R (V_{T\_HAB}-V_{ND})$, where R is related to the HAB/LAB binding affinity ratio; and iii) by the Occupancy plot $V_{T\_base}- V_{T\_block} =Occ(V_{T\_base}-V_{ND})$[4].

Results: A significant difference was found between the V_T of HABs and MABs across all ROIs (Figure 1). V_T was not quantifiable using 2TC for LABs in agreement with previous studies[5]. The test-retest variability (VAR: the mean of [2|test-retest|/[test+retest]) within a three-month period is around 25%. The V_{ND} estimated by the three methods was i) V_{ND}=1.38, ii) V_{ND}=1.92, and iii) V_{ND}=1.89, which implies the BP_{ND} in the normal human brain for HABs ranges from 1.75 to 3.04 in the ROIs examined and is consistent with the in silico biomathematical predictions of BP_{ND_HAB} = 3.99[2].

Conclusions: The in vivo TSPO signal of ^{11}C-PBR28 is consistent with the prediction from in vitro data, genetic data and an in silico biomathematical model. The tracer shows high specific signal in the healthy human brain.

References:

1. Owen et al. JCBFM, Vol.32, 2012

2. Guo et al. Neuroimage, Vol.60, 2012

3. Owen et al. Synapse. Vol.65, 2011

4. Cunningham et al. JCBFM, Vol.30, 2009

5. Fujita et al. Neuroimage, Vol.40, 2008

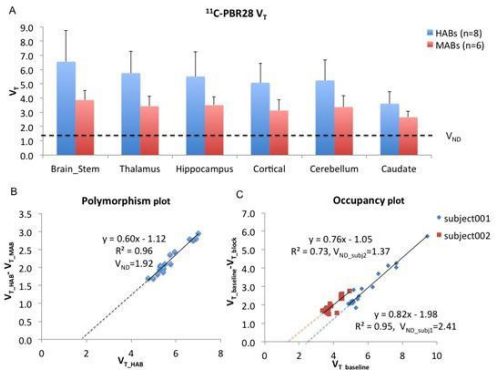

[Estimation of VND and BPND of [11C]PBR28 in humans]

[^{18}F]PF-05270430 AS A PET RADIOTRACER FOR IMAGING PHOSPHODIESTERASE-2A IN THE BRAIN: FIRST IN HUMAN EVALUATION AND ASSESSMENT OF TEST-RETEST VARIABILITY

M. Naganawa[1], N. Nabulsi[1], R.N. Waterhouse[2], A. Banerjee[2], S.-F. Lin[1], L. Zhang[2], T. Cass[1], J. Ropchan[1], A. Ogden[2], S. Tarabar[2], K. Zasadny[2], M. Skaddan[2], T.J. McCarthy[2], Y. Huang[1], R.E. Carson[1]

[1]Yale PET Center, Yale University, New Haven, [2]Pfizer Inc., Groton, CT, USA

Objectives: Phosphodiesterase-2A (PDE2A) is an enzyme that hydrolyzes the intracellular second messenger molecules cyclic AMP and cyclic GMP. PDE2A inhibitors have been shown to enhance memory [1] and cognitive function [2] in rats. [^{18}F]PF-05270430 is a novel PET radiotracer with high affinity and selectivity for PDE2A. The purpose of this study was to evaluate [^{18}F]PF-05270430 in the human brain and examine the test-retest variability of binding parameters measured with the tracer.

Methods: The radiotracer [^{18}F]PF-05270430 was synthesized via displacement of a tosylate precursor with K[^{18}F]. Five male healthy volunteers underwent 2 dynamic PET scans 3-5 days apart. PET images were acquired using an ECAT EXACT HR+ scanner with a scan time of 120 min. Arterial blood samples were collected for measurement of free fraction and radioactive metabolites, and for generation of the arterial input function. Brain regional time-activity curves (TACs) were measured in ten regions including striatum, neocortical regions, and cerebellum. TACs were analyzed with one- and two- tissue compartment models (1T and 2T) and the multilinear analysis method (MA1) to derive distribution volumes (V_T) and binding potentials (BP_{ND}) using the cerebellum as a reference region. Variability in model-derived tissue binding parameters was assessed using the following formula: %diff=100×|retest-test|/(test+retest)×2.

Results: [^{18}F]PF-05270430 was prepared in >99% radiochemical purity and specific activity of 124 ± 46 MBq/nmol (n = 10) at the end of synthesis. Plasma free fraction was 13 ± 3 % (n = 9). The fraction of [^{18}F]PF-05270430 in plasma decreased moderately over time, from 55 ± 8 % at 30 min to 40 ± 5 % at 120 min post tracer injection. Distribution of [^{18}F]PF-05270430 was heterogeneous in the human brain, with highest uptake in the putamen and caudate, followed by neocortical regions, and lowest in the cerebellum. Uptake of [^{18}F]PF-05270430 displayed a peak at ~5 min post injection, followed by rapid clearance in all regions. While 2T fits were better than those of the 1T model, the 2T parameters sometimes could not be reliably estimated. After excluding estimates with largest standard errors, there was an excellent agreement between the MA1 and 2T model estimates. Therefore, MA1 was chosen as the method of choice for modeling analysis. Reproducibility of estimates was similar across regions. Test-retest variability of V_T and BP_{ND} values in whole brain was 8 ± 4 % and 13 ± 11 %, respectively.

Conclusions: This is the first demonstration of a PDE2A-specific tracer suitable for the imaging and quantification of PDE2A binding sites *in vivo*. Evaluation in humans indicated that [^{18}F]PF-05270430 displayed several favorable properties as a PET tracer for the quantification of PDE2A binding sites, such as fast uptake kinetics, distribution in accordance to regional PDE2A densities, binding specificity, and excellent reproducibility of regional binding parameters. The cerebellum was used as a reference region due to its lowest uptake. However, a blocking study is required to evaluate the validity of the cerebellum as a reference region.

References:

[1] Rutten K *et al*., *Neuropsychopharmacol*, 2009; 34:1914-1925.

[2] Boess FG *et al*., *Neuropharmacology*, 2004; 47:1081-1092.

^{11}C-SSR180575 EVALUATED UNDER NORMAL AND PATHOLOGICAL CONDITIONS IN NONHUMAN PRIMATE BRAIN

N. Van Camp[1], S. Lavisse[1], L. Rbah-Vidal[1], R. Aron Badin[1], C. Jan[1], F. Dollé[2], T. Rooney[3], E. Brouillet[1], P. Hantraye[1]

[1]Life Science Department/I2BM, Molecular Imaging Research Center (MIRCen), Fontenay-aux-Roses, [2]Life Science Department/I2BM, Service Hospitalier Frédéric Joliot (SHFJ), Orsay, [3]Aging Therapeutic Strategic Unit, Sanofi-Aventis, Chilly-Mazarin Cedex, France

Objectives: The translocator protein 18kDa (TSPO) is the biomarker of interest for neuroinflammation in PET imaging. In search of specific and sensitive radioligands for

TSPO, the carbon 11 labelled SSR180575 ligand (Thominiaux et al. 2010) revealed highly specific binding in different rodent models of astrocytic activation (Lavisse et al. 2012) and neuroinflammation (Chauveau et al. 2011). Here we present a longitudinal follow up study in a non-human primate model of neuroinflammation evaluating the specificity and sensitivity of the ligand to detect early versus late inflammatory conditions.

Methods: Three cynomolgus monkeys underwent first a test-retest scan, followed by presaturation and displacement studies using different doses of PK11195 (1-5mg/kg). Dynamic PET data were acquired during 120 min (FOCUS220, Siemens) and imaging was performed under propofol anesthesia with constant monitoring of physiologic parameters. Then, an excitotoxic lesion was induced in the left striatum by stereotactic quinolinate injections. The animals were subsequently imaged at day 2, 9, 16, 23 and 46 after lesion and at the end of the study sacrificed for histological analysis. Brain PET data were coregistered to the corresponding T2-weighted MR images acquired on a 7T Varian scanner at different time points during the follow up study. Time activity curves extracted from different brain regions were expressed in SUV by normalizing for injected dose and body weight, allowing the comparison between and within animals over different time points. Total volume of distribution was calculated using the graphical method of Logan with fitted arterial input functions.

Results: In the healthy brain a specific and reversible binding of ^{11}C-SSR180575 was observed homogeneously all over the brain. Despite this ubiquitous distribution of the tracer in the normal condition, a clear increase in binding was observed in the quinolinate injected striatum as soon as 48h after excitotoxic lesion. The binding of the radioligand in the inflammatory lesion was visible up to two weeks after lesion, reaching a maximal contrast at nine days.

Conclusions: The present study reveals a promising specificity and sensitivity of ^{11}C-SSR180575 for the TSPO in vivo. Ongoing in vivo/postmortem correlations between the PET data and various immunohistological sections for GFAP, Iba1, CD68, TSPO and NeuN will yield complementary information regarding the cellular events associated with this increased binding. The early binding of ^{11}C-SSR180575 after the induction of the excitotoxic lesion, suggests binding to the TSPO in activated microglia in addition to the previously observed binding to the TSPO in activated astocytes (Lavisse et al.2012).

Chauveaux F. et al., Eur J Nucl Med Mol Imaging, 2011, 38 (3), 509-14

Lavisse S. et al. Journal of Neurosciences, 2012, 32(32), 10809-18

Thominiaux. et al. Journal of labelled compounds and radiapharmaceuticals, 2010, 53(13), 767-73

INITIAL EVALUATION OF [^{11}C]ITMM FOR MAPPING METABOTROPIC GLUTAMATE RECEPTOR TYPE 1 IN HUMAN BRAIN

M. Sakata[1], J. Toyohara[1], K. Oda[1], K. Ishii[1], M.R. Zhang[2], K. Ishiwata[1]

[1]Positron Medical Center, Tokyo Metropolitan Institute of Gerontology, Tokyo, [2]Molecular Imaging Center, National Institute of Radiological Sciences, Chiba, Japan

Objectives: Metablotropic glutamate receptor type 1 (mGluR1) has been reported to be a candidate of a drug target for the treatment of the central nervous system diseases, such as stroke, epilepsy, pain, cerebellar ataxia, Parkinson's diseases, anxiety, and mood disorders. *N*-[4-[6-(isopropylamino)pyrimidin-4-yl]-1,3-thiazol-2-yl]-4-[^{11}C]methoxy-*N*-methylbenzamide ([^{11}C]ITMM), recently developed by Fujinaga et al. [1], is a potential PET radioligand for mapping mGluR1 in the brain. In this study, we performed the initial clinical PET study using [^{11}C]ITMM.

Methods: Dynamic [^{11}C]ITMM PET scans (90-min) in two-dimensional mode were performed in five healthy male volunteers (23 ± 2 years old). The injected dose was 579 ± 48 MBq and the specific activity was 85 ± 23 MBq/nmol. During the scan, arterial blood was sampled at various time intervals, and the fraction of the parent compound in plasma was determined by HPLC analysis. ROIs were placed on the cerebellar and frontal cortices, thalamus, striatum, and pons. Total distribution volume (V_T) for each ROI was estimated by the two-tissue compartment model. The static [^{11}C]ITMM PET images (40-60 min after injection) were anatomically normalized and the mean images expressed as the standardized uptake value (SUV, g/mL) were calculated.

Results: [^{11}C]ITMM was much more stable peripherally in humans than in rodents; the percentage of unchanged form in the plasma remaining 62% ± 8% at 60 min after administration. The metabolite-uncorrected plasma radioactivity concentrations were higher than that of whole-blood suggesting plasma protein binding of [^{11}C]ITMM.

[^{11}C]ITMM heterogeneously distributed in the brain. Radioactivity in the cerebellar cortex was the highest and continuously increased over 30 min and then reached plateau. Radioactivities in the other regions were rapidly reached constant level, then remain plateau in the thalamus or slightly decreased in the frontal cortex, striatum, pons. The regional V_T was the highest in the cerebellar cortex (2.58 ± 0.27), followed by the thalamus (1.06 ± 0.18), frontal cortex (0.73 ± 0.09), pons (0.53 ± 0.19), and striatum (0.52 ± 0.11). This regional distribution pattern of V_T was consistent with the static SUV images and it was also consistent with the known distribution of mGluR1 in the primate brain [2].

Conclusion: [^{11}C]ITMM was suggested to be applicable for further evaluations as a PET radioligand for mapping mGluR1 in human brain.

References :

[1] Fujinaga M, et al., *J Med Chem*, 2012;55:2342-52.

[2] Hoestetler ED, et al., *Synapse*, 2011;65:125-35.

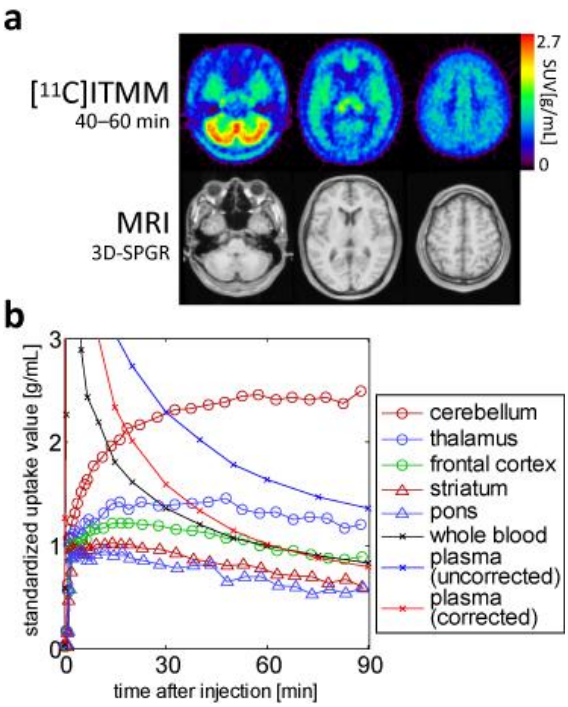

Figure:

(a) Anatomically normalized mean static images acquired for 40-60 min after injection with corresponding MRI and

(b) mean time-activity curves of [^{11}C]ITMM (n = 5).

FLUOXETINE ADMINISTERED TO PRE-PUBERTAL MONKEYS PERSISTENTLY UPREGULATES THE SEROTONIN TRANSPORTER INTO ADULTHOOD

S. Shrestha[1], **J.-S. Liow**[1], E.E. Nelson[2], R. Gladding[1], C.H. Lyoo[1], I. Henter[1], V.W. Pike[1], P.L. Noble[3], J.T. Winslow[4], S.J. Suomi[5], P. Svenningsson[6], E. Leibenluft[7], D. Pine[2], R.B. Innis[1]

[1]Molecular Imaging Branch, [2]Section Development & Affective Neuroscience, [3]Laboratory Neuropsychology, [4]Non-Human Primate Core, National Institute of Mental Health, [5]Section on Comparative Behavioral Genetics, National Institute of Child Health and Human Development, Bethesda, MD, USA, [6]Center for Molecular Medicine, Karolinska Institute, Stockholm, Sweden, [7]Section Bipolar Spectrum Disorders, National Institute of Mental Health, Bethesda, MD, USA

Background: Although selective serotonin reuptake inhibitors (SSRIs) are commonly

prescribed to treat mood and anxiety disorders in children, concerns have arisen regarding their routine use. Two of the safety concerns include the possible increased risk of suicidal thoughts [1] and the potential long-lasting effects on the developing brain. No prospective study to date has examined the long-term effects of SSRIs on the developing brain. This study examined the effects of prepubertal fluoxetine administration on serotonin transporter (SERT) and serotonin 1A (5-HT_{1A}) receptor in monkeys.

Methods: Thirty-two age- and weight-matched rhesus monkeys from four annual birth cohorts were randomly assigned to normal rearing or maternal separation conditions at birth. The rearing conditions for maternally-separated and normally-reared monkeys have been described elsewhere [2]. Fluoxetine was administered at age two and continued for one year. To rule out any confounding effects of residual SSRI in brain on our PET measurements, monkeys were scanned at least 1.5 years after drug washout. All monkeys (4.7 ± 0.3 yrs. and 7.5 ± 0.3 kg) underwent 2-hour scans on the microPET Focus 220 using two PET serotonergic radioligands: [^{11}C]DASB and [^{11}C]RWAY, selective for SERT and 5-HT_{1A} receptor, respectively. Dynamic PET images were co-registered to an MRI template. Time activity curves were generated from a set of predefined regions of interest for all regions except raphe where a manually drawn ROI was used. BP_{ND} was calculated using a multilinear reference tissue model with cerebellum as the reference. A full factorial ANOVA was performed using SPSS to examine the effects of rearing and treatment. Bonferroni post hoc tests were used to evaluate omnibus main effects. A two-tailed p value < 0.05 was considered statistically significant after correction for multiple comparisons. To visualize spatial pattern of the drug or rearing effect, voxel-wise SPM analysis was also performed on the parametric images.

Results: With regard to SERT, fluoxetine administration persistently upregulated BP_{ND} in both neocortex (19%, $p < 0.001$) and hippocampus (17%, $p < 0.02$). Voxel-wise SPM analysis found a highly significant effect of fluoxetine in the lateral temporal, cingulate and orbito-frontal cortices. No effect of rearing was observed. For 5-HT_{1A} receptors, raphe BP_{ND} increased by 23% in maternally-separated monkeys but was not significant after correcting for multiple comparisons. No effect of drug was observed. Two-way ANOVA did not show any significant rearing-by-drug interaction for both radioligands.

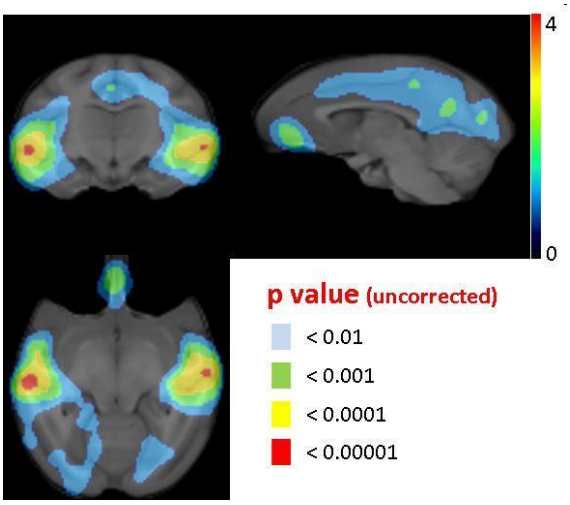

[Upregulation of SERT after fluoxetine treatment]

Conclusion: This study showed that fluoxetine had long-lasting effects in the developing brain. Specifically, monkeys receiving prepubertal fluoxetine administration showed persistently upregulated SERT binding despite 1.5 years of drug washout. The implications of this finding are presently unclear, and simplistic conclusions regarding whether the drug effects are either beneficial or toxic should be avoided. Both behavioral and biochemical studies with larger sample sizes in monkeys are warranted to further evaluate the functional significance of these persistent changes.

References:

1 FDA, *U.S. Food and Drug Administration: Labeling Change Request Letter for Antidepressant Medications.* 2007.

2. Nelson, E.E. and J.T. Winslow, *Non-human primates: model animals for developmental psychopathology.* Neuropsychopharmacology, 2009. **34**(1): p. 90-105.

CHANGES OF BRAIN PHOSPHODIESTERASE TYPE 4 MEASURED WITH ^{11}C-(*R*)-ROLIPRAM PET IN MAJOR DEPRESSIVE DISORDER

M. Fujita[1], C. Hines[1], S. Zoghbi[1], A. Mallinger[2], Y. Zhang[1], V. Pike[1], W. Drevets[3], C. Zarate[2], **R. Innis**[1]

[1]Mol. Imaging Branch, NIMH, [2]Exp. Ther. & Pathophysiol. Branch, NIMH, Bethesda, MD, [3]Psychiat., Univ. Oklahoma, Tulsa, OK, USA

Background: Phosphodiesterase type 4 (PDE4) selectively metabolizes cAMP in the brain. Basic studies have indicated that PDE4 and the cAMP cascade are downregulated in major depressive disorder (MDD) and that antidepressant treatment normalizes the activity of cAMP cascade to show antidepressant effects. The objectives of this study were to compare the binding of ^{11}C-(*R*)-rolipram, a PDE4 inhibitor, between unmedicated MDD patients and healthy controls and also to compare rolipram binding in patients with MDD before and after selective serotonin reuptake inhibitor (SSRI) therapy.

Methods: ^{11}C-(*R*)-Rolipram PET scans were performed in 34 unmedicated patients (37±11 years old; 11 females and 23 males) and 33 healthy controls (35±11y. o.; 10 F/23 M). The patients were moderately depressed with the Montgomery-Åsberg Depression Rating Scale (MADRS) score of 30±6. Sixteen patients repeated a scan 4−8 weeks after citalopram or sertraline treatment. To study the reproducibility of the PET measurement, eleven healthy controls had two scans with a similar interval without treatment. Total distribution volume normalized to plasma free fraction, V_T/f_P of ^{11}C-(*R*)-rolipram, was measured in 10 regions throughout the brain using unconstrained two-comp. model and metabolite-corrected arterial input function.

Results: Unmedicated patients showed lower V_T/f_P than controls in all regions with an average change of 18% (p=0.005). Although eleven healthy subjects showed similar V_T/f_P in two scans with retest variability of 12±7%, 16 patients who had two scans showed an increase of 18±40% after treatment across brain regions. Older patients showed significantly greater increase in V_T/f_P after SSRI with p< 0.001 for the regression of SSRI-induced increase in V_T/f_P (y) as a function of age (x) (y = 2.9x - 79) while seven of eight patients younger than 30 showed decrease rather than increase. When age was used as a covariate, the SSRI-induced increase in V_T/f_P in all 16 patients was significant with p=0.001. Those patients with lower V_T/f_P before medication showed a significantly greater increase after treatment (p=0.002) for the regression of increase in V_T/f_P (y) as a function of the baseline levels (x) (Fig. 1) indicating normalization of V_T/f_P by treatment. Seven male patients who were older than 30 showed a significant correlation between symptom improvement assessed with MADRS and the SSRI-induced increase in V_T/f_P in putamen and medial temporal cortex (Fig. 2. p=0.023).

Conclusions: The current study provide support for the cAMP theory of depression, specifically that this signal transduction cascade is downregulated in unmedicated patients with MDD and that antidepressant treatment normalizes the cAMP cascade. The current study suggests that MDD is potentially treated with PDE4 inhibitors, which directly stimulate the downregulated cAMP cascade.

Acknowledgement: This research was supported by the Intramural Research Program of NIMH.

Fig. 1

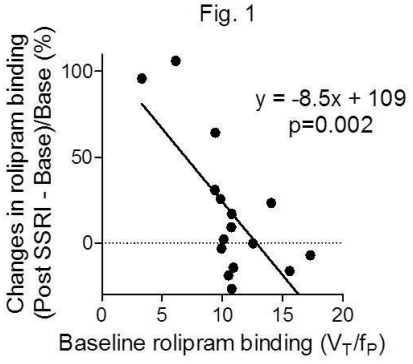

[Fig. 1]

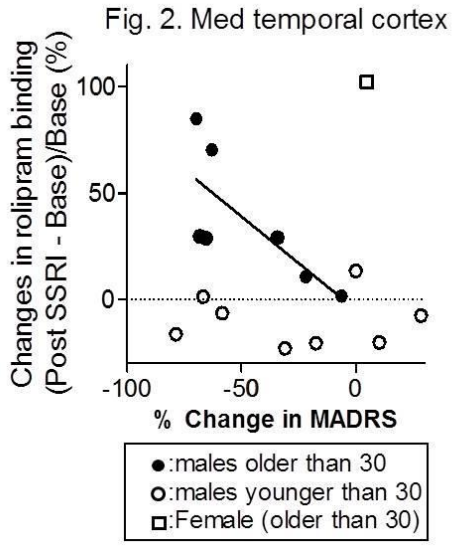

[Fig. 2]

SEROTONIN TRANSPORTER BINDING IN HEALTHY 5-HTTLPR S-ALLELE CARRIERS DOES NOT SHOW SEASONAL VARIATION

B. Mc Mahon[1], A.S. Andersen[1], M.K. Madsen[1], L. Feng[1], V. Frøkjær[1], S. Keller[2], S. da Cunha-Bang[1], M. Herth[1,2], P. Iversen[3], L. Hasholt[4], G.M. Knudsen[1]

[1]Neurobiology Research Unit and Center for Integrated Molecular Brain Imaging (CIMBI), Rigshospitalet and University of Copenhagen, [2]PET and Cyclotron Unit, Copenhagen University Hospital, Rigshospitalet, [3]CIMBI and Danish Research Centre for MR, Copenhagen University Hospital, [4]Department of Cellular and Molecular Medicine, Copenhagen University, Copenhagen, Denmark

Seasonal affective disorder is a common condition in the northern latitudes with an estimated prevalence of up to 10 % in Copenhagen residents. The disorder is caused by seasonal disruptions in the monoaminergic transmitter systems. We and others have in cross-sectional studies of healthy individuals observed that season dependent fluctuations in the cerebral serotonin transporter (SERT), with high striatal binding at winter solstice and low binding at summer solstice. In addition, we have identified a genotype-dependent interaction with SERT binding being dependent on the carrier status of the 5-HTTLPR promoter polymorphism *(Kalbitzer et al 2010*). This gene*environment interaction predicted the SERT fluctuations with a negative correlation between SERT binding and daylight minutes in carriers of the short 5-HTTLPR allele (S-allele), but less so in homozygote carriers of the long allele (L-allele). The aim of the present study was in a longitudinal design to investigate if seasonal SERT fluctuations could be confirmed in healthy S-allele carriers.

Methods: Participants were pre-screened for inclusion and 14 S-allele carriers entered the study (4 females and 9 males, age: 27 ±8, range 20-45 years, BMI: 22.8±2, range 19.1-25.9) that took place in Copenhagen. Exclusion criteria were significant medical history, known retinal pathology and the use of photosensitizing medications. All subjects had a normal neurological examination and ordinary blood biochemistry. Each participant had a structural brain MRI and a ^{11}C-DASB PET scan done in the summer (mean daylight min.:1026±28, 977-1052) and in the winter (mean daylight min.: 449±21, range:422-472), in randomized order. PET scans were conducted on a HRRT PET scanner (mean inj.dose: 596±10, range 556-612 MBq). Quantification was done with MRTM2 that generates the outcome parameter BP_{ND}; the primary region of interest was putamen.

Results: Summer and winter SERT BP_{ND} in putamen were compared using a Wilcoxon test. We found no season associated differences when comparing summer and winter SERT BP_{ND} (P=0.30) The mean change in putamen was 6.8±4.8% (-8.6-19.3%) which corresponds to test-retest values of ^{11}C-DASB scans observed with shorter intervals (4.8%, Kim et al 2006). There was a high correlation between individual's winter and summer k_2' (the clearance rate constant from cerebellum) (r=0.56, p< 0.001). However, modelling the summer and winter scan with the individuals average k_2' did not alter the main outcome (P=0.38).

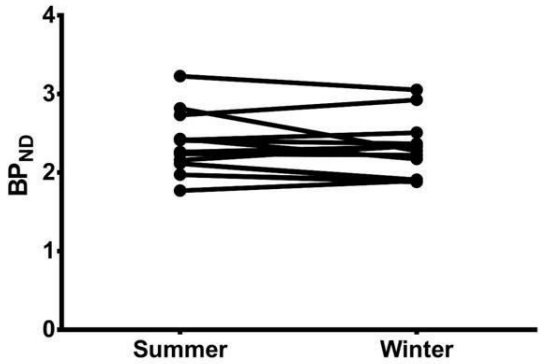

Table 1: Change of season did not change SERT BP_{ND} in fourteen healthy S-allele carriers.

[Table 1: Change of season did not change SERT BPND]

Conclusion: Previous cross-sectional studies have shown seasonal variations in putamen in healthy S-allele carriers but in this longitudinal study we unable to reproduce these findings. Here we found that the SERT stays stabile during the year with changes corresponding only to test-retest values.

CENTRAL 5-HT SYSTEM DETERMINES THE AMOUNT OF WEIGHT LOSS ACHIEVED WITH GASTRIC BYPASS

M.E. Haahr[1], D.L. Hansen[2], D.S. Stenbaek[1], T. Almdahl[3], C. Ratner[1], K. Madsen[1], J. Madsen[4], W.F. Baare[5], **G.M. Knudsen**[1]

[1]Neurobiology Reseach Unit, Rigshospitalet, Copenhagen University Hospital, Copenhagen, [2]Department of Endocrinology, Hvidovre University Hospital, Hvidovre, [3]Steno Diabetes Center, Gentofte, [4]PET and Cyclotron Unit, Rigshopitalet, Copenhagen, [5]Danish Research Centre for Magnetic Resonance, Hvidovre, Denmark

Backgroud and aims: Obesity increases morbidity and mortality and represents a serious public health problem in the plentiful modern societies. Bariatric surgery has proved highly successful at producing sustained weight loss, however, variability in treatment response persists. A better understanding of the pathophysiology of appetite and obesity may improve patient selection. Research into feeding behavior and satiety indicate that high cerebral serotonin (5-HT) levels reduce appetite. Further, alterations in brain 5-HT receptor and transporter availability as measured by PET has been found in obese subjects compared to controls. This may be due to a primary deficiency in 5-HT neurotransmission or to secondary 5-HT receptor and transporter regulation.

Here we aimed to determine if serotonergic neurotransmission is a trait marker of obesity and ultimately, if pre-surgical 5-HT marker activity can be used to identify those patients that will most likely benefit from bariatric surgery.

Patients and methods: Twenty-four obese adults (4 men) with BMI >35 kg/m^2 waiting for Roux-en-Y gastric bypass (RYGB) and ten lean (BMI< 27 kg/m^2) healthy controls (3 men), matched to the obese group in gender and age, were recruited for the study. We used [^{11}C]DASB and [^{18}F]altanserin PET and concurrently determined the levels of the 5-HT type 2A receptor (5-HT$_{2A}$R) and the 5-HT transporter in obese individuals before and after RYGB and in a lean control group at baseline.

The volumes of interest were neocortex for the 5-HT$_{2A}$R and the caudate-putamen-thalamus for the 5-HTT. Groups were compared with unpaired and paired t-test. Additionally, linear regression was used to investigate if the pre-surgical or the pre- to post-surgical changes in binding potentials of the two serotonergic markers predicted the amount of weight loss after RYGB. Time from surgery to PET rescan was included as a covariate in the models. Lastly, the association between 5-HT$_{2A}$R binding and 5-HTT binding was modeled using non-linear regression.

Results: We found significant higher pre-surgical 5-HT$_{2A}$R levels in obese than in lean participants (Obese: mean BP_P = 2.53 ± 0.97, lean: mean BP_P = 1.82 ± 0.46, p=0.035). Moreover, pre-surgical 5-HT$_{2A}$R, but not 5-HTT, levels predicted the amount of weight loss after RYGB (ß=2.63, R^2=0.39, p=0.029) (figure 1). Additionally, post-surgically change in 5-HT$_{2A}$R and 5-HTT binding predicted the change in BMI (ß=-0.08, R^2=0.42, p=0.023 and ß=-0.18, R^2=0.54, p=0.005). Finally, we observed an inverted U-shape association between the 5-HT$_{2A}$R binding in neocortex and the 5-HTT in the subcortical region, suggesting that a common regulator, presumably endogenous 5-HT, synchronizes the receptor and transporter regulation.

Conclusions: We find evidence for a globally altered serotonergic neurotransimisson in obesity. Moreover, pre-surgical 5-HT levels

and alterations post-surgically were predictive of the success of weight loss after a gastric bypass. This study provides novel evidence for the role of the central 5-HT system in the pathophysiology of obesity and obtainable weight loss after bariatric surgery. Our results may have important implications for the management of obesity, including the selection of patients for surgical procedures and the predictors of long-term outcomes following bariatric surgery.

CHANGES IN THE PRESYNAPTIC DOPAMINE METABOLISM OF NICOTINE DEPENDENT SUBJECTS: STATE OR TRAIT?

I. Vernaleken[1], L. Rademacher[1], S. Prinz[1], K. Henkel[1], C. Dietrich[1], O. Winz[2], S. Mohammedkhali[2], J. Schmaljohann[2], F. Mottaghy[2], G. Gründer[1]

[1]Department of Psychiatry, Psychotherapy and Psychosomatics, [2]Department of Nuclear Medicine, RWTH Aachen University, Aachen, Germany

Introduction: Several previous molecular and functional imaging investigations suggest a blunted effect of prodopaminergic stimuli in persons suffering from addiction whereas the sensitivity in respect to substance-related cues is increased. Most of the molecular imaging results were done with patients using agents which directly affect the dopamine transmission (e.g. cocaine). Only few molecular PET-investigations characterized dopaminergic effects of nicotine. None of these studies controlled for acute effects, disease related changes, and traits which might contribute to the vulnerability. The present [18F]FDOPA-PET investigation aims to detect nicotine related changes during continued smoking, after acute withdrawal, and after long-term treatment/abstinence. The latter condition should simulate the situation before the substance-dependent behaviour became apparent. The reversible inlet/outlet model for [18F]FDOPA-PET analysis was applied for better characterization of divers presynaptic dopaminergic parameters.

Methods: 30 male nicotine dependent subjects (age-range: 19-47 yrs.; mean: 28.3 ± 7.0) were included as well as 15 healthy control subjects (age-range: 19-46 yrs.; mean: 27.9 ± 7.5) which were free of any relevant nicotine consumption (less than 10 cigarettes during the life span). There was a strict matching for relevant factors that are associated with the individual's dopamine synthesis capacity (age, cognition, education). The control group underwent a single [18F]FDOPA-PET scan under baseline-conditions. One half of the patient-group underwent a first scan under withdrawal condition (>5 hours without smoking), the remaining subjects were scanned under continued smoking conditions. Afterwards, all patients attended at a smoking cessation program consisting of six psychotherapeutic interventions. 16/30 patients were able to remain abstinent for at least three months. This group was invited for a second scan under the same conditions. [18F]FDOPA scans were generally acquired for 124 minutes after a bolus infusion of 234 ± 23 MBq (controls) and 228 ±32 MBq (patients). All subjects underwent arterial blood withdrawal during the scanning procedure for obtaining activity input curves and [18F]FDOPA/[18F]OMFD ratios. The reversible inlet/outlet model of Kumakura et al. (2005) was applied in order to obtain the net blood/brain clearance (dopamine synthesis capacity, K), the loss of fluorinated metabolites (dopaminergic turn-over, kloss), and the total distribution volume (storage capacity, VD).

Results: Earlier results of positive correlations between the capacity of the dopaminergic transmission system and cognitive performance parameters could be replicated (TMT-B vs. VD in ventral caudate: r=-0.631, p=0.016). Smoking patients (without withdrawal) showed strong and significantly blunted dopamine synthesis capacity parameters in particular in the right (-16%, p=0.045) and left ventral caudate nucleus (-16%, p=0.050). The kloss sowed a reduction on trend-level. The long-term smoking cessation, nevertheless, normalized all presynaptic dopaminergic parameters in every region. Withdrawal showed a tendency toward reduced K and kloss which, however, did not reach statistical significance.

Discussion: According to our hypotheses, ongoing nicotine consumption results in a down-regulation of dopamine-synthesis capacity and turn-over. The complete normalization after 3 months of abstinence, however, was unexpected and does not claim an inefficient dopamine system to be a strong trait toward nicotine dependence.

INNATELY LOW D_2 RECEPTOR AVAILABILITY IS ASSOCIATED WITH HIGH NOVELTY-SEEKING AND ENHANCED BEHAVIOURAL SENSITIZATION TO AMPHETAMINE

N. Ginovart[1,2], B.B. Tournier[1], P. Millet[2], M. Moulin-Sallanon[2,3], P. Vallet[2], T. Steimer[2]

[1]Psychiatry, University of Geneva, [2]Psychiatry, University Hospitals of Geneva, Geneva, Switzerland, [3]INSERM Unit 1039, J. Fourier University, La Tronche, France

Objectives: High novelty-seeking has been related to an increased risk for developing addiction, but the neurobiological mechanism underlying this relationship is unclear. We investigated here whether differences in dopamine (DA) $D_{2/3}$-receptor ($D_{2/3}R$) availability and function underlies phenotypic divergence in novelty-seeking and vulnerability to addiction in the Swiss sublines of Roman high- (RHA) and low- (RLA) avoidance rats.

Methods: Ex vivo measures of $D_{2/3}R$ availability using the D_2R-preferring antagonist [^{18}F]Fallypride, and the D_3R-prefering agonist [^{3}H]-(+)-PHNO, and of DA-related gene expression and behaviours were used to characterize DA signalling in RHA and RLA rats, which respectively display high and low behavioural responsiveness both to novelty and psychostimulant exposure. In addition, the vulnerability of the ex vivo binding of [^{3}H]-(+)-PHNO to acute fluctuations in synaptic DA was assessed in both rat lines and compared to that of [^{18}F]Fallypride. Ex vivo binding for both radioligands was estimated by the specific binding ratio, defined as SBR=(%ID/g target region - %ID/g cerebellum)/(%ID/g cerebellum).

Results: When compared to RLA rats, high novelty-responding RHAs had lower levels of D_2R, but not D_3R, binding and mRNA in midbrain, and showed behavioural evidence of D_2-autoreceptor subsensitivity. Treatment with the DA-depleting agent reserpine has no effect on striatal [^{18}F]Fallypride binding but lead to significantly higher increases in striatal [^{3}H]-(+)-PHNO binding in RHAs (+45%; $p< 0.01$) than in RLAs (+23%; $p< 0.05$). Acute treatment with amphetamine reduced [^{18}F]Fallypride SBR to a similar extent in both lines (-25%; $p< 0.05$) but induced reductions in [^{3}H]-(+)-PHNO SBR that were significantly higher ($p< 0.05$) in RHA (-41%; $p< 0.01$) than in RLA (-18%; $p< 0.05$) rats. When compared to RLAs, RHA rats also exhibited lower availabilities and functional sensitivity of D_2R, but not D_3R, in striatum, that were inversely correlated with individual scores of novelty-seeking, which in turn predicted the magnitude of subsequent AMPH-induced behavioural sensitization.

Conclusion: The present study provides evidence that deficits in D_2R signaling in midbrain and striatum is associated with high novelty-seeking and enhanced susceptibility to develop addiction-related behaviours in rats. We propose that innately low D_2-autoR functioning in midbrain and the resulting increase in presynaptic DA tone and subsequent counteradaptative down-regulation of postsynaptic D_2R in striatum result in a specific pattern of DA signaling that may subserve novelty-seeking and vulnerability to drug use.

Research support: This work was supported by the Swiss National Science Foundation.

CHRONIC CEREBRAL HYPOPERFUSION DID NOT ACCELERATE [^{11}C]PIB-REACTIVE AB DEPOSITION IN AMYLOID PRECURSOR PROTEIN TRANSGENIC MICE

C. Seki, M. Higuchi, M. Tokunaga, B. Ji, M. Ono, M. Maruyama, J. Maeda, N. Nitta, I. Aoki, T. Suhara, H. Ito

Molecular Imaging Center, National Institute of Radiological Sciences, Chiba, Japan

Introduction: Mild cerebral hypoperfusion events are relevant in aged individuals. It has been reported that decreased cerebral blood flow can accelerate Alzheimer's disease (AD) related pathologies but the underlying mechanism has been still unclear. [^{11}C]PIB is a PET imaging probe for Aβ plaques and [^{11}C]PIB-PET can also detect the progression of Aβ amyloidosis with aging in living AD model mice[1]. Therefore the application of this method to an AD animal model with local cerebral hypoperfusion would reveal the impact of lowered regional cerebral blood flow (rCBF) on the Aβ plaque formation in living brains. In this study, unilateral hypoperfusion model was made on amyloid precursor protein transgenic (APP Tg) mice, and repeated [^{11}C]PIB-PET scans were performed to observe the progression of Aβ depositions and MRI scans for monitoring rCBF and ischemic infarction.

Methods: All of the following animal procedures were performed under anesthesia with 1.5% (v/v) isoflurane. The left common

carotid artery (ICCA) of an APP Tg mouse aged 18-20 months (n=3) was isolated from the adjacent vagus nerve and doubly ligated with a 6-0 silk suture. MRI scans with a 7T scanner were performed to evaluate rCBF with flow sensitive alternating inversion recovery method and formation of cerebral infarction with T2-weighted (T2W) and diffusion tensor imaging. [^{11}C]PIB-PET and MRI scans were performed 2 weeks before the ligation as the baseline, then repeatedly at 3 days to 4 or 6 months after the ligation to monitor longitudinal alternations of rCBF alternations and Aβ deposition. The distribution of Aβ deposition was evaluated with standardized uptake ratio (SUVR) map of [^{11}C]PIB-PET data averaged at 40-60 min using the cerebellum as a reference region.

Results and conclusion: The relative reduction of rCBF of ipsilateral neocortex by lCCA ligation was 42-58 % of contralateral neocortex at 3 days post ligation, then gradually increased up to 90 % after 6 months. There was no ischemic infarction observed in all animals based on the inspection of T2W images and apparent diffusion coefficient maps. The Aβ deposition increased and expanded over time without laterality related to hypoperfusion. The current results indicate that chronic cerebral hypoperfusion without formation of ischemic infarction detectable by MRI does not accelerate deposition of [^{11}C]PIB-reactive Aβ plaques.

1) Maeda J, et al., J Neurosci ; 27(41):10957-68, 2007

PROTEASOME INHIBITION MODEL OF PARKINSON'S DISEASE IN GOTTINGEN MINIPIG: COMBINED DOPAMINERGIC AND NORADRENERGIC EFFECTS

A.M. Landau[1,2], S. Jakobsen[2], A.K.O. Alstrup[2], A.C. Schacht[2], A. Møller[1,2], J.C. Sørensen[3], D.J. Doudet[2,4]

[1]Center of Functionally Integrative Neuroscience (CFIN) Mindlab, Aarhus University, [2]Department of Nuclear Medicine and PET Center, [3]Department of Neurosurgery, Aarhus University Hospital, Aarhus, Denmark, [4]Medicine/Neurology, University of British Columbia, Vancouver, BC, Canada

Objectives: Parkinson's disease (PD) is a multisystem disease with progressive deficits in multiple neurotransmitter systems, including dopamine (DA), noradrenaline (NA), serotonin and acetylcholine. Consequently, the interplay between transmitters and their actual contribution to symptoms and pathology remains poorly understood. None of the current animal models of PD recapitulate all its features. Here we use the *in vivo* capabilities of positron emission tomography (PET) imaging to evaluate the progression of neurotransmitter losses in a novel model of PD in minipig induced by the intracerebroventricular injection of an inhibitor of the ubiquitin proteasome system (UPS), lactacystin.

Methods: Four female minipigs were implanted in the cisterna magna with a catheter connected to a subcutaneous titanium injection port under sterile conditions. Six weeks after recovery from the catheter implant, and after injections of sterile saline alone to verify patency, minipigs were scanned at baseline with C-11 labeled dihydrotetrabenazine (DTBZ, a label of the vesicular monoamine transporter type 2 (VMAT2)) and yohimbine (a selective label of the alpha2 adrenergic receptors), in order to investigate *in vivo* the longitudinal effects of chronic exposure to a UPS inhibitor on the DA and NA projections. Pigs received weekly doses of 20 or 50 micrograms of the UPS inhibitor lactacystin dissolved in sterile saline, directly in CSF through the access port. They were scanned with DTBZ and yohimbine after the 2nd or 3rd and after the 5th or 6th dose of the UPS inhibitor. PET data were registered to an average minipig MRI atlas and processed using Montreal Neurological Institute software. The total volume of distribution (V_T) of yohimbine was obtained using the Logan graphical analysis during the 30-90 minute portion of the scan using plasma activity curve as input. The binding potential BP_{ND} of DTBZ was obtained with the Logan graphical analysis and cerebellum activity as input function.

Results: Depending on the dose received, the animals started developing mild symptoms (bradykinesia) after the 3rd to 4th injection of the UPS inhibitor. Striatal DTBZ binding to VMAT2 was not altered after 2-3 injections of lactacystin, but decreased on average by 35% after 4-6 injections of the proteasome inhibitor. On the other hand, yohimbine binding was increased by 15-25% in various brain regions after the 3rd injection, suggesting a very early upregulation of the receptors in response to NA neuron damage.

Conclusions: Decreased striatal binding of DTBZ is consistent with previous studies in other animal models of PD and in PD patients. Increased yohimbine binding to alpha2 adrenoceptors, may provide the first *in vivo* evidence for very early NA deficits, possibly preceding DA deficits, in the pre-symptomatic and early stages of the disease.

$5HT_{1B}$ RECEPTOR IMAGING AND COGNITION IN PARKINSON´S DISEASE

A. Varrone[1,2], P. Svenningsson[1,2], P. Marklund[2,3], H. Fatouros-Bergman[1], A. Forsberg[1], C. Halldin[1,2], L.-G. Nilsson[2,3], L. Farde[1,2]

[1]Department of Clinical Neuroscience, Karolinska Institutet, [2]Stockholm Brain Institute, [3]Department of Psychology, Stockholm University, Stockholm, Sweden

Objectives: The 5-HT_{1B} receptor (5-HT_{1B}-R) is a serotonin receptor subtype with potential as biomarker for brain imaging. Previous studies have shown that the serotonin system is affected in Parkinson´s disease (PD)[1], but data on the 5-HT_{1B}-R are not yet available. Impairment of cognitive function, frequently observed in PD, has been linked to the serotonin system. The aim of the present study was to examine whether the 5-HT_{1B}-R is affected in PD and whether the 5-HT_{1B}-R availability is associated with measures of cognitive function.

Methods: Twelve control subjects (7M/5F, age 65±7 years) and 11 PD patients (7M/4F, age 66±8 years, disease duration 6±3 years, Hoehn&Yahr stage 1.7±0.5, UPDRS-III 14.3±4.4) were included in the study. Cognitive function was evaluated by assessment of episodic, semantic, working memory, spatial span, creative ability (divergent thinking assessed with the alternative use task)[2], and visual attention. PET measurements were performed with the 5-HT_{1B}-R-radioligand [^{11}C]AZ10419369[3] and the HRRT system. Parametric images of binding potential (BP_{ND}) were generated using the wavelet-aided parametric imaging software[4] and the Logan graphical analysis, using the cerebellum as reference region. Differences between controls and PD patients in cognitive measures were assessed with multivariate analysis, with significance set at $p< 0.05$. Voxel-based analysis was performed with SPM, using a multiple regression model, to test the effect of group on the 5-HT_{1B}-R availability and the effect of cognitive variables on the 5-HT_{1B}-R, controlling for group. All analyses were performed controlling for age, gender and injected mass of the radioligand. Significance was set at corrected $p< 0.05$ at the cluster level and $p< 0.001$ at the voxel level.

Results: In PD patients significantly lower 5-HT_{1B}-R availability was found in the right orbitofrontal cortex when compared to controls. PD patients had statistically significant lower measures of episodic memory (15.4±4.0 vs. 18.6±3.1), and creative ability (12.5±6.3 vs. 18.6±7.1) and a trend towards lower measures of semantic memory (22.0±5.0 vs. 25.4±2.6, p=0.052). A statistically significant positive correlation was found between 5-HT_{1B}-R availability and creative ability in the left anterior cingulate/medial prefrontal cortex (BA32/BA9) and in the right cuneus and precuneus (BA18/BA19).

Conclusions: The orbitofrontal cortex is a region with dense serotonergic innervation and has an important role in reversal learning, a task frequently affected in PD. The decrease of 5-HT_{1B}-R availability in this region corroborates previous reports of a decrease in serotonin function in PD. Creative ability was significantly correlated with 5-HT_{1B}-R availability. Divergent thinking has been consistently associated with medial frontal lobe function and to some extent also to posterior parietal regions[5]. Although creativity has been conventionally linked to dopamine function, our findings suggest that the lower creative ability in PD might be also related to impaired serotonin function in the neural network involved in divergent thinking.

Acknowledgements: Support from Stockholm Brain Institute and Swedish Foundation for Strategic Research.

References:

1. Kish SJ. Brain 2008;131:120-131.

2. Guilford, J.P. Alternate uses: Manual of instructions and interpretation 1978.

3. Pierson, ME. Neuroimage 2008;41:1075-85.

4. Cselenyi Z. Neuroimage 2006;32:1690-708.

5. Shamay-Tsoory, S.G. Neuropsychologia 2011;49:178-185.

REPRODUCIBILITY OF PARKINSONISM-RELATED METABOLIC BRAIN NETWORK ACTIVITY IN A CHINESE PATIENT COHORT

Y. Ma[1], S. Peng[1], J. Wang[2], P. Wu[3], C. Tang[1], **C. Zuo**[3], V. Dhawan[1], D. Eidelberg[1]

[1]Center for Neurosciences, The Feinstein Institute for Medical Research, Manhasset, NY, USA, [2]Department of Neurology, [3]PET Center, Huashan Hospital, Fudan University, Shanghai, China

Introduction: PET with FDG has been used for differential diagnosis of parkinsonism by assessing metabolic brain network activity associated with Parkinson's disease (PD), multiple system atrophy (MSA) and progressive supranuclear palsy (PSP) [1]. We have previously shown that scores of brain network activity for PD-, MSA-, and PSP-related covariance patterns (i.e. PDRP, MSARP and PSPRP; Fig. 1) were highly reproducible in two independent cohorts of clinically-confirmed parkinsonian patients scanned on the GE Advance PET camera [2]. In this study, we evaluated the reproducibility of these disease-specific brain network scores in a Chinese cohort of patients with PD and atypical parkinsonism.

Methods: The Chinese cohort consisted of 33 patients with idiopathic PD and 33 age-matched healthy controls, 8 patients with MSA, 9 patients with PSP, and the same 10 age-matched healthy controls. The sample sizes for each parkinsonian condition were similar to those used in the original derivation cohorts at the Feinstein Institute. The patients were also age- and severity-matched in each disease category between the two centers. Each subject in the validation cohort was scanned on a Siemens Biograph 64 PET/CT system at the Huashan Hospital. For subjects in each patient group, we computed the corresponding network scores of each pattern using metabolic images on a prospective single-case basis.

Results: PDRP was characterized by relative metabolic increases in the pallidum, thalamus, pons, cerebellum, and sensorimotor cortex, covarying with metabolic decreases in the lateral premotor cortex (PMC) and parieto-occipital regions (Fig. 1). MSARP was characterized by covarying metabolic decreases in the putamen and cerebellum. PSPRP was characterized by covarying metabolic decreases in the medial prefrontal cortex (PFC), frontal eye fields, ventrolateral prefrontal cortex (VLPFC), caudate nuclei, medial thalamus, and upper brainstem.

PDRP scores were significantly elevated ($p < 0.0001$; Fig. 1) in the patients relative to the controls in the original derivation cohort at the Feinstein as well as in the prospective validation cohort at Huashan. Likewise, values of MSARP or PSPRP expression were also similarly elevated ($p < 0.0001$) in the two corresponding cohorts of patients and healthy controls from the Feinstein Institute and the Huashan Hospital, respectively.

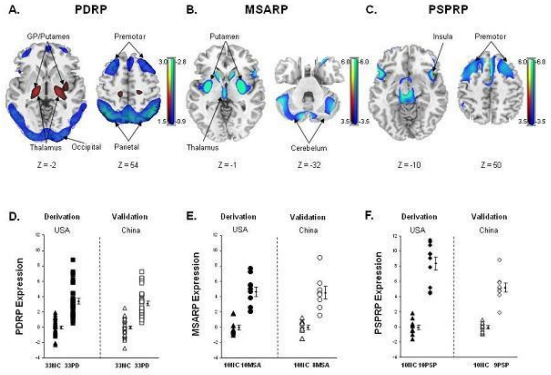

[Fig.1: Parkinsonism-related brain network scores.]

Conclusions: We demonstrated the reproducibility of our previously validated covariance patterns in parkinsonian patients scanned with FDG PET at the Huashan Hospital. Network scores of disease-related patterns in individual cohorts of parkinsonian patients and healthy controls were fully comparable and reproducible across the two centers in the USA and China. This study further validates the utility of these characteristic covariance patterns as viable network biomarkers regardless of patient cohorts and imaging instruments.

References:

1. Tang, CC et al (2010), 'Differential diagnosis of parkinsonism: a metabolic imaging study using pattern analysis'. *Lancet Neurol.*, 9:149-58.

2. Eckert, T et al (2008), 'Abnormal metabolic networks in atypical parkinsonism'. *Mov Disord.*, 23: 727-33.

[^{11}C]-(*R*)PK11195 UPTAKE AND TRANSLOCATOR PROTEIN EXPRESSION IN GLIOMAS: DIFFERENCES BETWEEN GRADES AND SUBTYPES

Z. Su[1], F. Roncaroli[2], A. Gerhard[1], R. Hinz[1], K. Karabatsou[3], D.J. Coope[3], F.E. Turkheimer[4], A. Jackson[1], K. Herholz[1]

[1]Wolfson Molecular Imaging Centre, University of Manchester, Manchester, [2]'John Fulcher' Neuro-Oncology Laboratory, Imperial College London, London, [3]Department of Neurosurgery, Salford Royal NHS Foundation Trust, Salford, [4]Department of Neuroimaging, Institute of Psychiatry, King's College London, London, UK

Background and aims: Gliomas are the most common brain tumours, consisting of two main histological subtypes: astrocytoma and oligodendroglioma. Translocator protein (TSPO), an 18 kDa mitochondrial molecule up-regulated in astrocytomas,[1, 2] can be imaged by PET using the selective radiotracer [^{11}C]-(*R*)PK11195. To date, only three PK11195 PET studies have been conducted on a small number of astrocytoma patients with inconsistent results.[3-5] We aimed to characterise [^{11}C]-(*R*)PK11195 uptake in human gliomas of different grades and subtypes, and explored the biology underlying the PET finding.

Methods: 23 glioma patients underwent perfusion MRI and dynamic [^{11}C]-(*R*)PK11195 PET scans. Radiotracer time-activity curves (TACs) were extracted from tumour regions and normal grey and white matter. Parametric maps of binding potential (BP_{ND}) were generated using the simplified reference tissue model[6] with a cerebellar input function. Co-registered MRI/PET was used to guide tumour biopsies. Tumour tissue was quantitatively assessed for TSPO expression and microglial infiltration by immunohistochemistry. The imaging and histopathologic parameters were compared amongst low-grade astrocytomas (LGAs), low-grade oligodendrogliomas (LGOs) and high-grade gliomas (HGGs).

Results: [^{11}C]-(*R*)PK11195 binding in HGGs was significantly higher than LGOs or LGAs. LGOs showed higher BP_{ND} than LGAs. The tracer kinetics also differed between LGOs and LGAs, where TACs in the former appeared more similar to grey matter whilst TACs in the latter similar to white matter. Four cases of HGG without obvious contrast enhancement on MRI demonstrated pronounced [^{11}C]-(*R*)PK11195 binding. Immunohistochemistry confirmed that TSPO in gliomas was expressed mainly by neoplastic cells. This expression correlated with BP_{ND} of the tumour (r=0.657). The intensity of TSPO immunoreaction was stronger in HGGs, and a trend towards increased density of TSPO positive neoplastic cells with tumour grade was observed. Microglial cells contributed minimally to the overall TSPO expression within gliomas, and the density of TSPO positive microglia did not differ between tumour grades or subtypes. A small portion of TSPO was also expressed in endothelial cells of normal vessels entrapped in the tumours, but no subtype-dependant difference was found, although tumour blood volume was higher in LGOs than LGAs.

Conclusions: Gliomas show differences in [^{11}C]-(*R*)PK11195 binding and kinetics that are related to tumour grade and subtype. [^{11}C]-(*R*)PK11195 PET has the potential to detect malignant transformation of non-enhancing gliomas and facilitate the targeting of aggressive areas in tumour biopsy. Neoplastic cells rather than microglia are the main cellular sources expressing TSPO and determine the [^{11}C]-(*R*)PK11195 binding in gliomas. The BP_{ND} difference between high- and low-grade gliomas was caused by different levels of TSPO expression in neoplastic cells, and the difference between LGAs and LGOs warrants further investigations.

References:

1. Vlodavsky E, Soustiel JF. J Neurooncol 2007; **81**: 1-7.

2. Miettinen H, et al. Cancer Res 1995; **55**: 2691-5.

3. Junck L, et al. Ann Neurol 1989; **26**: 752-8.

4. Pappata S, et al. J Nucl Med 1991; **32**: 1608-10.

5. Takaya S, et al. J Neurooncol 2007; **85**: 95-103.

6. Lammertsma AA, Hume SP. NeuroImage 1996; **4**: 153-8.

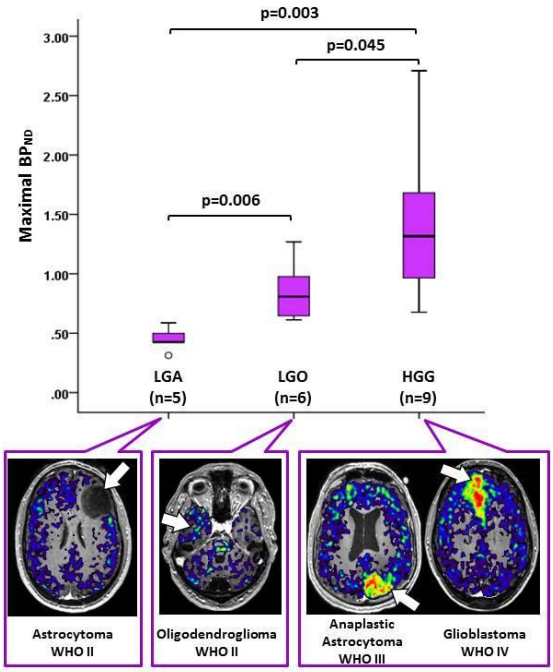

[BPND differences amongst LGAs, LGOs and HGGs]

MODIFICATIONS OF CHOLINERGIC FUNCTIONAL ANATOMY IN ALZHEIMER'S DISEASE ASSESSED BY AUTORADIOGRAPHY USING THE PET TRACER [^{18}F]FLUOROETHOXYBENZOVESAMICOL

J.-P. Soucy[1], M. Parent[2], M.-A. Bédard[3], A. Aliaga[2], N. Mechawar[4], P. Rosa-Neto[2]

[1]Montreal Neurological Institute, [2]Centre for Studies in Aging, McGill, [3]Unité de Recherche en Pharmacologie Cognitive, Université du Québec à Montréal, [4]Douglas Mental Health University Institute, McGill, Montreal, QC, Canada

Objectives: Early and significant alterations of septohippocampal and innominatocortical cholinergic systems have been repeatedly reported in Alzheimer disease (AD). These changes correlate well with the clinical manifestations of the disease (Dournaud). Based on thorough evaluation in rodents and primates (Kilbourn, Parent), PET imaging with the radiotracer [^{18}F]Fluoroethoxybenzovesamicol ([^{18}F]FEOBV) has been proposed as a tool to evaluate the density of these innervations *in vivo*. However, recent results (Ikonomovic) suggest that cholinergic anomalies in AD might not be linked to actual decreases in cholinergic innervation density, but rather to morphological alterations of cholinergic fibers. In the current study, we have investigated whether [^{18}F]FEOBV could in any case detect differences between postmortem brain samples from AD subjects and matched controls.

Methods: Frozen brain samples from 23 normal controls and 13 matched AD subjects were obtained from the Douglas-Bell Canada Brain Bank (Douglas Mental Health University Institute). Tissue sections from the striatum, prefrontal cortex and hippocampus were first incubated for 60 min. in high activity (>1100 Ci/mmol) [^{18}F]FEOBV, washed in cold buffer and dried. Imaging was performed using phosphor imaging plates (20 minutes of exposition). Seven subregions were analyzed on digitized sections: neocortical gray and white matter (the latter used as a non-specific binding reference area), caudate, putamen, and 3 hippocampal sectors (CA1, CA3, dentate gyrus). Averaged normalized binding values for each region were compared between groups (Controls *vs* AD) using a one-way ANOVA.

Results: Significant binding reductions were found in tissues from AD subjects in CA1 (20.13%; $F = 13.39$, $p = 0.001$), CA3 (25.16%; $F = 7.15$, $p = 0.014$), and in the PFC (24.5%; $F = 22.07$, $p < 0.0005$). Other areas (white matter, putamen, caudate nucleus and dentate gyrus) presented no significant anomaly.

Conclusions: AD-associated decreased [^{18}F]FEOBV binding in CA1, CA3 and PFC agrees with previously reported degeneration of septohippocampal and innominatocortical cholinergic systems in that disease. Maintained binding in the dentate gyrus of AD subjects might be explained by reactive sprouting of remaining cholinergic fibers (Scheff) or primary resistance of those fibers to degeneration. Overall, [^{18}F]FEOBV is indeed a promising marker for the detection of alterations in brain cholinergic systems, whether those are linked to changes in innervation density or to reversible structural/molecular modifications of cholinergic fibers.

References:

Dournaud P., et al. (1995). "Differential correlation between neurochemical deficits,

neuropathology, and cognitive status in Alzheimer´s disease". Neurobiol Aging **16**(5): 817-823.

Ikonomovic MD, et al. (2012). "Immunohistochemicla and biochemical analyses of cholinergic projections to the precuneus in normal aging, amnestic MCI and mild Alzheimer´s disease". Program No. 545.27, 2012 Neuroscience Meeting Planner, New Orleans, LA: Society dor Neuroscience, 2012. Online.

Kilbourn, MR, et al. (2009). "Positron emission tomography imaging of (2R,3R)-5-[(18)F]fluoroethoxybenzovesamicol in rat and monkey brain: a radioligand for the vesicular acetylcholine transporter". Nucl Med Biol **36**(5): 489-493.

Parent M, et al. (2012). " PET imaging of cholinergic deficits in rats using [^{18}F] fluoroethoxybenzovesamicol ([^{18}F]FEOBV)". NeuroImage 62: 555-561.

Scheff, S. (2003). "Reactive synaptogenesis in aging and Alzheimer´s disease: lessons learned in the Cotman laboratory". Neurochem Res **28**(11): 1625-1630.

A [^{11}C]DIPRENORPHINE STUDY OF THE HUMAN OPIOID SYSTEM DURING EXPERIMENTAL PAIN USING SIMULTANEOUS FMRI-PET

H.-Y. Wey[1], C. Catana[1], J.M. Hooker[1], D.D. Dougherty[2], G.M. Knudsen[3], B.R. Rosen[1], R.L. Gollub[2], J. Kong[2]

[1]Athinoula A. Martinos Center, Department of Radiology, [2]Department of Psychiatry, Massachusetts General Hospital, Harvard Medical School, Charlestown, MA, USA, [3]Neurobiology Research Unit, Rigshospitalet and University of Copenhagen, Copenhagen, Denmark

Objectives: BOLD fMRI has been used extensively in neuroscience research. However, fMRI lacks the ability to image neurotransmitter specific neural activity. Having an approach that is sensitive to neural responses and provides information about the underlying neurochemical events could be extremely helpful to better understand brain function. In this study, we present the first simultaneous fMRI-PET study in humans that investigated the engagement of the opioid system during experimental pain and how it compares to functional responses.

Methods: Eight healthy volunteers (4 males; age: 24.1±2.7) were included in this study.

MR-PET: All images were acquired on a 3T Siemens TIM-Trio with a BrainPET insert. BOLD imaging was acquired with GE-EPI (TR/TE=3000/30 ms and 3 mm isotropic resolution). A high-resolution anatomical image and a DUTE sequence (for attenuation map[1]) were acquired. Up to 12 mCi (10.83±1.45 mCi, N=16) of [^{11}C]Diprenorphine, a non-selective opioid receptor antagonist, was injected i.v. as a quick bolus for each scan. PET data were acquired for 90min in list mode and binned into 44 frames.

Stimulation: Intermittent pressure to achieve high-pain (15/20 Gracely intensity scale) was delivered to the subject's left calf muscle for 30 min. Baseline scans were acquired at low pressures.

Data Analysis: Data were processed using FSL, FreeSurfer, and PMOD. A standard GLM was used to generate fMRI activation map. Individual subject's anatomical image was processed through FreeSurfer reconstruction pipeline to generate atlas-based segmentations to be used for PET kinetic modeling (**Fig 1A**). PET data was analyzed using a non-invasive Logan model with bilateral occipital cortices as the reference tissues[2]. Quantitative binding potential maps (BP_{ND}) were calculated and co-registered to the MNI152 brain. Statistical group analysis was performed using two-group paired t-test ($Z>2.3$, $p< 0.05$ corrected).

Results: The pressure delivered to induce pain was 310±90 mmHg, which resulted in pain intensity rating of 13±2. fMRI showed robust responses to both pressure (no pain) and pain stimulation (data not shown). The group contrast of pain>no pain demonstrated significant activations in bilateral caudate, putamen, thalamus and brainstem **(Fig 1B, red-yellow)**.

Statistical comparison of BP_{ND} images revealed pain induced decreases in [^{11}C]DPN binding (interpreted as radioligand being displaced by the release of endogenous opioid peptides or by receptor internalization) in bilateral amygdala/parahippocampal area, insula, nucleus accumbens, hypothalamus, thalamus, and contralateral orbitofrontal cortex **(Fig 1B, purple-white)**. fMRI and PET

changes were observed in regions of the basal forebrain with percent BP_{ND} change of ~10-15%.

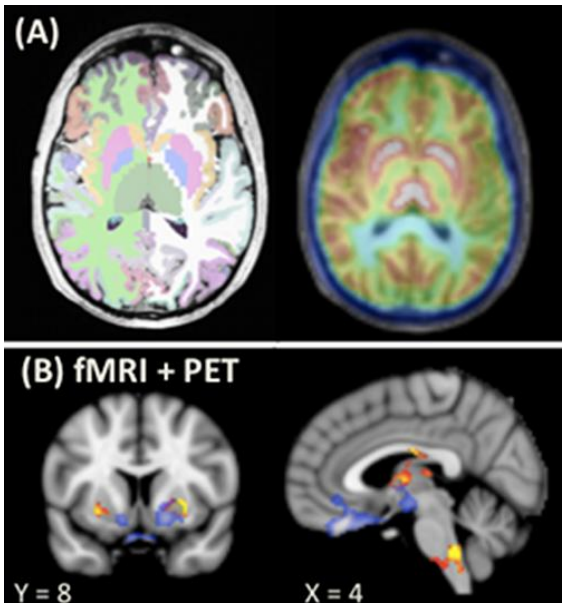

[Fig1]

Conclusions: We presented the first simultaneous fMRI-PET study of the human opioid system and showed fMRI-PET activations in regions related to opioid-mediated pain modulation. Simultaneous fMRI-PET data acquisition provides unique opportunity to relate neurochemical events (endogenous opioid release) to the functional responses (likely related to neural activation), and as such provides a powerful tool for studying the biology and pathology of the human brain.

References: 1. Catana C., et al., JNM, 2010. 2. Logan J, et al., JCBFM, 1996.

ENDOCANNABINOID MODULATION OF NORADRENALINE RELEASE REVEALED WITH [11C]YOHIMBINE MICRO-PET

A. Nahimi[1,2], A.M. Landau[1,3], M. Simonsen[1], G. Wegener[4], **A. Gjedde**[1,2]

[1]Department of Nuclear Medicine and PET Centre, Aarhus University Hospitals, Aarhus University, Aarhus, [2]Department of Neuroscience and Pharmacology, University of Copenhagen, Copenhagen, [3]Center of Functionally Integrative Neuroscience, Aarhus University, [4]Centre for Psychiatric Research, Aarhus University Hospitals, Aarhus, Denmark

Introduction: Endocannabinoid deficits in the brain contribute to severity of symptoms in several neuropsychiatric disorders, including depression, schizophrenia and anxiety. Importantly, CB_1 receptor density is increased in depressed suicide victims (Hugund et al., 2004), and inhibition of fatty acid amide hydrolase (FAAH), which increases the concentration of endogenous cannabinoids, exerts anxiolytic and antidepressant actions in animals (Kathuria et al. 2003, Gobbi et al., 2005). These beneficial effects of FAAH in depression and anxiety are poorly understood, but normalization of CB1 receptor activation and subsequent potentiation of monoaminergic neurotransmission has been suggested. Here, we test the hypothesis that FAAH-induced increase in CB1 receptor activity results in cortical and subcortical noradrenaline release and displacement of [^{11}C]yohimbine, as measured with micro-PET imaging.

Methods: Female Sprague Dawley rats (N=3) were anaesthetized and a femoral artery catheter was inserted for blood sampling. The rats received two 90 minute dynamic micro-PET scans with [^{11}C]yohimbine, an alpha-2 adrenoceptor antagonist which is sensitive to changes in noradrenaline release. One baseline scan and one challenge scan, approximately 60 minutes after treatment with URB 597 (0.03mg/kg, i.v.), a highly selective FAAH inhibitor were obtained. Summed PET images were manually registered to a digital high-resolution atlas of the rat brain (Toga, et al., 1995), and time activity curves were extracted for four volumes of interest including left striatum, right striatum, frontal cortex and cerebellum. We then calculated the volumes of distribution (V_T) by means of Logan graphical analysis (Logan et al., 1990), using individual

plasma curves as the input function. Because of lack of an appropriate reference region, we used the inhibition plot (Gjedde and Wong, 2000) to determine saturation of the receptors after FAAH inhibition. Data are presented as mean (± standard deviation).

Results: Administration of URB597 significantly reduced [^{11}C]yohimbine V_T in all VOIs (see Figure) compared to baseline. URB597 challenge reduced [^{11}C]yohimbine V_T from 1.99 (±0.956) to 0.816 (±0.197) in right striatum, from 1.874 (±0.839) to 0.7943 (±0.1470) in left striatum, from 1.268 (±0.541) to 0.5893 (±0.1097) in cerebellum and from 1.776 (±0.7991) to 0.7930 (±0.1590) in frontal cortex. Similarly, the inhibition plot yielded a 67% saturation of [^{11}C]yohimbine binding sites following administration of URB597.

Discussion: This preliminary study demonstrates important interactions between the endocannabinoid and noradrenergic systems. URB597 increases CB1 signaling by inhibiting the breakdown of endogenous agonists, such as anandamide. Increased activity of CB1 receptors located on both noradrenergic neurons in the locus coeruleus and on noradrenergic terminals hypothetically may increase noradrenaline release and reduce [^{11}C]yohimbine binding. This potentiating effect of FAAH inhibition on noradrenaline release supports the hypothesis that URB597 could have antidepressant and anxiolytic effects.

References:

Gjedde A. and Wong D., (2000) NeuroImage. 11, S48

Gobbi, G.,2005)., PNAS, 102(51), 18620-18625.

Hungund, B. L., et al., (2004). Molecular Psychiatry, 9(2), 184-190.

Kathuria, S., (2003)., Nature Medicine, 9(1), 76-81.

Logan J, et al., (1990) J Cereb Blood Flow Metab. 10:740-7

Toga W. A., (1995), Brain Research Bulletin, 38 (1), 77-85

ACUTE ETHANOL APPLICATION INCREASES A_1 ADENOSINE RECEPTOR AVAILABILITY IN THE HUMAN BRAIN

D. Elmenhorst, A. Matusch, T. Kroll, A. Bauer

Institute of Neuroscience and Medicine (INM-2), Forschungszentrum Juelich GmbH, Jülich, Germany

The fatiguing and sedating effects of alcohol in humans are supposed to be mediated partially by the inhibitory actions of cerebral adenosine, the main degradation product of ATP. Ethanol is known to increase extracellular adenosine several fold in the brain of rats by an increase in adenosine formation and a decrease of adenosine uptake. Interestingly, it has recently been reported that cerebral A_1 adenosine receptor (A_1AR) availability measured with [^{11}C]MPDX was increased after ethanol exposure in rats. In the present pilot study we investigated the impact of acute ethanol exposure on A_1AR availability in the human brain by the use of PET and the highly selective radioligand [^{18}F]CPFPX. This method has been proven to be suitable for quantifying A_1AR densities in the human brain. A bolus plus constant infusion for steady state quantification allows investigating acute drug interactions like the occupancy of A_1AR by caffeine.

In this ongoing study we administered 40 g of ethanol (corresponding to 1 L of beer, n=3) or placebo (n=1) during the steady state period of the PET experiment in healthy volunteers. Ethanol was diluted in 1 L of isotonic NaCl solution and infused intravenously between 80 and 110 min of the 140 min PET scan. Blood alcohol concentration peaked individually between 0.65 and 0.98 mg/mL 30 min after start of the infusion. Arterialized venous blood samples were collected to determine the distribution volume (V_T) of [^{18}F]CPFPX by calculating the ratio of the concentrations between tissue and plasma during steady state. The timespan of this ratio represented either baseline (60 to 80 min) or ethanol condition (120 and 140 min). The distribution volumes of various cortical and subcortical regions remained basically constant before and after placebo exposure (relative difference 3%). In contrast, distribution volumes in the ethanol group increased quickly by on average 29%.

Our preliminary data exhibit for the first time a rapid increase in cerebral A_1AR availability following acute intravenous ethanol application in humans.

QUANTIFICATION OF DOPAMINE D3 RECEPTORS AND DOPAMINE RELEASE IN THE FUNCTIONAL ZONES OF THE PALLIDUM

A.C. Tziortzi[1,2], G. Searle[2], G. Douaud[1], E. Rabiner[2], M. Jenkinson[1], R.N. Gunn[2]

[1]Clinical Neurosciences, FMRIB Centre, University of Oxford, Oxford, [2]Imanova Centre for Imaging Sciences, London, UK

Objectives: In non-human primates, the striatum sends projections to the pallidum imposing its functional organisation[1]. A recent study in humans, demonstrated that dopamine has a functional rather than an anatomical specificity[2]. Our objective is to study dopamine release (DR) and the D_3/D_2 receptors, in the connectivity-based functional subdivisions (CBFS) of the human pallidum, using probabilistic-tractography[3] and [^{11}C]PHNO PET.

Methods: Diffusion-weighted data and dynamic baseline and post-amphetamine [^{11}C]PHNO scans, were acquired in twelve healthy males to estimate the DR in the CBFS. To obtain the pallidal CBFS in each subject a two-step procedure was performed: A) The cortical-striatal connections were estimated using probabilistic-tractography to subdivide striatum into limbic, cognitive and sensorimotor as described in Tziortzi[2]. B) Connection probabilities from the striatal CBFS to the pallidum were estimated to subdivide pallidum into limbic, cognitive and sensorimotor.

The simplified reference tissue model (SRTM) was applied to the [^{11}C]PHNO data to estimate the binding potential (BP_{ND}) within the individual-subject pallidal CBFS. DR was assessed by calculating the change in BP_{ND} elicited by amphetamine.

For the dissection of the [^{11}C]PHNO signal into D_3/D_2 components, nineteen subjects received [^{11}C]PHNO at baseline and following administration of a D_3 antagonist. Dynamic PET data were analysed using SRTM. For this study Diffusion-weighted data were not available. The individual-subject CBFS obtained for the DR study were combined to construct a pallidal CBFS-atlas. The CBFS-atlas was then applied to the data to estimate the D_3 and D_2 BP_{ND} (BP^{D3} and BP^{D2}) as described in Searle[4].

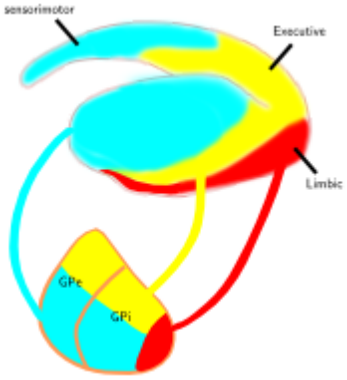

[Functional subdivision of the Pallidum]

Results: The functional organisation of the pallidum is congruent with non-human primate data. The limbic territory occupies the rostral ventral pallidum while the executive occupies the entire rostro-caudal extent with the highest connection probabilities observed in the dorsomedial pallidum. The sensorimotor projections reside in the ventrolateral pallidum.

The order of DR in the pallidal CBFS is the following: the highest DR was measured in the limbic followed by the sensorimotor and the lowest DR was measured in the executive region. In the limbic pallidum the BP^{D3}=2.60, in the cognitive BP^{D3}=2.10 whereas in the sensorimotor BP^{D3}=1.15. Notably the density of the D_2 is uniformly distributed in the functional subdivisions of the pallidum (BP^{D2}~1).

Conclusions: The order of the DR in the pallidum CBFS was the same with that found by Tziortzi[2] in the striatal functional zones. Tziortzi[2] also found that this order was independent of the ligand used and the relative distribution of the D_2/D_3 receptors. This is in agreement with our findings in the pallidum. Specifically, although the density of D_3 was higher in the cognitive as compared to the sensorimotor zone, the DR was higher in the sensorimotor CBFS. Moreover the highest BP^{D3} was in the limbic pallidum. This finding is in accord with theories that assign a primarily limbic role to the D_3 and justifies the efforts to target the D_3 for the treatment of addictive and other psychological disorders.

References:

[1] Parent, Brain-Research-Reviews, 1995

[2] Tziortzi, Cereb-Cortex, 2012

[3] Behrens, Nat-Neuro, 2003

[4] Searle, Biol-Psy, 2010

EFFECTS OF DOPAMINE D2 RECEPTOR AGONIST/ANTAGONIST CHALLENGES IN SIMULTANEOUS PET/FMRI

C.Y. Sander[1,2], J.M. Hooker[1], C. Catana[1], T. Witzel[1], D.B. Chonde[1], B.R. Rosen[1,3], J.B. Mandeville[1]

[1]A. A. Martinos Center for Biomedical Imaging, Massachusetts General Hospital and Harvard Medical School, Boston, [2]Electrical Engineering and Computer Science, Massachusetts Institute of Technology, [3]Health Sciences and Technology, Harvard-MIT, Cambridge, MA, USA

Introduction: [^{11}C]raclopride displacement studies have provided important insights into the dopamine system. However, such PET studies (mainly with amphetamine) have shown discrepancies to dopamine efflux from microdialysis due to prolonged raclopride displacement; an observation attributed to agonist-induced receptor internalization[1]. Simultaneous PET and functional MRI may provide further insight into these mechanisms *in vivo* as fMRI presumably depends upon the availability of non-internalized receptors. Hence, we employed PET/fMRI using a D2 agonist and antagonist at matched occupancies in order to test this hypothesis and evaluate whether prolonged PET displacement simultaneously induces a shortened hemodynamic response.

Methods: Dynamic PET/fMRI was acquired in an anesthetized rhesus macaque with [^{11}C]raclopride. A D2 agonist (quinpirole) or antagonist (raclopride) was employed in graded doses as within-scan challenges (0.1, 0.3mg/kg, quinpriole), or as bolus co-infusion paradigms (0.4, 1.4, 4.5, 16, 41µg/kg raclopride). Iron oxide was injected to improve fMRI contrast/detection and to deduce %CBV changes. PET/fMRI data were analyzed with the GLM. PET kinetic modeling employed MRTM2[2] with a time-dependent $k_{2a}(t)$ term[3], derived from a fit with a gamma or sigmoidal function by minimizing the χ^2/DOF. This was used to compute a time-dependent binding term, $DBP_{ND}(t)$.

Results: Voxelwise maps showed a consistent co-localization of PET specific binding and fMRI signal changes in the striatum (inhibition with quinpirole, excitation with raclopride). PET occupancies and fMRI peak magnitudes in putamen increased with higher doses of agonist or antagonist, although fMRI signs reversed for agonist/antagonist. PET time activity curves (TAC) showed a visible decrease in specific binding regions at the time of the challenge (Fig.1a). For a raclopride challenge with peak occupancy of 74%, changes in DBP_{ND} and CBV were very similar in time-to-peak and duration. However, for a quinpirole challenge that reached 78% occupancy, the decrease in DBP_{ND} was very prolonged relative to CBV changes (Fig.1b). With the antagonist, caudate exhibited a 2-fold smaller slope than putamen in relating CBV versus occupancy, whereas with the agonist, the slope in caudate was slightly larger. These results indicate that putamen has approximately twice the basal dopamine occupancy compared to caudate, consistent with literature values[4].

Conclusions: Understanding mechanisms of raclopride displacement is essential in order to quantitatively relate changes in raclopride binding to neurotransmission. While an antagonist-induced fMRI response roughly matches the temporal response of specific binding[5], the response to an agonist is severely abbreviated compared to raclopride displacement. These results implicate divergent mechanisms for agonists, which may induce receptor internalization, versus antagonists, which may not alter postsynaptic receptor concentrations. Further studies with graded agonist doses will help characterize the CBV-occupancy relationship. Understanding fMRI-occupancy relationships[5], however, can provide insights into basal occupancy - a measurement for which simultaneous PET/fMRI appears to be a promising methodology.

References:

[1]Ginovart *Mol Imaging Biol* 2005.

[2]Ichise et al. *JCBFM* 2003.

[3]Alpert et al. *Neuroimage* 2003.

[4]Skirboll et al. *Exp Neuro* 1990.

[5]Sander et al. *NRM2012*.

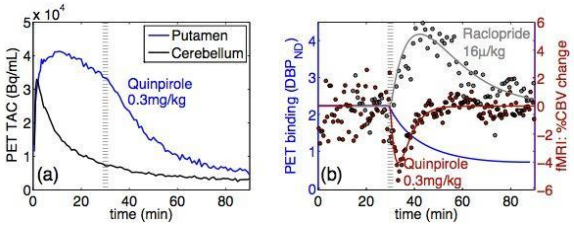

[Fig. 1]

Fig. 1: (a) Bolus TACs for an agonist challenge at 30min. (b) Corresponding decrease in PET binding is prolonged compared to fMRI signal.

PHARMACOLOGICAL INDUCED CHANGES IN GLUTAMATE LEVELS DO NOT AFFECT MGLUR5 RADIOLIGAND [11C]ABP688 BINDING IN THE RAT BRAIN

T. Wyckhuys[1], J. Verhaeghe[1], L. Wyffels[1,2], M. Schmidt[3], X. Langlois[3], S. Stroobants[1,2], S. Staelens[1]

[1]Molecular Imaging Center Antwerp, University of Antwerp, Wilrijk, [2]Nuclear Medicine, University Hospital Antwerp, Edegem, [3]Department of Neuroscience, Janssen Pharmaceutica NV, Beerse, Belgium

Objectives: Abnormal glutamate transmission is involved in the pathophysiology of various neurological disorders. However, there are no imaging techniques capable of measuring acute fluctuations in endogenous levels of glutamate in vivo. A recent study performed in baboons reported a significant decrease in binding of [11C]ABP688, a PET ligand that binds an allosteric site of mGluR5, when endogenous glutamate levels were increased following pharmacological challenge with N-Acetyl-cysteine (NAc) (Miyake N. et al., 2011). In our current study, we evaluated [11C]ABP688 binding in rats using small animal PET following pharmacological challenge with NAc and MK-801. Both compounds are known to induce increases in glutamate levels.

Methods: Three experiments were performed

i) rats (n=6) received two microPET (Inveon, Siemens) scans on two different days with either unlabelled ABP688 (3mg/kg, iv.) or vehicle pretreatment 10 minutes prior to tracer injection. Rats were injected with [11C]ABP688 (iv., < 3 nmol/kg) at the initiation of a dynamic microPET scan (1h). The order of administration of either unlabelled ABP688 or vehicle was randomized. The reconstructed images were normalized to a [11C]ABP688 rat brain template and time-activity curves (TAC) were extracted from a VOI-template containing the striatum and cerebellum. Non-displaceable binding potential (BP_{ND}) was calculated using the simplified reference tissue model (SRTM) with the cerebellum as reference region;

ii) rats (n=6) were scanned and analysed similarly as in the first experiment but were pretreated with NAc (50mg/kg/h infusion, iv.) or vehicle during 1h prior to tracer injection;

iii) rats (n=6) were treated similarly as in the first experiment but were pretreated with MK-801 (0.16mg/kg, ip.) or vehicle 20 min prior to tracer injection.

Results: Average BP_{ND} for the striatum was i) 2.39 +/- 0.13 and 0.15 +/- 0.05 ($p< 0.05$) for vehicle and unlabelled ABP688 pretreatment respectively; ii) 2.58 +/- 0.28 and 2.54 +/- 0.17 for vehicle and NAc respectively and; iii) 2.49 +/- 0.13 and 2.51 +/- 0.28 for vehicle and MK-801 respectively (Fig.). No significant difference was observed between NAc or MK-801 BP_{ND}s in comparison with their respective vehicle BP_{ND}s. The BP_{ND} observed in all vehicle microPET experiments closely resembled those observed in previous studies.

Figure: No significant changes in [11C]ABP688 binding are observed following administration of NAc or MK-801 in comparison with vehicle on

a) BP_{ND} eg. in caudate putamen and

b) microPET images

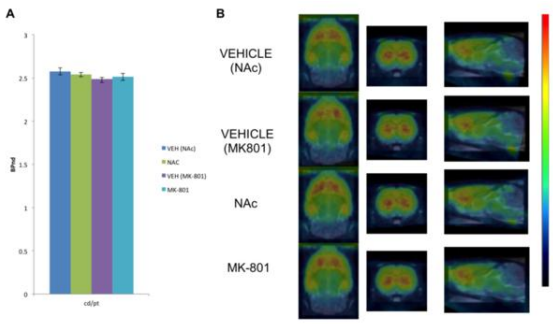

[Figure]

Conclusions: This study indicates that the vehicle BP_{ND} values for the [11C]ABP688 tracer correlate with literature findings and that microPET is able to discriminate for changes in [11C]ABP688 binding. Pharmacological challenge with both N-Acetyl-cysteine and MK-801, known to increase endogenous glutamate levels, did not affect the affinity of [11C]ABP688 for mGluR5 measured with microPET in the rat brain. This suggests that the affinity of [11C]ABP688 for the allosteric binding site is not modulated by glutamate binding onto the orthosteric site and that [11C]ABP688 is not capable of measuring (directly or indirectly) acute fluctuations in endogenous levels of glutamate in vivo in the rat brain.

Poster Session

THE INFLUENCE OF DEPRESSION ON THE SOCIAL BEHAVIOR OF RATS, THE EFFECT OF ANTIDEPRESSANT TREATMENT

M. Boyko, D. Porat, R. Kuts, I. Melamed, V. Zvenigorodsky, A. Zlotnik

Ben-Gurion University, Beer Sheva, Israel

Depression is a relatively prevalent disorder, and antidepressants are among the five commonly prescribed medication groups worldwide. While it affects many people as a primary disorder, depression commonly results in secondary complication of many other diseases, and significantly increases the rates of morbidity and mortality. Mechanisms leading to depression and the effects of this disorder on social behavior have evoked increasing interest in many research organizations; however they have not yet been thoroughly investigated.

The goals of this research are to study the effects of depression on the social organization of rats subjected to restricted access to food, and to test the efficiency of the antidepressant treatment. It includes inspection of the behavior of a group of rats, some of which were kept under depression-inducing conditions. We followed their behavior and group functioning as their access to food was limited by obstacles.

We found that the depressed rats were more competent to pass through obstacles to get food than the non-depressed rats. We believe that this is due to lower sense of fear under a state of depression. However, when these rats were treated with antidepressant, their behavior returned to normal as if they have never been exposed to depression-inducing conditions. This treatment had a consequence also on the social behavior in the group; while the depressed rats were those who went through the obstacles to fetch the food for the group at first, this duty is now distributed among all the other rats.

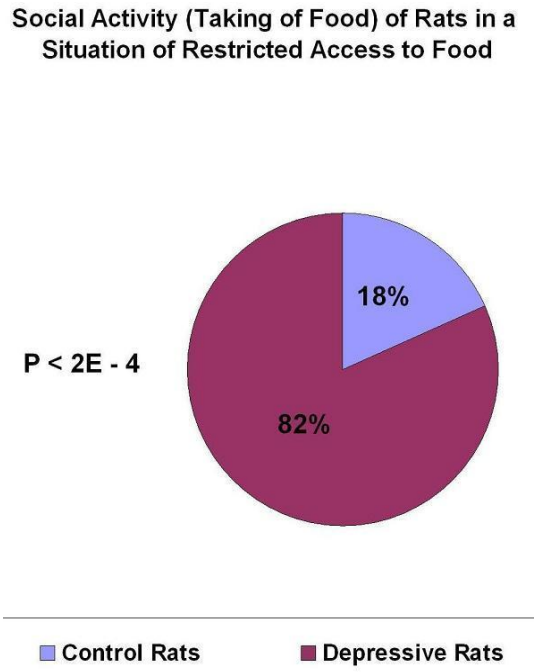

[Fig 1]

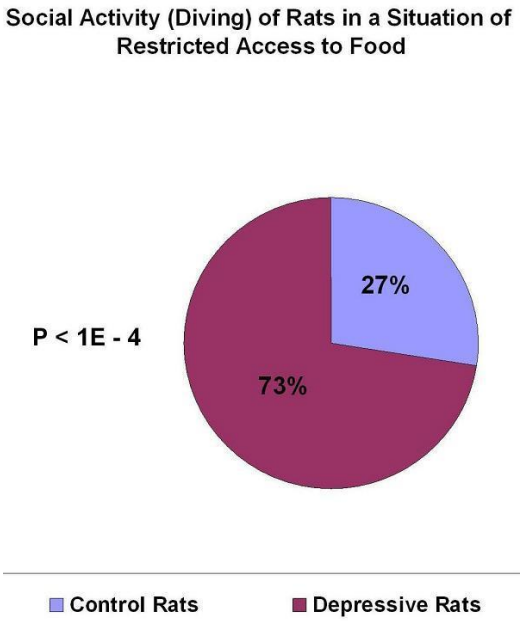

[Fig 2]

ESTABLISHMENT OF RAT MODEL OF POST-SUBARACHNOID HEMORRHAGE DEPRESSION

M. Boyko, R. Kuts, V. Zvenigorodsky, I. Melamed, D. Porat, A. Zlotnik

Ben-Gurion University, Beer Sheva, Israel

Introduction: While the pathophysiology of subarachnoid hemorrhage (SAH) has been studied extensively, the emotional consequences largely remain unclear. SAH has been described in humans to be associated with depression, anxiety and post-traumatic stress disorder. Yet, possibly due to the lack of experimental studies, little is known of the mechanism for post-SAH emotional and behavioral disturbances. Therefore, there is a great need for the development of animal models for post-SAH behavioral abnormalities. This study describes the neuro-behavioral profile of rats following both a single-injection and double-injection model of SAH.

Materials and methods: SAH was induced in 48 rats by 0.3 ml injection of autologous arterial blood into the cisterna magnum (single-injection model). Post-SAH vasospasm was induced in 24 of these rats by a second injection of blood into the cisterna magnum after 24 hours (double-injection model). 0.3 ml of saline was injected into the cisterna magnum of 24 additional rats (sham group). Neurological performance was measured at 24, 48 hours, 1, 2 and 3 weeks following SAH. 3 weeks after SAH, four behavioral tests were performed for the duration of 6 consequent days: open field test, sucrose preference test, elevated plus maze test and swimming test. The rats´ behavior was videotaped for post-recording analysis via Ethovision XT software.

Results: There was impaired neurological performance by 24 hours following SAH (P< 0.0001). For the open field test, the double-injection model was associated with less total travel distance (P< 0.005, Fig.1A), less travel distance in the central part of the field (P< 0.05, Fig. 1B), decreased time spent in the central part of the field (P< 0.05, Fig. 1C), and a reduced mean velocity (P< 0.005, Fig. 1D). Sucrose preference was impaired in both SAH groups compared to the control group (P< 0.01). For the plus maze test, the single-injection model was associated with less open arm entries (P< 0.005; Fig 2A), decreased time spent in open arms (P< 0.0005; Fig 2B), decreased closed arm entries (P< 0.01, Fig. 2C), and decreased platform entries (P< 0.005, Fig. 2E). In both models of SAH, there was decreased time spent on the platform (P< 0.005, Fig. 2D). There was more immobility time during the swimming test in both the single-injection group (P< 0.005) and double-injection group (P< 0.05) compared to the control group.

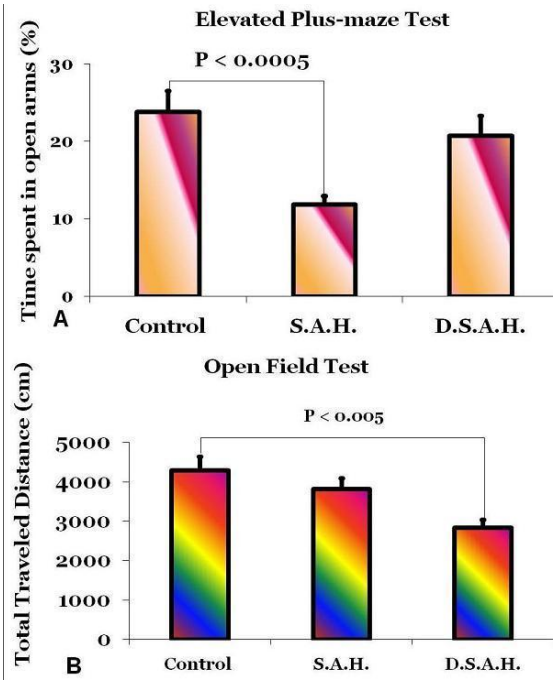

[Fig 1]

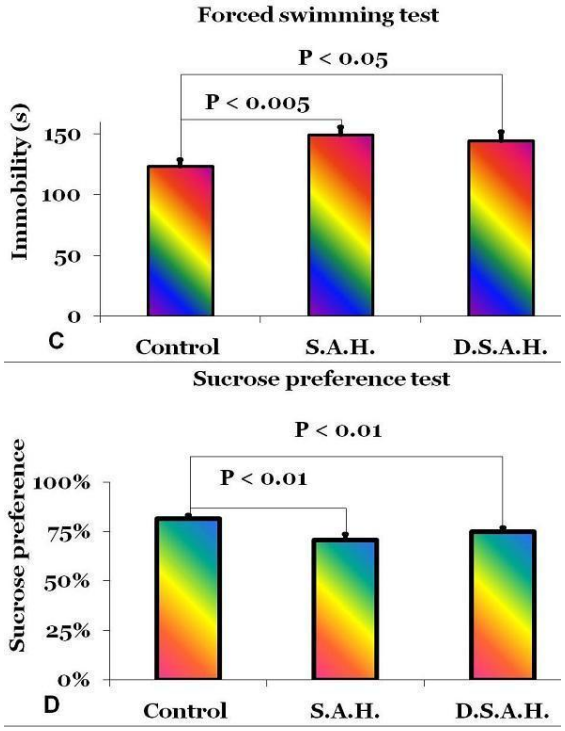

[Fig 2]

Conclusions: The mail finding of this study was that both, the single and double injection rat models of SAH, were associated with considerable behavioral disturbances including locomotor abnormalities, increased anxiety and depressive behavior.

ESTABLISHMENT OF ANIMAL MODEL OF DEPRESSION CONTAGION

M. Boyko[1], D. Porat[1], R. Kuts[1], V. Zvenigorodsky[1], Y. Kezerle[1], H. Severinovskaya[1], K. Baturova[2], A. Zlotnik[1]

[1]*Ben-Gurion University, Beer Sheva, Israel,* [2]*Dnepropetrovsk State University, Dnepropetrovsk, Ukraine*

Introduction: Shared paranoid disorder (SPD), also known as folie à deux, is a fairly uncommon disturbance characterized by the presence of similar psychotic symptoms in two or more individuals, while only one person has a genuine psychotic disorder, and the other suffers from induced symptoms, usually delusional. It is difficult to assess its prevalence in the population due to the difficulty of diagnosis, but hundreds of cases have been reported. Establishment of valid animal model of SPD may improve our understanding of mechanism and treatment of SPD.

Materials and methods: Ten social groups (each one containing 3 animals in it), where composed of a naïve rat and two rats which have been previously induced with depression were housed together for 5 weeks. After five weeks, all the rats where tested for depressive behavior using sucrose preference test and swimming test.

Results: In all the groups all three rats were identified as depressive (Fig.1).

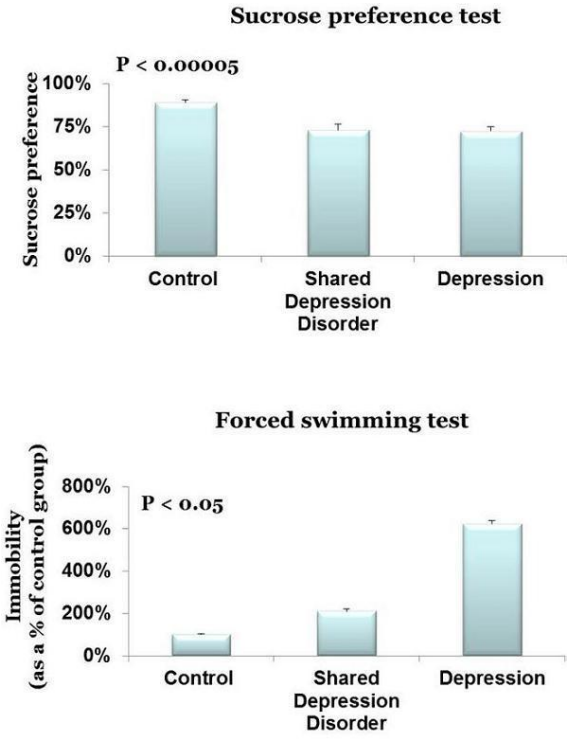

[Fig 1]

Conclusion: The rat which was initially non-depressive has picked up the same depressive behavior from the other two rats, merely due to sharing the same living space with them. Hopefully, a better understanding of the SPD among rats will help us build a model to the mechanism that this disorder takes place, which could eventually be applied to humans as well.

ENDOTHELIAL INJURY INITIATES THE PATHOLOGICAL CASCADE OF CEREBRAL SMALL VESSEL DISEASE IN SHRSP

C.Z. Büche[1], C. Garz[1], H.-J. Heinze[1,2,3], M. Goertler[1], K. Reymann[2,3], H. Braun[3], S. Schreiber[1]

[1]Department of Neurology, Otto-von-Guericke University, [2]Leibniz Institute for Neurobiology, [3]German Center for Neurodegenerative Diseases, Magdeburg, Germany

Objectives: In recent studies of spontaneously hypertensive stroke-prone rats (SHRSP) we assessed definite chronological stages of cerebral small vessel disease (CSVD) initiated by intravasal erythrocyte accumulations immediately followed by an age-dependent occurrence of blood-brain-barrier-disturbances. Microbleeds, arteriolar wall thickening and occlusion associated with tissue infarcts exhibit the final stages of CSVD. We now focused on the etiology of the initial microvascular dysfunction and assume, that those early erythrocyte accumulations are the consequence of an endothelial injury resulting in an activated coagulatory state.

Methods: Groups of SHRSP aged from 12 to 44 weeks and Wistar controls aged from 12 weeks to 3 years were investigated immunohistochemically (anti-thrombocyte-antibody, anti-von-Willebrand-factor(vWF)-antibody). Antibodies against the plasma proteins IgG and Fibronection served as marker for BBB breakdown.

Results: Erythrocyte accumulation occurred in the capillary and arteriolar bed and was detectable by red blood cell autofluorescence. Affected microvessels exhibited wall-adherent and perivascular accumulations of plasma proteins indicating an association between erythrocyte accumulation and BBB breakdown. Intravasal, between those accumulated erythrocytes, thrombocytes and threads of vWF were found. That thread-shaped vWF is activated by an exposure to the subendothelial matrix and effectively binds to thrombocytes.

Conclusions: We assume, that the initial microvascular dysfunction in CSVD is initiated by an early endothelial injury caused by arterial hypertension and age. The consecutive exposure of blood vWF to the subendothelial matrix leads to thrombocyte adhesion and aggregation. Erythrocytes stick in that network of vWF and thrombocytes and might indicate a local flow velocity reduction and thrombus formation. Accumulation of toxic hemoglobin products might further impair vessel wall integrity with subsequent vessel wall rupture and microbleeds initiating the terminal CSVD stages.

References:

Schreiber et al, J Cereb Blood Flow Metab. 2012 Feb;32(2):278-90 ,

Braun et al, J Neurol Sci. 2012 Nov 15;322(1-2):71-6,

Henning et al, J Cereb Blood Flow Metab. 2010 Apr;30(4):827-36,

Schneider et al, Proc Natl Acad Sci USA. 2007 May 8;104(19):7899-903,

Sukumari-Ramesh, Glia. 2010 Nov 15;58(15):1858-70

A NON-HUMAN PRIMATE MODEL OF TRANSIENT FOCAL CEREBRAL ISCHEMIA WITH VARIABLE DURATION DETERMINED BY SERIAL DIFFUSION MRI

S.-H. Cha[1], S.R. Lee[2], H.J. Lee[3], S.Y. Lee[1], K.S. Yi[1], K.-M. Kim[2], Y.J. Lee[2], K.-T. Chang[2]

[1]Radiology, Chung Buk National University Hospital, Cheongju, [2]National Primate Research Center, Korea Research Institute of Bioscience and Biotechnology, Ochang, [3]Medical Research Institute, Chung-Ang University College of Medicine, Seoul, Republic of Korea

Purpose: Among the researches of experimental stroke in non-human primates (NHPs) and a few transient focal cerebral ischemia models were documented. There is no NHP model which re-produce the infarction lesions of similar characteristics such as location and temporal evolution of ADC abnormality. This experimental study is to establish a non-human primate (NHP) model of transient focal cerebral ischemia with perfusion-diffusion match using transient endovascular occlusion of middle cerebral artery (MCAO) branch and repeated diffusion MRIs and to observe temporal changes of diffusion abnormality.

Methods: In each offour Rhesus monkeys,

after pre-MCAO brain MRIs, proximal M2 branch of right MCA were endovascularly occluded under the general anesthesia. Immediately after arterial occlusion, each animal was repeatedly imaged with 3 Tesla MRI. When diffusion abnormality in the occluded arterial territory did not grow for 30 minutes on consecutive MRIs, occluded artery was recanalized by removing intra-arterial device from the animal which remained in the MR magnet. Patency of the right MCA was confirmed on follow up MRA. The temporal evolution of lesion volume and apparent diffusion coefficient (ADC) in the ischemic lesions were investigated.

Results: The duration of arterial occlusion was 50, 80, 100, 120 minutes, respectively. Focal infarction volume was, initially at 30 minutes after ischemia, 35.87 %, 11.15 %, 8.66 %, 13.71 % of ipsilateral hemisphere (average = 17.35 %), peak volume prior to the recanalization was 37.85 %, 12.41 %, 14.68 %, 19.76 % (average = 21.18 %), respectively. After the reperfusion, in 3 cases, lesion volume decreased to 13.21 %, 3.42 %, 2.27 % (average = 6.30 %) at 6 hour.

Conclusion: Using temporary endovascular arterial occlusion, serial diffusion MRI and variable duration of transient focal cerebral ischemia, we developed a NHP model of with minimal perfusion-diffusion mismatch. This preliminary experience would lead to establish the NHP stroke model with localized hemispheric infarction of similar damage level.

EVOLUTION OF THE PENUMBRA IN AN ANIMAL STROKE MODEL DURING THE FIRST 12 HOURS AFTER STROKE ONSET

B. Hong-Goka[1,2], R. Sweazey[1], **F.-L. Chang**[1]

[1]Indiana University School of Medicine Fort Wayne, Fort Wayne, IN, [2]UCSF - Fresno Alzheimer's & Memory Center, Fresno, CA, USA

To facilitate translation of animal research on neuroprotection to treat human stroke we have proposed a penumbra-centric model using pimonidazole (HP-1) to delineate the penumbra, which represents hypoxic but still salvageable tissues, and is the target of neuro-intervention in clinical practice. There are four components of this model:

1. HP-1 staining to identify the hypoxic penumbra.

2. Within the penumbra, use of histochemical stains such as cresyl violet and changes of biomarkers representing components of the ischemic cascade such as albumin, ICAM-1, methionine sulfoxide (MetO), Hsp70 as outcome measures to evaluate treatment efficacy.

3. Study conducted within 12 hours from stroke onset to closely approximate clinically relevant time frame. Studies have shown a lack of benefit of reperfusion with delay of neuro-intervention beyond 12 hours.

4. Combination drug treatment to cover the entire spectrum of the ischemic cascade in contrast to a single agent. The current study examines the evolution of the penumbra within 12 hours after stroke onset to facilitate translation of animal model into clinical use.

This study is in compliance with NIH animal care guidelines and was approved by the Purdue Animal Care and Use Committee. Twenty-six Sprague-Dawley rats of both genders, aged 3-23 months were used. Intraluminal middle cerebral artery occlusion (MCAo) without reperfusion was induced under ketamine and xylazine. Physiologic parameters and blood gases were monitored. Core body temperature was maintained at 37^{o}C. Supplemental oxygen was administered to keep peripheral oxygen saturation at 99-100%. Cerebral blood flow was measured with a laser Doppler system. HP-1 (60mg/kg) was injected intraperitoneally 90 minutes before sacrifice.

We found a significant drop of penumbra area from 1 to 2 hours representing the early transformation of penumbra into core; this was followed by a continued shrinkage in penumbra size from 2 to 12 hours after stroke onset. Penumbra staining was most robust between 3 to 5 hours post-stroke. At 12 hours, little of the penumbra remained. During the same period, the adjacent core continued to expand into prior penumbra territory. We have previously demonstrated the loss of blood brain barrier integrity by the presence of serum albumin in the core as early as 1 hour after ischemia onset. This extravasation was confirmed by the detection of intravenously injected dextran-FITC in the neuropil. The core albumin labeling persists and slowly infringes on the penumbra with increased duration of ischemia. Cresyl violet staining showed shrunken neurons with pyknotic nuclei in the core, surrounded by healthy neurons with

vesicular nuclei in the penumbra. Immunostaining showed the presence of Hsp70, MetO, and ICAM-1 within penumbra.

Our study demonstrates the progressive disappearance of the penumbra over the first 12 hours in our rat stroke model. This effect closely parallels the current clinical impression of diminished benefits of intervention past 12 hours after stroke. Our study also demonstrates the feasibility of using biomarkers within the penumbra to study efficacy of various combination drug treatments for neuroprotection.

EFFECTS OF GINKGOLIDE ON EXPRESSION OF HO-1 IN CEREBRAL TISSUE OF SUBARACHNOID HEMORRHAGE AFTER BLOCKAGE OF CEREBRAL LYMPHATIC DRAINAGE RATS

C.Z. Cheng

Department of Rehabilitation, Traditional Chinese Medical Hospital of Taian, Taian City, Shandong, China

Objective: To investigate the effects of ginkgolide on expression of HO-1 protein in cerebral tissue following subarachnoid hemorrhage after cervical lymphatic blockage (CLB).

Methods: The 36 Wistar rats were divided into normal control, SAH group, SAH+CLB group, SAH+CLB+NS group, SAH+CLB + ginkgolide 20 mg, and SAH+CLB+ ginkgolide 80mg group. ginkgolide was given by intraperitoneal injection. One day after the induction of CLB model, SAH model was produced. On the third day after the second cisternal injection, the expression of HO-1 protein in brain tissue were determined by an immunofluorescence assay.

Results: An increased expression of HO-1 in brain sections was noted after SAH. The expression of SAH + CLB and NS group was more higher. The application of ginkgolides augmented the HO-1 expression. High-dose group of ginkgolides was significantly higher than low-dose group.

Conclusion: Ginkgolides could enhance the expression of HO-1 protein in SAH rat, especially in high dose group.

DIFFERENT SHAM PROCEDURES INDUCE CORRESPONDING INCREASES IN LEVELS OF TRAUMA MARKERS FOR RATS IN TRAUMATIC BRAIN INJURY EXPERIMENTS

Y.-H. Chiang[1,2], C.-C. Wu[1,3], K.-Y. Chen[1,2], W.-T. Chiu[1], C.-Y. Shiau[3]

[1]Department of Neurosurgery, [2]Department of Surgery, College of Medicine, Taipei Medical University, [3]Graduate Institute of Medical Sciences, National Defense Medical Center, Taipei, Taiwan R.O.C.

Introduction: In traumatic brain injury (TBI) animal models, sham or naïve control groups are often used for analysis of injured animals; however, the existence and/or significance of differences in the control groups has yet to be studied. In addition, recent controversies regarding the DECRA trial in which decompressive craniectomies in patients with severe traumatic brain injury and refractory increased intracranial pressure remains unsettled. While the report demonstrated that the procedure may result in less favorable long term outcomes despite the decrease in intracranial pressure and shorter length of ICU stay, the study has been criticized and the debate is still inconclusive partly due to a lack of mechanistic explanation. We have recently discovered Etk to exhibit upregulation after traumatic neural injury, and will compare the effects of craniectomy procedure to those of other procedures inducing different levels of severity.

Materials and methods: 4 groups of rats, receiving different procedures (controlled cortical impact, craniectomy, bicortical drilling, and unicortical drilling) were compared. PCR, Western blot analysis and immunoflorescence staining of Etk, S100, GFAP levels were used to analyze the results and compare the different groups.

Results: Etk Upregulation were statistically significantly between craniectomy group and unicortical drilling group. Level of change for GFAP and S100 were only significant when cortex was impacted.

Conclusions: Unicortical drilling may be preferable as a sham control procedure over craniectomy or bicortical drilling . Increases in the expression of Etk in the craniectomy group suggests a possible mechanism by which unfavorable outcome occur in patients receiving craniectomy procedures.

PROGRESSION OF A PHOTOTHROMBOTIC-INDUCED ISCHAEMIC INFARCT DETERMINED BY MRI AND HISTOLOGY

A. Craig, A. Krishnan, G. Housley

Department of Physiology, University of New South Wales, Sydney, NSW, Australia

Objectives: The mortality rate following a cerebellar infarction is 23% greater than for an infarct in any other part of the brain (Macdonell *et al.*, 1987). Moreover, vertebrobasilar stroke has a mortality rate of 85% (Kaye, 2011). Despite the deadly consequence of hindbrain strokes, there are limited animal models to aid investigations into novel therapeutic options. Currently, small animal models of stroke focus on middle cerebral artery occlusion or global ischaemia. Here we present a photothrombotic mouse model of cerebellar ischaemia with real-time imaging of thrombus development, magnetic resonance imaging (MRI) of the progression of these infarcts, and histological analysis of the tissue. Further, our data settles the controversy over whether this technique provides a thrombotic infarct, refuting the recent contention (Frederix et al., 2007; Kleinschnitz et al., 2008), that brain injury from photothrombotic infarct is independent of platelet aggregation-mediated occlusion of cerebrovascular microvessels, i.e. is due to photolytic action.

Methods: Photothrombosis in the cerebellum was achieved under isoflurane anaesthesia, by intravenous administration of rose bengal followed by illumination at 561nm directed to the region of interest within the cerebellum targeted for infarct (Watson *et al.*, 1985). The progressive clot formation was visualised by the intravenous administration of anti-CD42:Cy7-conjugate. Infarcts were examined by T2 weighted MRI at days 1, 4, and 7 post-ischaemia in situ. Following MRI, the tissue was paraffin embedded, sectioned, and stained with haematoxylin and eosin.

Results: The MRI scans resolved an area of acute infarction of approximately $1mm^3$ that specifically corresponded to the 561nm illuminated region of interest. This correlates to the anti-CD42 marker which is restricted to an area of the same size. The tissue damage is also evident in the histological sections. In control studies (rose bengal omitted), no thrombosis was evident and no brain damage occurred. The experiments followed protocols approved by the UNSW Animal Care & Ethics Committee.

Conclusion: Our results therefore confirm that the photo-thrombotic model of ischaemia delivers infarcts which can be defined with precise spatiotemporal control. These data indicated that endothelial activation by photo-sensitizing the cells with rose bengal was required for site-specific ischaemic brain injury. This model will enable study of neuroprotective signal pathways in the hind brain in the mouse model.

References:

Frederix K, Chauhan AK, Kisucka J, et al. (2007). Platelet adhesion receptors do not modulate infarct volume after a photochemically induced stroke in mice. Brain research 1185, 239-245.

Kaye V. (2011). Overview of Vertebrobasilar stroke, ed. Campagnolo D. medscape.com.

Kleinschnitz C, Braeuninger S, Pham M, et al. (2008). Blocking of platelets or intrinsic coagulation pathway-driven thrombosis does not prevent cerebral infarctions induced by photothrombosis. Stroke 39, 1262-1268.

Macdonell RA, Kalnins RM & Donnan GA. (1987). Cerebellar infarction: natural history, prognosis, and pathology. Stroke 18, 849-855.

Watson BD, Dietrich WD, Busto R, et al. (1985). Induction of reproducible brain infarction by photochemically initiated thrombosis. Annals of neurology 17, 497-504.

AJC is supported by a UNSW Vice Chancellor's post-doctoral Fellowship; funded by a UNSW Goldstar award.

PHOTOTHROMBOTIC MILD STROKE: MRI DETECTION OF CORE AND PERI-INFARCT INJURY

Q. Deng[1], M. Qiao[2], T. Foniok[3], D. Rushforth[3], U.I. Tuor[2,3]

[1]Department of Neuroscience, Hotchkiss Brain Institute, University of Calgary, [2]Department of Physiology and Pharmacology, Hotchkiss Brain Institute, University of Calgary, [3]Experimental Imaging Centre, Faculty of Medicine, University of Calgary, Calgary, AB, Canada

Introduction: A major stroke is often preceded by a transient ischemic attack or a minor stroke. The pathophysiology of minor stroke and its recurrence is difficult to study due to limited animal models available. The current objective was to establish an animal model of minor stroke using modifications of the photothrombosis method. Characterization of the severity of the modified photothrombotic ischemia was achieved using histological assessment, cerebral blood flow (CBF) measurement and magnetic resonance imaging (MRI).

Methods: For induction of an ischemic insult, Wistar rats (n=26) were injected with Rose Bengal (IV) to produce thrombosis within vessels under different conditions including varying the intensity of white light used for illumination, the duration of illumination and skull thickness. Cerebral blood flow was measured in the illuminated cortex using Laser Doppler flowmetry before and after illumination. At 24 hours after photothrombosis, MR scans in a subgroup animals (n=5) were acquired using a 9.4T Bruker MRI system. A set of 2 scans (10 slices, .7mm thick) were acquired consisting of a multi-echo spin-echo sequence (T2) and diffusion weighted images (5 b values) to obtain an ADC map. T2 and ADC were measured in regions of interest. Animals were perfused with fixative and brains were paraffin embedded and histological sections were stained with hematoxylin and eosin.

Results: Five minutes of illumination through a thinned skull produced a small stroke usually consisting of a wedge of infarction or pan-necrosis in the upper portion of cortex. Adjacent to it was a peri-infarct region with scattered cell death. Cerebral Blood Flow at the end of illumination was reduced to 50%±11% of baseline and this recovered to control levels (92%±11%) within 30-60 min. MRI measures within core and peri-infarct regions were different from contralateral (non-ischemic) cortex. ADC was reduced in the infarct core (68% $\pm$ 6% of the contralateral cortex; Students' t-test, $p < 0.01$) and to a lesser extent in the peri-infarct region (81% ± 6%; $p < 0.01$). Even greater changes were observed in T2 with increases in core to 232% ±30% of control ($p < 0.01$) and in the peri-infarct region to 139%±7% ($p < 0.01$). The T2 elevation in infarct core was greater than that in the peri-infarct region ($p < 0.01$).

Conclusion: Modifications of the photothrombosis method using Rose Bengal produced a small ischemic lesion with an infarct core and peri-infarct region of scattered cell death. This was associated with a transient decline of focal blood flow indicating a reperfusion in the illuminated area. The ischemic lesion had a decrease in ADC and increase in T2 that was greatest in the core and less marked in a region of selective cell death. These results support that the photothrombosis method can be modified to produce a minor stroke with a small infarct and a region of milder ischemic injury.

THE CORRIDOR TEST TO ASSESS SENSORIMOTOR NEGLECT FOLLOWING MIDDLE CEREBRAL ARTERY OCCLUSION

C.M. Diaz[1], R.C. Trueman[2], A.E. Rosser[1], S.B. Dunnett[1]

[1]Brain Repair Group, Cardiff University, Cardiff, [2]School of Biomedical Sciences, University of Nottingham, Nottingham, UK

Objectives: Stroke is a leading cause of death and disability in the developed world. Victims suffer an array of impairments such as motor, sensory and language deficits[1], and better therapeutics are urgently needed. To discriminate the various components of impairment, robust preclinical models and assays relevant to the human condition are required. MCAO-induced striatal damage in the rat offers a powerful animal model to assess behavioral and motor deficits following stroke and recovery after cell therapy[2]. However, robust tasks that are sensitive to discrete components of the impairment are required to test potential therapeutics. The corridor test provides a simple assessment of sensorimotor neglect that has been shown to be sensitive to deficits in rat models of Parkinson's[3] and Huntington's[4] diseases, but has not previously been used in stroke. In this study I report that MCAO lesioned animals exhibit a marked contralateral neglect on this task in comparison to sham animals.

Methods: Middle cerebral artery occlusion was performed on a cohort of 24 rats (17 lesions and 7 shams)[5]. Six weeks post-surgery, MCAO and sham animals underwent two consecutive days of corridor habituation followed by two consecutive days of corridor testing. The test involves placing the rat in an enclosed corridor (white Perspex 10cm wide x 100 cm long x 20cm high) lined with adjacent food wells on both sides[3]. The rat is free to move around and collect pellets from wells on

either side of the corridor. We record whether each well approached is to the left or right side of the rat's head and body axis, and compute the proportion of approaches to the contralateral side over the first 20 (ipsilateral + contralateral) approaches as the measure of side bias on each trial[3,4].

Results: Within one day of habituation, control rats rapidly approached and ate food pellets from both sides of the body, and on test days there was no indication of a preference for one side (see Fig). The rats with MCAO lesions were equally active in approaching and eating pellets from the food wells, but they exhibited a marked bias towards approaching wells on the ipsilateral side (under the control of the intact striatum, see Fig). Comparisons by Student's t-test confirmed that the asymmetry in the MCAO lesion group was significant (t_{22} = -2.80, p< 0.05).

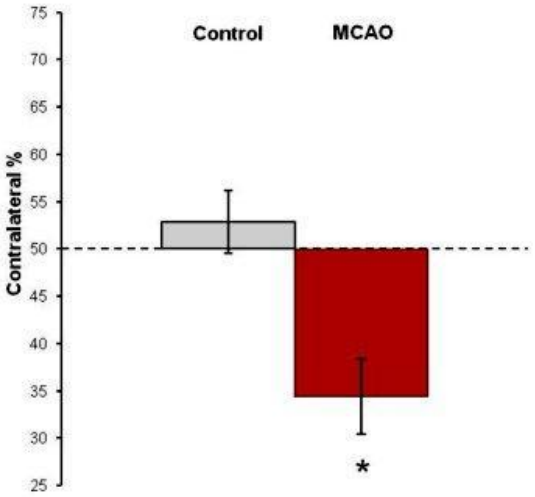

[Contralateral %]

Conclusions: Unilateral MCAO lesions induced a marked and significant sensorimotor neglect to the side contralateral to the lesion as assessed with the corridor test. These results corroborate the corridor test as a robust and sensitive method for assessing MCAO lesion deficits. This additional assay will assist in more effectively determining deficits in the MCAO model and refine the tools available for exploring and validating novel therapeutics.

References:

1. Hoffmann M, *et al*. J Stroke Cerebrovasc. 1997;6(3):114-120

2. Hossmann K-A. Cardiovasc Res. 1998;39(1):106-120

3. Dowd E, *et al*. Brain Res Bull. 2005;68(1-2):24-30

4. Döbrössy MD, *et al*. Behav Brain Res. 2007;179(2):326-330

5. Trueman RC, *et al*. Transl Stroke Res. 2011;2(4):651-661

INVESTIGATING THE TIME-COURSE OF MRI AND NEUROPATHOLOGICAL EFFECTS OF 45MIN MICROCLIP DISTAL MCA OCCLUSION (MD-TMCAO) IN THE SPONTANEOUSLY HYPERTENSIVE RAT

S. Ejaz[1], D.J. Williamson[2], T. Ahmed[1], S.J. Sawiak[2], J.-C. Baron[1,3]

[1]Department of Clinical Neurosciences, Stroke Research Group, [2]Wolfson Brain Imaging Centre, Department of Clinical Neurosciences, Addenbrooke's Hospital, University of Cambridge, Cambridge, UK, [3]INSERM U 894, Université Paris Descartes, Sorbonne Paris Cité, Paris, France

Background and objective: Selective neuronal loss (SNL) following reperfusion of the penumbra may hamper functional recovery and is attracting growing interest. Although brief proximal MCAo in rodents consistently results in predominantly striatal SNL[1], cortical SNL may have greater clinical relevance in the present era of thrombolysis. We previously reported that 45min md-MCAo in the spontaneously hypertensive rat (SHR) resulted in cortical SNL without pan-necrosis ('pure SNL') in 5/6 rats survived until day 14[2]. However, given previous reports suggesting possible delayed infarct maturation in SHRs[3,4], we aimed here to revisit the neuropathological sequelae in this model using various recovery durations.

Methods: 45min md-MCAo was performed in 16 anesthetized ~3-6-month old male SHRs according to our previously published procedures[2], followed by survival to days 14, 28 or 60 (n=3, 8 and 5 rats, respectively). Reperfusion was visually confirmed following clip removal and by MR angiography prior to brain collection. T2-weighted MRI was also

obtained on the same day. Immunohistochemistry included NeuN, OX42 and GFAP to appraise changes in neurons, microglia and astrocytes, respectively. Ischemic lesions were categorized as pan-necrosis, partial infarction or SNL[5].

Results: At day 14 post-MCAo, pure SNL was present in one rat and partial infarction in two (associated with SNL in both). T2w MR revealed typical hyperintense lesions in the latter two rats, but not in the former. At 28 days, pan-necrosis and/or partial infarction were present in 7 rats (consistently associated with some SNL) and pure SNL in one. T2w MR showed typical hyperintense lesions in all rats with pan-necrosis or partial infarction, but not in the rat with SNL. At 60 days, pan-necrosis was present in 5/5 rats (associated with bordering SNL in most) with typical hyperintense lesions on T2w. Microglial activation was conspicuous in all rats assessed on days 14 or 28, but faint or absent at day 60.

Conclusion: In this series of SHRs given 45min md-tMCAo, partial infarction was not observed beyond day 28, suggesting it is a temporary state en route to pan-necrosis. Regarding pure SNL, it was present in only 1/3, 1/8 and 0/5 rats killed at days 14, 28 and 60, respectively. Previously, we found pure SNL in 5/6, and pan-necrosis in 1/6 rats killed at day 14[2]. Thus, the 45min md-MCAo SHR model does not appear to consistently induce pure cortical SNL, and so is inadequate for this purpose, and shorter tMCAo durations need to be assessed (companion abstract, Ejaz et al). Further, the difference in outcome between the present and prior series[2] indicates major instability in outcome that may depend on slight differences in experimental protocol such as duration of early post-reperfusion anesthesia, which for logistical reasons was longer in the previous series. Finally, the lack of T2-weighted changes with pure SNL in this study is consistent with previous findings in striatal SNL[1].

References:

1. Sicard, Stroke, 2006, 37:2593;

2. Hughes, NeuroImage, 2010, 49:19;

3. Buchan A., 2001, in Delayed maturation of cortical infarction, p173;

4. Lehrmann, 1997, J Comp Neurol. 386**:**461;

5. Ejaz, Neurobiol. Dis., 2012 Nov 9.

A NOVEL RODENT MODEL OF PURE CORTICAL SELECTIVE NEURONAL LOSS FOLLOWING TEMPORARY MCA OCCLUSION (TMCAO): BEHAVIORAL, HISTOPATHOLOGICAL AND MRI CHARACTERIZATION

S. Ejaz[1], J. Emmrich[1], S.J. Sawiak[2], D.J. Williamson[2], J.-C. Baron[1,3]

[1]Department of Clinical Neurosciences, Stroke Research Group, University of Cambridge, UK, [2]Wolfson Brain Imaging Centre, Department of Clinical Neurosciences, Addenbrooke's Hospital, University of Cambridge, Cambridge, UK, [3]INSERM U 894, Université Paris Descartes, Sorbonne Paris Cité, Paris, France

Introduction and objectives: Selective neuronal loss (SNL) involving the rescued penumbra is attracting growing interest as an outcome of thrombolysed stroke. Although models of striatal SNL using proximal tMCAo are available[1], cortical damage may have greater clinical relevance given its enduring behavioral implications. In a companion abstract (Ejaz et al), we report that, as compared to longer occlusion times, 15min microclip distal tMCAo (md-tMCAo) in the spontaneously hypertensive rat (SHR) consistently induced pure cortical SNL on immunohistochemistry (IHC) at 28 days post-insult. Here we further characterized this model.

Methods: 15 min md-tMCAo was performed in 29 anesthetized male SHRs using published procedures[2]. Reperfusion was visually confirmed on clip removal and by MR angiography prior to brain collection. T2-weighted MR was also obtained on same day. In a first subset, 23 ~6-month old SHRs were allowed to survive for 7, 14, 28, 45 or 60 days (n=5, 5, 7, 3 and 3, respectively), and IHC appraised changes in neurons, microglia and astrocytes using NeuN, OX42 and GFAP, respectively. In another subset of six ~3-month old SHRs, behavior was assessed serially using both Garcia's Neuroscore and the modified sticky label test (mSLT) until sacrifice at day 28, and neurons and microglia were assessed using NeuN and Ib4 immunofluorescence, respectively. Ischemic lesions were categorized as pan-necrosis, partial infarction or SNL[3].

Results: Patchy SNL affected the MCA cortical territory to variable extent in 5/5, 5/5 and 7/7 subjects sacrificed at days 7, 14 and 28, respectively, with no instance of pan-necrosis or partial infarction. There were no pathological changes in rats survived to 45 or 60 days. Pure cortical SNL was present in 4/6 subset 2 animals. The Neuroscore was unchanged at any timepoint in any group, but the mSLT revealed significant bilateral effects ($p< 0.0001$), more pronounced contralaterally after day 7 ($p< 0.05$), with delayed recovery up to day 21. No T2w MRI changes were present in any subject of either subset.

Conclusion: The companion and present abstracts together confirm in a large sample that 15min md-tMCAo in the SHR is an appropriate model of pure cortical SNL, a pathology present in virtually all (21/23) rats killed before or at Day 28. Regarding later timepoints, the lack of tissue infarction tends to rule out 'delayed infarct maturation', while the lack of evident SNL suggests tissue remodelling such as dissipation of microglial activation and new neuron generation; formal cell counting is in progress. The lack of T2W changes is consistent with previous findings in striatal SNL[1]. While the unaffected Neuroscore is consistent with the absence of infarction, the mSLT disclosed subtle and long-lasting deficits matching the presence of neuronal damage. The bilateral effects are consistent with previously reported effects of cortical, as opposed to striatal, infarction[4]. These findings of long lasting, albeit mild, motor effects correlates of cortical SNL following very brief focal ischemia may have clinical relevance to TIAs.

References:

1. Sicard, Stroke, 2006, 37:2593;

2. Hughes, NeuroImage, 2010, 49:19;

3. Ejaz, Neurobiol. Dis., 2012 Nov 9;

4. Sharkey, Stroke, 1996, 27:2282.

DEVELOPMENT OF A MCA OCCLUSION RODENT MODEL OF PURE CORTICAL SELECTIVE NEURONAL LOSS: NEUROPATHOLOGICAL VALIDATION

S. Ejaz[1], D.J. Williamson[2], U. Jensen-Kondering[1], T. Ahmed[1], S.J. Sawiak[2], J.-C. Baron[1,3]

[1]Department of Clinical Neurosciences, Stroke Research Group, University of Cambridge, UK, [2]Wolfson Brain Imaging Centre, Department of Clinical Neurosciences, Addenbrooke's Hospital, University of Cambridge, Cambridge, UK, [3]INSERM U 894, Université Paris Descartes, Sorbonne Paris Cité, Paris, France

Introduction and objectives: Selective neuronal loss (SNL) in the reperfused penumbra may impact clinical recovery and is thus important to investigate. Although proximal MCAo models of pure/predominantly striatal SNL are available[1-3], cortical damage is particularly relevant given its behavioral implications and that thrombolysis mainly targets the cortex. Further, ^{11}C-flumazenil PET, the reference in vivo marker of SNL, is insensitive to striatal damage due to low receptor density relative to cortex[4]. We aimed to develop a rodent model of pure/predominantly cortical SNL using microclip distal temporary MCA occlusion (md-tMCAo) in the spontaneously hypertensive rat (SHR)[5].

Methods: md-tMCAo was performed in anesthetized ~6-month old male SHRs according to previously published protocols[6]. Given that 45min md-tMCAo resulted in pan-necrosis in 7/8 SHRs as assessed 28 days after reperfusion[4], three shorter MCAo durations were investigated here, namely 30, 22 and 15 mins (n=3, 3 and 7 rats, respectively). Reperfusion was visually confirmed following clip removal and by MR angiography just prior to brain collection at 28 ± 3 days. T2-weighted MRI was also obtained for characterization of ischemic lesions. Immunohistochemistry included NeuN, OX42, and GFAP to appraise changes in neurons, microglia and astrocytes, respectively. Ischemic lesions were categorized into three main types[4]: 1) pan-necrosis (tissue necrosis with absence of neurons, microglia and astrocytes; dissolved extracellular matrix; cavitations and tissue loss); 2) partial infarction (same as pan-necrosis but only mild volume

loss, relatively preserved extracellular matrix, no or few small cavitations, presence of dense activated microglia and elongated astrocytes); and 3) SNL (patchy loss of neurons with preserved tissue structure and presence of activated microglia and elongated astrocytes matching SNL).

Results: At post-mortem one 22min rat had an unusual MCA bifurcation and no tissue damage and was excluded post-hoc. Pan-necrosis and partial infarction were found in 3/3 and 2/2 of the 30min and 22min groups, respectively, but never in the 15min group. This distribution is statistically significant (Fisher $p < 0.001$). Pure SNL was present in 7/7 subjects of the 15min group. T2-MRI revealed characteristic hyperintense abnormalities in all rats with pan-necrosis or partial infarction, associated with marked or mild cortical thinning, respectively, whereas no change was observed in any 15min animal.

Conclusions: We found that in SHRs 15 min distal tMCAo consistently results in pure cortical SNL, whereas 22 and 30min tMCAo resulted in partial infarction and pan-necrosis, respectively. In a separate study, no infarcts were present in additional 15min rats survived up to day 60, ruling out delayed maturation. Our present results are consistent with earlier reports of mainly striatal SNL following proximal tMCAo[1-3], but apply here to cortical SNL. Cortical SNL was not associated with any abnormalities on T2-MRI, consistent with findings in striatal SNL[2]. Our model may prove of use to study the pathophysiology of cortical SNL and its prevention by appropriate interventions.

References:

1. Garcia, Stroke, 1997, 27:761-5;

2. Sicard, Stroke, 2006, 37: 2593-600;

3. Sicard, JCBFM, 2006, 26: 1451-62;

4. Ejaz, Neurobiol. Dis., 2012, Nov 9;

5. Buchan, Stroke, 1992, 23**:** 273-9;

6. Hughes, NeuroImage, 2012, 59: 2007-16.

DIRECT THETA BURST CORTICAL STIMULATION INDUCES LONG LASTING PLASTICITY-LIKE EFFECTS IN RAT

T.-H. Hsieh[1], C.-W. Peng[2], Y.-Z. Huang[3], A. Rotenberg[4], J.-J. Chen[5], J.-Y. Wang[6]

[1]Ph.D. Program for Neural Regenerative Medicine, Taipei Medical University, [2]Department of Physical Medicine and Rehabilitation, College of Medicine, Taipei Medical University, [3]Department of Neurology, Chang Gung Memorial Hospital and Chang Gung University College of Medicine, Taipei, Taiwan R.O.C., [4]Department of Neurology, Children's Hospital, Harvard Medical School, Boston, MA, USA, [5]Department of Biomedical Engineering, National Cheng Kung University, Tainan, [6]Graduate Institute of Medical Sciences, Taipei Medical University, Taipei, Taiwan R.O.C.

Objectives: Theta burst stimulation (TBS) protocols have been proposed as new repetitive transcranial magnetic stimulation (rTMS) paradigms for induction of motor cortical plasticity which might have therapeutic potential for neurological diseases [1]. However, TBS protocols in rodent models are still limited because the large size of the coil induces low spatial resolution in rodent´s brain [2]. To better understand the neural mechanism underlying varied TBS protocols and enable translational research in rodent disease models, we delivered direct electrical stimulation (DCS) to specific cortical area of anesthetized rats and examine the changes of long-term potentiation (LTP) or long-term depression (LTD)-like plasticity after TBS.

Methods: The rats were deeply anesthetized and equally assigned to sham control, intermittent and continuous TBS (iTBS and cTBS) group for testing immediate effect of TBS. The screw electrodes for DCS were implanted on the motor cortex of unilateral forelimb. The amplitude of motor evoked potentials (MEPs) reflecting LTP or LTD-like plasticity were measured from the brachioradialis muscle every 5 min until 30 min after the end of TBS.

Results: The amplitude of MEPs showed no obvious change at each measured time points in sham stimulation group. A clear reduction of amplitude of MEPs was found at each measured time points following cTBS when compared to shame TBS rats. A sustained

increase in amplitude of MEPs was found at 5 min following iTBS and remained enhanced for up to 30 min when iTBS was given.

Conclusions: We have developed a novel method of delivering TBS to produce consistent, rapid, and controllable electrophysiological changes in motor cortex. In particular, we have found that he LTP or LTD-like cortical plasticity can be modified in rat model after the specific TBS protocols. These results might have the clinical benefits for establishing the new therapeutic manipulation of brain plasticity.

References:

1. Huang YZ, Edwards MJ, Rounis E, Bhatia KP, Rothwell JC. Theta burst stimulation of the human motor cortex. Neuron 2005;45:201-206.

2. Lisanby SH, Luber B, Perera T, Sackeim HA. Transcranial magnetic stimulation: applications in basic neuroscience and neuropsychopharmacology. Int J Neuropsychopharmacol 2000;3:259-273.

INCREASED EXPRESSION OF SMALL HEAT SHOCK PROTEIN AB-CRYSTALLIN AFTER INTRACEREBRAL HEMORRHAGE IN ADULT RATS

K. Ke, L. Li

Affiliated Hospital of Nantong University, Nantong, China

αB-crystallin (αBC) not only acts as a molecular chaperone, but involves in many cellular activities, such as protection against stress and apoptosis. One attractive function of αBC is interfering transcriptional function of p53 and hampering subsequent induction of its pro-apoptotic target genes; besides, overexpression of it can induce neoplastic-like changes such as increased proliferation in vitro. Previous evidence has showed its anti-apoptotic and proliferation promoting effects in cancer cells, and indicated αBC might play a similar role in central nervous system (CNS) diseases. However, the distribution and function of αBC in CNS diseases are not fully investigated. To explore whether αBC participates in pathophysiology after intracerebral hemorrhage (ICH), we established an ICH model assessed by behavioral tests. Western blot and immunohistochemistry indicated a significant up-regulation of αBC around the hematoma. Immunofluorescent labeling showed αBC was strikingly increased in neurons and astrocytes compared with sham-operated group; and co-localization of αBC/PCNA and αBC/active-caspase-3 around the hematoma indicated αBC might involve in astrocytic proliferation and neuronal apoptosis. Additionally, the profiles of PCNA, p53, Bax and active-caspase-3 were parallel with that of αBC in a time-dependent manner. As shown above, we speculated αBC might exert an important function following ICH.

CONTRIBUTION OF ESTROGEN ALPHA AND BETA RECEPTORS IN NEUROPROTECTIVE EFFECTS OF ESTROGEN FOLLOWING TRAUMATIC BRAIN INJURY

M. Khaksari Haddad[1], S. Zahedi Asl[2], A. Siaposht Khachaki[3], N. Shahrokhi[1], S. Nourizade[4]

[1]Physiology Research Center, School of Medicine, Kerman University of Medical Sciences, Kerman, [2]Endocrine Research Center, Research Institute for Endocrine Sciences, Shaheed Beheshti University of Medical Sciences, Tehran, [3]Neuroscience Research Center, Kerman University of Medical Sciences, Kerman, [4]Nazlo, Oromie University of Medical Sciences, Oromie, Iran

Object: While there is evidence that the estradiol has neuroprotective effect after traumatic brain injury (TBI) in female rats, it is unclear which estrogen receptor (ER) subtype, ERα or ERβ, mediates this effect. We therefore examined the roles of the different ERs in this effect. Here we used the the ERα selective agonist PPT, and the ERβ selective agonist DPN alone and in combination in female rats, to investigate this question.

Methods: Before the Ovariectomized animals were injured using the TBI technique, they were randomly divided into 9 groups : Control ,Sham ,TBI ,Vehicle, E1 (physiological dose of 17-β estradiol) E2(pharmacological dose of 17-β estradiol) ,PPT , DPN, PPT+DPN. Levels of BBB disruption (5 h), water content (24 h) were evaluated after TBI induced by the Marmarou method. In groups receiving drugs or vehicle, treatment was administrated as a single dose intraperitonealy (i.p) 30 min after induction of brain trauma.

Results: Results showed that, brain edema or

brain water content after TBI was lower ($p< 0.001$) in the pharmacological dose of estrogen(E2), PPT, DPN, and PPT+DPN groups than vehicle group. After trauma Evans blue content or blood brain permeability (BBB) was significantly higher in TBI and vehicle groups ($p< 0.001$) than E2, PPT, DPN, and PPT+DPN. The inhibitory effects of PPT+DPN on brain water content, neurological scores, and Evans blue content were highest. Although both PPT and DPN increased neurological scores following TBI, but PPT appears to be more effective on increasing neurological scores.

Conclusion: Neuroprotective effects of estradiol on brain edema, BBB permeability, and neurological scores are mediated through both ERα and ER*β*. This may be suggesting therapeutic potential for the brain trauma of ER specific agonists.

DEPRESSION-LIKE BEHAVIOR IN A RAT MODEL OF CHRONIC CEREBRAL HYPOPERFUSION: FEASIBILITY AS AN ANIMAL MODEL FOR VASCULAR DEPRESSION

S.R. Lee[1], B.-R. Choi[1], S. Paul[2], J.-S. Han[2], **H.Y. Kim**[3]

[1]Neurology and Biological Sciences, [2]Biological Sciences, [3]Neurology, Konkuk University, Seoul, Republic of Korea

Background: Vascular depression is an emerging clinical hypothesis suggesting depression could be induced by chronic cerebrovascular injury. We investigated feasibility of rat model of chronic cerebral hypoperfusion as an animal model for vascular depression.

Methods: In Wistar rats, chronic cerebral hypoperfusion was modeled by permanent occlusion of bilateral common carotid arteries (BCCAo). Diverse behavioral tests were performed to characterize depression-like behaviors in this rat model of chronic cerebral hypoperfusion. Alteration of brain-derived neurotrophic factor (BDNF) expression or changes of hypothalamic-pituitary-adrenal (HPA) axis were evaluated. Results

More social withdrawal in the social interaction test ($p=0.038$), performed at the age of 12 month, and more sugar craving in the serial sucrose preference tests at the age of 6, 7, 8 month ($p=0.045$) were observed in BCCAo group, compared to sham group. Forced swimming test showed no difference between BCCAo and sham groups. In BCCAo group, blood levels of adrenocorticotropic hormone (ACTH) ($p=0.126$) and corticosterone ($p=0.034$), and protein level of receptors for glucocorticoid (GR) in the hippocampus were increased ($p=0.011$). BDNF expression in the hippocampus showed no difference.

Conclusion: Our experimental results support a clinical hypothesis that vascular depression could be induced by chronic cerebral hypoperfusion. Rat model of chronic cerebral hypoperfusion may be useful as an animal model for vascular depression.

ZEBRAFISH AS A NOVEL MODEL SYSTEM FOR STUDYING HYPOXIC-ISCHEMIC BRAIN DAMAGE

Y.V. Li, X. Yu

Biomedical Sciences, Ohio University, Athens, OH, USA

Objectives: Animal models provide an essential tool for understanding the complex cellular and molecular pathophysiology of stroke and for testing neuroprotective drugs in the pre-clinical setting. The objective is to test zebrafish as the novel models of global and focal ischemic stroke.

Methods: Manipulation of global hypoxic ischemia is easier yet more reliable on zebrafish than that on mammalians.

In aim 1: We built an air-proof chamber where nitrogen was applied to flush oxygen out with dissolved oxygen less than 0.6mg/L, proximate to complete hypoxia.

In aim 2: Zebrafish was tested as a photothrombotic model of ischemic stroke. After the hypoxic-ischemic treatment, mortality rate, brain injuries as well as behavioral recovery were measured and analyzed.

Results:

Aim 1: For global ischemic model, the zebrafish was placed in the hypoxia chamber, which is similar to the conditions in a complete global ischemic stroke. Zebrafish was hypoxia sensitive as erratic behaviors beginning were readily observed usually within 1 minute after being placed in the chamber, and was followed by loss of equilibriums in a few

minutes. The mean time from the start to the time when zebrafish was lying motionless on one side at the bottom of the chamber was 679.52 ± 90 seconds (mean ± SD, n =23), followed by transferring into a recovery beaker. Overall, 60.87% of subjects did not recover from hypoxia while 39% survived. Bilateral, moderate to complete TTC demarcation of the infarct brain damage was observed and there were a clear correlation between hypoxia time and brain damage.

Aim 2: For photothrombotic model, zebrafish was anesthetized by MS-222 (140 mg/ml) and intraperitoneally injected with Rose Bengal (50 mg/g), a commonly used in photothrombosis. The zebrafish was then placed in the upright posture. Cold light was placed right above the optic tectum (optic lobe) for 10-30 minutes. In the preliminary study, all zebrafish survived after the phtothrombosis, however, they experienced erratic movements including aberrant circling and rotating swimming. The zebrafish was observed for three days after the photothrombosis, and about 40% (n=15) dead during this observation period. The mortality rate was light exposure time-dependent. TTC stating confirmed that damaged brain area was in optical lobe.

Conclusions: Our studies indicate that zebrafish are susceptible to hypoxic attack and suggest that the models we present can be used as alternative models to evaluate hypoxia-induced brain damage. Besides its simplicity and susceptibility to ischemic brain damage, zebrafish offers several additional advantages for use as a model system: dissolved chemicals can be taken into its body through gills; no stress and tissue damage that are associated with rodent stroke models; a well studied set of genes and fully-sequenced genome; its behaviors (swimming) can be evaluated in three-dimensional analysis. The detail of these unique advantages will be further summarized in the conference.

References: Yu X, Li YV: Zebrafish as an alternative model for hypoxic-ischemic brain damage. *Int J Physiol Pathophysiol Pharmacol*. 2011;3:88-96. Yu X, Li YV: Neuroprotective effect of zinc chelators in a zebrafish model of hypoxic brain injury. *Zebrafish*. 2013; Accepted.

CURCUMIN REDUCES ABETA DEPOSITION IN THE APP/PS1 DOUBLE TRANSGENIC MOUSE THROUGH LXRB/RXRA/ABCA1 PATHWAY

X. Zhang[1], Z. Teng[2], C. Wang[2], J. Sun[2], **Y. Li**[1]

[1]Institute of Neuroscience, [2]Chongqing Medical University, Chongqing, China

Increased formation of the β-amyloid peptide (Aβ) plays an important role in the pathogenesis of Alzheimer's disease (AD). Aβ formationwere tightly related with high cholesterol level. The ATP-binding cassette transporter A1 (ABCA1) and high-density lipoprotein (HDL) promote cellular cholesterol mobilization. The gene expression of ABCA1 is regulated by liver X receptor/retinoid X receptor (LXR/RXR) ligands to mediate cholesterol efflux from cells. We fed the APP/PS1 double transgenic mouse for 6 months with different concentration of curcumin diet. Water maze test demonstrated that there was intellectual growth in those curcumin-diet mice. Colorimetric method was applied to detect the content of HDL in blood serum of transgenic mice, which showed markedly increased in high concentration of curcumin-diet mice. The expressive increase of ABCA1 and LXRβ/RXRα in the hippocampus of these mice had been proved by immunohistochemistry (SP) and western blot . We found that the passway's mRNA level had also obviously up-regulated via enhanced transcription with real-time PCR method. These data support the conclusions that curcumin can raise the expression of LXRβ/RXRα/ABCA1 passway and the content of HDL to lower the cholesterol level, resulting in decrease of amyloid deposition in the model of AD.

Acknowledgments: This work was supported by the National Natural Science Foundation of China (NSFC: 81271426, 30973154, 81100948).

CURCUMIN INDUCED MACROAUTOPHAGY EXPRESSION IN THE HIPPOCAMPUS OF THE APPSWE/PS1 DOUBLE TRANSGENIC MICE MODELS

X. Zhang[1], C. Wang[2], Z. Teng[2], J. Sun[2], **Y. Li**[1]

[1]Institute of Neuroscience, [2]Chongqing Medical University, Chongqing, China

Background: Autophagy is a degeneration process of eliminating the majority proteins with long half-life and organelles within the cells, and it is divided into microautophagy, macroautophagy and chaperone-mediated

autophagy. As well known that autophagy plays a key role in degradation of misfolded proteins and their aggregation, and its dysfunction or its transporting disorder is tightly related with the pathogenesis of Alzheimer's disease (AD). Curcumin is one kind of nature plant extraction, and has been reported to prevent and treatment with AD, but the mechanisms are not fully understood. The study aims to observe the effects of curcumin on the macroautophagy expression in the APPswe/PS1 double transgenic mice models and investigate the potential molecular mechanisms.

Methods: Thirty APPswe/PS1 double transgenic mice were enrolled in the study and randomly divided into three 3 groups: the control group (without curcumin), the low curcumin group (100ppm) and the high curcumin group (500ppm). All the mice were regularly fed with curcumin for six months. The Morris maze tests were carried out for detecting the effects of curcumin on the reference and spatial memory of the mice models. After sacrifice, the brains were immediately removed and fixed in the different fluids according to the request of the study. Immunohistochemistry (IHC) was for the expression of Abeta, immunofluorescence (IF) was for the expression of microtube associated protein-2 (MAP-2) and electron microscope was for autophagy vacuoles expression. The effects of curcumin on the expressions of PI3K, Akt (total Akt and p-Akt), mTOR (total mTOR and p-mTOR), LC3 and Beclin were detected with real-time PCR and Western blot.

Results: In the study, the Morris Maze test showed that in the AD mice models, curcumin could improve the impaired reference and spatial memory. Electron microscope results showed that after curcumin treatment the autophagy vacuoles were increased. IHC showed curcumin decreased the aggregation of Abeta, IF showed curcumin increased the expression of MAP-2. Real-time PCR and Western blot results showed curcumin induced the expression of LC3 and Beclin, and decreased the activity of PI3K/Akt and mTOR. Furthermore, all the changes were in a concentration-dependent manner.

Conclusion: Curcumin increases the expression of macroautophagy through inhibiting the activity of PI3K/Akt/mTOR pathway, and induces the autophagy axonal transport and promotes the clearance of autophagy and Abeta. Taken together, all the results provide a new target for AD treated with curcumin.

Acknowledgments: This work was supported by the National Natural Science Foundation of China (NSFC: 81271426, 30973154, 81100948).

THE INFLUENCE OF SYSTEMATIC HYPERTENSION ON GROWTH AND RUPTURE OF CEREBRAL ANEURYSM

J. Cai[1], T. Han[2], C. He[2], Y.-H. Bai[2], S.-P. Huang[1], Y. Huang[3], **F. Ling**[2]

[1]Department of Neurosurgery, Guangdong Provincial Hospital of Traditional Chinese Medicine, Hospital at Guangzhou Higher Education Mega Center, Guangzhou, [2]Department of Neurosurgery, Xuanwu Hospital, Capital Medical University, Beijing, [3]Department of Neurology, Guangdong Provincial Hospital of Traditional Chinese Medicine, Guangzhou, China

Systematic hypertension is widely deemed an independent risk factor for growth and rupture of cerebral aneurysms. In this study, we used a recently developed cerebral aneurysm (CA) model of rats to evaluate the influence of secondary hypertension on growth and rupture of experimental cerebral aneurysm. CA models were induced by ligation of the unilateral common carotid artery and the contralateral pterygopalatine and external carotid arteries. Some models were ligatured the bilateral posterior branches of renal arteries to produce secondary hypertension. One, two and three months after induction, the morphological changes in Willis Circle of animal models with or without hypertension were examined *in vivo* and *in vitro*. The incidence of CA in models with or without hypertension were similar, however, five rats of hypertension group died from CA rupture. According to the findings, we concluded systematic hypertension would rapid the growth and rupture of experimental CA.

UTILITIES AND CHALLENGES OF DIFFERENT MOUSE CEREBRAL ISCHEMIA MODELS

C. Liu[1], T. Kristian[2], B. Hu[2]

[1]Center for Shock, Trauma and Anesthesiology Research, University of Maryland, [2]Center for Shock, Trauma and Anesthesiology Research, Baltimore, MD, USA

Objectives: The availability of genetically engineered mice allows examination of the role of specific proteins in brain pathology processes. However, relative to rat models, mouse global brain ischemia models are technically more challenging to produce. This study is to present two effective mouse ischemic models.

Methods: Several methods were developed to achieve sufficient reduction of blood flow in the mouse brain that led to consistent ischemic brain damage.

Results: Occlusion of two carotid arteries only is inefficient to produce consistent brain damage in mice. More effective approaches are the bilateral common carotid occlusion that is combined with different approaches of reduction of mean arterial blood pressure. Furthermore a four-vessel occlusion model can be used or even a cardiac arrest model that has been developed for mouse.

Conclusions: All these models have specific problems, advantages, and clinical relevance. Thus the feasibility of using a particular model depends on the goal of the study and the outcome parameters assessed. Overall, the mouse models are valuable since they allow the study of ischemia-induced molecular mechanisms utilizing transgenic animals and also evaluate the effect of new neuroprotective compounds. This study is supported by NS040407 and NS03136 (BRH).

ANESTHETIC-DRUG INTERACTIONS IN RODENT PHARMACOLOGICAL MAGNETIC RESONANCE IMAGING OF THE SEROTONIN SYSTEM

C. Martin[1], **A. Spain**[1], A. Khrapichev[2], N.R. Sibson[2]

[1]Department of Psychology, University of Sheffield, Sheffield, [2]Department of Oncology, Oxford University, Oxford, UK

Objectives: Pharmacological magnetic resonance imaging (phMRI) studies map changes in brain function associated with the actions of administered pharmacological agents. However, the use of anesthetic agents in animal studies is problematic because anesthetics are themselves a pharmacological modulator of neuronal function, with actions that are more often complex and less well understood than those of the agent under investigation. The objective of this study was to determine the influence of choice of anesthetic agent upon the results of a pharmacological challenge of the serotonergic system. We report a comparison of blood oxygen level dependent (BOLD) phMRI signal changes in response to administration of the serotonin releasing agent fenfluramine under four different anesthetic regimes (halothane, isoflurane, urethane and alpha-chloralose).

Methods: Animals (n=5 per group) were anesthetized, tracheotomized for artificial ventilation and cannulated for administration of drugs and monitoring of physiological parameters. Imaging was performed on a 7-Tesla horizontal bore magnet. Anatomical scans to cover the whole brain were acquired using a T2-weighted fast spin-echo sequence (field of view 30X30mm, matrix size 128X128, slice thickness 0.5mm). Functional data were acquired using T2*-weighted multi-echo gradient-echo sequences (effective TE 12ms, field of view 30 X 30 mm, matrix size 128 X 64, slice thickness 0.5mm). Fenfluramine (10mg/Kg, in saline and administered in a volume of 1ml/Kg) was injected intravenously after 15 minutes of baseline data acquisition. Data processing was carried out using FEAT (FMRI Expert Analysis Tool) Version 5.92, part of FSL (FMRIB´s Software Library). Z statistic images were thresholded using clusters determined by Z>2.3 and a (corrected) cluster significance threshold of P=0.05.

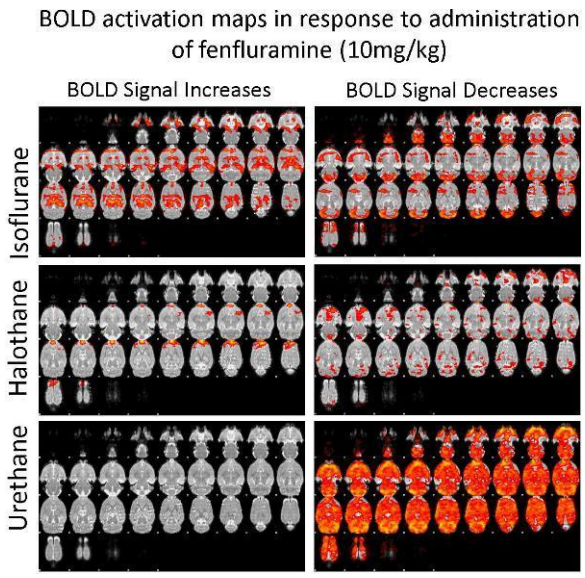

[Figure 1]

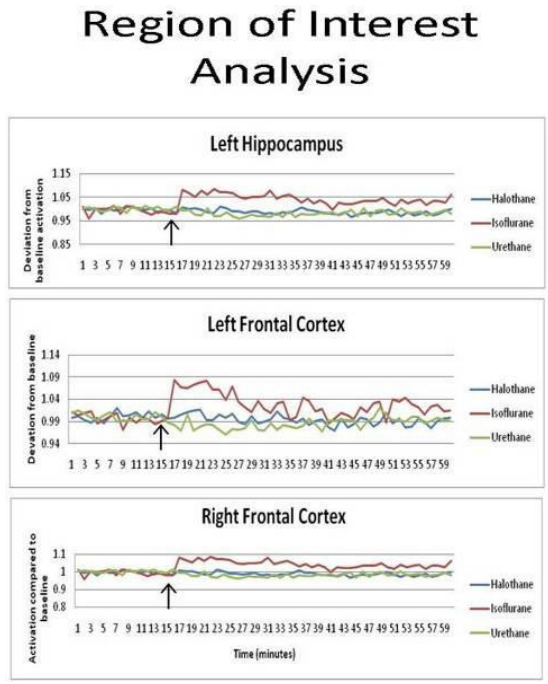

[Figure 2]

Results: Choice of anesthetic agent had pronounced effects on the fenfluramine phMRI activation maps (Figure 1) and time-series data extracted from structures of interest (Figure 2), including alterations in both the magnitude and directionality of blood oxygen level dependent signals. Overall, isoflurane and halothane anesthetic regimes resulted in similar patterns of activation, although the BOLD contrast to noise ratio was higher in the isoflurane condition. Urethane anesthesia resulted in widespread negative BOLD signal changes in response to fenfluramine administration.

Conclusions: These data demonstrate that the use of anesthesia per se, and the use of different anesthetic regimes in different laboratories, are major concerns for phMRI (and potentially fMRI) studies involving the serotonergic system in animal models. Ongoing research will extend these findings to include electrophysiological measures of fenfluramine induced changes in neuronal activity under different anesthetic regimes in order to determine the effects of anesthetic choice on neurovascular coupling and therefore our ability to interpret BOLD phMRI signal changes in terms of neuronal activity. Finally, we hypothesize that substantial neuroimaging anesthetic-drug interactions will occur in the context of other neurotransmitter systems and suggest that further research is needed to establish the validity of preclinical pharmacological neuroimaging research studies.

EFFECT OF ARGATROBAN ON LASER-INDUCED THROMBUS FORMATION IN MURINE BRAIN MICROVASCULATURE OBSERVED ON INTRAVITAL FLUORESCENCE MICROSCOPY

H. Maruyama, T. Fukuoka, T. Hayashi, Y. Nagamine, H. Sano, M. Hirayama, N. Tanahashi

Department of Neurology and Cerebrovascular Medicine, Saitama Medical University International Medical Center, Hidaka, Japan

Objective: Using a laser, we developed a technique to instantaneously induce thrombus formation in murine brain microvasculature. The purpose of this study was to observe the effect of argatroban (direct thrombin inhibitor) on the process of laser-induced thrombus formation and platelet behavior in the brain microvasculature of mice using intravital fluorescence microscopy.

Methods: C57BL/6J mice (n=15) were anesthetized with chloral hydrate. Eight mice were given continuously argatroban (0.3 mg/h/mouse) injected into femoral vein during the experiment (argatroban group). Seven mice served as controls (control group). Their head was fixed with a head holder, and a

cranial window was prepared in the parietal region. Platelets were labeled in vivo by intravenous administration of carboxylfluorescein succinimidylester (CFSE). Laser irradiation (1000 mA, DPSS laser 532 nm, TS-KL/S2; Sankei) was spotted for 4 seconds on pial arteries to induce thrombus formation. Labeled platelets and thrombus were observed continuously with a fluorescence microscope.

Results: After laser irradiation to the pial artery, the complete occlusion rate was significantly lower in the argatroban group (20%, 4/20 vessels, vessel diameter 26.2 ± 5.1μm) than in the control group (60%, 12/20 vessels, vessel diameter 28.3 ± 5.4μm). Thirty minutes after laser irradiation, the area of platelet thrombus was significantly smaller in the argatroban group (153 ± 94mm^2) than in the control group (358 ± 256mm^2).

Conclusion: Argatroban significantly inhibited laser-induced thrombus formation in mice pial arteries.

ACUTE HYDROCEPHALUS IN A RAT MODEL OF SUBARACHNOID HEMORRHAGE

S. Okubo[1,2], Y. Hua[1], N. Kawai[2], T. Tamiya[2], R.F. Keep[1], G. Xi[1]

[1]Neurosurgery, University of Michigan, Ann Arbor, MI, USA, [2]Neurosurgery, Kagawa University, Faculty of Medicine, Miki, Japan

Objectives: Acute hydrocephalus is a common complication of aneurysmal subarachnoid hemorrhage (SAH). Hydrocephalus can result in increased intracranial pressure that may lead to decreased cerebral blood flow and clinical deterioration. Here we report a rat model of acute hydrocephalus after SAH induced by endovascular perforation.

Methods: SAH was induced by endovascular perforation in adult male Sprague-Dawley rats (n=36). Sham rats (n=8) underwent the same procedure without perforation (1). MRI was performed 24 hours after SAH and the volume of the ventricular system and extent of T2* hypointensity lesions were measured (2). We defined hydrocephalus as ventricular volume greater than +3 standard deviations above the mean in sham animals. SAH grade was determined and brains were used for histology, immunohistochemistry, Perls' staining and Western blot analysis. Ventricular wall damage was defined as percentage of ependymal surface disruption.

Results: Endovascular perforation induced SAH in all survived cases (n=27) and results in ventricular enlargement at 24 hours (33.6±4.7 mm^3) compared with sham controls (13.5±1.4 mm^3, n=8, $p< 0.01$). The ventricular volume in SAH animals correlated with SAH grade ($r=0.48$, $p< 0.05$). Hydrocephalus was defined as ventricular volume greater than +3SD above the mean in sham animals and was present in 44% (12/27) of SAH animals. All animals with hydrocephalus (n=12) had intra-ventricular hemorrhage confirmed by MRI and histology. Rats with hydrocephalus had larger T2* hypointensity volume (4.9±1.8 mm^3, n=12) than the sham animals (0.6±0.1 mm^3, n=8, $p< 0.05$) and SAH animals without hydrocephalus (1.3±0.2 mm^3, n=15, $p< 0.05$). The percentage of ventricular wall damage was greater in SAH animals with hydrocephalus (7.4±1.2%, n=8) compared to those without hydrocephalus (1.1±0.2%, n=11, $p< 0.01$) and sham controls (0.6±0.2%, n=5, $p< 0.01$). Using Perls' staining, iron-positive cells were found in ependyma and subependyma of hydrocephalic SAH rats. Periventricular heme-oxygenase-1 (HO-1) and Iba-1 (a marker of microglia and macrophages) immunoreactivity was observed in hydrocephalic SAH animals. By Western blotting, HO-1 levels were increased in rats with hydrocephalus (4526±312 pixels) compared to sham controls (1370±191 pixels in the sham animals, n=3-4, $p< 0.01$). In addition, Iba-1 levels were increased in rats with hydrocephalus (4119±384 pixels) compared to sham controls (1911±348 pixels, $p< 0.05$) and those without hydrocephalus (1889±307 pixels, n=3-4, $p< 0.05$).

Conclusions: SAH causes ventricular enlargement in a rat endovascular perforation model, with hydrocephalus occurring in 44% of animals at 24 hours. Rats with hydrocephalus had more severe SAH, intraventricular hemorrhage and greater ventricular wall damage.

References:

1. Lee JY, Keep RF, He Y, Sagher O, Hua Y, Xi G. Hemoglobin and iron handling in brain after subarachnoid hemorrhage and the effect of deferoxamine on early brain injury. J Cereb Blood Flow Metab. 2010;30:1793-1803

2. Chen Z, Gao C, Hua Y, Keep RF, Muraszko K, Xi G. Role of iron in brain injury after

intraventricular hemorrhage. Stroke. 2011;42:465-470

deficiency of p62. Hence, p62 exerts neuroprotection against tau pathologies by eliminating nonfibrillar phospho-tau species primarily through selective autophagy and by sequestering other ubiquitinated components into aggresomes.

PIVOTAL ROLES OF P62 AND SELECTIVE AUTOPHAGY IN TAU DEPOSITION AND CONSEQUENT NEURODEGENERATION REVEALED WITH TAUOPATHY MOUSE MODELS

M. Ono[1], B. Ji[1], M. Tokunaga[1], M. Komatsu[2], T. Ishii[3], T. Suhara[1], M. Higuchi[1]

[1]Molecular Imaging Center, National Institute of Radiological Science, Chiba, [2]Protein Metabolism Project, Tokyo Metropolitan Institute of Medical Science, Tokyo, [3]Graduate School of Comprehensive Human Sciences, University of Tsukuba, Ibaraki, Japan

Here, we provide the first evidence that p62, ubiquitinated cargo receptor for selective autophagy, acts protectively against neuron death provoked by tau accumulation. In mice transgenic for P301S mutant human tau protein (P301S mice), autophagic activity in the hippocampus was higher than that in the brainstem, but this regional difference became unremarkable with aging, suggesting tau-induced impairment of autophagic processing in the hippocampus of old P301S mice. This could be associated with prominent neuronal loss observed in the hippocampus but not brainstem of old P301S mice. Genetic inactivation of p62 alone did not induce tau pathologies in mice, but P301S mice deficient in p62 (P301S/p62-KO mice) exhibited accelerated accumulation of soluble, phosphorylated tau as compared to P301S mice. Meanwhile, tau kinases (GSK-3β and Cdk5) remained unchanged, indicating that p62 serves autophagic clearance of pathologically phosphorylated tau. *In vivo* MRI demonstrated enhanced hippocampal atrophy in P301S/p62-KO mice relative to P301S mice. P301S mice progressively developed hippocampal aggresomes containing p62, ubiquitin and organelles but not phosphorylated tau. Notably, formation of these aggresomes was dramatically abolished in P301S/p62-KO mice, supporting the notion that p62-mediated packaging of ubiquitinated substrates such as damaged organelles and misfolded proteins except phosphor-tau into aggresomes is critical for neuronal survival. Finally, abundance of neurofibrillary tangles in P301S mice was not markedly altered by the

AMINO ACID TRACERS AS RELIABLE IMAGING BIOMARKER TO MONITOR TREATMENT RESPONSE OF GLIOBLASTOMAS TO TEMOZOLOMIDE THERAPY WITH INTERFERON-B AND BEVACIZUMAB

T. Ono[1], T. Sasajima[1], Y. Doi[2], S. Oka[2], M. Ono[2], M. Kanagawa[2], A. Baden[2], K. Mizoi[1]

[1]Department of Neurosurgery, Akita University Graduate School of Medicine, Akita, [2]Research Centre, Nihon Medi-Physics Co., Ltd, Chiba, Japan

Introduction: The aim of this study was to explore whether amino acid PET tracers (*trans*-1-amino-3-^{18}F-fluorocyclobutanecarboxylic acid (*anti*-^{18}F-FACBC), ^{11}C-methyl-L-mehionine (^{11}C-Met) are suitable to elucidate early response to temozolomide (TMZ) therapy with interferon-β (IFN) and bevacizumab (BV) in glioblastomas. We simultaneously analyzed uptake of the amino acid tracers (*anti*-^{14}C-FACBC and ^{3}H-Met, theoretically identical to *anti*-^{18}F-FACBC and ^{11}C-Met except for isotopes, respectively) in glioblastomas before and after treatment with single-agent (TMZ, BV) and combination therapy (TMZ/IFN, TMZ/BV, TMZ/IFN/BV) in vitro and in vivo.

Methods: In vitro experiments: Human glioblastoma U87MG (U87) was incubated with low dose TMZ to induce chemoresistance. MTT assay demonstrated a significant increase of surviving fraction in TMZ-resistant subline (U87R) compared to those of drug-naive cells (U87). Both *anti*-^{14}C-FACBC and ^{3}H-Met uptake were quantified using triple-label accumulation assay (*anti*-^{14}C-FACBC, ^{3}H-Met, ^{99m}Tc-DTPA) in U87 and U87R. Uptake values of tracers, which were corrected for extracellular fluid and damaged cells using ^{99m}Tc-DTPA, were quantified. Both *anti*-^{14}C-FACBC and ^{3}H-Met uptake profiles were fitted to a 2 compartment model and parameter for volume distribution (Vd) was determined. And the steady state accumulation rate of ^{3}H-thymidine (TdR) was calculated from the slope of the accumulation vs. time plot.

In vivo experiments: U87 and U87R cells were inoculated in the right- and left- basal ganglia of F344/N-rnu rats, respectively. We analyzed the efficacy of treatment with single-agent (TMZ, BV) and combination therapy (TMZ/IFN, TMZ/BV, TMZ/IFN/BV) in the orthotopic gliomas using MR imaging (T2-weighted image, Gd-postcontrast T1-weighted image), double-labeled autoradiographic images of *anti*-^{14}C-FACBC and ^{3}H-Met, and MIB-1 index, as a tumor proliferation marker, for preclinical research.

Results: In vitro experiments: ^{3}H-TdR accumulation rate and Vd for *anti*-^{14}C-FACBC and ^{3}H-Met of U87 significantly decreased after administration of TMZ alone, whereas those of U87R remained unchanged. Although treatment with a combination of TMZ and IFN significantly decreased the tracer accumulation of U87R as much as U87, no additional effect of BV was noted.

In vivo experiments: Inoculated U87R was shown as equivocal tumor without contrast enhancement on MR imaging, and both T2-high intensity lesions and enhancing lesions of U87 markedly decreased in size after treatment with BV alone and the combination therapy (TMZ/BV, TMZ/IFN/BV). In contrast, autoradiographic images using *anti*-^{14}C-FACBC and ^{3}H-Met clearly delineated tumor extension, which spread widely beyond T2-high intensity lesions and enhancing lesions on MR imaging. Treatment with TMZ alone significantly decreased amino acid tracer accumulation and proliferation of U87, whereas those of U87R remained unchanged. Treatment with a combination of TMZ and IFN significantly decreased the tracer accumulation and proliferation of U87R as much as U87, and in a combination with BV, those of both tumors decreased even further. *Anti*-^{14}C-FACBC and ^{3}H-Met uptake significantly related to MIB-1 index of the inoculated tumors. Contrarily, MR imaging was unsuitable for tumor delineation and assessment of treatment response after the antiangiogenic therapy using BV.

Conclusions: TMZ therapy with IFN and BV was effective to even TMZ-resistant glioblastoma. PET using amino acid tracers must provide important information on the early response of glioblastomas to the triple-agent combination therapy.

NEUROCHEMICAL SIGNALLING AND PARTICIPATION OF PAX6 IN FISHES POSTEMBRYONAL NEUROGENESIS

E.V. Pushchina[1], M.E. Stukanyova[2], D.K. Obukhov[3], A.A. Varaksin[1]

[1]Lab. Cytophysiology, A.V. Zirmunskii Institute of Marine Biology Far Eastern Branch of Russian Academy of Sciences, [2]School of Natural Sciences, Far Eastern Federal University, Vladivostok, [3]Department Cytology and Histology, Saint Petersburg State University, Saint Petersburg, Russia

The fishes brain has unique peculiarity among a vertebrates. It grows with organism during all their life. Thereby, the fishes are an attractive animal model for investigation of the embryonal and postembryonal central nervous system development and participation in this processes some neurochemical agents.

Pacific salmons *Oncorhynchus masou*, sturgeons *Acipencer schrenckii* and carps *Cyprinus carpio* were the objects of our investigation. The aim of our investigation is to explore the participation of some neurotransmitters (dopamine, GABA), gasotransmitters (NO and H_2S) and transcription factor Pax6 in the processes of postembryonal neurogenesis in fish.

In this work, we used methods of immunohistochemical labeling tyrosine hydroxylase, GABA, neuronal NOS, cystathionine β-synthase, transcription factor Pax6, proliferative nuclear antigen. The area, which contained apoptosis have been diagnosed by TUNEL - labeling.

Results of our research was established:

1. The population of undifferentiated cells, which producing a TH, NOS, Pax6 on the territory of matrix areas, which contained proliferative PCNA-ir cells in the brain of young *O. masou* 3-, 6- months and 1 year old was founded.

2. The expression of Pax6 in integrative brain centers (tectum and cerebellum) of *O. masou* in areas with cell migration and differentiation in 3, 6 months and 1 year. Diencephalic migration zone and neural migration zone containing Pax6-ir cells migrate into the largest sensory nuclei of diencephalon - pretectal and preglomerular nuclei and in territory of rhombencephalic medial reticular formation.

3. Existence of zones of proliferation and apoptosis in the brain of 3-year-old sturgeon.

The expression of neuronal NOS in sensory brain nuclei (V, VII,X), which contained proliferative PCNA-ir cells and TUNEL-labeled elements.

4. The expression of Pax6 in areas of proliferation, differentiation and migration in the brain integrative centers of adult carp. Colocolization of Pax6, TH and CBS in the matrix zone of the brainstem, cerebellum and of *lobus vagi*.

From the evidence presented it seems likely that in periventricular proliferative zones identified expression tyrosine hydroxylase, GABA, NO and H_2S, participating in the regulation of the basic histogenetic processes as morphogenetic factors, carrying out paracrinic and autocrinic regulation of cells-predecessors proliferation, migration of differentiating neurons and the expression of specific genes and synthesis.

A second conclusion that can be derived from the present investigation is that patterns of distribution tyrosine hydroxylase, GABA, Pax6, PCNA-expressing periventricular cellular zones in different periods of the post-embryonic ontogenesis mark neuromeric brain structure of salmon. The expression of transcription factor Pax6 determines the processes of regionalisation brain, not only in early post-embryonic (3 and 6 months), but in the later (1-3 years) periods.

In sensory and motor centers of the brain 3-year-old sturgeon is still a high level of proliferation and apoptosis, indicating the *neotenic* status of these structures. In the sensory centers: tectum and projections of nuclei V, VII and X of the nerves set different ratio between the levels of proliferation and apoptosis, showing the different rates of growth and differentiation of visual and chemosensory centers in sturgeons brain.

Supported by: Grant Far Eastern Branch Russian Academy of Science 12-III-A-06-095

DIAGNOSTIC SIGNIFICANCE OF NEWLY SYNTHESIZED AMINO ACID ANALOG *TRANS*-1- AMINO-3-FLUOROCYCLOBUTANECARBOXYLIC ACID (*ANTI*-FACBC) IN GLIOMAS

T. Sasajima[1], T. Ono[1], N. Shimada[1], Y. Doi[2], S. Oka[2], M. Kanagawa[2], A. Baden[2], K. Mizoi[1]

[1]Department of Neurosurgery, Akita University Graduate School of Medicine, Akita,
[2]Research Center, Nihon Medi-Physics Co., Ltd., Chiba, Japan

Introduction: Amino acid PET tracers have been promise for visualizing gliomas and evaluating early therapeutic effects of antitumor drugs in gliomas. To compare the diagnostic performance of *trans*-1-amino-3-^{18}F-fluorocyclobutanecarboxylic acid (*anti*-^{18}F-FACBC) with that of ^{11}C-methyl-L-mehionine (^{11}C-Met) in detection and early therapeutic response, we have used *trans*-1-amino-3-fluoro-1-^{14}C-cyclobutane carboxylic acid (*anti*-^{14}C-FACBC) and ^{3}H-methyl-L-methionine (^{3}H-Met), theoretically identical to *anti*-^{18}F-FACBC and ^{11}C-Met except for isotopes, respectively. We simultaneously analyzed uptake of the amino acid tracers in rat gliomas treated with and without temozolomide (TMZ) in vitro and in vivo.

Methods: In vitro experiments: C6 rat glioma was incubated with low dose TMZ to induce chemoresistance. MTT assay demonstrated a significant increase of surviving fraction in TMZ-resistant subline (C6R) compared to those of drug-naive cells (C6). Both *anti*-^{14}C-FACBC and ^{3}H-Met uptake were quantified using triple-label accumulation assay[1)] (*anti*-^{14}C-FACBC, ^{3}H-Met, ^{99m}Tc-DTPA) to examine relationship between amino acid tracer uptake and proliferation in C6 and C6R. Uptake values of tracers, which were corrected for extracellular fluid and damaged cells using ^{99m}Tc-DTPA, were quantified as corrected cell-to-medium concentration ratio. *Anti*-^{14}C-FACBC and ^{3}H-Met uptake profiles were fitted to a 2 compartment model and parameter for volume distribution (Vd) was determined. And the steady state accumulation rate of ^{3}H-thymidine (TdR) was calculated from the slope of the accumulation vs. time plot when the plot was linear.

In vivo experiments: C6 and C6R cells were inoculated in the right- and left- basal ganglia of rats, respectively. We analyzed the efficacy

of TMZ in the orthotopic glioma model using MR imaging (T2-weighted image, Gd-postcontrast T1-weighted image), autoradiographic images of *anti*-^{14}C-FACBC and ^{3}H-Met, and MIB-5 index, as a tumor proliferation marker, for preclinical research. Double-labeled autoradiographic technique using *anti*-^{14}C-FACBC and ^{3}H-Met was performed according to the modifications of previously reported methods[2)].

Results: In vitro experiments: ^{3}H-TdR accumulation rate and amino acid tracer uptake (Vd for *anti*-^{14}C-FACBC and ^{3}H-Met) by C6 significantly decreased 48 and 72 hours, respectively, after TMZ treatment, whereas those of C6R remained unchanged. Vd of *anti*-^{14}C-FACBC significantly correlated with Vd of ^{3}H-Met and ^{3}H-TdR accumulation rate.

In vivo experiments: In the intracerebral glioma model, autoradiographic images using *anti*-^{14}C-FACBC and ^{3}H-Met clearly delineated tumor extension, which spread widely beyond T2-high intensity lesions and enhancing lesions on MR imaging. Oral administration of TMZ significantly decreased *anti*-^{14}C-FACBC and ^{3}H-Met uptake and MIB-5 index of C6, whereas those of C6R remained unchanged. MIB-5 index of the inoculated tumors significantly related to *anti*-^{14}C-FACBC and ^{3}H-Met uptake. We revealed that TMZ inhibited amino acid tracer uptake and tumor proliferation earlier than morphological changes on MR imaging.

Conclusions: *Anti*-^{14}C-FACBC, as well as ^{3}H-Met, was more sensitive than postcontrast T1-wighted images on MR imaging in the detection of tumor extension and early tumor response for TMZ treatment. *Anti*-^{18}F-FACBC is believed to be a useful imaging biomarker not only for visualization of tumor extension but also for assessing effects of therapeutic agents in human gliomas.

References:

1) Sasajima T, et al (2004) Eur J Nucl Med Mol Imaging 31:1244-1256.

2) Sasajima T, et al (1997) J Neurooncol 34:123-129.

NEW MODEL OF MEDULLOBLASTOMA IN THE RAT TO DETERMINE THE ROLE OF TRANSIENT RECEPTOR POTENTIAL CHANNELS IN TUMOUR MICROENVIRONMENT

S. Serres[1], M. Glitsch[2], B. Claire[1], N.R. Sibson[1]

[1]Gray Institute for Radiation Oncology & Biology, Department of Oncology,
[2]Department of Physiology, Anatomy and Genetics, University of Oxford, Oxford, UK

Objectives: Recent work suggests that extracellular acidosis may contribute to tumour progression in medulloblastoma, through changes in intracellular Ca^{2+} signalling[1]. To establish whether the transient receptor potential channel (TRP), which mediates Ca^{2+} signalling, is important in modulating the tumour microenvironment in medulloblastoma, we have developed and characterized a new in vivo model using in vivo magnetic resonance imaging (MRI) and immunohistochemistry.

Methods: Nude rats were injected intracerebrally with human DAOY cells, a desmoplastic medulloblastoma cell, in the cerebellum. Animals underwent multimodal MRI at intervals over 12 weeks. T_2-weighted images were acquired to follow macroscopic structural changes, magnetization transfer ratio (MTR) maps generated to assess changes in the macromolecular pool, and post-gadolinium T_1-weighted images used to assess blood-brain barrier (BBB) integrity. Immunohistochemistry was performed at selected time-points to detect tumours, astrocyte and microglial activation, neuronal death and TRP expression.

Results: MRI revealed BBB breakdown (gadolinium enhancement), associated oedema accumulation (T_2 hyperintensity) and reduced MTR at the site of tumour cell injection by 5 weeks after induction. Clinical symptoms, such as hindlimb paralysis, were not evident until 10 weeks after induction. Immunohistochemistry of cerebellar sections showed medulloblastoma-like tumour structure and human vimentin staining confirmed the exogenous origin of the tumour cells. Medulloblastoma development induced astrocyte and microglial activation around the tumour and severe neuronal damage within

the tumour. Strong TRP expression was also found within the tumour.

Conclusions: We have developed a new model of medulloblastoma that will facilitate investigation of the role of the TRP in the tumour microenvironment. Histological correlation between the literature and our model supports this as a valid model of desmoplastic cerebellar medulloblastoma[2]. Multimodal MRI revealed longitudinal changes in the tumour environment, and may provide non-invasive biomarkers for tumour progression.

References:

1. Huang, W.C., et al., *Extracellular acidification elicits spatially and temporally distinct Ca2+ signals.* Curr Biol, 2008. **18**(10): p. 781-5.

2. Gilbertson, R.J. and D.W. Ellison, *The origins of medulloblastoma subtypes.* Annu Rev Pathol, 2008. **3**: p. 341-65.

A MODEL OF RAT EMBOLIC INTERNAL CAROTID ARTERY OCCLUSION WITH A QUANTIFIABLE, AUTOLOGOUS ARTERIAL BLOOD CLOT

N. Shimamura, J. Kikuchi, N. Matsuda, H. Ohkuma

Neurosurgery, Hirosaki University School of Medicine, Hirosaki, Japan

We developed novel model of rat embolic internal carotid artery occlusion with a quantifiable autologous arterial blood clot. The 0.15 ml of arterial blood were drawn from left femoral artery and mixed with 10 units of thrombin in 50 $\mu\ell$ saline. After 30 minutes the clot was suctioned into a 4-French tube. Three centimeters of a tube containing clot were prepared. A 24-gage catheter was inserted up through the internal carotid artery via a small incision in the external carotid artery stump. The 1 cm clot, at a volume of 7.2 mm^3, was pushed and inserted into the internal carotid artery via the catheter. After withdrawing the catheter the external carotid artery was ligated and the ICA blood flow recovered.

After 24 hours we checked the neurological status and measured the infarction volume by the TTC method. Two rats were not able to achieve an 80% reduction in CBF. One rat died due to cerebral infarction. The success rate in producing infarction was 82%. The surviving rats were analyzed for infarction volume and neurological score (1 ~ 15). The total infarction volume was 368.5 mm^3 ± 61.2 se, infarction volume of the basal ganglia was 126.5 mm^3 ± 26.0 se, infarction volume of the cortex was 242.1 mm^3 ± 36.1 se. Median neurological score was 6. The total volume of infarction for both the cortical infarction and basal ganglia infarction correlated significantly with the neurological score. We conclude that this embolic stroke model is useful in producing a human cardioembolic cerebral infarction, especially internal carotid occlusive severe embolic stroke.

PRENATAL STRESS MODULATES IGFBP-2 EXPRESSION IN HIPPOCAMPUS AND FRONTAL CORTEX

J. Slusarczyk, E. Szczesny, A. Basta- Kaim, K. Glombik, M. Leskiewicz, J. Detka, M. Kubera, B. Budziszewska, W. Lason

Experimental Neuroendocrinology, Institute of Pharmacology Polish Academy of Sciences, Krakow, Poland

Objectives: Pathogenesis of depression still remains under discerning investigation . Many authors suggest that weaker activity of growth factors, i.e. Insulin-like Growth Factor-1 (IGF-1) may play a key role in disturbances observed in depression. For instance, chronic antidepressant treatment increases IGF-1 protein levels in brains of experimental animals [1]. IGF-1 actions are regulated by a family of six binding proteins (IGFBP 1-6). Their presence in the circulation and extravascular fluids prolongs IGF's half-life, and modulates its interactions with receptors. IGFBP-2 is the main binding protein expressed in the CNS, and it has been postulated that in patients suffering from bipolar disorder expression of this binding protein is disturbed [2]. On the other hand, little is known about regulation of IGF-1 levels by IGFBP-2 in depressive disorder. The aim of present study was to determine, whether prenatal stress (approved animal model of depression) evokes changes in IGFBP-2 levels in hippocampus and frontal cortex in adult rats.

Methods: Pregnant Sprague- Dawley rats were subjected to stress sessions from 14th day of pregnancy until the delivery. Control pregnant females were left undisturbed in their home cages. After weaning, male rats from each experimental group were housed

collectively. At 3 months of age, the control and the prenatally stressed male rats were tested for behavioral changes in Porsolt test and elevated plus maze test. Some of animals were killed by rapid decapitation two days after the behavioral test and the hippocampi and frontal cortices were rapidly dissected out and stored at -80^{o}C. Levels of IGF-1mRNA were determined with RT-PCR. IGF-1 and IGFBP-2 were measured in hippocampus and frontal cortex tissue homogenates by ELISA assay.

Results: Prenatally stressed rats showed depression-like behavior: an increase in immobility time and decrease in climbing in Porsolt test and a decrease in the time spent in the open arm of the maze. There were no changes in the level of IGF-1 mRNA in the hippocampus and frontal cortex. Nevertheless, a significant decrease of IGF-1 protein was observed in both examined brain structures of prenatally stressed animals. Data obtained from ELISA analysis also revealed a reduction of IGFBP-2 levels in hippocampus and frontal cortex.

Conclusions: Data obtained from behavioral tests confirms the usefulness of prenatal stress model to examine the mechanisms involved in pathogenesis of depression. Reduction of IGFBP-2 in examined brain structures may be a cause of concurrently observed decrease in IGF-1 caused by prenatal stress. Thus changes in IGF system may be one of the mechanisms which trigger the onset of depression.

Acknowledgements: This work was supported by the Operating Program of Innovative Economy 2007-2013, grant No. POIG.01.01.02-12-004/09.

References:

[1] Khawaja X. et al.: Proteomic analysis of protein changes developing in rat hippocampus after chronic antidepressant treatment: Implications for depressive disorders and future therapies. J Neurosci Res. 2004, 75(4):451-460.

[2] Bezchlinnyk Y.B. et al.: Decreased expression of insulin-like growth factor binding protein 2 in the prefrontal cortex of subjects with bipolar disorder and its regulation by lithium treatment. Brain Res. 2007, 1147:213-217.

REGULATION OF IFN-GAMMA EXPRESSION BY SOCS-1 IN AN ANIMAL MODEL OF DEPRESSION

E. Szczesny[1], J. Slusarczyk[1], A. Basta- Kaim[1], A. Zelek-Molik[2], K. Rafa- Zablocka[2], K. Glombik[1], A. Kurek[1], B. Budziszewska[1], I. Nalepa[2], W. Lason[1]

[1]Experimental Neuroendocrinology, [2]Brain Biochemistry, Institute of Pharmacology Polish Academy of Sciences, Krakow, Poland

Objectives: It has been suggested that alterations in cytokine production observed in depressed patients may play a role in etiology of the disease. Moreover, IL-1, IL-2 and IFNs administration produces symptoms similar to those observed in major depression. On the other hand, stress may lead to changes in cytokine levels and functions, which can be important in the mechanism triggering the onset of depressive disorder [1]. One of the factors regulating cytokine expression is a family of Supressor of Cytokine Signalling proteins (SOCS). Among them, SOCS-1 is an inhibitor of IFN-gamma signaling, and its expression is evoked by some inflammatory cytokines and lipopolisaccharide (LPS) [2]. Nevertheless, there is very little data comprising the contribution of SOCS-1 to IFN-gamma level regulation in depression. The aim of present work was to examine whether prenatal stress (animal model of depression) and acute LPS administration may affect the expression of IFN-gamma and SOCS-1 in hippocampi of adult rats.

Methods: Pregnant Sprague- Dawley rats were subjected to stress sessions from 14th day of pregnancy until the delivery. Control pregnant females were left undisturbed in their home cages After weaning, male rats from each experimental group were housed collectively. At 3 months of age, the control and the prenatally stressed male rats were tested for behavioral changes in Porsolt test and locomotor activity test. Two days after behavioral test the animals were divided in four groups: control, control +LPS, prenatally stressed, prenatally stressed +LPS. 4 hours after lipopolysaccharide (250 ug/kg) was injected i.p., animals were killed by rapid decapitation. Hippocampi were dissected out and stored at -80^{o}C. SOCS-1 and IFN-gamma mRNA expression was measured with RT-PCR , while protein levels were assayed with ELISA method.

Results: Behavioral changes similar to depressive behavior were observed in prenatally stressed animals: increase of

immobility time in Porsolt test and increase in locomotor activity. An increase of IFN-gamma mRNA expression and protein level was observed in hippocampi of prenatally stressed rats. In all groups LPS administration altered IFN-gamma mRNA expression, but did not change protein levels. SOCS-1 mRNA level and protein expression remained unchanged in prenatally stressed animals, while acute LPS treatment caused an increase of SOCS-1 (mRNA and protein) in both groups.

Conclusions: Usefulness of prenatal stress in examination of the mechanisms involved in pathogenesis of depression was proved in behavioral tests. Hippocampal increase in SOCS-1 expression in both groups of animals treated with LPS may have resulted in lack of increase in IFN-gamma levels. No changes in SOCS-1 expression in hippocampi of prenatally stressed animals may be a cause of elevated IFN-gamma, and can be due to some sort of impairment evoked by prenatal stress.

Acknowledgements: This work was supported by the Operating Program of Innovative Economy 2007-2013, grant No. POIG.01.01.02-12-004/09.

References:

[1] Dunn AJ et al. Cytokines as mediators of depression: what can we learn from animal studies? Neurosci Biobehav Rev. 2005;29(4-5):891-909.

[2] Baker BJ et al.: SOCS1 and SOCS3 in the control of CNS immunity. Trends Immunol. 2009,30(8):392-400.

UNIFORM EXTENT AND DEGREE OF CEREBRAL ISCHEMIA AFTER MIDDLE CEREBRAL ARTERY OCCLUSION IN RATS: USE OF PROSPECTIVE DIFFUSION MRI

K.S. Yi[1], S.-H. Cha[1], S.Y. Lee[1], C. Lee[2], S.-R. Lee[3]

[1]Radiology, Chungbuk National University Hospital, Cheongju, [2]Division of Magnetic Resonance Research, Korea Basic Science Institute, [3]National Primate Research Center, Korea Research Institute of Bioscience and Biotechnology, Cheongwon, Republic of Korea

Purpose: For the translational research to evaluate therapeutic potential of any agent, there should be rat models with cerebral ischemia/infarction of very similar characteristics. And yet previous reports revealed middle cerebral artery occlusion (MCAO) models in rats presented very diverse results of cerebral infarction with the use of either sutures or macrospheres. This experimental study was to produce brain infarctions with uniform extent and level of ischemic damage after MCAO in rats.

Materials and methods: A total of 19 rats were subject to left MCAO using the suture technique. Immediately after occlusion, the animals were transferred into an MRI scanner (4.7 T) and diffusion weighted imaging (DWI) of axial and coronal planes was repeated every 10 minutes to post-occlusion 125 minutes (11 times). Every first MR imaging was started 15 minutes after stroke onset. Immediately after each DWI, the apparent diffusion coefficient (ADC) values were determined in the ischemic lesions and compared to the unaffected contralateral hemisphere. Successful MCAO was defined when the whole left MCA territory showed ADC abnormality on the first post-occlusion DWI at 15 minutes.

Results: Territorial infarction was induced successfully in nine rats (9/19, 47.4%), and MCAOs in 10 rats were classified as failure. On initial post-occlusion MR imaging at 15 minutes, the ADC values of the affected lesions were significantly lower than those of contralateral hemispheres (mean relative ADC value=0.77 ± 0.06), and remained stable in seven rats, however in two rats the ADC values decreased and reached lowest plateau in 45 and 55 minutes, respectively. Thus seven out of 19 MCAO cases had brain infarctions with very similar MR characteristics of lesion extent and temporal evolution of ADC abnormality.

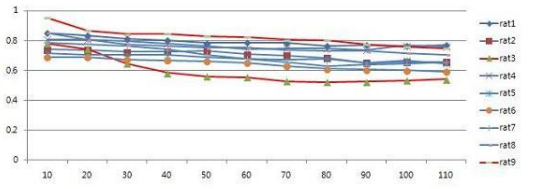

Fig 1. Temporal changes of relative ADC values.
In the ischemic lesions after left MCAO in nine cases, initially defined as successful. relative ADC values of the two showed different pattern of temporal evolution (red line) comparing to the those of the remaining seven (blue line).

[Temporal changes of relative ADC values]

Conclusion: Applying prospective diffusion

MRI and judging the success of modeling very early on after MCAO, we could exclude any inhomogeneity of brain infarctions and produce uniform extent and level of ischemic damage in rats. This technique would make it possible to obtain homogenous group of murine stroke models for the translational research.

LIPOPOLYSACCHARIDE/ISCHEMIA/HYPOXIA INDUCES DIFFUSE MYELIN/AXONAL INJURY AND FOCAL MYELIN/AB AGGREGATION IN RAT BRAIN

X. Zhan, C. Cox, B.P. Ander, G.C. Jickling, F.R. Sharp

Neurology, University of California at Davis, Sacramento, CA, USA

Background: Ischemia, Alzheimer's disease (AD) and white matter injury (White Matter Hyperintensities, WMH) often co-exist in the aging human brain. Though associated, it is not known if any one condition is predisposition to one of the others.

Methods: Sprague Dawley rats were given intraperitoneal injections of lipopolysaccharide (LPS, 3mg/kg). 24 hours later, rats were subjected to 20-minutes of focal middle cerebral artery ischemia (IS) using the suture/filament technique. This was followed by transient systemic hypoxia (H, 8% oxygen for 30 minutes). Subjects were allowed to survive up to 12 weeks. Controls included rats subjected to LPS, IS, H, LPS/IS, LPS/H, IS/H and naïve controls. The 5XFAD mouse Alzheimer's model was also studied. Immunohistochemistry and Western blot analysis were used to assess damage to myelin and deposition of β amyloid (Aβ) peptides.

Results:

1. Western blot analysis showed myelin basic protein (MBP) was degraded not only in the ischemic hemisphere, but also in the contralateral hemisphere. This was associated with a bilateral inflammatory response, with induction of microglial/monocyte IL-1β and Natural Killer Cell/Cytotoxic T Cell Granzyme B in both hemispheres that increased between 4 and 12 weeks post LPS/IS/H.

2. Diffuse dystrophic myelin sheaths in the cerebral cortex and hippocampus were identified bilaterally following LPS/IS/H. At one week, MBP staining was detected bilaterally throughout superficial layers of cortex in a pattern that resembled blood vessels. Double labeling showed that MBP was located in Caveolin1^{+} endothelial cells. By 4 weeks, focal tangles of dystrophic and disorganized myelin sheaths were identified throughout the cortex and the hippocampus that persisted up to 12 weeks post LPS/IS/H.

3. Axonal injury occurred in the cortex and corpus callosum suggested by abnormal staining of neurofilament light chain and βIII tubulin in the axons following LPS/IS/H compared to controls.

4. Myelin aggregates that stained for MBP and myelin associated glycoprotein (MAG) also stained for Aβ in the ischemic hemisphere following LPS/IS/H. In striatum and hippocampus, Aβ deposition occurred in areas absent of MBP. Cortical Aβ deposition usually occurred in MBP aggregates.

5. Myelin aggregates were identified in the amyloid plaques of the FAD mice by colocalization of MBP and FSB in the 8-month old mouse brain.

Conclusions: LPS/Ischemia/Hypoxia produces elements of AD and WMH pathologies in adult rat brains. LPS/IS/H leads to formation of myelin aggregates that appear to be foci for Aβ deposition that may lead to amyloid-like plaques. FSB stained amyloid plaques in a mouse AD model co-localize with myelin aggregates. These data suggest degraded myelin products might form the nidus for Aβ deposition and possibly for formation of amyloid plaques in both the LPS/IS/H model and a mouse AD model.

Acknowledgement: This study is supported by NIH grant RO1NS066845 (FRS), and Pilot Award Recipient (XZ) of NIH/NIA P30 AG010129-21.

ESTABLISHMENT AND EVALUATION OF AN EXPERIMENTAL ANIMAL MODEL OF HIGH ALTITUDE CEREBRAL EDEMA

Q.Q. Zhou[1,2], P. Guo[1,2], H. Luo[1,2], Y. Fan[1,2]

[1]Department of High Altitude Diseases, College of High Altitude Military Medicine, Third Military Medical University, [2]Key Laboratory of High Altitude Medicine, Ministry of Education, PLA, Third Military Medical University, Chongqing, China

Objective: The aim of our study was to establish a new animal model of high altitude cerebral edema in rats, by using a simulated high altitude acute hypobaric hypoxia environment combined with exhaustive exercise.

Methods: Forty healthy male Sprague-Dawley rats were randomly divided into a plains control group (PC group) and a plateau altitude hypoxia group (AH group). After 2 days of treadmill training adaptation under normoxic conditions, the AH group was housed in hypobaric conditions simulating 4000 m above sea level, and performed exhaustive exercise for 2 days. The simulated altitude was then changed to 8000 m for 3 days of simple hypobaric hypoxia exposure.There was no hypobaric hypoxia intervention treatment for the PC group.

Results: Compared with the PC group, water content and Evans blue staining in brain tissue were significantly greater in the AH group ($P < 0.01$). Ultrastructure Observation in the PC group, the brain microvascular endothelial cell basement membrane had a continuous linear distribution, and the structure of tight junctions was integral and not open. There was a high electron density of lanthanum particles locally deposited within the cerebral microvascular lumen, and the particles had not leaked out to the brain tissue space. The structure of the neurons, endothelial cells, and myelinated nerve fibers was normal. Compared with the PC group, the brain tissue structure of the AH group was extremely loose, the electron density of the capillary basement membrane was reduced, and the perivascular space of the cerebral blood vessels had increased. A large number of high electron density lanthanum particles had leaked from the widened tight junctions into the microvascular lateral wall and into the cerebral blood vessels. Mitochondrial swelling, mild expansion of the Golgi complex, and even vacuolar degeneration was seen in some neurons and glial cells. The nerve fibers were edematous and swollen. Detection of NF-κB Protein Expression was shown that the amount of NF-κB p65 in the frontal and parietal cortex was very low in the PC group (The expression level of PC group was considered as 100%); after exposure to acute hypobaric hypoxia the NF-κB p65 protein expression level in the cerebral cortex increased significantly (140.0 ± 40.7%). The NF-κB p65 level in the cerebral cortex in the AH group was significantly higher than that in PC group ($P < 0.05$).

Conclusion: Acute hypobaric hypoxia exposure with exhaustive exercise enabled successful establishment of an animal model of high altitude cerebral edema, in which the blood-brain barrier had increased permeability, leading to cerebral edema.

IN SEARCH OF AUTISM BIOMARKERS

D.M. Halepoto, **L.Y. Al-Ayadhi**

Autism Research and Treatment Centre, King Saud University, Riyadh, Saudi Arabia

Autism spectrum disorder (ASD) is a neurodevelopmental disorder characterized by impairments in social interaction, difficulty with communication, and restrictive and repetitive behaviors appearing during the first 3 years of life. Autism is currently affecting as many as 1 out of 88 individuals in the United States. There is growing evidence that autism may influenced by genetic, neurological, environmental and immunological factors, however its exact pathophysiology is unknown. The use of potential biomarkers that point to specific mechanism of ASD will help to diagnosis and tailor treatment or prevention strategies for disease rather than solely to a symptom category. Several studies have been carried out to find a candidate biomarker linked to the development of ASD, but up to date no reliable biomarker is available.

The aim of this poster is to provide an overview of the various potential autism biomarkers reported by our group to consider the future development in this area of research.

VALUE OF EXPRESSION LEVEL OF MICRORNA-1285 IN DIAGNOSIS OF AMYTROPHIC LATERAL SCLEROSIS

B. Cai, **D. Fan**

Neurology, Peking University Third Hospital, Beijing, China

Objective: To investigate the diagnostic value of plasma microRNA for amyotrophic lateral sclerosis (ALS).

Methods: Differential expression of plasma microRNA was detected by ABI miRNA microarray from 5 patients with ALS and 5 normal controls. The result of the microarray

was validated in plasma samples of 60 ALS patients and 53 normal controls by real-time PCR. ROC curve was used to evaluated the diagnostic value of microRNA for ALS.

Results: ABI miRNA microarry observed that the expression of microRNA-1285 was significantly lower in the plasma of ALS patients compared with the normal controls (RQ=0.4461, P=0.0332). By verifying it in larger sample, the expression quantity of microRNA-1285 was 0.75±0.50 in the ALS patients (n=60), which is significantly lower than 1.52±1.04 in the normal controls (n=53, $p=2.99*10^{-5}$). When 0.9463 was made as critical value for diagnosis, the sensitivity and specificity can be 0.736 and 0.683 respectively, and the area under curve of ROC was 0.728.

Conclusions: The expression of microRNA-1285 is down-regulated significantly in ALS. The microRNA-1285 may act as a biological marker for diagnosis of ALS.

MICRORNA EXPRESSION SIGNATURE IN HUMAN BRAIN ARTERIOVENOUS MALFORMATIONS AND BRAIN HEMANGIOBLASTOMA

J. Huang[1], W. Zhu[2], Q. An[2], Y. Wang[3], S. Zhang[2], T. Xu[2], G. Tang[1], Y. Li[1], Y. Liu[3], Y. Wang[1], G.-Y. Yang[1,3]

[1]Neuroscience and Neuroengineering Research Center, Med-X Research Institute and School of Biomedical Engineering, Shanghai Jiao Tong University, [2]Department of Neurology, Hua Shan Hospital, Fudan University, [3]Department of Neurology, Ruijin Hospital, School of Medicine, Shanghai Jiao Tong University, Shanghai, China

Objectives: Small noncoding microRNAs (miRNAs) play critical roles in many biological and pathological processes and are differentially expressed in normal tissue and diseased tissue.[1] Brain arteriovenous malformations (BAVM) and brain hemangioblastoma are cerebrovascular diseases involving in angiodysplasia. Yet, the function of miRNAs in regulating blood vessel development of these two diseases is unknown. In this study, we aim to investigate the miRNAs signature in human BAVM and human brain hemangioblastoma.

Methods: Total RNA from the surgical specimen of BAVM patients (n=6), hemangioblastoma patients (n=6) and healthy individuals (n=3) were assessed using EXIQON Kit arrays (microRNA Ready-to-Use PCR). 739 miRNAs were validated with qRT-PCR analysis in order to establish the miRNA expression signature. GenEx software was used to analyze all the preliminary qRT-PCR data. Ingenuity Pathway Analysis software was used to predict the potential miRNA targets and to analyze their functions.

Results: miRNA arrays revealed that 7 and 80 miRNAs expressed significantly different ($p< 0.05$ and passed Bonferroni correction) in BAVM patients and in brain hemangioblastoma patients compared to healthy controls, respectively. 23 miRNAs expressed significantly differently ($p< 0.05$ and passed Bonferroni correction) in the BAVM patients compared to the brain hemangioblastoma patients; of these significantly changed miRNAs, miR-137, miR-138, miR-431, miR-379 were down-regulated in both BAVM and hemangioblastoma patients compared to healthy controls while miR-451 was the only miRNA that is up-regulated in both patient groups. MiR-483-3p was greatly reduced in BAVM compared to the brain hemangioblastoma patients (Fold change=101.98, $p< 0.001$). Bioinformatic analysis indicated that miR-137, miR-138, miR-431, miR-379 and miR-451 were the potential miRNA targets that could be involved in angiodysplasia.

Conclusions: This study shows that there is a distinct miRNA expression signature in brain vascular diseases and health control. This finding provides valuable clue on the identification of miRNAs' function in cerebrovascular pathologic processes and the development of the therapeutic targets.

Reference:

1. Sharp FR, Jickling GC, Stamova B, Tian Y, Zhan X, Liu D, et al. Molecular markers and mechanisms of stroke: RNA studies of blood in animals and humans. J Cereb Blood Flow Metab 2011; 31: 1513-1531.

QUEST FOR ELECTROPHYSIOLOGICAL BIOMARKERS IN TRANSLATIONAL STROKE RESEARCH

J. Lückl[1,2], S. Major[1,2], U. Khojasteh[1,2], J.P. Dreier[1,2]

[1]Experimental Neurology, Charité University Medicine, [2]Center for Stroke Research Berlin (CSB), Charité University Medicine, Berlin, Germany

Objectives: Ample evidence has been accumulated on the pathophysiological role of spreading depolarizations in many brain injuries such as ischemic stroke, subarachnoid haemorrhage and traumatic brain injury. Analysing electrophysiological and blood flow data recorded in human studies imposes a huge work load on investigators. The complexity of the collected data raises the demand for simple biomarkers which would make data analysis faster and more effective. Accurate biomarkers would also allow clinicians to assess patient outcome at the bedside and may provide an opportunity for rapid intervention in the future.

Methods: Isoflurane anesthetized Sprague-Dawley rats (n=28) underwent 90 minutes of filament occlusion**.** Relative blood flow changes were monitored with a laser Doppler probe (4-5 mm lateral and 1-2 mm posterior to Bregma). Direct current (DC) potential and electrocorticogramm (ECoG) were recorded epidurally with two silver chloride electrodes (2 and 3 mm caudal to the laser Doppler probe). Another group of animals (n=12) underwent the same study protocol but with scalp electroencephalographic (EEG) recordings. The animals survived 72 hours and the infarct size was determined in hematoxylin-eosin stained slices. Physiological variables, relative blood flow changes and the electrophysiological data were recorded with a Spike data acquisition system and the data were processed further in LabChart7. The relative blood flow changes, the number of DC deflections, the integral of the DC curves, the relative changes of the ECoG/scalp EEG power and integral were calculated at different time points (10, 20, 30 ….90 minutes) after the occlusion. The different biomarkers were compared with the cortical infarct size by doing a series of regression analyses.

Results: The study revealed that all of the investigated biomarkers show a significant relationship (p values ranging from 0.05 to 0.001) with the histological outcome from the 20th minute of ischemia (**table**). Biomarkers like cerebral blood flow, power changes of the scalp EEG and the power/integral changes of the ECoG (posterior probe) can predict the outcome even after 10 minutes of ischemia.

Elapsed **time** after occlusion (min.)	Epidural recordings								Scalp recordings	
	No of DC		DC Integral		ECoG Integral		ECoG Power		EEG Power	
	ant	*post*	*ant*	*post*	*ant*	post	*ant*	*post*	*ant*	*post*
10	-	-	-	-	-	+	-	++	+	++
20	++	++	+	+	+	++	+	+++	-	++
30	++	++	++	+++	+	++	+	+++	+	++
40	++	++	+++	+++	+	++	+	+++	++	+++
50	++	++	+++	+++	+	++	+	+++	++	+++
60	++	++	+++	+++	+	++	+	++	++	+++
70	++	++	+++	+++	+	++	+	++	++	+++
80	++	++	+++	+++	+	++	+	+++	++	+++
90	++	++	+++	++	+	++	+	+++	++	+++

+ p< 0.05; ++ p< 0.01; +++ p< 0.001; - nonsignificant

[Figure]

Conclusions: Considering both the accuracy of the markers and simplicity of the analysis, we found that the ECoG/EEG power changes are promising biomarkers for clinical studies of subarachnoid haemorrhage.

CSF ALPHA-SYNUCLEIN TEMPORAL PROFILES PREDICT OUTCOME AFTER SEVERE TRAUMATIC BRAIN INJURY

S. Mondello[1], A. Buki[2], D. Italiano[3], A. Jeromin[1]

[1]Banyan Biomarkers, Inc., Gainesville, FL, USA, [2]University of Pecs, Pecs, Hungary, [3]University of Messina, Messina, Italy

Objectives: The study aims to examine alpha-synuclein (1) in the human cerebrospinal fluid (CSF) of patients with severe traumatic brain injury (TBI) and its relationship with clinical characteristics and long-term outcomes.

Methods: This prospective case-control study enrolled patients with severe TBI (Glasgow Coma Score [GCS] ≤8), who underwent ventriculostomy. CSF samples were taken from each TBI patient at admission and daily for up to 8 days after injury and successively assessed by ELISA. Control CSF was collected for analysis from subjects receiving lumbar puncture for other medical reasons. We used trajectory analysis to identify distinct temporal profiles of CSF alpha-synuclein that were compared with clinical outcomes.

Results: CSF alpha-synuclein was significantly elevated in TBI patients after injury as compared to controls (p=0.0008). Overall, patients who died had significantly higher concentrations (area under the curve) over 8 days of observation compared to those who survived at 6 months post injury (p= 0.002). Two distinct temporal alpha-synuclein profiles were recognized over time (Figure). Subjects who died had consistently elevated alpha-synuclein levels compared to those who survived with alpha-synuclein levels near controls. High-risk trajectory was a strong and accurate predictor of death with 100% specificity and a very high sensitivity (83%).

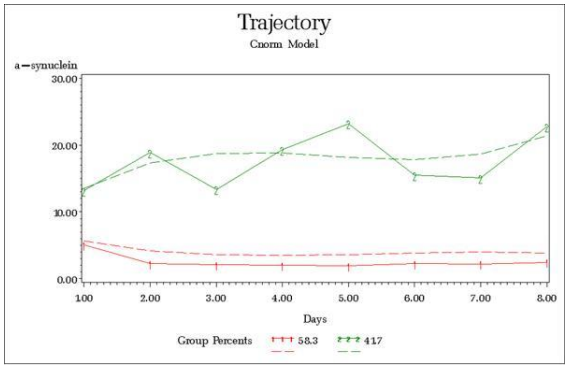

[Trajectory Analysis]

Conclusions: Taken together, these data support the hypothesis that in severe TBI patients, substantial increase of CSF alpha-synuclein may indicate widespread neurodegeneration (2) and reflect secondary neuropathological events occurring after injury. The determination of CSF alpha-synuclein may be a valuable prognostic marker, adding to the clinical assessment and creating opportunities for medical intervention.

References:

1. Vekrellis K, Xilouri M, et al. Pathological roles of alpha-synuclein in neurological disorders. Lancet neurology 2011;10:1015-1025.

2. Kramer ML, Schulz-Schaeffer WJ. Presynaptic alpha-synuclein aggregates, not Lewy bodies, cause neurodegeneration in dementia with Lewy bodies. J Neurosci 2007;27:1405-1410.

BLOOD GLUTATHIONE S-TRANSFERASE-PI AS A STOPWATCH OF STROKE ONSET

J.-C. Sanchez[1], X. Robin[1], J. Montaner[2], P. Burkhard[1], N. Turck[1]

[1]Human Protein Sciences, Geneva University, Geneva, Switzerland, [2]Stroke Unit, Vall d'Hebron Hospital, Barcelona, Spain

Background: Depending on the countries and studies, only 1 to 10% of acute ischemic stroke patients really benefit of recombinant tissue-plasminogen activator (rt-PA) therapy, the only established beneficial treatment for acute ischemic stroke. The main reason of this low access rate to thrombolytic therapies is related to the high proportion of stroke patients (up to 30%) excluded due to an undetermined time of stroke onset. The unknown time is also the main excluding factor of the treatment for all wake-up stroke patients. A few studies have recently reported that diffusion-weighted imaging (DWI), T2-weithed and fluid-attenuated inversion recovery (FLAIR) MRI sequences could be useful for estimating the time of stroke onset within the first few hours. However, immediate access to MRI machines as a surrogate marker for the early detection of stroke is likely to be limited, if not impossible, in most hospitals worldwide. We thus hypothesized that an early biomarker characterized by a rapid increase in blood after stroke onset may help defining better the time window during, which an acute stroke patient may be candidate for intravenous thrombolysis or other intravascular procedures.

Methods: The blood level of 30 proteins was measured by immunoassays on a prospective cohort of stroke patients (N = 103) and controls (N = 132). Mann-Whitney U tests, ROC curves and diagnostic odds ratios were applied to evaluate their clinical performances.

Results: Among the 30 molecules tested, GST-pi concentration was the most significantly elevated marker in the blood of stroke patients (p< 0.001). More importantly, GST-pi displayed the best area under the curve (AUC, 0.79) and the best diagnostic odds ratios (10.0) for discriminating early (N = 22, < 3 h of stroke onset) vs. late stroke patients (N = 81, >3 h after onset). According to goal-oriented distinct cut-offs (sensitivity (Se)-oriented: 17.7 µg/L or specificity (Sp)-oriented: 65.2 µg/L), the GST-pi test obtained 91%Se-50%Sp and 50%Se-91%Sp, respectively.

Conclusions: This study demonstrates that

GST-p can accurately predict the time of stroke onset in over 50% of early stroke patients. The ability of GST-p to predict the time window after stroke onset and consequently the potential eligibility for thrombolytic therapies may open new avenues for the management of stroke patients but also more specifically for the wake-up stroke patients, representing up to 30% of stroke events and traditionally excluded from treatment because of unknown time of symptom onset.

SERUM METABOLOMIC ANALYSIS RELIABLY DIFFERENTIATES BETWEEN MULTIPLE SCLEROSIS SUB-TYPES

N. Sibson[1], J.R. Larkin[1], A.M. Dickens[1,2,3], J.L. Griffin[4], A. Cavey[5], L. Matthews[5], B.G. Davies[3], T.D.W. Claridge[3], J. Palace[5], D.C. Anthony[2]

[1]Department of Oncology, [2]Department of Pharmacology, [3]Department of Chemistry, University of Oxford, Oxford, [4]Department of Biochemistry, University of Cambridge, Cambridge, [5]Nuffield Department of Clinical Neurosciences, University of Oxford, Oxford, UK

Objectives: Accurately determining when a multiple sclerosis (MS) patient progresses from a relapse-remitting (RRMS) to secondary progressive (SPMS) stage is currently challenging. To be clinically certain, a patient may be observed for periods up to a year. This uncertainty is unhelpful, as most MS-related disability accrues during the SPMS stage and effective therapy differs between the two stages.

The aim of our work was to establish whether a biofluid-based metabolomics approach, which we have previously used to distinguish distinct experimental neuropathologies[1], was able to differentiate between MS disease states.

Methods: Serum samples from three sets of RRMS and SPMS patients, and age-matched controls, were collected (Set A: n=15, 38 and 10; Set B: n=6, 10 and 7; Set C: n=5, 10 and 7, respectively). For Set A serum samples were also collected from 13 primary progressive (PP) MS patients. ^{1}H nuclear magnetic resonance (NMR) spectra were acquired for each sample and partial least squares discriminant analysis was used to identify differences between groups.

Results: Samples from Set A were used to build significantly predictive models that separated control volunteers from each stage of MS studied (SPMS (q^2=0.42), RRMS (q^2=0.61) and PPMS (q^2=0.70) where q^2>0.4 is considered significant). In addition, it was possible to separate RRMS and SPMS patients with a predictive model (q^2=0.45). In contrast, PPMS patients were not separated from either RRMS or SPMS patients (q^2< 0).

To corroborate these findings, a second set of models were constructed from samples in Set B. The same significant separations that were present in Set A were also present in Set B and the same metabolites were key in driving the separations. To further validate the models, the group membership of each patient in an independent Set C was predicted using the models produced from Set B. The models were highly predictive: RRMS vs. SPMS model, sensitivity = 0.9 and specificity = 0.8; RRMS and SPMS vs. control models, sensitivity and specificity = 1.0 ($p< 0.01$).

Conclusions: We have demonstrated for the first time that it is possible to distinguish between RRMS and SPMS patients in a predictive fashion using an objective biomarker, as well as being able to separate each class of MS patients from a control cohort. The separations are based on the complete metabolomic profile of each patient and are not biased towards one metabolite in particular.

References:

1. FEBS Lett 2004 568:49

CIRCULATING MICRORNA AS BIOMARKERS FOR STROKE SEVERITY: EVIDENCE FROM AN EXPERIMENTAL MODEL

A. Selvamani, M. Wright-Williams, R.C. Miranda, **F. Sohrabji**

Texas A&M Health Science Center, Bryan, TX, USA

Introduction: Stroke is the leading cause of adult disability and the 4th leading cause of mortality in the US. Treatment options are limited to one FDA-approved thrombolytic (tissue plasminogen activator [tPA]), however the vast majority of patients are usually not tPA-eligible, and are dependent on

rehabilitation services and supportive care. Hence, there is a critical need to accurately predict the future likelihood for neurological recovery in the early hours and days following a stroke, to better inform decisions about patient care and allocation of rehabilitative resources.

Aim: In this study we examined whether circulating microRNA could serve as prognostic markers of stroke outcome in an animal model. MiRNA are small non-coding RNAs that regulate the transcriptome by influencing mRNA transcript stability and gene translation. Initially considered an intracellular molecule, miRNA have now been detected in virtually all body fluids. Due to their high stability in circulation, tissue and disease specific expression profiles and availability of sensitive tools to measure them, circulating microRNAs are emerging as diagnostic markers in various diseases.

Methods: Young (5-6 months) and middle-aged (10-12 months) male and female Sprague Dawley rats (n=24) were subject to vasoconstrictive MCAo. At 2d post stroke, a blood sample was obtained from the saphenous vein and animals were terminated at 5d for infarct analysis by standard histological procedures. Qiagen miRNeasy Mini Kit was used for total RNA isolation from serum, and quantified using NanoDrop 2000 Spectrophotometer. For RT-PCR amplification of miRNA, Exiqon SYBR Green Universal RT was used in conjunction with Exiqon focus panels for serum microRNAs. Each focus panel contained 168 LNA microRNA primer sets that focus on serum/plasma relevant human microRNAs and 7 reference microRNAs. To develop a predictive model, we used regularized regression techniques to carry out feature selection among 168 miRNA, including sex and age as key variables.

Results: As reported previously, young females had infarct volumes that were one third smaller than those of middle-aged females ($p< 0.05$) and males had larger (1.8-fold) infarct volumes as compared to females ($p< 0.05$). Infarct volumes were positively correlated with performance on a sensory motor task (tape test) ($r=0.54$; $p< 0.05$). Thus our sample consisted of a broad range of stroke severity. Using a stepwise linear regression analysis, several predictive models were developed. The final selected model included a small cohort (6) of unique miRNA, normalized also for the sex of the subject. Internal validation of this predictive model returned a strong positive correlation (r^2: 0.93). MiRNA included in this model represent a combination of miRNA that have been implicated in stroke and cardiovascular neuroprotection (miR-223, miR-23b) and other unique miRNA not currently implicated in vascular disease.

Conclusion: Our results indicate that circulating miRNA, shed from endothelial, immune and neural sources into blood may contain composite information about stroke damage and tissue adaptation to damage, and can provide a unique disease biomarker.

DETERMINATION OF VISIN LIKE PROTEIN FOR DIAGNOSIS OF THE STROKE

D. Stejskal[1,2,3], M. Svestak[4], P. Kanovsky[3]

[1]Dept. of Laboratotory Medicine, Stredomoravska Nemocnici, Prostejov, [2]Institute of Medical Chemistry and Biochemistry, [3]Dept. of Neurology, Faculty of Medicine, Palacky University Olomouc, [4]Institute of Medical Chemistry and Biochemistry, Olomouc, Czech Republic

Background: Current diagnosis of stroke relies on clinical examination by a physician and is further supplemented with various neuroimaging techniques. A single set or multiple sets of blood biomarkers that could be used in an acute setting to diagnosis stroke, differentiate between stroke types, or even predict an initial/reoccurring stroke would be extremely valuable. Diagnosis of stroke is currently hampered by delaydue to lack of a suitable tool for rapid, accurate and analytically sensitive biomarker - based testing. There is a clear need for further assay development and clinical validation in this area (acute stroke setting) in order to improve patient outcomes and quality of life. Visinin like protein 1 (VILIP-1) is a newly discovered CNS-abundant protein which is very promising (by experimental studies) for early stroke diagnosis. There is no clinical study with measurement of VILIP-1 in sera as a marker of stroke.

Aim: To develop an assay for the determination of VILIP-1 in human serum, and to investigate its clinical relevance as a marker of ischemic stroke.

Design and methods: A new sandwich ELISA was developed, introduced and clinically tested. Mean spiking recovery was 98%. The

mean recovery for dilution linearity was 93%. The limit of detection of the assay was 0.01 mg/l; the intraassay and interassay coefficient of variation (CV) were always less than 10%. The study was approved by the Ethics Commission of the Hospital Prostejov, Czech Republic. A total of 17 healthy individuals (9 men and 8 women, age 64.0±13.0) and 44 individuals with ischemic stroke (26 men and 16 women, age 61.0±17.0) were recruited for our study. The criteria of stroke were proposed by the National Czech Standard. All individuals had blood samples drawn, and VILIP-1 analysis and CT and/or MRI were made.

Results: VILIP-1 serum level significantly differentiate healthy subjects from patients with stroke (P< 0.01). All of individuals with stroke had VILIP-1 serum values higher than > 0.05 µg/l, healthy had values below this value. Diagnostic efficacy of serum VILIP-1 was very significant (sensitivity 99%, specificity 97% at 0.093 mg/l VILIP-1 serum values, AUC 0,98 (CI 0.91-0.99, P< 0.01), Chi-square in frequency table was 31 (P< 0.01).

Conclusion: We introduce a new analytical tool for the study of VILIP-1. Our results support the hypothesis that serum VILIP-1 may be associated with ischemic stroke. The ELISA VILIP-1 assay offers a new research tool for diagnosis and pathophysiology of stroke or other CNS diseases.

NEUROVASCULAR OXIDATIVE STRESS THROUGH NITRIC OXIDE AND SOLUBLE LECTIN-LIKE OXIDIZED LOW-DENSITY LIPOPROTEIN RECEPTOR - 1 (SLOX-1) IN ACUTE STROKE

K. Suwanprasert[1], S.- Muengtaweepongsa[2]

[1]Physiology, [2]Neurology, Faculty of Medicine Thammasat University, Pathumthanee, Thailand

Objectives: Experiment stroke studies indicate that neurovascular oxidative stress is a major contributing factor to cerebral injury. Accumulating evidence suggests that LOX-1 plays a crucial role in atherosclerosis and can be cleaved from the cell surface and releases as sLOX-1. Elevated sLOX-1 level may be indicative of plaque instability. We hypothesize that cerebral endothelial dysfunction through NO release and sLOX-1 from plaque rupture may be potential distinguished marker of acute ischemic stroke. To test this, we investigated changes of nitric oxide (NO) and sLOX-1 levels during 72 hrs after onset of acute ischemic stroke.

Methods: Changes of plasma NO and sLOX-1 were studied within the first 72 hrs from symptoms onset in 65 acute stroke patients (age 62.5+ 14.4 yrs) and compared with those of basal levels in 18 control subjects with no underlying disease. All healthy subjects and patients gave informed consent according to the Declaration of Medicine Ethic Committee (MTU-EC-IM-4-018/54). Patients were divided into two groups, non-significant stenosis flow (NSSF, n = 59) and significant stenosis flow (n= 6) by carotid duplex. Plasma NO concentration was measured by electrochemistry technique and sLOX-1 by ELIZA.

Results: During first 72 hrs after onset, nitric oxide levels were significantly reduced while sLOX-1 levels were elevated in all groups when compared with those of control. Remarkably reduced NO levels were showed in SSF group. Higher sLOX-1 levels were appeared in both NSSF and SSF groups. Interestingly, sLOX-1 was drop suddenly during 67-72 hrs in NSSF and reached almost the same basal level. Meanwhile, nitric oxide was increased dramatically. An inverse association between sLOX-1 and nitric oxide of day 3 (67-72 hrs) in NSSF was noticed and might indicate neurovascular remodeling. Greater difference of nitric oxide and sLOX-1 was evident in SSF group and showed significant level.

Conclusion: The results indicate that sLOX-1 was extremely influenced by significant stenosis flow of large artery and may be potential neurovascular oxidative stress associated with NO. Further study is needed to clarify these findings.

Acknowledgement: This work was supported by National Research University Project of Thailand Office of Higher Education Commission and faculty of medicine, Thammasat University.

References:

1. Cherubini A, et al. Potential markers of oxidative stress in stroke. Free Radical Biology & Medicine, 2005, 39,841-852

2. Boo YC. et al. An improved method to measure nitrate/nitrite with an NO-selective electrochemical sensor. Nitric Oxide, 2007, 16, 306-312

3. Ueda A et al. Elisa for soluble form of LOX-1 , a novel marker of acute coronary syndrome. Clinical Chemistry, 2006, 52, 1210-1211

PSMB8 AS AN MTBI BIOMARKER

L.-J. Tsai[1], E.-Y. Lin[2], K.-Y. Chen[3], Y.-C. Chen[4], W.-T. Chiu[5], Y.-J. Chen[6], Y.-H. Chiang[7], J.-H. Chen[8]

[1]Graduate Institute of Medical Science, Taipei Medical University, Taipei, [2]Graduate Institute of Clinical Medicine, Taipei Medical University, Taipei City, [3]Department of Surgery, College of Medicine, Taipei Medical University Hospital, [4]Department of Surgery, College of Medicine, Taipei Medical University Hospital, [5]Department of Health, Executive Yuan, [6]Institute of Chemistry, Academia Sinica, [7]Neural Regenerative Medicine Doctoral Program, College of Medical Science and Technology, Taipei Medical University, [8]Center of Excellence for Cancer Research, Wan Feng Hospital, Taipei, Taiwan R.O.C.

Mild traumatic brain injury (mTBI) is complex damage to the brain that exhibits no clear clinical symptom. Neuroproteomics has been used in efforts to discover a biomarker for mTBI and has shown post-translational modification to be critical in protein regulation. This study evaluated S-nitrosylation proteomics combined with liquid chromatography—tandem mass spectrometry (LC-MS/MS) proteomics to find a biomarker for mTBI in a rat model. Proteins that exhibited significant abundance change were determined, and significant Kyoto Encyclopedia of Genes and Genomes (KEGG) pathways involved in this disease were also identified. Data analysis using the DAVID Bioinformatics Resources 6.7 revealed the significant KEGG pathways to be oxidative phosphorylation, systemic lupus erythematosus, arginine and proline metabolism, and phenylalanine metabolism. Based on the two proteomics studies and depending on proteasome function such as protein degradation and antigen presenting, we hypothesized that the proteasome plays an important role in the pathology of mTBI. The content of proteasome subcomponent was analyzed using western blot, which found that the proteasome subunit beta type 8 (PSMB8, also known LMP7) was significantly induced in mTBI. Through bioinformatics evaluation and literature mining, PSMB8 was found to be associated with metabolism of amino acids and derivatives involved in mild traumatic brain injury. Results of this study support the feasibility of using bioinformatics evaluation for finding candidates for an mTBI biomarker.

INCREASED CYSTATIN C AND DECREASED VEGF IN SERUM WITH LOW CEREBRAL GLUCOSE METABOLISM: PREDICTION FOR SEVERITY OF MALE PARKINSON'S DISEASE

H. Gao, Y. Xu, L. Long, Q. Wang

Neurology Department, The Third Affiliated Hospital of Sun Yat-Sen University, Guangzhou, China

Background: The clinical relevance of Cystatin C(Cys C) in patients with Parkinson's disease(PD) and Vascular Parkinsonism(VP) is unclear though it is hypothesized that there is a correlation of serum levels with disease severity, and possibly progression. This first study aimed to explore the association of Cys C with the severity of PD and VP.

Methods: A cross-sectional study was performed to compare plasma Cys C levels in normal subjects, PD, and VP patients. A receiver operating characteristic(ROC) curve was used to calculate its sensitivity and specificity. Patients were assessed for motor and nonmotor dysfunction, according to the NMS scale(NMSS), Mini-Mental State Examination(MMSE), modified Hoehn and Yahr staging scale(H&Y), and Unified Parkinson's Disease Rating Scale(UPDRS),respectively. Plasma IL-1B, VEGF, and cerebral metabolic rates of glucose(CMRGlc) were evaluated. Pearson's correlations were used to identify any associations between Cys C and motor/non-motor dysfunction in PD and VP.

Findings: A significant increase in Cys C was detected in VP(1.02 ±0.25 for VP, $p < 0.001$) and male PD(0.99 ±0.23 for male PD, $p=0.007$) when compared to normal subjects. This increase was significantly correlated with the H&Y(r_S = 0.345, p=0.049), UPDRS (I) (r_S=0.508, p=0.003), and gastrointestinal complaints(r_S=0.421, p=0.015) in male PD, and profoundly associated with H&Y(r_S=0.456, p=0.004) and UPDRS(r_S=0.491, p=0.002) in male VP. Increased plasma IL-1β and decreased VEGF levels in male PD/VP patients were observed. Moreover, these patients displayed a significant CMRGlc

decrease in the frontal cortex(p< 0.001) and caudate putamen(p< 0.001 for VP; p< 0.05 for PD) as compared to normal subjects.

Interpretation: This is the first study with strong evidence to show the role of Cys C in the development of VP and PD patients. High levels of Cys C may predict the risk for development, stratification and severity of VP and PD, especially in male patients. The decrease in CMRGlc in specific brain regions of VP and PD together with the increase in Cys C levels may be used as a potential biomarker in terms of prediction of disease onset, especially when only vague nonmotor symptoms are present.

IL-6 IS THE KEY PRO-INFLAMMATORY CYTOKINE IN PERIPHERAL INFLAMMATION RESPONSE TO CEREBRAL ISCHEMIA

L. Zeng[1,2], Y. Wang[2], J. Liu[1], L. Wang[1], S. Weng[1], K. Chen[2,3], E.F. Domino[4], G.-Y. Yang[1,2]

[1]Department of Neurology, Ruijin Hospital, School of Medicine, [2]Neuroscience and Neuroengineering Research Center, Med-X Research Institute and School of Biomedical Engineering, Shanghai Jiao Tong University, Shanghai, China, [3]Banner Alzheimer's Institute and Banner Good Samaritan PET Center, Neuroimaging, Phoenix, AZ, [4]Department of Pharmacology, University of Michigan, Ann Arbor, MI, USA

Objectives: The key circulating pro-inflammatory cytokines and their interaction in peripheral inflammation after acute cerebral ischemia are poorly understood. This study was designed to evaluate the relationship between the clinical features of strokes, the release of various cytokines, and to identify their interactions.

Methods: Circulating CD40L, IFN-γ, IL-1α, IL-1β, IL-6, IL-8, IL-17 and TNF-α were determined using multi-ELISA kit in stroke patients within 72 hours of an acute ischemic attack, and in age, gender, cardiovascular risk factor matched controls. Leukocyte mRNAs were determined using real-time polymerase chain reactions (PCR). Stroke severity and clinical outcomes were evaluated by National Institutes of Health Stroke Scores (NIHSS) and modified Rankin Scale (mRS). Plasma/mRNA cytokine interactions were analyzed using the Bayesian Network learning procedure.

Results: Compared to controls, stroke patients had higher IL-6, IL-8 and TNFα protein in plasma and lower IL-6, IL-8, TNFα, IL-1α, and IL-1β mRNA in leukocyte within 72 hours after stroke. However, only the elevation of IL-6 correlated with the severity and prognosis of their stroke. This was associated with a decreased IL-6 mRNA in leukocyte. Further study showed that Bayesian Network analysis revealed that changes in the other cytokines were subsequent to IL-6 leukocyte cytokine RNA. The change of other cytokines in plasma proteins after ischemic brain injury appeared secondary to IL-6.

Conclusions: Pro-inflammatory cytokines up-regulation in plasma and compensatory immunity depression in leukocyte involve in peripheral inflammation response to cerebral ischemia. IL-6 appears to be the key mediator of circulating pro-inflammatory cytokines.

CYCLOOXYGENASE-1 CONTRIBUTES TO BLOOD-BRAIN BARRIER DISRUPTION IN ISCHEMIC BRAIN INJURY BY MODULATING OF TIGHT JUNCTION PROTEINS

S.-H. Choi, F. Bosetti, A.C. Silva

NINDS/NIH, Bethesda, MD, USA

Objectives: Disruption of the blood-brain barrier (BBB) is a critical event in the development and progression of numerous neurological disorders[1,2]. Alterations in tight junction proteins have been previously correlated with alterations in BBB integrity[1],[2]. We recently found that two different isoforms of cyclooxygenase (COX) show distinctive roles in modulating BBB permeability during the acute neuroinflammatory response[3]. The main purpose of the present study is to determine whether these BBB permeability changes correlate with up- or down-regulation of the tight junction proteins in COX-1-deficient mice.

Methods: COX-1-deficient mice and wild-type mice received intracerebral injection of endothelin-1, a potent vasoconstrictive peptide, or lipopolysaccharide. Neuronal injury, brain edema, albumin extravasation, and tight junction protein expression were evaluated 24 hours after treatment using magnetic resonance imaging, FITC-albumin

leakage assays, microvessel isolation, Western blot analysis, quantitative PCR, flow cytometry, and immunofluorescent microscopy.

Results: COX-1-deficient mice showed a significant reduction in brain edema, infarct volume, and BBB permeability in the cerebral cortex compared with their wild-type mice after endothelin-1-induced ischemic brain injury. The specific COX-1 inhibitor SC-560 reduced the infarct volume and improved cerebral blood flow in wild-type mice. COX-1 knockout mice had a significant reduction in inflammatory response, vascular leakage, leukocyte infiltration, and metalloproteinase expression in response to lipopolysaccharide compared to wild-type mice. Alteration of BBB disruption and brain edema were associated with up-regulation of tight junction protein occludin and claudin-5 in cerebral microvessels.

Conclusions: These results indicate that COX-1 is actively involved in BBB disruption in inflamed brain through modulation of tight junction protein expression.

References:

[1]Hawkins BT and Davis TP 2005 Pharmacological review 57:173-185;

[2]Zlokovic BV 2008 Neuron 57:178-201;

[3]Aid S et al., 2010 J Cereb Blood Flow Metab 30:370-380.

PERMEABILISATION OF THE BLOOD-BRAIN BARRIER AT SITES OF METASTASIS ENABLES TARGETED THERAPY DELIVERY

J. Connell[1], G. Chatain[1], B. Cornelissen[1], K. Vallis[1], L. Seymour[1], D. Anthony[2], N. Sibson[1]

[1]Department of Oncology, [2]Department of Pharmacology, University of Oxford, Oxford, UK

Objective: It is estimated that 20-40% of cancer patients develop brain metastases and their prognosis is poor. Chemotherapeutic agents showing efficacy against primary systemic tumours have limited access to brain metastases owing to the presence of the blood-brain barrier (BBB). Therefore, the aim of this study was to permeabilise the BBB at sites of cerebral metastasis to facilitate drug entry.

Methods: A model of brain metastasis was generated by intracardiac injection of murine mammary carcinoma 4T1-GFP cells into female BALB/c mice. At day 13 after metastasis induction a bolus injection of tumour necrosis factor (TNF) or lymphotoxin (LT) was administered i.v. 2 to 24 hours prior to tracer or drug administration. BBB permeability was assessed in vivo using gadolinium-enhanced multi-slice T1-weighted magnetic resonance imaging (MRI) and was confirmed histologically by horseradish peroxidase (HRP) histochemistry. Brain uptake of the clinically relevant therapeutic, ^{111}In-trastuzumab, was determined using in vivo SPECT/CT.

Results: Systemic administration of TNF or LT significantly permeabilises the BBB, specifically at sites of metastasis in the brain, to exogenous tracers, horseradish peroxidase and gadolinium, and also to the relevant chemotherapeutic agent, trastazumab. Permeability of the BBB peaked at 6 hours post-cytokine treatment. The cerebral metastases displayed localised expression of TNF receptors TNFR1 and TNFR2 on either the vascular endothelium or associated leukocytes and microglia, respectively.

Conclusions: These findings demonstrate a new approach to detect currently invisible metastases in the brain and to facilitate access of chemotherapeutic agents specifically to sites of brain micrometastases, by exploiting the specific inflammatory profile of tumour-associated vasculature.

References: Seki T et al., 2011. Tumour necrosis factor-alpha increases extravasation of virus particles into tumour tissue by activating the Rho A/Rho kinase pathway. J Control Release.

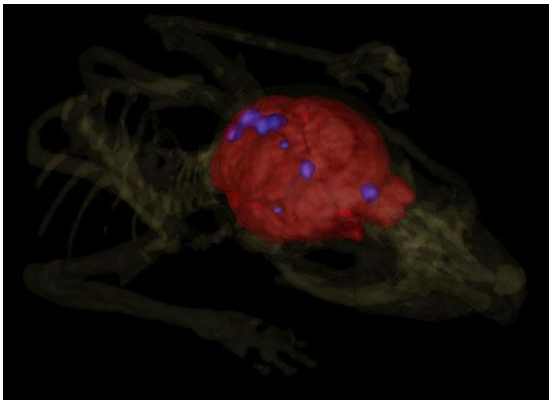

[Trastuzumab entry to brain mets.]

CAVEOLIN-1 REGULATES NITRIC OXIDE MEDIATED MATRIX METALLOPROTEINASES ACTIVITY AND BLOOD-BRAIN BARRIER PERMEABILITY IN FOCAL CEREBRAL ISCHEMIA AND REPERFUSION INJURY

Y. Gu, J. Shen

School of Chinese Medicine, University of Hong Kong, Hong Kong, Hong Kong S.A.R.

Objective: Nitric oxide is one of the key molecules that modulate blood-brain barrier (BBB) permeability and neuronal cell death during cerebral ischemia-reperfusion (I/R) injury. We previously reported that cav-1 was down-regulated and the production of nitric oxide (NO) induced the loss of cav-1 in focal cerebral ischemia and reperfusion injury. The present study aims to address whether the loss of caveolin-1 induced by NO production impacts on BBB permeability and matrix metalloproteinases (MMPs) activity during I/R injury.

Methods: Middle cerebral artery occlusion (MCAO) was used as I/R model. Microvessels from sham operation rats and model rats with vehicle and N^G-nitro-L-arginine methyl ester (L-NAME, a non-selective nitric oxide synthase inhibitor) treatment were isolated to observe the cav-1 expression level using western blot. MMP-2 and -9 activity and Zona Occludens 1 (ZO-1) were detected in cryo-sections of rats' brains with *in situ* zymography and immunostaining respectively. To determine the role of cav-1 in regulating MMPs activity, cav-1 was knocked-down with siRNA in primary cultured rat brain microvascular endothelial cells (BMECs) and the MMPs activity was determined in the conditional medium with gelatin gel zymography. Cav-1 knockout mice were also used to further study MMPs activity and BBB permeability (with Evans Blue leakage assay) *in vivo*.

Results: Expression of cav-1 in isolated cortex microvessels, hippocampus and ipsilateral cortex of ischemic brain was down-regulated after rats were treated with 2 hours of focal cerebral ischemia plus 6, 24 and 72 hours of reperfusion. The down-regulation of cav-1 was correlated with the increased activities of MMP-2 and -9, decreased level of tight junction protein ZO-1 and increased BBB permeability. Treatment of reserved the protein level of cav-1, inhibited MMPs activity and BBB permeability. Cav-1 knockdown remarkably increased MMPs activity in cultured medium of BMECs. Cav-1 deficiency mice displayed higher MMPs activity and BBB permeability than wild-type mice. Interestingly, the effects of L-NAME on MMPs activity and BBB permeability was partly reversed in cav-1 deficiency mice.

Conclusion: Our data suggest that cav-1 plays important roles in regulating MMPs and BBB permeability in focal cerebral ischemia and reperfusion injury. The effects of L-NAME on MMPs activity and BBB permeability are partly mediated by preservation of cav-1.

References:

1. Gu, Y., Dee, C. M. and Shen, J. (2011) Interaction of free radicals, matrix metalloproteinases and caveolin-1 impacts blood-brain barrier permeability. Front Biosci (Schol Ed), 3, 1216-1231.

2. Shen, J., Ma, S., Chan, P., et al. (2006) Nitric oxide down-regulates caveolin-1 expression in rat brains during focal cerebral ischemia and reperfusion injury. J Neurochem, 96, 1078-1089.

3. Gu, Y., Zheng, G., Xu, M. et al. (2012) Caveolin-1 regulates nitric oxide-mediated matrix metalloproteinases activity and blood-brain barrier permeability in focal cerebral ischemia and reperfusion injury. J Neurochem, 120, 147-156.

COMBINED MICROPET IMAGING AND MICRODIALYSIS IN A STUDY OF OXYCODONE ACTIVE UPTAKE IN RAT BRAIN

S. Gustafsson[1], J. Eriksson[2], S. Syvänen[3], O. Eriksson[2], J. Dunhall[1], M. Hammarlund-Udenaes[1], G. Antoni[2]

[1]Department of Pharmaceutical Biosciences, Translational PKPD, [2]Department of Medicinal Chemistry, Preclinical PET Platform, [3]Department of Public Health and Caring Sciences, Molecular Geriatrics, Uppsala University, Uppsala, Sweden

Objectives: The blood-brain barrier is a dynamic entity protecting the brain from toxic

insults and contributing to its normal function. Though, it constitutes an obstacle for the development of drugs aimed to act in the central nervous system (CNS), as various mechanisms efficiently prevent drugs from entering the brain to sufficient concentrations. However, previous microdialysis studies show that certain substances, like oxycodone, have a net active uptake into the brain from the blood as opposed to many other compounds [1]. To date, microdialysis is the gold standard method in measuring the unbound, pharmacologically active drug concentration in tissues, like brain, in living organisms. However, it is invasive and clinically only used in severe head injury patients. As a complement positron emission tomography (PET) is a minimally invasive technique and allows for the analysis of total drug concentrations within the brain. In comparison to PET which only gives the ratio of total concentration of drug in brain compared to total or unbound concentration in plasma, the so called Kp or Kp_u, microdialysis gives us the somewhat more relevant ratio of unbound concentration in brain versus unbound concentration in plasma, the so called Kp_{uu} [2]. The aim of this study was to set up simultaneous brain microdialysis sampling and microPET imaging to investigate if the active uptake of oxycodone, observed in microdialysis studies is also apparent in imaging studies. The study also aimed to combine results from simultaneous microdialysis and microPET measurements in an attempt to model and estimate the unbound concentration of drug from the total concentration achieved by PET imaging.

Methods: Animals were divided into two groups, where one group was analyzed with microPET only (n=5) and the other by combined microPET and microdialysis sampling (n=5). Anesthetized Sprague Dawley rats received a continuous i.v. infusion of [N-methyl-11C]oxycodone in a tracer dose together with a cold dose of oxycodone (0.3mg/kg/h) during 1h. Discrete blood sampling was performed during the infusion and 1h after the end of the infusion. Microdialysis and microPET imaging was performed during the entire experiment of 2h. Plasma and microdialysis samples were analyzed using LC-MS/MS.

Results: A protocol for simultaneous brain microdialysis sampling of oxycodone and microPET imaging of [N-methyl-11C]oxycodone in rats was successfully implemented. Brain and plasma pharmacokinetic profiles were obtained and preliminary analysis indicated that [N-methyl-11C]oxycodone is rapidly transported into the brain with a higher concentration in brain compared to blood. Oxycodone concentrations measured by microdialysis (unbound concentrations) and PET (total concentrations) differed in magnitude in the brain, but the ratio between the two types of measurements were fairly stable over time.

Conclusion: PET imaging is an important tool in drug development and an excellent method for the translation of in vivo animal data to clinical reality. Nevertheless, further optimization of the PET technique together with supporting techniques is needed for PET to reach its fullest potential as a translational tool.

References:

1. Bostrom, E. et al. Drug Metab Dispos, 2006. 34(9): p. 1624-31.

2. Hammarlund-Udenaes M. et al. Pharm Res, 2008. 25(8): p. 1737-50.

CORRELATIONS OF THE IMMUNOREACTIVITIES OF DYSTROGLYCAN COMPLEX AND LAMININ IN CEREBRAL VESSELS RELATED TO THE BLOOD-BRAIN BARRIER PERMEABILITY

M.G. Kálmán, J. Mahalek, S. Sadeghian, E. Faragó, N. Varga, K. Pócsai

Anatomy, Histology and Embryology, Semmelweis University, Budapest, Hungary

Introduction: Former studies revealed characteristic immunohistochemical alterations of cerebral vessels following lesions. Laminin which usually not detectable in the formaldehyde fixed intact brain tissue except some circumventricular organs (CVO) becomes detectable following lesions (Krum et al. 1991; Szabó and Kálmán, 2004), whereas the immunoreactivity of the lamina basalis-receptor beta-dystroglycan which delineates the vessels of intact brain disappeares (Szabó and Kálmán, 2008, Kálmán et al., 2011). These alterations are supposed to be indirect markers of gliovascular detachment which occurs following lesions and may have role in the impairment of blood-brain-barrier (BBB).

Aims:

a) to estimate the temporal and territorial correlations between the *post-lesion* exudate-penetrated area and the cerebrovascular immunoreactivities of the aforementioned substances;

b) to compare the vascular immunoreactivities of CVOs having 'leaky' BBB to that of the non-leaky intact cerebral vessels and to that of the 'leaky' vessels of the lesioned areas. Utrophin and alpha-dystrobrevin which belong to the dystroglycan complex were also studied.

Methods: Cryogenic lesions were performed in deep ketamine-xylazine anaesthesia with a copper rod cooled surrounded with dry ice and contacted the brain surface covered only with leptomeninx. Animals were transcardially perfused by buffered 4% paraformaldehyde under similar anaesthesia, and immunohistochemical reactions were performed in floating sections cut by Vibratome. *Post-lesion* exudation due to BBB impairment was estimated with immunohistochemical detection of plasma-fibronectin and immunoglobulins exudated and by filling the animals with rhodamine dye ten minutes before perfusion. Condition of vessels was estimated by the immunoreactivities of laminin, beta-dystroglycan as well as that of alpha-dystrobrevin and utrophin.

Results: The main results were: a) different markers mark similar areas of BBB leakage following lesion; b) in this area vessels became immunopositive to laminin but negative to beta-dystroglycan and alpha-dystrobrevin; c) where the tissue was not directly lesioned but the postlesional exudate extended (corpus callosum) over it only laminin immunoreactivity change but not that of dystroglycan; d) leaky CVO vessels are immunopositive to laminin (see also Krum et al., 1991) and utrophin like vessels in the territory of lesion but - unlikely - they were positive to dystroglycan and dystrobrevin (i.e. similar to the intact vessels); e) extracerebral (meningeal) vessels were laminin positive but dystroglycan- and dystrobrevin negative, similar to the vessels following lesions.

Conclusion: It suggests that alterations of the immunoreactivities studied here, although occur together in the lesioned vessels and probably parallel with alterations of gliovascular connections, may refer to independent steps of these alterations.

References:

Krum et al. (1991) Exp Neurol 111:151-165.;

Szabó and Kálmán (2004) Neuropath Appl Neurobiol 30:169-177;

Szabó and Kálmán (2008) Curr Neurovasc Res, 5: 206-213;

Kálmán et al. (2011) Histo Histopathol 26:1435-1452.

COMBINATORIAL ANTIOXIDANTS ATTENUATES BLOOD-BRAIN BARRIER DISRUPTION AFTER ISCHEMIC STROKE

J.E. Lee[1], J.Y. Kim[1], J.Y. Choi[1], S.-T. Lee[2], K.-M. Lee[2]

[1]Anatomy, Brain Korea 21 Project for Medical Science, Yonsei University, College of Medicine, [2]Neurology, Seoul National University, Seoul, Republic of Korea

Objectives: Cell to cell junction proteins in the brain endothelial cells plays an important role in maintaining the integrity of blood brain barrier (BBB) [1, 2]. Previous studies demonstrate that significant amounts of reactive oxygen species (ROS) /reactive nitrogen species (RNS) are trigger for many downstream pathways that directly mediate BBB compromise such as oxidative damage, and tight junction modification. These observations suggest that ROS are key mediators of BBB breakdown and implicate antioxidants as potential neuroprotectants in condition like ischemic stroke [3]. Among them, dehydroascorbic acid (DHA), oxidative form of vitamin C which is BBB penetrative, is considered to be a powerful agent to detoxify reactive oxygen species (ROS)-mediated damages. However, its effects are not investigated yet in the TJPs after cerebral ischemia. Therefore, in this study, we examined whether intravenous administration of DHA and other antioxidants could attenuate TJPs breakdown and BBB disruption after cerebral ischemia.

Methods: Sprague-Dawely rats (275±10g, 8w) were subjected to 60 min middle cerebral artery occlusion (MCAO) using an intra-luminal filament. Then, single dose of DHA (100mg/kg/ml), Glutathione (500mg/kg/ml), and Melatonin (10mg/kg/ml) were administered intravenously following MCAO. At 1st, 3rd, and 7th day following injury, behavior tests such as rotarod and limb placing test

were performed in experimental control and combinatorial antioxidants treated group. As well, TTC staining was conducted to measure the brain infarct volume. Finally, immunohistochemistry and western blotting were carried out to check TJPs regulatory factors after MCAO.

Results: Results show that combinatorial antioxidants significantly reduced the brain infarct volume and improved behavioral performance after cerebral ischemia. Of interest, the expression of TJPs and known as TJP regulatory factors were varied in combinatorial antioxidants treated group, probably implying that they are associated with the maintenance of BBB integrity under MCAO mediating damage.

Conclusions: Taken together, the present data suggest that combinatorial antioxidants treatment exerts protective effects on TJPs by reducing BBB disruption following stroke.

References:

[1] Histochem Cell Biol (2008) 130:55-70,

[2] Nat Cell Biol, vol (2008) 10. No.8 923-934,

[3] Free radical Res (2009) 43 (4): 348-364.

Support: This work was supportd by Basic Science Research Program through the National Research Foundation of KOREA (NRF) funded by the ministry of Education, Science and Technology (2012-0005827)

THE INTERACTIONS BETWEEN NITRIC OXIDE, CAVEOLIN-1 AND AUTOPHAGOSOME CONTRIBUTE TO OXYGEN-GLUCOSE DEPRIVATION-INDUCED CLAUDIN-5 DEGRADATION IN ENDOTHELIAL CELLS

J. Liu[1,2], J. Weaver[2], K. Liu[2], X. Jin[2], W. Liu[2]

[1]Tongji Hospital of Tongji University, Shanghai, China, [2]College of Pharmacy, University of New Mexico, Albuquerque, NM, USA

Objectives: Degradation of tight-junction proteins is a decisive step in hypoxic blood-brain barrier (BBB) breakdown in stroke (1). In BBB, claudin-5 plays a major role in forming tight junction strands to seal the intercellular space and maintain the function of paracellular barrier (2). In a recent study, we found that 2-hr oxygen-glucose deprivation (OGD) induced rapid translocation of claudin-5 in mouse brain microvascular endothelia cells bEND3, which was mediated by relocated caveolin-1 (Cav-1) (3). To further understand this process, the current study aimed to answer the following questions:

1) under OGD condition, what mediates Cav-1 translocation, and

2) what is the fate of translocated claudin-5 and Cav-1 if OGD continues to 4 hrs?

Methods: bEND3 cells were cultured in DMEM with 15% FBS on 60 mm dishes coated with collagen at 37°C in 5% CO_2/95% air. Cells at 80% confluence were exposed to OGD for 2 or 4 hrs without reoxygenation and glucose. Control cultures were incubated with normal DMEM without FBS. To verify a role of lysosome and autophagy in claudin-5 degradation, two lysosome inhibitors bafilomycin A1 (BFA1) and 3-Methyladenine (3-MA) were added to cells during OGD treatment. To demonstrate a role of iNOS-derived NO in mediating Cav-1 redistribution, the selective iNOS inhibitor 1400W and the NO scavenger Carboxy-PTIO were applied. Immediately after 2-hr OGD treatment, conditioned medium was collected for nitric oxide (NO) detection with electron paramagnetic resonance (EPR) (4, 5). The extraction of the total cellular lysates and subcellular fractions and detection of proteins by western blot were performed (3). Lysosome isolation kit was used to isolate lysosome from bEND3 cells according to manufacturer's protocol. The caveolae-enriched fractions were isolated as described previously (6).To determine whether Cav-1-mediated claudin-5 redistribution is a preceding step required for its subsequent degradation, knockdown of Cav-1 was done with Cav-1 siRNA (3). Coimmunoprecipitation was performed to determine the interaction of iNOS with Cav-1 and immunostaining were used to detect Cav-1 and claudin-5 (3).

Results: When OGD was prolonged to 4 hrs, claudin-5 was degraded. In this degrading process, we observed a transient colocalization of Cav-1, claudin-5 and LC3B (microtubule-associated protein light chain 3B) in autophagosome-enriched fractions as well as caveolae lipid raft fractions at 2-hr OGD, and this colocalization did not disappear at 4-hr OGD when the fusion of lysosome and autophagosome was inhibited by BFA1. Inhibition of lysosome or autophagy, but not

proteasome, blocked claudin-5 degradation after 4 hrs of OGD. Moreover, we found that iNOS-derived NO triggered rapid caveolin-1 translocation induced by 2-hr OGD, which was the important step preceding the degradation of claudin-5 by the lysosome.

Conclusions: Under OGD condition, NO triggers rapid translocation of caveolin-1 to the cytosol, which leads to the dissociation of claudin-5 from the cytoskeletal framework. When OGD continues, the translocated claudin-5 will be degraded in an autophagy-dependent manner.

Reference:

[1] PLoS One. 2011 Feb 22;6(2):e16760.

[2] J Cereb Blood Flow Metab. 2012 Jul;32(7):1139-51.

[3] J Neurosci. 2012 Feb 29;32(9):3044-57.

[4] Anal Biochem. 2001 Nov 1;298(1):50-6.

[5] J Biol Chem. 2004 Feb 6;279(6):3933-40.

[6] Anal Biochem. 2003 Feb 1;313(1):1-8.

THE PROTECTIVE ROLE OF TONGXINLUO ON BLOOD-BRAIN BARRIER AFTER ISCHEMIA-REPERFUSION BRAIN INJURY

Y. Liu[1], G. Tang[2], Y. Sun[3], G.-Y. Yang[1,2], J.-R. Liu[1]

[1]Department of Neurology, Ruijin Hospital, School of Medicine, [2]Neuroscience and Neuroengineering Research Center, Med-X Research Institute and School of Biomedical Engineering, Shanghai Jiao Tong University, [3]Department of Neurosurgery, Ruijin Hospital, Shanghai Jiao Tong University School of Medicine, Shanghai, China

Objectives: TXL is a compound prescription for the treatment of coronary heart disease,[1] and stabilizing the vulnerable plaques.[2] We focus on the effect of TXL on blood brain barrier (BBB) including edema formation and tight junction protein rearrangement, as well as inflammation response after transient middle cerebral artery occlusion (tMCAO). To explore the protection mechanism of TXL on ischemia induced BBB damage.

Methods: Adult CD1 male mice (n=132) were randomly divided into control group, TXL pretreatment group and TXL pre-post treatment group. Mice in TXL pretreatment group were given TXL solution by 1g/kg/day orally for 7 days. Mice in pre-post treatment group were continuously given TXL 7 days before and 14 days after tMCAO. Rotarod and neurological scores were evaluated at days 1, 3, 7 and 14 following tMCAO. Brains were harvested for infarct area, edema, and Immunofluorescence staining analysis following 1 and 3 days of tMCAO. Cytokines IL-6, IL-1β and TNF-α RNA expression, and BBB permeability were determined after tMCAO.

Results: TXL pretreatment and pre-post treatment improved rotarod behavior outcomes and neurological scores and decreased infarct size and hemispheric swelling compared to the control ($p< 0.05$). Reduced Evans blue extravasation and IgG leakage, fewer MPO positive cells and up-regulation of tight junction protein expression were also observed in both groups. Moreover, TXL pre-post treatment group showed a better recovery than TXL pretreatment group in BBB permeability, infarct volume, edema and tight junction protein integrity. IL-6, IL-1β and TNF-α in pre-post treatment group changed accordingly compared to the control ($p< 0.05$) while the expression in TXL pretreatment group increased ($p< 0.05$).

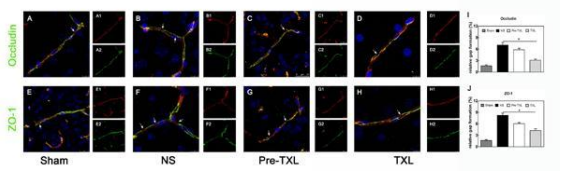

Figure 1. ZO-1 and Occludin disruption were rescued by TXL treatment. Tight junction protein ZO-1 and Occludin in sham group (**A, A1, A2** and **E, E1, E2**), in the control mice brains following 24 hours of tMCAO (**B, B1, B2** and **F, F1, F2**). in the TXL pretreatment group following 24 hours of tMCAO (**C, C1, C2** and **G, G1, G2**) and TXL pre-post treatment group (**D, D1, D2** and **H, H1, H2**). Scale bar=10 μm. Quantitative results of Occludin and ZO-1 measured gap length (**I, J**).

Conclusions: TXL pretreatment and pre-post treatment effectively protected the brain from BBB disruption, and pre-post treatment has better outcomes, suggesting that TXL should be continuously used after stroke rather than being a single prophylactic neuroprotective drug.

References:

1. Jia YL, Huang FY, Zhang SK. assessment of the quality of randomized controlled trials in treating coronary heart disease by chinese patent medicine. *Zhongguo Zhong Xi Yi Jie He Za Zhi* 2012; 32: 560-568.

2. Li Z, Yang YJ, Qin XW, Ruan YM, Chen X, Meng L, *et al.* effects of tongxinluo and simvastatin on the stabilization of vulnerable atherosclerotic plaques of aorta in aortic atherosclerosis and molecular mechanism thereof: A comparative study with rabbits. *Zhonghua Yi Xue Za Zhi* 2006; 86: 3146-3150.

EVALUATION OF PERMEABILITY AND METABOLISM OF 20(S)-PROTOPANAXADIOL IN AN IN VITRO BLOOD BRAIN BARRIER MODEL, HCMEC/D3 HUMAN BRAIN ENDOTHELIAL CELLS

W. Meng[1], C.A. Ortori[2], D.A. Barrett[2], W. Jia[3], A. Al-Shehri[4], T.L. Parker[1]

[1]School of Biomedical Sciences, [2]Centre for Analytical Bioscience, School of Pharmacy, University of Nottingham, Nottingham, UK, [3]Brain Research Centre, University of British Columbia, Vancouver, BC, Canada, [4]Directorate of Forensic Science, Riyadh, Saudi Arabia

Objective: 20(s)-Protopanaxadiol (PPD), one of ginseng's pharmacologically active components, has been shown to have anti-depressant[1] and antitumor properties[2]. However, despite its effects on the brain there is no information on the pharmacological interaction between PPD and capillary endothelial cells that from blood brain barrier (BBB). Therefore to clarify this possible interaction, cellular uptake, drug permeability and metabolism of PPD have been examined in an immortalized human brain endothelial cell line, hCMEC/D3.

Methods: The functional integrity of hCMEC/D3 barrier formation was assessed by immunocytochemistry determining tight junction-related proteins, zenula occludens-1 (ZO-1) and by measuring permeability coefficients (Pe) of fluorescent dextrans (4-40kDa) and [14C]-sucrose. PPD permeability experiments were performed using Transwell inserts where PPD was added to the upper (donor chamber) and transported PPD in lower (receptor chamber) analyised by LC-MS/MS. PPD was also incubated with hCMEC/D3 cells for various times periods and the intracellular and extracellular PPD concentration and its metabolites was analyzed by LC-MS/MS.

Results: The hCMEC/D3 cells formed tight junctions evidenced by positive immunostaining for ZO-1 and by TEM. The Pe for dextrans was in agreement with that found by Weksler et al.[3] PPD was transported via a combination of carrier-mediated and diffusion transport mechanisms. The cellular uptake of PPD reached saturation after 3 h. Over a period of 24 h, 19.8% of PPD penetrated through hCMEC/D3 cell layer. Metabolic studies suggested that the predominant metabolites of PPD formed via the oxidation of 24, 25-double bond to yield 24,25-epoxides followed by one of the oxygen atoms introduced into the either aglycone or side chain of the PPD. This metabolic mechanism is similar to the mechanism of PPD with microsome fractions from rat and human livers.[4]

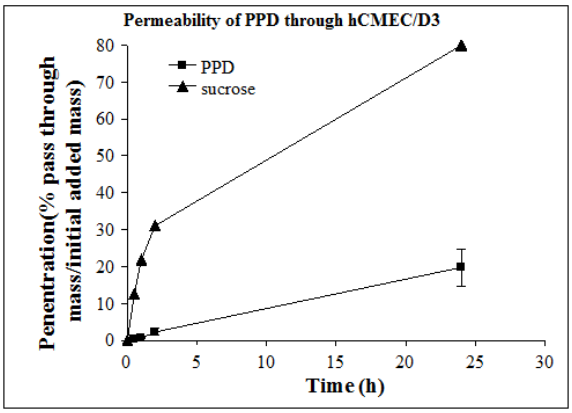

[permeability of PPD in hCMEC/D3]

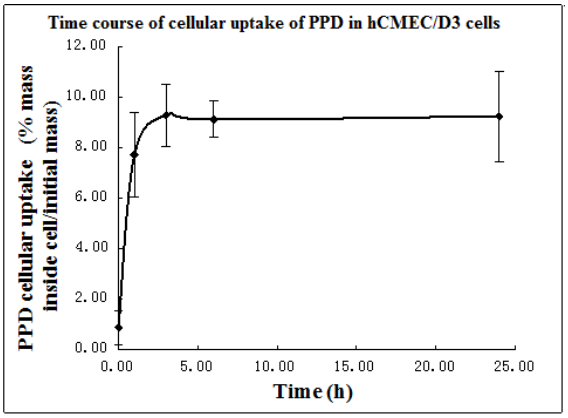

[cellular uptake of PPD in hCMEC/D3]

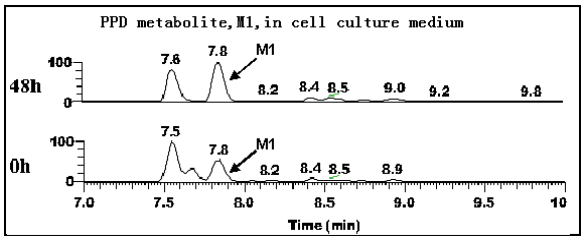

[Chromatogram of PPD metabolite]

Conclusions: At low concentrations and over a period of 24 h only 19.8% of the initial concentration of PPD was transported across the BBB. Of this only 20% was metabolised suggesting that the observed anti-depressant effects on the intact brain is due to the native PPD and not its metabolites.

References:

1. Liu GY, Bu X, Yan H, and Jia WW. 2007. J Nat Prod 70:259-264;

2. Hui YZ, Yang ZR, Yang ZQ, and Ge Q. 2006. inventors; CN-Know How Intellectual Property Agent Limited, assignee. China Patent CN 200610027507.1;

3. Weksler BB, Subileau EA, and et al . 2005. FASEB J 19:1872-1874;

4. Li L, Chen X, Li D, and Zhong D. 2011. Drug Metab Dispos 39:472-483.

DEVELOPMENT OF A BRAIN-TUMOUR-ENDOTHELIAL 3-D TRIPLE CO-CULTURE MODEL OF THE BBB FOR STUDIES ON TARGETING BRAIN TUMORS USING LIPID CARRIERS

T. Parker[1], A. Al Shehri[1], M.E. Favretto[2], H. Lu[3], W. Meng[2], P. Kallinteri[2]

[1]School of Biomedical Sciences, University of Nottingham, Nottingham, [2]Department of Pharmacy, University of Kent, Kent, UK, [3]Insititute of Neurobiology, School of Medecine, Xi´an Jiaotong Unversity, Xi´an, China

Objectives: To develop an in vitro 3-D model of the brain-tumor-endothelial interface to study transport of carrier born anti tumor drugs.

Methods: Construction of the triple co-culture model: hCMEC/D3 cells 1x 10^5 were grown to confluency over period of two days on transwell inserts; organotypic brain slices were prepared 7 day previously from 1day old rat pups (1) and added to the hCMEC/D3 and co-cultured for a further 7days. Pre-prepared spheroid cultures of medulloblastoma cells (DAOY) were then added to the brain slice and allowed to attach and invade the brain tissue over a period of 2 days (2). At the end of this period the triple co-culture models was ready for experimental use. The integrity and structure of the tight junctions between hCMEC/D3 was evaluated using fluorescent dextrans of mol weight ranging between 4Kd - 70kd and EM and immunocytochemistry Lipid carriers: The thin film method was used for preparation of liposomes from Distearoyl-phosphatidylcholine and Cholesterol encorporating either(Bodipy-DHPE or Rhod-DHPE) or tritiated cholesterol to label the liposomes (3).

Results: The hCMEC/D3 cells formed a uniform layer on the inserts onto which the brain slice firmly adhered with DAOY spheroids penetrating the brain slice (fig1).

Fig 1. Semi-thin section of triple co-culture of endothelial cells (E), brain slice (BS) and Daoy aggregate (Ag). Transwell membrane filter (F).

Immunostaining for zonula occluden-1 and EM micrographs showed extensive tight junction formation between hCMEC/D3 cells with a permeability coefficient of $8.02´10^{-3}$ cm/min $\pm 9.26´10^{-6}$ for 4 kDa FITC-dextran and $0.055´10^{-3}$ cm/min $\pm$ $6.96´10^{-6}$ for 70 kDa FITC-dextran . The culture integrity was maintained for several weeks. After a period of 2h and 5 hr uptake of labelled liposomes was 1.5% and 3.25% respectively. The liposomes were located in the hCMEC/D3 layer but interestingly only in cells not in contact with the brain slice indicating that the junctional complex might be tighter in these regions preventing liposome access.

Conclusion: The 3-D triple co-culture model more closely represents the in vivo conditions enabling better understanding of how drugs penetrate the BBB and as model for understanding metastatic tumor spread into the brain.

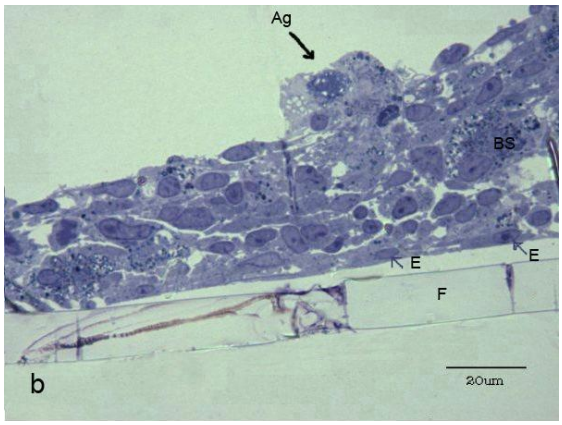

[Figure 1]

References:

1.Hai-xia, L., Levis, H., Liu,Y., Parker, T.L. (2011) Organotypic slices culture model for cerebellar ataxia: Potential use to study Purkinje cell induction from neural stem cells. Brain Research Bulletin 84 (2011) 169-173.

2.Meng, W., Kallinteri , P., D.A. Walker, Parker, T.L., Garnett, M.C. (2007) Evaluation of poly (glycerol-adipate) nanoparticle uptake in an in vitro 3-D Brain Tumour Co-Culture Model. Experimental Biology and Medicine 232 pp1100-1107

3.Favretto, ME; Marouf, S; Ioannou, P; Antimisiaris, SG; Parker, TL & Kallinteri, P (2009) Arsonoliposomes for the Potential Treatment of Medulloblastoma. Pharmaceutical Res. 26; pp2237-2246

EXACERBATION OF METHAMPHETAMINE-INDUCED NEUROTOXICITY IN DIABETES. NEUROPROTECTION BY NANODRUG DELIVERY OF NEUROTROPHINS

H.S. Sharma[1], J.V. Lafuente[2], R. Patnaik[3], D.F. Muresanu[4], A. Sharma[5]

[1]Surgical Sciences, Anesthesiology & Intensive Care Medicine, Uppsala University, Uppsala, Sweden, [2]Neuroscience, University of Basque Countries, Bilbao, Spain, [3]Biomaterials, School of Biomedical Engineering, National Institute of Technology, Banaras Hindu University, Varanasi, India, [4]Clinical Neurosciences, University of Medicine & Pharmacy, University Hospital, Cluj-Napoca, Romania, [5]Surgical Sciences, Anesthesiology & Intensive Care Medicine, Uppsala University, University Hospital, Uppsala, Sweden

The possibility that diabetes aggravates methamphetamine-induced neurotoxicity and neurotrophins could induce suitable neuroprotection was investigated in a rat model. Rats were made diabetic by administering streptozotocine (75 mg/kg, i.p. once daily for 3 days) that resulted in enhanced blood glucose level 22±4 mM/L within 2 weeks. Normal rats (blood glucose level 6±2 mM/L) were used as controls. Methamphetamine (METH) was injected in control or diabetic rats (40 mg/kg, i.p.) and the animals were allowed to survive 4 h after its administration. At the end of 4 h, blood-brain barrier (BBB) permeability to Evans blue (EBA) and radioiodine ($^{[131]}$ Iodine), brain electrolytes (Na^+, K^+, Cl^-) and water content, and brain pathology were examined using standard procedures.

Normal rats showed profound disruption of cortical BBB to EBA (+105 %) and radioiodine (+134 %) after METH administration as compared to the saline control group. METH intoxication also resulted in profound cortical edema formation (water content +1.5 % from control) and alterations in tissue electrolytes (increase in brain Na+ by 40 %) and K+ by 25 % and a decrease in Cl- by 30 %). The number of cortical neurons showing damages increased remarkably (+34 %) in METH treated animals from the control group. These pathological changes were markedly exacerbated in diabetic rats after identical METH administration, Thus, diabetic rats show about 230 % increase in EBA and 320 % in radioiodine extravasation in the cortical areas after METH administration compared to saline controls. The brain water also increased by +3.2% and electrolytes changes were most severe in diabetic rats (Na^+ + 64%, K^+ +42% and Cl^- - 44%) after METH. Neuronal injuries showed about 3- to 4- fold increase in diabetic rats following METH intoxication. Intravenous injection of a mixture of brain derived neurotrophic factor, BDNF (5µg/kg) and glia derived neurotrophic factor (GDNF, 5µg/kg) either 30 min before or 30 min after METH administration significantly reduced BBB disruption, brain edema formation and neuronal injuries in normal but not in diabetic rats. However, when these neurotrophins were tagged with TiO2 nanowires and administered in identical doses, diabetic rats also showed pronounced neuroprotection. Interestingly, nanowired neurotrophins were able to induce marked neuroprotection in normal and diabetic

rats even if they are administered 60 to 90 min after METH intoxication, a feature not seen by normal delivery of neurotrophins. Taken together, our results for the first time show that METH neurotoxicity was aggravated in diabetics and nanowired delivery of neurotrophins could induce pronounced neuroprotection.

CAVEOLIN-1 IS A CRUCIAL MOLECULAR TARGET IN BLOOD-BRAIN-BARRIER (BBB) DISRUPTION AND INFARCTION ENLARGEMENT DURING CEREBRAL ISCHEMIA-REPERFUSION INJURY

J. Shen, Y. Gu

School of Chinese Medicine, Research Centre of Heart, Brain, Hormone & Healthy Aging, The University of Hong Kong, Hong Kong, Hong Kong S.A.R.

Aims: Caveolin-1, a 22 kDa membrane integral protein, plays important roles in many pathological process but its roles in regulating BBB permeability are unknown yet. Our previously studies revealed that caveolin-1 were downregulated in ischemic rat brains and the loss of caveolin-1 is associated with nitric oxide (NO) production (J Neurochem 2006;96(4):1078). In present study, we aimed to explore the roles of caveolin-1 in regulating BBB permeability. We hypothesized that caveolin-1 might elevated BBB permeability though regulating NOS and matrix metalloproteinases (MMPs) pathway in cerebral ischemia-reperfusion injury.

Methods: SD rats were subject to different time courses of middle cerebral artery occlusion (MCAO). We investigated the expression of caveolin-1, the activations of MMP-9, tight-junction (TJ) protein, BBB permeability and infarction volume in rat and mouse models of cerebral ischemia-reperfusion injury in vivo and hypoxic rat brain microvascular endothelial cells (BMECs) in vitro.

Results:

(1) The decreased caveolin-1 expression was associated with the increases of NO and peroxynitrite production, MMP-2/9 activation, TJ protein degradation and BBB hyper-permeability;

(2) L-NAME, a non-selective NOS inhibitor, abolished the caveolin-1 reduction, MMP-2/9 activations, microvascular hyperpermeability and reduced infarction sizes in the ischemic brains;

(3) Cavolin-1 knockdown by siRNA increased the secretion of MMP-2 to the culture medium;

(4) After focal cerebral ischemia-reperfusion, cav-1 deficiency mice displayed higher MMPs activities and BBB permeability than wild-type mice;

(5) The effects of L-NAME on MMPs activity and BBB permeability was partly reversed in cav-1 deficiency mice.

Conclusion: Caveolin-1 can inhibit NOS and MMPs activity, protect TJ proteins from degradation and reduce the BBB permeability in cerebral ischemia-reperfusion injury. The interaction of reactive nitrogen species, caveolin-1 and MMPs forms a positive feedback loop which provides amplified impacts on BBB dysfunction during cerebral ischemia-reperfusion injury.

Acknowledgements: This work is supported by RGC GRF Grant (No. 777611M).

INTERACTION OF MELANOMA CELLS WITH BRAIN ENDOTHELIAL CELLS

I. Wilhelm, C. Fazakas, A.G. Végh, J. Haskó, J. Molnár, Á. Nyúl-Tóth, P. Nagyőszi, G. Váró, I.A. Krizbai

Institute of Biophysics, Biological Research Centre, Szeged, Hungary

Objectives: Brain tumours are life threatening pathologies with limited therapeutic options, representing an important cause of death in cancer patients. The majority of the tumours of the central nervous system (CNS) are metastases, among which melanoma is one of the most common. Since the CNS lacks a lymphatic system, tumor cells can only reach the brain parenchyma by hematogenous metastasis formation. During this process the first host cell type encountered by circulating melanoma cells are cerebral endothelial cells, which form the morphological basis of the blood-brain barrier (BBB). Despite the undisputable clinical importance, little is known about the mechanisms of extravasation of melanoma cells through the BBB. Therefore, our aim was to identify key molecules involved in the interplay between melanoma and brain endothelial cells during metastasis formation.

Methods: In order to study the routes and mechanisms of transendothelial migration of melanoma cells we have developed a transmigration experimental setup consisting of brain endothelial cells cultured on large pore size filter inserts and fluorescently labeled melanoma cells plated onto the apical side of the endothelial layer.

Results: We have shown that melanoma cells coming in contact with brain endothelial cells disrupted the tight junctions of endothelial cells and used (at least partially) the paracellular transmigration pathway. During this process melanoma cells produced and released large amounts of proteolytic enzymes, mainly gelatinolytic serine proteases including seprase. Inhibition of serine proteases decreased significantly the number of melanoma cells migrating through brain endothelial monolayers.

We have also investigated the role of the Rho/ROCK pathway in the interaction of melanoma and brain endothelial cells. ROCK inhibition using Y27632 induced a shift of melanoma cells to mesenchymal phenotype characterized by an elongated, fibroblastoid cell morphology with large actin-rich protrusions and several filopodia. We observed that the presence of Y27632 increased the number of melanoma cells attached to the brain endothelium, strengthened the adhesion force between melanoma and endothelial cells, and increased the number of melanoma cells migrating from the apical to the basolateral side of the brain endothelial monolayer. In vivo the ROCK inhibitor promoted formation of parenchymal brain metastases. In order to differentiate between the role of Rho/ROCK in endothelial and melanoma cells we used an irreversible Rho inhibitor and performed transmigration experiments. We have shown that melanoma-endothelial interaction is mainly influenced by the Rho/ROCK signaling in melanoma cells.

Conclusions: Our results indicate that release of serine proteases by melanoma cells and disintegration of the interendothelial junctional complex are main steps in the formation of brain metastases in malignant melanoma. We have also shown that shift of melanoma cells to the mesenchymal phenotype enhances adhesion to the brain endothelium and promotes transendothelial migration and brain metastasis formation.

EFFECT OF FASUDIL HYDROCHLORIDE ON NEURONAL APOPTOSIS AND BLOOD BRAIN BARRIER PERMEABILITY FOLLOWING FOCAL CEREBRAL ISCHEMIA IN RATS

H. Chen, Q.-H. Cui, **Y.-B. Zhang**, J.-M. Li

Dept of Neurology, Beijing Friendship Hospital, Beijing, China

Introduction and objectives: The mechanisms of the injury and protection of neurovascular unit (NVU) after cerebral ischemia are recently important issue in stroke research. The blood brain barrier (BBB) takes part in to form NVU, and Claudin 5 is a key determinant of transendothelial resistance at the BBB, and alterations in its interacting proteins can lead to the disruption of the barrier function. It is reported that Rho kinase inhibitor Fasudil hydrochloride has the effects of reducing cerebral vasospasm,antiinflammation and improving neurological funtion recovery after stroke. However, the effect of Fasudil hydrochloride on the expression of Claudin 5 has't been reported. We hypothesize that a Rho kinase inhibitor Fasudil hydrochloride can protect the integrity of the BBB via preserving tight junction (TJ) proteins after stroke. This would implicate that Rho kinase is involved in the pathophysiologic breakdown of the BBB after ischemia.

Methods: Focal cerebral ischemic model was established by using the intraluminal suture to let the right middle cerebral artery occlusion(MCAO) in SD rat. Rats were divided randomly into sham group (SG), ischemic model group(MG), physiologic saline group (PG) and Fasudil treatment group (FG). The later three groups were further divided into four subgroups according reperfusion time at 6h, 1d,3d and 7d. Fasudil was administrated immediately after reperfusion by 15 mg/kg abdominally and repeatedly once each day. The neurological deficit was evaluated by Longa´s method. The change of permeability of blood brain barrier (BBB) was tested by detecting the content of Evan's blue (EB). Neuronal apoptosis was tested by TUNEL method. The expressions of Rho A, GAP 43 and Claudin-5 were detected by immunohistochemistry and Western Blot.

Results: The results showed that Fasudil significantly improved neurological function recovery ($P < 0.01$). The EB content was

significantly lower in Fasudil group than that in PG at 24 h after ischemia($P < 0.01$). Compared with PG and MG, the number of apoptotic cells reduced significantly in FG on 1 d, 3 d and 7 d ($P < 0.01$). Fasudil also significantly suppressed the expression of Rho A, upregulating the expressions of GAP 43 and Claudin 5 at 7d after focal cerebral ischemia($P < 0.01$).

Conclusions: These suggested that Rho kinase inhibitor Fasudil hydrochloride protect neuron from apoptosis and ameliorate BBB permeability after focal cerebral ischemia. Rho kinase may play an important role in the injury of neurovascular unit. Rho kinase might be a new therapeutic target in the treatment of ischemic cerebrovascular disease.

PRECONDITIONING WITH SULFORAPHANE AND ALLYL ISOTHIOCYANATE TO INDUCE CEREBROVASCULAR PROTECTION

N. Zhou[1,2], J. Xiang[1], R. Keep[1]

[1]Neurosurgery, University of Michigan, Ann Arbor, MI, USA, [2]Pharmacology, Yunnan University of Traditional Chinese Medicine, Kunming, China

Objectives: This study examines the extent to which two natural dietary components, sulforaphane (SF; a component of cruciferous vegetables) and allyl isothiocynate (AITC; a component of mustard seed) may protect against the consequences of stroke. It particularly focuses on the cerebrovascular protective effects of preconditioning with these agents.

Methods: In vivo, male Sprague-Dawley rats were treated with SF (5 mg/kg, i.p), AITC (10 mg/kg, i.p) or vehicle. 24 hrs later the rats underwent 2 hours of middle cerebral artery occlusion (MCAO) with 2 hours of reperfusion. Rats were used either for brain edema measurement or assessment of blood-brain barrier (BBB) disruption with Evan's blue. The in vitro protective effects of SF were examined in brain endothelial cells (b.End3 cells). Cells were exposed to SF (1-20 µM) or vehicle for 24 hours prior to exposure to oxidative stress (0.5 mM H_2O_2, 4 hours). Cytotoxicity was assessed by determining lactate dehydrogenase (LDH) release. The effects of SF on cystine transport

(a determinant of GSH synthesis) were examined by determining the uptake of L-[^{35}S]cystine or L-[^{14}C]cystine.

Results: In vivo, SF and AITC, both markedly reduced the edema and BBB disruption induced by transient MCAO. Thus, while the % brain water content of the ipsilateral ischemic tissue in vehicle-treated rats increased by 2.47±0.34% compared to contralateral, this increase was only 0.86±0.34% ($P < 0.01$ vs. vehicle) and 1.27±0.35% ($P < 0.05$ vs. vehicle) in SF and AITC treated rats, respectively. Similarly, Evans blue leakage was 9.1±4.2 mg/g in vehicle treated rats vs. 0.18±0.15 and 0.40±0.45 mg/g in SF and AITC treated rats, respectively ($P < 0.01$ and $P < 0.05$ vs. vehicle). In vitro, pretreatment of b.End3 cells for 24 hours with 1, 5, 10 and 20 µM SF reduced H_2O_2-induced LDH release by 24±9, 55±4, 64±3 and 59±8%, respectively. SF induced a marked increase in endothelial cystine transport (a major determinant of cellular glutathione). Thus, cystine uptake was 287±49, 566±138 and 976±26% of control after 24 hours treatment with 1, 5 and 20 µM SF. The increase in cystine transport after SF exposure is delayed, i.e. cystine uptake was only 107±2 and 211±4% of control after 1 and 4 hours of SF treatment.

Conclusions: Two naturally occurring dietary components, SF and AITC, can protect the cerebrovasculature from a subsequent ischemic event. In vitro, concentrations of SF as low as 1 µM protected cerebral endothelial cells from oxidative stress and increased cystine transport. Plasma SF concentrations of 1 µM have been reported after ingestion of a bowl of broccoli soup (1).

References:

1. Al Janobi AA, Mithen RF, Gasper AV, Shaw PN, Middleton RJ, Ortori CA, Barrett DA. Quantitative measurement of sulforaphane, iberin and their mercapturic acid pathway metabolites in human plasma and urine using liquid chromatography-tandem electrospray ionisation mass spectrometry. J Chromatogr B 2006; 844:223-234.

INFLUENCE OF HYPOXIA ON THE PERMEABILITY OF BBB IN RAT AND PROTECTIVE EFFECT OF SODIUM AESCINATE ON BBB EXPOSURE HYPOXIA

Q.Q. Zhou[1,2], P. Guo[1,2], H. Luo[1,2]

[1]Department of High Altitude Diseases, College of High Altitude Military Medicine, Third Military Medical University, [2]Key Laboratory of High Altitude Medicine, Ministry of Education, PLA, Third Military Medical University, Chongqing, China

Objective: To explore the establishment method of animal model with experimental high altitude cerebral edema rats, for the study the pathogenesis and prevention and treatment measures of high altitude brain edema to provide experimental basis, and research the sodium aescinate on protective effect of blood brain barrier (BBB) under acute hypoxic exposure in rat.

Methods: The rats exposed to 4000m simulated high altitude hypoxia environment exhaustive exercise 2 days after placed in the 8000m altitude exposed for 3 days, to establishment the model of acute experimental brain edema. Using dry and wet method for determination the water content of brain, Evans blue (EB) tracer method measuring permeability of BBB, HE staining observation the pathological changes of brain tissue, and transmission electron microscopic of lanthanum nitrate tracer to observation the ultrastructure of tight junctions of BBB and brain tissue, immunohistochemical method and Western blot method for the detection the gene expression of occludin protein and claudin-5. Real-time fluorescent quantitative PCR assay for detection the gene expression of TJ associated molecular (ZO-1) and so on methods to evaluate the animal model.

Results: The rats after exhaustive exercise 2 days under hypoxia environment put on the 8000m exposure for 3 days,compared with the control group, results showed that brain water and Evans blue content of anoxia group rats are increased significantly ($P < 0.01$). light microscopically display the neurons is destroyed serious, tight junctions between endothelial cell of brain microvascular is open, lanthanum nitrate particles diffuse leakage into the brain interstitial, marked edema. sodium aescinate treatment after cerebral water content is decreased significantly ($P< 0.05$) in simple hypoxia group, EB detection results showed that EB leakage is reduced significantly. Neuronal serious depigmentation were observed by light microscopically in hypoxia group, sodium aescinate treatment after cellular edema decreased significantly, transmission electron microscopy shows that hypoxia group lanthanum particles diffuse deposition into the brain interstitial by through the opening of the TJ, capillaries around edema, sodium aescinate treatment group lanthanum particles to reduce significantly, the degree of leakage and edema is reduced significantly. Expression of Occludin mRNA and protein levels in hypoxia group was lowest, and compared with the control group were significantly different ($P< 0.01$), the highest expression in sodium aescinate treatment group, and compared with hypoxia group were significantly different ($P< 0.01$). At the same time, and compared with control group, hypoxia group expression of ZO-1 is decreased significantly ($P< 0.05$), claudin-5 were is lowed significantly, with sodium aescinate treatment after ZO-1, claudin-5 gene expression than simple hypoxia group increased significantly ($P< 0.01$).

Conclusion: The rats exposure to acute hypoxic to exhaustive exercise can successfully established the model of experimental high altitude cerebral edema; sodium aescinate can up-regulate the expression of Occludin protein and claudin-5 gene expression amount and thereby can reducing BBB permeability, therefore the sodium aescinate have protective obvious effect on blood brain barrier of hypoxic exposure.

ROLE OF ASTROCYTE NETWORK IN EDEMA FORMATION AFTER JUVENILE TRAUMATIC BRAIN INJURY

A.M. Fukuda[1,2], A. Adami[3], S. Ashwal[2], A. Obenaus[2,3,4], J. Badaut[1,2]

[1]Physiology, [2]Pediatrics, Loma Linda University School of Medicine, Loma Linda, [3]Neuroscience, University of California at Riverside, Riverside, [4]Radiation Medicine, Loma Linda University School of Medicine, Loma Linda, CA, USA

Introduction: In the U.S., traumatic brain injury (TBI) affects about 1.7 million people annually and contributes to 30.5% of all injury-related deaths. The vast majority of TBI occurs in children and young adults, but no effective

treatment exists for juvenile TBI (jTBI) to date. Edema is one of the pathological hallmarks after jTBI observed after blood-brain barrier (BBB) disruption. Aquaporin 4 (AQP4), a water channel protein, has been proposed as a key mediator in the edema process. Moreover, AQP4 and gap junctions are both located in perivascular astrocytic endfeet in contact with the vascular bed, and possibly involved in the control of water movement between the brain and blood in the BBB interface. Astrocytic gap junctions are composed by connexin 43 (Cx43) and Cx30. In vitro, siAQP4 has been shown to decrease the Cx43 expression. We propose that inhibiting AQP4 using small interfering RNA (siRNA) will result in better outcomes after jTBI, including improving BBB integrity through its actions on AQP4 and also gap junction proteins.

Objective: We tested whether injection of siRNA against AQP4 (siAQP4) after jTBI would result in reduced edema and BBB disruption, and improved behavioral outcomes. We then studied molecular and cellular changes by examining gap junction proteins after silencing AQP4.

Methods: Postnatal day 17 (P17) rats were injected with either siAQP4 or a non-targeted siRNA (siGLO) immediately after controlled cortical impact (CCI) injury, a model of jTBI. Diffusion weighted imaging (DWI) was used to monitor edema at 1 and 3 days (d) using (T2 weighted imaging) T2WI and (apparent diffusion coefficient) ADC values. Rotarod and foot-fault tests were performed at 1d and 3d to evaluate neurologic deficits. Immunohistochemical evaluation for AQP4, Cx43, Cx30, GFAP, IgG, and endothelial barrier antigen (EBA) was conducted at 3d.

Results: After jTBI, siAQP4-injected rats had significantly lower T2 (20% at 3d) and ADC values (21% and 24% less at 1d and 3d, respectively) around the lesion compared to siGLO-injected rats. The siAQP4 group also demonstrated improved gross motor activity via rotarod (40% increased time on rotarod before falling at 3d) and improved motor coordination via foot-fault tests (34% and 46% decreased number of foot-faults at 1d and 3d, respectively). We found a 30% decrease in IgG extravasation, signifying a more intact BBB, and 31% more EBA staining, signifying increased numbers of intact blood vessels. In the siAQP4 treated jTBI animals there was a 27% decrease in AQP4 expression, 28% decreased expression of Cx43, and 39% decreased GFAP immunoreactivity surrounding the lesion. No change was observed in Cx30 between groups.

Conclusions: We found that siAQP4 treatment after jTBI decreased markers of edema and BBB disruption around the lesion site, which resulted in improved behavioral recovery. We explored possible interactions between AQP4 and gap junction proteins and demonstrated that siAQP4 injection decreased AQP4 and Cx43 expression, which suggests that the siAQP4 is playing on the astrocyte network to limit the diffusion of the edema and the injury.

This work was supported in part by the NINDS grant R01HD061946 (JB).

EFFECTS OF PROPOFOL POST-TREATMENT ON BLOOD-BRAIN BARRIER INTEGRITY AND BRAIN EDEMA AFTER TRANSIENT CEREBRAL ISCHEMIA

B.-N. Koo, J.H. Lee, H.S. Cui

Yonsei University Health System, Seoul, Republic of Korea

Introduction: Cerebral edema is a serious complication that is associated with stroke. Recently, aquaporin (AQP) - transmembrane water channel protein- and matrix metalloproteinase (MMP) - extracellular matrix degrading enzyme- have been reported to be integral components of the pathophysiology of cytotoxic and vasogenic cerebral edema after ischemia. In addition, hypoxia-inducible factor (HIF)-1α, an upstream transcription factor induced by hypoxia, has been shown to be up-regulated in cerebral ischemia although its potential role after cerebral ischemia remains controversial. Thus, whether HIF-1α contributes to the formation of brain edema remains to be clarified. Although propofol has been reported to offer neuroprotection against cerebral ischemia, its impact on cerebral edema following ischemia is not clear. The objective of this investigation is to find out the effects of post-treatment of propofol on cerebral edema after transient cerebral ischemia and its mechanism of action, focusing on the modulation of AQPs, MMPs, and HIF-1α.

Methods: Adult male Sprague-Dawley rats (n=65) were allocated into three groups. The Sham group underwent sham operation; the EC group was subjected to middle cerebral artery occlusion (MCAO) for 1 hr followed by

reperfusion; the Pro group was subjected to MCAO/reperfusion and received 1 mg/kg/min of propofol for 1 hr when reperfusion was started. Brain edema and blood-brain barrier permeability were assessed 24 hr after MCAO (Fig.1). In addition, the expression of AQP-1, AQP-4, MMP-2, MMP-9, and occludin at 24 hr after MCAO, and HIF-1α at 8 hr after MCAO were analyzed using immunoblotting and immunofluoroscence.

Results: Compared to the EC group, the Pro group showed smaller volume of brain edema and lower brain water content ($p< 0.05$). The expressions of AQP-1, AQP-4, MMP-2, and MMP-9 were suppressed in the Pro group compared with the EC group ($p< 0.05$). On the other hand, occludin was expressed more in the Pro group than in the EC group ($p< 0.05$). Finally, the expressions of HIF-1α in the Pro group were lesser than those in the EC group ($p< 0.05$) at 8 hr after MCAO.

Conclusion: Post-treatment of propofol could attenuate cerebral edema after transient cerebral ischemia, which is associated with reduction in the expression of AQP-1, AQP-4, MMP-2, MMP-9, and HIF-1α.

ORDERED WATER WITHIN MOCROTUBULES (MTS) AS A SEPARATE AND SIGNIFICANT HYDRATION FRACTION TO BE MEASURED IN CEREBROVASCULAR BRAIN EDEMA

A.R. Kunz[1], C. Iliadis[2]

[1]Harvard University (Extension), Cambridge, MA, USA, [2]Department of Neurosurgery, University of Patras Medical School, Patras, Greece

Introduction: MRI's T_1 measures the rate nuclei in a magnetic field approach thermal equilibrium, dependent upon $Water_{total}$ + hydration fraction; the latter is the major source of uncertainty.

Methods: This paper explores the contribution of the hydration fraction within the intracellular microtubules' compartment to edema, using MRI's T_2, due to a theoretically describe quantum functioning of dipole-dipole interactions between *ordered water* and the MTs' protein, tubulin, endowing a coherence of increased order, a lower heat capacity, and a complexity of functioning.

Results and discussion: MTs are hollow cylinders 10^2-10^3 nm in length, with 25 nm exterior and 15 nm interior diameter(s); MTs represent 2-10% of the brain's protein; their concentration in axons and dendrites is 200 x 10^{-6}M. *Ordered water* fills the MTs' hollow core, 31% of the MTs by volume.

Three concepts support *ordered water* as separate water source; self-assembly is a property of living systems at the molecular level where the enzyme GTP carries electrons for tubulin's self-assembly into the MTs' hollow cylinders; *ordered water* fills this core, promoting **cooperative functioning.**

The MTs compose a hexagonal lattice of tubulin dimers, each with a dipole moment, a dielectric constant, and an electric field; these parameters determine order, spontaneously ordered at pH 7.2. *Ordered water's* own electric dipole couples with tubulin's quantized electromagnetic fields generating a quantum energy called solitons and coherent oscillations, travelling as a wave along the MTs non-linearly. Thus, *ordered water* functions to **self-focus electromagnetic energy**, called quantum coherence.

MTs are sensitive to electromagnetic fields, light and *heat*. The sequestration of water into an ordered structure results in a **lower heat capacity** and the quantum coherence maintains this new thermal-dynamic state. External negative charges isolate the MTs from thermal loss; the internal solitons' signals are non-dissipative waves, free from thermal noise and any loss.

In rat studies using T_2, which can separate out *ordered* and non-ordered water fractions, the mean fraction size of *ordered water* with the shortest T_2 was 13%. In man, upper limits of just 100 milliliters (mls), a 7-8% volume increase, are available to accommodate any brain edema. Yet, the low compliance of man's evolutionary significant gray matter tolerates only a 1.5%, or 18 mls increase.

Conclusion: In brain edema, the window to irreversibility is narrow; an inclusion of MTs' quantum functioning of *ordered water*, and measurement of this separate and significant hydration fraction, may bring options to management, and lead to the reversibility of life-threatening cerebrovascular brain edema.

MECHANISMS OF AQUAPORIN EXPRESSION FOLLOWING EXPERIMENTAL TRAUMATIC BRAIN INJURY

K. Rauen[1], R. Trabold[1], J. Badaut[2], V. Popp[2], N. Plesnila[1,3]

[1]Institute for Surgical Research & Dept. of Neurosurgery, University of Munich Medical Center, Munich, Germany, [2]Dept. of Pediatrics, Loma Linda University School of Medicine, Loma Linda, CA, USA, [3]Institute for Stroke and Dementia Research (ISD), University of Munich Medical Center, Munich, Germany

Objective: Brain edema formation and subsequent intracranial hypertension are well known to result in secondary brain damage and, hence, unfavorable outcome following traumatic brain injury (TBI). It is well known, that aquaporins (AQP), ubiquitous and highly specific water channels, mediate post-traumatic brain edema formation, but the mechanisms of their regulation in the brain remain still unclear.

Previously, we showed that pharmacological as well as genetic inhibition of arginine-vasopressin V_{1a} receptors reduces post-traumatic edema formation. In the current study, we quantified cerebral aquaporins on mRNA and protein levels in wild-type and V_{1a} receptor knock-out mice after experimental TBI to elucidate cerebral AQP function and possible molecular mechanisms via V_{1a} receptors.

Methods: Wild-type and V_{1a} receptor knock-out mice ($V_{1a}^{-/-}$) were not handled or subjected to controlled cortical impact (CCI: 8 m/s, 1 mm; n=10 per group). 15 min, 1, 3, 12 or 24 h after trauma AQP1 and 4 mRNA was quantified by RT-PCR and cellular AQP protein expression was identified by immunohistochemistry (+/- NeuN, GFAP). Regions of interest were perilesional to trauma and the contralateral hemisphere.

Results: AQP1 and 4 mRNAs were constitutively expressed in wild-type mouse brain. AQP1 was expressed on cortical neurons, while AQP4 was localized on cortical and subcortical glia cells. Following TBI AQP1 was significantly upregulated 4-fold (p=0.03) whereas AQP4 expression was not altered. In V_{1a} receptor knock-out mice AQP1 was not regulated on mRNA level.

AQP1 immunoreactivity increased significantly ($p< 0.05$) in the contralateral side, while AQP4 was mainly upregulated in the traumatized brain (p=0.04). AQP1 protein was not regulated in $V_{1a}^{-/-}$ mice; AQP4 did not increase immediately after trauma, but only 3 and 24 h thereafter.

Conclusion: AQP1 was found in neurons and AQP4 in glial cells. Both aquaporins were upregulated following TBI and this regulation was blunted in vasopressin V_{1a} receptor deficient mice. Our data therefore strongly suggest that V_{1a} receptors play a pivotal role in the regulation of cerebral aquaporins following brain injury. Thus, V_{1a} receptors may represent novel therapeutic targets for the treatment of aquaporin-mediated brain edema formation.

TEMPORAL AND SPATIAL DYNAMICS OF VASOGENIC BRAIN EDEMA FORMATION QUANTIFIED BY 2-PHOTON MICROSCOPY *IN VIVO*

S.M. Schwarzmaier[1,2,3], M. Gallozzi[1], N. Plesnila[1,2]

[1]Neurodegeneration, Royal College of Surgeons in Ireland (RCSI), Dublin, Ireland, [2]Institute for Stroke and Dementia Research (ISD), [3]Department of Anesthesiology, Ludwig-Maximilians University, Munich, Germany

Objectives: The formation of vasogenic brain edema is still one of the most important factors determining the fate of patients suffering from acute brain damage. So far, the quantification of vascular leakage, the pathophysiological basis of vasogenic edema, was difficult to achieve *in vivo*. In the current study we used *in vivo* 2-photon microscopy (2-PM) to investigate the spatial and temporal development of vasogenic brain edema formation in 3-D space. For that purpose we used an experimental model where vasogenic edema is prominent, i.e. traumatic brain injury (TBI).

Methods: 6-8 week old male C57/Bl6 mice (n=6 per group) were subjected to Controlled Cortical Impact (CCI) and a cranial window was prepared adjacent to the injury site. TMRM (40 mg/kg i.a., MW 40,000) was used to visualize the blood plasma. Intravascular and tissue TMRM fluorescence was monitored before and every 30 min from 2 h until 4 h post

CCI in 3 adjacent tissue volumes reaching from the brain surface to a depth of 300 µm. TMRM leakage over time was quantified with *ImageJ*.

Results: Vascular leakage could be detected as early as 2-4 h after CCI in all areas observed. Vascular leakage increased over time and was more pronounced closer to the primary contusion but was independent of tissue depth and vessel diameter. Arterioles, venules, and capillaries showed similar degrees of vascular leakage.

Conclusions: 3-D brain imaging with 2-PM microscopy is a feasible technique to quantify the formation of vasogenic brain edema *in vivo*. Vascular leakage occurs in large and small cerebral vessels and is similar in arteries and veins. This technique may therefore be used to investigate the mechanisms of vascular leakage in the brain and to develop novel therapies for brain edema formation.

AGE AND SIZE DEPENDENT NEUROPATHOLOGY OF NANOPARTICLES FROM METALS IN RATS ARE RELATED TO NITRIC OXIDE MEDIATED MECHANISMS

A. Sharma[1], D.F. Muresanu[2], R. Patnaik[3], H.S. Sharma[4]

[1]Surgical Sciences, Anesthesiology & Intensive Care Medicine, Uppsala University, Uppsala, Sweden, [2]Clinical Neurosciences, University of Medicine & Pharmacy, University Hospital, Cluj-Napoca, Romania, [3]Biomaterials, School of Biomedical Engineering, National Institute of Technology, Banaras Hindu University, Varanasi, India, [4]Surgical Sciences, Anesthesiology & Intensive Care Medicine, Uppsala University, University Hospital, Uppsala, Sweden

Previous studies from our laboratory show that chronic administration of engineered nanoparticles from metals, e.g., Cu, Ag, or Al (50-60 nm, 50 mg/kg, i.p. daily for 1 week) are able to induce profound blood-brain barrier (BBB) disruption, brain edema formation and brain pathology in adult rats (age 18 to 22 weeks). This effect was most pronounced by Ag followed by Cu and Al indicating that the constituents of nanoparticles play crucial roles in neurotoxicity. However, effects of size dependent neurotoxicity of nanoparticles in vivo situation are still unknown. In present investigation, we examined the effects of different size ranges of engineered nanoparticles from Cu, Ag and Al on brain pathology in rats. In view of the fact that age is also an important factor in brain pathology, we also evaluated age-related neurotoxicity of nanoparticles in our rat model.

Three different sizes of Cu, Ag or Al nanoparticles (20 to 30 nm; 50 to 60 nm, or 130 to 150 nm) were administered intraperitoneally (50 mg /kg, i.p.) in separate set of rats (n = 5 to 7) in 3 different age groups (9 to 10 weeks; 18 to 20 weeks or 30 to 35 weeks old). Saline treated rats served as controls. Breakdown of the BBB to Evans blue albumin (EBA) and radioiodine, brain water content, neuronal injury, astrocytic activation, myelin damages and nitric oxide synthase (NOS) immunoreactivity was examined using standard procedures.

Our results showed that brain pathology caused by different nanoparticles were inversely related to their sizes. Thus, smaller nanoparticles from Ag, Cu or Al induced most pronounced BBB breakdown (EBA +480 to 680%; radioiodine +850 to 1025%), brain edema formation (+4 to 6 %) as well as neuronal injuries (+30 to 40%), glial fibrillary acidic protein (GFAP) upregulation (+40 to 56% increase) and myelin vesiculation (+30 to 35 % damage) in youngest animals compared to controls. Interestingly, the oldest animals (30 to 35 weeks of age) also showed massive brain pathology as compared to young adults (18 to 20 weeks old). The Ag and Cu exhibited greater brain damage compared from Al nanoparticles in all age groups regardless of their sizes. This confirms that the composition of nanoparticles is important in neurotoxicity. The very young and elderly age groups exhibited greater neurotoxicity to nanoparticles suggests that children and elderly are more vulnerable to nanoparticles induced brain damage. The nanoparticles induced brain damage correlated well with the upregulation of neuronal and inducible NOS activity in the brain indicating that nanoparticles induced size and age dependent neurotoxicity could probably mediated via increased production of nitric oxide, not reported earlier.

NO EFFECT OF MANNITOL ON THE COURSE OF PERIHEMORRHAGIC EDEMA AFTER INTRACEREBRAL HEMORRHAGE

B. Volbers[1], W. Willfarth[1], S. Schwab[1], P. Gölitz[2], A. Doerfler[2], D. Staykov[1]

[1]Neurology, [2]Neuroradiology, University of Erlangen-Nuremberg, Erlangen, Germany

Objectives: Perihemorrhagic edema (PHE) after intracerebral hemorrhage(ICH) may exceed the initial hematoma volume by up to 600% thereby leading to increased intracranial pressure (ICP), clinical detoriation or even herniation(1). Intravenous hypertonic saline (HTS) has been shown to reduce PHE formation after ICH. Clinical data suggest that HTS may be superior to mannitol in lowering ICP(2). EUSI and ASA guidelines recommend the use of intravenous mannitol up to a serum osmolality (SO) of 320 mosmol/kg or HST in order to reduce elevated ICP(3, 4). We aimed to investigate the effect of mannitol and SO on the evolution of PHE after ICH.

Methods: 25 patients with supratentorial spontaneous ICH treated with 20% intravenous mannitol solution (125-250ml every 6h) for 5-10 days and 25 controls who did not receive mannitol or any other osmotic agents during the course of treatment were identified retrospectively from our institutional ICH database. Patients treated with mannitol and controls were matched for ICH-volume (±5ml). PHE volume was calculated on CT scans using a validated semiautomatic threshold based volumetric algorithm. Diagnostic CT and follow-up scans performed on days 1, 2-3, 4-6, 7-9 and 10-12 were analyzed. SO, concentration of sodium and glucose were obtained from patient records.

Results: Matching resulted in similar ICH-volumes in both groups (mannitol: 27.7±18.0ml, controls: 27.2±13.0ml). Mean age was 69(53-83) years in the mannitol group and 65(46-83) years in controls (p=0.2). Initial relative PHE did not differ significantly in both groups (mannitol: 1.03±0.6, controls: 0.90±0.4, p=0.35). Overall, there was no effect of mannitol treatment on the course of PHE (F=0.08, p=0.78). There was no significant correlation between SO and relative PHE at any timepoint of follow-up.

Conclusions: We found no effect of mannitol use and SO on the evolution of PHE. Other underlying mechanisms may explain the short-term effect of mannitol bolus administration on ICP in patients with spontaneous supratentorial ICH.

References:

1. Mayer SA, Sacco RL, Shi T, Mohr JP. Neurologic deterioration in noncomatose patients with supratentorial intracerebral hemorrhage. Neurology 1994;44:1379-1384.

2. Wagner I, Hauer EM, Staykov D, et al. Effects of continuous hypertonic saline infusion on perihemorrhagic edema evolution. Stroke 2011;42:1540-1545.

3. Steiner T, Kaste M, Forsting M, et al. Recommendations for the management of intracranial haemorrhage - part I: spontaneous intracerebral haemorrhage. The European Stroke Initiative Writing Committee and the Writing Committee for the EUSI Executive Committee. Cerebrovasc Dis 2006;22:294-316.

4. Morgenstern LB, Hemphill JC, 3rd, Anderson C, et al. Guidelines for the management of spontaneous intracerebral hemorrhage: a guideline for healthcare professionals from the American Heart Association/American Stroke Association. Stroke 2010;41:2108-2129.

ULINASTATIN ATTENUATES CEREBRAL ISCHEMIC NEUROINJURY VIA AQP4 AND NKCC1 MEDIATED ANTI-EDEMA ACTION

L. Zhang, Z. Fei

Xijing Hospital, The Fourth Military Medical University, Xi'an, China

Objective: Both AQP4 and NKCC1 have been shown to exert anti-edema effects associated with cerebral ischemic injury *in vitro* and *in vivo,* and a human urinary trypsin inhibitor-Ulinastarin (UTI) plays a broad spectrum of regulate apoptosis and autophy and is considered to have potential therapeutic applications. The aim of this study was to investigate the potential neuroprotective role of UTI against cerebral ischemic edema induced by middle cerebral artery occlusion (MCAO) in rats and the underlying mechanism.

Methods: Adult male BALB/c mice weighing 25 to 30g were subjected to 1h MCAO and pretreated with vehicle (0.9% isotonic Na

chloride), UTI alone, or UTI plus bumetanide (a specific NKCC1 inhibitor), TGN-020 (a specific AQP4 inhibitor) at 1-7d after the transient occlusion. Neurological deficit scores (NDS) and brain water content were assessed at 24h、72h and 7d after MCAO. Neuronal apoptosis, autophagy, AQP4 and NKCC1, activated caspase-3, CasthepinB, Beclin1 expression were also determined at 24h and 7d after MCAO.

Results: Administration of UTI on mice with MCAO-induced acute ischemic edema resulted in a significant decrease both the levels of apoptosis and water content of brain in the course of edema, and increased autophagy in the phase of acute ischemic edema (24h and 72h) and decreased autophagy in the phase of chronic ischemic edema (7d). Meantime, among AQP4, NKCC1 and activated caspase-3 expression were decreased and the expression of CasthepinB and Beclin1 were increased at 24h and 72h after MCAO. In contrary, the expression of AQP4 and NKCC1 were increased and CasthepinB and Beclin1 expression were decreased at 7d after ischemic edema. Furthermore, the neuroprotective effect of UTI was partly blocked by AQP4 inhibitor TGN-020 and NKCC1 inhibitor bumetanide.

Conclusions: In summary, these data suggested that UTI had neuroprotective effect against ischemic edema in vivo via AQP4 and NKCC1 mediated apoptotic and autophagic action, and the protection possibly was associated with regulated activation of AQP4 and NKCC1.

EFFECT AND INFLUENCING FACTORS OF FIRST AID AND TREATMENT ON THE SPOT FOR PATIENTS WITH HIGH ALTITUDE CEREBRAL EDEMA

Q.Q. Zhou[1,2], D. Yang[1,2], X. Zhang[1,2]

[1]Department of High Altitude Diseases, College of High Altitude Military Medicine, Third Military Medical University, [2]Key Laboratory of High Altitude Medicine, Ministry of Education, PLA, Third Military Medical University, Chongqing, China

Objective: To investigate the treatment method and pathogenic mechanism of acute high altitude cerebral edema, and evaluate the efficacy of emergency treatment on the spot in high altitude regions.

Methods: A total of 328 hospitalized patientswith high altitude cerebral edema in the past 50 yearswere reviewed , the case from the 1956 - 2005 in the Tibet Military Region General Hospital inpatient treatment of HACE case, In 328 HACE patients, 300 male cases,28 female patients, age 60 years old of maximum, minimum 1 years, an average of 30Years old; 98% Han Chinese migrants, 2% for other minority emigrated to Crowd. The onset of the height of 2800～5300 m, 4194 m on average; Early onset in 196 cases, and then back to their onset in 132 cases, moved to the time 35 years older, short 1 years, average moved to 5.25 years. Into the party Type: by car mostly by car into the pathogenesis, incidence of 190 Cases, 57.93% in all cases, flew into the incidence of 138 Cases, 42.07% in all cases. the efficacy of emergency treatment on the spots was evaluated, and the factors influencing therapeutic effect were analyzed.

Results: After emergency treatment on the spot for 328 patients with acute high altitude cerebral edema, 319 (97. 3%) patientswere successfully cured, and the average length of stay in hosp ital was 7. 1 days. The leading factor influencing therapeutic effect was multip le organ dysfunction syndrome (MODS). In those patients with MODS, 56 % had high altitude pulmonary edema, 41% had renal insufficiency, 14% had cardiac insufficiency, and 12. 5% had three - organ dysfunction.

Conclusion: First aid and treatment on the spot in high altitude regions is critical for the treatment of high altitude cerebral edema, and MODS was the main factor influencing therapeutic effect.

TLR4 AND SEIZURE GENERATION FOLLOWING ISCHEMIA WITH HYPERGLYCEMIA

Y. Liang[1], Z. Lei[2], H. Zhang[1], Z. Xu[1], Q. Cui[1], **Z.C. Xu**[2]

[1]Third Affiliated Hospital of Guangzhou Medical University, Guangzhou, China, [2]Anatomy & Cell Biology, Indiana University School of Medicine, Indianapolis, IN, USA

Diabetes is a risk factor for stroke and has adverse effects on the outcome of stroke patients. Seizure/epilepsy is a common sequel of cerebral ischemia and hyperglycemia markedly increases the onset of seizures after

ischemic insult. However, its underlying mechanism is unclear. It has been shown that toll-like receptor 4 (TLR4) pathway is involved in temporal lobe epilepsy. The present study investigated the possible involvement of TLR4 in pathogenesis of seizures following cerebral ischemia with hyperglycemia.

Global ischemia was produced in adult Wistar rats using four-vessel occlusion method for 15 min. Hyperglycemia (> 200 mg/dl) was induced by intraperitoneal injection of glucose (3g/kg) 15 min before ischemia. The animals were sacrificed at different time points after ischemia. Immunohistochemical staining using antibodies against TLR4 and HMGB1 were performed on animals with seizure following ischemia with hyperglycemia and compared with those with normal blood glucose levels. Lipopolysaccharide (LPS) was injected into the animal as positive controls.

Most rats in the hyperglycemic group developed tonic-clonic seizures after ischemia. The animals with seizures died of status epilepticus within 2 h after the onset of seizure. In naïve animals, TLR4 was expressed in interneurons of hippocampus and localized to plasmalemma or cytoplasm in hippocampus. HMGB1 was localized in the nucleus of neurons throughout the hippocampus. The intensity of TLR4 immunostaining was significantly increased in hippocampus in hyperglycemic group after ischemia as compared with normoglycemic group and control group. Meanwhile, a dramatic decrease of HMGB1 expression was observed in the hippocampus after hyperglycemic ischemia. No difference in the expression of TLR4 and HMGB1 was observed between hyperglycemic group and LPS group. The immunoreactivity of c-fos was also increased in hippocampal neurons in hyperglycemic animals after ischemia, suggesting the increase of neuronal activity.

These results suggested that TLR4 pathway is involved in the pathogenesis of seizures following cerebral ischemia with hyperglycemia, which provides a new direction to study the underlying mechanisms of seizures in stroke patients with diabetes.

The work was supported by grants from NIH (NS071238), AHA (GRNT4500000) and Guangdong Provincial Department of Science and Technology (2009B030801352).

NEUROPROTECTIVE EFFECT OF OSTHOLE AGAINST OXYGEN AND GLUCOSE DEPRIVATION IN RAT CORTICAL NEURONS: INVOLVEMENT OF MAPK PATHWAY

T. Chen, Z. Fei

Xijing Hospital, The Fourth Military Medical University, Xi'an, China

Osthole, a bioactive simple coumarin derivative extracted from many medicinal plants such as Cnidium monnieri (L.) Cusson, exerts a broad spectrum of pharmacological activities and is considered to have potential therapeutic applications. The aim of this study was to investigate the potential neuroprotective role of osthole against ischemic injury in vitro, as well as the potential mechanism. Cultured cortical neurons were exposed to oxygen and glucose deprivation (OGD) for 4 h followed by a 24h reperfusion. Osthole exhibited remarkable neuroprotection in a dose-dependent manner and the effect required presence of osthole during both OGD and reperfusion phases. Westernblot was used to examine the activation of three members of mitogen-activated protein kinases (MAPKs): extracellular signal-regulated kinase 1/2 (ERK1/2), c-Jun N-terminal kinase (JNK), and p38 kinase (p38). We found that osthole prolonged activation of ERK1/2 and prevented activation of JNK. Furthermore, we investigated the effects of MAPKs inhibitors on osthole-induced protection. The results demonstrated that the protection of osthole was partly reversed by PD98059, a selective inhibitor of ERK1/2, but further enhanced by the JNK inhibitor SP600125. In addition, osthole-induced reduction of neuronal apoptosis was abrogated by the ERK1/2 inhibitor PD98059, whereas the neuronal necrosis was further decreased by the JNK inhibitor SP600125. In summary, these data suggested that osthole had neuroprotective effect against ischemic injury in vitro via its anti-apoptotic and anti-necrotic activity, and the protection possibly was associated with prolonged activation of ERK1/2 and suppression of JNK activity.

CARDIAC ARREST DECREASES HIPPOCAMPAL CA1 NEURONS, INHIBITS PLASTICITY AND IMPAIRS SPATIAL MEMORY IN MIDDLE AGED RATS

C.H. Cohan, J.T. Neumann, M. Binkert, K.R. Dave, C.B. Wright, M.A. Perez-Pinzon

Neurology, University of Miami, Miami, FL, USA

Introduction: Cardiopulmonary arrest (CA) is a leading cause of death and disability in the US (1). Most CA research is performed in 2-3 month old rodents (equivalent of 13-18 year old humans, who represent 2% of CA cases). The histological, electrophysiological and behavioral deficits after CA are unknown in older rodent models. Here, we induce 6 minutes of asphyxia cardiac arrest (ACA) (2) in 9 month old Fischer 344 rats (30 human years) to characterize changes in cognition in this age group.

Objective: Characterize changes in hippocampal cell counts, synaptic plasticity and spatial memory in a middle-aged rodent model.

Aims: After ACA, examine Schaffer Collateral-CA1 synaptic changes with paired pulse response (PPR), quantify cell number in CA1 and subiculum (spatial memory areas), and determine spatial memory deficits.

Design: Animals are appropriately habituated, given a 6 min ACA, allowed to recover for 2 days, run on the Barnes maze spatial memory test for 4 days, and then sacrificed for histology or electrophysiology (Fig. 1A).

Methods: 6 minute ACA: Rats were anesthetized, ventilated, and injected I.V. with vecuronium. ACA was induced by disconnecting the intubation tube (6 minutes). Resuscitation was initiated with I.V. epinephrine and sodium bicarbonate. Ventilation was restored and manual chest compressions were performed.

Histopathology: Rats were perfused with formaldehyde, glacial acetic acid, and methanol mixture then paraffin embedded. Serial sections (10um) were obtained (-3.8 mm bregma). Nonpyknotic/eosinophilic cells were quantified.

PPR: 400um coronal slices were oxygenated in artificial cerebral spinal fluid at 36C. Excitatory post synaptic field potentials (fEPSPs) were recorded in the stratum radiatum of the CA1. PPR was conducted by stimulating Schaffer Collaterals 25-1000 ms apart with half maximal fEPSP 1 ms pulse.

Barnes Maze: Rodents use spatial cues to locate an escape tunnel. Incorrect holes, distance traveled, and latency till the escape box entrance were measured.

Results: 16/41 rats survived 7 days after ACA (39%) (Fig.1B). PPR was significantly increased at all time points (N=6 ACA, 5 Sham) (Fig.1C). Surviving cells were decreased after ACA in the CA1: Sham: 1273.44+/-70.41 SEM cells per slice, ACA: 888.06+/-80.89 SEM (p=.00504). Subiculum: Sham: 511.72+/-21.26 SEM, ACA: 399.28+/-40.57 SEM (p=.041) (N=6 ACA, 6 Sham) (Fig.1D). ACA significantly increased distance traveled (ACA 466.09cm+/-71.01 SEM, Sham 222.72+/-36.45 SEM p< .016) (Fig.1E), and latency till entering escape box (ACA 122.36 seconds+/- 19.65 SEM, Sham 56.24+/-17.11 SEM p< .0093, N=6 ACA, 7 Sham) on Barnes Maze day 2 (Fig.1F).

Conclusions: After ACA, PPR is increased, the CA1 and subiculum show a loss of surviving cells, and spatial memory acquisition is impaired. Cell death and modified synaptic plasticity (PPR) may disrupt spatial memory (Fig. 1G).

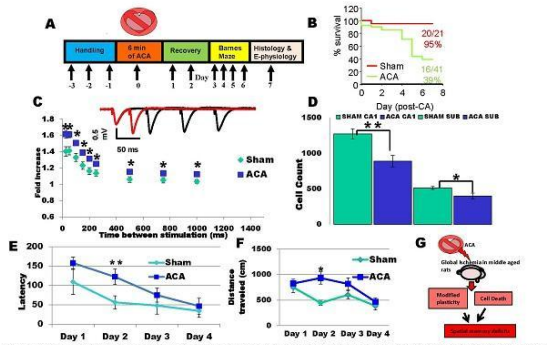

Figure 1: (A) Experimental design and timeline. (B) Animal survival Kaplan-Meier curve. (C). Example trace of paired pulse response and corresponding data. There was a significant increase in paired pulse response after ACA at all time points. (D) Count of viable neurons in the CA1 region and subiculum 7 days after ACA. There was a significant decrease in both the CA1 and subiculum. (E) Latency to entering escape box on Barnes maze spatial memory task. Latency was significantly increased on day 2 of Barnes maze trials after ACA compared to sham. (F) Distance traveled on Barnes maze spatial memory task. Distance was also significantly increased on day 2 after ACA compared to sham. (G) Proposed model of ACA induced spatial memory deficits.

[Fig.1]

References:

1. McNally B, *et al.*, Out-of-hospital cardiac arrest surveillance --- Cardiac arrest registry to enhance survival (CARES), United States,

October 1, 2005—December 31, 2010. MMWR Surveill Summ 2011, 60(8):1-19

2. Dave KR *et al*., Mild cardiopulmonary arrest promotes synaptic dysfunction in rat hippocampus. Brain research 2004, 1024(1-2):89-96

Funding: NIH NS45676, NS34774 and the Evelyn F. McKnight Brain Institute

GLOBAL CEREBRAL ISCHEMIA-REPERFUSION INDUCES STRIATAL T1-HYPERINTENSITY OF NEURONAL DEATH WITHOUT MICROBLEEDS IN HUMAN BRAINS: SWI STUDY ON CARDIAC ARREST SURVIVORS

M. Fujioka[1,2], T. Watanabe[3], T. Taoka[4], K. Okuchi[3]

[1]Neuroscience Unit, Emergency and Critical Care Medical CTR, Nara Medical University, Kashihara, [2]Neurosurgery, Osaka Saiseikai Ibaraki General Hospital, Ibaraki, [3]Emergency and Critical Care Medical CTR, [4]Radiology, Nara Medical University, Kashihara, Japan

Background: Global cerebral ischemia-reperfusion induces selective neuronal death in the hippocampal CA1 area, cerebellar cortex, dorsolateral striatum, and/or neocortical layers 3, 5, and 6 in animal models and in humans. Our previous MRI studies on patients resuscitated from cardiac arrest showed

1) bilateral neurodegeneration with hyperintensity on T1-weighted MRI in the striatum, thalamus, and/or substantia nigra (Stroke. 1994;25:2091-5., Neuroradiology. 1994;36:605-7.), and

2) specific hippocampal atrophy in the chronic stage (MRI volumetry) (Cerebrovascular Dis. 2000;10:2-7.). In the current study with susceptibility-weighted MRI (SWMRI), we investigated if the delayed T1-hyperintensity in the dorsolateral striatum consistently observed in cardiac arrest survivors represents minor hemorrhage (methemoglobin) or signifies selective neuronal death without bleeding reported as a specific type of ischemic neurodegeneration (Ann Neurol. 2003;54:732-47.).

Methods: We repeatedly studied eight vegetative patients resuscitated from unexpected out-of-hospital cardiac arrest using magnetic resonance (MR) imaging. We performed SWI study on the late-onset striatal T1-hyperintensity to investigate if the specific change represents iron accumulation derived from hemoglobin degradation products.

Results: In the eight patients, serial MR images demonstrated delayed T1-hyperintesity in the bilateral striatum from one to two weeks after the onset. The SWI study showed no hypointense change in the striatal T1-hyperintensity.

Conclusion: The SWI study in patients after cardiopulmonary resuscitation suggests that global brain ischemia-reperfusion induces delayed striatal injury with T1-hyperintensity without erythrocyte-extravasation in humans.

CIRCULATING NITRIC OXIDE AND AUTONOMIC IMPAIRMENT IN THERAPEUTIC HYPOTHERMIA AFTER CARDIAC ARREST

A. Jantanukul[1], S. Muengtaweepongsa[2], K. Suwanprasert[3]

[1]Medical Engineering Program, [2]Division of Neurology, [3]Division of Physiology, Faculty of Medicine, Thammasat University Rangsit Centre, Pathum Thani, Thailand

Objective: Although hypothermia is widely used to protect cells against injurious processes, oxidative stress through nitrite/nitrate formation has been reported. In this study, we hypothesize that nitric oxide (NO), a diffusible small molecule synthesized from those 3 isoforms of nitric oxide synthase (NOS), plays a crucial role as heart-brain axis modulator and oxidative stress marker derived reactive oxygen species (ROS) during therapeutic hypothermia. To test this, we studied changes of NO level and autonomic impairment determined by LF/HF ratio of heart rate variability (HRV).

Method: Fourteen cardiac arrest patients were recruited and studied in therapeutic hypothermia (age 55+/- 20.22, female: male 8:6) which all protocols were approved by local ethical committee (MTU-EC-PH-2-062/55). Plasma nitric oxide concentration was measured by electrochemistry technique and symphatho-vagal balance by LF/HF ratio of 5 minutes HRV analysis during four phases of treatment: cooling down, mild hypothermia, rewarm and recover to normothermia. All

patients were classified into survivors and non-survivors (7:7) by 30 days survival outcome.

Result: In all patients, NO levels associated with LF/HF ratio were gradually increased as seen in mild hypothermia to recover phase and reached significant level ($^{\#}p< 0.05$). There were no significant changes of both NO level and LF/HF ratio in non-survivors. In the survivors, remarkable increase in NO was found during recover phase and showed significance compared with rewarm phase ($^{\#}p< 0.05$). Interestingly, LF/HF ratio was significantly increased which compared with those of mild hypothermia, rewarm and recovering phases ($^{\#}p< 0.05$). Contrast to non survivors, NO level and LF/HF ratio patterns were dramatically increased in survivors.

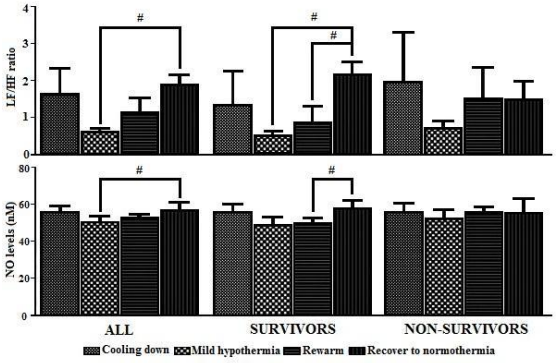

[NO and LF/HF ratio during therapuetic hypothermia]

Conclusion: An increasing NO level associated with autonomic improvement determined by LF/HF ratio may be predictor of cardiac arrest outcomein therapeutic hypothermia.

Acknowledgement: This work supported by National Research University Project of Thailand Office of Higher Education Commission and faculty of medicine, Thammasat University.

References:

1. Neil Herring, et al. Site specific cholinergic control of heart rate by nitric oxide is site specific. News Physiol Sci. 2002;17: 202-206

2. Ostadal P, et al. Nitrotyrosine and nitrate/nitrite levels in cardiac arrest survivors treated with endovascular hypothermia. Physiol Res. 2012; 61: 425-430

3. Pfeifer R, et al. Autonomic regulation during mild therapeutic hypothermia in cardiopulmonary resuscitated patients. Clinical Research in Cardiology, 2011; 100:797-805

MOVING FROM A RODENT MODEL TO THE CLINIC IN STUDYING GLOBAL CEREBRAL ISCHEMIA WITH HSP70 AND ICAM-1 AS EARLY BIOMARKERS

M. Jiang[1], E. Curfman[1], B.C. Hong-Goka[2], R.D. Sweazey[1], F.-L.F. Chang[1]

[1]Indiana University School of Medicine-Fort Wayne, Fort Wayne, IN, [2]UCSF-Fresno Alzheimer's & Memory Center, Fresno, CA, USA

Objectives: Cardiac arrest is often accompanied by global cerebral ischemia that subsequently causes a cascade of pathophysiological processes. Patients suffering an out-of-hospital cardiac arrest usually experience several minutes of global ischemia and have minimal cerebral blood flow (CBF). Most studies of global ischemia have focused on molecular events 24 hours after ischemia. However, to better understand, diagnose and treat global cerebral ischemia it is important to find early biomarkers that reflect underlying changes in the ischemic brain. To solve this problem, a modified 4-vessel occlusion (4-VO) was conducted in rats and molecular changes were examined as early as 3 hours after global ischemia.

Methods: This study is in compliance with NIH animal care guidelines and was approved by the Purdue University Animal Care and Use Committee. Six-minute global ischemia was produced in isoflurane-anesthesized Sprague Dawley rats using a modified 4-VO model followed by 3-hour reperfusion. Sham animals were processed using the same procedures except that the vertebral arteries were not cauterized and carotid arteries were not clamped. CBF and physiological parameters were monitored throughout the experiment. Core body temperature was maintained at 37^{o}C. Rats were sacrificed and alternate 2-mm coronal brain sections were stored either in RNAlater, or fixed in 10% buffered formalin, processed and paraffin-embedded. RNA was extracted, reverse transcribed, and analyzed by quantitative real-time PCR (qRT-PCR). Specific protein levels were examined by Western blot. Eight-micron sections were used

for immunostaining with Hsp70 and ICAM-1 antibodies.

Results: 4-VO produced a 80-90% drop in CBF and blood flow returned to its original value once reperfusion began. Both H&E and combined silver-cresyl violet staining showed neuronal damage in motor cortex (M1) and the CA4 regions of hippocampus suggesting ischemic damage occurs within three hours. The damage to CA1 was very light, which is inconsistent with most previous studies. A possible reason for this finding is the shorter survival time after reperfusion used in the current study. mRNA expression of four candidate genes (*Hsp70, ICAM-1, Hif-1α and MsrA)* by qRT-PCR with the comparative DDCt method normalized to β-actin and GAPDH showed >30-fold increased expression of *Hsp70* and >2.5 fold increase in *ICAM-1*. There were no significant changes in *Hif-1α* and *MsrA.* Immunostaining of Hsp70 and ICAM-1 found stronger staining in both M1 and CA4 regions of hippocampus compared to sham controls.

Conclusions: Our current 4-VO rat model showed that the M1 cortex and CA4 region of the hippocampus were the earliest and most affected areas. In contrast to studies using 24 hour reperfusion, the CA1 region showed less damage. Our study suggests that ICAM-1 and Hsp70 can be used as markers of global ischemic brain damage as early as 3 hours after reperfusion. These findings may assist in the translation of animal global ischemic models into effective clinical diagnosis and treatment.

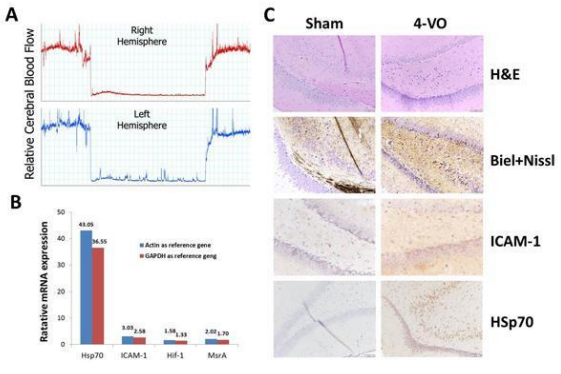

[CBF drop and biomarker changes in global ischemia]

EARLY MEK ½ INHIBITION AFTER TRANSIENT FOREBRAIN ISCHEMIA PREVENTS DELAYED UPREGULATION OF VASOCONSTRICTOR RECEPTORS IN RAT CEREBRAL ARTERIES

S.E. Johansson, S.S. Larsen, G.K. Povlsen, L. Edvinsson

Dept. of Clinical Experimental Research, Glostrup Research Institute, Glostrup, Denmark

Background: Cerebrovascular pathophysiology after global cerebral ischemia is associated with increased vasoconstriction and decreased global cerebral blood flow. The post-ischemic phase of cerebral hypoperfusion induces selective and delayed neuronal cell death, where the neurons in the CA1 region of the hippocampus are particularly vulnerable, resulting in persistent cognitive deficits in surviving individuals. Upregulation of contractile endothelin-B (ET_B) and 5-hydroxytryptamine 1B ($5\text{-}HT_{1B}$) has been demonstrated in cerebral artery smooth muscles 48 hours after experimental transient forebrain ischemia. On the basis of previous findings in other types of cerebral ischemia, we hypothesise that intracellular signalling via the mitogen-activated protein kinase kinase (MEK) - extracellular signal-regulated kinase ½ pathway is involved in this receptor upregulation after global cerebral ischemia in this model as well.

The aim of the present study was to characterize the time-course of changes in a) ET_B and $5\text{-}HT_{1B}$ receptors in cerebral arteries, b) neuronal cell damage and c) neurological deficits after experimental transient forebrain ischemia in rats. Moreover, the aim was to determine whether treatment with the MEK ½ inhibitor U0126 can prevent the cerebrovascular vasoconstrictor receptor upregulation after global cerebral ischemia.

Methods: Experimental transient forebrain ischemia was induced in male Wistar rats by 15 minutes occlusion of both common carotid arteries combined with concomitant hypovolemia, followed by reperfusion for 0, 1, 3, 5 and 7 days. The time-course of changes in contractile responses mediated by ET_B and $5\text{-}HT_{1B}$ receptors in cerebral arteries was evaluated by wire myography. Morphology and neuronal damage was studied in the hippocampus CA1 region by Hematoxylin/Eosin and TUNEL staining and neurological deficits were assessed by a rotating pole and a grip strength test. U0126 (30 mg/kg) or vehicle was administered

intraperitoneally at 0, 12, 24, 36, 48 and 60 hours post-ischemia. The effect of the U0126 treatment on contractile function and expression of vasoconstrictor receptors was evaluated at 3 days post-ischemia by wire myography and immunohistochemistry, respectively.

Results: The enhanced contractile function of ET_B and 5-HT_{1B} receptors reached its maximum peak in middle cerebral arteries (MCA) and anterior cerebral arteries (ACA) 3 days after transient forebrain ischemia. Neuronal cell damage appeared initially in the hippocampus after the third day of reperfusion and thereafter the cell damage developed and reached a maximal peak after 7 days. *In vivo* treatment with U0126 normalized the contractile responses in cerebral arteries of ischemic rats to levels in sham-operated rats. Protein expression of ET_B receptors in the cerebrovascular smooth muscles from ischemic rats treated with U0126 was also normalized to sham-operated levels.

Conclusions: Our data reveal new valuable information about delayed vasoconstriction in cerebral arteries following experimental global cerebral ischemia, demonstrating maximum enhancement of ET_B and 5-HT_{1B} contractile function at 3 days after the ischemic insult. The study also demonstrate that this enhanced cerebrovascular contractility, presumably involved in delayed cerebral hypoperfusion after global cerebral ischemia, could be prevented by treatment with the MEK ½ inhibitor U0126.

FATTY ACID METHYL ESTERS CONFER NEUROPROTECTION AFTER CEREBRAL ISCHEMIA

H.W. Lin, I. Saul, V.L. Gresia, S.V. Narayanan, J.T. Neumann, K.R. Dave, M.A. Perez-Pinzon

Neurology, University of Miami Miller School of Medicine, Miami, FL, USA

We previously showed that palmitic acid methyl ester (PAME) and stearic acid methyl ester (SAME) are simultaneously released from the sympathetic ganglion and PAME possesses potent vasodilatory properties which may be important in cerebral blood flow regulation after ischemia. Since PAME is a potent vasodilator simultaneously released with SAME, our hypothesis was that PAME and/or SAME confers neuroprotection in rat models of focal and global cerebral ischemia.

Asphyxial cardiac arrest (ACA, 6 min) was performed in male Sprague Dawley rats (260 - 280 g) 30 mins after PAME or SAME treatment (0.02 mg/kg, bolus, IV). 7 days after ACA, the rats were sacrificed, perfused with saline, and then a 40 % mixture of formaldehyde, glacial acetic acid, and methanol. The brain was removed from the skull and coronal brain blocks were embedded in paraffin with sections of 10 mm in thickness subsequently stained with hematoxylin and eosin. Hippocampal CA1 neurons were assessed by counting ischemic neurons at 18 fields/section along the medial to lateral extent of the CA1 region of the hippocampus 3.8 mm posterior to the bregma. Focal ischemia was induced in rats using an occluding intraluminal suture coated with poly-D-lysine (30 mm long segment of 3-0 nylon monofilament suture) with the tip rounded by a flame was inserted into the stump of the external carotid artery and advanced into the internal carotid artery ~19-20 mm from the carotid bifurcation to occlude the ostium of the middle cerebral artery for 2 hrs with 2 mins of reperfusion. Then, PAME or SAME was administered following reperfusion after 2 hrs of middle cerebral artery occlusion (MCAO). 2,3,5-triphenyltetrazolium staining of the brain was performed 24 hrs after MCAO and the infarct volume was quantified.

Following ACA, the number of surviving hippocampal neurons was enhanced in the presence of PAME (1143 ± 39.3 normal neurons) or SAME (1188 ± 57.8 normal neurons)-treated rats similar to the sham-operated group (1125 ± 41.5 normal neurons) as compared to ACA only (363 ± 15 normal neurons) or ethanol (0.005 %, vehicle) (432 ± 118 normal neurons)-treated groups (Figure 1A). Total infarct volume was decreased by PAME (69.24 ± 17.48 mm^3) or SAME (130.6 ± 22.85 mm^3) as compared to saline (408.6 ± 19.93 mm^3) or dimethylsulfoxide (276.1 ± 61.05 mm^3) (vehicles) in MCAO-treated animals (Figure 1B).

The use of both methods (MCAO or ACA models of cerebral ischemia) further validates the effectiveness of PAME or SAME-induced neuroprotection under global and focal ischemic conditions. PAME or SAME can provide hippocampal CA1 neuroprotection and reduce brain infarct volume (regional neuroprotection). With proper timing and dosage, administration of PAME and/or SAME

can be an effective therapy against cerebral ischemia.

This work was supported by: NS45676-05, NS054147-01A1, NS34773, NS073779, T32-NS007459-10, AHA-Philips 10POST4340011, AHA-13SDG13950014.

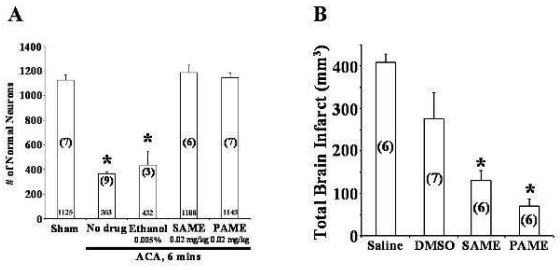

Figure 1. A) Rats pretreated with PAME (0.02 mg/kg) or SAME (0.02 mg/kg) provided neuroprotection in the CA1 region of the rat hippocampus 7 days after ACA. Rats were pretreated with PAME or SAME (IV bolus 30 mins before ACA). Sham (no ischemia), no drug (ACA only), and ethanol (vehicle control) groups were performed as internal controls. Neurons from the CA1 region of the hippocampus were counted and expressed in the bar graph shown in A. Numerical values in the bar graph represent the number of normal neurons counted. Numbers in parentheses indicate the number of animals used per group. B) Post-treatment with PAME or SAME after 2 hrs of MCAO decreased total rat brain infarct volume. Post-treatment with PAME (0.02 mg/kg, IV) or SAME (0.02 mg/kg, IV) decreased ipsilateral hemisphere volume as compared to saline and dimethylsulfoxide (DMSO) [vehicle for PAME, or SAME]. 2,3,5-Triphenyltetrazolium chloride (TTC)-treated brain slices were scanned and analyzed (Image J software) at the ipsilateral hemisphere. Total brain infarct volume is expressed as mm^3 ($n = 3$-9, *$p \leq 0.05$).

[figure 1abfinal]

IMPAIRED NMDA RECEPTOR FUNCTION IN PURKINJE NEURONS IN A MOUSE MODEL OF CARDIAC ARREST/CARDIOPULMONARY RESUSCITATION

N. Quillinan[1], K. Shimizu[1], H. Grewal[1], R.J. Traystman[1,2], P.S. Herson[1,2]

[1]Anesthesiology, [2]Pharmacology, University of Colorado Denver, Aurora, CO, USA

Objectives: Global ischemia caused by cardiac arrest results in neuronal damage and death in certain neuronal populations. Purkinje neurons are particularly sensitive to global ischemia and damage to these neurons results in motor coordination deficits. The purpose of this study is to assess NMDA receptor function and expression in mice that have been subjected to cardiac arrest and cardiopulmonary resuscitation (CA/CPR).

Methods: CA/CPR experiments performed in adult (8-10 week) C57Bl/6 mice. Cardiac arrest was induced by injection of KCl and after 8 min asystole, cardiopulmonary resuscitation was performed (CA/CPR). Mice were sacrificed at various time points following resuscitation (24 hrs, 7 days, 30 days) and acute parasagittal cerebellar slices were cut. Whole cell voltage clamp recordings were obtained from Purkinje cells (PCs) and synaptic NMDA receptor currents were recording following stimulation of the climbing fiber (stimulating electrode placed in granule cell layer). NMDA receptor expression was assessed using immunohistochemistry and quantitative real-time PCR from isolated PCs by laser capture microdissection.

Results: Analysis of NMDA mediated currents in PCs from sham controls and CA/CPR mice revealed a significantly reduced NMDA current 24 hr after resuscitation (-429.6± 198.9pA in control vs -165.5± 63.23pA 24 hr CA/CPR; $p< 0.05$) that did not recover at 7 days (-110.1± 45.01pA; $p< 0.05$) and partially recovered after 30 days (203.5±54.1; $p>0.05$). Immunohistochemistry and qRT-PCR revealed a decrease in NR2A expression at 24 hrs, 7 and 30 days and a decrease in NR2B expression at 24 hrs that recovered after 7 days.

Conclusions: Our data indicates that global cerebral ischemia causes a reduction in functional synaptic NMDA receptors in cerebellar Purkinje cells. This reduction is associated with decreases in NR2A expression and a transient decrease in NR2B expression. These data indicate that NMDA receptor-dependent processes, such as synaptic plasticity, may be impaired following global ischemia. Therefore, ongoing experiments are aimed at examining long-term depression, an NMDA receptor dependent form of synaptic plasticity, and motor coordination following CA/CPR.

ACTIVATION OF GLIAL CELLS AND REDISTRIBUTION OF WATER CHANNEL AQUAPRIN-4 IN RELATION TO BRAIN PATHOLOGY IN CARDIAC ARREST

H.S. Sharma[1], R. Patnaik[2], A. Sharma[1], L. Wiklund[1]

[1]Surgical Sciences, Anesthesiology & Intensive Care Medicine, Uppsala University, University Hospital, Uppsala, Sweden, [2]Biomaterials, School of Biomedical Engineering, National Institute of Technology, Banaras Hindu University, Varanasi, India

About 4 to 5 millions die every year due to cardiac arrest (CA) World Wide including 250 to 300k in the USA alone. Despite major developments in emergency medicine and resuscitation the survival rate of CA patients are very low. Those surviving CA exhibit neurological abnormalities that progresses

over time indicating that brain damage play important roles in disability of the victims.

The brain contains about 10 billion nerve cells that regulate cellular and system level functions to maintain homeostasis. However, the central nervous system (CNS) is also equipped with other non-neuronal cells, i.e., glial cells that are 6 to 10 times higher in number than the neuronal cells, and the endothelial cells that supply nutrients to the nerve cells also outnumber the glial cells. Thus, it is likely that non-neuronal cells play greater roles in maintaining neuronal functions during CA. This is evident from our findings that CA in a porcine model disrupts the blood-brain barrier (BBB) to serum proteins in different areas leading to neuronal damage. However, studies on glial cell functions e.g., astrocytes that support and regulate the BBB are not well known in CA. Breakdown of the BBB leads to entry of serum proteins into the CNS compartment causing edema. The water enters into the brain form the vascular comportment leading to brain swelling in a closed cranium causing instant death. Apart from endothelial cell leakage, special water channel proteins are present on the glial cells that regulate water transport across the brain. These water channel proteins known as aquaporins exist in various isoforms. The aqaporin4 (AQ4) regulates water transport in the brain and their expressions are altered in brain pathology. Our results in a porcine model show that 5 to 180 min of CA leads to massive activation of astrocytes in the areas of BBB leakage. These areas also exhibit AQ4 over expression. However, in many areas a downregulation of AQ4 was also seen. Upregulation of AQ4 denotes increased water transport into the cells and downregulation suggest either blockade of water transport or outward transport of water from the cell to maintain homeostasis. Both downregulation and upregulation of AQ4 suggest a tight regulation of water channel in brain during CA. Astrocytic activation seen using glial fibrillary acidic protein (GFAP) suggests that astrocytes are also maintaining water and ion transport in CA. Since neuroprotection caused by drugs e.g. methylene blue restores GFAP and AQ4 activation, it appears that in CA both glial cells and AQ4 plays important roles in regulating neuronal functions. Thus, in future therapeutic measures to restore glial cells and AQ4 function in CA is highly needed.

VENTILATORY PATTERN VARIABILITY IS ASSOCIATED WITH LONG-TERM SURVIVAL FOLLOWING CARDIAC ARREST AND RESUSCITATION IN RATS

K. Xu[1], Y. Kuang[2], T.E. Dick[3,4], F.J. Jacono[3,5]

[1]Neurology, [2]Physiology and Biophysics, [3]Medicine, [4]Neurosciences, Case Western Reserve University, [5]Medicine, Louis Stokes VA Medical Center, Cleveland, OH, USA

Introduction: High mortality is associated with cardiac arrest even following resuscitation [1]. Assessing mortality risk after cardiac arrest and resuscitation is essential for predicting outcomes and intervening to prevent mortality in high-risk patients. There may be changes in breathing patterns following cardiac arrest and resuscitation, such as what occurs in patients recovered from stroke. The changes in breathing patterns may reflect brainstem function with respect to cardio-respiratory regulation.

Objective: In this study we applied linear and nonlinear tools to assess ventilatory pattern variability (VPV) before and early recovery days following cardiac arrest an resuscitation with the goal of predicting long-term survival.

Methods: Male Wistar rats (3-month old) underwent cardiac arrest (12 min) and resuscitation. Spontaneous ventilation was recorded for 60 min using whole-body, flow-through plethysmography before cardiac arrest and day 0 and day 1 post-resuscitation. Ventilatory pattern was analyzed for non-linear-deterministic factors in variability by comparing original to surrogate data sets that had similar autocorrelation functions and measuring the differences in mutual information and sample entropy [2;3]. Overall survival was determined over a 4-day period.

Results: Consistent with previously reported [1], about 50% of rats subjected to cardiac arrest survived for 4 days. Before cardiac arrest, the ventilatory patterns were similar by our measures. However, after cardiac arrest and resuscitation VPV differed between survivor (survival for 4 days, n =15) and non-survivor (died before day 4, n =13) groups. The nonlinear complexity index (NLCI), a measure of deterministic similarity in ventilatory patterns, was similar between survivors and non-survivor (mean ± SD, 0.08 ± 0.03 vs.0.07± 0.03) before cardiac arrest. NLCI was significantly increased (about 3 folds) in the non-survivor group while remained unchanged in the survivors on day 0 and day 1 post-resuscitation. Traditional

measures such as respiratory rate and coefficient of variation of respiratory cycle length, cannot distinguish the difference in ventilatory pattern between the survivors and the non-survivors.

Conclusions: Our data showed that changes in VPV can distinguish survivor from non-survivor rats during early recovery phase, suggesting that VPV can be used as a non-invasive approach to predict outcome following cardiac arrest and resuscitation, therefore it may have translational potential to be used in clinical settings. Supported by NS 38632, HL 087377, VA Research Service.

References:

1. Xu,K.; LaManna,J.C. The loss of hypoxic ventilatory responses following resuscitation after cardiac arrest in rats is associated with failure of long-term survival. Brain Res. 1258: 59-64; 2009.

2. Dhingra,R.R.; Jacono,F.J.; Fishman,M.; Loparo,K.A.; Rybak,I.A.; Dick,T.E. Vagal-dependent nonlinear variability in the respiratory pattern of anesthetized, spontaneously breathing rats. J. Appl. Physiol 111: 272-284; 2011.

3. Jacono,F.J.; Mayer,C.A.; Hsieh,Y.H.; Wilson,C.G.; Dick,T.E. Lung and brainstem cytokine levels are associated with breathing pattern changes in a rodent model of acute lung injury. Respir. Physiol Neurobiol. 178: 429-438; 2011.

CYP2C19 POLYMORPHISMS AND ANTIPLATELET EFFECTS OF CLOPIDOGREL IN ACUTE ISCHEMIC STROKE IN CHINA

M. Zhang, Z. Chen, D. Jia, **Y. Xu**

Department of Neurology, Affiliated Drum Tower Hospital of Nanjing University Medical School, Nanjing, China

Background and purpose: Little research on genotypes and clopidogrel response in acute ischemic stroke has been published. The purpose of this study was to investigate whether the polymorphisms of receptors or enzymes which are involved in the process of clopidogrel metabolization affect clopidogrel response and prognosis in acute stroke.

Methods: Between Aug 2011 and July 2012, 263 acute ischemic stroke patients were enrolled in this prospective single-center study, including follow-up evaluations 3 to 6 months after clopidogrel treatment. CYP2C19 (636G>A, 681G>A), CYP3A4 (894C>T), P2Y12 (34C>T, 52G>T) were screened for mutations by a mutagenically separated polymerase chain reaction assay and genotyping microarray. Clopidogrel responsiveness was assessed using an ADP-induced platelet aggregation test, the National Institute of Health Stroke Scale (NIHSS) and the modified Rankin Scale (mRS).

Results: ADP-induced platelet aggregation, both in the intermediate metabolizers (IM) group and the poor metabolizers (PM) group, was significantly lower than the extensive metabolizers (EM) group (p=0.020 and 0.016 respectively). Patients in the EM group had better outcomes than the other two genotypes accessed by NIHSS and mRs scores 6 months after treatment. Regression analysis showed that CYP2C19 was an independent predictor of clopidogrel resistance.

Conclusions: CYP2C19 genotypes had significant impact on clopidogrel resistance and the prognosis of stroke patients. Screening the CYP2C19 gene may guide neurologists in treating stroke patients with clopidogrel, individually and collectively.

EFFECT OF MCI-186 ON THE INTRACELLULAR CALCIUM AND MEMBRANE FLUIDITY IN THE RATS WITH FOCAL CEREBRAL INFARCTION

M. Yu

Affiliated Hospital of Jiangsu University, Zhenjiang, China

Background: It has been proved that oxidative stress plays an important role in the pathogenesis of cerebral infarction and MCI-186 (3-methyl-1-phenyl-2-pyrazolin-5- one, adaravone), a novel free radical scavenger, can effectively remove hydroxyl radicals. It's reported that oxidative stress has a certain effect on homeostasis of the intracellular calcium ion and antioxidants also plays an important role in the prevention and treatment of cerebral infarction associated to abnormal Ca2+ mobilization induced by reactive oxygen species. Meanwhile, dysregulation of intracellular calcium signaling results in generation of excessive reactive oxygen species, then, membrane properties of

biological membranes are changed with the membrane fluidity having been decreased.

Aim: To determine the neuroprotective effect of MCI-186 through decreasing the concentration of intracellular calcium ([Ca2 +]i) and the mean microviscosity (MMV) in the rats with cerebral infarction.

Methods: Eighty male Wistar rats were randomly divided into 4 groups: normal control group, sham-operated group, focal cerebral infarction group, and MCI-186 treatment group. Focal cerebral infarction was successfully made with middle cerebral artery occlusion and neurological deficit score (NDS) was assessed with Zea Longa method. [Ca2+]i were respectively detected at 2h, 6h, 1d, 7d and 14d by Fura-2/AM fluorimetry. Membrane fluidity was also measured at above-mentioned time using fluorescence spectrophotometer. Neurons were enzymatically isolated and loaded with the fluorescent dye, DPH (1,6-diphenyl-1,3,5-hexatriene). MMV was used as index of membrane fluidity.

Results: [Ca2+]i, MMV and NDS increased in the focal cerebral infarction group from the 6th hour and reached the highest level at the 7th day compared with the normal control group and the sham operation group ($P < 0.01$). Compared with the focal cerebral infarction group, [Ca2+]i, MMV and NDS in MCI-186 treatment group significantly decreased from the 7th day to the 14th day ($P < 0.01$ or $P < 0.05$), but these indexes in MCI-186 treatment group never restored the normal level till the 14th day ($P < 0.01$ or $P < 0.05$).

Conclusion: MCI-186 can protect neurons in the rats with cerebral infarction through decreasing the intracellular calcium concentration and improving the membrane fluidity (that is, decreasing the mean microviscosity), which are probably important anti-oxidative mechanisms of MCI-186.

PROTECTIVE EFFECT OF DL-3-N-BUTYLPHTHALIDE ON RECOVERY FROM CARDIAC ARREST AND RESUSCITATION IN RATS

L. Zhang[1,2], Y. Kuang[1], K. Xu[3], J.C. LaManna[1]

[1]Physiology and Biophysics, Case Western Reserve University, Cleveland, OH, USA, [2]Neurology, Xiangya Hospital, Central South University, Changsha, China, [3]Neurology, Case Western Reserve University, Cleveland, OH, USA

Introduction: Dl-3-n-butylphthalide (NBP) was extracted as a pure component from seeds of Apium graveolens Linn, and was approved by the State Food and Drug Administration of China for clinical use in stroke patients in 2002. The molecular mechanisms of therapeutic effects of NBP are thought to include endothelial cells protection, enhanced angiogenesis, and increased cerebral microvessel density [1-3]. The similarities between the brain tissue damage mechanisms in stoke and cardiac arrest and resuscitation makes NBP a potential candidate for neuronal protection.

Objective: In this study we investigated the effect of NBP on the recovery from cardiac arrest and resuscitation in rats.

Methods: Male Wistar rats (3-month old) underwent cardiac arrest (12 min) and resuscitation. NBP was a gift from Shijiazhuang Pharma Grp NBP Co., LTD, Shijiazhuang, China. NBP was diluted into a solution of 10mg/ml in 0.5% Tween 80. Rats were randomly assigned to the following groups: sham non-arrested group; vehicle group, was given orally 0.5% Tween80 8ml/kg per day 7 days before cardiac arrest and 4 days post-resuscitation; NBP pre-treated group, was given orally 80 mg/kg of NBP per day 7 days before cardiac arrest; NBP post-treated group; was given 80 mg/kg i.p. for 4 days following cardiac arrest and resuscitation. Overall survival rates were determined in each group at the end of 4 days. Rats were sacrificed 4 days after resuscitation and the number of neurons surviving was evaluated in hippocampal CA1 region.

Results: Our data showed that NBP pre-treated group and NBP post-treated group had significantly higher survival rate (80%, 8/10 and 86%, 6/7 respectively) compared to that of

the vehicle group (50%, 6/12; $p < 0.05$, Wilcoxon survival analysis). At 4 days of recovery, only about 20% of hippocampal neurons were preserved in the vehicle group (mean ± SD, 23 ± 8, n = 12) compared to the sham non-arrested group (mean ± SD, 117 ± 2, n = 4). The hippocampal CA1 counts were significantly higher in the NBP pre-treated group and NBP post-treated group (mean ± SD, 76 ± 12, n = 10 and 61 ± 9, n =7, respectively) compared to the vehicle group.

Conclusions: NBP treatment improved the overall survival and hippocampal CA1 neuronal survival 4 days following cardiac arrest and resuscitation in rats. NBP has both preventive and therapeutic effect on improving outcomes following cardiac arrest and resuscitation.

References:

1. Chang,Q.; Wang,X.L. Effects of chiral 3-n-butylphthalide on apoptosis induced by transient focal cerebral ischemia in rats. Acta Pharmacol. Sin. 24: 796-804; 2003.

2. Li,L.; Zhang,B.; Tao,Y.; Wang,Y.; Wei,H.; Zhao,J.; Huang,R.; Pei,Z. DL-3-n-butylphthalide protects endothelial cells against oxidative/nitrosative stress, mitochondrial damage and subsequent cell death after oxygen glucose deprivation in vitro. Brain Res. 1290: 91-101; 2009.

3. Liao,S.J.; Lin,J.W.; Pei,Z.; Liu,C.L.; Zeng,J.S.; Huang,R.X. Enhanced angiogenesis with dl-3n-butylphthalide treatment after focal cerebral ischemia in RHRSP. Brain Res. 1289: 69-78; 2009.

NEURONAL DAMAGE AND GLIOSIS IN THE SOMATOSENSORY CORTEX INDUCED BY VARIOUS DURATIONS OF TRANSIENT CEREBRAL ISCHEMIA IN GERBILS

J.H. Ahn, D.H. Lee, B.C. Yan, J.H. Park, J.-C. Lee, M.-H. Won, J.H. Cho

Kangwon National University, Chuncheon, Republic of Korea

Objective: Although many studies regarding ischemic brain damage in the gerbil have been reported, studies on neuronal damage according to various durations of ischemia-reperfusion (I-R) have been limited. In this study, we examined neuronal damage/death and glial changes in the somatosensory cortex 4 days after 5, 10 and 15 min of transient cerebral ischemia using the gerbil.

Methods: To examine neuronal damage, we used Fluoro-Jade B (F-J B, a marker for neuronal degeneration) histofluorescence staining as well as neuronal nuclei (NeuN, neuronal marker) immunohistochemistry.

Results: In the somatosensory cortex, some NeuN positive ($^{+}$) neurons were slightly decreased only in layers III and VI in the 5 min ischemia-group, and the number of NeuN^{+} neurons were gradually decreased with longer ischemic time. F-J B histofluorescence staining showed a clear neuronal damage in layers III and VI, and the number of F-J B^{+} neurons was gradually increased with time of I-R: in the 15 min ischemia-group, the number of F-J B^{+} neurons was much higher in layer III than layer VI. In addition, we immunohistochemically examined gliosis of astrocytes and microglia using anti-glial fibrillary acidic protein (GFAP) and anti-ionized calcium-binding adapter molecule 1 (Iba-1) antibody, respectively. In the 5 min ischemia-group, GFAP immunoreactive astrocytes and Iba-1 immunoreactive microglia were distinctively increased in number, and their immunoreactivity was stronger than that in the sham-group. In the 10 and 15 min ischemia-groups, numbers of GFAP and Iba-1 immunoreactive cells were much more increased with time of I-R; in the 15 min ischemia-group, their distribution patterns of GFAP and Iba-1 immunoreactive cells were similar to those in the 10 min ischemia-group.

Conclusion: Our fining indicates that neuronal death/damage and gliosis of astrocytes and microglia were apparently increased with longer time of I-R.

OSTHOLE ATTENUATES CEREBRAL ISCHEMIC NEUROINJURY VIA ENOS DEPENDENT AND NITRIC OXIDE MEDIATED ANTI-APOPTOTIC ACTION

X.-D. Chao, Z. Fei

Xijing Hospital, The Fourth Military Medical University, Xi'an, China

Objective: Apoptosis contributes to cerebral ischemic injury, and both osthole and nitric oxide (NO) have been shown to exert anti-apoptotic effects *in vitro* and *in vivo*. However, interrelationship between two neuroprotective molecules remains completely unknown. The

present study investigated the neuroprotective effect of osthole on acute ischemic stroke induced by middle cerebral artery occlusion (MCAO) in rats and the underlying mechanism.

Methods: Adult male Sprague-Dawley rats weighing 250 to 280g were subjected to 2h MCAO and pretreated with vehicle (20% Tween-80), osthole alone, or osthole plus NG-nitro-L-arginine methyl ester (L-NAME, a nonselective NOS inhibitor), LY-294002 (a specific PI3K inhibitor) or GW9662 (a selective PPARγ antagonist) at 30min before the transient occlusion. Neurological deficit scores (NDS) and infarct volumes of brain were assessed at 24h and 72h after MCAO. Neuronal apoptosis, NO concentration and activated caspase-3, iNOS, nNOS, eNOS, phosphorylated eNOS (p-eNOS), Akt, phosphorylated Akt (p-Akt), Tumor necrosis factor-α (TNF-α) and arginase I proteins expression were also determined at 24h after MCAO.

Results: Pre-administration of osthole on rats with MCAO-induced acute ischemic stroke resulted in a significant decrease both in NDS and infarction volume at 24h and 72h and in the levels of neuronal apoptosis, activated caspase-3 and iNOS proteins expression at 24h after MCAO. In contrary, NO concentration and eNOS protein expression were increased. The neuroprotective effect of osthole was completely blocked by NOS inhibitor L-NAME. Furthermore, osthole-induced eNOS protein expression and phosphorylation was blocked by GW9662 and LY-294002 respectively. And the phosphorylation of eNOS had a greater effect on osthole neuroprotection than the expression of eNOS.

Conclusions: Our results provided direct evidence that osthole attenuates cerebral ischemic neuroinjury via eNOS-dependent and NO-mediated anti-apoptotic action in which both eNOS protein up-regulation and phosphorylation are involved, with the latter being the primary pathway.

RESP18 IS INVOLVED IN THE CYTOTOXICITY OF DOPAMINERGIC NEUROTOXINS IN MN9D CELLS

Y. Huang, J. Xu, F. Huang

State Key Laboratory of Medical Neurobiology, Shanghai Medical College and Institutes of Brain Science, Fudan University, Shanghai, China

RESP18 (Regulated endocrine-specific protein, 18kDa) was first identified as a dopaminergic drugs-regulated intermediate pituitary transcript. RESP18 protein is a unique endoplasmic reticulum (ER) resident protein. Its functions in the brain especially in the nervous system disorders remain unknown. ER stress (ERS) has been proved to be one of the important pathogenesis of neurodegenerative diseases, including Parkinson's disease (PD). Here, we explored the association of RESP18 and ERS in cell models of PD. Dopaminergic neurotoxin 1-methyl-4-phenyl-pyridinium ion (MPP^+), 6-hydroxydopamine (6-OHDA) and rotenone evoked dramatic MN9D cell death. The transcriptional expressions of RESP18 and two ERS markers---Binding immunoglobulin protein/glucose-regulated protein 78 (BiP/GRP78) and CCAAT/enhancer-binding protein homologous protein (CHOP) manifested differential changes in MN9D cells treated with MPP^+, 6-OHDA and rotenone. RESP18 protein levels increased in MPP^+ and 6-OHDA-treated cells, but did not change in the cells treated with rotenone, while the protein levels of ER molecular chaperone heat shock protein 90kDa beta member 1/glucose-regulated protein 94 (HSP90B1/GRP94) and BiP in the cells were up-regulated by MPP^+ and 6-OHDA, respectively. Salubrinal, an ERS inhibitor, significantly reduced MPP^+ and 6-OHDA-induced cell death. Moreover, ERS inducer---Thapsigarin and Tunicamycin, decreased the expression of RESP18, which is different from the changes of BiP, GRP94 and CHOP. Silencing RESP18 expression with Lenti-shRNA increased the expression of BiP, GRP94 proteins and alleviated MPP^+-induced cell death, while over-expression of RESP18 resulted in aggravated cell death induced by MPP^+ and 6-OHDA. Taken together, our results suggest that RESP18 is involved in the cytotoxicity of dopaminergic neurotoxins.

This work was supported by National Natural Science Foundation of China (81171188);

Grants from the Ministry of Science and Technology of China (2012CB966300); National Natural Science Foundation of China Specialized Research Fund for the Doctoral Program of Higher Education (20110071110039).

PROGRESSION FROM FOCAL ISCHEMIA TO INFARCT FORMATION AFTER BARREL CORTEX STROKE IN MICE

Q. Jiang, Y.Y. Zhao, T.C. Deveau, S.P. Yu, L. Wei

Anesthesiology, Emory University School of Medicine, Atlanta, GA, USA

Introduction: Stoke is the third most prevalent cause of death and the leading cause of long term disability with direct and indirect costs amounting to 34.3 billion annually in the United States. Focal barrel cortex stroke induced via permanent ligations of distal branches of the middle cerebral artery (MCA) and temporary bilateral common carotid (CCAo) occlusion results in an infarct restricted to the functionally defined whisker-barrel cortex[1]. This study aims to optimize the use of this model by characterizing the progression from ischemic insult to infarct formation which is currently fragmented.

Method: Adult C57/B6 male mice were subjected to permanent distal MCA occlusion with no CCAo, 4 min, 7 min, or 15 min CCAo. Infarct volume was measured 72 hrs later using 2,3,5-triphenyltetrazolium chloride (TTC) staining. Local cerebral blood flow (LCBF) was measured via laser Doppler scanning before, during stroke, and at the time of sacrifice. Furthermore, we quantified structural changes occurring post ischemia at time points of 6, 12, 24, 48, 72 hrs, and 7 days after stroke. Immunocytohistochemical analysis of cell death was visualized using terminal deoxyribonucleotidyl transferase-mediated dUTP nick end labeling (TUNEL), Hoescht, NeuN, and Glut1 staining.

Result: LCBF during MCA occlusion was reduced in a manner depending on CCA ligation. Without CCAo, LCBF was 44.0±1.0% of the basal flow, and 12.8±1.2%, 13.3±1.5%, 11.5±1.8% of baseline with 4, 7, and 15 min CAAo, respectively. Blood flow reduction without CCAo was statistically significant from groups with CCAo [$F(3,19)=126.8$, $p< 0.0001$]. Infarct volumes observed 72 hrs after stroke (indirect infarct ratios) were significantly smaller without CCAo [$F(3,12)=7.168$ $p=0.0051$] but no differences between other CCAo groups: no CCAo 0.019±0.011, 4 min CCAo 0.074±0.011, 7 min CCAo 0.069±0.011, 15 min CCAo 0.089±0.004. Immunocytohistochemistry characterization of cell death in the ischemic core showed TUNEL-positive cells appearing at 6 hrs, peaking at 48 hrs, and declining at 72 hrs after stroke. The percentage of TUNEL+ cells continued to rise steadily from 37.9 ± 7.5 % up to 96.4 ± 1.2 % by day 7. In the penumbra, less than 5% of neurons were observed to be TUNEL-positive at 24 hrs, 48 hrs, and 72 hrs.

Conclusion: The progression of neuronal damage after ischemia in this model follows a predictable time course. Characterization of the progression in the relevant brain structure enables the further investigation of morphological and functional correlations as well as tissue repair in a focal region of known function.

1. Wei L., Rovainen CM & Woolsey TA. Ministrokes in rat barrel cortex. Stroke 26:1459, 1995.

DIFFERENCES OF CALCIUM BINDING PROTEINS IMMUNOREACTIVITIES IN THE YOUNG HIPPOCAMPAL CA1 REGION FROM THE ADULT FOLLOWING TRANSIENT ISCHEMIC DAMAGE

I.H. Kim[1], J.-H. Cho[1], J.H. Park[1], J.H. Cho[1], Y.L. Lee[2], M.-H. Won[1], B.C. Yan[1]

[1]Kangwon National University, [2]Hallym University, Chuncheon, Republic of Korea

Objective and methods: It has been reported that the young were much more resistant to transient cerebral ischemia than in the adult. In the present study, we compared the chronological changes of CBPs (CB-D 28k, CR and PV) immunoreactivities and levels in the hippocampal CA1 region of the young gerbil with those in the adult following 5 min of transient cerebral ischemia induced by the occlusion of both the common carotid arteries.

Results: In the present study, we examined that about 90% of CA1 pyramidal cells in the adult gerbil hippocampus died at 4 days post-ischemia; however, in the young hippocampus, about 56% of them died at 7 days post-ischemia. We compared immunoreactivities and levels of calcium binding proteins (CBPs), such as calbindin 28k

(CB-D 28k), calretinin (CR) and parvalbumin (PV). The immunoreactivities and protein levels of all the CBPs in the young sham were higher than those in the adult sham. In the adult, the immunoreactivities and protein levels of all the CBPs were markedly decreased at 4 days post-ischemia, however, in the young, they were apparently maintained. At 7 days post-ischemia, they were decreased in the young, however, they were much higher than those in the adult.

Conclusion: In brief, the immunoreactivities and levels of CBPs were not decreased in the ischemic CA1 region of the young 4 days after transient cerebral ischemia. This finding indicates that the longer maintenance of CBPs may contribute to a less and more delayed neuronal death/damage in the young.

AGMATINE SUPPORTS COGNITIVE FUNCTION VIA ITS PRO-SURVIVAL ACTIVITY OF HIPPOCAMPAL NEURONS IN RATS EXPOSED TO STREPTOZOTOCIN

J.E. Lee[1], B.E. Hur[1], W. Yang[2]

[1]Anatomy, Brain Korea 21 Project for Medical Science, Yonsei University, College of Medicine, [2]Anatomy, Yonsei University, College of Medicine, Seoul, Republic of Korea

Objective: Alzheimer's disease (AD) is one of the most common neurological diseases which are characterized by progressive retardation of cognitive ability and memory loss due to the extensive neuronal death [1]. Agmatine is a polycationic and endogenous amine produced by arginine decarboxylase (ADC) [2]. Many studies have shown that it exerts neuroprotective effect as an antioxidant. Therefore, in this study, we explored the potentiality of agmatine to promote the survival of hippocampal neurons, which are relevant to cognitive function.

Methods: We used male rats (sprague-dawley) whose body weight ranges from 280 through 300g. Streptozotocin (STZ) was applied to produce cognitive impairment and hippocampal damage. Briefly, experimental groups of rats were divided into

(1) Sham,

(2) STZ (EC, 1.5mg/kg, 5μl, intra-cerebroventricular route, 1st and 3rd day from surgery [3]) and

(3) STZ with agmatine (100mg/kg, intra-peritoneal injection for 14 days).

All rats were sacrificed on 21 day after surgery for other analyses. Before being sacrificed, rats were subjected to behavioral tests (morris water maze [4] and radial arm maze) to evaluate cognitive abilities. After rats` brains were obtained, we performed western blotting to check protein levels of Bcl2, Bax, caspase-3 and cleaved caspase-3, PI3K, AKT, and Nrf2. As well, we did immunohistochemistry to examine caspase-3 and 8-oxo positivity in hippocampal tissue.

Results: STZ caused recognition disability as evidenced by water maze and radial arm maze tests indicating the impairment in spatial reference memory, whereas agmatine attenuated STZ-induced memory deficits. Concerning these, it was tested whether behavioral aberration is related with neural tissue damage. Both western blotting and immunohistochemical data indicate that STZ increases apoptotic proteins Bax, Bcl2, caspase-3 and cleaved caspase-3 and agmatine suppresses STZ triggering induction of these proteins in hippocampus. Then, it was further investigated how agmatine attenuates hippocampal neuronal damage by STZ. We found that agmatine elevates the protein levels of PI3K, P-AKT, and Nrf2 and declines 8-oxo immuno-fluorescence in hippocampal mitochondria of rats injected with STZ.

Conclusion: The present findings demonstrate that agmatine is able to support cognitive ability of rats exposed to STZ. Collectively, our data propose that agmatine might ameliorate cognitive function through the inhibition of hippocampal neuronal death implicated by oxidative stress.

References:

[1] Hyman et al., Annu Rev Public Health 10:115-140 (1998).

[2] Kim et al., Spin 36(25):2130-2138 (2011).

[3] Paxinos et al., The rat brain in stereotaxic coordinates 4th ed. San Diego, Academic press (1998).

[4] Morris, J Neuroscience Methods 11:47-60 (1984)

Support: This research was supported by Basic Science Research Program through the

National Research Foundation of Korea (NRF) funded by the Ministry of Education, Science and Technology(MEST) (2012-0005827)

EFFECT OF SHEXIANGBAOXIN PILL ON LEFT VENTRICLE IN PRESSURE-OVERLOADED HYPERTROPHY RAT

X. Liang[1], S. Li[2], L. Jinning[2]

[1]Qingdao University, School of Medicine, [2]Dept. of Chinese Medicine, Affiliated Yantai Yuhuangding Hospital, Qingdao University, School of Medicine, Yantai, China

AIM : To explore Shexiangbaoxin Pill (SXBXP), a traditional Chinese medicine which has been used to treat cardiovascular diseases for many years., on left ventricle in pressure-overloaded hypertrophy rats. And also the relationship between left ventricular hypertrophy (LVH) and cytokines, matrix metalloproteinases, apoptosis, and apoptosis genes.

Methods: IL-6, IL-10, MMP-2, MMP-9 were evaluated by ELISA means. TNF-alpha was measured with radioimmunoassays. Flow cytometer was used to measure the apoptosis ratio and the expression of Fas , Bcl-2 and Bax.

Results: 6 weeks after abdominal aortic coarctation operation, compared with the sham operated group, the weight of the left ventricle (0.983+0.316g) and heart weight/body weight (0.382+0.154) were significantly increased in control group. And also IL-6 (208.71+84.51pg/ml), TNF-α(1.983+0.842ng/ml), MMP-2 (74.63+37.62), MMP-9 (57.74+25.61), apoptosis ratio (8.47+4.18), and apoptosis genes (Fas, Bax, Bcl-2, Bcl-2/Bax) expression were increased, IL-10 (86.23+40.13pg/ml) decreased compared with sham operated group. The 3 groups with drugs (CP, LT, SXBXP) decreased the increasing weight of LV and ventricular weight/body weight; and inhibited the changes of influencing factors (IL-6, IL-10, TNF-α, MMP-2, MMP-9, apoptosis ratio, apoptosis genes expression), especially in the SXBXP group.

Conclusion: LVH might be related with many influencing factors. SXBXP may have the positive importance in the treatment and prevention of LVH,similar to ACEI and ARB.

PROTECTIVE EFFECT OF HOMER1A ON TUMOR NECROSIS FACTOR-A WITH CYCLOHEXIMIDE-INDUCED APOPTOTSIS IS MEDIATED BY MITOGEN-ACTIVATED PROTEIN KINASE PATHWAYS

P. Luo, Z. Fei

Xijing Hospital, The Fourth Military Medical University, Xi'an, China

Although Homer 1, of the postsynaptic density (PSD), regulates apoptosis, the signaling mechanisms are not fully elucidated. In this study, we found that tumor necrosis factor-α (TNF-α)/cycloheximide (CHX) treatment transiently increased Homer 1a (the short variant of Homer 1), but did not affect Homer 1b/c (the long variant of Homer 1). Overexpression of Homer 1a blocked TNF-α/CHX-induced apoptotic cell death, whereas inhibition of Homer 1a induction enhanced the pro-apoptotic effect of TNF-α/CHX treatment. Moreover, brain-derived neurotrophic factor (BDNF), as a potential activator of endogenous Homer 1a, inhibited apoptotic cell death after TNF-α/CHX treatment through induction of Homer 1a. Since three major mitogen-activated protein kinase (MAPK) pathways have important roles in apoptosis, we examined if Homer 1a is involved in the effects of MAPK pathways on apoptosis. It was shown that inhibition of the ERK1/2 pathway increased the expression and the protective effect of Homer 1a, but inhibition of the p38 pathway produced the opposite effect. Cross-talk among MAPK pathways was also associated with the regulation of Homer 1a during apoptotic cell death. Blocking the p38 pathway increased the activity in the ERK1/2 pathway, while inhibition of ERK1/2 pathway abolished the effect of p38 inhibitor on Homer 1a. Furthermore, Homer 1a reversely affected the activation of MAPK pathways. These findings suggested that Homer 1a plays an important role in the prevention of apoptotic cell death and contribute to distinct regulatory effects of MAPK pathways on apoptotic cell death.

THE ROLE OF THE A2A RECEPTOR IN CELL APOPTOSIS CAUSED BY MDMA

M. Mehdizadeh[1,2], M. Soleimani[1], M. Katebi[3]

[1]Cellular and Molecular Research Center, Tehran University of Medical Sciences, [2]Department of Anatomy, Tehran University of Medical Sciences, [3]Department of Anatomy, Hormozgan University, Tehran, Iran

Objective: Psychoactive recreational hallucinogenic substance and a major worldwide recreationaldrug. There are neurotoxic effects observed in laboratory animals and humans followingMDMA use. MDMA causes apoptosis in neurons of the central nervous system (CNS). Withdrawal signs are attenuated by treatment with the adenosine receptor (A2A receptor). This study reports the effects of glutamyl cysteine synthetase (GCS), as an A2A receptoragonist, and succinylcholine (SCH), as an A2A receptor antagonist, on Sprague Dawleyrats, both in the presence and absence of MDMA. Ecstasy, also known as 3, 4-methylenedioxymethamphetamine (MDMA), is a

Materials and methods: Dawley rats (200-250 g each). Each group was treated with daily intraperitoneal (IP) injectionsfor a period of one week, as follows:

i. MDMA (10 mg/kg);

ii. GCS (0.3 mg/kg);

iii.SCH (0.3 mg/kg);

iv. GCS + SCH (0.3 mg/kg each);

v. MDMA (10 mg/kg) + GCS (0.3 mg/kg);

vi. MDMA (10 mg/kg) + SCH (0.3 mg/kg); and

vii. normal saline (1 cc/kg) as the shamgroup. Bax (apoptotic protein) and Bcl-2 (anti-apoptotic protein) expressions were evaluatedby striatum using RT-PCR and Western blot analysis.In this experimental study, we used seven groups of Sprague.

Results: Group and a significant decrease in Bcl-2 protein expression in the MDMA+SCH groupThere was a significant increase in Bax protein expression in the MDMA+SCH ($p < 0.05$).

Conclusion: Bcl-2 pathways. An agonist of this receptor (GCS) decreases the cytotoxcity of MDMA, while the antagonist of this receptor (SCH) increases its cytotoxcity.

A2A receptors have a role in the apoptotic effects of MDMA via the Bax and Bcl-2 pathways. An agonist of this receptor (GCS) decreases the cytotoxcity of MDMA,

while the antagonist of this receptor (SCH) increases its cytotoxcity.

HEXOKINASE II-MEDIATED HYPOXIA TOLERANCE - A MOLECULAR SWITCH GOVERNING CELLULAR FATE DEPENDING ON THE METABOLIC STATE

P. Mergenthaler[1,2,3], J. Sünwoldt[1], K. Wendland[1], D.W. Andrews[4], A. Meisel[1,2,3]

[1]Department of Experimental Neurology, Charité University Medicine Berlin, [2]NeuroCure Clinical Research Center, NeuroCure Cluster of Excellence, [3]Center for Stroke Reasearch Berlin, Berlin, Germany, [4]Sunnybrook Research Institute, University of Toronto, Toronto, ON, Canada

The metabolic state of a cell is a key determinant in the decision to live and proliferate or to die. Hypoxia is a fundamental challenge of living organisms, interfering with homeostatic metabolism. It occurs physiologically during development or exercise and pathologically in vascular disease, tumorigenesis and inflammation.

We recently demonstrated that the hypoxia-inducible factor (HIF)-1-regulated glycolytic enzyme hexokinase II (HKII) functions as a molecular switch that determines cellular fate by regulating both cytoprotection and induction of cell death based on the metabolic state of the cell. We found HIF-1-dependent upregulation of HKII in primary rat brain cortical neurons upon hypoxic stimulation. We show that overexpression of HKII potently rescues neurons from hypoxic cell death. We further demonstrate that phosphoprotein enriched in astrocytes (PEA15) is a direct molecular interactor of HKII and show that together with PEA15, HKII inhibits apoptosis after hypoxia. In contrast, HKII accelerates cell death under glucose deprivation or in the absence of PEA15.

Furthermore, we present insight into the regulation of the HKII/PEA15 interaction as well as the functional consequences for neuronal fate under different states of metabolic stress.

In summary, HKII both protects neurons from cell death during hypoxia and functions as a sensor of glucose availability during normoxia, inducing apoptosis in response to glucose depletion.

SERIAL EXPRESSION OF HYPOXIA INDUCIBLE FACTOR-1A AND NEURONAL APOPTOSIS IN HIPPOCAMPUS OF RATS WITH CHRONIC ISCHEMIC BRAIN

C.T. Moon, Y.I. Chun, Y.C. Koh

Neurosurgery, Konkuk University Medical Center, Seoul, Republic of Korea

Objective: The purpose of this study is to investigate serial changes of hypoxia-inducible factor 1α (HIF-1α), as a key regulator of hypoxic ischemia, and apoptosis of hippocampus induced by bilateral carotid arteries occlusion (BCAO) in rats.

Methods: Adult male Wistar rats were subjected to the permanent BCAO. The time points studied were 1, 2, 4, 8, and 12 weeks after occlusions, with n = 6 animals subjected to BCAO, and n = 2 to sham operation at each time point, and brains were fixed by intracardiac perfusion fixation with 4% neutral-buffered praraformaldehyde for brain section preparation. Immunohistochemistry (IHC), western blot and terminal uridine deoxynucleotidyl transferase dUTP nick end labeling (TUNEL) assay were performed to evaluate HIF-1α expression, apoptosis.

Results: In IHC and western blot, HIF-1α levels were found to reach the peak at the 2nd week in the hippocampus, while apoptotic neurons, in TUNEL assay, were maximal at the 4th week in the hippocampus, especially in the cornu ammonis 1 (CA1) region. HIF-1α levels and apoptosis were found to fluctuate during the time course.

Conclusion: This study showed that BCAO induces acute ischemic responses for about 4 weeks then chronic ischemia in the hippocampus. These in vivo data are the first to show the temporal sequence of apoptosis and HIF-1α expression.

ZINC PROMOTES HYPOXIC ASTROCYTES DEATH BY INCREASE HIF-1A EXPRESSION VIA PARP-1

R. Pan[1], C. Chen[1], W. Liu[1], K. Liu[1,2]

[1]Department of Pharmaceutical Sciences, [2]Department of Neurology, University of New Mexico, Albuquerque, NM, USA

Objective: Pathological release of excess zinc has been implicated in ischemic brain cell death[1-5]. However, the underlying mechanism remains unclear. Exposing cells to hypoxia triggers response pathways based on regulating the hypoxia-inducible factor 1 (HIF-1) expression, which plays an important role in cell fate[6-9]. Overexpression of HIF-1α, the oxygen-dependent subunit, has been shown to exacerbate hypoxia-induced apoptotic cell death[10, 11]. We hypothesize that HIF-1 is involved in zinc-induced hypoxic astrocytes death.

Methods: Primary cortical astrocytes were isolated from the cortices of postnatal day 1 rat brains. Different concentrations of zinc chloride were added before hypoxia treatment. Cell death rate and protein expression were examined after 3hr hypoxic treatment.

Results: Exposure of astrocytes to hypoxia for 3hrs remarkably increased the protein level of HIF-1α, which was further augmented with the presence of $ZnCl_2$. Combination of 3hrs of hypoxia and 100μM of $ZnCl_2$ led to significant astrocytes death, while few cell dead under each treatment alone. Notably HIF-1α knockdown blocked zinc-induced astrocytes death. Moreover, Knockdown Poly(ADP-ribose) polymerase (PARP), another important protein in the response of hypoxia, attenuated the overexpression of HIF-1α and reduced the cell death rate.

Conclusions: Our studies show that zinc-induced cell death may be caused by the overexpression of HIF-1α via PARP-1 modification, which provides a novel mechanism for zinc-mediated ischemic brain injury.

References:

1. Nguyen, T., A. Hamby, and S.M. Massa, *Clioquinol down-regulates mutant huntingtin expression in vitro and mitigates pathology in a Huntington´s disease mouse model.* Proc

Natl Acad Sci U S A, 2005. **102**(33): p. 11840-5.

2. Weiss, J.H., S.L. Sensi, and J.Y. Koh, *Zn(2+): a novel ionic mediator of neural injury in brain disease.* Trends Pharmacol Sci, 2000. **21**(10): p. 395-401.

3. Frederickson, C.J., J.Y. Koh, and A.I. Bush, *The neurobiology of zinc in health and disease.* Nat Rev Neurosci, 2005. **6**(6): p. 449-62.

4. Cherny, R.A., et al., *Treatment with a copper-zinc chelator markedly and rapidly inhibits beta-amyloid accumulation in Alzheimer´s disease transgenic mice.* Neuron, 2001. **30**(3): p. 665-76.

5. Kauppinen, T.M., et al., *Zinc triggers microglial activation.* J Neurosci, 2008. **28**(22): p. 5827-35.

6. Jin, K.L., X.O. Mao, and D.A. Greenberg, *Vascular endothelial growth factor: direct neuroprotective effect in in vitro ischemia.* Proc Natl Acad Sci U S A, 2000. **97**(18): p. 10242-7.

7. Marti, H.J., et al., *Hypoxia-induced vascular endothelial growth factor expression precedes neovascularization after cerebral ischemia.* Am J Pathol, 2000. **156**(3): p. 965-76.

8. Bergeron, M., et al., *Induction of hypoxia-inducible factor-1 (HIF-1) and its target genes following focal ischaemia in rat brain.* Eur J Neurosci, 1999. **11**(12): p. 4159-70.

9. Chavez, J.C. and J.C. LaManna, *Activation of hypoxia-inducible factor-1 in the rat cerebral cortex after transient global ischemia: potential role of insulin-like growth factor-1.* J Neurosci, 2002. **22**(20): p. 8922-31.

10. Schofield, C.J. and P.J. Ratcliffe, *Oxygen sensing by HIF hydroxylases.* Nat Rev Mol Cell Biol, 2004. **5**(5): p. 343-54.

11. Fan, X., et al., *The role and regulation of hypoxia-inducible factor-1alpha expression in brain development and neonatal hypoxic-ischemic brain injury.* Brain Res Rev, 2009. **62**(1): p. 99-108.

THE CHANGES OF GENE EXPRESSION PROFILING AFTER CEREBRAL INFARCTION IN RATS

F.-F. Shi, P.-F. Huang, L. Yu, S.-S. Duan, **C.-C. Ren**

Neurology, Shanghai No 5 Hospital, Fudan University, Shanghai, China

Objective: To explore the changes of gene expression profiling of cerebral infarction in rats.

Methods: 6 SD rats was divided into ischemia and sham-operation group. Focal ischemia was generated by permanent occlusion of the left distal middle cerebral artery (dMCA) combined with 30 min of occlusion of both common carotid arteries (CCA) in rats. After cerebral ischemia for 1 hour, brain tissues was taken from the penumbra area in ischemic brains and the corresponding area in sham control brains.Total RNA was extracted from those brain tissues and was purified. Then the purified RNA was transcribed into complementary double-stranded DNA and mixed with ATP、GTP、CTP and aaUTP to synthesize cRNA. Next, cRNA was marked by CY5. The marked cRNA was hybridized with the Agilent gene expression profiling microarray and scanned by the Agilent scanner. The data that was obtained by scanning the chips was normalized and log2 transformed. The genes expressed differently was picked by the way of t-test ($p < 0.05$ and FC Abs>2).

Results: Except some genes expressed differently without names and functional annotation, totally, there were 127 genes expressed differently, among which 95 genes was up-expressed and 77 genes was down-expressed. And there were 20 genes up-expressed significantly and 3 genes down-expressed significantly. The standards for expressed differently significantly was p-value almost 0 and FC Abs higher than 7. By Gene Ontology analysis, we found that after acute cerebral infarction for 1 hour, there were 16 pathways in which all expressed differently genes were up-regulated, on the other hand, there were 4 pathways where all expressed differently genes were down-regulated, and there were 12 pathways which included genes up-expressed and down-expressed differently. The up-regulated molecular pathway were MAPK pathway, cellular factor-cellular factor

recptor pathway,and so on. Among which MAPK pathway included most up-expressed differently genes. Genes down-expressed differently spread in the vascular smooth muscle pathway, Cyt-P450 metabolism pathway and so on. The pathway including up- and down-expressed genes involved cellular adhesion molecular pathway, antigen processing and presenting pathway, and these pathways all included MHC genes, which were down-regulated in all pathways.

Conclusion: Acute cerebral ischemia induced neuronal inflammation and anti-inflammation, immune response and immune depression, the balance of them decided the outcome of cerebral ischemia injury.

INCREASED EXPRESSION OF TRPM7 CHANNELS IS ASSOCIATED WITH HYPERGLYCEMIA-MEDIATED INJURY OF VASCULAR ENDOTHELIAL CELLS

H.-W. Sun[1,2], T.-D. Leng[2], Z. Zeng[2], X.-R. Gao[1], K. Inoue[2], Z.-G. Xiong[2]

[1]Sun Yat-Sen University, Guangzhou, China, [2]Morehouse School of Medicine, Atlanta, GA, USA

Objectives: The study was aimed to investigate the involvement of transient receptor potential melastatin 7 (TRPM7) channels in hyperglycemia-mediated injury of human umbilical vein endothelial cells (HUVEC) and the potential underlying mechanisms.

Methods: HUVECs were cultured in the presence of normal (5.5 mM) or high concentration (30 mM) of D-glucose for 72h. L-glucose was used as an osmotic control. Cell viability and cytotoxicity were determined by MTT and LDH assays. TRPM7 mRNA was measured by reverse-transcription PCR and real-time PCR while TRPM7 protein was detected by Western blotting and immunofluorescence staining. TRPM7-like current was recorded by whole-cell patch-clamp recording. The levels of endothelial nitric oxide synthase (eNOS) protein expression and reactive oxygen species (ROS) generation were also examined.

Results: RT-PCR, real-time PCR, Western blotting, Immunofluorescence staining, and whole-cell patch-clamp recordings showed that TRPM7 mRNA, TRPM7 protein expression and TRPM7-like currents were increased in HUVECs cultured with high D-glucose for 72h. In contrast, cells cultured with high L-glucose did not show similar changes in TRPM7 mRNA/protein expression, or TRPM7-like currents. In addition, high D-glucose treatment increased ROS generation and cytotoxicity but decreased eNOS protein expression. These changes could be attenuated by knockdown of TRPM7 with TRPM7 siRNA. The protective effect of silencing TRPM7 against high glucose induced endothelial injury was abolished by U0126, an inhibitor of the extracellular signal-regulated kinase (ERK) signaling pathway.

Conclusions: These observations suggest that increased expression and function of TRPM7 channels play an important role in hyperglycemia induced injury of vascular endothelial cells and that ERK signaling pathway is likely involved.

This research was partially supported by NIH R01NS066027, NIMHD S21MD000101, U54RR026137, and AHA 0840132N.

REMARKABLE INCREASE OF CYTOCHROME C OXIDASE SUBUNIT I AFTER GLOBAL CEREBRAL ISCHEMIA

Y. Takahashi[1], T. Sugawara[1], T. Miyazaki[2], H. Itoh[2], K. Mizoi[1]

[1]Department of Neurosurgery, Akita University School of Medicine, [2]Department of Life Science, Faculty and Graduate School of Engineering and Resource Science, Akita University, Akita, Japan

Objectives: Cerebral ischemia is known to produce excessive reactive oxygen species (ROS) in mitochondria, and these radicals initiate radical chain reactions, causing cellular macromolecule damage and also promote mitochondrial apoptosis pathway, ultimately leading to cell death. However, little is known about the mitochondrial functional change after ischemia. We studied expression of cytochrome c oxidase (COX), a terminal, rate-limiting enzyme of the respiratory chain to generate ATP, after global cerebral ischemia in rats.

Methods: Transient global cerebral ischemia was induced for 5 min by bilateral common carotid artery occlusion and bleeding to lower the mean arterial pressure to 31-35 mmHg. Sublethal ischemia was induced for 3 min occlusion of bilateral common carotid artery.

The brain tissues were harvested at 1, 6 and 24 h after ischemia. Immunofluorescent staining and Western blot were performed to investigate the spatial and temporal changes in two important COX subunits, mitochondrial-encoded COX subunit I (COX I) and nucleus-encoded COX subunit IV (COX IV).

Results: In immunofluorescent staining, the intensity of COX I was increased at 6 h after 5 min ischemia, while COX IV intensity was not changed. In Western blot study, COX I of the hippocampal CA1 subregion showed significant increase at 1 h and 6 h after 5 min ischemia and then returned to the control level at 24 h. In contrast, there was no significant change in COX IV at 1, 6, and 24 h after 5 min ischemia compared with control. COX I and IV protein showed no obvious changes after 3 min ischemia.

Conclusions: This aberrant increase in COX I may be an early sign of delayed neuronal death or may predict later ETC dysfunction to generate ATP.

HEMIN-INDUCED PLASMALEMMA PERMEABILITY CONTRIBUTES TO AUTOPHAGIC CELL DEATH IN HT22 CELLS VIA REACTIVE OXYGEN SPECIES SIGNALING

L. Wang, T. Wang, M. Zhang, L. Zhang, Y. Wang, P. Chang, W. Dong, X. Chen, L. Tao

Institute of Forensic Medicine, Soochow University, Suzhou, China

Hemin, a breakdown product of hemoglobin after intracerebral hemorrhage (ICH), is toxic to neuronal cells. Growing evidences suggests that hemin causes lipid peroxidation which lead to plasmalemma permeability and subsequent to secondary cell death. However, the mechanisms and the type of hemin-induced cell death are not very clear. In this study, we established hemin toxic model in mouse hippocampal HT22 cells, cell death occurred when the cells exposed to hemin for 6 hours but the cell death suppressed by caspase inhibitor Z-VAD-FMK and autophagy inhibitor 3-MA respectively. Moreover, plasmalemma resealing agent Poloxamer 188 (P188) was used and the reactive oxygen species (ROS) signaling pathway was detected in this study. The results showed that the level of cellular ROS rapidly increased after hemin insult and antioxidant N-acetyl-L-cysteine (NAC) significantly suppressed ROS accumulation and thereby reduced the expression of apoptotic and autophagic associated proteins. Interestingly, P188 also reduced the level of cellular ROS, decreased hemin-induced cell death, and regulated the level of apoptotic and autophagic associated proteins, but did not provide further neuroprotective effect when ROS was eliminated by NAC. These data demonstrate that through oxidative stress signaling, hemin induces autophyagic cell death besides necrosis and apoptosis, and membrane resealing strategy may block hemin-induced ROS signaling to suppress cell death pathway.

IDUNA PROTECTS HT22 CELLS FROM HYDROGEN PEROXIDE-INDUCED OXIDATIVE STRESS THROUGH INTERFERING POLY (ADP-RIBOSE) POLYMERASE-1-INDUCED CELL DEATH (PARTHANATOS)

H.-X. Xu, Z. Fei

Xijing Hospital, The Fourth Military Medical University, Xi'an, China

Oxidative stress-induced cell death is common in many neurological diseases. However, the role of poly(ADP-ribose) (PARP) polymerase-1 (PARP-1) -induced cell death (parthanatos) has not been fully elucidated. Here, we found that hydrogen peroxide (H_2O_2) could lead to PARP-1 activation and apoptosis-inducing factor nuclear translocation in a concentration dependent manner. Iduna, as a novel regulator of parthanatos, was also induced by H_2O_2. Down-regulation of Iduna by genetic ablation promoted H_2O_2-induced cell damage. Up-regulation of Iduna reduced the loss of mitochondrial potential (MMP) and ATP and NAD+ production, but did not affect the mitochondrial dysfunction-induced cytochrome c release, increase of Bax/Bcl-2 ratio, and caspase-9/caspase-3 activity. In contrast, overexpression of Iduna inhibited activation of PARP-1 and nuclear translocation of AIF. Further study showed that PARP-1 specific inhibitor, DPQ, blocked the protective effect of Iduna against H_2O_2-induced oxidative stress. Moreover, in the presence of proteasome inhibitor (MG-132) or ubiquitin E1 inhibitor (PYR-41), protective effect of Iduna was significantly weaken. These results indicate that Iduna acts as a potential antioxidant by improving mitochondrial function and inhibiting oxidative stress-induced parthanatos, and these protective effects are dependent on the

involvement of ubiquitin-proteasome system (UPS).

EFFECTS OF PI3K/AKT SIGNALING PATHWAY ON MECHANICAL NEURONAL INJURY INDUCED AUTOPHAGY

M.-M. Zhao, Z. Fei

Xijing Hospital, The Fourth Military Medical University, Xi'an, China

Objective: To investigate autophagy induced by mechanical neuronal injury and the involvement of Phosphoinositide 3-kinase （PI3K）/ Protein Kinase B (PKB , also known as Akt) signaling pathway in this process.

Methods: Mouse cortical neurons were cultured for 2 weeks in vitro. After establishment of mechanical neuronal injury model, expression of microtubule-associated protein light chain 3 (LC3) Ⅰ/Ⅱ, Beclin-1, and p-Akt were measured by Western blot ; Neurons were pre-treated with PI3K inhibitor LY294002 for 1 hour before establishment of mechanical neuronal injury model, and then expressions of LC3Ⅰ/Ⅱ and Beclin-1 were measured by Western blot.

Results: LC3 Ⅱ, an autophagy related molecular, were gradually increased at 3 h after mechanical neuronal injury, but expression of Beclin-1 was stable; phosphorylation of Akt reached a peak at 3 h after mechanical neuronal injury, and then gradually returned to normal level; pretreatment with PI3K inhibitor LY294002 elevated the expression of LC3 Ⅱ and Beclin-1 after mechanical neuronal injury.

Conclusion: Autophagy can be induced by mechanical neuronal injury and PI3K/Akt signaling pathway may be involved in this process.

BAICALIN PROTECTS PC-12 CELL FROM DEATH DUE TO OXIDATIVE STRESS INDUCED BY HYDROGEN PEROXIDE VIA JAK/STAT SIGNALING PATHWAY

X. Cao, W.-X. Zheng, X. Yu, X. Hu

Wuhan University of Science and Technology, Wuhan, China

Objectives: To study the neuroprotective effects and possible mechanisms of baicalin on hydrogen peroxide.

Methods: Hydrogen peroxide (H2O2) is used to induce oxidative injury and represents valuable model for investigation of oxidative injury-driven neuronal death.

Results: Data of MTT reduction assay and flow cytometry revealed that exposure of PC12 cells to 400μM H2O2 caused an increase in viability loss and apoptotic rate. Pretreatment of PC12 cells with baicalin (2 μM, 5 μM) for 24h resulted in a reduction in viability loss and apoptotic rate. Baicalin (2 μM and 5 μM) was also found to increase superoxide dismutase (SOD) and Glutathione peroxidase (GSH-Px) activity, and to decrease Malonaldehyde (MDA) level in H2O2-treated PC12 cells. Results from Western blot and immunofluorescence microscopy also showed that baicalin increased the expressions of survivin, Bcl-2, and p-STAT3 and decreased caspase-3 expression in H2O2-treated PC12 cells.

Conclusions: The observed effects were attenuated by AG-490 (the inhibitor for JAK/STAT signaling pathway), indicating that the activation of JAK/STAT signaling pathway was involved in the antiapoptotic effects of baicalin.

References:

1. U. Singh, I. Jialal.Oxidativestress and atherosclerosis. Pathophysiology 2006;13: 129-142.

2. N. R. Madamanchi, A. Vendrov, M.S. Runge. Oxidative Stress and Vascular Disease. Arterioscler Thromb Vasc Biol2005;25 :29-38.

3. A. S. Darvesh, R. T. Carroll, A.Bishayee, W. J Geldenhuys, C.J V. Schy.Oxidative stress and Alzheimer's disease: dietary polyphenols

as potential therapeutic agents. Expert Review of Neurotherapeutics2010; 10:729-745.

4. Pawan K. Singal PhD, DSc, Neelam Khaper MSc, Firoozeh Farahmand MD, Adriane Belló-Klein PhD. Oxidative stress in congestive heart failure. Current Cardiology Reports2000;2:206-211.

5. In Koo Hwang, Ki-Yeon Yoo, Dae Won Kim, Choong Hyun Lee, Jung Hoon Choi,Young-Guen Kwon, Young-Myeong Kim, Soo Young Choi, Moo-Ho Won. Changes in the expression of mitochondrial peroxiredoxin and thioredoxin in neurons and glia and their protective effects in experimental cerebral ischemic damage. Free Radical Biology & Medicine 2010;48: 1242-1251.

6. RVandna Prasad, Anmol Chandele, Jayashree C., et al. OS-triggered caspase 2 activation and feedback amplification loop in β-carotene-induced apoptosis[J]. Free Radical Biology and Medicine, 2006, 41(3): 431-442.

THE EXPRESSION AND MECHANISM OF MMP-9 IN THP-1 CELLS INDUCED BY INJURED ENDOTHELIAL CELLS

F. Jiang, X. Qin, T. Tao, J. Feng

Department of Neurology, The First Affiliated Hospital of Chongqing Medical University, Chongqing, China

Background and objective: MMP-9（matrix metalloproteinase 9）is a well known inflammation factor involved in many physiological and pathological processes, including vascular endothelialization and restenosis after carotid artery stenting (CAS)[1]. Studies showed ERK1/2 involved in MMP-9 expression [2-4]. ELK-1 is one of important members of the Ets family, with MMP-9 binding epitopes [5]. Telmisartan can decrease inflammatory reaction and restenosis rate after artery stenting, but its mechanism is still unclear. Our aim was to investigate the effect of injured endothelial cell supernatant on THP-1 monocytes, and to observe the mechanism involved in MMP-9 expression.

Materials and methods: THP-1 cells treated with normal endothelial cell supernatant were used as negative control group. Transwell was used to evaluate the change of migration and invasion ability of THP-1 monocytes in each group. Immunofluorescence was applied to analyse the location of P-ERK1/2 expression. The expression of P-ERK1/2, P-ELK-1, MMP-9 in different time were determined by western blot. MMP-9 expression was also measured under condition of adding PD98059 （ERK inhibitor）or Telmisartan.

Results: Injured endothelial cell supernatant enhanced the ability of cell adhesion, migration and invasion ($P < 0.05$), and P-ERK1/2 translocated from cytoplasma into nuclei in THP-1 monocytes. The expression of P-ERK1/2、P-ELK-1 and MMP-9 reached to the peak at 15min,15min and 6 hours respectively. PD98059 can reduce the expression of P-ERK1/2, P-ELK-1 and MMP-9 ($P < 0.05$). Telmisartan can only suppressed the expression of ELK-1 and MMP-9 ($P < 0.05$).

Conclusions: Supernatant of injured endothelial cells can activate THP-1 monocyte effectively. ERK1/2 can regulate the MMP-9 expression of THP-1 cell induced by injury of endothelial cell supernatant through ELK-1. Telmisartan suppressed the expression of MMP-9 via inhibit the expression of ELK-1.

ZINC OVERLOAD OR CALCIUM OVERLOAD IN ISCHEMIC NEURONAL DEATH

Y.V. Li, C.J. Stork

Biomedical Sciences, Ohio University, Athens, OH, USA

Objectives: Current cellular models of ischemic injury center on calcium-mediated excitotoxicity. However, another divalent metal ion zinc (Zn^{2+}) has recently emerged as a cytotoxic signaling contributing to neural injury during ischemia and reperfusion. An important note is that the putative cell death signaling pathway triggered by zinc is strikingly similar to that reported to be triggered by calcium. Here, we sought to evaluate the specific contributions made by zinc and calcium toward the ischemic injury, and to decide which one exerts a more fundamental or decisive function in neuronal injury/death.

Methods: Ischemia was simulated by oxygen and glucose deprivation (OGD), followed by reperfusion in hippocampal slices. After baseline recordings, hippocampal slices were subjected to 30 min of OGD, and followed by 60 min reperfusion with normal oxygenated medium. Intracellular zinc and calcium was

measured with fluorescence microscopy, and colocalization analysis was carried out with confocal microscopy. Cell viability assays were studied to analyze cell death.

Results: Using confocal fluorescent microscopy, intracellular zinc accumulation was consistently met with the induction of OGD/R-induced cell injury. Using Calcium Green-1, a widely used calcium indicator, we detected increases in fluorescence intensity during OGD. The application of a zinc chelator at the peak of the 'calcium' fluorescence resulted in a significant drop, due to commonly used calcium indicators are sensitive to zinc than to calcium. Our data suggest that rising zinc is the primary source of the increasing calcium fluorescence, and is responsible for the ischemic neuronal cell death. Zinc chelation prevented cells from ischemic damage. Furthermore, we showed that zinc was also sequestered in thapsigargin/IP3-sensitive stores and was released upon agonist stimulation. In separate studies, calcium accumulation induced with high potassium (to open voltage-gated calcium channels) or ionomycin (a calcium ionophore) caused a moderate neuronal injury that was reduced by zinc chelator TPEN. In comparison, zinc accumulation, induced with the zinc ionophore pyrithione, resulted in significantly greater injury. The application of nimodipine and MK801 was shown to attenuate neuronal injury only from a mild (10 min) OGD insult. Neuronal injury from more severe (30 mins) OGD was not mitigated by the ion channel antagonists, whereas treatment with the zinc chelator TPEN did afford significant protection from cell injury.

Conclusions: Our results indicate that zinc overload contributes to conventionally recognized calcium overload, suggesting that the role of calcium in neurotoxicity described previously using calcium probes may need to be re-examined to determine whether effect previously attributed to calcium could, in part, be attributable to zinc. Finally, these results indicate that zinc mediated damage to be of greater consequence than calcium-mediated damage, and collectively support the suggestion that zinc accumulation may be a more significant causal factor of OGD/R-induced neuronal injury.

References:

Stork CJ, Li YV: Intracellular zinc elevation measured with a "calcium-specific" indicator during ischemia and reperfusion in rat hippocampus: a question on calcium overload. *J Neurosci.* 2006;26:10430-7.

Li YV: Zinc Overload in Stroke. In: *Metal Ion in Stroke*. Li YV, Zhang JH, (eds), pp. 167-89, 1st ed. Springer Science+Business Media, New York; 2012.

EFFECT OF ANGII ON APOPTOSIS AND MMPS IN ENDOTHELIAL AND SMCS, AND THE INFLUENCES OF XINKANG ON IT

X. Liang, S. Li, L. Jinning

Dept. of Chinese Medicine, Affiliated Yantai Yuhuangding Hospital, Qingdao University, School of Medicine, Yantai, China

Xinkang capsule, a preparation made of several Chinese medicinal herbs, has been successfully used to prevent or treat the cerebrovascular and cardiovascular diseases. The mechanisms of the effects remain uncertain.

Objective: To study the effects of angiotensin II in different concentrations and different action time on apoptosis ratio and the expression of cytokines in vascular endothelial cells, and on MMPs in vascular smooth muscle cells and the influences of Xinkang on it.

Methods: Flow cytometer was used to measure the apoptosis ratio and the expression of Fas , Bcl-2. RT—PCR, to measure the changes of MMPs. IL-6, IL-10 were evaluated by ELISA means.

Results:

(1)Apoptosis ratio and the expression of Fas, Bcl-2, IL-6 were induced and increased but IL-10, decreased by angiotensin II with the increase of concentrations and action time.

(2) MMPs were also induced and increased by angiotensin II in SMC, especially in high concentrations. And MMP-9 was earlier than MMP-1 and MMP-2.

(3)The effects of angiotensin II were significantly inhibited when cells were pretreated with Xinkang.

Conclusions: Xinkang capsule may have the inhibition effect against AngII, and also may have the regulative effect on apoptosis ratio

and the expression of Fas , Bcl-2, IL-6, IL-10, and MMPs.

CROSS-TALK REGULATION OF NTS NEURONS IN THE ELECTROACUPUNCTURE (EA) ANALGESIA EFFECT IN RAT WITH COLORECTAL DISTENTION (CRD)

K. Liu[1], L. Li[1], M.-D. He[2], X.-Y. Gao[1], B. Zhu[1], H. Ben[1]

[1]Physiology, China Academy of Chinese Medicine, [2]Beijing University of Chinese Medicine, Beijing, China

Objectives: Previous study demonstrated that acupuncture analgesia effect on visercal pain induced by colorectal distention related to neurons in spinal dorsal horn and thalamus (Rong, 2005; Zhang, 2003). Recent study revealed that NTS plays a role in visceral pain "parasympathetic" regulation (Ait-Belgnaoui, 2009). In our present study, we investigated the way of NTS neurons in the effect of electroacupuncture analgesia in rat colorectal distention induced visceral pain model.

Methods: The experiment was performed on 57 anesthetized male adult Sprague-Dawley rats. A 4cm ballon was placed in rectum connected to a pressure gauge to give stepping CRD conditioning stimulus from 20 to 80mmHg. Extracellular recording method was used to record spontaneous discharges of NTS neurons. And they were identified if their spontaneous activities excited (ON cell) or inhibited (OFF cell) by CRD and electroacupuncture test stimulus (2mA, 0.5ms, 10Hz) on auricular acupoint Heart (AA), Neiguan (PC6), Zusanli (ST36) was conducted for 30s for further discrimination.

Results: Totally 21 ON cell were identified to be gradient increased by stepping CRD conditioning stimulus, and 12 OFF cell were gradient decreased with statistical significance. A majority of the ON cell was inhibited and OFF cell was excited by EA test stimulus. There was no statistical difference among the three acupuncture points on changes of neuronal activity.

Conclusions: NTS neurons participate in the modulatory effect of EA on CRD induced visceral pain in anesthetized rat. Concerning the bilateral regulation of EA on the NTS neuronal activities excited or inhibited by CRD, there may exist cross-talk polysynaptic mechanism.

Support: This study was support by National Natural Scientific Foundation of China No. 81130063 to B ZHU, and No.81173345 to XY GAO.

THE KINASE INHIBITORY REGION OF SOCS-3 REDUCED INTERLEUKIN-6 INDUCED PHOSPHORYLATION OF STAT3 IN PC12

H.-X. Lu[1], L. Wang[1,2], Y.-Y. Wang[1], Q. Jiao[1], Z.-R. Li[2], Y. Liu[1]

[1]Institute of Neurobiology, Xi'an Jiaotong University College of Medicine, XI'an, [2]Department of Gynecology and Obstetrics, The Second Affiliated Hospital, Xi'an Jiaotong University College of Medicine, Xi'an, China

Suppressor of cytokine signaling (SOCS)3 is one of the negative feedback regulators of JAK/STAT3 signaling pathway[1]. It blocks the JAK/STAT3 signaling pathway through inhibition of JAK kinase activity via binding to the kinase domain through the N-terminal kinase inhibitory region (KIR) as well as the SH2 domain[2].

Objective: In current study, we are aiming to investigate whether the KIR domain of SOCS3 play essential roles in suppressing JAK/STAT3 signaling pathway.

Methods: Peptide KIR was constructed and intracellular delivered into PC12 cells through cell-penetrating peptide TAT. Different concentrations interleukin-6 (IL-6) was used to induce the inflammatory response via triggering JAK/STAT3 signalling pathway in PC12. After treated with IL-6, TAT-KIR and IL-6 /TAT-KIR, cell proliferation and phosphorylation level of STAT3 were detected by MTT assay and western blot assay.

Reuslts: It showed that KIR was successully deliverd into PC12 via TAT. In comparions with 50 and 200 ng/ml, IL-6 in 100 ng/ml significantly promoted the proliferation of PC12 that accompanied by dramaticaly increase of STAT3 phosphorylation ($P< 0.05$). TAT-KIR treatment did not significantly impair the proliferation and STAT3 phosphorylation in normal PC12. However, it significantly reduced the elevation of STAT3 phosphorylation that induced by IL-6 ($P< 0.05$).

Conclusion: These results suggested that KIR dormain of SOCS3 could successfully inhibite the IL-6 induced STAT3 phosphorylation. Intracellular delivery of fusion protein TAT-KIR could be a promising strategy to reduce the interleukin induced inflammatory response via suppressing the JAK/STAT signaling pathway.

References:

[1]. Croker, B.A., et al., SOCS3 negatively regulates IL-6 signaling in vivo. Nat Immunol , 2003. 4(6): p. 540-5.

[2].Doti, N., et al., New mimetic peptides of the kinase-inhibitory region (KIR) of SOCS1 through focused peptide libraries. Biochem J, 2012. 443(1): p. 231-40.

DOPAMINE D5 RECEPTOR MODULATE $G_{S/OLF}$/ADENYLYL CYCLASE-COUPLED D1 RECEPTOR PATHWAY AT PRESYNAPTIC SITES IN THE PRELIMBIC CORTEX

W. Luan, P. Zheng

Fudan University, Shanghai, China

Objectives: The AC and PLC pathways of dopaminergic D1-like receptors signaling are mediated through different receptor subtypes. We identified presynaptic sites in the prelimbic cortex that coexpress the dopamine receptor subtype-1 (DRD1) and the dopamine receptor subtype-5 (DRD5).

Methods: To interrogate function, by utilizing specific signaling inhibitors and biological agents in combination with the small interfering RNA (siRNA) approach, we investigated one pathway is active, whereas at higher levels of the intensity or longer durations of synaptic dopamine activity the second pathway is mobilized to supplant the base system at presynaptic sites.

Results: Elucidation of mechanism showed that the selective DRD5 agonist SKF83959 alone had no effect on the PKA activity, but could counteracted DRD1 agonist-induced PKA activation. The conventional PKC (cPKC), especially the PKCα, and the intracellular Ca^{2+} influx, Phospho-DARPP-32 Thr75 also play key roles in the effect of the SKF83959.

Conclusions: A clarification of the signaling relationship between dopamine and CDP-diacylglycerol could shed some new light on even some dopamine-associated disorders such as addiction, depression, and Parkinson disease.

MIR-324-3P INDUCES THE PROMOTER-MEDIATED EXPRESSION OF THE PRO-INFLAMMATORY RELA GENE AFTER ISCHEMIA

A. Dharap, C. Pokrzywa, S. Murali, G. Pandi, **R. Vemuganti**

Neurological Surgery, Univ. Wis. Madison, Madison, WI, USA

Recent studies have shown that microRNAs (miRNAs) can induce the expression of genes by targeting their promoters. To explore whether this phenomenon occurs in stroke, we conducted bioinformatics analyses for miRNAs that were altered significantly after stroke against the promoters of all rat protein-coding genes available in NCBI. The miR-324-3p which is known to be up-regulated after ischemia showed a strong target site in the RelA promoter. The expression of the RelA protein (a component of the pro-inflammatory transcription factor NF-κB family) is also known to increase swiftly, and correlates with inflammation and cell death following cerebral ischemia. We hypothesized that a sustained induction of miR-324-3p promotes the post-ischemic RelA gene expression. Co-transfection with miR-324-3p dose-dependently induced the expression of the rat RelA promoter plasmid in PC12 cells and this response was curtailed when the miR-324 target site in the RelA promoter was mutated. Furthermore, premiR-324-3p significantly increased the expression of the RelA mRNA and protein in PC12 cells and this effect was blocked when Ago2 was knocked-down with a siRNA. This indicates that miR-324-3p induces endogenous RelA promoter in a RISC dependent manner. Moreover, treatment with antagomiR-324-3p prevented the induction of RelA in PC12 cells subjected to oxygen-glucose deprivation and resulted in a ~20% increase in cell survival as compared to control. Thus, miR-324-3p upregulated after ischemia induces RelA expression by interacting with RelA promoter and this might be a mechanism of ischemic cell death.

SYNERGY OF PPARΓ AND MICRORNAS IN CNS

R. Vemuganti, A. Dharap

Neurological Surgery, Univ. Wis. Madison, Madison, WI, USA

MicroRNAs (miRNAs) are small non-coding RNAs that bind to the 8-bp target sequences in the 3-UTRs of mRNAs to induce post-transcriptional silencing. The miRNAs are formed as ~70-nt RNA stem-loop structures called primiRs which will be converted to 19 to 25-nt premiRs by RNAse III Drosha in the nucleus, transported into cytosol by exportin-5 and cleaved to mature 18 to 22-nt miRNAs by Dicer. The primiRs are thought to be transcribed by RNA polymerase II from the introns of protein-coding regions, and introns and exons of long noncoding RNA forming regions of DNA. The role of various transcription factors (TF) in miRNA biogenesis is not yet understood. PPARγ is a ligand-activated TF and its activation is known to induce neuroprotection following acute and chronic CNS insults by trans-repressing inflammatory genes and tarnsactivating anti-oxidant and heat-shock genes. To understand if PPARγ induces some of its pleiotropic beneficial effects by influencing miRNAome, we treated adult rats with rosiglitazone (a potent PPARγ synthetic ligand). Within a day after rosiglitazone treatment, 31 miRNAs were altered significantly (13 up- and 18 down-regulated; 3 to 119-fold change) in brain. In silico analysis of the PPAR/RXR binding sites in the putative promoter regions (500bp upstream of the TSS) of the altered miRNAs (with UCSC Genome Browser and MatInspector from Genomatix GmbH) showed that promoters of 24 miRNAs altered after rosiglitazone treatment contained 1 to 7 peroxisome proliferator response element signatures. Thus, our results show that a TF can control miRNA expression in CNS in vivo and will help to understand the neuroprotection induced by PPARγ in CNS.

INTERACTIONS BETWEEN SIRT1 AND MAPK/ERK REGULATE NEURONAL APOPTOSIS INDUCED BY TRAUMATIC BRAIN INJURY IN VITRO AND IN VIVO

Y.-B. Zhao, Z. Fei

Xijing Hospital, The Fourth Military Medical University, Xi'an, China

Traumatic brain injury (TBI) is a serious insult that frequently leads to neurological dysfunction or death. Silent information regulator family proteins 1 (SIRT1), as the founding member of nicotinamide adenine dinucleotide (NAD)-dependent deacetylases, has recently been demonstrated to have neuroprotective effect in several models of neurodegenerative diseases. The present study attempts to determine whether SIRT1 has a neuroprotective effect in the model of TBI, and further to investigate the possible regulatory mechanism of neuron death. Thus, we employ transection model in vitro and weight-drop model in vivo to mimic the insults of TBI. The study shows that the expressions of SIRT1, phosphorylation extracellular signal-regulated kinase (p-ERK) and cleaved Caspase-3 are induced after trauma injury in vitro or in vivo. Furthermore, inhibiting SIRT1 by pharmacological inhibitor salermide or SIRT1 siRNA significantly promotes apoptotic neuron death and reduces ERK1/2 activation induced by mechanical injury in vitro and in vivo. Inhibition of ERK1/2 activation with PD98059 or U0126 (two mitogen activated protein kinase kinase inhibitors) in vitro and in vivo significantly attenuates the SIRT1 and cleaved Caspase-3 expression to protect neuron against TBI-induced apoptosis. These results reveal that SIRT1 plays a neuroprotective effect against neuronal apoptosis induced by TBI. The interactions between SIRT1 and MAPK/ERK pathway regulate neuronal apoptosis induced by mechanical trauma injury in vitro and in vivo.

APT102, AN OPTIMIZED HUMAN APYRASE ALONE OR WITH RT-PA, IS BENEFICIAL IN THROMBOEMBOLIC STROKE MODELS

S.-M. Ting[1], X. Zhao[1], G.-H. Sun[1], R. Chen[2], S.S. Jeong[2], J.C. Grotta[1], **J. Aronowski**[1]

[1]Neurology, University of Texas, Medical School at Houston, Houston, TX, [2]APT Therapeutic Inc., St. Louis, MO, USA

Background: Inhibition of platelets after ischemic stroke could help to maintain vascular patency and assist rt-PA in recanalization. However, use of available platelet inhibitors may be associated with the increased risk of intracerebral hemorrhage (ICH).

Objective: Using two clinically relevant models of thromboembolic stroke [one using 24h mature clot (formed without use of exogenous thrombin) and one using fresh cloth (formed in presence of thrombin)] to establish the utility of a novel genetically engineered soluble human apyrase APT102 (which has improved enzymatic activity and more potent platelet inhibition capacity than the wild-type form), as agent synergizing with rt-PA without increased risk for ICH.

Method: In the mature clot thromboembolic stroke model, Long Evans rats were randomly divided into 4 treatment groups:

(1) control (saline treated);

(2) APT102 at 2.25 mg/kg,

(3) rt-PA (at 10 mg/kg) and

(4) APT102 at 2.25 mg/kg plus rt-PA. In the fresh clot stroke model, Sprague Dawley rats were randomly divided into 3 treatment groups:

(1) control (saline treated);

(2) APT102 at 0.75 mg/kg and

(3) APT102 at 2.25 mg/kg.

All treatments were initiated at 2 hours following thrombus injection into the internal carotid artery. Infarct volume, incidence of ICH and behavioral deficit were assessed at day 3 after the stroke.

Results: In the mature clot thromboembolic stroke model, although APT102 alone did not produce significant effect on stroke outcome as compared to saline control (123.1+/-19.9 vs. 119.9+/-26.4mm^3), APT102 combined with rt-PA significantly reduced infarct volume (71.2+/-16.1) compared to rt-PA alone and saline treated rats ($p< 0.05$). Analysis of behavioral deficit was performed on the same groups and APT102 combined with rt-PA reduced behavioral deficit as compared to rt-PA alone and saline treated rats ($p< 0.05$). Visual analysis of brains demonstrated that 2 out of 11 rats with saline and 5 out of 11 animals treated with rt-PA alone demonstrated petechial hemorrhages within the ischemia-affected aspects of the brain. In contrast, no hemorrhage was observed in any of 10 rats treated with APT102 with or without rt-PA.In the fresh clot stroke model, both APT 102 at 0.75 mg/kg or 2.25 mg/kg significantly reduced infarct volume compared to saline control (133.1+/-80.1 and 178.6+/-64.4 vs. 246.7+/-105.1, $p< 0.05$ and $p< 0.01$). Tripling the dose of APT 102 did not significantly produce additional effect on infarct volume. However, behavioral deficit scores for APT 102 at 2.25 mg/kg indicated a significant decrease against saline control ($p< 0.05$), while APT 102 at 0.75 mg/kg did not significantly reduce behavioral deficit as compared to saline control.

Conclusions: This study provides the first evidence that the optimized human apyrase used to inhibit platelets after ischemic stroke may be neuroprotective. Also, a combination of apyrase and rt-PA may have additive effects while decreasing the risk of ICH.

THE NEUROPROTECTIVE EFFECTS OF BLOOD GLUTAMATE SCAVENGING IN A RAT MODEL OF SUBARACHNOID HEMORRHAGE

M. Boyko[1], Y. Kezerle[1], I. Melamed[1], R. Kuts[1], D. Porat[1], A. Zhumadilov[2], S. Karibay[3], A. Zlotnik[1]

[1]Ben-Gurion University, Beer Sheva, Israel, [2]Department of Neuroanesthesiology and Critical Care, [3]Department of Neurosurgery, RSCEM, Astana, Kazakhstan

Introduction: Subarachnoid hemorrhage (SAH) is associated with significant morbidity and mortality. Glutamate scavengers have been shown to decrease glutamate concentrations in the blood and improve neurological outcome following ischemic stroke and traumatic brain injury in rats. This study examines the value of blood glutamate scavengers, pyruvate and oxaloacetate, as a therapeutic neuroprotective strategy in a rat model of SAH. We additionally investigated whether glutamate scavenging was the mechanism responsible for any resulting neuroprotection.

Materials and methods: SAH was induced in 60 rats by autologous arterial blood injection into the cisterna magnum. 20 additional rats served as the sham group, with a 0.3 ml saline

injection into the cisterna magnum. 60 minutes later, rats were treated with isotonic saline, 250 mg/kg oxaloacetate, or 125 mg/kg pyruvate by intravenous infusion for 30 minutes at a rate of 0.1 ml/100g/min. Prior to the induction of SAH (baseline) and 90 minutes after SAH, blood samples were collected. Rats´ neurological status was measured 24 hours following SAH. Glutamate concentrations in the CSF of half of the rats were also measured 24 hours following SAH. The blood brain barrier (BBB) permeability in the parieto-occipital and frontal lobes was assessed in the remaining half via histological analysis 48 hours following SAH.

Results: Blood glutamate levels were decreased in rats treated with pyruvate or oxaloacetate at 90 minutes following SAH ($p < 0.001$; figure 1). CSF glutamate was decreased in rats treated with pyruvate ($p< 0.05$). Neurological performance improved significantly in rats treated with pyruvate ($p< 0.01$) or oxaloacetate ($p< 0.05$). There was less BBB breakdown in the parieto-occipital lobes in rats treated with oxaloacetate ($p< 0.01$) or pyruvate ($p< 0.01$), and in the frontal lobe in rats treated with pyruvate ($p< 0.05$) (figure 2).

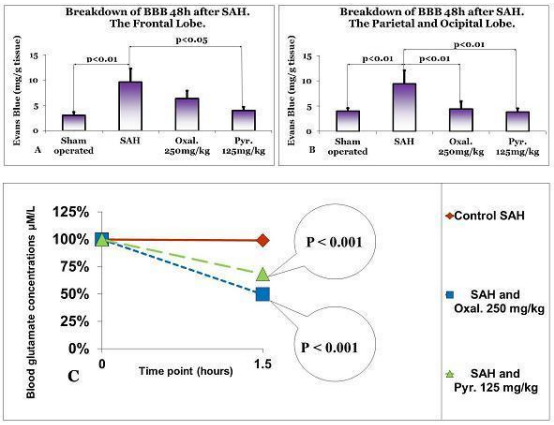

[Fig 1]

Conclusions: This study suggests the effectiveness of blood glutamate scavengers, pyruvate and oxaloacetate, in the treatment of SAH in rats. The data suggests that the observed neuroprotection with treatment of pyruvate or oxaloacetate is mediated via their blood glutamate scavenging effect.

THE LECTIN PATHWAY IN SUBARACHNOID HEMORRHAGE PATIENTS

M.-G. De Simoni[1], R. Zangari[1,2], T. Zoerle[2], F. Orsini[1], S. Parrella[1], V. Conte[2], N. Stocchetti[2], E.R. Zanier[1]

[1]Mario Negri Institute, [2]Department of Anaesthesia and Intensive Care, Ospedale Maggiore Policlinico, University of Milan, Milan, Italy

Objectives: Subarachnoid hemorrhage (SAH) is a severe condition due to the rupture of an intracranial aneurysm with a mortality rate of 45%. Brain ischemia is a main determinant of unfavourable outcome in these patients. It can play a role in the acute phase (day 1-3) as a consequence of the initial intracranial bleeding and/or at delayed stages as a consequence of cerebral vasospasm (day 4-14).

Recent evidence in ischemic stroke indicate that serum levels of mannose-binding lectin (MBL) and of ficolin-3, two recognition molecules of the lectin complement pathway are dysregulated in ischemic stroke (1,2). No data are available on this pathway in SAH.

In this study we analyzed MBL and ficolin-3 in SAH patients and their relationship with SAH severity, clinical vasospasm (VSP) and radiological findings.

Methods: SAH severity was assessed using World Federation of Neurological Surgeons grading scale. VSP was defined as neuro-worsening with angiographic confirmation of vessel narrowing. CT cerebral ischemia was defined as a hypodense lesion on CT scan performed before ICU discharge (3). We compared plasma levels of MBL, MBL/MASP-2 functional complexes, ficolin-3 and of complement factors (C3 and C5b-9) from 39 SAH patients and 20 healthy subjects. Plasma levels were determined in acute (1-3 day) and post acute phase (4-14 day) through western blot analysis and ELISA measurements.

Results: SAH patients showed a significant increase in C3 fragments and in C5b-9 concentrations indicating that the complement system is activated. In addition they showed a significant and persistent increase in plasma ficolin-3 concentrations. Importantly, ficolin-3 levels were related to brain injury severity. Namely, significantly lower levels of ficolin-3 were found in: 1) severe compared to mild patients, 2) patients with VSP compared to those without VSP; 3) patients with CT cerebral ischemia compared to those without

ischemia. MBL levels were not different between patients and controls.

Conclusions: In SAH patients:

1) ficolin-3 (but not MBL) acts as activator of the lectin pathway;

2) ficolin-3 levels are related to SAH severity as evaluated by clinical and structural parameters,

3) the pattern of ficolin-3 changes are in line with the concept that ficolin-3 decreases as a result of consumption through the binding to dying/injured cells during severe SAH-related events (1,4). These results show that the lectin pathway is important in SAH.

References:

1) Fust et al. *J.Neuroinflammation*, 2011

2) Orsini et al. *Circulation*, 2012

3) Zanier et al. *Intensive Care Medicine* 2011

4) Jensen et al. *Mol. Immunol*. 2007

COCHRANE SYSTEMATIC REVIEW: LUMBAR DRAINAGE OF CEREBROSPINAL FLUID FOR SUBARACHNOID HEMORRHAGE

W. Dong, S. Lin, D. Wang, B. Wu, Z. Hao, M. Liu

Neurology, West China Hospital, Sichuan University, Chengdu, China

Background: Subarachnoid hemorrhage(SAH) accounts for approximately 3-7% of all cerebral strokes. It is a devastating condition, often resulting in severe neurologic disability or death.Despite the rapid progress in medical science, effective SAH treatment is still lacking. DIND is a significant cause of morbidity and mortality in survivors of SAH. Lumbar drainage of cerebrospinal fluid is used to clear blood in subarachnoid space, in order to decrease DIND and improve functional outcome of SAH patients.There have been several randomized clinical trials published in the literature to suggest that drainage of cerebrospinal fluid through the lumbar cistern may be of some benefit in improving outcome of SAH patients. The aim of this review is to systematically analyse all the randomized controlled trials of CSF drainage for SAH patients to provide the best available evidence for clinical practice and further research strategies for SAH treatment.

Objectives: To assess the efficacy and safety of lumbar drainage of cerebrospinal fluid in patients with subarachnoid hemorrhage.

Methods: Types of studies: randomised controlled trials. Types of participants: patients of any age or sex with subarachnoid hemorrhage will be eligible. Types of interventions: trials evaluating lumbar drainage of cerebrospinal fluid regardless of the volume of drainage, the length of treatment period or medication injection during drainage(if any). The control interventions are standard therapies of SAH. Types of outcome measures: Primary outcomes: Unfavourable outcome (death, vegetative state, or severe disability (modified Rankin Scale (mRS) score 4 to 6) at 1,3 or 6 months after SAH. Secondary outcomes: prevalence of of DIND after SAH, recurrent haemorrhage, a sudden clinical deterioration with rebleeding, complications from the intervention. Electronic searches: Cochrane Stroke Group Trials Register; Chinese Stroke Trials Register; Cochrane Central Register of Controlled Trials (CENTRAL); MEDLINE; EMBASE (1980 to present); et al.

Results: This review is still ongoing and results will be presented in the conference.

MIRNA PROFILING OF CEREBRAL VESSELS AFTER SUBARACHNOID HAEMORRHAGE

A. Holt Müller, G.K. Povlsen, C.H. Bang-Berthelsen, L.S. Kruse, L. Edvinsson

Department of Clinical Experimental Research, Glostrup Research Institute, Glostrup, Denmark

Background: Subarachnoid haemorrhages (SAH) accounts for ~15% of all strokes and is most often caused by leakage of blood into the subarachnoid space from a ruptured aneurysm. This results in dramatically increased intracranial pressure and decreased cerebral blood flow. This acute phase can be followed by a phase of delayed cerebral ischemia 4-7 days after the initial SAH. The delayed cerebral ischemia is associated with pathological constrictions of cerebral arteries (cerebral vasospasms) and poor outcome. However, it is so far not possible to monitor in

a clinical setting the molecular changes in the cerebral vasculature that leads to development of vasospasms and it is therefore not possible to predict nor to prevent or treat the devastating cerebral vasospasms.

Biomarkers indicative of ongoing detrimental changes in the cerebral vasculature and of good vs. bad clinical outcome after SAH would be a highly valuable tool in prognosis and choice of individualized treatment. miRNAs have the potential to serve as such biomarkers, since miRNAs are often regulated very early upon disease onset and once transcribed they remain stable for several days. Most importantly, miRNAs are often secreted from the primary diseased tissue into the peripheral blood where they can be easily detected in a small sample.

Hypothesis: We hypothesise that miRNAs play a role in the cerebral vascular pathology after SAH leading to cerebral vasospasms and delayed cerebral ischemia. Additionally, we hypothesise that some of these miRNAs are secreted to the peripheral blood, where they can serve as biomarkers for the development of cerebral vasospasms and thus predictors of clinical outcome.

Aim: We aim at identifying blood borne miRNA biomarkers for outcome prognosis and prediction of SAH patients in high risk of developing cerebral vasospasms who would benefit from treatment specially targeted at prevention of vasospasms.

Methods: We utilized a rat SAH model in which autologous blood is injected into the prechiasmatic cistern on the base of the brain. miRNAs were isolated from both large cerebral vessels and peripheral blood. miRNAomes from cerebral vessel tissue were obtained using a qPCR based screen with primers for 752 known rat miRNAs. Selected SAH-regulated candidates are validated by single assay qPCR.

Results: 12 cerebral artery miRNAs were found to be regulated in the initial screen. Of these, miR-133a, miR-145 and miR191* were validated and showed significant up- or down-regulation after SAH. To pursuit the discovery of a bloodborne biomarker of changes in the cerebral vessels, serum from the same rats is currently being analyzed to identify any similar regulation of the three miRNAs in blood.

EFFECTS OF INTRAVENTRICULAR FIBRINOLYSIS ON CEREBRAL PERFUSION AND METABOLISM AFTER SEVERE INTRAVENTRICULAR HEMORRHAGE

J.B. Kuramatsu[1], S. Schwab[1], **H.B. Huttner**[2]

[1]University of Erlangen-Nuremberg, [2]Neurology, University of Erlangen, Erlangen, Germany

Introduction: Intraventricular hemorrhage (IVH) is an established independent predictor of poorer outcome in subarachnoid- and intracerebral- hemorrhage. Though, limited knowledge exists regarding the pathophysiologic mechanisms that may lead to cerebral injury and poorer outcome. This is the first report presenting in vivo data on cerebral blood flow and brain tissue metabolism during the occurrence of IVH and after intraventricular fibrinolysis (IVF).

Methods: A 78-year-old woman with severe subarachnoid hemorrhage (SAH), Hunt&Hess grade 3, modified Fisher Scale 4, was admitted to our neuro-critical care unit. Within the first 24 hours an extraventricular drainage was placed and a left-sided MCA aneurysm was coiled. After obtaining informed consent from the legal attorney, the patient received invasive multimodal neuro-monitoring, consisting of a cerebral blood flow (CBF)- and microdialysis- probe placed into the ipsilateral frontal white matter.

Results: Within 8 hours after probe placement we observed a significant drop of cerebral blood flow (CBF below 20 ml/100g/min) and an increase in L/P-ratio without significant changes in cerebral perfusion- or intracranial-pressure. Imaging revealed a re-hemorrhage into the ventricular system with blockage of the foramina of Monro and acute hydrocephalus. Consequently, therapeutic IVF was undertaken with 1 mg of rtPA which lead to sufficient clot resolution. After IVF we documented profound changes (Δ>20 ml/100g/min) in CBF and microdialysis parameters (L/P ratio: R^2=.739) leading to normalization of cerebral perfusion and metabolism.

Conclusions: This is the first report on IVH and its potential mechanisms that may contribute to secondary injury in the human brain. A decrease of cerebral blood flow and disturbance of cerebral metabolism was documented during the occurrence of IVH, supporting existing hypotheses of global impairment. Moreover, we could document profound treatment effects of IVF leading to a

restored CBF and a stable aerobic metabolism in the investigated brain tissue.

DIRECT THROMBIN INHIBITOR DABIGATRAN AS TREATMENT IN EXPERIMENTAL INTRACEREBRAL HEMORRHAGE BRAIN MODEL

S. Illanes[1,2], C. Urrutia[2], F. Vial[2], P. Conget[2]

[1]Neurology, [2]Instituto de Ciencias, Universidad del Desarrollo-Clínica Alemana, Santiago, Chile

Background and purpose: Intracerebral hemorrhage triggers several interrelated events, including cytotoxic edema, microvascular thrombosis, and tissue degeneration. Although the molecular mechanisms of cellular death in ICH have not been fully understood, blood-brain barrier leakage of serum constituents such as thrombin might exert a direct toxic effect on brain parenchyma. Thrombin activation plays a key role during ICH injury[1]. Thrombin has been shown to cause neuronal cell death both in vitro and in hemorrhage models in vivo. In hemorrhagic stroke models, continuous release of activated thrombin from existing clots would exert severe damage to the brain tissue, whereas infusion of argatroban, a direct inhibitor of thrombin, showed a reduced level of perihematomal infarction[2]. In addition, previous studies have related thrombin to blood-brain barrier damage and edema formation. Because preliminary data suggest that thrombin is a likely candidate to mediate vascular and tissue injury after stroke we aim to use the commercially available direct thrombin inhibitor Dabigatran etaxilate (Pradaxa®) as a treatment in a experimental ICH mice model.

Methods: In C57BL/6 mice receiving Dabigatran etaxilate (4.5 or 9.0 mg/kg), in vivo coagulation assay were measured in order to establish the optimal dose for these set of experiments. Because in the ICH mice model, there is no further hematoma expansion after 6 hours since the collagenase injection[3], mice received an intraperitoneal injection of dabigatran etaxilate (9.0 mg/kg) or saline six hours after the ICH induction. Behavioural tests, physiological parameters, hematoma volume and hemispheric water content was quantified on brains 24h after the ICH induction. A second group of animal received dabigatran etaxilate (9.0 mg/kg) or saline 6 and 24 hours after the ICH induction. Outcome was measured 48 hours after the ICH induction in this set of animals.

Results: We observed dabigatran anticoagulatory effect for more than 8 hours measured by an in vivo assay (lateral vein bleeding time). No further hematoma expansion was observed in dabigatran treatment group compared to controls. Water content was significantly reduced in dabigatran treatment group 24h (73.3% versus 78.7%. p< 0.001. n=10 per group) and 48h (77.2% vs. 79.2. p=0.02 n=9 per group) after ICH induction.

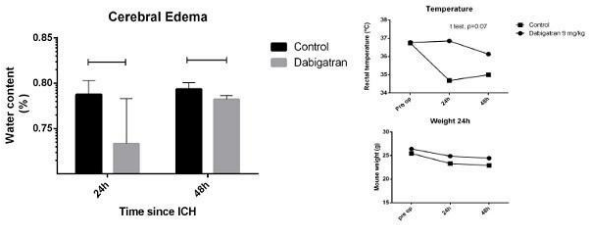

[Dabigatran effect 24 and 48h after ICH induction]

Conclusion: Administration of dabigatran etaxilate (Pradaxa ®) 6 and 24h after ICH induction reduces peri-hematoma edema development in the collagenase ICH mice model without further hematoma enlargement. This might be a good candidate for a clinical phase II study.

References:

1. Hua et al. Stroke. 2007;38:759-762

2. Nagatsuna et al. Cerebrovasc Dis 2005;19:192-200

3. Illanes et al. Brain Res. 2010 Mar 12;1320:135-42.

ADIPONECTIN PREVENTS THE INTRACEREBRAL HEMORRHAGE THROUGH STAT3 AND NF-KB MEDIATED MECHANISM

H. Jang[1,2], B.-J. Kim[1,2], Y.-J. Kim[1,2], J. Noh[1,2], S. Yang[1,2], S.-H. Lee[1,2], B.-W. Yoon[1,2]

[1]Neurology, Seoul National University Hospital, [2]Clinical Research Center for Stroke, Biomedical Research Institute, Seoul National University Hospital, Seoul, Republic of Korea

Objectives: Adiponectin is a fat-derived 30-kDa circulating plasma protein that has beneficial actions on cardiovascular disorders. In addition, Adiponectin has emerged as a key vasculoprotective molecule with insulin-sensitizing, anti-inflammatory, and anti-atherogenic properties, thereby suppressing pro-inflammatory gene expression in macrophages. Furthermore, after intracerebral hemorrhage, plasma adiponectin level was increased until 2 days and then gradually decreased; implying adiponectin may have an important role after ICH. Therefore, we investigated the role of adiponectin following ICH injury in mice, and clarified its mechanism.

Methods: To explore the role of adiponectin in the intracerebral hemorrhage, we investigated a collagenase-induced mouse model of ICH. Mice were administered either vehicle or adiponectin at 30 minutes after ICH induction. At 48 hours after ICH, mice were sacrificed for further experiments: immunohistochemistry, western blotting, and measuring brain edema. For further clarification of its mechanism, we treated adiponectin together with or without hemolysates in the astrocytes and endothelial cells.

Results: At 48 hours after ICH, adiponectin administration resulted in a significant reduction of hematoma volumes relative to the contralateral hemisphere (adiponectin-treated group 40.29±4.1% vs. saline-treated group 57.81±6.2%, p=0.03). Interestingly, Vascular endothelial growth factor (VEGF) expression was significantly repressed in the hemorrhagic brain tissue. In addition, phosphorylation of STAT3 is repressed upon the administration of adiponectin, which is required for VEGF expression. In the beginning of ICH, VEGF has a role for increasement of brain edema, up-regulating Matrix metalloproteinses (MMPs). Furthermore, NF-kB activation was repressed and increased phosphorylation of eNOS in the adiponectin-treated hemorrhagic brain, indicating the anti-inflammatory effect.

Conclusion: Adiponectin reduced the hematoma after intracerebral hemorrhage, regulating STAT3 mediated VEGF expression, NF-kB mediated MMP expression, and eNOS phosphorylation. Our data suggested that adiponectin could be applied for an effective therapeutic treatment for the hemorrhage stroke.

References:

1. Nishimura, M., Izumiya, Y., Higuchi, A., Shibata, R., Qiu, J., Kudo, C., Shin, H. K., Moskowitz, M. A., and Ouchi, N. (2008) *Circulation* **117**, 216-223

2. Kondo, M., Shibata, R., Miura, R., Shimano, M., Kondo, K., Li, P., Ohashi, T., Kihara, S., Maeda, N., Walsh, K., Ouchi, N., and Murohara, T. (2009) *J Biol Chem* **284**, 1718-1724

3. Shimano, M., Shibata, R., Tsuji, Y., Kamiya, H., Uchikawa, T., Harata, S., Muto, M.,

Ouchi, N., Inden, Y., and Murohara, T. (2008) *Circ J* **72**, 1120-1124

4. Ouchi, N., and Walsh, K. (2008) *Arterioscler Thromb Vasc Biol* **28**, 1219-1221

5. Weis, S. M., and Cheresh, D. A. (2005) *Nature* **437**, 497-504

6. Wang, J., and Tsirka, S. E. (2005) *Brain* **128**, 1622-1633

INCREASED EXPRESSION OF EHD2 AFTER INTRACEREBRAL HEMORRHAGE IN ADULT RATS

K. Ke[1], Y. Rui[2]

[1]Department of Neurology, Affiliated Hospital of Nantong University, [2]Nantong University, Nantong, China

EHD2, a member of the Eps15 homology domain (EH domain) family, is important for protein interactions during vesicular trafficking. It can regulate trafficking from the plasma membrane in the process of endocytosis. However, its function in central nervous system diseases is still unknown. In this frame, we have found the EHD2 expression is increased in the perihematomal region in adult rats after performed intracerebral hemorrhage (ICH). Double immunofluorenscence staining revealed that EHD2 was co-expressed with neurons and activated microglias after ICH. Besides, we detected that neuron apoptosis marker (Tunnel and Caspase-3) and microglia activation marker CD68 were co-located with EHD2. Moreover, we have found the expression of EHD2 was up-regulated in microglia activation in vitro and knockdown EHD2 may suppress microglia activation via affecting NF-κB activation. All our findings suggested that EHD2 may be involved in the pathophysiology of ICH.

SPONTANEOUS CORTICAL SPREADING DEPRESSION AFTER ACUTE SUBDURAL HEMATOMA IN RATS: INFLUENCE OF BLOOD CONSTITUENTS ON CSD AND LESION

O. Kempski, M. Plath, S. Tretzel, A. Heimann, B. Alessandri

Institute for Neurosurgical Pathophysiology, University Medical Center of the Johannes Gutenberg-University Mainz, Mainz, Germany

Traumatic brain injury is closely associated with acute subdural hemorrhage (ASDH) that worsens outcome massively. Responsible factors are increased ICP, wide-spread ischemia underneath the hemorrhage and blood constituents. Recently we demonstrated the occurrence of spontaneous cortical depression (CSD) after ASDH (1). The goal of the present study was to extend our former data and to find out whether blood constituents play a role in triggering CSD following ASDH.

Male Sprague-Dawley rats were anesthetized with chloral hydrate and surgically prepared for ASDH by inserting an L-shaped needle underneath the dura mater. ASDH was induced by infusion of 300 µl autologous venous blood. In a second group blood was replaced by 300 µl of paraffin oil in order to eliminate all blood constituents. Spontaneous CSDs were measured in all rats by means of impedance (IMP) electrodes (CSD causes cell swelling that leads to IMP increase paralleling DC-changes (2)). Half of the animals received contralateral ICP or CBF measurements for 180 min. Histological outcome was assessed at day 7 post-injury (all values = mean ± SEM).

ASDH with blood and paraffin oil caused an immediate IMP and ICP increase and a CBF decrease during infusion. Thereafter, IMP decreased to around 105% of baseline values within 25-40 min.

Spontaneous CSDs were observed in 11 out of 20 rats receiving blood infusion (5.8 ± 1.4 CSD). Lesion volume was 51.8 ± 3.8 mm^3 (with CSD) and 20.5 ± 4.0 mm^3 (without CSD); t-test $p< 0.001$). Only 3 of 7 paraffin-infused rats showed spontaneous CSDs (4.0 ± 2.1 CSD), but no difference in lesion volume was found (4.7 ± 2.6 vs. 4.4 ± 1.7 mm^3).

Independent of blood or paraffin oil infusion, ASDH induced spontaneous CSDs in 50% of all cases. On average blood induced more CSDs and a larger lesion than paraffin oil. The significantly larger lesions of rats with blood infusion and CSD suggest an influence of CSD on lesion development after ASDH or vice versa. Data from paraffin-infused rats, however, suggest that blood constituents are important for lesion growth but play a minor role in CSD induction in the early phase after ASDH.

(1) Alessandri et al. (2012) Spontaneous cortical spreading depression and intracranial pressure following acute subdural hematoma in a rat. Acta Neurochir Suppl 114: 373-6

(2) Otsuka H et al. (2000) Effects of cortical spreading depression on cortical blood flow, impedance, DC-potential, and infarct size in a rat venous infarct model. Exp. Neurol 162: 201-214

SECONDARY LESION EXPANSION FOLLOWING ACUTE SUBDURAL HEMORRHAGE IN RATS

O. Kempski, E. Amoruso, A. Heimann, B. Alessandri

Institute for Neurosurgical Pathophysiology, University Medical Center of the Johannes Gutenberg-University Mainz, Mainz, Germany

Secondary lesion growth is a process that is initiated following traumatic brain injury (TBI) or stroke. It enlarges not only lesion size but defines also the time window for successful treatment. Following focal contusion in mice brain damage expands by 32% and 67% within 6h and 24h, respectively (Zweckberger et al., 2006). An acute subdural hemorrhage (ASDH) is a devastating consequence of TBI and worsens outcome of TBI patients additionally. As a possible factor for this we characterized secondary lesion growth in a rodent ASDH model.

Male Sprague-Dawley rats were anesthetized with chloral hydrate and surgically prepared for measurement of mean arterial blood pressure and cerebral blood flow and ASDH that was induced with 300 µl autologous venous blood. Rats were randomly assigned to groups surviving for 15 min or 1, 2, 6 or 24 hours (n=10/group). Brains were processed for cresyl violet, hematoxylin-eosin or fluoro-jade B (FJB) staining.

Conventional histology showed an initial damage of 3.7 ± 0.4 mm^3 at 15 min post-

ASDH. Thereafter lesion increased to 6.8 ± 1.4 mm^3 at 1h, to 7.9 ± 1.7 mm^3 at 2h, to 12.4 ± 1.5 mm^3 at 6h and to 22.0 ± 2.8 mm^3 at 24h post-ASDH ($p < 0.05$ all vs. 6h and 24h). FJB-positive cells were found mainly in the cortex at 15 min post-ASDH. FJB staining expanded to hippocampal and basal regions at later time points, but disappeared within the growing ischemic damage. Total number of FJB-positive cells increased from 177 ± 28 (contralateral 13 ± 1) at 15 min to 270 ± 16 (contralateral 63 ± 19) at 6h post-ASDH and decreased to 227 ± 57 (contralateral 6 ± 5) at 24h.

In conclusion, ASDH induced a rapid lesion expansion by 115% from 15 min to 2h, by 61% from 2h to 6h and by additional 73% from 6h to 24h post-ASDH. This massive secondary lesion expansion (495% from 15 min to 24h) is a major factor likely to worsen outcome of TBI patients with an ASDH.

MODIFIED CLIPPING TECHNIQUE OF THE SMALL CAROTID CAVE ANEURYSMS USING FENESTRATED CLIPS THROUGH SMALL INCISION ON THE CAVERNOUS SINUS ROOF

J. Kim, J. Cheong, C. Kim

Neurosurgery, Hanyang University Guri Hospital, Guri, Republic of Korea

Background: Recently, through the better comprehensive skull base microanatomical knowledge, it is more convenient to neurovascular surgeons to adopt the extensive opening of the cavernous sinus (CS) in paraclinoid aneurysm surgery. However, the wide opening of the CS is more harmful and it remains the various complications to the patients. Also in the direct microsurgical clipping of small carotid cave aneurysms, less extensive exposure of the CS is required. The author used the modified surgical technique instead of the wide exposure of the CS in the small carotid cave aneurysms.

Methods: We have directly obliterated five small unruptured carotid cave paraclinoid aneurysms. In all cases, the tailored orbito-zygomatic craniotomies with extradural and/or intradural clinoidectomy were performed. For proximal control, the cervical internal carotid arteries (ICAs) were exposed in all cases. After completion of the anterior clinoidectomy, optic canal unroofing, the right angled fenestrated clips had been advanced parallel to the clinoid ICA through the small opening on the carotid trigone of CS roof. The anterior clip blade was carefully stuck into the carotid cave and posterior clip blade into the small opening on the CS roof. The efficacy of the surgical clipping was evaluated with the postoperative digital subtraction angiography (DSA) and computed tomography (CT) angiography. The author reviewed our surgical experiences in direct surgical clipping of the carotid cave aneurysms especially in dealing with the anterior clinoidectomy, distal dural ring resection, optic canal unroofing, clipping techniques, and surgical complications.

Results: Five all small carotid cave paraclinoid aneurysms were completely obliterated with direct neck clipping. There was no surgery related complication. Postoperative brain CT angiographic scans and 3-demensional DSA images revealed complete obliteration of carotid cave aneurysms. Postoperatively, the patients recovered uneventfully.

Conclusions: The key feature of modified clipping technique is using right-angled fenestrated clip through the small incision on the cavernous sinus roof. The goal of this technique is the complete obliteration of the aneurysms with minimal manipulation of the CS and decrease of the morbidity. Multiple tandem clipping method using the multiple fenestrated clips is occasionally useful in selected cases.

EXSANGUINATION POSTCONDITIONING OF ICH - USING THE LANCET TO TREAT THE BLEED: PRELIMINARY STUDY IN RODENTS

T. Lekic, W. Rolland, P. Krafft, J. Tang, J. Zhang

Loma Linda University School of Medicine, Loma Linda, CA, USA

Introduction: Cerebral iron overload contributes to the free-radical damage and secondary brain injury following intracerebral hemorrhage (ICH)(1-7) . Phlebotomy most effectively removes iron for the human body, compared to any pharmacological agent (e.g. chelator (8)). For centuries, this approach was mainstay treatment for stroke (9-11). To date, this is the first scientific evaluation using this approach after ICH.

Methods: Femoral catheterization occurred at

thirty minutes following collagenase infusion. Three different exsanguination volumes (1ml, 2ml, 3ml) were compared with ICH and sham controls. Routine (12-13) brain water content, hemorrhage size, and Neuroscore were measured twenty-four hours later.

Results: Phlebotomy significantly decreased brain edema and hemorrhagic size; however neurobehavioral outcome was not significantly improved at one day after ICH.

Conclusion: Exsanguination after ICH using the traditional phlebotomy approach may ameliorate the early brain injury (hemorrhage and edema), despite equivocal changes in the short-term neurological functional ability. Thus studies must further delineate the involvement of specific neuroprotective molecules, sympathetic responses, hemodynamic-vasoactive molecules, or neuro-endocrine factors involved in this rodent postconditioning of ICH.

References:

1. Nakamura T, Keep RF, Hua Y, Nagao S, Hoff JT, Xi G. Iron-induced oxidative brain injury after experimental intracerebral hemorrhage. Acta Neurochir Suppl. 2006;96:194-8.

2. Chen Z, Gao C, Hua Y, Keep RF, Muraszko K, Xi G. Role of iron in brain injury after intraventricular hemorrhage. Stroke. 2011;42(2):465-70.

3. Hua Y, Keep RF, Hoff JT, Xi G. Brain injury after intracerebral hemorrhage: the role of thrombin and iron. Stroke. 2007;38(2 Suppl):759-62.

4. Hua Y, Nakamura T, Keep RF, Wu J, Schallert T, Hoff JT, et al. Long-term effects of experimental intracerebral hemorrhage: the role of iron. J Neurosurg. 2006;104(2):305-12.

5. Wu J, Hua Y, Keep RF, Nakamura T, Hoff JT, Xi G. Iron and iron-handling proteins in the brain after intracerebral hemorrhage. Stroke. 2003;34(12):2964-9.

6. Huang FP, Xi G, Keep RF, Hua Y, Nemoianu A, Hoff JT. Brain edema after experimental intracerebral hemorrhage: role of hemoglobin degradation products. J Neurosurg. 2002;96(2):287-93.

7. Okauchi M, Hua Y, Keep RF, Morgenstern LB, Xi G. Effects of deferoxamine on intracerebral hemorrhage-induced brain injury in aged rats. Stroke. 2009;40(5):1858-63. PMCID: 2674519.

8. Adams PC, Barton JC. How I treat hemochromatosis. Blood. 2010;116(3):317-25.

9. Weinberg F. Bloodletting. Can Fam Physician. 1994;40:131-4. PMCID: 2380011.

10. Morabia A. Pierre-Charles-Alexandre Louis and the evaluation of bloodletting. J R Soc Med. 2006;99(3):158-60. PMCID: 1383766.

11. Parapia LA. History of bloodletting by phlebotomy. Br J Haematol. 2008;143(4):490-5.

12. Lekic T, Hartman R, Rojas H, Manaenko A, Chen W, Ayer R, et al. Protective effect of melatonin upon neuropathology, striatal function, and memory ability after intracerebral hemorrhage in rats. J Neurotrauma. 2010;27(3):627-37.

13. Lekic T, Rolland W, Manaenko A, Krafft PR, Kamper JE, Suzuki H, et al. Evaluation of the hematoma consequences, neurobehavioral profiles, and histopathology in a rat model of pontine hemorrhage. J Neurosurg. 2012.

ATORVASTATIN INDUCES CEREBRAL HEMORRHAGE BY DAMAGING BLOOD VESSEL STABILITY VIA MEVALONATE AND SRC/VE-CADHERIN PATHWAYS IN HUMAN ENDOTHELIAL CELL AND ZEBRAFISH

S. Li[1], Z.Y. Zhou[1], M.P.M. Hoi[1], W.C. Hang[2], Y.W. Kwan[3], S.W. Chan[4], G.P.H. Leung[5], S.M.Y. Lee[1]

[1]State Key Laboratory of Quality Research in Chinese Medicine, Institute of Chinese Medical Sciences, Macao, [2]Department of Clinical Oncology, The Chinese University of Hong Kong, [3]School of Biomedical Sciences, Faculty of Medicine, The Chinese University of Hong Kong, [4]State Key Laboratory of Chinese Medicine and Molecular Pharmacology, Department of Applied Biology and Chemical Technology, The Hong Kong Polytechnic University, [5]Department of Pharmacology and Pharmacy, Faculty of Medicine, The University of Hong Kong, Hong Kong, China

Objectives: Statins are a class of drugs used to lower hypercholesterolemia and to prevent

its complications such as cardiovascular diseases by inhibiting the enzyme HMG-CoA reductase. However, a Stroke Prevention by Aggressive Reduction in Cholesterol Levels (SPARCL) study showed that statins appeared to increase the risk of intracerebral hemorrhage (ICH), particularly in elderly patients with history of ICH, and it did not seem to correlate with low-density lipoprotein (LDL) levels 1. Statins induced-cerebral bleeding, mediated by rupture vessel integrity, could be reproduced in zebrafish model2 . Loss of integrity of the vascular endothelium can result in the rupture of blood vessels and hemorrhage into interstitial spaces. Therefore, we employed human endothelial cells *in vitro* and zebrafish larvae *in vivo* to study the mechanisms of change of vascular integrity and endothelium permeability underlying the atorvastatin-induced cerebral bleeding process.

Methods: 1 days post fertilization (dpf) wild-type as well as Tg (fli1:EGFP)y1 and Tg (Gata1:dsRed) double transgenic zebrafish embryos treated with atorvastatin were used to mimic the cerebral hemorrhage in human. Vascular integrity and endothelium permeability were investigated in atorvastatin treated Human Umbilical Vein Endothelial Cells (HUVECs).

Results: Our present study showed that atorvastatin did not affect the cholesterol levels in zebrafish larvae measured in the body fluids isolated from larvae homogenates. Furthermore, the cerebral hemorrhage and decreased locomotor activity in zebrafish larvae induced by atorvastatin could be reversed by Mevalonic acid (MVA) exposure to the embryos but not cholesterol. The results suggest that atorvastatin causes bleeding through vessel rupture in zebrafish via the mevalonate pathway but is unrelated to cholesterol. Besides, our results showed that atorvastatin induced loss of cell-cell junctions and increase of endothelial cell monolayer permeability by derangement of both actin cytoskeleton and VE-cadherin (VEC) distribution. VA treatment could completely recover actin cytoskeleton derangement, cell shrinkage and VEC distribution impairment induced by atorvastatin. In addition, we found that atorvastatin activated phosphorylation of Src and VE-cadherin on residues Tyr-658 and Tyr-731. Thus, PP2 (Src inhibitor) was used to challenge vessel rupture and endothelial cell-cell junction break in atorvastatin treated zebrafish and HUVEC. Interestingly, PP2 not only completely prevented atorvastatin-induced bleeding and locomotor deficit in zebrafish and also recovered the atorvastatin induced abnormal cell permeability by blocking actin cytoskeleton derangement, cell shape shrink and VEC redistribution in HUVEC. Moreover, PP2 also inhibited the phosphorylation of VEC on Tyr-658 and Try-731, strongly suggesting that Src is involved in atorvasvatin-induced VEC phosphorylation.

Conclusions: Taken together, the present study showed that atorvastatin damaged blood vessel stability through mevalonate and Src/VE-cadherin pathways. It implies that inhibition of Src should offer a new therapy strategy in the management of cerebral vasospasm in statins treatment.

1 Huisa, B. N., Stemer, A. B. & Zivin, J. A. Atorvastatin in stroke: a review of SPARCL and subgroup analysis. Vasc Health Risk Manag 6, 229-236 (2010).

2 Gjini, E. et al. Zebrafish Tie-2 shares a redundant role with Tie-1 in heart development and regulates vessel integrity. Dis Model Mech 4, 57-66, doi:Doi 10.1242/Dmm.005033 (2011).

TREATMENT RESULT OF THE DISTAL INTERNAL CAROTID ARTERY ANEURYSM, MICROSURGICAL VS ENDOVASCULAR THERAPIES

D.-J. Lim, S.-H. Kim, S.-D. Kim, S.-K. Ha

Neurosurgery, Ansan Hospital, Korea University, Ansan-si, Republic of Korea

Objective: Distal internal carotid artery (ICA) aneurysms are feasible for both microsurgical and endovascular treatment. We report the surgical result of the distal ICA aneurysms.

Materials and methods: Between July 2008 and December 2011, 57 (60 aneurysms) patients with distal ICA aneurysms were treated. Eleven (18.3%) aneurysms were unruptured ones. Forty-eight (80%) aneurysms were treated using microsurgical strategy. We compared patient´s characteristics, radiologic features, and surgical results between microsurgical group and endovascular one.

Results: Most aneurysms treated with endovascular technique were unruptured ones. Patients underwent endovascular therapy were older than those with microsurgery. The management outcome was

mainly associated with the preoperative status of the patients. Surgical morbidity between clipping and coiling was not comparable. Two patients with coiling needed another session of coiling procedures. An important cause of surgical morbidity was the occlusion of the branches such as posterior communicating artery or anterior choroidal artery.

Conclusions: Both microsurgical clipping and endovascular coil embolization are feasible for the treatment of the distal ICA aneurysms. Although both strategies have pros and cons, the selection of the management strategy is mainly up to the doctor´s preference. Whatever the strategy, the preservation of the branching arteries is important for the better surgical result.

ROLE OF ENDOTHELIUM DERIVED FACTORS IN CORTICAL SPREADING ISCHEMIA INDUCED VASOCONSTRICTION OF ISOLATED RAT MCA

U. Lindauer[1], I. Eskina[1], S. Pinkernell[1], B. Meyer[2]

[1]Experimental Neurosurgery, Department of Neurosurgery, [2]Department of Neurosurgery, Klinikum rechts der Isar, Technical University Munich, Munich, Germany

Objective: Under normal conditions, cortical spreading depolarisation (CSD) goes along with strong vasodilation. However, in the diseased brain, CSD can induce severe vasoconstriction (cortical spreading ischemia, CSI) [1]. CSI can be modelled in the isolated middle cerebral artery (MCA) by application of combined extraluminal ion changes according to changes of the extracellular milieu during CSI [2]. Vascular endothelial cells release vasoactive factors responsible for normal smooth muscle cell function and vascular tonus, as the arachidonic acid metabolites EETs or the gaseous factor H_2S. We investigated the role of these endothelial factors in vascular reactivity to CSI.

Methods: Rats were anesthetized and decapitated. The MCA was dissected, cannulated and pressurized. Vascular reactivity to CSI was tested under baseline conditions and under P450-epoxygenase inhibition with MS-PPOH ($5x10^{-6}$M), or under DL-Propargylglycine (PAG, 10^{-3}M), an irreversible inhibitor of the H_2S synthesizing enzyme cystathionine-γ-lyase (CSE). MS-PPOH application was followed by L-type channel inhibition with nimodipine (10^{-7}M), and vascular reactivity to CSI was tested again.

Results: In response to CSI cocktail the arteries significantly dilated from 79+/-11µm to 94+/-14µm. During MS-PPOH application, CSI cocktail induced vasoconstriction from 95+/-10µm to 86+/-15µm, and application of the L-type channel antagonist nimodipine reestablished vasodilation to CSI cocktail (MS-PPOH + nimodipine: baseline: 113+/-12µm, CSI cocktail: 123+/-11µm). Under CSE inhibition, arteries still dilated to CSI (PAG baseline: 92+/-21µm, PAG CSI cocktail: 100+/-21µm).

Conclusions: Endothelium released arachidobic acid metabolites of P450-epoxygenase prevent vasoconstriction during CSI. During inhibition of the H_2S releasing enzyme, CSI still induces vasodilation. Following subarachnoid hemorrhage, endothelial cell dysfunction and cell death has been shown, which may be responsible for CSD induced exacerbation of tissue damage. It has to be further evaluated whether endothelial cell protection may represent an effective approach to reverse CSD induced ischemic events within the microcirculation [3].

References:

[1] Dreier JP et al.; J Cereb Blood Flow Metab 18, 978-990 (1998)

[2] Windmüller O et al.; Brain 128: 2042-2051 (2005)

[3] Lauritzen M, Dreier JP, Fabricius M, et al.; J Cereb Blood Flow Metab 31, 17-35 (2011)

ANTI-MITOGENIC TREATMENTS VIA SRC INHIBITION IN INTRAVENTRICULAR HEMORRHAGE

D.Z. Liu, B.P. Ander, X. Zhan, B. Stamova, G.C. Jickling, F.R. Sharp

Department of Neurology, University of California at Davis, Sacramento, CA, USA

Increasing evidence reveals anti-mitogenic strategy that has been widely practiced in cancer therapeutics can be useful to prevent death of neurons in treatment of neurological diseases, such as intraventricular hemorrhage (IVH). However, anti-mitogenic therapy might produce global mitosis inhibition that block proliferation of neural progenitor cells (NPCs),

astrocytes and brain microvascular endothelial cells (BMVECs) and thus not affect ongoing processes of neurogenesis, blood brain barrier (BBB) self-repair and other cellular responses important during the recovery stage in IVH. Therefore, we plan transient anti-mitogenic treatment (using single administration of the oncogene Src inhibitor PP2 or nanoparticle-based siRNAs) should prevent IVH-induced brain injury at acute stage, but not affect cellular proliferation and self-repair at recovery processes in IVH.

Using the rat *in vivo* IVH model (i.c.v. thrombin or fresh blood), we show that single administration of Src inhibitor PP2 (1mg/kg, i.p., given immediately after IVH) prevents IVH-induced neurotoxicity including astrocyte and endothelial cell injury, BBB disruption, brain edema, death of hippocampal neurons, and cognitive deficits assessed on the Morris Water Maze. However, delayed and lasting administration of PP2 (1mg/kg, i.p., given once a day from day 2 through day 7) prolongs BBB self-repair and brain edema resolution. Moreover, PP2 (1mg/kg, i.p.) alone did not affect proliferation of NPCs and did not affect cognition as assessed using the Morris Water Maze. Since there are several Src subtyes in brain, we are now targeting specific SFK subtypes using a newly developed *in vivo* nanoparticle-based siRNA transfection system. One day after injections of nanoparticle-siRNAs (100µg, i.c.v.) for the Fyn, Lck and c-Src SFK family members into the left lateral cerebral ventricle, Fyn, Lck and c-Src mRNAs decrease in rat hippocampus by 22%, 37% and 43%, respectively.

Our ongoing studies are testing whether blocking Fyn, Lck or c-Src with nanoparticle-based siRNAs prevents IVH-induced brain injury in rats. This could provide a novel therapy for treating IVH patients, as the FDA approved nanoparticle-based siRNA approach is able to provide heightened specificity for targeting and silencing a single Src gene.

Acknowledgements: This study was supported by NIH grant NS054652 (FRS), and AHA Beginning Grant-in-Aid 12BGIA12060381 (DZL).

THROMBIN HAS A ROLE IN HYDROCEPHALUS DEVELOPMENT AFTER INTRAVENTRICULAR HEMORRHAGE

F. Liu, Z. Chen, Y. Hua, R.F. Keep, **G. Xi**

University of Michigan, Ann Arbor, MI, USA

Objectives: Hydrocephalus after intracranial hemorrhage is a common and important complication that causes clinical deterioration and affects recovery. The precise mechanisms underlying the development of hydrocephalus are still not clear. Previous studies demonstrated that thrombin and iron are two important factors that cause brain injury after intracerebral hemorrhage [1]. Our recent studies showed that iron has a role in hydrocephalus development following intraventricular hemorrhage (IVH) [2] or subarachnoid hemorrhage [3]. This study investigated the effect of thrombin on hydrocephalus in a rat intraventricular hemorrhage model.

Methods: There were two parts in this study. First, three groups of male Sprague-Dawley rats had a 200 µl injection of either autologous blood, heparinized autologous blood or saline into the right lateral ventricle and had MRI scanning at different time points. Rats were euthanized at day 28 and the brains used for histological analysis. Second, rats had an injection of 5U thrombin dissolved in 50 µl saline or saline alone, and were euthanized at 24 hours after MRI scanning. Ventricle volume was measured and the brains were used for Western blotting and histological analysis.

Results: Intraventricular injection of autologous blood caused hydrocephalus (day 1: 61.7 ± 5.7 vs. 8.4 ± 1.3 mm^3 in saline controls, $p< 0.01$; day 28: 40.4 ± 6.8 vs. 10.1 ± 8.0 in saline controls, $p< 0.01$). Blood-induced ventricle enlargement was reduced by co-injection of heparin (day 1: 38.2 ± 13.0 mm^3, $p< 0.05$; day 28: 16.9 ± 3.3 mm^3, $p< 0.05$). Intraventricular injection of thrombin also caused significant ventricular enlargement (40.9 ± 3.3 vs. 8.8 ± 1.3 mm^3 in saline controls, $p< 0.01$). Western blotting and histological analysis demonstrated that thrombin but not saline caused significant blood-brain barrier damage and activation of c-Jun-terminal kinases in the periventricular region.

Conclusions: Heparin reduces IVH-induced hydrocephalus and intraventricular injection of thrombin causes ventricular enlargement. These results suggest that thrombin generation during hematoma formation has a role in hydrocephalus development after intracranial hemorrhage, and thrombin may be a therapeutic target for hydrocephalus.

References:

1. Keep, R.F., Hua, Y. & Xi, G. Intracerebral haemorrhage: mechanisms of injury and therapeutic targets. Lancet Neurol 2012;11, 720-731.

2. Chen, Z., et al. Role of iron in brain injury after intraventricular hemorrhage. Stroke 2011;42, 465-470.

3. Okubo, S., Strahle, J., Keep, R.F., Hua, Y. & Xi, G. Subarachnoid Hemorrhage-Induced Hydrocephalus in Rats. Stroke 2012 Dec 4. [Epub ahead of print].

S100B PLAYS A KEY ROLE IN SUBARACHNOID HEMORRHAGE (SAH)-ASSOCIATED CEREBROVASCULAR DYSFUNCTION AND NEUROPATHOLOGY

C. Paisansathan, H. Xu, P. Polak, D. Pelligrino

Neuroanesthesia Research Laboratory, Department of Anesthesiology, University of Illinios-Chicago, Chicago, IL, USA

Objective: Elevations in the CSF and serum levels of the astrocytic protein, S100B, in association with SAH is well documented. However, it remains unclear as to whether that increase simply reflects the presence of brain damage (biomarker function) or actually contributes to intracerebral cytotoxicity. Preliminary findings by us[1], in rats, indicated that: (A) cisternal CSF levels of S100B increased post-SAH, peaking at 48h; and (B) expression of the receptor for advanced glycation end products (RAGE) in cortical tissue rose over the same timeframe. Since S100B is a major RAGE ligand, these findings implied that post-SAH S100B engagement with RAGE promoted an enhanced inflammatory state resulting in a repressed microvascular dilating function and an accompanying neuropathology. Thus, in the present study, a S100B antisense oligodeoxynucleotide (AS-ODN) knockdown strategy was applied to SAH- rats to examine: (A) whether chronic AS-ODN intracerebroventricular (icv) administration decreases SAH-associated-S100B elevation in CSF; and (B) whether AS-ODN-associated S100B knockdown leads to the restoration of cerebrovascular dilating dysfunction and an associated reduction in neurologic deficits in rats subjected to SAH.

Methods: A rat anterior cerebral artery perforation model was used to elicit SAH. Rats were divided into 3 groups:

(1) sham surgical control,

(2) S100B missense ODN (MS-ODN)-treated SAH, and

(3) S100B AS-ODN-treated SAH.

In the last 2 groups, rats received icv infusion of MS-ODN or AS-ODN via an osmotic pump started 24 h before SAH. At 48 hours after SAH or sham surgical operation, rats from each group were evaluated for neurological deficits, pial arteriolar dilating (PAD) function (intravital microscopy via closed cranial window), and S100B levels in cisternal CSF (via ELISA).

Results: Compared to shams, we observed much higher S100B levels in the cisternal CSF at 48h post-SAH (1370 ± 332 pg/ml in MS-ODN-treated SAH vs 579 ± 110 pg/ml in sham controls). S100B AS-ODN application significantly blunted SAH-induced S100B elevation in CSF (600 ± 118 pg/ml). Relative to sham, a marked neurological deficit was seen in MS-ODN-treated rats (10.5 ± 1.3 in MS-ODN vs 20.5 ± 0.5 in sham control). This was significantly reversed by S100B knockdown via AS-ODN (15.7 ± 0.8). The vasodilating responses to hypercapnia, sciatic nerve stimulation (SNS), and topically-applied vasodilators (acetylcholine, adenosine, S-nitroso-N-acetyl penicillamine) were completely lost at 48 h-post SAH in MS-ODN-treated rats. AS-ODN knockdown of S100B restored all PAD dysfunction, except SNS-induced vasodilation, which was not altered.

Conclusion: Enhanced S100B is a major contributor to cerebrovascular dysfunction and neuropathology following SAH.

References: 1) Xu, et al. Soc. Neurosci Abstr; Program No. 849.14 (2012)

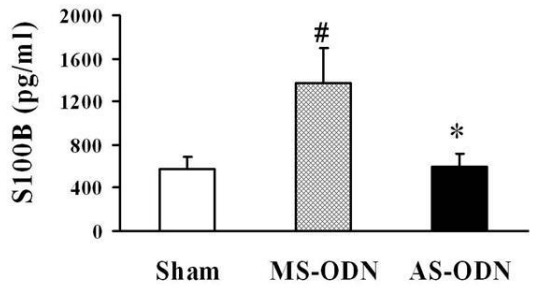

Fig 1. SAH-associated S100B elevation in cisternal CSF was substantially suppressed by intracerebroventricular application of S100B antisense oligodeoxynucleotide (AS-ODN). CSF samples were harvested at 48 h post-SAH. #, p<0.05 vs sham, *, p<0.05 vs S100B missense oligodeoxynucleotide (MS-ODN).

[Effect of AS-ODN on SAH-related S100B elevation]

GENE SIGNATURE AND CO-OCCURRENCE OF TRANSCRIPTION FACTOR BINDING MOTIFS IN SUBARACHNOID HAEMORRHAGE

A.K. Samraj, A.H. Mueller, L. Edvinsson

Clinical Experimental Research, Copenhagen University, Glostrup, Denmark

Background and aim: Subarachnoid hemorrhage (SAH) is a form of stroke that brings severe disability or death. The aim of the study is to understand the cellular and molecular mechanisms following SAH, which would help to develop therapies to reduce the damage caused to the brain thereby increasing quality of life.

Methods: We performed gene expression profiling at an early (6h) and late (24h) time point in the cerebral arteries of SAH rat model. Differential gene expression pattern was compared between SAH and sham operated animals. Transcription Factor Binding Site (TFBS) analyses were performed for the presence of highly conserved and enriched binding sites in the promoter regions of the differentially regulated genes. *Ingenuity* Systems Pathway Analysis was employed to identify potential canonical candidates as pharmacological target.

Results: We have identified several differentially regulated genes that are known to participate in regulating inflammation, cell cycle, chemotaxis, vascular tone, oxidative stress response, extracellular matrix degradation and vascular remodelling. TFBS analyses of differentially expressed gens revealed a significant enrichment of binding sites for IK1, STAT3, STAT5A, ETS, AP1, AP4 and NFkB and Toll like receptor (TLR) signalling. In addition, we identified ERK2 as an upstream regulator.

Conclusions: In this study we have identified transcription factors that might be playing pivotal role in the pathophysiology of SAH. ERK2 has been identified as a canonical candidate that orchestrates the pathophysiology of SAH. The Identified candidate transcription factors are currently under investigation for further evaluation as potential pharmacological targets.

DELETION OF THE PROSTAGLANDIN E2 EP1 RECEPTOR AGGRAVATES HEMORRHAGIC INJURY AND COGNITIVE DEFICITS

N. Singh[1], B. Ma[2], S. Narumiya[3], S. Doré[4]

[1]Anesthesiology, Center for Translational Research in Neurodegenerative Disease, University of Florida, Gainesville, FL, [2]Neurogenetics Divison, National Institute on Aging, Bethesda, MD, USA, [3]Pharmacology, Kyoto University, Kyoto, Japan, [4]Anesthesiology, Neuroscience, Neurology and Psychiatry, University of Florida, Gainesville, FL, USA

Objective: Prostaglandin E2 (PGE2) has been described to have various cytoprotective or toxic properties in acute and chronic conditions including stroke, Parkinson's, Alzheimer and other neurodegenerative diseases. However, the precise role of the PGE2 EP1 receptor in intracerebral hemorrhage (ICH)-induced brain injury is unknown. Therefore, this study was performed to investigate the role of the EP1 G protein-coupled receptor in hemorrhagic stroke.

Methods: Striatal intracerebral hemorrhage was induced in adult male wildtype (WT) and EP1 C57BL/6 mice by stereotactic injection of collagenase. Following ICH, mice were evaluated for neurological deficits using a 24 point scale, as well as functional impairments using Rotarod, Open Field and Adhesive Removal tests. Following behavioral testing, mice were euthanized for quantification of lesion volume and brain swelling with Cresyl Violet staining, cell death/survival with Fluoro-Jade staining and 8-hydroxyguanosine staining, and microglial activation with

immunohistochemical labeling of Iba1. Data were expressed as mean±SEM, and the number of cells/field was calculated by averaging four different regions proximal to the hematoma.

Results: This ICH model produced a reproducible hematoma that was primarily restricted to the striatum. Neurological deficits were worsened in EP1 knockout mice compared to WT mice 72h after ICH. Interestingly, deletion of EP1 receptor exacerbated lesion volume and brain swelling compared to WT mice. Behavioral testing indicated that WT mice recovered faster compared to EP1 mice, showing reduced time to remove adhesive tape, increased distance traveled in open field and increased latency to fall on the Rotarod task. Fluoro-Jade staining demonstrated that cell death was higher in EP1 knockout mice compared to WT controls, and 8-hydroxyguanosine staining showed that neuronal survival was reduced in EP1 mice. Additionally, quantification of Iba1 immunoreactivity showed a significant increase in microglial activation in WT mice compared to EP1 knockout mice.

Conclusion: These results demonstrate that, the PGE2 EP1 receptor deletion worsens anatomical and functional outcomes following ICH. (This study was supported by grant 2RO1NS046400 from NIH/NINDS).

EFFECT OF HUMAN ALBUMIN IN CEREBRAL BLOOD FLOW, DELAYED CEREBRAL ISCHEMIA, AND CEREBRAL INFARCTION IN SUBARACHNOID HEMORRHAGE (ALISAH STUDY)

J. Suarez[1], R.H. Martin[2], E. Calvillo[1], The ALISAH Study Investigators

[1]Neurology, Baylor College of Medicine, Houston, TX, [2]Division of Biostatistics and Epidemiology, Medical University of South Carolina, Charleston, SC, USA

Objectives: The neuroprotective effects of human albumin have been demonstrated in animal models of stroke and humans with various intracranial disorders. We investigated the effect of 25% human albumin (ALB) on mean cerebral blood flow velocities (MCBFV), delayed cerebral ischemia (DCI), and cerebral infarctions.

Methods: We studied patients from the Albumin in Subarachnoid Hemorrhage (ALISAH) Pilot Clinical trial. ALISAH intended to investigate the safety and treatment effect of 4 different dosages of ALB of increasing magnitude (0.625 g/Kg: Tier 1; 1.25 g/Kg: Tier 2; 1.875 g/Kg: Tier 3; and 2.5 g/Kg: Tier 4). Each dosage was to be given to 20 adult subjects daily for 7 days. We found that ALB up to 1.25 g/Kg/d x 7 days was tolerated by SAH patients with improved outcomes and the study was stopped after 47 subjects were enrolled (20 in tier 1, 20 in tier 2, and 7 in tier 3). We collected data on MCBFV as measured by transcranial Doppler ultrasound (TCD), incidence of DCI, and cerebral infarctions on head CT scan at 90 days. TCD vasospasm was defined as MCBFV > 120 cm/sec. DCI was defined as neurological decline within 4-14 days after SAH not attributable to hydrocephalus, rebleeding, seizures, or systemic derangements. Cerebral infarctions were classified as new or old compared to post-aneurysm treatment. Statistical analysis is mainly descriptive as the assignment of subjects to dosage tier was not randomized but in a dose-escalation manner and after clearance by the Data and Safety Monitoring Board.

Results: We found that 15 subjects (75%) in dosage tier 1, 11 (55%) in dosage tier 2, and 2 (28.6%) in dosage tier 3 had TCD signs of vasospasm during the monitoring period. DCI was present in 4 (20%) subjects in tier 1, 3 (15%) in dosage tier 2, and 1 (14.3%) in dosage tier 3. We collected head CT scan data on 33 subjects: 9 in tier 1, 18 in tier 2, and 4 in tier 3. Cerebral infarctions were seen in 5 (45%) subjects in dosage tier 1 (3 new - 27%), 3 (16%) in dosage tier 2 (all new), and 1 (25%) in dosage tier 3 (old). All strokes in tier 1 and 3 involved the middle cerebral artery territory (MCA). In dosage tier 2 one stroke involved the MCA and 2 the anterior cerebral artery.

Conclusions: ALB administration was associated with decreased incidence of TCD vasospasm, DCI, and cerebral infarctions at 90 days in a dose-dependent manner. These findings may explain the good clinical outcomes of subjects enrolled in ALISAH. Preparations for ALISAH II (Phase II futility study) are currently underway.

References:

1. Suarez JI, Martin RH, Calvillo E et al. The Albumin in Subarachnoid Hemorrhage (ALISAH) multicenter pilot clinical trial: safety

and neurologic outcomes. Stroke 2012;43:683-90

2. Suarez JI, Martin RH. Treatment of subarachnoid hemorrhage with human albumin: ALISAH study. Rationale and Design. Neurocrit Care 2010;13:263-77

3. ALSAH was funded by NINDS (1R01NS049135-01, PI: Suarez JI)

SITUATIONAL REVIEW OF ABNORMAL MOTOR EVOKED POTENTIAL (MEP) DURING ANEURYSM CLIPPING

J.H. Sung, J. Huh, S.W. Lee

Neurosurgery, St. Vincent's Hospital, The Catholic University of Korea, Suwon, Republic of Korea

Introduction: It has been well-known that intraoperative monitoring of motor evoked potential (MEP) can detect compromised motor function during operative procedures. During aneurysm surgery, many factors can compromise cerebral perfusion and immediate correction is critical for patients' safety. We retrospectively review various situations of abnormal MEP and briefly discuss its causes and pitfalls.

Material and method: From 2010 Nov. to 2012 Feb., total 98 cases of aneurysm neck clipping were performed by pterional or supraorbital approach with the guidance of MEP monitoring. The NIM Eclipse intraoperative nerve monitor system (Medtronic, USA) was used. Briefly, C3-C4 scalp electric stimulator was applied at each side of skull vertex. Needle electrodes were inserted to both side hands (abductor pollicis brevis and abductor digiti minimi) and feet (abductor hallucis and abductor digiti quinti). The stimuli characteristics were as follows; intensity of 200-400V, duration of 50μs, biphasic polarity with pulse train. The criterion of abnormal recording was 1) reduction of amplitude less than 50%, or 2) increase of latency more than 10%, or 3) no response after increased stimulation intensity. The check out list of abnormal change was

1) deep anesthesia,

2) hypotension,

3) electrode error,

4) true intraoperative problem.

The abnormal MEPs were grouped according to anticipated one (group 1) and unexpected one (group 2).

Results: Among 98 cases, 18 cases of abnormal MEP were recorded (18.4%). The mean age was 58.4±11 years and most of patients were females(15 cases). The ruptured aneurysms were 9 cases (50%).

The group 1 had 10 cases (55.6%). Most common cause was premature rupture/temporary clipping (7 cases; 38.9%), followed by clipping error (3 cases; 16.7%).

The group 2 had 8 cases (44.4%). Most common cause was unknown (5 cases; 27.8%), followed by careless brain retraction (2 cases; 11.1%) and arterial kinking (1 cases; 5.6%). The aneurysm rupture or approach route did not influence MEP change. Final restoration of MEP amplitude was confirmed in 16 cases (88.9%). In 2 cases, it was not restored. One case was giant MCA aneurysm and mild hemiparesis was followed. The other one showed uneventful recovery despite of unsatisfactory final MEP. Briefly, in 13 cases of “known” causes, intraoperative MEP restored after appropriate rescue procedures (72.2%).

Conclusion: Intraoperative MEP monitoring is reliable safeguard for temporary clipping. It can detect unexpected surgical errors inducing compromise of blood flow, but the false positive results should be considered.

NLRP3 INFLAMMASOME MEDIATED BY MITOCHONDRIA ROS CONTRIBUTES TO INFLAMMATORY RESPONSE FOLLOWING INTRACEREBRAL HEMORRHAGE IN MICE

J. Tang, Q. Ma, J.H. Zhang

Loma Linda University School of Medicine, Loma Linda, CA, USA

Objective: Inflammation plays a critical role in cerebral injury after intracerebral hemorrhage. NLRP3 inflammasome is a key component of innate immune system, which releases active caspase-1 and IL-1 β after activation, thereby amplifying the inflammatory response. Here, we investigated whether the knockdown of NLRP3 inflammasome decreases neutrophil infiltration, reduces brain edema and improves

neurological function in an ICH mouse model. We also determined whether mitochondrial ROS governed by mitochondrial permeability transition pore (mPTP) mediates NLRP3 inflammasome activation following ICH.

Methods: ICH was induced by autologous arterial blood (30 µl) injection into mice brain. NLRP3 siRNAs were administered 24 hours before ICH. A mPTP inhibitor (TRO-19622) or a specific mitochondria ROS scavenger (Mito-TEMPO) was co-injected with blood. In naïve mice, TRO-19622 or Mito-TEMPO was delivered following rotenone, a respiration chain complex I inhibitor injection into brain. Post-assay included neurological deficits evaluation, brain edema measurement, ELISA, western blot, in vivo chemical cross linking, in vitro ROS detection and immunostaining.

Results: ICH markedly upregulated NLRP3 inflammasome components. NLRP3 knockdown reduced brain edema and improved neurological functions at 24-72 hours as well as lessening the MPO level at 24 hours following ICH. TRO-19622 or Mito-TEMPO reduced ROS, NLRP3 inflammasome components and MPO level following ICH. In naïve animals, rotenone administration induced mPTP formation, ROS generation and NLRP3 inflammasome components upregulation, which were reduced by TRO-19622 or Mito-TEMPO.

Conclusion: NLRP3 inflammasome may amplify the inflammatory response by releasing proinflammatory factors and promoting neutrophil infiltration following ICH. Mitochondria ROS may be one of the major triggers of NLRP3 inflammasome components upregulation and activation. Our study provided a possible interpretation of the sources of inflammation following ICH.

ROLE OF FERRIC IRON TRANSPORTERS WHEN IRON ACCUMULATION IN BRAIN AFTER RAT INTRACEREBRAL HEMORRHAGE

G. Wang, S. Meng, W. Hu

Neurology, Shanxi Medical University, Taiyuan, China

Background and purpose: Iron accumulation after hemolysis in intracerebral hemorrhage(ICH) trigger several pathways to transport and metabolize this iron. There have been few studies on the fate of iron after ICH and on the spatio-temporal relationship between iron overloading and iron-handling proteins that may regulate iron. There are few data in iron handling pathways after ICH. Our study is to observe the dynamic expression of the ferric iron deposit, the transferrin (Tf) /transferrin receptor(TfR) and ceruloplasmin (CP) in different time after ICH and their spatio-temporal patterns.

Methods: Sprague-Dawley rats received an infusion of CollagenaseⅣ into the right basal ganglia and were killed at 1, 3, 7, 14 day. MALLORY's method was used for ferric iron staining, and brain iron deposits was determined. Brain Tf /TfR /CP around hematoma were examined by immunohistochemistry ((IHC)).

Results: ICH resulted in ferric iron overload in the brain. A marked increase in brain iron was not cleared within 14 days. The expression of Tf in all groups increased and TfR/CP at 1 day ,3 day and 7 day intensified in ICH compared with the operation controls, and they reached a plateau at 3-7 day in ICH models. Correlations test showed that iron sediment granules positively correlated with Tf /TfR（r=0.468-0.521, P< 0.01）; CP expression is paralleled with Tf and TfR (r=0.521-0.634, P< 0.01).

Conclusions: Iron excessive accumulation after ICH activate Tf /TfR/CP expression. Tf /TfR/CP may play a role in clearing away iron when iron overload in brain.

UROCORTIN REDUCES BRAIN INJURY FOLLOWING CEREBRAL HEMORRAGE PARTIALLY VIA PI3K/AKT AND GSK-3B SIGNALING PATHWAYS

J.-Y. Wang[1], H. Liew[2], C. Pang[2], G.S. Chen[3]

[1]Graduate Institute of Medical Sciences, Taipei, [2]Dept. of Medical Res., Tzu Chi General Hosp., Hualien, [3]Graduate Institute of Life Sciences, Taipei Med. Univ., Taipei, Taiwan R.O.C.

Introduction: Intracerebral hemorrhage (ICH) remains a serious clinical problem lacking effective treatment. ICH frequently causes brain edema which worsens brain injuy and neurological outcomes. Increasing evidence suggests that inflammatory cascades are involved in ICH-induced brain injury.Urocortin 1 (UCN), a member of the corticotropin-

releasing factor family, protects ischemic cardiomyocytes and dopaminergic neurons.

Objective: We examined the therapeutic effect of UCN on ICH-induced neurological deficits and neuroinflammation.

Methods: ICH was induced in male Sprague-Dawley rats by intrastriatal infusion of bacterial collagenase VII-S or autologous blood. At 1 h after the induction of ICH, UCN either administered intracerebroventricularly (5μg, icv) or intraperitoneally (2.5 or 25 μg/kg) reduced neurological deficits from 1 to 7 days post-ICH.

Results: Although a higher dose (25 μg/kg, i.p.) also reduced the functional deficits associated with ICH, it is significantly less effective than the very low dose (2.5 μg/kg, i.p.). Beneficial results with the low dose of UCN also included a reduction in brain edema, BBB disruption, lesion volume, microglial activation and neuronal loss 3 days post-ICH, and suppression of TNF-a, IL-1β, and IL-6 production 1, 3 and 7 days post-ICH. Systemic post-ICH treatment with UCN reduced striatal injury and neurological deficits, likely via suppression of microglial activation and inflammatory cytokine production. We further demonstrated that the fluorescently label-UCN penetrated more prominent into the neurons than microglia, but not astrocytes. Both PI3K/Akt and GSK-3β signaling pathways participate in the UCN-mediated protection against ICH-induced brain injury.

Conclusion: Post-injury treatment with UCN reduces the injury area, brain edema, and BBB permeabilityand improves neurological deficits in ICH rats and provides a protential as a therapeutic agent for patients with ICH or other brain injuries.

(Supported by NSC 99-2320-B-038-006-MY3, Taiwan)

CHARACTERISTICS OF ETIOLOGICAL DIAGNOSTIC WORKUP ACROSS THE PAST 10 YEARS IN PATIENTS WITH SPONTANEOUS INTRACEREBRAL HEMORRHAGE IN A CHINESE HOSPITAL

Q. Wang

Department of Neurology, West China Hospital ,Sichuan University, Chengdu, China

Background: Based on former studies and knowledge, patients could benefit more from a quick diagnosis of etiology in spontaneous intracerebral hemorrhage (SICH) and vascular source was considered the most urgent treatable cause. It is unclear what the status of diagnostic workup is in Chinese hospitals which treat the majority of the hemorrhagic patients in the world.

Aims: We aim to demonstrate characteristics on diagnostic workup we get used to do in both departments of Neurology and Neurosurgery in patients with SICH, to decide whether it is sufficient in diagnosis of etiology. And we planned to predict if having an examination of vascular associated with time and different departments.

Methods: We enrolled patients with SICH from January 2002 to December 2011 from Chengdu stroke registry, which included patients from either in departments of Neurology or Neurosurgery. Data on diagnostic workup were extracted. Our collected workup include: CT, MRI, special sequences of CT, special sequences of MRI, CTA, MRA, DSA, blood pressure in admission, lipid, immunological detection, serological test, coagulation screen, erythrocyte sedimentation rate, tumor marker, CSF, bone marrow aspiration, pathological examination and carotid duplex ultrasound. Logistic regression models were used to predict whether the fullfillment of diagnostic workup was associated with diffferent departments and time. We also planned to use Chi-square and Fisher exact tests to demonstrate the differences between departments of Neurology and Neurosurgery.

Results: A total of 2264 patients diagnosed as SICH with rapid CT scan were included. The patients were admitted in departments of Neurology or Neurosurgery (36.5% vs 63.5%). Following diagnostic workup were more frequently undertaken in the Neurological

Department than in the neurosurgical Department: special sequences of MRI or CT (P=0.000), special sequences of MRI (P=0.001), special sequences of CT (P=0.045), MRA (P=0.000), immunological detection (P=0.000), serological test (P=0.000), ESR (P=0.000), tumor markers (P=0.000), carotid duplex ultrasound (P=0.000). However, CT (P=0.000), CT/MRI (P=0.000), CTA (P=0.002), coagulation screen (P=0.000) were implemented more in the Neurosurgery Department. DSA stood the same importance in two departments. From a perspective of intracranial vascular examination, contains whichever in CTA, MRA and DSA, department of Neurosurgery had more advantages (P=0.000).Department of Neurosurgery (p=0.006) and the year 2011 (p=0.000) were independent predictors of more complementations of diagnostic workup on vascular.

Conclusion: Department of Neurosurgery and the year 2011 associated with more thorough diagnostic workup aiming at vascular etiology. Data of our study showd the implemention of diagnostic workup is scant to clarify each cause of SICH. The department of Neurology prefer diagnostic workup aiming at hematological source while department of Neurosurgery laid more emphasis on vascular. Since patients could benefit more from a quick diagnosis of etiology, it was an urgent to explore a practical scheme of diagnostic workup of etiology for SICH, and that is in the schedule of our following study.

COAGULATION STATUS AND MMPS DID NOT CORRELATE TO BRAIN MICRO BLEEDINGS IN CIRRHOTIC PATIENTS

J. Ding, D. Lin, **X. Wang**

Department of Neurology, Zhongshan Hospital, Fudan University, Shanghai, China

Background and objectives: Intracranial hemorrhage is common complication in hepatic cirrhotic patients. But no evidence for micro bleeding in cirrhotic patients has been present. Our study aimed to detect micro bleeding in patients with hepatitis B virus (HBV) infection-related cirrhosis and to explore the relationship between bleeding, coagulation status and blood barrier disruption.

Methods: Forty HBV-related cirrhotic patients were enrolled. Micro bleeding was detected by susceptibility weighted phase imaging technique using 3T MRI. Liver function was graded by Child-Pugh classification and serum albumin level. Coagulation status, including platelet count, prothrombin time (PT), activated partial thromboplastin time (APTT) and INR were tested. Matrix metalloproteinase (MMPs) as blood-brain barrier dysfunction indicator were also measured in serum.

Results: Patients' mean Child-Pugh Score was 6.47±2.02. HBV-related cirrhotic patients had increased APTT, PT, INR as well as decreased platelet count compared to normal range. Eleven out of forty Cirrhotic patients (27.5%) were found brain micro bleeding by susceptibility weighted phase imaging. There was no significant difference in PT, APTT, INR and serum MMPs between patients with micro bleeding and without micro bleeding.

Conclusion: In our study, 27.5% HBV-related cirrhotic patients had micro bleedings. These micro bleedings do not correlate with systemic coagulation status and blood-brain barrier disruption. Other etiology, such as weakening the walls of blood vessels, should be suspected.

EFFECTS OF LYMPHATIC DRAINAGE PATHWAY ON NEURAL STEM CELLS PROLIFERATION, DIFFERENTIATION AND PLASTICITY AFTER SUBARACHNIOD HEMORRHAGE

L. Xichang, B.-L. Sun

Penglai People's Hospital, Penglai, China

Objective: To approach effect of cerebral lymphatic blockade (CLB) on never stem cells proliferation, differentiated and plasticity after Subarachniod Hemorrhage (SAH).

Method: adult male wistar rat were used as experimental animals,Cisterna magna injection twice of freshly autologous arterial blood was used to induce SAH in rats, and CLB model in rats was established by occlusion of cervical lymphatic tubes and removal of cervical lymphatic nodes. The rats were divided into: normal group; SAH group; SAH+CLB group. NSCs were signed by Brdu, express of Brdu+,GFAP+, Neurod+ and PSA-NCAM+ cells were detected by means of immunofluorescence double staining, laser confocal microscopy was used for observed their express.

Results:

BrdU+,NeuroD+/BrdU+,GFAP+/BrdU+ and PSA-NCAM+/BrdU+ cells of SAH group were more than normal groups. Compared with SAH group, BrdU+ and $GFAP^+$/ $Brdu^+$ cells in CLB+SAH group were remarkably increased, while Neurod+ /Brdu+ and PSA-NCAM+/BrdU+ cells were decreased.

Conclusion: Brain lympha drainage blockage were able to facilitated proliferation of NSCs, but disadvantaged to differentiation and plasticity of NSCs.

EFFECT OF GINKGOLIDES AGAINST BRAIN EDEMA AND NEURON ULTRASTRUCTURAL INJURY ON SAH RATS WITH CEREBRAL LYMPHATIC BLOCKADE

L. Xichang, B.-L. Sun

Penglai People's Hospital, Penglai, China

Objective: To determine the effect of cerebral lymphatic drainage pathway on brain water content and neuronic ultrastructure secondary to subarachnoid hemorrhage (SAH), and to observe the protective role of Ginkgolides.

Methods: 90 mature male Wister rats were randomly divided into six groups: negatived control group, SAH group, Cerebral lymphatic blockade (CLB)+SAH group, CLB+SAH+ Normal Sodium (NS) group, CLB+SAH+20mg/kg Ginkgolides group (Gl_{20}) and CLB+SAH+80mg/kg Ginkgo ides group (Gl_{80}). Cistern magna injection twice of freshly autologous arterial blood was used to induce SAH in rats, and CLB model in rats was established by occlusion of cervical lymphatic tubes and removal of cervical lymphatic nodes. 24h and 72h after induction of SAH, brain water content was detected. Electron microscope was used to observe neuronal ultrastructures 72h after SAH model inducted.

Results: SAH increased brain water content. Increasing of brain water content were more severe in CLB+SAH group than that in others group. Compared with SAH+CLB group, brain water content in CLB+SAH+Gl groups were decreased, brain water content were a remarkable decreased in SAH+CLB+Gl_{80} groups. The neuronal ultrastructures of the rats showed different extent of destruction except for the ras of negatived control group. The destruction of neuronal ultrastructures were more severe in CLB+SAH group.

Conclusions: Brain lymphatic drainage pathway might play important role in brain edema and neuronal ultrastructure injury after SAH. Ginkgolides may relieve brain edema and injury of neuronal ultrastructure after SAH rats with CLB.

S100B, BUT NOT HMGB1, MEDIATES SUBARACHNOID HEMORRHAGE (SAH)-ASSOCIATED CEREBROVASCULAR DYSFUNCTION AND NEUROPATHOLOGY

H. Xu, C. Paisansathan, P. Polak, D.A. Pelligrino

Anesthesiology, University of Illinois at Chicago, Chicago, IL, USA

Objective: SAH accounts for nearly 25% of cerebrovascular deaths. Approximately 65 - 80 % of SAH patients either die or suffer severe disability. Although findings from multiple basic science studies and clinical trials related to SAH have been published, few clinically effective treatments have resulted. Our preliminary data revealed that enhanced activity of the receptor for advanced glycation end-products (RAGE) plays a key role in mediating SAH-related pial arteriolar (PA) dysfunction[1] and neuropathology. Besides S100B, High-Mobility Group Box-1 (HMGB1) protein, another important RAGE ligand, merits consideration[2]. This study was designed to test whether S100B and/or HMGB1 are involved in SAH-related neuropathology and PA dysfunction.

Methods: Rats were randomized into 7 groups: (A) sham surgical controls; (B) vehicle-treated (saline, ip) SAH rats; (C) vehicle (aCSF)-treated (icv, osmotic pump) SAH rats; (D) ONO-2506 (S100B-selective inhibitor)-treated (ip) SAH rats; (E) BoxA (selective HMGB1 blocker)-treated (icv) SAH rats; (F) Oxpapc (TLR2/4 blocker)-treated (icv) SAH-rats; and (G) soluble RAGE (sRAGE)-treated (icv) SAH rats. The SAH model involved suture perforation of the anterior cerebral artery. PA dilatory responses and neurobehavioral function were assessed 48h post-SAH. Neurological function evaluations included spontaneous activity, muscle tone, and neurologic reflex. The PA response, viewed through a closed cranial window, is presented as the % PA diameter changes in the presence of hypercapnia, sciatic nerve stimulation, and topically-applied vasodilators

(acetylcholine, adenosine, S-nitroso-N-acetyl penicillamine).

Results: Compared to sham rats, substantial suppression of the PA response and significant neurological deficits were seen in the 2 vehicle-treated groups. Rats treated with either S100B inhibitor (ONO-2506) or the RAGE blocker (sRAGE) displayed a marked improvement in neurological function and dramatic recovery in PA dilatory function. On the other hand, blocking of HMGB1 (via BoxA) or TLR (via Oxpapc), yielded no significant protective effect with respect to both neuropathology and PA dilating function.

Conclusion: SAH-associated cerebrovascular dilating dysfunction and neuropathology is largely mediated by enhanced RAGE activation, which is initiated via S100B-RAGE engagement. HMGB1, another key RAGE ligand, however, is not involved in SAH-related vasculopathy or neuropathology.

References:

(1) Britz GW, et al. Stroke (2007) 38:1329-1335.

(2) Ohnishi M, et al. Neuropharmacology (2011) 61:975-980.

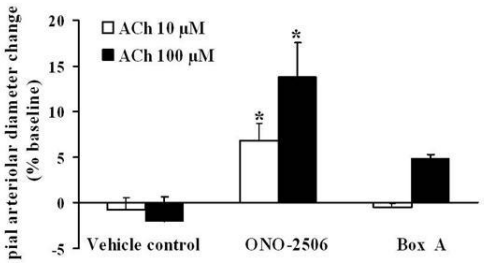

Fig1. Effect of ONO-2506 (S100B selective inhibitor) and Box A (HMGB1 selective blocker) on pial arteriolar response to acetylcholine (ACh) in rats subjected to SAH. Pial arteriolar dilation was assessed at 48 h post-SAH. *, p<0.05 vs vehicle control.

[Effect of ONO2506 or BoxA on ACh-induced dilation]

COMPARISON BETWEEN THE FORMULA 1/2ABC AND 2/3SH IN INTRACEREBRAL PARENCHYMA HEMORRHAGE

J. Yan[1], K. Zhao[2], J. Sun[3], W. Yang[1], Y. Qiu[4], T. Kleinig[5], Y. Fu[1], S. Chen[1]

[1]Department of Neurology & Institute of Neurology, Ruijin Hospital, Shanghai Jiaotong University School of Medicine, [2]Department of Neurosurgery, Changhai Hospital of Shanghai, [3]Department of Neurology, Gongli Hospital, [4]Shanghai Jiaotong University School of Public Health, Shanghai, China, [5]Royal Adelaide and Lyell McEwin Hospitals, University of Adelaide, Adelaide, SA, Australia

Objectives: The 1/2ABC formula is the method most commonly used in clinical practice to rapidly estimate Intracerebral Hemorrhage (ICH) volume. We aimed to compare this method with the alternative '2/3Sh' formula for both regularly and irregularly-shaped hematomas.

Methods: Computed Tomography (CT) images from 344 ICH patients (median volume 16.66mL) were retrospectively reviewed. According to the maximum slice, the shape was classified into regular or irregular (multilobular, conical and other). Volumes as determined by the 1/2ABC and 2/3Sh formulas were compared against the gold standard, computer-assisted planimetry, for various hematoma shapes.

Results: With the 1/2ABC method, errors were seen non-significantly more frequently for irregularly-shaped hematomas (OR 2.85 [95% CI 0.65-12.50]). The 1/2ABC method misclassified a greater proportion of hematomas as greater or less than 30mL in volume (7.0% [95% CI 6.0-9.9%] vs 1.2% [95% CI 0.4-3.2%]). Both the 1/2ABC and 2/3Sh formulas correlated well with gold standard (correlation coefficients >0.9 for each shape). While there was no statistically significant measurement error bias for either method, the 95% confidence intervals of the limit of agreement for 2/3Sh were tighter (-0.22mL [-4.7 to 4.25mL] vs 2.50mL [-10.35 to 15.34mL]). Measurement errors were significantly greater with the 1/2ABC method, for both regular and irregular hematomas (1.17mL [0.48-2.83mL] vs 0.88mL [0.42-1.68mL], and 2.65mL [1.07-5.88mL] vs 0.99mL [0.47-2.28mL]; P< 0.001, respectively), although the magnitude of error

would only rarely be clinically relevant for regular hematomas. Errors were most evident in assessing multilobular-shaped hematomas (6.49mL [3.35-13.98mL] vs 1.86mL [0.96-9.94mL]; P< 0.001).

Conclusions: The 2/3Sh formula leads to fewer clinically-relevant hematoma volume misclassifications than the 1/2ABC formula, and is particularly superior in estimating volumes of irregularly-shaped hematomas.

FINGOLIMOD REDUCES CEREBRAL LYMPHOCYTE INFILTRATION IN EXPERIMENTAL MODELS OF RODENT INTRACEREBRAL HEMORRHAGE

W. Rolland, T. Lekic, P. Krafft, Y. Hasegawa, O. Altay, R. Hartman, R. Ostrowski, A. Manaenko, J. Tang, **J. Zhang**

Loma Linda University School of Medicine, Loma Linda, CA, USA

Objectives: T-lymphocytes promote cerebral inflammation, thus aggravating neuronal injury after stroke (Yilmaz et al. 2006; Lo 2009; Shichita et al. 2009). Fingolimod, a sphingosine 1-phosphate receptor analog, prevents the egress of lymphocytes from primary and secondary lymphoid organs (Chiba 2005). Based on these findings, we hypothesized that fingolimod treatment would reduce the number of T-lymphocytes migrating into the brain, thereby ameliorating cerebral inflammation following experimental intracerebral hemorrhage (ICH).

Methods: We investigated the effects of fingolimod (1.0mg/kg, given IP) in two well-established mouse models of ICH, implementing intrastriatal infusions of either bacterial collagenase (cICH) or autologous blood (bICH). Furthermore, we tested the long-term neurological performance in a collagenase-induced rat model of ICH.

Results: Fingolimod, in contrast to vehicle administration alone, improved neurological functions and reduced brain edema at 24 and 72 hours following experimental ICH in CD-1 mice (n=103; p< 0.05). Significantly fewer lymphocytes were found in blood and brain samples of treated animals when compared to the vehicle group (p< 0.05). Moreover, fingolimod treatment significantly reduced the expression of intercellular adhesion molecule-1 (ICAM-1), interferon-gamma (INF-γ), and interleukin-17 (IL-17) in the mouse brain at 72 hours post-cICH (p< 0.05 compared to vehicle). Long-term neurocognitive performance and histopathological analysis were evaluated in Sprague-Dawley rats between 8 and 10 weeks post-cICH (n=28). Treated rats showed reduced spatial and motor learning deficits, along with significantly reduced brain atrophy and neuronal cell loss within the basal ganglia (p< 0.05 compared to vehicle).

Conclusions: We conclude that fingolimod treatment ameliorated cerebral inflammation, at least to some extent, by reducing the availability and subsequent brain infiltration of T-lymphocytes, which improved the short and long-term sequelae after experimental ICH in rodents.

References:

Chiba, K. (2005). "FTY720, a new class of immunomodulator, inhibits lymphocyte egress from secondary lymphoid tissues and thymus by agonistic activity at sphingosine 1-phosphate receptors." Pharmacol Ther 108(3): 308-319.

Lo, E. H. (2009). "T time in the brain." Nat Med 15(8): 844-846.

Shichita, T., Y. Sugiyama, et al. (2009). "Pivotal role of cerebral interleukin-17-producing gammadeltaT cells in the delayed phase of ischemic brain injury." Nat Med 15(8): 946-950.

Yilmaz, G., T. V. Arumugam, et al. (2006). "Role of T lymphocytes and interferon-gamma in ischemic stroke." Circulation 113(17): 2105-2112.

A STUDY OF CORRELATION BETWEEN HYPOPERFUSION OF THE LANGUAGE CENTER AND APHASIA IN PATIENTS WITH MOYAMOYA DISEASE

L. Duan

Department of Neurosurgery, 307 Hospital, PLA., Beijing, China

Background and purpose: Lingustic function is one of vulnerable aspects of moyamoya disease, which may have destructive effects on patients' communicative and daily life. Claimed in previous studies as well, those with aphasia have poor long-term functional outcome, reduced probability of returning to

work, and an increased mortality rate. However, few studies emerged concerning the aphasia caused by Moyamoya disease. It is more conducive to find possible problems , If we can discuss the aphasia in accordance with different types of cerebrovascular disease. Therefore, this paper investigates the relationship between hypoperfusion of the language center and aphasia in patients with Moyamoya disease ,using SPECT.

Materials and methods: Sixty unilingual Chinese-speaking patients with Moyamoya disease were classified aphasia with the Aphasia Battery of Chinese (ABC). Not only MRI was used to decide the pathological site but also the perfusion of language center was analysed by SPECT within 1 week after all patients'admission. All collected data was compared between aphasia and nonaphasia groups.

Results: It is difficult to find any significance between aphasia and nonaphasia groups regarding the age, gender, MMD type, and Suzuki stage; The types of aphasia and lesion locations do not always accord with the classical clinical-anatomic correlations as identified by MRI; Meanwhile, for SPECT image analysis, we discovered that the hypoperfusion of lesion appeared strikingly related to the aphasia group compared with the group without aphasia($p< 0.00$).

Conclusion: The worse decreased perfusion status, the probability of aphasia incidence becomes more in Moyamoya disease. As the possibility of languge center perfusion declines , consequently the possibility of aphasia increases. That is a potential mechanism of aphasia in MMD patients. Thus, our study suggests that taking policies to improve perfusion maybe a good intervention.

DYNAMIC MODELING OF LAYER SPECIFIC CORTICAL TEMPERATURE FOR QUANTITATIVE FMRI

A. Gaglianese[1,2], P. Herman[1], P. Pietrini[2], F. Hyder[1,3]

[1]Department of Diagnostic Radiology - Magnetic Resonance Research Center, Yale University School of Medicine, New Haven, CT, USA, [2]Laboratory of Clinical Biochemistry and Molecular Biology, University of Pisa, Pisa, Italy, [3]Department of Biomedical Engineering, School of Engineering and Applied Science, Yale University, New Haven, CT, USA

Objective: Alterations in blood flow (CBF) and oxygen consumption (CMR_{O2}) both at rest and during function lead to local changes in brain temperature and contribute to the BOLD effect. The goal of the present study was to derive a reliable model for temperature dynamics in cerebral cortex. If successful, we believe that by combining CBF mapping with arterial-spin labeling (ASL) and temperature mapping of water chemical shift, high-resolution CMR_{O2} maps can be obtained without the need for calibrated fMRI.

Methods: Multimodal measurements were acquired from Upper (U), Middle (M), Lower (L) layers of the S1FL cortex of adult male rats (n=40; Sprague-Dawley; 200-300g) under α-chloralose (~40 mg/kg/hr) during forepaw stimulation (0.3ms, 2mA, 3Hz fs, lasting 30s). BOLD images were acquired with gradient echo EPI sequence (25.6x25.6x2 mm, 64x64 in plane mapping) on a 11.7T scanner. Quantitative changes in CBV and CBF data were measured by a plasma-borne MRI contrast agent, arterial-spin labeling, and laser Doppler flowmetry [1]. Temperature was measured with a copper-constantan thermocouple wire. Finally, changes in CMR_{O2} were calculated with calibrated fMRI [2]. We defined the generalized Pennes heat equation on the columnar direction of the brain in terms of heat metabolism in the brain [3]. We modeled dynamic temperature changes by the heat transferred from blood flow and the heat due to the oxygen consumption [4-5]. We applied Newton's law of cooling for the upper boundary between tissue and air and Dirichlet condition of prescribed temperature for the lower boundary (brain core). Temperature solution $T(x,t)$ was obtained by finite element method.

Results: Measured and estimated layer-specific temperature profiles in time are shown in Figure 1. The model estimation was in agreement with measured values. Resting baseline temperature increased from the upper to the lower layer (+0.33 M and +0.41 L respect to U, respectively), while ΔT measured during activation decreased from upper to lower respectively (U + 0.09, M +0.06, L +0.02). Since the difference between arterial blood (constant across layer) and baseline temperature decreased from U to L, the cooling effect of heat by blood flow was enhanced and, consequently, the increase in temperature during activation decreased. Our

temperature changes are in agreement with literature values [4-5].

Conclusions: Combining multimodal measurements of CBF, BOLD signal and CMR_{02}, our model is able to predict temperature dynamic both during resting and functional activation. Our results suggests that high resolution CMR_{02} maps can be obtained through the combination of CBF and temperature mapping in vivo.

[1] Herman P. et Al., 2009a, JCBFM, vol. 29, pp. 19-24

[2] Hyder F. et Al., 2012, NeuroImage, vol. 62, n.2, pp. 985-994

[3] Pennes H.H. et Al., 1948, Journal of Appl Physiol, vol. 1,pp. 93-122

[4] Truebel H. K.F. et Al., 2006, JCBF, vol. 26, pp. 68-78.

[5] Collins C. M., 2004, J Appl Physiol, vol.97, pp. 2051-2055

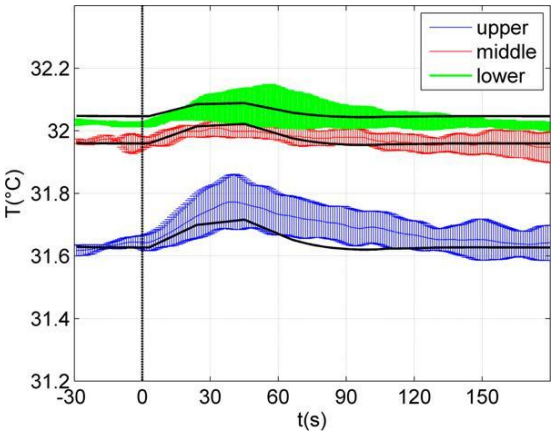

[Fig.1 : Temperature profile]

EFFECTS OF GLP-1 ON GLUCOSE TRANSPORT AND PHOSPHORYLATION CAPACITIES IN HUMAN BRAIN

M. Gejl[1], S. Lerche[1], L. Egefjord[1], J.J. Holst[2], B. Brock[1], N. Møller[3], J. Rungby[1], **A. Gjedde**[2]

[1]Aarhus University, Aarhus, [2]Copenhagen University, Copenhagen, [3]Aarhus University Hospital, Aarhus, Denmark

In hyperglycemia, glucagon-like-peptide-1 (GLP-1) lowers brain glucose concentration (C_{tissue}) together with increased net blood-brain clearance and brain metabolism, but it is not known whether this effect depends on the prevailing plasma glucose (PG) concentration. In hypoglycemia, glucose depletion potentially impairs brain function. Here, we test the hypothesis that moderate hypoglycemia eliminates the effect of GLP-1. To test the hypothesis, we determined glucose transport and consumption rates in seven healthy men in a randomized, double-blinded placebo-controlled cross-over experimental design. The acute effect of GLP-1 on glucose transfer in the brain was measured by positron emission tomography during a hypoglycemic clamp (3 mM PG) with ^{18}F-fluoro-2-deoxy-glucose as tracer of glucose. In addition, we jointly analyzed cerebrometabolic effects of GLP-1 from the present hypoglycemia study and our previous hyperglycemia study to estimate the Michaelis-Menten constants of glucose transport and metabolism. The GLP-1 treatment lowered the vascular volume of brain tissue. Loading data from hypo- to hyperglycemia into the Michalis-Menten equation, we found increased maximum phosphorylation velocity (V_{max}) in the grey matter (GM) regions of cerebral cortex, thalamus, and cerebellum, as well as increased blood-brain glucose transport capacity (T_{max}) in GM, white matter, cortex, thalamus, and cerebellum. In hypoglycemia, GLP-1 had no effects on net glucose metabolism, C_{tissue}, or blood-brain glucose transport. Neither hexokinase nor transporter affinities varied significantly with treatment in any region. We conclude that GLP-1 changes blood-brain glucose transfer and brain glucose metabolic rates in a PG concentration-dependent manner. One consequence is that hypoglycemia eliminates these effects of GLP-1 on brain glucose homeostasis.

GLUTAMATERGIC FUNCTION IN RESTING HUMAN BRAIN DEMANDS UNIFORMLY HIGH OXIDATIVE ENERGY

F. Hyder, R.K. Fulbright, R.G. Shulman, D.L. Rothman

Department of Diagnostic Radiology - MRRC, Yale University, New Haven, CT, USA

Introduction: Rodent ^{13}C MRS studies show that glutamatergic signaling requires high oxidative energy in the awake resting state **[1]** and allowed calibration of fMRI signal in terms of energy relative to the resting energy **[2]**. Here we derived energy used for

glutamatergic signaling in the awake resting human. The magnitude of neuronal signaling in the human brain, and by inference the commensurate energy demand, underscores the functional relevance of resting activity and has profound implications for interpreting fMRI experiments in humans. Given the rapidly increasing use of resting-state fMRI in mapping networks - defined as a subset of cortical and/or subcortical gray matter regions that function together - it is important to quantitatively establish if in the resting human the metabolic demand for neuronal signaling is high, as has been established for the rodent, and to what extent metabolic demand varies across gray matter regions.

Methods: We analyzed human data of EEG, PET maps of CMR_{O2} and glucose CMR_{glc} utilization, and calibrated fMRI from a variety of experimental conditions.

Results: CMR_{glc} and EEG in the visual cortex were tightly coupled over several conditions, showing that the oxidative demand for signaling was 4 times greater than the demand for non-signaling events in the awake state. Variations of CMR_{O2} and CMR_{glc} from gray matter regions and networks were within ±10% of means, suggesting that most areas required similar energy for ubiquitously high resting activity. Human calibrated fMRI results suggest that changes of fMRI signal in cognitive studies contribute at most ±10% CMR_{O2} changes from rest. PET data of sleep, vegetative state, and anesthesia show metabolic reductions from rest, uniformly >20% across, indicating no region is selectively reduced when consciousness is lost.

Discussion: These results demonstrate that oxidative demand for glutamatergic signaling in the resting human is globally high, whereas detectable cortical activity fluctuations in cognitive fMRI studies are small in comparison and the lowered global energy is correlated with overt behavioral changes. The use of small average metabolic differences across regions as evidence that some networks have greater functional importance than others (e.g., default mode network **[3]**) does not seem justified given the much larger underlying activity that all networks and regions share **[4]**. Our meta-analysis of cerebral energy consumption and its coupling with neuronal activity suggests that metabolic energy is quite uniform in gray matter space of the human brain. This conclusion does not make any claims about uniformity of cellular density because the measured metabolic data from PET are susceptible to partial volume effects arising from either white matter and/or varying cortical thickness.

Conclusion: Given the importance of ubiquitously high oxidative energy demand for supporting conscious human behavior, we propose that clinical fMRI studies could take advantage of quantitative measures of metabolic energy when evaluating patients.

References:

[1] Hyder F et al (2006) J Cereb Blood Flow Metab. 26:865-877.

[2] Hyder F et al (2010) Front Neuroenergetics. 2,pii:18.

[3] Vaishnavi SN et al (2010) PNAS USA. 107:17757-17762.

[4] Hyder F et al (2013) J Cereb Blood Flow Metab. (in press).

CONSERVED CORTICAL ENERGY DEMANDS OF SIGNALING AND NON-SIGNALING COMPONENTS ACROSS ACTIVITY LEVELS IN MAMMALIAN BRAIN

F. Hyder[1,2], D.L. Rothman[1,2], M.R. Bennett[3]

[1]Department of Diagnostic Radiology - MRRC, [2]Biomedical Engineering, Yale University, New Haven, CT, USA, [3]Brain and Mind Research Institute, University of Sidney, Sidney, NSW, Australia

Introduction: The continuous need for ion gradient restoration across the cell membrane, a prerequisite for cortical signaling, is believed to be a major factor for brain's high oxidative demand **[1,2]**. But do energy requirements of signaling and non-signaling components of cortical neurons and astrocytes vary with activity levels and across species? **[3]**

Objective: We derived oxidative ATP demand associated with signaling (P_s) and non-signaling (P_{ns}) components in the cerebral cortex using species-specific physiologic and anatomic data.

Methods: Briefly, the measured neuronal activity data were used to calculate glucose oxidation and then compared with measured glucose oxidation to determine values of P_s and P_{ns}. In rat's cerebral cortex, we calculated

glucose oxidation rates from layer-specific neuronal activity measured across different states, spanning from isoelectricity to awake and sensory stimulation. We then compared these calculated glucose oxidation rates with measured glucose metabolic data for the same states as reported by 2-deoxy-glucose autoradiography. We then calculated glucose oxidation rates from human electroencephalogram data acquired under various conditions using fixed P_s and P_{ns} values derived for the rat.

Results: Table 1 compares the results of this study **[3]** with results from other studies **[1,2]**. First, we found that single values for P_s and P_{ns} were able to predict the entire range of states in the rat. Second, the calculated metabolic data in human cerebral cortex compared well with glucose metabolism measured by positron emission tomography. Independent of species, linear relationship was established between neuronal activity and neuronal oxidative demand beyond isoelectricity (**Figure 1**).

Table 1	**η_N**	**η_A**	**$R_{in,N}$**	**$R_{in,A}$**	**$P_{ns,N}$**	**$P_{ns,A}$**	**P_s**
This study (rat) [1]	4.75	4.75	74	74	9.20	6.85	4.81
This study (human) [1]	1.83	1.83	74	74	9.20	6.85	4.81
Ref [2] (rat)	9.2	9.2	200	500	3.42	1.02	0.71
Ref [3] (human)	4.0	3.8	79	163	8.6	3.1	2.4

Average values of cortical density of neurons (η_N, $\times 10^7$ neuron/cm^3) and astrocytes (η_A, $\times 10^7$ neuron/cm^3)densities, input resistances of neurons ($R_{in,N}$, MΩ) and astrocytes ($R_{in,A}$, MΩ), rate of ATP use for non-signaling per neuron ($P_{ns,N}$, $\times 10^8$ ATP/neuron/s) and astrocyte ($P_{ns,A}$, $\times 10^8$ ATP/astrocyte/s), and ATP use per signaling event per neuron (P_s, $\times 10^9$ ATP/spike/neuron)

[Table 1]

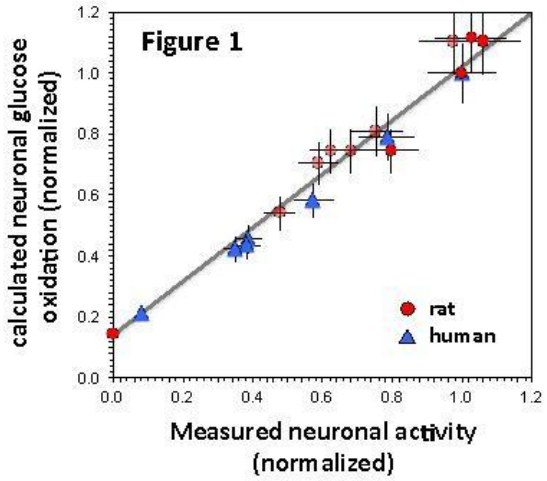

[Figure 1]

Discussion: Cortical signaling requirements dominated energy consumption in the awake state, whereas the non-signaling requirements were ~20% of awake resting value. These predictions are supported by recent ^{13}C magnetic resonance spectroscopy results.

Conclusion: We conclude that energy demands of signaling and non-signaling components in cerebral cortex are conserved across activity levels in mammalian species. A constant inter-species ATP demand of cortical activity emphasizes the relevance of animal testing in experimental neuroscience studies.

References:

[1] Attwell D, Laughlin SB (2001) J Cereb Blood Flow Metab. 21:1133-1145.

[2] Lennie P (2003) Curr Biol. 13:493-497.

[3] Hyder F, Rothman DL, Bennett MW (2013) PNAS USA. (in press).

SCALING OF BRAIN METABOLISM AND HEMODYNAMICS IN RELATION TO CAPILLARY SCALING

J. Karbowski[1,2]

[1]IBIB Polish Academy of Sciences, [2]University of Warsaw, Warsaw, Poland

Introduction: Brain is one of the most energy demanding organs in mammals, and its total metabolic rate scales with brain volume raised

to a power of around 5/6. This value is significantly higher than the more common exponent 3/4 relating whole body resting metabolism with body mass and several other physiological variables in animals and plants.

Aim: This study investigates the reasons for brain allometric distinction on a level of its microvessels.

Results: Based on collected empirical data of mammalian species it is found that regional cerebral blood flow CBF across gray matter scales with cortical volume V with an exponent -1/6, brain capillary diameter scales with V with an exponent 1/12, and density of capillary length decreases with V with an exponent -1/6. It is predicted that velocity of capillary blood is almost invariant, capillary transit time scales with exponent 1/6, capillary length increases with V with power 1/6+epsilon, and capillary number with power 2/3-epsilon, where epsilon is typically a small correction for medium and large brains, due to blood viscosity dependence on capillary radius. It is shown that the amount of capillary length and blood flow per cortical neuron are essentially conserved across mammals.

Conclusions: These results indicate that geometry and dynamics of global neuro-vascular coupling have a proportionate character. Moreover, cerebral metabolic, hemodynamic, and microvascular variables scale with allometric exponents that are simple multiples of 1/6, rather than 1/4, which suggests that brain metabolism is more similar to the metabolism of aerobic than resting body. Relation of these findings to brain functional imaging studies involving the link between cerebral metabolism and blood flow is also discussed.

References:

1) Karbowski J (2007). Global and regional brain metabolic scaling and its functional consequences. BMC Biology 5: 18.

http://dx.doi.org/10.1186/1741-7007-5-18

2) Karbowski J (2011). Scaling of brain metabolism and blood flow in relation to capillary and neural scaling. PLoS ONE 6(10): e26709.
http://dx.doi.org/10.1371/journal.pone.0026709

CEREBRAL BLOOD FLOW RESPONSE OF INTRAVENOUS ADENOSINE INFUSION

J.M. Lynch[1], E. Buckley[2], P. Schwab[3], M. Feldman[4], M. Harris[5], D.J. Licht[3], A.G. Yodh[1]

[1]Department of Physics & Astronomy, University of Pennsylvania, Philadelphia, PA, [2]Department of Radiology, Massachusetts General Hospital, Boston, MA, [3]Department of Neurology, The Children's Hospital of Philadelphia, Philadelphia, PA, [4]University of Rochester School of Medicine, Rochester, NY, [5]Department of Cardiology, The Children's Hospital of Philadelphia, Philadelphia, PA, USA

Intravenously administered adenosine is well-known to have vasodilatory effects on the coronary arteries, but its cerebral effects are poorly understood. To address this knowledge gap, we employ diffuse correlation spectroscopy (DCS) to quantify cerebral blood flow (CBF) changes during a six-minute adenosine infusion in a pediatric population (N=17) undergoing a clinical cardiac stress test. DCS employs the temporal fluctuations of scattered near-infrared light to rapidly (~3 seconds) monitor tissue blood flow. Here, the relative changes in CBF (rCBF) due to adenosine administration are quantified by comparing a two-minute average prior to the infusion with a two-minute average at the end of the infusion period. The rCBF response due to adenosine is observed to be dependent on the anesthetized state of the subject. Figure 1 shows a boxplot of changes in rCBF for the subjects that were awake during the adenosine administration (N=12) and for those that were under general anesthesia (N=9) (sevoflurane). We find significant ($p < 0.01$) difference between the CBF responses of these two groups. These results take first steps towards elucidating the effects of adenosine on the cerebral vasculature, particularly whether variables, such as general anesthetics, can affect its action.

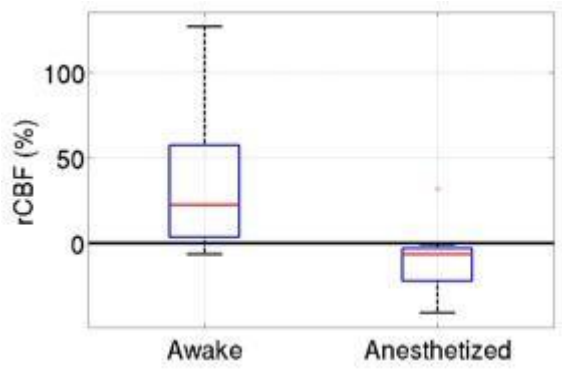

[

Figure 1. Changes in CBF due to intravenously administered adenosine in subjects that were awake and fully anesthetized during the administration. The red line represents the median CBF response of each group. The edges of the box represent the 25^{th} and 75^{th} percentiles. The whiskers extend to the most extreme non-outlier data points, and the outliers are plotted individually.

COMPARISON OF NITRIC OXIDE PRODUCTION BETWEEN ANGIOTENSIN II TYPE 1A RECEPTOR KNOCKOUT MICE AND TYPE 2 RECEPTOR KNOCKOUT MICE

R. Nishioka, M. Yamazato, Y. Ito, A. Miyake, M. Hirayama, K. Ishizawa, M. Sawada, Y. Asano, N. Araki

Department of Neurology, Saitama Medical University, Saitama, Japan

Introduction: Nitric oxide (NO) and angiotensin II play an important role in the regulation of cerebral blood vessels. Pretreatment with angiotensin II type 1 receptor antagonists protects against cerebral ischemia. Moreover, a significant correlation was found between brain NO synthase and AT1 receptor mRNAs. Meanwhile, it is well known that angiotensin II type 2 receptor increases expression under the condition of brain infarction. Therefore, we examined the generation of NO metabolites during global ischemia and reperfusion in angiotensin II type 1a receptor knockout mice and in angiotensin II type 2 receptor knockout mice using an *in vivo* microdialysis technique.

Methods: Male angiotensin II type 1a receptor knockout mouse (AT1a-KO group, n=8), angiotensin II type 2 receptor knockout mouse (AT2-KO group, n=5) and wild type C57BL/6 (n=6: used as a control group) were anesthetized with 0.5-1% halothane. A microdialysis probe was inserted into left striatum and perfused with Ringer's solution at a constant rate of 2 ml/min. After 2 hours equilibrium period, fractions were collected every 10 minutes. A laser Doppler probe was placed on the right skull surface. Global ischemia was produced by clipping both common carotid arteries for 10 minutes using Zen clips. The levels of nitrite (NO_2^-) and nitrate (NO_3^-) in the dialysate samples were measured by the Griess reaction.Animals (AT1a-KO group (n=3), AT2-KO group (n=7), wild type C57BL/6 (n=6)) were euthanized to get pathological findings 72 hours after 10 minutes global ischemia under same anesthesia condition. The brains were removed and stained by Hematoxyline-Eosin staining. Ischemic findings of hippocampus CA1 area were described by counting survival cells/(survival cells +dead cells) rate.

Results:

(1) Blood Pressure: Mean arterial blood pressure (MABP) in AT1a-KO (50±8.0 mmHg, mean±SD) was significantly lower than that of controls (71±8.0 mmHg). MABP in AT2-KO (82.1±10.4 mmHg, mean±SD) was significantly higher than that of controls.

(2) CBF: Cerebral blood flow decreased to 11.7±10.3 % in AT1a-KO group, 11.3±11.5 % in AT2-KO group and 15.9±11.0 % in control group during ischemia. After reperfusion, cerebral blood flow transiently returned to baseline values and then decreased significantly in all group. There were no significant differences among the three groups.

(3) NO Metabolites: No significant differences were observed in NO_2^- levels in the dialysate among the three groups. Baseline NO_3^- levels in the dialysate in AT1a-KO group (1.09±0.14 mmol/L) was significantly lower than that of the control group (1.61±0.61) ($p< 0.05$). After reperfusion (between 30 minutes and 60 minutes after the start of reperfusion), NO_3^- levels in the dialysate in AT1a-KO group were significantly lower than those of control group. No significant differences were observed in NO_3^- levels in the dialysate between AT2-KO group and control group.

(4) Hippocampus CA1 area cell counts : There were no significant differences among the AT1a-KO group (63.9±6.3%), AT2-KO group (67.3±9.8%) and control group (63.4±23.9%) in the number of survival cells in the hippocampus CA1 area.

Conclusion: These data suggest that angiotensin II may be related to nitric oxide metabolism not only in baseline but also in ischemia/reperfusion.

EFFECT OF NON-STEROIDAL ANTI-INFLAMMATORY DRUG CELECOXIB ON CEREBRAL GLUCOSE METABOLISM IN RAT BRAIN SLICES AS MEASURED BY DPAT

T. Asai[1,2], S. Fukumoto[1,2], W. Wang[1], **H. Okazawa**[1]

[1]Biomedical Imaging Research Center, University of Fukui, Eiheiji-cho, [2]Department of Nuclear Power and Energy Safety Engineering, University of Fukui, Fukui, Japan

Background: Celecoxib (CXB) is a non-steroidal anti-inflammatory drug (NSAID) that specifically inhibits cyclooxygenase 2 and thus is used widely as a drug with less gastric side effects. The use of aspirin, a nonselective NSAID, was once associated with acute brain dysfunctions in children [1]. Recent studies indicate that NSAIDs including CXB increase intracellular Ca^{2+} concentration and cause apoptosis in various tumor cells. We have examined whether CXB has any effect on the cerebral metabolic rate of glucose in rat brain slices by measuring [^{18}F]FDG uptake using dynamic positron autoradiography technique.

Methods: Sagittal brain slices (300-µm thickness) were prepared from Wistar rats (6-7 weeks old). The slices were incubated in a chamber with the bottom made from polyvinylidene chloride film that was penetrable to positron of ^{18}F. The chambers were filled with oxygenated Krebs-Ringer solution kept at 36°C, and 100 kBq/mL of [^{18}F]FDG was added at the start of recording. Sequential images of [^{18}F]FDG uptake were obtained every 15 min by replacing imaging plates (BAS-MS2040, Fuji Photo Film, Tokyo, Japan). The imaging plate was scanned with an image analyzer (FLA-7000, Fuji Photo Film, Tokyo, Japan) to measure radioactivity signals on the imaging plate from the frontal cortical region of the slices. The relative uptake value of [^{18}F]FDG which was an index of cerebral metabolic rate of glucose was calculated by dividing the radioactivity signal from the frontal cortex by that from the external solution.

Results: Application of CXB (10-100 µM) increased [^{18}F]FDG uptake rate gradually with time over 2 hours and the degree of the CXB-induced increase was concentration dependent (Figure 1). Addition of membrane-permeable Ca^{2+} chelator BABTA-AM (50 µM) caused a slight decrease in [^{18}F]FDG uptake rate and inhibited the effect of CXB. On the other hand, removal of Ca^{2+} from the external solution did not suppress the CXB-induced increase in [^{18}F]FDG uptake rate.

Conclusion: CXB caused an increase in the brain glucose metabolism by elevating the intracellular Ca^{2+} concentration that were most likely released from the internal Ca^{2+} stores such as endoplasmic reticulum and/or mitochondria.

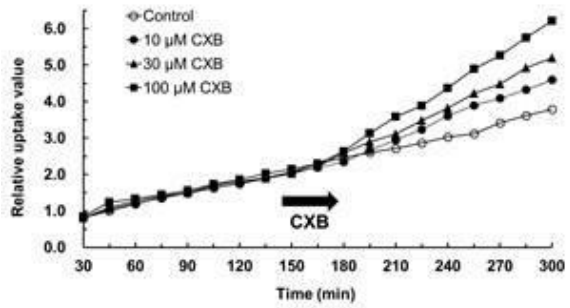

[Figure 1]

Figure legend: Application of CXB at 150 min increased [^{18}F]FDG uptake rate in a concentration-dependent manner.

References:

[1] Bhutta AT, et al.,; *Southern Med J* **96**: 43-45 (2003)

CIGARETTE SMOKING SIGNIFICANTLY ALTERS WHOLE BRAIN CEREBRAL BLOOD FLOW AND OXYGEN CONSUMPTION

M.S. Vafaee[1], P. Cumming[2], N. Imamirad[3], K. Vang[4], A. Gjedde[1]

[1]Dept. of Neuroscience and Pharmacology, University of Copenhagen, Copenhagen, Denmark, [2]Dept. of Nuclear Medicine, Maximillian University, Munich, Germany, [3]Dept. of Lung Medicine, Aarhus Univeristy Hospital, [4]PET Center, Aarhus University Hospital, Aarhus, Denmark

Introduction: Tobacco is the most widely abused substance, and overwhelming evidence links the abuse to the nicotine content of tobacco (Wayne et al., 2006). However, it remains uncertain whether

cerebrometabolic effects of smoking can be attributed to the psychopharmacological properties of nicotine. To understand the effects of smoking on brain metabolism, we studied smokers who resumed smoking after overnight abstention. We predicted that effects of renewed smoking would include transient changes of cerebral blood flow (CBF) in a network of cortical regions revealed by previous positron emission tomography (PET) studies (Zubieta et al., 2005), as well as increased cerebral oxygen consumption ($CMRO_2$) in brain regions rich with nicotinic receptors.

Methods and results: To test the predictions, we acquired paired PET maps of baseline values of CBF and $CMRO_2$ from 14 smokers and again at intervals during the first 90 minutes after smoking. At 15 and 60, and 105 minutes post-smoking, the global values of CBF and $CMRO_2$ in grey matter rose significantly with a linear trend as time progressed. The resting state values of aged-matched non-smokers significantly exceeded the baseline CBF and $CMRO_2$ values of the smokers, which in turn rose post-smoking and reached the baseline values of the non-smokers. In contrast, the numerical values of CBF and $CMRO_2$ were lower or higher after smoking than before in several cortical and subcortical regions. However, the numerical decreases or increases did not reach to a statistical significance level and spatial pattern of rising $CMRO_2$ values after smoking did not match the known distribution of nicotinic receptors in human brain.

Conclusion: The findings imply that smokers stimulate otherwise their depressed values of CBF and $CMRO_2$ by means of tobacco use.

References:

1. Wayne GF, Connolly GN, Henningfield JE. (2006) Assessing internal tobacco industry knowledge of the neurobiology of tobacco dependence. Nicotine Tob Res. 6(6):927-40. Review.

2. Zubieta JK, Heitzeg MM, Xu Y, Koeppe RA, Ni L, Guthrie S, Domino EF. (2005) Regional cerebral blood flow responses to smoking in tobacco smokers after overnight abstinence. Am J Psychiatry. 162(3):567-77.

TIME TO INCLUDE THE NITRATE TO NO PATHWAY IN CEREBROVASCULAR PHYSIOLOGY

R. Aamand[1], T. Dalsgaard[2], Y.-C. Lynn Ho[1], A. Møller[1,3], A. Roepstorff[4], T.E. Lund[1]

[1]Department of Clinical Medicine, Aarhus University, Aarhus C, [2]Department of Biomedicine, Cardiovascular and Pulmonary Pharmacology, Aarhus University, Aarhus, [3]PET Center, Aarhus University Hospital, [4]Institute of Culture and Society, Aarhus University, Aarhus C, Denmark

Objectives: Nitrate has for a long time been considered to be a toxic compound with deleterious effects on human health. However the last 20 years of research has shown that nitrate, via its enzymatic conversion to nitrite and nitric oxide (NO), has a positive role to play in mammalian physiology as well. E.g. dietary nitrate lowers blood pressure (Larsen et al 2006), protects against ischemia/reperfusion injury (Bryan et al 2007), is vasoprotective and lowers platelet adhesion (Webb et al 2008), and increases mitochondrial oxygen efficiency (Larsen et al 2011).

In neurovascular coupling the only producer of NO has been believed to be NO synthases that produce NO from L-Arginine. Contrary to this view a recent study has indicated that NO from nitrite can act as a source of NO in rats if the NO synthases are blocked pharmacologically (Piknova et al 2011).

In light of this therapeutic effect of nitrite, we wanted to study if dietary nitrate had an inherent physiological effect on the cerebrovascular response to visual stimulation in young healthy human volunteers.

Methods: To study this, we increased and decreased the nitrate intake in two groups of healthy human volunteers in a crossover design (n=18). Our measure of cerebrovascular response to visual stimulation was the BOLD response measured in an MR scanner.

Results: We observed significant nitrate-induced decreases in the BOLD amplitude (7.9 +/- 4 %), the hemodynamic lag to peak amplitude (7.0 +/- 2 %), and in the voxelwise variation in both measures (15.3 +/- 7 % and 12.3 +/- 4 % respectively). (Results are provide as mean +/- SEM).

Conclusions: This strongly indicates that dietary nitrate is of importance when cerebral

vessels responds to neuronal processing and suggest that dietary nitrate could be an important secondary entry point for NO production in the brain.

References:

Bryan NS, Calvert JW, Elrod JW, Gundewar S, Ji SY, Lefer DJ (2007) Dietary nitrite supplementation protects against myocardial ischemia-reperfusion injury. Proceedings of the National Academy of Sciences 104:19144-9

Larsen FJ, Ekblom B, Sahlin K, Lundberg JO, Weitzberg E (2006) Effects of dietary nitrate on blood pressure in healthy volunteers. N Engl J Med 355:2792-3

Larsen FJ, Schiffer TA, Borniquel S, Sahlin K, Ekblom B, Lundberg JO, Weitzberg E (2011) Dietary Inorganic Nitrate Improves Mitochondrial Efficiency in Humans. Cell Metabolism 13:149-59

Piknova B, Kocharyan A, Schechter AN, Silva AC (2011) The role of nitrite in neurovascular coupling. Brain Res 1407:62-8

Webb AJ, Patel N, Loukogeorgakis S, Okorie M, Aboud Z, Misra S, Rashid R, Miall P, Deanfield J, Benjamin N, MacAllister R, Hobbs AJ, Ahluwalia A (2008) Acute blood pressure lowering, vasoprotective, and antiplatelet properties of dietary nitrate via bioconversion to nitrite. Hypertension 51:784-90

QUANTIFICATION OF COLLATERAL FLOW DYNAMICS BY DOPPLER OCT FOLLOWING STROKE IN A MOUSE MODEL OF TYPE 2 DIABETES

Y. Akamatsu[1], C.C. Lee[1], L. Shi[2], R. Wang[2], **J. Liu**[1]

[1]Neurological Surgery, UCSF and SFVAMC, San Francisco, CA, [2]Bioengineering & Ophthalmology, University of Washington, Seattle, WA, USA

Introduction: As a major vascular risk factor, type 2 diabetes mellitus (T2DM) worsens the outcome of stroke. During acute flow obstruction, some parts of the brain tissue suffer from ischemia while others are sustained by collateral flow through pre-existing adjacent collateral arteries. It is unclear whether T2DM associated-poor outcome after stroke is related to unfavorable collateral flow recruitment, although increased collateral vessels were previously reported in the rat model of T2DM. The current study sought to determine the effect of T2DM on collateral blood flow dynamics and stroke outcome.

Method: Adult male db/db and db/+ mice (12-16 weeks of age) were subjected to temporary distal middle cerebral artery occlusion (tMCAo). Hemodynamics was evaluated by laser doppler flowmetry. In vivo imaging of blood flow and flow velocity was performed with Doppler optical coherence tomography (DOCT). Motor function impairment was assessed by sticky-tape removal and horizontal ladder tests at one week after stroke. The numbers of connecting collateral vessels were quantified by DiI-labeling and infarct volume determined using H&E stained sections.

Results: On average db/db mice displayed lower rCBF in the core of the MCA territory at 24 hours after MCAO compared to db/+ mice. db/db mice also had a larger infarct volume, correlated with worse neurological outcomes compared to db/+ mice. Data with DOCT suggest that during occlusion of the MCA, db/+ mice showed more robust retrograde filling of several distal branches of the MCA from ACA than db/db mice. However, we did not observe a significant difference in the number of connecting collateral arteries between groups in this age group.

Conclusion: Our results demonstrate that T2DM is associated with impaired collateral flow recruitment between the MCA and ACA vascular networks, resulting in reduced rCBF during the acute phase of tMCAo, which might in part, contribute to the worse outcome observed in the db/db mice. Ongoing experiments will investigate whether there is an age-related decline in collateral flow recruitment or the number of connecting collateral vessels between MCA and other vascular networks in the T2DM mice.

MAPPING REGIONAL RATE OF CHANGE IN CBF IN RESPONSE TO CHANGES IN PACO2: A COMBINED MR-ASL AND PHASE-CONTRAST STUDY

N. Alperin, A. Bagci

University of Miami, Miami, FL, USA

Introduction: Limited information is available regarding how different regions in the brain response to global change in arterial blood flow. Invasive studies in patients during anesthesia demonstrated differences in the degree of auto regulation between the anterior and posterior circulation [1]. A practical noninvasive protocol for assessment of regional CBF response to global change in PaCO2 may provide a more direct means for assessing regional blood flow autoregulation and regional cerebral vulnerability. The proposed protocol utilizes whole brain Pulsed Arterial Spin Labeling (PASL) and phase contrast MRI in conjunction with 3D-T1W anatomical scan to assess mean CBF in selected anatomical regions. Phase contrast MRI (PCMR) measurements of total arterial inflow (tCBF) are used to quantify the subject's response to change in PaCO2. Therefore, this approach is noninvasive as it eliminates the need to measure PaCO2. Manipulation of the tCBF over a wide range is obtained by manipulating the end tidal pCO_2 level with the application of continuous positive airways pressure.

Methods: Five healthy subjects (ages 24 to 39 years) underwent MRI scans using 3T (Verio, Siemens Healthcare). Scans were repeated at 3 physiological states: rest, moderate (6mmHg) and high (12 mmHg) continuous positive airway pressures. End tidal pCO_2 level ranged from 45 to 20 mmHg. CBF in a normal subject is reduced by 3% per mmHg. Total cerebral blood flow (tCBF) from PCMR was obtained by summation of the arterial inflow through the two internal carotids and vertebral arteries [2]. In addition, regional mean CBF (perfusion values in mL/min/100gm) were calculated separately for the following regions: cerebral GM and WM, thalamus, Palladium, hippocampus, putamen and the amygdala. The brain masks for the selected brain regions were obtained using FreeSurfer.

Results: Fig. 1 demonstrates the relationship between ASL-derived whole brain CBF and the PC tCBF values from all 5 subjects (each subject is shown in different colors). A strong linear correlation with R value of 0.94 demonstrates the reliability of PCMR based tCBF measurement as a surrogate measure for the change in PaCO2. Regional CBF regulation is estimated by the slope of the mean regional ASL derived CBF vs. the global blood flow, i.e., tCBF. The steeper the slope the less is the degree of flow regulation. Mean slopes ranged from 0.075 (vulnerable) to 0.001 (protected) regions.

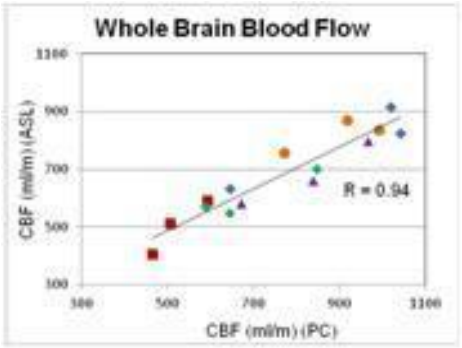

[Whole Brain ASL Blood Flow vs. tCBF by PC]

Conclusions: Large differences in CBF response to changes in PaCO2 were found across different brain regions. For example, a significantly larger mean slope (0.075) was found for the thalamus compared with the putamen (0.023). This difference can be attributed to the fact that the thalamus is supplied by the vertebrobasilar arterial system which is part of posterior circulation, which has less sympathetic innervations compared with the anterior circulation. The putamen is supplied by branches of the middle cerebral arteries, which is part of the anterior blood supplies.

References:

[1] Rozet I et al, Anesth Analg 2006;102:560 - 4.

[2] Alperin NJ and Lee SH, Magn Reson Med 2003;49:934-944.

CEREBROVASCULAR DYSFUNCTION IN NEWBORNS WITH HYPOXIC ISCHEMIC ENCEPHALOPATHY (HIE): CAN "NON-RESPONDERS" BE IDENTIFIED DURING THERAPEUTIC HYPOTHERMIA (TH)?

L. Chalak[1], P. Sanchez[1], R. Zhang[2]

[1]Pediatrics, [2]Neurology, UT Southwestern Medical Center, Dallas, TX, USA

Background: The relationship between cerebrovascular dysfunction, electrical activity and brain injury has been understudied in newborns with HIE receiving systemic hypothermia therapy.

Objectives: To

1) determine whether increasing severity of encephalopathy (mild, moderate, and severe) is associated with increasing alterations in cerebral near infrared spectroscopy (NIRS) and amplitude integrated EEG (aEEG), and

2) determine whether alterations in NIRS and aEEG are predictive of abnormal outcomes in newborns with HIE undergoing hypothermia therapy.

Methodology: All infants in this prospective cohort study (6/2010-6/2011) had aEEG and NIRS continuous monitoring between 12-78 hours after birth. Staging of HIE (mild, moderate [mod[or severe [sev]) was based on exam at < 6 hours of age. NIRS measures were cerebral oxygen saturation (rO_2)and fractional O2 extraction (FTOE).

aEEG background was categorized by visual inspection as normal or abnormal (burst suppression, low voltage, flat), and ANALYZE software was used to calculate voltage, percent discontinuity and the presence of cycles (SWC). The entire NIRS and aEEG recordings were analyzed to derive a representative value. The primary outcome was any Bayley III cognitive, language or motor score < 70 assessed at 12-18 months of age for infants with moderate or severe HIE.

Results: Enrolled infants (n=30) had a gestational age of 39±2 wks, were inborn, 75% Hispanic and all survived. Ten infants with mild HIE did not receive TH and served as a reference; all had a normal aEEG with SWC throughout and a median rO_2 of 76% (interquartile range, IQR 73-79). Infants with mod (n=17) or sev (n=3) HIE received TH, had an abnormal aEEG in 5 (25%), and delayed appearance of SWC to > 72hrs in 6(30%).aEEG border voltages differed between mild, mod and sev HIE, respectively: lower border (8±1 vs. 7±1, vs. 5±1mcv, p=0.01) upper border (19±4 vs. 15±3, vs. 11±2mcv, p=0.006) and % discontinuity in tracing (0.5%±1 in mild, 9%±15 in mod vs. 52%±10 in sev HIE, p=0.01). Median rO_2 for mod and sev HIE was 81, IQR (73-85) and was similar between stage. Of the 4 (15%) infants with abnormal outcome (3 mod, 1 sev), 3 had delayed SWC and discontinuous aEEG, and 3 had hyperemic rO2 (median 94%, IQR 84, 95).

Conclusions: Increasing severity of HIE stage at is associated with progressive aEEG abnormalities over 78hrs but without parallel rO_2 changes.

The significance of increased cerebral rO2 in a subset of infants with abnormal outcome require further study as it could represent manifestations of secondary energy failure with hyperemic cerebral oxygen saturation (rO_2) and depressed electrocortical activity.

References:

1.Zhang R, Zuckerman JH, Giller CA, Levine BD. Transfer function analysis of dynamic cerebral autoregulation in humans. Am J Physiol. Jan 1998;274(1 Pt 2):H233-241.

2. Chalak LF, Rouse DJ. Neuroprotective approaches: before and after delivery. Clin Perinatol. Sep 2011;38(3):455-470.

NEURAL OVER-EXPRESSION OF ACE2 DECREASES MCAO-INDUCED CEREBRAL INJURY PARTIALLY THROUGH BP-INDEPENDENT MECHANISMS

J. Chen[1], S. Chen[1], J. Wang[1], C. Zhang[1], X. Xiao[1], W. Zhang[1], B. Zhao[2], Y. Chen[1]

[1]Pharmacology/Toxicology, Wright State University, Dayton, OH, USA, [2]Clinical Research Center and Department of Neurology, The Affiliated Hospital of Guangdong Medical College, Zhanjiang, China

Objectives: The angiotensin converting enzyme 2 (ACE2) converts angiotensin II (Ang II) into Ang (1-7). Accumulating evidence suggest that the ACE2/Ang (1-7)/Mas signaling pathway counteracts the effect of

ACE/Ang II/AT1 axis in many aspects. In this study, we investigated the role of ACE2 in counteracting the effect of Ang II/AT1on ischemic damage as well as the blood pressure (BP)-independent mechanisms.

Methods: Transgenic mice over-expressing human rennin and angiotensinogen (R+A+) and over-expressing ACE2 in neurons in R+A+ mice (R+A+ACE2+) were used for the study. There were three groups (n=6/group): R+A+ACE2+ control, R+A+ACE2+ "clamping" and R+A+. A radiotelemetric probe was implanted to record BP for analysis of mean arterial pressure (MAP). Chronic infusion of noreadrenine (NE, 5.6 mg/kg/day, minipump) was used to "clamp" the BP in R+A+ACE2+ mice to the same level as that in R+A+ mice within 5 days. In "clamping" control group, mice were infused with normal saline solution. After 7 days recovery, mice were subjected to middle cerebral artery occlusion (MCAO) surgery for induction of focal ischemic stroke. The cerebral blood flow (CBF) was recorded immediately before and after MCAO using laser Doppler flowmetry. Mice were sacrificed at 48 hrs after MCAO surgery. Animals were perfused with 4% paraformaldehyde to obtain fixed brain samples for histology analysis. Ischemic damage was determined by staining brain slides with Fluoro-J. In the parallel experiments, fresh brain samples were collected for isolating blood vessel and vessel-depleted brain parenchyma fractions. The levels of Ang II and Ang (1-7) in the fractions and plasma were determined by using ELISA assays.

Results: We found that

1) After "clamping", the MAP in R+A+ACE2+ mice significantly increased by about 14 mmHg (from 121 ± 3 mmHg to 135 ± 7 mmHg, $P< 0.05$) to a similar level (135 ± 9 mmHg, $P>0.05$) of R+A+ mice.

2) As expected, the MCAO-induced infarct volume in R+A+ACE2+ mice was less than in R+A+ mice. The infarct volume in R+A+ACE2+ "clamping" group was more than that in R+A+ACE2+ control group (17.2 ± 0.5% and 15.3 ± 0.6%, $P< 0.05$), but was less than that in R+A+ group (21.5 ± 1.0%, $P< 0.05$).

3) The CBF in the peri-infarct area of R+A+ACE2+ mice were more than that in R+A+ mice. The level of CBF in R+A+ACE2+ "clamping" group was less than in R+A+ACE2+ control group (48.5 ± 2% and 51.3 ± 3%, $P< 0.05$), but was more than that in R+A+ group (40.5 ± 2%, $P< 0.05$).

4) ELISA data (Table 1) showed that the Ang II level was lower while the Ang (1-7) level was higher in the brain parenchyma fraction of R+A+ACE2+ mice than that of R+A+ mice.

Table 1. Ang II/Ang (1-7) balance in R+A+ and R+A+ACE2+ mouse

	R+A+	R+A+ACE2+
Plasma (pg/ml)		
Ang II	225±43	209±41
Ang (1-7)	128±33	107±33
Ang II/Ang (1-7)	1.75±0.26	1.95±0.24
Brain parenchyma (fmol/mg)		
Ang II	110±22	89±15**
Ang (1-7)	79±20	110±28**
Ang II/Ang (1-7)	1.32±0.10	0.81±0.10**
Cerebral vessel (fmol/mg)		
Ang II	58±15	55±16
Ang (1-7)	40±11	42±18
Ang II/Ang (1-7)	1.45±0.10	1.22±0.11

**$P<0.01$, *vs.* R+A+; Data are mean ± SEM, n=6/group.

[Table 1]

Conclusions: Neural ACE2 over-expression prevents the brain from ischemic injury by changing the balance of Ang II/Ang (1-7) in control of local CBF which is partially independent of BP.

WAVELET CROSS-CORRELATION ANALYSIS ON RELATIONSHIP BETWEEN CEREBRAL OXYHAEMOGLOBIN AND ARTERIAL BLOOD PRESSURE

R. Cui, W. Li, W. Zhou, L. Lu, Q. Han, Y. Gao, Z. Li

Shandong University, Jinan City, China

Background and aims: Five characteristic frequencies related to the activities of metabolic (0.008-0.02Hz), neurogenic (0.02-0.06Hz), myogenic (0.06-0.15Hz), respiratory (0.15-0.4Hz) and cardiac (0.4-2.0Hz) of cerebral oxyhaemoglobin (O_2Hb) as measured

with near-infrared spectroscopy (NIRS) and mean arterial blood (MAB) pressure signals were extracted using wavelet transform. The relationship between O_2Hb and MAB need to be analyzed using an effective method.

Material and methods: The relationship between cerebral oxyhaemoglobin and arterial blood pressure was studied using the method of wavelet cross-correlation (WCC). The signals of O_2Hb and MAB of 45 volunteers were collected to be analyzed. The signals of MAB whose sampling frequency is 100Hz are resampled to 10Hz which is the sampling frequency of O_2Hb.

Results: High synchronization with high common power existing between O_2Hb and MAB was found in each frequency between two signals from the results. Average angle of the phase angle of the cross-wavelet power in time series of each frequency appears to be close to 1, which supposes to mean high synchronization rate.

Conclusion: The wavelet cross-correlation provides a useful approach to analyze the relationship between the signals of NIRS O_2Hb and MAB.

References:

A. Grinsted, J.C. Moore and S. Jevrejeva : Application of the cross wavelet transform and wavelet coherence to geophysical time series Nonlinear Process. Geophys. Vol. 11(2004), p. 561-6.

A.B. Rowley, S.J. Payne: Synchronization between arterial blood pressure and cerebral oxyhaemoglobin concentration investigated by wavelet cross-correlation. Physiol. Meas. Vol. 28(2007), p. 161-173.

A. Stefanovsk, M. Bracic, H. D. Kvernmo: Wavelet analysis of oscillations in the peripheral blood circulation measured by laser Doppler techni que. IEEE Trans. Biomed. Vol. 46 (1999), p. 1230-1239.

ABBREVIATED TITLE: 20-HETE SYNTHESIS EXPLAINS REDUCED CBF AFTER CSD

J. Fordsmann[1], R. Koh[2], H.B. Choi[2], K.J. Thomsen[1], B.M. Witgen[1], C. Mathiesen[1], M. Lønstrup[1], H. Piilgaard[1], B. Macvicar[2], **M. Lauritzen**[1]

[1]University of Copenhagen, Copenhagen, Denmark, [2]Brain Research Centre, Vancouver, BC, Canada

Cortical spreading depression (CSD) is associated with release of arachidonic acid (AA), impaired neurovascular coupling, and reduced cerebral blood flow (CBF), caused by cortical vasoconstriction. We tested the hypothesis that the released AA is metabolized by the cytochrome P450 enzyme to produce the vasoconstrictor 20-hydroxyeicosatetraenoic acid (20-HETE), and that this mechanism explains cortical vasoconstriction and vascular dysfunction after CSD. CSD was induced in the frontal cortex of rats and the cortical electrical activity and local field potentials (LFPs) recorded by glass microelectrodes, CBF by laser Doppler flowmetry, and tissue oxygen tension (tpO2) using polarographic microelectrodes. 20-HETE synthesis was measured in parallel experiments in cortical brain slices exposed to CSD. We used the specific inhibitor HET0016 (N-hydroxy-N'-(4-n-butyl-2-methylphenyl)formamidine) to block 20-HETE synthesis. CSD increased 20-HETE synthesis in brain slices for 120 min, and the time course of the increase in 20-HETE paralleled the reduction in CBF after CSD in vivo. HET0016 blocked the CSD-induced increase in 20-HETE synthesis and ameliorated the persistent reduction in CBF, but not the impaired neurovascular coupling after CSD. These findings suggest that CSD-induced increments in 20-HETE cause the reduction in CBF after CSD, and that the attenuation of stimulation-induced CBF responses after CSD has a different mechanism. We suggest that blockade of 20-HETE synthesis may be clinically relevant to ameliorate reduced CBF in patients with migraine and acute brain cortex injuries.

RETROGRADE DIASTOLIC BLOOD FLOW IN THE MIDDLE CEREBRAL ARTERIES DURING NEUROCARDIOGENIC SYNCOPE

A. Gergont, M. Kacinski, A. Biedron

Chair of Children and Adolescents Neurology, Jagiellonian University, Krakow, Poland

Case report:

Objectives: Neurally mediated syncope is one of the most common paroxysmal events and the head-up tilt table test has become a widely accepted tool in the clinical evaluation of patients presenting with syncopal symptoms. Numerous published reports provide a substantial base of experience supporting the diagnostic utility of the monitoring of the blood flow in the middle cerebral arteries during tilting. The common change detected during syncope was the preferential decrease in diastolic velocity in the middle cerebral artery. We will present unusual data of diastolic retrograde blood flow in the middle cerebral arteries recorded during neutrally mediated syncope.

Methods: The passive head upright tilt table test with cerebrovascular Doppler monitoring added to standard blood pressure and heart rate measurements was performed in a-16-year old boy with recurrent syncopes. Epilepsy was excluded as well as disorders of cardiac muscle. The tilting at the angle 70^{o} was performed with continuous monitoring of peak systolic and end diastolic velocities in the middle cerebral arteries using Nicolet Companion III with special tool to stabilize a device (2 MHz).

Results: Normal results of cerebrovascular Doppler examination were recorded before tilting. Presyncope accompanied by arterial hypotension and bradycardia occurred after 10 minutes of tilting. Transcranial Doppler monitoring revealed the progressive decrease in the diastolic velocity in the middle cerebral arteries, however systolic blood flow velocities did not decrease. The short retrograde blood flow during early diastole occurred before neurally mediated syncope. The reactive increase in velocities of the blood flow was recorded in the lying position after test termination.

Conclusions: The diastolic retrograde flow in the middle cerebral arteries during the neutrally mediated syncope reflects the critical decrease in cerebral blood flow. The complex nature of syncope makes it imperative that continued research into the pathophysiology is performed with examination of cerebral circulation.

References:

1. Albina G., Cisneros LF., Laino R., et al.: Transcranial Doppler monitoring during head upright tilt table testing in patients with suspected neurocardiogenic syncope. Europace 2004, 6, 63-9.

2. Dan D., Hoag JB., Ellenbogen KA., et al.: Cerebral blood flow velocity declines before arterial pressure in patients with orthostatic vasovagal presyncope. J Am Cardiol 2002, 20, 1039-45.

3. Eberhardt H., Foelsing R., Herterich R., Letzqus A.: Value of transcranial Doppler sonography during tilt table test in children. Ultrashall Med 2002, 23, 379-82.

4. Sung RY., Du ZD., Yu CW., et al.: Cerebral blood flow during vasovagal syncope induced by active standing or head up tilt. Arch Dis Child 2000, 82, 154-8.

DYNAMIC CEREBRAL BLOOD FLOW MEASUREMENTS DISTINGUISH UPSTREAM BLOOD SUPPLY FROM LOCAL MICROVASCULAR TONE

R. Graf[1], M. Takagaki[2], H. Backes[1], M. Gramer[1], **D. Feuerstein**[1]

[1]MPI for Neurological Research, Cologne, Germany, [2]Osaka University Graduate School of Medicine, Osaka, Japan

Objectives: Regional cerebral blood flow (rCBF) is the product of upstream blood supply and local microvascular tone. While rCBF can be directly measured it is difficult to distinguish between upstream blood supply, which represents the maximum available amount of blood that can be delivered to the tissue, and microvascular tone, which distributes blood supply locally so as to adjust rCBF to local energy needs. Since diseases can affect each of these two factors, diagnostics and treatment could benefit from discriminating between the two.

Here, we monitored rCBF at high time resolution, using Laser Speckle Imaging (LSI)

experimentally and Laser Doppler Flowmetry (LDF) clinically. We measured the rCBF changes in response to cortical spreading depression (CSD), a high-energy demanding event that occurs in physiopathological conditions, such as migraine (1) and brain injury (2). We first developed a method that could discriminate between local microvascular tone and upstream blood supply in controlled experiments. We then applied this method to predict tissue conditions dynamically in cases of experimental ischemic stroke and in two patients suffering from acute brain injury.

Methods: LSI was performed through thinned skull in 15 male Wistar rats. In group 1 (n=5), we modified the microvascular tone by changing anesthesia regimens from isoflurane (a vasodilator) to propofol. In group 2 (n=5), we modified the blood supply to the brain by consecutively ligating the left and right common carotid arteries under isoflurane. In each condition of basal rCBF levels, we induced cortical spreading depression (CSD) by a needle prick and measured the rCBF response for 60 minutes. In group 3 (n=5), we induced focal ischemic stroke by occlusion of the middle cerebral artery (3). We observed spontaneous rCBF waves that propagated around the ischemic insult during 3 hours after occlusion.

We monitored two patients requiring an emergency craniotomy after traumatic brain injury or sub-arachnoid hemorrhage. We recorded electrocorticography and rCBF from a subdural strip implanted over the peri-infarct tissue for electrocorticography or LDF recordings. CSDs were identified by their ECoG signature (4). rCBF changes recorded by LDF in close temporal vicinity to the identified CSDs were characterised.

Results: The rCBF responses to induced CSDs were identical under altered basal local vascular tones (group 1), while the responses were strongly affected by the basal conditions of upstream blood supply (group 2). In particular, the increase in blood flow per unit of time in response to CSD, which we refer to as the hyperemic slope, was linearly correlated to the upstream blood supply. We found, both experimentally (group 3) and clinically, that the hyperemic slope correlated well with electrophysiological activity, whereas perfusion levels did not.

Conclusions: We conclude that assessing tissue conditions purely based on perfusion may be misleading. Instead, markers for upstream blood supply, such as the hyperemic slope associated with cortical spreading depression, may be of better clinical value.

References:

1. Lauritzen, *Brain*, 1994

2. Dohmen *et al.*, *Annals of Neurology*, 2008.

3. Kumagai *et al.*, *JCBFM*, 2010.

4. Fabricius *et al.*, *Brain*, 2006.

STATE-DEPENDENT RESTING-STATE COHERENCE BETWEEN NEURAL ACTIVITY AND BLOOD FLOW

P. Herman[1], R.N.S. Sachdev[2,3], Y. Yu[2,4], B.G. Sanganahalli[1], H. Blumenfeld[2,5], D.A. McCormick[2,3], **F. Hyder**[1,6]

[1]Department of Diagnostic Radiology, [2]Department of Neurobiology, [3]Kavli Center of Neuroscience, Yale University, New Haven, CT, USA, [4]Centre for Computational Systems Biology, Fudan University, Shanghai, China, [5]Department of Neurology, [6]Biomedical Engineering, Yale University, New Haven, CT, USA

Introduction: Central hypothesis of functional neuroimaging is that task-induced increased neural activity triggers hemodynamic responses [1,2]. Certain, but weak correlations between components (e.g. frequency range) of resting neural activities and fluctuations of spontaneous hemodynamic signals (BOLD, CBF, or CBV) were shown [3,4,5]. We proposed a non-linear convolution approach to prove the validity of neurovascular coupling in resting state. Using convolution to model the neurovascular coupling we found that there was very strong dependence between neural and hemodynamic signals, even when linear correlation methods were not feasible. We examined the relationship between neocortical spontaneous activity and concurrently measured local blood flow in awake and anesthetized rodents.

Methods: We used anesthetized Sprague-Dawley rats (α-chloralose and medetomidine in separate groups). For awake state we used black cbl57 mice. Tungsten microelectrodes together with a micro laser-Doppler probe (200 μm in diameter) were inserted up to layer 4 (~1mm depth) with stereotaxic manipulators in

the somatosensory region (S1). Individual spiking events were extracted from multi-unit activities (MUA). 300s long segments were selected for analysis. Spiking events were used as input signals for convolution analysis, while the LDF signals were considered as output. We defined transfer functions as a modified gamma variate functions (GVF) [6]. We systematically changed the parameters of GVF to create series of transfer function (n=80000) to find where correlation of simulated and measured LDF signals is the highest.

Results: The GVF had three parameters: the constant amplitude (A=1), the peak time (t_p) and the exponential decay parameter (α). t_p and α were significantly different in awake than in anesthetized states ($p< 0.002$) and showed difference between anesthetic states ($p< 0.06$). The parameters of the averaged transfer functions were t_p=4.77s, α=5.4 for α-chloralose anesthesia, t_p=3.83s, α=9.5 for medetomidine anesthesia and t_p=3.1s, α=20, for awake animals. Using these parameters, the state dependent transfer functions created simulated LDF signals which were highly correlated (r>0.5) to the measured signal (Figure).

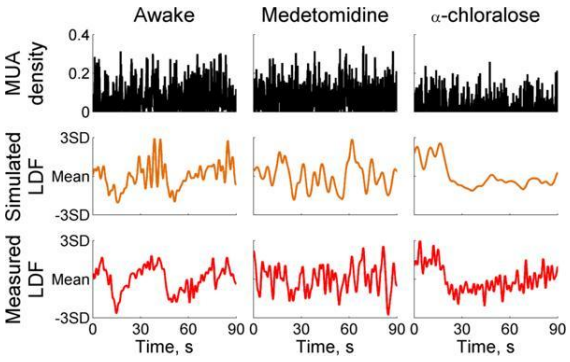

[Figure]

Discussion: Resting neural activities and CBF signals were linearly correlated only if the neurovascular transfer function was fast and narrow. The fastest and narrowest neurovascular connection was in awake state. The slower transfer function of anesthetized states could completely eliminate the linear correlation between neural and vascular signals, while the nonlinear correlation remained the same as in awake state. In summary, depth of anesthesia attenuated not only the intensities of neurovascular signals, but the dynamic of their coupling as well.

References:

[1] Sanganahalli et al. (2009) *J Neurosci* 29:1707-1718

[2] Herman et al. (2009) *J Neurochem* 109:73-79

[3] Shmuel and Leopold (2008) *Hum Brain Mapp* 29:751-761

[4] Schölvinck et al. (2010) *PNAS* 107:10238-10243

[5] Liu et al. (2011) *Cereb Cortex* 21:374-384

[6] Madsen (1992) *Phys Med Biol* 37:1597-1600

Acknowledgement: Supported by NIH (R01 MH-067528, P30 NS-52519) and the The Kavli Institute for Neuroscience.

CEREBRAL ARTERIAL PULSATION DRIVES PARAVASCULAR CEREBROSPINAL FLUID-INTERSTITIAL FLUID EXCHANGE

J. Iliff[1], M. Wang[2], M. Nedergaard[3]

[1]Department of Anesthesiology and Peri-Operative Medicine, Oregon Health & Science University, Portland, OR, USA, [2]Department of Neurology, Tongji Hospital of Tongji University, Wuhan, China, [3]Center for Translational Neuromedicine, University of Rochester Medical Center, Rochester, NY, USA

The clearance of waste from the interstitial space is a basic aspect of organ function, and in the brain is critical for the maintenance of optimal extracellular environment and neural function. Many neurodegenerative diseases, such as Alzheimer's disease, are characterized by the failure of interstitial solute clearance and the resulting deposition of neurotoxic aggregates. We recently described a brain-wide paravascular pathway along which subarachnoid cerebrospinal fluid (CSF) exchanges with brain interstitial fluid (ISF), facilitating the clearance of interstitial solutes such as amyloid β. CSF entered the brain parenchyma primarily via paravascular channels surrounding penetrating cerebral arteries, while ISF was cleared from the brain primarily along paravascular spaces surrounding large draining veins. Because

CSF influx was so strongly polarized to para-arterial pathways, in this study we tested the hypothesis that arterial pulsation is a key driver of paravascular CSF-ISF exchange. Using in vivo 2-photon imaging, we measured vascular wall pulsation at all levels of the cerebral surface and parenchymal vasculature. We observed that unilateral internal carotid artery ligation reduced vascular wall pulsation in penetrating cerebral arteries by 48%. When CSF-ISF exchange was quantified 30 min after intracisternal fluorescent CSF tracer injection, unilateral internal carotid artery ligation reduced CSF influx by 20%. Conversely, when the β_1 adrenergic agonist was administered systemically, the pulsation of cerebral arterial walls increased by 115% while CSF influx increased 19%. These data suggest that cerebral arterial pulsation is one factor contributing to the paravascular exchange of CSF and ISF. One implication of these findings that in the aging or diseased brain, reduced cerebral arterial wall compliance may contribute to the failure of interstitial waste clearance and potentially to the onset and progression of neurodegenerative disorders such as Alzheimer's disease.

RELATION BETWEEN HEART RATE VARIABILITY AND NITRIC OXIDE TO CEREBRAL AUTOREGULATION DURING BREATH HOLDING INDUCED-HYPERCAPNIA IN HEALTHY SUBJECTS

K. Intharakham[1], K. Suwanpraser[2]

[1]Medical Engineering Program, [2]Division of Physiology, Department of Preclinical Science, Faculty of Medicine, Thammasat University, Patumtani, Thailand

Objectives: Impaired cerebral autoregulation and endothelial dysfunctions leading to reduced cerebral reserve function are thought to play an important role in small artery ischemic stroke. In this study, we investigated the relation between endothelial dysfunction through circulating nitric oxide (NO) and autonomic modulation by heart rate variability (HRV) to cerebral autoregulation during breath holding induced-hypercapnia.

Methods: 16 healthy volunteers (5 men, 11 women, age 27.33 $\pm$3.85) were recruited. All healthy subjects gave informed consent according to the Declaration of Medicine Ethic Committee (MTU-EC-PH-6-076/55). 30 sec breath holding induced-hypercapnia experiment was carried out as before experiment (basal phase) and during experiment (during phase). Mean cerebral blood flow velocity (mCBFV) by transcranial Doppler, The one minute HRV analysis by lead II ECG recording and plasma NO by real time electrochemistry measurement were performed. Sympatho-vagal balance and potential modulation of parasympathetic control were examined in term of LF/HF ratio and Sample Entropy (SampEn), respectively.

Results: Values of mean arterial pressure between basal and during breath holding phases are closely. Plasma NO level, mCBFV and LF/HF ratio were increased significantly during breath holding when compared to basal phase ($p< 0.05$). Good correlation among NO, mCBFV, LF/HF ratio and SampEn was showed (table).

Characteristics (mean ±SD)	**Healthy (n=16)**			
Age:	27.33 ± 3.85			
Pearson´s Correlation Coefficient (r)	**Basal**		**During**	
	mCBFV	NO	mCBFV	NO
mCBFV:	-	0.38	-	-
NO:	-	-	0.91	-
LF/HF ratio:	-0.40	-0.12	0.49	0.56
SampEn:	0.20	0.42	0.82	0.42

[Pearson's Correlation Coefficient (r)]

Conclusions: This finding suggests that NO play a crucial role in cerebral autoregulation and autonomic modulation in healthy subject and indicates the normal cerebral reserve function.

Acknowledgement: This work was supported by National Research University Project of Thailand Office of Higher Education Commission and faculty of medicine, Thammasat University.

References:

1. Salahuddin L, Cho J, Jeong MG, Kim D. Ultra short term analysis of heart rate variability for monitoring mental stress in mobile settings. Conf Proc IEEE Eng Med Biol Soc. 2007;2007:4656-9.

2. Lavi S, Egbarya R, Lavi R, Jacob G. Role of nitric oxide in the regulation of cerebral blood flow in humans: chemoregulation versus mechanoregulation. Circulation. 2003 Apr 15;107(14):1901-5.

3. Julian F.R. Paton SKaDJP. Nitric oxide and autonomic control of heart rate: a question of specificity. TRENDS in Neurosciences 2002 Dec;25(12): 626-631.

CORTICAL SPREADING DEPRESSION EVOKED CHANGES IN OXYGEN CONSUMPTION AND CEREBRAL BLOOD FLOW IN NMRI AND C57BL6/J MICE

L. Khennouf, B. Gesslein, M. Lauritzen

Neuroscience and Pharmacology, Copenhagen University, Copenhagen, Denmark

Cortical spreading depression (CSD) is a transient slow propagating depolarization wave of cortical neurons and glial cells. CSD may induce a brief period of anoxia during return to normal of the ionic gradients, which causes no harm in the normal brain, but in the damaged brain with compromised blood supply and energy metabolism CSD may expand ischemic lesions. Previous study of CSD in mice has suggested that the first episode induces a strong vasoconstriction that limits the supply of oxygen and glucose in the recovery phase. In this study we sought to reproduce these findings by examination of electrical function, cerebral blood flow (CBF) and cerebral metabolic rate of oxygen ($CMRO_2$) during and after CSD in NMRI and C57bl6/j mice.

CSD was evoked by pressure injection of potassium acetate (1 M) into the posterior part of the somatosensory cortex. Propagation was monitored by a glass microelectrode that recorded electrocorticographic (ECoG) activity, while CBF was monitored by using a laser-Doppler probe and tissue oxygen tension by using a Clark type microelectrode about 4 mm from elicitation point. In addition, to monitor the putative elicitation of a CSD during craniotomies we recorded CBF with laser-Doppler techniques via an optic fiber glued to the skull. The oxygen consumption ($CMRO_2$) was calculated from corresponding values of CBF and tpO_2. Neurovascular coupling before and after CSD was evaluated following whisker pad stimulation and concurrent recordings of local field potentials, CBF and tPO_2.

CSD in NMRI (n=5) and C57bl6/j (n=5) mice triggered a rise in CBF at the same time as the tpO_2 dropped to null. CBF first increased by 113±4%, in most cases it was followed by a vasoconstriction of 48±13%, then it increased again of 252±57%. These phases took 1-2 minutes to develop and varied slightly between mice. Whether the initial vasoconstriction occurred or not was independent of the mouse strain (tested on NMRI and C57bl6/j), of the brain region (tested on the frontal lobe and the parietal lobe), of the blood flow measurement technique (either on top of the skull with an optic fiber or directly on top of the cortex) and more, it was independent of the CSD order (it was seen for the first CSD as well as for the second CSD). Subsequently, CBF was reduced by 19±6% of baseline in both mouse strains for 45-60 mins, and in both strains the $CMRO_2$ was elevated indicating a high demand for oxygen and a great turnover of ATP. We noticed that repeated CSD waves triggered a pronounced reduction of CBF (35±15%) that lasted for 2 hours (n=4). Another effect of the CSD was the impairment of neurovascular coupling. After a CSD the CBF responses were significantly lower than in normal conditions (p=0.034 in C57bl6/j and p=0.041 in NMRI).

These results provides insight into the vascular reactions to CSD in mice by providing evidence for a sequence of CBF changes that are reminiscent of what has been observed in rats.

ENDOTHELIAL DYSFUNCTION IN HYPERTENSIVE RATS HAMPERS THE EFFECT OF G-CSF ON PIAL ARTERIOGENESIS

K. Kitagawa, Y. Sugiyama, Y. Yagita, T. Yukami, N. Oyama, T. Sasaki, H. Mochizuki

Department of Neurology, Osaka University, Suita, Japan

Objectives: Pial collateral development, arteriogenesis, plays an important role on attenuating infarct size after middle cerebral artery occlusion (MCAO). Previously, we have demonstrated that

(1) chronic hypoperfusion by unilateral common carotid artery occlusion (CCAO)

induces development of pial collateral circulation[1-3], and

(2) treatment with granulocyte colony stimulating factor (G-CSF) enhances arteriogenesis through recruitment of circulating mononuclear cells in normal mice[4]. However, activation of endothelial cells by fluid shear stress is the first step on arteriogenesis.

In fact, endothelial dysfunction often underlies the etiology of human ischemic stroke. Thus the purpose of this study is to examine the effect of G-CSF on pial arteriogenesis in spontaneously hypertensive rats (SHR), that showed endothelial dysfunction of the brain.

Methods: Adult male Wistar rats (aged 7-10 weeks, n=30) and SHR (aged 10-11 weeks, n=30) were obtained from Charles River, Inc. Both rats received left CCA occlusion or sham surgery. In the first experiment, the level of phosphorylation of endothelial nitric oxide synthase (eNOS), a marker of endothelial function, was measured using the normal cerebral cortex samples with immunoblotting. The level of total eNOS was used as control. In the second experiment, G-CSF (100 mg/kg/day) or vehicle was administered after left CCA occlusion for five days. Rats with sham-operation received only vehicle. Seven days after CCA occlusion or sham surgery (N=5, each group), latex compound mixed with carbon black was injected through left ventricle to visualize the leptomeningeal anastomoses. The vessel diameter was measured at the point where the distal MCA joined the distal anterior or posterior cerebral artery. Other rats (N=5, each group) were perfused transcardially with 4% paraformaldehyde and the brains were fixed in the same solution. To examine the accumulation of monocyte/macrophages around the borderzone leptomeningeal arteries, immunostaining was performed using CD68 antibody. In the control WKY and SHR (n=10, each group), blood was obtained after G-CSF (n=5, each group) or vehicle (n=5, each group) administration for 5 days, and absolute blood monocyte, granulocyte, and lymphocyte counts were calculated.

Results: The level of eNOS phosphorylation was significantly lower in the brain sample of SHR than in Wistar rats. In both Wistar rats and SHR, treatment with G-CSF increased the number of circulating monocytes about four times. In both rat groups, treatment with vehicle did not enlarge the diameter of anastomosis vessel 7 days after CCA occlusion. In Wistar rats, G-CSF treatment enhanced accumulation of CD68-positive cells in the leptomeningeal arteries and promoted collateral growth after CCA occlusion, but in SHR G-CSF did not show any effect on accumulation of CD68-positive cells or vessel diameter of leptomeningeal anastomosis.

Conclusions: G-CSF enhanced arteriogenesis in chronic brain hypoperfusion in normal rats. However, the effect of G-CSF on arteriogenesis diminished in SHR. Our findings suggested that preservation of endothelial function is crucial for enhancement of pial arteriogenesis by G-CSF.

References:

1. Kitagawa K et al., *Stroke*, 2005:36: 2270-2274.

2. Todo K et al., Stroke, 2008:39:1875-1882.

3. Omura-Matsuoka E et al., J Neurosci Res, 2011:89: 108-116.

4. Sugiyama Y et al., *Stroke*, 2011, 42:770-5

POSTNATAL DEVELOPMENT OF NEUROVASCULAR COUPLING AT A CELLULAR AND MICROVASCULAR LEVEL

M.G. Kozberg[1], L.E. Grosberg[2], E.M.C. Hillman[2]

[1]Neurobiology and Behavior, [2]Biomedical Engineering, Columbia University, New York, NY, USA

Objectives: Localized changes in brain blood flow are the basis of signals measured using functional magnetic resonance imaging (fMRI). In adults, this 'hemodynamic response' consists of an increase in blood delivery to activated regions in response to somatosensory stimulation. However, prior work from our laboratory in a rodent model demonstrates that the neonatal hemodynamic response may be inverted with respect to the adult response, consisting of early oxygen consumption and delayed decreases in local blood flow caused by arterial constriction. This response then matures via a gradual development of a blood delivery phase, eventually masking oxygen consumption and balancing arterial constriction.

Although the adult hemodynamic response has been well-characterized, the precise

cellular mechanisms involved have yet to be defined. An understanding of these mechanisms could provide valuable insights into conditions with a suspected neurovascular basis, including age-related neurodegeneration and Alzheimer's disease. Our observation that stimulus-evoked hyperemia increases gradually with age provides a framework with which to explore the corresponding changes in vascular and cellular morphology that correlate with the ability of the cortex to induce blood flow increases. The development of neurovascular coupling may include

1) the maturation of the vasculature and perivascular cellular populations, and

2) establishment of signaling within the vascular endothelium.

The goal of this study is to identify components of the neurovascular unit that contribute to the post-natal development of the hemodynamic response to stimulation.

Methods: This study used neonatal rat pups, focusing on two younger age groups:

1) postnatal day 12 to 13, assumed to be equivalent in age to human newborns, and

2) postnatal day 15 to 18. These age groups exhibited fully inverted and bi-phasic hemodynamic responses to stimulus respectively in our prior work. Results from these age groups were compared to adult controls (P80+).

High-speed, high-resolution optical imaging was used to determine the developmental stage of each rat's hemodynamic response. In-vivo two-photon microscopy was then used in the same animals to explore the vascular and cellular correlates of the changing hemodynamic response. Novel volumetric and multi-plane techniques were also used to investigate the depth-dependent onset dynamics of vasodilation in the cortex as a function of age.

Results and conclusions: Preliminary results demonstrate that the vascular morphology of the neonatal brain is strikingly different from that of the adult. Additionally, functional data obtained with optical imaging and in-vivo two-photon microscopy suggest that the developing initial hyperemia phase of the hemodynamic response is localized to the capillary beds and diving arterioles of the cortex before developing the ability to recruit upstream pial arteries. In comparison, in adults we have observed strong pial arterial dilations. We will present the results of our continued analysis.

BOLD FMRI OF CEREBROVASCULAR RESERVE IN PATIENTS WITH SEVERE ARTERIAL STENOSIS: A LATERALITY INDEX APPROACH

A. Krainik[1,2], A. Attye[1,2], O. Detante[2,3], F. Tahon[1], I. Troprès[4], L. Lamalle[4], J. Pietras[4], J.-L. Magne[5], J.-F. Le Bas[1,2,4]

[1]Neuroradiology and MRI, University Hospital of Grenoble, [2]Grenoble Institute of Neurosciences, [3]Neurology, University Hospital of Grenoble, [4]IRMaGe, University Joseph Fourier, [5]Vascular Surgery, University Hospital of Grenoble, Grenoble, France

Background and aims: Functional MRI of cerebrovascular reserve (CVR fMRI) using vasoreactivity to hypercapnia may identify patients at risk of hemodynamical stroke among those with severe arterial stenosis. Because absolute quantification remains challenging, we aimed to propose a laterality index to better identify abnormal CVR in clinical practice.

Patients and methods: 18 patients (5 females; 60.6±16.4years) with severe arterial stenosis of the right (n=9) or left (n=9) internal carotid (ICA) (n=9) or middle cerebral artery (MCA) (n=9) were examined using BOLD CVR fMRI with a block-design hypercapnic challenge (CO2 7%) at 3T. Averaged end-tidal CO2 pressure (EtCO2) was used as a physiological regressor for statistical analyses with a general linear model (SPM8). We conducted regions of interest (ROI) measures of %BOLD signal change/mmHg EtCO2 on segmented gray matter of the middle cerebral arteries (MCA) territories. We calculated a laterality index with LI_{MCA}=(Left_CVR_{MCA}-Right_ CVR_{MCA})/(Left_ CVR_{MCA} +Right_ CVR_{MCA}). Basal perfusion was assessed using dynamic susceptibility contrast to estimate cerebral blood flow (CBF) and volume (CBV), and mean transit time (MTT).

CVR fMRI data obtained in patients were compared to those of 100 volunteers (40 females; 49.5±21.4 years) without cervico-encephalic arterial stenosis.

Results: No adverse reaction to hypercapnia was detected during and after CVR fMRI.

In controls, CVR values ranged from 0.14 to 0.48 with m±sd=0.26±0.07 %BOLD/mmHg EtCO2. The mean laterality index (LI) was 0.01 with an interval of fluctuation that covered 0.00. The standard deviation was 0.026. Thus, 99% confidence interval of LI was ±0.07. LI values were independent of age.

In patients, CVR values ranged from 0.01 to 0.36 with m±sd=0.21±0.08. Among these 18 patients, 9 patients with ICA (n=4) or MCA stenosis (n=5) had a normal $|LI_{MCA}|< 0.08$ ranging from 0.03 to 0.07 (0.04±0.01), and 9 patients with ICA (n=5) or MCA stenosis (n=4) had an abnormal $|LI_{MCA}| \geq 0.08$ ranging from 0.08 to 0.91 (0.28±0.27). All abnormal LI values identified the MCA territory ipsilateral to the stenosis. CVR values and LI were not correlated to basal perfusion parameters. Both figures depict patients with severe left MCA stenosis (arrow) revealed by stroke. Figure 1 shows an additional poststenotic aneurysm. Basal CBF were normal out of the stroke sequellae. Figure 1 shows a normal CVR whereas Figure 2 shows a significant CVR impairment in the left MCA territory.

Conclusions: Subjects without cervico-encephalic arterial stenosis have an absolute value of LI_{MCA} below 0.08 with a 99% probability. Among patients with severe stenosis of ICA or MCA, half of the patients had an abnormal $|LI_{MCA}|$ in the territory ipsilateral to the stenotic artery. In pathological conditions, the absence of correlation between CVR and basal perfusion also suggests that significant CVR impairment might be an independent predictor of the risk of hemodynamic stroke. Thus, CVR fMRI may help to better define the treatment strategy, including intravascular stenting.

References:

Markus and Cullinane Brain 2001;124:457-467

Mazighi et al. Neurology 2006;66:1187-1191

Mandell et al. Stroke 2008; 39:2021-2028

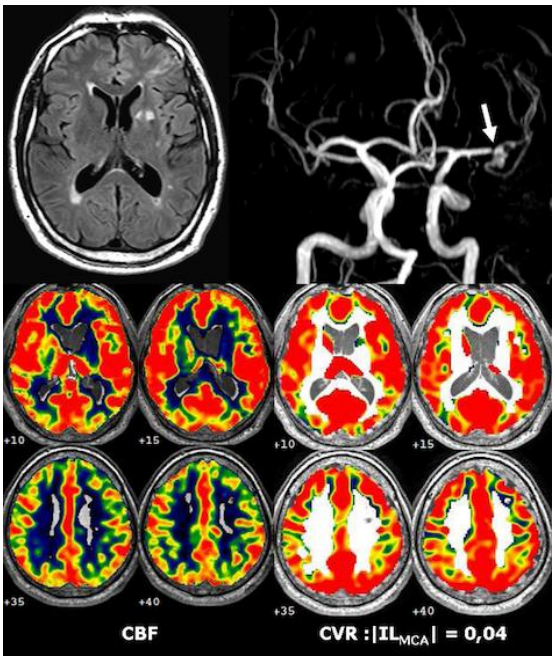

[Fig 1]

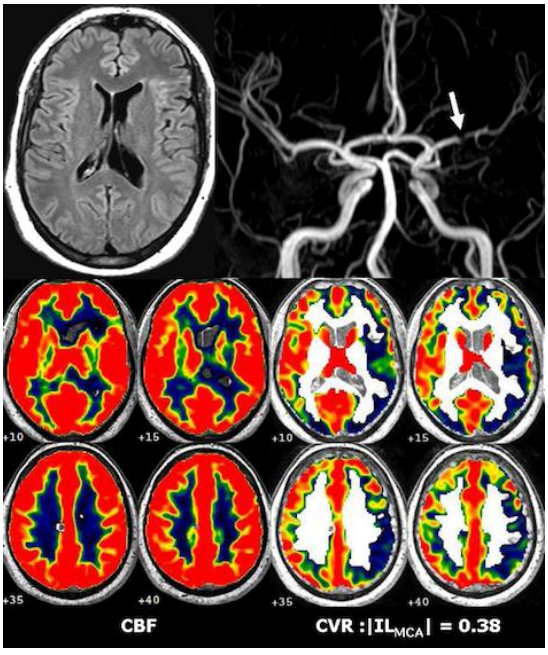

[Fig. 2]

MICRO-VASCULAR CBF RESPONSE TO HYPERCAPNIA IN HEALTHY ADULTS AT ELEVATED HEAD-OF-BED POSITION (HOB)

C. Lindner[1], U. Weigel[1], P. Zirak[1], J. Tercero[2], I. Gracia[2], E. Carrero[2], R. Valero[2], N. Fabregas[2], T. Durduran[1]

[1]Medical Optics, ICFO - The Institute of Photonic Sciences, Castelldefels, [2]Department of Anesthesiology, Hospital Clínic, Barcelona, Spain

Objectives: Elevated HOB position is known to decrease baseline cerebral perfusion pressure and possibly effect the cerebral auto-regulation which in turn may decrease CBF. Different HOB are utilized during surgeries and in the management of neuro-critical patients. Therefore, we sought to investigate whether micro-vascular mCBF is altered at raised HOB by utilizing hypercapnia challenge.

Methods: Micro-vascular CBF was measured bilaterally on the frontal poles of six healthy volunteers (3 Male, 3 Female, 25-37 y/o, mean weight=68kg, height=171cm, BMI=23.6) before, during and after hypercapnia (inspired CO_2 ≈ 6.8 − 8%, O_2 ~ 30%) at supine and 50° HOB. An end-tidal CO2 ($EtCO_2$) increase >20mmHg and two minutes of hypercapnia was necessary for inclusion. Arterial oxygen saturation (SpO2), the heart rate (HR) were recorded. Changes in CBF were measured by diffuse correlation spectroscopy (DCS) which utilizes near-infrared light to non-invasively measure micro-vascular CBF [1]. CBF response to hypercapnia (during first 30 seconds and 2 minutes) was evaluated in both positions. The temporal profile was characterized by the rise time (t_{rise}) relative to the onset of the CBF increase after $\Delta EtCO_2$ > 20mmHg as determined by the time-point CBF rose beyond the baseline mean+3σ. The recovery time (t_{rec}) is the time difference between the recovery of $EtCO_2$ until the CBF fell below the post-baseline plus 3σ. Cases of total mCBF response below 3σ of pre- or post-baseline were discarded. Both hemispheres were evaluated separately, compared statistically by a paired ttest - for t_{rise},t_{rec} by a Wilcoxon ranksum test - before averaging over both hemispheres.

Results:

	supine position	50° sitting position
$\Delta EtCO_2^{30s}\,[mmHg]$	33 ± 8	27 ± 45
$\Delta EtCO_2^{2min}\,[mmHg]$	36 ± 7	27 ± 5
$\Delta HR^{30s}\,[bpm]$	6 ± 11	2 ± 4
$\Delta HR^{2min}\,[bpm]$	6 ± 10	1 ± 4
$t_{rise}\,[s]$	26 ± 21	20 ± 24
$\Delta mCBF^{30s}\,[\%]$	122 ± 28	113 ± 11
$\Delta mCBF^{2min}\,[\%]$	158 ± 38	156 ± 37
$mCBF_{norm}^{30s}\,[\%/mmHg]$	0.8 ± 1	0.5 ± 0.4
$mCBF_{norm}^{2min}\,[\%/mmHg]$	2 ± 1	2 ± 1
$t_{rec}\,[s]$	43 ± 30	50 ± 19
$\Delta SpO_2^{30s}\,[\%]$	2.3 ± 0.5	2.1 ± 0.5
$\Delta SpO_2^{2min}\,[\%]$	2.8 ± 1	2.4 ± 0.6

[Summary of study results]

The table shows the results indicating that there was no statistically significant difference in mCBF between two positions. As expected [2], mCBF increased. The results characterized by the percent mCBF change per mmHg change in $EtCO_2$ are at the lower end of the expectations of 2−3.6%/mmHg [3]. Previously, DCS was utilized in healthy adults in supine position ($\Delta CBF/\Delta EtCO_2$ ≈ 2.4 ± 0.4%/mmHg [1]) and was validated in neonates and children with congenital heart defects in supine position reporting a total $\Delta CBF/\Delta EtCO_2$ ≈ 3.1±1.9%/mmHg [4] and 1.8%/mmHg [5] during mild hypercapnia. While we have used a higher than usual CO_2 concentration, we have applied it briefly and did not reach the plateau.

Conclusions: Cerebrovascular reactivity to hypercapnia was the same at the supine and 50° positions. This can indicate that the cerebrovascular response to hypercapnia seems to be rather independent of posture and cerebral auto-regulation in healthy individuals exhibits an immediate measurable response in the cortex approximately within the first 30s and maintains CBF in normal values.

Funded by Fundació Cellex Barcelona, Marie Curie IRG , ISCIII, MICINN, Institució CERCA , Generalitat de Catalunya, FEDER and LASERLAB.

References:

[1] T Durduran et al. Reports on Progress in Physics, 73(7):076701, 2010

[2] L. Sokoloff. Anesthesiology, 21:664-673, 1960

[3] A. Kastrup et al. Magnetic Resonance Imaging, 19(1):13 - 20, 2001

[4] T. Durduran et al. Journal of Biomedical Optics, 15(3):037004-037004-10, 2010

[5] E. Buckley et al. Journal of Biomedical Optics, 17(3):037007-1-037007-8, 2012

ECDYSTERONE ATTENUATES METABOLITE ABNORMALITIES AND GLUTAMATE DISORDERS IN SUBARACHNOID HEMORRHAGE RABBIT: A MICRODIALYSIS STUDY

Z. Liu, Y. Chen, Z. Chen, H. Feng

Department of Neurosurgery, Southwest Hospital, The Third Military Medical University, Chongqing, China

Objectives: With the development of surgery and interventional therapy, aneurysm could be cure at the first time. However, cerebral ischemia following aneurysmal subarachnoid hemorrhage (SAH) is becoming the big challenge, which could determine prognosis of SAH patients. Ecdysterone seemed to be an effective medicine for subarachnoid hemorrhage in previous studies. The present study was carried out in order to investigate whether the protective effect of ecdysterone on brain injury of subarachnoid hemorrhage involves changes of energy metabolite depletion, or alterations in the extracellular release of glutamate.

Methods: 30 male rabbits were divided into 5 groups randomly. They were sham group, SAH group (treated with alcohol), Nimodipine group (2.5mg/kg), Ecdysterone 1.5mg/kg group (1.5 mg/kg, 4/d) and 3mg/kg group (3 mg/kg EDS, 4/d). Microdialysis was applied to monitor the levels of glucose, lactate, pyruvate and glutamate of hippocampus and lactate/pyruvate (L/P) ratio were calculated.

Results: There were no significant differences of glucose, lactate, pyruvate, lactate/pyruvate and glutamate concentrations between ipsi- and contralateral hippocampus ($P>0.05$). The glucose level of all groups showed almost no change throughout the trial. Lactate level increased after SAH, peaked at 3 days after SAH and decreased 7 days after SAH, but did not recover to the baseline level ($P< 0.05$). It decreased significantly at day 7 in treatment, and returned to control level in EDS 3mg/kg treatment group. There were no differences between pyruvate levels of all groups. L/P ratio increased after SAH and decreased in 7 days after SAH. Its level in EDS 3mg/kg group at 3d after SAH was lower than that in other groups. Glutamate concentration was increased dramatically after SAH. Moreover, it recovered more quickly in EDS 3mg/kg group than Nimodipine treatment group.

Conclusions: Hippocampus of rabbits undergoing a metabolite abnormalities and glutamate accumulation which could alleviate by ecdysterone and its effect could be compared with even better than that of nimodipine.

AUTOREGULATION OF CEREBRAL CIRCULATION IN PROGRESSIVE HEART FAILURE AND ITS RELATIONSHIP TO SEIZURE READINESS

M. Mamalyga

Moscow State Pedagogical University, Moscow, Russia

Objectives: Study the peculiarities of changes autoregulation of cerebral hemodynamic depending on the degree of cardiac decompensation activities with the progressive heart failure (HF), as well as to assess its relations with the manifestation of the convulsion.

Methods. Experiments conducted on a white male rats Wistar, weight 200-220 g. For research used doxorubicin-induced model of heart failure (HF). Ultrasound examination allowed to examine the influence of progressive HF in the brain hemodynamic in three groups of animals:

I - with compensated HF;

II - with early stage of decompensation HF;

III - severe stage of decompensation HF.

To identify compensated and decompensated stages HF every three days with the help of echocardiography. The adequacy of brain perfusion at different stages of HF studied according to the linear speed of the blood flow with transcranial dopplerography basilar artery. For an objective estimation of potential possibilities of autoregulation of cerebral haemodynamics in clinical practice widely used hypercapnia and compression functional stress tests. Magnetic resonance imaging studies were conducted on a "Bruker Biospec 70/30" with the induction of the magnetic field

of 7 T and induction coil diameter of 72 mm. Statistical analyses were performed with the help of computer program «Statistica 6.0».

Results: In the early stage of cardiac decompensation does not change the blood flow in the carotid and basilar arteries, but seizure readiness (SR) of the animals increased. Preservation of reactivity to hypercapnic and compression tests, suggests that the increase in SR is not associated with circulatory disorders in the brain. Exacerbation of HF leads to severe decompensation, including a decrease in blood flow in the carotid and basilar arteries. Metabolic cascade of autoregulation in these animals areactive and myogenic greatly reduced. In this case revealed a progressive increase in the SR. Inefficiency of the heart at different stages of HF is not the same effect on the reserves of the autoregulation of cerebral hemodynamics, which affects the formation and aggravation of SR. Moreover, its rise in various stages of decompensation is not always caused by cerebral ischemia.

Conclusions: Inefficient work of the heart in the early and severe stages of cardiac decompensation varies greatly affects the reserve possibilities of autoregulation of cerebral hemodynamics and the level of convulsion of the brain. And increase seizure activity manifests itself stage of early HF, i.e., on the background of adequate cerebral blood flow. The progression of HF, there is a significant decrease in cerebral hemodynamics, which entails compounded by hypoxia and even more pronounced than in early HF, lowering the threshold of convulsive readiness. The results of the studies suggest that increasing the convulsion of the brain when HF is not always due to hypoxia, but its severity depends on the stage of cardiac decompensation.

HEMODYNAMIC CHANGES DURING WHISKER STIMULATION IN AWAKE AND ANESTHETIZED MICE EXAMINED BY LASER-DOPPLER FLOWMETRY

T. Matsuura[1,2], H. Takuwa[2], T. Obata[2], H. Kawaguchi[2], I. Kanno[2], H. Ito[2]

[1]Department of Chemistry and Bioengineering, Iwate University, Morioka, [2]Molecular Imaging Center, National Institute of Radiological Sciences, Chiba, Japan

Objectives: The mechanisms of regional hemodynamic response during neural activation, including the concept of neurovascular coupling, have been investigated using anesthetized rodents as models. However, anesthesia significantly affects the physiological state, including the regulation of cerebral circulation. To eliminate the physiological effects of anesthesia, a system for an awake animal experiment to study brain microcirculation is required. Longitudinal measurement using laser-Doppler flowmetry (LDF) and laser-speckle flowmetry in awake-behaving mice has been reported in our previous study [1]. In the present study, we investigated changes in cerebral blood flow (CBF), red blood cell (RBC) velocity, and RBC concentration in cerebral microvessels using LDF to explore changes in hemodynamic characteristics during resting and neuronal activation states in awake and anesthetized mice.

Methods: Eighteen male C57BL/6J mice (20-30 g, 7-11 weeks) were used in this study. A custom-made metal plate with a 7-mm diameter hole in the center was attached to the animal's skull with dental resin. The animals were allowed to recover from anesthesia and housed for at least 1 week before initiation of the experiments. The animal was then placed on a styrofoam ball that was floating with the help of a stream of air. This allowed the animals to exercise freely on the ball while their heads were fixed to the apparatus. LDF recording was started under the awake condition, followed by 1.5% isoflurane-anesthetized condition. Changes in hemodynamic characteristics in the somatosensory cortex during whisker stimulation were measured with an LDF system. The tail artery of these mice was cannulated to evaluate the blood gas values under the awake and anesthetized conditions.

Results: The increases in CBF, RBC velocity, and RBC concentration were 20.2 ± 6.3%, 18.4 ± 7.5%, and 1.7 ± 2.9%, respectively, in the awake condition and 4.8 ± 2.7%, 3.4 ± 2.9%, and 1.4 ± 1.0%, respectively, in the anesthetized condition. The increases in CBF and RBC velocity in the anesthetized condition were significantly lower than those in the awake condition ($P < 0.01$), whereas no significant difference was observed in the increase in RBC concentration between the anesthetized and awake conditions. During the resting condition, no significant differences in baseline CBF, RBC velocity, and RBC concentration between the awake and

anesthetized mice were observed. There were significant differences in PaO_2 and $PaCO_2$ between the awake and anesthetized mice because isoflurane anesthesia was administered with O_2 and N_2.

Conclusion: Isoflurane-induced anesthesia attenuates the increase in CBF during stimulation mainly caused by an increase in RBC velocity rather than RBC concentration, indicating the decreased energy demand in the brain. As a result, the attenuation of neuronal activity due to anesthesia might inhibit the increase in CBF during stimulation. RBC measurement techniques in awake animals are useful for the investigation of hemodynamic characteristics resulting from changes in neural activity or other chemical factors such as $PaCO_2$.

References:

[1] Takuwa H., et al, (2011) Reproducibility and variance of a stimulation-induced hemodynamic response in barrel cortex of awake behaving mice. Brain Res. 1369, 103-111.

EFFECTS OF BRAIN PARTIAL ISCHEMIA ON MITOCHONDRIAL FUNCTION AND MICROCIRCULATORY BLOOD FLOW IN BRAIN AND SMALL INTESTINE UNDER HEMORRHAGIC HYPOTENSION

M. Mandelbaum-Livnat[1], E. Barbiro-Michaely[1], **A. Mayevsky**[2]

[1]Faculty of Life Sciences, Bar Ilan University, [2]The Mina & Everard Goodman Faculty of Life Sciences and The Gonda Multidisciplinary Brain Research Center, Bar-Ilan University, Ramat Gan, Israel

Objectives: During hemorrhage, blood is redistributed in favor of the vital organs and on the expense of the less vital organs. Bilateral carotid occlusion (BCO) is an animal model of arteriosclerosis..

The purpose of the present study was to investigate how BCO influences the responses of the brain (vital organ) and small intestine (less vital organ) to hemorrhagic hypotension.

Methods: Rats were bled until reaching mean arterial pressure (MAP) of 40mmHg, with or without BCO 24 hours prior to the bleeding session. MAP level was maintained for 15 minutes, after which the animals were resuscitated with the withdrawn blood. Metabolic and hemodynamic monitoring from both organs were carried out using the Multi-Site Multi-Parametric system, which simultaneously monitors tissue blood flow using Laser Doppler Flowmeter and mitochondrial NADH redox state using surface fluorometry.

Results: While hemorrhage under normoxic conditions caused a decrease in blood supply (30±7%, $p< 0.01$) and mitochondrial dysfunction (132±10% ($p< 0.01$) to the intestine, the brain preserved its normal function. However, under ischemic conditions hemorrhage caused deterioration in both organs. Blood supply to both brain and intestine rapidly decreased and remained low for the entire hemorrhage period (79.5±8% ($p< 0.001$) and 56±10% ($p< 0.001$), respectively). In addition, mitochondrial dysfunction was observed in both brain (137±9%, $p< 0.01$) and intestine (145±12%, $p< 0.01$). Furthermore, the responses of the cerebral parameters to hypotension, exhibited Ischemic-Depolarization (ID) and Secondary Reflectance Increase (SRI) - biphasic changes, where the immediate response was followed by a further response.

Conclusions: The Impaired blood supply to the brain decreases cerebral autoregulation abilities and therefore decreases its protection during hemorrhage. The ID demonstrates the severity of the ischemic damage to normal mitochondrial function under combination of partial ischemia and hemorrhagic hypotension, while the SRI implicates the severity of the damage to normal hemodynamic. These highlight the importance of adequate cerebral perfusion for the maintenance of body homeostasis.

References:

Mandelbaum MM, Barbiro-Michaely E, Tolmasov M and Mayevsky A. Effects of Severe Hemorrhage on In Vivo Brain and Small Intestine Mitochondrial NADH and Microcirculatory Blood Flow. Journal of Innovation in Optical Health Sciences 1: 177-183, 2008

BRAIN METASTASIS INDUCES ASTROCYTE ACTIVATION AND ALTERS NEUROVASCULAR COUPLING IN THE RAT

S. Serres[1], M. Sarmiento Soto[1], C.J. Martin[1,2], C. Escartin[3], G. Bonvento[3], N.R. Sibson[1]

[1]Gray Institute for Radiation Oncology & Biology, Department of Oncology, University of Oxford, [2]Department of Psychology, University of Sheffield, Oxford, UK, [3]MIRcen, URA CEA CNRS 2210, Fontenay-aux-Roses, France

Objectives: Astrocytes play a central role in neurovascular coupling between local neural activity and associated changes in cerebral blood flow (CBF). In secondary cancer (metastasis) of the brain, astrocytes become activated and this may have significant consequences for neurovascular coupling and brain function. The aim of this study was to determine the effects of astrocyte activation on the cortical hemodynamic responses to either stimulation of the whisker-barrel pathway or hypercapnic challenge in the rat brain using both functional magnetic resonance imaging (fMRI) and laser speckle contrast imaging (LSCI).

Methods: Two cohorts of BD-IX rats were injected intracortically in one node of the whisker barrel cortex pathway; the barrel field somatosensory cortex. One cohort was injected with a lentivirus expressing ciliary neurotrophic factor (Lv-CNTF) known to switch astrocytic phenotype to an activated state; animals were used from 6 weeks after injection. The second cohort was injected with metastatic ENU1536 cells (an *N*-ethyl-*N*-nitrosourea-induced mammary adenocarcinoma) to determine the effect of metastatic progression on astrocytic control of blood flow; animals were used one week after injection. All animals underwent T_2*-weighted imaging to measure the blood oxygenation level dependent (BOLD) response and LSCI to measure the CBF response, to both electrical stimulation of the whisker pad and hypercapnic (CO_2) challenge. Immunohistochemical assessment was performed to detect metastases (H&E), astrocyte activation (GFAP) and neuronal death (NeuN).

Results: In both cases, a persistent activation of astrocytes, revealed by strong upregulation of GFAP, was observed in the injected cortex and associated with minimal neuronal damage. CBF responses to whisker pad stimulation or CO_2 challenge were greatly reduced (~50%) in the injected cortex compared to the non-injected cortex, as recorded by LSCI, for both Lv-CNTF and ENU1536 cell injected animals. Similarly, BOLD responses measured by fMRI to whisker pad stimulation were reduced in the Lv-CNTF or ENU1536 cell injected cortex, confirming modulation of neurovascular coupling.

Conclusion: Our findings suggest that astrocyte activation occuring in brain metastasis is a major cause of altered neurovascular coupling when neuronal damage are minimal. Further, these data indicate that astrocytes may play an important role in the control of blood flow during hypoxia. These findings may help to better understand the mechanisms of neurovascular coupling, and yield new therapeutic and diagnostic targets in brain metastasis.

REGULATION OF BASAL CEREBRAL BLOOD FLOW BY DIETARY NITRITE AND ASCORBIC ACID IN OSTEOGENIC DISORDER SHIONOGI (ODS) RATS

B. Piknova[1], J.W. Park[1], S.E. Todd[1], A.N. Schechter[1], **A.C. Silva**[2]

[1]NIDDK, [2]NINDS, National Institutes of Health, Bethesda, MD, USA

Objectives: Nitric oxide (NO) has a key role in maintaining CBF and as a mediator of neurovascular coupling [1]. NO can be synthesized in situ by NO synthase (NOS), or supplied by conversion of its precursor nitrite [2], although the specific pathways for reduction of nitrite into active NO in vivo are still under investigation. One possible catalytic agent is ascorbic acid (AA), which exists in brain tissue at high enough concentrations (2-10mM) to facilitate such reduction [3].

In the present work, we investigated whether AA is involved in producing NO from nitrite by regulating the amount of available dietary nitrite and AA in a strain of rats that does not synthesize AA, the Osteogenic Disorder Shionogi (ODS) rat.

Methods: The amount of bioavailable nitrite and AA was manipulated in four groups of ODS rats (n=12) kept on either a standard or low nitrite/nitrate (NOx) diet (3 weeks), and with or without (1 week) AA supplementation.

CBF was measured with arterial spin labeling in a 7T/30cm MRI system in rats anesthetized with chloralose. NO was inhaled at 5 different concentrations (0-63ppm) to acutely manipulate the amount of bioavailable NOx. Mean arterial blood pressure (MABP) was continuously monitored and methemoglobin (metHb) measured at each NO concentration. NOx were measured from brain tissue by chemiluminescence.

Results: Low NOx diet decreased nitrite levels by 50% ($p< 0.05$), but not nitrate. For animals on the standard diet, deprivation of AA increased the amounts of both nitrite and nitrate, but had no effect on their levels in groups on low NOx diet.

Resting CBF was dramatically decreased to ~50% in rats on low NOx diet compared to those on a standard diet ($p< 0.05$). NO inhalation did not change resting CBF in rats on standard diet supplemented by AA or in groups on low NOx diet. However, NO inhalation caused a robust linear increase of CBF in the ODS group fed a standard diet but lacking AA ($p< 0.05$).

MABP was significantly higher in groups on low NOx diet, but NO inhalation caused a significant decrease of MABP. Animals kept on a standard diet had a lower MABP, which increased significantly with NO inhalation. AA deprivation had no effect on MABP ($p>0.05$).

AA deprivation caused a significant increase in metHb in rats on the standard diet, but not in those on the low NOx diet ($p< 0.05$). In all groups, the amount of metHb increased with NO inhalation.

Conclusions: Together these results suggest that:

1. Dietary NOx are directly involved in basal CBF regulation;

2. In certain circumstances, AA modulates CBF, either by playing a role in the nitrite conversion into NO or by maintaining functionality of the NO cycle by a still unknown mechanism;

3. NOx and AA could be considered for human supplementation in situations of compromised CBF.

References:

[1] Toda N, Ayajiki K, Okamura T (2009) Pharmacol Rev. 61(1):62-97.

[2] Piknova B, Kocharyan A, Schechter AN, Silva AC (2011) Brain Res 1407:62-8.

[3] Millar J (1995) Med Hypotheses. 45:21-6.

TRPM7 REGULATES VASCULAR ENDOTHELIAL CELL ADHESION, MIGRATION AND ANGIOGENESIS

Z. Zeng[1,2], **H.-W. Sun**[1], T.-D. Leng[1], X.-C. Feng[1], L. Zhu[2], K. Inoue[1], Z.-G. Xiong[1]

[1]Morehouse School of Medicine, Atlanta, GA, USA, [2]Soochow University, Soochow, China

Objective: Transient receptor potential melastatin 7 (TRPM7) is a non-selective cation channel possessing α-kinase domain in its c-terminal. As a channel-kinase, it is involved in diverse physiological/pathological processes such as Mg^{2+} homeostasis, hypoxic neuronal injury, and cell proliferation. Increasing evidence suggests that TRPM7 also plays a role in the physiology/pathology of vascular system. For example, we demonstrated previously that silencing TRPM7 promotes growth/proliferation of human umbilical vein endothelial cells (HUVECs). However, the potential effects of TRPM7 on other functions of vascular endothelial cells such as adhesion, migration and angiogenesis were unclear.

Methods: We silenced TRPM7 in HUVECs by TRPM7-siRNA and studied its effect on the morphology of HUVECs. Transwell migration and wound healing assays were used to determine the effect of TRPM7 on cell migration and motility. The effects of TRPM7 on cell adhesion to matrigel and tube formation (as an indication of angiogenesis) were also investigated.

Results: We show that inhibition of TRPM7 function in HUVECs alters cell morphology. Silencing TRPM7 by small interference RNA (siRNA) promotes cell migration and tube formation. In contrast, adhesion of HUVECs to the extracellular matrix is decreased by TRPM7 silencing. We further demonstrate that extracellular signal regulated kinase (ERK) pathway is involved in the change of cell morphology and increased migration of HUVECs induced by TRPM7 silencing. In addition, we show that silencing TRPM7 enhances the phosphorylation of myosin light

chain (MLC) which might be involved in the enhancement of cell motility.

Conclusions: Our data suggest that TRPM7 channels play an important role in the functions of vascular endothelial cells.

References: Inoue K and Xiong ZG. Cardiovascular Res, 2009, 83(3):547-57.

This research was partially supported by NIH R01NS066027, NIMHD S21MD000101, U54RR026137, and AHA 0840132N.

AUTOREGULATORY VASODILATATION AND REDUCED CEREBRAL CIRCULATION RESERVE DUE TO CAROTID ARTERY OCCLUSION MEASURED BY TWO-PHOTON LASER MICROSCOPE IN MICE

Y. Tajima, H. Takuwa, H. Kawaguchi, J. Taniguchi, Y. Ikoma, K. Masamoto, C. Seki, I. Kanno, H. Ito

Molecular Imaging Center, National Institute of Radiological Sciences, Chiba, Japan

Objectives: Reduced cerebral perfusion pressure (CPP) due to occlusive cerebrovascular disease causes autoregulatory vasodilation to maintain cerebral blood flow (CBF) [1]. The autoregulatory vasodilation causes reduced cerebral perfusion reserve which can be estimated by vascular responsivity to hypercapnia or vasodilatory substance, i.e., acetazolamide [2]. However, autoregulatory vasodilatation and vascular response to hypercapnia in microvasculature has not been investigated in detail. In the present study, autoregulatory vasodilatation due to steno-occlusive vascular lesion was evaluated using two-photon laser scanning microscopy (TPLSM) in awake mice. The vascular response to hypercapnia in microvasculature was also evaluated.

Methods: CBF at rest and during hypercapnia was measured by Laser-Doppler flowmetry (LDF) through a chronic cranial window in awake C57/BL6 mice before (baseline) and at 1, 3, 7, 14 and 28 days after right common carotid artery occlusion (N=6). The diameters of arteriole, venule and capillary vessels at rest and during hypercapnia was also measured by TPLSM through a chronic cranial window in awake C57/BL6 mice before (baseline) and at 1, 3, 7, 14 and 28 days after right common carotid artery occlusion (N=2).

Result: CBF values decreased to 82.2 ± 9.6%, 84.2 ± 7.6%, 79.1 ± 5.4%, 85.7 ± 8.5% and 82.5 ± 5.0% of baseline at 1, 3, 7, 14 and 28 days after occlusion, respectively. Vascular responses to hypercapnia were 15.0 ± 3.9%, 6.1 ± 2.2%, 4.5 ± 1.7%, 9.1 ± 3.3%, 9.8 ± 4.3% and 8.2 ± 5.7% at baseline (before occlusion) and at 1, 3, 7, 14 and 28 days after occlusion, respectively. The changes to hypercapnia in diameter of arteriole, venule and capillary vessels at baseline (before occlusion) were 24.1 - 29.4%, 0.8 - 2.4% and 9.5 - 13.4%, respectively. After occlusion, all three vascular components, i.e., arteriole, venule and capillary vessels were dilated by 27.1 - 77.2%, 5.0 - 31.2% and 29.6 - 76.5%, respectively at 1 to 28 days. Moreover, the changes to hypercapnia in diameter of arteriole and capillary vessels decreased at 1 to 28 days after occlusion (Graph 1).

Discussion: Both the autoregulatory vasodilatation and the vascular response to hypercapnia were prominent in arteriole and capillary vessels. Further study is required to evaluate which parts of arteriole and capillary vessels are especially responsive to autoregulation and vascular response.

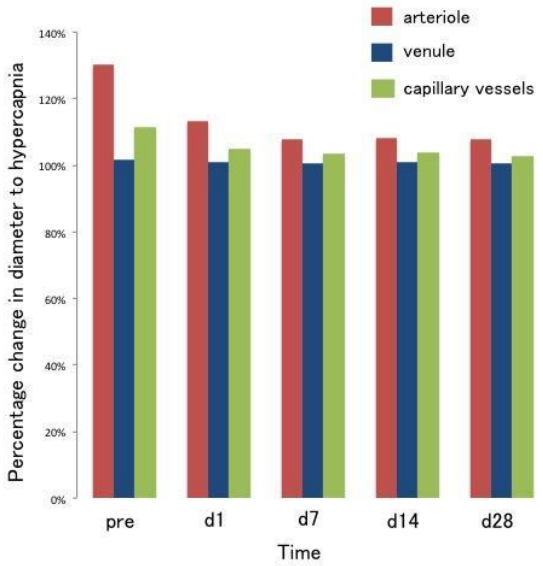

[The percentage change in diameter]

References:

[1] Gibbs JM et al. Lancet 1984; 1: 310-314.

[2] Ito H, et al. Ann Nucl Med 2005; 19: 65-74.

HEMODYNAMIC CHANGES IN CROSSED CEREBELLAR DIASCHISIS MEASURED BY LASER-DOPPLER FLOWMETRY IN AWAKE MICE

H. Takuwa[1], Y. Tajima[1], H. Kawaguchi[1], J. Taniguchi[1], Y. Ikoma[1], K. Masamoto[1,2], C. Seki[1], I. Kanno[1], H. Ito[1]

[1]Molecular Imaging Center, National Institute of Radiological Sciences, Chiba, [2]Center for Frontier Science and Engineering, University of Electro-Communications, Tokyo, Japan

Objectives: Neural activation has been reported to cause larger increase in cerebral blood flow (CBF) than cerebral blood volume (CBV) in humans using PET [1] and has been reported to cause larger increases in red blood cell RBC velocity than RBC concentration in mice using Laser-Doppler flowmetry (LDF) [2]. Crossed cerebellar diaschisis (CCD) caused by contralateral supratentorial lesions can be considered as a condition of neural deactivation, and hemodynamic changes in CCD measured with positron emission tomography (PET) in humans have been reported to show almost the same degree of decrease in CBF and CBV [3]. In the present study, we developed a new mouse model of CCD and measured the change in RBC velocity and concentration due to CCD using LDF.

Methods: RBC velocity and concentration were measured with LDF through a chronic cranial window at the cerebellum in awake mice (C57BL/6J mice, 27-30g, N=6) riding our custom-made apparatus [4]. This apparatus consisted of a head holder and styrofoam ball float on a jet of air under the mice. This allows the mice to walk freely on the ball during LDF measurement. RBC velocity and concentration in bilateral cerebellum were measured at baseline and one day after permanent occlusion of contralateral middle cerebral artery (MCAO) which can cause CCD. The ratio of CCD side to unaffected side in cerebellum for measures by LDF was calculated.

Results: The ratio of CCD side to unaffected side in cerebellum for CBF corresponding to RBC velocity multiplied by RBC concentration after MCAO was decreased by 18% as compared to that of baseline. The ratio of CCD side to unaffected side in cerebellum for RBC concentration after MCAO was decreased by 23% as compared to that of baseline. However, no significant changes in the ratio of CCD side to unaffected side in cerebellum were observed for RBC velocity.

Discussion: The present results indicate that reduction of CBF induced by neural deactivation was mainly caused by the decrease in RBC concentration. The relationship between changes in RBC velocity and concentration due to a neural deactivation is opposite to those due to a neural activation [3]. If RBC concentration can be used as an indicator of CBV, hemodynamic changes due to neural activation and deactivation measured by LDF might be in good agreement with PET measurement in humans previously reported [1,3]. It is likely that our newly established mouse model of CCD will be useful for investigation of the effects of neural deactivation on cerebral microcirculation using two-photon laser microscope and animal PET.

References:

[1] Ito H, et al. J Cereb Blood Flow Metab 2005; 25: 371-377.

[2] Takuwa H, et al. Brain Res. 2012; 1472; 107-112

[3] Ito H, et al. Ann Nucl Med 2002; 16: 249-254.

[4] Takuwa H, et al. Brain Res. 2011; 1369; 103-111

NORADRENERGIC MODULATION OF THE SENSORY-EVOKED NEUROVASCULAR COUPLING RESPONSE IN THE RAT

X. Toussay, E. Hamel

Montreal Neurological Institute, McGill University, Montreal, QC, Canada

Background and objectives: Neuronal activity and cerebral blood flow (CBF) are tightly coupled to ensure adequate oxygen and glucose supply to neurons at work, a process known as neurovascular coupling or functional hyperemia. The neuronal network and vasoactive mediators governing the cortical neurovascular coupling response to sensory stimulation have been partially elucidated. The locus coeruleus-noradrenergic (LC-NA) system is known to enhance activity in cortical neurons and astrocytes (1, 2) and to promote synaptically evoked neuronal excitation (3). Here, we investigated whether or not the LC-

NA pathway modulates the neurovascular coupling response to sensory (whisker) stimulation, and alters the neuronal network underlying this hemodynamic response.

Methods: Changes in cortical CBF were measured using Laser Doppler Flowmetry in urethane-anesthetized (1.1 g/kg, i.p.) male Sprague-Dawley rats. Sensory stimulation was induced by mechanical stimulation of the whisker (8-10 Hz). Increase in cortical NA release was achieved with yohimbine (6 mg/kg, i.p.) or desipramine (25 mg/kg, i.p.), whereas central NA levels were reduced with the selective noradrenergic neurotoxin DSP-4 (60 mg/kg, i.p.). Additionally, in a subset of rats, a sub-maximal activation of LC-NA system was induced by electrical stimulation of the LC (10Hz train of 3 spikes/train every 3s). Activation of barrel cortex neurons was identified by immunochemistry for c-Fos in paraformaldehyde-fixed brain sections.

Results: The CBF response to whisker stimulation was significantly increased following pharmacological enhancement of NA release by yohimbine (+20%, $p< 0.05$) or desipramine (+30%, $p< 0.01$) administration. Similarly, electrical stimulation of the LC-NA afferent pathway that did not significantly alter baseline cortical CBF significantly potentiated the whisker-evoked CBF responses (+35%, $p< 0.01$). DSP-4 treatment drastically reduced NA innervation in the cerebral cortex, and potently decreased (-60%, $p< 0.001$) the CBF response evoked by whisker stimulation. Qualitative analysis of C-Fos immunostaining in DSP-4-treated rats revealed a smaller area of activated (c-Fos-positive) neurons in the barrel cortex compared to saline-injected animals. In contrast, despite the enhanced CBF responses, no change in the extent of c-Fos-positive cells in the barrel cortex was observed in rats treated with yohimbine or desipramine relative to saline controls.

Conclusions: The data show that the CBF response evoked by sensory stimulation is enhanced under conditions of increased cortical NA levels whereas it is decreased in conditions of low NA tone to the cerebral cortex, confirming that NA drives these modulatory effects. The NA-potentiating effects on the neurovascular coupling response to sensory stimulation is in line with the reported facilitating effects of LC on activity of barrel field somatosensory neurons. Moreover, the c-Fos data support the continuous recruitment of new neurons in the facilitated ensemble to replace those suppressed or eliminated from the activated pool (4).

References:

1. Berridge CW and Foote SL (1991) J Neurosci 11:3135-3145

2. Bekar L et al., (2008) Cereb Cortex 18:2789-2795

3. Waterhouse BD et al., (1998) Brain Res 790:33-44

4. Devilbiss DM and Waterhouse BD (2004) J Neurosci 24: 10773-10785.

Supported by the Canadian Institutes of Health Research (CIHR, grant MOP-84209, EH).

DIFFERENT RESPONSE IN DIAMETER OF PIAL VESSELS AND IN CEREBRAL BLOOD FLOW ASSOCIATED WITH CORTICAL SPREADING DEPRESSION IN ANESTHETIZED MICE

M. Unekawa[1], Y. Tomita[1], H. Toriumi[1], T. Osada[1,2], **K. Masamoto**[3,4], H. Kawaguchi[4], Y. Itoh[1], I. Kanno[4], N. Suzuki[1]

[1]Neurology, Keio University School of Medicine, Tokyo, [2]Neurology, Tachikawa Hospital, Tachikawa, [3]Center for Frontier Science and Engineering, University of Electro-Communications, Chofu, [4]Molecular Imaging Center, National Institute of Radiological Sciences, Chiba, Japan

Objectives: Cortical spreading depression (CSD), a propagating phenomenon of depolarizing neurons and astroglia, dramatically affects cortical cerebral blood flow (CBF) by still undetermined mechanisms. We previously reported suppression of red blood cell (RBC) velocity flowing in capillaries conversely in the region of neuronal activation [(1,2)]. To further understand the mechanisms of CBF control during CSD, we examined temporal pattern of diametric changes in pial vessels and CBF.

Methods: To visualize blood vessels, we used Tie2-GFP transgenic mice (N=16), in which specifically vascular endothelial cells emit fluorescence. Under urethane anesthesia and artificial ventilation, a cranial window was installed on the temporo-parietal region of the cerebral cortex. KCl (1 M) was applied on the brain surface through a burr hole posterior to

the cranial window to elicit CSD. Diameters of pial arteries, veins and capillaries were measured with the confocal laser-scanning fluorescence microscopy and an image analysis software ImagePro. DC potential was simultaneously recorded next to the window along with CBF by laser Doppler flowmeter. The fluorecent flow in cerebral vessels was recorded on a video after the intravenous bolus injection before and after CSD elicitation. Pixel-by-pixel microflow values (a reciprocal of mean transit time: 1/MTT) were calculated from the temporal intensity change by the in-house Matlab software KEIO-IS1 in the same region of interest [3].

Results: Application of KCl induced biphasic response, first constriction of pial arteries (-35.4±18.8%) during DC potential deflection and then dilation (5.2±12.6%). CBF increased with transient drop observed at the peak time of vasoconstriction.There was no significant correlation between baseline diameters of the pial arteries and their % changes during CSD (r=0.342). Pial veins and capillaries showed small but significant dilation. Second and third waves of CSD also elicited vasodilation but the response was diminished (4.8±10.9% and 1.9±7.4%, respectively), whereas CBF increase (29.6±14.5% and 27.7±12.0%) without transient drop was repeatedly observed without diminution. Mild vasoconstriction was observed only in limited cases (n=25/40 and 10/30). After CSD, CBF decreased and reached a plateau below the baseline level (-19.7±9.2%) (post-CSD oligemia), whereas 1/MTT decreased only 12.4±11.6% and became stable with diameter of pial vessels returning to the baseline levels.

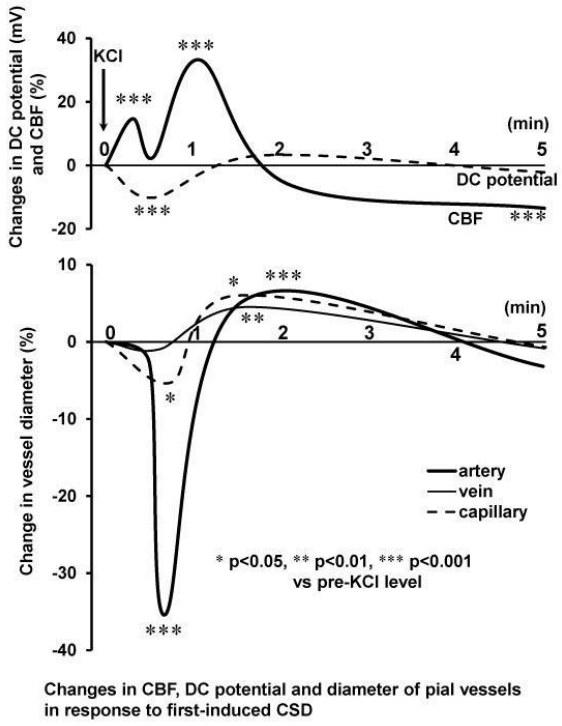

Changes in CBF, DC potential and diameter of pial vessels in response to first-induced CSD

[Figure]

Conclusion: Initial increase in CBF during first CSD may be counteracted with vasoconstriction induced through mechanisms different from flow-metabolism coupling. Diametric responses in pial vessels were diminished, whereas increase in CBF was repeatedly observed. Thus, cerebrovascular control in response to CSD might be largely affected by peripheral vessels from the pial artery such as penetrating arteries. Together with our previous reports of suppressed RBC flow [1,2], it is suggested that diameter of pial artery and cortical CBF are controlled differently during CSD.

References:

(1) Unekawa M et al, Microcirculation, 19:166-74, 2012.

(2) Unekawa M et al, J Neurosci Res, in press.

(3) Tomita Y et al, Brain Res, 1372:59-69, 2011.

HUK EXERTS A NEUROPROTECTIVE EFFECT BY REGULATING GLUCOSE METABOLISM IN EXPERIMENTAL STROKEV

J. Li, **Y. Xu**

Department of Neurology, Affiliated Drum Tower Hospital of Nanjing University Medical School, Nan Jing, China

Objectives: The kallikrein-kinin system (KKS) exerts beneficial effects on ischemic brain injury by enhancing neovascularization and restoring regional blood flow [1]. Human Urinary Kallidinogenase (HUK), a key member of KKS, has been used for more than 4 years in clinic for treating ischemic stroke patients in China, however, the protective mechanism is still unclear. The present study was undertaken to investigate whether the HUK treatment can regulate glucose metabolism in experimental stroke .

Methods: Rats with or without HUK were subjected to 2-hour MCAO and followed by 1d, 3d and 18d of reperfusion. Neurofunctional recovery was assessed using Longa scores. The cerebral glucose metabolism of rats was detected by micro-PET. Scans were reconstructed iteratively with OSEM3D algorithm. At various time post-reperfusion, brains were removed and stained with 2,3,5-triphenyltetrazolium chloride (TTC) for infarct size. Statistical analyses were performed using ANOVA and post hoc Fisher's PLSD tests, with $P< 0.05$ considered statistically significant.

Results: HUK treatment significantly decreased infarct size following ischemia and lowered Longa mean scores at 3 and 18 d ($P< 0.05$). FDG uptake was decreased in MCAO groups ($P< 0.05$, versus sham group), but HUK treatment resulted in enhanced FDG uptake at 3 and 18 d ($P< 0.05$). No differences in blood pressure, SpO2 and heart rate were observed between MCAO group and HUK group.

Conclusions: Neovascularization induced by HUK treatment enhanced cerebral glucose metabolism following experimental stroke, which contributes to the protection of HUK.

References:

[1] Xia CF, et al. Kallikrein Protects Against Ischemic Stroke by Inhibiting Apoptosis and Inflammation and Promoting Angiogenesis And Neurogenesis. Human Gene Therapy .2006 ;17:206-219.

DYSFUNCTION AND RECOVERY OF ENDOTHELIAL TRPV4 CHANNELS IN PATHOLOGIES OF THE CEREBRAL CIRCULATION RELATED TO ALZHEIMER'S DISEASE

L. Zhang, E. Hamel

Laboratory of Cerebrovascular Research, Montreal Neurological Institute, McGill University, Montréal, QC, Canada

Background and objectives: Transient receptor potential vanilloid type 4 (TRPV4) channels expressed in endothelial cells (EC) regulate vascular tone in systemic vessels [1]. Particularly, Ca^{2+} influx via TRPV4 channels causes dilation by activating EC intermediate- and/or small-conductance (IK and/or SK) Ca^{2+}-sensitive K^+ (K_{Ca}) channels [2]. Impaired endothelial dilation is a key landmark of amyloid-β (Aβ)-induced cerebrovascular dysfunction in mouse models of Alzheimer's disease (AD), and has been imputed to Aβ-induced oxidative stress [3]. Here, we investigated whether TRPV4 channels contribute to the dilation of cerebral arteries, and if they are altered in

i) mice that overexpress a mutated form of the human amyloid precursor protein (APP mice) and recapitulate the Aβ pathology of AD,

ii) mice that overexpress transforming growth factor-β1 (TGF mice) and recapitulate the cerebrovascular fibrotic pathology of AD [4], and

iii) APP/TGF mice that combine these two pathologies [5]; and whether TRPV4 channel function is sensitive to antioxidant therapy.

Methods: Dilations to acetylcholine (ACh) or the selective TRPV4 channel agonist GSK1016790A (GSK) were measured by online videomicroscopy [3] in isolated and pressurized posterior cerebral artery (PCA) segments from three month-old mice. Dilations were measured either after endothelium-denudation, in presence of the TRPV4 selective antagonist HC-067047 (HC), the SK and/or IK blocker apamin and/or charybdotoxin (ChTx), or after exposing vessels to the antioxidant superoxide dismutase (SOD) or

catalase. Smooth muscle cell integrity was tested with the nitric oxide (NO) donor sodium nitroprusside (SNP).

Results: Compared with WT mice, ACh- and GSK-induced cerebral dilations were significantly reduced (-50%) in APP, TGF and APP/TGF mice. In WT mice, these dilatory responses, but not that induced by SNP, virtually disappeared after endothelium removal. The ACh-induced dilation was impaired (-50-60%) and that of GSK almost abolished by HC (10^{-6}M), apamin (10^{-8}M) or by a combination of apamin (10^{-8}M) and ChTx (5.10^{-8} M) in WT brain arteries. In contrast, these treatments had no or only modest effects on the ACh-induced dilation in APP, TGF or APP/TGF mouse brain vessels. Superfusion of SOD or catalase completely normalized the ACh- or GSK-induced dilations in APP brain arteries, whereas it had no effect on these dilatory responses in vessels from WT, TGF and APP/TGF mice.

Conclusions: We conclude that endothelial TRPV4 channels are important mediators of dilatory function in brain vessels, that they are altered in various models of cerebrovascular pathology, and that they are sensitive, albeit in the reversible manner, to Aβ-induced oxidative stress. In contrast, antioxidant therapy has no benefit on TRPV4 channel function in pathologies that involve vascular fibrosis as seen in TGF and APP/TGF mice.

Supported by: The Canadian Institutes of Health Research (CIHR, grant MOP-84275, EH).

References:

1. Zhang DX et al., J Cardiovasc Pharmacol 2011, 57: 133-9.

2. Sonkusare SK et al., Science 2012, 336: 597-601.

3. Tong XK et al., J Neurosci 2005, 25: 11165-11174.

4. Wyss-Coray T et al., Am J Pathol 2000, 156: 139-150.

5. Ongali B et al., Am J Pathol 2010, 177: 3071-3080.

COMPARISON OF BLOOD VELOCITY AND VOLUMETRIC FLOW IN MIDDLE CEREBRAL AND INTERNAL CAROTID ARTERY DURING STEPWISE CHANGES IN BLOOD PRESSURE

J. Liu[1,2], C. Hill[1], K. Armstrong[1], T. Tarumi[1,2], A.M. Stowe[3], **R. Zhang**[1,2,3]

[1]Institute for Exercise and Environmental Medicine, Texas Health Presbyterian Hospital Dallas, [2]Department of Internal Medicine, [3]Department of Neurology and Neurotherapeutics, University of Texas Southwestern Medical Center, Dallas, TX, USA

Objectives: To determine whether changes in cerebral blood flow velocity (CBFV) in the middle cerebral artery reflect the volumetric changes in cerebral blood flow (CBF) during stepwise decreases and increases in arterial pressure in older adults.

Methods: Twenty six healthy subjects (14 females, 67 ± 6 yr) participated. Mean arterial pressure (MAP) was decreased stepwise by intravenous infusion of sodium nitroprusside and then increased by phenylephrine. Transcranial Doppler and color-coded duplex ultrasonography were used to measure CBFV in the middle cerebral artery (MCA) and volumetirc CBF in the internal carotid artery (ICA) respectively, with end-tidal CO_2 recorded simultaneously. Changes in CBFV and CBF as well as calculated cerebrovascular resistance (CVR = MAP/CBF) or resistance index (CVRi = MAP/CBFV) in response to changes in MAP were used to assess cerebral autoregulation (CA) by linear regression analysis. The relationship between changes in the ICA diameter and MAP was also assessed. All values were normalized as percentage change from baseline (%).

Results: The range of changes in MAP induced by drug infusion was from -26% to 35%. Changes in CBFV and CVRi in response to changes in MAP were linear and the magnitudes were similar in the MCA and ICA. However, CBF in the ICA remained unchanged during stepwise changes in MAP associated with a greater increase in CVR relative to CVRi. The differences between changes in CBFV and CBF could be attributed to the changes of the ICA diameter in response to changes in MAP ($r = -0.39$, $P < 0.05$).

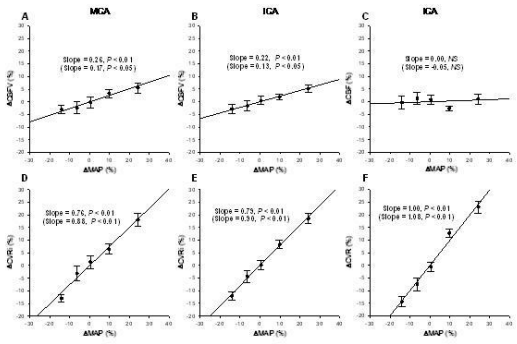

[Figure 1]

Conclusions: Changes in CBFV measured in the MCA reflect changes in volumetric CBF in the ICA. However, the cerebral autoregulatory capability may be underestimated using CBFV and CVRi instead of CBF and CVR. The inverse relationship between changes in the ICA diameter and MAP suggests that large cerebral artery involves in CA.

Figure 1. Percentage changes in cerebral blood flow velocity (CBFV), volumetric CBF (top row), cerebrovascular resistance (CVR) and cerebrovascular resistance index (CVRi)(bottom row) in the middle cerebral artery (MCA) and internal carotid artery (ICA) during stepwise changes in mean arterial pressure (MAP). Note: Values in parentheses are adjusted for changes in end-tidal CO_2.

INTRACRANIAL TUMORS IN INFANTS: A FORTY-THREE YEAR REVIEW OF A SINGLE INSTITUTION EXPERIENCE IN SASKATCHEWAN, CANADA

K. Ali

Pediatric Oncology, Saskatchewan Cancer Agency and University of Saskatchewan, Saskatoon, SK, Canada

Introduction: Central nervous system tumors constitute the most common group of malignant solid tumors in the pediatric population. While the experience with this malignancy is well documented in children, adolescents, and young adults, there are a limited number of published studies on infants under one year of age with intracranial tumors (ICT).

Objectives: To determine the distribution, treatment and outcomes of ICT in infants under one year of age diagnosed at the Saskatoon Cancer Centre, Saskatchewan, Canada.

Methods: An archival review was conducted of health records on infants with ICT diagnosed between 1 January 1970 and 14 December 2012 at the Saskatoon Cancer Centre. Data capture items included, among others, age at diagnosis, sex, tumor type, treatments received, and outcomes.

Results: A total of 16 infants were diagnosed with ICT before their first birthday. Median age at diagnosis was 9 months (range 5 days - 11 months). There were 9 females, and 7 males. Brain tumors (BT) comprised 10 cases; there were 5 cases of retinoblastoma (RBMA), and 1 case of malignant ectodermal tumor of infancy.

Of the 10 infants with BT, 5 underwent surgery (SX) alone; the remaining 5 were treated with a combination of SX and radiation therapy (XRT) - none received chemotherapy. Five were confirmed deceased; 4 long term survivors (LTS) were followed for up to 17 - 28 years.

Among the 5 infants with RBMA, 3 were bilateral (2 - synchronous). Both infants with synchronous bilateral tumors eventually underwent bilateral enucleations. XRT was administered as external beam irradiation in 2 patients, 1 of whom was also treated with brachytherapy, One infant with metachronous RBMA was treated with enucleation of the first affected eye, and cryotherapy to the second.

Second malignant neoplasms (SMN), all within XRT portals, were documented in 3 LTS, The first was a meningioma that occurred 28 years post-treatment in a BT patient, The second, a basal cell carcinoma of skin, occurred 17 years later, also in a BT patient, The third, with primary bilateral RBMA, succumbed to a malignant fibrous histiocytoma 17 years later.

Conclusions: Infants under one year of age diagnosed with ICT comprise a special subgroup of pediatric patients in terms of distribution of tumor types and unique management challenges, and in whom cures are attainable. Open-ended, long term follow up is required to monitor their transition into adulthood, and for surveillance of SMN with onset in the second and third decades of life.

EMBRYOLOGIC ASSOCIATION OF TOMWALDT'S CYST WITH CEREBRAL ARTERY ABNORMALITIES

A. Badr[1], M.F. Osborn[1], N. Akle[2], J. Zhang[1,3]

[1]Anesthesiology, [2]Radiology, [3]COE for Neuroscience, Biomedical Sciences, Texas Tech University Health Science Center, El Paso, TX, USA

Objectives: Tornwaldt's cysts, also known as pharyngeal bursae, are rare midline cysts found in the nasopharynx. These cysts are usually incidental findings on imaging studies of the head and neck region. The embryologic origin of Tornwaldt's cysts derives from the period of transformation of the notochordal process into the solid notochord between days 16 and 22 of development. During this time, the ventral wall of the notochordal process fuses with the endoderm to form a notochordal plate. After the plate is formed at the cranial end, the notochordal plate infolds and forms a solid rod, the notochord. Failure of complete infolding leads to the development of a Tornwaldt's cyst, a remnant of the notochord attached to the endoderm. The notochord's role is to induce and modulate the development of the early embryo. This occurs through various cellular signaling mechanisms. The notochord is also involved in dorsal-ventral patterning and induction of the development of various tissues. The notochord is in close proximity to the developing vasculature, most notably the dorsal aortae, two primitive vessels that run the length of the embryo. These vessels lie on either side and slightly ventral to the notochord, and dorsal to the gut tube. The cranial extensions of the dorsal aortae form the distal portions of the internal carotid artery including the middle cerebral arteries. In addition to these cranial vessels, the dorsal aortae fuse to form the descending aorta.

Methods: Based on a case of a twelve-year-old Hispanic female who was diagnosed with both an ischemic stroke due to middle cerebral artery abnormalities and a Tornwaldt's cyst, we performed a literature search to examine the possibility of notochordal dysfunction leading to cerebral vascular abnormalities which might predispose an individual to stroke.

Results: Based on the embryology of the notochord and its relationship to the forming vasculature during early development, we propose a link between this patient's Tornwaldt's cyst and the irregularity in the M1 segment of the middle cerebral artery (MCA). Notochord-derived signaling molecules such as (hedgehog, Hh) are essential cues for the specification and differentiation of multiple tissues and organs during embryonic development. Perturbation of the notochord, similar to the events causing the formation of a Tornwaldt's cyst during development, could result in dysfunction of endoderm development or of cell signaling during vasculogenesis/angiogenesis. Through the remnant of the notochord in the gut tube, there could be further interaction with the dorsal aortae at the level of the remnant through persistent, inappropriate or absent cell signaling in this region. These defective processes could result in a cystic or atretic deformity in the MCA, leading to abnormal vasculogenesis/angiogenesis, which would predispose an individual to stroke. Our hypothesis is further supported in this case by the family history of stroke.

Conclusions: Our case study suggests a possible etiologic connection between Tornwaldt's cyst and cerebral vasculature abnormalities by way of notochordal signaling perturbation, a predisposition to cerebral vascular accidents. This report provides evidence for the association between notochordal dysfunction (as in Tornwaldt's cyst) and vascular abnormalities.

CLINICAL FEATURES, SURGICAL TREATMENT, AND LONG-TERM OUTCOME IN ADULT PATIENTS WITH MOYAMOYA DISEASE IN CHINA

L. Duan

Department of Neurosurgery, 307 Hospital, PLA, Center for Cerebral Vascular Disease, Beijing, China

Background: Moyamoya disease develops mostly in Asian countries including Japan, Korea, mainland China and Taiwan. However, there was few detailed demographic and clinical data about Chinese patients with moyamoya disease. Currently, the most effective treatment in adult patients with moyamoya disease is unknown. There have only been a few small case series reporting on Encephalo-duro-arterio-synangiosis (EDAS) in an adult population. Here we describe the clinical features, surgical treatment, and long-term outcome of adults with moyamoya disease treated at a single institution in China.

Methods: Our cohort included 470 adult patients with moyamoya disease. The

demographic and clinical characteristics were obtained by retrospective chart review and long-term outcome was evaluated using the stroke status. A modified Rankin Scale (mRS) was used to determine the neurological functional outcome. Univariate and multivariate logistic regression analyses were performed to determine risk factors for postoperative morbidity and functional outcome. Risk of subsequent stroke was determined using the Kaplan-Meier method and Cox regression was used to determine risk factors for postoperative or subsequent strokes.

Results: The median (range) age for the onset of symptoms was 36.8 (18 to 59) years. The ratio of female to male patients was 1:1(231/239). Familial occurrence of moyamoya disease was 2.3%. The most common initial symptom was a cerebral ischemic event. The incidence of postoperative ischemic events or hemorrhage was 5.9% (9.8% of patients). Older age of symptom onset, PCA involvement and present of TIA were identified as predictors of adverse postoperative events. The Kaplan-Meier estimate stroke risk was 10.1% in the first 2 years, and the 5-year-Kaplan-Meier risk of stroke was 13% after surgery for all patients treated with surgical revascularization. Older age of symptom onset, PCA involvement, and present of TIA were identified as predictors of postoperative or subsequent strokes. Overall, 73.2% of patients had an independent life with no significant disability and the strongest predictor being the preoperative mRS score.

Conclusion: Clinical characteristics of adult moyamoya disease in China are different from that in other Asian countries. EDAS in adult patients with moyamoya disease carries a low risk, is effective at preventing future ischemic events, and improves quality of life.

A RETROSPECTIVE STUDY ON THE DIAGNOSES AND TREATMENT OF 4462 CASES WITH SEVERE TRAUMATIC BRAIN INJURY

Z. Fei

Xijing Hospital, The Fourth Military Medical University, Xi'an, China

Objective: To analyse and summarize the diagnostic and treatmental modality in order to increase the cure rate and survival rate for patients with severe traumatic brain injury (STBI).

Methods: A retrospective study was made on the diagnoses and treatment of 4462 cases with STBI. There were 3298 male and 1164 female in this group. The most frequent cause for injury was traffic accident(35. 5%). Closed head injury happened in 3654(81.9%) cases and open head injury in 808(18.1%) cases. The most commen clinical manifestations unconsciousness, changes of pupils and life signs. In this group, 1158 cases (26.0%) were found to have injury to other organs and 1356 cases (30.4%) with complications. All the cases underwent first aid, surgery or conventional treatment. Emphasis was put on the treatment of secondary insults.

Results: Surgery was made on 3023 cases (67.7%) with a mortality of 17.9%, and conventional treatment on 1439 cases (32.3%) with a mortality of 23.7%. There were 2462 cases (55.2%) with fair recovery, 508 cases (11.4%)with mild disability, 339 cases (7.6%) with severe disability, 272 cases (6.1%)in vegetative state and 881 case（19.7%） of death in this group on discharge according to the Glasgow outcome scale.

Conclusion: Active diagnoses and treatment, strict rules for medication and prevention and treatment for secondary insults may be the keys for the higher cure rate and lower morbidity as well as mortality of STBI.

EFFICACY AND LIMITATIONS OF INTRAOPERATIVE MOTOR EVOKED POTENTIAL MONITORING IN CEREBRAL ANEURYSM SURGERY

N. Higashiyama, T. Yanagisawa, T. Sugawara, T. Sasajima, K. Mizoi

Department of Neurosurgery, Akita University Graduate School of Medicine, Akita, Japan

Objective: Intraoperative neuromonitoring (IOM) has been proposed as a method to reduce perioperative neurologic complications. We performed direct cortical stimulation motor evoked potentials (DCS-MEP) monitoring in patients undergoing cerebral aneurysm surgery, and investigated its efficacy and limitations.

Methods: We reviewed DCS-MEP monitoring records of 137 consecutive patients (mean age: 61.8 years, 37 male and 100 female) who

underwent cerebral aneurysm surgery between Dec 2004 and Aug 2012. DCS-MEP monitoring was performed using multipulse direct cortical stimulation under total intravenous anesthesia, and electromyograms were monitored at abductor pollicis brevis and abductor hallucis muscles contralateral to the surgical side. More than 50% decrement of MEP amplitudes compared with baseline recordings was regarded as a threshold for a warning sign.

Results: Assessable and reproducible MEP waves were obtained in all cases. Intraoperative reduction in amplitude of at least 50% for DCS-MEP was seen in 45 of the 137 cases. Forty one of the 45 patients showed recovery of MEP amplitude by the end of the operation, and none showed any motor deficits after surgery. Four of the 45 patients did not show recovery of MEP amplitude, and had postoperative motor deficits. The sensitivity and specificity of our warning criteria were 100% and 69.2%, respectively, in detection of postoperative motor deficits.

Conclusion: The DCS-MEP monitoring was noninvasive, and simple method for IOM. For warning criteria, a threshold of 50% reduction in amplitude obtained high sensitivity and specificity for postoperative motor deficits.

LONG-TERM ONGOING CORTICAL REMODELING AFTER CONTRALATERAL C7 NERVE TRANSFER

X.-Y. Hua, W.-D. Xu

Department of Hand Surgery, Huashan Hospital, Shanghai, China

Objective: Contralateral C7 nerve transfer is developed for the treatment of brachial plexus injury patients. In the surgical procedure, the affected recipient nerve would connect to the ipsilateral motor cortex and the dramatic peripheral alteration may trigger extensive cortical reorganization. But little is known about the long term results after such specific nerve transfer. The purpose of this study is to investigate the long term cortical adaptive plasticity after brachial plexus injury and contralateral C7 nerve transfer.

Methods: In this study, nine healthy male volunteers and five male patients who suffered from right BPAI and underwent contralateral C7 transfer for more than 5 years were involved. fMRI was used for the investigation of the long-term cerebral plasticity.

Results: The neuroimaging results suggested that the ongoing cortical remodeling procedure after contralateral C7 nerve transfer could last for a long period, at least for 5 years. The motor control of the reconstructed limb may finally transfer from the ipsilateral hemisphere to the contralateral hemisphere solely instead of the bilateral neural network activation.

Conclusions: It was believed that the cortical remodeling may last for a long period after peripheral rearrangement and the successful cortical transfer is the foundation of the independent motor recovery.

LONG TERM FOLLOW-UP RESULTS IN 142 ADULT PATIENTS WITH MOYAMOYA DISEASE ACCORDING TO MANAGEMENT MODALITY

P.W. Huh

Department of Neurosurgery, Uijeongbu St. Mary's Hospital, The Catholic University of Korea, School of Medicine, Ujieongbu, Republic of Korea

Background: To clarify the most beneficial treatment of the management modality based on our experience with adult moyamoya disease (MMD).

Methods: From 1998 to 2010, clinical results of 142 patients (ischemic 98, hemorrhagic 44) with adult MMD were investigated according to management modality. Revascularization surgery (direct, indirect, and combined bypass) was performed in 124 patients. We observed the clinical course of 18 patients who treated conservatively. Clinical outcome, angiographic features, hemodynamic change and incidence of recurrent stroke were preoperatively and postoperatively investigated.

Results: In patients with ischemic MMD, direct and combined bypass were more effective treatments to prevent recurrent ischemic stroke than indirect bypass surgery ($P < 0.05$). In patients with hemorrhagic MMD, rebleeding was less likely to occur in patients who had undergone bypass surgery. But, no significant difference was observed in the rebleeding rate between patients with and those without

revascularization surgery (P > 0.05). An angiogram after bypass surgery comparing the extent of revascularization and reduction of moyamoya vessels in patients treated with direct, indirect and combined bypass showed a significant difference (P < 0.05) in favor of direct and combined bypass. Postoperative angiographic changes and SPECT results demonstrated significant statistical correlation (P < 0.05).

Conclusion: Although, the effect of direct and combined bypass on the prevention of recurrent an ischemic event in adult patients with ischemic MMD has been statistically confirmed in this study, there is still no clear evidence that revascularization surgery significantly prevents rebleeding in adult MMD. More significant angiographic changes were observed in direct and combined bypass compare to indirect bypass. In addition, postoperative angiographic change was well correlated with postoperative SPECT results.

LONG TERM RESULT OF THE REVASCULARIZATION SURGERY IN THE HEMORRHAGIC MOYAMOYA DISEASE

P.W. Huh

Department of Neurosurgery, Uijeongbu St. Mary's Hospital, The Catholic University of Korea, School of Medicine, Ujeongbu, Republic of Korea

Background and purpose: Revascularization surgery for moyamoya patients is believed to prevent cerebral ischemic attacks by improving cerebral blood flow. However, Surgical treatment protocol of hemorrhagic moyamoya in patients have not yet been established in the literature due to the low rate of hemorrhage onset as well as the originally limited numbers of patients with moyamoya disease, poor understanding of the clinical course of rebleeding, correct surgical management, and outcome. This study represents part of a therapeutic survey of hemorrhagic moyamoya disease, and we examined the preventive effect of bypass surgery on rebleeding, clinical course and outcome.

Methods: This study included 28 moyamoya patients with episodes of intracranial hemorrhage between 20000 and 2009. The mean follow-up period was 8.07 years. There were 11 males and 17 females, aged 13 to 80 years (mean 44.4 years). Cerebral angiography and CT scans were performed for all patients. Surgical treatment was performed in 22 patients (78.6%), and 20 patients (71.4%) underwent revascularizatio n surgery. We observed the clinical course of all 28 patients. We also studied the relationship between the efficacy of surgical treatment and long-term outcome.

Result: Three of the 28 patients (10.7%) died of the initial intracranial hemorrhage, and 2 patients died of rebleeding. Rebleeding occurred in 5 of the remaining 25 patients (20.0%). The interval to rebleeding ranged from 1 to 19 years (mean 10.0 years). Of these 5 patients, 2 died of rebleeding. Rebleeding was observed in 4 of 20 patients who underwent bypass surgery and in 2 of 8 patients who did not, which suggested that rebleeding was less likely to occur in patients who had undergone bypass surgery. However, there was no significant difference in rebleeding ratio or mortality between patients with and those without revascularization surgery (P=0.55).

Conclusions: In this study, we compiled the results of meticulous follow-up conducted over the past 10 years for patients with hemorrhagic moyamoya disease. Because hemorrhagic moyamoya disease is known for its high rate of mortality at the time of rebleeding and often causes rebleeding long after the initial episode (as much as 20 years later), implementation of long-term preventive measures for rebleeding is necessary. This suggests that a long-term prospective study of a large number of patients with hemorrhagic moyamoya disease is required to determine whether bypass

surgery prevents rebleeding of hemorrhagic moyamoya disease.

PRACTICAL CLINICAL USE OF DSC-MRI FOR SURGICAL TREATMENT OF MOYAMOYA DISEASE

Y. Ishii[1], T. Nariai[2], Y. Tanaka[2], M. Mukawa[2], M. Inaji[2], T. Maehara[2], K. Ohno[2]

[1]Neurosurgery, Kushiro Kojinkai Memorial Hospital, Kushiro, [2]Neurosurgery, Tokyo Medical and Dental University, Tokyo, Japan

Background and purpose: In the indirect bypass surgery for Moyamoya disease (MMD), precise evaluation of hemodynamic stress is important. We explored whether perfusion

imaging with dynamic susceptibility contrast MR imaging (DSC-MRI) could predict the effect and risk of indirect bypass surgery on MMD.

Methods: Between 2001 and 2009, we performed indirect bypass surgery on 115 hemispheres of 69 patients. All of them underwent DSC-MRI and 46 of them underwent digital subtraction angiography (DSA) before and after the surgery. We examined correlation of their ischemic events and revascularization with DSC-MRI-measured mean transit time (MTT) using cerebellum as a control we termed as MTT delay".

Results: Ischemic events disappeared in 58 (84%) and ameliorated in 7 (10%) patients after surgical treatment. Between hemispheres responsible and non-responsible for ischemic events, there was a significant difference on their preoperative MTT delay (2.66 vs 1.57 seconds, p< 0.001), and the postoperative MTT delay of responsible hemispheres was significantly reduced in cases whose symptoms disappeared compared with the preoperative one (2.61 vs 1.35 seconds, p< 0.0001). More excellent revascularization was induced in the area with larger MTT delay. In four hemispheres among 115 (3.5%), perioperative infarction occurred. MTT delay of these hemispheres was significantly larger than the others (3.97 vs 2.38 seconds, p=0.0213) and all exceeded 3 seconds.

Conclusion: DSC-MRI was a practical clinical imaging method for patients with MMD. It can be used to select the operative candidates by setting a threshold value in MTT delay. It can predict an effect and a risk of surgery by using MTT delay as indicator.

CEREBRAL HAEMODYNAMICS DURING SEIZURES IN UNCONSCIOUS CHILDREN

F. Kirkham, C. Newton

Neurosciences Unit, UCL Institute of Child Health, London, UK

Introduction: Seizures and status epilepticus are common in unconscious patients, but although associated with poor outcome, the pathogenesis of neurological damage is unclear. Ischaemic brain damage might occur if cerebral blood flow (CBF) does not increase sufficiently to match the increased metabolic demand during seizures.

Aims: As an ancillary component of an observational study of spontaneous seizures in unconscious children,[1] we aimed to document change in CBF velocity (CBFV) in the middle cerebral artery before, during and after individual seizures.

Patients and methods: From a total of 204 children with impaired consciousness who underwent continuous EEG monitoring,[1]CBFV was monitored in the middle cerebral artery using transcranial Doppler ultrasound during 159 spontaneous clinical or electroencephalographic seizures in 32 children. Change in CBFV was compared with time to localize pain and to sit as well as with mortality.

Results: Median ictal increase from pre-ictal CBFV was 13% (range -69 to 215%), significantly lower than reported in the literature. CBFV did not increase >5% during 61 (38%) seizures (all types including generalized tonic-clonic). In univariable multilevel analysis of 159 seizures within 32 patients, lower pre-ictal CBFV, longer seizure duration, longer time since admission, higher pre-ictal MAP, lower temperature, higher glucose, higher pCO_2 and lower pH were significantly associated with a greater percentage change in CBFV during a seizure. In the multivariable model, lower pre-ictal CBFV (coefficient -1.070, 95% confidence intervals (CI) -1.30, -0.84; p=0.00001), higher pre-ictal MAP (coefficient 0.313, 95%CI 0.01, 0.62; p=0.0435) and longer seizure duration remained independently associated with increased percentage change in CBFV. Seventeen children survived, 3 with poor outcome. In Cox regression, greater minimum percentage change in CBFV during the seizures observed over the first 5 days predicted shorter time to localize (hazard ratio 1.013, 95%CI 1.004, 1.022) and to sit (hazard ratio 1.011, 95%CI 1.001, 1.018). For time to death, only hypoxic-ischaemic aetiology was an independent predictor (HR 2.92, 95%CI 1.0006, 8.48, p=0.049).

Conclusions: In unconscious children the increase in CBFV is lower than expected, perhaps because the cerebral circulation is close to maximal vasodilatation. Matching of CBF to metabolic demand during seizures cannot be assumed and reduced haemodynamic reserve is a possible mechanism for ischaemic brain damage and poor neurological outcome in survivors.

1: Kirkham FJ, Wade AM, McElduff F, Boyd SG, Tasker RC, Edwards M, Neville BG,

Peshu N, Newton CR. Seizures in 204 comatose children: incidence and outcome.

Intensive Care Med. 2012 May;38(5):853-62.

CORTICAL GLUCOSE HYPOMETABOLISM CORRELATES WITH DECREASED CORTICAL THICKNESS IN CORTICOBASAL DEGENERATION: [18F]FDG PET AND MRI STUDY

C.S. Lee[1], S.M. Kim[1], S.J. Kim[1], J.S. Kim[2], J.M. Lee[3]

[1]Neurology, [2]Nuclear Medicine, University of Ulsan College of Medicine, Asan Medical Center, [3]Biomedical Engineering, Hanyang University, Seoul, Republic of Korea

Background: Corticobasal degeneration (CBD) is uncommon tau parkinsonian disorder, characterized by asymmetric limb apraxia and parkinsonism along with impairment in speech and cognition. Pathology shows asymmetric frontoparietal atrophy with a varying extent of neural degeneration in the basal ganglia and thalamus. We investigated regional pattern of cortical atrophy *in vivo* using [18F]FDG PET and 3.0T MRI.

Methods: We studied 29 patients with CBD (age=70.1±5.5 years, mean±SD) and 18 patients with progressive supranuclear palsy (PSP; age=68.4±7.0). Fifteen healthy subjects were included as normal control group (age=60.3±6.34). [^{18}F]FDG PET and 3.0T MRI were performed for all subjects. Regional glucose metabolism was obtained from the ratio using V1 area as a reference. Cortical thickness was obtained from MRI data using automated surface-based analysis. Z-scores were obtained in each region for correlation analysis of glucose metabolism and cortical thickness.

Results: In [^{18}F]FDG PET studies, CBD patients showed highly significant hypometabolism ($p< 0.01$) in middle and inferior frontal gyri, medial superior frontal gyrus, supplementary motor area, and anterior cingulate cortex. In contrast, patients with PSP showed significant hypometabolism only in superior frontal gyrus, caudate and thalamus. In MRI studies, CBD patients showed highly significant reduction of cortical thickness ($p< 0.01$) in superior and middle frontal gyri, supplementary motor area, pre- and postcentral gyri, inferior parietal lobule, and middle cingulate cortex. PSP patients showed highly significant reduction of cortical thickness only in superior medial frontal cortex. In CBD patients, regression analysis of z-scores revealed significant correlations between glucose hypometabolism and cortical thickness in each region with significant changes.

Conclusions: Glucose hypometabolism in [^{18}F]FDG PET and cortical thickness obtained from MRI showed similar regional pattern of cortical atrophy in CBD, with significant correlation between the two measurements. These data indicate that both measurements can be used to assess cortical atrophy *in vivo* in patients with CBD.

SUBSTANCE P LEVEL AS A MARKER OF DYSPHAGIA IN POST-STROKE PATIENTS

S. Matsumoto[1,2], M. Shimodozono[1], R. Miyata[1], K. Toyama[2], K. Kawahira[1]

[1]Department of Rehabilitation and Physical Medicine, Kagoshima University, [2]Department of Rehabilitation, Kirishima Rehabilitation Center of Kagoshima University Hospital, Kirishima City, Japan

Background and aim: Aspiration pneumonia is a serious health concern in post-stroke patients. Neurogenic components, such as neurotrophic factors and neuropeptides, are probably involved in the pathogenesis of dysphagia via the neurological system. Substance P (SP) is an excitatory neuropeptide that acts via the neurokinin-1 (NK-1) in the nervous system. Thus, we hypothesized that SP would be associated with declined swallowing function in post-stroke patients. The aim of this study was to evaluate the levels of SP in the plasma of post-stroke patients and to examine their possible correlation with swallowing function.

Methods: We measured plasma levels of SP by an immunoenzymatic assay in 60 patients with stroke (mean age ± standard deviation [SD], 64.8 ±10.2 years), and compared them with 32 age-matched post-stroke patients without dysphagia as the controls (mean age ± SD, 62.2 ± 9.8 years). The severity of the swallowing function in post-stroke patients was evaluated using the dysphagia handicap index (DHI).

Results: Patients with dysphagia had significant decreases in plasma levels of SP compared with controls (43.8 ± 20.4 pg/mL vs. 92.2 ± 30.2 pg/mL, P < 0.01). There was a significant correlation of plasma SP levels and severity of swallowing function.

Conclusions: These findings suggested the need for intensive observation for prevention of aspiration pneumonia in post-stroke patients. In addition, these data are valid to support the hypothesis of a systematic involvement of SP in post-stroke patients. Therefore, SP may be useful markers of dysphagia in patients with stroke.

THIRD VENTRICLE MORPHOLOGY AS A PREDICATOR OF ENDOSCOPIC THREE VENTRICULOSTOMY SUCCESS

X.F. Min

Neurosurgery, Taishan Medical University, Taian, China

Object: To explore the anterior three ventricular wall and the lower wall morphology in predicting whether endoscopic three ventriculostomy success or not.

Method: Pre-and postoperatong image, combined wth measuring f anterior and inferior wall shift distance and the preoperative and postoperative Evan´ index, were analysed restrospectively. Their correlation were discussed.

Results: The floor of the three ventricle appears bulge shape change and their clinical symptoms improved greatly, There is statistical significance between the three ventricle shift distance and Evan´ index

Conclusion: Three ventricle wall bulge can be used as a predictive indicators success of three ventriculostomy in obstructive hydrocephalus.

HEMISPHERIC ASYMMETRY OF CEREBROSPINAL FLUID CIRCULATION AND OF SKULL BIOMECHANICS

Y.E. Moskalenko[1], G.B. Weinstein[1], N.A. Ryabchikova[2], P. Halvorson[3], T.C. Vardy[4], T.I. Kravchenko[5]

[1]Brain Circulatory Laboratory, Sechenov Institute Russian Academy of Sciences, St. Petersburg, [2]Biological Faculty, Moscow State University, Moscow, Russia, [3]Research, PCOM, Philadelphia, PA, USA, [4]Faculty of Health, Queensland University of Technology, Brisbane, QLD, Australia, [5]Clinical Deprtment, Russian School of Osteopathic Medicine, St. Petersburg, Russia

Introduction: The craniospinal space filled with cerebrospinal fluid (CSF) represents a unified system when comparatively slow CSF circulatory processes are considered, but during rapid CSF replacements some anatomical peculiarities of the brain cavities and their interconnections, as well as peculiarities of skull structures, play a definite role. The resulting right-left asymmetry of CSF circulation inside the hemispheres may influence volume compensation by cerebrovascular control processes. This study aims to reveal on the systemic level and by non-invasive means the presence of hemispheric asymmetry of CSF circulation and skull biomechanical properties and to evaluate their possible role in cerebral circulatory-metabolic supply under normal conditions and in cases of pathology.

Methods: Investigations of hemispheric asymmetry of CSF circulation and skull biomechanics were conducted using Transcranial Dopplerography(TCD) - “MultiDop-P”(Germany) and Rheoencephalography(REG) - ”Mitsar”(Russia). The TCD probe was focused on basement of the MCA; REG electrodes were placed in the fronto-mastoid position. These methods were applied to both brain hemispheres simultaneously to regions supplied by the MCA. The signals recorded, via analogue-digital transformer “PowerLab-8”(AD Instrument, Australia) were input to PC“Windows XP”. Data was analysed using “PowerLab -8”(Chart 5) adapted for the study allowing calculation in standardized units of the coefficients of pulsatile skull pliability and CSF movements and evaluation of low frequency intracranial fluctuations. Slow

fluctuations of investigated processes was evaluated spectrum analysis. 46 healthy persons of both sexes between ages 20-55 were investigated. Recordings were sampled at rest and during functional tests directed to the cerebrovascular system using hypoxic, hyperoxic and hypercapnic gases and to the CSF system via the Stookey and Valsalva manoeuvres.

Results: Under resting conditions the indices of CSF mobility and skull biomechanics, evaluated by its pliability to intracranial pressure, are characterized by marked inter-hemispheric asymmetry, which expresses the differences of CSF mobility. The coefficient of asymmetry (right/left ratio of CSF mobility) was found to be 1.25—1.45 in healthy middle-age persons. The coefficient of hemispheric asymmetry of skull pliability was 0.75—0.95. These coefficients are characterized by reciprocal relationships. They demonstrate no dominance related to right/left hemispheres. No correlation with neuro-physiological indices was found. Functional tests gave rise to significant changes of these values and the dominance of asymmetric coefficients. In older subjects the magnitudes of these coefficients decreased. Low frequency (0.10-0.25Hz) spectral diagrams, presumably associated with brain metabolism, were obtained from 90s of simultaneous TCD-REG fragments. Hemisphere asymmetry was observed in the spectrum as different amplitudes (up to 50%) of certain peaks and, in some cases, the appearance of additional peaks in only one hemisphere. Hemispheric asymmetry decrease with age and significantly diminish in ages after 60-ty.

Conclusion: The source of inter-hemisphere asymmetry of the CSF dynamics and skull biomechanical properties may lie in structural peculiarities of the skull and intracranial media. Hemispheric asymmetry may reflect a special mechanism contributing to the process of circulatory-metabolic support of brain functioning.

Reference: Yu Moskalenko et al. “Changes of circulatory-metabolic indices and skull biomechanics with brain activity during aging” Journal of Integrative Neuroscience, Vol. 10, No. 2 (2011) 131-160.

IMPROVED CEREBRAL HEMODYNAMICS AND FUNCTION OF MOYAMOYA DISEASE WITH USE OF PET GUIDED INDIRECT-BYPASS SURGERY

T. Nariai[1], M. Inaji[1], S. Image[1], M. Mukawa[1], Y. Ishii[1], T. Kudo[1], Y. Tanaka[1], T. Maehara[1], K. Ishiwata[2], K. Oda[2], K. Ishii[2]

[1]Neurosurgery, Tokyo Medical and Dental University, [2]Positron Medical Center, Tokyo Metropolitan Institute of Gerontology, Tokyo, Japan

Introduction: We have been using positron emission tomography (PET) to treat patients with moyamoya disease (MMD) in these 20 years. We reported that PET measured parameters is useful to evaluate the degree of hemodynamic impairment and degree of neovascularization induced by indirect-bypass surgery (Nariai et al. Stoke 1994 and JNNP 2005). In these ten years, we started to use PET prospectively to determine the surgical indication and the methods of surgery.

Methods: From 1991 to the present, 190 patients with MMD (9-58 y/o) underwent quantitative PET measurement of cerebral blood flow (CBF), blood volume (CBV), oxygen extraction fraction (OEF) and cerebral metabolic ratio for oxygen ($CMRO_2$) by inhalation of ^{15}O-oxygen gases and arterial blood sampling. Using the data of earlier 57 patients, threshold value of each parameters was set to determine the surgical indication with indirect bypass surgery. Surgical strategy after 2001 was also modified and the area showing hemodynamic stress (elevated OEF and CBV) was operated with combined use of several indirect bypass techniques. Post operative PET scan was performed in all operated patients approximately 1 year after surgery.

Results:

1) In the earlier period, 30 of 57 (53%) patients were operated based on clinical symptom. In the latter period, 42 of 133 (32 %) patients were operated using PET data as determinant.

2) Pre- and Post-operative PET data of patients treated before 2001 indicted that CBF significantly increased among frontal lobe, but $CMRO_2$ significantly decreased in parieto-occpital lobe. In the recent patients, CBF and $CMRO_2$ significantly increased among frontal,

temporal, parietal and occipital lobe together with significantly decreased OEF.

4) In both periods, CBV significantly decreased among widespread cerebral area including basal ganglia.

5) Permanent deficit caused by perioperative infarction decreased in recently treated cases (2 out of 30 (6.6%) in earlier and 0 in recent cases). Surgical mortality was 0 in both periods.

Conclusions: Quantitative measurement of cerebral hemodynamics of MMD with PET and surgical treatment using indirect bypass technique based on them was useful in selecting surgical candidates and in performing effective and safe surgery to ameliorate cerebral blood flow and function.

GLYCO-PROTEOMIC STUDY OF THERAPEUTIC HYPOTHERMIA IN GLOBAL ISCHEMIC BRAIN INJURY POST CARDIAC ARREST

J. Cao, F.S. Buonanno, K. Feeney, M. Elia, H. Koop, D. McMullin, S.-Z. Guo, K. Arai, E.H. Lo, **M. Ning**

Neurology, Clinical Proteomics Research Center and Neuroprotection Research Laboratory, Massachusetts General Hospital, Harvard Medical School, Boston, MA, USA

Background: Global ischemic brain injury post cardiac arrest is prevalent with dismal prognosis -- less than 10% survive to hospital discharge. Therapeutic hypothermia (TH) is an efficacious neuroprotective treatment, protects against multi-organ damage, doubles the chance of good neurologic outcome and decreases mortality by 25%, but is grossly underutilized (< 5%). We use a glyco-proteomic approach to better understand and predict TH response, because: 1) glycosylation is one of the most important and common extracellular post-translational modifications in immunity and coagulation, and is crucial in TH-related side effects such as sepsis and bleeding; 2) it occurs rapidly over the time window of treatment; and 3) it can be used to focus proteomic profiling by targeting specific plasma signals.

Methods: Lectin array and various lectin immunoblots were used to study plasma glycosylation patterns of TH patients (24 hrs post cardiac arrest) with good vs poor clinical outcome (evaluated at 3 months post event). To identify and enrich candidate plasma proteins with potential clinical utility, specific lectin affinity chromatography and LC-MS/MS were performed.

Results: Plasma glycosylation patterns differ dramatically with respect to clinical outcome in TH-treated patients. On screening lectin blots (figure), whereas SBA showed little change, RCA (decreased around 35-100kD - in box) and ConA (increased around 40-150kD - in box) were different in a wide range of MW, and WGA identified unique banding around 100kD (in box) in TH responders. In lectin affinity pull-down, more than 400 specific glycoproteins were identified showing significant changes with respect to TH outcome.

Conclusion: A glyco-proteomic approach is promising to help predict neurologic outcome, select TH responders, and triage hypothermic therapy in global ischemic brain injury patients post cardiac arrest. Further studies are under way to investigate these exploratory findings.

PLASMA PROTEOMIC CHANGES PERSIST IN LONG TERM FOLLOW-UP OF PATENT FORAMEN OVALE RELATED STROKE PATIENTS AFTER PFO CLOSURE

M. Ning, M. Lopez, D. Sarracino, K. Feeney, M. Thayer, M. Elia, H. Koop, D. McMullin, Z. Demirjian, I. Inglessis-Azuaje, S. Silverman, G.W. Dec, I. Palacios, E.H. Lo, F.S. Buonanno

Neurology, Clinical Proteomics Research Center and Neuroprotection Research Laboratory, Massachusetts General Hospital, Harvard Medical School, Boston, MA, USA

Introduction: Paradoxical embolism from patent foramen ovale (PFO), a heterogeneous multi-organ condition involving brain, lung, heart and blood, lacks consensus for treatment options due to variability among individual patients. Clinical proteomic approaches may be promising for such complex diseases, where the disease process can be monitored in clinically accessible fluid such as blood. Here, we apply a pharmaco-proteomic approach to study PFO endovascular closure, an intervention that requires better risk stratification and monitoring of therapeutic efficacy to individualize treatment. Previously, we found that plasma small molecule signals such as serotonin (5HT) -- which may avoid pulmonary filtration via PFO -- decrease immediately in

the systemic circulation after effective PFO closure. Now we study the long-term effect of PFO endovascular closure.

Methods and results: To reduce confounders in an inherently complex system, the most robust clinical proteomic comparisons are those of profiles taken over time from the same individual. Accordingly, in consecutively recruited patients who underwent PFO closure, we analyze venous blood obtained prior to closure and in long-term followup (>1 year) post closure. None of the subjects experienced recurrent TIA or strokes. More than 1 year post closure, plasma protein profiles continue to show a statistically significant ($p< 0.05$) decrease of coagulation markers such as fibrinogen, fibrinogen fragments, D-dimer and others. Moreover, markers of inflammatory changes such as hsCRP, apolipoproteins and various immunoglobulins also remain decreased.

Conclusion: We found that a pharmaco-proteomic approach is clinically feasible and may help to monitor therapeutic efficacy, improve patient selection, and ensure more precise clinical phenotyping for clinical trials in PFO-related stroke. More than 1 year post PFO closure, inflammatory and coagulation factors remain lowered after adjusting for other confounders such as medication changes. Further studies are needed to explore the utility of proteomic profiling to help individualize treatment in PFO-related strokes.

DURAL ARTERIOVENOUS FISTULA ASSOCIATED WITH HEMANGIOPERICYTOMA IN TRANSVERSE SINUS

M. Oda[1], T. Sasajima[1], M. Takahashi[1], T. Ono[1], S. Takahashi[2], K. Mizoi[1]

[1]Department of Neurosurgery, [2]Department of Radiology, Akita University Graduate School of Medicine, Akita, Japan

Introduction: The pathogenesis of dural arteriovenous fistura (dAVF) is still unclear, while various mechanisms of the development of these lesions have been proposed. Although some dAVFs discovered during infancy may be congenital, most lesions are thought to be acquired. The coexistence of intracranial tumors and dAVFs has been reported and tumor causing occlusion of major sinuses is rarely associated with dAVF. Experimental studies suggested a role of angiogenic growth factors (vascular endothelial growth factor: VEGF, basic fibroblast growth factor, etc) in the genesis of dAVF. We report a rare case of thrombosis of the transverse sinus associated with a hemangiopericytoma, which demonstrated positive staining for VEGF, resulting in a transverse-sigmoid sinus dAVF.

Case description: A 37-year-old male presented with a one-week history of vertigo and nausea. Neurological examination revealed left-sided dysmetria. Contrast-enhanced T1-weighted MR imaging revealed a homogeneously enhancing tumor in the left cerebellum and hydrocephalus. The tumor had a broad attachment to the left transverse sinus and invaded it, leading to its severe stenosis and presumably resulting in an associated dAVF. Vertebral angiogram demonstrated moderate tumor staining fed by left superior cerebellar artery (SCA) and posterior inferior cerebellar artery. The fistura was fed by not only tumor feeding arteries but also the left occipital, middle meningeal, auricular and ophthalmic arteries and drained into the left sigmoid sinus and occipital cortical veins (Cognaud type II a+b). First, the patient underwent transarterial embolization of the left occipital artery preoperatively and partial removal of the cerebellar tumor followed by continuous ventricular drainage. The histological diagnosis was hemangiopericytoma. We observed moderate staining for VEGF in the tumor cells. The MIB-1 positive rate was 13.7%. Neurological symptoms were improved after the initial operation. Second, the patient underwent transarterial embolization of a branch of left SCA and total removal of the residual tumor and affected sinus with tumor invasion. The tumor was completely resected and immunoreactive for VEGF. The MIB-1 positive rate was 19.4%. Fourteen months after postoperative radiotherapy (60Gy to the tumor bed), the patient has been free of symptoms, showing no evidence of tumor recurrence on follow-up MR imaging. Two weeks after the second operation, MR digital subtraction angiography (DSA) revealed residual dAVF draining into the left sigmoid sinus, but no residual dAVF has been noted on MR DSA 3 months after the second operation. We encountered a case of the disappearance of residual dAVF of the transverse-sigmoid sinus after removal of the associated hemangiopericytoma, and speculated that the VEGF secreted by the tumor as well as venous outflow obstruction might contribute to occurrence of the acquired dAVF.

Conclusions: The findings of present case supports that dAVFs are acquired and induced lesions and not only venous hypertension due to venous obstruction but also the VEGF secreted by the tumors may participate in genesis of dAVF. In hemangiopericytomas associated with the dural sinuses, diagnostic evaluation for possible dAVFs should be considered. Treatment of these lesions should be based on contributing factors, since spontaneous resolution after tumor excision has been documented.

FOLLOW-UP STUDY OF SPONTANEOUS INTRACRANIAL ARTERIAL DISSECTIONS

H. Ono, H. Nakatomi, H. Imai, N. Saito

Department of Neurosurgery, Faculty of Medicine, The University of Tokyo, Tokyo, Japan

Background: Symptoms of spontaneous intracranial dissection (IAD) are mainly divided into hemorrhagic and non-hemorrhagic ones, the former is subarachnoid hemorrhage (SAH) and the latter are headaches or ischemic stroke. For patients with SAH, early repair of the affected vessels by open surgery or endovascular technique tends to be performed, while conservative treatments has been advocated for non-hemorrhagic IAD. However, the long-term clinical course of IAD, which should influence clinical decision-making, is poorly understood. In this study, we performed follow up of 143 patients with acute IAD.

Method: From April 1980 to December 2000, 143 patients were diagnosed with acute IADs at our institutions. All cases satisfied one of the three diagnostic criteria for acute IAD: 1) the typical pearl and string or double lumen sign at a non-branching site of the intracranial cerebral arteries on angiography; 2) fusiform dilatation with retention of contrast medium or angiographic steno-occlusive lesions accompanied by intramural hemorrhage detected on MRI at the same region; or 3) histopathologically confirmed IAD. We defined symptomatic recurrence as any neurological symptoms due to recurrent arterial dissections after initial stroke.

Result: The ages of the 143 patients ranged from 7 to 83 years (mean 50.7 years). There were 85 men and 58 women. 31 cases of IADs were located in the anterior circulation, while 112 cases were in the posterior circulation. The patients were divided into two groups based on their initial presentation: the hemorrhagic group presenting with SAH (86 patients, 60%), and the non-hemorrhagic group presenting with headache or neurological symptoms caused by brain ischemia (57 patients, 40%). The mean ages of the hemorrhagic and non-hemorrhagic groups were 52.8 and 47.5 years, respectively. Male patients were predominant in both groups. Follow-up periods ranged from 1 day to 25 years (mean 8.2 years). The recurrence occurred 0 day to 7 years after the initial dissection. Of 86 cases initially presenting with hemorrhage (SAH), 35 developed hemorrhagic recurrence with a mean interval of 4.8 days, and 2 developed non-hemorrhagic recurrences after 21 and 85 months, respectively. Of 10 patients initially presenting with non-hemorrhagic symptoms, 1 developed SAH 4 days after the initial ischemic event, and 9 developed non-hemorrhagic recurrence with a mean interval of 8.6 months. Clinical characteristics of patients with symptomatic recurrence and significant risk factors of patients with recurrent intracranial arterial dissections are shown in table1 and 2, respectively.

Table 1. Clinical characteristics of patients with symptomatic recurrence

Initial presenting symptom	Recurrent dissection	Case number	Recurrent presenting symptom	Case number	Time to recurrence (mean, range) (days)
Hemorrhagic: 86	No	49	N/A	49	N/A
	Yes	37	Hemorrhagic:	35	4.8, 0-26
			Non-hemorrhagic: minor stroke	1	630, N/A
			Non-hemorrhagic: mass effect	1	2555, N/A
Non-hemorrhagic: 57	No	47	N/A	47	N/A
	Yes	10	Non-hemorrhagic	9	257, 2-1377
			Hemorrhagic	1	4, N/A
N/A, data not available					

[Table 1]

Table 2. Significant risk factors of patients with recurrent intracranial arterial dissections			
Hemorrhagic group			
	Recurrence(+): 37	Recurrence(-): 49	p-value
Initial clinical grade: WFNS>3	27	22	*0.0081
GOS (>6 months): independent	9	38	*< 0.0001
Age >50	26	21	*0.0100
Non-hemorrhagic group			
	Recurrence(+): 10	Recurrence(-): 47	p-value
Lesion location: ICA	3	2	*0.0334
NIHSS >6	5	8	*0.0383
WFNS, World Federation of Neurological Surgeon's clinical grade; GOS, Glasgow outcome scale; ICA, internal carotid artery; NIHSS, National Institute of Health Stroke Scale; *Statistically significant on either the chi-square test or Fisher's exact probability test.			

[Table 2]

Discussion: The present study demonstrated that IAD is a disease carrying a relatively high risk of symptomatic recurrence (33%), which occurs in three phases: early recurrence within 1 month, mainly causing hemorrhagic events; late recurrence mainly presenting with non-hemorrhagic symptoms; and chronic fusiform aneurysm transformation. Knowledge on this three-phase recurrence patterns is important in decision-making of treatment and follow-up of IAD.

Reference: Ono H, Nakatomi H, et al. Stroke 2012 Nov 29. [Equb ahead of print]

CYTOFLAVIN ANTIOXIDANT THERAPY IMPROVES CLINICAL, MRI AND ELECTROENCEPHALOGRAPHY PARAMETERS IN ACUTE ISCHEMIC STROKE

A. Orlova[1], S. Rumiantseva[2], E. Silina[1], S. Bolevich[1]

[1]I.M. Sechenov First Moscow State Medical University (MSMU), [2]The Russian National Research Medical University named after N.I. Pirogov (RNRMU), Moscow, Russia

Objective: To evaluate the efficiency of Cytoflavin (CF), a metabolic drug with antihypoxic and antioxidative properties in acute ischemic stroke based on clinicopathologic and electroencephalographic parameters.

Patients and methods: Thirty six patients admitted to the hospital within 24 hours of acute cerebral ischemic stroke were randomized to Control group (n=17, age 58,6±11,2, male 52,9%) receiving conventional therapy, and Intervention group (n = 19, age 62,4±9,6, male 57,9%) receiving conventional therapy plus CF (days 1-10 - 20 ml iv; days 11-35 - 2 tab. orally twice a day).

Neurological status on NIHSS scale, Glasgo scale, Rankin scale, Bartel index; MRI and EEG were assessed on days 1, 5, 10, 20 and 35. FR formation in plasma was measured by oxidative (chemiluminescence intensity index - basal (CIIb) and zymosane-stimulated (CIIs)) and lipid peroxidation markers (anti-peroxide plasma activity (APA), malondialdehyde (MDA).

Results: Improved recovery of consciousness and neurological function in intervention group was observed by day 20. There was a smaller infarct volume increase in the intervention group compared to the control group both on day 5 (control group, 35,9%; intervention group 26,7%, p< 0,05 compared to control group), and on day 20, (control group: 16%, intervention group: 1%, p< 0,05 compared to control group). Hemorrhagic transformation showed strong correlation with MDA (day 5, r=0,565; p< 0,05), CIIb (day 1 r=-0,311; day 10 r=-0,548; both p< 0,05), CIIs (day 1 r=-0,349; day 10 r=-0,501; both p< 0,05). Increase of infarct volume on day 1-20 correlated strongly with APA (r=-0,516; p< 0,05), MDA (r=0,624; p< 0,05) and CIIb (r=-0,517; p< 0,05) plasma levels. . On day 1 EEG revealed changes of basal rhythm with increase in total power of slow-wave activity and appearance of pathologic focal activity in 94% of patients. Total signal power on days 1,5,10 and 20 was 149, 132, 121, 116 relative units in control group and 156, 128, 115, 102 r.u. in intervention group, which correlated with decreased period of unconsciousness in patients, receiving CF. On discharge in intervention group on EEG dominated beta-activity of moderate magnitude, reflecting more preserved haemodynamics. Spectrum analysis of EEG revealed marked asymmetry of alfa-rhythm in 59% of patients, by day 20 it decreased to 41% in intervention group and 49% in control group. CF treatment resulted in improved functional outcome in stroke patients on days 20 and 35 (p< 0,05 vs. control group).

Conclusion: Indices of free radical formation are considered early markers of morphologic changes in ischemic stroke lesion, with APA and MDA being the most sensitive ones. Early energocorrective and antioxidant treatment with CF in addition to conventional therapy in patients with acute cerebral infarction has a favourable effect on clinico-morphologic, EEG values and treatment outcome.

ELEVATED THYROID AUTOANTIBODIES IN YOUNG STROKE PATIENTS WITH INTRACRANIAL LARGE ARTERY STENOSIS (ILAS): A RETROSPECTIVE STUDY

Z. Shi, X. Zhang, Z. Chen, M. Lou

Department of Neurology, The 2nd Affiliated Hospital of Zhejiang University, School of Medicine, Hangzhou, China

Objectives: To investigate the association between thyroid autoantibodies and intracranial large artery stenosis in young stroke patients with apparent euthyroid states.

Methods: We retrospectively reviewed the first-onset ischemic stroke patients (age≤55) consecutively admitted to our department. Intracranial large artery stenosis (ILAS) was defined as a reduction of ≥50% in luminal diameter of any of the intracranial large arteries. We compared demographic profiles, risk factors, thyroid function test, and thyroid autoantibodies including antithyroperoxidase antibody (TPO-Ab), and antithyroglobulin antibody (TG-Ab)) between patients with and without ILAS. We also performed multivariate logistic regression analysis to evaluate the association between thyroid autoantibodies and ILAS.

Results: A total of 360 patients were analyzed. The mean age of the patients was 47.1±7.7 (range,10-55 years) and 257 (71.4%) patients were male. We identified ILAS in 107 patients (29.7%). Patients with ILAS showed a higher frequency of elevated TG-Ab levels and elevated TPO-Ab levels respectively in comparison with non-ILAS group (9.3% versus 2.4%, p< 0.01; 20.6% versus 2.8%, p< 0.001, respectively). After adjusting for covariates, the presence of elevated TPO-Ab levels (OR:11.719; 95% CI: 4.325-31.758, p< 0.001), age (OR: 1.052; 95% CI: 1.013-1.093, p=0.008) and current smoker (OR:0.504; 95% CI: 0.298-0.850, p=0.01) were independently associated with ILAS.

Conclusions: Thyroid autoantibodies may be associated with the development of intracranial large artery stenosis in young stroke patient, which may help to explore the immune pathogenesis of intracranial large artery stenosis and allow the clinician to evaluate intracranial vessels in young patients with elevated thyroid autoantibodies.

MONTREAL COGNITIVE ASSESSMENT FOR TRAUMATIC BRAIN INJURY PATIENTS WITH INTRACRANIAL HAEMORRHAGE

G.K.C. Wong[1], K. Ngai[2], W.S. Poon[2]

[1]Neurosurgery, [2]The Chinese University of Hong Kong, Hong Kong, Hong Kong S.A.R.

Objective: In recent years, the Montreal Cognitive Assessment (MoCA) has been developed to assess patients with ischemic stroke. However, it has not been validated for use on traumatic brain injury patients with intracranial hemorrhage (tICH). Our aim was to evaluate the psychometric properties of the MoCA (MoCA) in such patients.

Research design and method: We carried out a cross-sectional observational study on 40 controls and 48 tICH patients recruited in Hong Kong. Concurrent validity was assessed by a comprehensive battery of neuropsychological tests and the Mini-Mental State Examination (MMSE). Criterion validity was assessed by the differentiation of tICH patients from controls.

Main outcome and results: In tICH patients, cognitive z scores (β=0.579; p< 0.001) and MMSE (β=0.366, p=0.012) significantly correlated with performance in the MoCA after adjustment for age, gender, and total score for the Geriatric Depressive Scale. For the differentiation of tICH patients from controls, analysis of receiver operating characteristics curves in the MoCA revealed an optimal balance of sensitivity and specificity at 25/26 with an area under the curve of 0.704 (p=0.001). MoCA is applicable to and significantly correlated with excellent neurological outcome in tICH patients.

Conclusions: MoCA is a useful and psychometrically valid tool for the assessment of gross cognitive function in tICH patients.

EXTENT OF EARLY CEREBRAL INFARCTION AFTER ANEURYSMAL SUBARACHNOID HEMORRHAGE: RISK FACTOR AND PROGNOSTIC SIGNIFICANCE

G.K.C. Wong[1], J. Leung[2], J. Yu[2], D. Siu[2], S. Lam[3], W.S. Poon[3]

[1]Surgery, The Chinese University of Hong Kong, [2]Prince of Wales Hospital, [3]The Chinese University of Hong Kong, Hong Kong, Hong Kong S.A.R.

Background: Aneurysmal subarachnoid hemorrhage (SAH) is a serious disease with high case fatality and morbidity. Delayed cerebral infarction was proposed to be the surrogate if not an important cause of poor outcome. Recently, early cerebral infarction was recognized as a risk factor for poor outcome.

Objectives: We aimed to assess the impact of extent of early and delayed cerebral infarction on outcomes of aneurysmal subarachnoid hemorrhage at three months.

Methods: We prospectively enrolled consecutive aneurysmal subarachnoid hemorrhage (SAH) patients presenting to an academic neurosurgical referral center (Prince of Wales Hospital, the Chinese University of Hong Kong) in Hong Kong. The study was approved by Joint CUHK-NTEC Clinical Research Ethics Committee. All images are reviewed by 2 blinded radiologists. Extent of early and delayed cerebral infarction was the sum scores of the bilateral modified ASPECTS (Alberta Stroke Programme Early CT Score) and posterior circulation Acute Stroke Prognosis Early CT Score (pc-ASPECTS). A third radiologist adjudicator independently assessed the infarct extent when discrepancy arose among the 2 reviewers. Clinical outcome assessments were carried out 3 months after ictus by trained research assistants (psychology graduates) blinded to other clinical data.

Results: Cerebral infarction occurred in 24(48%) patients, in which 14(27%) were early and 14(28%) were delayed respectively. Extent of early cerebral infarction correlated with CT Hijdra SAH Score (OR -0.06, 95%CI: -0.13 to 0.00, P=0.050), while extent of cerebral infarction correlated with Glasgow Coma Scale on admission (OR -0.21, 95%CI: -0.34 to 0.02, P=0.030). After adjustments for age and admission World Federation of Neurosurgical Societies grade, extent of early cerebral infarction predicted outcome at three months [modified Rankin Scale (OR 0.42, 95%CI: 0.19 to 0.65, P=0.001), Lawton Instrumental Activity of Daily Living (OR -1.61, 95%CI: -2.66 to -0.57, P=0.003), Mini-Mental State Examination ((OR -2.29, 95%CI: -4.04 to -0.54, P=0.012), and Montreal Cognitive Assessment]. (OR -2.61, 95%CI: -4.31 to -0.91, P=0.004). Extent of delayed cerebral infarction was not significant in the multivariable analyses.

Conclusions: Our data supported that early cerebral infarction was related to the severity of subarachnoid hemorrhage and had prognostic significance.

PERIPHERAL CROSS-NEUROTIZATION INDUCING UNAFFECTED HEMISPHERE REORGANIZATION TO ENHANCE THE MOTOR CONTROL OF THE SPASTIC HEMIPLEGIC HAND IN CENTRAL NEUROLOGIC INJURY

W.-D. Xu

Department of Hand Surgery, Fudan University, Shanghai, China

Background: Central neurologic injury resulting from different etiological factors (stroke, traumatic brain injury, cerebral palsy) is the main cause of long-term disability. Spontaneous motor recovery would occur at the acute stage predominantly in the initial weeks to the first three months, but continue at a slower pace throughout the years. The activation of ipsilateral motor structures, including primary motor and premotor cortex has been reported to be beneficial to the performance in the chronic stage of central neurologic injury. It could be a novel approach to the medical problem to enhance the unaffected hemisphere control. Our research on brachial plexus roots avulsion demonstrated that ipsilateral motor cortex was capable of controlling both the affected and healthy hand following the peripheral cross-neurotization. Based on the discovery, peripheral cross-neurotization was performed to treat the hemiplegic hands after central neurologic injury for the first time.

Methods: The peripheral cross-neurotization was performed on six spastic hemiplegic patients suffering from different etiological factors such as peri-operative stroke, perinatal asphyxia and central nervous system infection,

whose affected arm's function had made little improvement despite their regular outpatient physical and occupational therapies. The six patients were examined for a 24-month period of follow-ups, the spastic evaluation conducted using Modified Ashworth Scale (MAS); the functional use of the affected arm evaluated based on Quality of Upper Extremity Skills Test (QUEST); the peripheral regeneration examined via electromyography; and the cortical reorganization investigated with transcranial magnetic stimulation (TMS), positron emission tomography (PET) and functional magnetic resonance imaging (fMRI).

Results: After a 24-months period of follow-ups, all the patients showed evident improvements in extension of the elbows and wrists; 2 of them showed great improvements in forearm rotation. Scores in both QUEST and MAS tests had been significantly improved at final visit, reflecting the peripheral cross-neurotization could strengthen extension power and improved the motor coordinate of the whole upper extremity in hemiplegia. Longitudinal PET correlation results showed that the intact hemisphere contributed to the motor recovery after surgical treatment. TMS and fMRI studies demonstrated that a new motor control focus of the paralyzed arm occurred in the ipsilateral motor area.

Conclusion: Peripheral cross neurotization to induce intrahemispheric cortical reorganization, as a novel surgical approach, could help control the affected hand in hemiplegia resulting from central neurologic injury. As indicated by the literature, it was the first time to treat the central neurologic injury at a peripheral level.

RISK FACTORS FOR VERTEBRAL ARTERY STENT-TREATED STROKE PATIENTS TO DEVELOP IN-SENT RESTENOSIS

J. Li, Y. Lin, M. Zhang, L. Qian, **Y. Xu**

Department of Neurology, Affiliated Drum Tower Hospital of Nanjing University Medical School, Nan Jing, China

Preventing stroke through endovascular treatment with vertebral artery stenting (VAS) remains a great challenge for the occurrence of an in-stent restenosis (ISR) and a lack of randomized controlled trials.

Methods: In this study, we conducted a retrospective analysis of 163 patients (191 arteries) that had been treated with stent between January 2004 and December 2011 in Nanjing Drum Tower Hospital. Patients were followed up at 3 months, 6 months, and 1 year after treatment and annually thereafter. We compared the cumulative long-term incidence of VSA and also identified risk factors for the development of ISR. DNA was extracted from blood for genotyping CYP2C19 (636G>A, 681G>A), CYP3A4 (894C>T), P2Y12 (34C>T, 52G>T).

Results: Our data demonstrated that a higher growth rate of in-stent restenosis were mainly within the first year after VAS treatment (4.05%), while no sharp increase occured in the long-term follow-up. A multiple binominal regression analysis showed that stroke patients with the habit of smoking, or complicated with hypertension or hyperlipidemia were easy to develop ISR (smoking 28.3% versus 50%, p=0.024; hypertension 77.2% versus 89.2%, p=0.038; Hyperlipidemia 26.9% versus 46.4%, p=0.039). The strongest statistically significant predictor for the development of a subsequent ISR after Logistic regression analysis was Hyperlipidemia (OR 4.305, 95% CI 2.988-18.761, p=0.042), and CYP2C19 (OR 0.521, 95% CI 0.17-0.699, p=0.035).

Conclusions: Higher growth rate of ISR occurs mainly within the first year after VAS treatment. Hyperlipidemia and CYP2C19 impotency are risk factors for VAS treated ischemic patients to develop ISR.

DIABETES-SPECIFIC ENTERAL NUTRITION MODULATION THE IMMUNE-FUNCTION AND INSULIN RESISTANCE AFTER ACUTE ISCHEMIC STROKE

X. Zhang, W. Heng, Y. Xu

Nanjing Drum Tower Hospital, Nanjing, China

Inflammation and insulin resistance (IR) both are important contributing mechanisms in ischemic stroke. However, little clinical study has been made to evaluate the influence of enteral nutrition on the immune status and IR after acute ischemic stroke. From January 2012 to June 2012, 90 acute brain infarction patients within 72 hours of onset with swallow dysfunction have been enrolled in this single-center, open-label study. All the patients were randomized to the diabetes-specific enteral nutrition treated group (dsEN) and normal enteral nutrition treated group (nEN). Both two

groups received the same foundation treatment. The circulating levels of nutritional markers, immune markers and the IR markers were compared at 0 (base line) and 14 days. In both two groups, the circulating levels of nutritional markers like prealbumin, transferring and albumin decreased after 14 days, but the changes were not significantly different compared to the base line. However, only in dsEN group, total cholesterol and HOMA-IR showed significant decrease between 14 days and the baseline (for TC decreased from 4.52±1.21mmol/L at baseline to 3.66±1.08 at 14 days, $p< 0.05$, HOMA-IR decreased from 5.77±7.42 at baseline to 4.72±3.02 at 14 days, $p< 0.05$). The percent of CD3+CD4+ T cells was 39.92±7.25 at baseline, and significantly increased to 45.96±10.27 after 14 days in dsEN group, and ratio of CD3+CD4+/CD3+CD8+ T cells also had an significant increase from 1.78±0.72 to 2.41±1.11 at 14 days ($p< 0.05$). While in nEN group, there were no changes about immune marker between baseline and 14 days later. The results of this study suggest that AeEN and nEN have a similar effect on nutrition, but the EN could reduce the insulin resistance and enhance the immune statue after acute ischemic stroke. However, these findings, warrant further studies on a larger scale, and evaluate the prognosis of the patients.

FAS LIGAND INDUCED BRAIN INFLAMMATION AFTER ISCHEMIC STROKE AND ATTENUATES BY HUMAN URINARY KALLIDINOGENASE

X. Zhang, Y. Xu

Nanjing Drum Tower Hospital, Nanjing, China

Inflammation is an important contributing mechanism in ischemic stroke. Fas ligand plays a critical role in post-stroke inflammatory responses. However, little progress has been made in clinical therapy, especial the treatment of inflammation after ischemic stroke. From 2010-2012, acute brain infarction patients within 72 hours of onset in the territory of anterior circulation artery have been enrolled in this study. All the patients were randomized to the HUK treated group (HP) and non HUK treated group (control group, CP). Both two groups received the same foundation treatment. In HP group, the patients received an intravenous transfusion of HUK once a day, for 10 days. The NIHSS index were used to evaluate neurological deficit at both day 0, days 10 and day 90. All patients were imaged with 3.0T MRI at both day 0 and day 10. The ischemic lesion area was measured by both DWI, PWI and FLAIR. The brain edema extent were compared. The blood samples were taken by all the patients for sFAL and inflammation factors detection at day 0, day 10 and day 90. We found: 1) 206 patients were enrolled in this study, 117 patients were in HP group and 89 patients were in CP group. The NIHSS index and brain edema extent show no significant difference between the HP group and CP group at day 2) sFAL could be detected in peripheral blood, and the level of sFAL had an significant increase at day 10 compared to day 0. Both inflammation cells and inflammation factors were increased at day 10 as compared to day 0. 3) As patients which received the HUK treatment, we observed the obvious improvement of NIHSS score, brain edema as well as inflammatory mediators. sFAL induced inflammation might contribute to the brain injury after ischemic stroke, and HUK protects against ischemic brain injury by inhibiting inflammatory response.

STREPTOCOCCUS PNEUMONIAE INFECTION DRIVES ATHEROGENESIS AND AUGMENTS CEREBROVASCULAR PATHOLOGIES IN ISCHAEMIA VIA IL-1- AND PLATELET-MEDIATED SYSTEMIC INFLAMMATORY MECHANISMS

A. Denes[1,2], J. Pradillo[1], C. Drake[1], P. Warn[3], K.N. Murray[1], B. Rohit[4], D. Dockrell[4], S. Francis[4], B. Nieswandt[5], N. Rothwell[1], S.M. Allan[1]

[1]Faculty of Life Sciences, University of Manchester, Manchester, UK, [2]Laboratory of Molecular Neuroendocrinology, Institute of Experimental Medicine, Budapest, Hungary, [3]University of Manchester, Manchester, [4]Department of Cardiovascular Science, Medical School, University of Sheffield, Sheffield, [5]Chair of Vascular Medicine, University Hospital and Rudolf Virchow Center for Experimental Biomedicine, University of Würzburg, Würzburg, UK

Objectives: Common bacterial infections contribute to the development of diverse non-communicating diseases and impair outcome after myocardial infarction or stroke. Infection by *Streptococcus pneumoniae* (S. *pneumoniae*) is a major cause of prolonged hospitalization and death of patients worldwide, but the mechanisms by which it

influences cardio- and cerebrovascular pathologies are not understood.

Methods: C57BL/6 and ApoE$^{-/-}$ mice fed high fat or control diet were intranasally infected with increasing doses of *S. pneumonia*e three times, over a six days course. Carotid atherosclerosis, systemic inflammatory changes were examined. In separate experiments, mice and obese, atherosclerotic corpulent rats were infected with *S. pneumoniae* and then subjected to transient middle cerebral artery occlusion to investigate the effects of preceding bacterial infection on stroke outcome.

Results: Persisting pulmonary infection by *S. pneumoniae* in rodents triggered atherogenesis, led to systemic upregulation of the cytokine interleukin-1 (IL-1) and profoundly (by 50-90%) exacerbated ischaemic brain injury in mice and rats. Infection-mediated cerebrovascular inflammation after experimental stroke was more severe in combination with old age and atherosclerosis. Systemic blockade of IL-1 with IL-1 receptor antagonist (IL-1Ra) fully reversed infection-mediated exacerbation of brain injury and impairment of sensori-motor function after cerebral ischaemia. Infection also facilitated platelet activation and microvascular coagulation in the brain after cerebral ischaemia. Blockade of GPIbα, a major adhesion molecule on platelets, reduced brain injury after experimental stroke in infected mice. Both GPIbα blockade and IL-1Ra reversed the induction of microglia associated IL-1α in response to cerebral ischaemia in infected animals. No evidence for induction of plaque rupture acutely by *S. pneumoniae* in atherosclerotic animals was found.

Conclusions: *S. pneumoniae* augments atherosclerosis and exacerbates experimental ischaemic brain injury via IL-1 and platelet-mediated systemic inflammation. These mechanisms may contribute to diverse cardio- and cerebrovascular pathologies in humans.

CNS-IMMUNE INTERACTIONS DURING CHRONIC STRESS AND ITS REGULATION BY NITRIC OXIDE (NO) IN RATS

A. Ray, K. Gulati

Department of Pharmacology, Vallabhbhai Patel Chest Institute, University of Delhi, Delhi, India

Stress in any external or internal stimulus capable of disrupting homeostatic mechanisms and influencing both neurobehavioral and immune functions. A bi-directional link exists between the central nervous system (CNS) and immune systems and such CNS-immune interactions play a crucial role in health and disease. Complex neurochemical mechanisms regulate stress responses and nitric oxide (NO) is widely documented as a unique, multidimensional messenger molecule with neuromodulatory properties. Acute and chronic stressors elicit distinctly different nature of biological responses and the neural basis of chronic stress responses as less widely studied. The present study thus evaluated the role nitric oxide (NO) and its signaling pathways in CNS-Immune interactions during chronic stress. Wistar rats (170-200 g) were used for the study and restraint stress (RS) was used as the experimental stressor. Neurobehavioral activity was studied by the elevated plus maze (EPM) test and markers of adaptive immunity (humoral and cell mediated) as well as cytokine (TNF-α and IL-4) were assessed. Brain and plasma levels of NO metabolites (NOx), ADMA, and MDA levels were used as biochemical markers. Exposure to chronic RS (x15) suppressed neurobehavioral activity in the EPM suggestive of an anxiogenic response, and this was associated with suppressions in brain NOx and elevations in brain ADMA (endogenous NOS inhibitor) activity. Pretreatment with the NO mimetic, L-arginine attenuated both behavioral responses and brain biochemical markers, whereas, the NO synthase inhibitor, L-NAME, aggravated them. Assessment of immune markers revealed that antibody responses and delayed type hypersensitivity reactions were inhibited after chronic RS and differential modulations of cytokines (TNF-α and IL-4) were observed. These changes were accompanied by reductions in NOx and enhancements in MDA levels in both brain homogenates and plasma. The chronic RS induced immunological and oxidative changes were also attenuated by L-arginine and aggravated by L-NAME pretreatments. Such chronic RS induced biological changes were gender dependent with female rats showing greater resistance to anxiogenic and immunosppressive responses, and these were associated with lesser extent of changes in brain NOx and MDA levels, as compared to males. Similarly, `high emotional` rats showed greater stress susceptibility in behavioral and immune responses as also lower levels of brain and plasma NOx as compared to `low emotional` rats. It is

suggested that RS may be effectively used as a unique model for studying CNS-immune reactions during stress and further indicates the involvement of NO in the regulation of such interactions.

NEUROPEPTIDE -Y CONTRIBUTES TO HYPOXIC REMODELING OF OVINE MIDDLE CEREBRAL ARTERIES

O.O. Adeoye, J. Silpanisong, K. Latschaw, J.M. Williams, W.J. Pearce

Center for Perinatal Biology, Loma Linda University, Loma Linda, CA, USA

Objectives: Exposure of the fetal brain to hypoxia either in-utero, during labor or after birth frequently results in acute complications and/or chronic defects of varying severity. These complications often involve alterations in cerebral artery structure and function through mechanisms that are yet to be fully elucidated. Hypoxic induction of HIF-1a upregulates angiogenic genes for molecules such as VEGF and its receptors. Although VEGF is known traditionally to induce angiogenesis, recent studies suggest its involvement in vascular remodeling. VEGF potentiates growth and differentiation of perivascular sympathetic nerves, which in turn can exert potent trophic effects on cerebral arteries. Whereas NE is the most prominent adrenergic neuroeffector, our previous experiments have demonstrated a potent guanethidine-resistant trophic influence arising from the ovine cerebrovascular adrenergic innervation. Based on these findings, this study explores the hypothesis that hypoxic alteration of cerebrovascular structure and function is mediated, at least in part, through NPY release from perivascular nerves and action on Y-1 receptors in adjacent smooth muscle.

Methods: Pregnant sheep kept at an altitude of 3820m for the final 110 days of gestation and control sheep kept at sea level were used for this study. In both normoxic and hypoxic groups, a unilateral superior cervical ganglionectomy was performed on the exteriorized fetus on day 124 of gestation. Denervated fetuses were returned back into the uterus and maintained for 14 days. Middle cerebral arteries (MCA) on both denervated side and intact sides were harvested on day 138 of gestation and used fresh or following organ culture for 24 hours in the presence or absence of NPY ± BIBP3226, a Y-1 receptor antagonist.

Results: Immunohistochemical analyses revealed that chronic hypoxia significantly increased expression of NPY and that sympathectomy eliminated NPY in both normoxic and hypoxic arteries. In fresh middle cerebral arteries, denervation decreased spontaneous myogenic reactivity by 62%. Organ culture with 100 nM NPY decreased myogenic reactivity by 83% in intact arteries, but increased reactivity by 183% in denervated arteries. Co-culture with NPY and 5 µM BIBP3226 reversed effects of NPY in denervated arteries only, suggesting the presence of Y-2 receptors in intact but not sympathectomized arteries. Correspondingly, culture with NPY decreased wall thickness by 16% in intact arteries, but increased wall thickness by 15% in sympathectomized arteries.

Conclusions: These results demonstrate that chronic hypoxia increases NPY content in perivascular cerebrovascular nerves, and also suggest that through action on Y-1 receptors, release of NPY supports myogenic reactivity and contributes to hypoxic increases in wall thickness in ovine fetal middle cerebral arteries. These findings support the hypothesis that NPY contributes to hypoxic remodeling of ovine middle cerebral arteries. NPY thus appears to be an important factor that dynamically influences changes in cerebrovascular structure and function in response to both physiological and pathophysiological stimuli, and could play a role in the fetal cerebrovascular complications associated with peripartum hypoxia.

PROFOUND NEUROPROTECTIVE EFFECTS OF TRKB RECEPTOR AGONIST 7,8-DHF IN FEMALE THAN MALE MICE AFTER PERINATAL HYPOXIA AND ISCHEMIA

V. Chanana[1], K. Uluc[2], P. Kendigelen[1,3], L. Zhang[1], D. Kintner[1], E. Akture[1,2], K. Ye[4], P. Ferrazzano[1,5], D. Sun[6], P. Cengiz[1,5]

[1]Pediatrics, [2]Neurosurgery, Univ. Wis. Madison, Madison, WI, USA, [3]Anesthesiology and Critical Care, Afsin State Hospital, Kahramanmaras, Turkey, [4]Patholgy and Laboratory Medicine, Emory University School of Medicine, Atlanta, GA, [5]Waisman Center, Madison, WI, [6]Neurology, Univ. of Pittsburgh, Pittsburgh, PA, USA

Objectives: Hypoxia ischemia (HI) is a common cause of mortality and chronic morbidity in neonates. BDNF, one of the important nerve growth factors, is neuroprotective via activation of tyrosine kinase B (TrkB) receptor-mediated signaling transduction pathways following HI. However, the bioavailability of systemically administered BDNF is poor. In this study, we investigated 1) whether post-injury administration of a bioactive high-affinity TrkB receptor agonist 7,8-dihydroxyflavone (7,8-DHF) has neuroprotective effects after neonatal HI; 2) whether 7,8-DHF has differential effects in male and female mice after HI.

Methods: HI was induced by using Vannucci-Rice method in P9 mice (C57/Black6). Left common carotid artery was cauterized and then mice were exposed to 10% O_2 for 50 min at 37°C. Animals were randomly assigned to HI-vehicle control group [phosphate buffered saline (PBS), intraperitoneally (i.p.)] or HI + 7,8 DHF-treated groups (5 mg/kg in PBS, i.p at 10 min, 24 h, or with subsequent daily injections up to 7 days after HI). Rotarod and Morris Water Maze (MWM) tests were performed at 3 months and animals were sacrificed to detect changes of Fluoro Jade-C, staining and immunofluorescence staining of microtubule associated protein 2 (MAP2), GFAP, myelin basic protein (MBP) and neurofilament (NF).

Results: The HI-vehicle control mice exhibited neuronal degeneration in the ipsilateral hippocampus and cortex with increased Fluoro-Jade C positive staining and loss of MAP2 expression. In contrast, the 7,8 DHF-treated mice showed less hippocampal neurodegeneration and astrogliosis, with more profound effects in female than in male mice. Moreover, 7,8 DHF-treated mice improved motor learning and spatial learning at P30-60 compared to the HI-vehicle control mice. Diffusion tensor imaging of *ex-vivo* brain tissues at P90 after HI revealed less reduction of fractional anisotropy values in the ipsilateral corpus callosum of 7,8 DHF-treated brains, which was accompanied with better preserved MBP and CA1 hippocampal structure. Moreover, phosphorylation of TrkB receptors in the ipsilateral hippocampi was six-fold higher in the 7,8 DHF-treated female mice than male mice. 7,8 DHF-treated female mice not only exhibited less ipsilateral hippocampal lesion at 3 day post-HI but also demonstrated better spatial learning and memory in the MWM test ($p=0.03$).

Conclusion: In this study, we showed that post-injury application of a bioactive high-affinity TrkB agonist 7,8-DHF is neuroprotective in neonatal mice after HI. Stimulating TrkB receptor activity with 7,8-DHF has more profound effects on decreasing delayed hippocampal neurodegeneration and improving spatial memory and learning in female mice than in male mice after neonatal HI.

Funding: Supported by UW Dept. of Pediatrics R & D Grant (Cengiz P), 9U54TR000021 from the Clinical and Translational Science Award program of NCATS (Cengiz P, Ferrazzano P), NIH grants RO1NS38118 and RO1NS48216 (Sun D), and NIH P30 HD03352 (Waisman Center).

AGE-DEPENDENT MICROGLIAL RESPONSES AFTER HYPOXIA-ISCHEMIA

V. Chanana[1], K. Uluc[2], E. Fidan[1], E. Akture[1], D. Kintner[1], P. Cengiz[1], D. Sun[3], P. Ferrazzano[1,4]

[1]Pediatrics, [2]Neurosurgery, Univ. Wis. Madison, Madison, WI, [3]Neurology, Univ. of Pittsburgh, Pittsburgh, PA, [4]Waisman Center, Madison, WI, USA

Objectives: Cerebral ischemia affects over 20,000 infants and children every year in the US. Survivors frequently suffer from lasting neurologic impairments, and treatment options are limited. Therapies that mitigate the neuroinflammatory response to ischemia have been recognized as a promising neuroprotective strategy. However, the microglia-mediated inflammatory response to ischemia in the developing brain is not well understood, limiting development of this therapy for infants and children. In the present study, we tested whether the ongoing differentiation of microglia in the immature brain results in more robust microglial activation and pro-inflammatory responses than juvenile brains following hypoxia-ischemia (HI).

Methods: HI was induced by using Vanucci-Rice method in P9 and P30 mice (unilateral carotid artery ligation and subsequent exposure to 10% O_2 for 50 min at 37°C). Under HI and normoxic conditions, microglial activation profiles were assessed using flow cytometry in postnatal day 9 and postnatal day 30 mice (P9 and P30) by analyzing relative expression levels of CD45 in $CD11b^+/CD45^+$ microglia/macrophages. Immunofluorescence

staining for CD11b and Microtubule associated protein 2 (MAP2), was performed at day-2 and day-9 post-HI. Expression of cytokines (TNF-a, IL-1b and IL-10) and cleaved caspase-3 release were measured by ELISA.

Results: Flow cytometry analysis revealed that the hippocampi of P9 and P30 brains exhibited higher baseline levels of CD45 expression in $CD11b^+/CD45^+$ cells than the cortex and striatum. In response to HI, there was an early increase in number of $CD11b^+/CD45^+$ microglia/macrophages in the ipsilateral hippocampus of P9 mice. Immunostaining revealed that $CD11b^+$ microglia transformed from a "ramified" to an "amoeboid" morphology in the CA1 region, which was accompanied by a loss of MAP2 expression. The peak response of microglial activation in the ipsilateral hippocampus of P9 mice occurred on day 2 post-HI, which was in contrast to a delayed and persistent microglial activation in the cortex and striatum (peak on day 9 post-HI). P9 brains demonstrated a 2-3 fold greater increase in microglia counts than P30 brains in each region (hippocampus, cortex, and striatum) during day 1-17 post-HI. P9 brains also showed more robust expression of pro-inflammatory cytokines (TNF-α and IL-1β) than P30 brains after HI.

Conclusion: Differential microglial responses to HI in P9 and P30 mice suggest that age-dependent differences in microglial responses may impact the efficacy of anti-inflammatory treatment strategies after HI. The P9 brains demonstrated a dramatic increase in microglia activation and a predominantly pro-inflammatory cytokine response early after HI, suggesting that inhibition of microglia may provide benefit in immature brains when administered soon after injury. In contrast, despite similar levels of apoptotic cell death early after injury, the P30 mice demonstrated less microglia activation and a more balanced pro- vs. anti- inflammatory response after HI, suggesting that inhibition of microglia in juvenile brains may be less effective or possibly worsen outcome after HI.

COMPARISON OF THE IMMUNOREACTIVITIES OF NMDA RECEPTORS BETWEEN THE YOUNG AND ADULT HIPPOCAMPAL CA1 INDUCED BY TRANSIENT CEREBRAL ISCHEMIA

B.H. Chen[1], C.H. Lee[2], J.H. Park[2], M.-H. Won[2], J.H. Cho[2], Y.L. Lee[1]

[1]Hallym University, [2]Kangwon National University, Chuncheon, Republic of Korea

Objective and methods: Young gerbils are much more resistant to transient cerebral ischemia than the adult. In the present study, we confirmed that about 90% of CA1 pyramidal cells in the adult hippocampus died at 4 days post-ischemia; however, about 56% of them in the young hippocampus died at 7 days post-ischemia. To compare excitotoxicity between them, we carried out immunoreactivities of NMDA receptor 1 (NMDAR1) and NMDAR2A/B in the hippocampal CA1 region (CA1) induced by 5 min of transient cerebral ischemia in the young and adult gerbils.

Results: NMDARs immunoreactivities and protein levels in the young sham-group were much lower than those in the adult sham-group. Four days after ischemia-reperfusion, they were significantly decreased in the adult ischemia-group; however, in the young ischemia-group, they were much higher than those in the adult. Seven 7 days after ischemia-reperfusion, NMDAR1 immunoreactivity and its level in the young were much higher than those in the adult; NMDAR2A/B immunoreactivity and its level in the young were lower than the adult.

Conclusion: These results indicate that the increases of inflammatory cytokines and their receptors in the aged spinal cord might be related to maintaining a balance of inflammatory reaction in the spinal cord during normal aging.

MODELLING BLOOD FLOW AND METABOLISM IN THE PIGLET BRAIN DURING HYPOXIA-ISCHAEMIA: SIMULATING INTRACELLULAR PH

T. Hapuarachchi[1,2], T. Moroz[1,2], A. Bainbridge[3], S. Faulkner[4], D. Price[3], E. Powell[4], T. Zhu[1], E. Baer[1], K.D. Broad[4], D. Thomas[5], E. Cady[3], N. Robertson[4], X. Golay[5], **I. Tachtsidis**[1]

[1]Medical Physics and Bioengineering, [2]Centre for Mathematics and Physics in the Life Sciences and Experimental Biology (CoMPLEX), University College London, [3]Medical Physics and Bioengineering, University College London Hospitals, [4]Institute for Women's Health, [5]Institute of Neurology, University College London, London, UK

Introduction: Neonatal brain injury can result from hypoxic-ischaemia (HI) due to in-utero or intrapartum complications. To investigate the cerebral physiological and metabolic responses in such circumstances, we have created a computational model of cerebral blood flow and metabolism. The model has successfully predicted near-infrared spectroscopy (NIRS) and magnetic resonance spectroscopy (MRS) measurements during brief anoxias in piglets [1]. We expanded the model recently to simulate HI caused by carotid artery occlusion and to investigate intracellular pH.

Aim: In this study we apply our extended model to integrate our brain tissue multimodal measurements of NIRS and MRS during HI in the neonatal preclinical model. In particular, we investigate the brain tissue pH changes as measured with phosphorus (^{31}P) MRS.

Methods: HI was induced by reducing inspired oxygen and reversibly inflating bilateral carotid artery occluders. NIRS measured changes in cerebral oxygenated (HbO_2) and deoxygenated (HHb) haemoglobin and changes in the oxidation state of cytochrome-c-oxidase (ox-CCO). CCO is the terminal electron acceptor of the mitochondrial electron transfer chain, which in turn provides a driving force for ATP synthesis. ^{31}P MRS measured intracellular inorganic phosphate (Pi), phosphocreatine (PCr), and nucleotide triphosphate (NTP, mostly ATP). In addition, ^{31}P MRS can estimate intracellular pH using the Pi or ATP chemical shifts [2].

Our simulation model is composed of differential equations and algebraic relations describing cerebral blood flow and oxygenation, and oxygen and energy metabolism at a cellular level. The simulation currently includes ~100 parameters and ~25 variables. Figure 1(a) shows a schematic of the model. To simulate intracellular pH, we have included the main dynamics of H^+ ions in both mitochondria and cytoplasm. Model inputs are arterial blood pressure (P_a), arterial oxygen saturation (SaO_2) and arterial carbon dioxide (P_aCO_2). The model then simulates NIRS and ^{31}P MRS measurements as well as e.g. cerebral metabolic rate of oxygen ($CMRO_2$) and cerebral autoregulation (Figure 1(b)).

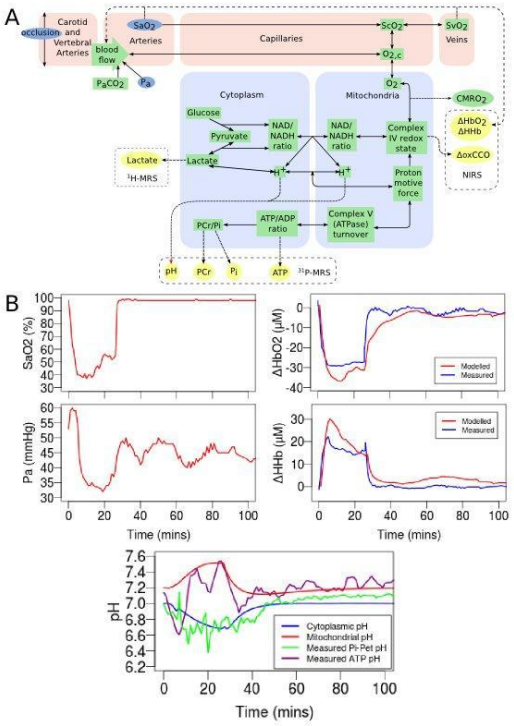

[Figure 1]

Results: The model successfully simulates our NIRS and MRS measurements during HI. In the model simulations, cytoplasmic pH was more acidic during HI whereas mitochondrial pH was more alkaline (Figure 1(b)). MRS intracellular pH measured using Pi corresponded to the simulated cytoplasmic pH whereas MRS pH measured using ATP was comparable to the simulated mitochondrial pH.

Discussion: We present a novel computational model of the piglet brain

capable in simulating NIRS and MRS measurements during HI. The model predicts that MRS pH measured using ATP correlates with mitochondrial pH during HI, perhaps shedding further light on the main origin of that MRS measurement. The model is a useful tool enabling integration of multimodal measurements and testing of physiological and metabolic hypothesis.

References:

[1] Moroz T. et al. (2012) J. R. Soc. Interface, 9(72):1499-1509

[2] Cady E.B. et al. (2008) Journal of neurochemistry, 107(4):1027-1035

NEURAL STEM CELLS WITH HIGH MITOTIC ACTIVITY EXIST IN THE INJURED AREA OF NEONATAL BRAIN AFTER HYPOXIC ISCHEMIC INSULT

J. Kido[1], K. Momosaki[1], D. Fujisawa[1], H. Mori[1,2], S. Matsumoto[1,2], H. Mitsubuchi[1,2], F. Endo[1], **M. Iwai**[1,2]

[1]Pediatrics, [2]Neonatology, Kumamoto University, Kumamoto, Japan

Background and purpose: Hypoxia/ischemia induces neurogenesis via stimulation of neural stem/progenitor cells proliferation and acceleration of their migration to ischemic injured area in neonatal brain. Although migrated neural progenitor cells can be detected using histological method with their specific maker, neural stem cells cannot be detect because of lack of its specific marker. Therefore, the fate and property of the neural stem cells in ischemic injured area is still unclear. The aim of this study is to confirm presence of neural stem cells and acceleration its mitotic activity in the ischemic injured area after neonatal hypoxia ischemia (HI).

Methods: HI brain injury was induced in 7-days-old rat pups by the left common carotid artery occlusion followed by 120 minutes exposure to 8% oxygen. Three days after HI, the brain is removed and sliced at 2 mm thickness, and then six columns are punched out from various infarct areas for cell culture using neurosphere method. The cell clusters are analyzed by immunocytochemistry and mRNA expression for neuron, astrocyte and oligodendrocyte. Also, the cell clusters are investigated the ability of induction for neuron, astrocyte and oligodendrocyte.

Results: The numbers of neurosphere-like cell clusters from infarct areas at 3 days after HI are dramatically increased compared with those from sham control animals. Four and 30 days incubation of the cell clusters provided various types of cells positive for BrdU, Nestin, NG2, β-III-tubulin, GFAP, O4, Vimentin or Iba1. These cell clusters expressed mRNA such as Nanog, Sox2, Oct3/4 and Rex1 as same as ES cell. Also these cell clusters could be differentiated into neurons, astrocytes or oligodendrocytes, and expressed mRNA such as Nestin, βIIItubulin, GFAP and MBP.

Conclusion: We have isolated injury-induced neural stem cells form ischemic injured area after neonatal HI. This cell has a potential to use as a source for new neurons driving CNS repair after neonatal HI.

HYPOXIC PRECONDITIONING PREVENTS THE LOSS OF MYELIN FOLLOWING HYPOXIC-ISCHAEMIC INJURY IN THE NEWBORN RAT

N.M. Jones, E. Suryana

Pharmacology, School of Medical Sciences, University of New South Wales, Sydney, NSW, Australia

Objectives: Myelination is an essential process in development that is carried out by oligodendrocytes in the central nervous system. Hypoxic-ischaemic (HI) events such as birth asphyxia can disrupt myelination by causing oxidative stress, inflammation, excitotoxicity, and disruption to normal mitochondrial function; resulting in the loss of myelin as well as cells of the oligodendrocyte lineage (Huang et al, 2009; Segovia et al, 2008). Previous studies have shown that preconditioning with hypoxia can protect the newborn brain against a subsequent injury, and this protection is due to changes in hypoxia-inducible gene expression (Jones & Bergeron, 2001). In addition, hypoxia can increase the expression of glutamate transporters and antioxidant enzymes in the brain, therefore may also be able to prevent white matter damage after HI. To date, there have been no studies investigating the effects of hypoxic preconditioning on myelination and cells of the oligodendrocyte lineage after an HI insult.

Methods: Sprague Dawley rat pups (postnatal day (P) 6) of both sexes were placed in control

or hypoxic preconditioned (8% oxygen, 3 hours) groups. On P7, pups were further separated into HI and sham surgery groups. HI surgery pups were anesthetised with 1.5% isofluorane and underwent a permanent unilateral right common carotid artery occlusion and then maintained at 8% oxygen for 3 hours. Sham pups underwent the same procedure without occlusion and were maintained in room air. Brains were removed 5 days post-surgery for histological analysis with cresyl violet and immunohistochemical staining using the myelin basic protein (MBP) antibody.

Results: HI alone (n=17) resulted in an increase in brain injury when compared to controls (n=8; 32.2 ± 9.8% loss in brain tissue; P< 0.05, 1-way ANOVA). Exposure to hypoxic preconditioning, 24 hours prior to HI (n=13) protected the brain from injury when compared to HI alone (6.4 ± 1.8% loss in brain tissue; P< 0.05, 1-way ANOVA). HI alone also reduced the amount of myelin when compared to controls (40.1 ± 8.8% loss in MBP staining in the ipsilateral hemisphere; P< 0.001, 1-way ANOVA), while hypoxic preconditioning prior to HI prevented the loss of myelin compared to HI alone (14.8 ± 2.8% loss in MBP staining in the ipsilateral hemisphere; P< 0.05, 1-way ANOVA).

Conclusions: These results indicate that hypoxic preconditioning not only reduces the degree of neuronal damage in the brain as a result of HI, but is also able to prevent against damage to myelin. We found that hypoxic preconditioning prevented the loss in MBP staining caused by HI, which may be attributed to direct protection of myelin or by preventing the maturational arrest of the cells of the oligodendrocyte lineage which has been shown to occur after HI.

References:

Huang et al (2009) Brain Research **1301:** 100-9

Jones & Bergeron (2001) JCBFM **21:** 1105-14

Segovia et al (2008) Annals of Neurology **63:** 520-30

TRANSIENT POSTNATAL HYPOXIA INCREASES CORTICAL CAPILLARY DENSITY IN MICE

J.C. LaManna[1], C. Tsipis[1], X. Sun[1], T. Radford[1], G. Babcock[1], W.F. Boron[1], K. Xu[2]

[1]Physiology and Biophysics, [2]Neurology, Case Western Reserve University, Cleveland, OH, USA

Introduction: Brief hypoxic exposure in early life has led to persistent structural and functional changes in brain [1]. Furthermore, hypoxic/ischemic events during infancy may, through epigenetic mechanisms, result in greater vulnerability to subsequent challenges in adulthood, such as hypoxic exposure or ischemic insult.

Objectives: In this study we investigated the effect of early life hypoxia (+/- hypercapnia) conditioning on brain capillary density and hypoxic adaptation in 3-month old adult mice.

Methods: Mouse pups at postnatal day 2 (P2) were randomly assigned to the P2 Hypoxic or Hypoxic+Hypercapnic groups and exposed to hypoxia (5% O_2 balanced in N_2) or hypoxia+hypercapnia (5% O_2, 8% CO_2 balanced in N_2), respectively, in a normobaric Oxycycler chamber (Biospherix, Redfield, NY) for 2 hours. Normoxic littermates were maintained in an adjacent chamber open to room air and used as controls. All mice will be maintained in normoxia until P60. At P60, mice are exposed to either normobaric hypoxia (8% O_2 balanced with 92% N_2) or normoxia for 21 days.

Cortical capillary density (N/mm^2) was determined by identifying GLUT-1 positive capillaries via immunohistochemistry [2] and reported as mean ± S.E.M .

Results: Capillary density baseline in P2-Hypoxia mice was significantly increased (554 ± 28, n = 6) compared to P2-Normoxia (425 ± 17, n = 12). P2-Hypoxia+Hypercapnia group had similar baseline capillary density (436 ± 23, n = 6). Consistent with previously reported observations [3], cerebral capillary density was significantly increased after 21 days of normobaric hypoxic exposure (8% O2 balanced in N2) in P2-Normoxia adult mice (513 ± 15, n = 15). Chronic hypoxia induced a proportionally smaller increase in microvascular density (~10%) in P2-Hypoxic

adults (611 ± 24, n = 5), and potentially due to a significant elevation in baseline density. However, no change was observed in the P2-Hypoxia+Hypercapnia group after chronic moderate hypoxia (450 ± 18, n = 6) in the adult.

Conclusions: These data suggest that early postnatal hypoxic versus hypoxic+hypercapnic stress result in different angiogenic response in mouse brain and subsequent adult hypoxic adaptation.

References:

1. Akers,K.G.; Nakazawa,M.; Romeo,R.D.; Connor,J.A.; McEwen,B.S.; Tang,A.C. Early life modulators and predictors of adult synaptic plasticity. Eur. J. Neurosci. 24: 547-554; 2006.

2. Pichiule,P.; LaManna,J.C. Angiopoietin-2 and rat brain capillary remodeling during adaptation and deadaptation to prolonged mild hypoxia. J. Appl. Physiol 93: 1131-1139; 2002.

3. Benderro,G.F.; LaManna,J.C. Hypoxia-induced angiogenesis is delayed in aging mouse brain. Brain Res. 1389: 50-60; 2011.

NEUROPROTECTIVE EFFECTS OF GLYCINE AGAINST HYPOXIC-ISCHEMIC BRAIN INJURY IN NEONATAL RATS

K. Momosaki, H. Mori, J. Kido, M. Iwai

Pediatrics, Kumamoto University, Kumamoto, Japan

Neonatal hypoxia-ischemia is a major cause of perinatal brain injury in human newborns. Amino acids have recently been shown to be neuroprotective in experimental models of adult stroke. In this study, we investigated whether amino acids were neuroprotective in an experimental model of neonatal hypoxic-ischemic brain injury. Amino acids were administered just prior to inducing hypoxia, and glycine was found to have the strongest neuroprotective effect against hypoxic-ischemic brain injury. A dosage of 800 mg/kg was found to be optimal and glycine significantly reduced the percentage of brain tissue loss in the lesioned hemisphere compared with the unlesioned hemisphere (saline group 30.53 ± 5.02%; glycine group 8.35 ± 3.00%). Immunohistological analysis showed that glycine significantly suppressed the reactivity of astrocytes and microglia, and significantly decreased the number of TUNEL-positive apoptotic cells in the peri-lesioned brain area 3 days after the hypoxic-ischemic insult. In RT-PCR analysis, the glycine group showed significant inhibition of TNFα mRNA expression in the injured brain hemisphere 12 and 24 h following the insult compared with the saline group. Our results suggest that glycine is neuroprotective against neonatal hypoxia-ischemia and its neuroprotective effect is likely mediated in part by inhibition of TNFα-induced inflammation. Our findings suggest glycine may be clinically relevant for the treatment of hypoxic-ischemic brain injury in human newborns.

A SLICE CULTURE MODEL OF PERINATAL HYPOXIA-ISCHEMIA SHOWS NEUROPROTECTION BY HYPOTHERMIA

A. Phillips[1,2], M. Porambo[3], M.A. Wilson[1], I. Shats[4], J.D. Rothstein[4], M.V. Johnston[1,4], A. Fatemi[1,4]

[1]Kennedy Krieger Institute, [2]Neurology, Johns Hopkins Medical Institutions, [3]Neuroscience, Kennedy Krieger Institute, [4]Johns Hopkins Medical Institutions, Baltimore, MD, USA

Introduction: Brain injury due to perinatal hypoxia-ischemia (HI) is a major public health problem. A HI event leads to an excito-oxidative cascade followed by an inflammatory response. Rodents are used to model HI related injury but show significant variability which limits evaluation of therapeutics. We have therefore adopted an organotypic hemispheric brain slice culture system from neonatal mice that allows for precise control of injury conditions while isolating the effects of peripheral modulators such as the immune system.

Objective: The objective of this study is to determine whether hypothermia protects from injury due to oxygen-glucose deprivation in these organotypic slice cultures.

Materials and methods: Organotypic slice cultures were prepared from P3 CD-1 mouse brain hemispheres. Slices of cortex containing the dorsal hippocampus, 350μm thick, were transferred and maintained on cell culture inserts in medium. Five to seven days later slices were exposed to O_2 deprivation in a glucose free buffer (OGD) for 2hr followed by 36hr reoxygenation under either hypothermia (33.5°C) or normothermia (37°C). Conditioned medium and buffer were collected at various time points post OGD and assayed for lactate

dehydrogenase (LDH) to determine cell viability. Assays for glutamate release, soluble GFAP secretion and propidium iodide (PI) exclusion were also performed. Slices were also probed for immunoreactivity to the cell death marker activated caspase 3.

Results: Slices that were exposed to OGD revealed increased PI uptake particularly in the region of the hippocampus. Hypothermia conferred protection to slices under all conditions. Control slices maintained under optimal conditions that received hypothermia showed the least cell death and slices under OGD and normothermia revealed the greatest level of cell death. Assays for glutamate release were analyzed as well.

Conclusions: Our data suggest that organotypic brain slice cultures respond in a similar manner to in vivo models of HI-mediated injury. Slices exposed to 36hr hypothermia show reduced injury, but whether injury is averted or delayed is still being determined. The protective effect of hypothermia alone may be a delayed response due to temperature induced reduction of metabolic activity, however this may still be clinically relevant since it provides a larger window for administering neuroprotective drugs. Studies are underway to identify clinically relevant biomarkers of HI induced injury and to explore whether hypothermia in tandem with select pharmacologic agents can be used to induce recovery from injury.

PERINATAL ASPHYXIA DECREASES NEURONAL BRANCHING AND SYNAPTOGENESIS IN RAT HIPPOCAMPUS. IMPLICATION OF ASTROCYTE REACTIVITY AND HIF-1ALPHA

E. Rojas-Mancilla[1,2], T. Neira-Peña[1,2], C. Kraus[1,2], B. Rivera[1,2], R. Pérez[1,2], Á. Álvarez[2], D. Bustamante[1,2], P. Morales[1,2], L. Leyton[2], M. Herrera-Marschitz[1,2]

[1]Programme of Molecular and Clinical Pharmacology, [2]Biomedical Neuroscience Institute, University of Chile, Santiago, Chile

Perinatal asphyxia is a main cause of long-term neurological damage, requiring pharmacological targets to protect the neonatal central nervous system (1-3). During hypoxic conditions, branching and neurite length is reduced, possibly affecting synaptogenesis in the developing brain (4, 5). The transcription factor Hypoxia Inducible factor 1 alpha (HIF-1α) is accumulated in the cytoplasm and translocated to the nucleus (6). Indeed, severe hypoxia induces HIF-1α-dependent neurotoxic processes, possibly affecting synaptic plasticity (7, 8). Both the role of astrocytes in synapsis impairment following asphyxia and HIF-1α-dependent astrocyte reactivity have not been elucidated.

Objectives: In our work we determined the effect of asphyxia on

(i) neurite branching,

(ii) synaptogenesis,

(iii) astrocyte reactivity and

(iv) HIF-1α activity *in vitro* and *in vivo*.

Methods: *In vivo*, asphyxia was induced by immersing G22 foetuses into a water bath at 37°C for 21 min. *In vitro*, primary cultures of hippocampal neurons from asphyxia-exposed rats were obtained. Neurite branching and cell viability was evaluated every 2 days. Primary cultures of astrocytes were exposed to hypoxia during 4h. HIF-1α, astrocyte reactivity (GFAP, bystin, Aldh1L1) and synaptic (synaptophysin, PSD95) protein levels were determined by Western-blot and immunocytochemistry.

Results: Following asphyxia *in vivo*, neurite branching and length were reduced. HIF-1α levels increased immediately after birth (0h), while bystin and GFAP levels increased 1 and 8h after, respectively. Furthermore, synaptophysin and PSD-95 levels increased at P7 but decreased at P30. Synaptic contacts were decreased at P7. *In vitro*, GFAP, bystin and HIF-1α levels increased immediately after a 4h period of hypoxia, together with an increase of morphological parameters of astrocyte reactivity. Also, intracellular calcium is increased and sustained in time in hypoxia-exposed astrocytes.

Conclusions: The present results suggest that the increase of HIF-1α activity during asphyxia leads to astrocyte reactivity, reduced neurite branching and long-term synaptic plasticity in hippocampus tissue. The causal relationship and potential reversion by pharmacologically and molecular induced HIF-1α down-regulation remains to be determined.

References:

1. M. de Haan et al., Dev Sci 9, 350 (2006).

2. S. Sarkar, J. D. Barks, I. Bhagat, S. M. Donn, J Perinatol 29, 558 (2009).

3. E. Strackx et al., Behav Brain Res 208, 343 (2010).

4. P. Morales et al., Neuroscience letters 348, 175 (2003).

5. V. Klawitter et al., Amino Acids 28, 149 (2005).

6. G. L. Wang, B. H. Jiang, E. A. Rue, G. L. Semenza, Proc Natl Acad Sci U S A 92, 5510 (1995).

7. S. M. Curristin et al., Proc Natl Acad Sci U S A 99, 15729 (2002).

8. Y. F. Huang, C. H. Yang, C. C. Huang, M. H. Tai, K. S. Hsu, J Neurosci 30, 6080 (2010).

Acknowledgments: Supported by FONDECYT-Chile 1110263 (PMR), 1120079 (MHM), 1110149 (LL); Millenium Institute (BNI P09-015-F). ER-M is a CONICYT PhD Fellow. TN-P is a MECESUP (UCH0714) PhD Fellow.

NEUROPROTECTIVE EFFECTS OF METHANE IN AN NEONATAL HYPOXIA-ISCHEMIA RAT MODEL

Y. Zhou Heng[1], J. Shi[1], Z. Kang[2], X. Sun[1]

[1]Diving Medicine, [2]Second Military Medical University, Shanghai, China

Objectives: Cerebral hypoxia-ischemia (HI) represents a major cause of brain damage in neonates. Our study aimed to examine the short and long-term neuroprotective effects of methane gas in a neonatal rat HI model.

Methods: Seven-day-old rat pups were subjected to left common carotid artery ligation and then 150-min hypoxia (10% oxygen at 37℃). Inhalation of methane (2.5%) was done immediately after HI insult. At 24 h after HI, the pups were sacrificed and the brain was collected for 2,3,5-triphenyltetrazolium chloride (TTC) staining, Nissl staining, and TUNEL staining. Acute cell death, inflammation and oxidative stress were evaluated by detecting caspase-3 activity and MDA content as well as immunochemistry for Iba-1 in the brain.

Results: Our results showed the post-HI methane treatment significantly reduced apoptosis, caspase activity, MDA content, Iba-1 expression as well as infarct ratio.

Conclusion: Methane has potentials in the clinical treatment of HI.

NON-INVASIVE IN-VIVO BRAIN BIOMARKERS IN PERINATAL HYPOXIA-ISCHAEMIA

I. Tachtsidis[1], A. Bainbridge[2], S. Faulkner[3], D. Price[2], E. Powell[3], T. Zhu[1], E. Baer[1], K.D. Broad[3], D. Thomas[4], E. Cady[2], N. Robertson[3], X. Golay[4]

[1]Medical Physics and Bioengineering, University College London, [2]Medical Physics and Bioengineering, University College London Hospitals, [3]Institute for Women's Health, [4]Institute of Neurology, University College London, London, UK

Background: Neonatal encephalopathy following hypoxic-ischaemia (HI) is associated with high mortality and morbidity rates worldwide. Using magnetic resonance spectroscopy (MRS), our newborn piglet model previously defined the biphasic pattern of energy disruption during and after HI [1]. However, the precise relationship between energy failure and cell death remains unclear. To investigate this we have integrated two non-invasive techniques broadband near-infrared spectroscopy (NIRS) and MRS [2]. Broadband NIRS can measure changes in brain tissue oxygenation and the oxidation state of cytochrome-c-oxidase (Δ[oxCCO]). CCO is the terminal electron acceptor of the mitochondrial electron transfer chain (ETC) which catalyses over 95% of oxygen metabolism.

Aim: In this study we investigated changes in brain oxygenation, oxCCO and energy-resources during transient HI and recovery using simultaneous broadband NIRS and phosphorus (^{31}P) MRS in the neonatal preclinical piglet model.

Methods: Twenty-two healthy piglets (aged < 24 hr) were anaesthetised and physiologically monitored. Transient cerebral HI (duration 20 minutes) was induced by reducing the inspired oxygenation and reversibly inflating bilateral carotid artery occluders. ^{31}P MRS measured inorganic phosphate (Pi)/epp, phosphocreatine

(PCr)/epp, and nucleotide triphosphate (NTP)/epp (epp=exchangeable phosphate pool=Pi+PCr+3NTP). NIRS measured cerebral concentration changes of oxy-haemoglobin ([HbO_2]) and deoxy-haemoglobin ([HHb]), and [oxCCO]. In addition we estimated the percentage recovery fractions of our signals following HI and compared them to clinical outcome.

Results: HI rapidly reduced brain oxygenation (Δ[Hbdiff]=Δ[HbO_2]-Δ[HHb])) closely followed by a fall in Δ[oxCCO]. PCr/epp fell, and Pi/epp rose, quickly while NTP/epp was buffered initially and only declined when Δ[oxCCO] was significantly lowered. During recovery, metabolic markers returned to baseline levels for 13 of the 22 piglets but not in 9 piglets suggesting the latter endured a severe insult. Group analysis of the recovery fractions between the NIRS and the ^{31}P MRS measurements demonstrated significant correlations. oxCCO % recovery demonstrated the highest correlations with metabolic MRS % recovery markers and in particular NTP/epp (Figure 1(a)). In addition our results suggested that if NTP/epp and oxCCO % recovery is not above 70% following HI unfavourable outcome is likely. The correlation between HbDiff % recovery and NTP/epp % recovery was not as high and there was a poor association with outcome (Figure 1(b)).

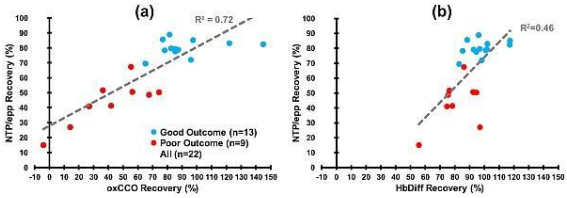

[Figure 1: Recovery fractions of NIRS versus MRS]

Discussion: During transient HI, CCO becomes reduced due to oxygen depletion; NTP (mainly adenosine triphosphate) levels are initially preserved by the creatine kinase reaction leading to PCr decline whereas energy utilisation without oxidative phosphorylation leads to increased Pi. During recovery we have observed high associations between Δ[oxCCO] and ^{31}P MRS measurements. Complementary MRS and NIRS improve understanding of the cerebral metabolic response to HI and can help prognosticate cerebral injury and evaluate early interventional therapies. In addition the portability of the NIRS system can potentially enhance clinical bedside prognosis.

References:

[1]Lorek A. et al. Pediatr.Res.,36,699-706(1994).

[2]Tachtsidis I. et al. Biomedical Optics (BIOMED) 2012 JM3A.27 2012.

G-CSF-INDUCED PROTECTION AGAINST HYPOXIC-ISCHEMIC BRAIN INJURY IN NEONATAL RATS INVOLVES CORTICOSTERONE SYNTHESIS INHIBITION VIA JAK2/PI3K/PDE PATHWAY AND CAMP DEGRADATION

J. Tang, M. Charles, J.H. Zhang

Loma Linda University School of Medicine, Loma Linda, CA, USA

It has been reported that granulocyte-colony stimulating factor (G-CSF) influences the activity of the hypothalamic-pituitary-adrenal axis (HPA), primarily the hormones adrecorticotropic hormone (ACTH) and glucocorticoids. G-CSF was shown to inhibit corticosterone in rodents after a hypoxic-ischemic event; the rodent specific glucocorticoid known to exacerbate injury after an insult. The manner in which G-CSF interacts with corticosterone biosynthesis remains to be examined. In this study, we investigate for the first time the underlying mechanism of G-CSF on corticosterone biosynthesis in a neonatal rat model of hypoxic-ischemic (HI)-induced brain injury and a rodent Y1 adrenal cortical cell line. Systemic G-CSF (50 μg/kg) administration reduced brain infarction at 24 hours post HI injury. Neuroprotection of G-CSF was neutralized by ACTH or IBMX (phosphodiesterase 3B (PDE3B) inhibitor)). In vitro study, cholera toxin was used to agonize corticosterone synthesis by constitutively increasing cAMP. Corticosterone and cAMP were quantitatively assayed by ELISA. Janus Kinase 2 (JAK2)/Phosphatidylinositol-3-kinases (PI3K)/Protein kinase B (Akt), the downstream signaling components of G-CSF receptor activation, their phosphorylated forms and Phosphodiesterase 3B (PDE3B) were detected by western blot. G-CSF at 30 ng/ml inhibited corticosterone synthesis by Y1 adrenal cortical cell. The inhibitory effect of G-CSF was conferred by interfering with the cAMP signaling via the activation of

JAK2/PI3K/PDE3B pathway, as verified with respective inhibitors. The degradation of cAMP by G-CSF signaling reduced corticosterone. We conclude that G-CSF-induced neuroportection is associated with inhibition of corticosterone synthesis at the adrenal level via JAK2 activation by degrading intracellular cAMP.

THE EFFECTS OF HYPOXIC POSTCONDITIONING IN A NEONATAL RAT MODEL OF HYPOXIC-ISCHAEMIC BRAIN INJURY

J.D. Teo, M.J. Morris, N.M. Jones

Pharmacology, School of Medical Sciences, University of New South Wales, Sydney, NSW, Australia

Objective: Neonatal hypoxic-ischaemic (HI) brain injury has been shown to cause a range of long term consequences including memory and motor deficits. Previous animal studies have shown that exposure to mild hypoxia before injury can prevent subsequent damage to the brain and this protection involves changes in levels of hypoxia-responsive genes[1], and promotion of anti-inflammatory[2] and anti-apoptotic[3] mechanisms. More recently, the neuroprotective actions of post-injury treatment (or postconditioning = PC), with mild hypoxia was reported in adult rat brain[4]. Here, we have examined whether PC with mild hypoxia can reduce the extent of damage and prevent gliosis caused by HI injury in newborn rats.

Methods: Postnatal day (P) 7 Sprague Dawley rat pups were exposed to HI treatment, which included a unilateral carotid artery occlusion with hypoxia (7% oxygen for 3 hours). Non-injured sham controls (C) underwent identical surgery procedures without occlusion. Postconditioning started 24 hours after HI and consisted of daily exposure to 8% oxygen for 1 hour for 5 days following surgery. Normoxic controls (N) were exposed to room air for the same duration. Brains were fixed on P13, sectioned and brain injury was quantified using cresyl violet staining of serial sections and the difference in volume between the ipsilateral and contralateral hemispheres was measured. Immunohistochemical staining for glial fibrillary acidic protein (GFAP) was performed to examine brain inflammation. Sections were scored by comparing the intensity of staining and activation of astrocytes in the ipsilateral (injured) hemisphere to the contralateral (non-injured) hemisphere.

Results: Control animals did not show any visible brain damage, with injury volumes as indicated (C+N: -0.17±1.26mm^3 (n=8); C+PC: -1.47±1.05mm^3 (n=8)). HI+N treated pups demonstrated a significant degree of injury affecting the ipsilateral hemisphere compared to controls (-15.67±4.37mm^3, n= 15, $p< 0.05$, 1-way ANOVA), and the extent of injury was reduced by PC (HI+PC: -5.15±2.6mm^3, n=16, $p < 0.05$, 1-way ANOVA). HI+N increased gliosis, as indicated by the increase in GFAP staining with the glial cells appearing hypertrophic compared to other groups. HI+PC reduced gliosis compared to HI+N and minimal differences were noted between C+N and C+PC treatments.

Conclusion: This study has demonstrated the neuroprotective actions of PC with mild hypoxia in the neonatal rat brain and confirmed that PC alone does not cause brain damage. The mechanism responsible for neuroprotection offered by PC appears to involve a reduction in glial cell activation and reduced inflammation[5]. Further studies will elucidate the mechanisms involved in this novel neuroprotective phenomenon, and examine the effects of PC on neurons and glial cells.

References:

[1]Jones, NM & Bergeron, M (2001) *JCBFM* **21** 1105-14

[2]Yin W, *et al.* (2007) *Stroke* **38** 1017-24

[3]Park HK, *et al.* (2011) *J Korean Med Sci* **26** 1495-500

[4]Leconte C, *et al*. (2009) *Stroke* **40** 3349-55

[5]Winerdal M, *et al*. (2012) *PLoS One* **7**(5):e36422

DOPAMINE D1- AND ADENOSINE 2A-RECEPTOR ANTAGONISTS HAVE ADDITIVE NEUROPROTECTION IN NEONATAL HYPOXIA-ISCHEMIA

B. Wang, Z.-J. Yang, A.C. Larsen, J.L. Jamrogowicz, E. Kulikowicz, L.J. Martin, R.C. Koehler

Johns Hopkins University School of Medicine, Baltimore, MD, USA

Objectives: Neonatal hypoxic-ischemic (HI) encephalopathy is a clinically significant disorder with long-term morbidity. The implementation and clinical efficacy of therapeutic hypothermia are limited. Striatal neurons at term are highly vulnerable to HI, and their degeneration occurs rapidly. Because initiation of therapeutic hypothermia is often delayed, it is important to search for adjunct treatments that can be readily administered to protect the rapidly evolving injury in newborn striatum. Approximately half of the medium spiny neurons express D1 receptors, and half express adenosine 2A (A_{2A}) receptors with little co-localization. Previous work with a D1 receptor antagonist showed striatal neuroprotection, but protection was less than 50% [1]. Therefore, we tested the hypothesis that combined D1 and A_{2A} receptor antagonist treatment after HI would provide greater striatal neuronal protection than either antagonist alone.

Methods: Anesthetized newborn male piglets were subjected to 40 minutes of ventilation with 10% O_2 followed by 7 minutes of airway occlusion. At 5 minutes after reoxygenation, piglets were given four different treatments: 1) vehicle (0.5% DMSO in saline); 2) the D1 antagonist SCH23390 administered as a 0.5 mg/kg loading dose followed by a continuous infusion for 6 hours (0.2 mg/kg/h, iv); 3) the A_{2A} antagonist SCH58261 administered as a 0.1 mg/kg loading dose and a continuous infusion for 6 hours (0.033 mg/kg/h, iv); 4) combined treatment with SCH23390 and SCH58261. At 4 days of recovery, the brains were perfused with fixative and processed for histology. The total number of viable neurons in putamen was measured by unbiased stereology on cresyl violet-stained sections. Additionally, neurobehavioral assessments were performed at 1, 2, 3, and 4 days after HI. Neurologic deficits, including consciousness, sensory responses, motor function, spatial orientation and clinical seizure activity, were graded on a scale with a maximum deficit score of 154 and a normal score of 0.

Results: None of the drug treatments affected arterial blood pressure, blood gases, blood glucose and rectal temperature. Stereological analysis did not detect a difference in the volume of the putamen among the sham-operated and four HI groups at 4 days of recovery. The total number of viable neurons in the whole putamen in the HI group treated with vehicle was decreased to 19±10% (±SD, n=8) of that in the sham-operated group (100±11%, n=5). However, the total number of viable neurons was significantly increased to 45±9% (n=7) and 49±4% (n=7) in the SCH23390- and SCH58261-treated groups, respectively. Furthermore, combining SCH23390 with SCH58261 produced additive neuroprotection (74±22%, n=8) that was significantly greater than either treatment alone. Neurologic deficit scores after treatment with SCH23390 (32±6) or SCH58261 (30±6) were significantly reduced compared with those of the vehicle-treated group (37±7). Moreover, the drug combination reduced the deficit score (27±5) more than either treatment alone after HI.

Conclusion: Early implemented, combined post-treatment with A_{2A} and D1 antagonists provides additive neuroprotection in highly vulnerable putamen in a large animal model of neonatal HI and may provide a useful clinical adjunct therapy with hypothermia.

References:

1. Yang et al J Cereb Blood Flow Metab (2007) 27: 1339-51.

ADENOSINE 2A RECEPTORS CONTRIBUTE TO STRIATAL INJURY AFTER NEONATAL HYPOXIA-ISCHEMIA

Z. Yang[1], B. Wang[1], H. Kwansa[1], K.D. Heitmiller[1], G. Hong[1], L.J. Martin[2,3], R.C. Koehler[1]

[1]Department of ACCM, [2]Pathology, [3]Neuroscience, Johns Hopkins University, Baltimore, MD, USA

Objectives: Postsynaptic adenosine 2A (A_{2A}) receptors coupled to adenylate cyclase and PKA activation are enriched in medium spiny striatal neurons that project to globus pallidus. Although A_{2A} receptors are thought to contribute to neurodegeneration in ischemia in adult brain, data in immature rodents has been divergent (1, 2). Here, we used a large animal model of neonatal hypoxia-ischemia (H-I) to test the hypothesis that the A_{2A} receptor antagonist SCH58261 would attenuate PKA-dependent phosphorylation on dopamine- and cAMP-regulated phosphoprotein-32 (DARPP-32), NMDA receptor NR1, and Na,K-ATPase and provide protection of striatopallidal neurons after H-I.

Methods: Piglets underwent sham surgery without H-I or surgery followed by H-I, which involved 40 min hypoxia (10% O_2) plus 7 min

of asphyxia. At 5 min after reoxygenation, piglets received intravenous injections of vehicle or 1 of 3 doses of SCH58261 (0.01, 0.1, or 1 mg/kg) followed by a continuous infusion for 6 h (0.0033, 0.033, or 0.33 mg/kg/h, iv, respectively). Animals were survived 4 days for histology or 3 hours for measurements of protein phosphorylation and the oxidative and nitrative stress markers, nitrotyrosine and protein carbonyl formation. A separate set of piglets without H-I received direct infusion of the A_{2A} receptor agonist CGS21680 via microdialysis into the putamen to determine if phosphorylation changes observed in H-I could be replicated by A_{2A} receptor activation.

Results: At 4 days of recovery, profile counting indicated that the density of viable neurons in putamen in the H-I group treated with vehicle was 19±9% (±SD; n=7) of the sham value (n=8). Neuronal density was significantly increased to 33±8%, 43±11%, and 40±9% in the SCH58261 groups treated with the low (n=7), medium (n=8), and high doses (n=7), respectively. Stereological results also showed that medium dose of SCH58261 increased the viable putamen neurons from 0.85×10^6 to 1.62×10^6 at 4 days after H-I. Further analysis indicated that administration SCH58261 after H-I improved early neurological recovery and protected preferentially striatopallidal neurons in putamen. Western blotting showed that treatment with medium dose of SCH58261 attenuated the H-I-induced phosphorylation of the PKA-sensitive sites Thr34 DARPP-32, Ser897 NR1, and Ser943 Na, K-ATPase, but had no effect on phosphorylation of the PKC-sensitive sites Ser896 NR1 or Ser23 Na, K-ATPase at 3 h of recovery. SCH58261 also improved Na,K-ATPase activity and blunted H-I-induced increases in nitrotyrosine immunoreactivity and carbonyl formation. In addition, post-treatment with SCH58261 did not alter the recovery of laser-Doppler flow, which returned to baseline levels within 1 h. The A_{2A} receptor agonist CGS21680 increased phosphorylation of Na, K-ATPase and NR1 selectively at PKA-sensitive sites but not at PKC-sensitive sites in normal putamen tissue.

Conclusions: A_{2A} receptor activation promotes neurodegeneration in putamen after reoxygenation from H-I. The mechanism of toxicity may be related to DARPP-32-dependent phosphorylation of PKA-sensitive sites on NR1 and on Na,K-ATPase, thereby augmenting excitotoxic-induced oxidative stress after reoxygenation.

References:

1. Aden et al. (2003) Stroke 34: 739-44.

2. Bona et al. (1997) Neuropharmacology 36: 1327-38.

INTRANASAL ADMINISTRATION OF CALCITONIN GENE-RELATED PEPTIDE ALLEVIATES CEREBRAL VASOSPASM IN RATS FOLLOWING SUBARACHNOID HEMORRHAGE

B.-L. Sun[1], F.-P. Shen[1], M.-F. Yang[1], D.-W. Li[1], Z.-Y. Zhang[1], H. Yuan[1], F.-M. Xie[1], J. Chen[2], F. Zhang[1,2]

[1]Key Lab of Cerebral Microcirculation in Universities of Shandong, Department of Neurology, Affiliated Hospital, Taishan Medical University, Taian, China, [2]Center of Cerebrovascular Disease Research, University of Pittsburgh School of Medicine, Pittsburgh, PA, USA

Objectives: Subarachnoid hemorrhage (SAH) is a devastating disease because of its super-acute nature, high mortality rate and striking at a relatively young age. The incidence of cerebral vasospasm after SAH is high, and its subsequent early brain injury and delayed cerebral ischemia are the major reasons of neuronal death, cerebral infarct and overall poor clinical conditions. The clinical management of vasospasm is far from satisfactory. Calcitonin gene-related peptide (CGRP) is a potent endogenous vasodilator, and CGRP is depleted after SAH. Supplements of CGRP were able to prevent or attenuate vasoconstriction induced by SAH in both experimental and clinical settings. However, clinical application of CGRP is limited by its low BBB permeability and cardiovascular side effects. Intranasal drug delivery has recently emerged as a promising approach to deliver drugs to the brain. In this experiment, we investigate if intranasal delivery of CGRP is an appropriate approach to alleviate cerebral vasospasm after SAH.

Methods: Male adult Wistar rats were used in the experiments. A femoral catheterization was made to monitor blood pressure and blood gases and to collect arterial blood for cisternal injection to induce SAH (Suzuki's double-blood injection model). Intranasal administration was made via a segment of PE-50 tube inserted into nasal cavities, and a total

of 1 mg of CGRP in 50 microliters of water was administered per rat through 10 injections. Iodine-125-labeled CRGP (^{125}I-CGRP) and liquid scintillation were also used to measure CGRP distribution in venous blood, CSF and brain tissues. The diameter of the basilar arteries and regional cerebral blood flow (rCBF) were monitored. Circulating endothelial cells were counted and immunohistochemically stained using anti-CD31 antibody. RT-PCR was performed to detect VEGF mRNA and Westerns blots were performed to detect VEGF protein.

Results: Comparing to intravenous injection, intranasal delivery led to a 10-fold higher level of CGRP in the brain. Intranasal CGRP administration significantly ameliorated cerebral vasospasm, indicated by increased diameters of basal arteries and improved cerebral blood flow. Consequently, cortical neuronal death was reduced and the numbers of circulating endothelial cell were also decreased. In addition, intranasal CGRP application increased the levels of vascular endothelial growth factor and stimulated angiogenesis in the brain.

Conclusions: Our data demonstrated that intranasal administration of CGRP is more efficient than IV in the delivery of CGRP to CNS. CGRP also stimulates VEGF expression and angiogenesis. Take together, these results suggest that intranasal application of CGRP could be a practical approach to diminish the vasospasm and early ischemic brain injury after SAH.

NEURO-CAPILLARY COUPLING IN VIVO

J. Lee, W. Wu, D.A. Boas

Martinos Center for Biomedical Imaging, Massachusetts General Hospital, Harvard Medical School, Charlestown, MA, USA

Background and aims: Neurovascular coupling traditionally focuses on how local neuronal activity adjusts arteriolar tone (and thus local CBF) to meet metabolic needs [1]. This paradigm has recently been extended to consider manipulation of capillaries in response to neuronal activity; so called neuro-capillary coupling. Recent studies showed that contractile cells called pericytes can control the diameter of capillaries [2], but their responses to neurotransmitters have only been demonstrated in vitro and their role for regulating blood flow has not been observed. Here we demonstrate in vivo capillary flow regulation in response to neural activation.

Methods: We developed a novel optical imaging technology for systematic measurement of the capillary network flow pattern in a cranial window preparation of rats. An optical speckle statistics-based metric of quantifying flow speed has been proposed and validated. This metric has been integrated with optical coherence tomography, enabling us to measure the blood flow speed over hundreds of capillaries at the same time (Fig. 1B). Therefore, we were able to obtain a time series of 3D maps of flow speed over a reasonably large volume embracing several hundred capillaries, with a sufficiently high temporal resolution for tracing fast hemodynamic responses (~1 s). In addition, a range of algorithms have been developed to automatically identify and vectorize individual capillaries from the flow speed volume data, permitting flow speed averaging over capillary segment lengths and thus improving the statistical significance of the speed measurements (Fig. 1C).

Results: Using the technologies, we monitored changes in the blood flow pattern of the cerebral capillary network while applying electrical stimulation to the forepaw. The mean flow speed averaged across capillaries increased in response to neural activation, only in the region at the center of activation (Fig. 1D). Interestingly, the standard deviation of the capillary flow decreased (n=3, see Table in Fig. 1). Furthermore, this flow homogenization occurred significantly earlier than both the mean capillary flow increase ($p< 0.01$, n=3) and the arteriole flow increase (data not shown). When looking into individual capillary responses (Fig. 1E), high-baseline-speed capillaries statistically exhibited early drops (Fig. 1F). This flow speed reduction in high-baseline capillaries results in the early capillary flow homogenization. The observed flow homogenization might lead to larger tissue oxygen extraction [3].

Conclusion: Our results suggest that capillaries may regulate blood flow towards homogenization in response to neural activation, in support of active capillary control by pericytes.

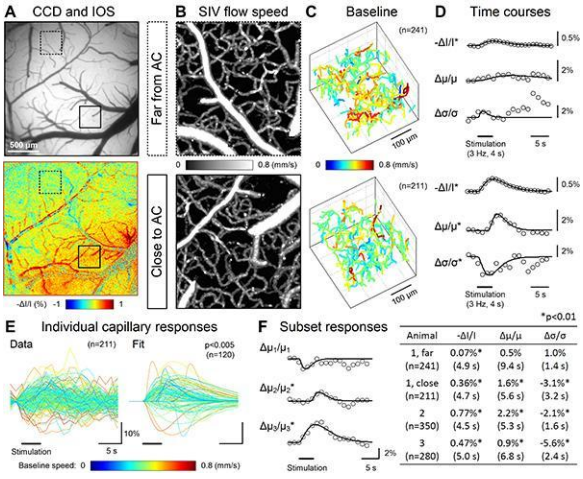

Animal	-ΔI/I	Δμ/μ	Δσ/σ
1, far (n=241)	0.07%* (4.9 s)	0.5% (9.4 s)	1.0% (1.4 s)
1, close (n=211)	0.36%* (4.7 s)	1.6%* (5.6 s)	-3.1%* (3.2 s)
2 (n=350)	0.77%* (4.5 s)	2.2%* (5.3 s)	-2.1%* (1.6 s)
3 (n=280)	0.47%* (5.0 s)	0.9%* (6.8 s)	-5.6%* (2.4 s)

[Fig. 1]

[1] D. Attwell, A. M. Buchan, S. Charpak, M. Lauritzen, B. A. MacVicar, and E. A. Newman, “Glial and neuronal control of brain blood flow,” Nature 468, 232-243 (2010).

[2] C. M. Peppiatt, C. Howarth, P. Mobbs, and D. Attwell, “Bidirectional control of CNS capillary diameter by pericytes,” Nature 443, 700-704 (2006).

[3] S. N. Jespersen and L. Ostergaard, “The roles of cerebral blood flow, capillary transit time heterogeneity, and oxygen tension in brain oxygenation and metabolism,” J Cereb Blood Flow Metab 32, 264-277 (2012).

CORTICAL REGIONS RELATED TO APRAXIA IN PATIENTS WITH CORTICOBASAL DEGENERATION: [18F]FDG PET AND MRI STUDY

C.S. Lee[1], S.M. Kim[1], S.J. Kim[1], J.S. Kim[2], J.M. Lee[3]

[1]Neurology, [2]Nuclear Medicine, University of Ulsan College of Medicine, Asan Medical Center, [3]Biomedical Engineering, Hanyang University, Seoul, Republic of Korea

Background: Corticobasal degeneration (CBD) is uncommon tau parkinsonian disorder, characterized by asymmetric limb apraxia and parkinsonism along with impairment in speech and cognition. Pathology shows asymmetric fronto-parietal atrophy with a varying extent of neural degeneration in the basal ganglia and thalamus. Apraxia, which is most characteristic symptom of CBD, is defined as loss of the ability to execute learned purposeful movements, or loss of dexterity, without dementia, ataxia, weakness and sensory loss. It is derived from disturbance of cortical motor circuits, including motor engrams and production-execution system. We explored apraxia-related cortical regions by comparing cortical atrophy between the more- and less-affected side in patients with early CBD, who presented with unilateral limb apraxia. Cortical atrophy was assessed *in vivo* by [18F]FDG PET and 3.0T MRI.

Methods: We studied 29 patients with CBD (age=70.1±5.5 years, mean±SD). Fifteen healthy subjects were included as normal control group (age=60.3±6.34). [^{18}F]FDG PET and 3.0T MRI were performed for all subjects. Regional glucose metabolism was obtained from the ratio using V1 area as a reference. Cortical thickness was obtained from MRI data using automated surface-based analysis. Z-scores were obtained in each region for correlation analysis of glucose metabolism and cortical thickness.

Results: In [^{18}F]FDG PET studies, comparison of FDG uptake between cerebral hemispheres corresponding to the side with apraxia and to the side without apraxia sides showed highly significant glucose hypometabolism ($p< 0.01$) in Brodmann area 44 (pars opercularis of inferior frontal gyrus; part of Broca's area), and Brodmann area 40 (supramarginal gyrus). In MRI studies, more affected side (corresponding to apraxic limb) showed highly significant reduction of cortical thickness ($p< 0.01$) in inferior parietal lobule, Heschl gyrus, rolandic opercular region, superior medical frontal gyrus, supplementary motor area, and cingulate gyrus. Z-scores of regional glucose uptake correlated with z-scores of cortical thickness of the corresponding region in opercular part of inferior frontal gyrus ($r=0.511$, $p=0.004$), rolandic opercular region ($r=0.551$, $p=0.002$), insula ($r=0.670$, $p< 0.0001$), middle frontal gyrus ($r=0.531$, $p=0.003$), supramarginal gyrus ($r=0.453$, $p=0.013$), and superior temporal gyrus ($r=0.375$, $p=0.044$).

Conclusions: We provided evidence that apraxia in patients with CBD is associated with cortical atrophy in opercular area of inferior frontal gyrus (part of Broca's area), inferior parietal lobule and superior temporal gyrus. These findings indicate that the cortical regions associated with apraxia are close to regions related to language, or to human mirror neuron system.

HONOKIOL FOR NEUROPROTECTION IN THE DEVELOPING RAT BRAIN

A. Woodbury[1], S.-P. Yu[1], L. Wei[1,2]

[1]Anesthesiology, [2]Neurology, Emory University, Atlanta, GA, USA

Introduction: We recently showed that neonatal inflammatory pain causes neuronal cell death and has long-term deleterious effects [1]. This raises a concern for pediatric and neonatal patients exposed to multiple painful procedures in intensive care units [2]. Simultaneously, recent identification of detrimental neurological consequences from anesthetic exposure during early life stages leads to the search for neuroprotective analgesic/anesthetic agents for the pediatric population. Honokiol is a naturally-occurring lignan previously shown to have neurotrophic and analgesic effects [3]. Its proposed mechanism of action is multifactorial, including blocking NMDA receptors and inflammatory pain, increasing the 5HT/5-HIAA ratio, and modulating GABA-A [4]. We hypothesize that honokiol could enhance analgesia and attenuate insults on the developing brain produced by pain and inflammation.

Materials and methods: Post-natal day 7 (P7) rat pups were subjected to the paw-lick test following acute injection with intraplantar formalin plus intraperitoneal (i.p.) honokiol treatment or corn oil control. To evaluate for chronic, severe pain responses, rats were injected with either i.p. honokiol or corn oil vehicle 1 hr prior to intraplantar formalin injection to all 4 paws for 3 days (P4-P6) and later underwent evaluation for delayed stress and pain responses. Behavioral tests included hot plate testing (P17), open field testing (P20), defensive-withdrawal testing (P20), and novel object recognition testing (P20). Brains were harvested and sectioned at P21. Immunohistochemistry for BrdU and NeuN co-labeling was performed to look for neurogenesis, and microglia were labeled with Iba1 as a marker of inflammation.

Results: Honokiol decreased recuperation time by ~ 60% at 30 min following formalin injection in the paw-lick test ($p < 0.05$). Honokiol decreased signs of thermal hyperalgesia in hot plate testing ($p < 0.05$), demonstrated by a greater than 50% increase in latency to jumping in the treatment group. Honokiol did not show a significant effect on open field testing or defensive withdrawal, however there was a trend to increased exploratory behavior in the treated group. In the hippocampus, honokiol treatment increased neurogenesis 33%, decreased cell death 20%, and decreased microglia 50% relative to control ($p < 0.05$). In the thalamus, honokiol increased neurogenesis 60%, decreased cell death 33%, and reduced microglia 25% relative to control ($p < 0.05$).

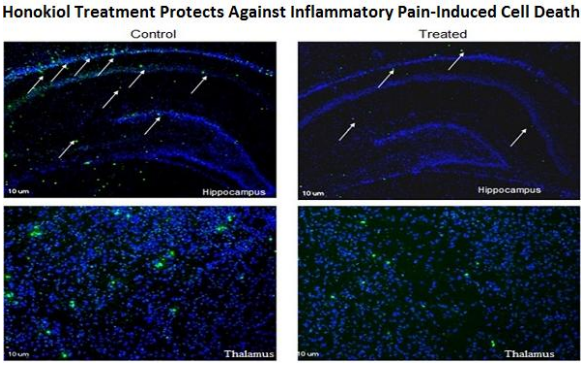

[Honokiol Protects Against Neuronal Death]

Conclusions: Honokiol prevents pain-induced neuronal death, increases neurogenesis, decreases inflammatory responses, and prevents both acute pain sensation and chronic thermal hyperalgesia, while attenuating long-term stress-related behavioral responses. Honokiol could be a potent analgesic and neuroprotectant for the developing neonate.

References:

1. Mohamad et al.: Erythropoietin reduces neuronal cell death and hyperalgesia induced by peripheral inflammatory pain in neonatal rats. *Mol Pain* 2011, 7(51):1-15.

2. Mitchell and Boss: Adverse effects of pain on the nervous systems of newborns and young children: a review of the literature. *J Neurosci Nurs* 2002, 34(5):228-236.

3. Fukuyama et al.: Neurotrophic activity of honokiol on the cultures of fetal rat cortical neurons. *Bioorg & Med Chem Lett* 2002, 12:1163-1166.

4. Lin et al.: Antinociceptive actions of honokiol and magnolol on glutamatergic and inflammatory pain. *J Biom Sci* 2009, 16(94):1-10.

ASTROCYTIC HMGB1 PROMOTES ENDOTHELIAL PROGENITOR CELL ACCUMULATION AND FUNCTIONAL RECOVERY AFTER ISCHEMIC STROKE

K. Hayakawa[1], L.D. Pham[1], Z.S. Katusic[2], K. Arai[1], E.H. Lo[1]

[1]Massachusetts General Hospital, Harvard Medical School, Boston, MA, [2]Mayo Clinic College of Medicine, Rochester, MN, USA

Objectives: Crosstalk between the brain and systemic responses in blood is increasingly suspected of playing critical roles in stroke. But how this communication takes place remains to be fully understood. Emerging data suggest that reactive astrocytes may contribute to neurovascular remodeling, in part via the release of high-mobility group box1 (HMGB1) (Hayakawa *et al* 2010a; Hayakawa *et al* 2010b). Recent study suggests that HMGB1 may enhance endothelial progenitor cells (EPCs) homing after tissue injury (Chavakis *et al* 2007). EPCs play an important role for tissue vascularization and endothelium homeostasis in stroke. Here we assessed the effects of small interference RNA (siRNA) for HMGB1 on EPCs accumulation in a mouse model of stroke recovery.

Methods: Primary rat cortical astrocytes and rat spleen-derived EPCs were prepared. Conditioned media from IL1β-stimulated astrocytes were transferred into EPC cultures to assess the proliferation. Whether EPCs promoted angiogenesis in brain endothelial cells was evaluated by *in vitro* matrigel assay. In an *in vivo* study, 5 days after cerebral ischemia, mice were stereotaxically injected control siRNA or HMGB1 siRNA in intra-cerebro-ventricular (i.c.v.). To detect accumulated EPCs in the ischemic brain, Flk1 and CD34 double positive cells were measured in the peri-infarct cortex by using FACS analysis over the course of 14 days after stroke. Behavioral tests were also performed over 14 days post-stroke.

Results: Conditioned media from reactive astrocytes increase EPC proliferation in vitro. siRNA suppression of HMGB1 in astrocytes prevents this effect. FACS analysis showed that cultured EPC expressed growth factors (FGF2 and BDNF). Conditioned media from EPC increased angiogenic response in brain endothelial cells through PI3K/Akt pathway. In a mouse model of focal cerebral ischemia, reactive astrocytes in peri-infarct cortex upregulate HMGB1 at 14 days post-stroke, along with an accumulation of endogenous EPCs. In vivo siRNA suppression of HMGB1 blocks this EPC response, reduces peri-infact angiogenesis, and worsens neurological deficits.

Conclusions: Astrocytic HMGB1 contributes to EPC migration into the ischemic peripheral region and promote endogenous stroke recovery through EPCs-mediated vasculogenesis, Modulating this process may provide a novel repair strategy in stroke therapy.

References:

Chavakis E, Hain A, Vinci M, Carmona G, Bianchi ME, Vajkoczy P, Zeiher AM, Chavakis T, Dimmeler S (2007) High-mobility group box 1 activates integrin-dependent homing of endothelial progenitor cells. *Circ Res* 100:204-12

Hayakawa K, Arai K, Lo EH (2010a) Role of ERK map kinase and CRM1 in IL-1beta-stimulated release of HMGB1 from cortical astrocytes. *Glia* 58:1007-15

Hayakawa K, Nakano T, Irie K, Higuchi S, Fujioka M, Orito K, Iwasaki K, Jin G, Lo EH, Mishima K, Fujiwara M (2010b) Inhibition of reactive astrocytes with fluorocitrate retards neurovascular remodeling and recovery after focal cerebral ischemia in mice. *J Cereb Blood Flow Metab* 30:871-82

ASTROCYTIC HMGB1 PROMOTES ADHESIVE INTERACTION BETWEEN BRAIN ENDOTHELIUM AND ENDOTHELIAL PROGENITOR CELLS

K. Hayakawa[1], L.D. Pham[1], Z.S. Katusic[2], K. Arai[1], E.H. Lo[1]

[1]Massachusetts General Hospital, Harvard Medical School, Boston, MA, [2]Mayo Clinic College of Medicine, Rochester, MN, USA

Objectives: Emerging data now suggest that endothelial progenitor cells (EPCs) contribute to neurovascular repair after stroke and brain injury. But in order for this to take place, the circulating EPCs must first adhere to and then transmigrate across targeted endothelium. Recent studies suggest that high-moblity-group-box-1 (HMGB1) may enhance endothelial progenitor cells (EPCs) homing after tissue injury (Chavakis *et al* 2007; Hayakawa *et al* 2012). Here, we test the hypothesis that activated astrocytes release

HMGB1 that promotes EPC-endothelial adhesive interactions.

Methods: Primary rat cortical astrocytes, rat brain endothelial cells (RBE.4), and rat spleen-derived EPCs were used in this study. To count the number of EPCs in both assays for adherence and migration, EPCs were labeled by DiI-ac LDL. Cell adhesion and trans-endothelial migration assays were performed between EPCs and RBE.4 monolayers. The numbers of adhered cells were quantified at 45 min after co-culture by counting the number of ac-LDL positive cells in 4 random microscopic fields (x20). For migration assays, IL-1β-stimulated astrocytes or recombinant HMGB1 protein were set in the lower chamber. After 24 h of incubation at 37°C, the lower side of the filter was washed with PBS and fixed with 4% PFA. Labeled EPCs migrating into the lower chamber were directly counted in 4 random microscopic fields (x20).

Results: EPCs stimulated with IL-1β demonstrate high adhesion to RBE.4 cells, in parallel with increasing β2 integrin expression. Pre-incubation of EPCs with neutralizing β2 integrin antibody significantly reduced adherence rates. The receptor for advanced glycation endproduct (RAGE) is known as β2 integrin receptor. Blocking endothelial RAGE also reduced IL-1β-stimulated EPC adherence to RBE.4 endothelial cells. To assess whether reactive astrocytes enhanced this mechanism, co-culture experiments were performed using transwell systems. The RBE.4 monolayer was prepared onto collagen-coated membrane in the upper chamber. Interestingly, high-mobility group box 1 (HMGB1) released from IL-1β-stimulated astrocytes or HMGB1 itself in lower chamber enhanced the adhesion of EPCs. Endothelium Egr1 suppression with siRNA confirmed that RBE.4 stimulated by HMGB1 up-regulated RAGE expression mediated by Egr1.

Conclusions: Astrocytic HMGB1 contributes to enhance the crosstalk between EPC and brain endothelial cells, and the increased adhesion and trans-endothelial migration of EPCs may promote neurovascular remodeling during stroke recovery.

References:

Chavakis E, Hain A, Vinci M, Carmona G, Bianchi ME, Vajkoczy P, Zeiher AM, Chavakis T, Dimmeler S (2007) High-mobility group box 1 activates integrin-dependent homing of endothelial progenitor cells. *Circ Res* 100:204-12

Hayakawa K, Pham LD, Katusic ZS, Arai K, Lo EH (2012) Astrocytic high-mobility group box 1 promotes endothelial progenitor cell-mediated neurovascular remodeling during stroke recovery. *Proc Natl Acad Sci U S A* 109:7505-10

LEVODOPA INDUCED ATTENUATION OF ADAPTIVE IMMUNE RESPONSE ENHANCES RECOVERY AFTER STROKE

E. Kuric, T. Wieloch, K. Ruscher

Department of Clinical Sciences, Lund University, Lund, Sweden

Introduction: Treatment with levodopa/benserazide combined with physical therapy has been shown to improve motor learning and recovery of function in stroke patients [1, 2]. Similarly, we have shown that delayed treatment with levodopa/benserazide improves lost neurological function in rats subjected to experimental stroke and proposed that non neuronal cells may contribute to levodopa/benserazide induced recovery [3].

Inflammation is a central process in the ischemic brain and has a significant impact on mechanisms of tissue reorganization and recovery. A persistent pro-inflammatory milieu may perpetuate detrimental processes for recovery such as secondary neurodegeneration. Dopamine has been recognized as an immunomodulator. Functional dopamine receptors, dopamine synthesis and uptake systems, have been identified on glial and diverse immune cells [4, 5].

Objective: This study, thererfore, was conducted to investigate the effects of levodopa on central and peripheral inflammation induced by experimental stroke and the contribution of these effects to recovery.

Methods: Male Sprague Dawley rats were subjected to transient occlusion of the middle cerebral artery (tMCAO) for 2 hours, treatment with levodopa (20mg/kg)/benserazide (15mg/kg) was initiated at day 2 post occlusion and continued for additional 5 or 12 days. One week after tMCAO, brains, blood and spleens were collected; immune cells were isolated

and processed for flowcytometry. Two weeks post tMCAO, cytokines were analyzed in the ischemic hemisphere and levels of major histocompability complex two (MHC II) proteins and amyloid precursor protein (APP) were determined.

Results: Levodopa/benserazide treatment reduced the total immune cell load in the ischemic hemisphere. In particular, we found a significant increase in CD3+/CD25+ regulatory T-cells and a nonsignificant reduction of MHCII+/CD11b+ cells (p=0.06) in the ischemic hemisphere after treatment with levodopa/benserazide. We also observed reduced levels of MHCII molecules, pro-inflammatory cytokines IL-1β and IFN-γ in the ischemic core/peri-infarct zone 2 weeks post tMCAO upon levodopa treatment suggesting a central immunosuppressive action of levodopa. The number of T-lymphocytes in the blood of levodopa/benserazide treated rats after tMCAO were similar to levels found in sham operated animals, in contrast to reduced numbers in vehicle treated rats after tMCAO. Moreover, we found reduced levels of amyloid precursor protein in the contralateral cortex indicative for a reduced secondary neurodegeneration of transcallosal fibers in levodopa/benserazide treated rats after tMCAO.

Conclusion: Our data strongly suggest anti-inflammatory and recovery enhancing actions of levodopa in the ischemic hemisphere by modulation of resident glial cells and peripheral immune cells. Recovery of T-lymphocytes in the blood suggests crosstalk between the brain and the immune system mediated by central dopamine.

References:

1. Rosser, N., et al. Arch Phys Med Rehabil, 2008. **89**(9): p. 1633-41.

2. Scheidtmann, K., et al. Lancet, 2001. **358**(9284): p. 787-90.

3. Ruscher, K., E. Kuric, and T. Wieloch. Stroke, 2012. **43**(2): p. 507-13.

4. Basu, S. and P.S. Dasgupta. J Neuroimmunol, 2000. **102**(2): p. 113-24.

5. Sarkar, C., et al. Brain Behav Immun, 2010. **24**(4): p. 525-8.

NEURONAL REGENERATION WITHIN SUBVENTRICULAR ZONE OF ADULT RAT AFTER CYTOSINE ARABINOSIDE INTRAVENTRICULAR INJECTION

T. Ochi, H. Nakatomi, H. Ono, S. Miyawaki, H. Horikawa, A. Ito, H. Imai, N. Saito

Neurosurgery, University of Tokyo, Bunkyo-ku, Japan

Considering previous reports, stimulating intrinsic stem/progenitor cells seems to be useful approach. The proliferation kinetics of neural stem cells after brain damage, however, is still not known well.

To investigate the cell kinetics of neural regeneration after brain damage, we focused on the subventricular zone of the lateral ventricules. Within the area Neuronal production persists throughout life, which bear a striking resemblance to the ventricular zone in the embryonic neuroepithelium. SVZ neural stem cells(Type B cells) function as the primary precursors of rapidly dividing transit-amplyfying Type C cells, which generate neuroblast(Type A cells). Each types of cells is known to express specific transcription factors, which also bear a striking resemblance to the expression of transcription factors in the embryonic neuroepithelium.

Using the cytosine arabinoside(Ara-C) intraventricular injection model of adult rats, which aimed to kill the dividing cells, we investigated chronological change of the cells within the SVZ with immunohistological analysis of transcriptional factors in combination with BrdU labeling.

Immediately after Ara-C injection, neither dividing cells nor Tuj-1+ cells was seen and a few Sox2+/GFAP+/Nestin+ cells were seen within SVZ. After some period of time, Prox1+/BrdU+ dividing cells started to appear first. Next, Ascl1+ cells and NeuroD1 cells could be seen. Finally, Tuj-1+ cells reappeared in this area.

Our results suggest that, after Ara-C injection, reappearance of cell populations involved in neuronal production within SVZ may occur not simultaneously but according to the order, in which remaining type B cells become typeC cells which generate type A cells.

So our results also imply that neuronal regeneration after brain damage may occur in the same manner with the development of the embryonic neuroepithelium.

MINING THE "NEW PENUMBRA" TO IDENTIFY TARGETS FOR PROTECTION AND REPAIR FOLLOWING STROKE: FOOL´S GOLD OR HIDDEN TREASURE?

R. Ratan

Burke-Cornell Medical Research Institute, Department of Neurology and Neuroscience, Weill Medical College of Cornell University, White Plains, NY, USA

It has been established for more than 50 years that excessive activation of NMDA receptors leads to cell death, a biological term referred to by Olney and colleagues as excitotoxicity. An apparent paradox also highlighted by work of Olney is that NMDA receptor blockade can itself lead to cell death. Initially this parabolic response was attributed to a window of calcium homeostasis congruent with survival. In this scheme, too low levels of cytosolic calcium (NMDA receptor blockade) or too high levels of calcium were thought to be responsible for this dichotomy. Another formulation has recently been developed is that suggests that it is “the location” of NMDA receptors that determines whether their activity is coupled to pro survival or pro death signals. Our main thesis is that the location of NMDA receptors not only determines pro-survival vs. pro-death signals, but also determines pro-regenerative versus anti-regenerative signals. Specifically, we hypothesize that blockade of extrasynaptic glutamate receptors will not only enhance survival of neurons post stroke, but also enhance plasticity of neurons post stroke. A further extension of this model is that activation of extrasynaptic glutamate receports or hypoactivation of synaptic glutamate receptors will impair transcriptional mechanisms that foster recovery signals.

Recently it has been shown that memantine at “low doses” can selectively block extrasynaptic glutamate receptors, leaving synaptic glutamate receptor activity intact. This block can prevent a feed-forward loop involving CREB, the coactivator Torc, and their downstream gene target, PGC1alpha. PGC1alpha is a coactivator that stimulates the expression of genes involved in mitochondrial biogenesis and antioxidant defense. Elegant new data shows that PGC1alpha deletion can itself promote extrasynaptic NMDA receptor activity. Although it is tempting to speculate that this increased activity comes via increased expression of Nr2b receptors (thought to be enriched in extrasynaptic sites) or Nr2b activity, available data argues against this. Equally plausible is the effect of this PGC1alpha on redox status, energy availability or calcium levels. I will discuss the implications of this finding for brain repair and several potential targets.

A major challenge moving forward is to develop appropriate preclinical models in vitro and in vivo that allow one to define approaches in humans that can selectively block extrasynaptic glutamate receptors. We propose to meet this challenge using a combination mature neuronal cultures and clinically relevant models of stroke. The goal of this approach is to develop methods to enhance acute and subacute survival of neurons while simultaneously enhancing their regenerative and plastic capacity. Thus, the need for concern about excacerbating acute injury with an intervention geared to stimulate recovery is minimized if not alleviated.

EXPRESSION REGULATION AND PROTEOLYTIC CLEAVAGE OF L1CAM FOLLOWING EXPERIMENTAL TRAUMATIC BRAIN INJURY IN MICE

M. Schaefer, L. Dangel, A. Sebastiani, E.-V. Schaible, C. Luh, S. Thal, C. Werner

University Medical Center Mainz, Mainz, Germany

The neural cell adhesion molecule L1CAM participates in neuronal migration, axon growth and pathfinding as well as synapse formation and plasticity in the developing and adult brain. The importance of L1CAM is reflected by human pathological mutations causing the L1 syndrome. Several studies demonstrated a role of the neural cell adhesion molecule L1CAM to maintain and reinstate neural homeostasis in mice models for acute and chronic neurodegeneration. In this study the CNS expression regulation of L1CAM was investigated after experimental traumatic brain injury in mice. qRT-PCR analyses revealed L1CAM downregulation up to 5 days after lesion. Expression levels increased 7 days after lesion suggesting a role in neural regeneration. Immunoblot analyses revealed enhanced proteolytic cleavage of L1CAM 24 hours after lesion leading to nuclear translocation of its cytoplasmic domain. These results suggest that proteolytic cleavage of L1CAM plays a pathophysiological role and modulates gene transcription after TBI.

TREATMENT OF CLINICAL CASES OF ALZHEIMER'S DISEASE WITH ZINC SULPHATE AND VITAMINS

K.S. Dhillon[1], **J. Singh**[1], J.S. Lyall[2]

[1]Punjab Agricultural University, [2]Punjab Council of Medical Services, Ludhiana, India

Objective: Alzheimer's Disease (AD) is the most common and complex disease of elderly people which typically presents a slow and progressive loss of cognitive functions and memory. The exact cause and treatment of AD are yet elusive. While delving disparately into the literature extant on this subject the most probable cause converged to the mineral(Copper, Iron and Zinc) dyshomeostasis generating free radicals and causing oxidative degeneration the brains of the affected persons. Hence, conceptually and logically the treatment of AD patients stated above was undertaken.

Materials: Eleven cases in the early stages of AD (4men and 7 women) visiting the clinics were diagnosed on the basis of history, age, progressive loss of memory and dementia. A questionnaire was prepared for further recording of clinical signs regarding progression/ regression of the disease after initiation of the medication. The treatment comprised of 100mg of Zinc sulphate dissolved in about 100 ml of drinking water one hour after meals daily for three months. In addition to this treatment one capsule of Vitamin A/E was given daily for the first fifteen days. The patients were interviewed fortnightly along with their attendant and observations were recorded on the questionnaire. At the end of three months another such schedule of this treatment was repeated and observations recorded. The side effect(s) of the treatment, if any, was also observed.

Results: The patients showed subtle signs of recovery from dementia which became apparent around 10-12 weeks after the start of medication. The patients presented remarkably pleasant behavior and confidence with further progression of treatment period i.e., up to six months. The caretakers and some relations contacted thereafter also remarked positively towards improvement in memory and previous behavior of frequent repetitive talking and forgetfulness. The patients were followed-up for a period of two years after six months of treatment and found to be in very good condition of memory. However, all the patients were advised to take this treatment once-a-week during the period of follow-up. None of the patients thus treated show any side effect of the medication.

Conclusion: The patients showed spectacular recovery from AD and dementia after treatment with 100mg of Zinc sulphate and one capsule of Vitamin A/E for a period of six months. Nevertheless, it is recommended that such trials on larger populations with placebo controlled investigations be undertaken before these results are applied in the clinical practice.

INTRANASAL ADMINISTRATION OF CART PEPTIDE INDUCES NEUROREGENERATION IN STROKE RATS

S.-J. Yu, H. Shen, Y. Yang, **B. Hoffer**, Y. Wang

NIDA, NIH, Baltimore, MD, USA

Objective: Utilizing a classic stroke model in rodents, middle cerebral artery occlusion (MCAo), we describe a novel neuroregenerative approach entailing the repeat intranasal administration of cocaine- and amphetamine-regulated transcript (CART) peptide starting from day 3 post-stroke by enhancing the functional recovery of injured brain.

Methods: Adult rats were separated into 2 groups with similar infarction sizes, measured by MRI on day 2 after MCAo, and were treated with CART or vehicle delivered into the nostrils. Proliferation and migration of endogenous neuroprogenitor cells (NPCs) as well as re-innvervation to the lesioned cortex were examined using cell culture, qRT-PCR, Western, immunohistochemistry, and MRI.

Results: CART treatment increased CART level in brain, improved behavioral recovery, and reduced neurological scores. In the subventricular zone (SVZ), CART enhanced immunolabeling of bromodeoxyuridine (BrdU), the neural progenitor cell marker Musashi-1, and the proliferating cell nuclear antigen, as well as upregulated BDNF mRNA. AAV-GFP was locally applied to the SVZ to examine migration of SVZ cells. CART enhanced migration of GFP(+) cells from SVZ toward the ischemic cortex. In SVZ culture, CART increased the size of neurosphere formation. CART -mediated cell migration from SVZ explants was antagonized by anti-BDNF

blocking antibody. Using 1H-magnetic resonance spectroscopy, increases in N-acetylaspartate levels were found in the lesioned cortex after CART treatment in stroke brain. CART increased the expression of GAP43 and fluoro-ruby fluorescence in the lesioned cortex.

Conclusion: CART enhances reinnervation in the lesioned cortex via several molecular mechanisms. Intranasal CART may provide a non-invasive and longer treatment window of days after stroke occurrence.

STEM CELL FACTOR AND GRANULOCYTE-COLONY STIMULATING FACTOR COMBINATION TREATMENT IN CHRONIC STROKE ENHANCES NEURAL NETWORK REMODELING IN AGED BRAIN

L.-R. Zhao[1], L. Cui[1,2], S. Murikinati[3], X. Zhang[2], W.-M. Duan[4], Brain Repair after Stroke

[1]Neurology/Cellular Biology and Anatomy, Louisiana State University Health Sciences Center, Shreveport, LA, USA, [2]Neurology, Second Hospital of Hebei Medical University, Shijiazhuang, China, [3]Neurology, [4]Cellular Biology and Anatomy, Louisiana State University Health Sciences Center, Shreveport, LA, USA

Objectives: Stroke has a high incidence in the elderly. Chronic stroke is the timing beyond 3 months after stroke onset. No treatment is currently available for chronic stroke other than physical therapy. In our early study, we reported that the combination of two hematopoietic growth factors, stem cell factor (SCF) and granulocyte-colony stimulating factor (G-CSF) (SCF+G-CSF) showed therapeutic effects on chronic stroke[1]. However, it remains unclear how SCF+G-CSF repairs brain in chronic stroke. In the present study, we have determined the effects of SCF+G-CSF in neuronal network remodeling in the aged brain in the phase of chronic stroke.

Methods: Sixteen to eighteen months old transgenic mice (equal to 62-69 years old human) expressing yellow fluorescent protein in layer V pyramidal neurons were subjected to cortical brain ischemia. SCF and G-CSF were subcutaneously injected for 7 days beginning at 3.5 months post-ischemia. A multiphoton microscope was used for acquiring brain images in live animals, and the live brain imaging was performed before treatment, 2 and 6 weeks after treatment. After the final imaging at week 6, brain sections were processed for immunohistochemistry.

Results: We observed that SCF+G-CSF increased the mushroom-type spines on the apical dendrites of layer V pyramidal neurons adjacent to the infarct cavities 2 and 6 weeks after treatment. Moreover, SCF+G-CSF promoted dendritic branching and functional synapse formation in the cortex adjacent to the infarct cavities 6 weeks after treatment.

Conclusions: SCF+G-CSF treatment in chronic stroke can re-establish stable and functioning neural circuits in the aged brain. This study offers new insights into the contribution of hematopoietic growth factors in brain repair and provides supporting evidence for developing a new therapeutic strategy to treat chronic stroke.

This study was supported by The National Institutes of Health, National Institute of Neurological Disorders and Stroke (NINDS), R01 NS060911 to L.R.Z.

Reference: 1. Zhao, L.R., Berra, H.H., Duan, W.M., Singhal, S., Mehta, J., Apkarian, A.V., and Kessler, J.A. Beneficial effects of hematopoietic growth factor therapy in chronic ischemic stroke in rats. *Stroke.* 2007, 38: 2804-2811.

POST-INJURY ADMINISTRATION OF DOCOSAHEXAENOIC ACID REDUCES ER STRESS RESPONSE AND IMPROVES NEUROLOGICAL FUNCTION AFTER TRAUMATIC BRAIN INJURY IN RATS

G. Begum[1], H.Q. Yan[2], A. Singh[1], C.E. Dixon[2], D. Sun[1]

[1]Dept. of Neurology, University of Pittsburgh, [2]Dept. of Neurosurgery, Brain Trauma Research Center, University of Pittsburgh, Pittsburgh, PA, USA

Objectives: Endoplasmic reticulum (ER) stress and abnormal protein accumulation are associated with activation of the unfolded protein response (UPR) and cell death during the acute phase of traumatic brain injury (TBI). Interestingly, in this study, we detected a prolonged UPR at 3-21 days post-TBI. Our recent study has shown that docosahexaenoic acid (DHA) blocked ER Ca^{2+} depletion and ER stress in astrocytes in response to ischemic

stress (Begum et al., *J Neurochem* 120: 622-630). Here, we investigated whether post-injury administration of DHA can reduce ER stress, abnormal protein aggregation, and axonal injury and improve neurological function in rats after TBI.

Methods: TBI was induced in Sprague-Dawley rats by the controlled cortical impact injury device. Sham control animals underwent identical surgical procedures but without receiving TBI. Either DHA (16mg/kg) or vehicle DMSO (1ml/kg) was administered interperitonially (i.p) once a day for 3, 7 or 21 days. Brain tissues were harvested at 3, 7 or 21 days post TBI for immunoblotting and immunocytochemical analysis of ER stress marker proteins ATF4, peIF2a and CHOP. Expression of ubiquitin, Aβ APP, and p-Tau was measured by immunocytochemistry. Sensorimotor function recovery after TBI was assessed with beam balance task and beam walking task at 1-5 days after TBI. Morris water maze test was performed at day 14-20 post TBI to assess the spatial learning and memory deficits.

Results: Western blot analysis revealed that TBI triggered prolonged activation of the UPR marker proteins p-eIF2a, ATF4 and CHOP in the ipsilateral cortex at 3 to 21 days after TBI. Moreover, prolonged ER stress was accompanied with accumulation of abnormal protein aggregates in the ipsilateral frontal cortex peri lesion at day 3 and 7 after TBI. Interestingly, post TBI administration of DHA attenuated expression of all ER stress proteins and reduced the expression of ubiqutinated proteins. Increased expression of Aβ APP and pTau was detected as early as day 3 and persisted upto 4 weeks post TBI. Moreover, the injured cortex, striatum, and corpus callosum exhibited significant axonal accumulation of APP/p-Tau. Most importantly, none of these pathological changes were detected in the DHA -treated brains. The DHA-treated animals exhibited an earlier recovery of the motor function and an improved spatial learning.

Conclusions: TBI triggers sustained ER stress and UPR activation during the chronic post-injury recovery phase. The prolonged ER stress, abnormal protein accumulation, and axonal injury contribute to the development of neurological deficits after TBI. To date, there are no effective treatments proven to improve the long term neurological function recovery after TBI. Our study demonstrates that post-injury administration of DHA reduces prolonged ER stress and abnormal accumulation of protein aggregates. These findings suggest that DHA may enhance the long term neurological function recovery after TBI via reducing ER stress and abnormal protein accumulation.

MANNOSE BINDING-LECTIN IS ASSOCIATED WITH INJURED VESSELS IN CLINICAL AND EXPERIMENTAL TRAUMATIC BRAIN INJURY AND ITS DELETION IS PROTECTIVE

M.G. De Simoni[1], F. Orsini[1], L. Longhi[1,2], S. Parrella[1], D. De Blasio[1], R. Zangari[1], F. Ortolano[2], N. Stocchetti[2]

[1]Mario Negri Institute, [2]Department of Pathophysiology and Transplantation, University of Milano, Fondazione IRCCS Ca' Granda, Ospedale Maggiore Policlinico, Milano, Italy

Objectives: Mannose binding lectin (MBL) is the activator of the lectin complement pathway. After cerebral ischemia MBL inhibition has been associated with neuroprotection with a wide therapeutic window (1). Instead in the setting of traumatic brain injury (TBI) MBL deficiency has been reported to be detrimental (2). We

1) characterized MBL activation following experimental TBI and in human contusions and

2) tested the hypothesis that its inhibition is associated with reduced behavioral deficits and histologic damage after experimental TBI.

Methods:

1) Male C57/Bl6 (WT) mice received intraperitoneal anesthesia (Pentobarbital, 65 mg/kg) followed by the controlled cortical impact model of TBI (injury parameters: velocity of 5 meter/s and 1 mm depth of deformation). MBL immunostaining was evaluated at 30 min, 6, 12, 24, 48, 96 hrs and 1 week after TBI using anti MBL-A and MBL-C (the two isoforms present in rodents) antibodies. MBL immunostaining was also evaluated in cerebral contusions of TBI patients that underwent surgical evacuation of the contusion for mass effect.

2) The effects of MBL inhibition were evaluated in WT and MBL-A and -C double knockout (-/-) mice. Functional outcome was

tested using the Neuroscore and Beam Walk test weekly for 4 weeks postinjury. Histologic outcome was evaluated by neuronal cell count in the cortex adjacent to the contusion.

Results: After experimental TBI we observed MBL-C positive immunostaining in the injured cortex starting at 30 minutes postinjury and up to 1 week, suggestive of an activation of this pathway. MBL-C was observed both at endothelial and tissue level. MBL-A was detected in the injured brain but its staining was much lower compared to that of MBL-C.

We found MBL positive immunostaining also in the injured cortex of TBI patients up to 4 days postinjury.

Injured WT and MBL (-/-) mice showed motor deficits up to 4 weeks postinjury when compared to their controls. Motor deficits were reduced in MBL (-/-) compared to WT mice at 2-4 weeks postinjury ($p < 0.01$ for Neuroscore and Beam Walk). Moreover we observed a reduced cortical cell loss at 4 weeks postinjury in MBL (-/-) mice compared to WT ($p < 0.05$).

Conclusions: We observed:

1) MBL deposition/synthesis on injured vessels and in the brain tissue after both clinical and experimental TBI.

2) Functional neuroprotection associated with MBL deficiency, suggesting that MBL modulation might be a potential therapeutic target after TBI.

References:

1) Orsini et al. Circulation. 2012 Sep 18;126(12):1484-94

2) Yager et al. J Cereb Blood Flow Metab. 2008 May;28(5):1030-9

OMEGA-3 POLYUNSATURATED FATTY ACID SUPPLEMENTATION IMPROVES NEUROLOGICAL RECOVERY AND ATTENUATES WHITE MATTER INJURY FOLLOWING EXPERIMENTAL TRAUMATIC BRAIN INJURY

H. Pu[1], W. Zhang[1], J. Zhang[1], L. Huang[1], G. Wang[1], A. Liou[2], J. Chen[1,2], **Y. Gao**[1]

[1]State Key Laboratory of Medical Neurobiology and Institute of Brain Science, Fudan University, Shanghai, China, [2]Department of Neurology and Center of Cerebrovascular Disease Research, University of Pittsburgh School of Medicine, Pittsburgh, PA, USA

Background: Traumatic Brain Injury (TBI) is a neurological disorder that leads to short and possibly long term motor and cognitive dysfunction with no effective therapeutic agent to date. Dietary supplementation with omega-3 fatty acids has been shown to confer protection against various neurological disorders. In this study, we characterized the protective effect of omega-3 polyunsaturated fatty acids (w-3 PUFAs) on controlled cortical impact (CCI) injury.

Methods: TBI was induced in C57/BL6 mice by a controlled cortical impact mouse model. w-3 PUFAs was administered in the diet for 2 months before CCI. For outcome assessments, sensorimotor deficits (hang wire, cylinder and foot fault tests) were determined at 1-35 days after TBI and cognitive performance was detected in the Morris water maze tests at 22-27 days post-TBI. Cresyl violet (CV) staining was used to assess the size of cortical lesion and calculate survival neurons at CA3. Microglial activation was measured using a microglial marker (Iba1), microglial pro-inflammatory response was detected by Real-time PCR and western blot of various pro-inflammatory cytokines. White matter injury was evaluated by immunohistochemistry staining of myelin basic protein (MBP) and SMI32 monoclonal antibody, western blot of MBP. Electron microscopic studies were taken to document myelinated or unmyelinated fiber damage in the corpus callosum post-TBI. The conductivity of the myelinated nerve fibers in the corpus callosum surrounding brain regions were evaluated Compound action potentials (CAPs).

Results: Our results indicate that inclusion of

w-3 PUFAs for 2 months in the diet attenuated short and long-term motor deficits as measured by the hanging wire, cylinder, and foot fault tests. w-3 PUFAs also prevented the loss of cognitive ability in the Morris water maze test at 22-27 days post-injury. Although w-3 PUFAs did not change cortical lesion volume, the dietary supplementation did protect against hippocampal neuronal loss following CCI and reduced the number of activated microglia as well as cytokine release. Finally, w-3 PUFAs prevented the loss of myelin basic protein (MPB), preserved the integrity of the myelin sheath, and maintained nerve fiber conductivity.

Conclusion: w-3 PUFAs elicit multifaceted protection against behavioral dysfunction, hippocampal neuronal loss, inflammation, and loss of myelination and impulse conductivity. Thus, w-3 PUFAs warrant further investigation as a therapeutic agent for traumatic brain injury.

PHARMACOLOGICALLY INDUCED HYPOTHERMIA ATTENUATES BRAIN INJURY AFTER TRAUMATIC BRAIN INJURY IN NEONATAL RATS

X. Gu[1], Z. Wei[1,2], A.R. Espinera[1], L. Wei[1,2], S.P. Yu[1]

[1]Department of Anesthesiology, Emory University School of Medicine, [2]Department of Neurology, Emory University School of Medicine, Atlanta, GA, USA

Introduction: Neonatal brain injury is a neurological disorder that can result in serious long-term disabilities. Mild to moderate hypothermia has shown strong neuroprotective effects in both pre-clinical and clinical studies after ischemic stroke. However, the benefits of hypothermic therapy for traumatic brain injury (TBI) have not been as thoroughly investigated. Since conventional physical cooling methods are not efficient and often impractical for acute stroke patients, we investigated pharmacologically induced hypothermia with a novel neurotensin receptor 1 compound, ABS-201. It is a blood-brain barrier permeable compound that shows few side effects in rodents and monkeys. We previously demonstrated that ABS-201 induced dose-dependent hypothermia and was neuroprotective against ischemia-induced cell death and improved functional recovery after ischemic stroke in mice (Choi, Hall et al. 2012). In the present investigation, we tested the hypothesis that pharmacological hypothermia is a neuroprotective treatment after TBI in a neonatal rat model.

Methods: Neonatal rats at post-natal day 9 (P9) were subjected to a controlled cortical impact (CCI), followed by ABS-201 injection (2 mg/kg, i.p.) 20 min after the onset of TBI. Additional injections were given to maintain the hypothermia for 6-9 hours. Animals were sacrificed at 6, 12, 24 and 72 hours after TBI. The blood-brain barrier (BBB) integrity, contusion volume, and brain swelling were measured. Cell death and cell survival assays were performed by immunochemistry, qRT-PCR and Western blot.

Results: ABS-201 reduced brain and body temperature from 37^{o}C to 33^{o}C within 30-60 min of injection without causing noticeable shivering and, after last injection the temperature gradually returned to the normal level without overshoot. ABS-201-treated pups showed much less BBB damage measured by Evans Blue assay after TBI compared to saline control pups. Pharmacological hypothermia significantly reduced the contusion volume and cell death. Specifically, the TUNEL/NeuN- colabeled cells in the injury core and the peri-injury regions were significantly decreased in ABS-201-treated rats. Western blot showed that ABS-201 treatment diminished caspase-3 activation and increased the Bcl-2 expression as well as the Bcl-2/Bax ratios in injury regions. Additionally, pharmacological hypothermia attenuated inflammatory gene expression including tumor necrosis factor-α (TNF-α), interleukin-1β (IL-1β) and IL-6.

Conclusions: These results support that pharmacological hypothermia induced by ABS-201 show multiple benefits by attenuating TBI-generated brain damage. Pharmacological hypothermia provides a promising therapeutic approach for the treatment of neonatal TBI and possibly other brain injuries such as ischemic stroke.

Reference: Choi, K. E., C. L. Hall, J. M. Sun, L. Wei, O. Mohamad, T. A. Dix and S. P. Yu (2012). A novel stroke therapy of pharmacologically induced hypothermia after focal cerebral ischemia in mice. FASEB Journal **26**: 2799-2810, 2012.

HYPERBARIC OXYGEN THERAPY IMPROVES NEUROIMAGING OUTCOMES IN A RAT MODEL OF REPETITIVE MILD TRAUMATIC BRAIN INJURY

L. Huang[1,2], J.S. Coats[3], A. Mohd-Yusof[3], J.H. Zhang[1,2,4], R.D. Martin[1], A. Obenaus[3,5,6]

[1]Anesthesiology, [2]Physiology & Pharmacology, [3]Pediatrics, Loma Linda University School of Medicine, [4]Neurosurgery, Loma Linda University, Loma Linda, [5]Cell, Molecular & Developmental Biology, University of California at Riverside, Riverside, [6]Neuroscience, University of California at Riverside, Loma Linda, CA, USA

Objective: Mild traumatic brain injury (mTBI) is an important medical concern that accounts for upwards of 75% of all TBI patients each year. Repetitive mTBI (rmTBI) can result in cumulative brain injury, leading to exacerbation of tissue damage and long lasting psychosocial outcomes (McCrory, 2011). Given cellular metabolic perturbations may underline the pathological processes following mTBI (Barkhoudarian, 2011), a neuroprotective approach favoring cerebral aerobic metabolism could be beneficial in the setting of rmTBI. Hyperbaric oxygen (HBO) fulfills this requirement and has been explored as a novel therapeutic approach for management of TBI (Huang, 2011). In this study, we investigated both prophylactic and therapeutic HBO strategies in a rat model of rmTBI using multi-modal magnetic resonance imaging (MRI), correlated to histopathology.

Methods: Sprague Dawley adult male rats were randomized into nine groups: Sham, rmTBI 3d and 7d apart with or without HBO intervention including pre-treatment or post-treatment. A mild controlled cortical impact was delivered to the parietal cortex. For animals receiving rmTBI, a second CCI was delivered at the same location 3 or 7 days later. Sham animals underwent the same surgical procedures without CCI. HBO (100% oxygen at 2 ATA) was given 1hr daily for 3 consecutive days either prior to (pre-treatment) or 24 hrs post (post-treatment) the initial TBI. T2 weighted imaging (T2WI) and susceptibility weighted imaging (SWI) were acquired on 4.7T Bruker Biospin in vivo 24hrs after each impact and at 14 days post-1st CCI. Total lesion and hemorrhage volumes were quantified. At 14 days post-1st CCI, glial responses were examined using immunohistochemistry staining of Glial Fibrillary Acidic Protein (GFAP) for astrocytes and Ionized Calcium Binding Adaptor Molecule 1 (IBA1) for microglia.

Results: In the rmTBI 3d apart but not 7d apart group, the second injury significantly increased T2WI-dervied lesions and SWI-identified hemorrhage volumes at 24 hrs post rmTBI, persisting to 14 days post the injury. Both HBO pre-treatment and post-treatment reduced lesion volumes compared to non-treated rmTBI animals. The most dramatic decrease were seen in rmTBI 3d apart HBO treated animals where there was a 3-fold decrease in hemorrhage volumes. Histopathology correlated with in vivo MRI findings demonstrating HBO pre- or post-treatment associated reduction in astrocyte and microglial activation following rmTBI.

Conclusions: The brain appears to exhibit heightened vulnerability to a second mild traumatic insult within 3 days after an initial mTBI. Both prophylactic and therapeutic HBO provide a potential neuroprotective strategy that can be applied to rmTBI patients.

References:

1. McCrory, P. Sports concussion and the risk of chronic neurological impairment. Clinical Journal of Sport Medicine. 2011; 21, 6-12.
2. Barkhoudarian, G., Hovda, D.A., Giza, C.C., 2011. The molecular pathophysiology of concussive brain injury. Clinics in Sports Medicine. 30, 33-48, vii-iii.
3. Huang, L., Obenaus, A. Hyperbaric oxygen therapy for traumatic brain injury. Med Gas Res. 2011; 1: 21

HYPERBARIC OXYGEN TREATMENT IS NEUROPROTECTIVE AGAINST REPETITIVE MILD TRAUMATIC BRAIN INJURY

L. Huang[1,2], M. Hamer[3], K. Tasi[4], A. Obenaus[3], R. Applegate[1], J.H. Zhang[1,2,5]

[1]Anesthesiology, [2]Physiology & Pharmacology, [3]Pediatrics, Loma Linda University School of Medicine, Loma Linda, [4]Biology, University of California at Riverside, Riverside, [5]Neurosurgery, Loma Linda

University School of Medicine, Loma Linda, CA, USA

Objectives: Repetitive mild traumatic brain injury (mTBI) is an important public health issue in the pediatric population participating in sports. Individuals who sustain repetitive mTBI endure emotional, sensor and/or cognitive deficits. Hyperbaric oxygen (HBO) therapy has been shown to be neuroprotective against moderate-severe TBI (Huang et al, 2011). A genome microarray study suggested that activation of nuclear factor E2-related factor 2 (Nrf2) might one of the primary mechanisms underlying HBO included-cytoprotective response (Godman et al., 2010). In the present study we investigated the treatment effect of HBO and its Nrf2 activation in an adolescent rat model of repetitive mTBI (rmTBI).

Methods: Sprague Dawley adolescent male rats (30 days old) were randomized into Sham, Sham+HBO, rmTBI, mTBI+HBO. A mild controlled cortical impact (CCI) was induced to generate mTBI. HBO (2.0ATA×1h/day) were administered at 24 hrs post 1st CCI for 3 consecutive days. For animals receiving rmTBI, the second identical CCI was delivered at 3 days later at the same site. Sham animals underwent the same surgical procedures without CCI. CCI lesions were evaluated in vivo 24hrs after each impact and 14 days post-1st CCI using T2 weighted images (T2WI) and susceptibility weighted images (SWI) on a 4.7T Bruker Biospin. Total lesion volumes including edema and bleeding were identified by T2WIs. Regions of interest for hemorrhages were derived on SWIs. Immunohistochemistry examinations included Glial Fibrillary Acidic Protein (GFAP) staining for astrocytes and Ionized Calcium Binding Adaptor Molecule 1 (IBA1) for microglia; Neuronal Nuclei (NeuN) for neuron co-staining with Nrf2.

Results: Compared to non-treated rmTBI animals, HBO treatment significantly reduced the T2WI-defined lesion volumes and SWI-defined hemorrhage volumes at 24 hours after the 2nd mTBI. Correlated to neuroimaging findings, there were significantly lesser cortical astrocyte gliosis and microglia activation in HBO-treated rmTBI at 14 days post-initial mTBI. At 24 hrs post 2nd mTBI, increased nuclear expressions of Nrf2 in neurons with ipsilateral cortex were associated with HBO treatment.

Conclusions: HBO provides a potential neuroprotective strategy that can be applied to pediatric population at high risk for repetitive mTBI. MRI is a sensitive neuroimaging biomarker for monitoring experimental and clinical treatment effects within the setting of rmTBI.

References:

1. Huang, L., Obenaus, A. Hyperbaric oxygen therapy for traumatic brain injury. Med Gas Res. 2011; 1: 21
2. Godman CA, Chheda KP, Hightower LE, Perdrizet G, Shin DG, Giardina C. Hyperbaric oxygen induces a cytoprotective and angiogenic response in human microvascular endothelial cells. Cell Stress Chaperones. 2010;15:431-442

AQUAPORIN-4 (AQP4) DYSREGULATION IN A CLOSED-SKULL MURINE MODEL OF MILD AND MODERATE TRAUMATIC BRAIN INJURY

J. Iliff[1], Z. Ren[2], L. Yang[2], M. Nedergaard[2]

[1]Department of Anesthesiology and Peri-Operative Medicine, Oregon Health & Science University, Portland, OR, [2]Center for Translational Neuromedicine, University of Rochester Medical Center, Rochester, NY, USA

Cerebral edema is a major driver of morbidity after traumatic brain injury (TBI). Since first being implicated in the genesis of cerebral edema after ischemic stroke, the astrocytic water channel aquaporin-4 (AQP4) has been the subject several TBI studies, as its potential role in the post-traumatic edema formation and resolution has been evaluated. Each of these studies has utilized an open-skull model of moderate to severe TBI. In these preparations, changes in intracranial pressure (ICP), cerebral edema and AQP4 expression are likely altered from what occurs in the closed-skull injuries that are most prominent clinically. Additionally, no prior studies have evaluated changes in AQP4 expression after mild traumatic brain injury. In the present study, we utilize a novel closed-skull model of traumatic injury termed 'Hit & Run' TBI to characterize the dynamics of AQP4 expression after mild and moderate injury. We observe that after moderate TBI, blood brain barrier disruption, cerebral edema and ICP peak 3 days post-injury, then resolve prior to 7 days post-injury. AQP4 dysregulation, which is characterized by a depolarization of AQP4 localization away

from perivascular astrocytic endfoot processes to the broader somal compartment, does not peak until 7 days after moderate TBI. This suggests that AQP4 dysregulation likely does not drive cerebral edema formation, but rather may represent a compensatory mechanism to support edema clearance and ICP normalization after moderate TBI. For the first 14 days post-injury, AQP4 dysregulation after mild and moderate TBI are indistinguishable from one another. However, after mild TBI AQP4 dysregulation largely resolves 3-4 weeks post-injury. In contrast, AQP4 is chronically dysregulated after moderate TBI, including dramatic overexpression of AQP4 in the developing glial scar. These findings demonstrate that the dynamics of post-traumatic AQP4 dysregulation are more complex than suggested by prior TBI studies, and differ markedly between mild and moderate grades of TBI.

CEREBRAL HEMODYNAMICS OF MILD TRAUMATIC BRAIN INJURY AT THE ACUTE STAGE

Z. Kou[1], H. Doshi[2], W. Wang[3], V. Mika[2], R. Welch[2], E.M. Haacke[1]

[1]Biomedical Engineering and Radiology, [2]Wayne State University School of Medicine, Detroit, MI, USA, [3]Computer Science, South-Central University for Nationalities, Wuhan, China

Introduction and objective: There are more than 1.7 million reported traumatic brain injury (TBI) cases every year in the United States alone. There is little data showing the effect of mTBI on cerebral hemodynamic changes at the acute stage. The objective of this study is to get a global picture of brain hemodynamic at the acute stage. Particularly we will measure changes in the arterial cerebral blood flow (CBF), by using Arterial Spin Labeling (ASL), and venous oxygen saturation, by using Susceptibility Weighted Imaging and Mapping (SWIM) techniques.

Materials and methods: The main criteria for patient recruitment were the definition of mTBI by American Congress of Rehabilitation Medicine (ACRM) and Glasgow Coma Scale (GCS) of 13-15 at the time of arrival. A short neurocognitive instrument called standard assessment of concussion (SAC) was used to assess the patients' neuro-cognitive status, including orientation, attention and memory. Patients were scanned on 3T Siemens VERIO scanner with 32-channel head coil. Imaging sequence protocol includes SWI, ASL, DTI and baseline structural imaging. Fourteen patients were scanned for SWI, among which 9 also had ASL. Nine patients had 1-month follow-up.

ASL data were processed to measure cerebral blood flow in Thalamus, Caudate, Putamen, Striatum, Globus Paddilum, Frontal, Occipital, Parietal and Temporal lobes. The normalized ASL data was registered to the T1 template and the lobe/structure specific ROIs were projected back to the native space using inverse transform. SWIM processing was performed on the SWI data [1]. Blood oxygen saturation in 8 major veins was measured on SWIM images. Student's t-test was performed in both ASL and SWI data analysis to compare the patient and control group.

Results: Patient group showed significant lower SAC score than control group ($p=0.05$). The difference is more significant in delayed recall ($p=0.02$). In SWIM data, two major veins, left thalamo-striate vein and right basal vein of Rosenthal showed significantly lower oxygen saturation at acute stage than controls (See Figure 1). These oxygen saturation levels came back to control levels at the follow-up. ASL data shows significantly higher cerebral blood flow in the Caudate nucleus, Putamen and Striatum at the acute stage.

Discussion and conclusion: This study shows that, after head injury, the increased cerebral blood flow is followed by more oxygen left in the venous side of the same striatum region. However lower SAC scores shows neurocognitive problems. This suggests that there might be some deficiency in that part of the brain in which condition brain works hard and generates higher demand of blood supply. Weather the amount of changes in cerebral blood flow is in proportion with the increased oxygen saturation in the veins needs to be studied in more details. Changes in CMRO2 at the acute stage and variations in brain activity during this stage also need to be studied more comprehensively.

Reference:

1. Haacke EM, Tang J, Neelavalli J, and Cheng YCN. Susceptibility Mapping as a Means to Visualize Veins and Quantify Oxygen Saturation. JMRI, 32:663-676 (2010).

THE PROTECTIVE EFFECT OF PHARMACOLOGICALLY INDUCED HYPOTHERMIA AFTER TRAUMATIC BRAIN INJURY IN ADULT MICE

J.H. Lee, L. Wei, S.P. Yu

Anesthesiology, Emory University School of Medicine, Atlanta, GA, USA

Objectives: Traumatic brain injury (TBI) is a severe disorder resulting in high mortality and disability. Currently there is no effective therapy for the treatment of acute TBI patients. However, mild to moderate hypothermia is considered to be a promising TBI and stroke treatment [1]. Nonetheless, forced cooling by physical methods in patients is inefficient, cumbersome and often impractical for acute stroke and TBI patients. Our recent study tested pharmacologically induced hypothermia using a novel neurotensin receptor 1 (NTR1) agonist, ABS-201 that is blood-brain barrier (BBB) permeable and effectively reduces body/brain temperature 3-5^{o}C in the 30-60 min after administration. ABS-201-induced hypothermia has shown significant neuroprotection against ischemic damage [2]. In the present investigation, we examined the efficacy of ABS-363, a second generation NTR1 agonist in a TBI mouse model.

Methods: Adult male mice were anesthetized and subjected to a controlled cortical impact (CCI) (velocity=3m/s, depth=1.0 mm, contact time=150 ms) to the exposed cortex. ABS-363 (0.3 mg/kg, i.p.) injection in both the control mice and TBI mice induced a mild-to-moderate hypothermia (3-5 °C reduction). Additional injections maintained the hypothermia for up to 6 hrs. TBI-induced brain injury, cell death, blood brain barrier disruption, inflammatory response, and sensorimotor functional deficit were measured at 12 hrs and 3 days after TBI.

Results: At 3 days after TBI, ABS-363 treatment significantly reduced the contusion volume. ABS-363 treatment diminished the activated casapse-3, Bax expression, and TUNEL-positive cells in the peri-contusion cortical region at 12hrs after TBI. To examine whether ABS-363-induced hypothermia prevented BBB damages, we examined the extravasation of Evans blue (EB) dye and Immunoglobulin G (IgG). ABS-363 significantly reduced the volume of EB leakage, attenuated the upregulated expression of IgG, and the expression of MMP-9 after TBI. TBI triggered a significant increase in ionized calcium binding adaptor molecule 1 (iba1)-positive microglia within the core and penumbra regions. This increase was attenuated by ABS-363 treatment. qRT-PCR experiments revealed that ABS-363 decreased the expression of tumor necrosis factor-a (TNFα) and interleukin-1b (IL-1b), but increased IL-6 and IL-10. In addition, delayed hypothermia for up to 2 hrs after TBI also showed the protective effect of reducing the contusion volume and TUNEL-positive cells. Finally, compared to the control mice, the TBI mice with either early or delayed administration of ABS-363 showed better sensorimotor functional recovery in the adhesive removal test 3 days after TBI.

Conclusions: ABS-363 is an effective pharmacological hypothermic compound and may be used for treating TBI and stroke. The therapeutic window of at least 2 hours after the onset of TBI insult in the animal model is of clinical significance. These findings support that pharmacological hypothermia should be further explored in pre-clinical and clinical investigations.

References:

1. Dietrich WD, Bramlett HM (2010) The evidence for hypothermia as a neuroprotectant in traumatic brain injury. Neurotherapeutics 7: 43-50.

2. Choi KE, Hall CL, Sun JM, Wei L, Mohamad O, et al. (2012) A novel stroke therapy of pharmacologically induced hypothermia after f multifaceted ocal cerebral ischemia in mice. FASEB J 26: 2799-2810.

MICRORNA EXPRESSION PROFILE DURING SECONDARY LESION EXPANSION AFTER TRAUMATIC BRAIN INJURY

L. Meissner[1,2], M. Gallozzi[2], S. Schwarzmaier[1,2], M. Balbi[1,2], N. Terpolilli[3], **N. Plesnila**[1,2]

[1]Institute of Stroke and Dementia Research, University of Munich Medical Center, Munich, Germany, [2]Department of Neurodegeneration, Royal College of Surgeons in Ireland (RCSI), Dublin, Ireland, [3]Institute for Surgical Research, University of Munich Medical Center - Campus Großhadern, Munich, Germany

Objectives: MicroRNAs play a pivotal role in the regulation of protein expression in the brain[1]. Recent studies revealed that microRNA expression is changed after traumatic brain injury (TBI)[2,3], however, the temporal and

spatial profile are still unclear. Therefore we performed a temporal profile of microRNA expression during secondary expansion of the lesion in a cortical contusion impact (CCI) model of traumatic brain injury in mice and validated the resulting hits by in situ hybridization.

Methods: Microarray analysis of microRNA profile was performed on RNA samples isolated from the cortical penumbra at 1, 6, 12 h after CCI. The expression profile was compared to sham operated and untreated animals. The most significant results obtained by the microarray were validated by qPCR and in situ hybridization.

Results: Hierarchical clustering of 410 microRNAs analyzed by microarray screening revealed a clustering of microRNA profiles corresponding to the different time points after TBI. Untreated healthy animals clustered with sham operated animals. qPCR validation of the 5 most significantly upregulated and the 4 most significantly downregulated microRNAs compared to sham operated animals correlated with the data obtained by the array. In situ hybridization demonstrated that the most significantly upregulated microRNA (miR-2137) is highly expressed in neuronal cells in the penumbra of the contusion.

Conclusions: This study identified interesting candidates for further functional analysis and drug development. Highly upregulated candidates such as miR-2137 might be new targets for the treatment of secondary brain damage after traumatic brain injury.

References:

1. *Saugstadt, J. MicroRNAs as effectors of brain function with roles in ischemia and injury, neuroprotection, and neurodegeneration. JCBFM 30 (9), 1564-76 (2010).*
2. *Redell, JB., Liu, Y., Dash PK.Traumatic brain injury alters expression of hippocampal microRNAs: potential regulators of multiple pathophysiological processes. J Neurosci Res. 87(6),1435-48 (2009).*
3. *Lei, P., Li, Y., Chen, X., Yang, S., Zhang, J.Microarray based analysis of microRNA expression in rat cerebral cortex after traumatic brain injury.Brain Res. (1284), 191-201 (2009).*

GLYCYRRHIZIN THERAPY FOR TRAUMATIC BRAIN INJURY

Y. Okuma[1,2], K. Liu[2], H. Wake[2], K. Teshigawara[2], J. Haruma[1,2], I. Date[1], M. Nishibori[2]

[1]Neurosurgery, [2]Pharmacology, Okayama University Graduate School of Medicine, Dentistry and Pharmaceutical Sciences, Okayama, Japan

High mobility group box-1 (HMGB1) plays an important role in triggering inflammatory responses in many types of diseases. Previously we found that anti-HMGB1 mAb efficiently reduced acute brain edema after traumatic brain injury (TBI) through protection of the blood brain barrier (BBB) and inhibition of the inflammatory responses. It has been shown that Glycyrrhizin binds directly with HMGB1 by interacting with two shallow concave surfaces formed by the two arms of both HMG boxes in HMGB1.

In this study, we examined whether or not Glycyrrhizin inhibited HMGB1 binding to sRAGE. We also investigated the ability of intravenously administered neutralizing Glycyrrhizin to attenuate brain injury induced by TBI. Traumatic brain injury was induced in rats or mice by fluid percussion. Glycyrrhizin was administered intravenously after TBI. Glycyrrhizin remarkably inhibited HMGB1 binding to sRAGE. Glycyrrhizin significantly inhibited fluid percussion-induced brain edema in rats associated with inhibition of HMGB1 translocation, protection of blood-brain barrier (BBB) integrity, suppression of inflammatory molecule expression and improvement of motor function. Experiments using RAGE-/- mice suggested the involvement of RAGE as the predominant receptor for HMGB1.

Glycyrrhizin may provide a novel and effective therapy for TBI by protecting against BBB disruption and reducing the inflammatory responses induced by HMGB1.

SMALL MOLECULAR HGF MIMETIC REDUCES TBI INDUCED MOTOR DEFICIT AND TISSE DAMAGE IN MICE

H. Sheng[1], M. Lu[2], M. Izutsu[1], D. Smith[3], I. Goldberg[3], D.S. Warner[4]

[1]Anesthesiology, Duke University Medical Center, Durham, NC, USA, [2]Anesthesiology, Second Affiliated Hospital, Zhengzhou University, Zhengzhou, China, [3]Angion Biomedica Corp, Uniondale, NY, [4]Anesthesiology, Neurobiology and Surgery, Duke University Medical Center, Durham, NC, USA

Objectives: Hepatocyte growth factor (HGF) serves as a potent angiogenic and neurotrophic factor and has been found to attenuate cerebral ischemia injury (1, 2) and promote neuronal differentiation of stem cells (3). This translational study was designed to define if small molecular HGF mimetic, BB3, can be used in treating traumatic brain injury (TBI) induced motor functional deficit and tissue damage in mice.

Methods: The institute approved this study. Under isoflurane anesthesia, mice were intubated and ventilated. Normal body temperature was maintained. 40 C57Bl/6J mice were subjected to cortical controlled impact injury in left parietal brains at 5m/s, 1 mm depth and 200 ms dwell time. Additional 8 mice had same procedure without cortical injury. Post-surgery mice were randomly assigned to one of experimental groups and received BB3 (6mg/kg) or saline i.p. daily beginning at 1 hour after surgery for 28 days. Rotarod test and beam walking were performed at 1, 3, 7, 14, 21 and 28 days. Morris Water maze was performed at 29-34 days. At the end of experiment, brains were perfused and paraffin embedded for histological analysis. Person blind to treatment performed functional tests and measured lesion size. Data were expressed as mean ± SD and analyzed with ANOVA or unpaired T test.

Results: Injured mice had motor deficit in fixed rotarod test (32 rpm) at post-injury day 1 ($p < 0.01$). BB3 treatment improved the latency to fall at post-injury day 3 (BB3 n=20, 160 ± 113 sec, Vehicle n=20, 86 ± 81 sec, p= 0.02, unpaired T test). Latency to fall was not different at post-injury day 28. However, BB3 treated mice had a better performance in fine beam walking at post injury 28 days (BB3 = 2.25 ± 0.9, Vehicle = 1.6 ± 0.9, p= 0.03, sham = 3.5 ± 0.8). Injured mice had a longer latency to find the platform in Morris water maze (p= 0.004) and however, BB3 treatment did not shorten the latency. Histological analysis showed that cortical lesion size in vehicle group was larger compared to BB3 treated mice (BB3 = 1.71 ± 0.46 mm3, Vehicle = 2.23 ± 0.54 mm, p= 0.0025). Ipsilateral hippocampal size was significantly reduced in injured mice ($p < 0.01$, sham= 3.02 ± 0.37 mm3, BB3 = 1.01 ± 0.61 mm3, vehicle = 1.12 ± 0.64).

Conclusions: These data demonstrated that BB3 treatment effectively improves TBI-induced motor deficit in performing fine beam walking and early rotarod test. Cortical tissue damage was also reduced. Failure to improve post-injury cognitive function was probably due to too severe hippocampus injury in this injury setting. Further exposure of the use of HGF mimetic in TBI is encouraged. The treatment window and dose response effect will be tested in near future to systemically evaluate its therapeutical potential in TBI treatment.

References:

1. Shimamura M et al. Circulation 2004, 109: 424-31

2. Date I et al. Biochem Biphys Res Commun 2004, 319:1152-8

3. Kato M et al. Neuroport 2004, 15:5-8

PATHOBIOLOGY AND TREATMENT OF CLINICAL CASES OF AUTISM IN CHILDREN

J. Singh

Punjab Agricultural University, Rocklin, CA, USA

Objective: Autism is a complex neurodevelopment brain disorder in children. The clinical signs include impairment of communication skills, social interaction, repetitive behavior and differences in sensory processing. Autism affects one in 110 children and tens of millions worldwide are currently suffering from this malady and the number is still increasing. Its putative causes are multifactorial as genetics, environmental, oxidative stress but remains enigmatic. While delving disparately into the literature extant on this disease it appears to be an imbalance

among different trace minerals in the affected kids (Jory and McGinnis, 2008). This imbalance appear to cause oxidative stress and neuronal degeneration in affected subjects which is expressed as Autism Spectrum Disorder. Hence, it was conceptually and logically hypothesized to attempt medication with some trace elements and antioxidants to alleviate the clinical signs of this malady.

Methods: Eleven children (7 boys and 4 girls) aged 4-9 years visiting the clinics were diagnosed with Autism depending on the signs. Their parents or caretakers were also interviewed and the information was recorded in a proforma relating to age, approximate period of appearance of signs, treatments given and its outcome. Each child received 75mg of zinc sulfate in drinking water + one capsule of vitamin A daily for three weeks when the assessment of effect of this treatment was made. Two children who had muscular weakness and could not stand on their feet were also given 200mg of magnesium sulfate and/or copper sulfate after an intervening period of one week. This schedule continued with six such regimens. The patients and their parents/ caretakers were interviewed after each schedule and observations recorded. The side effect, if any, from the medication was also enquired and duly recorded.

Results: All the kids thus treated showed discernible improvement in their signs after first three weeks of medication. The parents especially mothers reported that there was a lot of improvement in gastrointestinal troubles as diarrhoea/constipation and general behavior. These signs further improved with the progression of treatment. Two kids having muscular weakness also revealed some improvement as they started putting weight on their feet with assistance at the end of three schedules of medication. The overall assessment at the end of six-three week schedules of treatment showed 50-60 percent recovery in the clinical signs.

Conclusions: It was inferred that clinical cases of Autism responded positively to this treatment and did not show any side effect(s) from the medication.

References: Jory J and McGinnis WR. Red-cell trace minerals in children with Autism. Am J Biochem Biotech 2008; 4(2): 101-104.

NOTCH SIGNALING PATHWAY MEDIATES NEUROPROTECTIVE EFFECT IN MOUSE CORTICAL NEURONS AFTER TBI

N. Su, Z. Fei

Xijing Hospital, The Fourth Military Medical University, Xi'an, China

Traumatic brain injury (TBI) in humans leads to neuronal death and neurological dysfunction. Reducing the necrosis and apoptosis of neurons can improve the survive rate after TBI. Notch signaling contributes to a variety of cell-fate decisions during development. Our aim is to investigate whether Notch activation could influence the apoptosis of neurons after TBI in vitro. Cultured cortical neurons were injured by physical damage. Western-blot and immunohischemistry was used to examine the activation of Notch, Notch intracellular domain (NICD) and caspase 3. Neurons exhibited substantially increased levels of NICD and caspase 3. Furthermore, blockage of the Notch pathway by a γ-secretase inhibitor significantly reduced NICD induced by TBI. Meantime, the apoptosis of neurons was reduced. These data suggest that Notch signaling pathway maybe mediates the survival of neurons after TBI.

ENDOPLASMIC RETICULUM STRESS FOLLOWING TRAUMATIC BRAIN INJURY

V.P. Nakka, **R. Vemuganti**

Neurological Surgery, Univ. Wis. Madison, Madison, WI, USA

Following translation, proteins are folded and sorted in the endoplasmic reticulum (ER). Cellular stress disrupts this process leading to accumulation of unfolded/misfolded proteins in ER. To cope-up with this, cells initiate an unfolded protein response (UPR) that leads to ER stress. The positive aspect of the ER stress is the induction of chaperones to transport the defective proteins out of ER to ubiquitin-proteasomal system for degradation. However, when the ER is overloaded, the negative effects of ER stress kicks-in. The ER transmembrane protein PERK is a major effector of ER stress response. PERK activation phosphorylates the down-stream eif2α which repress translation to reduce protein load on ER. However, p-eif2α allows translation of certain proteins like transcription factor ATF4 due to the specific arrangement of uORF2 in ATF4 mRNA (transcript-specific translational control). ATF4 induces its down-

stream transcription factor CHOP and further GADD34. GADD34 activates PP1c which dephosphorylates p-eif2α leading to translational recovery. We currently report that traumatic brain injury in adult rats induces the protein expression of PERK, CHOP and GADD34 in addition to increasing the phosphorylation of eif2α. Furthermore, treating rats with salubrinal (a GADD34 inhibitor) after TBI induced a significant neuroprotection by allowing eif2α to stay in a phosphorylated form. Thus, these studies indicate the presence of ER stress after TBI in adult rats and a major role played by PERK/eif2α CHOP/GADD34 pathway.

CORTICAL THICKNESS FINDINGS IN PATIENTS WITH PERSISTENT SYMPTOMS AFTER MILD TRAUMATIC BRAIN INJURY

O. Wu[1], E. McIntosh[1], B.L. Edlow[2], J.C. Sherman[3], A. van der Kouwe[1], S. Stufflebeam[1], M. Purohit[4], D.M. Greer[2,5], B. Fischl[1], R. Zafonte[4]

[1]Athinoula A Martinos Center for Biomedical Imaging, Massachusetts General Hospital, Charlestown, [2]Department of Neurology, [3]Department of Psychiatry, Massachusetts General Hospital, [4]Department of Physical Medicine and Rehabilitation, Spaulding Rehabilitation Hospital, Boston, MA, [5]Department of Neurology, Yale University School of Medicine, New Haven, CT, USA

Objectives: Approximately 75% of traumatic brain injury (TBI) patients have mild TBI (MTBI) and typically exhibit few if any abnormalities on conventional brain imaging, but display a broad spectrum of neurocognitive dysfunction, including confusion, inattention and amnesia. The majority of MTBI patients recover within a few months, but for up to 15% symptoms persist, with a devastating impact on school, work, and interpersonal relationships, potentially leading to long-term disability. Cortical thickness analyses[1] have shown promise for identifying regions of thinning associated with cognitive impairments in patients with moderate to severe TBI[2, 3] and in patients many years after sports concussion injuries.[4] We therefore investigated whether differences existed in cortical thickness in subjects with persistent post-concussion syndrome after MTBI.

Methods: Ten MTBI patients symptomatic for at least 3 months were recruited from a sports concussion clinic along with 10 healthy controls. All subjects were required to be at least 16 years old. All subjects were imaged on a 3T MRI. 3D T1-weighted MPRAGE were acquired with 1x1x1 mm^3 resolution, using a field-of-view of 256 mm and 176 sagittal slices. Cortical thickness analyses[1] were performed between control and MTBI subjects taking into consideration age and correcting for multiple comparisons (P=0.05) by Monte Carlo cluster-wise simulations using FreeSurfer. A 30-minute neurocognitive assessment was performed after MRI. The protocol included Hopkins Verbal Learning Test-R, Symbol Digit Modalities Test, Digit Span, Trail Making Test (Parts A and B), Stroop Color and Word Test, FAS/Animals, Cancellation Test (WAIS-IV). Test scoring was normalized to age and education.

Results: The MTBI group was 60% male with mean±SD age 17.6±1.6 years old. IMPACT Symptom scale at time of MRI was median 9 [IQR 6-41], with time to MRI from last injury being 159 [144-240] days. The 10 healthy controls were 40% male, and 20.4±1.9 years old. Significant differences (P< 0.05) between the controls and MTBI subjects were found in tests of working memory (Digit Span, P=0.02), controlled word association (FAS, P< 0.002), Trails B (P=0.03), and HVLT-R total recall (P=0.003). Cortical thickness analyses identified significant group differences between control and MTBI subjects primarily in the left inferior temporal lobe (red cluster in Figure). No significant differences in cortical thickness were found in the right hemisphere.

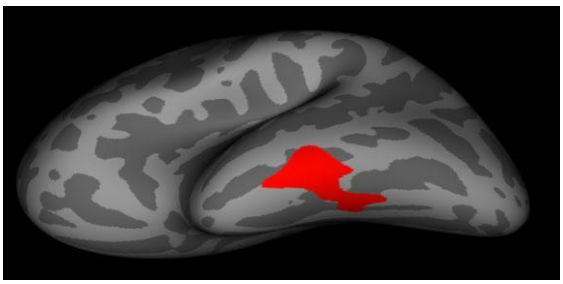

[Cortical thickness differences]

Conclusions: Previous studies have shown reduced cortical thickness several years after sports concussion injury.[4] Studies in moderate to severe TBI have shown changes as early as 3 months post-injury.[2,3] Although the observed reduced cortical thickness may be a direct sequela of the injury, another potential explanation is that individuals with reduced neuronal reserve as reflected by the observed

reduced cortical thickness may be especially susceptible to post-concussion syndrome. Further studies with larger sample sizes will be needed to test our hypotheses.

References:

1. Fischl B, et al. *Neuroimage.* 1999; 9, 195-207.

2. Wilde EA, et al. *Int J Dev Neurosci.* 2012; 30, 267-76.

3. Palacios EM, et al. *Cortex.* 2012; Epub.

4. Tremblay S, et al. *Cerebral Cortex.* 2012; Epub.

CEREBROLYSIN IMPROVES LONG-TERM COGNITIVE FUNCTIONAL OUTCOME IN RATS AFTER MILD CLOSED HEAD INJURY

Y. Xiong[1], M. Chopp[2,3], Y. Zhang[1], Y. Meng[1], T. Schallert[4], E. Doppler[5], A. Mahmood[1], Z.G. Zhang[2]

[1]Neurosurgery, [2]Neurology, Henry Ford Health System, Detroit, [3]Physics, Oakland University, Rochester, MI, [4]Psychology, Institute for Neuroscience, Austin, TX, USA, [5]Clinical Research and Pharmacology, EVER Neuro Pharma GmbH, Oberburgau, Austria

Objectives: Traumatic brain injury (TBI) is a major public-health problem for which mild TBI (mTBI) comprises the majority of cases. Memory dysfunction is a common clinical observation following mTBI. Other than rehabilitation, there is no pharmacological treatment for TBI. Cerebrolysin is a peptide preparation which mimics the action of neurotrophic factors and is widely used in the treatment of stroke, TBI, and dementia. The aim of the present study was to investigate whether Cerebrolysin therapy improves long-term cognitive function in rats after mTBI.

Methods: Adult male Wistar rats (n=30) were subjected to mild closed head injury (CHI) induced by using the Marmarou impact-acceleration injury model. CHI rats received intraperitoneal (ip) injection of saline (n=11) or Cerebrolysin (2.5 ml/kg, EVER Neuro Pharma, Austria, n=11) starting 24 hour post injury and daily for 28 days. Animals with surgery but without injury and treatment served as sham controls (n=8). To evaluate spatial learning and memory function, the modified Morris water maze (MWM) test was performed monthly up to 3 months post mTBI. Novel object recognition tasks relying on the natural tendency of rats to explore unfamiliar objects were measured by a social odor-based task at 45-46 days and 89-90 days post mTBI.

Results: All sham animals acquired the MWM learning task as demonstrated by their ability to significantly reduce their escape latencies and increase the percent time spent in the correct quadrant following the 5-day test ($p< 0.05$, vs the first day trial). However, rats that suffered mTBI showed profound and long-term learning and memory deficits as detected at 1, 2, and 3 months following injury. Cerebrolysin treatment significantly reduced the escape latencies and increased the percent time spent by injured rats in the correct quadrant ($p< 0.05$, vs saline treatment), even when Cerebrolysin was discontinued. Forty-five and ninety days after mTBI, singly-housed rats had four wooden beads placed in their home cage: three beads containing odors from their home cage (H beads) and one bead from a cage of another rat (N1 bead). Exploration times for each bead were recorded during three 1-min habituation trials separated by 1-min intervals. Twenty-four hours later, a 1-min memory test was conducted, in which animals were presented with two H beads, one N1 bead, and one bead from another novel animal (N2). All rats showed similar, progressive decreases in exploration time for the N1 bead during the habituation trials, indicating equivalent short-term olfactory habituation to the novel odor. However, during the subsequent memory test, both sham rats and Cerebrolysin-treated TBI rats spent significantly more time exploring the N2 bead than the N1 bead ($p< 0.05$, N2 vs N1), while saline-treated TBI rats did not show this preference ($p>0.05$, Cerebrolysin-treated group vs Saline-treated group). These results show that mTBI impairs long-term memory for the previously experienced odors.

Conclusions: mTBI impairs long-term spatial learning and memory in rats as demonstrated by the modified MWM test and the novel social odor-based test. Cerebrolysin treatment significantly improves cognitive function after mTBI, suggesting that Cerebrolysin has potential therapeutic value in mTBI.

HYDROGEN SULFIDE REDUCES HISTOPATHOLOGY AND IMPROVES FUNCTIONAL OUTCOME AFTER TRAUMATIC BRAIN INJURY IN MICE

M. Zhang[1], L. Tao[2]

[1]Nantong University, Nantong, [2]Soochow University, Suzhou, China

Introduction: Hydrogen sulfide (H_2S) is a lipid-soluble, endogenously produced gaseous messenger molecule collectively known as gasotransmitter. Over the last several decades, gasotransmitters have emerged as potent cytoprotective mediators in various models of tissue and cellular injury.

Objectives: To investigate changes of H_2S after traumatic brain injury and its possible role, mouse traumatic brain injury (TBI) model was established.

Methods: Expression of Cystathionine-β-synthase (CBS) mRNA as H_2S-producing enzymes in mouse brain was determined by reverse transcriptase-polymerase chain reaction (RT-PCR). This study examines the neuroprotective effects of Hydrogen sulfide by lesion volume, motor performance and Morris water maze test after TBI in mice.

Results: From the results of RT-PCR, it was found that the expression of CBS was down-regulated in mouse brain cortex and hippocampus after brain injury. Western blot analysis revealed that CBS was present in normal mouse brain cortex and hippocampus. Hydrogen sulfide in the cortex and hippocampus exhibited dynamic changes after brain injury, in parallel with CBS mRNA and protein expression. Moreover, pretreatment with the H_2S donor (NaHS) could protect the neuron against the injury induced by TBI. Noticeably, the H_2S donor NaHS could reduce TBI-induced injury assessed with lesion volume, motor performance and Morris water maze test.

Conclusions: These data suggested that H_2S may have a therapeutic potential against neuron damage and improves functional outcome improves functional outcomeimproves functional outcome improves functional outcome.

ASSOCIATION OF METABOLIC SYNDROME AND ISCHEMIC STROKE IN THE HISPANIC POPULATION ON THE US-MEXICO BORDER

A. Badr[1], M.F. Osborn[1], C.C. Miller[2], J. Zhang[1,3]

[1]Anesthesiology, [2]Biomedical Sciences, [3]COE for Neuroscience, Biomedical Sciences, Texas Tech University Health Science Center, El Paso, TX, USA

Objectives: Stroke represents a major health burden in the United States in both morbidity and mortality. Evidence has shown that the Hispanic population is disproportionately affected by this condition, while the prevalence of diabetes, hypertension, dyslipidemia and obesity is coincidently on the rise in the same group, making it increasingly important to understand the impact of these clinical conditions on the risk of stroke in the Hispanic population. In this study, we hypothesized that these factors, known as the metabolic syndrome, significantly increase the risk of ischemic stroke in the Hispanic population.

Methods: To test our hypothesis, we used stroke patient data from the *ElPasoStroke* (n=505) database that we created in our stroke epidemiological study in El Paso, TX, USA, and matching subject data from the *NHANES* database (n=1010) to assess the effects of the metabolic syndrome risk factors on the pathogenesis of ischemic stroke among the Mexican Hispanic population. Subjects were classified as obese if BMI ≥ 30, and as having the metabolic syndrome if they had three or more of following criteria: obesity, diabetes, hypertension, dyslipidemia and low HDL cholesterol. Odds ratios (OR) and 95% confidence interval (CI) between different groups and age stratified groups were calculated for the evaluation of pathogenic effects of individual components of metabolic syndrome, as well as other risk factors for stroke. Multivariable logistic regression was also performed to assess these risk factors in the pathogenesis of stroke in this Hispanic population.

Results: Our results show that the metabolic syndrome substantially increases the odds of suffering ischemic stroke among the Mexican Hispanic population, with the risk being greatest in the younger age groups. The metabolic syndrome and its components, specifically hypertension, diabetes, and dyslipidemia play a greater role in the pathogenesis of stroke and combined put Hispanics at nearly eighteen times the risk of

suffering a stroke. Hypertension alone has the most significant impact, putting Hispanics at nearly forty times the risk of suffering stroke. We also found that a more profound impact of hyperlipidemia on ischemic stroke and there is an increased risk of ischemic stroke among Mexican Hispanics with diabetes. In conclusion, the metabolic syndrome significantly increases the risk of ischemic stroke in the Mexican Hispanic population.

Conclusions: Early studies indicated that there is an increased risk of stroke among individuals who have the metabolic syndrome, among Hispanic group which was primarily Dominican, and Puerto Rican, Cuban, and Central and South American. Using a specific and well defined large Mexican Hispanic population exclusively from the US-Mexico border, our study demonstrates the metabolic syndrome and its components have more profound effects in the pathogenesis of ischemic stroke among the Mexican Hispanics than the Non-Hispanics. Our data indicate a significant correlation between the metabolic syndrome and ischemic rather than hemorrhagic stroke in the Mexican Hispanic population. Future efforts to prevent ischemic stroke and limit its impact in the Mexican Hispanic population ought to primarily be targeted at controlling key components of the metabolic syndrome, especially hypertension and diabetes.

PREDISPOSED CHRONIC PERIPHERAL INFECTION IN AGED MICE AGGRAVATES ISCHEMIC STROKE INDUCED BRAIN DAMAGE

H. Dhungana[1], T. Malm[1], A. Denes[2,3], P. Valonen[1], S. Wojciechowski[1], J. Magga[1], E. Savchenko[1], R. Grencis[2], J. Koistinaho[1,4]

[1]Department of Neurobiology, University of Eastern Finland, Kuopio, Finland, [2]Faculty of Life Sciences, University of Manchester, Manchester, UK, [3]Laboratory of Molecular Neuroendocrinology, Institute of Experimental Medicine, Budapest, Hungary, [4]Department of Oncology, Kuopio University Hospital, Kuopio, Finland

Objectives: Ischemic stroke is associated with a number of co-morbid risk factors such as atherosclerosis, diabetes and infections which alter the peripheral inflammatory processes, thereby affecting the outcome of stroke. Inflammation triggered by prior infections has also been shown to exacerbate ischemic brain damage and influence the clinical outcome (1). Yet the regulation of the profound interaction between ageing and infection-related inflammation and its contribution to the outcome of brain ischemia still remains elusive. In this study, we investigated the effect of predisposed systemic chronic infection on stroke outcome in aged mice.

Methods: Systemic infection was modeled by *T. muris* parasite infection, which leads to chronic Th-1 polarized immune response through up regulation of several pro-inflammatory cytokines (2). *T.Muris* parasite eggs were administered to 4- and 18-month-old C57BL/6j mice. The mice underwent permanent cerebral artery occlusion (pMCAO) one month after the infection when Th-1 polarized immune response has been shown to peak. The effect of systemic infection on the cortical infarct size, brain gliosis and brain and plasma cytokine profiles was analyzed.

Results*: T. muris* infection significantly exacerbated the size of the ischemic lesion in aged but not in young mice at 24 hours post ischemia. Aged mice showed increased neutrophil infiltration into the ischemic brain parenchyma and the extent of neutrophil infiltration significantly correlated with the lesion size. In addition, aged infected mice showed up regulation in plasma levels of IL-17A and TNFa and altered brain cytokine profile. However, brain gliosis was unaffected by either age or infections.

Conclusions: Chronic peripheral infection status together with advanced aged trigger ischemia-induced neuronal damage likely by enhancing the infiltration of neutrophils into the site of the ischemic damage and altering the inflammatory status in both the brain and periphery. Our results suggest that predisposed chronic infection altering the inflammatory response in aged animal should be taken into account when modeling the disease of elderly patients.

References:

1. Emsley HCA, Hopkins SJ. Acute ischaemic stroke and infection: recent and emerging concepts. *Lancet Neurol*. 2008; 7:341-353.

2. Dénes Á, Humphreys N, Lane TE, Grencis R, Rothwell N. Chronic Systemic Infection Exacerbates Ischemic Brain Damage via a CCL5 (RANTES) Mediated Proinflammatory Response in Mice. *J. Neurosci.* 2010;30:10086-10095

THE IMPACT OF AGING ON PERI-INFARCT DEPOLARIZATIONS INDUCED BY FOCAL CEREBRAL ISCHEMIA IN THE RAT BRAIN

A. Institoris[1], D. Clark[2], Z. Bere[1], E. Farkas[2], U.I. Tuor[3], F. Bari[2]

[1]Department of Physiology, Faculty of Medicine, [2]Department of Medical Physics and Informatics, Faculty of Medicine, University of Szeged, Szeged, Hungary, [3]Departments of Physiology and Pharmacology, Clinical Neurosciences and Radiology, University of Calgary, Calgary, AB, Canada

Introduction: Spreading depolarization (SD) is a slowly propagating wave of transient neuronal and glial depolarization, coupled with cerebral blood flow (CBF) changes, which occurs in the brain during migraine or after injury. During ischemia, repetitive SD-like peri-infarct depolarizations (PIDs) can impair tissue by worsening the disparity between CBF and metabolism. Although the largest predictor of stroke in patients is advanced age, there are few studies examining PIDs in aged animals. The purpose of the current study was to identify and characterize electrophysiological and hemodynamic changes in young (6-week-old; n=7), middle-aged (9-month-old; n=7) and old (2-year-old; n=7) male Wistar rats exposed to mild focal ischemia, utilizing multi-modal imaging of the rat cerebral cortex through a closed cranial window.

Methods: A cranial window was mounted over the right parietal bone. Transient focal ischemia was achieved by 30 minutes of middle cerebral artery occlusion (MCAO) using a microaneurysm clip. A CCD camera captured images of the parietal cortex illuminated with light-emitting diodes at wavelengths either preferentially absorbed by deoxygenated hemoglobin or isobestic for deoxygenated and oxygenated hemoglobin (representing total hemoglobin). A second CCD camera recorded laser speckle contrast images and florescence images of a voltage sensitive dye (RH-1838). This multi-modal strategy allowed for the study of synchronous changes in: membrane potential (detected with the voltage sensitive dye), cerebral blood volume, local blood oxygen saturation, and CBF (laser-speckle imaging).

Results: A similar decrease in CBF was observed immediately following MCAO in young (53.8±8.1%), middle-aged (52.2±10.9%) and old rats (51.6±6.4%). Age significantly altered the total number of PIDs during and after MCAO and pair-wise comparison showed both middle-aged and old rats had significantly fewer PIDs than young ($p < 0.05$). Depolarizations were categorized into two groups: PIDs associated with recovery of membrane potential (SD-like PIDs) and those without apparent recovery (terminal PIDs). Young animals had more frequent SD-like PIDs than middle-aged or old rats ($p < 0.05$). Old animals experienced significantly fewer SD-like PIDs but more terminal PIDs than either middle-aged or young ($p < 0.05$). All terminal PIDs were associated with a sustained reduction in local CBF (inverse hemodynamic response) but SD-like PIDs were associated with: spreading hyperemia (normal hemodynamic response), no apparent flow response, or a period of reduced local CBF. Hyperemia was associated with SD-like PIDs more frequently in young (85%) compared to old rats (58%).

Conclusion: Age significantly altered the number, shape and hemodynamic responses of PIDs during mild stroke. Young animals had frequent PIDs, mostly associated with membrane repolarization and increased CBF. Terminal depolarizations were often observed in old rats, coupled with a lasting decrease in local blood flow. The occurrence of such depolarization events likely compromises the cortical tissue of aged animals exposed to even a short duration of focal ischemia.

Acknowledgements: This work was supported by grants from NFM, NNF 78902, OTKA K81266, HURO/0901/137/2.2.2.HU-RO-TRANSMED, and HURO/0901/069 HURO-DOCS. DC was supported by Canadian Heart and Stroke Fellowship.

CEREBROLYSIN REDUCES EXACERBATION OF BLOOD-BRAIN BARRIER BREAKDOWN, EDEMA FORMATION AND BRAIN PATHOLOGY IN DIABETIC AND HYPERTENSIVE RATS AFTER HYPERTHERMIA

D.F. Muresanu[1], A. Sharma[2], R. Patnaik[3], H. Moessler[4], H.S. Sharma[5]

[1]Clinical Neurosciences, University of Medicine & Pharmacy, University Hospital, Cluj-Napoca, Romania, [2]Surgical Sciences, Anesthesiology & Intesnive Care medicine, Uppsala University, University Hospital, Uppsala, Sweden, [3]Biomaterials, School of Biomedical Engineering, National Institute of

Technology, Banaras Hindu University, Varanasi, India, [4]Ever NeuroPharma, Oberburgau, Austria, [5]Surgical Sciences, Anesthesiology & Intensive Care medicine, Uppsala University, University Hospital, Uppsala, Sweden

Nitric oxide synthase (NOS) upregulation in the CNS is a common phenomena following hypertension or diabetes. Previous reports from our laboratory showed marked upregulation of neuronal and inducible NOS in different brain regions in rats brain after 4 h heat stroke at 38° C. This NOS upregulation correlates well with blood-brain barrier (BBB) breakdown, edema formation and brain pathology. When diabetic or hypertensive arts were subjected separately to identical heat stress, BBB disruption and brain pathology were exacerbated as compared to normal rats. However, the states of NOS expression in these diabetic or hypertensive animals after heat stress are still not known. In clinical situations, stroke is associated with both diabetes and hypertension. Thus, it would be interesting to examine whether a combination of diabetes and hypertension could further aggravate brain damage following heat stress. In this investigation chronic hypertensive rats (two kidney one clip 2K1C for 6 weeks) were made diabetic by administering streptozotocine (50 mg/kg, i.p./day for 3 days in week 3 during 2K1C) so after 6 weeks these rats were both diabetic (20-30 mM/L Blood Glucose) and hypertensive (180-200 mmHg mean arterial blood pressure, MABP) akin to clinical situation. When these diabetic and hypertensive arts were subjected to 4 h heat stress at 38°C, they demonstrated massive increase in BBB breakdown to proteins and neuronal injuries (850% from normal and 350 to 420 % higher than diabetic or hypertensive rats alone) in the whole brain. In these animals nNOS or iNOS expression increased over 600 % from the normal rats about 250 to 340 % higher than diabetic or hypertensive rats alone. Interestingly, in normal rats after heat stress nNOS expression was higher than iNOS expression. However, in diabetic or hypertensive rats iNOS expression superseded than nNOS upregulation. Cerebrolysin in high doses (10-ml/kg, i.v. instead of 5-ml/kg) induced significant neuroprotection and downregulation of nNOS and iNOS in diabetic and hypertensive animals whereas normal animals need only 5-ml/kg doses for this purpose. Our observations demonstrate that co-morbidly factors exacerbate brain damage in HS through NOS expression and require double dose of cerebrolysin for neuroprotection as compared to normal rats, not reported earlier.

PREFERENTIAL DECREASE IN HIPPOCAMPAL MITOCHONDRIAL RESPIRATION IN COCKAYNE SYNDROME B MICE, A MOUSE MODEL OF PRE-MATURE AGING

K. Thomsen[1], N. Sherazi[1], T. Yokota[2,3], V. Bohr[4], M. Lauritzen[1,5]

[1]Institute of Neuroscience and Pharmacology, [2]Center for Healthy Aging, Dept. of Biomedical Sciences, University of Copenhagen, Copenhagen, Denmark, [3]Dept. of Cardiovascular Medicine, Hokkaido University Graduate School of Medicine, Sapporo, Japan, [4]Laboratory of Molecular Gerontology, National Institute of Aging, National Institutes of Health, Bethesda, MD, USA, [5]Dept. of Clinical Neurophysiology, University Hospital at Glostrup, Glostrup, Denmark

Objective: In humans, the devastating progeria Cockayne syndrome (CS) is characterized by neurodegeneration and cachetic dwarfism with an average life expectancy of 12 years. 80% of CS cases have a mutation in the CS complementation group B. $CSB^{-/-}$ mice display a mild phenotype of this progressive condition with neurodegeneration of the spiral ganglion of the inner ear (1). Reduced spine density in the frontal and parietal cortices (2) and widespread dysmyelination and cerebellar Purkinje cell degeneration are found in $CSB^{-/-}$ mice that also lack global genomic repair (3; 4). Thus $CSB^{-/-}$ mice have been used as a model of premature aging and dementia. As the mitochondrial theory of aging proposes that mitochondrial dysfunction is the basis of the aging process, we examined mitochondrial respiration in the cerebral cortex and hippocampus of $CSB^{-/-}$ mice (14 months), comparing them to the same brain areas of young (2 months) and middle-aged (14 months) WTs (C57Bl/6).

Methods: We used acute brain slices (200 µm thick; Vibratome) from which we took biopsies (final size: 0.42 mm^3) of the frontal/parietal cortex and the hippocampus. Mitochondrial respiration in the brain biopsies was examined using a Oxygraph O2k (Oroboros Instruments). Maximal respiration was achieved with glutmate+malate+succinate+ADP as subsequent addition of the uncoupler, FCCP

(Carbonyl cyanide-4-(trifluoromethoxy)phenylhydrazone) did not significantly increase it. The function of F_0F_1ATPase and Complex III was evaluated using oligomycin and antimycin A.

Results: We found that hippocampal state 3 respiration (glutamate+malate+ADP) and maximal respiration with glutamate+malate+succinate+ADP were significantly reduced in middle-aged $CSB^{-/-}$ mice compared to young WTs. The values for these parameters for middle-aged WTs lay between those of young WTS and middle-aged $CSB^{-/-}$ mice, and were not significantly different from either. State 2 respiration in the presence of glutamate+malate, state 4o respiration in the presence of all substrates+oligomycin, and respiration in the presence of antimycin A did not differ between the three groups. In the hippocampus, the respiratory control index (state 3/state 2 respiration) was unchanged between young and middle-aged WTs, but was significantly reduced in middle-aged $CSB^{-/-}$ mice compared to both groups of WTs. In the cortex, none of the above parameters was significantly different between groups.

Conclusions: In conclusion, we have found that mitochondrial respiration in the hippocampus of middle-aged $CSB^{-/-}$ mice is reduced at a time when cortical respiration is unimpaired, indicating that the aging process may initially occur in the hippocampus. In contrast to the reduction in hippocampal respiration demonstrated here, an earlier study has shown that fibroblasts from $CSB^{-/-}$ mice have increased mitochondrial respiration due to accumulation of defective mitochondria (1). This may explain our findings in the cortex where mitochondrial respiration from neither middle-aged WTs nor $CSB^{-/-}$ mice was significantly different from young WTs.

References:

1. Scheibye-Knudsen et al, *J of Experimental Medicine*, 209(4): 855-869, 2012

2. Wong et al, *Neuropathology and Applied Neurobiology*, in print.

3. Revet et al, *Proc Natl Acad Sci U S A*, 109:4627-4632, 2012

4. Laposa, Huang and Cleaver, *Proc Natl Acad Sci U S A*, 104(4): 1389-1394

DYSFUNCTION OF ANNEXIN A2 CONTRIBUTES TO HYPERGLYCEMIA-INDUCED FIBRINOLYTIC ACTIVITY REDUCTION ON HUMAN ENDOTHELIAL CELLS

H. Dai[1,2], Z. Yu[2], X. Fan[2], N. Liu[2], M. Yan[1], Z. Chen[1], K.A. Hajjar[3], E.H. Lo[2], **X. Wang**[2]

[1]The Second Affiliated Hospital, Zhejiang University School of Medicine, Hangzhou, China, [2]Departments of Neurology and Radiology, Massachusetts General Hospital and Harvard Medical School, Charlestown, MA, [3]Departments of Cell and Developmental Biology, Weill Cornell Medical College, New York, NY, USA

Background and purpose: Diabetes is an established independent risk factor for atherothrombotic cardiovascular and cerebrovascular diseases. Impaired fibrinolysis on the surface of endothelial cells has been identified as one of the key pathogenic factors contributing to the thrombotic vascular complications in patients with diabetes. Annexin A2, a superfamily of calcium-dependent phospholipid binding proteins, has been identified on endothelial cells as a co-receptor of t-PA and plasminogen that functions in accelerating plasmin generation. Interestingly annexin A2 was recently discovered as one of a few key endothelial plasmalemma-associated proteins forming early glucose adducts, which might cause dysfunction of annexin A2 in plasmin generation process on the endothelial cell surface under hyperglycemia. The possibility of fibrinolytic activity impairment by the dysfunction of annexin A2, called annexinopathy has not yet been well studied but is of great interest. In this study we tested our hypotheses that hyperglycemia may cause dysfunction of endothelial cell membrane protein annexin A2, that at least partially responsible to the reduction of fibrinolytic activity on the cell surface.

Methods: Cultured human brain microvascular endothelial cells (HBMEC) were exposed to hyperglycemia (25 mmol/L D-glucose) for 7 days. Fibrinolytic activity was assessed by plasmin activity assay. Tissue type plasminogen activator (t-PA) and its inhibitor-1 (PAI-1), p11 and annexin A2 expressions were examined by RT-PCR and western blot analyses. Total cell and membrane AGE-related form of annexin A2 production were measured by immunoprecipitation and western blot analysis. Effects of adding exogenous t-PA, plasminogen, annexin A2 and AGE-related

annexin A2 in rescuing the reduced plasmin activity was tested and compared.

Results: Hyperglycemia for 7 days did not significantly affect cell viability and cell number counting, but significantly decreased fibrinolytic activity on the cell surface. The hyperglycemia significantly decreased t-PA, plasminogen and annexin A2, but increased PAI-1 mRNA and protein expressions. No changes of p11 mRNA and protein expression were detected. There were significant increases of AGE-related forms of total cellular and membrane annexin A2 protein under hyperglycemia. The hyperglycemia-induced fibrinolytic activity reduction can be fully restored by incubation with recombinant annexin A2 protein (rA2) but not by AGE-related annexin A2 or exogenous t-PA. Disturbance of annexin A2 binding to plasminogen disabled the rescue effects of the adding rA2 to the impaired fibrinolytic activity.

Conclusions: Despite the decreased t-PA expression and upregulated PAI-1 expression by hyperglycemia, annexin A2 dysfunction associated with the decreased Annexin A2 protein expression and increased AGE-related annexin A2 production, which might partially contribute to the hyperglycemia-induced fibrinolytic activity reduction on the surface of cultured HBMEC. Further investigations to elucidate the underlying molecular mechanisms and pathophysiological implications might ultimately lead to better understanding of impaired vascular fibrinolysis mechanisms and development of new intervention strategies for the thrombotic vascular complications in diabetes.

NEURAL EFFECTS OF GERIATRIC DEPRESSION AND AMNESTIC MILD COGNITIVE IMPAIRMENT ON THE HIPPOCAMPAL FUNCTIONAL CONNECTIVITY NETWORK IN THE NON-DEMENTED ELDERLY

C. Xie[1,2], J. Goveas[3], W. Li[2], G. Chen[2], T. Zhai[2], G. Chen[2], M. Franczak[4], P.G. Antuono[4], J.L. Jones[4], S.-J. Li[2], Z. Zhang[1]

[1]Neuropsychiatry, Zhongda Hospital, Southeast University, Nanjing, China, [2]Biophysics, [3]Psychiatry and Behavioral Medicine, [4]Neurology, Medical College of Wisconsin, Milwaukee, WI, USA

Introduction: Late-life depression (LLD) and cognitive impairment (CI) are frequently reported to be concurred in the elderly, and this comorbidity is associated with increased risk for the subsequent dementia. However, neural basis implicated in this comorbidity remains unclear. Currently, the purpose of this study was to characterize the neurocricuits implicated in this comorbidity of LLD and CI with resting-state fMRI (R-fMRI) approach in non-demented elderly.

Methods: Eighteen LLD, 17 aMCI, 12 depressed aMCI (dMCI), and 25 age-matched cognitively normal (CN) subjects were recruited in this study and completed neuropsychological battery tests and fMRI scan. Consent written forms were obtained from each of subject. The intrinsic connectivity of bilateral hippocampus was measured by the R-fMRI approach at a 3.0 T GE scanner. Analysis of covariance (ANCOVA) was used to examine the main effects and interactive effects of LLD and CI on the bilateral hippocampal functional connectivity networks (HFCNs) among four group subjects, after controlling the effects of age, gender, education and gray matter atrophy. Linear regression analysis was employed to detect the relationship between the intrinsic connectivity strength of bilateral HFCNs and depressive severity, which measured by Geriatric Depression Scales (GDS) scores, and memory deficits, which measured by delayed recalled scores, in all four group subjects, after controlling the above covariates of no interest.

Results: Significant differences from ANOVA analysis were found in MMSE score, dementia ratio scale-2 scores, immediate and delayed-recalled memory scores, and GDS scores. Voxelwise 2×2 ANCOVA analysis revealed that the main effects of depression on the bilateral HFCNs in the affective-related regions, including bilateral dorsolateral prefrontal cortex (DLPFC), dorsomedial prefrontal cortex (DMPFC), thalamus, dorsal striatum; main effects of CI on the bilateral HFCNs were seen in cognition-related regions, including bilateral DLPFC, DMPFC, inferior prefrontal cortex (IPC), posterior cingulate cortex (PCC), and dorsal anterior cingulate cortex (dACC); The interactive effects of depression and CI on the right HFC network were identified in the bilateral ventromedial PFC (vmPFC), dACC, and right DLPFC. Additionally, we did not find significantly interactive effects of depression and CI on the left HFC network. Main effect of the GDS scores on the bilateral HFCNs were located in regions that included bilateral DLPFC,

DMPFC, dACC, thalamus, and dorsal striatum; main effect of the memory scores on the bilateral HFCNs were found in the bilateral vmPFC, PCC, left DLPFC; Significantly interactive effect of the GDS and memory scores on the bilateral HFCNs were identified in the bilateral IPC, dACC, PCC, left thalamus, and right cuneus.

Conclusion: Specific neurocircuitries implicated in the geriatric depression and cognitive impairment. Importantly, neural basis of interaction between LLD and cognitive impairment were also identified. In addition, behavioral significance of bilateral HFCNs also showed that the distinct neural pathways and common pathogenic circuits were involved in depressive symptoms severity and memory deficits as well as their interaction, after controlling gray matter atrophy. Malfunction of these neurocircuitries may increase the susceptibility for depression- or cognitive impairment-specific neuroadaptive changes and facilitate the individual to progress to dementia.

SKF83959 IS A POTENT ALLOSTERIC MODULATOR OF SIGMA-1 RECEPTOR

L. Guo[1], J. Zhao[2], B. Zhao[2], G. Jin[3], G. Wang[4], A. Zhang[1], X. Zhen[4]

[1]Shanghai Institute of Materia Medica, Shanghai, [2]Department of Neurology, The Affiliated Hospital of Guangdong Medical College, Zhanjiang, [3]Shanghai institute of Materia Medica, Shanghai, [4]College of Pharmaceutical Sciences, Soochow University, Suzhou, China

SKF83959, an atypical dopamine receptor-1(D_1 receptor) agonist, has showed many D_1 receptor-independent effects such as neuroprotection, blockade of Na^+ channel, and promotion of spontaneous glutamate release, which somehow resembled the effects of the sigma-1 receptor activation. In the present work, we explored the potential modulation of SKF83959 on the sigma-1 receptor. The results indicated that SKF835959 dramatically promoted the binding of ^{3}H(+)-pentazocine (a selective sigma-1 receptor agonist) to the sigma-1 receptor in brain and liver tissues, but produced no effect on ^{3}H-progesterone binding (a sigma-1 receptor antagonist). The saturation assay and the dissociation kinetics assay confirmed the allosteric effect. We further demonstrated that the SKF83959 analogs such as SCH22390 and SKF38393 also showed the similar allosteric effect on the sigma-1 receptor in the liver tissue but not in the brain tissue. Moreover, all three tested chemicals elicited no significant effect on ^{3}H-1,3-di(2-tolyl)-guanidine(^{3}H-DTG) binding to the sigma-2 receptor. The present data uncovered a new role of SKF83959 and its analogs on the sigma-1 receptor, which, in turn, may reveal the underlined mechanism for the D_1 receptor-independent effect of the drug.

ACTIVATION OF ENDOGENOUS STEM CELLS AFTER FOCAL VENOUS CEREBRAL ISCHEMIA AND CORTICAL SPREADING DEPRESSION

A. Heimann[1], K. Horiuchi[1,2], S. Nieraad[1], B. Alessandri[1], O. Kempski[1]

[1]Institute for Neurosurgical Pathophysiology, Johannes Gutenberg-University, Mainz, Germany, [2]Neurosurgery, Nara Medical University, Nara, Japan

Objective: Ischemia-induced neurogenesis is reported in regions that are not a direct source of neurogenic precursors as the hippocampus, cerebral cortex and striatum. That implicates that newly born neurons can migrate toward damaged regions and replace injured neurons. Neurogenesis was studied after venous stroke in the adult rat. The focus was to examine whether cortical spreading depression (CSD) in combination with venous ischemia increases migration and differentiation of neural stem cells in the subventricular zone (SVZ), dentate gyrus (DG) and cortex more than ischemia alone.

Material and methods: Sixty-two male adult Wistar rats were randomly divided into four experimental groups (naïve, sham, venous ischemia, venous ischemia combined with artificial induced CSDs). In order to analyze the time course of stem cell induction sub-groups with 1, 2, 4 and 9 days survival were randomized. Two adjacent bridging veins were permanently occluded by fiber optically induced photothrombosis (2-VO, n=23) for induction of ischemia. To analyze the effect of cortical spreading depression ten artificial CSDs were induced by KCl-microinjection in addition to venous ischemia (150mM, 5µl; 2-VO+CSD, n=24). All animals were physiologically monitored (blood-pressure, cerebral blood flow, blood gases) and received BrdU daily after intervention in order to label in vivo proliferating cells. Brains were removed and coronary slices (40 µm) evaluated

qualitatively and quantitatively. Predefined regions of interest in the subventricular zone, dentate gyrus and cortex were analysed for newly formed cells (BrdU-positive) and newly formed neurons (BrdU-positive cells co-labeled for DCX, Doublecortin) by immunofluorescence combined with ApoTome-Axiovision software (Axio-Vision, Zeiss, Germany).

Results: In the SVZ immunofluorescence analysis did not reveal any differences in neurogenesis between experimental groups. In the DG the number of newly formed cells and newly formed neurons was significantly higher 9 days after 2-VO and 2-VO+CSD compared to naïve and sham. Analogously, only few fluorescent cells were observed in naïve and sham operated animals in the cortex, irrespectively of the hemisphere and survival time. In contrast, at day 1, 2, 4 and 9 newly born cells ($BrdU^+$) as well as newly born neurons ($BrdU^+/DCX^+$) were induced in the ipsilateral cortex by ischemia alone and by its combination with CSD, increased over time and peaked at day 4 and 9 compared to day 1. In addition significantly more BrdU/DCX-double stained cells were seen in the region close to the infarct compared to ROIs far from the infarct.

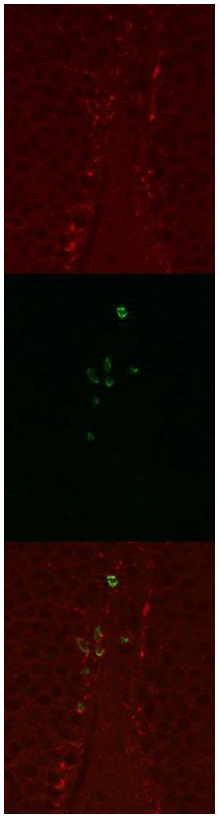

[Fig 1]

Conclusion: The current study provides evidence that ischemia triggers the early activation of cortical endogenous stem cells, which is not further increased by CSD.

MIRNA-424 PROMOTES NEUROPROTECTION AGAINST FOCAL CEREBRAL ISCHEMIA INJURY IN MICE THROUGH SUPPRESSING MICROGLIAL ACTIVATIONV

H. Zhao, L. Gao, X. Liu, Z. Gao, Z. Tao, X. Ji, **Y. Luo**

Cerebrovascular Diseases Research Institute, Xuanwu Hospital of Capital Medical University, Beijing, China

Background and purpose: We investigate that whether microRNA-424 (miR-424), which was found significantly decreased in the expression profiling of miRNAs in circulating lymphocytes of acute ischemic stroke patients, affect ischemic brain injury in mice through regulation of microglial activation, the immune cells of the brain.

Methods and results: Real-time PCR showed that miR-424 levels were reduced in the plasma of acute ischemic stroke patients, as well as in the plasma and ipsilateral brain tissue at 4h, 8h and 24h after ischemia in mouse middle cerebral artery occlusion (MCAO) model. In situ hybridization and real-time PCR demonstrated that miR-424 levels were reduced respectively in the cortex, hippocampus and basal ganglia at 8h after ischemia. Reversely, lentiviral overexpression of miR-424 decreased cerebral infarction size, brain edema and neuronal apoptosis. Meanwhile, miR-424 overexpression inhibited microglial activation including suppressing Iba1-immunoreactivity and protein level, and reduced TNF-α production depicting by immunofluorescence staining, western blot and ELISA. Furthermore, miR-424 overexpression caused G1 phase cell cycle arrest detected by flow cytometry and inhibited BV-2 microglial activity determined by CCK-8 kit. Real-time PCR and western blot showed that miR-424 overexpression reduced the mRNA and protein levels of key activators of G1/S transition including CDC25A, Cyclin D1 and CDK6, which were upregulated in cerebral ischemic brain or BV2 microglial cells under oxygen-glucose deprivation.

Conclusions: We proved that miR-424 overexpression prevented ischemic brain injury through suppressing microglial activation by translational depression of key activators of G1/S transition, suggesting a novel miR-based therapeutic strategy for stroke.

GENOME-WIDE SURVEY REVEALS ISCHEMIC POST-CONDITIONING PARTIALLY REVERSES CELL CYCLE REACTIVITY FOLLOWING ISCHEMIA/REPERFUSION INJURY

R. Wang, H. Zhao, X. Liu, F. Yan, X. Ji, **Y. Luo**

Cerebrovascular Diseases Research Institute, Xuanwu Hospital of Capital Medical University, Beijing, China

Background and purpose: The neuroprotective effects of ischemic postconditioning (IPostC) are well established but the underlying mechanism is still unknown. We began to explore this critical gap in the field by genomic comparison of ischemic rat cortex following transient middle cerebral artery occlusion (tMCAO) alone or plus IPostC.

Methods and results: Microarray analysis revealed that tMCAO-induced transcriptional changes in 40 cell cycle regulators were ameliorated by IPostC, suggesting that IPostC reversed neuronal cell cycle re-entry. RT-PCR, immunoblotting, and immunofluorescence were subsequently used to quantify or localize the cell proliferation marker proliferating cell nuclear antigen (PCNA), positive and negative cell cycle regulators, and related signaling molecules. As expected, IPostC reversed the rise in mRNA levels of positive cell cycle regulators cdcb1, cdk1, cdca2, cadca3, and cdca7. Elevations in cyclin D1 and neuronal cyclin A2 were similarly inhibited. tMCAO-induced phosphorylation of extracellular signal-regulated kinase (p-ERK), glycogen synthase kinase-3β (p-GS3K3β), and cAMP response element binding protein (p-CREB) were also all depressed by IPostC. Furthermore, p-ERK colocalized with neuronal cyclin A2.

Conclusions: The present study demonstrates the potent inhibitory effect of IPostC treatment on tMCAO-induced cell-cycle reentry and on ERK/CREB and GSK3β/CREB signaling. Because neuronal cell cycle re-entry is pro-apoptotic, these findings lend insight into potential mechanisms underlying neuroprotection with IPostC.

DELTA-OPIOID RECEPTOR MEDIATED UP-REGULATION OF EXCITATORY AMINO ACID TRANSPORTERS IN MOUSE ASTROCYTES

J. Liang[1,2], H.K. Sandhu[1], D. Chao[1,2], D.H. Kim[1], **Y. Xia**[1,2]

[1]The University of Texas Medical School at Houston, Houston, TX, [2]Yale University School of Medicine, New Haven, CT, USA

Introduction: Cerebral ischemia/hypoxia causes an imbalance in the neural release and uptake of excitatory amino-acids, e.g., glutamate. This results in neuroexcitotoxicity due to their accumulation in the extracellular space. A family of high-affinity sodium-dependent excitatory amino acid transporters (EAATs) plays an important role in the uptake regulation of excitatory amino-acids, thereby buffering against excitotoxicity. So far five high-affinity EAATs have been cloned in the mammals, namely EAAT1 (GLAST), EAAT2 (GLT1), EAAT3 (EAAC1), EAAT4, and EAAT5. Of these, EAAT1 and EAAT2 are predominantly expressed in the glial cells and at moderate-to-low levels in forebrain, cerebellum and hippocampus. Under normal circumstances, astrocytes regulate the extracellular concentrations of excitatory amino-acids through EAAT1 and EAAT2, thus preventing neuronal injury.

Objective: Since we have demonstrated that activation of δ-opioid receptor (DOR) offers neuroprotection against glutamate-induced injury and hypoxic/ischemic encephalopathy, we further investigated if DOR-protection is associated with the function of astrocytic EAAT1 and EAAT2. However, a possible link between DOR neuroprotection and astrocytic EAATs has not been established. In fact, there is no published report on the effect of DOR on EAAT regulation in astrocytes. In this work, we aim at investigating if DOR activation regulates astrocytic EAAT expression and function.

Methods: We used UFP-512, a potent and specific DOR agonist, to treat pure astrocyte-rich cultures prepared from newborn C57BL/6J mice brain. Quantitative RT-PCR and Western blot analysis were used to measure mRNA and protein expression of EAAT1 and EAAT2 after DOR activation. The DOR-induced changes in EAAT1 and EAAT2 expression

were further determined following application of Naltrindole (a DOR antagonist) and intracellular signaling inhibitors for PKC, PKA, phosphatidylinositol 3-kinase, p38, MEK and ERK inhibitors, respectively. All comparisons were subjected to statistical significance.

Results: We found that DOR activation increased the astrocytic mRNA and protein expression of EAAT1 and EAAT2, thereby enhancing glutamate transportation. DOR-induced EAAT1 and EAAT2 expression was significantly suppressed by the inhibitors of MEK, ERK and p38. However, the inhibitors of PKA, PKC or PI3K had no appreciable effect on the DOR-induced expression of EAAT1 and EAAT2.

Conclusions: These data suggest that the activation of DOR up-regulates EAAT expression and function in the astrocytes through a MEK-ERK-p38 dependent pathway. Our salient observations are the first to provide a novel basis for an association between DOR activation and EAATs in neuroprotection against excitotoxic injury.

This work was supported by NIH (HD-034852; AT-004422) and Vivian L. Smith Neurologic Foundation.

ANGIOTENSIN-(1-7) MODULATES RENNIN-ANGIOTENSIN SYSTEM ASSOCIATED WITH REDUCING OXIDATIVE STRESS AND ATTENUATING NEURONAL APOPTOSIS IN THE BRAIN OF HYPERTENSIVE RATS

Y. Zhang, T. Jiang

Department of Neurology, Nanjing Hospital of Nanjing Medical University, Nanjing, China

Objectives: Angiotensin-(1-7) [Ang-(1-7)] has beneficial effects against hypertension-induced damage in peripheral organs, but its effect(s) in brain is not clear as yet. The effect of Ang-(1-7) on the physiopathologic changes caused by hypertension in brain of spontaneously hypertensive rats (SHRs) was investigated in this study.

Methods: Wistar-Kyoto rats received intracerebroventricular (I.C.V) infusion of artificial cerebrospinal fluid (aCSF) (0.25 µL/h) and SHRs received I.C.V infusion of Ang-(1-7) (0.1 nmol/0.25 µL/h, 1.1 nmol/0.25 µL/h or 11.1 nmol/0.25 µL/h) or aCSF (0.25 µL/h) for 4 weeks. Brain tissues were collected and analyzed by western blotting, enzyme immunoassay, spectrophotometric assays and terminal deoxynucleotidyl transferase-mediated dUTP end-labeling (TUNEL) staining.

Results: Infusion of Ang-(1-7) for 4 weeks significantly reduced the expression of Angiotensin II and AT_1R in SHR brain. It also decreased the levels of malondialdehyde and total superoxide dismutase activity accompanied by reductions of NADPH oxidase subunit $gp91^{phox}$ and inducible nitric oxide synthase in the brain of SHR. The hypertension-induced increase in the percentage of TUNEL-positive neurons and Bax to Bcl-2 ratio in SHR brain was also attenuated by Ang-(1-7). These effects were independent of blood pressure reduction.

Conclusion: Those findings demonstrated that treatment with Ang-(1-7) for 4 weeks modulated the component of renin-angiotensin system accompanied by reducing oxidative stress and attenuating neuronal apoptosis in the brain of SHRs, without affecting blood pressure. It is suggested that chronic treatment with Ang-(1-7) may be beneficial to attenuate hypertension-induced physiopathologic changes in brain and prevent hypertension related cerebrovascular diseases.

CLASSIFYING INTRACRANIAL MAJOR ARTERY STENOSIS/OCCLUSION BASED ON THE GENOTYPE OF *RNF213*, THE SUSCEPTIBLITY GENE FOR MOYAMOYA DISEASE

S. Miyawaki, H. Imai, H. Ono, S. Takayanagi, H. Horikawa, T. Ochi, A. Ito, A. Mukasa, H. Nakatomi, N. Saito

Department of Neurosurgery, The University of Tokyo, Bunkyo-ku, Japan

Objective: The c.14576G>A variant in ring finger protein 213 (*RNF213*) was recently identified as a susceptibility gene variant for moyamoya disease (MMD). We assumed that the c.14576G>A variant could be the cause of a wide spectrum of phenotypes of intracranial major artery stenosis/occlusion (ICASO) including MMD, and so some cases of ICASO originally considered to originate from atherosclerosis might be associated with the c.14576G>A variant in *RNF213*. In this study, the occurrence of c.14576G>A variant was evaluated in patients with ICASO without signs of MMD (non-MMD ICASO), as well as in

patients with MMD and other cerebrovascular diseases as controls.

Methods: This single-hospital-based case-control study was completed in 7 months (from October 2011-April 2012) at Department of Neurosurgery, The University of Tokyo Hospital. The occurrence of c.14576G>A variant was analyzed in 41 patients with non-MMD ICASO, in 48 with MMD, in 21 with cervical disease, in 61 with cerebral aneurysm, and in 25 normal subjects.

Results: Nine of 41 patients (21.9%) with non-MMD ICASO and 41 of 48 (85.4%) with MMD had the c.14576G>A variant. One of 61 patients (1.6%) with cerebral aneurysm and no patients with cervical disease or normal subjects had the variant. Comparison of each phenotype group with the normal subjects showed that presence of c.14576G>A variant had significant associations with MMD (odds ratio [OR], 292.8; 95% confidence interval [CI], 15.4-5153.0; P< 0.0001) and with non-MMD ICASO (OR, 14.9; 95% CI, 0.82-268.4; P=0.01), but no association with either cerebral aneurysm (OR, 1.2; 95% CI, 0.04-32.0; P=1.00) or cervical disease (OR, 1.1; 95% CI, 0.02-62.3; =1.00) [1].

	MMD	ICASO Non-MMD	Cerebral Aneurysm	Cervical Disease	Control
Total number of patinets	48	41	61	21	25
Number of patients with c.14576G>A variant (G/A + A/A)	41	9	1	0	0
Rate (%)	85.4	21.9	1.6	0	0
P Value	<0.0001	0.010	1.00	1.00	0
Odds Ratio	282.2	14.9	1.2	1.1	
95% confidence interval	15.4-5153.8	0.82-268.4	0.04-32.0	0.02-62.3	

[Rate of the occurence of c.14576G>A]

Conclusions: The present study indicates that a particular subset of Japanese patients with non-MMD ICASO has a genetic variant associated with MMD. Therefore, we propose the existence of a new entity of ICASO caused by the c.14576G>A variant in *RNF213*, *RNF213* variant-related ICASO, which can be differentiated from ICASO caused by atherosclerosis only by using genetic analysis.

1. Miyawaki S, Imai H, Takayanagi S, Mukasa A, Nakatomi H, Saito N. Identification of a genetic variant common to moyamoya disease and intracranial major artery stenosis/occlusion. Stroke; a journal of cerebral circulation. 2012;43:3371-3374

DEVELOPMENT OF GENETIC STUDY BY USING GROUPING SYSTEM FOR STROKE CARE (MEDICAL TREATMENT/NURSING SERVICE/WELFARE) IN THE REMOTE PLACE

K. Takenaka[1], K. Hayashi[2], M. Kato[2], T. Yamada[2]

[1]Neurosurgery, [2]Takayama Red Cross Hospital, Takayama, Japan

Introduction: Grouping system for stroke care (medical treatment/nursing service/welfare) has been introducing for developing genetic study and the regional healthcare cooperation in the remote place, such as Hida area in Japan,. This area is a wide and a rural area which has many elder people. Population is 110,000 and aging rate (over 65-years-old) is 29%, and wideness is almost same size of metropolitan Tokyo area, which means population uneven distribution area. Our hospital is a center hospital which has emergency department and critical care center in regional medicine of this area. It has also building acute disease, skilled nursing facilities (SNF), healthcare facility for the aged, and home nursing visit to perform in-home nursing care.

Methods: Candidate gene for cerebrovascular disease (e.g. familial subarachnoid hemorrhage, familial arterial venous malformation, familial moyamoya disease) was researched by using genomic DNA, and MRA data and regiolan medical history by groupin members.

Results: Five hundreds forty seven new in-patients were admitted to our department. Of all, number of stroke patients is 303 cases in admission, which contain subarachnoid hemorrhage (22 cases, 7.3%), intracranial cerebral hemorrhage (86 cases, 28.4%), and cerebral infarction (195 cases, 64.4%). Intravenous tissue plasminogen activator (rt-PA) was administered in 12 patients in a year. Due to high incidence of stroke and the elder patients in this area, we need to construct grouping system and consortium to achieve seamless medical service. To prevent of stroke, detection of candidate gene and comfort study were examined by group system. They involve in faculties of the hospital, primary care physician, the administration, and professor as pro bono publico, Hida regional health authority, and public heath department. They also communicate with each others about many issues (e.g. care system of the disable people, large amount of money in medical care and support expense system). Some suspected genes were reviewed in subarachnoid hemorrhage and arterial malformation patients. Some genetic factors may exist In this area.

Conclusion: Collaboration of medical service and nursing care system is important for performance of researching of genetic factor of stroke and post stroke patients in the remote place.

This activity is supported by program of eradication of lifestyle disease in Hida regional health authority in 2011 and 2012.

1) Katsunobu Takenaka, Katsuhiko Hayashi, Masayasu Kato, Masaki Nishihora, Toshihiko Wani: Collaboration with medical staffs and pharmacists in Hida area. Annual report of Takayama Red Cross Hospital 34: 27-30, 2010 (in Japanese)

2) Inoue S, Liu W, Inoue K, Mineharu Y, Takenaka K, Yamakawa H, Abe M, Jafar JJ, Herzig R, Koizumi A.: Combination of linkage and association studies for brain arteriovenous malformation. Stroke. 2007 38(4):1368-1370.

NOVEL CELLULAR ROLES OF CCM SIGNALING COMPLEX DURING NEUROVASCULAR ANGIOGENESIS

J. Zhang[1,2], S. Shen[1], Y. Qu[1], A. Badr[1]

[1]Anesthesiology, [2]COE for Neuroscience, Biomedical Sciences, Texas Tech University Health Science Center, El Paso, TX, USA

Objectives: Cerebral cavernous malformation (CCM) is a microvascular disease in the central nervous system (CNS) marked by venous sinusoids that predispose to intracranial hemorrhage and stroke. CCMs occur in approximately 0.5% of the population and represent 10% of all vascular malformations. CCM lesions have shown gaps between endothelial cells (ECs) processing with exposure of the basal lamina directly to the lumen of the sinusoids, suggesting a perturbation of both endothelial cell-extracellular matrix interactions at focal adhesions and cell-cell interactions at tight and adherent junctions. Resultant abnormalities of the blood-brain barrier (BBB) might contribute to the pathophysiology of CCMs. Therefore, CCM is a disease of abnormal angiogenesis in the brain, affecting the neurovascular unit at its most fundamental level.

CCM is a genetic disorder with an autosomal dominant trait. This disease is genetically heterogeneous with three currently known contributing genetic loci, CCM 1-3. Researchers have now established that all three CCM proteins interact with each other to form a CCM complex that, in turn, interacts with other cellular proteins. Based on our latest data, we define this complex as CCM Signaling Complex (CSC). The critical importance of CSC is evidenced by the observation that at least one of its major components is disrupted in most cases of human CCM. Our goal is to understand the molecular mechanisms of microvascular angiogenesis and blood-brain barrier (BBB) function regulated by CSC with regard to vessel malformation and angiogenesis

Methods: Since the precise molecular and cellular mechanism of the CSC modulation of the microvascular angiogenesis and the integrity of blood-brain barrier (BBB) remains elusive, we hypothesized that additional genetic component within *CSC* may contribute to the pathophysiology of CCM. In this report, we employed molecular genetic approaches,

such as rapid amplification of cDNA ends (RACE), nested PCR and real-time quantitative PCR (RT-PCR), genomic analysis and proteomic analysis, such as in-vitro and in-vivo protein-protein interaction assays, to identify novel cellular component in CSC. Further we also investigated the interlaced relationship of CSC proteins to try to define the specific and dynamic role of each factor in CSC during microvascular angiogenesis, using both genomic and proteomic approaches.

Results: Multiple novel cellular factors of CSC were identified. Our new data indicate that CSC contains many more complicated networks of cellular factors which contribute to CSC function in different signaling pathways through their specific interaction and position within various cellular signal pathways. We further analyzed the newly redefined CSC and found that the CSC plays an essential role via their interaction with integrins during angiogenesis.

Conclusions: Our data indicate that newly identified cellular factors in the CSC plays essential roles in the vascular angiogenesis through their interactions with EC beta integrins (ITGBs) and cell receptor tyrosine kinases (RTKs), further validating our previous belief that CSC regulates vascular angiogenesis through modulating EC signaling activities of integrins and other key cellular signaling molecules. Our data further suggest that CSC may also involve in other important cellular events through regulating signaling pathways among integrins and between integrins and other cellular factors.

ASTROCYTE REACTIVITY IS ASSOCIATED WITH DECREASED OF N-ACETYL-ASPARTATE LEVELS IN ABSENCE OF NEURODEGENENERATION IN THE RAT BRAIN

M.-A. Carrillo-de Sauvage, L. Ben Haim, M. Guillermier, J. Valette, C. Escartin

Laboratoire de Maladies Neurodégénératives, CEA, DSV, I²BM, MIRCen and CNRS URA 2210, Fontenay-aux-Roses, France

Purpose: N-Acetyl-Aspartate (NAA) is one of the most abundant metabolite in the brain and constitutes the major peak detected by magnetic resonance spectroscopy (MRS) in vivo. Although its function in the brain is still unclear, this neuronal metabolite has received considerable interest as a biomarker for neurodegeneration and a decrease in its concentration is classically interpreted as neuronal death or dysfunction [1]. However, there is not clear evidence that other cell types, specifically astroglia, could contribute to change in NAA levels in the brain.

Astrocyte reactivity occurs in response to many pathological brain situations [2], including neuronal degeneration. Reactive astrocytes display morphological and functional changes that could result in changes in the concentration of some brain metabolites localized both in astrocytes but also in neurons. In this study, we aimed at dissecting the MRS signature associated with astrocyte reactivity per se. We took advantage of a model of selective astrocyte activation using overexpression of the cytokine ciliary neurotrophic factor (CNTF, [3]). CNTF leads to a selective activation of astrocytes in absence of detectable effects on neurons. Using this model, we show that, contrary to the classical interpretation, a decrease in the NAA can occur in absence of neurodegeneration.

Methods:

Animal model: Experiments were performed using a rat model (N=10) of astrocyte activation induced by stereotactic injection of lentiviral vectors encoding for CNTF (lenti-CNTF) into the right striatum [3]. The contralateral striatum was injected by a control lentiviral vector that encodes for beta-galactosidase (lenti-LacZ).

NMR Experiments: MRS data were acquired on a 7 T Agilent magnet in two voxels positioned in each striatum. A LASER (Localization by Adiabatic Selective Refocusing) sequence with echo time TE=40 ms was used. Repetition time was 2 s. Chemical shift localization error was less than ±5% over the 2-4 ppm range. Concentrations were measured using LCModel software for NAA, myo-inositol, choline, glutamate and taurine relative to absolute creatine (tCr) signal.

Results: Lenti-CNTF injection promotes a sustained, extensive and selective activation of astrocytes, as evidenced by overexpression of GFAP and vimentin and cellular hypertrophy (Fig.1). Importantly, neurons displayed unaltered morphological, molecular and electrophysiological features, as described previously [3,4]. Our result confirmed significant changes in metabolite concentration in this model: in the lenti-CNTF injected

striatum, levels of the astrocyte metabolites myo-inositol and choline were increased (+38% and +19%, respectively), whereas levels of the neuronal metabolite NAA and glutamate were decreased (-17% and -12%, respectively). Importantly, the absolute tCr signal (arbitrary units) was identical in both groups.

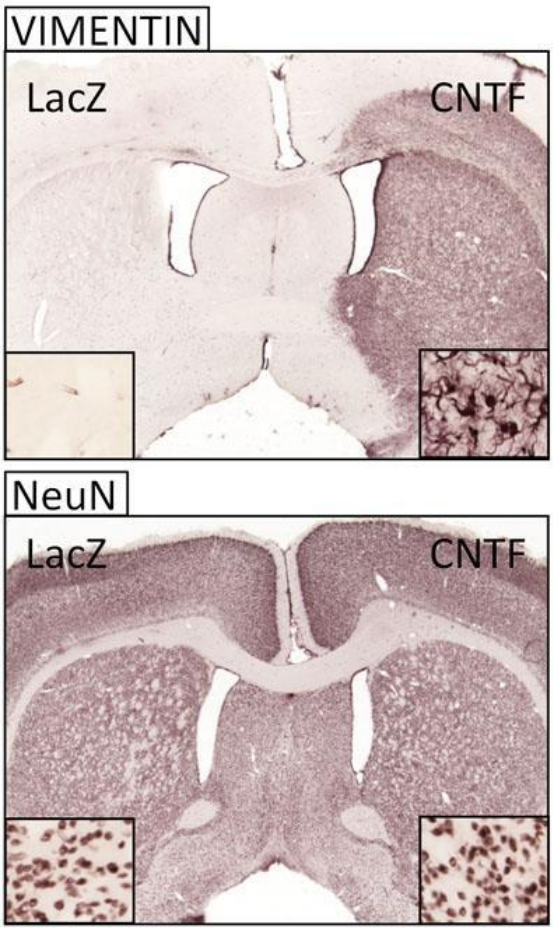

Fig.1. *lenti-CNTF injection leads to astrocyte activation (upper image) with no detectable effect on neurons (bottom image).*

[Fig.1]

Conclusion: Our results suggest that reactive astrocytes alone result in alterations of metabolite concentrations detectable by NMR. Although the mechanisms by which activated astrocytes regulate neuronal metabolism remain to be elucidated, our work challenges the MRS dogma of decreased neuronal metabolites associated with neuronal degeneration.

References:

[1] Moffet et al. (2007): Prog. Neurobiol. 81:89-131.

[2] Escartin and Bonvento (2008): Mol. Neurobiol. 38:231-41.

[3] Escartin C et al. (2006): J Neurosci 26:5978-5989.

[4] Beurrier C et al. (2010): PLoS One 5:e8550.

BAICALEIN INDUCES ASTROCYTE-SPECIFIC PRODUCTION OF INTERLEUKIN 6 VIA ACTIVATION OF PI3K/AKT SIGNALING PATHWAY FOR NEUROPROTECTION

S.-H. Lin[1], **H.-Y. Chuang**[1], Y.-Y. Sun[2], Y.-H. Lee[1]

[1]Physiology, National Yang-Ming University, Taipei, Taiwan R.O.C., [2]Pediatrics and Neurology, Emory University School of Medicine, Atlanta, GA, USA

Objectives: Our previous study first demonstrated that baicalein protects neurons against excitotoxicity (Lee et al.,2003), and further investigation revealed that the effect involves the activation hypoxia-inducible factor 1α (HIF-1α) in neurons. Recent studies indicated that baicalein activates PI3K/Akt to protect against ischemic stroke (Liu et al., 2010), but its downstream effectors for its neuroprotection remains undetermined. Further, the involvement of astrocytes, the most abundant cell type in the brain, in the baicalein neuroprotection has been poorly studied. The objective of this study was to investigate how baicalein-activated PI3K/Akt signaling in astrocytes contributes to its neuroprotection via regulating the production of IL6 and TNFα, both cytokines are proinflammatory and also reported to be neuroprotective.

Methods: Primary cultured rat brain astrocytes were used and treated with baicalein to examine the expression and release of IL6 and TNFα using quantitative RT-PCR and ELISA, respectively. The involvement of PI3K/Akt pathway in the baicalein-mediated cytokine expression was examined by performing Akt phosphorylation assay and PI3K isoform inhibitor effects on

baicalein-induced IL6/TNFα expression. Finally, conditioned medium collected from baicalein-treated astrocytes transfected with siRNA for IL6 mRNA was applied to primary cultured cortical neurons to examine the impact of baicalein-induced astrocytic IL6 on the NMDA-induced neuronal apoptosis.

Results: Our data show that baicalein at 10 and 35 μM profoundly induced the expression and release of IL6, but not TNFα, from astrocytes. This IL6-elevating effect was not observed in neurons, and was accompanied by the increase of phosphorylated Akt. Both the pan-PI3K inhibitor and class I PI3K isoform inhibitors attenuated its IL6-elevating effect. Furthermore, unlike in neurons, baicalein did not induce HIF1a target gene expression in astrocytes, and HIF1α activator DMOG did not induce IL6 expression, suggesting that HIF1α is not involved in the IL6 induction. Finally, knockdown of baicalein-induced IL6 production in astrocytes by siRNA attenuated the protective effect of the obtained baicalein-conditioned astrocyte medium on primary cultured cortical neurons under excitotoxic NMDA insult.

Conclusion: Baicalein-activated PI3K/Akt signaling pathway is causally related to its cell type-specific induction of IL6 in astrocytes. This baicalein-induced glial IL6 neuroprotection provides promising direction for its application in the prevention and therapy of the neurodegenerative process in brain injury and diseases.

References:

Lee HH et al. (2003) Differential effects of natural polyphenols on neuronal survival in primary cultured central neurons against glutamate- and glucose deprivation-induced neuronal death. Brain Res. 986:103-13.

Liu C et al. (2010) Neuroprotection by baicalein in ischemic brain injury involves PTEN/AKT pathway. J Neurochem 112:1500-12.

ASTROCYTES - A TARGET FOR THE ACTION OF THROMBIN AND ACTIVATED PROTEIN C

L. Gorbacheva[1,2], S. Strukova[1], A. Ivanova[1], V. Pinelis[3], G. Reiser[4]

[1]The Lomonosov Moscow State University, [2]The Russian National Research Medical University named after N.I. Pirogov (RNRMU), [3]Scientific Centre for Children`s Health RAMS, Moscow, Russia, [4]Institute for Neurobiochemistry, Otto-von-Guericke University, Magdeburg, Germany

Astrocytes are the most common cell in the human brain. Many pathological processes in brain are accompanied with structural and functional changes of astrocytes. It is known that reactive astrogliosis observed during various viral and inflammatory diseases, encephalopathies, acute brain injuries and neurodegenerative pathologies (e.g. Alzheimer´s). Thrombin (Th) and activated protein C (APC) - serine proteinases of hemostasis play importent role in coagulation. These proteinases have anti(pro)-apoptotic and pro-(anti)-inflammatory properties. The high concentration of thrombin that occur during inflammation, injuries, etc. can find in brain and causes a reactive astrogliosis which is associated with proliferation and morphological changes (Nicole et al., 2005). The marker of reactive astrogliosis is a expression of protein S100. However, the participation of APC in regulation of astrocyte function is not clear. The influences of APC on the thrombin-induced activation of astrocytes are in a focus of our research.

Studies were performed using primary culture of astrocytes from cortex of Wistar rat pups brain. In 14 DIV astrocytes cultures fluorescence immunostaining revealed that expression of S100B was higher in cells that received the continuous application of the high concentration of Th (100 nM, 20 h) than in untreated control astrocytes. Thrombin in lower concentration (1 and 10 nM) did not influence on the level of S100 in astrocytes. The incubation of astrocytes with 1 nM APC before and during thrombin treatment led to decrease of S100B level. These data are consistent with data of Western blot.

By confocal microscopy we showed the increase of free fields in astrocyte cultures under Th (100 nM) application. It is point to

Th-induced cellure migrational and morphological changes in astrocytes. When the 10 nM APC presents in culture medium, numbers of cell free fields were lower then during the incubation of astrocytes with high concentration of Th alone. Staining with fluorescence-conjugated phalloidin revealed that continuous application of 10-100 nM Th caused actin cytoskeletal rearrangements. APC also exchanged the thrombin-induced modification of astrocyte cytoskeleton. Thus APC prevents the thrombin-induced activation of cultured astrocytes. APC has not only neuroprotective effects but also can prevent the activation of astrocytes and astrogliosis during pathological condition. Our results demonstrate new aspects of APC as a protective agent for brain at trauma and neuropathology.

A MAJORITY OF ASTROCYTES SHOW RAPID STIMULUS-EVOKED CA^{2+} ACTIVITY, FAST ENOUGH TO CONTRIBUTE TO THE HEMODYNAMIC RESPONSE IN VIVO

B.L. Lind[1], A. Brazhe[1,2], S.B. Jessen[1], F.C.C. Tan[1], M. Lauritzen[1,3]

[1]Department of Neuroscience and Pharmacology, University of Copenhagen, Copenhagen, Denmark, [2]Faculty of Biology, Moscow State University, Moscow, Russia, [3]Department of Clinical Neurophysiology, Glostrup Hospital, Glostrup, Denmark

Neural activity in the brain is observed as increases in local blood flow in functional imaging techniques. Cerebral blood flow (CBF) is regulated by messengers released from neurons and astrocytes as a result of Ca^{2+}-dependent mechanisms. Astrocytes are ideally suited to vascular control because of their close connections to both synapses and blood vessels. Thus far only slow-developing Ca^{2+} increases have been reported from astrocytes in vivo. For these slow dynamics it has not been possible to prove that stimulation-induced increases in astrocytic Ca^{2+} were sufficiently fast to be relevant for blood flow regulation. We determine stimulation-evoked increases in astrocytic Ca^{2+} sufficiently fast to provide control of blood flow during activation.

Mouse sensory whisker barrel cortex was activated *in vivo* by stimulation of the contralateral whisker pad and studied through a craniotomy drilled over the right hemisphere (n=31 mice). The frequency dependent activity in layer II/III was studied by 2-photon microscopy based Ca^{2+} imaging, microelectrode recordings of extracellular potentials, CBF changes with laser Doppler and electrographic recordings of the tissue oxygen tension. The tissue was bulk-loaded with the Ca^{2+} indicator Oregon green bapta in combination with sulphorhodamine 101 which is taken up selectively by astrocytes. This allowed for the distinction between Ca^{2+} activity in astrocytic and neuronal structures. Animals were anesthetized with α-chloralose during imaging. Blood-pressure, blood-gasses and CO_2 in the expired air was monitored during the experiment, to ensure that the animal was kept under physiological conditions.

We observed fast, brief Ca^{2+} signals in 70% of astrocytes (n=151 in 31 animals), which peaked within 100-200 ms., prior to blood flow initiation. Fast Ca^{2+} rises were observed in astrocyte processes, end-feet and somas. The high incidence of fast astrocytic Ca^{2+} signals suggests that astrocytes detect single synaptic events similarly to neurons and may equally contribute to blood flow control. Fast Ca^{2+} increases in astrocytes have been suspected to be contamination from neuropil fluorescent signals. We demonstrate that the fast calcium responses are genuinely astrocytic, by laminar analysis of calcium signals in cortical astrocytes and the surrounding neuropil, combined with an assessment of the point spread function of our system. Fast Ca^{2+} signals in astrocytes were also observed with the use of Rhod2, a calcium indicator that is taken up by only astrocytes. In addition we observed a time delay between the fast, brief Ca^{2+} increases in neuropil and the Ca^{2+} signals formed in astrocyte soma less than 20 ms later, which precluded that the source of the fast astrocyte Ca^{2+} signal was the neuropile.

The sum of fast Ca^{2+} increases in astrocytes correlated with the amplitude of stimulation-induced CBF responses. This suggests that stimulation-induced CBF responses requires preserved Ca^{2+} activity in and interaction between neurons, astrocytes, and blood vessels. Our results will prompt a re-consideration of the connection between neuronal activity and the increase in blood flow that underlies functional imaging techniques.

A VICIOUS CIRCLE OF AGING, HYPOXIA, AND ASTROGLIA CALCIUM WAVES

C. Mathiesen[1], A. Brazhe[2], K. Thomsen[1,3], M.L. Lauritzen[1,3]

[1]Center for Healthy Aging, Department for Neuroscience and Pharmacology, University of Copenhagen, Copenhagen, Denmark, [2]Department for Biophysics, Moscow State University, Moscow, Russia, [3]Department for Clinical Neurophysiology, Glostrup Hospital, Glostrup, Denmark

Astroglial calcium waves (AGCW) constitute a means to spread signals between astroglial cells and to neighboring neurons and blood vessels. AGCW occur spontaneously in Bergmann glia (BG) of the mouse cerebellar cortex *in vivo*. Here we tested three hypotheses: 1) Aging and reduced blood oxygen saturation alters AGCW activity; 2) AGCWs change cerebral oxygen metabolism; 3) AGCWs change vessel diameter; and 4) neuronal and AGCWs activities are correlated.

We used in vivo two-photon microscopy in the cerebellar cortex of adult (8-15-week-old) and aging (48-80-week-old) ketamine-anaesthetized mice after bolus-loading with OGB-1/AM and SR101. The multiscale vision model was used for detection and reconstruction of glial Ca^{2+} waves. Local tension partial oxygen (tpO_2) was recorded with a modified Clark-type polarographic oxygen microelectrode. Blood vessel diameter was assessed by using post-hoc line-scans.

We report that:

1) the occurrence of spontaneous AGCW is 70 times more frequent in the cerebellar cortex of aging (N=11) as compared to adult mice (N=14), which correlated with a reduction in resting tpO_2.

2) In adult mice, spontaneous AGCWs increased during light hypoxia, and ATP-evoked AGCWs reduced the tissue O_2 tension (N=5).

3) ATP-evoked waves were associated with a small but significant increase in oxygen consumption (N=7).

4) When spontaneous AGCWs collided with blood vessels a constriction by 4.3-11.5% was observed in 3/43 capillaries (N=8). Dilation was observed once in pial arteriole.

5) Finally, although spontaneous Purkinje cell (PC) activity was not associated with increased AGCW activity (N=36 events, 4 mice), spontaneous AGCW did affect intracellular Ca^{2+} activity in PCs (N=336 events, 4 mice).

Present data demonstrate that the aging compared to the adult brain has increased spontaneous AGCW activity and a low resting tpO_2 in the cerebellar cortex, suggesting a relationship between AGCW and brain energy. ATP-evoked AGCW were associated with a time-locked reduction in tpO_2 implying increased local oxygen consumption. AGCW tends to induce vasoconstriction. Lastly, we report that AGCW activity was triggered independently of principal neuron Ca^{2+} activity.

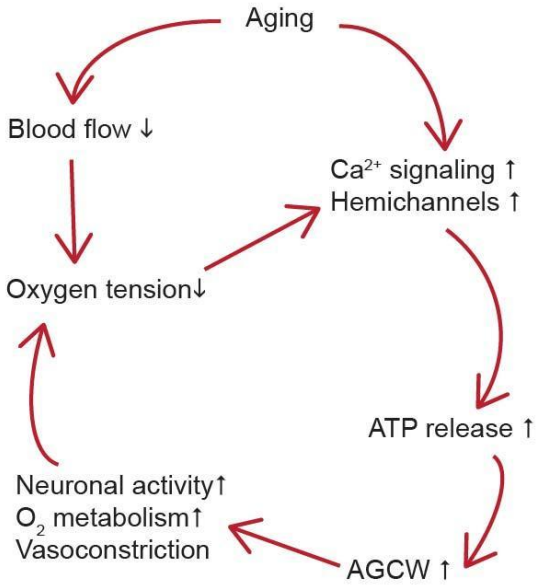

Figure 1. Vicious circle

[Figure 1.]

Our results indicate that the aging brain is more vulnerable and has a large oxidative demand relative to oxygen supply that makes it susceptible to the initiation of a vicious cycle of AGCW and hypoxia (Figure 1).

STIMULATION OF NA^+/H^+ EXCHANGER ISOFORM 1 PROMOTES MICROGLIAL MIGRATION

Y. Shi[1,2], H. Yuan[1], D. Kim[1], V. Chanana[3], A. Baba[4], T. Matsuda[4], P. Cengiz[3], P. Ferrazzano[3], D. Sun[1,2,5]

[1]Department of Neurology, University of Pittsburgh, Pittsburgh, PA, [2]Neuroscience Training Program, [3]Waisman Center, University of Wisconsin, Madison, WI, USA, [4]Graduate School of Pharmaceutical Sciences, Osaka University, Osaka, Japan, [5]Department of Neurological Surgery, University of Wisconsin, Madison, WI, USA

Objectives: Microglia patrol the central nervous system (CNS) with their surveillant function and migrate to the site of injury or inflammation under pathological conditions. However, it remains poorly understood how microglial migration is regulated. In this study, we proposed that Na^+/H^+ exchanger isoform 1 (NHE-1) is important in microglial migration via maintaining intracellular pH (pH_i) homeostasis, interacting with cytoskeletal proteins ezrin and actin, and stimulating reverse mode operation of Na^+/Ca^{2+} exchange (NCX_{rev}).

Methods: Primary microglia or murine BV2 microglial cell line were treated by bradykinin (BK) as a stimulant for motility. Cell movement and morphological changes were monitored, and intracellular H^+, Ca^{2+} and Na^+ concentrations were measured. Immunostaining and immunoprecipitation were performed to investigate the interaction between NHE-1 and cytoskeletal proteins. Pharmacological inhibition, siRNA knockdown or genetic knockout of NHE-1 or NCX was used to evaluate their function.

Results: NHE-1 protein was co-localized with cytoskeletal protein ezrin in lamellipodia of primary or murine BV2 microglia and maintained its more alkaline pH_i. BK increased lamellipodial area and protrusion rate of microglia, but reduced lamellipodial persistence time. Interestingly, blocking NHE-1 activity with its potent inhibitor HOE 642 not only acidified microglia, abolished the BK-triggered dynamic changes of lamellipodia, but also reduced microglial motility and microchemotaxis in response to BK. In addition, NHE-1 activation resulted in intracellular Na^+ loading as well as intracellular Ca^{2+} elevation mediated by NCX_{rev}.

Conclusions: Our study shows that NHE-1 protein is abundantly expressed in microglial lamellipodia and maintains alkaline pH_i in response to BK stimulation. In addition, we demonstrated that NHE-1 and NCX_{rev} play a concerted role in BK-induced microglial migration via Na^+ and Ca^{2+} signaling.

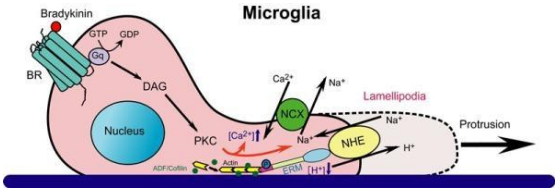

[Microglial migration]

ACTIVITY-DEPENDENT CA^{2+} SIGNALS IN HIPPOCAMPAL ASTROCYTES OF ADULT MICE REVEALED BY GCAMP5

W. Tang[1,2], K. Szokol[1], V. Jensen[1], Ø. Hvalby[3], P.J. Helm[4], L. Looger[5], R. Sprengel[2], E. Nagelhus[1]

[1]Center for Molecular Medicine Norway, University of Oslo, Oslo, Norway, [2]Molecular Neurobiology, Max Planck Institute for Medical Research, Heidelberg, Germany, [3]Department of Physiology, [4]Center for Molecular Biology and Neuroscience, University of Oslo, Oslo, Norway, [5]Janelia Farm Research Campus, Howard Hughes Med. Inst., Ashburn, VA, USA

Neuronal activity evokes a localized increase in blood flow. Being interposed between neurons and the vasculature, astrocytes are in a strategic position to mediate neurovascular coupling. A vast amount of literature based on bulk loading of synthetic fluorescent Ca^{2+} indicators indicates that Ca^{2+} signals in astrocytes can be evoked by synaptic activity and in turn modulate vascular diameter. However, the use of synthetic Ca^{2+} indicators has key limitations - difficult loading procedure, incomplete cleaving and compartmentalization issues - when using AM-ester loading in adult animals and low sensitivity for detecting Ca^{2+} signals in distal astrocytic processes. In this study, the genetically encoded Ca^{2+} indicators GCaMP5 and Lck-GCaMP5 (a membrane-tethered version of GCaMP5) were delivered by rAAV virus mediated gene transfer in order to monitor the spatial and temporal pattern of astrocytic Ca^{2+} signals in acute hippocampal slices of adult mice. Two to three weeks post infection, spontaneous Ca^{2+} activities from the

GCaMP5 transduced astrocytes could be detected with 2-photon imaging. Stimulation of the Schaffer collateral/commissural fibers triggered robust $[Ca^{2+}]_i$ responses in astrocytic cell bodies and processes, including the delicate endfoot processes along blood vessels. The responses typically occurred after a delay of >2 seconds and showed $(\Delta F/F)_{max}$ of 4-6. The activity-evoked astrocytic Ca^{2+} signals could be completely abolished upon application of tetrodotoxin, indicating their dependence on action potentials. Application of (*RS*)-*a*-methyl-4-carboxyphenylglycine (MCPG) and 2-methyl-6-(phenylethynyl)pyridine (MPEP) only partly blocked the signals, indicating a minor role of metabotropic glutamate receptors (mGluRs). Taken together, the genetically encoded Ca^{2+} indicator GCaMP5 delivered by a viral gene transfer can be used to study the role of Ca^{2+} signals in neurovascular coupling.

CORTICAL $GABA_A$ RECEPTOR BINDING POTENTIAL PATTERNS DISPLAY SMALL-WORLD CHARACTERISTICS

N.W. Duncan[1], C. Wiebking[1], P. Gravel[2], A.J. Reader[2], G. Northoff[1]

[1]Mind, Brain Imaging and Neuroethics, Institute of Mental Health Research, University of Ottawa, Ottawa, ON, [2]McConnell Brain Imaging Centre, Montreal Neurological Institute, McGill University, Montreal, QC, Canada

Objectives: Neuroimaging has revealed a picture of the brain as a massively connected network, giving insight into its functional and structural organisation and specialisations. More recently, graph theoretical approaches have been applied to the brain´s structural and functional connectivity, revealing important insights into the organisation of the brain at these levels (Bullmore and Bassett, 2011). Little is known, however, about the network organisation of receptors for neurotransmitters across the cortex.

Methods: To investigate this, ^{18}F-flumazenil PET was used to map $GABA_A$receptor binding potentials (BP_{ND}) in healthy humans (25 participants - 10 females and 15 males; mean age 22.67 yrs, range 18-32 yrs), revealing the distribution of this receptor across the cortex. The cortex was segmented into 68 anatomically defined regions using Freesurfer and BP_{ND} values, corrected for grey-matter density, extracted from each. Receptor distribution networks were then calculated using correlation and an FDR-corrected significance threshold of p = 0.05 (He et al., 2007). Standard graph-theoretical measures were then applied to the receptor distribution networks identified with these maps using the Brain Connectivity Toolbox (Rubinov and Sporns, 2010).

Results: The pFDR = 0.05 threshold produced a graph with a sparsity of 16%. In line with structural and functional networks, it was found that the regional BP_{ND} connectivity network followed a small-world organisation (sigma = 1.74, Figure 1A). Nodes with a high degree were concentrated in the frontal and temporal cortices whilst those with a high betweenness centrality were located in the cortical midline. Finally, the overall network was found to be composed of four sub-modules, including a visual module and a midline-insular module, that correspond with known functional networks (Figure 1B).

Conclusions: These findings provide information as to the organisation of $GABA_A$ receptors in the human brain. The correspondence seen between these receptor networks and known functional and structural ones provides a potential link between structure and function in the human brain.

References:

Bullmore, ET, Bassett, DS (2011). Brain graphs: graphical models of the human brain connectome. Ann Rev Clin Psych 7, 113-140.

He, Y, et al. (2007). Small-world anatomical networks in the human brain revealed by cortical thickness from MRI. Cereb Cortex 17, 2407-2419.

Rubinov, M, Sporns, O (2010). Complex network measures of brain connectivity: uses and interpretations. NeuroImage 52, 1059-1069.

USEFULNESS OF BRAIN PERFUSION SPECT IMAGING IN CHILDREN CORTICAL VISUAL IMPAIRMENTS EXPLORATION

K. Farid[1], C. Cavezian[2], F. Caetta[2], N. Caillat Vigneron[1], S. Chokron[2]

[1]Nuclear Medicine, Hôtel Dieu University Hospital, [2]Fondation Ophtalmologique Rothschild, Paris, France

Introduction: Cortical visual impairments (CVI) in children are considered as a major source of interference with school achievements. However, the brain abnormalities underlying these disorders are not systematically sought, possibly because of morphological abnormalities are not always found using conventional brain imaging (CT-Scan and MRI).

Objective: To investigate the neuro-anatomical correlates of cortical visual impairments in children.

Methods: Sixteen children (10 years old ± 2) were included. They all present CVI ranging from visual field defects to more visual cognitive deficits such as visual analysis or visual attention impairments. All included patients had structural MRI and perfusion brain SPECT (99ECD-SPECT).

Results: In 11 children out of the sixteen presenting CVI, brain MRI did not reveal significant morphological abnormality although the brain perfusion SPECT revealed hypoperfusion in the prefrontal cortex as well as in associative cortical areas in particular in the occipital and in the parietal lobes.

In 4 out of the 16 children with CVI, 4 presented both a visible morphological lesions of the posterior cortical areas on MRI and parieto-occipital hypoperfusions revealed by the brain perfusion SPECT. And finally, only in one child, CVI was observed although morphological MRI as well as brain perfusion SPECT did not reveal any lesion or perfusion abnormality.

Discussion: Brain perfusion SPECT is an imaging method that is able to reveal functional abnormalities consistent with clinical symptoms (ie, hypoperfusion in the posterior cortical regions underlying the visuo-spatial information processing). These functional abnormalities were detected even in the absence of morphological brain abnormalities in the vast majority of children with CVI.

Conclusion: These preliminary results raise the question of the use of brain functional imaging examinations in order to support the neuro-functional correlates in patients suffering from cortical visual impairment.

References:

Cavézian C, Vilayphonh M, de Agostini M, Vasseur V, Watier L, Kazandjian S, Laloum L, Chokron S. Assessment of visuo-attentional abilities in young children with or without visual disorder: toward a systematic screening in the general population. Res Dev Disabil. 2010 Sep-Oct;31(5):1102-8

HIGH-RESOLUTION IN VIVO SPECT-IMAGING OF ACTIVITY-DEPENDENT CHANGES IN REGIONAL CEREBRAL BLOOD FLOW IN MOUSE BRAIN

J. Goldschmidt[1], A. Kolodziej[1], J. Neubert[2], F. Angenstein[3], A. Pethe[4], O.S. Grosser[4], H. Amthauer[4], U.H. Schroeder[1], K.G. Reymann[3], H. Scheich[1], F.W. Ohl[1]

[1]Leibniz-Institute for Neurobiology, Magdeburg, [2]Institute of Cell Biology and Neurobiology, Charite-Universitaetsmedizin, Berlin, [3]German Center for Neurodegenerative Diseases (DZNE), [4]Otto-von-Guericke-University, Clinic for Radiology and Nuclear Medicine, Magdeburg, Germany

Objectives: Large-scale (whole brain) in vivo imaging of spatial patterns of neuronal activity in mouse brain still poses methodological challenges. Measurements of blood-oxygenation level dependent (BOLD) signals using magnetic resonance imaging (MRI) requires the animals to be restrained inside scanners severely limiting the range of applications. Images of activation patterns in unrestrained behaving animals can be obtained using tracers that accumulate in the brain in an activity-dependent manner, show no redistribution after accumulation and can be mapped after stimulation as in 18F-2-fluoro-2-deoxyglucose positron emission tomography (18F-FDG PET). Spatial resolution in 18F-FDG-PET, however, usually does not exceed about 1 mm and is finally limited by positron flight. Single-photon emission computed tomography (SPECT) imaging of regional cerebral blood flow (rCBF) is an additional option but its use for mapping spatial patterns of neuronal activity in mice has remained largely unexplored.

Methods: Here we used 99m-technetium hexamethylpropylene amine oxime (99mTc-HMPAO) multipinhole-SPECT for imaging spatial patterns of neuronal activity in mouse brain during electrical stimulation of the medial forebrain bundle (mfb). We intravenously injected awake behaving mice with the flow tracer 99mTc-HMPAO via chronically implanted jugular vein catheters during five minutes of intracranial self-stimulation or

experimenter-induced stimulation of the mfb. After stimulation we mapped the 99mTc-brain distribution using a dedicated small-animal SPECT-scanner equipped with 1 mm multipinhole apertures. In addition, proof-of-concept experiments were performed using 0.3 mm apertures.

Results: We achieved spatial resolutions of 770 micrometers isotropic voxel sizes using the 1 mm apertures and 400 micrometers using the 0.3 mm apertures. Upon intracranial self-stimulation and experimenter-induced stimulation focal increases in blood flow at the stimulation site and anatomically related brain structures could be observed. Small brain structures such as the mfb were clearly delineated.

Conclusions: 99mTc-HMPAO-SPECT using continuous intravenous tracer-injection during ongoing behavior is a novel tool for in vivo imaging of spatial patterns of neuronal activity in mouse brain. Similar to 18F-FDG-PET, images of spatial patterns of neuronal activity can be obtained from awake behaving unrestrained mice. Both temporal and spatial resolutions, however, are higher with 99mTcHMPAO-SPECT than with 18F-FDG-PET.

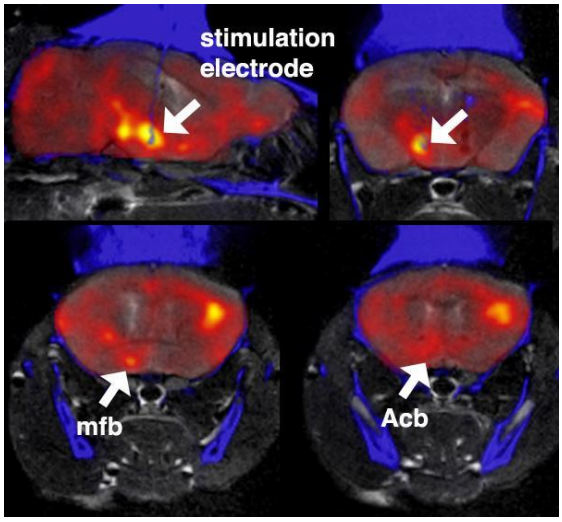

[Fig. 1]

Fig. 1: 99mTc-HMPAO SPECT-images of rCBF during intracranial self-stimulation in mouse brain. SPECT (red to yellow) images are overlaid on MR (grey level) and CT (blue) images. Note focal increase in blood flow at the stimulation site (upper row, sagittal section left, frontal section right). Note also increases in rCBF in medial forebrain bundle (mfb) and accumbens nucleus (Acb).

DUAL ENERGY VIRTUAL NON-CONTRAST TECHNIQUE OF DUAL SOURCE HEAD CTA IN DIAGNOSISI OF MENINGIOMAS

D. Han, X. Xie, Y. Deng, X. Zeng, S. Kang

Kunming Medical University, Kunming, China

Objective To investigate the clinical value of the dual energy CT angiography (CTA) in the preoperative examination of meningioma. Methods CT images of 50 cases pathologically confirmed as meningiomas were retrospectively analyzed. Conventional non-contrast (CNC) and dual energy CTA scan were performed and virtual non-contrast (VNC) and iodine-enhanced images were obtained with postprocessed technology. The mean CT value, signal-to-noise ratio (SNR), image quality, lesions detectability and radiation dose were compared between VNC and CNC images. The supply artery of tumor and relationship between tumor and adjacent intracranial vessel was observed on head CTA image from head bone removal using dual energy technique. Results CT value, SNR, and image quality scores of CNC were higher than those of VNC (all P< 0.05). The image quality scores of VNC were all above 3, which could meet the diagnostic requirements. There were no statistical differences in the size, shape, intratumoral calcification, necrosis and peritumoral edema of lesions between CNC and VNC images. The ability of VNC to display calcification inside meningiomas was limited. The radiation dose of dual energy CTA was 1.71 mSv (61.07%) lower than that of CNC and conventional enhancement scan. Conclusion Dual source CT dual energy technique can obtain VNC, iodine-enhanced and CTA images by single enhanced scan, and it is excellent in preoperative examination for meningiomas.

PHYSIOLOGICAL CORRELATES OF CEREBRAL BLOOD FLOW AT THE ONSET OF THE STEADY-STATE EXERCISE: A PET STUDY

M. Hiura[1,2], T. Nariai[2], K. Ishii[3], M. Sakata[3], K. Oda[3], J. Toyohara[3], K. Ishiwata[3]

[1]Faculty of Sports and Health Studies, Hosei University, [2]Department of Neurosurgey, Tokyo Medical and Dental University, [3]Neuroimaging Team, Tokyo Metropolitan Institute of Gerontology, Tokyo, Japan

Objectives: The present study aimed to investigate the changes of cerebral blood flow (CBF) during the steady-state cycling exercise and focused on regulating factors of CBF during exercise in addition to arterial carbon dioxide tension (P_aCO_2).

Methods: The study group consisted of ten young healthy male volunteers (22.7 ± 1.8 years; mean height, 175 ± 5.0 cm; mean body mass, 65.9 ± 9.8 kg). The quantitative images of regional CBF (rCBF) were investigated by oxygen-15-labelled H_2O (H_2 ^{15}O) PET. The individual cerevrovascular response to CO_2 (CVR to CO_2) was determined by performing PET scans at the rest and during the inhalation of CO_2. The rCBF was assessed at the rest (*Rest*), at the 3 min (*Ex1*) and 13 min (*Ex2*) from the onset of exercise. The pulmonary oxygen uptake ($\dot{V}O_2$), cardiac output (CO), heart rate (HR), blood pressure (BP) and $P_aCO_2$were measured as well.

Results: The CVR to CO_2 for the global CBF was 6.9 ± 5.6 % /mmHg. The work rate of the steady-state cycling was 71 ± 11 watt. The$\dot{V}O_2$, CO, HR and $P_aCO_2$increased from the *Rest* to the *Ex1* and these variables, except for CO, did not change from the *EX1* to the *Ex2*. The mean BP did not change from the *Rest* to *Ex2*. The global CBF significantly increased at the *Ex1* (from 52.5 ± 10.5 to 67.2 ± 20.6 ml/min/100g, P < 0.05) and decreased to the resting level (53.0 ± 8.9 ml/min/100g) at the *Ex2*. For the further anlysis, the absolute values of rCBF were corrected using the individual CVR to CO_2 so that the influence of $P_aCO_2$could be excluded. The statistical parametric mapping analysis (SPM8) indicated that the clusters representing CBF increases at the *Ex1* were widely distributed in the temporal, parietal cortical regions, the basal ganglia, the cerebellum and the brainstem (P< 0.05) and especially in the primary sensory and motor cortex of the legs ($S1_{Leg}$and $M1_{Leg}$) of the legs, the supplementary motor area (SMA), the left insular cortex and the vermis (P< 0.01). At the *Ex2,* CBF increased only in the $S1_{Leg}$ and $M1_{Leg}$, the SMA and the vermis. The absolute rCBF values in the $M1_{Leg}$ increased by 68.6 % at the *Ex1*and by 34.5% at the *Ex2*. A correlation analysis for the rCBF data of the *Rest* and *Ex1* revealed correlation coefficient between the vermis, the M1 and the left insular cortex and $\dot{V}O_2$ of 0.68, 0.67 and 0.55, respectively and between the vermis and $M1_{Leg}$ and HR of 0.58 and 0.54, respectively. These correlations were diminished when the analysis included the *Ex2*.

Conclusions: As the previous study described that the insular cortex and vermis correlated with the autonomic cardiovascular arousal (Critchley et al., 2000), the present study demonstrated that the same regions correlated with $\dot{V}O_2$ and HR only at the *Ex1.* This findings imply that the increase of rCBF would be confined to the initiation of exercise and that the changes in these phyiological variables would be assumed as the regulating factors of rCBF during exercise.

QUANTITATIVE ASSESSMENT OF REST- AND ACETAZOLAMIDE CBF USING QSPECT AND DUAL-TABLE ARG METHOD - INTER-INSTITUTIONAL CONSISTENCY OF NORMAL VALUES

M. Yamauchi[1], E. Imabayashi[2], H. Matsuda[2], J. Nakagawara[3], M. Takahashi[4], E. Shimosegawa[5], J. Hatazawa[5], H. Iwanaga[6], M. Suzuki[7], K. Fukuda[3], **H. Iida**[8]

[1]Department of Investigative Radiology, National Cardiovascular Center-Research Institute, Suita, [2]Department of Nuclear Medicine, Saitama Medical University International Medical Center, Saitama, [3]Department of Neurosurgery, National Cerebral and Cardiovascular Center, Suita, [4]Department of Radiology, Nakamura Memorial Hospital, Sapporo, [5]Department of Nuclear Medicine, Osaka University School of Medicine, Suita, [6]Departmenf of Radiological Technology, [7]Department of Neurosurgery, Yamaguchi University School of Medicine, Yamaguchi, [8]Department of Investigative Radiology, National Cerebral and Cardiovascular Center, Suita, Japan

Introduction: Recently, a novel technique has been developed, and integrated as a software package (QSPECT), to provide quantitative

images of the radioactivity distribution from original projection data acquired using a standard, commercially available SPECT systems. Application of this technique to a clinical imaging protocol demonstrated that the quantitative CBF values were consistent with results from PET both at rest and after acetazolamide challenge [1,2], and that quantitative CBF values were reproducible between the first and the second studies within a month interval, at 9 institutions [2]. Further, Yoneda et al. [3], demonstrated that the CBF and CVR values were well reproducible, both in the quantitative values and also in relative distributions, when obtained from the same patients but at different institutions equipped with different SPECT systems. As an extension of those previous works, this study was intended to evaluate the inter-institutional consistency of quantitative CBF images at rest and after acetazolamide challenges.

Methods: Three institutions carried out a series of SPECT scanning on 32 healthy volunteers, following a standardized protocol for the recently proposed Dual-Table autoradiography (DTARG), which involved dual administration of ^{123}I-iodoamphetamine (IMP). Intra-institute and inter-institute variations of CBF values at rest and after acetazolamide were evaluated. Regional differences among institutions were also investigated using SPM5. Contribution of equalization of spatial resolution among the institutions was also investigated.

Results: SPECT scans have been successfully performed at all institutions, to provide quantitative CBF images at rest and after acetazolamide. Intra-institutional variation of 10-20% at rest and after acetazolamide was consistent with those in previous reports. Quantitative CBF values were not significantly different among institutions in all regions, except of the white matter region. Relative CBF distribution both at rest and after acetazolamide showed small institutional differences, and the differences vanished after equalization of the spatial resolution.

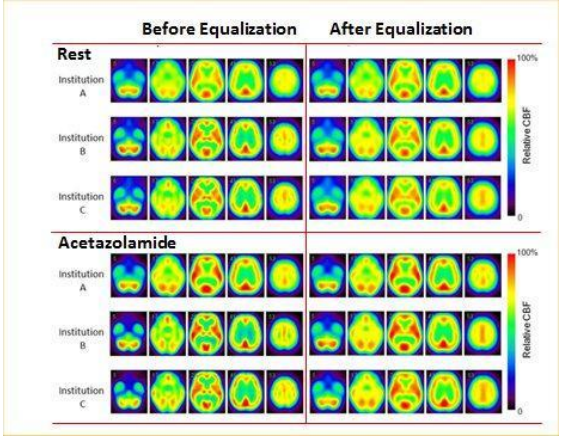

[Impact of spatial-resolution equalization]

Conclusions: Quantitative CBF images which were identical among institutions equipped with different SPECT devices can be obtained if one follows the standardized procedures. It has been considered that SPECT can provide images intrinsically independent of the geometric design of SPECT devices [4]. This concept has been strongly supported by the present study. Use of existing SPECT systems is therefore valid in multicenter clinical studies.

[1] Kim KM et al., Neuroimage, 2006; 46: 689-696

[2] Iida et al., J Nucl Med 2010; 51: 1624-31

[3] Yoneda H et al., JCBFM 2012; 32(9): 1757-64

[4] Graham LS et al., Nuc Med Comm1995; 22: 401-9.

MEASUREMENTS OF CBV AND CBF IN GRAY AND WHITE MATTER FROM BRAIN PERFUSION CT IMAGES IN UNILATERAL ARTERIAL STENOSIS PATIENTS

Y.-H. Kao[1], M.M.H. Teng[2,3], H. Wang[1], Y.-T. Kao[1]

[1]Biomedical Imaging and Radiological Sciences, [2]School of Medicine, National Yang Ming University, [3]Department of Radiology, Taipei Veterans General Hospital, Taipei, Taiwan R.O.C.

Objective: Brain perfusion CT imaging technique is used for evaluating local brain perfusion in patients with cerebral arterial

stenosis or ischemic stroke. Hemodynamic parameters such as cerebral blood volume (CBV) and flow (CBF) are calculated for the evaluation of local brain perfusion. We hypothesis that normal gray matter and white have different CBV and CBF value, and different thresholds are needed for identifying gray and white matter with delayed perfusion.

Methods: On CT images, gray matter contains more water (oxygen) and less lipid (carbon) as compared with white matter. The photoelectric absorption effect is increased and attenuation coefficient is also increased. The brain perfusion CT images of 15 patients with unilateral arterial stenosis were segmented into vessels, cerebrospinal fluid, gray matter, and white matter. The CBV and CBF for gray matter and white matter on the normal and stenotic sides were measured and compared.

Results: As shown in Figure 1, CBV and CBF values for normal gray matter are about twice of the values of normal white matter. The CBV and CBF are different for gray matter, as well as white matter, on the normal and stenotic sides.

Conclusion: In analyzing brain perfusion CT images, different CBV and CBF thresholds are needed to identify gray and white matter with delayed perfusion.

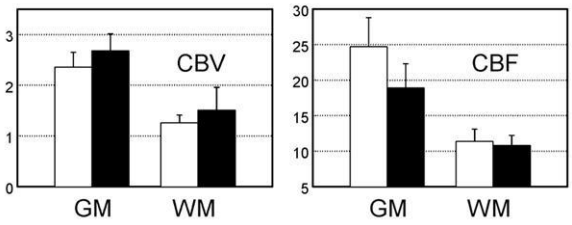

[Figure 1]

The CBV (mL/100 g) and CBF (mL/100 g/min) for gray matter (GM) and white matter (WM) measured on the normal side (white box) and stenotic side (black box).

USEFULNESS OF BRAIN PERFUSION SPECT FOR DIFFERENTIATION BETWEEN IDIOPATHIC PARKINSON'S DISEASE AND MULTIPLE SYSTEM ATROPHY

H.-J. Kim[1], I.-U. Song[1], Y.-A. Chung[2]

[1]Department of Neurology, [2]Department of Nuclear Medicine, Incheon St. Mary's Hospital, Incheon, Republic of Korea

Objectives: Statistical parametric mapping was performed to investigate differences in regional cerebral blood flow (rCBF) between patients with idiopathic Parkinson's disease (IPD), patients with multiple system atrophy (MSA), and healthy volunteers.

Methods: Tc-99m HMPAO SPECT was performed on 23 IPD patients (10 men, 13 women; age, 57-80 y), 9 MSA patients (4 men, 5 women; age, 60-83 y), and 12 age-matched healthy volunteers (5 men, 7 women; age, 56-81 y).

Results: Significant hypoperfusion was observed in IPD compared with healthy subjects in a symmetric subcortical-cortical network including the basal ganglia, thalami, prefrontal and lateral frontal cortex, and parietal cortex (voxel size: 50, corrected $P < 0.001$).

For MSA, only symmetric hypoperfusion was seen in the both prefrontal cortices with respect to healthy subjects and to IPD (voxel size: 50, corrected $P < 0.001$).

Conclusions: Tc-99m HMPAO perfusion SPECT shows detailed differences between IPD and MSA, which may be of use in the differentiation of both disease entities.

ACCURACY OF CENTRAL BENZODIAZEPINE RECEPTOR BINDING POTENTIAL/ CEREBRAL BLOOD FLOW SPECT IMAGING FOR DETECTING MISERY PERFUSION

H. Kuroda

Neurosurgery, Iwate Prefectural Chubu Hospital, Kitakami, Japan

Purpose: The aim of the present study was to determine whether central benzodiazepine receptor binding potential (BRBP)/cerebral

blood flow(CBF) or a combination of CBF and cerebrovascular reactivity (CVR) to acetazolamide on single-photon emission computed tomography (SPECT) more accurately detects misery perfusion, indicating elevation of absolute value of oxygen extraction fraction (OEF) on positron emission tomography(PET), in patients with unilateral major cerebral artery occlusive diseases.

Methods: In 84 patients, OEF, CBF, CVR to acetazolamide, and BRBP were assessed using ^{15}O-PET and *N*-isopropyl-*p*-[^{123}I]-iodoamphetamine and [^{123}I]-iomazenil SPECT, respectively. A region of interest was automatically placed in the middle cerebral artery territory using a 3-dimensional stereotactic region of interest template.

Results: Sensitivity, specificity, and positive and negative predictive values for the affected side-to-contralateral side asymmetry on SPECT-BRBP/CBF to detect the abnormally elevated PET-OEF in the affected hemisphere were 100%, 86.4%, 66.7%, and 100%, respectively. Area under the receiver operating characteristic curve in detecting the abnormally elevated PET-OEF in the affected hemisphere did not differ between analysis of the combination of SPECT-CBF and SPECT-CVR in the affected hemisphere (0.89; 95% confidence interval, 0.80-0.94) and that of the affected side-to-contralateral side asymmetry on SPECT-BRBP/CBF (0.93; 95% confidence interval, 0.86-0.97). The combination of the 3 detected abnormally elevated PETOEF with 97.0% specificity and 90.0% positive predictive value.

Conclusions: The accuracy of central BRBP/CBF asymmetry on SPECT is equivalent to that of the combination of CBF and CVR to acetazolamide on SPECT for detecting misery perfusion in patients with unilateral major cerebral artery occlusive disease.

STATISTICAL IMAGING ANALYSIS USING 3D-SSP OF ^{123}I-IMZ SPECT FOR DIAGNOSIS OF HIGHER BRAIN DYSFUNCTION IN PATIENTS WITH ADULT MOYAMOYA DISEASE

J. Nakagawara[1], K. Iihara[2], H. Kataoka[2], K. Morita[2], K. Itoh[2], N. Kobayashi[2], D. Ishii[2], D. Maruyama[2], N. Hashimoto[2], H. Iida[3]

[1]*Integrative Stroke Imaging Center, Neurosurgery,* [2]*Neurosurgery, National Cerebral and Cardiovascular Center,* [3]*Investigative Radiology, National Cerebral and Cardiovascular Center Research Institute, Suita, Japan*

Background: ^{123I}-Iomazenil (IMZ) is a specific radioligand for the central benzodiazepine (BZ) receptor that could be used as a marker of cortical neuron loss after cerebral ischemia using SPECT[1)]. In this study, based on the statistical imaging analysis for IMZ-SPECT, relationship between higher brain dysfunction and cortical neuron loss in medial frontal lobes was estimated to establish confirmatory diagnosis of higher brain dysfunction in patients with adult moyamoya disease.

Subjects and methods: Eighteen patients with adult moyamoya disease (3 male, 15 female with average age of 39.3±9.0 years) in the chronic stage were included to this study. All patients have a clinical history of transient ischemic attack (TIA) or stroke episodes and type of brain attack in these patients was classified into TIA, ischemic stroke (ISC), intraventricular hemorrhage (IVH), intracerebral hemorrhage (ICH). Surgical revascularization was performed in 16 of 18 patients, and long-term follow-up was achieved in all patients. Relatively mild higher brain dysfunction, observed in 6 patients within these subjects, was confirmed by neuropsychological tests. IMZ-SPECT was estimated by 3-dimensional stereotactic surface projections (3D-SSP) [2)]. Cortical neuron loss was analyzed using stereotactic extraction estimation (SEE) method (level 3: gyrus level) [3)] for 3D-SSP Z-score maps (Z-score>2). Extent of pixels with significant reduction of BZ receptor density within the target gyri (i.e. bilateral MFG and ACG) was calculated.

Results: In 6 patients with higher brain dysfunction, significant cortical neuron loss was observed in bilateral MFG in 4 patients, unilateral MFG in 1 patient, and bilateral ACG in 2 patients. In 12 patients without higher brain dysfunction, significant cortical neuron loss was not observed at bilateral MFG or ACG, and mild loss was observed at bilateral MFG in 2 patients, unilateral MGF in 4 patients, and unilateral ACG in 2 patients.

Conclusions: Long-standing mild hemodynamic ischemia in the anterior circulation of patients with adult moyamoya disease could lead to incomplete brain infarction within medial frontal lobes. Statistical imaging analysis using 3D-SSP and SEE methods for IMZ-SPECT could demonstrate

significant cortical neuron loss in bilateral frontal medial cortex involving MFG and/or ACG which correlate with higher brain dysfunction in patients with adult moyamoya disease. Multi-center investigation based on standardization of statistical image analysis is necessarily to confirm diagnostic contribution.

References:

1) Nakagawara J, et al: Incomplete Brain Infarction of Reperfused Cortex May Be Quantitated With Iomazenil. Stroke 28: 124-132, 1997

2) Minoshima S, et al: A diagnostic approach in Alzheimer's disease using three-dimensional stereotactic surface projections of fluorine-18-FDG PET. *J Nucl Med* 36: 1238-1248, 1995

3) Mizumura S, et al: Three-dimensional display in staging hemodynamic brain ischemia for JET study: objective evaluation using SEE analysis and 3D-SSP display. Annals of Nuclear Medicine 18: 13-12, 2004

VOXEL ANALYSIS OF CT PERFUSION MAPS IN ACUTE ISCHEMIC STROKE

E.M. Nemoto[1], M. Malkoff[1], J. Kawano[2], T. Lee[3], H. Yonas[1]

[1]Neurosurgery, [2]Neurology, University of New Mexico, Albuquerque, NM, USA, [3]Radiology, University of Western Ontario, London, ON, Canada

Objective: Presently, clinicians examining the results of CT or CT perfusion scans are left to their best estimate in assessing the volume of tissue affected from CT perfusion scans where the distribution of disturbed tissue can be scattered among normal tissue. The objective of this study was to quantitatively define tissue volumes of hypoperfusion or increased blood brain barrier permeability by voxel analysis of CT perfusion maps.

Methods: Nine patients emergently being evaluated for acute ischemic stroke with consideration for thrombolytic therapy were subjected to CT perfusion in a Siemens Somatom Definition 64 slice scanner using the VPCT protocol. We scan 123 images with the Dynamulti perfusion protocol - for approximately 2 cm coverage. The Dynamulti perfusion protocol acquires the scan in 9.8 mm slices and acquires three images per second for a 40 second scan time. Voxel analysis comparisons of cerebral blood flow (CBF), cerebral blood volume (CBV), mean transit time (MTT) and blood brain barrier permeability (PS) were compared between the ipsilateral and contralateral hemispheres. The acquired DCE-CT data over 60s was analyzed with the CT Perfusion 4D (GE Healthcare) to generate functional maps including blood flow, blood volume and blood-brain barrier (BBB) permeability surface (PS) product. The map generation algorithm is based on the Johnson-Wilson model where the impulse residue function (IRF) is modeled as a rectangular function with an exponential washout. The BBB PS is then calculated with the Christian-Crone relationship with the known blood flow and extraction efficiency from the determined IRF.

Results: The results (Figure) show that quantitative tissue volumes of reduced Blood Flow and Blood volume and increased permeability surface product can be objectively differentiated between the stroke and contralateral hemispheres.

Conclusions: Clinicians making decisions based on scanning CT perfusion images of CBF, CBV, MTT and PS have to rely on their experience rather than quantitative thresholds. The conversion of the data from the maps to frequency histograms will greatly enhance the ability to experimentally define these thresholds that can be established for clinicians making these decisions.

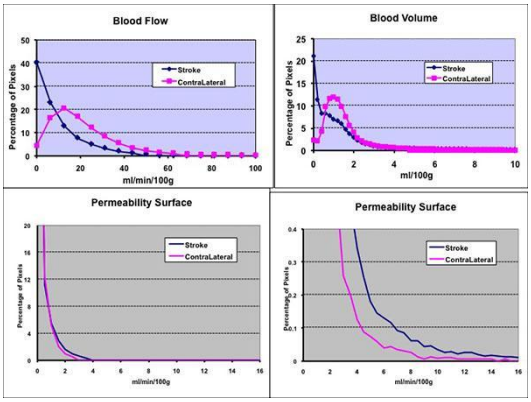

[CT Perfusion]

STABLE XENON CEREBRAL BLOOD FLOW QUANTITATIVELY REFLECTS CT DENSITY IN ACUTE ISCHEMIC STROKE

E.M. Nemoto[1], T. Zhang[2], H. Yonas[1]

[1]Neurosurgery, [2]Neurology, University of New Mexico, Albuquerque, NM, USA

Objective: To determine whether voxel-wise comparison of quantitative stable xenon cerebral blood flow (CBF) and CT density are correlated in a monkey model of acute focal ischemia by middle cerebral artery occlusion.

Methods: In a protocol approved by the Institutional Animal Care and Use Committee of the University of Pittsburgh, eight rhesus monkeys (*Macaca mulatta*), five females and three males, weighing 8.5 ± 3 kg were subjected to transorbital occlusion of the left middle cerebral and internal carotid arteries after two baseline CT and stable Xenon CT CBF measurements (29% xenon) (ref). The measurements were made at four levels beginning at the orbito-meatal line in 5 mm thick contiguous slices. Measurements were repeated 30 min after occlusion and hourly thereafter for up to 6 hrs after focal ischemia. Arterial blood pressure and blood gases were continuously monitored (Nemoto et al, Transl. Stroke Research (2012) 3:369-374). For voxel analysis for each level and scan, the corresponding CT density data were used to detect the edge of the brain, using the Laplacian of Gaussian method in Matlab. A brain mask and midline were then found by above procedure. The left and right masks were applied to both CBF and CT data at the same scan, resulting in the CBF and CT density for both hemispheres in comparison.

Results: Hemispheric voxel-wise analysis of the baseline CT scan in houndfield units (HU) and cerebral blood flow values were done using MatLab. In a representative sample, a plot of CT density versus CBF showed a straight linear correlation with CT density values achieving lower values in the ischemic left hemisphere compared to the right (Figure). CT density values in the normal brain range in the order of 20-30 for white matter and 37 to 45 for gray matter.

Conclusions: These results show that in acute ischemic stroke for up to 6-8 hrs, quantitative stable Xenon CBF measurements reflect CT density where low CBF values < 20 ml/100g/min are correlated with CT densities < 20 HU reflecting brain edema.

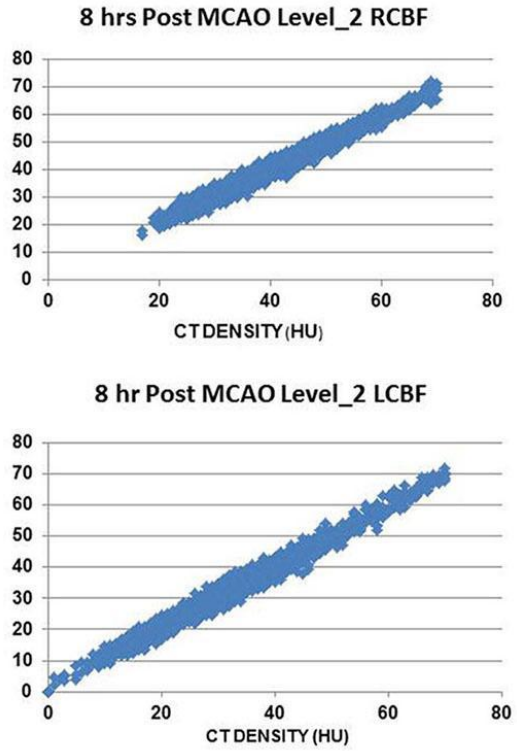

[XeCBF vs CT Density (HU)]

HOW DO GABA AND GLUTAMATE MODULATE THE BRAIN'S INTRINSIC ACTIVITY AND SUBSEQUENT STIMULUS-INDUCED ACTIVITY ON A REGIONAL LEVEL?

G. Northoff, C. Wiebking, P. Qin, N. Duncan

University of Ottawa Institute of Mental Health Reserch, Ottawa, ON, Canada

Background: The cellular level of neural activity is characterized by the balance between neural excitation and inhibition, the excitation-inhibition balance (EIB). The EIB is supposed to crucially mediated by the excitatory transmitter Glutamate and the inhibitory GABA including their respective receptors. While much research has been done on the biochemical modulation of the EIB on the cellular level, the neuro-biochemical mechanisms underlying the EIB on the regional level of neural activity remain largely unknown. I therefore present a series of multimodal imaging studies that combine fMRI or EEG with biochemical measures as obtained in MRS or PET.

Method: We investigated a series of healthy subjects in fMRI. That was combined with biochemical measures of Glutamate and GABA as in MRS or measurement of GABA-A receptors as in 18-F-Flumazenil-PET. Resting state activity was measured during eyes closed (5 minutes). While measurement of stimulus-induced activity included different task-related paradigm including self-relatedness, reward, and interoceptive awareness.

Results: We could show that the resting state concentration of Glutamate (MRS) in the medial prefrontal cortex (MPFC) predicted the degree of neural activity in MPFC during the resting state, e.g., intertribal interval, as distinguished from reward-related activity in the same region. Moreover, our studies show that the concentration of MPFC Glutamate predicted the degree of neural activity in (and functional connectivity to) subcortical regions like the thalamus, the striatum, and the pons. Analogous trans-regional effects of MPFC Glutamate were also observed on the cortical level with MPFC Glutamate predicting stimulus-induced activity in anterior cingulate cortex. Though our results show correlation between the concentrations of GABA and Glutamate, only Glutamate correlated with neuronal measures of the resting state. However, we observed that GABA resting state concentration (MRS) and GABA-A receptors (PET) in for instance MPFC, insula, and visual cortex predicted the degree of stimulus-induced activity in the same regions during intero- or exteroceptive awareness or basic visual input.

Discussion: Our results suggest different roles for GABA and Glutamate in constituting the EIB on the regional level. Glutamate seems to be strongly involved in mediating intra- and trans-regional effects during the resting state (and subsequent stimulus-induced activity).In contrast, GABA seems to act more on the rest-stimulus interaction and the shaping of the stimulus-induced activity in different regions and their respectively associated psychological functions. Based on our and others findings, a model for the constitution of the EIB on the regional level of neural activity is presented.

EFFECTIVE BRAIN CONNECTIVITY IN GRN-RELATED MONOGENIC FRONTOTEMPORAL DEMENTIA: A PATH MODELING ANALYSIS

B. Paghera[1], A. Alkhraisheh[1], E. Premi[2], M. Grassi[3], B. Borroni[2], A. Padovani[2], R. Giubbini[1]

[1]Department of Nuclear Medicine, Spedali Civili Hospital and University of Brescia, [2]Center for Aging Brain and Dementia Department of Neurology, University of Brescia, Brescia, [3]Health Sciences Section of Medical Statistics and Epidemiology, University of Pavia, Pavia, Italy

Background: It has been suggested that monogenic Frontotemporal Dementia (FTD) due to Granulin (GRN) mutations present a specific pattern of atrophy, involving parietal regions, as compared to FTD GRN-negative disease. Recent literature have suggested that the study of functional neural networks, rather than regional structural damage, might better elucidate the underlying pathogenic mechanisms, showing complex relationship among structural alterations observed with conventional neuroimaging techniques.

Objective: To evaluate effective brain connectivity in FTD patients carrying GRN mutations (FTD GRN+), as compared to FTD patients without pathogenetic GRN mutations (FTD GRN-), and healthy controls (HC).

Methods: Thirty FTD patients (15 GRN+ and 15 GRN-, matched for age, gender and clinical phenotype) and 15 age and gender-matched HC underwent brain perfusion single photon emission tomography at rest. Brain regions specifically involved in FTD, i.e. dorsolateral cortex, anterior cingulate cortex, orbitofrontal cortex, posterior temporal cortex, temporal pole, and parietal cortex, were used as volume-of-interest (VOI) to identify functionally interconnected areas using voxel-wise covariance analysis. A path model was defined by means of effective connectivity analysis within the Bayesan Modeling and Structural Equation Modeling framework. Statistically significant differences between the three groups on the identified model were carried out.

Results: The best fitting was obtained by the data-driven approach, and brain connectivity pathways resembling the state-of-art

anatomical knowledge were obtained. Signature of FTD (both GRN+ and GRN- subgroups) was the disconnection of dorsolateral and temporal cortices, as compared to HC. When GRN+ and GRN- groups were considered, the former presented a selective bilateral parieto-temporal disconnection in respect to GRN- patients. Furthermore, in FTD GRN+ patients, an increased compensative connectivity of the temporal regions, i.e. temporal pole and posterior temporal cortices, was observed.

Conclusions: The present work suggests that impairment of effective functional connectivity of the parieto-temporal regions is the hallmark of GRN -related FTD. Compensative mechanisms, which should further investigated, may however occur.

THE USE OF ^{201}THALLIUM-DIETHYLDITHIOCARBAMATE-SPECT FOR IN-VIVO IMAGING OF EARLY STROKE INDUCED ALTERATIONS IN CEREBRAL POTASSIUM METABOLISM

F. Stöber[1,2], U. Dirnagl[1], K.G. Reymann[3,4], U.H. Schröder[3], H. Scheich[2,4], A. Wunder[1,5], J. Goldschmidt[2]

[1]Department of Experimental Neurology Center for Stroke Research Berlin, University Medicine Berlin, Berlin, [2]Department Auditory Learning and Speech, [3]Project Group Neuropharmacology, Leibniz Institute for Neurobiology, [4]German Center for Neurodegenerative Diseases (DZNE), Magdeburg, [5]Boehringer Ingelheim Pharma GmbH & Co. KG Translational Medicine Experts, Biberach an der Riss, Germany

Objectives: Cerebral ischemia is accompanied by severe alterations in potassium (K^+)-metabolism in the affected region. Within the first minutes after oxygen- and glucose-deprivation neurons lose their ability to accumulate K^+ and to maintain the intra- to extracellular K^+-gradients due to decline of energy dependent K^+-pump activity. Imaging these alterations in-vivo could be of substantial interest in preclinical research as well as for diagnostic purposes in humans, since they are sensitive indicators of tissue damage and may serve to distinguish salvageable from irreversibly damaged tissue at very early time points. We here present a novel approach for imaging K^+-metabolism in focal cerebral ischemia using the radioactive K^+-analogue ^{201}thallium ($^{201}Tl^+$). This isotope has been used for decades for SPECT-imaging of myocardial infarction. Due to the poor blood-brain barrier (BBB) permeability of K^+ and K^+-analogues, however, little use has been made thus far of this tracer for imaging K^+-metabolism and tissue viability in the CNS. Recently, we have shown using histochemical methods that it is possible to study cerebral K^+-metabolism when the lipophilic chelate complex thallium-diethyldithiocarbamate (TlDDC) is used instead of water-soluble thallium salts. After crossing the BBB Tl^+ is released from TlDDC prior to activity dependent neuronal and glial uptake.

Methods: We intravenously injected mice and rats with ^{201}TlDDC after inducing of focal cerebral ischemia by temporary occlusion of the middle cerebral artery (MCA) using the filament model in mice and the Endothelin-I model in rats. The $^{201}Tl^+$-distribution was monitored in brains in-vivo using a small-animal SPECT/CT scanner. In dual-isotope studies, we combined these measurements with ^{99m}TcHMPAO-SPECT-imaging of regional cerebral blood flow (rCBF). The definite structural tissue damage was determined by MRI. In addition, we mapped the Tl^+-distribution for different MCA occlusion times histochemically with single-cell resolution and compared it with an established marker for cell death, Propidium-Iodide (PI) and Nissl stain.

Results: SPECT-imaging showed a reduced $^{201}Tl^+$-content on the lesioned side as well as a continuous loss of $^{201}Tl^+$ from the lesioned area during the first hours after stroke onset. The lesioned areas differ in their size for the different occlusion times. The final areas of reduced $^{201}Tl^+$ content matched with the structural damage as detected with MRI (see pic_01), histochemistry and PI.

In addition, we found mismatches between ^{99m}Tc- and $^{201}Tl^+$-content in the affected areas early after stroke onset. At later time points, 24 hours after stroke onset respectively, the $^{201}Tl^+$-signal matches the ^{99m}Tc-signal. ^{99m}Tc-measurements matched with the final lesioned area already at early time points.

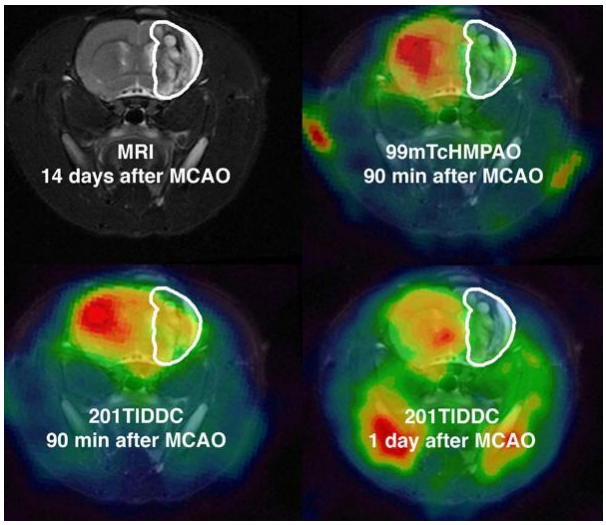

[Dual isotope study of 99mTcHMPAO and 201TlDDC]

Conclusion: Our findings suggest that ^{201}TlDDC is a useful tracer for mapping alterations of K^+-metabolism early in the time course of cerebral ischemia and prior to structural damage. Small-animal ^{201}TlDDC-SPECT can provide novel insights into the spatiotemporal dynamics of K^+-metabolism and can give information about the lesion growth and lesion size in the acute and hyperacute phase. ^{201}TlDDC-SPECT appears to be a promising technique to determine tissue viability and tissue that might be rescued and to monitor therapeutic effects in cerebral ischemia.

NON INVASIVE ASSESSMENT OF HYPOXIA WITH [^{18}F]-FMISO PET IN TWO EXPERIMENTAL HUMAN GLIOMA MODELS

S. Valable[1,2], A. Corroyer-Dulmont[1,2], E.A. Pérès[1,2], E. Petit[1,2], L. Durand[1,2], L. Marteau[1,2], J. Toutain[1,2], S. Roussel[1,2], L. Barré[1,3], M. Bernaudin[1,2]

[1]CNRS, UMR ISTCT 6301, CERVOxy Group, Université de Caen Basse-Normandie, [2]CEA, DSV/I2BM, UMR ISTCT 6301, CERVOxy Group, [3]CEA, DSV/I2BM, UMR ISTCT 6301, LDM-TEP Group, Caen, France

Introduction: Despite therapies, GBM patients still have a poor prognosis. At the preclinical level, numerous glioma models are used for the development of new therapies but also to optimize conventional ones. Given the significance of hypoxia in drug and radiation resistance and that hypoxia is widely observed among glioblastoma patients, mapping hypoxia *in vivo* may contribute to optimize translation of new therapies.

The aim of this study was to compare the hypoxic status of two commonly used human orthotopic glioma models using non-invasive hypoxia imaging with [^{18}F]-FMISO-µPET. In parallel, given the relationships between angiogenesis and hypoxia, we used MRI and histology to characterize the vasculature. Finally, to explore in further detail the difference in hypoxia between both models, we analyzed at the molecular level the expression of hypoxia inducible genes.

Methods: Human U87 and U251 orthotopic glioma models were implanted in nude rats. Imaging (MRI and PET) were performed on Days 15 or 16 after cell implantation for the U87 model and Days 24 and 25 for the U251 models. µMRI was performed on a 7 teslas horizontal magnet. The tumor-associated edema was detected using a T2w sequence. The vasculature was characterized by MRI by measuring perfusion after a bolus injection of contrast agent (P904®, 200µmol/kg, Guerbet Research), (ii) Cerebral Blood Volume (CBV), (iii) vessel size, and (iv) vascular permeability after injection of Dotarem® (200µmol/kg, Guerbet SA). Glucose metabolism and hypoxia were studied after intravenous injection of 66 MBq.kg^{-1} of [^{18}F]-FDG and [^{18}F]-FMISO-PET using a µPET (Inveon, Siemens). At the time of the last µPET session, anesthetized rats were euthanized, brains were removed, immediately snap frozen and stored at -80°C. Coronal sections were cut on a cryostat. Standard hematoxylin and eosin (H&E) staining was used for histological examination and molecular studies. Immunohistochemical staining for Rat Endothelial Cell Antigen (RECA)(Abcam, 0.4µg/ml) was used to characterize glioma vascularization. RT-qPCR was performed to analyze the expression of EPO, CAIX and VEGF.

Results: Both tumor models were detectable in T2w MRI and [^{18}F]-FDG-µPET. FDG uptake was not significantly different between both models. In contrast, only the U251 model exhibited [^{18}F]-FMISO uptake. In accordance with these results, the U251 tumors exhibited a low vasculature as compared to the U87 tumors (rCBV measured with MRI = 2.17 ± 0.34 and 1.49 ± 0.30 for U87 and U251 models respectively, $p < 0.01$). These results

were confirmed with RECA immunohistochemistry which demonstrated fewer vessels in the U251 tumor as compared to the U87 model. Finally, at the molecular level, the expression of hypoxia inducible genes. EPO was not differentially expressed between both models; however, we observed an increase in the mRNA expression of VEGF and CAIX in the U251 relative to the U87 model.

Conclusions: This study demonstrates differences between glioma models and emphasizes the importance of using non invasive imaging of hypoxia at the preclinical level. Indeed, given the importance of oxygen for chemo- and radio-therapies in GBM patients, it is essential to find the most reliable preclinical models for translation of new therapies to clinic.

UNDERSTANDING MECHANISMS OF ENERGY FAILURE USING ^{15}OXYGEN AND [^{18}F]FLUOROMISONIDAZOLE POSITRON EMISSION TOMOGRAPHY FOLLOWING HEAD INJURY

T.V. Veenith[1], T. Geeraerts[2], J. Grossac[1], E. Carter[1], V. Newcombe[1], J. Outtrim[1], G. Gee[3], R. Smith[4], F.I. Aigbirhio[4], T. Fryer[3], D. Menon[1], Y. Hong[3], J. Coles[1]

[1]Division of Anaesthesia, University of Cambridge, Cambridge, [2]Départements d'Anesthésie Réanimation, CHU Purpan, Toulouse, [3]Wolfson Brain Imaging Centre, University of Cambridge, [4]Wolfson Brain Imaging Centre, University of Cambridge, Cambridge, UK, Cambridge, UK

Introduction and objectives: Using ^{15}oxygen positron emission tomography (^{15}O PET) we have shown evidence of classical ischaemia associated with poor outcome within 24 hours of traumatic brain injury (TBI).[1] Other PET studies have demonstrated non ischaemic metabolic derangements associated with chronic cerebral atrophy.[2] Post-mortem studies show widespread microvascular occlusion and perivascular oedema in TBI, associated with selective neuronal loss.[3] The relevance of these findings is explained by our TBI studies with ^{15}O PET and brain tissue oximetry ($BtpO_2$), which show increased vascular to tissue gradients for oxygen tension.[4] This suggests evidence of regional tissue hypoxia secondary to microvascular ischaemia but requires confirmation through demonstration of a mismatch between the distributions of classical ischaemia and tissue hypoxia. Tissue hypoxia can be imaged using the PET tracer [^{18}F]Fluoromisonidazole ([^{18}F]FMISO), which is trapped in hypoxic but viable tissue through oxygen dependent bioreduction, but has not been used following TBI. The aim of this study was to compare evidence of classical ischaemia to the distribution of tissue hypoxia secondary to microvascular ischaemia using [^{18}F]FMISO binding within the injured brain.

Material and methods: Ten patients with deterioration in Glasgow Coma Score < 12, and 10 controls under went ^{15}O and [^{18}F]FMISO PET imaging. Following [^{18}F]FMISO injection arterial data were acquired. Arterial plasma input function was used for kinetic analysis and binding was quantified using BAFPIC (a basis function approach to non-linear least square two tissue irreversible compartmental modelling[5]) and Patlak graphical analyses to derive kinetic parameters from the dynamic [^{18}F]FMISO PET emission. We calculated the burden of classical ischaemia based on regional OEF through calculation of the ischaemic brain volume (IBV),[1] and the 99% confidence interval (CI) for [^{18}F]FMISO binding in controls was used as a threshold to identify the burden and spatial distribution of tissue hypoxia in patients.

Results: The mean (range) IBV for patients was 95 (7 - 266) ml, while the volume of brain with k_3 [^{18}F]FMISO that exceeded the 99% CI of controls was 243 (114 - 490) ml. The distribution of [^{18}F]FMISO binding was typically located within the brain tissue adjacent to visible contusions (figure, TBI, GCS 5 within 24 hours of injury).

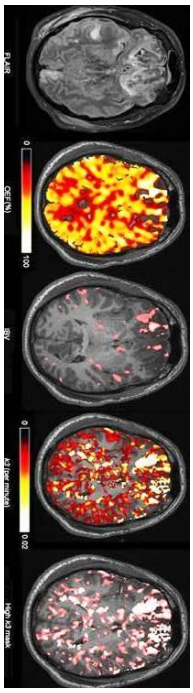

[PET images within 24 hours of TBI]

Conclusion: The volume of brain with physiology consistent with classical ischaemia in patients was variable, and did not match the volume of brain with increased [^{18}F]FMISO uptake. This suggests evidence of tissue hypoxia in the absence of high OEF. Although such regions may already be irreversibly injured it suggests evidence of microvascular ischaemia resulting in lesion expansion due to ongoing neuronal injury.

References:

(1) Coles JP et al. JCBFM 2004

(2) Vespa P et al. JCBFM 2010

(3) Stein et al. Neurosurgery 2004

(4) Menon et al. CCM 2004

(5) Hong YT et al NeuroImage 2010

HYPOPERFUSION OF CONSECUTIVE BRAIN SPECT IMAGES WITH MCI BY 3 ALTERNATED MR-BASED PARTIAL VOLUME CORRECTION ALGORITHMS

H.J. Yoon[1], Y.J. Jeong[2], D.-Y. Kang[2]

[1]Department of Nuclear Medicine, Dong-A University Medical Center, [2]Department of Nuclear Medicine, Dong -A University Medical Center, College of Medicine, Busan, Republic of Korea

Purpose: Partial volume correction (PVC) can be applied to brain SPECT image in order to improve quantitative accuracy of measured radioactivity concentrations(1). The localized regions of hypo-perfusion using Tc-99m-HMPAO brain SPECT image were examined on subtraction of consecutive images before and after PVC using MR images of the brain. The aim of this study was to investigate the effects of subtraction images acquired by 3 alternated MR-based PVC methods (Meltzer, Mueller-Gartner(MG)(2), modified MG (mMG)) using MR-based including count normalization and spatial normalization(3).

Methods: The consecutive brain SPECT images were acquired on the patients with mild cognitive impairment (MCI) using 2 head gamma camera who were severely decreased perfusion after injection of 925 MBq Tc-99m-HMPAO. The subtraction of 2 consecutive images was calculated by SPM8 implemented Ictal-interictal Subtraction Analysis by Statistical Parametric Mapping (ISAS) and Subtraction Ictal SPECT Co-registred to MRI (SISCOM) algorithms. We applied the influence of 3 alternated MR-based PVC algorithms on SPM analysis of the ISAS and SISCOM. The software implemented 3 alternated algorithms (Meltzer, MG, mMG) was used to improve a degree of accuracy in the brain SPECT image.

Results: The brain SPECT images were affected by the partial volume effect and the statistical results of ISAS were changed before and after PVC. The regions of the hyper- and hypo-perfusion by subtraction were focused after correction of the partial volume effect. The patient showed hypo-perfusion by SISCOM in the limbic lobe, temporal lobe, anterior lobe, frontal lobe, left parietal lobe ($p< 0.01$ uncorrected, $k>100$). Three alternative methods for PVC produced similar localizations, but they did not agree with each

other on the value and region of the threshold. The subtracted region for consecutive images without PVC was very similar to the region by Meltzer method, the result by MG method focused the hyper- and hypo-perfusion region, and finally the region noise was eliminated by mMG method.

Conclusion: The importance of combining anatomy and function in the analysis of ISAS and SISCOM for the patient with hypo-perfusion should be considered. We have tested 3 PVC algorithms analyzing the brain SPECT image with MR. The subtracted regions by 3 methods of PVC had similar hyper- and hypo-perfusion and PVC was represented to compare the quantitative accuracy of subtracted analysis performed on Tc-99m-HMPAO consecutive brain SPECT images.

References:

(1) Rousset O, Zaidi H. Correction for partial volume effects in emission tomography. Quantitative Analysis in Nuclear Medicine Imaging 2006:236-271.

(2) Muller-Gartner HW, Links JM, Prince JL, Bryan RN, McVeigh E, Leal JP, et al. Measurement of radiotracer concentration in brain gray matter using positron emission tomography: MRI-based correction for partial volume effects. Journal of Cerebral Blood Flow & Metabolism 1992;12(4):571-583.

(3) Quarantelli M, Berkouk K, Prinster A, Landeau B, Svarer C, Balkay L, et al. Integrated software for the analysis of brain PET/SPECT studies with partial-volume-effect correction. Journal of Nuclear Medicine 2004;45(2):192-201.

DETERMINING THE LOCALIZATION OF CONSECUTIVE BRAIN SPECT IMAGES USING SISCOM, ISAS AND ISAS HN METHOD

H.J. Yoon[1], Y.J. Jeong[2], D.-Y. Kang[2]

[1]Department of Nuclear Medicine, Dong-A University Medical Center, [2]Department of Nuclear Medicine, Dong-A University Medical Center, College of Medicine, Busan, Republic of Korea

Purpose: The regions of hyper- and hypoperfusion change in two consecutive brain SPECT images were investigated in individual patients and compared with their results, according to each numerical algorithm.

Methods: Tc-99m-HMPAO brain SPECT images were acquired on the known 3 MCI patients (converted to PDD) and 28 MCI patients (non-converted) over a 2 or 3-year period using a two-head gamma-camera(1). The subtraction of two consecutive images was calculated by SPM8 and BioImage Suite 2.6(2). These algorithms for the subtraction were used in Subtraction Ictal SPECT Co-registred to MRI (SISCOM)(3), Ictal-Interictal Subtraction Analysis by Statistical Parametric Mapping (ISAS)(4), ISAS half normal distribution (ISAS HN). Three analysis methods of SISCOM, ISAS with SPM8 and ISAN HN with BioImage Suite were compared.

Results: The codes by three algorithms produced similar localization of the right cerebellum anterior lobe, left cerebrum *parahippocampa gyrus*, right superior temporal gyrus, left and right inferior frontal gyrus, left middle occipital gyrus, right middle temporal gyrus, and right paracentral lobule BA 31 ($p < 0.01$) for one patient. The two algorithms of ISAS and ISAS HN had a similar hyper- and hypoperfusion region, but they did not agree with each other on the value of the threshold. The subtraction images from SISCOM were in agreement with another two algorithms in the most significantly activated area. The scan order bias in the estimation of the normal variation had no major effect on the results.

Conclusion: Three analysis methods were available to compare two consecutive perfusion images and were compared with each subtraction result according to algorithm. The codes by three algorithms had similar hyper- and hypoperfusion regions in the patient. ISAS-type analysis in SPM8 is recommended to diagnose for the patient with perfusion changes because it has a statistical significance, while SISCOM has not, and it is more familiar than ISAS HN BioImage Suite.

References:

(1) Yoon HJ, Park KW, Jeong YJ, Kang DY. Correlation between neuropsychological tests and hypoperfusion in MCI patients: anatomical labeling using xjView and Talairach Daemon Software. Ann.Nucl.Med. 2012:1-9.

(2) Scheinost D, Teisseyre TZ, Distasio M, DeSalvo MN, Papademetris X, Blumenfeld H. New open-source ictal SPECT analysis

method implemented in BioImage Suite. Epilepsia 2010;51(4):703-707.

(3) Hogan RE, Kaiboriboon K, Bertrand ME, Rao V, Acharya J. Composite SISCOM perfusion patterns in right and left temporal seizures. Arch.Neurol. 2006;63(10):1419.

(4) McNally KA, Paige ALB, Varghese G, Zhang H, Novotny Jr EJ, Spencer SS, et al. Localizing value of ictal-interictal SPECT analyzed by SPM (ISAS). Epilepsia 2005;46(9):1450-1464.

DETECTION OF HEMODYNAMIC RESPONSE WITH FUNCTION MRI USING REPEATED MEDIAN NERVE STIMULATION

L. Ai[1], X. Gao[2], J. Xiong[3]

[1]*Department of Biomedical Engineering, University of Iowa, Iowa City, IA, USA,* [2]*Department of Medical Imaging, Suzhou Institute of Biomedical Engineering & Technology, Suzhou, China,* [3]*Department of Radiology, University of Iowa, Iowa City, IA, USA*

Purpose: The coupling relationship of cerebral hemodynamics and neuronal activity is the foundation of fMRI. Median nerve stimulation has been closely studied with direct electrical recordings, but not with BOLD fMRI. In this study, we investigate the BOLD response with similar stimulation, which may also offer some insight on the coupling relationship.

Methods:

Stimulation Paradigm: Unilateral stimulations were delivered to the right median nerve using a Grass S48 stimulator (Grass Technologies, USA). The stimulation intensity was adjusted to 15V above the minimum required to obtain a thumb twitch. A block design with four and a half off/on cycles was used with a randomized inter-stimulation interval (ISI) of 1.5-2.5 seconds. The volunteers were asked to stay still and awake for the duration of the scan. No task was actively performed during the scan.

Data Acquisition: The MRI data was acquired on a Siemens 3T Trio scanner (Siemens Medical Solutions, Erlangen, Germany). A gradient echo EPI pulse sequence was used to acquire the BOLD fMRI images. Each run was six minutes in length with 180 images captured. Each scanning session was composed of seven runs.

Data Analysis: The MRI images were processed using Analysis of Functional NeuroImages (AFNI). All images were aligned to Talriach space (www.bic.mni.mcgill.ca). Cross correlation analysis was performed to generate a statistic map with a statistical threshold of Z = 3 (p = 0.0013, uncorrected).

Results: Inter-run habituation is shown in figure 1. The data was averaged across all ten subjects. Only the first run showed significant activations in the left S1/M1.

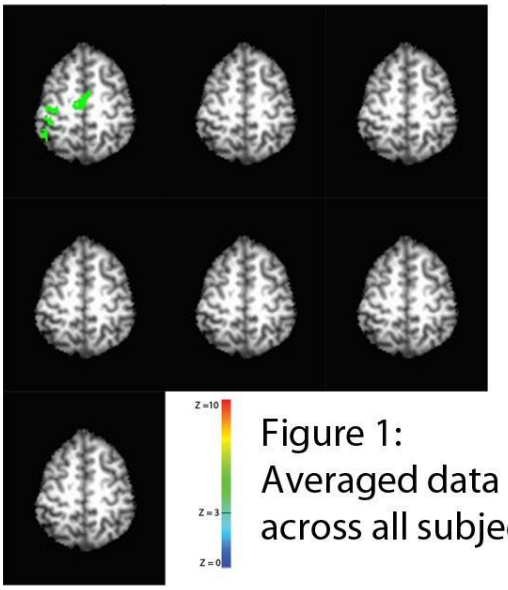

Figure 1: Averaged data across all subjects

[Figure 1]

Figure 2 shows the average activation volume in the left M1/S1 area across all seven runs. It appears that there is a consistent rapid decrease in the cluster volumes of statistical significance (ANOVA, F = 2.59, p< 0.05).

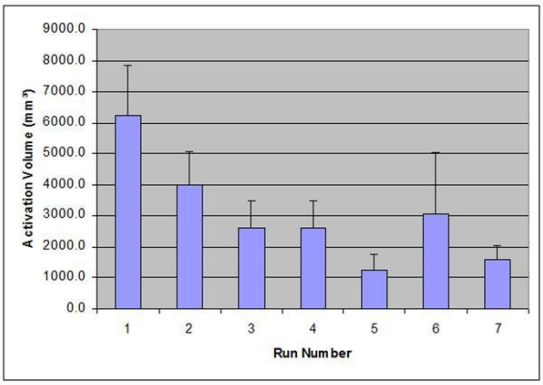

Figure 2: Graph of average activation volumes

[Figure 2]

Discussion and conclusions: Using median nerve stimulation, we observed hemodynamic habituation in the BOLD response. The BOLD signal was detectable only in the first of seven runs. It would not be unreasonable to conclude that there is a strong habituation associated with median nerve stimulation. Direct cortical recordings are often considered to be the gold standard when measuring neuronal activity, but such studies have not seen the same habituation (Thees et al, 2003). Combining direct cortical recordings with the BOLD offers an opportunity to study the dynamic coupling between neuronal activity and cerebral hemodynamics. Further studies are required to study this relationship.

Funding: This study was funded by the National Institutes of Health, USA (R21 MH 082187-01) and the International Science and Technology Cooperation Plan of Suzhou, China. (SH201210).

References:

Thees S, Blankenburg F, Taskin B, Curio G, and Villringer A (2003). Dipole source localization and fMRI of simultaneously recorded data applied to somatosensory categorization. NeuroImage 18(3): 707-719.

DYNAMIC SUSCEPTIBILITY CONTRAST MRI ABSOLUTE QUANTITATIVE CBF ISCHEMIC VOLUMES CLOSELY MIRRORS NIHSS SEVERITY IN ACUTE ISCHEMIC STROKE

J.R. Alger, G. Ahadi, D.J.J. Wang, D.S. Liebeskind

Neurology, University of California, Los Angeles, CA, USA

Objective: Dynamic Susceptibility Contrast Magnetic Resonance Imaging (DSC-MRI) is frequently used in the evaluation of the acute stroke patient. It is possible to derive absolute quantitative cerebral blood flow (aqCBF) images using DSC-MRI, but this is rarely done because of computational complexity and issues with CBF accuracy. Penumbra identification with DSC-MRI would be greatly enhanced if a reliable method to calculate aqCBF from DSC-MRI data were available. Accordingly we have been experimenting with various aqCBF calculation techniques. This study hypothesized that an accurate, reliable aqCBF calculation method would produce aqCBF images that could be segmented for ischemia using a simple CBF threshold and that the so defined ischemic volume would have a statistically significant correlation with the contemporaneous National Institutes of Health Stroke Scale (NIHSS) measure.

Methods: The study used 27 archived DSC-MRI data sets obtained at a single institution, but with multiple MRI scanners, for an indication of acute ischemic stroke within 24 hrs of symptom onset for which contemporaneously acquired NIHSS results were also available. Studies showing uncorrectable head movement and poor contrast agent delivery (arterial input function (AIF) full width at half maximum > 12 sec) to the contralateral middle cerebral artery were not used. The CBF calculation used

1) AIF measurement,

2) VOF correction for partial volume

3) A field dependent AIF/VOF correction factor

4) AIF deconvolution and

5) CBF measured as maximum of the Residue function.

Ischemic volumes were measured using ischemic CBF thresholds between 1 and 50 cm^3/100 g/min. Correlation and significance between ischemic volume expressed as a fraction of brain volume and NIHSS were evaluated at each threshold using Spearman Rank Statistics.

Results: The figure provides

1) the correlation plot for the optimal ischemic CBF threshold (top)

2) a plot of the relationship between correlation coefficient and ischemic CBF threshold (middle) and

3) a plot of the relationship between correlation significance and ischemic CBF threshold (bottom).

The optimal ischemic correlation threshold was 4 cm^3 /100 g/min (Spearman rho = 0.63 P < 10^{-3}. A second evaluation of only patients with left hemisphere ischemia showed a much higher correlation between ischemic CBF

volume and NIHSS (Optimal Threshold = 6.0 cm3/100 g/min Spearman rho = 0.84, $P < 10^{-4}$)

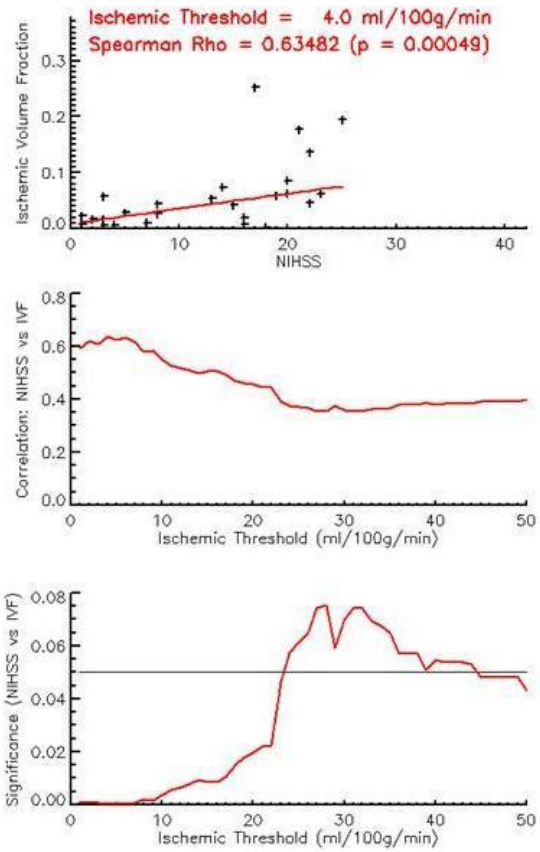

[FinalFigJPG]

Conclusions: With proper attention to detail and elimination of poor technical quality studies, it is possible to obtain DSC-MRI aqCBF images that can be segmented to produce ischemic CBF volumes that correlate closely with NIHSS and that reflect the known sensitivity of the NIHSS to left hemisphere stroke compared to right. The most significant correlation between ischemic CBF volume and NIHSS occurs at a CBF level that would be classically-defined ischemic core.

ASSOCIATION OF TAU PROTEIN PATHWAYS AND DISRUPTED CORTICO-CEREBELLAR LOOPS IN AMNESTIC MILD COGNITIVE IMPAIRMENT

F. Bai[1], W. Liao[2], C. Yue[3], M. Pu[3], Y. Shi[1], H. Yu[3], Y. Yuan[1], L. Geng[3], Z. Zhang[1]

[1]Department of Neurology, Affiliated Zhongda Hospital of Southeast University, Nanjing, [2]Center for Cognition and Brain Disorders, Hangzhou Normal University, Hangzhou, [3]Department of Neurology, Medical School of Southeast University, Nanjing, China

Background: Tau hypothesis have been raised regarding pathophysiology of Alzheimer's disease (AD). However, little is known about test polymorphisms in multiple functionally-related genes for strengthening the confidence in imaging genetics associations and generating the tau protein pathways framework.

Methods: 43 aMCI and 30 healthy controls underwent resting-state functional magnetic resonance imaging, and tau protein pathways-based approach to investigate changes in the topological organization of the brain function in aMCI.

Results: Topologically convergent and divergent functional alterations patterns within multiple functionally-related genes, and disrupted cortico-cerebellar loops were associated with tau protein pathways-genes in aMCI patients. The associations of networks and behavioural significance implicated direct or indirect interactions were between tau protein pathways genes.

Conclusions: Tau pathway-based approaches could strengthen the confidence in imaging genetics associations and generate the pathway framework, which are potentially powerful for providing new insights into the neural mechanisms underlying of aMCI.

THE HUMAN PARAHIPPOCAMPAL REGION: II. PERIRHINAL CORTEX CYTOARCHITECTONIC AND MRI CORRELATION

X. Blaizot, F. Mansilla, A.M. Insausti, A. Salinas-Alaman, R. Insausti

Department of Health Sciences, School of Medicine, University of Castilla-La Mancha, Albacete, Spain

Introduction: The parahippocampal region, made of the perirhinal (PC), posterior parahippocampal and temporopolar cortices[1], plays a key role in learning, memory, spatial navigation, emotion, and social behavior. The general cytoarchitectonic features of the PC in humans were described by Brodmann's[2] Area 35 and 36. The PC is a key struture because of its location within the temporal lobe and its connexions with the neighbouring areas such as the posterior parahippocampal, and entorhinal cortices, the amygdala, hippocampus and temporal pole. The PC is particulary affected in Alzheimers'disease by the neurofibrillary tangles[3].

Objectives: We aim at providing a more precise delimitation of the human PC organization to determine with the highest possible accuracy its real extent in the human brain taking into consideration the variability in the sulcal pattern[4]. Description of the PC subfields and their corresponding extent within the PC, will be based mainly on their cytoarchitecture, but also with their spatial relationship to anatomical landmarks within the temporal lobe. These references would greatly facilitate the correlation with MR and other neuroimaging techniques. The data will also be compared to those observed in other nonhuman primate species (macaque and baboon) to explore the homology of the PC among these species.

Methods: The basic analysis has been performed from the brain of 9 healthy subjects. The brains were serially sectioned and stained with thionin to determine cytoarchitectonic boundaries. Two-dimensional maps of the size, extent and topological relationships of the parahippocampal gyrus were made. T1-weighted MR images obtained in healthy controls were also analyzed in reference to the neighboring anatomical landmarks. The volumetric segmentation of the PC, was performed in 24 additional control cases from the 3D-T1 weighted MR sequence on a computer from coronal images with the corresponding location on the axial and sagittal MR images on the same screen.

Results: Histologically, the PC is made up of two subareas, area 35 (agranular and with large and darkly stained neurons in layer V, with 3 subfields namely 35o, 35d, 35v for the olfactory, dorsal and ventral portions) and area 36 subdivided in 36r, more rostral, with clumps of neurons in layer II, and 36c, more caudal, more akin to neocortex. Compared to nonhuman primates, lamination is as little or less clear in humans. The PC represents 41.25% of the volume and 37.4% of the surface of the whole parahippocampal region, and its size is similar between both hemispheres.

Conclusions: This organization is quite similar but more complex (lamination and gyrification degree) to nonhuman primates. These observations suggest that the relative size and complexity of the PC may contribute to declarative memory development in humans.

The correlation between cytoarchitecture of the PC and MR images allows the delimitation of the subfields of the PC, which should be helpful in the interpretation of neurofunctional imaging such as fMRI or PET.

References:

[1]Scharfman et al. 2000, Ann N Y Acad, Sci. 911:ix—xiii

[2]Brodmann K. 1909.Leipzig (Germany): Barth.

[3]Arnold SE et al. 1991, Cereb Cortex. 1:103—116

[4]Ono et al. 1990. Stuttgart (NY): Georg Thieme verlag.

PROBABILISTIC MRI BRAIN ANATOMICAL ATLASES BASED ON 1,000 CHINESE SUBJECTS

N. Chen, K. Li, X. Wang

Radiology, Xuan Wu Hospital, Capital Medical University, Beijing, China

Brain atlases are designed to provide a standard reference coordinate system of the brain for neuroscience research. Existing

human brain atlases are widely used to provide anatomical references and information regarding structural characteristics of the brain. The majority of them,however, are derived from one paticipant or small samples of the Western population. This poses a limitation for scientific studies on Eastern subjects. A total of 1,000 Chinese volunteers ranging from 18 to 70 years old participated in this study. 10 new Chinese brain atlases for different ages and genders were constructed using MR anatomical images based on HAMMER (Hierarchical Attribute Matching Mechanism for Elastic Registration). There was a significant difference in brain volume between females and males in each group (18-30, 31-40, 41-50, 51-60 and 61-70 years) $p< 0.01$). Furthermore, volumetric brain parameters were larger in males than females, and an age-related decline in brain volume was observed. These population-specific brain atlases represent the basic structural characteristics of the Chinese population. Comparatively, the Chinese brain templates are generally smaller in length and height than the MNI template of the Western society, while the width/length ratio for the average Chinese brain is larger than the MNI brain template. They may be utilized for basic neuroscience studies and clinical diagnosis, including evaluation of neurological and neuropsychiatric disorders, in Chinese patients and those from other Eastern countries.

NEW IN VIVO APPROACH FOR IMAGING INTRACELLULAR NAD CONTENTS AND NAD^+/NADH REDOX STATE IN LIVING BRAINS

W. Chen, M. Lu, X.-H. Zhu

Center for Magnetic Resonance Research, Radiology Department, University of Minnesota, Minneapolis, MN, USA

Objectives: Nicotinamide adenine dinucleotide (NAD) plays vital roles in cellular energy metabolism and various biological processes. It exists in oxidized (NAD^+) or reduced (NADH) form; and their ratio reflects the intracellular redox state. The ability to study NAD and NAD^+/NADH redox state is essential for understanding the basis of cellular metabolism and regulation in health and disease[1-3]. However, noninvasive assessment of these parameters *in vivo* has never been successful in brains due to technical challenges. Here we report a novel *in vivo* ^{31}P MRS approach for quantitative and non-invasive imaging of intracellular NAD concentrations and NAD^+/NADH redox ratio (RX) in animal and human brains under physiopathological conditions.

Methods: A ^{31}P MRS-based quantification model was developed to describe and quantify the resonance signals of NAD^+, NADH and α-ATP at any given magnetic field strength. By least-square fitting of the model outputs to the resonance signals obtained from *in vivo* ^{31}P spectrum, signal intensity and linewidth of each phosphorus peak were determined. The cerebral contents of NAD^+ and NADH were quantified by normalizing their peak integrals to that of baseline α-ATP, which has a stable, known pool size of ~2.8 mM in normal brain[4]. Thus, the absolute concentrations of cerebral α-ATP, NADH, NAD^+, total NAD ($[NAD]_{total}=[NAD^+]+[NADH]$) and RX were obtained. Anesthetized cats and rats were scanned at 9.4 Tesla (T) or 16.4T. Healthy human volunteers were scanned at 7T. Localized *in vivo* ^{31}P MR spectra were acquired using either RF surface coil localization or chemical shift imaging.

Results: Figure 1 shows a typical localized ^{31}P MR spectrum of rat brain under physiological condition. Excellent sensitivity and spectral quality achievable at ultrahigh field ensured the reliable detection and quantification of the brain NAD signals *in vivo*. The total signals of α-ATP, NAD^+ and NADH determined by the model fitting matched well to the original ^{31}P signals with a very low residual, and the individual fitting components provided quantitative measures of the intracellular $[NAD^+]=0.36\pm0.02$mM (mean±std; n=6), $[NADH]=0.12\pm0.01$mM, $[NAD]_{total}=0.49\pm0.02$mM and $RX=3.1\pm0.5$ in the anesthetized rat brains, that are consistent with the literature reports based on the tissue extracts and chemical assay[5]. Similar values were found in the cat visual cortex; and were relatively lower in the visual cortex of healthy human subjects. The alterations of the NAD contents and redox states to the physiopathological perturbation in animals and age dependence in humans were also studied and observed.

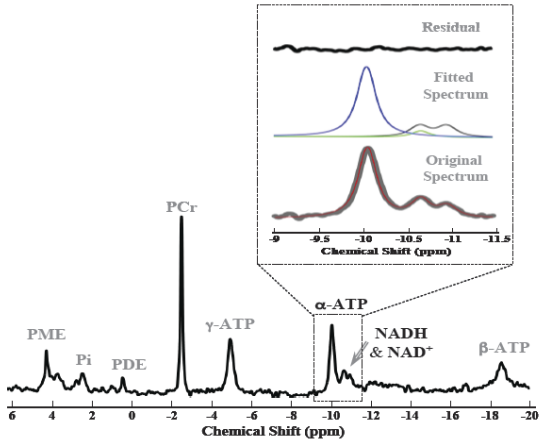

Figure 1. Localized *in vivo* ^{31}P MR spectrum of a representative rat brain measured at 16.4T with 9min acquisition. The inserts display the chemical shift range of -9 to -11.5ppm with the original ^{31}P signals (in gray color) and the total signals (red trace) of the α-ATP, NAD^+ and NADH determined by the model fitting. The individual fitting component of α-ATP (blue), NAD^+ (black), NADH (green) and the residual signal of the fitting are also displayed.

[Figure 1]

Conclusions: The results indicate that the new NAD imaging approach can provide reliable measures of cerebral NAD contents and redox state and is sensitive to the changes associated with normal aging and physiopathological alterations in brain energy and metabolism; thus, provides an invaluable tool for basic biomedical research and potential for clinical translation. Moreover, the same approach can be applied to other organs.

References:

[1] Siesjo, B. K. *Brain Energy Metabolism* (1978);

[2] Ying, W. *Antioxid Redox Signal* **10**,179-206 (2008);

[3] Belenky et al. *Trends Biochem Sci* **32**, 12-19 (2007);

[4] Du et al. *PNAS* **105**, 6409-6414 (2008);

[5] Klaidman et al. *Anal Biochem* **228**, 312-317 (1995).

HYPOINTENSIVE DEEP MEDULLARY VEINS CORRELATES WITH HYPOPERFUSION IN ISCHEMIC STROKE PATIENTS: A 3T SUSCEPTIBILITY-WEIGHTED IMAGING (SWI) STUDY

M. Lou, **Z. Chen**, H. Hu, Y. Lin, J. Wan, S. Yan, Z. Shi

Department of Neurology, The 2nd Affiliated Hospital of Zhejiang University, Hangzhou, China

Purpose: We hypothesize that the hypointensive deep medullary veins on susceptibility weighted imaging (SWI) may be related to the hypoxic status after acute ischemic stroke. We thus investigated the relationship between hypointensive deep medullary veins and hypoperfusion after acute ischemic stroke.

Methods: We retrospectively analyzed our prospectively collected thrombolytic data from Aug 1, 2009 to Jul 31, 2012. A total of 197 patients received intravenous rtPA therapy during this period. Thirty-six anterior circulation acute stroke patients were included, who had complete baseline and 24 hour follow-up multi-model MRI image. We defined asymmetry index (AI) of deep medullary veins as a ratio of voxel numbers between the ipsilateral and contralateral hemispheres. We compared the correlation between baseline variables and AI. Multiple linear regression was then used to determine the independent factors for the AI score. We also investigated the change of AI (ΔAI) between baseline and 24 hour after intravenous rtPA therapy in patients with or without recanalization/reperfusion.

Results: AI was significantly correlated with both DWI lesion volume (r_s = 0.358, P=0.032) and PWI lesion volume (r_s = 0.557, P=0.000). Multiple linear regression analysis showed that PWI lesion volume was the only independent factor for Box Cox transformed (λ= -1) AI (F = 4.060; P=0.004). Both absolute and relative ΔAI were higher in patients with recanalization (absolute ΔAI: P=0.000; relative ΔAI: P=0.000) and reperfusion (absolute ΔAI: P=0.002; relative ΔAI: P=0.005) than those without recanalization or reperfusion.

Conclusion: Higher AI score on SWI are associated with severer hypoperfusion, which indicates that the hypointensive deep medullay

veins may reflect the hypoxic status following hypoperfusion.

MOLECULAR IMAGING OF SELECTIN EXPRESSION AFTER STROKE

T. Farr[1], D. Grünstein[2], C.-H. Lai[2], A. Barandov[2], C.-C. Wang[2], G. Laettig[1], P.H. Seeberger[2], C. Harms[1]

[1]Department of Experimental Neurology, Center for Stroke Research Berlin (CSB), Charité University Medicine, [2]Department of Biomolecular Systems, Max-Planck Institute of Colloids and Interfaces, Berlin, Germany

Objectives: Molecular imaging of specific targets in the intact and diseased brain is of high interest but is also inherently challenging as direct access to the brain is inhibited by the blood brain barrier. As such, vascular components represent attractive targets. Increases in selection expression after brain injury were observed with magnetic resonance imaging (MRI) using glyconanoparticles that were coated with carbohydrate ligands specific to selectins (van Kasteren, *et al*., 2009. PNAS. 106: 18-23). The purpose of the present study was to examine the potential of similar particles in the stroke brain.

Methods: Magnetic nanoparticles (MNPs) were constructed by coating magnetite with silica and rendering them neutral for *in vivo* administration. Sub-populations of particles were then covalently bound to sugar moieties that contain either ligands with no known targets (MNPs + L^X) or the ligand sialyl $Lewis^X$ (MNPs + sLe^X) which targets E and P selectin. Male C57/BL6 mice (n=18) received 60min of middle cerebral artery occlusion (MCAO) and 4hrs later randomly received one of the 3 types of MNPs (n=6, each) i.v. (1000µmol Fe/kg) while inside the magnet. T_1, T_2, and T_2* weighted images were acquired at 4 and 24hrs post MCAO. Organs and brains were processed for immunohistochemistry and Prussian blue staining (for iron).

Results: All of the iron formulations exhibited a strong blood pool effect immediately after injection and 24hrs later the brains contained many small punctuate regions of signal loss. There were no differences between groups in overall brain signal to noise ratios (SNRs), and no differences in SNRs between the infarcted volumes when compared to the mirrored region in the intact hemisphere. To account for partial volume effects, the number of dark voxels in each volume of interest was measured. A greater number of dark voxels were present in the infarcted volumes of all groups when compared to the mirrored region in the intact hemisphere (MNP: 237.5 ± 109.7 vs 142.9 ± 76; MNPs + L^X: 95.3 ± 81.7 vs 46.5 ± 32.3; MNPs + sLe^X: 246.1 ± 95 vs 122 ± 35). The greatest effect was in the MNPs + sLe^X treated animals, though this failed to reach statistical significance on account of the high degree of variability. Interestingly, in 3 of the 5 mice that received naked MNPs, there was a large spot of iron accumulation.

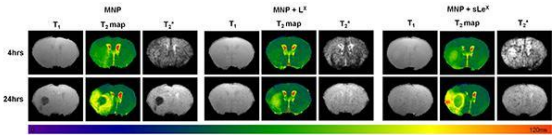

Figure 1. T_1-weighted images, T_2 maps, and T_2*-weighted images from an animal in each of the groups at 4 and 24hrs post MCAO. Note: the blood pool effect of the iron formulations directly after injection and the punctuate regions over the entire brain 24hrs later.

Conclusions: These preliminary results indicate that, when compared to the appropriate control conditions, functionalized MNPs may not work as well as previously reported. Ongoing work aims to establish specificity of the MNPs to the target and determine under which conditions molecular imaging can be most useful.

NEUROIMAGING AND BEHAVIOURUAL CHARACTERIZATION OF A MOUSE MODEL OF VASCULAR COGNITIVE IMPAIRMENT

T.D. Farr[1], M.P. Brinckmann[1], M. Foddis[1], A. Kunz[1], C. Po[2], U. Dirnagl[1], M. Füchtemeier[1]

[1]Department of Experimental Neurology, Center for Stroke Research Berlin (CSB), Charité University Medicine, Berlin, Germany, [2]Imagerie par Résonance Magnétique Médicale et Multi-Modalités, Université Paris-Sud, Orsay, France

Background and aims: Vascular cognitive impairment (VCI) is a group of cognitive disorders that share a vascular origin. Despite its prevalence in the clinic, little attention has been given to small vessel disease in preclinical research. Chronic hypoperfusion to the brain was proposed as a mouse model of VCI (Shibata, *et al*., 2004, Stroke. 35: 2598-

03) and studies have reported spatial and working memory impairments, hippocampal atrophy and white matter damage in these mice (Reimer, *et al*., 2011. JNeurosci. 31: 18185-94; Yoshizaka, *et al*., 2008. ExpNeurol.210: 585-91). Our group is currently working to characterize this model using multimodal imaging, a battery of behavioral tests and histology. Preliminary results are presented here.

Methods: Chronic hypoperfusion (or sham (n=10 each)), was induced by wrapping microcoils (180µm diameter) around both carotid arteries in male C57/BL6 mice. Mice performed the pole test one week before and at 7 and 14d after the surgical procedure. At 21d, animals were trained for a week in a standard hidden platform (place) task in the Morris water maze with probe trial on the final day. At this time, magnetic resonance imaging (T_2-weighted and time-of-flight angiography sequences) was performed in most of the mice and tissue harvested for histological analysis. Cerebral blood flow (CBF) was monitored continuously in a subgroup of microcoil mice (n=8) using arterial spin labeling.

Results: Microcoil mice did not display sensorimotor impairments in the pole test or learning deficits in the water maze, though they spent significantly less time in the target quadrant compared to shams in the probe trial ($t(18)= -3.018$, $p=0.007$). There was a significant increase in T_2 in the corpus callosum of microcoil animals (53ms ± 4.1) when compared to shams (49ms ± 0.8; $t(7.8)= -2.332$, $p=0.04$) and a trend towards the same response was observed in the striatum. There was some variability in water maze performance and T_2 values in the microcoil group, which could be explained by the fact that only half of the mice exhibited a substantial decrease in CBF following microcoil implantation. Some of the microcoil mice exhibited evidence of vascular remodeling in angiography, such as dilation and growth of the Circle of Willis and other major cerebral vessels. Detailed analysis is currently pending. No micro-infarctions or overt evidence of neuronal pathology was observed in the tissue sections, though a few of the microcoil animals exhibited white matter degeneration (Luxol blue staining) and reactive gliosis (GFAP) in the striatum.

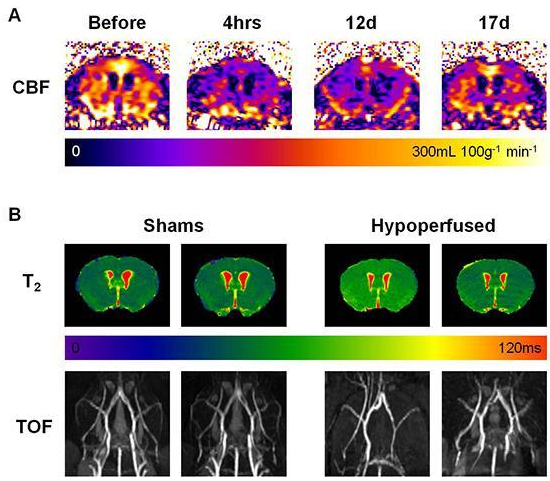

[

Figure 1. A: A timecourse of CBF maps from a mouse before and at 4hrs, 12 and 17d after microcoil implantation. B: T_2 maps and angiography projections from two sham and hypoperfused mice at 4 weeks after microcoil implantation.

Conclusions: These preliminary results indicate that this model might be more variable than previously reported. Ongoing work aims to establish selection criteria for model success at different timepoints, and to gain mechanistic insight into the observed pathology.

DWI STUDY REVEALS VERY-DELAYED CYTOTOXIC EDEMA IN THE PULVINAR AND MEDIAL NUCLEI OF THALAMI IN HUMAN BRAINS AFTER HYPOGLYCEMIC COMA

M. Fujioka[1,2], S. Suzuki[3], K. Okuchi[4], Y. Tada[4], T. Watanabe[4], T. Seki[4], T. Taoka[5], Y. Kitazawa[3]

[1]Neuroscience Unit, Emergency and Critical Care Medical CTR, Nara Medical University, Kashihara, [2]Neurosurgery, Osaka Saiseikai Ibaraki General Hospital, Ibaraki, [3]Emergency and Critical Care Medical CTR, Kansai Medical University, Hirakata, [4]Emergency and Critical Care Medical CTR, [5]Radiology, Nara Medical University, Kashihara, Japan

Background: Experimental studies have shown that profound hypoglycemia induces a purely neuronal lesion of the neocortex (layers 2 and 3), the hippocampus (CA1 region and dentate gyrus), and dorsolateral crescent of the caudoputamen in rat brains in the acute stage. Our MRI study in humans indicated that

hypoglycemic coma produces slowly-progressive neuronal death and glial proliferation (astrocyte and microglia) with paramagnetic effect (Ann Neurol 2003;54:732-47) in the striatum, neocortex, hippocampus, and/or substantia nigra, but not in the thalamus (Stroke 1997;28:584-87). These studies have shown a particular resistance of the thalamus against hypoglycemic injury. Here we investigated if diffusion-weighted (DW) MRI can depict a specific change with time in the thalamus of humans after hypoglycemic coma.

Methods: We repeatedly studied MRI in three adult patients in a vegetative state for two months after profound hypoglycemia.

Results: In all patients, serial MR images revealed symmetrical lesions of hyperintensity and hypointensity on T1- and T2-weighted images, respectively, in the striatum, neocortex, and/or hippocampus from 17 days after onset, but not in the thalamus. In these patients, DWI in the early stage showed hyperintensity in the neocortex and basal ganglia except for thalamus. However, with the DWI hyperintensity in these areas subsiding over time, the pulvinar and medial nuclei of thalami bilaterally appeared bright on DWI study from one month after the severe hypoglycemic stress.

Conclusion: The thalamic lesion after hypoglycemia may represent a delayed cytotoxic edema caused by secondary remote effects from the neocortex/striatum via axonal and/or transsynaptic mechanisms.

EVALUATING NEURODEGENERATIVE DISEASE WITH ASL PERFUSION: COMPARISON WITH FDG-PET

S.H. Fung[1,2], C. Karmonik[2,3], M.F. Dulay[2,3], B. Pascual[2,4], D.Y. Lee[1,2], S.B. Chiang[1,2], R.E. Fisher[1,5], R.G. Grossman[2,3], B.M. Spann[2,4], G.C. Roman[2,4]

[1]Radiology, The Methodist Hospital, Houston, TX, [2]Weill Cornell Medical College, New York, NY, [3]Neurosurgery, [4]Neurology, The Methodist Hospital, [5]Baylor College of Medicine, Houston, TX, USA

Purpose: To compare regional and voxel-level cerebral blood flow (CBF) estimated from arterial spin labeling (ASL) to 18F-fluorodeoxyglucose (FDG) activity from positron emission tomography (PET) in elderly patients evaluated for neurodegenerative disease.

Methods: Twenty-four patients (ages 62-84, M:F 1.2) evaluated for cognitive impairment (including MCI, AD, FTD, DLB, PPA, NPH, vascular and mixed dementia) had brain MRI and FDG-PET within 24 hours. Brain MRI was performed on a 3.0 T clinical scanner with CBF (mL/min/100g) estimated using pseudo-continuous ASL (pCASL) with post-labeling delay of 2.5 s. ASL was acquired twice during the 20 min MRI session, once in the beginning and again in the end of the imaging session, to determine test-retest reproducibility of ASL. A subset of patients were instructed to keep eyes open and then closed during the initial and repeat ASL scan, respectively, to test perfusion variability in the visual cortex. High-resolution anatomical images were also obtained using SPGR for registration of CBF maps and PET images. Brain FDG-PET was performed on a clinical PET/CT scanner 0.75-1.5 hours after intravenous injection of 7.3-11.3 mCi FDG. Standard uptake value (SUV) maps were generated from CT attenuation-corrected PET images. FSL was used for image registration, gray matter (GM)/white matter (WM) segmentation, and image analysis. Overall visual inspection, regional and voxel-level comparison, and histogram analysis were performed.

Results: CBF maps from ASL were noisier and less visually pleasing to interpret than FDG-PET images. With the exception of the occipital lobe, regional hypoperfusion on ASL correlated with regional hypometabolism on PET with good voxel-level CBF-SUV correlation in intrasubject comparisons. With the exception of the occipital lobe, regional comparison of normalized cortical CBF to normalized cortical SUV also correlated well in intersubject comparisons. In all subjects, FDG activity was consistently highest in the occipital lobes (visual cortex), whereas occipital perfusion on ASL was more variable. Test-retest ASL data showed good voxel-level reproducibility in all cortical regions, including the occipital lobe with no significant difference in visual cortical perfusion between eyes open and closed states within limits of test-retest variance. Histogram analysis demonstrated unimodal distribution of whole brain CBF in contrast to bimodal distribution of whole brain SUV, consistent with smaller mean difference and larger variance of GM and WM CBF relative to that of SUV.

Conclusion: In most cases, hypoperfusion

pattern on ASL correlates well with hypometabolism pattern on FDG-PET and can be used to distinguish various neurodegenerative diseases. Given ease and repeatability of ASL acquisitions, ASL-MRI should be considered an additional imaging technique for evaluating neurodegenerative diseases. One caveat is the relatively poor correlation between ASL and FDG-PET in the occipital lobe, which may be secondary to decreased arterial spin labeling efficiency in the posterior circulation versus physiologic causes but does not appear to correlate with eyes open/closed state. Caution should be made with interpreting occipital hypoperfusion with ASL, especially when considering DLB, which can have both hypoperfusion and hypometabolism in the occipital lobe. In such cases, occipital hypoperfusion on ASL should be confirmed with corresponding hypometabolism on FDG-PET.

THE HUMAN HIPPOCAMPUS AND AMYGDALA: PROBABILISTIC ATLASES IN A STEREOTAXIC SPACE, AND QUANTITATIVE COMPARISON OF SPATIAL NORMALIZATION STRATEGIES

C. Vial[1,2,3], M. Belgacem[1,2,3], R.A. Heckemann[2,4], J.A. Yankam Njiwa[2], R. Allom[4], C.-H. Chen[4], N. Costes[1], **A. Hammers**[2,4,5]

[1]CERMEP - Imagerie du Vivant, [2]Functional Neuroimaging, Neurodis Foundation, [3]Ecole Polytechnique Universitaire - ISTIL, Lyon 1 University, Lyon, France, [4]Division of Brain Sciences, Imperial College London, [5]Department of Clinical and Experimental Epilepsy, University College London, London, UK

Background: It is often necessary to determine whether a neuroimaging result belongs to a given structure in standard (stereotaxic, Montreal Neurological Institute (MNI)) space. There are no probabilistic maps for the hippocampus (HC) or amygdala (Am), two important structures of the limbic system.

Various spatial normalisation methods exist for registration of an image from its native (acquisition) space to MNI space. Few quantitative data exist to compare these strategies.

Materials and methods: *Participants:* 30 healthy subjects, with normal MRI scans, from the database of the Epilepsy Society MRI unit (University College London, UK); 15 women; median age 30 years. HC and Am have been manually delineated following published protocols.[1,2]

Spatial normalisation: HC and Am were extracted from the original atlases. Three spatial normalisation strategies were tested within the Statistical Parametric Mapping software (SPM8; www.fil.ion.ucl.ac.uk/spm), all based on registration of the MRI associated with each of the 30 atlases:

1) standard spatial normalisation (NORM).

2) "Unified normalisation" combining tissue classification, bias correction, and spatial normalisation (UNIF).[3]

3) Diffeomorphic normalisation with a large number (~6.4M) of degrees of freedom (DARTEL).[4]

All HC and Am in MNI space were averaged to obtain probability maps with values between zero and one. Centres of gravity were determined. To evaluate spatial normalisation strategies, each probabilistic atlas (HC and Am, respectively) was thresholded at 6% (i.e. all voxels in MNI space labelled as the structure based on at least two subjects) and 100% (all voxels labelled as the structure based on all subjects). The smaller the 6%/100% ratio, the more effective the spatial normalisation strategy has been.

Results: Probabilistic maps for HC and Am have been created. An example for each structure, created via the DARTEL method, is shown in Figures 1 and 2. The centres of gravity were significantly more anterior on the right, by 1.4-1.5mm.

In the comparison of spatial normalisations, DARTEL had the smallest 6%/100% ratio, followed by UNIF and NORM (HC: 10/17/32; Am: 7/10/28).

Conclusion: Our results provide further evidence for using the DARTEL method.[5] The probabilistic maps will be useful for the localisation of results from group analyses in neuroimaging studies of memory, neurodegeneration, epilepsy, and emotion.

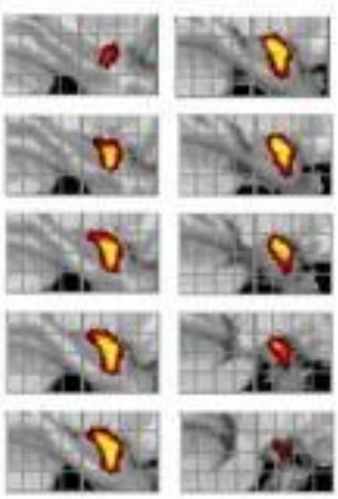

Figure 1: Probabilistic maps, right Am (sagittal slices, MNI space). Slices shown every 2mm from x=+58mm (top left) to x=+77. Note contour of frontal cleft of temporal horn (Klingler J 1948).

Figure 2: Probabilistic maps of HC (coronal slices, MNI space). Slices shown every 3-5mm from y=+97mm (top) to y=+120mm. Note extension more anteriorly on right (image #6, bottom) and more posteriorly on left (#1). High resolution showing vertical digitation[1] (#4, 5) and intralimbic gyrus (#3, 4).

References:

(1) Niemann K, Hammers A et al., Psych Res Neuroimaging 2000,

(2) Hammers A, Allom R et al., Hum Brain Mapping 2003,

(3) Ashburner J and Friston K, Neuroimage 2005,

(4) Ashburner J, Neuroimage 2007,

(5) Klein A et al., Neuroimage 2009

EARLY CHANGE IN FERUMOXYTOL-ENHANCED MAGNETIC RESONANCE IMAGING SIGNAL SUGGESTS UNSTABLE HUMAN CEREBRAL ANEURYSM. A PILOT STUDY

D. Hasan

University of Iowa, Iowa City, IA, USA

Background: Imaging with magnetic resonance imaging (MRI) 72 hours after infusion of ferumoxytol demonstrated maximal uptake by macrophages in the wall of human cerebral aneurysms. The clinical significance of early (i.e. within the first 24 hours) uptake of ferumoxytol by macrophages in the wall of human cerebral aneurysms is not clear. The purpose of this study was to determine whether early uptake of ferumoxytol, which may indicate inflammation, suggests unstable cerebral aneurysm.

Methods: 30 unruptured aneurysms in 22 patients were imaged with MRI 24 hours after infusion of ferumoxytol. Eighteen aneurysms were also imaged 72 hours after infusion of ferumoxytol. Aneurysm dome tissue was collected from four patients with early MRI signal changes, five patients with late signal changes, and five other patients with ruptured aneurysms. The tissue was immunostained for expression of cyclooxygenase-1 (COX-1), cyclooxygenase-2 (COX-2), microsomal-prostaglandin-E2 synthase-1 (mPGES-1) and macrophages.

Findings: In 23% (7/30) of aneurysms, there was pronounced early uptake of ferumoxytol. Four aneurysms were clipped. The remaining three aneurysms which were managed conservatively with observation, all ruptured within six months. In 53% (16/30) of aneurysms, there was pronounced uptake of ferumoxytol at 72 hours. Eight aneurysms

were surgically clipped and eight were managed conservatively; none ruptured or increased in size in six months. With immunostaining, expression of COX-2, mPGES-1, and macrophages was similar in unruptured aneurysms with early uptake of ferumoxytol and ruptured aneurysms. Expression of these inflammatory molecules was significantly higher in aneurysms with early uptake of ferumoxytol than in aneurysms with late uptake.

Interpretation: Unstable aneurysms, suggested by early uptake of ferumoxytol in aneurysm walls (within the first 24 hours) and inflammation, are generally large and warrant early intervention. Larger clinical studies are indicated to validate this preliminary observation.

EFFECTS OF ARTERY INPUT FUNCTION ON (K^{TRANS}) AND (V_E) OF DYNAMIC CONTRAST ENHANCED MRI FOR DETERMINING GRADES OF GLIOMAS

B. Hou[1], N. Zhang[2], J.S. Carpenter[1]

[1]Radiology, WVU, Morgantown, WV, USA, [2]Paul C. Lauterbur Research Center for Biomedical Imaging, Institute of Biomedical and Health Engineering, Shenzhen, China

Introduction: In this study, we compared the values of K^{trans} and V_e obtained by using different AIFs in four grades of gliomas (determined by biopsy) for evaluating impacts of the AIFs on grading the tumors.

Material and methods: 28 patients with histologically confirmed gliomas were examined using a 1.5 T MRI scanner. Histopathologically 14 of the 28 gliomas were low grades (8 grade I and 6 grade II) and 14 high grades (6 grade III and 8grade IV). AIFs from ACA, MCA, and PCA were respectively derived from the time courses of the DCE scans. K^{trans} and V_e were calculated from a modified model with the AIFs, and were compared using Two Related Samples Tests (TRST) and Mann-Whitney U-test in the low and high grades with a value of $P< 0.05$ regarded as statistically significant.

Results: Individual AIFs of ACA, MCA, and PCA of a patient with representative grade I glioma were plotted in Figure 1. In Figure 2, mean values of K^{trans} and V_e corresponding to the AIFs were respectively plotted against the four grades. K^{trans} and V_e increased with the increase of histological grades from I to IV. P values of TRST for comparing K^{trans} and V_e between any two AIFs in the low or high grade were summarized in Table 1. P values of Mann-Whitney U-test for the K^{trans} and Ve derived from the AIFs of ACA, MCA, and PCA in the low vs high grades and grade II vs III groups were listed in Table 2. Specificity and Sensitivity of the K^{trans} and V_e to differentiate the low with high grade gliomas were calculated and the corresponding ROC curves were drawn in Figure 3. The areas under the ROC curves of the AIFs of ACA, MCA, and PCA for K^{trans} and $V_{e,}$ were 0.983, 0.983, and 0.942, and 0.908, 0.942, and 0.892, respectively.

Discussion: The peak height (PH) value of an AIF was lower for PCA than for AMA and MCA (Figure 1), resulting in the higher values of K^{trans} and V_e derived from PCA than the ones from ACA and MCA in all histological grades (Figure 2), and the difference was statistical significance (Table 1). This may result from partial volume effect (PVE) for which reduces the accuracy of generating the AIF from the PCA. Whether existed difference of values of these two tracer kinetic parameters among the AIFs of ACA, MCA, and PCA, they all increase with the histological grades from I to IV (Figure 2), and can be applied to distinguish the low from high grades (Table 2, $p< 0.05$) with high sensitivity and specificity (Figure 3). The ROC curves (Figure 3) indicated that K^{trans} of ACA and MCA were better indicators to distinguish the low from high grades since they had a better sensitivity and specificity. However, for distinguishing grade II with III, the data in the Table 2 suggest that only K^{trans} derived from the AIF of MCA has a p value less than 0.05.

FMRI OF GLUCOSE INGESTION

C. Huerta, J. Li, T. Duong

UTHSCSA, San Antonio, TX, USA

Objectives: Dysfunction of neural circuitries controlling food intake has been implicated in eating disorders. The majority of studies to date used fMRI of visual food cues to map neural circuitries involved in satiety. This approach maps many cognitive components of satiety regulation but not the physiological effects of food ingestion. Few have investigated the satiety circuitry associated with food ingestion per se and most of these studies reported changes only in the hypothalamus. The goal of this study was to

use fMRI to investigate the neural networks responding to ingestion of a glucose solution while the subjects were in the MRI scanner.

Methods: Healthy lean subjects (4 M, 3 F, 20-35 yo, BMI = 18-25 kg/m^2) fasted overnight (8 hours). None of the subjects were on any diet program or recently lost weight. Whole-brain fMRI was acquired using EPI at 3T with TR = 3000ms, TE = 30 ms, 1.7 x 1.7 mm, 5-mm sagittal slices. The total scan lasted 65 mins with an initial 10-min period of baseline of pre-glucose ingestion acquisition, followed by 55 mins of post-glucose ingestion acquisition. Subjects ingested a standard glucola solution (75 g of glucose, 296 ml) in a self-pace manner over 4.5 ± 0.75 min via a peroral rubber tube. Blood glucose were measured every 10 min. Correlation analysis of the fMRI signals with blood glucose temporal profile was performed using the FSL software (FEAT tool).

Results: The basal blood glucose was 90 ± 10 mg/dL. The mean blood glucose started to elevate 15 mins after glucose ingestion, peaked 30 mins after glucose ingestion, and remained elevated during the entire fMRI study. The temporal profile of blood glucose peaking about 30 mins post glucose ingestion is consistent with previous findings[1]. The activated brain structures that showed correlation with blood glucose measurements were: the hypothalamus, caudate, orbitofrontal cortex (BA 47), medial frontal gyrus (BA 6), cerebellum, thalamus, cingulate gyrus (BA 31), precuneus (BA 7) and insula (BA 13).

Conclusion: Hypothalamus, implicated in food intake, was activated, in agreement with previous fMRI studies of glucose ingestion[2,3]. However, these studies did not report other activated structures. By contrast, we detected activated structures in the reward circuitries, including caudate[4], orbitofrontal cortex, Insula, cingulate gyrus, medial frontal gyrus, cerebellum and thalamus. In conclusion, we found glucose ingestion evoked a large neural network that regulates satiety. This approach offers a reliable method to study neural circuitries involving food intake. Future studies will examine subjects with eating disorders and correlate with temporal profiles of other blood markers (such as c-peptide) and behavioral data of satiety.

References:

(1) Tschrtter et al. 2003.

(2) Vidardottiret al. 2007.

(3) Liu Y et al. 2000.

(4) Alexander G.E. et al. 1990.

(5) Nioche et al. 2000.

(6) Dreher et al 2012.

(7) Small et al. 2010.

DIFFERENTIAL FMRI RESPONSES TO VISUAL FOOD CUES BETWEEN LEAN AND OBESE SUBJECTS

C. Huerta, P. Sarkar, T. Duong

UTHSCSA, San Antonio, TX, USA

Objectives: Obesity is at an epidemic proportion, affecting one-third of American adults and 17% of American children. Obesity increases the risk of cardiovascular diseases, such as stroke and heart diseases, cancer and diabetes regardless of race and gender. To better understand how the brain responds to food intake, we used fMRI to probe the neural responses to visual food cues in obese and lean subjects during “fasted” and “satiated” state.

Methods: BOLD fMRI at 3T was performed on ten lean subjects (5M and 5F, 20-41yo, BMI=22.1±2.1kg/m2, fasting glucose level=82±8mg/dL) and the obese subjects (5M and 5F, 22-47yo, BMI=31.3±1.6kg/m^2, fasting glucose level= 91.4±11.8mg/dL). Each fMRI trial consisted of participants viewing high-caloric content food versus non-food pictures over 15 mins. fMRI was performed in the fasted state. The subjects were then asked to drink a standard glucola solution (75g glucose in 296 ml) via a peroral tube over 5 min while in the scanner. The second fMRI trial was repeated starting after glucola ingestion.

Results: Obese relative to lean displayed increases reactivity in orbitofrontal cortex (BA 47), precuneus (BA 18), fusiform gyrus (BA 19) and inferior frontal gyrus (BA 46), but reduced activity in caudate, precuneus (BA 7), lentiform nucleus, thalamus, parahippocampus and precentral gyrus (BA 2 and 6) in the fasted condition. Obese showed increased reactivity in precuneus (BA 31), superior temporal gyrus (BA 22), inferior parietal lobe (BA 40) and orbitofrontal cortex (BA 47) but reduced

activity in the precuneus (BA 7), lentiform nucleus, parahippocampus and cerebellum in the satiated condition.

Conclusion: Obese subjects exhibited increased reactivity in orbitofrontal cortex, fusiform gyrus and inferior frontal gyrus compared to lean in the fasting sate. Except for the inferior frontal gyrus, these structures belong to the motivation component of food intake regulation. Fusiform gyrus is part of the secondary visual cortex and it has been implicated in attention tasks. This finding suggests that obese are more attentive to food cues in comparison with lean subjects. Orbitofrontal cortex is responsible for reward value assessment and reward error prediction[1]. Activation of this area has been reported to correlate positively with individual's subjective ratings of pleasantness of food, suggesting that highly palatable foods cause a stronger response in obese compared to lean[2]. Obese subjects exhibited increased reactivity in orbitofrontal cortex, superior temporal gyrus and inferior parietal lobe compared to lean in the satiated condition. Our findings showed that the orbitofrontal cortex activation did not decrease after eating. These findings suggest there are strong neural correlates, particularly of the reward/craving circuitry, in patients with eating disorders.

References:

(1) Drehet et al. 2012.
(2) Martin et al. 2010.
(3) Karhumen et al. 1997.
(4) Fisher et al. 2006.
(5) Smeets et al. 2006.

FEASIBILITY OF USING PULSED CONTINUOUS ARTERIAL SPIN LABELING TECHNIQUE FOR QUANTITATIVE EVALUATION OF CEREBRAL BLOOD FLOW

M. Isozaki[1], H. Okazawa[2], A. Tada[1], S. Yamada[1], H. Arai[1], H. Takeuchi[1], H. Kimura[3], K. Kikuta[1]

[1]Department of Neurosurgery, Faculty of Medical Sciences, University of Fukui, [2]Biomedical Imaging Research Center, University of Fukui, [3]Department of Radiology, Faculty of Medical Sciences, University of Fukui, Fukui, Japan

Objectives: In recent years, arterial spin labeling (ASL) magnetic resonance imaging, a non-isotopic technique, has been introduced as a noninvasive technique to evaluate cerebral hemodynamics. Recent reports suggested that modified ASL techniques were useful for quantitative measurement of cerebral blood flow (CBF). This study aimed to investigate the accuracy of pulsed continuous ASL (PCASL) technique for quantitative evaluation of CBF in comparison with N-isopropyl-p-[^{123}I]iodoamphetamine (^{123}I-IMP) single- photon emission computed tomography (SPECT).

Methods: Between February 2010 and September 2012, 14 patients with internal carotid artery (ICA) stenosis (>50%) were admitted to our hospital for carotid endarterectomy. Among these patients, 9 patients (all men; age, 69 ± 8 y), who had undergone both PCASL and ^{123}I-IMP SPECT were included in this study. Regional values obtained from the parametric images of all patients were determined using multiple regions of interest (ROIs) placed on the cortical territories of the bilateral cerebral and cerebellar hemisphere. The post-labeling delay time (PLD), during which blood flows from the tagged region into the ROIs, was set to 1.5 seconds. We analyzed the correlation between the quantitative CBF values obtained using PCASL and ^{123}I-IMP SPECT. The asymmetry index (AI) was also calculated for PCASL and ^{123}I-IMP SPECT.

Results: The mean quantitative global CBF values of PCASL and ^{123}I-IMP SPECT were 31.7 ± 6.14 and 50.0 ± 16.5, respectively. Although PCASL overestimated regional CBF values, there was significant correlation between the quantitative CBF values obtained using PCASL and ^{123}I-IMP SPECT in all ROI plots ($r = 0.52$, $y = 1.4x + 6.0$). The mean CBF-AI values of PCASL and ^{123}I-IMP were 1.43±1.15 and 1.10±1.07, respectively. The correlation of AI values showed better ($r = 0.75$, $y = 1.4x - 0.4$) than that of quantitative CBF values.

Conclusion: A good correlation was observed between the CBF-AI values measured using the PCASL technique and those measured using ^{123}I-IMP SPECT. The PCASL technique was reflected distribution of regional CBF in the hemisphere, although previous study reported that the quantitative accuracy of the PCASL technique depends on the vascular territories, such as the anterior or posterior circulation. Therefore, it is important to note this point when quantitative PCASL evaluation

of CBF values is performed in patients with ICA stenosis.

Reference:

[1] Deqiang Qiu et al. J. Magn. Reson. Imaging 2012; 36: 110-119.

[2] Hanna Järnum et al. Neuroradiology 2010; 52: 307-317.

[3] Peter Jan van Laar et al. Radiology 2008; 246: 2: February.

DETECTION OF EARLY WHITE MATTER REORGANIZATION USING MRI Q-SPACE DTI

Q. Jiang[1,2,3], G. Ding[1], S. Pourabdollah Nejad D.[1], C. Qu[4], A. Mahmood[4], L. Li[1], Q. Li[1], M. Chopp[1,2]

[1]Neurology, Henry Ford Health System, Detroit, [2]Physics, Oakland University, Rochester Hills, [3]Neurology, Wayne State University, [4]Neurosurgery, Henry Ford Health System, Detroit, MI, USA

Introduction: Cell-based treatment of traumatic brain injury (TBI) promotes white matter (WM) reorganization and functional recovery. However, dynamic monitoring of treatment induced WM reorganization is a challenge. In the current study, we evaluated the effects of cell-based treatment of TBI on WM reorganization using MRI. We demonstrate that fractional anisotropy (FA) and fiber tracking from conventional Gaussian DTI can correctly identify white matter reorganization in the brain tissue with a preponderance of single oriented axons after TBI. However, Q-space DTI, such as standard deviation (SD)[1], Kurtosis and q-ball need to be employed to detect WM reorganization if fiber crossing is present in the recovery tissue.

Materials and methods: Male Wistar rats (n=17) were treated either with superparamagnetic particle labeled bone marrow stromal cell (MSC) or with saline after TBI. MRI measurements T_1, T_2, FA, fiber orientation, q-ball, apparent kurtosis coefficient (AKC), and SD were performed two days, and weekly for 6 consecutive weeks after TBI. To detect white matter reorganization, brain sections were stained using Bielshowsky and Luxol fast blue immunoreactive staining.

Results: The labeled MSCs selectively migrated toward injured boundary regions where white matter reorganization was detected on MRI and immunoreactive staining. Cell-based treatment promotes WM reorganization, confirmed by an increase in axons and myelination, which reflected elevated FA ($p< 0.01$ at 6 weeks) in the TBI recovery region, decreased T_2 ($p< 0.01$ at 2, 3, and $p< 0.05$ at 4, 6 weeks) in TBI core, and improved functional recovery ($p< 0.05$, ≥ 2 weeks) compared with untreated animals after TBI. WM reorganization after cell-based treatment of TBI is predominantly located in the extended area of the corpus callosum. The fiber tracking map revealed reorganized connections between white matter reorganized regions separated by the TBI lesion. Although conventional Gaussian DTI exhibited promising results in detecting WM reorganization in the recovery regions where the fiber orientation map exhibited more single oriented axons than crossing axons, FA did not detect the increase in axons in the TBI lesion boundary where axon crossing was detected by the q-ball orientation map. In contrast with FA, the SD and AKC maps exhibited increased SD and AKC in the WM remodeling region with more crossing axons, which is consistent with histological confirmation of increased axonal density.

Discussion: Our data suggests that MRI can detect white matter reorganization, reconnection, and labeled cell migration and distribution after cell-based treatment of TBI. Although FA shows promise in differentiating white matter reorganized brain tissue from other TBI damaged tissues, FA does provide error information if crossing axons are predominant in the white matter reorganized region. Since crossing axons are dominant during the early stage of WM reorganization, our data suggest that we may provide information about the stage of white matter remodeling in the injured brain, with increased SD or AFC alone (without FA elevation) representing an early recovery stage with more crossing axons, while the increased FA identifies more mature linear axons.

References:

1. Jiang Q, et al. PlosONE, 2012, 7:e42845

QUANTITATIVE ASSESSMENT OF CEREBRAL BLOOD VOLUME AND FLOW FROM BRAIN PERFUSION MR IMAGES WITH THE REMOVAL OF VESSEL VOXELS

Y.-H. Kao[1], M.M.H. Teng[2,3], I.-C. Cho[1], F.-Y. Chiu[1], F.-C. Chang[3]

[1]Biomedical Imaging and Radiological Sciences, Yang-Ming University, [2]School of Medicine, National Yang Ming University, [3]Department of Radiology, Taipei Veterans General Hospital, Taipei, Taiwan R.O.C.

Objective: Cerebral blood volume (CBV) and cerebral blood flow (CBF) are calculated from dynamic-susceptibility-contrast MR images to evaluate the deficiencies in local brain perfusions. The CBV and CBF are usually overestimated in perfusion MRI technique compared to computed tomography and positron emission tomography, because the difficulty in finding a voxel containing 100% blood as a reference and the inclusion of vessel voxels in the measurements. An automatic segmentation technique was developed to improve the quantitative assessment of CBV and CBF in the brain from perfusion MRI.

Methods: Relative CBV images were calculated by using the area under the concentration-time curve for each voxel. Relative CBF images were calculated by using the concentration-time curve of an arterial voxel and the singular value decomposition technique (1). Normal brain parenchyma was automatically segmented with the time-to-peak criteria after cerebrospinal fluid removal and preliminary vessel voxel removal. Two scaling factors were calculated by comparing the relative CBV and CBF of the segmented normal brain parenchyma with the absolute values in the literature. Using the scaling factors, the relative CBV and CBF were converted to the absolute CBV and CBF. Voxels with either CBV > 8 mL/100 g or CBF > 100 mL/100 g/min (2) were segmented as vessel voxels and were excluded from the quantitative measurements.

Results: The segmented brain parenchyma with normal perfusion was consistent with the angiographic findings for each patient. Measurements of CBV and CBF on the normal brain hemisphere were in agreement with data reported in the literature. The CBV and CBF were slightly reduced after CSF removal. The CBV and CBF were greatly reduced after the removal of vessel voxels. There was a significant difference in the measured data of the normal hemisphere before and after removal of both CSF and vessel voxels.

Conclusions: The benefits of our proposed technique are as follows:

1) the inter-observer and intra-observer variability associated with identifying brain tissue with normal perfusion can be eliminated by using the automatic segmentation technique;

2) the individual differences in the CBV and CBF of the normal brain parenchyma can be normalized, and a quantitative comparison can be achieved;

3) there is no need to find a voxel containing 100% blood as a reference.

References:

1. Ostergaard L, Weisskoff RM, Chesler DA, et al. High resolution measurement of cerebral blood flow using intravascular tracer bolus passages: part I. mathematical approach and statistical analysis. Magnetic Resonance in Medicine 1996;36:715-725.

2. Murphy BD, Fox AJ, Lee DH, et al. Identification of penumbra and infarct in acute ischemic stroke using computed tomography perfusion-derived blood flow and blood volume measurements. Stroke 2006;37:1771-1777.

IDENTIFICATION OF BRAIN SUB-NETWORKS DURING THE INITIATION OF WILLED MOVEMENT

C. Karmonik[1], A. Verma[2], M. Dulay[1], S. Fung[3], R.G. Grossman[1]

[1]Neurosurgery, [2]Neurology, [3]Radiology, The Methodist Hospital Neurological Institute, Houston, TX, USA

Introduction: Brain regions were differentiated into a sub-network processing a visual stimulus that evoked an emotional response and a sub-network performing a willed movement using a visually presented approach-avoidance paradigm. This paradigm investigates the neural events occurring from switching from the so-called 'default mode state' to an active, goal-directed state of the brain.

Methods: Images of ten faces (10 seconds) separated by a green background (50 seconds) were presented to the subjects (n=10). If perceived as unpleasant, the subject was told to remove the image of the face by pressing a button, i.e. by a willed movement. Utilizing differentional correlation analysis of the Talairach-transformed BOLD activation maps (AFNI) with time-signal intensity curves extracted from the visual cortex and from the motor cortex, brain regionswere correlated with the visual stimulus and performing of the willed movement, respectively. Graph-theoretical clustering was used to identify brain regions synchronized with both these sub-networks.

Results: All subjects identified 5 faces as unpleasant and pressed the button with the right (dominant) hand. Highest activation correlated with visual cortex activation included bilaterally the lingual gyrus, the inferior and middle occipital gyrus, the declive, the culmen of vermis, the cuneus, the red nucleus and the ventral anterior thalamic nucleus. On the left, highest activation occurred in the substantia nigra and the uvula.On the right, in the lateral geniculate and the medial globus pallidus.

Highest activation correlated with performing the willed movement occurred bilateraly in the precentral and postcentral gyrus, in the inferior parietal lobule, the insula, the transverse temporal gyrus, the claustrum. Highest activated regions on the left included the supramarginal gyrus, the ventral posterior medial thalamic nucleus, the superior parietal lobule and the paracentral lobule and on the right, the inferior parietal lobule, the dentate, the cerebellar lingual and the fastigium (figure 1). Graph cluster analysis identified bilateral declive, culmen, substantia nigra and left lentiform nucleus as brain regions synchronized with both sub-networks.

Conclusions: Two distinct sub-networks of brain areas can be identified that appear to be linked in performing the transition from the default state to a goal-directed activity state of the brain.

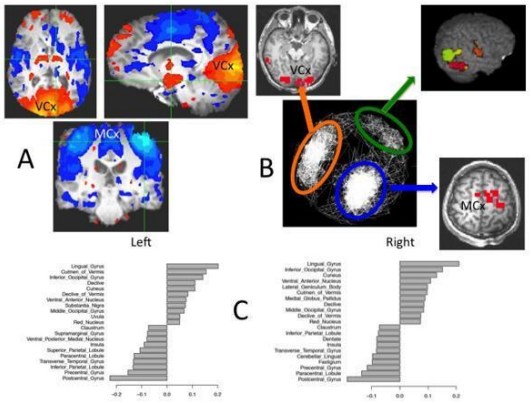

Figure 1: A: Average BOLD activation maps identifying brain regions participating in the stimulus processing only (red/orange, VCx: visual cortex) and brain regions performing the willed movement (blue, MCx: motor cortex). B: Graph network for subject #10 illustrating the separation into two sub-network (orange, blue) interconnected by central brain regions (green) **C:** Brain regions with highest activation (determined by the differential correlation analyis) for stimulus processing only are listed with positive values and brain regions involved in performing the motor task with negative values (left and right hemispheres separately).

STANDARDIZATION OF PRECLINICAL STROKE IMAGING

A. Kranz[1,2], J. Boltze[2,3], D.-C. Wagner[2,4]

[1]Experimental Imaging, Fraunhofer Institute for Cell Therapy and Immunology, [2]Translational Centre for Regenerative Medicine, University Leipzig, [3]Department of Cell Therapy, [4]Ischemia Research Unit, Fraunhofer Institute for Cell Therapy and Immunology, Leipzig, Germany

Objectives: T2 turbo spin-echo (TSE) magnetic resonance (MR) imaging is widely used to measure infarct size in preclinical stroke studies. Valid results can be obtained beginning from eight hours after stroke onset and are highly correlated to histological gold standards. However, despite the advantages of *in vivo* imaging, only few groups may have access to specialized small animal scanners. Here we report an approach that allows preclinical imaging by a standard clinical MR imaging system. Special emphasize was thereby given to quality assurance aspects such as intra- and inter-observer variability and sample size calculation.

Methods: All measurements were performed in a clinical 1.5 T Phillips MR scanner using a routine 47mm small loop microscopy RF-coil and minor modifications of the standard T2-TSE sequence. In 25 animals the middle cerebral artery was permanently occluded and MR investigation was performed on days 1, 8, 29 and 60 after onset of ischemia. To determine the intra- and inter-observer differences, final calculations of the infarct size were done by five independent observers using the open source software ImageJ. To furthermore compare the predictivity of the four experimental time points we defined the following parameters for the sample size calculation: alpha = 0.05 ; beta = 0.2 ; effect size = 15%.

Results: The method described here is feasible and reproducible to determine the infarct volume in small animals using a clinical MR imaging system. We observed a low intra-observer, but a significant inter-observer variability indicating that such analyses should be preferentially performed by only one blinded investigator. Moreover, by simulating sample size calculations we found that the chosen endpoint (i.e. the infarct size at variable time points of investigation) had a considerable impact on the calculated group sizes. This is most likely due to different stages of the infarct development and hence different underlying pathophysiological mechanisms that ultimately result in differing variability. Hence, this phenomenon should be considered when scheduling further imaging experiments.

VENTROMEDIAL PREFRONTAL CORTEX IN CONTROL OF PHYSIOLOGICAL AROUSAL: THE EFFECTS OF IMPULSIVITY

S. Zhang, **C.-S.R. Li**

Psychiatry and Neurobiology, Yale University School of Medicine, New Haven, CT, USA

Background: Numerous previous studies implicate the ventromedial prefrontal cortex (vmPFC) in the regulation of physiological arousal. However, the findings report a correlation but do not establish a causal relationship between regional activities and indices of arousal such as skin conductance. Here, we use Granger causality analyses to evaluate whether vmPFC fMRI signals "Granger cause" skin conductance level during a cognitive task. An additional goal of the study is to evaluate whether and how an impulsive personality trait influences this regulatory mechanism.

Subjects and methods: Twenty-three healthy adults participated in fMRI of the stop signal task with simultaneous recording of skin conductance using a Biopac setup (Zhang and Li, 2012, NeuroImage). Imaging data were processed with Statistical Parametric Mapping. A linear regression with skin conductance level (SCL) was performed for individual subjects. Data from all subjects were combined with random effects analyss.

Results: A one-sample t test identified areas in the vmPFC including the subgenual anterior cingulate cortex where the BOLD signals are negatively correlated with SCL. In contrast, the BOLD signals of the dorsal anterior cingulate cortex are positive correlated with SCL, in accord with many previous studies (e.g., Nagai et al., 2004, NeuroImage). We used Granger causality analyses to evaluate whether vmPFC BOLD and SCL time series are causally related. The results showed that vmPFC BOLD signals Granger cause SCL, thus establishing the direction of influence. Furthermore, greater causality (as indexed by the F value) is negatively correlated with skin conductance response (SCR) elicited by stimulus events during the stop signal task (e.g., correlation with SCR of stop trials: $p< 0.0004$, Spearman regression). Also, impulsivity personality as assessed by the Barratt Impulsivity Scale-11 is associated with a smaller causality and greater event-related SCR across subjects.

Conclusions: These results demonstrate that vmPFC activities causally regulate physiological arousal. A greater regulatory influence is associated with less autonomic responses to salient environmental events. These findings may advance our understanding of the etiologies of mental illnesses that implicated vmPFC dysfunctions and altered affective processing.

ALTERERED NEUROVASCULAR COUPLING OF CEREBRAL BLOOD FLOW AND NEURONAL RESPONSES TO SENSORY STIMULATION BY THE SEROTONIN RECEPTOR AGONIST PSILOCIN

A. Spain[1], C. Howarth[2], M. Maczka[3], T. Sharp[4], N.R. Sibson[2], C. Martin[1]

[1]Department of Psychology, University of Sheffield, Sheffield, [2]Department of Oncology, [3]Department of Statistics, [4]Department of Pharmacology, Oxford University, Oxford, UK

Objectives: Accurate interpretation of functional MRI signals as evidence for stimulus or task-evoked changes in neuronal activity depends upon neurovascular coupling, whereby alterations in the activity of neurons drive local changes in cerebral hemodynamics. Whilst empirical work to date has focused upon the role for excitatory, glutamate-mediated neurotransmission in neurovascular coupling, very little research has addressed whether and how an important modulatory neurotransmitter such as serotonin (5-HT) might alter the relationship between neuronal activity and the hemodynamic events that are responsible for fMRI signals. Our objective in this study was to investigate the effect of a specific 5-HT receptor agonist, psilocin, on the relationship between concurrently measured neuronal activity and cerebral blood flow (CBF) responses to sensory stimulation in rats. We also used a carbon dioxide challenge (hypercapnia) to determine any effect of the drug upon cerebrovascular reactivity.

Methods: Rats were anesthetised, tracheotomised and the femoral vessels cannulated for monitoring and maintenance of physiological parameters and drug infusion. The skull overlying left somatosensory cortex was thinned to translucency for laser speckle imaging of CBF changes and insertion of a bipolar recording electrode. Cerebral blood flow and local field potential changes were measured concurrently n response to (a) electrical stimulation of the corresponding whisker pad, which consisted of a 2s stimulation at frequencies ranging from 1Hz to 40Hz, randomly interleaved, and (b) hypercapnia, which consisted of a 30s epoch of 10% carbon dioxide added to the animals air supply. Data collection was repeated after i.v. administration of the 5-HT receptor agonist psilocin (2mg/kg).

Results: Our initial data presents strong evidence for alterations in the relationship between stimulus evoked neuronal activity and CBF responses attributable to action of the 5-HT receptor agonist psilocin. Specifically, over a range of stimulation parameters (frequency) hemodynamic responses were augmented by the drug (Figure 1, showing trial-averaged CBF responses) whereas neuronal responses were reduced (Figure 2, showing average local field potential responses to a single stimulus pulse).

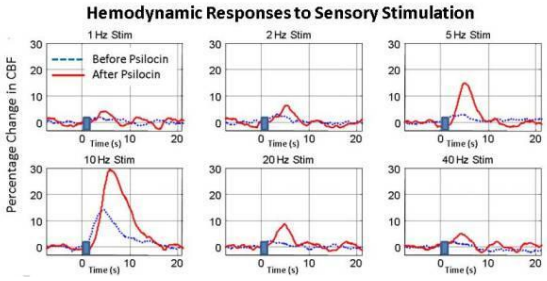

[Figure 1]

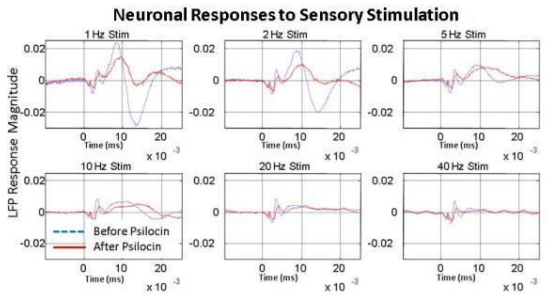

[Figure 2]

There was no change in cerebrovascular reactivity as determined by hypercapnia (Figure 3A, showing trial-averaged CBF responses). By plotting mean CBF response maxima against summed neuronal activity (area under the curve) for each stimulation condition, we also find evidence that the relationship between the CBF responses and their underlying neuronal activity was altered by psilocin (Figure 3B).

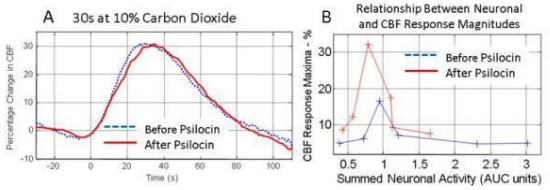

[Figure 3]

Conclusions: Alterations in neurovascular coupling by changes in the function of the 5-HT neurotransmitter system may have important implications for the application of functional MRI to investigate drug action or disease mechanisms that involve 5-HT systems. In particular, these findings may complicate the interpretation of BOLD fMRI data as a proxy measure of neuronal activity differences between subject groups where differences in the functionality of the 5-HT system are known or expected (e.g. affective disorder). Ongoing studies will further characterize these effects and investigate the mechanisms that might underlie them.

HEMODYNAMIC EVALUATION OF MIDDLE CEREBRAL ARTERY IN PATIENTS WITH ISCHEMIC STROKE DETECTED BY 3.0TESLA MRI

A. Mizuma, N. Kajihara, H. Takano, K. Endo, M. Kawakata, H. Nishio, T. Horie, T. Yanagimachi, S. Takizawa

Tokai University School of Medicine, Isehara, Japan

Purpose: Atherosclerotic lesions in carotid artery, coronary artery, ascending aorta/aortic arch, renal artery, and peripheral artery have been known to be important factors as ischemic stroke risk factors. On the other hand, transcranial doppler ultrasonograhy has been used to evaluate hemodynamic change of intracranial artery. However, it is limited to detect intracranial artery clearly because of bony artifact, especially in Japanese. Thus, there were few reports about the relationship between atherosclerotic lesion of intracranial artery and ischemic stroke risk factors. The purpose of this study is to assess atherosclerotic change of intracranial artery including dynamic change in patients with ischemic stroke using 3.0 Tesla MRI.

Subjects and methods: Six ischemic stroke patients (classified as branch atheromatous disease in middle cerebral artery (MCA) branch, without MCA stenosis in MRA) and four healthy volunteers (control group: they had no atherosclerotic risk factors and past history of vascular disease) were investigated. We measured the cross sections in MCA (just on horizontal part, distal and proximal parts) in both systolic and diastolic phases by synchronizing with heart beats, as well as the maximum flow velocity (peak systolic velocity (PSV), end-diastolic velocity (EDV) and time-averaged maximum velocity (TAMV)), using cine mode MRI. We examined differences in cross-sectional area of systolic and diastolic phases (Stiffness parameterβ:In(systolic blood pressure/diastolic blood pressure) ・systolic vessel diameter / (systolic vessel diameter-diastolic vessel diameter)), maximal flow velocity (pulsatility index (PI: (PSV-EDV)/TAMV), resistance index (RI:(PSV-EDV) / PSV)) for each part between two groups.

Results: In ischemic stroke patients and healthy volunteers, all parameters (PSV, EDV, TAMV, PI, RI, and Stiffness parameter β) were not significant difference among horizontal, distal and proximal parts. PI (0.98 vs 0.48, P< 0.05) and RI (0.60 vs 0.39, P< 0.05) were significantly larger in ischemic stroke patients than those in distal part in healthy volunteers. But Stiffness parameterβ were not significant difference.

Conclusion: Hemodynamic evaluation, especially in PI and RI, using 3.0T MRI may be useful for predicting the atherosclerotic change in MCA, even if there was no atherosclerotic lesion.

EVALUATION OF PHASE UNWRAPPING METHODS IN MRI FOR ASSESSMENT OF OEF IN TRANSIENT ISCHEMIC BRAIN TISSUE IN RATS

K. Nakamura[1], J. Kawamura[2], Y. Kondoh[3], H. Miyata[2], T. Kinoshita[1]

[1]Radiology & Nuclear Medicine, [2]Neuropathology, [3]Neurology, Akita Research Institute for Brain and Blood Vessels, Akita, Japan

Introduction: Susceptibility phase image in MRI has been used for oxygen extraction fraction (OEF) assessment [1,2]. Macroscopic susceptibility effects from non-uniform background field are shown as low-spatial frequency components in phase images. The

effects should be removed before OEF quantification. A polynomial fit [1,3] and a high-pass filter (HPF) [2,4] are two notable procedures to eliminate the background field. We evaluated the difference between polynomial fit and HPF of phase unwrapping for quantification of OEF in ischemic brain tissue in rats.

Methods: Forty-nine male Sprague-Dawley rats were used. Sixty minutes of transient ischemic regions were induced by occluding the left middle cerebral artery with embolic thread. One day after the reperfusion diffusion-weighted image (DWI) and gradient echo image were acquired in a 4.7-T MRI. HPF phase image was extracted from reconstructed HPF image from original FID divided by a low-pass filtered FID (32, 64, and 96 points Hanning filter) in gradient echo image. 2D polynomial functions (4^{th}, 8^{th}, and 12nd order) were used for unwrapping the phase images. Macroscopic polynomial fitted images subtracted from the original phase data were used for polynomial fit images. The mean value of apparent diffusion coefficient (ADC) in the healthy right caudate-putamen (N-Cpu) was considered to be 100% of relative ADC (rADC). Voxels in both sides of the caudate-putamina were then classified as ischemic core (< 70% rADC), ischemic penumbra (70% to 90% rADC) or normal (>90% rADC). Phase difference change ($\Delta\phi$) between mean value of N-Cpu and each voxels were then calculated and mean value of each classified region was evaluated in each rat.

Results: Figure 1 shows phase difference of mean and standard deviation from all rats. Three different Hanning filter and polynominal fit as a function of rADC value were shown. The phase differences differ with filter size in HPF image. Polynomial fit of 8^{th} and 12nd order are almost same profile. It indicates polynomial fit images are useful for quantification of susceptibility phase difference.

Discussion: HPF effect on the phase difference in ischemic brain tissue in rats is not negligible and therefore it is not simple to perform a quantitative estimation of OEF from HPF phase image. On the other hand, higher order of polynomial fit is stable and it is better to use polynomial fit of phase unwrap in MRI for OEF estimation

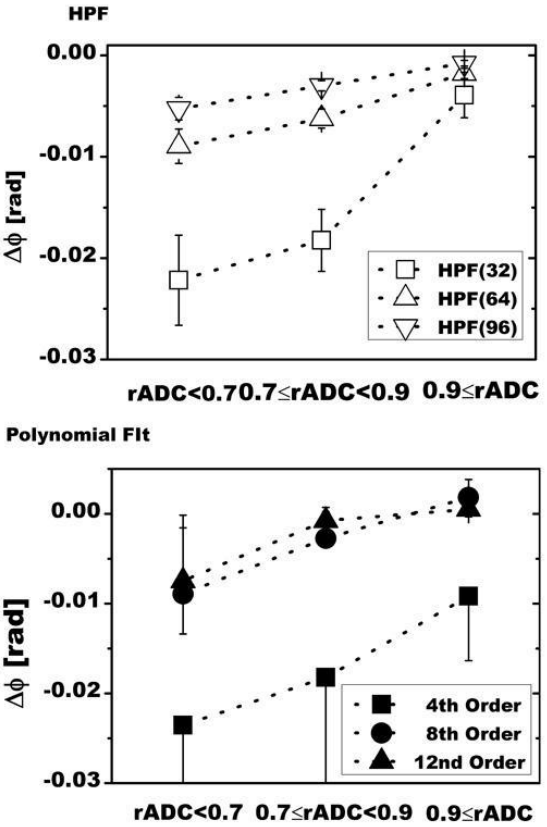

[Figure1]

References:

[1] X He et al., MRM 57; 115 - 126 (2007)

[2] DS Bolar et al., MRM 66; 1550 - 1562 (2011)

[3] JH Duyn et al., PNAS 104; 11796 - 11801 (2007)

[4] Y Shen et al., MRI 25; 219 - 227 (2007)

DEPRESSIVE MOOD MODULATES ANTERIOR LATERAL CA1 DURING A PATTERN SEPARATION TASK IN HEALTHY INDIVIDUALS: A FUNCTIONAL MRI STUDY

T. Fujii[1,2], D.N. Saito[1,2], H.T. Yanaka[2,3], H. Kosaka[1,4], **H. Okazawa**[1,2]

[1]Research Center for Child Mental Development, [2]Biomedical Imaging Research Center, [3]Research and Education Program for

Life Science, [4]Department of Neuropsychiatry, University of Fukui, Eiheiji-cho, Japan

Background: Although patients with major depressive disorder show reduction of hippocampus volume especially in the Cornu ammonis1 (CA1), animal studies suggest depressive mood is related with neurogenesis in the dentate gyrus (DG). To clarify which subregion in the hippocampus is related with depressive mood in human, we conducted a functional MRI (fMRI) study with a delayed matching-to-sample task and compared with scores of depressive mood.

Methods: Twenty-seven healthy volunteers participated in this study. They performed a modified version of a delayed matching-to-sample task in a 3T-MRI scanner (Signa Excite; General Electric, Milwaukee, USA) to investigate pattern separation related activity [1]. The pattern separation is a process to prevent interference of similar memory. They also completed the Beck Depression Inventory (BDI), a questionnaire about depressive mood, outside the scanner. Functional MR images were acquired with high spatial resolution, covering only around the hippocampus, to evaluate and compare BOLD signal in small subregions of the hippocampus precisely.

Results: Depending on the similarity between the sample cues, the DG/CA3 and medial CA1 in the anterior hippocampus changed their activities during encoding in different ways. Furthermore, the DG/CA3 was active in successful encoding trials relative to false trials. The activity in the lateral CA1 in the anterior hippocampus was negatively correlated with the BDI score (Figure 1), and this tendency was enhanced by the pattern separation of similar inputs.

Conclusion: Depressive mood reduced the encoding-related activity in the lateral CA1, even in the sub-clinical condition, and this tendency was enhanced by the pattern separation of similar inputs. The activity under pattern separation in the lateral CA1 observed in high resolution fMRI may predict depressive mood, which is different from the DG/CA3, the core region of the pattern separation.

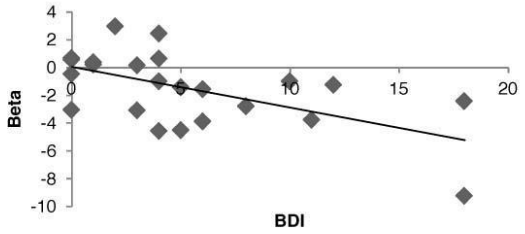

[Figure 1]

Figure legend: Scatterplot between regional activity in the lateral CA1 and depressive mood showed a significant negative correlation.

Reference:

[1] Bakker A, Kirwan CB, Miller M, Stark CEL. Pattern separation in the human hippocampal CA3 and dentate gyrus. Science (2008); 319:1640-1642.

EFFECTS OF TRANSIENT FUNCTIONAL BRAIN DISRUPTION ON GLOBAL NEURAL NETWORK STATUS IN RATS

W.M. Otte, K. van der Marel, R.M. Dijkhuizen

Biomedical MR Imaging and Spectroscopy Group, Image Sciences Institute, University Medical Center Utrecht, Utrecht, The Netherlands

Objectives: Permanent focal brain damage can have critical remote effects on the function of distant brain regions, which relate to constrained behavioral output and cognitive comorbidities[1-2]. However, the effects of transient disturbances on global brain function are largely unknown. Recently, transient ischemic attack (TIA) has been associated with transient cognitive impairment and depression, suggestive of global functional network modifications[3]. Our goal was to map the impact of transient functional brain impairment on large-scale neural networks in the absence of structural damage.

Methods: We developed a rat model of transient functional hemispheric disruption using unilateral focal anesthesia, similar to the intracarotid sodium amobarbital procedure for the 'Wada test' in humans. Healthy adult rats

were mechanically ventilated with 2% isoflurane, and the right carotid artery was catheterized. Resting state fMRI (rs-fMRI) was acquired (4.7T; gradient-echo; TR/TE=500/19 ms; 15 min acquisition; n=3) at 1% isoflurane. After 7.5 minutes 2 mg/kg pentobarbital was injected intracarotidly. Lastly, perfusion MRI was acquired (TR/TE=100/25 ms) in combination with an intracarotid bolus injection of gadobutrol (1.0 mmol/mL). In two animals, EEG was recorded in the bilateral somatosensory cortices.

Rs-fMRI images were motion-corrected, spatially smoothed, band-pass filtered between 0.01 and 0.1 Hz, and nonlinearly matched with an atlas for functional connectivity (FC) analysis. The first (pre-barbital injection) and last (post-barbital injection) 500 images were used to extract time series for 65 bilateral regions-of-interest (ROIs), and to calculate pair-wise FCs (correlation coefficient *r*). We focused on the presence of highly connected network hubs (i.e., 'Rich-club' organization; which reflects a network's capacity to efficiently segregate and integrate multisensory information[4]).

Results: Results are summarized in the Figure.

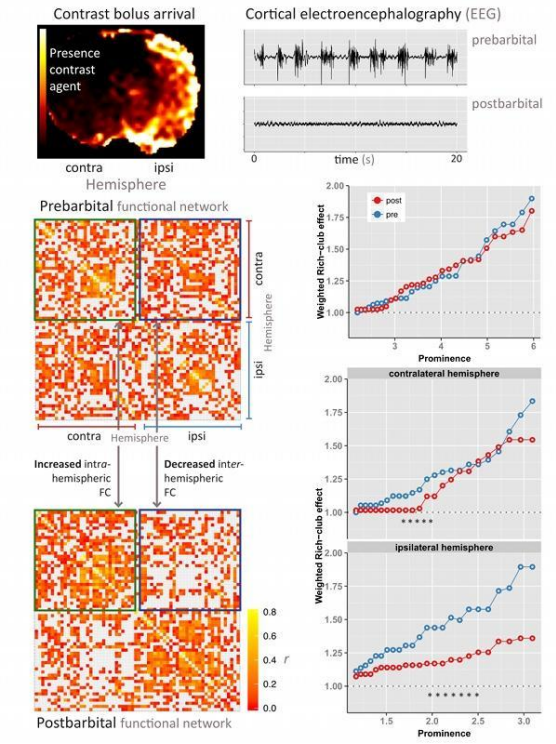

[Figure]

Perfusion MRI data demonstrated that the catheterized carotid artery effectively supplied the ipsilateral hemisphere allowing for selective hemispheric brain silencing with pentobarbital. Low-frequency interhemispheric EEG synchronization decreased after unilateral pentobarbital injection. The average prebarbital FC network-calculated from rs-fMRI-displayed strong connectivity within and between hemispheres, whereas the disrupted hemisphere revealed increased intrahemispheric connections with concomitant decrease of interhemispheric FC. The bilateral FC network was characterized by a strong 'Rich-club' effect (value >1.0), which was not affected by ipsilateral functional disruption. Nevertheless, the 'Rich-club' value was significantly decreased in the ipsilateral hemisphere and to a lesser extent contralaterally over a range of prominence thresholds (*p< 0.01, 'Rich-club' difference).

Conclusions: Our study shows that transient functional network disruptions can be effectively studied using a straightforward rodent model in combination with rs-fMRI. Our data support the concept that densely connected 'Rich-club' regions play a central role in global brain communication. In addition, we found the network hub configuration to be significantly affected by temporary functional disruption of one hemisphere, which may reflect an underlying mechanism of neurological impairments found in TIA patients.

References:

[1]Carter et al, *Ann Neurol*. 67(2010)

[2]Van Meer et al, *J Neurosci*. 28(2012)

[3]Luijendijk et al, *Stroke*. 42(2011)

[4]Van den Heuvel et al, *PNAS*. 109(2012)

QUANTIFICATION OF CEREBRAL HAEMODYNAMICS BEYOND CBF USING NON-PARAMETRIC CPI METHOD FOR DYNAMIC SUSCEPTIBILITY CONTRAST MRI

S.J. Payne[1], A. Mehndiratta[1], D.E. Crane[2], B.J. MacIntosh[2], M.A. Chappell[1]

[1]*Institute of Biomedical Engineering, Department of Engineering Science, University of Oxford, Oxford, UK,* [2]*Sunnybrook Research Institute, University of Toronto, Toronto, ON, Canada*

Objective: It should be possible to study cerebral haemodynamics by estimation of tissue residue function, *R(t)* from DSC-MRI perfusion analysis. But the most widely used Singular Value Decomposition (SVD) deconvolution methods cannot provide a physiologically interpretable residue function because of oscillations in the solution. In this study our motivation was to use a recently proposed non-parametric deconvolution technique (Control Point Interpolation, CPI) that offers regularised residue function estimates along with accurate perfusion values.

Methods: DSC data were acquired from 8 patients (65yrs [47-85], M:F=5:3) with atherosclerotic disease, using Diffusion Weighted Imaging (DWI) and GRE-DSC: TR/TE=1.5s/30ms, 128x128x22x78 matrix with 0.1 mmol/kg Magnevist. DSC images were analysed using the oSVD and with CPI deconvolution. In the CPI method the *R(t)* was estimated non-parametrically using a set of control points and cubic spline interpolation to generate the complete smooth function. *R(t)* characteristics were evaluated over regions of interest (ROI) based on DWI and perfusion images acquired pre- and post- carotid endarterectomy under two criteria: contralateral healthy (normal) and infarcted (DWI+) tissue. 32 ROIs were selected from eight patients under normal and 18 under DWI+ group. *R(t)* obtained from CPI deconvolution were analysed for variation in shape and heterogeneity. In order to characterise the monotonically decreasing residue function, we measured the time for it to drop to 50% and 10% of its maximum value, referred to as *R50* and *R10* respectively. Transit time distribution (*h(t)*) was calculated from the residue functions (using, $h(t) = -dR(t)/dt$).

Results: Considerable differences in the shape of residue function were observed with CPI for healthy and infarcted brain tissue (figure). The residue function from DWI+ group showed a slower decay compared to the normally perfused contralateral hemisphere (figure). *R50* and *R10* values of the healthy and DWI+ tissue were found to be significantly different ($p < 0.05$). Mean *R50* values pre-surgery for healthy and DWI+ tissue were 1.21s, 4.17s respectively which became 1.20s and 1.76s post-surgery; *R10* changed from 3.59s, 15.72s to 3.83s and 5.99s respectively.

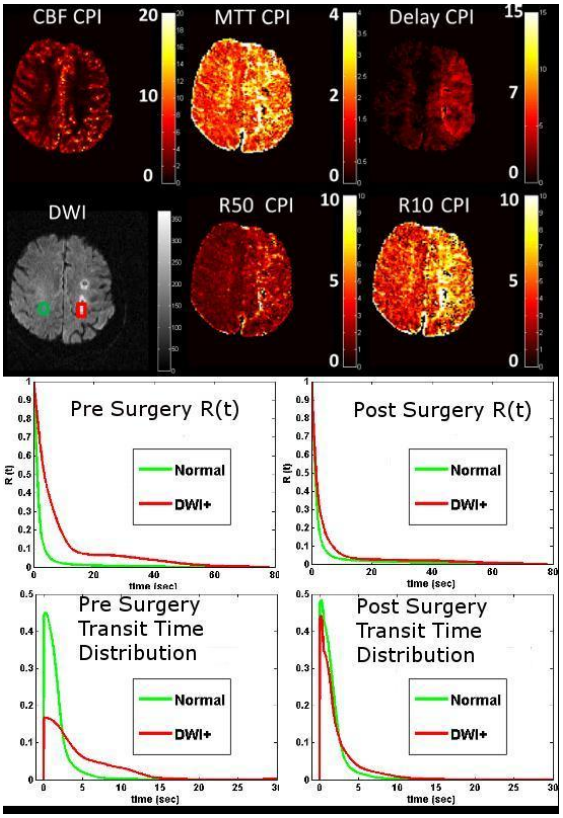

[Figure]

Conclusion: Tissue residue function shape is critical in clinical image analysis as it allows the potential information on flow heterogeneity and tissue oxygen delivery to be assessed. The CPI formulation allowed physiologically realistic smooth functions to be estimated. Significant differences in normal brain parenchyma and ischemic tissue haemodynamics were observed in a patient group. *R50* and *R10* could serve as clinically useful quantitative measures with higher sensitivity to pathological variation than the more widely used MTT parameter. *R50* and *R10* parametric maps were found to provide

information in addition to standard perfusion and diffusion imaging.

EXPERT SYSTEM DEVELOPMENT FOR THE FANN BASED DIAGNOSIS OF BRAIN TUMOR

N. Pradhan[1], A.K. Sinha[2]

[1]*Department of Electronics and Communication Engineering, Dronacharya Group of Institutions, Gautam Buddh Nagar,*
[2]*Information Technology, ABES Engineering College, Ghaziabad, India*

Objective: The objective of this research paper is to develop an expert system using an integrated approach, which segments, and labels pathological tissue tumor and edema separately, in FLAIR magnetic resonance images of the human brain. The expert system using machine learning is developed in which knowledge base is acquired from clinical symptoms, results obtained from neurological tests and cerebrospinal fluid tests and feature vectors extracted from brain magnetic resonance images.

Method: A new approach to the development of an Expert System for the diagnosis of Brain Tumor has been presented in this paper. The knowledge has been acquired from clinical symptoms, neurological tests, Cerebrospinal fluid (CSF) tests and feature vectors extracted from fluid attenuated inversion recovery (FLAIR) brain magnetic resonance (MR) images of the brain tumor patients. For processing of brain MR images composite feature vectors, comprising of empirically developed higher order wavelet function using Daubechies wavelet transform and statistical functions, are extracted from the blocks of size 4×4 pixels of intra-cranial brain image. Fuzzy C-mean is used for segmentation of intra cranial image. Knowledge base thus acquired is used for machine learning using fuzzy artificial neural network (FANN) and validated with real data collected from hospitals.

Results: A comprehensive expert system is implemented with the data of substantial number of patients and shown in figure.

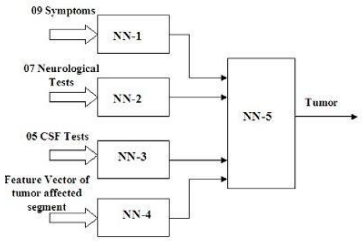

[Expert System]

The result of proposed approach is very promising and efficiently applied for tumor diagnosis. Trained and validated system is tested with the data of 12 unknown brain tumor patients with 90 samples out of which in 82 cases tumor tissue diagnosis is matching with the opinion of radiologists and neurologists. Block wise segmentation of MR images improves the computational speed of the segmentation process.BPA based Fuzzy ANN offers promising results in the task of classifying brain tissues.

Conclusions: In this paper an expert system is developed which can be efficiently applied for brain tumor diagnosis. Performance of system is evaluated and found that for 91.11% samples correct diagnosis is done. The Expert system developed here can be used for the diagnosis of brain tumor and can be very helpful to the neurologists and radiologists for the definitive diagnosis of tumor.

References:

1. Zhang, Desai(2001) 'Segmentation of Bright Targets Using wavelets and Adaptive Thresholding" in IEEE transaction on Image Processing, VOL.- 10,No. 7.

2. Prastawa, Bullitt etal (2004) "A brain tumor segmentation framework based on outlier detection" Elsevier's Medical Image Analysis 8, 275-283

3. N. Benamrane et al (2005)"A Hybrid Fuzzy Neural Networks for the Detection of Tumors in Medical Images" in Americal Journal of Applied Sciences2(4): 892-896, ISSN 1546-9239

4. M.H.Fazel Zarandi et al (2011) "Systmatic

image processing for diagnosing brain tumors : A Type-II fuzzy expert system approach" in ScienceDirect Applied Soft Computing, Volume 11,issue 1, Pages 285-294

SPONTANEOUS ACTIVITY AND THE SELF - AN INTERACTION STUDY BETWEEN DIFFERENT OPERATIONAL RESTING STATES AND SELF-SPECIFIC STIMULI

P. Qin[1], S. Grimm[2], M. Bajbouj[2], G. Northoff[1]

[1]*University of Ottawa Institute of Mental Health Research (IMHR), Ottawa, ON, Canada,* [2]*Cluster Languages of Emotion, Free University Berlin, Berlin, Germany*

Objectives: Previous studies suggest that there may be specific interaction of self-specific stimuli with spontaneous brain activity (Beer, 2007;Northoff et al., 2010;Qin and Northoff, 2011). The aim of the present study is to directly test the interaction of self- and non-self-specific stimuli with different operational resting state, e.g., eyes closed and eyes open which could modulate spontaneous brain activity.

Methods: Using fMRI, we applied a 2x3 rest-stimulus interaction design by investigating neural activity during auditory name perception with three different names (own, familiar and unknown) in two different (operational) resting state conditions, eyes open (EO) and eyes closed (EC). Additionally, we used a block-design experiment with two conditions (EO and EC) to define brain activity differences between EO and EC.

Results: The interaction between self- and non-self-specific stimuli and two resting state conditions (EC, EO) showed a significant effect in auditory cortex. Only other names (familiar and unknown) induced significantly different signal changes during EO when compared to EC. In contrast to other names, the own name did not induce differential signal changes in the two resting state conditions. This was observed despite the fact that eyes open by itself induced higher signal change in auditory cortex when compared to eyes closed (Figure 1). Unlike in auditory cortex, we did not observe interaction effect in other brain regions like the cortical midline structures.

Conclusions: Our results may suggest differential reactivity of self- and non-self-specific stimuli to changing spontaneous brain activity levels in auditory cortex. Hence our data contribute to not only better understand the relationship between self-specific stimulus processing and spontaneous brain activity but, more generally, how different spontaneous brain activity levels can impact stimulus processing.

References:

Beer, J.S. (2007). The default self: feeling good or being right? Trends Cogn Sci 11, 187-189.

Northoff, G., Qin, P., and Nakao, T. (2010). Rest-stimulus interaction in the brain: a review. Trends Neurosci 33, 277-284.

Qin, P., and Northoff, G. (2011). How is our self related to midline regions and the default-mode network? Neuroimage 57, 1221-1233.

FMRI BOLD SIGNAL OF MICE IN RESPONSE TO PROLONGED SENSORY STIMULATION SHOWS NONLINEARITIES WHICH DEPEND ON THE ANESTHETIC REGIME

F. Schlegel[1], A. Schröter[1], M. Rudin[1,2]

[1]*Institute for Biomedical Engineering, ETH and University Zürich,* [2]*Institute of Pharmacology and Toxicology, University Zürich, Zürich, Switzerland*

Objectives: Considering the many genetically engineered mouse lines available for studying the nervous system, fMRI in the mouse has become an attractive tool for investigating hemodynamic and metabolic changes underlying the measured signal. Such studies are relevant for the interpretation of human fMRI data of physiological and pathological conditions. Yet, animal fMRI studies are typically carried out under anesthesia, where interactions of anesthetics with neural and vascular function generate additional complexity[1]. This leads to deviations from linear behavior, which becomes problematic when standard statistical tools like the general linear model are incautiously applied to mouse fMRI. Here, we investigated the influence of several anesthetics on temporal characteristics of stimulus-induced fMRI responses in the mouse.

Methods: Female C57Bl/6 were artificially ventilated (90% air/10% oxygen) and paralyzed (pancuronium bromide i.v.). The following anesthetics were used: isoflurane

(1%), urethane (1.5g/kg i.p.), medetomidine (0.1mg/kg bolus + 0.2mg/kg/h infusion i.v.) and propofol (30mg/kg bolus + 150mg/kg/h infusion i.v.). Measurements were carried out using a 9.4T Bruker BioSpec 94/30 (Bruker BioSpin MRI, Germany) system with a four-element receive-only cryogenic phased-array coil (Bruker BioSpin AG, Switzerland). BOLD responses were acquired with GE-EPI (TE/TR=10/1000ms, acquisition time: 1s) for 12 axial slices (voxel dimensions: 185x312x500um^2). Electrical stimuli (1mA, 5Hz) were delivered by needle electrodes placed subcutaneously in the hindpaw. Data were extracted from the contralateral somatosensory hindlimb area.

Results: Hemodynamic response functions (HRFs) for a single stimulus pulse are shown for isoflurane (Fig.1a) and urethane anesthesia (Fig.1d). Negative BOLD signal components (initial dip, post-stimulus undershoot) were pronounced under urethane but absent under isoflurane. Modeling the BOLD response for 20s stimulation blocks led to major deviations between predicted and measured response using linear convolution. For isoflurane (Fig.1b), the initial slope was correctly predicted but total signal duration was underestimated. For urethane (Fig.1e) there were severe deviations regarding the temporal characteristics. Improved models were generated by introducing simple assumptions regarding adaptation of neural and vascular responses to repetitive stimuli: For isoflurane (Fig.1c), the assumption that the amplitude of each HRF decayed exponentially for subsequent stimuli, while time-to-peak increased accordingly, led to a significantly improved agreement between the experimental and predicted signal. For urethane (Fig.1f), the measured signal could be explained by a linear increase of time to peak and time to maximal post-stimulus undershoot. Area under HRF elicited by each stimulation pulse was kept constant throughout.

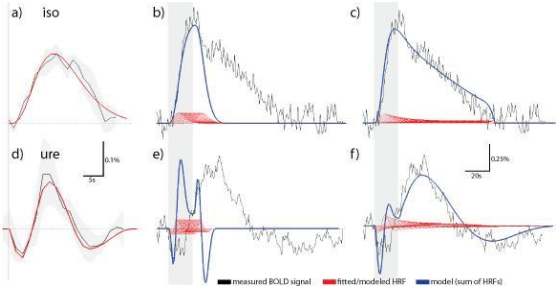

Fig.1: HRFs (a,b), linear convolution models (b,e) and improved models (c,f) for isoflurane (top) and urethane (bottom).

Conclusions: Different anesthetics introduce considerable variations in the BOLD response in mice, which can be investigated by supplementary measurements of cerebral blood flow, blood volume or neural signals. For the interpretation of the fMRI results, anesthetic specific HRF have to be used. Moreover, our experimental data indicate deviations from linear behavior, which have to be considered when analyzing the temporo-spatial characteristics of the BOLD signals.

References:

[1] Masamoto et al. Anesthesia and the quantitative evaluation of neurovascular coupling. *J. Cereb. Blood Flow Metab*. 32, 2012

DEFINING THE HUMAN HYPOTHALAMUS *IN VIVO* BY ULTRA-HIGH FIELD 7 TESLA MRI

S. Schindler[1], L. Schmidt[1], M. Strauß[1], A. Anwander[2], P.-L. Bazin[2], H. Möller[2], R. Trampel[2], U. Hegerl[1], R. Turner[2], S. Geyer[2], **P. Schönknecht**[1]

[1]Psychiatry, University Hospital of Leipzig, [2]Max Planck Institute for Cognitive and Brain Sciences, Leipzig, Germany

Introduction: *Post mortem* studies have shown a volume deficit of the hypothalamus in depressive patients. With ultra-high field (7 Tesla) MRI this effect can now be investigated *in vivo* in detail. But to benefit from the sub-millimeter resolution a segmentation procedure was required that overcomes limitations of existing procedures, in particular schematic approximations.

Methods: Using 7 Tesla T1 images the traditional anatomical landmarks of the hypothalamus were refined. A detailed segmentation algorithm (unilateral hypothalamus) was developed for colour coded, histogram-matched images and evaluated in a sample of 10 subjects. Intra- and interrater reliabilities were estimated in terms of intra- and interclass-correlation coefficients (ICC).

Results: The computer-assisted segmentation algorithm ensured test-retest reliabilities of ICC ≥ .97 and interrater-reliabilities of ICC ≥

.94. There were no significant volume differences between the tracers and between the hemispheres (paired t-tests). The estimated volume of the hypothalamus (tracer 1, first run) was 1130.64 mm^3 ± 103.48mm^3.

Conclusion: We present a computer-assisted algorithm for the manual segmentation of the human hypothalamus on ultra-high field 7 Tesla MR images. With very high intra- and interrater reliabilities it outperforms former procedures established with 1.5 T or 3 T MRI. The estimated volumes lie between previous histological and neuroimaging results. The algorithm provides an excellent basis for the investigation of our larger neuropsychiatric sample. It can be used by fellow researchers and it can serve as a gold standard for future automated procedures.

DIFFERENCES IN BRAIN FUNCTION BETWEEN PHONEMIC FLUENCY AND SEMANTIC CATEGORY VERBAL TESTS

A. Shiino[1], T. Watanabe[2], Y. Shirakashi[2], K. Tanigaki[3], T. Inubushi[1]

[1]Biomedical MR Science Center, Shiga University of Medical Science, Ohtsu, [2]Division of Neurological and Cerebrovascular Disease Center, Takeda Hospitala, Kyoto, [3]Research Institute, Shiga Medical Center, Moriyama, Japan

Introduction: Verbal fluency tests (VFT) are roughly divided into two methods; phonemic fluency or letter cue (LC) tasks and semantic category or category cue (CC) tasks. In this study, we aimed to identify differences in brain regions associated with LC and CC tasks. We found that hippocampal atrophy was tightly related to the results of CC tasks. Before VFT, we compared the results of memory-testing (by Wechsler Memory Scale-Revised, WMS-R) to the z-scores of anatomical regions of interest (ROIs) seen by magnetic resonance imaging (MRI) to assess base-line conditions.

Subject and methods: We tried to find the relation between the degree of focal brain atrophy and the results of psychological tests. More than 500 consecutive patients who visited our hospital with complaints indicating cognitive impairment participated. All subjects underwent psychological examination and MRI. Patients diagnosed with Alzheimer's diseases (AD) fulfilled the modified NINCDS-ADRDA criteria for probable AD. Patients with dementia who did not fulfill AD criteria, or who showed a tendency to depression were excluded from the study. As a result, 239 patients with AD, 30 patients with amnestic mild cognitive impairment (aMCI), and 204 subjects without dementia were selected.

T1-weighted 3D MR imaging was performed using spoiled gradient-recalled (SPGR) acquisition. We developed a batch program called “BAAD” (Brain Anatomical Analysis using Dartel) for evaluation of focal brain atrophy. BAAD calculates z-scores from t-valuesacquired from voxel-based morphometry (VBM) analyses using SPM 8 statistical parametric mapping software, and it calculates mean z-scores in 90 brain regions using automated anatomical labeling mapping.

Results: The results of VBM showed functional impairment most closely correlated with brain atrophy in the following pattern: general memory to the left hippocampus; verbal memory to the left hippocampus; delayed recall to the left hippocampus; and visual memory to the right hippocampus. The Logical Memory II subtest within WMS-R, which was thought to be a useful subscale for early detection of cognitive impairment was related to left hippocampal atrophy. CC-VFT scores were most strongly related with a region of the right hippocampus overlapping with and very similar to the region related to general memory test results. On the other hand, LC-VFT was most related to the right insular cortex. On multiple regression analysis among CC-VFT, LC-VFT, general memory and age, the regions highly related to the results of LC-VFT were the prefrontal and lateral temporal cortices, but not the medial temporal region.

Conclusion: We found that general memory and delayed memory were closely related to hippocampal functioning, as the degree of hippocampal atrophy was closely related to memory test scores. There seemed to be a significant difference between the brain regions associated with CC- and LC-VFT. CC-VFT was related to hippocampal functioning, but LC-VFT was shown to be related to prefrontal and lateral temporal functioning.

INVESTIGATING AUDITORY PROCESSING IN CONSCIOUS AWAKE COMMON MARMOSETS USING FMRI

C.R. Toarmino[1], C.C.-C. Yen[2], D.A. Leopold[3], C.T. Miller[1], **A.C. Silva**[2]

[1]Department of Psychology, University of California at San Diego, La Jolla, CA, [2]NINDS, [3]NIMH, National Institutes of Health, Bethesda, MD, USA

Introduction: Human natural behavior is heavily reliant on the perception and production of vocal and other types of sounds. Understanding the processing of sounds by the brain is a major goal in neuroscience. The common marmoset (Callithrix jacchus) is a New World non-human primate that has gained increased popularity in experimental neurobiology. Like humans, marmosets are a social species that utilizes a vast array of vocalizations to communicate within their groups and with other species. Although auditory processing in common marmosets has been extensively studied with electrophysiology [1] the use of non-invasive imaging techniques would allow the simultaneous investigation of the multiple brain areas involved in the perception, interpretation, and generation of sounds.

Here, we propose the use of non-invasive fMRI to investigate auditory processing in common marmosets. Therefore, our goals are two-fold: 1) to develop a technique for auditory stimulation in marmosets and 2) to show significant activation of marmoset auditory cortex.

Methods: Adult male common marmosets (n= 2) were first acclimated to being restrained according to a three-week schedule as previously described [2]. Each subject's head was restrained with individual custom-made helmets designed to fit the contours of each subject. Subjects were placed in a 7T/30cm MRI where auditory stimulation was delivered directly to the ear canals. Two surface RF coils were placed above auditory cortex to acquire the MRI signal. A total of three different stimuli with a length of 4s each were presented: a burst of white noise, a phee call, and a frequency sweep ranging from 1kHz-20kHz. BOLD fMRI data were acquired using a gradient-echo echo-planar imaging sequence at the end of each stimulus according to a sparse-sampling paradigm to avoid any interaction between scanner noise and the signal due to auditory stimulation. The location of the auditory cortex was identified using the anatomical structure of lateral sulcus (LS). Other acquisition parameters were: FOV: 3.84 x 2.88 cm^2, Matrix: 128 x 96, Slice thickness: 1 mm, 8 slices, and TE/TR=27ms/16s.

Results: Figure 1 shows the BOLD functional map of 3 slices immediately below the lateral sulcus (LS). Bilateral activation of the primary auditory cortex was robustly detected. The time course of activation is strongly correlated to the stimulations, and a small difference in activation could be observed between noise and either the phee call or a frequency sweep.

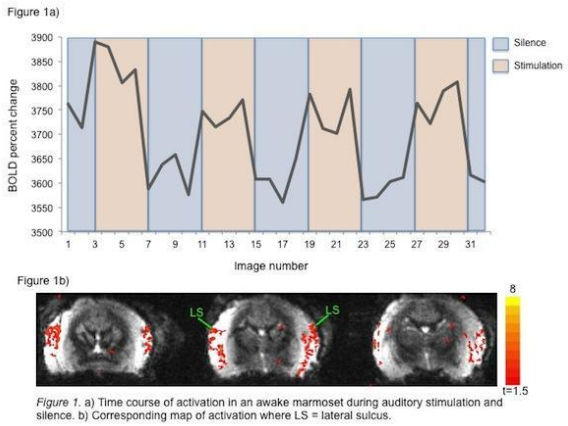

Figure 1. a) Time course of activation in an awake marmoset during auditory stimulation and silence. b) Corresponding map of activation where LS = lateral sulcus.

[Figure 1]

Conclusions: To the best of our knowledge, this is the first study to employ fMRI to investigate auditory processing in awake, conscious marmosets. These results will allow future research to focus on the functional mapping marmoset auditory cortex in a non-invasive manner.

References:

[1] Wang, X., et al. Nature 435: 341-346 (2005).

[2] Silva A. C., et al. Methods Molecular Biology 711, 281-302.

BRAIN PERFUSION MEASUREMENT IN PATIENTS WITH STENO-OCCLUSIVE DISEASE USING ARTERIAL SPIN LABELLING: CURRENT STATUS AND PERSPECTIVES

J. Sobesky[1,2], M. Mutke[1], S. Martin[1], V. Madai[1], F. Samson-Himmelstejrna[1], O. Zaro Weber[1], M. Guenther[3]

[1]Center for Stroke Research (CSB) Berlin, [2]Neurology, Charite - University Medicine Berlin, Berlin, [3]Fraunhofer Institute, Bremen, Germany

Objectives: In patients with chronic hemodynamic compromise, the assessment of hypoperfusion provides clinically relevant information to guide therapeutic decisions. Arterial spin labeling (ASL) magnetic resonance imaging (MRI) offers a non-invasive technique to measure surrogates of cerebral blood flow (CBF). However, several methodological constraints are currently focussed and the optimal sequence is a matter of debate. We evaluated two different ASL protocols to assess CBF in patients with chronic steno-occlusive disease in comparison to dynamic susceptibility contrast (DSC) perfusion weighted MRI.

Methods: In a prospective imaging study, 40 patients with chronic steno-occlusive disease were imaged by DSC-MRI and two different ASL sequences (3 T Magnetom Trio, Siemens, Erlangen). In 27/40 patients, a commercially available (PICORE Q2 TIPS sequence, single inflow time point, scanner-based software; Group A) was applied, in 13/40 patients, a research software (3D GRASE sequence, multiple inflow time points, calculation off-line; Group B) was applied. For DSC-MRI, images were analyzed off-line and maps of time-to-peak (TTP) and of CBF were calculated. Maps of DSC-CBF, DSC-TTP and ASL-CBF were analyzed by visual rating as well by a region of interest based approach (cortical ROIs, 20 mm diameter in 7 representative slices per patient) using Spearman`s rho and Bland-Altman (BA) plot.

Results: Average age of the patient sample was 58 years, occlusions were found in 22/40 patients, high graded stenoses were found in 18/40 patients. In 80% of the patients, a TTP delay, in 70% of the patients a CBF decrease was identified in the hemisphere ipsilateral to the vessel pathology. The visual analysis showed a fair agreement for group A and a good agreement for group B with respect to the identification of hypoperfusion. In both groups, regions with a TTP delay were well identified by ASL. The quantitative analysis of group A showed no correlation of DSC-CBF and ASL-CBF values. One major confounder was the arterial transit delay artefact with very low intensity values and/or with very high intravascular intensity values in the area of TTP delay with or without CBF decrease. Accordingly, the BA plot showed a wide spread of values. The quantitative analysis of group B showed a significant correlation for CBF values (rho 0.6, $p < .0001$) with clearly improved values for the BA plot.

Conclusions: ASL offers a valuable non-invasive estimate of CBF in stroke patients with steno-occlusive disease. However, the arterial transit delay artefact is a major confounder that well indicates TTP delay but causes errors in the assessment of quantitative CBF. This error can be attenuated by improved ASL sequences which acquire multiple inflow time points.

PHARMACOLOGICAL MRI (PHMRI) OF THE SEROTONIN (5-HT) RECEPTOR AGONIST PSILOCIN IN THE RAT: POTENTIAL FAST-ONSET THERAPY FOR AFFECTIVE DISORDERS

A. Spain[1], C. Howarth[1], A. Khrapitchev[1], T. Sharp[2], N.R. Sibson[1], C. Martin[3]

[1]Department of Oncology, [2]Department of Pharmacolgy, University of Oxford, Oxford, [3]Department of Psychology, University of Sheffield, Sheffield, UK

Introduction: Current pharmacological treatments for affective disorders are of limited use in an acute setting as several weeks of treatment are required before relief of symptoms. This is a major shortcoming, given that affective disorders are associated with a high degree of disability and significant mortality through suicide . Reports from psychedelic-assisted therapy carried out in the 1960s as well as recent pilot studies, suggest that “magic” mushrooms and their active constituent, psilocin, may give rapid symptom relief, with effects that persist for weeks beyond initial treatment. Recently, Cahart-Harris *et al*. reported widespread decreases in BOLD MRI and cerebral blood flow following psilocin administration in humans[1]. Adaptation of this imaging model to rats would allow

further study of the physiological effects of this drug.

Aim: The aim of this study, therefore, was to determine the phMRI responses to the 5-HT receptor agonist, psilocin, in the rat.

Methods: Male Sprague-Dawley rats underwent 60 minutes of BOLD MRI in a 9.4T horizontal bore magnet (Varian). After 15 minutes baseline acquisition either psilocin (2 or 0.03mg/kg) or vehicle (N=6/group) was administered intravenously. 45 minutes after imaging ended rats were terminated by perfusion fixation.

Results: Rats given 2mg/kg psilocin showed an increased BOLD response compared to vehicle in olfactory and limbic regions (Fig. 1A), as well as in the hypothalamus and connected hindbrain regions. At the same time, decreased BOLD responses compared to vehicle were observed in psilocin-treated animals in the prelimbic and cingulate cortex (Fig. 1B), dorsal thalamic nuclei, fimbria, habenula, areas of motor and sensory cortices, posterior hippocampus and elements of the visual system. In contrast, rats given 0.03mg/kg psilocin did not show robust changes in BOLD signal compared to vehicle.

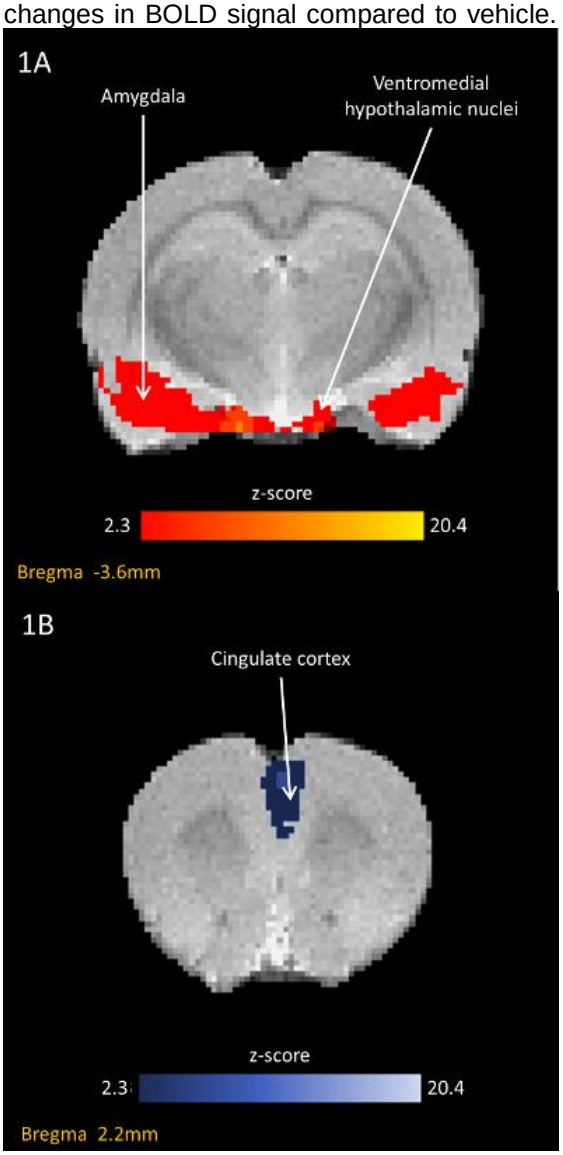

[Figure 1]

Conclusions: The bidirectional BOLD responses to psilocin administration observed in this study are in contrast to the exclusively decreased responses seen in humans[1], although certain areas, with high relevance in affective disorders (e.g. limbic areas, cingulate cortex) showed significant changes in both studies. Staining of brain sections from rats in this study for an immediate early gene marker of neuronal activity will be performed to probe whether these BOLD changes are due to the neuronal effects of the drug. Direct measurement of the CBF response to psilocin will further aid in identifying the vascular contribution to the observed BOLD signal changes.

References:

FUNCTIONAL MAGNETIC RESONANCE IMAGING FOR DETECTION OF CORTICAL REORGANIZATION IN PEDIATRIC-ONSET MULTIPLE SCLEROSIS

R.O. Suarez[1], M.P. Gorman[2], M. Matson[2], S.P. Prabhu[1], S.K. Warfield[1]

[1]Radiology, [2]Neurology, Harvard Medical School, Boston Children's Hospital, Boston, MA, USA

Introduction: Pediatric-onset Multiple Sclerosis (POMS) leads to debilitating language, and motor impairments. Longitudinal MRI to monitor lesion burden is done in clinical disease management along with standard neuropsychological evaluations to monitor performance levels. Functional MRI (fMRI) presents a unique view of cortical functional recruitment in disease progression; however, presently this important disease-monitoring technology is not utilized in POMS disease management.

Objective: We performed a comparative study of POMS patients against age- and gender-matched healthy controls in order to test the hypothesis that POMS patients will demonstrate abnormal brain function in language, and primary motor systems resulting from disease-induced cortical reorganization. We designed novel fMRI metrics and statistical analysis procedures to quantify abnormal cortical recruitment in POMS patients compared to controls. We evaluate predictive strength of the fMRI metrics based on their correlation to performance scores derived from standard neuropsychological testing in the patients.

Methods: Establish normative fMRI localization and lateralization metrics for language, and primary-motor tasks in control volunteers. Evaluate fMRI maps in POMS patients to test for atypical language, and primary-motor activation patterns. Correlate fMRI metrics in POMS patients with their performance on neuropsychological evaluations. Evaluate fMRI activation patterns to detect abnormal cortical recruitment and by this means predict performance decline in POMS patients.

Results: Using a motor-specific task in controls—systematic tapping of the fingers of the right and then left hands—we observed the normative motor-specific activation pattern expected of this task. This normative activation pattern is characterized by contralateral activation of primary motor cortex in the frontal lobes. We detected atypical motor-specific activation patterns in 2 out of 5 POMS tested; abnormal activation patterns were detected in: POMS1 and POMS4 (Figure 1). Importantly, POMS1 and POMS4 suffer from motor deficits.

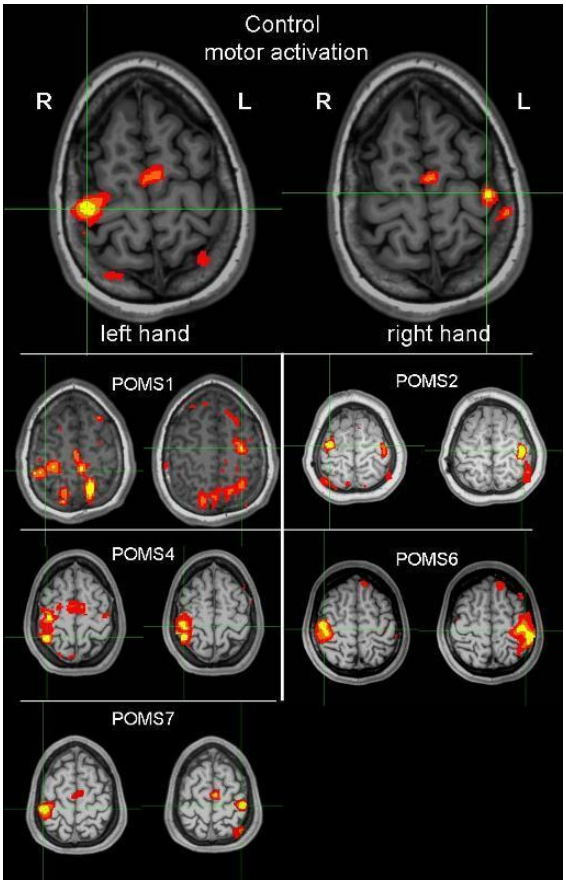

[Figure 1: FMRI of motor in controls and POMS.]

Using a vocalized antonym-generation task, we observed the normative language activation pattern expected of this task—characterized by left-dominant activation of language centers of the inferior frontal gyrus (expressive) and of the temporoparietal region (receptive), as well as bilateral activation of primary and secondary visual cortices consistent with visual presentation of words. We detected atypical language fMRI activation patterns in 4 out of 6 POMS tested; abnormal activation patterns were observed in: POMS2, POMS3, POMS4, and POMS6 (Figure 2).

Importantly, POMS2, POMS3, and POMS6 suffer from mild language impairments.

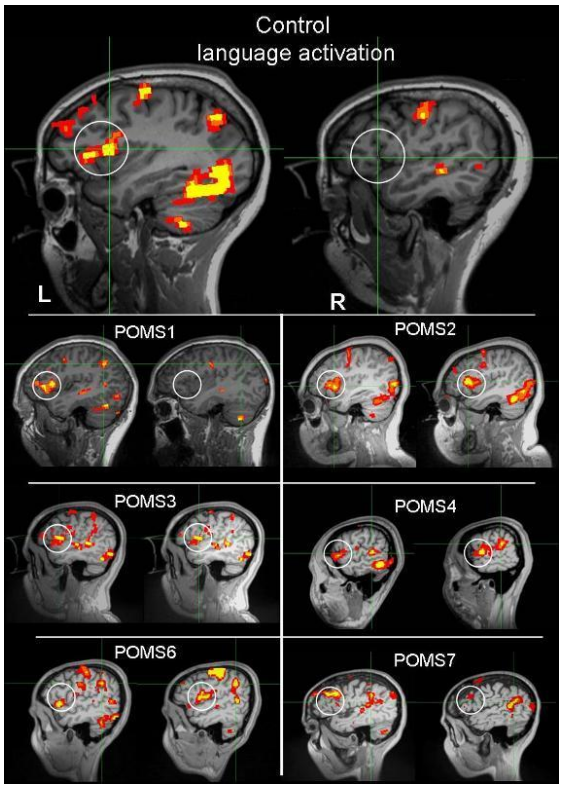

[Figure 2: FMRI of language in controls and POMS.]

Conclusions: Given that typical MS disease time course is highly variable in individuals, there is generally no specific timeline for the treatment regiment, until specific deficits are presented. Measures derived from neuropsychological examinations are helpful in that respect; however, the application of fMRI in the assessment of POMS cortical reorganization provides more advanced monitoring that is highly complimentary to the current standards. In this study, we demonstrate that fMRI motor and language activation patterns are indicative of performance decline in most of the POMS patients tested. This proof-of-concept has stimulated our increased recruitment and systematic study of cortical reorganization in larger MS populations.

Acknowledgement: Funded by NMSS Pilot Award PP1625 and NIH grant R01 LM010033

REGIONAL GRAY AND WHITE MATTER VOLUME INCREASES IN ADULT RAT BRAIN FOLLOWING 7 DAYS VOLUNTARY WHEEL RUNNING

A. Sumiyoshi[1], Y. Taki[1,2], H. Nonaka[1], H. Takeuchi[1], R. Kawashima[1]

[1]Institute of Development, Aging and Cancer, [2]Tohoku Medical Megabank Organization, Tohoku University, Sendai, Japan

Objectives: Multiple recent voxel-based morphometry (VBM) studies have identified structural brain changes in adult humans under various intervention protocols [1-3]. The comparable neuroimaging techniques in non-human animals need to be established so that one can investigate the underlying cellular and molecular mechanisms behind such structural brain plasticity [4]. In this study, we examined whether VBM in rats detect possible structural brain changes following voluntary wheel running.

Methods: Twelve pairs of adult male Wistar rats, one for exercise and the other for non-exercised control, were scanned in a 7.0-T MRI scanner at 3 time points, before exercise, after 7 days exercise, and at 7 days follow-up. The MRI images were analyzed using the rat atlas template and tissue prior probability maps that were recently published by our laboratory [5].

Results: Longitudinal VBM analysis revealed significant increases in regional gray and white matter volume of exercising rats. The most significant effects ($p < 0.05$ corrected for multiple comparisons) were localized in the left primary motor cortex. The changes of gray matter volume in the left motor cortex were significantly correlated with the total running distance ($p < 0.05$). The less significant effects ($p < 0.001$ uncorrected) were localized in the bilateral primary and secondary motor cortices, bilateral primary somatosensory cortices, right secondary visual cortex, right dorsolateral striatum, right laterodorsal thalamus, and midline cerebellum.

Conclusions: These results support the utility of longitudinal VBM study in rats and may lead to an alternative avenue for understanding the nature of structural brain plasticity in humans.

References:

1. Draganski et al. (2004) Neuroplasticity: changes in grey matter induced by training. Nature 427:311-312.

2. Colcombe et al. (2006) Aerobic exercise training increases brain volume in aging humans. J Gerontol A Biol Sci Med Sci 61:1166-1170.

3. Ilg et al. (2008) Gray matter increase induced by practice correlates with task-specific activation: a combined functional and morphometric magnetic resonance imaging study. J Neurosci 28:4210-4215.

4. Zatorre et al. (2012) Plasticity in gray and white: neuroimaging changes in brain structure during learning. Nat Neurosci 15:528-536.

5. Valdés-Hernández et al. (2011) An *in vivo* MRI template set for morphometry, tissue segmentation, and fMRI localization in rats. Front Neuroinform 5:26.

Acknowledgements: This study was supported by a Grant-in-Aid for Young Scientists (B) (KAKENHI 24791271) from the Ministry of Education, Culture, Sports, Science and Technology in Japan.

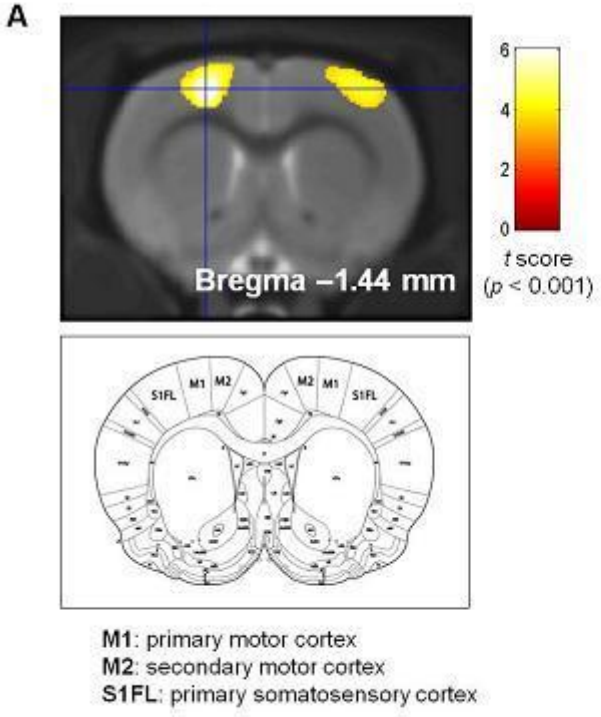

Figure: Regional gray matter volume increases following 7 days voluntary wheel running in adult rat brains.

(A) Red and yellow voxels represent clusters of significant regional gray matter volume increase ($p < 0.001$ uncorrected) from scan 1 to scan 2, superimposed on the mean T2-weighted image across all subjects. Note that the crosshair represents the left primary motor cortex.

(B) Mean and standard errors of the gray matter volume changes within the peak located in the left primary motor cortex.

(C) Correlation between the gray matter volume changes and the total running distance during 7 days voluntary wheel running.

NORMAL TIME-TO-PEAK BRAIN MAP - ANOTHER PARAMETRIC IMAGE FOR EVALUATION OF BRAIN PERFUSION

M.M.H. Teng[1], Y.-H. Kao[2], I.-C. Cho[2], F.-C. Chang[3], C.-J. Lin[3], C.-B. Luo[3], W.-Y. Guo[3]

[1]Radiology, National Yang Ming University, Taipei Veterans General Hospital, [2]National Yang Ming University, [3]Radiology, Taipei Veterans General Hospital, Taipei, Taiwan R.O.C.

Objective: We describe a new parameter to evaluate the brain perfusion, the normal TTP brain voxel map, or the normal TTP brain mask.

Material and methods: To produce the normal TTP brain voxel map, we did cerebrospinal fluid removal, and initial vessel voxels removal first. The criteria of normal TTP brain map is TTP values between the (TTP_{median} - 3 sec) and TTP_{median}. The TTP_{median} is the median of the TTP. If the TTP of the brain voxel is between (TTP_{median} - 3 sec) and TTP_{median}, the brain voxel is coded "1" if it is outside of the interval, the voxel is coded "0".

We evaluated the normal TTP bain voxel map of MR perfusion in 44 patients with cerebrovascular disease retrospectively.

Results: The normal TTP brain masks were consistent with the patients´ arterial and clinical conditions in all these patients. The bilateral hemispheres in the normal brain mask are grossly symmetrical in patients with bilateral normal arteries or unilateral slight stenosis. The normal brain mask is slightly asymmetrical in patients with unilateral moderate stenosis or unilateral severe carotid stenosis with good collateral circulation. They are obviously asymmetrical, with no or few voxels on the side with severe unilateral

carotid stenosis and poor collateral circulation at the Willis' circle or severe unilateral stenosis at M1.

Conclusion: The normal TTP brain mask is correlated with the patient's angiographic and clinical condition, and can be used for evaluation of vascular supply of the brain.

Reference:

Kao YH, Teng MMH, Zheng WY, et al. Removal of CSF voxels on brain MR perfusion images using first several images and Otsu's thresholding technique. Magn Reson Med 2010; 64:743-748.

LONGITUDINAL DIFFUSION KURTOSIS IMAGING OF NORMAL WHITE MATTER DEVELOPMENT IN RATS

K. van der Marel, W.M. Otte, U.S. Rudrapatna, A. van der Toorn, R.M. Dijkhuizen

Biomedical MR Imaging and Spectroscopy Group, Image Sciences Institute, University Medical Center Utrecht, Utrecht, The Netherlands

Objectives: Understanding alterations of neural tissue properties during and beyond adolescence may help to identify developmental deficits underlying neuropsychiatric illness[1]. Diffusion Tensor Imaging (DTI) conventionally captures structural integrity and architecture of anisotropic neural tissue, in particular white matter. Recently, Diffusion Kurtosis Imaging (DKI) has been introduced to also inform on (directional) kurtosis[2], potentially providing higher sensitivity for alterations during post-natal brain development[3]. The aim of the present study was to assess the sensitivity of tissue kurtosis parameters for capturing developmental alterations in white matter through adolescence (25-46 days) into adulthood (>60 days) by serially applying DKI.

Methods: Male Wistar rats (*n*=20) underwent MRI (4.7T) at post-natal day (P)25,32,46,60,88,123,158,200, and 284. Animals were anesthetized (isoflurane) and mechanically ventilated. DKI was acquired (*b*=650,1285,1919,2518s/mm^2, 30 directions/*b*-value), and quantitative of diffusion (FA=fractional anisotropy, MD=mean diffusivity) and kurtosis parameters (MK=mean kurtosis, $K_{parallel}$=parallel kurtosis, $K_{perpendicular}$=perpendicular kurtosis) were obtained after tensor fitting[4]. Additionally, T_2-maps and myelination-sensitive Magnetization Transfer Ratio (MTR)-maps were obtained. White matter tissue segmentation was achieved using a supervised classification algorithm[5] that was trained on T_2, FA, MD, and spatial features of cerebral white matter delineations from a separate study. Parameter averages weighted by the white matter probabilities were calculated. Spline regression was then applied to model the time course of parameter changes, with the spline degrees of freedom optimized (AIC). Fits were also obtained for parameters in mid-cortical gray matter, and for the ratio between parameters in white and gray matter.

Results: Cerebral white matter volume increased on average by 98% between P25-P88 (from 95±7.3mm^3 to 189±6.3mm^3), and overall by 143% to 230±12.3mm^3 at P284. Panel **A** shows fits and 95% confidence intervals for FA (R^2=0.53), MD (R^2=0.15), MK (R^2=0.66), $K_{parallel}$ (R^2=0.53), $K_{perpendicular}$ (R^2=0.68), MTR (R^2=0.69), T_2 (R^2=0.85), and white matter volume (R^2=0.96). MTR, $K_{perpendicular}$ and MK displayed the largest changes in early adulthood (**B**). At around 21 weeks, FA started to decrease, while kurtosis parameters and MTR continued to increase. In absolute terms, FA exhibited the highest contrast, with opposite trajectories of equal magnitude in gray and white matter (**C**). However, $K_{perpendicular}$ and MTR showed more rapid and larger increases in contrast properties. MK, MD, and T_2 had similar white and gray matter profiles.

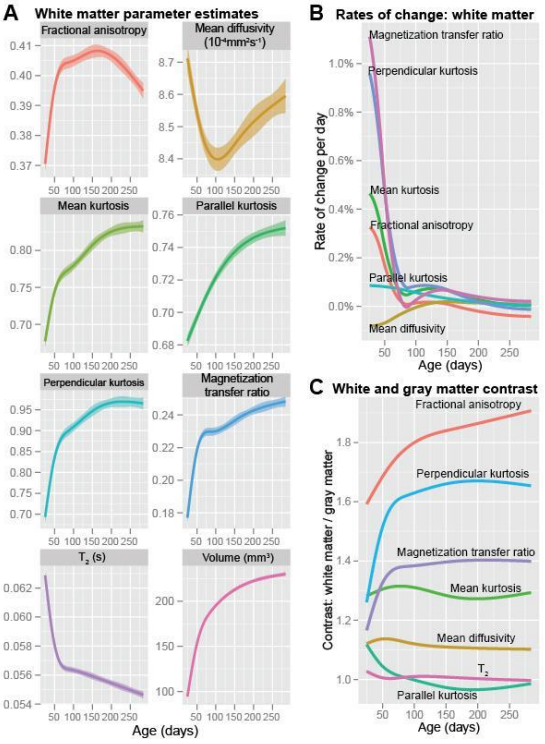

[Parameter trajectories in gray and white matter]

Conclusions: Our findings of increased white matter volume and diffusion parameters values are in line with reports of DTI in young rats[6] and humans[7]. This has been associated with continued myelination or increases of axonal caliber[7]. We found that rates of change of kurtosis parameters (mainly $K_{perpendicular}$) and their contrast properties are different from conventional diffusion measures, particularly during early life. The similarity between $K_{perpendicular}$ and MTR trajectories may indicate a higher sensitivity of kurtosis measures for detection of myelin development.

References:

[1]Andersen, *Neurosci.Biobehav.Rev.* **27**(2003);

[2]Wu and Cheung, *NMR.Biomed.* **23**(2010);

[3]Cheung *et al.*, *Neuroimage* **45**(2009).

[4]Tabesh *et al.*, *Magn.Reson.Med.* **65**(2011);

[5]Breiman, *Machine Learning* **45**(2001);

[6]Bockhorst *et al.*, *J.Neurosci.Res.* **86**(2008);

[7]Schmithorst and Yuan, *Brain.Cogn.* **72**(2010).

MOLECULAR MRI OF ICAM-1 EXPRESSION AT DIFFERENT STAGES AFTER EXPERIMENTAL STROKE IN MICE

G.A. Van Tilborg[1], L.H. Deddens[1], K. van der Marel[1], H. Hunt[1], A. van der Toorn[1], H.E. de Vries[2], R.M. Dijkhuizen[1]

[1]Biomedical MR Imaging & Spectroscopy Group, Image Sciences Institute, University Medical Center Utrecht, Utrecht, [2]Department of Molecular Cell Biology and Immunology, VU University Medical Center, Amsterdam, The Netherlands

Introduction: Recent studies have demonstrated the potential of molecular MRI for in vivo detection of neurovascular inflammation in rodent models of neurological disorders. Expression of endothelial cell adhesion molecules, such as P- and E-selectin and VCAM-1, can be directly targeted with functionalized contrast agents, allowing their detection after experimental brain injuries.[1,2] In contrast to the abovementioned cell adhesion molecules, ICAM-1 is not only expressed on (inflamed) endothelium, but also on leukocytes. Molecular MRI of ICAM-1 would therefore provide an interesting opportunity to image endothelial activation as well as leukocyte invasion in relation to stroke pathophysiology and (anti-inflammatory) treatment.

Objective: The goal of the current study was to determine the potential of a novel molecular MRI probe for in vivo imaging of vascular ICAM-1 expression and leukocyte infiltration at different stages after transient unilateral stroke in mice.

Material and methods: Antibody-functionalized MR contrast agent was obtained by incubation of micron-sized iron oxide particles (MPIO) with murine ICAM-1 antibody (αICAM-1) or irrelevant immunoglobulin G antibody (IgG). Transient focal cerebral ischemia was induced in isoflurane-anesthetized C57Bl/6 mice by unilateral 30-min intraluminal middle cerebral artery occlusion (MCAo).

T_2- and T_2*-weighted MRI were at 9.4 T before and 1 h after intravenous injection of IgG-MPIO or αICAM-1-MPIO under isoflurane anesthesia. MRI was done at 1 (n=6/4), 2 (n=5/5), 3 (n=4/5), 7 (n=4/4), or 21 (n=4/5) days post-stroke. Brain lesions, lesion borderzones and contralesional tissue were

were outlined, and the volume percentage of contrast-enhanced (CE) voxels within these regions was calculated.

After MRI scan, mice were sacrificed for immunohistochemical staining for ICAM-1, CD45 and iron.

Results: Substantial post-contrast hypointensities, particularly in the ipsilesional hemisphere, were observed after injection of αICAM-1-MPIO at day 1 and day 2 and, to lesser extent, at day 3 post-stroke (Figure, left). No contrast enhancement was detected at 7 days post-stroke. At day 21, pre-contrast hypointense areas marginally enlarged after αICAM-1-MPIO injection. IgG-MPIO injection resulted in neglible contrast effects at all time-points.

Significant increase in the volume of hypointense voxels was observed in the lesion core at days 1, 2 and 3 post-stroke after αICAM-1-MPIO injection, and in lesion borderzone and contralesional tissue at post-stroke day 2 (Figure, right). No significant MPIO-induced enlargement of hypointense volume was detected at days 7 or 21 post-stroke.

At post-stroke days 1 and 2, MPIO were abundantly present in the lesion territory, and strictly confined to ICAM-1-positive vessels. Some MPIO co-localized with CD45-positive leukocytes. At day 21, massive cellular infiltration was evident. Considerable amounts of MPIO were found throughout the lesion core, associated with leukocytes. Tissue from animals that received IgG-MPIO revealed no MPIO presence.

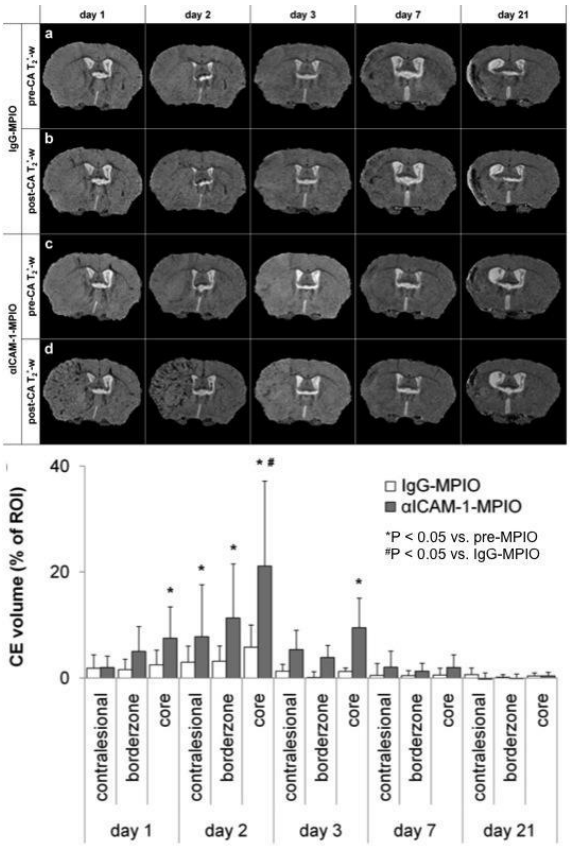

Conclusions: This study shows that molecular MRI with αICAM-1-MPIO offers a unique approach for *in vivo* imaging of endothelial ICAM-1 expression and vascular leukocyte adhesion after experimental stroke. However, accumulation of iron-containing cellular infiltrates may hamper the detection of MPIO at chronic stages.

References:

1. Sibson et al., Methods Mol Biol 2011;711:379-396

2. Deddens et al., Cerebrovasc Dis 2012;33:392-402

INTER SUBJECT VARIABILITY, WITHIN AND BETWEEN SESSION REPRODUCIBILITY OF DIFFUSION TENSOR IMAGING AND IMPORTANCE IN INTERVENTIONAL AND LONGITUDINAL STUDIES

T. Veenith[1], E. Carter[1], J. Grossac[1], V. Newcombe[1], J. Outtrim[1], V. Lupson[2], G. Williams[2], D. Menon[1], J. Coles[1]

[1]Division of Anaesthesia, [2]Wolfson Brain Imaging Centre, University of Cambridge, Cambridge, UK

Background and aim: Diffusion tensor imaging (DTI) has been used to identify neuronal injury and predict outcome in a variety of neurological disorders such as traumatic brain injury, multiple sclerosis, Alzheimer's dementia and psychiatric disorders.The aim of these studies was to provide reference data on intersubject variability and reproducibility of diffusion tensor imaging.

Methods: Healthy controls underwent imaging on two occasions using the same 3T Siemens Verio magnetic resonance scanner. At each session two identical diffusion tensor sequences were obtained along with standard structural imaging. Fractional anisotropy, apparent diffusion coefficient, axial and radial diffusivity parameters were created and regions of interest applied in normalised space. The baseline data from all 26 controls were used to calculate intersubject variability, while within session reproducibility was calculated separately for the baseline and follow up sessions within six months in 25 and 22 controls respectively. Between session reproducibility was calculated for 22 volunteers who completed both sessions. The data were also used to calculate the 95% confidence interval for zero change within the same and different imaging sessions.

Results: The within and between session reproducibility data were lower than the values for intersubject variability, and were different across the brain. The mean (range) coefficient of variation figures for within session reproducibility were 1.9 (0.9 - 4.7%), 1.3 (0.4 - 3.6%), 1.2 (0.4 - 3.5%) and 1.8 (0.6 - 4.3%) for fractional anisotropy, apparent diffusion coefficient, axial and radial diffusivity, and were lower than between session reproducibility measurements (2.8 (1.0 - 5.5%), 2.3 (1.0 - 5.3%), 2.0 (1.1 - 4.6%) and 3.5 (1.6 - 6.9%); $p < 0.001$). The calculated 95% prediction intervals for zero change for the within and between session datasets were similar.

Conclusions: This study provides additional reference data concerning intersubject variability and reproducibility of DTI conducted within the same imaging session (within session) and different imaging sessions (between session) in a group of healthy volunteers. While overall DTI measurements were relatively stable the CoV for repeated DTI sequences obtained during the same session (within session) were lower than those obtained from measurements obtained in a different imaging session separated by up to six months. These data can be used to calculate the 95% prediction interval for zero change and utilised in interventional studies to quantify change within a single imaging session, or to assess the significance of change in longitudinal studies of brain injury and disease.

RELIABILITY OF 2D AND 3D PSEUDO-CONTINUOUS ARTERIAL SPIN LABELING PERFUSION MRI IN ELDERLY POPULATIONS - COMPARISON WITH 15O-WATER PET

D.J. Wang[1], E. Kilroy[1], L. Apostolova[1], C.Y. Liu[1,2], L. Yan[1], J. Ringman[1]

[1]Neurology, UCLA, [2]Neurology, Univ of Southern California, Los Angeles, CA, USA

Objective: Arterial spin labeling (ASL) perfusion MRI is an appealing approach for measuring perfusion in dementia by utilizing magnetically labeled arterial blood water as an endogenous tracer (1). The purpose of this study was to investigate the reliability and accuracy of two pseudo-continuous ASL (pCASL) sequences, using 2D gradient-echo echo planner imaging (EPI) and 3D gradient and spin echo (GRASE) as the readout respectively (2), and to compare them with 15O-water PET.

Materials and methods: MRI was performed on a Siemens 3T Trio scanner. Each sequence was performed twice four weeks apart on 6 normal control subjects, 6 elderly subjects with mild cognitive impairment (MCI), and one participant with Alzheimer's' disease (AD)(mean age = 68 ± 5.8). Imaging parameters were: FOV=220mm,

matrix=64x64, labeling duration=1.5s, post-labeling delay (PLD)=1.5s, TR=4s, rate-2 GRAPPA, TE=11/22ms for EPI and GRASE.

Eight of these subjects also underwent $H_2{}^{15}O$ PET scans using a whole-body ECAT EXACT HR+ Siemens PET scanner, on the same day or proximal to their second MRI scan. 10-15mCi of 15O-water was injected as a rapid bolus (< 5 sec). A series of dynamic frames were acquired for a total of 2min following injection, and 3-4 injections were performed in each subject with a 10min break between each. The longitudinal repeatability of EPI and GRASE pCASL were evaluated with the intra-class correlation coefficient (ICC) and within-subject coefficient of variation (wsCV). The accuracy was evaluated by correlating ASL CBF and PET CBF across regions-of-interest (ROI) based on the automated anatomical template as well as across brain pixels.

Results: The ICCs of global perfusion measurements were 0.697 and 0.413 for GRASE and EPI based pCASL respectively (Table 1).

	EPI pCASL	EPI pCASL	EPI pCASL	EPI pCASL	GRASE pCASL	GRASE pCASL	GRASE pCASL	GRASE pCASL
	CBF Scan1	CBF Scan2	ICC	CV	CBF Scan1	CBF Scan2	ICC	CV
Grey Matter	54.33 ± 10.84	54.72 ± 8.99	0.404	0.102	48.02 ± 10.37	52.33 ± 9.95	0.718	0.099
White Matter	25.75 ± 7.85	25.16 ± 10.50	0.424	0.256	31.56 ± 7.90	33.55 ± 7.30	0.623	0.117
Whole Brain	47.58 ± 9.96	48.01 ± 8.45	0.413	0.106	43.29 ± 9.55	47.20 ± 8.43	0.697	0.103

[Table 1.Test-retest results of mean CBF]

GRASE pCASL also demonstrated a higher longitudinal repeatability for regional perfusion measurements across 24 regions-of-interests (ICC=0.707, wsCV=10.9%) compared to EPI pCASL (ICC=0.362, wsCV=15.3%). When compared to PET, EPI pCASL showed a higher degree of spatial correlation with PET than GRASE pCASL (pCASL EPI r= .53, SD= .06, $p < .001$, pCASL GRASE r=.51, SD= .08, $p < .001$) , although the difference was not statistically significant.

Conclusion: PCASL with 3D readout may provide a reliable imaging marker for the evaluation of disease progression and treatment effects in MCI and early AD subjects. Further technical developments are needed for minimizing spatial blurring in 3D acquisitions.

References:

1) Alsop DC et al, Journal of Alzheimer´s disease 2010;20(3):871-880

2) Fernandez-Seara MA et al, Magn Reson Med 2008;59(6):1467-1471

PHARMACOLOGICAL MRI AND TENSOR-BASED MORPHOMETRY IN THE 6-OHDA RAT MODEL OF PARKINSON'S DISEASE

R. Westphal[1], C. Simmons[1], M. Mesquita[1], T.C. Wood[1], W.R. Crum[1], D. Duricki[1], A. Vernon[2], S.C. Williams[1], D. Cash[1]

[1]Neuroimaging Department, Institute of Psychiatry, [2]Psychosis Studies, Institute of Psychiatry, King's College London, London, UK

Introduction: The neurotoxin 6-hydroxydopamine (6-OHDA), when administered into the medial forebrain bundle of rats, damages the dopaminergic nigrostriatal pathway. This models parkinsonian features such as reduced dopamine and dopaminergic neural terminals in the striatum[1]. The 6-OHDA rat has been widely used as a test-bed for many symptomatic and neuroprotective agents. The aim of this study was to further evaluate the 6-OHDA rat in terms of structural and functional brain abnormalities in order to identify new biomarkers and provide new targets for therapeutic interventions.

Methods: Male adult Sprague-Dawley rats were lesioned by a stereotaxic unilateral injection of 11.76 µg 6-OHDA (n=18) or saline (sham group, n=18) into the left medial forebrain bundle (AP -4.4, ML +1, DV -7.8). Serial structural MR images were acquired before surgery (baseline) and at 48 hours, 1, 3 and 5 weeks post-surgery. Images were

analyzed using a tensor-based morphometry (TBM) approach[2, 3]. Resulting statistical parametric maps (SPM's) are of significant ($p < 0.01$, uncorrected) difference between the lesioned and the sham group. At the final (5th week) time-point, pharmacological MRI (phMRI) was performed using a BOLD contrast-sensitive gradient echo technique.The rats were continually imaged for 30 min before and 60 min after the administration of dopamine agonist apomorphine (0.1 mg/kg sc). PhMRI data were pre-processed and statistically analysed [regressor based on behavioural data (not shown)] by SPM8 software (Wellcome Trust Centre for Neuroimaging).

Results: PhMRI revealed a stronger BOLD signal in the lesioned (ipsilateral) than in contralateral side of the 6-OHDA rat brains in several regions including thalamus, frontal cortex and the brain stem, in contrast to the shams where only the bilateral thalamic BOLD signal increase was observed, with very small changes in the other areas (Fig 1). The TBM analysis showed an apparent tissue volume contraction in the ipsilateral brain stem at 2 days and 5 weeks post-surgery, and in the ipsilateral frontal cortex at 5 weeks (Fig 2).

Conclusion: The structural changes in the brain stem that coincide with functional abnormality in the same area give rise to a structure-function relation which has been shown to be true in PD patients[4]. Moreover, it could be postulated that in addition to striatal dopamine depletion, brain stem degeneration enforces thalamic impairment seen by phMRI. Thus, the visualization of structural and functional alterations in the integrity of thalamus, frontal cortex and brain stem in this animal model lends further credence to the validity of 6-OHDA rat for modelling multiple aspects of human PD and may broaden its application for therapeutic intervention targeting the brain stem-thalamo-cortical pathway.

References:

1. Duty et al, 2011, Br J Pharmacol 164:1357-1391,

2. Vernon et al, 2011, PLoS One 6:e17269,

3. Crum et al, 2005, Physics in Medicine and Biology 50:5153-5174,

4. Hirsch et al, 1987, Proc Natl Acad Sci U S A 84:5976-5980.

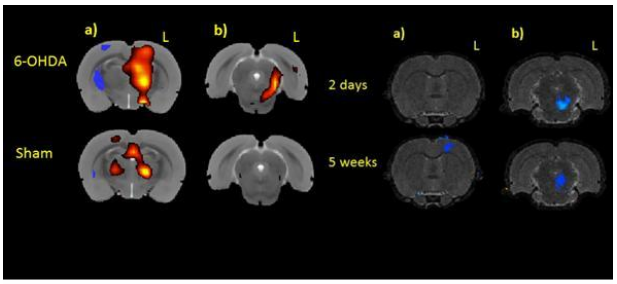

Fig 1: BOLD signal of apomorphine-induced activations in thalamus and frontal cortex (a) and brain stem (b). SPM's ($p<0.01$, uncorrected) depict increases (red-yellow) and decreases (blue-green). L=lesioned side (ipsilateral).

Fig 2: Structural comparison between the shams and 6-OHDA rats mean normalised MR images for 2 days and 5 weeks post-surgery ($p<0.01$, uncorrected). Blue-green indicates local tissue volume contraction. Frontal cortex (a), brain stem (b).

[phMRI and structural MRI results]

INCREASED COX ACTIVITY IN MELAS IS LINKED TO SEVERE SKELETAL ENERGY FAILURE BY 31P-MRS

F. Niu[1], L. Zhuo[2], F. Chen[3], **Y. Xu**[2]

[1]Department of Pathology, Drum Tower Hospital of Nanjign University Medical School, [2]Department of Neurology, Affiliated Drum Tower Hospital of Nanjing University Medical School, [3]Department of Radiology, Drum Tower Hospital of Nanjign University Medical School, Nanjing, China

Objectives: Mitochondrial myopathy, encephalopathy, lactic acidosis, and stroke-like episodes (MELAS) syndrome is a mitochondrial encephalopathy subgroup. Until now, the pathogenesis of MELAS is unclear. Previous studies proposed that mtDNA mutation induced mitochondrial neuropathy as the underlying causes. But this theory can not fully explain the clinical phenotype and relationship with the molecular defect. Recently another interesting hypothesis suggested that the residual cytochrome c oxidase (COX) activity lead to energy production dysfunction, because ragged-red fibers (RRFs) and succinate dehydrogenase-reactive vessels (SSVs) seen in MELAS are typically COX positive, while those seen in MERRF or CPEO are mostly COX negative. The purpose of this study is to determine if the abnormal increasing COX activity in MELAS, as detected by muscle biopsy, could result in abnormal ATP energy metabolism in resting and after exercise, compared to CPEO and control subjects by 31P-MRS at 3T.

Methods: Patients selection: From January 2008 to December 2012, 21 patients with suspected mitochondrial encephalomypathies were recruited from Drum Tower Hospital of Nanjing University Medical School, 7 cases were diagnosed as MELAS and 6 cases were CPEO by muscle biopsy and gene detection.

31P-MRS: Measurements were performed on 13 patients either with MELAS or CPEO and 10 healthy men using a 3T MRS scanner. Quadriceps femoris muscle was chosen to measure high-energy phosphate before, during and after 6 minute plantar flexion exercise in a supine position. The plantar flexion exercise was performed with a constant load of maximal voluntary contraction. The ratio of Pi/PCr, and mitochondrial ATP production were calculated.

Results: Muscle biopsy: Tab. 1 showed the detailed clinical information of these patients. Fig. 1 showed the muscle biopsy examination: in MELAS patients the ragged-red fibers and vessel walls are typically COX positive, while in CPEO patients these RRF are mostly deficient for COX histochemical staining, suggested that the MELAS patients may have more residual respiratory chain activity relative to CPEO patients.

31P-MRS: Fig. 2 shows maximal voluntary contraction (MVC) load in our healthy volunteers and patients groups. Fig. 3 shows the ratio change of Pi/Pcr, and ATP before, during ,and after 6 minutes plantar flexion exercise in a supine position with sand bags. Our results suggested patients with MELAS/CPEO disorders displayed rapid phosphocreatine (PCr) depletion during exercise and a delay in PCr recovery after exercise, compared to controls. Moreover, in MELAS patients we observed lower ratio of ATP and more declined PCr after exercise recovery , suggesting that MELAS patients might have severe dysfunction of skeletal muscle energy metabolism than CPEO patients.

Tab 1 MELAS

Patients	Total	COX+		COX-	
		RRF+	SSV+/SDH N	RRF+	SSV+/SDH N
1	918	29	159	11	84
2	2275	56	215	19	124
3	1556	43	204	27	111
4	864	37	171	30	64
5	1728	61	218	46	83
6	1320	26	120	10	72
7	1853	52	188	25	109

CPEO

Patients	Total	COX+		COX-	
		RRF+	SDH N	RRF+	SDH N
1	2486	0	21	42	168
2	1683	0	16	33	147
3	749	1	3	19	92
4	943	4	9	44	73
5	3014	2	18	56	115
6	1947	3	25	51	189

Fig 1

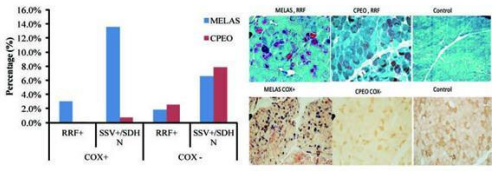

[attachment figure-01]

Fig 2

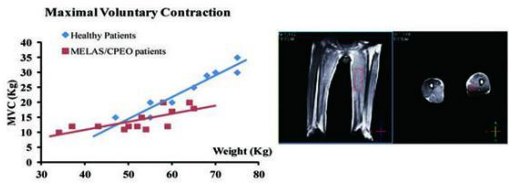

[attachment figure-02]

Fig 3

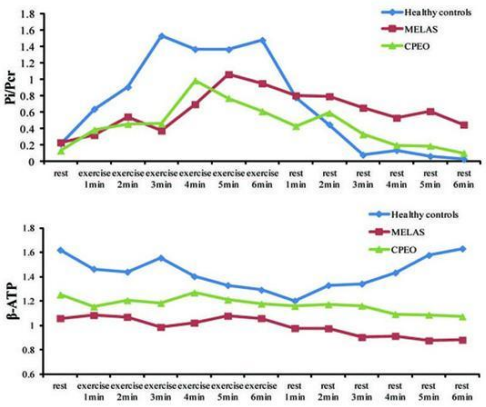

[attachment figure-03]

Conclusions: Unlike the most mitochondrial disorders such as MERRF and CPEO, COX (comples IV) histochemical activity is only partially reduced in muscle of MELAS patients. This observation suggested that there is a relative preservation of respiratory chain activity in MELAS. However, our results were contrary to this hypothesis. Using 31P-MRS we found that MELAS patients had a significant depletion of high-energy phosphoate (ATP and PCr) after exercise compared to CPEO patients, suggesting that MELAS patients may have a severe respiratory defect.

METABOLIC CHANGES IN SYMPTOMATIC ATHEROSCLEROTIC LARGE-ARTERY OCCLUSIVE DISEASE EVALUATED BY PROTON MAGNETIC RESONANCE SPECTROSCOPY

T. Yagi[1], K. Hashimoto[1], S. Yagi[2], M. Shimizu[2], T. Shimizu[2], T. Horikoshi[1], H. Kinouchi[1]

[1]Department of Neurosurgery, Interdisciplinary Graduate School of Medicine and Engineering, University of Yamanashi, Chuo, [2]Kanto Neurosurgical Hospital, Kumagaya, Japan

Objectives: Proton MR spectroscopy (MRS) is valuable for identifying metabolic changes occurring during brain ischemia. Although N-acetylaspartate (NAA) measurement by MRS is shown to be useful to detect neuronal damage in acute stage of cerebral ischemia, clinical significance and the availability of the NAA measurement in chronic stage of cerebral ischemia are still obscure. [1-3] We examined a serial change of NAA/Creatinin (Cr) ratio in patients who underwent EC-IC bypass in chronic stage of ischemia and investigated the influence of revascularization surgery on the brain metabolism.

Material and methods: Between October 2009 and December 2010, 14 patients with symptomatic athelosclerotic large-artery occlusive disease were treated in our institute. Nine patients who underwent EC-IC bypass, five patients who received conservative treatment, and three healthy volunteers were studied. ^{1}H-MRS was obtained using Philips Achieva 3.0T. Multi-voxcel spectra were recorded using a SE-2D-CSI sequence (TR/TE = 2000/288 ms). The volume of interest was placed in the frontal white matter of both hemispheres axially above the lateral ventricles. Surgery was done on average 45 days after the onset. ^{1}H-MRS was performed before and 1week, 1 and 3 months after surgery. In the conservative treatment group, ^{1}H-MRS was performed 1, 2 and 4 months after the onset of cerebral infarction. Serial change of ischemia/contralateral side ratio (I/C ratio) of NAA/Cr between bypass group and conservative treatment group was compared.

Results: In the healthy volunteer group, laterality of NAA/Cr and the serial change were not seen. Six patients in bypass group had significant lower NAA/Cr on the affected side compared to the contralateral side at 1 month after onset. In these patients, I/C ratio of NAA/Cr was increased 11 percentage point after 3months from surgery. All patients in the conservative treatment group also had significant lower NAA/Cr on the affected side, but I/C ratio of NAA/Cr was increased 3 percentage point in duration of 3 months after onset. The improvement range of I/C ratio of NAA/Cr was significantly higher in bypass surgery group.

Conclusions: The present study demonstrated that decreased NAA/Cr shown in the chronic stage of cerebral ischemia is reversible. MRS may provide useful information of impaired metabolic state in patients with chronic stage of cerebral ischemia.

References:

[1] M. Hund-Georgiadis, D.G. Norris, T. Guthke, D.Y. von Cramon, Characterization of cerebral small vessel disease by proton spectroscopy and morphological magnetic resonance, Cerebrovasc. Dis. 12 (2001) 82-90.

[2] S. Muñoz Maniega, V. Cvoro, F.M. Chappell, P.A. Armitage, I. Marshall, M.E. Bastin, et al., Changes in NAA and lactate following ischemic stroke: a serial MR spectroscopic imaging study, Neurology. 71 (2008) 1993-1999.

[3] A. Nitkunan, R.A. Charlton, T.R. Barrick, D.J.O. McIntyre, F.A. Howe, H.S. Markus, Reduced N-acetylaspartate is consistent with axonal dysfunction in cerebral small vessel disease, NMR Biomed. 22 (2009) 285-291.

NETWORK ASYMMETRY OF VISUAL AREAS REVEALED BY RESTING-STATE FUNCTIONAL MRI

L.-R. Yan[1], Y.-B. Wu[2]

[1]Department of Information, Wuhan General Hospital of Guangzhou Command, [2]Department of Unmanned Aerial Vehicle, Wuhan Mechanical Technology College, Wuhan, China

Objectives: There are ample functional magnetic resonance imaging (fMRI) studies on functional brain asymmetries, but the network asymmetry is little known. Brain network embodies the brain dynamics, i.e., the temporal characteristic, while brain asymmetry

represents an effect-hemisphere interaction, i.e. the spatial characteristic. So far the unified analysis of these two characteristics is less established.

Methods: An automatic network asymmetry analysis schema was formulated. The network asymmetry was defined as the difference between the left and right part of a particular default mode network (DMN) in the resting state. DMN was described using the functional connectivity MRI (fcMRI) analysis. Visual areas, including primary and secondary visual areas (Brodmann's area (BA) 17, 18) were regions of interest (ROIs). The following steps were included: (i) spatial preprocessing; (ii) ROI definition and timeseries extraction; (iii) the first-level analysis, to detect the DMN corresponding to the ROIs; (iv) modification of the contrast images and (v) the second level and asymmetry analysis, to detect the areas with network asymmetry. Twelve healthy male subjects with mean age 29.8±6.4 were studied. They were all right-handed and had no neurological or physical disorder. Data were acquired in a GE Signa System operating at 1.5 T with a gradient echo EPI sequence.

Results: For left and right BA 17, the DMN asymmetry existed in several consistent foci including left precentral gyrus (with the peak value near [-52 4 48]), medial frontal gyrus ([-24 24 58], [-42 46 30]), inferior parietal lobe ([-52 -36 54]), and right lingual gyrus ([4 -98 2]), cuneus ([6 -78 26]) and cingulated gyrus ([14 -60 16]). It is noted that the left side of the resulting images represents 'left > right' asymmetry, while the right side represents 'right > left' asymmetry in neurological display convention. For left and right BA 18, the DMN asymmetry existed in several consistent foci including the right insula (with the peak value near [40 -6 6]), cerebellum posterior lobe ([34 -42 -40), and cuneus ([6 -90 26]).

Conclusions: There existed asymmetries of DMN for the visual areas in the resting state. The primary visual areas had stronger connectivity with the left hemisphere, and the secondary visual areas had stronger connectivity with right hemisphere. The foci in the left hemisphere included precentral gyrus, parietal lobe related with the processing of visual sensory information. The foci in the right hemisphere included lingual gyrus, cuneus, cingulated gyrus, and insula related with visual attention and visual memory. There results imply the left hemisphere dominance for junior visual information processing and right hemisphere dominance for senior visual information processing.

References:

1. Greicius MD, Krasnow B, Reiss AL, Menon V. Functional connectivity in the resting brain: A network analysis of the default mode hypothesis. Proc Natl Acad Sci USA 2003, 100(1):253-258.

2. Theorina A, Johanssona RS. Zones of bimanual and unimanual preference within human primary sensorimotor cortex during object manipulation. NeuroImage 2007, 36:T2-T15.

3. Seghier ML. Laterality index in functional MRI: methodological issues. Magn Reson Imaging 2008, 26:594-601.

CONTRAST-ENHANCED MRI OF INTRA- AND PERILESIONAL VASCULAR CHANGES AFTER FOCAL CEREBRAL ISCHEMIA IN RATS

P. Yanev, P. Seevinck, M. Bouts, U. Rudrapatna, A. van der Toorn, R.M. Dijkhuizen

Biomedical MR Imaging & Spectroscopy Group, Image Sciences Institute, University Medical Center Utrecht, Utrecht, The Netherlands

Objective: After acute ischemic stroke, reorganization of neural tissue may contribute to reinstatement of lost function.[1] This metabolically demanding process may be supported by ongoing remodeling of the associated cerebrovasculature. Uncovering the spatiotemporal characteristics of vascular changes in reorganizing brain tissue increases our understanding of endogenous repair mechanisms[2], which may be exploited for development of neuroreparative therapies to enhance post-stroke recovery.

Our goal was to noninvasively characterize the nature and pattern of vascular remodeling in and around the primary lesion from subacute to chronic time-points after experimental focal cerebral ischemia.

Methods: Focal cerebral ischemia was induced by 60-min unilateral middle cerebral artery occlusion with an intraluminal filament in isoflurane-anesthetized male Wistar rats.

MRI was conducted on a 4.7 T MR system at 1 (n=5), 7 (n=5), 21 (n=9) or 70 days (n=9) after stroke. Multislice steady-state susceptibility contrast-enhanced MRI was performed using multiple spin-echo ($TR/TE_1/\Delta TE$=3500/13/13 ms) and multiple gradient-echo ($TR/TE_1/\Delta TE$=1800/4/4 ms) imaging, before and after injection of ultrasmall particles of iron oxide (16.5 mg/kg). Subsequently, ΔR_2^* and ΔR_2 were calculated as measures of total and microvascular cerebral blood volume (CBV), respectively.[3]

Lesioned tissue was identified on pre-contrast T_2 maps (2SD above the mean contralateral tissue T_2), followed by image processing (i.e., erosion and dilation) to select three ipsilateral regions-of-interest (ROIs): 1. lesion core; 2. intralesional borderzone; and 3. extralesional borderzone (figure A). A contralateral ROI encompassing cortical and subcortical tissue was also defined. Voxels with significantly increased ΔR_2^* and ΔR_2 inside ROIs were identified by thresholding at 2SD above the mean value in the contralateral ROI. Relative volumes of tissue with elevated ΔR_2^* and ΔR_2 were calculated for each ROI.

Results: Vascular contrast-induced ΔR_2^* (total CBV) and ΔR_2 (microvascular CBV) values revealed a heterogeneous spatiotemporal profile between days 1 and 70 after stroke (figures B and C). The percentage of tissue with elevated ΔR_2^* was significantly raised at days 1 and 7 after stroke in the lesion borderzone ($P< 0.05$ vs. contralateral), which normalized at subsequent time-points. One day post-stroke the lesion core and intralesional borderzone had significantly reduced areas with high ΔR_2 as compared to contralateral. Significantly enlarged areas with elevated ΔR_2 appeared between one and three weeks in the intra- and extralesional borderzone, which persisted in the extralesional borderzone up to day 70.

Conclusions: At early time-points following transient cerebral ischemia, increased total CBV in and around the ischemic tissue lesion may signify vasodilation, while decrease of the area of high microvascular CBV may be associated with (edema-related) vascular collapse. Gradual increase of areas with elevated microvascular CBV in the lesion borderzone between one and ten weeks post-stroke may be related to ongoing angiogenesis, which could contribute to restoration of neuronal networks.

References:

[1]Murphy et al. Nat Rev Neurosci. 2009;10:861-72.

[2]Yanev and Dijkhuizen. Stroke. 2012;43:3436-41.

[3]Seevinck et al. Angiogenesis. 2010;13:101-11.

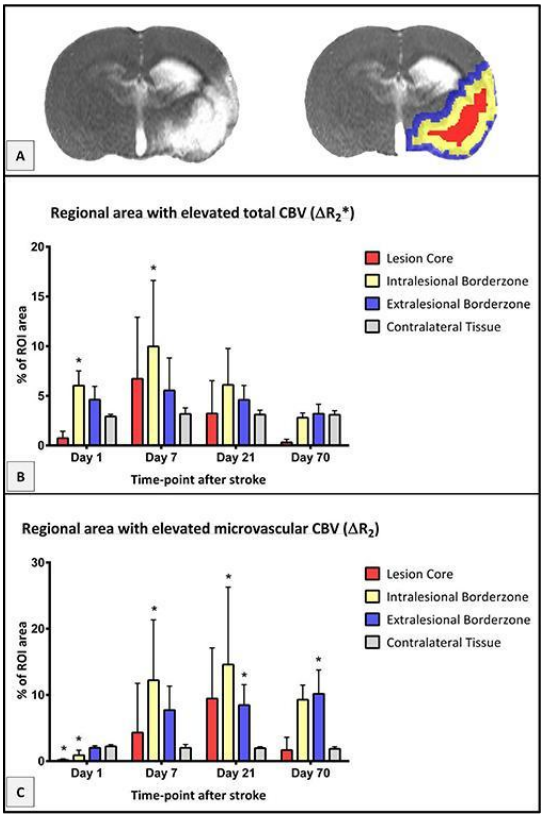

INTRAOPERATIVE HEMODYNAMIC MONITORING IN THE ARTERIOVENOUS MALFORMATION SURGERY: THE ROLE OF INTRAOPERATIVE MRI

F. Zhu[1], Y. Mao[2], D. Song[2], W. Zhu[2], Y. Gu[2], B. Xu[2], J. Wu[2], L. Zhou[2]

[1]Department of Neurosurgery, Huashan Hospital, [2]Fudan University, Shanghai, China

Objective: In a series of six patients diagnosed of intracerebral AVM which was operated under intraoperative MRI (iMRI) guidance, we evaluated the efficacy of iMRI guidance for intraoperative hemodynamic monitoring.

Methods: iMRI, including 3D time-of-flight (TOF) magnetic resonance angiography (MRA), diffusion weighted imaging (DWI), perfusion weighted imaging (PWI), were used to monitor the surgical treatment of each patient with intracerebral AVM. Intraoperative DWI and PWI were used for real-time hemodynamic monitoring for AVM surgery.

Result: In all the patients, MRA demonstrated the angioarchitecture of AVM, DWI and PWI demonstrated no evidence of brain ischemia. Integrated FLAIR and MRA data sets were used for image guidance and revealed complete elimination of the AVM without conventional catheter angiography. One subject in which intraoperative PWI revealed elevated CBF posterior to the resection cavity suffered from re-bleeding two days after the operation (see Graph 1). All patients recovered well without neurological deficits.

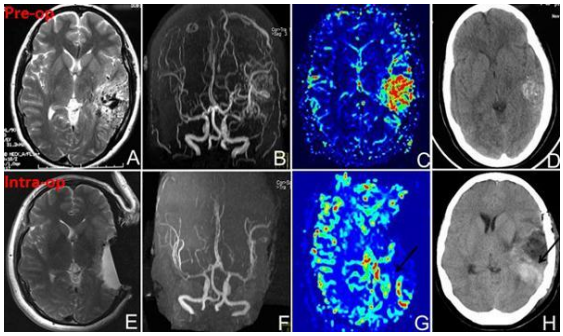

[iMRI-guided AVM resection]

Conclusions: iMRI for surgical guidance of intracerebral AVM can enhance intraoperative orientation and detect early ischemic and hemorrhagic risk, may be used for intraoperative hemodynamic monitoring in the microsurgical treatment of AVM.

INTRAOPERATIVE HEMODYNAMIC CHANGE AND BRAIN REPERFUSION AFTER CAROTID ENDARTERECTOMY EVALUATED BY INTRAOPERATIVE MRI

F. Zhu[1], Y. Mao[2], D. Song[2], Y. Gu[2], B. Xu[2], W. Zhu[2], J. Wu[2], L. Zhou[2]

[1]Department of Neurosurgery, Huashan Hospital, [2]Fudan University, Shanghai, China

Objective: To use intraoperative magnetic resonance imaging (iMRI) to monitor the hemodynamic change and brain reperfusion after carotid endarterectomy (CEA).

Methods: 8 patients with severe ICA stenosis were treated with CEA in the iMRI suite. iMRI, including intraoperative quantitative magnetic resonance angiography (MRA), diffusion-weighted imaging (DWI), perfusion-weighted imaging (PWI), was used to monitor the real-time hemodynamic change and prevent reperfusion injury after CEA operation.

Results: In all the patients, intraoperative MRA demonstrated the stenosed ICA restored to its patency immediately after the operation. Intraoperative quantitative MRA quantified the blood flow of the ipsilateral ICA and MCA. Diffusion-weighted studies demonstrated no evidence of brain ischemia. Intraoperative PWI revealed the brain reperfusion soon after the CEA operation. All patients recovered well without new neurological deficits, acute ischemic or hemorrhagic stroke by controlled hypotension after the operation under the guidance of hemodynamic analysis.

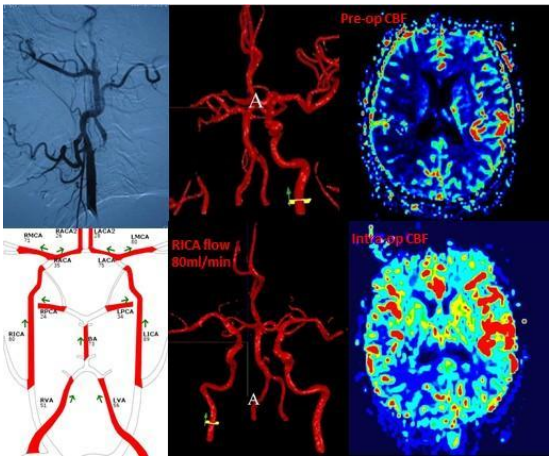

[pre and intra-op quantitative MRA]

Conclusion: Intraoperative MRI can be used to quantitatively monitor the hemodynamic change after CEA surgery for ICA stenosis by performing quantitative MRA analysis. It may be a useful adjunct to prevent brain reperfusion and to document the intraoperative vascular flow.

TARGETING EVALUATION OF FA-NIR797 MAGNETIC ALBUMIN NANOSPHERES IN VITRO AND IN VIVO

Y.-L. An[1], Q.-S. Tang[2], D.-F. Liu[2], G.-J. Teng[1]

[1]Jiangsu Key Laboratory of Molecular and Functional Imaging, Department of Radiology, [2]Southeast University, Nanjing, China

Objective: To explore the targeting effect of FA-NIR797 magnetic albumin nanospheres on C6 rat glioma cells and investigate the feasibility of monitoring with FA receptor-mediated targeted delivery system by 7.0 Tesla MRI in vitro cellular level. To research the targeting effect, security and feasibility of real-time monitoring the delivery process of FA-NIR797 magnetic albumin nanospheres on xenograft glioma tumor-bearing nude mice by using the 7.0 Tesla MRI in vivo experiments.

Methods:

①In vitro experiment: C6 cells were incubated with FA targeting groups (FA-NIR797 magnetic albumin nanospheres), non-FA targeting groups (NIR797- magnetic albumin nanospheres) and FA suppressing groups (FA-NIR797 magnetic albumin nanospheres and FA) for 24 hours respectively, prussian blue staining and MRI were used to observe the FA-mediated targeting effect on C6 cells.

②In vivo experiment: 48 mice were randomly divided into FA targeting groups which were injected FA-NIR797 magnetic albumin nanospheres through tail vein, non-FA targeting groups injected NIR797-magnetic albumin nanospheres and FA suppressing groups injected FA-NIR797-magnetic albumin nanospheres with FA and applied dose was 5 mg Fe/kg mouse. MRI imaging were performed to measure T_2WI and T_2*WI signal strength of the regions of interest (tumor and muscle tissue) before injection and after injection at different time points (1 h, 2 h, 4 h, 8 h, 24 h, 48 h, 72 h) respectively and calculate the signal change rate. Histopathological examination included HE staining and prussian blue staining.

Results:

①In vitro experiment: Prussian blue staining demonstrated that C6 cells which were incubated with FA targeting groups had high cellular iron density while no obvious iron particles were found within the cells incubated with non-FA targeting groups and FA suppressing groups. The MRI T_2 signal intensity of C6 cells decreased significantly after incubating with FA targeting groups, but did not show obvious decrease after incubating with non-FA targeting groups and FA suppressing groups.

②In vivo experiment: As in vivo MRI imaging, the T_2 and T_2^* signal intensity and signal change rate of the tumor tissue of FA targeted groups decreased significantly at different time points after injection and the change had significant difference. The signal intensity of non-FA targeting groups and FA suppressing groups also slightly decreased immediately, at 1 h and at 2 h after injection, but the MRI signal intensity was lower than FA targeted groups and the duration time of signal was shorter than FA targeted groups. Pathological examination: prussian blue staining showed that much more intracellular iron particles existed in FA-targeted tumor tissue, while intracellular iron particles of the non-FA targeting groups and FA suppressing groups were almost invisible.

Conclusions: In vitro experiment, FA-NIR797-magnetic albumin nanospheres had a better targeting effect on rat glioma C6 cells; in vivo experiment, it had a better targeting effect on nude mice bearing rat glioma xenograft tumor.

FROM ASTRONOMY TO ASTROCYTES: MULTISCALE VISION MODEL FOR DETECTION OF GLIAL CALCIUM WAVES IN TWO-PHOTON IMAGING DATA

A. Brazhe[1,2], C. Mathiesen[2], M. Lauritzen[2,3]

[1]Department of Biophyics, Biological Faculty, Moscow State University, Moscow, Russia, [2]Neuroscience and Pharmacology, University of Copenhagen, Copenhagen, [3]Department of Clinical Neurophysiology, Glostrup Hospital, Glostrup, Denmark

Intercellular glial calcium waves (GCW) constitute a signaling pathway which can be visualized by fluorescence imaging of cytosolic calcium changes. Reliable detection of calcium waves in multiphoton imaging data is challenging because of low signal-to-noise ratio. We extend an image processing technique, originally used for astronomical images, but never applied to biological data before. As a proof of concept we demonstrate how this technique has led us to new insights

to glial calcium waves — a concerted way of intercellular calcium signaling among astrocytes.

Dynamic fluorescent imaging is the daily bread of neuroscience today. Imaging data, especially *in vivo*, are characterized by low signal-to-noise ratio, high data dimensionality, and often sporadic and transient nature of the studied signals which also have a wide range of spatio-temporal characteristic scales. Consequently, there is a high demand for tools of sensitive and noise-resistant detection, segmentation and characterization of the observed patterns in the imaging data.

We note that the mentioned challenges are also common in processing of astronomical images, where the light sources are inherently faint and can be distributed over large range of spatial scales. Accordingly, we tested if a wavelet-based technique, designed specifically to detect and quantize different objects in noisy astronomical images, could be transferred to the field of biological imaging. We implemented and extended the original algorithm (multiscale vision model, MVM) to be able to work with time-lapse image series.

Using the modified MVM algorithm we were able to successfully detect and analyze spontaneous glial calcium waves (GCWs) in mouse cerebellum *in vivo*. The new analysis approach allowed to describe peculiarities of the GCW evolution, such as triggering secondary GCWs from the expanding wave front, rebound calcium rises in the origin of the GCW, and interaction with vessel walls. These observations extend the existing understanding of a GCW in cerebellum as a simple response to ATP diffusion from the point source and suggest secondary ATP release events, refractory period for GCW generation and two-way nonlinear interaction with the surrounding tissue.

REPERFUSION IN MANNOSE-BINDING LECTIN KNOCK-OUT MICE FOLLOWING MIDDLE CEREBRAL ARTERY OCCLUSION

A. Kristoffersen[1], X. de la Rosa Siles[2], C. Valdés[1], C. Justicia[2], **A.M. Planas**[2], T. Durduran[1]

[1]ICFO - The Institute of Photonic Sciences, Castelldefels, [2]IDIBAPS-The August Pi i Sunyer Biomedical Research Institute, Barcelona, Spain

The role that the biology of reperfusion plays in the outcome of long term injury and functional impairments following ischemic stroke is not yet fully understood. It has been shown that Mannose-binding lectin (MBL) deficiency is beneficial in experimental brain ischemia in mice.[1] In an earlier study [1] we have shown that the infarct volume in MBL-knock out (KO) mice is known to be smaller at 48 hours following ischemia compared to wild type (WT) mice, despite having similar reduction in CBF during occlusion, as measured by laser Doppler. This result has also been related to clinical studies in humans showing that stroke patients with MBL-low genotypes have a better outcome than MBL-sufficient genotypes [1]. One question that arises from this research is what happens to the hemodynamics in the first hours following reperfusion?

We have conducted a longitudinal study comparing relative cerebral blood flow (rCBF) changes of five male C57BL/6J wild-type (WT) and five male MBL-null mice (B6.129S4-Mbl1tm1Kata Mbl2tm1Kata/J) mice during 6 hours following occlusion using a combined laser speckle imaging and intrinsic optical signals (LSF-OIS) which simultaneously tracks rCBF, and changes in Hb and HbO_2 concentrations. With this technique we can identify different zones of CBF reduction during ischemia and monitor the evolution of the hemodynamics.

Mice were anesthetized with isofluorane. A 15 minute baseline was measured prior to ischemia. Ischemia was induced with a ninety minute middle cerebral artery (MCA) occlusion, as previously reported [2]. The reduction of CBF was verified by laser Doppler in the first 30 minutes of occlusion. The final 30 minutes of the occlusion were monitored with LSF-OIS. Following reperfusion, hemodynamics were monitored with the LSF-OIS device for one hour, and again at 4 and 6 hours after occlusion.

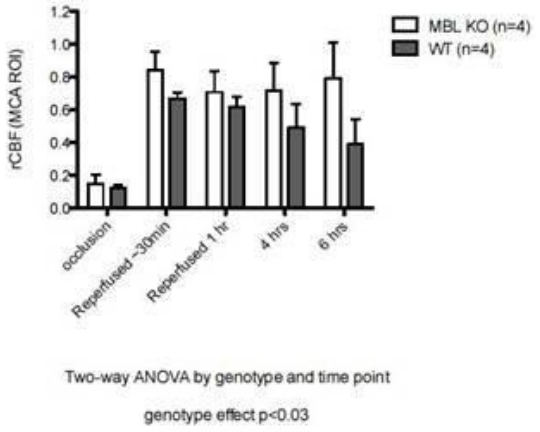

[rCBF near ischemic core]

The presented data shows n=4 for both groups. During occlusion, the change in CBF is seen to be similar between groups, with an rCBF of 12±2% for the WT and 15±5% for MBL-KO. However, as time progresses, the difference between the two groups increased dramatically. At 4 hours, the rCBF seen in the WT group is 49±14%, whereas in the MBL-KO group, the rCBF has recovered to 72±17%. A two-way Anova analysis gives $p< 0.03$ between groups. After the final time point, the mice were sacrificed and the biological zero due to Brownian motion was measured. The infarct volume was obtained by TTC staining, and was found to be 51 ±7 mm^3 in the WT group, and 31±21mm^3 in the MBL-KO group. The changes in concentration for Hb and HbO_2 are also followed and $CMRO_2$ was calculated and no significant difference between groups was found.

[1] Cervera A, et al. (2010) Genetically-Defined Deficiency of Mannose-Binding Lectin Is Associated with Protection after Experimental Stroke in Mice and Outcome in Human Stroke. PLoS ONE 5(2): e8433. doi:10.1371/journal.pone.0008433

[2] Justicia C, et al. (2006) Anti- VCAM-1 antibodies did not protect against ischemic damage neither in rats nor in mice. J Cereb Blood Flow Metab 26: 321-322.

CHANGES IN EFFECTIVE DIFFUSIVITY FOR OXYGEN DURING NEURAL ACTIVATION AND DEACTIVATION ESTIMATED FROM CAPILLARY DIAMETER MEASURED BY TWO-PHOTON LASER MICROSCOPE

H. Ito[1], H. Takuwa[1], Y. Tajima[1], H. Kawaguchi[1], K. Masamoto[1], J. Taniguchi[1], Y. Ikoma[1], C. Seki[1], M. Ibaraki[2], I. Kanno[1]

[1]Molecular Imaging Center, National Institute of Radiological Sciences, Chiba, [2]Akita Research Institute of Brain and Blood Vessels, Akita, Japan

Objectives: According to a model for the regulation of cerebral oxygen delivery proposed by Hyder et al. [1], the relation between cerebral blood flow (CBF) and cerebral oxygen extraction fraction (OEF) can be expressed using the effective diffusivity for oxygen in the capillary bed (D) as OEF=1-exp(-D/CBF). The D value is proportional to capillary blood volume, and therefore changes in D can be estimated from changes in capillary diameter. The discrepancy between the increases in CBF and cerebral metabolic rate of oxygen ($CMRO_2$) during neural activation and deactivation observed in crossed cerebellar diaschisis (CCD) caused by contralateral supratentorial lesions has been reported to causes a significant decrease and increase in OEF using positron emission tomography (PET) in humans, respectively [2, 3]. In the present study, changes in D during neural activation and deactivation were estimated from changes in capillary diameter measured by in vivo two-photon laser microscopic imaging in mice, and compared with those calculated from measures by PET in humans reported previously.

Methods: The cortical vasculature was imaged with two-photon laser microscope through a chronic cranial window at the somatosensory cortex and cerebellum in awake mice (C57BL/6J mice, N=4) after intraperitoneal administration of sulforhodamine 101 (10 mM, 8 μL/g) for labelling blood plasma. First, capillary vessels diameter in the somatosensory cortex was measured at baseline and during sensory stimulation (Whisker stimulation: 10Hz). Second, capillary vessels diameter in the cerebellum was measured at baseline and one day after permanent occlusion of contralateral middle cerebral artery which could cause

CCD. Changes in capillary diameter during neural activation and deactivation were calculated, and then changes in D were estimated. Changes in D during neural activation and deactivation caused by motor task and CCD, respectively, were also calculated as OEF=1-exp(-D/CBF) from measures by PET in humans previously reported [2, 3].

Results: Changes in capillary diameter were 6 ± 2% and -10 ± 3%, and changes in D were 13 ± 5% and -20 ± 6% during neural activation (somatosensory cortex) and deactivation (cerebellum) in mice, respectively. Changes in CBF, $CMRO_2$, and OEF during neural activation by motor task reported in humans were 47%, 11%, and -24%, respectively, in the primary motor cortex, and therefore change in D calculated was 7% [2]. Changes in CBF, $CMRO_2$, and OEF during neural deactivation by CCD reported in humans were -20%, -12%, and 8%, respectively, and therefore change in D calculated was -11% [3].

Conclusions: The degree of changes in D during both neural activation and deactivation were larger in mice than in humans, however the degree of changes in D during neural activation were smaller than during neural deactivation for both mice and humans. This might indicate the validity of a model for the regulation of cerebral oxygen delivery proposed by Hyder et al. [1].

References:

[1] Hyder F, et al. J Appl Physiol 1998; 85: 554-564.

[2] Ito H, et al. J Cereb Blood Flow Metab 2005; 25: 371-377.

[3] Ito H, et al. Ann Nucl Med 2002; 16: 249-254.

CHRONIC IMAGING OF CORTICAL BLOOD FLOW USING MULTI-EXPOSURE SPECKLE IMAGING

S.M.S. Kazmi, A.K. Dunn

The University of Texas at Austin, Austin, TX, USA

Objectives: Chronic imaging of cerebral blood flow (CBF) is an important tool for investigating vascular remodeling following injury such as focal cerebral ischemia. Although techniques such as laser speckle contrast imaging (LSCI) have emerged as valuable tools for imaging cerebral blood flow in acute experiments, their utility for chronic measurements or comparisons across animals has been limited. Recently, an extension to laser speckle contrast imaging, called Multi-Exposure Speckle Imaging (MESI), was introduced that increases the quantitative accuracy of CBF images. In our work, we examine the chronic accuracy of flow dynamics predicted by MESI compared to those from traditional single-exposure LSCI.

Methods: We evaluate the accuracy of the MESI flow estimates using high speed Red Blood Cell (RBC) reflectance tracking as an absolute flow calibration in cranial window implanted mice. Specifically, we compute the deviation of the MESI and LSCI flow predictions from the RBC velocity changes obtained in surface vasculature over several days. Subsequently, we examine the speckle techniques' ability to map changes in blood flow after photothrombosis of selected cortical vasculature. We assess the CBF dynamics within the stroke induced animals to characterize the extent of infarct, changes in flow distribution, and turnover of vasculature over one week relative to physiological baseline.

Results: In our work, we demonstrate that estimates of chronic blood flow changes are better with MESI than traditional LSCI. The flow measures computed using the MESI and LSCI techniques were found to be on average 10% and 27% deviant (n = 201 measurements, 9 animals), respectively, compared to velocity changes estimated using RBC tracking. We also used MESI to map CBF dynamics after photo-thrombosis of selected microvasculature, akin to studies that induce strokes in similar animal models. Correlations of flow estimates to RBC tracking were closer with MESI (*r=0.88*) than LSCI (*r=0.65*), exhibited by accurate characterization of CBF dynamics up to two weeks from baseline with MESI.

Conclusions: The MESI computed flow measure can go beyond qualitative observations of vascular remodeling by providing a reliable spatial perfusion index to help characterize patho-physiology. We assessed the CBF dynamics due to induced vascular occlusions in mice to determine the extent of the infarct, changes in flow distribution, and turnover of vasculature relative to an accurately estimated

physiological baseline. This comparison is now possible because of the increased quantitative accuracy of the MESI technique. Beyond observing baseline flows, the ability to quantitatively characterize post-occlusion CBF dynamics via intrinsic optical flow-measurements in a chronic setting provides a platform for assessing the efficacy of therapies for flow restoration.

References:

Ashwin B. Parthasarathy et al., "Robust Flow Measurement with Multi-exposure Speckle Imaging," Optics Express 16, no. 3 (February 4, 2008).

Ashwin B. Parthasarathy, S. M. Shams Kazmi, and Andrew K. Dunn, "Quantitative Imaging of Ischemic Stroke Through Thinned Skull in Mice with MultiExposure Speckle Imaging," Biomedical Optics Express 1, no. 1 (2010).

Donald D Duncan et al., "Absolute Blood Velocity Measured with a Modified Fundus Camera," Journal of Biomedical Optics 15, no. 5 (October 2010).

REAL TIME CEREBRAL BLOOD FLOW MONITORING IN RAT MIDDLE CEREBRAL ARTERY OCCLUSION SURGERY BY LASER SPECKLE IMAGING

L. Yuan, H. Lu, **Y. Li**, S. Tong

Shanghai Jiao Tong University, Med-X Research Institute, Shanghai, China

Introduction: Middle cerebral artery occlusion (MCAO) in the rat by intraluminal suture is one of the most used models for ischemic stroke study. Yet the surgery protocol is complicated and the dynamics of the cerebral blood flow (CBF) during MCAO surgery is usually monitored by laser dopploer flowmetry (LDF), which provides CBF information in very limited locations. It is desireable to monitor the CBF changes in a more comprehensive way to study the cerebral hemodynamics during MCAO surgery. Laser speckle imaging (LSI) provides full field CBF information with high spatial and temporal resolution. We designed a miniaturized head-mounted LSI system which could perform real time monitoring of CBF changes during MCAO surgery.

Methods: The head-mounted LSI imaging system consists of a multimode optical fiber bundle for laser light delivery and a printed circuit board with a CMOS sensor embedded along with image acquisition and transferring circuits. The entire imager weighs about 20 g and is 3.1 cm high, which is fixed onto the rat skull using glass ionomer cement. In this work, the system was used to monitor the real-time CBF from the beginning of MCAO surgery until 30 minutes after the occlusion. The images were captured at 50 frames per second rate. Ten adult Sprague-Dawley rats were prepared randomly with the same type of 5 mm suture head silicone coating for MCAO models. Moreover, we performed correlation analysis between the CBF changes and the infarct size at 24 hours after the surgery.

Results: We mainly observed the CBF changes in the ipsilateral hemisphere during the surgery and compared them with baseline data collected before the surgery. After the ligature being made in the common carotid artery (CCA), the blood flow in the arteries and veins decreased about 20% and 10% from baseline respectively ($p < 0.05$). There were no significant further changes in CBF when the filament was introduced until the occlusion. Right after the occlusion of MCA (within 1 minute), the CBF in arteries within the affected region in ipsilateral hemisphere reduced about 70% from baseline ($p < 0.05$). The veins showed 20% less decline than the arteries, which decreased 50% from baseline upon occlusoin. The correlation between the CBF right after occlusion (within 1 minute) and the infarct volume calculated at 24 hours after the surgery was significant ($R^2 = 0.65$, $p < 0.01$).

Conclusions: The ultimate goal of this work is to obtain the real time full field CBF information during intraluminal filament MCAO surgery, which can provide more informative pathophysiological indicators during MCAO modeling.

References:

1.E. B. Ringelstein, R. Biniek, C. Weiller, et al. Type and extent of hemispheric brain infarctions and clinical outcome in early and delayed middle cerebral artery recanalization. Neurology, 1992; 42: 289-298.

2.J. D. Briers, A. F. Fercher. Retinal blood-flow visualization by means of laser speckle photography. Invest Ophthalmol, 1982, 22: 255-259.

3.P. Miao, H. Lu, Y. Li, et al. Laser speckle contrast imaging of cerebral blood flow in

freely moving anmials. Journal of Biomedical Optics, 2011;16(9).

UNDERSTANDING CEREBRAL NEUROVASCULAR COUPLING FUNCTIONS OF THE PHOTOTHROMBOTIC STROKE VIA NOVEL ELECTROCORTICOGRAPHY-FUNCTIONAL PHOTOAOCUSITC MICROSCOPY (ECOG-FPAM)

L.-D. Liao[1], H.-Y. Lai[2], V. Tsytsarev[3], N.V. Thakor[1,4], Y.-R. Lin[5], Y.-Y.I. Shih[2], M.-L. Li[6], Y.-Y. Chen[7]

[1]Institute for Neurotechnology, National University of Singapore, Singapore, Singapore, [2]Experimental Neuroimaging Laboraory, Neurology and Biomedical Research Imaging Center, University of North Carolina, Chapel Hill, NC, [3]Anatomy and Neurobiology, University of Maryland School of Medicine, [4]Biomedical Engineering, Johns Hopkins University, Baltimore, MD, USA, [5]Changhua Christian Hospital, Emergency Medicine, Changhua, [6]Electrical Engineering, National Tsing Hua University, [7]Biomedical Engineering, National Yang Ming University, Hsinchu, Taiwan R.O.C.

Objectives: Studying the functional neurovascular roles of individual cerebral cortical arterioles in maintaining both the structure and function of cortical regions during and after photothrombotic stroke attacks is an important issue [1]. The combination of ECoG and fPAM enables simultaneously studying of the neural activations and their corresponding hemodynamic changes, with the potential to understand the neurovascular coupling functions after stroke attack and optimize treatment [2]. The goal of this study was to characterize the functional hemodynamic changes in single cerebral vessels before/after photothrombotic stroke by using a custom-made ECoG-fPAM system.

Methods: Six male Wistar rats were anesthetized with pentobarbital (50 mg/kg, ip.). A cranial window of approximately 4×2 mm under right S1FL was drilled for PA acquisition and two epidural cortical electrodes were secured in the skull around the cranial window for ECoG recordings [3]. Rose Bengal (10 mg/kg) was injected for 2 min within 5-min 532-nm CW laser onset. Cerebral HbT, CBV, SO_2 and SSEPs changes associated with the induced stroke in selected arterioles were imaged/recorded by present ECoG-fPAM system [4-6]. Averaged SSEP was subdivided into two most commonly observed SSEP components: P1 (the first maximum voltage) and N1 (the minimum voltage).

Results: The PA images of A1 (upstream), A2 (occluded blood vessel) and A3 (neighboring) arterioles showed significant differences between before and after stroke (**Fig. A**). Averaged functional HbT (i.e., R_{HbT}), CBV (i.e., R_{CBV}) and SO_2 (i.e.,R_{SO2}) changes in the A1, A2 and A3 arterioles as a function of the difference between cases are shown in **Fig. B**. The amplitudes of P1 and N1 showed the significant changes after stroke and P1 and N2 peak-latencies become longer after stroke between C3 and C9 (**Fig. C**). Both increasing of the latency and decreasing of the amplitude of the somatosensory evoked potentials elicited by embarrassing of the synaptic transmission in the occlusive area. Increasing of the evoked potentials amplitude, which was observed in some cases, probably can be explained by suppression of the inhibitory neurons in occlusive area [7].

Conclusion: This study demonstrates functional changes of the nearby cortical arterioles can be observed immediately after photothrombotic stroke. The results demonstrated that no significant changes were observed in neighboring and upstream arterioles from the brain region of a specific clotted arteriole. For the first time, the present ECoG-fPAM system complements existing imaging techniques and has the potential to offer a favorable tool for explicitly studying cerebral hemodynamics in small animal models of photo-induced ischemic stroke.

References:

[1] T. H. Murphy and D. Corbett, Nat Rev Neurosci, 2009 10:861.

[2] L. V. Wang, Nature Photonics, 2009, 3:503

[3] Paxinos and Watson, The Rat Brain in Stereotaxic Coordinates, 2007.

[4] L.-D. Liao et al. NeuroImage 2010, 52:562.

[5] L.-D. Liao et al. JCBFM 2012, 32:938

[6] L.-D. Liao et al. J Biomed Opt 2012, 17: 061210-1.

[7] N. M. Branston et al, Exp Neurol, 1974, 45:195.

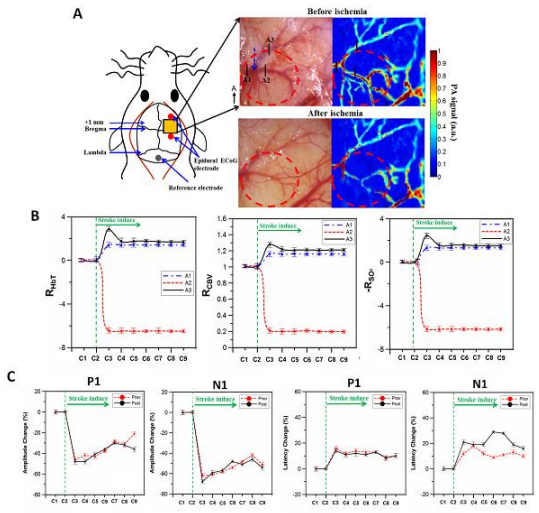

[Fig1]

Figure. Functional cerebral HbT, CBV, SO_2 and SSEPs changes before and after stroke.

IN VIVO OPTICAL IMAGING FOR EVALUATING THE EFFICACY OF EDARAVONE AFTER TRANSIENT CEREBRAL ISCHEMIA IN MICE

N. Liu, J. Shang, T. Yamashita, Y. Omote, K. Deguchi, Y. Ikeda, K. Abe

Department of Neurology, Okayama University Graduate School of Medicine, Dentistry and Pharmaceutical Sciences, Okayama, Japan

Detection and protection of apoptosis, autophagy and neurovascular unit (NVU) are essentially important in understanding and treatment for ischemic stroke patients. In this study, we have conducted an in vivo optical imaging for detecting apoptosis and activation of matrix metalloproteinases (MMPs), then evaluated the profective effect of 2 package types of free radical scavenger edaravone (A and B) on apoptosis, autophagy and NVU in mice after transient middle cerebral artery occlusion (tMCAO). As compared to vehicle treatment, edaravone A and B showed a significant improvement of clinical scores and infarct size at 48 h after 90 min of tMCAO with great reductions of in vivo fluorescent signal for MMPs and early apoptotic annexin V activations. Ex vivo imaging of MMPSense 680 or annexin V-Cy5.5 showed a fluorescent signal, while which was remarkably different between vehicle and edaravone groups, and colocalized with antibody for MMP-9 or annexin V. Edaravone A and B ameliorated the apoptotic neuronal cell death in immunohistochemistry, and activations of MMP-9 and aquaporin 4 with reducing autophagic activations of microtubule-associated protein 1 light chain 3 (LC3) in Western blot. In this study, edaravone in both packages showed a similar strong neuroprotection after cerebral ischemia, which was confirmed with in vivo and ex vivo optical imagings for MMPs and annexin V as well as reducing cerebral infarct, inhibiting apoptotic/autophagic mechanisms, and protecting a part of neurovascular unit.

VALIDATION OF OPTICALLY MEASURED CEREBRAL VENOUS OXYGEN SATURATION IN HUMANS

J.M. Lynch[1], E. Buckley[2], P. Schwab[3], M.E. Putt[4], B.D. Hanna[5], D.J. Licht[3], A.G. Yodh[1]

[1]Department of Physics & Astronomy, University of Pennsylvania, Philadelphia, PA, [2]Department of Radiology, Massachusetts General Hospital, Boston, MA, [3]Department of Neurology, The Children's Hospital of Philadelphia, [4]Department of Biostatistics, University of Pennsylvania, [5]Department of Cardiology, The Children's Hospital of Philadelphia, Philadelphia, PA, USA

Diffuse Optical Spectroscopy (DOS) is a well-established and widely accepted modality for non-invasively measuring concentrations of oxy- and deoxy-hemoglobin ([HbO_2] and [Hb]) in tissue. Specifically, it is well suited for measurement of cerebral tissue oxygen saturation. However, while cerebral tissue oxygen saturation provides some insight into how oxygen is being utilized by the brain, quantification of cerebral oxygen extraction requires separate measurements of arterial and venous saturations. Measures of cerebral arterial oxygen saturation are easily attainable, but cerebral venous oxygen saturation is much more difficult to measure, especially non-invasively and without potentially dangerous perturbations such as venous occlusion.

To isolate the venous component of the DOS signal without a perturbation, a method has been proposed previously that utilizes the oscillations of the venous blood volume at the respiration rate.[1,2] However, direct comparison against a gold standard measurement in humans has not been performed. To this end, we validate this method against the gold standard invasive measurement of central venous saturations.

We compare the optically measured SvO_2 against an oxygen saturation measured from a blood sample taken from the superior vena cava (SVC) in a pediatric population (N=9) for which this invasive measurement is part of clinical care. The SVC saturation exhibits good agreement with the optical measurements (R^2=0.79, p< 0.01, slope=1.1±0.5), thereby demonstrating the ability to non-invasively measure cerebral SvO_2 unambiguously with DOS.

References:

1. Wolf, M., et al., *Continuous noninvasive measurement of cerebral arterial and venous oxygen saturation at the bedside in mechanically ventilated neonates.* Critical Care Medicine, 1997. **25**(9): p. 1579-1582.

2. Franceschini, M.A., et al., *Near-infrared spiroximetry: noninvasive measurements of venous saturation in piglets and human subjects.* Journal of Applied Physiology, 2002. **92**(1): p. 372-384.

IN VIVO TWO-PHOTON IMAGING OF CORTICAL MICROVASCULAR DYSFUNCTION IN ANIMAL MODELS OF ESSENTIAL THROMBOCYTHEMIA AND POLYCYTHEMIA VERA

T.P. Santisakultarm[1], C.Q. Paduano[1], T. Stokol[2], N. Nishimura[1], T.L. Southard[3], R.C. Skoda[4], W.L. Olbricht[5], A.I. Schafer[6], R.T. Silver[6], **C.B. Schaffer**[1]

[1]Biomedical Engineering, [2]Population Medicine and Diagnostic Services, [3]Biomedical Sciences, Cornell University, Ithaca, NY, USA, [4]Biomedicine, University Hospital Basel, Basel, Switzerland, [5]Chemical and Biomolecular Engineering, Cornell University, Ithaca, [6]Medicine, Weill Cornell Medical College, New York, NY, USA

Objectives: Essential thrombocythemia (ET) and polycythemia vera (PV) are among the myeloproliferative neoplasms (MPNs), a group of disorders with bone marrow hyperactivity. They share a common $JAK2^{V617F}$ mutation in hematopoietic cells, leading to excessive production of platelets in ET, and red blood cells (RBCs), leukocytes, and platelets in PV. These additional components alter rheology and lead to coagulation problems in large vessels. Although evidence suggests microcirculatory dysfunction as well, direct observations have not been made. Because disruption to cortical circulation is linked to cognitive decline and dementia, we quantify the alterations in cerebral circulation in ET and PV mice and determine the mechanisms that disrupt blood flow in microvessels, with the goal of identifying potential therapeutic targets.

Methods: $JAK2^{V617F}$ transgenic mice were used as donors for bone marrow transplantation into wildtype mice. The recipient mice were classified as ET or PV based on a complete blood count. In order to understand the contribution of elevated RBCs alone, another group of wildtype mice received erythropoietin injections (Epo, 10-100 IU for 5 days) to enhance erythrocytosis. All animals were anesthetized and imaged through an implanted cranial window using two-photon excited fluorescence microscopy. Texas-red dextran, Rhodamine 6G, and Hoechst 33342 were intravenously injected to reveal vascular topology and label leukocytes and platelets. Cortical capillaries were determined to be flowing or stalled by recording the position of blood cells in individual vessels over time. For flowing arterioles, capillaries, and venules, flow speed was measured.

Results: The hematocrits of control, ET, Epo-injected, and PV groups were 44±1.4% (mean±SEM), 42±1.9%, 58±2.3%, 66±3.0%, respectively. The fraction of microvessels stalled in the top 350 μm of the cortex increased from 3±0.6% in controls (5,167 vessels, 17 mice) to 16±5%, 19±4%, and 28±5% in ET (4,692 vessels, 8 mice), Epo-injected (5,840 vessels, 15 mice), and PV (8,959 vessels, 11 mice), respectively (Figure 1). The stalls were frequently associated with leukocytes and platelets that firmly adhered to the endothelium. The median persistent time for leukocyte and platelet stalls were 30 and 8 min in ET, and 38 and 59 min in PV, respectively. Flow speeds significantly decreased by 24% in PV (77 vessels, 7 mice) relative to the control (149 vessels, 18 mice) while only a trend toward slower flow in ET and Epo-injected groups was observed. No significant difference in capillary diameters was found. Given the vascular density of 8,937±1,492 (mean±SD), 8,030±727, 9,897±3,073, and 8,890±1,615 vessels/mm3 in control, ET, Epo-injected, and PV, we estimate ~30%, 17%, and 34% reduction in perfusion, respectively.

Conclusions: Our study suggests cerebral microcirculation problems may be a neglected feature of ET and PV. While hematocrit is the most predictive factor for the proportion of

capillaries stalled, leukocyte and platelet adherence play a crucial role in obstructing cortical perfusion in MPNs. Targeting leukocyte and platelet activation and adhesion may be clinically important in patients to restore normal cerebral microcirculation.

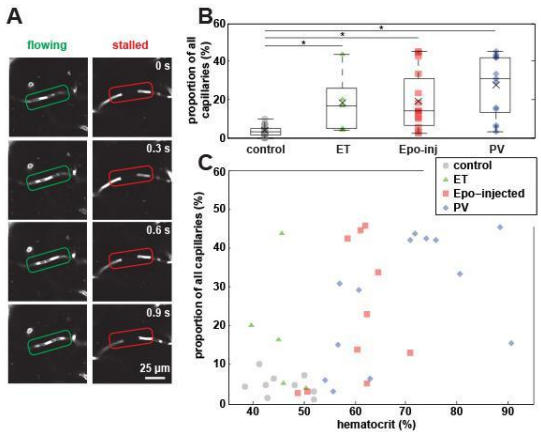

[Figure1]

AN APPLICATION OF THE FIBERED FLUORESCENCE MICROSCOPY TO CONTINUOUSLY MONITOR THE RAT CEREBRAL NEURONS *IN VIVO*

Y. Shi, L. Chen, M. Jiang

Institutes of Brain Science and State Key Laboratory of Medical Neurobiology, Fudan University, Shanghai, China

Introduction: Fiber-optic fluorescence imaging has become increasingly versatile in recent years. Fibered-based fluorescence microscopy includes a point-scanning laser confocal system and a fiber-optic microscopy which uses a small-diameter fiber-optic probe to provide real-time image. The microprobe is made of several tens of thousands of flexible optical fibers, micro-optics and a proprietary connector. This unique structure makes minimally invasive high-resolution imaging in conscious animals into reality.

Objectives: To trace the fluorescent signals of neurons in living animals in a direct and rapid approach with the application of fiber-optic fluorescence microscopy.

Methods: To visualize cortical neurons, recombinant virus vectors containing GFP were microinjected into the cerebral cortex in SD rats with the help of stereotaxie apparatus. Seven days later, by applying fibered fluorescence microscopy technology, an approach that uses 650 micrometer-diameter fiber-optic probe to acquire real-time fluorescent images, we continuously examined and recorded fluorescent signals of rat cerebral cortical neurons transfected with GFP *in vivo*. To confirm the observation, we recorded the fluorescence signals of GFP using fluorescence microscopy on brain slices of the same animal.

Results:

1. Real-time images were recorded in rat cerebral cortex by fibered fluorescence microscopy at a rate of 12 frames per second.

2. Neurons marked with GFP in cerebral cortex of rat brain slices were recorded by a fluorescence microscope.

Conclusion: Fiber-optic fluorescence microscopy is ideal for imaging structures of the deep brain and make *in vivo* tracking of neuronal migration, cell division, promoter activity, and other relatively protracted processes amenable to study.

References:

1.Jacobs RE, Cherry SR. Complementary emerging techniques:high resolution PET and MRI. Curr Opin Neurobiol 2001; 11:621-629.

2.Helmchen F, Denk W. New developments in multiphoton microscopy. Curr Opin Neurobiol 2002; 12:593-601.

3.Jung JC, Mehta AD, Aksay E, Stepnoski R, Schnitzer MJ. In vivo mammalian brain imaging using one- and two-photon fluorescence microendoscopy. J Neurophysiol 2004; 92: 3121-3133.

4.Levene MJ, Dombeck DA, Kasischke KA, Molloy RP, Webb WW. In vivo multiphoton microscopy of deep brain tissue. J Neurophysiol 2004; 91: 1908-1912.

5.Vincent P, Maskos U, Charvet I, Bourgeais L, Stoppini L, Leresche N, Changeux JP, Lambert R, Meda P, Paupardin-Trutsch D. Live imaging of neural structure and function by fibered fluorescence microscopy. EMBO reports 2006; 7(11): 1154-1161.

6.Paxinos G, Watson C. The Rat Brain in Stererotaxic Coordinates. 4th ed. San Diego: Academic Press, 1999, 96-101.

7.Moriyoshi K, Richards LJ, Akazawa C, O´Leary DDM, Nakanishi S. Labeling neural cells using adenoviral gene transfer of membrane-targeted GFP. Neuron 1996; 16: 255-260.

8.Flusberg BA, Cocker ED, Piyawattanametha W, Jung JC, Cheung ELM, Schnitzer MJ. Fiber-optic fluorescence imaging. Nat Methods 2005; 2(12): 941-950.

9.Davenne M, Custoday C, Charneau P, Lledo PM. *In Vivo* imaging of migrating neurons in the mammalian forebrain. Chem Senses 2005; 30(suppl 1):i115-i116.

NEUROVASCULAR COUPLING STUDIED IN AWAKE RATS BY DOI/EEG MEASUREMENTS

J. Sutin[1,2], W. Wu[1], C. Chang[1], L. Ruvinskaya[1], M.A. Franceschini[1]

[1]*Athinoula A. Martinos Center for Biomedical Imaging, Massachusetts General Hospital, Harvard Medical School, Charlestown,* [2]*Pathology, Boston University, Boston, MA, USA*

Objective: Our previous Diffuse Optical Imaging (DOI) and EEG neurovascular studies in anesthetized rats observed profound impacts of anesthetics on brain hemodyamics and electrical activity [1]. Recently, functional optical measurements have been shown to be feasible in awake rats during electrical stimulation [2-4]. In this work, we have developed an implantable electro-optical probe for simultaneous DOI/EEG measuments in fully awake rats. We are using this new probe and associated methods to study neurovascular coupling free from the effects of anesthetics in order to develop a neurovascular coupling model which can be extended to humans.

Methods: Neuronal activity is monitored by transcranial EEG while hemodynamic functional changes are measured by a CW6 system (TechEn Inc., Milford, MA). We developed a novel probe to accommodate stimulus and EEG electrodes, NIRS optodes and head restraint. The probe itself is a composite device consisting of a 3D-printed, ABS plastic support structure and 4-META/MMA-TBB dental resin cement. The probe is surgically implanted onto the bare skull of 250 gram female Sprague-Dawley rats under sterile conditions. In this manner, EEG recordings are taken from screws inserted into the skull over the whisker and forepaw sensory regions, referenced against screws in interparietal bone. Changes in oxyhemoglobin and deoxyhemoglobin are determined from light absorbance measurements at 690 and 830 nm from source and detector fibers located between the screw electrodes. A set of stimulus electrodes is chronically implanted from the probe into the body right whisker pad and measurements are made both contralaterally and ipsilaterally to stimulation. Rats are trained by operant conditioning to remain still in a custom tubular restraint during measurements.

Results: As expected, awake rats exhibit different electrical and larger hemodynamic evoked responses. However, a lower signal-to-noise ratio of the evoked response due to higher spontaneous activity and subject motion require increased signal averaging compared to experiments under anesthesia. Quantitative measurements are still on-going with longitudinal measurements continuing on the same individuals for over 3 months post-surgery.

Conclusion: Simultaneous EEG and DOI measurements are feasible in awake rats, removing the strong effect of anesthetics from neurovascular coupling studies.

References:

[1] MA. Franceschini, H. Radhakrishnan, K. Thakur, W. Wu, L. Ruvinskaya, S. Carp, D. Boas. The effect of different anesthetics on neurovascular coupling *NeuroImage*, *51*(4), 1367-1377 (2010).

[2] J. Berwick, C. Martin, J. Martindale, M Jones, D Johnston, Y Zheng, P. Redgrave, et al. Hemodynamic response in the unanesthetized rat: intrinsic optical imaging and spectroscopy of the barrel cortex. *Journal of cerebral blood flow and metabolism: official journal of the International Society of Cerebral Blood Flow and Metabolism*, *22*(6), 670-679 (2002).

[3] C. Martin, J Martindale, J Berwick, J. Mayhew. Investigating neural-hemodynamic coupling and the hemodynamic response function in the awake rat *NeuroImage*, *32*(1), 33-48 (2006).

[4] M. Holzer, C. Schmitz, Y Pei, H Graber, R Abdul, J Barry, R. Muller, R., R. Barbour 4D

functional imaging in the freely moving rat. *Conf Proc IEEE Eng Med Biol Soc*, *1*, 29-32 (2006).

IN VIVO IMAGING OF CEREBRAL ENERGY METABOLISM WITH 2-PHOTON FLUORESCENCE LIFETIME MICROSCOPY OF NADH AND PO2

M.A. Yaseen, S. Sakadžić,, B. Fu, W. Wu, D.A. Boas

Martinos Center for Biomedical Imaging, Massachusetts General Hospital/ Harvard Medical School, Charlestown, MA, USA

Objectives: Understanding the role of altered cerebral energy metabolism in the aging process and progression of neurodegenerative disorders such as Alzheimer's Disease requires measurement methods with high spatial and temporal resolution. Here, we utilize 2-photon (2P) lifetime microscopy to perform minimally-invasive, in vivo measurements of cerebral oxygen pressure and various enzyme-bound formulations of reduced nicotinamide adenine dinucleotide (NADH). The enzymatic formulations, or species, of NADH constitute more specific indicators of glycolysis or oxidative metabolism. These species are measured in the cerebral cortices of rats and mice during various metabolic manipulations and correlated with measurements of extracellular oxygen pressure (pO_2).

Methods: 2P imaging was performed through cranial windows in male Sprague Dawley rats or C57BL/6 mice , primarily over the somatosensory cortex. Animals were mechanically ventilated, anesthetized, and cannulated, and their blood pressure, body temperature, and blood gases were monitored continuously. For pO_2 measurements, the novel 2P-excitable oxygen sensitizer, PtP-C343 was pressure-injected directly into the cortical tissue, roughly 300 µm below the brain surface, with a micropipette [1, 2]. The 2P portion of our custom-designed, multimodal imaging system was utilized to measure the phosphorescence lifetime and fluorescence lifetimes of PtP-C343 and various species of endogenous NADH, respectively. NADH and pO_2 were monitored while manipulating the amounts of inspired oxygen to induce metabolic changes.

Results: Multiple, disparate lifetimes of NADH are indicative of variations in enzyme bound state, including free, unbound NADH or NADH bound to metabolic enzymes such as lactate dehydrogenase, malate dehydrogenase, or mitochondrial complex I. Four distinct NADH species, with fluorescence lifetimes ranging from picoseconds to nanoseconds, were distinguished using custom-designed multi-exponential fitting software. Each species responded differently to brief periods (45s) of anoxia. Anoxia causes reversible changes in relative amounts of NADH species. Longer periods of mild hypoxia (10 min, 14% FIO_2) induces irreversible changes, suggestive of a HIF1α-induced metabolic-shift from oxidative metabolism to glycolysis. To further substantiate these observations, we propose to couple these NADH measurements with high resolution extracellular pO2 measurements, enabling detailed correlation between available oxygen and the relative contributions of glycolysis and oxidative metabolism.

Conclusions: 2P fluorescence lifetime imaging allows for resolution between different enzyme-bound states of NADH, extending its utility to indicate metabolic activity with greater specificity. Future in vivo experiments to monitor NADH species representing glycolysis or oxidative metabolism in astrocytes and neurons will help reveal the role of cerebral metabolic changes in senescence and neurodegeneration.

References:

1. O. S. Finikova, A. Y. Lebedev, A. Aprelev, T. Troxler, F. Gao, C. Garnacho, S. Muro, R. M. Hochstrasser, and S. A. Vinogradov, "Oxygen Microscopy by Two-Photon-Excited Phosphorescence," ChemPhysChem 9, 1673-1679 (2008).
2. S. Sakadžić, E. Roussakis, M. A. Yaseen, E. T. Mandeville, A. Devor, E. H. Lo, S. A. Vinogradov, and D. A. Boas, "Imaging of oxygen partial pressure in cerebral vasculature and tissue using a two-photon-enhanced phosphorescent nanoprobe," Nat. Methods 7, 755-759 (2010).

NON-INVASIVE EVALUATION OF NEURONAL VIABILITY IN ORGANOTYPIC BRAIN CULTURES USING OPTICAL COHERENCE MICROSCOPY

F. Li[1], Y. Berdichevsky[1,2], M.D. Feldman[3], **C. Zhou**[1,2]

[1]Electrical and Computer Engineering, [2]Bioengineering Program, Lehigh University, Bethlehem, [3]Department of Pathology & Laboratory Medicine, Perelman School of Medicine, University of Pennsylvania, Philadelphia, PA, USA

Objectives: Organotypic brain cultures are increasingly used as a model system to develop better treatments for epilepsy, trauma, stroke, ischemia, and other neurological conditions. Neuron morphology and number in organotypic brain cultures are key parameters that are assessed to determine the degree of insult and/or rescue [1-2]. Typical methods to evaluate neuronal viability include histology and 3D confocal microscopy, which require tissue fixation and staining, making it difficult to assess neuronal viability at multiple time points in the same specimen. In this study, we present a non-invasive 3D optical imaging technology, optical coherence microscopy (OCM) [3-5], which provides micro-scale image resolution and is suited for evaluating neuronal viability in organotypic brain cultures without tissue processing and staining.

Methods: A spectral-domain OCM system was developed using a super-continuum light source centered at 800nm, which enables 1.5μm axial resolution in tissue. A 20x objective was used to provide < 2um transverse imaging resolution. The OCM system was operated at 20,000 A-scans per second and achieved a sensitivity over 100dB. Organotypic brain slices (~100um in thickness) were dissected from the hippocampus region of 7-days old Sprague-Dawley rats (Charles River), maintained at an air-culture interface and incubated in humidified 5% CO_2 at 37°C. 3D-OCM images were obtained from the brain slices on 6, 13, 18, 24 and 30 days *in vitro* (DIV). After imaging, these brain slices were fixed in 10% formaldehyde and were processed with H&E histology.

Results: Figure 1 shows representative OCM images from brain slices at DIV 6, 13, 18, 24 and 30, and corresponding histology from DIV 18. The CA3, CA1 and the dentate gyrus (DG) regions are clearly identified from the OCM images. Viable neurons present in OCM images as hyposcattering circular regions with a well-defined boundary and can be readily identified from images acquired on DIV-6 and DIV-13. Starting from DIV-13, the neuron boundary became diffusive, suggesting that the membrane integrity of some of the neurons had been compromised as DIV increased. These findings were confirmed by H&E histology obtained from the same brain slices. Quantitative analysis to correlate features visible in OCM images and histology is currently underway.

Conclusions: We demonstrate OCM as a promising non-invasive 3D optical imaging technique that can be used to evaluate neuronal viability in organotypic brain cultures. This enables longitudinal studies using the same brain slices and opens up new possibilities to investigate treatment mechanism for various neurological conditions using organotypic brain cultures.

References:

[1] J Noraberg, et al, Brain Research Protocols, 3(3):278-290,1999.

[2] L Lossi, et al, Progress in Neurobiology, 88(4):221-245,2009.

[3] D Huang, et al. Science, 254:1178-81,1991.

[4] JA Izatt, et al, Optics Letters, 19:590-2,1994.

[5] VJ Srinivasan, et al, Optics Express, 20(3):2220-2239,2012.

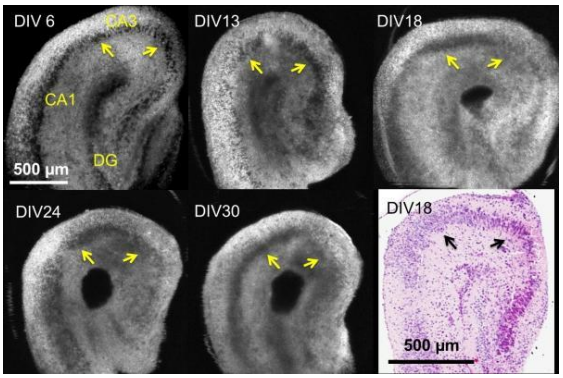

[Figure 1, OCM brain slice images]

Figure 1, Representative OCM images from brain slices at DIV 6, 13, 18, 24 and 30, and

corresponding histology from DIV 18. Arrows in the figure indicate neuronal layers.

SEGMENTATION OF MOUSE BRAIN MICROVASCULATURE FROM MICRO-CT IMAGES USING GABOR FILTER AND LOCAL ENTROPY THRESHOLDING

Y. Ding[1], W. Ward[1], T. Parker[2], S. Nakagawa[2], L. Buttery[3], L. White[3], L. Bai[1]

[1]Computer Science, [2]Biomedical Sciences, [3]Pharmacy, University of Nottingham, Nottingham, UK

Objectives: Vascular pathology is present in most human diseases, so there has been intense research in the past in MRI for diagnosis and treatment of vascular diseases. Recently the role of neurovascular dysfunction in pathogenesis of neurological diseases has been identified, including Alzheimer's Diseases (AD). Most significant is the finding that vascular abnormalities, characterized by abnormal cerebral microvasculature, and angiogenesis, could potentially serve as an early biomarker of the diseases. This new theory has opened up new avenues for research, with laboratory research worldwide gaining momentum and the lack of computational tools becoming increasingly apparent. To validate the theory linking microvasculature to pathology of neurodegenerative conditions on large datasets, the only feasible way is to develop automated computational analysis methods.

However, existing algorithms for image analysis have mostly been developed for segmenting large vessels, and analysis of these vessels has been limited to measuring curvature and diameter of individual vessels, which are unsuitable for microvasculature. Imaging devices such as micro-CT can achieve resolutions on the order of several µm, allowing imaging the three dimensional (3D) microvasculature down to the capillary level. The main weakness of using micro-CT for vascular research is considered to be the lack of software for 3D quantification of microvasculature. We aim to automatically segment and analyse 3D microvasculatures from micro-CT images.

Methods: A corrosion casting method was used to prepare 3D resin casts of the microvasculature of wild type and transgenic Alzheimer´s mice model brains. The resin casts were freeze dried for micro-CT (Skyscan 1174) scanning. Resin casts, contained within 20 ml universal tubes, were mounted on a stage within the imaging system and scanned. Measurements were obtained at a voltage of 40 kV, current of 800 µA and voxel resolution of 24 µm. The segmentation method presented in this paper represents our preliminary work on the dataset that uses a combination of Gabor filtering and local entropy thresholding (LET) to segment the microvasculature. The Gabor-filter is a wavelet-based filter, used to preprocess images to remove noise and improve image contrast for vessel detection and feature extraction. LET is a method to find a threshold for each pixel based on local spatial distributions of intensity levels.

Results: The segmentation algorithm was applied to the dataset consisting of over 300 micro-CT slices. The segmentation result is accurate by visual inspection, with few misidentified pixels, as shown in a randomly selected result below. Microvessels were also detected.

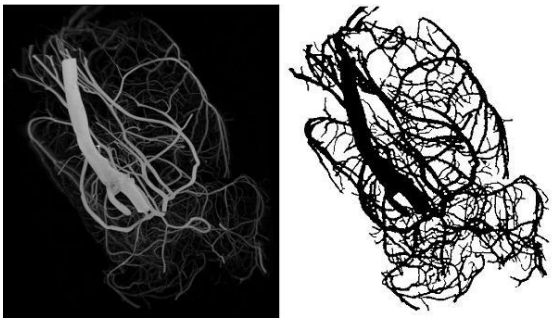

[micro-CT image of rodent brain and segmentation]

Conclusions: With the results obtained from the available dataset, we can demonstrate that our method is computationally efficient for automated segmentation of the brain microvasculature for analysis. Currently we are extending the segmentation framework to 3D micro-CT images.

References:

Bedford L, et al (2008). Depletion of 26S proteasomes in mouse brain neurons causes neurodegeneration and Lewy-like inclusions resembling human pale bodies. J Neurosci. 28(33):8189-98.

Chanwimaluang,T. et al. “An efficient blood vessel detection algorithm for retinal images

using local entropy thresholding." IEEE ISCAS, Vol. 5 (2003)

VIRTUAL NAVIGATOR - NEW MODALITY FOR INTRAOPERATIVE FUSION IMAGING OF BRAIN TUMORS

M. Filip[1], P. Linzer[2], F. Šámal[2], P. Jurek[1], D. Skoloudik[3]

[1]Dept.of Neurosurgery, [2]Dept. of Neurosurgery, Teaching Hospital T. Bati, Zlín, [3]Clinic of Neurology, Faculty Hospital Ostrava, Ostrava, Czech Republic

Virtual Navigator - new technology allows the real-time intraoperative ultrasound imaging in correlation with CT/MR images. It offers more confidence in assessing the morphology in US images, because of image fusion. Using the technology *improves the accuracy of the diagnosis,* allowes *ultrasound-navigated burr-hole biopsies,* and helps with orientation during brain tumor surger. This metod is used in diagnosis of some neurological diseases since 2009. We have been using the technology in our department in brain tumor surgery since 2011.

Methods: Utilization of virtual navigator for brain surgery.

1. Navigation before and during the main operation, where the probe is used lika a pointer.
2. Standard intraoperative ultrasound scanning 2D, 3D + flow modes.
3. When the reading of US imag is not clear the possibility of fusion with MRI may be very helpfull for orientation in brain structures and anatomy situation.

Summary: Virtual navigator has been used in brain tumor surgery by our department since June 2011. (Gliomas 3x, Metastasis 1x, Cavernoma 1x, Meningeoma 1x) Visibility of the lesion may be improved by colour flow maping or use of contras agent. Early experiences with this technology show this modality as valuable alternative to other intraoperative imaging with good price/performance ratio. Disadvantage of the technology is in design of electromagnetic positioning device which was made for diagnostics not for intraoperative imaging. This year alternative devices of other producers will be clinically tested and evaluted and companies will develop usefull instruments dedicated for this type of procedure.

USEFULNESS OF HIGH SPATIAL RELATION THREE-DIMENSIONAL FUSION IMAGE IN THE ANTERIOR APPROACH FOR THE RESECTION OF SPINAL HEMANGIOBLASTOMA

D. Nakagawa[1], T. Kin[1], K. Ishii[1], H. Imai[1], M. Yoshino[1], H. Oyama[2], N. Saito[1]

[1]Neurosurgery, [2]Clinical Information Engineering, The University of Tokyo Graduate School of Medicine, Tokyo, Japan

Objective: To perform surgical simulations using high spatial relation three-dimensional (3D) fusion image in a patient with spinal hemangioblastoma.

Methods: Spinal hemangioblastoma was identified in a female patient in her thirties with progressive partial paralysis on the right side. High-resolution images were extracted by performing CT scanning and three-dimensional rotational angiography to 3D computer graphics (3DCG). The normalized mutual information method was adopted for registration. Based on an originally developed threshold-processing method to apply multiple thresholds to a single tissue, each tissue was reconstructed as an independent 3D model using the surface rendering method. Surgical simulations were performed on workstation by rotating and scaling the obtained 3D image fusion, and removing bone with it.

Results: With 3DCG based on the our proposed method, it was possible to depict the anterior spinal artery, minute feeding vessels, and emissary veins, which are difficult to grasp using conventional 3-D imaging methods, with high spatial resolution, facilitating the recognition of the anatomical construction of the lesion and its periphery. Consequently, the anterior approach was predicted as the most appropriate in this case. Considering that it is occasionally necessary to observe spinal cord tumors during the unusual anterior approach, 3-D image fusion may facilitate such intuitive and instantaneous recognition of the anatomical construction of surgical view. Further, in the study, surgical simulations were performed with it to determine the surgical approach, extent of bone removal, and site of lesion resection, and this contributed to the development of a minimally-invasive surgical plan. It was particularly useful to perform such

simulations in order to determine the minimum necessary and most appropriate extent of vertebrectomy, and set resection margins while conserving the anterior spinal artery.

Conclusion: It may be useful to perform surgical simulations based on high spatial relation three-dimensional (3D) fusion image in the anterior approach for spinal hemangioblastoma treatment in order to develop appropriate pre- and intraoperative plans.

References:

1.Gauvrit JY,et al. 3D rotational angiography: use of propeller rotation for the evaluation of intracranial aneurysms. AJNR 2005;26:163-5

2.Kin T,et al. prediction of surgical view of neuromuscular decompression using interactive computer graphics. Neurosurgery 2009;65:121-128

NOVEL INDANONE DERIVATIVES AS PROBES FOR SENILE PLAQUES IN ALZHEIMER'S DISEASE

D. Nan[1], C. Gan[2], C. Wang[1], J. Qiao[1], J.-N. Zhou[1]

[1]CAS Key Laboratory of Brain Function and Disease, School of Life Sciences, University of Science and Technology of China,
[2]Engineering Research Center of Bio-Process of Ministry of Education, Hefei University of Technology, Hefei, China

Objectives: Senile plaques (SPs) is one of the main pathological feature of Alzheimer´s disease that composed of β-amyloid (Aβ) protein aggregates [1]. Noninvasive detection of SPs is an effective method for the early diagnosis of Alzheimer's disease. In our published work, we developed a series of indanone derivatives with high affinity to senile plaques in vitro and ex vivo [2]. Based on that, several novel indanone derivatives were synthesized with optimization in functional groups.

Methods: We designed and synthesized two indanone derivatives. The K_i value was measured by the competitive radioligand binding assay with $A\beta_{1-40}$ aggregates, and the radioligand was [^{125}I]IMPY [3]. Fluorescent staining of Br-NID and I-NID to human AD brain tissue slices was detected by fluorescence microscope [3]. [^{125}I]I-NID was synthesized, and purified by HPLC [4]. Partition Coefficient Measurement was obtained from [^{125}I]I-NID. Biodistribution of [^{125}I]I-NID was measured by ICR mice in different period. [^{125}I]I-NID was mixed with tissue homogenates and detected by HPLC to study the stability in vitro. Human AD brain tissue slice was labeled by [^{125}I]I-NID and exposed to X-ray film to obtain the autoradiography in vitro.

Results: Br-NID and I-NID exhibited the K_i value of 6.65 and 11.83 nM with $A\beta_{1-40}$ aggregates competed with [^{125}I]IMPY. In AD brain tissue fluorescent staining, both Br-NID and I-NID were specific binding to SPs. The log P value of [^{125}I]I-NID is 3.45. In biodistribution in ICR mice, [^{125}I]I-NID displayed the concentration of 5.28%ID at 2 min and 0.84%ID at 60min post-injection in brain. In human AD and control brain homogenates, the percentage of unchanged [^{125}I]I-NID is 98% at 60min and 95% at 120min. [^{125}I]I-NID labeled SPs of human AD brain tissue slice in vitro autoradiography.

Conclusions: The K_i value shows high affinity of Br-NID and I-NID to $A\beta_{1-40}$ aggregates, and the increase of log P value leads to the improvement of initial brain uptake. [^{125}I]I-NID is stable in human AD and control brain homogenates from 2 min to 120 min. Fluorescent staining and autoradiography demonstrates the specific character of Br-NID and I-NID to SPs. The analysis above suggests that I-NID has the potential to become a useful probe for detecting senile plaques for diagnosis of AD by PET or SPECT.

References:

[1]. Roberson, E.D. and L. Mucke, 100 years and counting: prospects for defeating Alzheimer´s disease. Science, 2006. 314(5800): p. 781-4.

[2]. Qiao, J.P., et al., Novel indanone derivatives as potential imaging probes for beta-amyloid plaques in the brain. Chembiochem, 2012. 13(11): p. 1652-62.

[3]. Kung, M.P., et al., Binding of two potential imaging agents targeting amyloid plaques in postmortem brain tissues of patients with Alzheimer´s disease. Brain Res, 2004. 1025(1-2): p. 98-105.

[4]. Newberg, A.B., et al., Safety, biodistribution, and dosimetry of 123I-IMPY: a

novel amyloid plaque-imaging agent for the diagnosis of Alzheimer´s disease. J Nucl Med, 2006. 47(5): p. 748-54.

NOVEL DERIVATIVES CONTAINING (E)-1-PHENYL-3-(4-((E)-STYRYL)PHENYL)PROP-2-EN-1-ONE CORE AS POTENTIAL IMAGING AGENT FOR SENILE PLAQUES

C. Wang, D. Nan, X. Wang, J. Qiao, J.-N. Zhou

CAS Key Laboratory of Brain Function and Disease, School of Life Sciences, University of Science and Technology of China, Hefei, China

Objectives: Senile plaques (SPs) is a major neuropathological feature of Alzheimer's disease (AD). Non-invasive detection of SPs by imaging agents may be a useful strategy for early diagnosis of AD.[1] In the present study, we designed a novel core structure termed (E)-1-phenyl-3-(4-((E)-styryl)phenyl)prop-2-en-1-one and then synthesized a iodo-compound termed (E)-3-(4-((E)-4-iodostyryl)phenyl)-1-(4-methoxyphenyl)prop-2-en-1-one as a new potential agent for SPs imaging.

Methods: The affinity of a series of compounds to postmortem human AD patient brain homogenates and $A\beta_{1-40}$ aggregates was measured by competitive radioligand binding study using ^{125}I-IMPY as a radiolabeled standard.[2] ^{125}I labeled compound was synthesized and then purified by HPLC. Furthermore, several experiments like autoradiography of SPs in human AD patient brain adjacent sections, partition coefficient measurement and biodistribution in normal mouse was also investigated.

Results: Competitive radioligand binding assay data were calculated and the best Ki value is 30nM. Autoradiography of SPs in human AD patient brain adjacent sections reveals that this iodo-compound could bind to SPs in a manner similar to ^{125}I-IMPY. Furthermore, the log P value of the iodo-compound is 3.31. In Biodistribution experiment, the iodo-compound displayed concentrations of 2.86% ID/g in the brain at 2 min, and 0.25% ID/g at 60 min post-injection, respectively.

Conclusions: The preliminary results suggest that this new core structure is worthy for further study and might be used as a SPs imaging agent for early detection of AD. Preparation and in vivo investigation of new derivatives based on this core structure are currently underway.

References:

[1].Mathis, C.A., Y. Wang and W.E. Klunk, Imaging beta-amyloid plaques and neurofibrillary tangles in the aging human brain. Curr Pharm Des, 2004. 10(13): p.1469-92.

[2].Zhuang, Z.P., et al., Structure-activity relationship of imidazo[1,2-a]pyridines as ligands for detecting beta-amyloid plaques in the brain. J Med Chem, 2003. 46(2): p. 237-43.

EVOLUTION MODELING OF BRAIN MEMORY FUNCTIONAL SMALL WORLD NETWORK

L. Zhang[1,2], Y. Tang[2], B. Sun[3]

[1]School of Information and Engineering, Taishan Medical University, Taian, [2]Institute of Neuroinformatics, Dalian University of Technology, Dalian, [3]Life Sciences Research Centre, Taishan Medical University, Taian, China

Objectives: In order to explore the small-world character evolution mechanism of complex brain memory functional network, discuss how to change the abstract and unordered memory phenomena into the visual and ordered scientific explanations. We focus on the memory model of the brain functional network, especially the small-world network, and discuss the evolution mechanism of small-world memory network.

Methods: We adopt deterministic modeling to set up the brain memory functional small-world network based on the graph theory, complex network theory and neural network.

Graph theory provides the network modeling methods by abstracting the node and edge. The complex network provides the network topology dynamics characters' computation so as to discuss the small-world character and verify memory characters. The neural network provides the memory association mechanism derived from memory phenomena. The deterministic modelling provides a visual and direct method to recognize the evolution mechanism of the brain memory network.

Results: We set up a brain memory functional network model by deterministic modeling algorithm, then compute the network topology characters and get the small-world network with high clustering and small average path length.

Conclusions: The brain structural and functional systems have features of complex network. Recent developments in the quantitative analysis of brain functional networks in according with small-world topology have been rapidly translated to the studies of the brain functional network simulation. In order to serve well of the simulation, we apply the deterministic modeling method to simulate the brain memory functional network based on memory factor and path compression, then discuss the computing and simulating of the model such as degree distribution, clustering coefficient and average path length. The simulation of the brain memory functional network by that way have the properties of small-world such as high clustering coefficient, especially the average path length that indicates exclusively shorter close to a constant independent on the node scale.

References:

[1] Jason W. Bohland, Ali A. Minai, Efficient associative memory using small-world architecture, Neurocomputing 38-40(2001)489-496.

[2] Olaf Sporns, Christopher J. Honey, Small worlds inside big brains, Proc. Natl. Acad. Sci. USA 103(2006)19219-19210.

[3] Ed Bullmore, Olaf Sporns, Complex brain networks: graph theoretical analysis of structural and functional systems, Nat. Rev. Neurosci. 10(2009)186-198.

[4] Christopher J. Honey, Jean-Philippe Thivierge, Olaf Sporns, Can structure predict function in the human brain?, NeuroImage 52(2010)766-776.

[5] Hana Burianova, Anthony R. McIntosh, Cheryl L. Grady, A common functional brain network for autobiographical, episodic, and semantic memory retrieval, NeuroImage 49(2010)865-874.

[6] Ginestet CE, Simmons A, Statistical parametric network analysis of functional connectivity dynamics during a working memory task, NeuroImage, 55(2011):688-704.

[7] Stevens AA, Tappon SC, Garg A, Fair DA, Functional Brain Network Modularity Captures Inter- and Intra-Individual Variation in Working Memory Capacity, PLoS ONE 7(2012): e30468.

A PC-BASED AUTORADIOGRAPHIC IMAGING SYSTEM FOR ANIMAL STROKE OR TRAUMA STUDY

W. Zhao[1,2]

[1]Biomedical Engineering, University of Miami, Coral Gables, [2]Neurology and Radiology, University of Miami Miller School of Medicine, Miami, FL, USA

Introduction: In animal experiments, brain physiology is crucially important to reveal information for animals subjected to normal condition or pathological insults (cerebral ischemia or brain trauma). Macro-scaled imaging modalities used to measure physiological information include MRI, CT, PET or autoradiography. Although autoradiographic imaging has been used to label cerebral blood flow, glucose utilization, brain protein synthesis or in situ hybridization gene expression for three decades, its applications in experimental neuroscience has been dramatically reduced in last ten years. Part of the reason is the invasive nature of the technique. However, more importantly, it is the sophisticated calibration procedure and inconvenient data processing operation that limit the technique being popularly used. Advantages of autoradiography, a functional imaging modality, are superior to other imaging techniques, including high image resolution, quantitative physiological information, and dynamic data acquisition.

Objective: Free downloadable software to conduct autoradiography is unavailable. In addition, many user-required image processing features are usually not included in common image processing software. In order to use the autoradiographic imaging technique easily in laboratory, we aimed to develop a personal computer based autoradiographic imaging system which can establish customized issue-equivalent calibration standards, acquire numerical data, process scanned images by various scientific or engineering implementations.

Materials and experimental description: This system requires a film digitizer (either a regular optical scanner or a CCD camera system). Autoradiogram with tissue sections and radiation calibration standards are digitized and converted into image format. The PC is equipped with common hardware components (3GHz CPU, 2GB RAM and a 250GB hard drive). The PC is running Fedora Linux operating system. The software is written by plain C language and uses xwindows and associated Xlib functions as graphical interface.

Methods: The system is designed to have following modules and functions:

Calibration Module:

1) Commercial radiation standards can be calibrated by Lab-made tissue-radioisotope mixture to establish tissue equivalent radiation standards.

2) For each experiment, the system generates image intensity vs. physiology calibration curve by computing radiation dose (tissue-equivalent) vs. image intensity curve and physiology data (collected through liquid scintillation counter) vs. radiation dose curve.

Processing Module:

1) 3D reconstruction is built by aligning sequentially cut tissue sections.

2) Image processing includes image averaging, statistical analysis and arithmetic operations.

3) Output function includes exporting processed data set and region-of-interest (ROI) data.

Display Module: All display functions provide online data acquisition and section or volume rendering.

Results: We have conducted a number of experimental neuroscience experiments by using the developed system. Examples will be given in the presentation. 3D reconstructed image data set reveals information that cannot be appreciated by 2D image. Arithmetic operation, such ratio image, difference image, and statistical image, quantitatively present the coupling/uncoupling effect, protection/treatment effect, etc. Atlas-based image mapping provides efficient and unbiased ROI data collection.

Conclusion: An easy-operated autoradiographic imaging system for animal laboratory has been developed and used for experimental neuroscience studies. We will expand the system's processing capability for more imaging modalities. A downloadable version will soon be available.

PROSTAGLANDIN D2 DP1 RECEPTOR ACTIVATION RESCUES THE ISCHEMIC BRAIN THROUGH IMPROVED CEREBRAL BLOOD FLOW

A. Ahmad[1,2], T. Maruyama[3], S. Narumiya[4], S. Dore[1,2,5]

[1]Department of Anesthesiology, [2]Center for Translational Research in Neurodegenerative Disease, University of Florida, Gainesville, FL, USA, [3]Discovery Research Institute I, Ono Pharmaceutical Co Ltd, Osaka, [4]Department of Pharmacology, Kyoto University Faculty of Medicine, Kyoto, Japan, [5]Departments of Neuroscience, Neurology, and Psychiatry, University of Florida, Gainesville, FL, USA

Background and purpose: Identification and use of tPA as a thrombolytic agent provided the much needed relief; however, its side effect leading to intracranial bleeding limits its usage. Therefore, the pursuit of an effective, multifaceted intervention to rescue the “stunned brain” still continues. PGD2 is the most abundant prostaglandin in the brain therefore its association with vasculature and blood makes it a prime candidate to be investigated in stroke. We have reported earlier that characterization of cerebral vessels in C57BL/6 wildtype (WT) and DP1-/- mouse brain show no major differences however DP1-/- have greater brain damage after middle cerebral artery occlusion (MCAO) and NMDA-induced acute excitotoxicity. Here, we test whether activation of DP1 receptor by selective agonist BW245C post-treatment after stroke improves cerebral blood flow (CBF), consequently minimizes anatomical and functional deficits.

Methods: First, to determine if BW245C can change basal CBF, WT and DP1-/- mice were anesthetized and a laser Doppler flow probe was affixed to the skull to record CBF. After the baseline, WT and DP1-/- mice were given single i.p. injection of vehicle or 0.02, 0.2, 2.0mg/kg BW245C, and CBF was recorded for

2h. Next, to determine whether BW245C can prevent brain damage after MCAO, WT and DP1-/- mice were subjected to 60min MCAO and 96h reperfusion. Immediately at reperfusion, mice were given a single i.p. injection of vehicle or 0.02, 0.2, 2.0mg/kg BW245C. The functional and anatomical outcomes were determined at 96h. Further, to determine if the beneficial effect of BW245C is through CBF, BW245C was given during occlusion and changes in peri-infarct and core CBF were continuously recorded. Finally, to address any potential compensatory mechanisms, effect of BW245C on stroke outcomes was also tested in DP1-/-.

Results: The basal CBF after BW245C treatment significantly increased in WT whereas in DP1-/- it remained unchanged. The infarction volume was significantly ($p< 0.05$) reduced to 38.7±8.1% in 0.2mg/kg BW245C treatment group as compared with the control group (51.2±7.1%) and vehicle group (52.7±8.6%). The BW245C treatment also reduced the functional deficits significantly. Interestingly, BW245C also resulted in considerable increase in peri-infarct and core CBF immediately before reperfusion. Analysis revealed a strong correlation between attenuation in infarction and CBF improvement in peri-infarct immediately at reperfusion ($p< 0.02$) and at 60min after reperfusion ($p< 0.005$). The infarction in DP1-/- was significantly higher (66.3±11.4%) than the WT control mice (51.2±7.1%), and BW245C treatment didn't change the final outcome in DP1-/-.

Conclusions: Accumulating data suggests that stimulation of the DP1 receptor after stroke improves CBF, and minimizes brain damage and functional deficits. This ongoing work provides novel mechanistic pathways to better explain the neuroprotective mechanisms of DP1 receptor in stroke.

References:

1-Kiriyama et al. Br J Pharmacol 1997; 122:217.

2-Eguchi et al. PNAS 1999; 96:726.

3-Narumiya et al. Physiol Rev 1999; 79:1193.

4-Hayaishi and Urade. Neuroscientist 2002; 8:12.

5-Liang et al. Neurochem 2005; 92:477.

6-Bate et al. Neuropharmacology 2006; 50:229.

7-Saleem et al. Eur J Neurosci 2007; 26: 73.

8-Li et al. Neurochem Res. 2008; 33:490.

9-Ahmad et al. Age 2010; 32: 271.

DIMINISHED ET_B RECEPTOR-MEDIATED VASOCONSTRICTION BY MEK1/2 INHIBITION IS ASSOCIATED WITH IMPROVED NEUROLOGICAL FUNCTION AFTER CEREBRAL ISCHEMIA IN FEMALE RATS

H. Ahnstedt[1], F. W Blixt[1], R. Thiagarajah[1], K. Warfvinge[1], D.N. Krause[2], L. Edvinsson[1]

[1]Clinical Sciences, Experimental Vascular Research, Lund University, Lund, Sweden, [2]Pharmacology, School of Medicine, University of California, Irvine, CA, USA

Introduction: Sex differences are well-known in cerebral ischemia as demonstrated by the higher incidence of stroke in men throughout much of the lifespan. The sex difference persists well beyond the menopausal years, up to 80 years, suggesting that intrinsic biological sex differences play a major role beside the hormonal effects [1]. Experimental stroke and organ culture induce upregulation of contractile ET_B receptors in vascular smooth muscle cells of cerebral arteries from male rat [2]; thereby further reducing blood flow and increasing tissue damage after ischemia. Treatment with the MEK1/2 inhibitor U0126 attenuates ET_B receptor upregulation, reduces infarct size and improves neurological function in male rats [3, 4], however, responses in females are not known.

Objectives: The present study aims to investigate i) whether ET_B receptor upregulation occurs in female rats, ii) if receptor upregulation is mediated by activation of the MEK/ERK1/2 pathway, and iii) if the MEK1/2 inhibitor U0126 attenuates ET_B receptor upregulation and show benefit in female rats after cerebral ischemia.

Methods: Transient middle cerebral artery occlusion was performed in female rats with and without U0126 treatment administered at 0 h and 24 h (30 mg/kg i.p.). Additionally, in vitro organ culture of isolated cerebral arteries from female rats was studied as a model for

ET_B receptor upregulation. Stroke infarct volumes were assessed with neuron-specific nuclear protein NeuN staining and neurological examination was performed with 6-point neuroscore. ET_B receptor-mediated contraction was studied with wire myograph, and protein expression with immunohistochemistry and Western blot, respectively.

Results: Cerebral ischemia in female rat resulted in increased ET_B receptor expression and vasoconstriction. U0126 treatment attenuated ET_B receptor-mediated vasoconstriction, prevented the ischemia-induced ET_B receptor expression and improved the neurological function.

Conclusion: The present study demonstrates for the first time increased ET_B receptor-mediated vasoconstriction in female middle cerebral arteries after focal cerebral ischemia. MEK1/2 inhibition attenuated ischemia-induced ET_B receptor upregulation and improved neurological function, but did not significantly reduce the brain damage. Our findings may indicate somewhat less effects to stroke treatment with the MEK1/2 inhibitor U0126 in females, compared to earlier reports in males.

References:

1. Turtzo, L.C. and L.D. McCullough, Future Neurol, 2010. **5**(1): p. 47-59.

2. Povlsen, G.K., et al., Exp Brain Res, 2012. **In Press**.

3. Henriksson, M., et al., Exp Brain Res, 2007. **178**(4): p. 470-6.

4. Maddahi, A. and L. Edvinsson, BMC Neurosci, 2008. **9**: p. 85.

POST-ISCHEMIA ETHANOL (PIE) THERAPY IS HIGHLY NEUROPROTECTIVE IN ACUTE STROKE BY REDUCING OXIDATIVE INJURY THROUGH IMPROVED METABOLIC FUNCTION

K. Asmaro[1], C. Peng[1], R. Kochanski[1], T. Higashida[1], I. Lee[2], M. Hüttemann[2], M. Guthikonda[1], Y. Ding[1]

[1]Department of Neurological Surgery, [2]Center for Molecular Medicine and Genetics, Wayne State University School of Medicine, Detroit, MI, USA

Objectives: Our recent study (*Stroke. 2012, 43(1):205-10*) has demonstrated a strong neuroprotective effect of ethanol (EtOH) in ischemic stroke. The underlying mechanisms, however, remain to be determined. Balanced energy metabolism is critical for neuronal survival. Previous studies have shown EtOH to decrease whole-brain metabolism, suggesting its potential to ameliorate metabolic dysfunction following ischemia, thereby serving as a possible neuroprotective agent for stroke therapy. The purpose of this study was to determine whether EtOH attenuates and normalizes hyperglycolytic and oxidative metabolism, thereby reducing oxidative damage in ischemic stroke.

Methods: Sprague-Dawley rats underwent right middle cerebral artery occlusion (MCAO) for 2 h. EtOH (1.5 g/kg, reaching a blood concentration equivalent to the legal driving limit) was administered at the onset of reperfusion. Levels of reactive oxygen species (ROS) and apoptotic cell death were measured to assess oxidative injury. Levels of lactate, lactate dehydrogenase (LDH), glucose transporters (GLUT-1 and -3), and phosphofrucktokinase-1 (PFK-1) were measured to assess cerebral glycolysis. Levels of pyruvate dehydrogenase (PDH) as well as activities of NADPH oxidase (NOX) and cytochrome c oxidase (CcO) were assayed to assess mitochondrial oxidative metabolism. NAD/NADH ratio, ADP/ATP ratio, and Na+/K+ ATPase activity were measured to assess overall cellular function.

Results: Oxidative damage determined by increased ROS production and apoptotic cell death was significantly reduced by EtOH at 3 and/or 24 h after reperfusion. At 3 h post-reperfusion, production of ATP and NADH, as well as Na+/K+ ATPase activity were decreased in the ischemic rat; EtOH, however, normalized these parameters to control-matched levels, suggesting a restoration of cellular function by EtOH. EtOH treatment reduced the higher levels of lactate and LDH, as well as the expression of GLUT-1 and -3, and PFK-1 after ischemia, suggesting an attenuation of hyperglycolysis during reperfusion. Furthermore, a significant decrease in PDH expression and an increase in NOX and CcO activities after stroke were largely reversed by EtOH treatment, suggesting an improved and well controlled oxidative metabolism.

Conclusions: Acute administration of EtOH after stroke regulates cellular glucose and

oxidative metabolism, producing favorable outcomes with reduced ROS generation and apoptotic cell death. Aside from expanding upon the pathophysiology of stroke, this study helps validate an ancient drug for a new therapeutic application and proposes new therapeutic mechanisms in stroke.

Reference: Wang, F., Wang, Y., Geng, X., Asmaro, K**.**, Peng, C., Sullivan, J.M., Ding, J.Y., Ji, X., Ding, Y., 2012. Neuroprotective effect of acute ethanol administration in a rat with transient cerebral ischemia. Stroke. 43**,** 205-10.

IDENTIFICATION OF ISCHEMIC PENUMBRA USING FDG POSITRON EMISSION TOMOGRAPHY

H. Backes[1], M. Walberer[2], H. Endepols[1], B. Neumaier[1], K. Wienhard[1], R. Graf[1], G. Mies[1]

[1]Max Planck Institute for Neurological Research, [2]Neurology, University Hospital Cologne, Cologne, Germany

Objectives: The penumbra is characterized by reduction of cerebral blood flow (CBF) and preserved energy metabolism. Penumbral tissue will eventually result in brain infarction but may be salvaged by therapeutic intervention. Therefore, the non-invasive definition of penumbral tissue is a prerequisite for evaluating new therapies of acute stroke.

With positron emission tomography (PET) CBF and metabolism can be measured non-invasively using [15O]H2O and [15O]O2 as tracer. Identification purely based on CBF levels as well as identification by mismatch of diffusion and perfusion weighted MRI fails. However, due to the short half-life of [15O] (2 minutes) applicability of this method is restricted to only a small number of PET centres with an onsite cyclotron.

We show that reduced CBF and preserved energy metabolism can alternatively be measured using [18F]2-fluoro-2-deoxy-D-glucose (FDG) as PET tracer. Since this compound is available to every PET centre, the potential for the penumbra identification is highly increased.

Methods: Remote occlusion of the middle cerebral artery was induced in 10 Wistar rats by injection of 4 TiO2 macrospheres. 60 Minutes after occlusion CBF was measured with [15O]H2O-PET followed by a 60 minutes FGD-PET scan. FDG kinetic parameters were determined by kinetic modelling of the data with a two-tissue-compartment model. [15O]H2O-PET data and FDG kinetic parameters were compared with structural MRI and histology at 24 hours.

Results: Comparison of CBF measured with [15O]H2O and the unidirectional rate constant for FDG transport from blood to tissue (K1) shows - as expected from theory - that K1 is equal to CBF in the limit of low flow. The hypo-perfused area can therefore be identified by the FDG parameter K1. We calculated glucose consumption rate (CMRG) as a function of K1 and the net influx rate constant Ki of FDG. In contrast to the commonly used autoradiographic method for calculating CMRG from FDG, this method does not lose validity in pathologic tissue. The penumbra can then be identified as a region of reduced K1, increased Ki, and preserved CMRG in analogy to identification with 15O tracers where the penumbra shows reduced CBF increased oxygen extraction fraction and preserved CMRO2. The combined core (low K1 and low CMRG) and penumbra region determined from the FDG data agreed well with the total infarct volume defined by MRI or histology 24 hours past occlusion.

Conclusion: With the described method the ischemic penumbra can be identified non-invasively using FDG-PET. The reduction in glucose delivery (and CBF) is compensated by an increase in hexokinase activity and thus preserves CMRG and extends tissue viability.

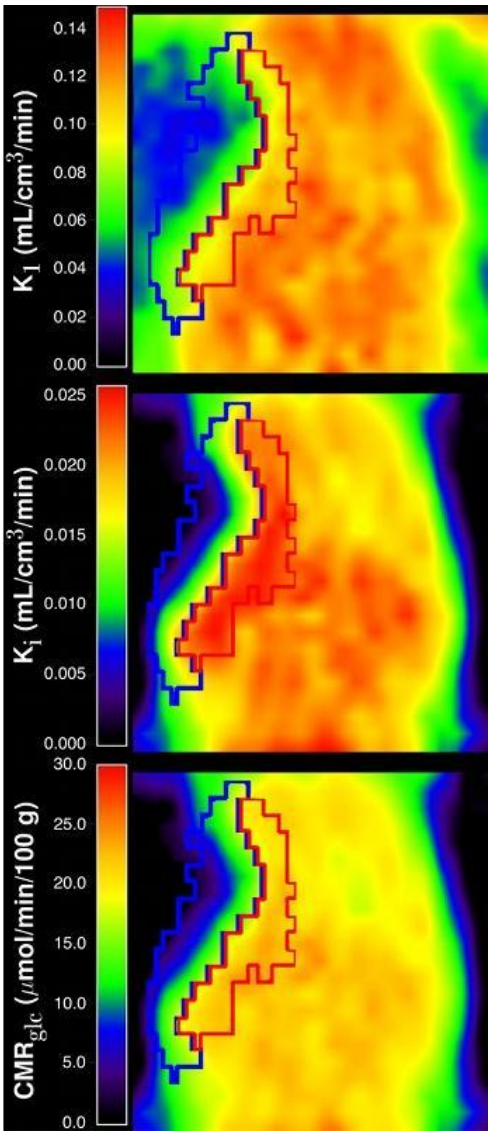

[Penumbra detection with FDG kinetic parameters]

Parametric images of FDG kinetic parameters from a rat after occlusion of the middle cerebral artery enable the detection of the ischemic penumbra (red contour) and core (blue contour).

QUANTIFYING LEPTOMENINGEAL COLLATERAL BLOOD FLOW DURING MIDDLE CEREBRAL ARTERY OCCLUSION IN THE RAT

D.J. Beard[1,2], D.D. McLeod[1,2], C.L. Logan[1], M. Imtiaz[1,2], N.J. Spratt[1,2]

[1]School of Biomedical Sciences and Pharmacy, University of Newcastle, Callaghan, [2]Hunter Medical Research Institute, New Lambton, NSW, Australia

Leptomeningeal collateral blood flow is a powerful clinical predictor of stroke size, major reperfusion and stroke outcome. Therefore collateral vessels are an extremely attractive therapeutic target for stroke. In order to trial "Collateral Therapeutics" a preclinical model with quantitative assessment of collateral flow is needed. Our aim was to develop an animal model permitting quantitative assessment of collateral blood flow during middle cerebral artery occlusion (MCAo) and reperfusion.

Methods: Fluorescent 1 µm microspheres were visualised through a closed cranial window during MCAo in Wistar rats (n= 4). A high-speed microscope-mounted recording camera was used. Microsphere velocity and vessel diameter were calculated using Image J software. Individual vessel collateral flow was calculated before, during and after MCAo.

Results: Baseline collateral flow was bidirectional (from anterior cerebral artery (ACA) and MCA) at 166 ± 85 nl/min/vessel (mean ± SE). Where the opposing flows met, spheres dived into penetrating arterioles. Immediately following MCAo, flow within the MCA reversed and dramatically increased, to 513 ± 159 nl/min/vessel at 1 min after MCAo, and peaked at 890 ± 273 nl/min/vessel at 90 minutes after occlusion. Immediately following reperfusion collateral flow was predominantly from MCA to ACA; this subsequently returned towards baseline levels at 10 min after reperfusion (257 ± 78 nl/min/vessel), and then rose again at 15 min post-reperfusion (502 ± 178 nl/min/vessel).

Conclusions: A large but highly variable increase in flow was seen during MCAo, similar to that seen angiographically in patients. Contrary to previous reports, we found persistent blood flow through collateral vessels following reperfusion. The ability to quantify absolute blood flow will permit better

modelling of the key regulators of collateral flow, and targeted investigation of potential collateral therapeutic strategies.

IMPROVING QUALITY AND PREDICTIVENESS OF TRANSLATIONAL BRAIN RESEARCH: STATE-OF-THE-ART METHODS AND FUTURE PERSPECTIVES

J. Boltze[1,2], J. Jolkkonen[3], A. Denes[4,5], G. Metz[6], M. Macleod[7], U. Dirnagl[8,9]

[1]Department of Cell Therapy, Fraunhofer Institute for Cell Therapy and Immunology, Leipzig, Germany, [2]Massachusetts General Hospital and Harvard Medical School, Boston, MA, USA, [3]Institute of Clinical Medicine, Neurology, University of Eastern Finland, Kuopio, Finland, [4]Faculty of Life Sciences, University of Manchester, Manchester, UK, [5]Institute of Experimental Medicine, Hungarian Academy of Sciences, Budapest, Hungary, [6]Canadian Centre for Behavioural Neuroscience, University of Lethbridge, Lethbridge, AB, Canada, [7]Department of Neuroscience, Centre for Clinical Brain Sciences, University of Edinburgh, Edinburgh, UK, [8]Departments of Neurology and Experimental Neurology, [9]Center for Stroke Research Berlin, Charité University Medicine, Berlin, Germany

Rational and summary: Despite thorough preclinical and clinical research activities, thrombolysis by tissue plasminogen activator (tPA) remains the only approved treatment option for ischemic stroke so far. In fact, the development of novel stroke therapies is hampered by a continuous failure to translate experimental findings and treatment strategies to the clinic.

Since a lot of clear parallels have been reported and relevant clinical results were predicted by well-designed preclinical trials, there is no good reason to assume that our animal models are generally incapable of reflecting the pathophysiology of human stroke. However, there is a strong demand for the proper use of these models, adequate behavioral tests and more realistic preclinical study designs to resemble the clinical situation and to thereby improve our research strategies. Moreover, understanding the translational failure in neuroprotection should also prevent in repeating same mistakes in restorative studies.

This symposium will discuss biostatistical problems being related to use of neurofunctional tests in stroke. It will present strategies to optimize the predictive power of such tests and will give examples for unexpected, but translationally relevant preclinical results regarding later clinical trials. It also provides knowledge about best models and behavioral outcome measures and gives concrete evidence that our preclinical research approaches can be designed to be highly predictive.

We will also suggest and discuss novel preclinical trail design models as their implementation in future research endeavors to reach a higher level of predictiveness and should therefore be of interest for the basic and translational stroke research community.

Speakers and session details: Johannes Boltze (Fraunhofer-Institute for Cell Therapy and Immunology, Leipzig, Germany / Massachusetts General Hospital and Harvard Medical School, Boston, USA) will introduce the speaker and highlight the particular challenges and solutions to be discussed throughout the session.

Jukka Jolkkonen (University of Eastern Finland, Kuopio, Finland) will review widely used stroke models and discuss potential reasons for the previous failure of translating neuroprotective therapies to the clinic.

Adam Denes (University of Manchester, United Kingdom / Institute of Experimental Medicine, Budapest, Hungary) will provide novel insights to state-of-the-art brain disease modeling with special emphasis on confounders and relevant comorbidities to be considered in preclinical stroke research.

Gerlinde Metz (Department of Neuroscience, University of Lethbridge, Canada) will discuss proper neurofunctional assessment techniques for rodents as well as their meaningful implementation in experimental therapeutic studies.

Malcolm Macleod (Department of Neuroscience, Centre for Clinical Brain Sciences, University of Edinburgh, Scotland, United Kingdom) will introduce the concept of international, multicenter, randomized and controlled 'phase III' preclinical trials and the expected impact on stroke research.

Finally, Ulrich Dirnagl (Center for Stroke Research Berlin / Departments of Neurology and Experimental Neurology at the Charité,

Berlin, Germany) will summarize the main findings reported as well as the central hypotheses an solutions suggested to open the scientific discussion.

APOPTOTIC AND NECROTIC PROCESSES IN A RAT ORGANOTYPIC HIPPOCAMPAL SLICE CULTURE MODEL OF ISCHEMIC STROKE WITHOUT REPERFUSION

A.I. Martin[1], P.I. Huynh[1], R.D. Sweazey[1], B.C. Hong-Goka[2], **F.-L.F. Chang**[1]

[1]Indiana University School of Medicine Fort Wayne, Fort Wayne, IN, [2]UCSF - Fresno Alzheimer's & Memory Center, Fresno, CA, USA

Organotypic hippocampal brain slice cultures (OHCs) are one of the most widely used *in vitro* models of ischemic stroke. Using an *in vitro* method of culturing, this model simulates an *in vivo* environment where neurons retain their cellular connections and functions. Detection of neuronal cell death is a standard procedure to assess the severity of damage in tissue culture models of neurodegenerative diseases. However, information about the time course of injury during an ischemic event is limited and experiments documenting apoptotic processes that occur in the ischemic penumbra, where cells are still salvageable, are lacking. Therefore we examined the time course of apoptosis and necrosis in a rat OHC model of ischemia. Characterization of apoptotic tissue *in vitro* is needed to further therapeutic targeting and prevention of apoptosis in the penumbra, thereby limiting the expansion of infarct volume and improving outcome after stroke.

We exposed OHCs from postnatal day 6-9 Sprague Dawley rats to varying periods of oxygen and glucose deprivation (OGD) (0, 2, 4, 6, 8 and 16 hours) at 37°C to mimic conditions following cerebral ischemia. All analytical tests were run immediately after OGD to avoid reperfusion effects, a condition we believe to be more clinically relevant than the more traditional *in vitro* reperfusion models since the majority of stroke patients do not experience reperfusion. The viability of the hippocampal slices exposed to OGD was determined qualitatively and quantitatively using YO-PRO 1 iodide which stains apoptotic cells and propidium iodide (PI) which stains necrotic cells.

Apoptosis in the OHCs increased gradually with increased time of OGD. Image analysis of YO-PRO 1 iodide fluorescent intensity showed that after 1 hour of OGD an increase in YO-PRO 1 staining was already apparent in the CA1 and dentate gyrus with maximum staining intensity occurring between 4 and 8 hours of OGD. In parallel, quantitative analysis showed a small number of PI stained cells which could also be detected as early as 1 hour following OGD, but notable increases were not observed until at least 6 hours of OGD. Along with the changes in fluorescent intensity of the two viability stains, we also observed gross changes in the morphology of the slice under light microscopy. The data gathered from these experiments suggest that the most suitable length of ischemia without reperfusion for the maximization of apoptosis in our OHC model is between 4 and 8 hours. Within this time frame we see a large increase in apoptotic cells which are potentially salvageable and are easily accessible for application and assessment of neuroprotective interventions.

In conclusion, our *in vitro* model is easy and results are stable and reliable. It provides us with the unique opportunity (1) to select the severity of the ischemic insult by varying the period of OGD, (2) to estimate the amount of damage by evaluating the effects on viability through generation of apoptotic and necrotic cells, and (3) to test potential new treatments for hypoxic-ischemic stroke.

CALRETICULIN AND CAROTID PLAQUES STABILITY

B.-L. Chen, Y. Xu, Z.-Z. Wu, X.-B. Li

Nanjing Drum Tower Hospital Clinical College of Nanjing Medical University, Nanjing, China

Aims: Carotid plaques stability plays a important role in the pathological process of stroke. In this study, we investigated the relationship between calreticulin and plaque stability, as well as the possible mechanism.

Method: 19 patients were underwent carotid endarterectomy. Plaques were stained with hematoxylin and eosin and immunohistochemically before being classified into stable and instable groups based on their pathological aspects. Calreticulin expression was detected by immunostaining and western blotting.

Result: Necrosis, hemorrhage and thrombus

in instable plaques is more likely to lead to stroke. Higher expression of calreticulin was in instable plaques than that in the stable plaques by immunostaining and western blotting.

Conclusion: The results indicated that high expression of calreticulin in instable plaques which is correlated to the pathomechanism of destabilization.

THE INVOLVEMENT OF PROGRAMMED CELL DEATH 5（PDCD5）IN THE REGULATION OF APOPTOSIS IN CEREBRAL ISCHEMIA/REPERFUSION INJURY

C. Chen[1], Z. Jiang[1], X. Yang[1], J. Yan[1], L. Yang[1], K. Wang[1], Y. Chen[2], J.H. Zhang[3], C. Zhou[1]

[1]Peking University Health Science Center, Beijing, [2]Peking University Center for Human Disease Genomics, Beijng, China, [3]Loma Linda University, Loma Linda, CA, USA

Programmed Cell Death 5 (PDCD5) is a protein that accelerates apoptosis in different types of cells in response to various stimuli, and is down-regulated in many cancer tissues. In this study, we found for the first time that PDCD5 plays an essential role in brain ischemic injury in a rat focal cerebral ischemia model. We hypothesized that down-regulating PDCD5 can protect the brain from ischemic damage by inhibiting PDCD5 induced apoptotic pathway. Results showed that PDCD5 siRNA reduced the infarct volume, improved neurological deficits and reduced Evans blue extravasation. Meanwhile, over-expression of PDCD5 protein using recombinant human PDCD5 (rhPDCD5) had the opposite effect. But unfortunately, changed PDCD5 expression had no significant effect on mortality. Immunohistochemistry and western blot demonstrated PDCD5 siRNA decreased expressions of key pro-apoptotic proteins such as p53, Bax/Bcl-2 and cleaved casepase-3 in the infarcted areas, whereas PDCD5 overexpression attenuates cell apoptosis. Double fluorescence labeling showed PDCD5 positive immunoreactive materials were partly colocalized with MAP2, GFAP, p53 and caspase-3 in the injured cerebral cortex. In conclusion, we found in this study that PDCD5 induced apoptosis and over-expression of PDCD5 is harmful to the ischemic neurons in vivo. Meanwhile, inhibition of PDCD5 may be protective via reducing the apoptotic-related protein such as p53, Bax and caspase-3. This observation may have potential for the treatment of ischemic cerebral stroke.

THE REGENERATIVE EFFECTS OF DANSHENSU AFTER ISCHEMIC STROKE IN ASMA-GFP TRANSGENIC MICE

D. Chen[1], J. Li[2], D. Drury-Stewart[1], L. Wei[1,3]

[1]Dept Anesthesiol., Emory Univ. Sch. of Med., Atlanta, GA, USA, [2]Dept of Neurology, Beijing Friendship Hospital, Beijing, China, [3]Dept Neurol, Emory Univ. Sch of Med., Atlanta, GA, USA

Objective: Danshen, the dried root of *Salvia miltiorrhiza*, is a popular traditional Chinese medicine that has been widely used in both Asian and Western countries for promoting circulation and vasodilatation of the heart. Danshensu (Salvianic acid A) is a major active hydrophilic component from Danshen, which has been shown to dilate coronary arteries, inhibit platelet aggregation and improve microcirculation. In this study, we tested the hypothesis that Danshensu stimulates neurovascular repair and improves cerebral blood reperfusion after ischemic stroke.

Method: To visualize the brain arteries, transgenic mice expressing GFP under the control of the αSMA promoter were used in our study. Permanent focal ischemia was induced by occluding the right middle cerebral artery in WT C57/BL6 and αSMA-GFP mice. Danshensu extract (700 mg/kg, i.p.) was injected 10 min after the stroke induction and also daily until the mice were sacrificed. 5-Bromo-2'-deoxyuridine (BrdU, 50 mg/kg, i.p.) was injected daily starting 3 days after ischemia to label proliferating cells . Local cerebral blood flow after stroke was measured by PeriScans laser Doppler imaging. Immunostaining and Western blot were also performed to examine neurogenesis, angiognesis and arteriogenesis after ischemic stroke.

Results: More newborn neurons (NeuN and BrdU co-labeled cells) in peri-infarct cortex were found in Danshensu-treated mice 28 days after stroke. Furthermore, Danshensu remarkably increased proliferating endothelial cells and smooth muscle cells, enlarged the diameter of collaterals (Figure 1) and enhanced the local cerebral blood flow recovery after stroke. Danshensu significantly increased the expression of neurotrophic

factors such as VEGF, SDF-1, BDNF as well as eNOS expression in the peri-ischemic cortex. Danshensu-treated animals showed more doublecortin (DCX)-positive neurons in the peri-ischemic cortex and more newborn DCX-positive cells in the migratory tract from the SVZ to peri-infarct region 14 days after stoke.

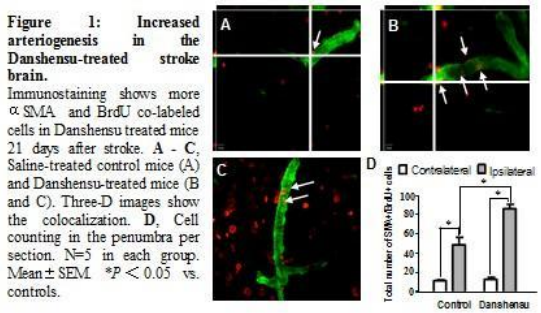

Figure 1: Increased arteriogenesis in the Danshensu-treated stroke brain.
Immunostaining shows more α SMA and BrdU co-labeled cells in Danshensu treated mice 21 days after stroke. **A - C**, Saline-treated control mice (A) and Danshensu-treated mice (B and C). Three-D images show the colocalization. **D**, Cell counting in the penumbra per section. N=5 in each group. Mean ± SEM. *$P < 0.05$ vs. controls.

[Increased arteriogenesis by Danshensu]

Conclusions: These results suggest that Danshensu promotes neurogenesis, angiogenesis and arteriogenesis, and enhances local blood flow in the post-ischemic brain which may contribute to the overall functional recovery after ischemic stroke.

References:

1. Wei L et. al. Ministrokes in rat barrel cortex. Stroke 26: 1459, 1995.

2. Wei L et al., Collateral growth and angiogenesis around cortical stroke. Stroke 32: 2179, 2001.

3. Li Y et al., Enhanced neurogenesis and cell migration following focal ischemia and peripheral stimulation in mice. Dev Neurobiol, 68:1474, 2008.

NEURORESTORATIVE THERAPY FOR STROKE IN TYPE ONE DIABETIC RATS USING APX3330

T. Yan[1], M. Chopp[1], A. Zacharek[1], R. Ning[1], X. Qiao[2], M.R. Kelley[3], C. Roberts[1], **J. Chen**[1]

[1]Neurology, [2]Ophthalmogy, Henry Ford Hospital, Detroit, MI, [3]Herman B Wells Center for Pediatric Research, Indiana University School of Medicine, Indianapolis, IN, USA

Objectives: Diabetes mellitus (DM) is associated with both microvascular and macrovascular disease and leads to a 3-4 fold higher risk of experiencing ischemic stroke and arteriosclerosis. Hyperglycemia and diabetes instigate a cascade of events leading to vascular endothelial cell dysfunction, increased vascular permeability, a disequilibrium of angiogenesis and poor recovery after ischemic stroke. In addition, DM stroke patients are more prone to develop more and earlier white matter (WM) high-intensity lesions than non DM stroke patients. APX3330, a small molecule inhibitor of apurinic apyrimidinic endonuclease redox effector factor-1 (APE1/Ref-1) redox activity, inhibits hypoxia-inducible factor 1α (HIF1a) and nuclear factor kappa-light-chain-enhancer of activated B cells (NFκB) activity. APX3330 decreases retinal angiomatous proliferation (RAP)-like neovascularization and also facilitates neuronal protection against ionizing radiation-induced toxicity. In this study, we are the first to investigate whether APX330 treatment of stroke in Type one diabetic (T1DM) rats promotes neurorestorative effects and improves functional outcome.

Methods: Adult male Wistar rats (225-250g, 3 months) were used to induce T1DM by a single intraperitoneal injection of streptozotocin (STZ, 60mg/kg). Diabetes was defined by fasting blood glucose >300mg/dl. Rats were used 2 weeks after diabetes induction. T1DM rats were subjected to 2h transient middle cerebral artery occlusion (MCAo) and treated with or without APX3330 (10mg/kg, gavage) initiated at 24h after MCAo daily for 14 days. Rats were sacrificed at 14 days after MCAo. To test brain blood barrier (BBB) leakage, Evan's blue dye was injected at 4h before sacrifice. Rats were sacrificed at 5 days after MCAo for BBB leakage assay. A battery functional tests, and vascular and WM changes and protein expression were measured in the ischemic brain.

Results: The data show that APX330 treatment of stroke did not decrease lesion volume and BBB leakage; however, treatment with APX330 significantly improved functional outcome after stroke ($p< 0.05$). APX3330 treatment significantly decreased total vessel density, but increased smooth muscle cell rounded vessel number as well as enhanced axonal density, oligodendrogenesis and synaptic protein expression measured by Luxol fast blue, neuron-glial antigen 2 (NG2,oligodendrocyte progenitor cell marker), 2´,3´-cyclic-nucleotide 3´-phosphodiesterase (CNPase) and Synaptophysin expression, respectively. We also found that APX3330

significantly decreased receptor for Advanced Glycation Endproducts (RAGE, 5 fold), Matrix Metallopeptidase 9 (MMP9, 3 fold), monocyte chemotactic protein-1 (MCP1, 3 fold) and macrophage inflammatory proteins 1 α (MIP-1α, 4 fold) levels measure by Angiogenic ELISA array. Using in vitro primary cortical neuron (PCN) and oligodendrocyte (OL) culture model, we found that high glucose and Advanced Glycation Endproducts (AGE), both increase PCN and OL cell death and decrease PCN neurite outgrowth. APX3330 treatment significantly decreases PCN and OL cell death and promotes PCN neurite outgrowth in high glucose condition.

Conclusion: Decreasing RAGE and inflammatory factors expression may promote vascular and white matter remodeling and facilitate APX3330 induced neurorestorative effect after stroke in T1DM rats.

CHARACTERIZATION OF HYPOXIA INDUCIBLE FACTOR PATHWAY IN NEUROPROTECTION AND NEURORESTORATION FOLLOWING CEREBRAL ISCHAEMIA

R. Chen[1,2], S. Nagel[2,3], M. Papadakis[2], P. Ratcliffe[4], C. Pugh[4], C. Schofield[5], A. Buchan[2]

[1]School of Pharmacy, Keele University, Stoke, [2]Nuffield Department of Medicine, University of Oxford, Oxford, UK, [3]Department of Neurology, University of Heidelberg, Heidelberg, Germany, [4]Henry Welcome Building for Molecular Physiology, [5]Department of Chemistry, University of Oxford, Oxford, UK

Activation of the hypoxia inducible factors (HIF) pathway confers protection against ischemia / reperfusion injury and can be induced by inhibition of the HIF prolyl-4-hydroxylase enzymes (PHD1-3). To successfully apply PHD inhibitors for neuroprotection in ischaemic stroke, the precise function of each PHDs (1-3) was investigated by using mice with each isoform genetically suppressed as well as by applying a novel hypoxia mimetic agent - FG2216. FG2216 has higher specificity on PHD than FIH (factor inhibiting HIF) and is currently being studied for clinical trials on anaemia (www. Fibrogen.com/programs/fg-2216).

Middle cerebral artery occlusion (MCAO)(45min ischaemia/24h reperfusion) was performed on male, 8-12 week old $PHD1^{-/-}$, $PHD2^{+/-}$ and $PHD3^{-/-}$ mice and their wild type (WT) littermates, and C57/B6 mice with/without FG2216 treatment. During the experiments, regional cerebral blood flow (rCBF) was recorded by laser Doppler flowmetry. Behaviour was assessed at 24h after reperfusion with a common neuroscore. Infarct volumes, blood brain barrier (BBB) disruption, cerebral vascular density, reactive oxygen species (ROS) and apoptosis were then determined using histological and immunohistochemical techniques.

When compared to their WT littermates, $PHD2^{+/-}$ mice had significantly more effective restoration of rCBF upon reperfusion, better functional outcomes (Neuroscores: 1.9±0.5 vs 4.3±0.5, $p< 0.01$) and higher activity rates at 24h after MCAO, there were significantly fewer apoptotic cells in the penumbra and less BBB disruption, with a trend towards reduced infarct volume (26.7±6.7% vs 40±5.5%, $p=0.15$) at 24h after MCAO but no difference in ROS formation; $PHD3^{-/-}$ mice had impaired rCBF upon early reperfusion but comparable functional outcomes; $PHD1^{-/-}$ mice did not show any significant changes following MCAO.

When receiving FG2216 one day before the MCAO, C57/B6 mice had better neuroscores and smaller infarct volumes than those receiving the vehicle, with only the low-dose (20 mg/kg) comparison reaching statistical significance (Neuroscores: 2.0±0.6 vs 4.5±0.3, Infarct volumes: 27.0±8.1% vs 47.4±5.3%, both $p< 0.05$). When FG2216 was given immediately before the MCAO, mice had similar neuroscores and infarct volumes to those receiving the vehicle with either low or high dosages.

Genetic inhibition of PHD enzymes produces different effects on outcome after transient cerebral ischemia. Notably, partially knock-out PHD2 confers neuroprotection for cerebral ischaemia. These effects are seen following lifelong PHD deficiency and thus reflect a composite of developmental changes, affecting features such as vessel density and overall sympathetic tone, and perhaps more acute effects amplifying the hypoxic stimuli inherent in this model. Only these latter effects can contribute to the observed protection entrained by the specific PHD inhibitor - FG2216 administration one day before, but not acutely at the time of cerebral ischemia. HIF activation upon ischaemic injury is swift, but the HIF transcription is delayed. Taken together it is possible that pharmacological inhibition of PHD2 would stimulate adaptations

that provide protection against damage from a subsequent stroke. Specific inhibitors of PHDs can be developed as drugs for ischaemic diseases once potential systemic side effects of PHD manipulation are delineated. Our study needs to be considered in optimizing therapeutic effects of PHD inhibitors, particularly when isoform specific inhibitors become available.

IMMUNE CELL INFILTRATION AFTER PERMANENT CEREBRAL ISCHEMIA

H.X. Chu[1], H.A. Kim[1], S. Lee[1], M. Gelderblom[2], T.V. Arumugam[3], G.R. Drummond[1], C.G. Sobey[1]

[1]Department of Pharmacology, Monash University, Melbourne, VIC, Australia, [2]Department of Neurology, University Medical Center Hamburg-Eppendorf, Hamburg, Germany, [3]Department of Pharmacology, University of Queensland, St Lucia, QLD, Australia

Objectives: The temporal profile of leukocyte infiltration in the brain following transient focal cerebral ischemia has recently been described (Gelderblom *et al.*, 2009). However, little is known about whether significant leukocyte infiltration occurs following cerebral ischemia in the absence of reperfusion. Thus, our aim was to profile the numbers and subtypes of immune cells infiltrating the brain within the first 24 h after permanent middle cerebral artery occlusion (pMCAO).

Methods: C57BL6/J male mice (8-12 weeks old) underwent pMCAO, as described previously (Brait *et al.*, 2010). Briefly, focal ischemia was induced by intraluminal filament occlusion of the right MCA. The filament was kept in place for 3 h or 24 h. Sham-operated and and naïve animals were also included as controls. Flow cytometric analyses were used to identify immune cells in the brain.

Results: Briefly, there was an approximate 4-fold increase in the number of leukocytes ($CD45^+_{high}$) in the ischemic hemisphere at both 3 h and 24 h after pMCAO. These infiltrated leukocytes consisted of ~60% lymphoid cells (which were increased by 2-fold) and ~40% myeloid cells (which were increased by 4-fold). Among the various cell subtypes examined, there was a 5.3-fold increase in neutrophils ($Ly6G^+$) and a 2.5-fold increase in monocytes/macrophages ($Ly6C^+_{high}$ or $F4/80^+$) at 3 h, both of which were sustained at 24 h. B lymphocytes ($B220^+$) were increased by 5.3-fold at 3 h but this decreased to 2.3-fold at 24 h. T lymphocytes ($CD3^+$) were increased by 2.4-fold at 3 h and by 4.4-fold at 24 h. Of these, $CD8^+$ T cells were increased by 5.6-fold at 3 h but by only 3.5-fold at 24 h, whereas $CD4^+$ T cells were not increased at 3 h, but were 4.9-fold more numerous at 24 h. Regulatory T cells ($CD4^+CD25^+$) were unchanged at 3 h but increased 4.5-fold at 24 h. NKT cells ($NK1.1^+CD3^+$) were also unchanged at 3 h and were increased by 3.7-fold at 24 h, whereas NK cells ($NK1.1^+CD3^-$) were increased by 2.2-fold at 3 h but returned to baseline at 24 h. Dendritic cells ($CD11b^+CD11c^+$) were unchanged at 3 h but were increased by 4-fold at 24 h. Brain microglia ($CD45^+_{med}CD11b^+F4/80^+$) were unchanged at either time point.

Conclusions: There is a substantial degree and complex pattern of infiltration of multiple immune cell types into the ischemic brain hemisphere following pMCAO. This pattern seems to differ from that occurring following transient ischemia (see Gelderblom et al., 2009). For example, neutrophils appear to be a prominent infiltrating cell type present early after pMCAO, whereas this is not the case after transient ischemia. Together, such information may inform the development of therapies to selectively target culprit immune cells that may differentially contribute to post-ischemic inflammatory injury depending upon whether or not early reperfusion is successfully achieved.

References:

Gelderblom et al., *Stroke* 2009;40:1849-1857.

Brait et al., *J Cereb Blood Flow Metab* 2010;30:1306-1317.

HIGH-FAT DIET INDUCES OBESETY, CEREBRAL VASCULAR REMODELING AND INCREASED ISCHEMIC BRAIN INJURY IN MICE

J. Deng[1,2], L. Xiong[2], Z. Zuo[1]

[1]Anesthesiology, University of Virginia, Charlottesville, VA, USA, [2]Anesthesiology, Xijing Hospital, The Fourth Military Medical University, Xi'an, China

Objective: Ischemic stroke is a fatal disease that affects 795,000 people each year in the U.S. Of all the risk factors, obesity has the

highest prevalence (35.7% adults in the US). However, how obesity may affect the severity of ischemic brain injury is still unclear. This study was to determine whether high fat diet-induced obesity would induce cerebral vascular remodeling and worsen ischemic brain injury in mice and whether the degree of hyperlipidemia would affect the neurological outcome after a stroke.

Methods: Two groups of six-week old CD1 mice were used in this study. They were fed with high fat diet (4.7 kcal/gm, HF) or regular diet (RD). At the age of 16 weeks, 9 animals from each group were perfused with warm saline after deep anesthesia with 5% isoflurane and rapidly perfused with 3 ml 20% freshly made vascular casting resin (PU4ii) with blue dye. Vascular tortuosity and number of collaterals in the middle cerebral artery (MCA) were determined. Another set of animals received a 90-min MCA occlusion (n=11 for RD group and n=10 for HF group). Motor coordination (rotarod index ratio) was assessed at 72 h after the brain ischemia. Blood was collected for lipid profiling and brains were harvested for edema and infarction evaluation with 2,3,5-triphenyltetrazolium chloride (TTC) staining.

Results: Significant increase in body weight was found in HF diet-fed animals (P< 0.0001, 50.4±5.5 g vs. 38.9±2.7 g). The tortuosity index of cerebral arteries was found increased (P=0.029, figure 1-A) in HF animals but the number of collaterals was not affected. Blood glucose was elevated during ischemia in HF animals (228.7±57.2 vs. 162.1±44.2, P=0.007, Figure 1-B). Rotarod index ratio was decreased in HF animals (0.217 ± 0.055 vs. 1.182 ± 0.374, P=0.02). Edema index (1.130±0.017 in HF vs. 1.076±0.016 in RD, P=0.034) and infarct volume (47.1%±4.1% in HF compared to 33.5%±3.4% in RD group, P=0.02, Figure 1-C) were significantly increased in HF animals. The infarct volume at 72 h after reperfusion was significantly correlated with blood cholesterol level [P=0.03, 95% CI: (0.05475, 0.7759). Figure 1-D], low density lipoprotein (LDL)/high density lipoprotein (HDL) ratio [P=0.01, 95% CI: (0.1613, 0.8154)], and LDL/cholesterol ratio [P=0.02, 95% CI: (0.1088, 0.7967)], but not with blood glucose during ischemia [P=0.1478, 95% CI: (-0.1259, 0.6911)].

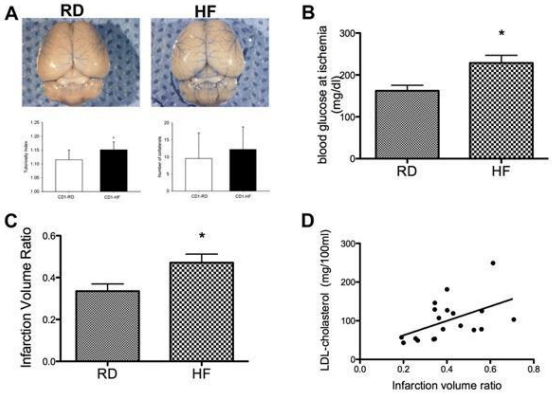

[Figure 1]

Conclusion: High fat diet induces obesity and hyperglycemia in CD1 mice. It can also increase cerebral artery tortuosity and worsen ischemic brain injury. Furthermore, Blood LDL level, LDL/HDL ratio and LDL/cholesterol ratio were all significantly correlated to infarct volume after stroke. Thus, hyperlipidemia increases the severity of ischemic brain injury.

EARLY TREATMENT OF TYPE 2 DIABETIC MICE WITH PIOGLITAZONE REVERSED CEREBRAL VASCULAR REMODELING AND ISCHEMIC BRAIN INJURY AGGRAVATION

J. Deng[1,2], L. Xiong[2], Z. Zuo[1]

[1]Anesthesiology, University of Virginia, Charlottesville, VA, USA, [2]Anesthesiology, Xijing Hospital, The Fourth Military Medical University, Xi'an, China

Objective: To investigate whether type 2 diabetes could induce cerebral vascular remodeling and aggravate brain damage after brain ischemia-reperfusion and the effect of pioglitazone on these changes.

Methods: Four- to five-week old db/db mice and their control db+ mice were obtained from Jackson Lab. After db/db mice developed hyperglycemia at ages of 5-6 weeks, animals in treatment group were given 100 mg/kg pioglitazone (Actos) or equal volume of dimethyl sulfoxide (DMSO) intraperitoneally once every other day for 3 times. Then random blood glucose (RBG) was monitored once every week and a supplemental dose of Actos was given if RBG exceeds 200 mg/dl in animals of dbdb+Actos group.

In the vascular remodeling study, four groups of animals were used: db+ (control mice, n=9), db/db (n=9), db/db+Actos (n=9) and db/db+DMSO (n=8). At age of 9-10 weeks, animals were perfused with warm saline under deep anesthesia followed by 3 ml 20% vascular casting resin (PU4ii). Brain vascular tortuosity and number of collaterals on the middle cerebral artery (MCA) were calculated.

In the stroke outcome study, mice were randomly divided into four groups: db+ (n=11), db++Actos (n=9), db/db (n=8) and db/db+Actos (n=9). Animals in db++Actos group received Actos at the same time of paired animals in db/db+actos group. At age of 9-10 weeks, all animals were given MCA occlusion for 45 min. Motor coordination dysfunction (rotarod index ratio) was assessed at 24 h after ischemia. Then brains were harvested for edema and infarction evaluation with 2,3,5-triphenyltetrazolium chloride (TTC) staining.

Results: Body weight and RBG were significantly increased in the db/db animals and RBG but not body weight increase was reversed after Actos treatment. Neither DMSO injection for db/db mice nor Actos injection for db+ mice changed blood glucose when compared to db/db or db+ animals, respectively (data not shown). The tortuosity index but not number of collaterals of cerebral arteries was increased in the db/db and db/db+DMSO groups (P< 0.05 vs. db+ group). Actos treatment reversed this change (figure 1-A). In the stroke outcome study, Actos injection did not affect any parameter for neurological outcome in db+ mice. Rotarod index ratio was decreased in db/db group (P< 0.01 vs. db+) and this decrease was reversed in the db/db+Actos group (P=0.02 vs. dbdb group). Edema index was increased in db/db animals (1.098±0.017 vs. 1.031±0.004 in db+ group, P< 0.01) but was not changed in db/db+Actos animals (P=0.1245 vs. db+ group). Infarction volume was significantly increased to 37.6%±2.5% in db/db group compared to 23.8%±2.9% in db+ group (P=0.0032) and this change was reversed by Actos treatment (23.7%±4.5% in the db/db+Actos group, P=0.0199 vs. db/db group. Figure 1-B and 1-C).

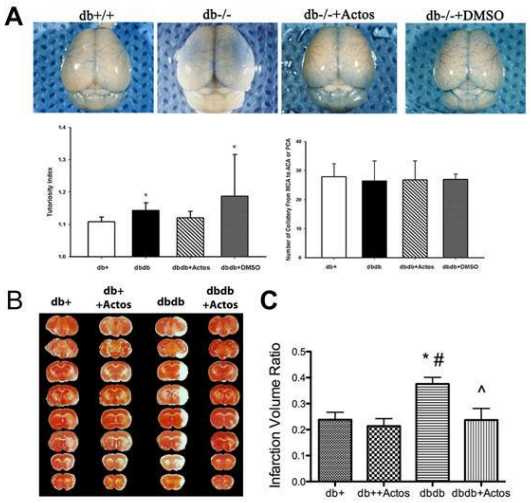

[Figure 1]

Conclusion: Type 2 diabetic animals exhibit spontaneous hyperglycemia and overweight after the age of 5 weeks. Early treatment with pioglitazone could lower blood glucose but does not affect body weight. Db/db mice exhibited cerebral vascular tortuosity increase and aggravation of ischemic brain damage. Both deteriorations were reversed by early treatment with pioglitazone.

DEVELOPMENT OF A CUSTOM-DESIGN MICROWIRE FOR ENDOVASCULAR OCCLUSION OF MIDDLE CEREBRAL ARTERY IN RATS VIA TRANSFEMORAL APPROACH

A.A. Divani[1], X. Wang[2], R. Chow[3], X.-H. Zhu[2], J. Nordberg[1], A. Murphy[1], T. Acompanado[4], J. Tokarev[1], Y. Zhang[2], W. Chen[2]

[1]Neurology, [2]Radiology, [3]Mechanical Engineering, University of Minnesota, Minneapolis, [4]Lake Region Medical, Chaska, MN, USA

Objectives: The objective of this study was to develop a reliable/repeatable method of inducing focal middle cerebral artery occlusion (MCAo) in rats without ligation of external carotid artery (ECA), that can alter cerebral blood flow, and reducing the risk of developing subarachnoid hemorrhage (SAH).

Methods: We prototyped microwires with different diameters (0.0120”, 0.0115”, and 0.0110”), materials, and construction methods

(coil on core and extruded polymer jacket on core). Under fluoroscopy guidance and using a femoral artery access, the microwires were navigated into the right internal carotid artery (ICA) of male Wistar rats (n=70, weight [Mean±SD]=421.5±18.7 g) to occlude the tip of the right MCA for 1 and 1.5 hours. We determined the optimal microwire diameter (0.0115") and design (polyurethane jacket on a Nitinol core) that provided the most successful outcome (i.e., repeatable ipsilateral MCA territory infarction without developing SAH).

MRI measurements were performed on a 9.4T/31cm animal scanner (Varian) with a ^{1}H RF surface coil. T_2-weighted images were acquired with a fast spin echo sequence (TE=10ms; TR=4sec; FOV=3.2×3.2cm; matrix=256×256; thickness=0.25 mm; 8 echo train length). Bipolar diffusion gradients in three dimensions were inserted between the GE excitation pulse and data acquisition to obtain the diffusion images (TE=14ms; TR=250ms; FOV=3.2×3.2cm; image matrix=128×128; 1 mm thickness). Two *b* factors (b_1=10.8 and b_2=1007 $s \cdot mm^{-2}$) were used for obtaining apparent diffusion coefficient (ADC) maps. Cerebral blood flow (CBF) images were acquired with the continuous arterial spin labeling (CASL) method (TE=20ms; TR=3sec; FOV=3.2×3.2cm; image matrix=64×64; 1 mm thickness).

Results: Figure 1 shows positioning of the microwire in the aorta, navigating toward the right ICA and blocking the tip of the MCA. 3D rendered images of a MRI are shown in Figure 2. A sample MRI study revealing a subcortical lesion (indicated by the arrows) on the side of MCAo (right) is shown in Figure 3, where hyperintensity in T_2-weighted images was observed as compared with the control (left side of the brain). Both ADC and CBF in the lesion area decreased dramatically.

[Figure 1]

Figure 1: Positioning of the microwire passing through the aorta and right CCA to the right ICA.

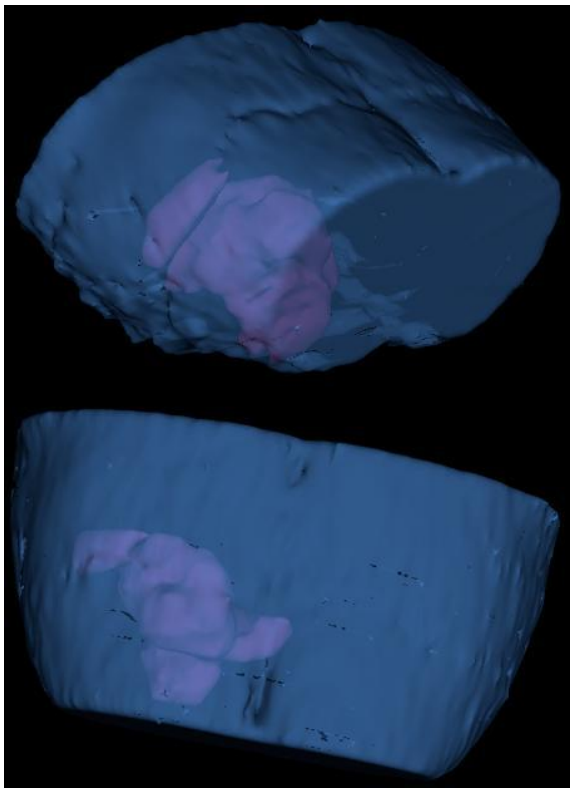

[Figure 2]

Figure 2: 3D rendered MRI images showing the volume of the infarcted tissue.

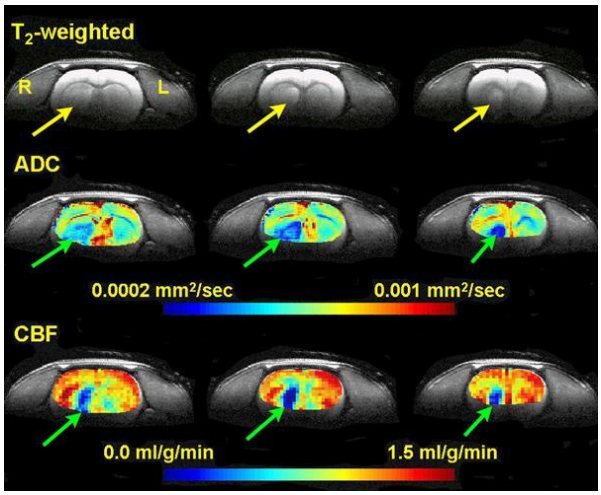

[Figure 3]

Figure 3: Lesions created by 1 hour MCAo. MRI scans were obtained 1 day after the occlusion.

Interestingly, the peri-infarct region demonstrated an increase in CBF. For shorter occlusion time (1h), we observed that the infarcted tissue was confined to the subcortical region. However, with longer occlusion time (1.5h) the infarct extended into the brain cortex.

Conclusions: We have developed a reliable/repeatable MCAo method in rats that allows for a precise occlusion of MCA under direct fluoroscopy visualization without altering cerebral hemodynamics. Permanent ligation of ipsilateral ECA that is routinely done in filament models can lead to CBF augmentation in the ipsilateral brain hemisphere with subsequent effect on the outcome of MCAo.

THE EFFECT OF FLUVOXAMINE, ENVIRONMENTAL ENRICHMENT AND DIETARY RESTRICTION ON EXPERIMENTAL STROKE IN RATS

D.A. Duricki, A.L. Dixon, K. Galley O'Toole, C. Simmons, M. Mesquita, S.C. Williams, D. Cash

Neuroimaging, Institute of Psychiatry, King's College London, London, UK

Objectives: Stroke remains one of the leading causes of neurological disability worldwide. In stroke the key goal is to protect the brain from the associated inflammatory response and to restore any lost function. This study aimed to promote neuroprotection and neurogenesis *via* a combination of treatments following stroke: environmental and dietary modification, and the selective serotonin reuptake inhibitor (SSRI) fluvoxamine. It is known that following stroke, stem cells in the adult brain divide and the new neurons can migrate to damaged areas. This process of neurogenesis can be enhanced by a variety of environmental and dietary modifications.

Methods: A transient middle cerebral artery occlusion (MCAO) model of stroke was used whereby the MCA was occluded for 90 minutes by an intraluminal thread in 38 adult male SD rats (9-10 per group). The rats were treated with fluvoxamine (25 mg/kg, ip) or vehicle twice: 30 min before MCAO and at reperfusion. T2-weighted MRI was acquired at 24 hours and 9 weeks to assess lesion volume changes. One week following stroke the rats were assigned to normal housing and standard diet or a combination of dietary restriction (food every other day) and

environmental enrichment (toys in the cage) and BrdU, a marker of neurogenesis, was injected on 5 consecutive days. Rats were euthanized 9 weeks after stroke and the BrdU positive cells quantified by immunohistochemistry within the dentate gyrus.

Results: In a preliminary experiment in the naïve rats, we show that enhancement of neurogenesis by environmental enrichment and dietary restriction was augmented when these two are combined (Fig 1a). Previously we showed that the selective serotonin reuptake inhibitor (SSRI) fluvoxamine was slightly neuroprotective in an MCAO rat model, presumably via the ability of SSRI's to suppress inflammation, increase cell survival and promote neurogenesis (Galley O'Toole et al., 2011). In this study neither fluvoxamine nor environmental enrichment and dietary restriction reduced lesion volume, however in combination led to a significant reduction in lesion volume (Fig. 1b). There was increased neurogenesis within the dentate gyrus following stroke with environmental enrichment and dietary restriction alone, and also following stroke with the combination of fluvoxamine, environmental enrichment and dietary restriction (Fig 1c).

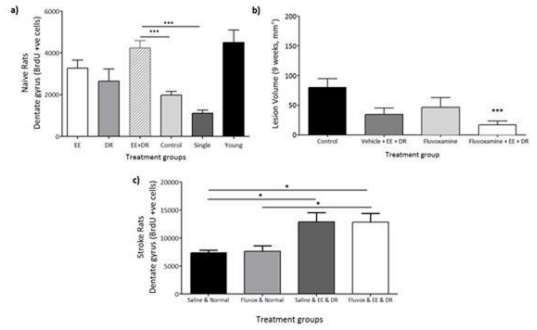

[Figure 1]

Conclusions: Firstly, we have demonstrated that neurogenesis can be enhanced in naïve rats that undergo either environmental enrichment and/or dietary restriction and that is significantly augmented when the two paradigms combined. Similarly, neurogenesis was enhanced by these treatments in animals following stroke. Following stroke, we also show a significant decrease in lesion volume upon treatment with the SSRI, fluvoxamine in combination with dietary restriction and environmental enrichment. Interestingly, fluvoxamine alone or in combination with the environmental enrichment and dietary restriction did not further augment neurogenesis, maybe suggesting the effect fluvoxamine does not modify neurogenesis alone following stroke. Together these results suggest a promising combinatorial approach for stroke therapy by both significantly reducing the lesion volume and by enhancing the level of neurogenesis within the brain.

References: Galley O´Toole K, et al (2011) Int Symposium on Cerebral Blood Flow, Metabolism and Function (Brain11), Barcelona.

MIGRAINE PROPHYLACTIC DRUGS LAMOTRIGINE AND TOPIRAMATE SUPPRESS PERI-INFARCT DEPOLARIZATIONS AND IMPROVE STROKE OUTCOMES

K. Eikermann-Haerter[1], J.H. Lee[2], A. Daneshmand[1], E.S. Yu[1], A. Can[1], B. Sengul[1], Y. Zheng[1], N. Yalcin[1], C. Ayata[1,3]

[1]Radiology, Massachusetts General Hospital and Harvard Medical School, Charlestown, MA, USA, [2]Drug Discovery Research, Korea Research Institute of Chemical Technology, Yuseonggu, North Korea, [3]Neurology, Massachusetts General Hospital, Boston, MA, USA

Introduction: Migraine is the most common neurological disease in adults affecting 10-20% of the population, and is an independent stroke risk factor. Stroke is the second leading cause of death and a major cause of disability. Epidemiological studies indicate that a history of migraine increases stroke risk up to 10-fold, particularly in otherwise healthy persons without cardiovascular risk factors.

Background and aims: Excitatory mechanisms have been implicated in pathogenesis of both migraine and stroke. We recently showed that migraine mutations increase brain vulnerability to ischemia via excitatory mechanisms[1]. Migraine mutant mice developed a higher number of peri-infarct depolarizations (PIDs) upon experimental stroke, associated with accelerated infarct growth and worsened outcomes. PIDs are related to spreading depression (SD), the electrophysiologic event underlying migraine aura, and enlarge infarcts by worsening the metabolic mismatch. We tested whether migraine prophylactic drugs that reduce

susceptibility to SD also inhibit PIDs and thereby protect against ischemic stroke.

Material and methods: Using C57 mice, we examined the effect of the migraine prophylactic and antiepileptic drugs lamotrigine (LTG; 30mg/kg/d p.o.) and topiramate (TPM; 80mg/kg/d p.o.) compared to vehicle (ORA) on SD, PID, and stroke phenotype after chronic treatment (6 weeks). In electrophysiological studies, mice were ventilated, and blood pressure and blood gas monitored and maintained within normal range. Data are mean ± standard deviation. *p< 0.05 vs. vehicle.

Results: Chronic treatment with LTG or TPM suppressed SD susceptibility in mice. A stronger electrical stimulus was necessary to induce SD, and the cumulative SD duration upon topical KCl was reduced.

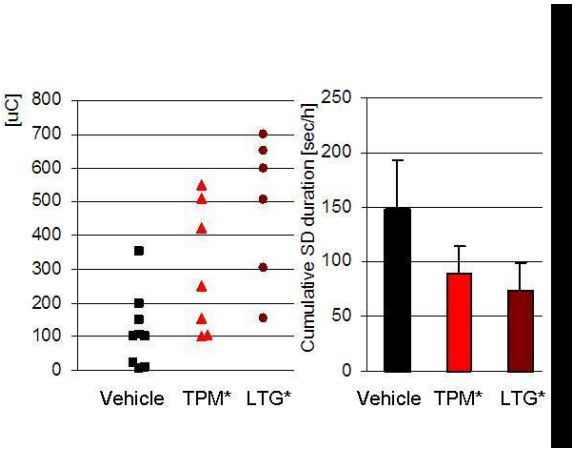

[[LTG and TPM suppress SD]]

Both drugs inhibited PIDs upon transient filament occlusion of the middle cerebral artery (fMCAO). LTG and TPM increased the latency to the onset of anoxic depolarization after occlusion, and reduced the frequency and cumulative duration of PIDs when recorded for 2 hours during ischemia (n=8 each).

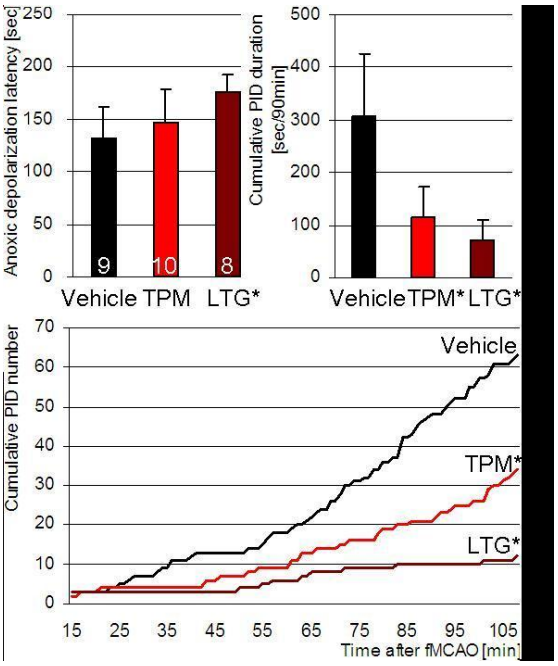

[[LTG and TPM suppress PID]]

Both drugs also improved stroke outcomes by reducing infarct size (infarct and ischemic swelling volumes; colored and white bars, respectively) and improving neurological function 24 hours after ischemia.

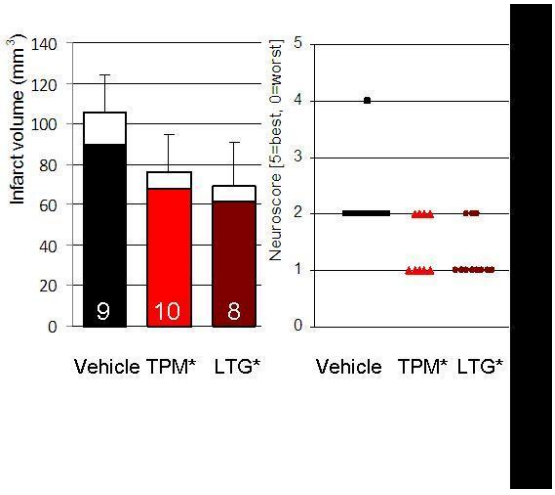

[[LTG and TPM improve stroke outcomes]]

Conclusions: These data further support the notion that increased stroke risk in migraineurs is related to enhanced susceptibility to ischemic depolarizations, and suggest that migraine prophylaxis may improve stroke outcomes.

[1] Eikermann-Haerter K, Lee JH et al. Migraine Mutations Increase Stroke Vulnerability by Facilitating Ischemic Depolarizations. *Circulation* 2012;125: 803-812.

CITALOPRAM ENHANCES NEUROVASCULAR REGENERATION AND SENSORIMOTOR FUNCTIONAL RECOVERY AFTER ISCHEMIC STROKE IN MICE

A.R. Espinera[1], Z. Wei[1,2], M.E. Ogle[1], X. Gu[1], A.C.H. Yu[2], L. Wei[1]

[1]Departments of Anesthesiology and Neurology, Emory University School of Medicine, Atlanta, GA, USA, [2]Neuroscience Research Institute and Department of Neurobiology, School of Basic Medical Sciences, Peking University, Beijing, China

Introduction: Recent clinical trials have demonstrated that treatment with selective serotonin reuptake inhibitors (SSRIs) after stroke enhances motor functional recovery; however, the underlying mechanisms remain to be further elucidated. Our previous investigations have demonstrated enriched environment and drug-enhanced angiogenesis, neurogenesis and cell migration following ischemia (Li et al., 2007, 2008, Ogle et al., 2012). SSRIs enhance neuronal plasticity and neurogenesis through an increase in neurotrophic factors such as brain derived neurotrophic factor (BDNF). We hypothesized that daily administration of the clinical drug citalopram would produce these functional benefits via enhancing neurovascular repair in the ischemic peri-infarct region.

Methods: Focal ischemic stroke was induced in male C57/B6 mice by permanent ligation of distal branches of the middle cerebral artery (MCA) to the barrel cortex and 7-min occlusion of the bilateral common carotid arteries (CCA) (Li et al., 2007, Ogle et al., 2012). Citalopram (10 mg/kg, i.p.) was injected 24 hrs after stroke and daily thereafter. BrdU (bromodeoxyuridine) was injected daily beginning 3 days after stroke utile 14, 21 and 28days. Functional recovery was assessed using the adhesive removal task. Latency and removal times were assessed prior to surgery, 3 and 14 days post-stroke. Western blotting techniques were utilized to analyze BDNF protein expression in the ischemic penumbra. Both immunohistochemical and functional assays were performed to elucidate cellular and sensorimotor changes after stroke in response to citalopram treatment.

Results: Citalopram-treated mice had better functional recovery than saline-treated controls 3 and 14 days after stroke in the adhesive removal test. Increased expression of BDNF was detected in the peri-infarct region 7 days after stroke in citalopram-treated animals. The number of proliferating neural progenitor cells and the distance of neuroblast migration from the SVZ towards the ischemic cortex were significantly higher in citalopram-treated mice at 7 days after stroke. Immunohistochemical staining and 3-D imaging showed that citalopram-treated animals generated an increased number of new neurons and microvessel density in the peri-infarct region 21 and 28 days after stroke.

Conclusion: Taken together, these results suggest that citalopram promotes post-stroke sensorimotor recovery while enhancing neural cell migration, proliferation, indicated neurogenesis, and the angiogenesis support in the peri-infarct region of the ischemic brain. Further, our data support the idea that post-stroke treatment using SSRIs such as citalopram could potentially offer a new, safe avenue for stroke therapy.

References:

1. Wei Ling , Rovainen C, Woolsey TC. Ministrokes in rats barrel cortex. Stroke 26(8):1459- 1462, 1995.

2. Li WL, Yu SP, Ogle ME, Ding XS, Wei L (2008) Enhanced neurogenesis and cell migration following focal ischemia and peripheral stimulation in mice. Dev Neurobiol 68:1474-1486.

3. Li Y, Lu Z, Keogh CL, Yu SP, Wei L (2007) Erythropoietin-induced neurovascular protection, angiogenesis, and cerebral blood flow restoration after focal ischemia in mice. J Cereb Blood Flow Metab 27:1043-1054.

4. Ogle ME, Gu X, Espinera AR, Wei L (2012) Inhibition of prolyl hydroxylases by dimethyloxaloylglycine after stroke reduces ischemic brain injury and requires hypoxia inducible factor-1alpha. Neurobiol Dis 45:733-742.

THE POLY (ADP-RIBOSE) POLYMERASE INHIBITOR PJ34 COUNTERACTS BLOOD BRAIN BARRIER DAMAGES INDUCED BY RT-PA AFTER ISCHEMIC STROKE IN MICE

T. Fei[1], V. Beray-Berthat[1], B. Coqueran[1], C. Lesbats[2], B. Palmier[1], M. Garraud[1], C. Bedfert[1], N. Slane[1], D. Scherman[2], M. Plotkine[1], B.-T. Doan[2], C. Marchand-Leroux[1], I. Margaill[1]

[1]Equipe de Recherche 'Pharmacologie de la Circulation Cérébrale' (EA 4475), Université Paris Descartes, Sorbonne Paris Cité, Faculté des Sciences Pharmaceutiques et Biologiques, [2]Unité de Pharmacologie Chimique et Génétique et d'Imagerie (CNRS, UMR 8151, Inserm, U 1022), Université Paris Descartes, Sorbonne Paris Cité, Faculté des Sciences Pharmaceutiques et Biologiques, France et ENSCP Chimie-Paritech, Paris, France

Objective: Thrombolysis with recombinant tissue plasminogen activator (rt-PA) is presently the only pharmacological treatment approved for ischemic stroke patients. However, rt-PA increases the risk of hemorrhagic transformations (HT). The aim of this study was to determine whether the nuclear enzyme poly (ADP-ribose) polymerase (PARP) is implicated in the vascular toxicity of rt-PA, especially on interendothelial jonctions of the blood-brain barrier (BBB).

Methods: Permanent focal cerebral ischemia in male Swiss mice (anesthetized with ketamine (50 mg/kg) and xylazine (6 mg/kg)) was performed by endovascular occlusion of the left middle cerebral artery. Six hours after the onset of ischemia, mice were given an intravenous perfusion of rt-PA (10 mg/kg). PJ34 (N-(6-oxo-5,6-dihydrophenanthridin-2-yl)-2-(N,N-diméthylamino)acétamide), a powerful PARP inhibitor, was administrated twice, immediately and 4 hours after ischemia onset (1 or 3 mg/kg *via* intraperitoneal route). Twenty-four hours after ischemia, expression of the tight junction proteins claudin-5, occludin and zonula occludens-1 (ZO-1), and of the adherens jonction protein VE-cadherin were studied by Western blotting. Expression of basement membrane proteins, laminin and collagen-IV, were studied by immunohistochemistry. The HT were evaluated by magnetic resonance imaging (MRI) and Western blotting of intraparenchymal brain hemoglobin. Cerebral edema was assessed by MRI and brain water content. Sensorimotor deficits of mice were also evaluated using a battery of tests.

Results: Administration of rt-PA (10 mg/kg, iv) 6 hours after ischemia led to an increase in HT. This effect was associated with an aggravation of the post-ischemic degradation of ZO-1 (32%), claudin-5 (25%) and VE-cadherin (29%) proteins, but without modification of the expression of occludin, collagen IV and laminin. Furthermore, ischemia-induced functional deficits were also aggravated by rt-PA. Combining PJ34 with rt-PA preserved the expression of ZO-1, claudin-5 and VE-cadherin, reduced HT and improved sensorimotor performances. Cerebral edema was modified neither by rt-PA nor PJ34 alone or in association.

Conclusions: Our results showed that PARP is implicated in post-ischemic damages of the BBB induced by rt-PA. Thus PARP inhibition would be a promising strategy to associate with rt-PA for the treatment of ischemic stroke.

ADAMTS13: A NOVEL THERAPEUTIC DRUG CANDIDATE FOR ACUTE STROKE AND FOR DELAYED CEREBRAL ISCHEMIA

M. Fujioka[1,2], C. Muroi[1,3], K. Mishima[3], Y. Fujimura[4], K. Okuchi[5], M. Fujiwara[3], B.K. Siesjo[6]

[1]Neuroscience Unit, Emergency and Critical Care Medical CTR, Nara Medical University, Kashihara, [2]Neurosurgery, Osaka Saiseikai Ibaraki General Hospital, Ibaraki, [3]Neuropharmacology, Fukuoka University, Fukuoka, [4]Blood Transfusion Medicine, [5]Emergency and Critical Care Medical CTR, Nara Medical University, Kashihara, Japan, [6]Laboratory for Experimental Brain Research, Lund University, Lund, Sweden

Stroke research has highlighted basic mechanisms that damage brain cells since the phenomenon `delayed neuronal death` was discovered. We have studied brain ischemia-reperfusion injury according to this research line (Stroke 1994;25:2091-5., Ann Neurol.2003;54:732-47., Stroke.2008;39:951-58., Blood. 2010;115:1650-3.). However, a main treatment clinically proved effective for acute ischemic stroke is thrombolysis with tissue plasminogen activator. Further, with a concept of "neurovascular unit" emerging, stroke research has more emphasized an importance to study how blood vessels and brain cells communicate with each other. In this context, ADAMTS13(A disintegrin and metalloproteinase with thrombospondin type-1

motifs 13) may become a new therapeutic option against ischemic brain injury. ADAMTS13 cleaves von Willebrand factor (VWF) and down-regulates the VWF biological activities, depending on increased shear stress related to high blood flow velocity due to artery narrowing. VWF is, upon mechanical and/or biochemical stimuli, released from Weibel-Palade-body in vascular endothelial cells, contributing to platelet thrombus formation and leukocytes extravasation on the activated vascular endothelium. Therefore, ADAMTS13 may protect brain from ischemia by reducing microthrombosis and inflammation. We have been working on this subject (Blood.2010;115:1650-3., NeurolSci.2012Jan3.). In a mouse focal cerebral ischemia, ADAMTS13-gene-deletion aggravates ischemic brain injury. The administration of ADAMTS13 enzyme reduces the size of brain infarction. In addition, recently we have found that in mice ADAMTS13 can improve the delayed ischemic brain damage due to cerebral microthrombosis after subarachnoid hemorrhage. Herein, we review the possible neuroprotective effects and mechanisms of ADAMTS13 in acute and in delayed cerebral ischemia.

T CELLS CONTRIBUTE TO STROKE-INDUCED LYMPHOPENIA IN RATS

L. Gu[1], X. Xiong[2], X. Gao[2], S. Krams[2], H. Zhao[2]

[1]Hangzhou Normal University, Hangzhou, China, [2]Stanford University, Stanford, CA, USA

Stroke-induced immunodepression (SIID) results when T cell and non-T immune cells,

such as B cells, NK cells and monocytes, are reduced in the peripheral blood and

spleen after stroke. We investigated the hypothesis that T cells are required for the

reductions in non-T cell subsets observed in SIID. Our results showed that focal

ischemia resulted in similar cortical infarct sizes in both wild type (WT) Sprague Dawley

(SD) rats and nude rats with a SD genetic background, which excludes the possibility

of different infarct sizes affecting SIID. Numbers of total peripheral blood mononuclear

cells (PBMCs) and lymphocyte subsets, including T cells, CD4+ or CD8+ T cells, B

cells and NKT cells, as well as monocytes in the blood and spleen, were decreased 3

days after stroke. In nude rats, however, total number of PBMCs and absolute

numbers of NK cells, B cells and monocytes were increased in the peripheral blood

after stroke; nude rats are athymic therefore they have few T cells present. Adoptive

transfer of WT splenocytes into nude rats before stroke resulted in lymphopenia after

stroke similar to WT rats. Moreover, in vitro T cell proliferation stimulated by

concanavalin A was significantly inhibited in WT rats as well as in nude rats receiving

WT splenoctye adoptive transfer, suggesting that T cell function is indeed inhibited

after stroke. In conclusion, T cells are required for stroke-induced reductions in non-T

immune cells and they are the most crucial lymphocytes for SIID.

BNIP3 AND OGD-INDUCED OLIGODENDROCYTE DEATH: ROLE IN WHITE MATTER INJURY IN CEREBRAL ISCHEMIA

T. Guan[1], C. Li[2], J. Kong[1]

[1]Department of Human Anatomy and Cell Science, University of Manitoba, Winnipeg, MB, Canada, [2]Department of Histology and Embryology, The Thrid Military Medical University, Chongqing, China

Objectives: Oligodendrocytes (OLs), the major myelin-forming cells in the central nervous system and are highly vulnerable to ischemic insult(1). OLs undergo a complex pattern of death in cerebral ischemia with an early loss from excitotoxicity via the glutamate AMPA receptors(2), and die at more delayed time points via apoptosis(3). Since OLs death and white matter damage contribute to functional deficits following cerebral ischemia,

enhancing the long-term survival of mature and newly born OLs could promote white matter function at delayed time points following ischemic injury. Studies have shown that BNIP3, a proapoptotic member of the Bcl-2 family of death-regulating proteins, mediates necrosis-like cell death by mitochondrial PT pore opening, independently of association with other Bcl family proteins through BH3 domains(4). Therefore, it is possible that an increase in BNIP3 expression enhances susceptibility to OLs. We sought to identify potential role of BNIP3 in the intrinsic pathway of programmed cell death in cerebral ischemic white matter damage.

Methods: Primary cultures of rat OLs were subject to oxygen-glucose deprivation and reoxygenation. Middle cerebral artery occlusion (MCAO) was induced in BNIP3 knockout (KO) and wild type (WT) mice with 1, 3 or 7 d of reperfusion. Cell death was quantitatively assessed by LIVE/DEAD viability assay and TUNEL assay. Stage-specific OL cultures were identified by immunocytochemical characterization. Expression and level of proteins were examined using immunohistochemistry and immunoblotting.

Results: Survival assays revealed that oligodendrocyte precursor cells (OPCs) and later-stage precursors were highly vulnerable. Exposure of OLs to OGD resulted in a significant increase in BNIP3 expression. Down-regulation of BNIP3 with shRNA or pharmacological inhibition with necrostatin-1 reduced OGD-triggered OL apoptosis. After tMCAO/R, loss of OLs was detected at ipsilateral external capsule (EC) concurrent with highly BNIP3 expression. TUNEL showed greater cell death in EC in WT mice when compare with KO mice. Both PDGFR-α and GalC level was significantly increased in WT and KO ipsilateral white matter. Moreover, the increase in KO mice was significantly higher than WT.

Conclusions: Our results suggested BNIP3 deficiency may promote OPCs proliferation and protect the immature OLs from ischemic injury. These studies unveil BNIP3 as an important mediator in OLs death, which may contribute to a better understanding of white matter injury in stroke.

References:

1. Pantoni L, Garcia JH, Gutierrez JA. Cerebral white matter is highly vulnerable to ischemia. Stroke; a journal of cerebral circulation. 1996;27(9):1641-6; discussion 7. Epub 1996/09/01.

2. McDonald JW, Althomsons SP, Hyrc KL, Choi DW, Goldberg MP. Oligodendrocytes from forebrain are highly vulnerable to AMPA/kainate receptor-mediated excitotoxicity. Nature medicine. 1998;4(3):291-7. Epub 1998/03/21.

3. Dewar D, Underhill SM, Goldberg MP. Oligodendrocytes and ischemic brain injury. Journal of cerebral blood flow and metabolism : official journal of the International Society of Cerebral Blood Flow and Metabolism. 2003;23(3):263-74. Epub 2003/03/07.

4. Vande Velde C, Cizeau J, Dubik D, Alimonti J, Brown T, Israels S, et al. BNIP3 and genetic control of necrosis-like cell death through the mitochondrial permeability transition pore. Molecular and cellular biology. 2000;20(15):5454-68. Epub 2000/07/13.

PROTECTION OF ELECTROACUPUNCTURE AGAINST CEREBRAL ISCHEMIA THROUGH ADIPONECTIN SIGNALING PATHWAY IN STREPTOZOTOCIN-INDUCED DIABETIC MICE

F. Guo, Q. Wang, L. Xiong

Xijing Hospital, The Fourth Military Medical University, Xi'an, China

Objectives: Hyperglycemia is known as an exacerbating factor in stroke and many beneficial methods for treating cerebral ischemia-reperfusion injury have been proved blunting in the diabetic models. We have previously proved that electroacupuncture (EA) pretreatment induces cerebral ischemic tolerance in normal animal models. However, it is unknown whether or not EA can attenuate cerebral ischemia reperfusion injury in diabetic mice, while the possible underlying mechanism is still unrevealed.

Methods: Male C57BL/6 mice were subjected streptozocin (STZ) for diabetic models. Focal cerebral ischemia was induced by middle cerebral artery occlusion for 60 minutes following 24 hours reperfusion. The neurobehavioral scores, infarction volumes, neuronal apoptosis and the expression of Bcl-2 and Bax were evaluated after reperfusion injury. Malondialdehyde (MDA), reactive

oxygen species (ROS) levels, superoxide dismutase (SOD) and NADPH oxidase activation were measured in the ischemic penumbra. The expression of plasma and cerebral adiponectin (APN) levels were measured, as well as the cerebral adiponectin receptor 1 (AdipoR1) and 2 (AdipoR2) expression. Phosphorylation of GSK-3β at 9ser [p-GSK-3β (9ser)] was also evaluated.

Results: EA pretreatment reduced infarct size, improved neurological outcome, inhibited neuronal apoptosis and oxidative reaction in the diabetic mice. Plasma and cerebral APN levels were increased accompanied by enhanced AdipoR1 in the brain. The protective effect of EA was abolished by pretreatment of AdipoR1 knockdown. Further, our results revealed that EA pretreatment increased p-GSK-3β (9ser) in the ipsilateral penumbra. Augmented phosphorylation of GSK-3β induced similar neuroprotective effects as did EA pretreatment. By contrast, inhibition of PI3K dampened the levels of p-GSK-3β (9ser), and reversed the neuroprotective effect of EA pretreatment. In addition, Regulation of GSK-3β by EA pretreatment was abolished following treatment with an AdipoR1 knockdown.

Conclusions: We conclude that pretreatment with EA increases the production of APN, which elicits protective effects against cerebral ischemia reperfusion injury through AdipoR1 and GSK-3β signaling pathway. These results suggest a novel mechanism of EA pretreatment-induced tolerance to diabetic cerebral ischemia.

DO DIFFERENCES IN THE METABOLIC RESPONSES TO STROKE IN OBESE AND LEAN MICE EXPLAIN THE 'OBESITY PARADOX'?

M. Haley, C. Lawrence

Faculty of Life Sciences, University of Manchester, Manchester, UK

Obesity is a risk factor for stroke and worsens outcome in animal models. However, studies in patients are conflicting, with some reporting better stroke recovery in the obese. Since inflammation is usually detrimental to stroke outcome, and obesity features a raised inflammatory profile, this finding has been called the 'obesity paradox'. A suggested mechanism for this protective effect is that obesity may improve tolerance to post-stroke weight loss (cachexia). Therefore, the aim of this study was assess whether there are metabolic differences in the responses of obese and lean mice to ischaemic stroke.

Focal cerebral ischaemia was induced by intraluminal filament occlusion of the middle cerebral artery in 16-to-20-week-old obese *ob/ob* and control (ob/-) mice. Ischaemic damage was assessed at 4 and 24 hours post-stroke, as were the metabolic and inflammatory responses to stroke. Lipid metabolism was assessed in the blood and in epididymal fat pads. Metabolomic analysis was performed on cardiac blood samples.

Obese mice suffered increased ischaemic brain damage, and had clear differences in a range of metabolites after stroke. In particular, obese mice showed increased concentrations of plasma fatty acids and up regulation of lipolytic enzymes in adipose tissue. This suggests stroke may differentially affect lipid metabolism in obese and lean mice. This may have implications for understanding the 'obesity paradox', but may also mediate the increased ischaemic damage seen in obese mice since pathological concentrations of fatty acids may be pro-inflammatory.

PH-WEIGHTED IMAGING IN ACUTE STROKE: HOW DOES IT COMPARE TO CONVENTIONAL TECHNIQUES?

G.W.J. Harston[1], Y.K. Tee[2], M. Chappell[2,3], N. Blockley[3], T. Okell[3], J. Levman[2], F. Sheerin[4], M. Cellerini[4], P. Jezzard[3], S. Payne[2], J. Kennedy[1]

[1]Radcliffe Department of Medicine, [2]Institute of Biomedical Engineering, Department of Engineering Science, [3]Oxford Centre of Functional MRI of the Brain, Nuffield Department of Clinical Neurosciences, University of Oxford, [4]Department of Neuroradiology, Oxford University Hospitals NHS Trust, Oxford, UK

Objectives: Magnetic resonance imaging (MRI) characterization of cerebral intracellular pH changes could provide an indication of metabolic stress and improve the understanding of the evolution of the ischaemic penumbra.[1] The objective of this study is to examine how pH weighted imaging changes are linked to tissue outcome in acute stroke patients.

Methods: Patients with ischaemic stroke are

recruited within 6hrs of symptom onset and undergo serial MRI, on presentation, at 1 day, and 1 week. MRI protocols include diffusion-weighted imaging (DWI), fluid attenuated inversion recovery (FLAIR), and single slice pH-weighted imaging using chemical exchange saturation transfer (CEST) MRI.[2] Perfusion using arterial spin labeling is also measured. Cerebral intracellular pH is estimated by model fitting of the z-spectrum to define the proton transfer ratio between amide and water.[3] pH signal is normalized relative to the intracellular pH in the unaffected contralateral hemisphere. Tissue outcome was defined using co-registered DWI lesion on presentation and at 24hrs, and FLAIR lesion at 7 days. Final infarct volume was defined by the day 7 FLAIR scan. Core infarct was defined as DWI positive, FLAIR positive (DWI+FLAIR+) and the mismatch between core and final infarct as DWI negative, FLAIR positive (DWI-FLAIR+).

Results: The data of the first 2 patients in whom pH-weighted imaging was used are presented. In both patients, a relative pH signal reduction to below 85% of normal identified core infarct at the time of presentation. DWI-FLAIR+ tissue had greater, but nevertheless low, pH values at that time (85-91% of normal). pH increased in both patients by 24hrs. Despite normalization of cerebral pH in patient 2 by 24hrs the tissue progressed to infarction by 1 week.

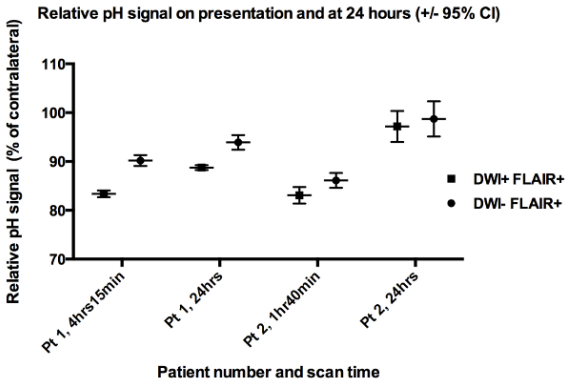

[Graph]

Conclusions: These data suggest that intracellular acidosis occurs early in ischaemic stroke and an initial pH drop may predict final infarct volume better than DWI. The normalization of acidosis in patient 2 by 24 hours may represent a return of normal metabolism in tissue that nonetheless progresses to infarction. It is not clear whether this subsequent infarction is due to a second insult or delayed injury responses. The data support the hypothesis that the magnitude of acidosis predicts tissue outcome.

Recruitment is ongoing to assess whether thresholds of tissue acidosis can determine reversibly injured penumbral tissue, which may be amenable to intervention. The relationship between perfusion and pH is also being explored using serial perfusion imaging.

References:

1. Hossmann KA. Viability thresholds and the penumbra of focal ischemia. Ann Neurol. 1994; **36**(4): 557-65.

2. Zhou J, Payen JF, Wilson DA, Traystman RJ, van Zijl PC. Using the amide proton signals of intracellular proteins and peptides to detect pH effects in MRI. Nat Med. 2003; **9**(8): 1085-90.

3. Chappell MA, Donahue MJ, Tee YK, Khrapitchev AA, Sibson NR, Jezzard P, et al. Quantitative Bayesian model-based analysis of amide proton transfer MRI. Magn Reson Med. 2012 (in press).

DIFFERENCES IN THE SPECTRAL PARAMETERS OF SKIN-SURFACE LASER-DOPPLER SIGNALS BETWEEN STROKE AND NORMAL SUBJECTS

H. Hsiu[1], C.-T. Chen[2], F.-C. Lin[3], C.-L. Hsu[4], Y.-S. Liu[5]

[1]Graduate Institute of Biomedical Engineering, National Taiwan University of Science and Technology, [2]Department of Traditional Chinese Medicine, [3]Department of Rehabilitation, Taipei City Hospital RenAi Branch, [4]Graduate Institute of Applied Science and Technology, National Taiwan University of Science and Technology, [5]Department of Rehabilitation, Taipei City Hospital Ren Ai Branch, Taipei, Taiwan R.O.C.

Objectives: Stroke is often accompanied with a reduced walking activity; identifying improvements in walking has been suggested to be a primary rehabilitation goal in stroke patients [1]. Laser Doppler flowmetry (LDF) is a popular method for monitoring microcirculatory blood flow (MBF) with attractive clinical features, such as noninvasiveness and allowing the

measurement of rapid responses that exploits Doppler shifts in laser light produced by moving red blood cells, and has been widely used to monitor the MBF condition in patients with various diseases. Spectral analysis of LDF signals reveals that blood-flow oscillations at frequencies of 0.01-1.6 Hz might reflect various physiological rhythms [2]. The present study used skin-surface LDF measurements and spectral analysis with the aim of discriminating the MBF characteristics in stroke subjects subdivided into two groups according to their walking ability.

Methods: LDF probes were attached to the skin surface of the bilateral sites at around 2.5cm lateral to the canthus to monitor the MBF condition of the underlying cerebral vascular beds. 20-minute LDF measurements were performed in the following groups: Group A (cannot walk independently), Group B (can walk independently), and Group C (healthy controls). Wavelet transform with Morlet mother wavelet was applied to the measured LDF signals; the energy density within each frequency band was calculated, which are suggested to be influenced by the endothelial activity of the vessel wall, the neurogenic activity of the vessel wall, the intrinsic myogenic activity of vascular smooth muscle, the respiration, and the heartbeat, respectively [2-4].

Results: There is a decreasing trend for Groups A-C in the energy density of the neural-related frequency band; it illustrated that in stroke patients, the worse MBF perfusion condition might be correlated with the vasoconstriction induced by the increased sympathetic neural activities at local vascular beds. Furthermore, energy density of.the myogenic-related frequency band were smaller in both stroke groups than in Group C.

Conclusions: The present finding demonstrates the feasibility of using spectral LDF index to discriminate between stroke subjects with different walking abilities and between stroke and normal subjects. The present analysis provides a noninvasive and real-time method for discriminating MBF characteristics and understanding the underlying microcirculatory regulatory mechanisms, and thus may be pertinent to noninvasive monitoring of the disease progress and the recovery stages in stroke.

Reference:

1. N.M. Salbach, S.J. Guilcher, S.B. Jaglal, Physical therapists´ perceptions and use of standardized assessments of walking ability post-stroke, J Rehabil Med 43(6) (2011), 543-549.

2. H. Hsiu, S.M. Huang, C.T. Chen, C.L. Hsu, and W.C. Hsu, Acupuncture stimulation causes bilaterally different microcirculatory effects in stroke patients, Microvasc Res 81(3) (2011), 289-294.

3. L. Bernardi, M. Rossi, P. Fratino, G. Finardi, E. Mevio, C. Orlandi, Relationship between phasic changes in human skin blood flow and autonomic tone, Microvasc Res 37(1) (1989), 16-27.

4. P. Kvandal, S.A. Landsverk, A. Bernjak, A. Stefanovska, H.D. Kvernmo, K.A. Kirkeboen, Low-frequency oscillations of the laser Doppler perfusion signal in human skin, Microvasc Res 72(3) (2006), 120-127.

GINSENOSIDE RD BLOCKS AIF MITOCHONDRIO-NUCLEAR TRANSLOCATION AND NF-KB NUCLEAR ACCUMULATION BY INHIBITING POLY(ADP-RIBOSE) POLYMERASE-1

G. Hu, M. Shi, G. Zhao

Xijing Hospital, The Fourth Military Medical University, Xi'an, China

Objectives: Our previous clinical and basic studies have demonstrated that ginsenoside Rd (GS-Rd) has remarkable neuroprotective effects after cerebral ischemia but the underlying mechanisms are still unknown. In our latest studies, we revealed that GS-Rd could prevent mitochondrial release of apoptosis-inducing factor (AIF) and reduce inflammatory response following transient focal ischemia in rats. Poly(ADP-ribose) polymerase-1 (PARP-1) is required for both AIF release from mitochondria and NF-κB-mediated inflammation. Here, we investigated whether GS-Rd could act on PARP-1 and subsequently affect AIF translocation and NF-κB activation.

Methods: Sprague-Dawley rats were treated with GS-Rd (10 mg/kg) 30 min before surgery with the right middle cerebral artery occlusion, and at different time points following cerebral ischemia, brain tissues were collected for western blotting analysis.

Results: Our results showed that GS-Rd

significantly attenuated ischemia-triggered increased levels of Poly(ADP-ribose), an enzymatic product catalyzed by PARP-1, but not altered the expression of PARP-1 per se. Meanwhile, GS-Rd pretreatment reduced AIF mitochondrio-nuclear translocation and inhibited NF-κB p65 subunit nuclear accumulation after cerebral ischemia.

Conclusions: Therefore, our finding provide the first evidence that GS-Rd can inhibit PARP-1 activity and sequential AIF translocation and NF-κB nuclear accumulation, which may be responsible for GS-Rd's neuroprotection against both neuronal cell death and inflammation after ischemic stroke.

References: Ye R, Zhang X, Kong X, Han J, Yang Q, Zhang Y, Chen Y, Li P, Liu J, Shi M, Xiong L, Zhao G. Ginsenoside Rd attenuates mitochondrial dysfunction and sequential apoptosis after transient focal ischemia. Neuroscience. 2011 Mar 31;178:169-80.

EARLY SUPERFICIAL TEMPORAL ARTERY TO MIDDLE CEREBRAL ARTERY BYPASS IN ACUTE ISCHEMIC STROKE

P.W. Huh

Department of Neurosurgery, Uijeongbu St. Mary's Hospital, The Catholic University of Korea, School of Medicine, Ujeongbu, Republic of Korea

Background: To evaluate the effect and safety of superficial temporal artery-middle cerebral artery (STA-MCA) anastomosis in the early stage after acute ischemic event in patients with intracranial atherosclerotic occlusive disease.

Methods: From 2006-2010, 20 patients (15 males and five females) with atherosclerotic ICA or MCA stenosis or occlusion were treated by STA-MCA bypass. All patients presented with acute hemodynamic insufficiency and stroke in progress despite maximal medical therapy. STA-MCA bypass were performed within 2 weeks from symptom onset. Clinical outcome and hemodynamic study were preoperatively and postoperatively investigated and we compared our results with those of other studies on delayed STA-MCA bypass.

Results: Among 20 patients who underwent early STA-MCA bypass, fourteen (70%) patients achieved a good functional outcome (mRS 0, n=2; mRS 1, n=8; mRS 2, n=4). Before surgery, the mean rCBF and CVR in the symptomatic hemisphere were 37.3 ± 4.3 mL/100g/min and 57.8 ± 6.7%. The mean basal rCBF and CVR significantly increased postoperatively. No reperfusion-induced hemorrhage occurred. In pooled analysis, no statistical differences were observed in clinical outcome (P =0.328) and incidence of postoperative complication (P =0.516) between patients who underwent early STA-MCA bypass and patients who underwent delayed STA-MCA bypass in other studies.

Conclusions: In this series of carefully selected 20 patients with acute ischemic stroke, early STA-MCA bypass appears to be both safe and effective, and in some cases resulted in rapid neurological improvement. Early STA-MCA bypass appears to be beneficial for the selected patients who have acute hemodynamic ischemic stroke.

METFORMIN PROMOTES FUNCTIONAL RECOVERY FOLLOWING EXPERIMENTAL STROKE VIA INDUCING ALTERNATIVE POLARIZATION OF MICROGLIA

J. Jia[1], Q. Jin[2], J. Cheng[3], X. Zhen[2]

[1]Department of Pharmacology, College of Pharmaceutical Sciences, Soochow University, Institute of Neuroscience, [2]Department of Pharmacology, College of Pharmaceutical Sciences, Soochow University, [3]Institute of Neuroscience, Soochow University, Suzhou, China

5'-AMP-activated protein kinase (AMPK), a critical sensor of cellular energy, is increasingly recognized to be involved in pathogenesis of neurodegenerative diseases. However, the role of AMPK in cerebral ischemia remains controversial [1, 2]. Emerging data suggest that AMPK activation is a master switch that induces alternative polarization (M2) of microglia /macrophages and that M2 polarization of microglia/macrophages promotes brain repair following injuries [3-5] . Thus, we investigated if post-ischemic administration of metformin, a well-established AMPK activator, promotes post-ischemic functional recovery and neurogenesis by inducing M2 polarization of microglia in the ischemic brain.

Adult male mice were subjected to 1 hour middle cerebral artery occlusion (MCAO), followed by daily intraperitoneal injection of

metformin (50mg/kg/day), starting at 24 hours after MCAO. Western blot was performed to characterize metformin effects on AMPK activation in the ischemic brain. Functional recovery was monitored with behavioral tests over 30 days after MCAO. Quantitative PCR (qPCR) and immunohistochemical staining were performed to monitor M1 and M2 markers of microglia/macrophages following MCAO. To assess neurogenesis in the subventricular zone (SVZ), immunohistochemistry was used to detect cells co-labeled with bromodeoxyuridine (BrdU) and the newborn neuronal marker doublecortin (DCX) at 14 days after MCAO.

Metformin activated AMPK both in the ischemic brain and a microglial cell line. Compared to mice treated with the vehicle, metformin-treated mice displayed improved neurobehavioral deficits as indicated by neurological severity scores as well as better performance in the corner test and rotarod test since 7 days following MCAO. qPCR and immunohistochemistry showed that metformin significantly reduced the expression of M1 microgilal markers (CD32, IL-1β) and increased that of M2 markers (CD206, Arginase 1) in the ischemic brain at 3, 7, 14 and 30 days after MCAO. Using ELISA technique, we further showed that metformin increased cerebral levels of IL-10, a critical effecter produced by M2 macriphages/microglia, in the ischemic brain following MCAO. Consistent with our expectation, we found that metformin reduced brain atrophy 30 days after MCAO and increased post-ischemic neurogenesis in the SVZs at 14 days after MCAO.

In conclusion, our data suggest that post-ischemic administration of the AMPK activator metformin promoted functional recovery and brain repair following MCAO via pivoting the phenotype of microglia/macrophages to a skewed M2 polarization.

1. Li J, Benashski SE, Venna VR, McCullough LD: **Effects of metformin in experimental stroke**. *Stroke* 2010, **41**(11):2645-2652.

2. Li J, McCullough LD: **Effects of AMP-activated protein kinase in cerebral ischemia**. *J Cereb Blood Flow Metab* 2010, **30**(3):480-492.

3. Kigerl KA, Gensel JC, Ankeny DP, Alexander JK, Donnelly DJ, Popovich PG: **Identification of two distinct macrophage subsets with divergent effects causing either neurotoxicity or regeneration in the injured mouse spinal cord**. *J Neurosci* 2009, **29**(43):13435-13444.

4. Lu DY, Tang CH, Chen YH, Wei IH: **Berberine suppresses neuroinflammatory responses through AMP-activated protein kinase activation in BV-2 microglia**. *J Cell Biochem* 2010, **110**(3):697-705.

5. Hu X, Li P, Guo Y, Wang H, Leak RK, Chen S, Gao Y, Chen J: **Microglia/Macrophage polarization dynamics reveal novel mechanism of injury expansion after focal cerebral ischemia**. *Stroke* 2012, **43**(11):3063-3070.

GENOMIC ANALYSIS OF LEUKOCYTE MRNA SUGGESTS IMMUNE PREDISPOSITION TO HEMORRHAGIC TRANSFORMATION IN ISCHEMIC STROKE

G.C. Jickling[1], B.P. Ander[1], B. Stamova[1], X. Zhan[1], D. Liu[1], L. Rothstein[1], P. Verro[1], J. Khoury[2], E.C. Jauch[3], A. Pancioli[4], J.P. Broderick[4], F.R. Sharp[1]

[1]Neurology, University of California at Davis, Sacramento, CA, [2]Biostatistics and Epidemiology, Cincinnati Children's Hospital Medical Center, Cincinnati, OH, [3]Emergency Medicine, Medical University of South Carolina, Charleston, SC, [4]Neurology, University of Cincinnati, Cincinnati, OH, USA

Objective: Hemorrhagic transformation (HT) is a major complication of ischemic stroke that worsens outcomes and increases mortality. Disruption of the blood brain barrier is a central feature to HT pathogenesis, and leukocytes may contribute to this process. We sought to determine whether ischemic strokes that develop HT have differences in leukocyte RNA expression within 3 hours of stroke onset prior to treatment with thrombolytic therapy.

Methods: Stroke patient blood samples were obtained prior to treatment with thrombolysis, and leukocyte RNA assessed by microarray analysis. Strokes that developed HT (n=11) were compared to strokes without HT (n=33) and controls (n=14). Genes were identified (corrected p-value < 0.05, fold change ≥|1.2|) and functional analysis performed. RNA prediction of HT in stroke was evaluated using cross-validation, and in a second stroke cohort (n=23).

Results: Ischemic strokes that developed HT

had differential expression of 29 genes in circulating leukocytes prior to treatment with thrombolytic. A panel of 6 genes could predict strokes that later developed HT with 86.4% accuracy. Key pathways involved in HT of human stroke are described, including amphiregulin, a growth factor that regulates matrix metalloproteinase-9; a shift in transforming growth factor-beta signaling involving SMAD4, INPP5D and IRAK3; and a disruption of coagulation factors V and VIII.

Conclusions: Identified genes correspond to differences in inflammation and coagulation that may predispose to HT in ischemic stroke. Given the adverse impact of HT on stroke outcomes, further evaluation of identified genes and pathways is warranted to determine their potential as therapeutic targets to reduce HT and as markers of HT risk.

TRANSGENIC NAMPT OVEREXPRESSION PROTECTS AGAINST CEREBRAL ISCHEMIC STROKE

Z. Jing[1,2], J. Xing[2], F. Zhang[2], Y. Gan[2], J. Chen[1,2], G. Cao[1,2]

[1]GRECC, VA Pittsburgh Healthcare System, [2]Neurology, University of Pittsburgh School of Medicine, Pittsburgh, PA, USA

Objectives: Nicotinamide phosphoribosyltransferase (NAMPT) is the rate-limiting enzyme of nicotinamide adenine dinucleotide biosynthesis, and plays a key role in the regulation of energy metabolism and stress responses. Lentivirus-mediated NAMPT overexpression[1] or genetic NAMPT depletion[2] indicated a neuroprotection of NAMPT against ischemic brain injury. However, the mechanism underlying its protective effect remains largely unknown. The objective of this project is to further examine the protective effect of NAMPT and its potential mechanism against ischemic stroke, utilizing a novel neuron-specific NAMPT transgenic mice line.

Methods: NAMPT transgenic mice line was constructed using Thy-1 promoter which allows for NAMPT overexpression (tagged with HA) in a neuron-specific pattern. Transgenic mice and littermates were subjected to transient occlusion of the middle cerebral artery (MCAO) for 60 min followed by reperfusion. Infarct volume and white matter injury (WMI) were evaluated at 72h after MCAO.

Results: NAMPT was exclusively found in the brain in NAMPT transgenic mice, with 3-fold expression level as compared to that of littermates. Immunohistochemistry staining showed that transgenic NAMPT was expressed within the whole brain region, and highly expressed in layers 5 and 6 pyramidal neurons in the cortex and striatal fiber bundles. The majority of HA positive cells are neurons. NAMPT overexpression in the brain does not alter body weight and blood glucose level, or causes other phonotype changes. To determine whether NAMPT has neuroprotective effects, NAMPT transgenic mice were subjected to transient MCAO for 60 min followed by reperfusion. Infarct volume was determined by triphenyltetrazolium chloride staining, and neurological deficiency score was evaluated 72 hr after MCAO. Transgenic NAMPT overexpression significantly reduced infarct volume (by 65%, $p=0.018$) and improved neurological deficit scores ($p< 0.05$) compared to littermates. Physiological parameters (blood pressure, blood gases, and blood glucose) did not shown significant changes between transgenic mice and littermates. Cortical blood flow as determined using two-dimensional Laser Speckle Contrast Imaging showed no significant difference between groups during and after MCAO. Interestingly, NAMPT expression was dramatically induced after ischemia in striatal fiber bundles and the corpus callosum after ischemia, a strong hint that NAMPT may be related to white matter injury. In line with this, Luxol Fast Blue staining indicated that transgenic NAMPT overexpression dramatically increases the area of myelinated fibers in the striatum as compared to littermates ($^{**}p< 0.01$).

Conclusions: Transgenically overexpressed NAMPT confers not only neuroprotective effect, but also white matter protection against ischemic brain injury. Our novel finding suggests that NAMPT protects brain against ischemia via a multiple mechanisms.

Reference:

1. Wang, P., et al. Ann Neurol. 69:360-74 (2011)

2. Zhang, W., et al. J Cereb Blood Flow Metab. 30:1962-71 (2010)

IS THERE SOMETHING WRONG HOW WE PRODUCE STROKE IN RODENTS?

J. Jolkkonen

Institute of Clinical Medicine, Neurology, University of Eastern Finland, Kuopio, Finland

Experimental models are indispensable in understanding the pathology and brain repair in stroke on which development of new therapies is based. Producing cerebral ischemia is in principal straightforward. Next I will refer to the transient MCAO model (filament), which is perhaps the most common stroke model. Although craniectomy is not needed, yet the model is invasive and complicated by high variability in lesion size and location, hemorrhage and high mortality, which are difficult to overcome even in skillful hands.

Anesthesia used during ischemia operation varies a lot between laboratories, but usually gas anesthesia and isoflurane is used. However, isoflurane is neuroprotective (compared to halothane), it is vasodilative and it causes damage to the blood-brain barrier. Another variable possibly affecting results is postoperative care of the animals, including the administration of painkillers, which should be used to lessen suffering from the operation. Also an inherited complication in the MCAO model are difficulties in swallowing and drinking leading to severe loss of body weight, which bias all food rewarded behavioral tests at acute phase.

The methods used to measure tissue damage (e.g., TTC staining) may also contribute to translational failure. The stained tissue may seem to be viable, but in fact it is not functional as shown by fMRI. Thus, sensitive behavioral tests could be used as an additional and often more reliable measure of neuroprotection. In addition, one overlooked difference between rodents and humans is the secondary pathology in the thalamus (e.g., accumulation of β-amyloid and calcium), which further exacerbate the inflammation and neuronal damage and is likely to affect the long-term outcome in rodents.

Maybe there is not that much wrong in our stroke models, but the procedures how we induce stroke and how we assess outcome need adjusting. Most of the issues raised here could be overcome if the stroke community put forces together to establish common standard operating procedures. This should result in more reliable and consistent data and hopefully prevent translational failures in future.

DEPLETED BRAIN TISSUE POTASSIUM AT THE ISCHEMIC EDGE, BUT NOT THE CENTRAL ISCHEMIC CORE, LIMITS INFARCT EXPANSION

S.C. Jones[1,2,3], V.E. Yushmanov[1], A. Kharlamov[1]

[1]Anesthesiology, [2]Neurology, Allegheny-Singer Research Institute, Drexel University College of Medicine, [3]Radiology, University of Pittsburgh School of Medicine, Pittsburgh, PA, USA

Objectives: Pathological progression in ischemic stroke is presumed, with few exceptions (1), to occur uniformly within the ischemic region. However, pathophysiologic events such as edema formation, brain tissue $[Na^+]$ (2) and $[Ca^{2+}]$ increase (3), and loss of MAP2 (4) occur in the peripheral regions within the ischemic core, termed the Ischemic Edge. Tissue sampling methods show a consistent decrease in brain tissue $[K^+]$, $[K^+]_{br}$, in ischemic cortex (5), but K^+-staining imaging shows excessive K^+ decreases (3) in the Ischemic Edge compared to the central ischemic core. These Ischemic Edge changes are at the crux of ischemic pathology with K^+ being a central player: K^+-mediated depolarization is the hallmark of ischemic depolarization, having been used to define the initial descriptions of the ischemic threshold (6) and penumbra (7). We suggest that these greater decreases of $[K^+]_{br}$ at the Ischemic Edge limit peri-infarct depolarization (PID)-mediated infarct expansion (8,9).

Methods: In two groups of rats (isoflurane anesthesia) (Group I: Time-course of K^+-depletion, n=12 and Group II: Infarct volume, Amount of K^+-depletion, Moderate hypertension, CBF, n=8) focal ischemia was induced via MCA transection and both CCAo. Brain sections were quantitatively stained for K^+ (10) and the cortical ribbon was analyzed for differences in $[K^+]_{br}$ in the normal cortex, NC, central ischemic core, ICc, and K^+-depleted-Ischemic Edge, IEdep, over 2.5 to 5 h with linear regression (Group I) or, at 2 h for Group II, for the amount of K^+ lost (IEdep volume x ($[K^+]$-ICc - $[K^+]$-IEdep). In Group II, moderate hypertension induced with phenylephrine (Phe group, n=5, 132 mmHg) (11) doubled laser speckle-determined CBF (11.2% vs 6%, p=0.03) in the Ischemic Edge

compared to the control (Con, n=3, 102 mmHg).

Results: In Group I, accelerated K^+-depletion occurred in the IEdep, compared to ICc region, and then slowed after 2.5 h (6.2 vs 14 mEq/kg/h, p< 0.01, see Fig.). In the IEdep region of Group II twice as much K^+ was lost in the Phe vs. Con group and this K^+-loss was associated with significant infarct volume reduction (11±2% Con vs. 5.9±1% Phe group, p=0.02). We suggest that hypertension increased the K^+-loss via increased collateral flow, thus limiting the severity and frequency of PIDs because of their need for K^+, which in turn mitigated PID-induced infarct expansion.

Conclusions: Our results of ischemic core differences in K^+-depletion over time combined with increased K^+-loss under moderate hypertension suggest that vascular infarct protection is at least partially accomplished through reduced PID-mediated infarct expansion.

Support: NIH NS30839, NS30839-14S1, NS66292

References:

1. Del Zoppo et al. 2011;JCBFM 31:1836-1851

2. Yushmanov et al. 2009;JMRI 30:18-24

3. Kato et al. 1987;ExpNeurol 96:118-126

4. Kharlamov et al. 2001;JNeurosciMethods 111:67-73

5. Schuier et al. 1980;Stroke 11:593-601

6. Astrup et al. 1977;Stroke 8:51-57

7. Branston et al. 1977;JNeurolSci 32:305-321

8. Sasaki et al. 2009;NeurosciLett 449:61-65

9. Lauritzen et al. 2011;JCBFM 31:17-35

10. Mies et al. 1984;AnnNeurol 16:232-237

11. Shin et al. 2008;Stroke 39:1548-1555

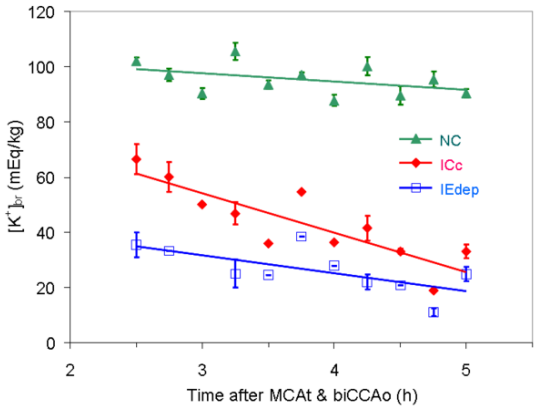

[The time-course of [K+]br -depletion]

REAL TIME SPREADING DEPOLARIZATION IN HYPERACUTE PHASE OF STROKE USING PERFUSION MRI

Y.-C.J. Kao[1], H.-Y. Lai[1], W. Lin[2], Y.-Y.I. Shih[1]

[1]Department of Neurology and Biomedical Research Imaging Center, [2]Department of Radiology and Biomedical Research Imaging Center, University of North Carolina, Chapel Hill, NC, USA

Objectives: Spreading depolarization (SD) is a series of propagating electric waves that appear under noxious condition including the hyperacute phase of stroke (within 30 min after stroke onset in rodents) [1]. Optical imaging and EEG/ECoG recording allow identification of SD, but both techniques are depth-limited and cannot provide volumetric tissue information with clinically relevant indices. SD in stroke model has never been characterized by MRI due to relatively long setup time and a lack of consecutive imaging data with high temporal resolution. This study aimed to characterize SD using quantitative perfusion MRI with high temporal resolution.

Methods: Seven Sprague Dawley rats were anesthetized with 1.5% isoflurane, ventilated and paralyzed. A home-made MR-compatible optic fiber (200 µm) was placed above the primary somatosensory cortex of forelimb (S1fl). An 8 m optic patch cable was used to deliver green-light laser (532 nm, 10 mW) for 8 min. Rose Bengal (10 mg/kg) was intravenously administered 1 min after the laser onset for 2 min. MRI was performed on a Bruker 9.4T Biospec scanner with a home-

made surface coil (ID=2 cm) and a separate neck coil for arterial spin labeling (ASL). CBF acquired by continuous ASL with 3 s temporal resolution was measured for 60 min including 20 min baseline. T2-weighted images were acquired 24 h after stroke. Significant level was set at $p< 0.05$. Error bars were SEM.

Results: This study demonstrates a modified photothrombotic stroke model (**Fig. A**) capable of producing a localized stroke (**Fig. B**) inside the MRI. After laser illumination, the CBF in the target area dropped 50% within 10 min. We showed for the first time that post-SD oligemia [1,2] is not restricted to the SD territory but occurs on a whole-brain scale (**Fig. C&D**). The oligemia occurred upon the first SD and exacerbated after the subsequent SDs (**Fig. E**). An average of 3.7±2.31 (mean±SD) SDs was observed within 30 min. SD in our study was characterized by spreading-hyperemia (**Fig. D**), in which CBF rises more than 100% due to energy demand to restore homeostasis as observed by optical imaging [3]. The SDs initiated around the implanted region, propagated outward, and then vanished when reaching the corpus callosum and the brain midline at a propagation velocity of ~2 mm/min, and were confined to the ipsilesional cortex [1,3,4] (**Fig. E**).

Conclusions: This study demonstrates a modified photothrombotic stroke model for visualization the CBF changes before, during and after stroke onset. SD and post-SD oligemia were revealed for the first time by high resolution perfusion MRI.

References:

[1] Dreier, Nat Med, 2011, 17:439.

[2] Lauritzen, Brain, 1994, 117:199.

[3] Ayata et al., JCBFM, 2004, 24:1172.

[4] Nakamura et al., Brain, 2010, 133:1994.

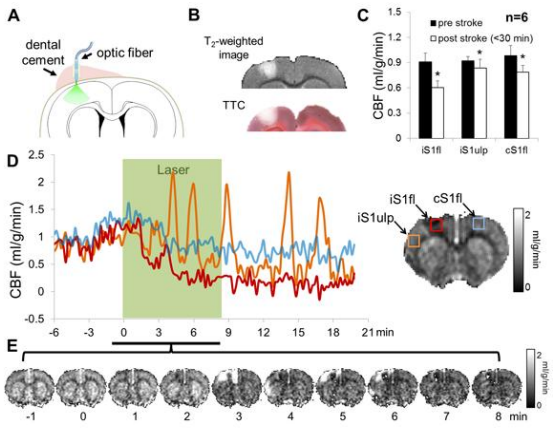

Figure:

(A) The modified photothrombotic model.

(B) T2-weighted image and TTC stain in the same subject.

(C) Group-averaged CBF changes,

(D) continuous CBF data with 3 s, and

(E) CBF images with 1 min temporal resolution during the stroke onset.

*indicates significant difference from pre-stroke values.

ENDOGENOUS STEM CELL ACTIVATION THERAPY FOR ISCHEMIC STROKE USING NERUOMODULATORY DRUGS IGF-1 AND ATROVASTATIN: A MULTI-DISCIPLINARY TRANSLATIONAL MEDICINE APPROACH

S. Kapoor, S. Rallabandi, G. Revathy, P.K. Roy

Computational Neuroscience & Neuroimaging, National Brain Research Centre, Gurgaon, India

Aim of study: To develop a translational-medicine model of cell-based therapy for Transient Ischemic Attack (TIA) using a multi-disciplinary approach combining computational tools with in-vivo verification to translate the results to patients. Most stroke patients incur residual disability despite treatment, needing newer approaches of non-invasive regenerative medicine. In our study, the phenomena of neurogenesis, synaptogenesis and progenitor cell migration with induced

angiogenesis from the sub-ventricular zone, under influence of therapeutic growth factor introduced interventionally, were employed as model parameters.

Material and methods: A predictive mathematical model was designed to discretize the steps involved in neural stem cell proliferation, migration and differentiation and angiogenesis leading to neurorestorative recovery. The optimal dosage and time-point at which the drugs should be administered were computed. A robust ischemia model using the Middle Cerebral Arterial Occlusion technique was created to verify the efficacy and accuracy of the design. The effect of optimal dose of combination of IGF-1 with Atorvastatin was checked. MRI, MR Angio, Perfusion and Diffusion imaging is done to ensure causation of similar ischemic lesions across subjects, changes in blood vasculature, and thus alteration of hypoxic volume post therapy. Behavioural recovery using a battery of sensory-motor tests is correlated with biochemical and cellular changes.

Results: On analysis of the effect of applying the computed therapeutic agent dose at an optimal time point, on neural progenitor cell dynamics we observed a strong peak of synaptic recovery. Experimental findings based on animal experiments, MRI and histopathology exhibit similar trends thus establishing this approach to be useful for optimizing cellular recovery in neurological dysfunction.

Conclusions: Given that the ischemic brain has evolved an incisive way to partly recoup itself by increasing the production of endogenous stem cell niches, an approach to augment this performance by suitably optimizing the dosage and its temporal scheduling is the main aim of this study. Our efforts can be seen as the 1st endeavour of incorporating endogenous NSC processes influenced by neuro-modulators in a robust model that allows for incorporation of patient specific parameters that would be indicators and hence influence recovery which could be monitored effectively by non-invasive imaging and pathological bio-markers.

References:

1. Thored P, Arvidsson A, Cacci E, *et al.* Persistent Production of Neurons from Adult Brain Stem Cells During Recovery after Stroke, *Stem cells*; **24**:739-47 (2006)

2. Yamashita T, Ninomiya M, Acosta PH, *et al*. Subventricular zone-derived neuroblasts migrate and differentiate into mature neurons in the post-stroke adult striatum. *J. Neuroscience*; **26**:6627-36 (2006)

3. Minger S, Ekonomou A, Carta E *et al*. Endogenous neurogenesis in the human brain following cerebral infarction, *Regenerative Med.,* **2(1):** 69-74 (2007)

4. Chen J, Zhang ZG, Li Y, *et al.* Statins induce angiogenesis, neurogenesis, and synaptogenesis after stroke. *Ann. Neurol*; **53**:743-51 (2003)

5. Chopp M, Zhang ZG, Jiang Q. Neurogenesis, angiogenesis, and MRI indices of functional recovery from stroke. *Stroke*; **38**:827-31 (2007)

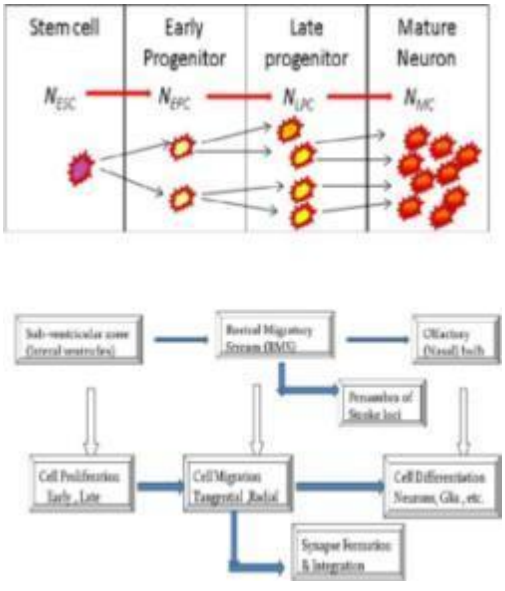

[Stem cell dynamics during Stroke injury]

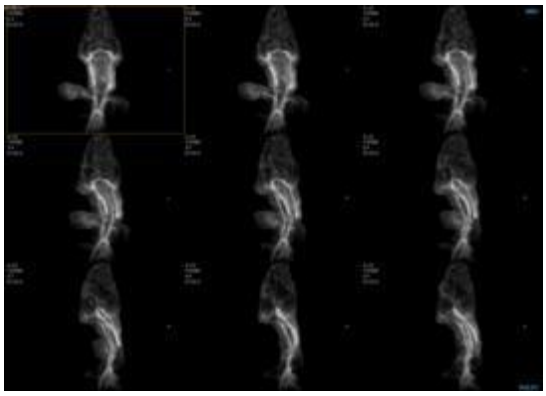

[Imaging of Rat Model]

THE ROLE OF THE INNATE IMMUNE AND INFLAMMATORY SYSTEM, TRIGGERING RECEPTOR EXPRESSED BY MYELOID CELLS-2 (TREM2), IN THE HYPOTHERMIC THERAPY

M. Kawabori, M. Hokari, X.N. Tang, Z. Zheng, C. Calosing, **M.A. Yenari**

Neurology, University of California San Francisco (UCSF) and San Francisco VA Medical Center (SF VAMC), San Francisco, CA, USA

Hypothermia is neuroprotective against many acute neurological insults. We and others have previously shown that protection by hypothermia is associated with the suppression of the inflammatory response that accompanies stroke. However, the roles of the phagocytic process by immune cells in the setting of ischemic stroke have not been fully elucidated. In this study, we subjected early and delay hypothermia for mouse permanent ischemic stroke model and compare the relationship between the effect and anti-inflammatory response. We subjected male mice to permanent middle cerebral artery occlusion (MCAO). We identified 2 cooling paradigms, one where cooling (rectal temp=30C) began at the onset of MCAO (early) and a second where cooling began 1h later (delayed). In both cases, cooling was maintained for 2h. A 3rd group was maintained at normothermia as a control (38C). Mice survived 1, 3, 7, 14 & 30d (n=6/group/time point). Mice from the normothermia and delayed groups had similar ischemic lesions sizes and neurological performance, but mice cooled early showed marked protection as evidenced by smaller lesion size and few neurological deficits ($P< 0.05$) at all time points. Immunostains for microglia and macrophages among animals exposed to delayed hypothermia did not show any difference from that of normothermic group, but these immune cells were markedly decreased in the early group ($P< 0.01$). Expression of the Triggering receptor expressed by myeloid cells-2 (TREM2) which is thought to be involved in phagocytosis of the injured neurons was increased only in the early hypothermia group at Day 7. Immune cells were reduced only where hypothermia was protective and we conclude that inflammation is related to the amount of injury present, and not whether cooling occurred.

POSITRON EMISSION TOMOGRAPHY STUDY DURING INTERNAL CAROTID ARTERY TEST OCCLUSIONS: FEASIBILITY OF RAPID QUANTITATIVE MEASUREMENT OF CBF AND OEF/$CMRO_2$

N. Kawai[1], M. Kawanishi[1], A. Shindou[1], N. Kudomi[2], T. Tamiya[1]

[1]Department of Neurological Surgery, [2]Department of Medical Physics, Kagawa University, Faculty of Medicine, Kita-gun, Japan

Objectives: Occlusion of the internal carotid artery (ICA) is sometimes necessary to treat giant ICA aneurysms and tumors encasing the ICA. Balloon test occlusion (BTO) of the ICA combined with cerebral blood flow (CBF) study is a sensitive test for predicting the outcome of permanent ICA occlusion. However, false negative result sometimes occur using single photon emission tomography (SPECT). We have recently developed a rapid positron emission tomography (PET) protocol that measures not only the CBF but also the cerebral oxygen metabolism before and during BTO in succession within 15 minutes. In this presentation, we report our initial experiences of PET study for evaluating the cerebral blood flow and metabolism before and during BTO, especially describing the feasibility of rapid quantitative measurement of the CBF and OEF/$CMRO_2$.

Methods: We measured acute changes in regional CBF and OEF/$CMRO_2$ before and during BTO in 3 cases with large or giant cerebral aneurysms using the rapid PET protocol. The PET protocol was originally

developed as the dual tracer autoradiographic (DRAG) method [1], in which $^{15}O_2$ and $H_2{}^{15}O$ (or $C^{15}O_2$) are sequentially administered during a single PET scanning to measure the $OEF/CMRO_2$ and CBF. The method was further improved by eliminating the need for CBV data so that the total scan time is shortened to less than 15 min [1].

Results: Although no patients showed ischemic symptoms during BTO, PET studies exhibited mildly to moderately decreased CBF (13% and 34%) compared to the values obtained before BTO in 2 cases. The average OEF during BTO was significantly increased (21% and 43%) than that of before BTO in the 2 cases. The 2 cases were considered to be non-tolerant for permanent ICA occlusion and treated with partial obliteration of the aneurysm without ICA sacrifice. Another case showed mild CBF reduction (9%) without significant OEF elevation. This case was considered to be tolerant for permanent ICA occlusion and treated with ICA occlusion without acute or later neurological deficits.

Conclusions: Measurement of the CBF and $OEF/CMRO_2$ using a rapid PET protocol before and during BTO is feasible and can be used for accurate assessment of tolerance prediction in ICA occlusion.

This study was published in Interventional Neuroradiology [2].

References:

1. Kudomi N, Watabe H, Hayashi T, Iida H. Separation of input function for rapid measurement of quantitative CMRO2 and CBF in a single PET scan with a dual tracer administration method. Phys Med Biol. 2007; 52: 1893-1908.

2. Kawai N, Kawanishi M, Shindou A, Kudomi N, Yamamoto Y, Nishiyama Y, Tamiya T. Cerebral blood flow and metabolism measurement using positron emission tomography before and during internal carotid artery test occlusions: feasibility of rapid quantitative measurement of CBF and OEF/CMRO(2). Interv Neuroradiol 2012; 18: 264-274.

PARAMETERS OF TRANSIENT POST-STROKE HYPOTENSION ASSOCIATED WITH PERI-INFRACT DEPOLARIZATIONS

A. Kharlamov[1], V.E. Yushmanov[1], **S.C. Jones**[1,2,3]

[1]Anesthesiology, Allegheny Singer Research Institute, Allegheny General Hospital, [2]Neurology, Allegheny Singer Research Institute, [3]Radiology, University of Pittsburgh School of Medicine, Pittsburgh, PA, USA

Objectives: Peri-infarct depolarizations (PIDs) are a major mechanism of infarct expansion in experimental and human stroke, subarachnoid hemorrhage, and brain trauma (Dijkhuizen et al., 1999; Dreier, 2011). Our preliminary data demonstrated that 59% of PIDs observed after focal brain ischemia in rats were associated with episodes of post-stroke transient hypotension (PSTH). These data suggest that PSTH of certain parameters can exacerbate the hypoperfusion in ischemic tissue and trigger additional PIDs which in turn contribute to infarct expansion. The purpose of this study is to measure parameters of PSTH associated with PID initiation.

Methods: Permanent unilateral focal ischemia in male Sprague-Dawley rats (n=5) was induced under isoflurane anesthesia via three vessel occlusion (unilateral middle cerebral artery and bilateral common carotid artery occlusion). After stroke induction, the animal was placed in an animal-bore ClinScan 7 T magnet for fast ADC brain mapping with continuous mean arterial blood pressure (MABP) monitoring with continuous intravenous infusion of gallamine triethiodide (1 mg/kg/h in 1 ml/h saline). Trace ADC maps were reconstructed with the isotropic resolution (0.5x0.5x0.5 mm voxel size). PID occurrences and tracking were performed by analysis of transient expansion of low-ADC regions in whole 3D brain using AMIDE software (Loening and Gambhir, 2003).

Results: After stroke, MABP was unstable, and 59% of PIDs were associated with PSTH (87±2 mmHg MABP during PID vs. 123±2 mmHg pre-PID MABP, $p \leq 0.001$, n=33), while spontaneous PIDs (i.e., the other 41%) occurred during normotension (112±4 mmHg MABP during PID vs. 112±3 mmHg pre-PID MABP, $p \geq 0.1$, n=25). Fig. 1 illustrates: 1) that episodes of PSTH associated with PIDs lasted 150±17 s; 2) that the interval between PSTH

and the subsequent PID is 66±15 s; 3) PIDs are triggered when MABP is 75±2 % of pre-PID-MABP; and 4) the speed of MABP drop associated with PIDs initiation was 13±1 mmHg/min. The detrimental effect of PIDs manifested itself in the growth of the volume of low ADC values (≤570 $\mu m^2/s$) as a marker for low CBF in the ischemic core and eventual infarct from 1 to 4 h after stroke from 70.5 mm^3 to 97.5 mm^3 ($p \leq 0.01$) at an average rate of 1.8 mm^3 per PID.

Conclusions: These data suggest that PSTH with certain parameters can contribute to infarct expansion by amplifying the hypoperfusion in ischemic tissue and triggering PIDs. Preventing episodes of PSTH with these parameters that trigger additional PIDs may improve stroke outcome.

Support: NIH NS30839, NS30839-14S1, NS66292

References:

1. Dijkhuizen RM, Beekwilder JP, van der Worp HB, Berkelbach van der Sprenkel JW, Tulleken KA, Nicolay K (1999) Correlation between tissue depolarizations and damage in focal ischemic rat brain. Brain Res 840:194-205

2. Dreier JP (2011) The role of spreading depression, spreading depolarization and spreading ischemia in neurological disease. Nat Med 17:439-447

3. Loening AM, Gambhir SS (2003) AMIDE: a free software tool for multimodality medical image analysis. Mol Imaging 2:131-137

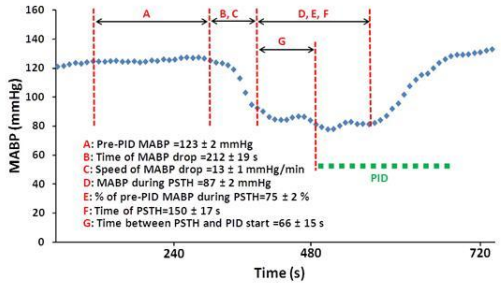

Fig 1. *Parameters of MABP (blue) during PSTH associated with PID (green)*

BRAIN INFARCT VOLUME AFTER PERMANENT FOCAL ISCHEMIA IS NOT DEPENDENT ON NOX2 EXPRESSION

H.A. Kim, V.H. Brait, S. Lee, T.M. De Silva, H. Diep, A. Eisenhardt, G.R. Drummond, C.G. Sobey

Department of Pharmacology, Monash University, Clayton, VIC, Australia

Introduction: Reactive oxygen species (ROS) generated by Nox2 oxidase are reported to contribute to infarct damage following cerebral ischemia-reperfusion. Experimental studies investigating mechanisms of post-stroke brain injury have mostly utilized models of ischemia with reperfusion. Hence, they are most relevant for elucidating the pathology occurring in ischemic stroke cases receiving clot-buster therapy or where there is spontaneous reperfusion. It is thus important to clarify if Nox2 oxidase is also a valid therapeutic target in ischemia without reperfusion. We examined the role of Nox2 expression in outcome following permanent focal cerebral ischemia.

Methods: Male wild-type (WT) C57Bl6/J and $Nox2^{-/y}$ mice were anesthetized with i.p. ketamine-xylazine (80 and 10 mg/kg, respectively). Cerebral ischemia was induced using a monofilament to cause middle cerebral artery occlusion (MCAO) for 24 h. Regional cerebral blood flow was reduced by ~85 % in all mice. Neurological deficit and hanging wire grip time was assessed, and infarct and edema volumes were estimated using thionin-stained brain sections at 24 h. In separate mice, Nox2 expression was measured in the ischemic hemisphere using Western blotting.

Results: Nox2 expression was increased in the ischemic versus non-ischemic hemisphere of WT mice 24 h after MCAO (1.77 ± 0.31 versus 1.00 ± 0.09; n=9-10, $P < 0.05$). However, genetic deletion of Nox2 had no effect on any outcome measures at 24 h after permanent MCAO. WT and $Nox2^{-/y}$ mice had similar neurological deficit scores and hanging times. Similarly, the edema volume and total, cortical, and subcortical infarct volumes did not differ between WT and $Nox2^{-/y}$ mice.

Conclusions: ROS production by Nox2 oxidase activity plays no significant role in the pathophysiology of cerebral ischemia in the absence of reperfusion. Nox2 oxidase was first found to be expressed in phagocytic cells, but it is now known to be constitutively expressed in all of the major cell types present in brain tissue (i.e. neurons, astrocytes, microglia and vascular endothelial cells). Moreover, the key

cell types involved in Nox2-dependent neuronal injury following cerebral ischemia and reperfusion may include resident brain cells (e.g. neurons and microglia) and infiltrating leukocytes. The findings may highlight the importance of ROS production by Nox2 oxidase-containing leukocytes that enter the ischemic brain specifically if reperfusion is instituted.

CEREBROPROTECTION BY HESPERETIN IS ASSOCIATED WITH RESTORATION OF TRYPTOPHAN METABOLIC ENZYME SYSTEM IN MOUSE

S.J. Kim, S.Y. Kim, Y. Fang, W.S. Lee

Department of Pharmacology, Pusan National University School of Medicine, Yangsan, Republic of Korea

The tryptophan metabolic enzyme systems of indoleamine 2,3-dioxygenase (IDO) and tryptophanyl-tRNA synthetase (TrpRS), which are involved in L-tryptophan catabolism and its use in protein synthesis, respectively, are associated with the neuroinflammation and immune response to acute cerebral ischemia. Hesperetin, a citrus flavanone, is known to help prevent tissue damage from oxidative stress in the brain. However, the exact cerebroprotective mechanism of hesperetin remains unclear. In this study we investigated the mechanisms involved in cerebroprotective action of heseperetin in connection with the tryptophan metabolic enzyme systems. Posttreatment with hesperetin significantly reduced the infarct size including infarct area and volume. Ischemic insult markedly altered the tryptophan metabolic enzyme systems, i.e. an increase in the expression of IDO, CD11b, and CD11c, and a simultaneous decrease in that of TrpRS. Hesperetin significantly decreased the expressions of IDO, CD11b, CD11c, p-JAK2 and p-STAT1 via increasing the expression of TrpRS. Hesperetin significantly restored the tryptophan metabolic enzyme system, inhibiting JAK/STAT signaling activation. These results suggest that the cerebroprotective effects of hesperetin might be associated with the increase in the TrpRS expression as well as the suppression of the IDO expression.

TPA THROMBOLYTIC THERAPY FOR ACUTE ISCHEMIC STROKE IN JAPAN

S. Kono[1], K. Deguchi[1], T. Kurata[1], T. Yamashita[1], Y. Manabe[2], Y. Takao[3], K. Kashihara[4], K. Abe[1]

[1]Okayama University, [2]Okayama National Hospital Medical Center, [3]Kurashiki Heisei Hospital, [4]Okayama Kyokuto Hospital, Okayama, Japan

Objectives: A recombinant tissue plasminogen activator (tPA), alteplase, was approved for patients with acute ischemic stroke within 3h of onset in Japan in October 2005 at a dose of 0.6 mg/kg. The aim was to assess safety and efficacy of alteplase in Japan.

Methods: The 114 consecutive patients who admitted to our 4 hospital groups received intravenous tPA within 3h of onset from October 2005 to December 2009. Clinical backgrounds and outcomes were investigated.

Results: When total patients were chronologically divided into 2 groups, the mean time from arriving at hospital to start of treatment was significantly reduced in latter group from 82.6 to 70.9 min compared to former group. Intracerebral hemorrhage (ICH) group involved in 26 patients (22.8%) had significantly greater proportion of cardiogenic embolism (CE; 88.5% vs. 58.0%), had taken warfarin (26.8% vs. 6.8%) than non-ICH group, showed higher score of NIHSS on admission (16 vs. 10), 3 days (14 vs. 5) and 7 days (13.5 vs. 3) after onset and showed lower DWI-ASPECTS (7.8 vs. 9.1). Patients with edaravone showed higher recanalization rate (77.7% vs. 36.4%) than non-edaravone group, but the rate of hemorrhagic transformation did not differ between these 2 groups, suggesting the possibility that edaravone can prevent hemorrhagic transformation.

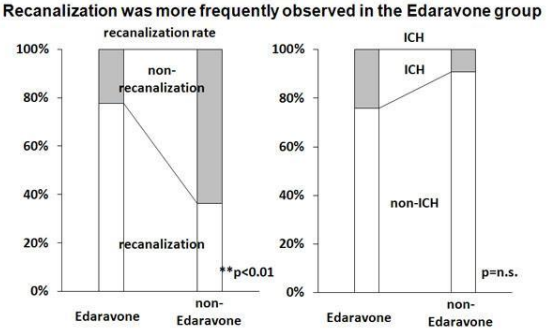

[edaravone study]

Conclusions: These data suggest that intravenous alteplase (0.6mg/kg) within 3h of onset was safe and effective, that DWI-ASPECTS and NIHSS were useful predictors of ICH after tPA administration, that warfarin-treated patients are more likely to develop symptomatic ICH despite INR less than 1.7. Edaravone may be a good partner for combination therapy with tPA to enhance recanalization and to reduce hemorrhagic transformation.

References:

Yamaguchi T, Mori E, Minematsu K, et al. Alteplase at 0.6 mg/kg for acute ischemic stroke within 3 hours of onset: Japan Alteplase Clinical Trial (J-ACT). Stroke 2006; **37**: 1810-1815.

Abe K, Yuki S, Kogure K. Strong attenuation of ischemic and postischemic brain edema in rats by a novel free radical scavenger. Stroke 1988; **19**: 480-485.

Yamashita T, Kamiya T, Deguchi K, et al. Dissociation and protection of the neurovascular unit after thrombolysis and reperfusion in ischemic rat brain. Journal of Cerebral Blood Flow & Metabolism 2009; **29**: 715-725.

GHRELIN GENE-DERIVED PEPTIDES HAVE PROTECTIVE ROLES IN THE CEREBRAL CIRCULATION, AND IN THE BRAIN AFTER ISCHEMIC STROKE

J. Ku[1], T.M. De Silva[1], G. Drummond[1], C. Sobey[1], S. Spencer[2], Z. Andrews[3], A. Miller[1]

[1]Department of Pharmacology, Monash University, [2]School of Health Sciences, RMIT University, [3]Department of Physiology, Monash University, Melbourne, VIC, Australia

Objectives: Cerebrovascular dysfunction - primarily deficits in nitric oxide (NO·) function and Nox2-oxidase-dependent oxidative stress- occurs after ischemic stroke, which may accelerate neuronal cell death. Despite progress in understanding mechanisms of neuronal death during ischemia, translation of that knowledge into effective stroke therapies has been unsuccessful. Consequently, an increased focus on targeting vascular as well as neuronal mechanisms for improving stroke outcome has been advocated. The ghrelin gene is expressed in the stomach where it ultimately encodes for three peptides-acylated-ghrelin, desacylated-ghrelin and obestatin. Acylated-ghrelin acts on the growth hormone secretagogue receptor 1a (GHSR1a) in the hypothalamus to regulate body homeostasis, whereas the receptors for desacylated-ghrelin and obestatin are unknown. Importantly, emerging evidence suggests that these peptides may have neuroprotective and vasoprotective functions. However, their roles in protecting the brain and its vasculature against ischemic stroke have not been tested. Therefore, in the present study we examined whether ghrelin gene-derived peptides exert protective cerebrovascular effects; and protect against brain injury and cerebrovascular dysfunction after ischemic stroke.

Methods: Cerebral arteries (basilar and middle cerebral [MCA]) were isolated from male, wild-type (WT, n=88) or ghrelin gene knockout ($Ghr^{-/-}$, n=22) mice. NO· function was assessed in a myograph via the vasoconstrictor response to L-NAME (NO· synthase inhibitor; 100 mmol/L), and Nox2 activity was assessed by measuring superoxide levels in response to the Nox2 activator, phorbol 12,13-dibutyrate (PDBu; 10 µmol/L). Stroke was induced in WT and $Ghr^{-/-}$ mice by transient MCA occlusion (tMCAo) for 0.5h followed by reperfusion (23.5h). At 24h, neurological and sensorimotor function, infarct and oedema volumes, and cerebrovascular Nox2 activity were evaluated.

Results: The magnitude of L-NAME-induced constrictions of MCA from $Ghr^{-/-}$ mice (D diameter = -27.4±2%; n=5, $P< 0.05$) were lower by ~36% when compared to WT mice (-42.7±2%; n=5). PDBu-stimulated superoxide production was 2-fold higher in $Ghr^{-/-}$ mice (Ghr-/-: 412.7±87.6 vs. WT: 178.5±35.8, 10^3 counts/s/mg, n=7, $P< 0.05$). In WT mice, exogenous desacylated-ghrelin or obestatin (100 fmol/L-10 nmol/L; n=5-8) elicited concentration-dependent cerebral vasodilatations (Rmax: desacyl: 69.8±9.7%; obestatin: 88.4±5.1%), which were virtually abolished in the presence of L-NAME (n=4-7, $P< 0.05$). Furthermore, the vasodilator effect of either peptides (100 fmol/L-10 nmol/L; n=4) were sustained in the presence of the GHSR1a antagonist, YIL-781 (0.5 µmol/L, n=4). By contrast, acylated-ghrelin (n=6) had a modest constrictor effect on tone (Cmax: -28.8±19.3%). Desacylated-ghrelin (1 nmol/L-

10 nmol/L), but neither acylated-ghrelin nor obestatin, inhibited PDBu-stimulated superoxide levels (desacyl: 375±63 vs. control: 550±43, 10^3 counts/s/mg, n=5, *P*< 0.05). After tMCAo, $Ghr^{-/-}$ mice tended to have worse neurological and sensorimotor impairment, and had significantly larger infarct ($Ghr^{-/-}$: 37.7±3.9 vs. WT: 26.3±2.7, mm^3, n=8-10, *P*< 0.05) and oedema ($Ghr^{-/-}$: 7.8±1.7 vs WT: 4.03±0.6, mm^3, n=8-10, *P*< 0.05) volumes. Furthermore, PDBu-stimulated superoxide levels in ischemic MCA of $Ghr^{-/-}$ mice were ~2-fold higher ($Ghr^{-/-}$: 829±195 vs. WT: 373±104, 10^3 counts/s/mg, n=8-9, *P*< 0.05).

Conclusion: These data reveal previously unrecognised protective roles for ghrelin gene-derived peptides in the cerebral circulation and brain after ischemic stroke, and highlight their potential as novel approaches for the treatment of cerebral artery dysfunction and ischemic stroke.

THE ROLE OF NEUROVASCULAR COUPLING IN STROKE RECOVERY

E. Lake[1,2], R. Janik[1,2], J. Chaudhuri[1], G. Stanisz[1,2], B. Stefanovic[1,2]

[1]*Imaging Research, Sunnybrook Health Science Center,* [2]*Medical Biophysics, University of Toronto, Toronto, ON, Canada*

Objectives: Treatment for ischemic stroke is limited to clot dissolving drugs that are effective only within 3-4.5 hours following the onset of symptoms (utilized in 2% of patients) and physiotherapy.[1] The majority of stroke survivors suffer significant disabilities and up to 1/3 are institutionalized making stroke the leading cause of permanent neurological disability.[2] Effective rehabilitation is hindered by uncertainty surrounding the underlying mechanisms of recovery. Whereas much is known about the acute stage, the changes in the neurovascular unit in the peri-infarct zone during the days and weeks following ischemic insult are not well understood. The present work combines functional MRI with behavioural testing to assess the effect of well-timed, low dose GABA antagonism on recovery in the chronic stage in a well established rat model of focal ischemia.[3]

Methods: Focal ischemic stroke was induced in 6 adult male rats using intracranial injections of endothelin-1 (ET-1), a potent vasoconstrictor.[4,5] This model permits targeting of specific cortical domains in a manner that is not achievable with most other stroke models and affords kinetics of perfusion decrease and restoration that more faithfully reproduce those seen in human ischemic stroke.[4,5] Left forelimb sensorimotor deficits were evaluated at weekly intervals following stroke and compared to baseline reaching ability.[6] MRI was performed prior to stroke and at weekly intervals following ischemia for a three week period. Animals were anaesthetized with a continuous IV infusion of propofol. At each imaging session, structural and functional continuous arterial spin labelling images were collected. Functional hyperemia was elicited bilaterally via electrical forepaw stimulation. Beginning 7 days following stroke, and continuing for a 14 day period, animals underwent daily subcutaneous pill implantations. Animals either received pills containing 58.5mg of HPMV and 1.5mg of a novel GABA antagonist L-655,708 (treated group) or 60mg of HPMV (control group).[7]

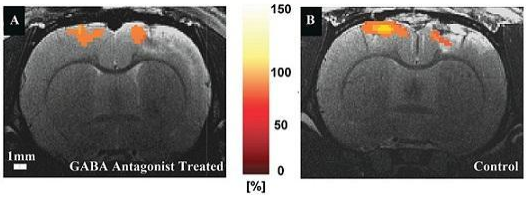

[Changes in Perfusion Response to Paw Stimulation]

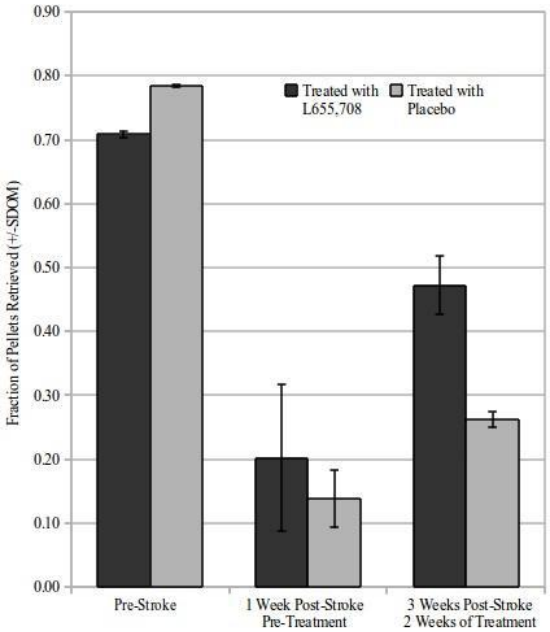

[Skilled Forelimb Reaching Test Results]

Results: ET-1 microinjection into the right somatosensory cortex caused a pronounced deficit in left forelimb reaching ability 1 week following injury. After 2 weeks of daily pill implantations, GABA antagonist treated animals (N_T=3) exhibited significantly more recovery than that shown by the control group (N_C=3). The ratio of ipsi- to contra-lesional perfusion responses across all responding voxels (in all slices) for GABA antagonist treated was 0.89+/-0.05 and 0.52+/-0.05 in control animals. These data demonstrate that ET-1 ischemia induces long-term compromises in functional hyperemia and that GABA antagonist treatment results in the partial normalization of the ipsi-to-contra-lesional perfusion response ratio.

Conclusion: The present work builds upon the exciting finding that continuous, low dose treatment with a novel GABA antagonist in the chronic stage of stroke recovery may ameliorate some of the deleterious effects of ischemic injury.[3] The current data show beneficial effects of this treatment in rats on behavioural recovery, in agreement with prior work done in mice,[3] and further suggests that the improved behavioural recovery is accompanied by the partial normalization of functional hyperemia.

References:

[1]Buchan,CMAJ[2005;172(10):1307-1312]

[2]Morris,Neuroepidemiology[2001;20(2):65-76]

[3]Carmichael,Nature[2012;468(7321):305-309]

[4]Corbett,ExpNeurol[2006;201(2):324-334]

[5]Lei,MagnResonMed[2001;46(4):827-830]

[6]Montoya,NeurosciMethods[1991;36:219-228]

[7]Clarke,DrugMetabDisposition[2006;34(5):887-893]

STUDIES ON THE KALLIKREIN-KININ SYSTEM IN THE CEREBRAL VESSELS, MICROVESSELS AND BRAIN TISSUE AFTER BRAIN ISCHEMIA DAMAGE

N.E. Lapina, N. Weinzierl, L. Schilling

Division of Neurosurgical Research, Department of Neurosurgery, Medical Faculty Mannheim, Heidelberg University, Mannheim, Germany

Pathological processes in the brain such as ischemia-reperfusion damage result in increase of blood-brain barrier permeability leading to brain edema and swelling. The pathophysiology post-ischemic brain is edema a multifactorial process, and release of bradykinin (Bk) following activation of the kallikrein-kinin system (KKS) appears to play a major role. However, the source of Bk is still not yet clear. Therefore, in the present study we focused on the KKS activation and compared the changes of gene expression in brain tissue, in the middle cerebral artery (MCA), and in MVs.Male Sprague-Dawley rats (300-350g) anesthetized with isoflurane (2.5-3.0%) underwent right-sided filament of the MCA occlusion (MCAO) for 2h followed by reperfusion. The experiments were terminated 24h after MCAO by in-situ perfusion with pre-cooled physiological saline solution containing 1% Evans blue. After removal of the brain both MCAs were isolated. Serial coronal sections were obtained from the brain and the MVs isolated using a purely mechanical protocol at 4ºC. The yield and integrity of total RNA obtained were determined using a chip-based method. After reverse transcription real time PCR was performed to describe the levels of gene expression of the Bk receptor subtypes 1 and 2 (B1R, B2R), angiotensin converting enzyme (ACE), kininogen (KIN), and kallikrein 6 (KAL) using elongation factor-1 (EF-1) as house-keeping gene. All PCR assays were obtained from Applied Biosystems.The ΔCt values obtained under physiological conditions (control) are indicated in the table as mean±SD along with the fold changes after MCAO (mean value and the 95% confidence intervals).

	B1R (ΔCt)		B2R	ACE	KIN	KAL
Tissue (cont	Not detectable	(ΔCt)	12.9± 2.0	5.7± 0.5	12.7± 1.3	3.0± 1.0

rol)						
Tissue (after MCAO)	11.0±2.4	(fold change)	x32 (3.6-282)	x4.3 (1.6-11.3)	x2521 (2048-3104)	x3.5 (1.6-7.5)
MCA (control)	Not detectable	(ΔCt)	3.7±0.8	-5.2±0.9	-0.7±1.7	2.0±1.1
MCA (after MCAO)	0.5±0.9	(fold change)	x56 (20-158)	x4 (1-16)	x194 (60-630)	x0.9 (0.4-3.0)
MVs (control)	Not detectable	(ΔCt)	9.4±1.0	4.0±0.8	10.4±3.1	2.2±0.9
MVs (after MCAO)	10.1±1.9	(fold change)	x8 (3-21)	x6 (3-9)	x294 (158-549)	x1 (0.7-1.4)

[The ΔCt values obtained under physiological condit]

Under physiological conditions the KKS displays marked tissue-specific differences in the expression levels with a clear-cut preponderance in the arterial over the MV and the parenchymal compartment. Following transient ischemia there is

(i) a de novo expression of the B1R mRNA and

(ii) a marked upregulation of B2R and of KIN mRNA in the parenchymal, macro- and microvascular compartments.

Unexpectedly, an upregulation of KIN mRNA was also observed in the contralateral hemisphere.Our results suggest the presence of a complete KKS in the macro- and microvascular compartments of the brain and activation of the expression following MCAO. Thus, a highlocal concentration of Bk in the vascular wall is to be expected, and this concentration might well account for the pathophysiological effects of Bk.

MATHEMATICAL MODEL OF GLUTAMATE RELEASE DURING ISCHAEMIA

S. Laranjeira, J. Palace, M. Symmonds, **S. Payne**, P. Orlowski

Oxford University, Oxford, UK

Objectives: Treatment of neurodegenerative diseases (NDs) is inefficient and mostly symptomatic incurring large costs. Research focuses on understanding the pathophysiology of the diseases in view of the design of new drugs, identification of biomarkers and improving treatment planning. Glutamate is central to mechanisms behind learning and memory; common targets of NDs. Stroke and Multiple Sclerosis (MS) are respectively responsible for ischaemia and for the damage of membrane water channels. Both of these lead to glutamate excitotoxicity which precedes neuronal death (apoptosis, necrosis). Therefore, we aim to implement a model relating the two mechanisms to glutamate kinetics in order to better understand their pathophysiologies.

Methods: The metabolism model in [1] was updated with a state of the art model of glutamate kinetics [2]. Three modes of glutamate release are included: synchronous, asynchronous and spontaneous release. The key trigger of glutamate release is set to be an increase above the baseline value of the intracellular calcium concentration. This indeed occurs during membrane depolarisation in stroke and oedema in MS [3],[4]. The combined model was further updated with a three glutamate pool system inside the neuron and a model of the dynamics between them.

Results: In order to mimic the experimental data from [5] stroke was simulated by reducing cerebral blood flow (CBF) by 80-95% for 5min followed by full re-perfusion. The rate of release and peak extracellular glutamate concentrations ([GLU]e) varied exponentially with CBF drop. The shape of the change of glutamate levels agreed with experiments yet the simulated values differed by up to several orders of magnitude depending on the level of perfusion with the largest discrepancies occurring during severe depolarisation. With intent of improving the results an oedema model governed by osmotic pressure was included. In fact the behaviour of the model exhibited a better agreement with the data

than before (Fig1.). A final hypothesis was tested where vesicle recycling is disabled during stroke. Here even at 95% CBF reduction [GLU]e reaches a lower value than the data (bold-line Fig1.). In all three tests fast cell depolarization occurred for CBF drops above 90% and was in good agreement with experimental studies (increase of 55mV in 4 and 10 minutes in the experiment and in the simulation respectively).

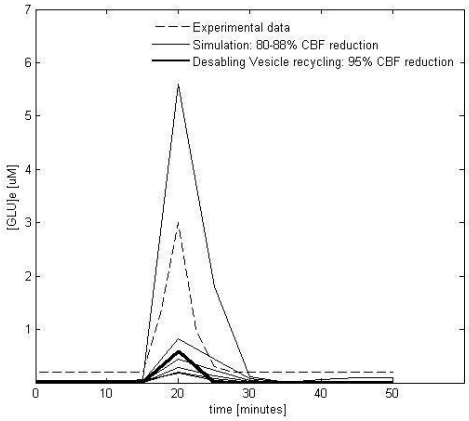

[Fig.1]

Conclusion: The metabolism model predicts the depolarisation level with qualitative agreement with experimental data. We are currently expanding the model to reduce the differences between measured and predicted glutamate levels. The main areas will focus on are:

1. understanding the mechanisms behind vesicle recycling (its dependence on ATP might limit the glutamate available for release)

2. Develop a model of astrocyte controlled spontaneous release of glutamate (relevant aspect in the case of M.S.).

As the model develops, this will help to interpret the many complex interacting processes that are implicated in NDs, assisting in developing better therapy planning.

References:

[1] Orlowski, P.et al. *Interface Focus* **1**,408-416,2011.

[2] Sun, J.et.al. Nature **450**,676-682,2007.

[3] Dirnagl, U.et.al. Trends Neurosci. **22**,391-397,1999.

[4] Srinivasan, R.et.al. Brain, **128**,1016-1025,2005

[5] Mitani, A.et.al. Neuroscience **48**,307-313,1992

CHANGES OF GENE EXPRESSION IN FOCAL CEREBRAL ISCHEMIA WITH MICROARRAY ANALYSIS

J.E. Lee[1], S.Y. Cheon[1,2], K.J. Cho[1,2], G.W. Kim[2]

[1]Anatomy, [2]Neurology, Brain Korea 21 Project for Medical Science, Yonsei University, College of Medicine, Seoul, Republic of Korea

Objectives: Understanding of gene expression after cerebral ischemia is needed to develop new therapeutic strategies for treating ischemic stroke. Identification of novel single gene, gene network or molecular pathway helps reveal the complex mechanisms. To provide and characterize the information of genes that associated with the pathogenesis of cerebral ischemia, DNA microarray analysis was performed.

Methods: Male C57BL/6 mice used in our study were subjected to occlusion of the middle cerebral artery (MCA) for 1 hour, followed by reperfusion for 8 hours. The group was divided to non-ischemia and ischemia group. Total RNA extracted from the striatum and cortex in each group was converted to cDNA and gene expression was analyzed by using GeneSpring 7.3. Genes were classified with apoptosis, angiogenesis, cell cycle, cell differentiation, cell proliferation, DNA repair, inflammatory response, response of oxidative stress and transcription according to Gene Ontology Consortium (http://www.geneontology.org/index) by GeneSpringGX7.3. All data was normalized and selected genes equal or greater than 2 fold.

Results: We identified that at 8 hours after cerebral ischemia, the levels of 5165 genes were found to be altered significantly in ischemic striatum. Of 39429 genes, 4165 genes (10.64%) were upregulated and 1000 genes (2.54%) were downregulated in striatum of the ischemia group, more than non-ischemia group. Also, 7095 genes were

significantly changed in ischemic cortex. The genes 6618 (16.78%) were upregulated and 477 genes (1.21%) were downregulated in ischemia group as compared to that of non-ischemia group. Most of these upregulated and downregulated genes were associated with cell proliferation, apoptosis, and transcription. Also, in our data of ischemic striatum, members of cc chemokine family were increased and MTMR15, Dnase1, GPR8 were specially decreased. In the cortex, ATF3, HSP70, TIMP were upregulated and CDK1, ADLRA2A and Gli3 were significantly downregulated as compared to non-ischemia group.

Conclusions: Our data suggest that several genes caused by ischemia. To our knowledge, modulation of these genes after cerebral ischemia may determine cell fate and these findings may provide a potential targets for novel therapies of ischemic stroke.

Reference: Gene Ontology Consortium (http://www.geneontology.org/index).

Support: This research was supported by Basic Science Research Program through the National Research Foundation of Korea (NRF) funded by the Ministry of Education, Science and Technology (MEST) (2011-0017276).

(-)-EPICATECHIN IMPROVES FUNCTIONAL OUTCOMES FOLLOWING PERMANENT FOCAL ISCHEMIA AND PROTECTS NEURONS THROUGH THE TRANSCRIPTIONAL FACTOR NRF2

C.C. Leonardo[1,2], M. Agrawal[1,2], N. Singh[1,2], S. Dore[1,2,3]

[1]Anesthesiology, [2]Center for Translational Research in Neurodegenerative Disease, [3]Neurology, Psychiatry, Neuroscience, University of Florida, Gainesville, FL, USA

Background and purpose: Stroke remains the fourth leading cause of death in the United States (second worldwide) and a leading cause of long-term disability, resulting in a total direct and indirect cost of approximately $73.7 billion annually. The failure of novel therapies in clinical trials demonstrates that the complex neural response to stroke must be targeted at multiple levels. Polyphenolic natural compounds have shown potential in the prevention and treatment of cardiovascular disease. As means of identifying mechanism, our laboratory has been investigating the flavanol (-)-epicatechin (EC). Due to its abundance in various dietary sources including cocoa, green tea and red wine, as well as the demonstrated safety of these and other EC-containing extracts, EC represents a promising natural compound to boost endogenous cellular protection. Indeed, EC has been recognized for its ability to promote vascular function, and the consumption of EC-containing extracts is associated with reduced risk for stroke. Despite promising epidemiological data, few studies have combined *in vivo* and *in vitro* ischemic models to link functional efficacy with mechanisms of action. The objectives of this study were to evaluate the efficacy of EC in improving the neuroanatomical and functional outcomes following experimental stroke, and to begin identifying the mechanisms by which EC affords neuroprotection.

Methods: For *in vivo* experiments, 3 month old male C57BL/6 mice were administered vehicle (methylcellulose) or EC (5, 10 or 15mg/kg) by oral gavage 90 minutes prior to permanent distal middle cerebral artery occlusion (pdMCAO). Mice were then evaluated post-stroke for functional deficits, as measured by Grip Strength and Adhesive Removal tests, and neuroanatomical outcomes including infarct volume, microglia/macrophage activation and reactive astrogliosis. For *in vitro* experiments, mouse cortical neurons isolated from 0-1 day old C57BL/6 wildtype or $Nrf2^{-/-}$ pups were pretreated with media or EC (50 or 100µM) and subjected to 4 hours of oxygen glucose deprivation followed by 24 hours reoxygenation. Cultures were then assessed for viability, protein carbonyl levels and the induction of Nrf2-regulated proteins.

Results: Mice subjected to pdMCAO displayed grip strength deficits of 13.3±3.6% 7 days after stroke, while EC-treated mice showed no deficits. Forelimb impairments, reflected by a greater than threefold increase in latency to remove adhesive tape 1 day following pdMCAO, were dose-dependently reduced following EC treatment. Additionally, EC reduced infarct volume by up to 54.5±8.3% and Iba1 immunoreactivity by up to 56.4±13.0% at 7 days post-stroke. In culture, primary neurons treated with EC increased expression of cytoprotective proteins regulated by the transcriptional factor Nrf2, including heme oxygenase 1, ferritin light chain and biliverdin reductase. EC also reduced protein carbonyl levels and increased cell viability by 40.2±14.1% following oxygen glucose

deprivation, and this protection was negated in cells derived from Nrf2$^{-/-}$ mice.

Conclusions: These data support the prophylactic use of EC and demonstrate a protective mechanism through activation of the Nrf2 pathway. Future studies combining pharmacokinetics, efficacy and mechanism are needed to further explore the therapeutic potential of EC and EC-containing extracts.

References:

Leonardo et al., *Nutr Neurosci* 2011; 14(5):226. Shah et al., *JCBFM* 2010; 30(12):1951.

ELEVATED LEVELS OF HEPARANASE AND A POTENTIAL ROLE IN ANGIOGENESIS AFTER ISCHEMIC STROKE IN EXPERIMENTAL MOUSE MODEL AND STROKE PATIENTS

J. Li[1], L. Wang[1], Y. Zhao[1], J. Sun[1], L. Wei[2]

[1]Department of Neurology, Beijing Friendship Hospital, Capital University of Medical Sciences, Beijing, China, [2]Department of Neurology, Emory University School of Medicine, Atlanta, GA, USA

Objective: Heparanase (Hpa) is the only mammalian endo-β-D-glucuronidase that specifically cleaves heparan sulfate proteoglycans. It has been shown that Hpa accelerates angiogenesis in multiple normal and pathological conditions. We undertook this study to determine the expression pattern of Hpa after ischemic stroke and to test the hypothesis that Hpa contributes to angiogenesis after ischemic stroke. Data from an focal ischemic stroke model and human stroke patients were collected and analyzed in this investigation.

Methods: A focal ischemic stroke targeting the whisker barrel cortex was induced in mice according to previously performed procedures (Whitaker et al., 2007). Real time reverse transcription-polymerase chain (RT-PCR) was performed to detect the mRNA expression of Hpa, vascular endothelial growth factor (VEGF) and angiopoietin-2 (Ang-2). Brain tissues were collected in and around the ischemic region. 10μm thick coronal fresh frozen sections were stained with immunohistochemistry and incubated with specific primary and secondary antibodies. Peripheral stimulation was achieved by mechanical stimulation of the whiskers on the left face for 15 min at about 140 strokes per min. Hospitalized patients with acute ischemic stroke but non-lacunars infarction with a mean age of 62 years and counterpart controls were analyzed. Blood was draw at different time points according to the research plan. The level of serum Hpa was detected by an enzyme-linked-immunosorbnent assay (ELISA). Comparisons between two groups were achieved by Student's t-test.

Results: In the stroke model, ischemia led to upregulation of Hpa, VEGF and Ang-2. The expression of Hpa mRNA was significantly enhanced from 3 days after stroke compared to controls ($p< 0.05$), and reached a peak level around 14 days after stroke ($p< 0.01$). The expression of VEGF and Ang-2 mRNA were also markedly upregulated at 3 days after stroke ($p< 0.01$). The VEGF expression maintained high levels while the Ang-2 expression decreased thereafter. At early time points, Hpa expression was largely confined to proliferating vascular endothelial cells. At 14 days after ischemia, this expression had shifted to astrocytes in the same region. Immunohistochemical staining revealed that Hpa-positive, neuronal-like cells around ischemic region increased in mice that had received peripheral stimulation 14 days after stroke. ELISA assay of the blood samples from stroke patients showed time-dependent increases in the level of Hpa during the 14 days observation. The increases reached a peak level around 4-7 days after stroke and then started to decline gradually.

Conclusion: Cerebral ischemic stroke increases Hpa mRNA expression in and around the ischemic region, accompanied with enhanced expression of angoigenetic factors VEGF and Ang-2. Hpa levels increase in endothelial cells and then in astrocytes. These data suggest a possible link between ischemia-induced Hpa expression and angiogenic activity. The increased Hpa level in the peripheral blood of stroke patients suggests a possible brain ischemia marker and a potential angiogenic response.

Reference: Whitaker VR, Cui L, Miller S, Yu SP, Wei L. Whisker stimulation enhances angiogenesis in the barrel cortex following focal ischemia in mice. J Cereb Blood Flow Metab. 27(1):57-68, 2007.

MKP-1 GENE DELETION EXACERBATES STROKE OUTCOME IN MICE

S. Doran, S. DiMauro, B. Manwani, L. Capozzi, V. Scranton, L. McCullough, **J. Li**

University of Connecticut Health Center, Farmington, CT, USA

Objectives: It has been well recognized that inflammatory response contributes neuronal death follow stroke. Mitogen-activated protein kinase phosphatase-1 (MKP-1) has been identified as a critical inhibitor of inflammation by inhibiting the activation of microglia (1), which is a major contributor of the inflammatory response in stroke. Indeed, MKP-1 is indispensable for the neuroprotection induced by endocannabinoid anandamide in co-culture of organotypic brain slices and microglia exposed to NMDA toxicity (1). Interestingly, it was reported that MKP-1 is up-regulated in rat brains in a model of focal ischemia (2), further suggesting an important role of this protein in stroke. Therefore, we tested the hypothesis that MKP-1 gene deletion in mice may worsen stroke outcome by increasing stroke induced inflammatory response.

Methods: MKP-1 knockout (MKP-1 KO) mice were obtained from Dr. Carol Pilbeam Lab at UCHC. Confirmation of genotype was made through PCR analysis. Transient 60-minute middle cerebral artery occlusion was performed on male 7-8 week MKP-1 KO mice and WT controls. For outcome studies, a cohort was sacrificed at 72 hours post stroke after functional assessments and brains were harvested for TTC staining. Serum was also collected for cytokine analysis via ELISA. Another cohort of mice was sacrificed at 6 hours post stroke for comparative cytokine and western blot analysis. Data was presented as mean±SEM and mean comparisons were performed using Student's t-test.

Results: A dramatic induction of MKP-1 protein expression was observed in mice brain at 6 hours after the onset of stroke. MKP-1 KO mice showed significantly larger infarct volumes than wild type counterparts. This increase in infarct volume (n=10 KO, n=7 WT) was observed across the cortex (KO 76.3±1.8% vs. WT 48.1±10%, $p< 0.05$), striatum (KO 88.9±2.5% vs. WT 68.3 ± 7.3%, $p< 0.05$), and total hemisphere (KO 71.5±2.8% vs. WT 43.6±8.1%, $p< 0.05$). The detrimental effect of MKP-1 gene deficiency was reflected in functional assessment using corner test (KO 0.71±0.033 vs. WT 0.60 ± 0.025, $p< 0.05$). MKP-1 deficient mice additionally showed significantly higher levels of circulating IL-6 cytokine at 72 hours when compared to wild type mice subjected to the ischemic model (72 h: KO 32.9±3.1 vs. WT 10.3 ± 0.18 pg/ml, $p< 0.05$, n=3 KO, n=2 WT). Levels of IL-10 were three times higher in KO mice at 6 hours post stroke compared to the expression in wild type with a trend towards statistical significance (6h: KO 206 ± 62 vs. WT 56 ± 32 pg/ml, n=3 p/g, p=0.16).

Conclusions: We demonstrated that MKP-1 deletion led to larger infarct volumes and worse functional recovery after cerebral ischemia. This was associated with higher levels of pro-inflammatory cytokines. Our data suggests MKP-1 may function to hinder the inflammatory response in stroke and targeting MKP-1 might have therapeutic potential for stroke disease.

References:

1. Eljaschewitsch et al. Endocannabinoid anandamide protects neurons during CNS inflammation by induction of MKP-1 in microglial cells. Neuron. 2006, 49(1):67-79.

2. Koga et al. Over-expression of map kinase phosphatase-1 (MKP-1) suppresses neuronal death through regulating JNK signaling in hypoxia/re-oxygenation. Brain Res. 2012, 1436:137-46.

URSOLIC ACID PROMOTES THE NEUROPROTECTION BY ACTIVATING NRF2 PATHWAY AFTER CEREBRAL ISCHEMIA IN MICE

L.-T. Li

Department of Neurology, Hebei General Hospital and Second Hospital of Hebei Medical University, Shi Jia Zhuang, China

Background: Oxidative and inflammatory damage have been suggested to play an important role in cerebral ischemic pathogenesis, and provide promising therapeutic strategies for stroke. Nuclear factor-erythroid 2-related factor 2 (Nrf2), a pleiotropic transcription factor, has been shown to play a key role in protecting cells against oxidative injury in cerebral ischemia. In this study, we demonstrated the hypothesis that ursolic acid (UA), a natural pentacyclic triterpenoid acid, isolated from edible plants in the Oleaceae family, a well-known anti-oxidative and anti-inflammatory reagent,

protects the brain against ischemic injury by activating the Nrf2 pathway.

Methods: Nrf2$^{-/-}$ and Wild-type (WT) mice were induced into focal cerebral ischemia by transient middle cerebral artery occlusion (MCAO), and received UA treatment immediately after MCAO. The behavioral dysfunction, infarct size, and the expression of Nrf2, HO-1 and inflammatory factors (TLR4 and NF-κB) in ischemic brain were measured at 24 h after stroke.

Results: UA treatment significantly improved neurological deficit and reduced infarct size in WT mice after MCAO. Administration of UA also decreased the product of lipid peroxidation, promoted the activation of Nrf2 pathway and decreased the expression of TLR4 and NF-KB after stroke in WT mice. However, Nrf2$^{-/-}$ mice demonstrated more severe neurologic deficits, infarct size and inflammatory damage after MCAO, and did not benefit from the protective effect of UA.

Conclusion: The results indicated that UA protected the brain against ischemic injury in mice by anti-oxidative and anti-inflammatory effects after MCAO. Activation of the Nrf2 pathway contributes to the neuroprotective effects induced by UA in cerebral ischemia.

CYSTAMINE EFFECTIVELY PROMOTES FUNCTIONAL RECOVERY BY INCREASING BRAIN-DERIVED NEUROTROPHIC FACTOR LEVELS IN BRAIN AFTER STROKE IN MOUSE

P.-C. Li[1], Y. Jiao[2], W. Zhou[3], G.-J. Teng[1]

[1]Jiangsu Key Laboratory of Molecular and Functional Imaging, Department of Radiology, Zhongda Hospital, Medical School, Southeast University, [2]Jiangsu Key Laboratory of Molecular and Functional Imaging, Medical School, Southeast University, [3]Southeast University, Nanjing, China

Objectives: Cystamine has been reported it is neuroprotective in Huntington disease (HD) mice by increasing Brain-derived neurotrophic factor (BDNF) levels in brain. BDNF which is mainly synthesized by neurons, plays a crucial role in neuronal survival, synaptic plasticity,learning and memory, and neuroplasticity. Thus, the beneficial effects of rehabilitation in promoting functional recovery after stroke may also depend on BDNF. The aim of this study was to examine whether cystamine could promote functional recovery after stroke in mouse by increasing brain levels of BDNF.

Methods: Adult male C57B/6J mice (n=60) were subjected to photothrombotic model of focal stroke or sham operation. Cystamine (100mg/kg/day, i.p.) or saline was administered for 7 days initiated at 24 h after onset of stroke. We also administered ANA-12, a low-molecular weight TrkB antagonist that prevented activation of the receptor by BDNF with a high potency, to examine the mechanisms for rehabilitation by cystamine.The expression of BDNF mRNA and the secretion of BDNF protein in brain were examined by RT-PCR and enzyme linked immunosorbent assay at 1, 3, and 7 days after stroke. T2-weighted imaging, diffusion tensor imaging (DTI) and functional motor measurements were performed to detect lesion volumes, axonal remodeling and functional recovery from 24 h to 6 weeks after stroke. After the mouse euthanasia, brain sections were immunostained for semiquantitative analysis of myelin basic protein, synaptophysin, neurogenesis and quantification of infarct volumes.

Results: Cystamine significantly increased BDNF levels in brain. Cystamine-treated animals had better functional motor recovery compared with all other groups($p< 0.05$). Cystamine treatment induced axonal remodeling in the ischemic border zone and synaptophysin expression within the contralateral cortex 6 weeks after ischemia ($P< 0.05$). Cystamine treatment also doubled both the number of new mature neurons and immature neurons adjacent to the stroke. Infarct volumes were not different between the groups 1 or 6 weeks after ischemia.

Conclusions: Cystamine treatment improves functional recovery after photothrombotic stroke in mouse and induces neurogenesis and axonal remodeling by increasing BDNF levels in brain . Cystamine may be a promising pharmacological therapy for promoting recovery of function after stroke. Together, our results provide a novel drug to promote recovery after stroke and possibly other brain injuries.

ASSESSMENT OF SPONTANEOUS OSCILLATIONS IN CEREBRAL OXYGENATION HEMODYNAMICS IN SUBJECTS WITH HYPERTENSION

Z. Li[1], M. Zhang[2], Q. Xin[1], S. Luo[1], W. Zhou[1], R. Cui[1], L. Lu[1]

[1]Shandong University, Jinan, [2]The Hong Kong Polytechnic University, Hong Kong, China

Purpose: The objective of this study was to assess the spontaneous oscillations in subjects with hypertension based on the wavelet transform of cerebral oxygenation signal measured with near-infrared spectroscopy (NIRS) signals.

Methods: Continuous recordings of NIRS and arterial blood pressure (ABP) signals were obtained from simultaneous measurements in 20 normal subjects (age: 70.8 ± 5.2 years) and 22 subjects with hypertension (age: 72.5 ± 6.8 years).

Results: Using spectral analysis based on wavelet transform, five frequency intervals were identified (I, 0.005-0.02 Hz; II, 0.02-0.06 Hz; III, 0.06-0.15 Hz; IV, 0.15-0.40 Hz; and V, 0.40-2.0 Hz). The amplitudes of Δ[Hb] and Δ[HbO_2] in interval III, IV and V were significantly higher in hypertensive patients, who have increased mean flow velocity in middle cerebral artery (MCA), compared to that in the normal subjects ($p< 0.01$). The amplitudes of the ABP in frequency intervals I and III were significantly higher in hypertensive patients than in the normal subjects ($p< 0.01$).

Conclusions: The present findings revealed that hypertension and increased mean flow velocity in MCA have significant interaction on the cerebral oscillations. The presence of higher cerebral oscillations was affected by the intracerebral atherosclerosis in response to systemic hypertension. In addition, the higher spontaneous oscillations in interval I and III in ABP indicate a metabolic regulation and myogenic response to hypertension.

Acknowledgement: This project was supported by the National Natural Science Foundation of China (Grant No. 81071223), Shandong Provincial Natural Science Foundation (ZR2010HM024) and Independent Innovation Foundation of Shandong University （IIFSDU, 2010JQ007）

THE MODIFICATION AND INHIBITION OF PROTEIN DISULFIDE ISOMERASE BY CYCLOPENTENONE PROSTAGLANDIN 15D-PGJ_2: IMPLICATIONS FOR POST-ISCHEMIC NEURONAL INJURY

H. Liu[1,2], W. Li[1,2], J. Chen[2], M. Rose[1,2], S. Shinde[2], B. Mutus[3], M. Balasubramani[4], G. Uechi[4], S. Graham[1,2], R. Hickey[5]

[1]Geriatric Research, Educational and Clinical Center, VA Pittsburgh Healthcare System, [2]Department of Neurology, University of Pittsburgh, Pittsburgh, PA, USA, [3]Department of Chemistry and Biochemistry, University of Windsor, Windsor, ON, Canada, [4]Genomics and Proteomics Core Lab, University of Pittsburgh, [5]Department of Pediatrics, University of Pittsburgh School of Medicine, Pittsburgh, PA, USA

Objectives: Protein disulfide isomerase (PDI) is an abundant protein in the endoplasmic reticulum facilitating disulfide bond formation and isomerization of disulfide bonds in nascent and denatured proteins; it may play an important role in the ER stress response following hypoxic-ischemic (HI) brain injury[1]. The cyclopentenone prostaglandins (CyPGs) are bio-active metabolites of PGD_2 and PGE_2 that covalently modify proteins via Mecheal addition[2]. The present study aims to 1) detect the generation of CyPGs in post-ischemia rat brains and its relationship with COX-2 activation; 2) assess the modification of CyPGs on PDI and its biological effects on post-hypoxia/ischemia neuronal injury.

Methods:

1) Global ischemic brain injury was induced by asphyxial cardiac arrest (ACA), and brain CyPG concentrations were measured with UPLC-MS/MS [2,3].

2) The modification of PDI by CyPG 15d-PGJ_2 was detected in vitro by MS with recombinant PDI and in primary cortical neurons by avidin pull-down assay with biotin labeled 15d-PGJ_2. Immunocytochemistry and confocal microscopy were performed to detect the co-localization of PDI and 15d-PGJ_2 in primary neuron.

3) The effect of 15d-PGJ_2 modification on PDI activity was measured with thiol reductase activity assay. PDI activity was aslo measure in the post-ischemia rat brain samples with or without COX-2 inhibitor pretreatment.

4) LDH assay and cell viability assay were performed to assess the effects of PDI over-expression or inhibition on the hypoxia induced primary neuronal cell death.

Results: Here we report that the concentrations of CyPGs, including 15d-PGJ_2, PGJ_2 and Δ12-PGJ_2, significantly increased in rat brain 24h following ACA, and this effect was abrogated by the COX-2 inhibitor SC58125 pre-treatment. The CyPG 15d-PGJ_2 is the most abundant J_2-series CyPG present in post-ischemic rat brain. 15d-PGJ_2 can covalently modify PDI via its reactive cyclopentenone moiety as shown by in vitro binding and immunoprecipitation assays using biotin labeled 15d-PGJ_2. Confocal microscopy of primary neuronal culture incubated with biotin labeled 15d-PGJ_2 showed co-localization with PDI. Tandem mass spectroscopy showed 15d-PGJ_2 modifies cysteine residues within the active catalytic thioredoxin-like domain of PDI. This was substantiated by experiments showing decreased PDI activity in

1) recombinant PDI incubated with 15d-PGJ_2 to and,

2) immunoprecipitated PDI from primary neuronal culture incubated with 15d-PGJ_2.

Activity was also decreased in immunoprecipitated PDI from primary neuronal culture exposed to anoxia and rat brain homogenate following resuscitation from cardiac arrest. Impaired PDI activity in both anoxic primary neuronal culture and rats resuscitated from cardiac arrest is partially restored by treatment with a COX-2 inhibitor. Treatment with the PDI inhibitor nitazoxanide increases susceptibility to anoxic death in primary neuronal culture, while over-expression of PDI is protective.

Conclusions: These results suggest that,

1) excessive production of CyPGs can exacerbate ischemic injury by covalent modification and inhibition of PDI and

2) the neuroprotective effects of COX-2 inhibitors may, in part, be secondary to protection of PDI activity.

References:

1. Kam KY, et al. Mol Cells, 2011, 31:209-15

2. Liu H, et al. Neurobiology of Disease, 2011; 41: 318-28.

3. Fink EL, et al. Pediatr Crit Care Med, 2004; 5: 139-44.

DYNAMIC CHANGES OF MITOCHONDRIAL FUSION AND FISSION PROTEINS AFTER TRANSIENT CEREBRAL ISCHEMIA IN MICE

W. Liu, F. Tian, T. Yamashita, K. Deguchi, Y. Ikeda, T. Kurata, K. Abe

Neurology, Graduate School of Medicine, Dentistry and Pharmaceutical Sciences, Okayama University, Okayama, Japan

With fusion or fission, mitochondria alter their morphology in response to various physiological and pathological stimuli resulting in either elongated, tubular, interconnected or fragmented form, respectively. Immunohistochemistry and Western blot analysis were performed at 2 d, 7 d, 14 d and 28 d after 90 min of transient middle cerebral artery occlusion (tMCAO) in mice. This study first showed that mitochondrial fission protein Dynamin-related protein 1 (Drp1) and fusion protein optic atrophy 1 (Opa1) were both upregulated in the ischemic penumbra with the peak at 2 d after tMCAO, while phosphorylated-Drp1 (P-Drp1) progressively increased with a peak at 14 d after tMCAO. Double immunofluorescent analysis showed many Drp1/cytochrome c oxidase subunit I (COX1) double positive cells and Opa1/COX1 double positive cells in the ischemic penumbra, and also showed some double positive cells with Drp1/terminal deoxynucleotidyl transferase-mediated dUTP-digoxigenin nick end labeling (TUNEL) and Opa1/TUNEL in the ischemic penumbra. In contrast, both Drp1 and Opa1 showed progressive decreases until 2 d after tMCAO in the ischemic core due to necrotic brain damage. The present study suggests that there happened a continuous mitochondrial fission and fusion during these periods in the ischemic penumbra after tMCAO probably in an effort for mitophagy and cellular survival.

MIRNA-124 REGULATES IASPP AND AGGRAVATES BRAIN DAMAGE IN THE EARLY STAGES OF EXPERIMENTAL STROKE

X. Liu[1], F. Li[1], S. Zhao[2], F. Yan[1], Y. Luo[1], X. Ji[1]

[1]Cerebrovascular Diseases Research Institute, Xuanwu Hospital of Capital Medical University, [2]Beijing Tongren Hospital, Capital Medical University, Beijing, China

The apoptosis stimulating proteins of p53 (ASPP) family, comprising three proteins-ASPP1, ASPP2 and iASPP (inhibitory member of the ASPP family), interact with and modulate the behavior of p53 family. Recent evidence has shown that microRNAs (miRNAs) play a pivotal role in the development of brain and neurological diseases including stroke. Here, we studied the function of the ASPP family and one brain-specific miRNA, miRNA-124 (miR-124) and elucidated iASPP is a potential target of miR-124. Focal cerebral ischemia was induced in C57/B6 mice by permanent middle cerebral artery occlusion (MCAO). Expression level of ASPP1, ASPP2 and miR-124 in MCAO group was significantly higher than that of the sham-operated group respectively by quantitative real-time polymerase chain reaction and/or Western blot. However, the protein expression of iASPP decreased in MCAO group, which was not in accordance with its mRNA expression. Meanwhile, miR-124 directly bound to the predicted 3'-UTR target sites of iASPP genes. Moreover, excess miR-124 effectively decreased iASPP protein level in Neuro-2a cells and mouse stroke model; whereas miR-124 inhibitor increased iASPP protein levels in Neuro-2a cells and mouse stroke model. Furthermore, miR-124 inhibitor protected the brain from ischemic injury. Thus, miR-124 was up-regulated in the early stages of focal cerebral ischemia and down-regulated the levels of iASPP, which may be useful in future research and therapeutic applications.

AXONAL PLASTICITY OF CORTICOSPINAL TRACT IN THE SPINAL CORD IS CRUCIAL FOR MOTOR RECOVERY AFTER ISCHEMIC STROKE IN ADULT MICE

Z. Liu[1], M. Chopp[2], X. Ding[2], Y. Cui[2], X. Shang[2], Y. Li[2]

[1]Neurology Research, [2]Henry Ford Hospital, Detroit, MI, USA

Objectives: Since the hemiparesis after stroke is a consequence of the loss or interruption of motor signals from the motor cortex to the spinal motoneurons, reestablishment of synaptic connections between cerebral neurons and their peripheral targets provides a physical substrate for functional recovery. However, the mammalian central nervous system fails to regenerate their damaged axons. Our previous studies demonstrate that axonal remodeling of the corticospinal tract (CST) originating from the contralesional cortex in mice subjected to unilateral pyramidotomy (PT) followed by middle cerebral artery occlusion (MCAo) contributed to motor recovery after stroke. To specifically investigate the contributions of the bilateral descending CST to functional outcome after stroke, we perform a bilateral pyramidotomy (BPT) to eliminate the selected CST fibers in the cervical spinal cord in mice with transgenic Yellow Fluorescent Protein (YFP) CST labeling.

Methods: Adult male CST-YFP mice (n=30) were subjected to 1-hour right MCAo followed by BPT at the medulla level or sham surgery without CST transection. A Foot-fault test and a single pellet reaching test were performed 3 days after MCAo and weekly thereafter to monitor skilled motor functional deficit and recovery. The animals were euthanatized 14 and 28 days after MCAo, respectively. The medulla and cervical cord were processed for vibratome sectioning. Immunofluorescent staining was performed on cervical sections with primary antibodies against growth-associated protein 43 (GAP43), growth cone and synaptophysin, and Cy3-conjugated secondary antibodies. A laser scanning confocal imaging system was used to detect the YFP and Cy3 labeling.

Results: Progressive functional improvements were evident during the 4 week experimental period in MCAo only mice (n=10, $p < 0.01$, 28 days vs 3 days). Mice subjected to MCAo-BPT

(n=10) were able to walk and attempt to catch food pellets; however, the skilled fine movement of stroke-impaired left forepaw lost accuracy and no significant recovery was detected until 28 days. The CST-YFP axonal densities in the stroke-affected side of the cervical gray matter was significantly increased 28 days after MCAo compared with that in the mice subjected to MCAo and sacrificed at 14 days (n=10, $p< 0.05$). In addition, the numbers of CST-YFP axons in the stroke-affected side co-stained with $Cy3^+$GAP43 or $Cy3^+$growth cone were significantly increased compared with that in the intact side of the spinal cord at 14 days after stroke, and the CST-YFP axonal terminals co-stained with $Cy3^+$synaptophysin was significantly increased at 28 days compared with that at 14 days after MCAo ($p< 0.05$) in MCAo alone mice. There was no CST regeneration detected in the spinal cord in mice subjected to MCAo-BPT.

Conclusions: Our data suggest that there is no compensation on skilled fine motor functional recovery without CST remodeling in the spinal cord; therefore, the CST axonal plasticity in the spinal cord is crucial to the recovery of voluntary movement after stroke, which may provide a treatment target to develop rational restorative therapeutic approaches.

THE EFFECT OF TLR9 AGONIST ON BRAIN DAMAGE AND CYTOKINES EXPRESSION IN THE WALLS OF CEREBRAL ARTERIES FOLLOWING CEREBRAL ISCHEMIA

A. Maddahi, L. Edvinsson, Vascular Research Group

Clinical Sciences, Lund University, Lund, Sweden

Objective: Cerebral ischemia is one of the leading causes of death and disability in the world. Cerebral ischemia from middle cerebral artery occlusion (MCAO) results in increased expression of cerebrovascular pro-inflammatory cytokines (TNF-α, IL-6 and IL-1ß) and activation of the cell signalling pathways such as mitogen-activated protein kinas (MAPK) and toll -like receptors (TLRs) pathways. TLRs are signalling receptors in both innate and adaptive immunity. In this study, we hypothesised that treatment with a specific oligodeoxynucleotides, which is a TLR9 agonist, would induce the tolerance to ischemic cell death by altered in the expression of cerebral vascular pro-inflammatory cytokines leading to reduce infarct size and improve neurological score.

Methods: Rats were subjected to 90 minutes MCAO followed by reperfusion for 48 hours. A specific immunomodulatory oligonucleotide, IDX-9059 (TLR9 agonist) was injected intraperitoneally in rats at 0 or 2 hours after reperfusion and repeated at 24 hours. After 48 hours, the rats were sacrificed. The middle cerebral arteries (MCA) were harvested and the expressions of interleukin-1ß (IL-1ß), interleukin-6 (IL-6), tumour necrosis factor-α (TNF-α), phosphorylated p38 and transcription factor NF-κB were analysed using immunohistochemistry and real-time PCR. The brain damage and infarct volume were measured using TTC staining.

Results: We observed that injection of IDX-9059 started immediately after reperfusion significantly reduced the infarct volume (12.24 ± 2%,$^*P < 0.05$) and improved the neurological scores (2 ± 0.6, $P < 0.05$) as compare with control (vehicle) group. Immunohistochemistry revealed enhanced expression of IL-1β, IL-6, TNF-α, p-p38 and pNF-κB in the walls of MCAs after MCAO. Treatment with IDX-9059 given at zero but not at 2 hours after reperfusion, decreased the p-p38 and pNF-κB immunoreactivities and reduced the protein levels of cytokines expression.

Conclusion: Our results show that administered of a specific TLR-9 agonist immediately after reperfusion decreased the phosphorylated p38 and NF-κB, vascular pro-inflammatory cytokines expression, reduced the infarct volume and improved neurological scores.

References:

1. Cerebral ischemia induces microvascular pro-inflammatory cytokine expression via the MEK/ERK pathway. Maddahi A, Edvinsson L. J Neuroinflammation. 2010 Feb 26;7:14

2. Toll-like receptors in cerebral ischemic inflammatory injury. Yang-Chun Wang, Sen Lin and Qing-Wu Yang. J Neuroinflammation. 2011, 8:134

THE DETRIMENTAL EFFECT OF DIET-INDUCED OBESITY ON STROKE OUTCOME IN MICE IS INFLUENCED BY THE DURATION OF THE ISCHEMIC INSULT

S. Maysami[1], B. McColl[2], **C.B. Lawrence**[1]

[1]Faculty of Life Sciences, University of Manchester, Manchester, [2]The Roslin Institute, University of Edinburgh, Midlothian, UK

Obesity, with increasing prevalence in western societies, positively correlates with an increased risk for ischemic stroke. We have previously demonstrated that the infarct size and severity of injury is significantly increased in leptin deficient obese mice (ob/ob)[1]. Here we used a more translational model to evaluate the effect of long term diet-induced obesity on stroke outcome using a model of transient ischemic stroke and determined whether the extent of ischaemia influenced outcome[2]. Male C57BL/6 mice were maintained on either a high-fat (HFD, 60%-fat) or control (12%-fat)] diet for 28±2 weeks. Blood pressure, heart rate, blood glucose and body weight were monitored throughout the study. The right middle cerebral artery was transiently occluded (MCAo) for either 20 or 30min[2] and cerebral blood flow (CBF) was monitored during, 5min prior and 10min after MCAo. After 24h reperfusion mice were culled and brains were collected. After 28 weeks of diet, mice receiving HFD had significantly higher body weight at the time of stroke compared to the controls (45±2g vs 33±3g respectively). Blood pressure, blood glucose and heart rate were not significantly different between study groups prior to induction of ischemic stroke. After 20min MCAo there was no significant difference in the extent of ischemic infarct in HFD study group compared to control mice (28±7 mm^3 vs 21±11 mm^3, p = 0.57 respectively). However after 30min MCAo a significant increase in infarct volume was observed in HFD animals compared to the controls (53±8 and 23±6 respectively, p = 0.01) but no haemorrhagic transformation was detected in any study groups. The increase in infarct volume was mainly due to a significant increase in infarct in the cortex and hippocampus in HFD animals compared to the controls (29±4 mm^3 vs 8±4 mm^3 respectively, $p < 0.01$ and 6.6mm^3 vs 0.1mm^3 respectively, p = 0.02). Hence, diet-induced obesity worsens stroke outcome, but this effect is dependent on the length/severity of the ischaemic insult. This detrimental effect of diet-induced obesity on stroke outcome was not due to a change in blood pressure, heart rate and/or blood glucose. Further investigations are in progress to evaluate the impact of HFD on immune profile and peripheral organs prior and after ischemic stroke.

This study is funded by Wellcome Trust Fund.

1. McColl BW, Rose N, Robson FH, Rothwell NJ, Lawrence CB. Increased brain microvascular MMP-9 and incidence of haemorrhagic transformation in obese mice after experimental stroke. *J Cereb Blood Flow Metab* 2010; 30(2): 267-72.

2. Longa EZ, Weinstein PR, Carlson S, Cummins R. Reversible middle cerebral artery occlusion without craniectomy in rats. *Stroke; a journal of cerebral circulation* 1989; 20(1): 84-91.

VALIDATING A METHOD FOR MEASURING LEPTOMENINGEAL COLLATERAL FLOW IN RATS DURING MIDDLE CEREBRAL ARTERY OCCLUSION

D.D. McLeod[1,2], D. Beard[1,2], M. Imtiaz[1,2], N. Spratt[1,2]

[1]School of Biomedical Sciences & Pharmacy, University of Newcastle, Callaghan, [2]Hunter Medical Research Institute, New Lambton, NSW, Australia

Background: We have developed a method to quantify absolute leptomeningeal collateral blood flow during middle cerebral artery occlusion and reperfusion in the rat using a cranial window, fluorescent microspheres, and a high-speed camera. Bench studies were performed to test the accuracy of microsphere absolute flow measurements compared to a gold-standard flow measurement. This comparison was performed over the range of *in vivo* flow measurements made recently in our laboratory in rat collateral vessels during experimental stroke (unpublished data).

Methods: Fluorescent microspheres diluted in heperainised blood were infused at multiple rates via syringe driver through a 127 µm internal diameter polyurethane tube. At each infusion rate, the end of the tube was positioned inside a new Eppendorf tube to measure the volume of blood exiting the tube over a given time period (µl/min). During collection of blood at each infusion rate, a

section of tubing was simultaneously imaged through a x10 objective fluorescent microscope using a 300-frames/sec digital video camera to capture microspheres passing through the tube. Using Image J measurement tools, microsphere velocity was calculated at multiple points across the tube diameter to account for the observed laminar parabolic flow profile. Absolute microsphere flow (µl/min) was calculated by multiplying the mean velocity of microspheres by the cross-sectional area of the tubing. Linear regression analysis was performed to test the accuracy of absolute microsphere flow measurements.

Results: Regression analysis for microsphere absolute flow measurement in blood indicated that the relationship between the gold-standard flow measurement and microsphere flow was linear (r^2= 0.99). There was no difference between the slope and the y-intercept of the regression line and the line of identity (P = 0.76 slopes; P = 0.93 y-intercepts).

Conclusions: The calculation of flow using the microsphere technique is accurate in predicting absolute blood flow in our *in vitro* preparation. This measurement technique may be used *in vivo* to calculate leptomeningeal collateral blood flow during middle cerebral artery occlusion in the rat.

SEQUENTIAL MRI STUDIES OF BRAIN ALTERATIONS BEFORE AND DURING STROKE IN A MODEL OF RENOVASCULAR CHRONIC ARTERIAL HYPERTENSION IN RATS

B. Ménard[1,2,3], L. Chazalviel[1,2,3], S. Roussel[1,2,3], M. Bernaudin[1,2,3], O. Touzani[1,2,3]

[1]CNRS, UMR 6301 ISTCT, CERVOxy, GIP CYCERON, [2]Université de Caen Basse-Normandie, UMR 6301 ISTCT, CERVOxy, [3]CEA, DSV/I2BM, UMR 6301 ISTCT, CERVOxy, Caen, France

Introduction: Although chronic arterial hypertension (CAH) is known to be the major risk and aggravating factor for stroke in human, very few animal studies integrate this factor in the investigation of brain ischemia. The majority of those studies employ spontaneously hypertensive rats (SHR), the disadvantage of which is a susceptibility to ischemic damage independently of arterial hypertension (Lecrux et al., 2007; stroke). To overcome this problem, we use a renovascular model of hypertension to examine, with magnetic resonance imaging (MRI), brain alterations during the development of hypertension and after brain ischemia. The apparent diffusion coefficient (ADC) and fractional anisotropy (FA), two parameters of the diffusion tensor imaging (DTI) that are easily acquired by MRI, can provide information on the microstructure of tissues.

Aims: In this context, the aim of the study was to rely on the use of sequential MRI in a renovascular model of CAH in rats in order to analyze the effects of arterial hypertension on ADC and FA values, and to examine whether these MRI-derived parameters could predict the extent of brain damage induced by transient focal cerebral ischemia.

Material and methods: Hypertension was induced in Sprague Dawley rats according to the Golblatt model. Multiparametric MRI (DTI, Angiography, T2, and T2*) was carried out sequentially at 3 weeks, 1 week and 1 hour before ischemia and at 10 min and 50 min following ischemia and at 10 min following the reperfusion. One-hour cerebral ischemia was induced by intraluminal occlusion of the middle cerebral artery (MCAo) 12 week following the induction of hypertension.

Results: At eight weeks after the induction of hypertension, awake hypertensive animals showed higher systolic pressure values than control animals (respectively 240±30 mmHg (n=5) and 170±15 mmHg (n=7), p< 0.001). These values remained stable along the experimental protocol. Before ischemia and at all the time points examined, global analysis of ADC and FA did not show any difference between normotensive and hypertensive rats. However, hypertensive animals displayed larger ischemia-induced lesions as soon as 10 min following MCAO (294±79 mm^3 versus 54±60 mm^3, p< 0.0006). Following reperfusion, the ADC values in the lesion recovered better in normotensive rats compared to hypertensive ones ($6,09^{-04}$±$6,19^{-05}$$mm^2$/s versus $5,35^{-04}$±$3,49^{-05}$$mm^2$/s, p< 0.05). Three of 5 hypertensive rats showed hypertension induced pre-ischemic lesions, the size of which correlated to the amount of damage induced by stroke (R^2=0.99).

Conclusion: The data show that renovascular model of hypertension displays many pathological features found in man with hypertension. The use of this model is relevant and highly desirable in combination with SHR for stroke studies. Our data also suggest that

ADC and FA derived from global analyses could not be used as putative predictors of ischemic outcome in hypertensive subjects. Analyses of theses parameters in discrete brain regions are underway.

Acknowledgments: CNRS, Interreg IV A-2 seas zeeëns TC2N (Trans-Channel Neuroscience Network), ERDF (European Regional Developmental Fund), Conseil Régional de Basse-Normandie and the University of Caen Basse-Normandie.

I am 24 PhD student and I would like to be considered for the travel stipend.

NEURAL SUBSTRATES OF MOTOR IMAGERY BASED BRAIN-COMPUTER INTERFACE TRAINING IN UPPER LIMB PARALYSIS FOR STROKE PATIENTS

L. Mingfen, **J. Jie**

Department of Rehabilitation, Huashan Hospital, Fudan University, Shanghai, China

Objective: There is now sufficient evidence that using Motor Imagery based Brain-Computer Interface (MI-BCI) training can lead to enhanced functional recovery of paralyzed upper limb for stroke patients. However, the underlying neurophysiological mechanism is not available. Thus this study tries to explore the potential neurophysiological mechanism following the recovery of upper limb motor function for stroke suffers.

Methods: 14 stroke patients with sever hemiparesis were randomly divided into MI-BCI group (*n*=7) and control group (*n*=7). Both two groups received the routine rehabilitation therapy and drug therapy while MI-BCI group was treated with MI-BCI rehabilitation training for 2 months. The MI-BCI group conducted MI-BCI training three times per week and it lasted for 1.5 hours each time. A set of clinical measures including Fugl-Meyer motor assessment (FMA) and Action Research Arm Test (ARAT) were applied to assess the two groups' upper limb functional recovery. The Event-Related Desynchronization (ERD) over both hemispheres during motor imagery involving imaging the affected limb was analyzed among MI-BCI group.

Results: After MI-BCI training, positive improvements in the clinical measures were significantly observed in MI-BCI group($P< 0.05$). For most patients, significant ERD phenomenon over both sensorimotor areas of the cortex and parietal lobe was observed during motor imagery, whereas the affected hemisphere showed significant greater depression of sensory motor rhythm.

Conclusions: MI-BCI training as a novel rehabilitation protocol shows potential in improving the motor function of upper limb for stroke patients and can yield neural plasticity contributing to the restoration of motor function following stroke.

DELAYED NEURONAL LOSS AND PERSISTENT REACTIVE GLIOSIS IN A MOUSE MODEL OF MULTI-LACUNAR INFARCTS

W. Minghuan[1,2]

[1]*Translational Neuromedicine, University of Rochester School of Medicine, Rochester, NY, USA,* [2]*Tongji Hospital, Huazhong Universitiy of Science and Technology, Wuhan, China*

Microinfarcts are a common clinical feature of the aging brain, particularly in patients with cognitive decline, vascular or Alzheimer's dementia. However, the natural history of these lesions remains largely unexplored. Here we describe a mouse (C57BL/6J) model of multiple diffuse microinfarcts induced by unilateral internal carotid artery injection of cholesterol crystals (40-70µm). Microinfarcts were spread throughout the deep cortex, subcortical tissue and hippocampus and were comprised of a CD68 (a marker for reactive microglia and macrophages)-positive core surrounded by large regions of GFAP-positive reactive astrogliosis. Widespread reactive gliosis, including mis-localization of the astrocytic water channel aquaporin-4 (AQP4) persisted long after injury, recovering only after 1 month post-stroke. Within the cortex, neuronal cell death progressed gradually over the first month, from ~35% at 3 days to 60% at 28 days post-stroke. Delayed demyelination was also observed in lesions, beginning 28 days post-stroke. These findings demonstrate that microinfarct development follows a distinct course compared to larger regional infarcts such as those induced by middle cerebral artery occlusion. The long-lasting gliosis, delayed neuronal loss and demyelination suggest that the therapeutic window for microinfarcts may be much wider (perhaps days to weeks) than for larger strokes.

QUANTITATIVE PROTEOMIC PROFILE OF TISSUE PLASMINOGEN ACTIVATOR (TPA) RESPONDERS

M. Ning, J. Cao, M. Lopez, D. Sarracino, D. McMullin, K. Feeney, M. Thayer, M. Elia, H. Koop, F.S. Buonanno, X. Wang, E.H. Lo

Neurology, Clinical Proteomics Research Center and Neuroprotection Research Laboratory, Massachusetts General Hospital, Harvard Medical School, Boston, MA, USA

Background: The utilization of IV tPA remain low after more than a decade of FDA approval. We aim to widen the therapeutic window for tPA by understanding clinical thrombolysis response. Besides its intended role in clot lysis, tPA is also a pleiotrophic signaling protease in the blood, whose efficacy may potentially be monitored by proteomic profiles directly in stroke patients.

Method and results: To study thrombolysis response, we mapped quantitative profiles of all proteins pre and post IV tPA administration in plasma of stroke patients with good clinical outcome at 3 months. Plasma was sampled from stroke patients immediately before and 6-12hrs after tPA administration. Quantitative changes of proteins pre and post tPA were mapped by isotopic methods and analyzed on LC-MS. While both intra- and extracellular proteins were found, most were known plasma proteins, as seen on IPA analysis (Figure). Of 191 proteins found, 48 changed significantly post tPA (fold ratio in parenthesis). Compared to pre-tPA levels, we found significantly increased post-tPA levels of thrombolysis-related proteins such as fibrinogen gamma chain (↑11x), α-2-antiplasmin (↑4x), and a decrease in factor X (↓7x) etc. Changes were also found in factors outside of standard thrombolytic pathways, such as α-2-macroglobulin (↑2.3x); CD14 (↓2x) and GPX3 glutathione peroxidase 3 (↓2x) etc.

Conclusion: In order to study thrombolysis response and monitor thrombolysis efficacy at the bedside, we mapped quantitative protein fold changes of IV tPA responders and found a coordinated change not only in reported thrombolysis pathways, but also in other important proteolytic pathways in patient plasma. These early results are a step toward attempts to monitor clinical thrombolysis response in acute stroke patients in real time. Further studies are under way to compare plasma profiles of tPA-treated stroke patients with respect to different clinical outcome and imaging findings of reperfusion.

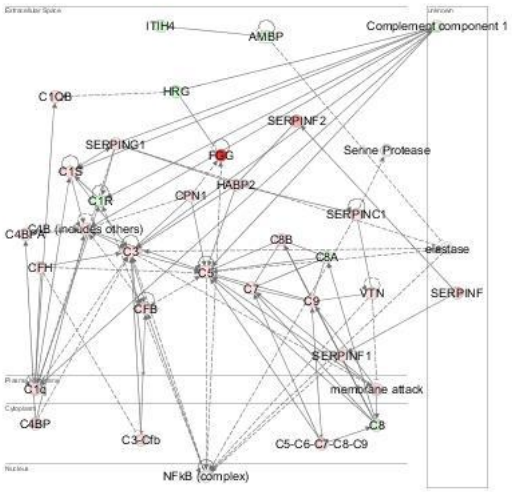

[IPA Analysis With Respect to Cellular Compartments]

CLINICAL AND PATHOLOGICAL IMPROVEMENT IN STROKE-PRONE SPONTANEOUS HYPERTENSIVE RATS RELATED TO PLEIOTROPIC EFFECT OF CILOSTAZOL

Y. Omote, K. Deguchi, F. Tian, H. Kawai, T. Kurata, T. Yamashita, Y. Ohta, Y. Ikeda, K. Abe

Neurology, Graduate School of Medicine, Dentistry and Pharmaceutical Sciences, Okayama University, Okayama, Japan

Background and purpose: This study investigated the efficacy of anti-platelet drugs on stroke, and motor and cognitive functions in relation to oxidative stress markers and insulin-like growth factor 1 receptor (IGF-1R).

Methods: Stroke-prone spontaneously hypertensive rats (SHR-SP) were treated with vehicle, aspirin, clopidogrel and cilostazol from 8 to 10 weeks of age. Physiological parameters, regional cerebral blood flow (rCBF), motor and cognitive functions were evaluated. Spontaneous infarct volume, oxidative stress markers and the IGF-1R positive cell ratio in the hippocampus were immunohistochemically examined. IGF-1R expression in the hippocampus was assessed by western blotting.

Results: Cilostazol and clopidogrel reduced the spontaneous infarct volume more than

aspirin. Only cilostazol improved motor and cognitive functions with a significant increase ($p < 0.05$) in the memory-related IGF-1R positive ratio and IGF-1R expression in the hippocampus. Cilostazol reduced oxidative stress markers in affected neurons regardless of blood pressure or rCBF.

Conclusion: The present results suggest that a possible pleiotropic effect of cilostazol resulted in the reduction of spontaneous infarct volume and preservation of motor and cognitive functions. The increase of IGF-1R positive cells in the hippocampus could partly explain the preservation of cognitive function in SHR-SP.

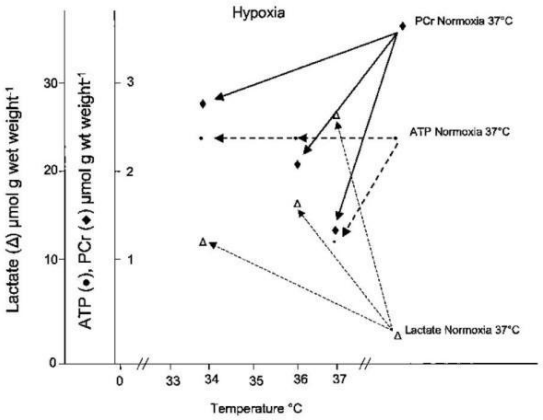

[Figure1]

A MODEL OF THE IMPACT OF HYPOTHERMIA ON CELL SURVIVAL DURING ISCHAEMIC STROKE

P. Orlowski, F. Kennedy, **S. Payne**

University of Oxford, Oxford, UK

Objectives: Treatment of ischaemic stroke by the injection of t-PA is recommended up to four hours from stroke onset. Beyond this point most of the brain damage is assumed to have occurred. We aim to design a mathematical model of brain metabolism during ischaemia to estimate by how much fever prevention or hypothermia may extend the window of opportunity and thus potentially suggest new treatment directions in stroke.

Methods: The brain metabolism model presented in [1] was adapted to incorporate the dependence of reaction rates and ion diffusion on temperature. The Q10 rule was used to set the reaction rate temperature dependence. Heat production by an element of brain tissue was set to depend on both metabolic rate and the level of perfusion. Cell death was assumed to occur after severe membrane depolarization.

Results:

Change of metabolite concentrations under stroke and hypothermia: The change of lactate, ATP and phosphocreatine concentration was simulated at an 80% and 90% reduction of cerebral blood flow (representing stroke) and at tissue temperatures ranging from 34° C to 37° C. The simulation results were in good agreement with experimental results in [2], as shown in Figure1.

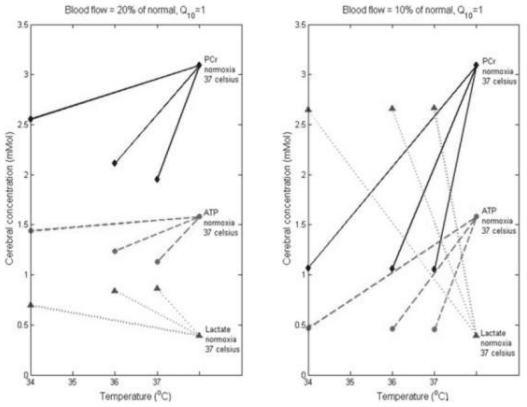

[Figure1b]

Figure 1. Comparison of experimental and simulation results for the change of phosphocreatine, ATP and lactate for different levels of ischaemia and hypothermia levels ranging from 34° C to 37° C.

Cell death during stroke and hypothermia: For Q10=1 and 80% blood flow reduction, a temperature decrease of at least 1°C induced within 50 minutes of stroke onset will extend the lifetime of the hypoperfused cells indefinitely. However, if the metabolic temperature dependence is Q10=3, just a 0.5°C fall in cerebral tissue temperature applied within 80 minutes of stroke onset will protect the cells of the model indefinitely. In infarct core tissue (90% blood flow reduction), if Q10=1 even a 3°C decrease in cerebral tissue temperature, applied at stroke onset, will have almost no effect on cell survival time; cell survival time in the infarct core in that case

will increase by no more than half an hour. There is thus a clear potential benefit to hypothermia, the therapeutic effect relies mostly on blood flow and to a smaller extend to the Q_{10} which is poorly characterised in the literature.

Conclusions: The model predicts metabolic changes during ischaemia and hypothermia in good agreement with experimental studies. Results predicting cell death delay encourage further refinement of the model and a search for optimal methods and tools to induce hypothermia.

References:

[1] Orlowski, P. et al. *Interface Focus* **1**, 408-416, 2011.

[2] L. Berntman et al. *Anesthesiology,* vol. 55, pp. 495-498, 1981 1981.

A MODEL OF OEDEMA DURING ISCHAEMIC STROKE

P. Orlowski, D. O'Neill, V. Grau, Y. Ventikos, **S. Payne**

University of Oxford, Oxford, UK

Objectives: Treatment of ischaemic stroke is associated with a haemorrhage risk. Therefore identification of salvageable brain tissue is necessary to compare treatment benefits and risks and to assist intervention planning. Our aim is to introduce a physiological model at the cellular and tissue levels which will predict brain decay through oedema and necrosis based on quantitative imaging of perfusion in order to guide treatment planning.

Methods: Cell volume change is set to depend on osmosis based on the kinetics of sodium, potassium, calcium, chloride and bicarbonate ions. The brain metabolism model in [1] is adapted to relate ion kinetics to changes in perfusion characteristic for stroke. Regulation of bicarbonate kinetics by a pH buffer is implemented. State rates of change are set to depend on cell volume change. Porosity α and tortuosity λ of the extracellular matrix are used to characterise the effect of the observed changes on diffusion in the extracellular space at tissue level. α has typically a narrow range in the brain and λ can be modelled as a function of α and thus these paramaters are not likely to have to be measured for the individual patient. An adapted version of Fick's law is then used to model the arising reaction-diffusion problem.

Results:

Simulation of cell growth during stroke: Change in cell volume (Figure 1) after a reduction of blood flow by 90 % shows a decrease of the extracellular space fraction from 0.3 to a minimum of 0.1 in ~3000 s. These results are in line with studies [3] and [4] which report values of α between 0.04 and 0.10 in mice models with first sign of oncotic oedema observed within 30 minutes from stroke onset.

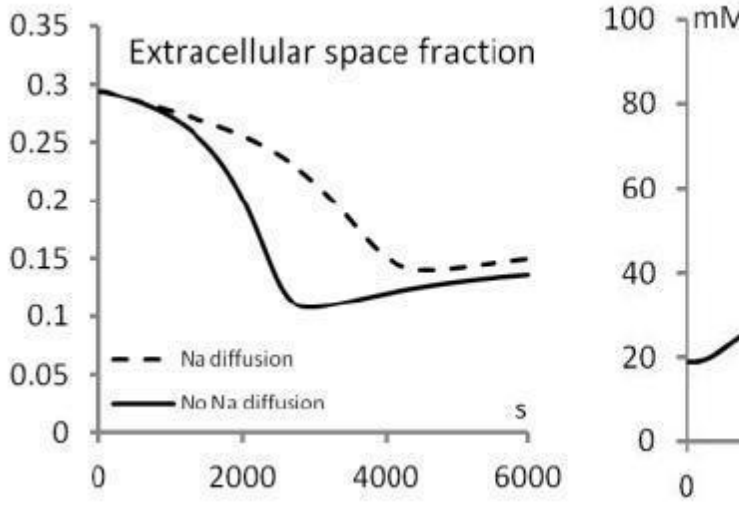

[Figure 1. Extracellular space and sodium change]

Diffusion simulation: To illustrate the role of diffusion of an individual group of ions during oedema, sodium diffusion was enabled. As a result the minimum extracellular volume fraction was reached ~1000s later. A cubic mesh with 1000 cubic cells for $1000cm^3$ of volume was created to simulate diffusion in ischaemic tissue. Diffusion of all metabolies was enabled. Simulation results suggest that diffusion between the ischaemic and non-ischaemic tissue expands the decay region. We further refine the characterization of this process.

Conclusions: The model predicts volume change in good agreement with experimental studies. Diffusion affects the speed and scale of cell volume change which suggests that cell death models should be set at the tissue scale. Oedema is a generic mechanism for the pathophysiology of many neurodegenerative

diseases thus its accurate model may lead to new drug developments, identification of biomarkers and improve treatment planning.

References:

[1] Orlowski, P. et al. *Interface Focus* **1**, 408-416, 2011.

[2] Nicholson C. *Rep. Prog. Phys.* 64:815-884, 2001.

[3] Lundbaek J.A. et.al. *Acta Physiol Scand.***146**:473-84, 1992.

[4] Syková E. et al *J Cereb Blood Flow Metab.* **14**:301-11, 1994.

STRENGTHENING OF STRUCTURAL INTERCONNECTIVITY IN THE UNAFFECTED HEMISPHERE CHRONICALLY AFTER EXPERIMENTAL UNILATERAL STROKE

W.M. Otte, K. van der Marel, M.P. van Meer, R.M. Dijkhuizen

Biomedical MR Imaging and Spectroscopy Group, Image Sciences Institute, University Medical Center Utrecht, Utrecht, The Netherlands

Objectives: Post-stroke loss of function is a major cause of adult disability. Nevertheless, partial recovery may occur in the weeks and months following onset. This maybe attributed to large-scale reorganization in functional neural networks, involving ipsi- and contralesional brain areas[1]. Highly connected network regions (i.e., 'hubs') play a critical role in functional networks[2]. Our goal was to measure the degree of interconnection strength between most significant hubs in the unaffected contralesional hemisphere chronically after experimental stroke.

Methods: Stroke was induced by transient occlusion of the right middle cerebral artery in male rats. Age-matched rats served as controls (Control; n=10). Ischemic lesion size and location were measured at 3 days post-stroke with T_2-weighted MRI, and animals were assigned to groups represented by subcortical ($Stroke_{Medium}$; n=9), or subcortical and cortical lesions ($Stroke_{Large}$; n=4). Ten weeks post-stroke, rats were euthanized and transcardially perfused. High-resolution diffusion tensor imaging (DTI) of post mortem brains was conducted at 9.4T. Maps of tissue fractional anisotropy (FA) were calculated and aligned to a rat brain atlas. Whole-brain tractography was achieved from seeds in each voxel with FA>0.2 using an interpolated streamline algorithm, with a 35° angle threshold (10 random seeds/voxel). Structural connectivity networks were calculated from fiber tracts expressing structural connectivity among 42 contralesional cortical and subcortical gray matter regions. Network edges between the regions were defined and weighted by the FA along the connecting tracts. We focused on the presence of highly connected network hubs (referred to as 'Rich-club' organization[3]; which reflects a network's capacity to segregate and integrate information between different network parts) in the averaged networks.

Results: Results are summarized in the Figure.

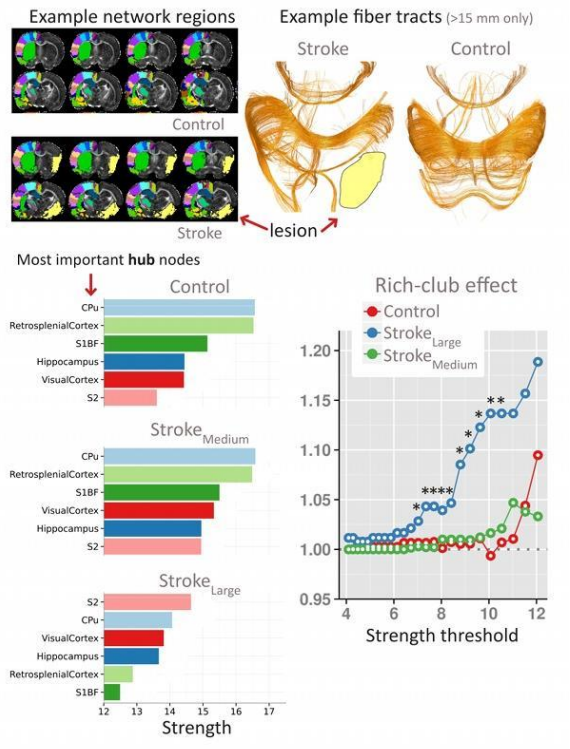

[Figure]

The caudate-putamen complex (CPu) was the most strongly interconnected contralesional hub in the Control and $Stroke_{Medium}$ groups, whereas the secondary somatosensory cortex (S2) had highest interconnection strength in the $Stroke_{Large}$ group. The contralesional network was characterized by a strong 'Rich-club' effect in the $Stroke_{Large}$ group (value>1.0,

*p< 0.01 vs. Control). The 'Rich-club' effect was less pronounced in the Control and $Stroke_{Medium}$ groups.

Conclusions: Our post mortem DTI study shows that rat brain, similar to human brain, expresses 'Rich-club' organization, in line with the concept that regions with high connection density are central to global brain communication. In addition, our data demonstrates significant modifications in contralesional network hubs chronically after stroke, in animals with large cortical and subcortical infarctions. The strengthening of interconnectivity in the contralesional hemisphere, particularly involving S2, reflects structural brain remodeling that may improve global brain communication and contribute to post-stroke functional recovery.

References:

[1]Dijkhuizen et al. Transl Stroke Res 3(2012)

[2]Bullmore and Sporns. Nat Rev Neurosci 13(2012)

[3]Van den Heuvel and Sporns. J Neurosci 31(2011)

DYNAMICS OF BRAIN OXYGEN DELIVERY THROUGH MODELLING OF THE CEREBRAL MICROVASCULATURE

C.S. Park, S.J. Payne

Institute of Biomedical Engineering, Department of Engineering Science, University of Oxford, Oxford, UK

Objectives: The brain requires a constant supply of oxygenated blood to maintain its function. Understanding the dynamics of oxygen delivery to changes in capillary network properties will provide valuable information of the effects of oxygen supply to different pathological conditions, such as ischaemic stroke. The mass transport equation is solved here for general capillary networks to quantify the effects of the properties of the capillary network on the oxygen extraction fraction (OEF) and hence the cerebral metabolic rate of oxygen (CMRO2). This model could be used to provide useful information on the capillary networks from imaging results and thus link modelling and imaging techniques.

Methods: An artificial capillary network matching both length and radial distributions of the cerebral microvasculature is created using a previously developed algorithm [1]. The unsteady one-dimensional mass transport equation is solved using the Laplace transform, assuming Poiseuille flow, that the concentration is convection driven and that the oxygen diffuses into the tissue at a rate proportional to the oxygen concentration. An analytical solution for the concentration can be obtained for a single vessel which can then be solved for the entire capillary network. Both the OEF and CMRO2 can then be solved with the knowledge solely of the individual vessel transit times [2].

Results: A specific signal is considered at the inlet of our capillary network in order to observe the signal produced at the outlet, and hence to calculate the dynamic OEF of the network. Figure 1 shows the dynamic OEF with time for a unit step concentration of 1mol at the inlet. A general decay is observed with time, the decay being dependent on the permeability of the walls (λ). The decay reaches a steady state value, which is also determined by the permeability of the walls. Mathematical analysis show that the time to reach this steady state value of the OEF is unaffected by the permeability, but solely by the properties of the network.

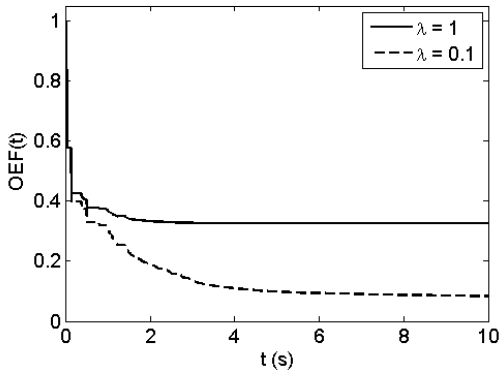

[Figure 1]

Conclusions: We have presented a model to quantify the OEF within the vessels in a simple capillary network. Preliminary results show that the model responds in a first order way. The OEF decays with time, with the permeability determining the steady state value. We next plan to investigate how different networks respond and thus to characterize the response in terms of the network properties, such as vessel length and

radius distribution. This will be very helpful in quantifying the effects of oxygen supply to different pathological conditions such as local ischaemia and improve our understanding of the effects of reperfusion.

References:

[1] Su *et al.*, *Microcirculation,* 19:175-187, 2012.

[2] Park *et al.*, *Interface Focus*, under review.

CAN WE INFER CEREBRAL MICROVASCULATURE PROPERTIES FROM THE RESIDUE FUNCTION?

C.S. Park, S.J. Payne

Institute of Biomedical Engineering, Department of Engineering Science, University of Oxford, Oxford, UK

Objectives: Clinical measurements of perfusion are very widely used to assess cerebrovascular disease. It is however, difficult to relate these measurements to the properties of the microvasculature due to the difficulties in generating accurate inter-connected networks. In our recent work, we developed a model of the cerebral microvasculature in terms of its residue function and thus opened up the possibility of exploring in detail the behaviour of such networks. An inverse analysis could then be performed such that it would be possible to determine the properties of the capillary network from data acquired by imaging, such as ASL and dynamic susceptibility MRI. Such a model would provide potentially very valuable information and also allow us to improve our understanding of post stroke dynamics.

Methods: 16 artificial capillary networks were created using a previously developed specific algorithm [1]. The unsteady one-dimensional mass transport equation was solved using the Laplace transform for the created capillary networks, assuming Poiseuille flow and that the concentration is solely driven by convection [2]. This was then used to solve for the residue function. The results from the capillary networks were characterised to quantify the effects of the properties of the capillary network structure on the residue function. The effects of the length distribution on the residue function are considered here.

Results: A bigamma distribution was used to characterise the residue function for each of the networks generated. Table 1 shows the mean and standard deviation of the parameters from the bigamma distribution, which can be used to characterise the residue functions. k_i, α_i and β_i represent the weighting, shape parameter and time constant of the bigamma distribution. Two different cases are considered, one matching experimental vessel length distributions [3] and the other replacing the short distance vessels (L< 25μm) with specific vessel lengths (40μm< L< 100μm), thus increasing the mean vessel length. The results show that there is a general increase in the mean shape parameters and time constants with a decrease in the cerebral blood flow (CBF). The paired t-test shows a significant difference ($p< 0.05$) between the mean values of the smaller time constant and its respective shape parameter, as well as for both of the weighting terms and CBF (represented with an asterisk on the table).

	k_1 (*)	α_1 (*)	α_2	β_1 (*)	β_2	CBF (*)
Matching experimental length distribution	0.57 ± 0.12	1.47 ± 0.93	1.04 ± 0.11	0.32 ± 0.29	3.04 ± 0.89	52.95 ± 12.91
Replacement of shorter vessels	0.70 ± 0.17	2.37 ± 1.66	1.54 ± 1.54	0.83 ± 0.54	4.14 ± 1.89	43.04 ± 4.30

[Table 1]

Conclusions: We have presented a model to quantify the effects of the properties of the microvasculature on the residue function. Preliminary results show that changes in network length distribution do have significant effects. We next plan to investigate how the residue function varies with different network properties, such as network connectivity and blockages. This will be very valuable in interpreting clinical imaging data.

References:

[1] Su *et al.*, *Microcirculation,* 19:175-187, 2012.

[2] Park *et al.*, *Interface Focus*, under review.

[3] Cassot *et al.*, *Microcirculation*, 13:1-18, 2006.

REGULATION OF BLOOD-BRAIN BARRIER PERMEABILITY BY ISCHEMIC PRECONDITIONING VIA EXTRACELLULAR SIGNAL-REGULATED KINASE ACTIVATION

E.-M. Park[1,2], J.A. Shin[1,2], H.-S. Kim[2,3]

[1]Pharmacology, [2]Tissue Injury Defense Research Center, [3]Molecular Medicine, School of Medicine, Ewha Womans University, Seoul, Republic of Korea

Objectives: Activation of extracelluar signal-regulated kinase 1 and 2 (ERK1/2) has been reported to have a role in neuroprotection by ischemic preconditioning (IP) against ischemic stroke. However, the protective mechanism of ERK1/2 activation by IP has not been clearly defined. ERK1/2 is one of major signaling pathways regulating tight junction (TJ) of blood-brain barrier (BBB) and affecting neuronal survival after ischemic stroke. This study was aim to examine whether the protective effect of IP was associated with modulation of TJ proteins via ERK1/2 activation.

Methods: IP of brief bilateral common carotid artery occlusion (BCCAO) was induced in male C57BL/6 mice 24 h before transient middle cerebral artery occlusion (MCAO). A specific ERK1/2 inhibitor U0126 was given to some of mice 1 h before MCAO to examine the role of ERK1/2 in the preconditioned brain. Behavior tests (neurological score and hanging wire test) were performed and infarct volume was measured 3 days after reperfusion. To asses BBB break down, the amount of Evans blue in the brain was measured at 24 h later. Levels of TJ proteins, pro-inflammatory cytokines were analyzed by Western blot. Activation of microglial/macrophage was examined by immunofluorescence staining with Iba1. Also TJ structural changes were examined by ransmission electron microscopic analysis.

Results: During the ischemic tolerance period, protein levels of TJs were reduced and TJ structures were deteriorated with the increase of inflammatory response. ERK1/2 activation was also specifically increased. The inhibition of activated ERK1/2 by U0126 normalized TJ protein levels, structural changes of TJ and inflammatory responses during tolerance periods. Moreover, the neuroprotective effects induced by IP on infarct volume, edema formation, BBB permeability and behavioral outcome were abolished by inhibition of ERK1/2 activation.

Conclusions: The findings suggest that neuroprotective effects of IP are mediated by modulation of BBB permeability through ERK1/2 activation. Therefore, targeting ERK1/2 activation can be a useful therapeutic strategy to regulate BBB permeability.

Acknowledgements: This research was supported by the National Research Foundation of Korea (NRF) grant funded by the Korea government (MEST) (2010-0029354 and 2012-0009854).

UP-REGULATION OF HEMEOXYGENASE-1 ATTENUATES BRAIN DAMAGE AFTER CEREBRALISCHEMIA VIA SIMULTANEOUS INHIBITION OF SUPEROXI DEPRODUCTION AND PRESERVATION OF NO BIOAVAILABILITY

Y. Qu

Xijing Hospital, The Fourth Military Medical University, Xi'an, China

Cerebral ischemia exacerbates neuronal death and neurological dysfunction, Evidence supports the involvement of oxidative/nitrative stress in the pathophysiology of cerebral ischemia, Heme oxygenase-1 is a rate-limiting enzyme in heme catabolism, possessing prteint anti-oxidant and anti-apoptosis effects, In transgenic mice.HO-1 overproduction is neuroprotective against cerebral ischemia injury, but by unclear nechamisms. The present study determined whether treatment with adenoviral vector overexpressing HO-1(Ad-HO-1)at-tenuates post-ischemic brain damage via reduction of oxidative/nitrative stress. After focal cerebral ischemia, at-Ad-HO-1 reduced lipid peroxidation and protein nitration,decreased infarct volume, and attenuated neurologic deficits. Zinc protoporphyrinI X (ZnPPIX, aspecific HO-1 inhibitor) blocked Ad-HO-1 mediated effects against ischemic brain damage. Although Ad-HO-1 slightly reduced ischemic brain NO concentrations, Ad-HO-1 treat-ment significantly inhibited cerebral expression of iNOS protein expression, without significant effectup on nNOS or eNOS expressi on compared to vehicle after focal cerebral ischemia. Ad-HO-1 preserved NO bioavailabil-ity by increasing eNOS phosphorylation during ischemia compared to vehicle. Together, ourresults suggest that Ad-HO-1attenuates post-ischemic brain damage via simultaneous

reduction of oxidative/nitrative stress and preservation of NO bioavailability;

INTEREST OF THE ASSOCIATION OF MESENCHYMAL STEM CELLS WITH PHARMACOLOGICALLY ACTIVE MICROCARRIERS FOR THE CEREBRAL ISCHEMIA TREATMENT IN RAT

M.-S. Quittet[1,2], O. Touzani[1,2], L. Sindji[3], F. Fillesoye[1,2], J.-P. Karam[3], M. Lecocq[1,2], L. Marteau[1,2], J. Toutain[1,2], D. Divoux[1,2], S. Roussel[1,2], C. Montero-Menei[3], M. Bernaudin[1,2]

[1]CNRS, UMR 6301 ISTCT, CERVOxy Group, Université de Caen Basse-Normandie, [2]CEA, DSV/I2BM, UMR 6301 ISTCT, CERVOxy Group, Caen, [3]Lunam Universite, INSERM U 1066, MINT 'Micro et Nanomedecines Biomimetiques', Angers, France

Introduction: To date, no effective therapy is available to treat brain neurological disorders consecutive to stroke. Transplantation of Mesenchymal Stem Cells (MSCs) has shown promising results at preclinical and clinical levels. However, growing evidence suggests that the implantation of MSCs with a carrier may improve their survival and their differentiation abilities. The aim of this study was to associate MSCs with Pharmacologically Active Microcarriers (PAMs), a cellular biomimetic support of MSC which is able to deliver trophic molecules, and evaluate their effects on functional recovery and brain damage when administrated into the ischemic lesion.

Material and methods: One day after a transient middle cerebral artery occlusion (90min), male rats received 8µL of vehicle solution (vehicle), PAMs, MSCs or MSCs adhered onto PAMs (MSC-PAM) in the ischemic striatum. The lesion volume was evaluated using T2-MRI (7 teslas, PharmaScan, Bruker) at days 2 and 22 post-occlusion. Functional recovery was sequentially assessed using several cognitive and sensorimotor tests. Immunohistochemical analyses were performed to evaluate neurogenesis, astrogliosis and apoptosis.

Results: As expected, volumes of infarction at 2 and 22 days were not different between the different groups. However, the immunohistology revealed that MSCs grafted on PAM further express mature neuronal marker (NeuN) compared to MSCs alone (Student test, p=0.003). Interestingly, this treatment may improve functional recovery and in particular sensori-motor functions.

Conclusion: These preliminary data suggest that association of MSCs with PAMs may be an interesting regenerative strategy for the treatment of cerebral ischemia.

Acknowledgments: CNRS, French Ministère de l'Enseignement Supérieure et de la Recherche, Interreg IV A-2 mers seas zeeëns TC2N (Trans-Channel Neuroscience Network), European union (FEDER) and the University of Caen Basse-Normandie.

Due to the fact I'm 25 years old PhD student, I would like to be integrated in the eligible student list for the young investigator student bursary.

OPTICAL COHERENCE TOMOGRAPHY MAPS HEMODYNAMICS AND CELL VIABILITY DURING ACUTE ISCHEMIC STROKE

V.J. Srinivasan[1,2], **H. Radhakrishnan**[1], K. Eikermann-Haerter[3,4], C. Ayata[3,4]

[1]Biomedical Engineering, University of California at Davis, Davis, CA, [2]Radiology, [3]Stroke and Neurovascular Regulation Laboratory, Department of Radiology, Massachusetts General Hospital, Harvard Medical School, Charlestown, [4]Stroke Service and Neuroscience Intensive Care Unit, Department of Neurology, Massachusetts General Hospital, Harvard Medical School, Boston, MA, USA

Objective: The capability to image the spatiotemporal evolutions of injury and recovery during both the acute and chronic stages of ischemic stroke *in vivo* in mice is desired; however suitable techniques are lacking. The goal of this study was to develop and validate high resolution, optical imaging techniques to map hemodynamics [1] and cell viability [2] using intrinsic scattering signatures. In particular, we used Doppler Optical Coherence Tomography (OCT), OCT angiography, and OCT signal slope analysis to achieve this goal. These novel techniques represent microscopic, optical analogs of diffusion weighted and perfusion weighted Magnetic Resonance Imaging. In this study, we investigate hemodynamic and cellular scattering changes during acute ischemic stroke using a transient filament middle

cerebral artery occlusion (fMCAO) mouse model.

Methods: Thinned-skull, glass coverslip-reinforced cranial windows were created in C57BL/6 mice (N = 4). After baseline imaging of both hemispheres, mice were placed in a prone position and the common carotid artery was exposed. An incision was made through which a filament was advanced to the origin of the middle cerebral artery. During fMCAO, the ipsilateral hemisphere was imaged. Forty-five minutes later, animals were briefly re-anesthetized with isoflurane, and the filament was withdrawn. Imaging of both hemispheres was performed again approximately 60 minutes after reperfusion. Imaging was performed using a 1310 nm spectral/Fourier domain OCT system with either a 5x or a 10x long-working distance infrared objective.

Results: Figure 1 shows OCT angiograms at baseline, during fMCAO, and 60 minutes after reperfusion (A-C). During fMCAO (B), a capillary non-perfused region is apparent, and demarcated with a solid white line. OCT cross-sectional images on a logarithmic scale show differences in signal penetration in the lateral portion of the cranial window, which become pronounced after reperfusion (D-F). Images of the concavity of the OCT signal vs. depth reflect this evolution (G-I). In (H-I), the capillary non-perfusion boundary from (B) is shown as a dotted white line. Remarkably, the tissue with anomalous scattering properties (i.e., the log OCT signal is concave down vs. depth) after reperfusion corresponds well to the capillary non-perfused tissue during fMCAO. No comparable changes were observed in the contralateral hemisphere.

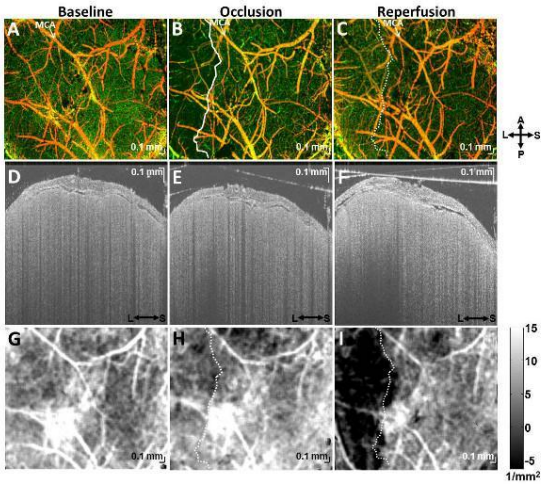

[fMCAO hemodynamic and cellular scattering maps]

Conclusion: Our results have shown the capability to independently map both hemodynamics and cell viability simultaneously using dynamic and static optical scattering changes. In particular, capillary non-perfusion during fMCAO predicts changes in scattering properties that are indicative of infarction. Using this imaging platform we will identify biomarkers for tissue that is at risk but not yet destined for infarction, representing an important therapeutic target.

References:

1. Srinivasan, V.J., et al., *Quantitative cerebral blood flow with optical coherence tomography.* Opt Express, 2010. **18**(3): p. 2477-94.

2. Srinivasan, V.J., et al., *Optical coherence microscopy for deep tissue imaging of the cerebral cortex with intrinsic contrast.* Opt Express, 2012. **20**(3): p. 2220-39.

TAKING NEUTROPHILS OUT OF PLAY IN DEVELOPING SECONDARY NEURONAL DAMAGE BY ANTI VLA-4 TREATMENT

M. Riek-Burchardt[1], J. Neumann[2], R. König[3], H. Hütten[4], K.G. Reymann[3], M. Gunzer[5]

[1]PG Neuropharmacology, Leibniz Institute for Neurobiology, [2]Clinic for Neurology, Otto-von-Guericke University, [3]German Center for Neurodegenerative Diseases (DZNE), [4]Clinic for Hematology and Oncology, Otto-von-Guericke University, Magdeburg, [5]Institute of Experimental Immunology and Imaging, University of Duisburg-Essen, University Hospital, Essen, Germany

Objective: Ischemic stroke is accompanied by a marked early infiltration of neutrophil granulocytes into the injured parenchyma. We assume this event as neurotoxic and their contribution to the secondary neuronal damage after ischemia.

Methods: We investigated the association of neutrophil granulocytes and inflamed vessels within the penumbra 24 h after permanent occlusion of the middle cerebral artery by using Lys-M-eGFP-mice and intracranial two-photon microscopy.

Results: We found within the penumbra in close proximity to the ischemic core especially

strongly elevated slow rolling of neutrophil granulocytes on the endothelium. After setting a vessel lesion (irritation, thrombus, bleeding) we found a shift to firm adhesion and later an infiltration into the brain parenchyma. In the penumbra, more close to the healthy parenchyma just a few neutrophil granulocytes had been detected on the endothelium, but there was a dramatic recruitment to the vessel wall after setting distinct pathological events (see above) in contrast to healthy conditions where recruitment had not been observed. This indicates the highly alertness of the interplay between inflamed vessels and neutrophil granulocytes and in turn potentially contribution to secondary neuronal damage. Using an approach of intravenously application of VLA-4-antibody 24 hours after ischemia during two-photon microscopy imaging, we showed for the first time the effectiveness of shifting adhesion and slow rolling of neutrophil granulocytes to fast rolling or detachment from the endothelium by this treatment, and thus potentially avoiding infiltration.

Conclusions: This approach would be suitable for a potential clinical application as add on therapy after stroke to reduce the development of secondary neuronal damage by taking neutrophil granulocytes out of play.

DECREASED LEVELS OF SIRT6 IN CEREBRAL ISCHEMIA

J. Shao[1], T. Liu[1], T. Zhang[1], W. Xia[1,2]

[1]School of Biomedical Engineering and Med-X Research Institute, Shanghai Jiao Tong University, [2]Clinical Stem Cell Center, Renji Hospital, Shanghai Jiao Tong University School of Medicine, Shanghai, China

Objectives: Stroke is a major cause of mortality and morbidity worldwide. Caloric restriction (CR) has been shown to protect against ischemic injury[1].The benefits of caloric restriction are mediated by a family of NAD-dependent deacetylases called sirtuins, which include SIRT1-7 in mammals. In this study we investigated the role of SIRT6 in experimental ischemia stroke.

Methods: For in vivo experiments, 24 adult male ICR mice were subjected to sham operation or transient middle cerebral artery occlusion (tMCAO)[2]. Protein and RNA samples from striatum were collected at 12 h, 24 h or 72 h after ischemia-reperfusion and Sirt6 levels were detected by immunoblotting or quantitative PCR. For in vitro experiments, astrocytes were isolated from cortex of post-natal day 1 Sprague Dawley rats and underwent oxygen and glucose deprivation (OGD) for 6 h. Proteins were collected at 6 h, 12 h, and 24 h after re-oxygenation and Sirt6 levels were detected by Western blot.

Results: Sirt6 protein and mRNA levels were decreased at 12 h and 24 h while had no significant change at 72 h after ischemia-reperfusion. In addition, OGD for 6 h caused a significant reduction in Sirt6 levels in astrocytes.

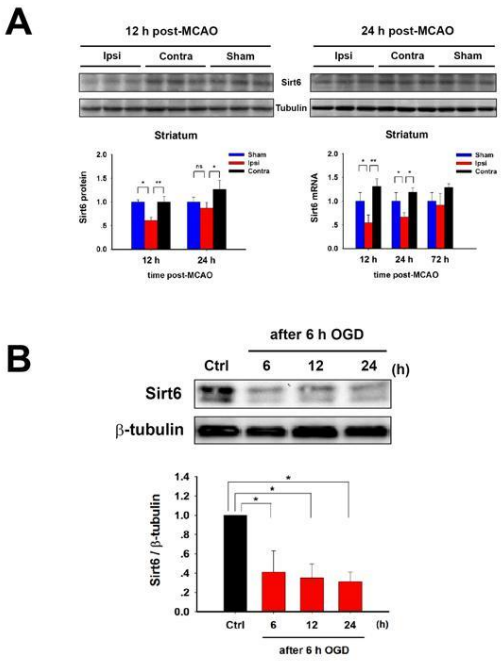

Figure 1.

A. Sirt6 protein and mRNA levels were detected at 12 h, 24 h, 72 h after ischemia-reperfusion. (sham, n=6; 12 h or 24 h after tMCAO, n=7 respectively; 72 h after tMCAO, n=4). Ipsi-ischemic hemisphere; contra-undamaged hemisphere. *p< 0.05, **p< 0.01 by one-way ANOVA.

B. Sirt6 protein levels were detected at 6 h, 12 h and 24 h after OGD in astrocytes. *p< 0.05 by one-way ANOVA.

Conclusion: We demonstrated that Sirt6 levels were decreased after ischemia-reperfusion and oxygen glucoase deprivation, suggesting intervention of Sirt6 levels in ischemic stroke might be of therapeutic value. This work is currently under investigation.

References:

1. Kahlilia C Morris, Hung Wen Lin, John W Thompson and Miguel A Perez-Pinzon. Pathways for ischemic cytoprotection: Role of sirtuins in caloric restriction, resveratrol, and ischemic preconditioning. J*ournal of Cerebral Blood Flow & Metabolism* (2011) 31, 1003-1019

2. Yang, G., Chan, P.H., Chen, J., Carlson, E., Chen, S.F., Weinstein, P., Epstein, C.J., Kamii, H. Human copper -zinc superoxide dismutase transgenic mice are highly resistant to reperfusion injury after focal cerebral ischemia. *Stroke* 1994; 25, 165- 17

A NOVEL NEUROPROTECTIVE STRATEGY USING METHYLENE BLUE: A LONGITUDINAL MRI STUDY

Q. Shen[1], F. Du[2], S. Huang[1], Y.V. Tiwari[1], T.Q. Duong[1]

[1]Research Imaging Institute, University of Texas Health Science Center at San Antonio, San Antonio, TX, [2]Morehouse School of Medicine, Atlanta, GA, USA

Objectives: Methylene blue (MB), has unique energy-enhancing and antioxidant properties.[1] It has been recently demonstrated that MB substantially reduces infarct size in transient focal cerebral ischemia in rats by histology.[2] As the next logical step, in this work, we evaluated MB's neuroprotective effects using MRI to longitudinally evaluate ischemic evolution. Comparisons were made with functional changes using neurological assessments.

Methods: Twelve male rats (250-300g) were subjected to 60-min transient middle cerebral arterial occlusion using intraluminal suture occlusion method. Using a randomized and double-blinded experimental design, either vehicle or MB was administered (1 mg/kg, i.v. infusion over 30 mins) immediately after reperfusion, and again 3-hr post-occlusion (0.5mg/kg), day-2 and day-7 (1 mg/kg). Quantitative CBF (cerebral blood flow) and ADC (apparent diffusion coefficient) were measured using continuous arterial spin labeling and diffusion-weighted EPI. T2 maps were acquired using fast spin echo sequence in day-2. Behavioral tests were performed at acute phase, day-1, 2, 7 and 28. Animals were scored neurologically according to a 6-point scale (0 = no deficit and 5 = dead). Based on 30-min ADC and CBF maps, ischemic core, perfusion/diffusion mismatch and normal tissues were classified using automated clustering ISODATA method.[3] Initial lesion volumes were defined by the core tissue volumes. Final infarct volumes were derived from day-2 T2 maps using threshold of mean T2 value of normal hemisphere plus two times of standard deviation. Edema correction was applied. Day-2 data was co-registered to acute phase data for pixel-by-pixel tissue fate tracking. Paired or equal variance t-test was used for statistical test. Data showed are mean ± SEM.

Results: The initial lesion volumes of the vehicle- and MB-treated group were not significantly different (P=0.92). In the vehicle-treated group, the initial lesion volume grew larger at day 2 (19±6%, N=6, P=0.03). By contrast, in the MB-treated group, the initial lesion volume became smaller at day 2 (-17±5%, N=6, P=0.02). The MB-treated infarct volume was significantly smaller than vehicle-treated infarct volume at day 2 by 30% (P=0.03). Pixel-by-pixel analysis further showed that MB salvaged more initial core pixels compared to controls (22±3% vs 11±3%, P=0.03), and MB also salvaged more mismatch pixels compared to vehicle (83±3% vs 61±8%, P=0.02). The mean NINDS stroke scores of the MB- and vehicle-treated rats were, respectively, 1.5 and 2 at day 2 (P=0.04), and 1.0 and 1.7 at day 7 (P=0.01), indicative of improved neurological status.

Conclusions: Our results showed that MB significantly reduces infarct size and behavioral deficit in the 60-min cerebral ischemia in rats. Such neuroprotective effect is consistent with MB's unique properties as a metabolic enhancer and an antioxidant. Future studies will investigate different occlusion durations, chronic stroke, embolic stroke model with combination therapy with rtPA, as well as incorporate fMRI and other MRI measurements. MB is already clinically approved for other indications, which should enable speedy translation to clinical trials.

References:

[1] Zhang X, et al, Neurotox Res 2006;9:47.

[2] Wen Y, et al, J Biol Chem 2011;286(18):16504.

[3] Shen Q, et al, J Cereb Blood Flow and Metab 2004;24:887.

THE ROLE OF BNIP3 IN BRAIN ISCHEMIA/REPERFUSION: REGULATING MITOPHAGY AND APOPTOSIS IN DELAYED NEURON DAMAGE

R. Shi, J. Kong

Human Anatomy and Cell Science, University of Manitoba, Winnipeg, MB, Canada

Introduction: Physiological level of autophagy is essential for the cellular recycling and homeostasis, and is believed to promote neuronal survival in ischemic stroke. The pathological role of apoptosis (type I programmed cell death) in delayed neuronal death in stroke has been well-established by many studies. In this study, we show that the pro-apoptotic BCL-2 family member BNIP3 is an important upstream regulator for both processes. Specifically, deletion of BNIP3 gene is neuroprotective by affecting both mitophagy and apoptosis pathways.

Methodology: We performed immunohistochemistry, western blot, co-ip, ELISA, and cell transfection to analyze the regulation of BNIP3 on mitophagy and apoptosis processes in cortical neurons and ischemic brains. Both BNIP3 wild-type and knock-out transgenic mice were used for tissue collection.

Results: In primary neuronal cultures exposed to oxygen and glucose deprivation (OGD) and reperfusion (RP), the death-inducing gene BNIP3 was highly expressed in primary cortical neurons, and the time course and expression levels of apoptosis-related proteins (i.e. active caspase-3, cytochrome C, and BAX) as well as autophagy-related proteins (i.e. LC3, Beclin-1, and LAMP-2) were positively regulated by BNIP3 expression. Promoting or inhibiting autophagy activities by using specific inducer or inhibitor didn't affect the expression patterns of BNIP3. Thus, BNIP3 is an upstream regulator of the elevated neuronal apoptosis and autophagy in ischemia/hypoxia (I/H). Then, we measured the brain damage of neonatal cerebral I/H in transgenic animals. By using TTC staining, we found that the infarct volume of the ischemic brains was significantly reduced in BNIP3 knock-out mice compared to wild-type mice upon 3-7 days recovery. Furthermore, deletion of BNIP3 gene in cortical neurons of knock-out mice activated a robust autophagic response. This increased autophagic response in BNIP3-null neurons was simultaneously accompanied by a decreased apoptotic response, which may coordinately contribute to the neuroprotection in the knock-out animals.

Conclusion: Our results indicate that BNIP3 is an important upstream regulator for both autophagy and apoptosis processes in delayed neuron damage in stroke.

IMAGING NEUROVASCULAR FUNCTION AND FUNCTIONAL RECOVERY AFTER STROKE IN THE RAT STRIATUM USING FOREPAW ELECTRICAL STIMULATION UNDER ISOFLURANE ANESTHESIA

Y.-Y.I. Shih[1], S. Huang[2], Y.-Y. Chen[3], H.-Y. Lai[1], F. Du[2], Y.-C.J. Kao[1], E.S. Hui[2], T.Q. Duong[2]

[1]Department of Neurology and Biomedical Research Imaging Center, University of North Carolina at Chapel Hill, Chapel Hill, NC, [2]Research Imaging Institute, University of Texas Health Science Center at San Antonio, San Antonio, TX, USA, [3]Department of Biomedical Engineering, National Yang-Ming University, Taipei, Taiwan R.O.C.

Objectives: The striatum is the major relay of the basal ganglia circuit that involves in various aspects of brain signaling. Recent studies showed that negative cerebral blood volume (CBV) functional magnetic resonance imaging (fMRI) response can be evoked in the bilateral striatum in rats by using forepaw electrical stimulation [1-2]. This unique negative response is related to intrinsic regulation of the dopamine system because injecting D_2-like receptor antagonist [1,3] or lesion of the dopamine neurons in the substantia nigra with 6-hydroxydopamine [4] significantly attenuated the evoked fMRI response. The current study aimed to investigate the neurovascular coupling/uncoupling in this model and establish a protocol that can longitudinally evaluate striatal function and functional recovery in the same subject after stroke.

Methods: In the first study, 11 rats were used to determine the optimal CBV fMRI responses with 9 different pulse-widths (0.1-30 ms) under isoflurane anesthesia and 5 rats were used to investigate the corresponding local field potential responses under the same experimental conditions. In the second study, two groups of 5 rats each were used to longitudinally study the striatal function and functional recovery after 20- and 45-min

middle cerebral artery occlusion (MCAO) followed by reperfusion. MR images were longitudinally acquired at *Control* time point, (3-5 days before MCAO), on *Day 0* (immediately after MCAO and reperfusion), *Day 7* and *Day 28*.

Results: Tight neurovascular coupling was found in the ipsilateral and contralateral cortex (r=0.89 and r=0.95, respectively, both *P*< 0.05) to forepaw stimuli. The striatal CBV responses were neither positively, nor negatively correlated with field potential (r=0.04, *P*< 0.05), indicating regional neurovascular uncoupling but related to the integrity of the dopamine receptor function [1,3,4]. The optimal stimulus parameter was 3 ms combined with 12 Hz and 10 mA which was then translated to study functional recovery after MCAO followed by reperfusion (**Fig. A&B**). No fMRI response was found in the ipsilateral striatum in both groups on Day 0. The striatal fMRI responses in the 20-min MCAO group were hyper-responsive on Day 7 compared to the pre-stroke baseline condition and also the matched time point in the 45-min MCAO group (*P*< 0.05). The Day 28 data in the 20-min MCAO group showed improved striatal functional recovery compared to the 45-min MCAO group (*P*< 0.05) and showed no significant difference compared to the contralateral striatum as well as pre-stroke baseline (both *P*>0.05). This fMRI technique provided additional information than traditional diffusion and perfusion data (**Fig. C&D**).

Conclusions: This study demonstrates intrinsic striatal neurovascular functions and functional recovery using hemodynamic fMRI under isoflurane anesthesia. These findings shed light on a unique brain neurovascular uncoupling mechanism and make longitudinal imaging of the striatal function possible in preclinical rat model by using forepaw stimulation.

References:

[1] Shih et al., J Neurosci 2009, 29:3036.

[2] Shih et al., JCBFM 2011, 31:832.

[3] Shih et al., Exp Neurol 2012, 234:382.

[4] Chen et al., Neurobiol Dis 2012, 49C:99.

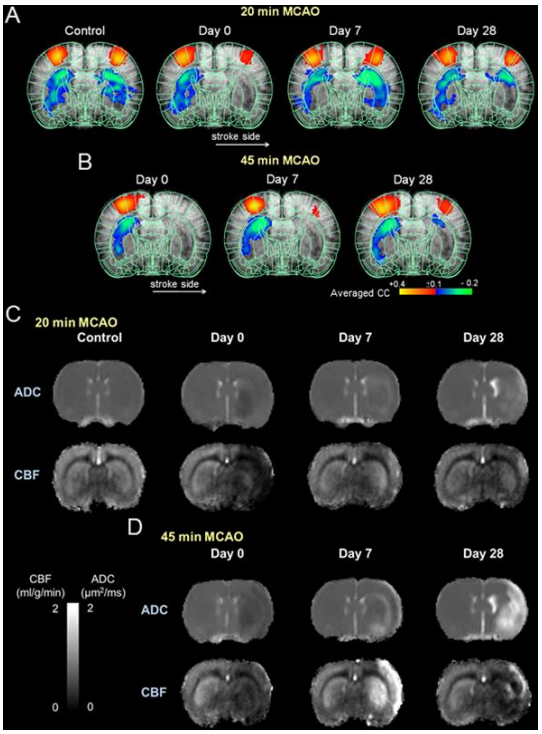

[Figure]

NEUROPROTECTIVE EFFECT OF OLIVE OIL IN FOCAL CEREBRAL ISCHEMIA MODELS

J. Song[1], D.H. Lee[1], J.G. Choi[2], H. Lee[2], D. Lee[2], S.K. Moon[3], H. Kim[1]

[1]Department of Herbal Pharmacology, College of Korean Medicine, Kyung Hee University, [2]Korea Institute of Science and Technology for Eastern Medicine (KISTEM), NeuMed Inc., [3]Department of Cardiovascular & Neurologic Diseases (Stroke Center), College of Korean Medicine, Kyung Hee University, Seoul, Republic of Korea

Olive oil consumption is associated with decreased risk of ischemic stroke, suggesting a neuroprotective effect. Previous studies have demonstrated that oleic acid, the main component of olive oil, protects neuronal cell death in rodent models of stroke. Though olive oil has been reported to exert neuroprotective effects when administered before an ischemic insult, it is not known whether postischemic treatment with olive oil is beneficial. The aim of this study was to determine whether olive oil exerts neuroprotective effect against focal cerebral ischemia in rodents. Focal cerebral ischemia was induced by middle cerebral

artery occlusion (MCAo) and photothrombotic vascular occlusion. Sprague-Dawley rats were subjected to 90 min of MCAo followed by referfusion. The skull of C57BL/6 mice was irradiated with cold white light for 15 min after intraperitoneal injection of rose bengal. Olive oil was administered once via tail vein at the onset of occlusion. Infarct volume in rodents was evaluated by 2, 3, 5-triphenyltetrazolium chloride staining 24 hours after ischemic insults. Intravenous treatment of olive oil 200 mg/kg significantly reduced infarct volume by 47.8 % ($p< 0.05$) in MCAo rats. Intravenous treatment of olive oil 1000 mg/kg significantly reduced infarct volume by 32.9 % ($p< 0.001$) in photothrombosis mice. These findings suggest that olive oil has neuroprotective effect against focal cerebral ischemia and could be of therapeutic value against stroke.

RESTORATION OF INTRACORTICAL AND THALAMOCORTICAL CIRCUITS AFTER TRANSPLANTATION OF BONE MARROW MESENCHYMAL STEM CELLS INTO THE ISCHEMIC BRAIN OF MICE

M. Song, O. Mohamad, X. Gu, L. Wei, S.P. Yu

Emory University School of Medicine, Atlanta, GA, USA

Objectives: Stem cell transplantation therapy has emerged as a promising regenerative therapy for tissue repair and functional recovery after ischemic stroke. Among many cell types, bone marrow mesenchymal stem cells (BMSCs) have a superior therapeutic capacity because of their autologous availability, multipotent potential, and documented clinical safety. As a therapeutic strategy to achieve functional recovery, the repair of ischemia-damaged neural networks and neuronal connections in the peri-infarct region is necessary. A clear demonstration of these therapeutic effects in stem cell therapy however, has been challenging and rarely reported.

Method: Adult male C57BL/6 mice were induced ischemic stroke in the barrel cortex (Li et al., 2007). BMSCs were isolated from the femoral and tibial bones of green fluorescent protein (GFP) transgenic Wistar rats. Based on our previous investigations (Theus et al., 2008; Hu et al., 2011), all BMSCs were subjected to a hypoxic preconditioning treatment before transplantation to increase cell survival/ trophic factor release. A total of 100,000 BMSCs were infused into two different sites in the penumbra; the injection was repeated twice at 1 and 7 days after stroke. The functional deficit and recovery were evaluated using the corner test. The activity of intracortical and thalamocortical circuit was assessed by recording of field potentials in the thalamocortical brain slices. The cellular mechanisms of circuit repair were demonstrated by immunohistochemical staining and Western blotting analysis.

Result: Two days after the BMSC transplantation (3 days after stroke), TTC staining showed a significantly smaller infarct in BMSC-treated mice compared to vehicle-treated stroke mice. Six weeks after stroke, BMSC treatment significantly improved recovery of sensorimotor function. Field potential recording in the peri-infarct region shows that the ischemia-disrupted intracortical activity from layer 4 to layer 2/3 was noticeably recovered in BMSC-treated mice, and the thalamocortical circuit connection was also partially restored. Little recovery was seen in stroke control animals. Immunohistochemical staining showed a higher density of neurons, axons and blood vessels in the peri-infarct region of BMSC-treated mice, accompanied with enhanced local blood flow recovery as measured with laser Doppler blood flow imaging. Western blotting showed that BMSC treatment increased the expression of stromal cell-derived factor-1 (SDF-1), vascular endothelial growth factor (VEGF) and brain-derived neurotrophic factor (BDNF) in the peri-infarct region. The expression of the axonal growth associated protein-43 (GAP-43) was markedly increased whereas the axonal growth inhibiting proteins ROCK II and NG2 were suppressed in the BMSC-treated brain. BMSC transplantation also promoted directional migration and survival of doublecortin (DCX)-positive neuroblasts in the peri-infarct region.

Conclusion: We provide novel evidence that BMSC transplantation has the potential to repair the ischemia-damaged neural networks and restore lost neuronal connections.

Reference:

Li, Y, Lu Z, Keogh CL, Yu. S.P. and Wei L. J Cereb Blood Flow Metab, 27:1043-1054, 2007

Theus, M. H.; Wei, L.; Cui, L.; Francis, K.; Hu, X.; Keogh, C.; Yu, S. P. Exp Neurol 210:656-670; 2008.

Hu, X.; Wei, L.; Taylor, T. M.; Wei, J.; Zhou,

X.; Wang, J. A.; Yu, S. P. Amer J Physiology (Cell physiology) 301:C362-C372; 2011.

ROLE OF MIR-15B SUPPRESSION OF BCL-2 IN CEREBRAL ISCHEMIC INJURY AND ITS REVERSAL BY THE PRECONDITIONING OF SEVOFLURANE

B.-L. Sun[1], H. Shi[2], S. Lu[2], P. Zhang[2], H. Wang[2], Q. Yu[2], R.A. Stetler[2,3], P.S. Vosler[2,3], J. Chen[2,3], Y. Gao[2]

[1]Key Lab of Cerebral Microcirculation in Universities of Shandong, Department of Neurology, Affiliated Hospital of Taishan Medical University, Taishan Medical University, Taian, [2]Department of Anesthesiology of Huashan Hospital, State Key Laboratory of Medical Neurobiology and Institute of Brain Sciences, Fudan University, Shanghai, China, [3]Center of Cerebrovascular Disease Research, University of Pittsburgh School of Medicine, Pittsburgh, PA, USA

Background and aims: Ischemic neuroprotection afforded by sevoflurane preconditioning has been previously demonstrated, yet the underlying mechanism is poorly understood and likely affects a wide range of cellular activities. Accumulating evidence suggest that microRNAs contribute to the pathogenesis of cerebral ischemia. However, the particular microRNA(s) that could emerge as potential therapeutic targets are not well defined and are likely to be highly context-specific under different neuroprotective strategies. However, several individual microRNAs have been implicated in both the pathogenesis of cerebral ischemia and cellular survival, and are capable of affecting a range of target mRNA. Conceivably, sevoflurane preconditioning may lead to alterations in ischemia-induced microRNA expression that may subsequently exert neuroprotective effects. The study was carried out to investigate the microRNA expression profile following transient cerebral ischemia in rats and the impact of an identified miRNA on neuroprotection afforded by sevoflurane preconditioning.

Materials and methods: Transient focal cerebral ischemia was induced in adult male Sprague-Dawley rats by filament occlusion of the left middle cerebral artery (MCAO) for 120 minutes and then reperfusion for the indicated durations. Sham-operated rats were used as controls. Animals subjected to MCAO underwent neurological evaluation at 24 hr and 48 hr after ischemia. Preconditioning with sevoflurane was induced by subjecting rats to 1.0 minimum alveolar concentration (MAC) sevoflurane (2.4% sevoflurane in air) for 30 min per day on 4 consecutive days, with the final exposure occurring 24 h prior to MCAO. Differential microRNA expression in the cortex was determined using both microarray analysis and real time PCR, and target protein expression was assessed by western blot and immunofluorescence staining. The selective Bcl-2 inhibitor TW-37 (0, 2.5 or 5□g) or vehicle was infused intracerebroventricularly for 5 min occuring1 h prior to MCAO or sham operation. For in vitro studies, oxygen-glucose deprivation and sevoflurane preconditioning were performed in cultured cortical neurons. Lentiviral vectors overexpressing mouse miR-15b or the inhibitor miR-15bI were transduced 2 d prior to sevoflurane/OGD. Cell death and viability were assessed.

Results: Microarray analysis revealed that 3 microRNAs were up-regulated (>2.0 fold) and 9 were down-regulated (< 0.5 fold) following middle cerebral artery occlusion (MCAO) compared to sham controls. In particular, miR-15b was robustly upregulated after MCAO. Preconditioning with sevoflurane significantly attenuated the upregulation of miR-15b at 72h after reperfusion. Bcl-2, an anti-apoptotic gene involved in the pathogenesis of cerebral ischemia, has been identified as a direct target of miR-15b. Consistent with the observed downregulation of miR-15b in sevoflurane-preconditioned brain, post-ischemic Bcl-2 expression was significantly increased by sevoflurane preconditioning. We identified the 3'-UTR of Bcl-2 as a target for miR-15b in neuronal cells. Molecular inhibition of miR-15b was capable of mimicking the neuroprotective effect of sevoflurane preconditioning, suggesting that the suppression of miR-15b due to sevoflurane contributes to its ischemic neuroprotection.

Conclusions: Sevoflurane preconditioning may exert its anti-apoptotic effects by reducing the elevated expression of miR-15b following ischemic injury, allowing its target proteins, including Bcl-2, to be translated and expressed at the protein level.

GLUTATHIONE LEVELS ARE ALTERED FOLLOWING CEREBRAL ISCHEMIA BUT ITS MODULATION DOES NOT AFFECT CELL DEATH IN ASTROCYTES OR NEURONS

B.A. Sutherland[1], Z.B. Redzic[1,2], G.L. Hadley[1], T. Rabie[1], M. Papadakis[1], A.M. Buchan[1]

[1]Acute Stroke Programme, Radcliffe Department of Medicine, University of Oxford, Oxford, UK, [2]Department of Physiology, Faculty of Medicine, Kuwait University, Kuwait, Kuwait

Objectives: Glutathione (GSH), a tripeptide with antioxidant and neuroprotective properties [1], may also control cerebral blood flow. These properties make GSH an attractive therapeutic target for ischaemic stroke. We examined *in vivo* whether GSH levels and expression of its regulatory enzymes were affected in the core or penumbra following focal cerebral ischaemia. Both astrocytes and neurons utilise GSH, but GSH levels may be differentially affected by cerebral ischaemia in these two cell types [2]. Therefore, we investigated whether modulation of astrocytic or neuronal GSH levels individually *in vitro* could alter cell death following oxygen glucose deprivation (OGD) and recovery.

Methods: Male Wistar rats (226-348g) were subjected to sham, permanent middle cerebral artery occlusion (pMCAO) or 90 minute transient MCAO (tMCAO). 24 hours following ischaemic onset, brains were dissected into cortical and striatal regions of both hemispheres. Protein expression of GSH peroxidase-1 (GPx-1) and glutamylcysteine synthetase (GCS) was assessed using Western blots. GSH levels were determined using a kinetic assay (Assay Designs). Primary cultures of rat astrocytes and neurons were prepared as previously described [3, 4]. Astrocytes and neurons were exposed to OGD or control conditions for 6h and 2h, respectively, followed by 24h recovery. To attenuate GSH levels, astrocytes were treated with 100µM buthionine sulfoximine (BSO) for 12 hours prior to OGD. To promote GSH levels, neurons were treated with 200µM N-acetylcysteine during recovery. For all *in vitro* experiments, cell death was assessed using a lactate dehydrogenase activity assay (Promega).

Results: pMCAO resulted in a cortical and striatal infarct that had significantly attenuated GSH levels compared to sham. tMCAO predominantly produced striatal infarcts which also had significantly decreased GSH levels compared to sham, while there was no change in GSH in the penumbral cortex. Striatal and cortical GPx-1 and GCS expression were not affected 24 hours following tMCAO. In astrocytic cultures, 6h OGD and 24h recovery had no effect on GSH levels compared to controls. Although BSO treatment abolished GSH levels, this had no effect on astrocytic cell death following 6h OGD and 24h recovery. Interestingly, BSO treatment increased cell death in control conditions. In neuronal cultures, cell death following 2h OGD + 24h recovery was not affected by N-acetylcysteine administration.

Conclusions: GSH levels were significantly decreased in the core following cerebral ischaemia with no change in the penumbra, which may reflect a reduction in viable cells in this region, or augment the susceptibility of these cells to oxidative stress. Since modulation of GSH in astrocytes and neurons individually did not affect cell death following OGD, GSH may require the interaction of many cells types to produce an effect. Further experiments examining these cellular interactions will determine if modulation of GSH is a viable strategy for treating cerebral ischaemia.

References:

1 Khan, M. *et al*. *J Neurosci Res* **76**, 519, (2004).

2 Bragin, D.E. *et al*. *J Cereb Blood Flow Metab* **30**, 734, (2010).

3 Abbott, N.J. *et al*. *Methods Mol Biol* **814**, 415, (2012).

4 Stefanis, L. *et al. J Neurosci* **19**, 6235, (1999).

RECOMBINANT TISSUE PLASMINOGEN ACTIVATOR AFFECTS NEURONAL DEATH IN VITRO BUT NOT INFARCT VOLUME IN VIVO FOLLOWING CEREBRAL ISCHAEMIA

B.A. Sutherland[1], C.N. Hall[2], A.M. Buchan[1]

[1]Acute Stroke Programme, Radcliffe Department of Medicine, University of Oxford, Oxford, [2]Department of Neuroscience, Physiology & Pharmacology, University College London, London, UK

Objectives: Recombinant tissue plasminogen activator (rtPA) is a thrombolytic that restores blood flow to improve neurological function following ischaemic stroke. rtPA is dissolved with L-arginine, the biological substrate for nitric oxide production, and most studies investigating rtPA do not compare its effects to its appropriate L-arginine control. Acting as a thrombolytic, rtPA is neuroprotective in thromboembolic models of stroke [1]. However, in mechanical models of stroke not requiring thrombolysis, rtPA may produce neurotoxicity [2]. Here, we examined the neurotoxic effects of rtPA following cerebral ischaemia *in vitro* and *in vivo* independent of thrombolysis, and attempted to delineate the contribution of L-arginine.

Methods: For *in vitro* experiments, cortical organotypic slices from P8 Sprague- Dawley rats were cultured for 7-9 days *in vitro* and then exposed to 45 mins oxygen glucose deprivation (OGD) or control conditions. Upon restoration of oxygen and glucose, slices were treated with rtPA (2 or 20µg/mL), L-arginine (70 or 700µg/mL) or PBS. Slices were labelled with propidium iodide and imaged to assess cell death at 6, 24 and 48 hours following OGD. For *in vivo* experiments, male Wistar rats (243-338g) were subjected to 90 minutes middle cerebral artery occlusion (MCAO) using an intraluminal filament [3]. Upon reperfusion, rtPA (1 or 10mg/kg), L-arginine (35 or 350mg/kg) or saline were administered as a 10% i.v. bolus and 90% i.v. infusion for 60 mins. Cerebral blood flow (CBF) was monitored using laser Doppler flowmetry. 24 hours following ischaemic onset, neurological function and infarct volume were determined.

Results: In slices, OGD significantly increased cell death compared to control. Treatment with L-arginine (either dose) following OGD significantly reduced cell death compared to PBS. However, treatment with rtPA (20µg/mL) reversed the protective effect of L-arginine. *In vivo*, rtPA treatment (with either dose) following transient MCAO led to a 19% mortality while the other treatment groups had < 5% mortality. CBF during the first 60 mins of reperfusion never recovered to pre-ischaemia levels, and there was no change in CBF with any treatment. Furthermore, no difference in percentage weight loss or neurological function was observed between treatments 24 hours following transient ischaemia. rtPA had no effect on striatal, cortical and total infarct volume compared to both L-arginine and saline treatments.

Conclusions: Since rtPA is dissolved with L-arginine, the comparison between rtPA and its L-arginine vehicle solution is critically important. Our data showed that *in vitro*, L-arginine was protective against cell death following OGD, which was reversed by rtPA, suggesting that rtPA may counteract any protective effect of L-arginine. However, these results were not replicated *in vivo* as rtPA had no significant effect on infarct volume following transient mechanical cerebral ischaemia compared to L-arginine or saline. This would indicate that, in our hands, rtPA does not produce any neurotoxic effects in vivo, supporting its further use as a treatment for acute ischaemic stroke.

References:

[1] Zivin, J.A. *et al*. *Science* **230**, 1289, (1985).

[2] Harston, G.W.J. *et al*. *J Cereb Blood Flow Metab* **30**, 1804, (2010).

[3] Longa E.Z. *et al*. *Stroke* **20**, 84, (1989).

A CASE OF CARDIAC RUPTURE AFTER TISSUE PLASMINOGEN ACTIVATOR (TPA) ADMINISTRATION FOR ACUTE CEREBRAL INFARCTION

K. Takenaka[1], N. Tsugita[2], K. Hayashi[1], M. Kato[1]

[1]Neurosurgery, Japanese Takayama Red Cross Hospital, [2]Cardiology, Takayama Red Cross Hospital, Takayama, Japan

Introduction: This is a first autopsy case report of cardiac rupture after tissue plasminogen activator (tPA) administration for acute cerebral infarction.

Case report: A case of a 90-year-old-female

with diagnosed atrial fiblillation was admitted to our hospital suffering from right hemiparalysis and aphasia. Initial NIHSS (NIH Stroke Scale) was 25 points. On diffusion-weighted imaging (DWI) of MRI, diffuse high intensity area was detected in left insular cortex. Intravenous thrombolysis using tissue plasminogen activator (tPA) (40kg, 24mg) administered at 1hour and 45minutes of symptom onset, which was caused by acute embolic cerebral infarction. After this treatment, her motor weakness and NIHSS were improved by 17 points within 90 minutes. However, just after, she suddenly became the state of shock (maximal blood pressure was 60 mmHg) and she became coma. On head and whole body CT scan, intracranial hemorrhage was not detected, but large volume of pericardial effusion resulting in cardiac tamponade was detected. She died in 215 minutes after Intravenous thrombolysis treatment and a pathological autopsy was performed. The recent myocardial infarction and blow-out-type cardiac rupture were reviewed on the cardiac posterior wall.

Conclusion: We should pay attention the cardiac complication in treatment of tPA.

References:

1) Fessler AJ,Albets MJ. Stroke treatment with tissue plasminogen activator in the setting of aortic dissection. Neurology 2000 ; 54 : 1010

2) Culie V, Mirie D, Eterovie D: Correlation between symtomatology and site of acute myocardial infarction. Int J Cardiol 77: 163-168, 2001

3) Gaul C,Dietrich W,Friedrich I,Sirch J,Erbguth FJ. Neurological symptoms in type A aortic dissections. Stroke 2007 ; 38 : 292-297

4) Dhand A. Nakagawa K, Nagpal S. et al: Cardiac rupture after intravenous t-PA administration in acute ischemic stroke. Neurocrit Care 13: 261-262, 2009

OVINE MIDDLE CEREBRAL ARTERY OCCLUSION REPRODUCES KEY FEATURES OF CLINICAL STROKE

R.J. Turner, A.V. Leonard, A.J. Wells, R. Vink

Adelaide Centre for Neuroscience Research, The University of Adelaide, Adelaide, SA, Australia

Objectives: Worldwide, more than 15 million individuals suffer a stroke each year with death, disability and dementia common outcomes. Despite this, clinical translation of stroke therapies from animal models to human patients has been extremely poor, with treatment options limited to tissue plasminogen activator. A number of factors may have contributed to this, one of which is the choice of animal model. Rodents have a small lissencephalic brain with a small amount of white matter. In contrast, sheep have a large human-like gyrencephalic brain with a large proportion of white matter. Utilising large animal models such as the sheep may more accurately predict efficacy in humans. Accordingly, we have recently developed a model of MCA occlusion in the sheep where both permanent and reperfused strokes can be achieved. The aim of the present study was to characterise the sheep MCAO model with respect to tissue oxygenation, intracranial pressure (ICP) and magnetic resonance imaging (MRI), lesion size and histological assessment.

Methods: Merino sheep (n=18) were subject to either sham surgery or MCA occlusion achieved by either diathermy (permanent) or the application and subsequent removal of an aneurysm clip (2h occlusion) under Isoflurane and ketamine anaesthesia. Brain tissue oxygenation (Licox®), intracranial pressure (ICP), blood pressure and blood gases were recorded for 24hrs after the induction of stroke. At 24hrs animals underwent magnetic resonance imaging (MRA, T1, T2, DWI) followed by perfusion with cold tris-saline. Brains were then removed for infarct volume assessment by tetrazolium chloride (TTC) staining and then processed for histological assessment by H&E, weil and albumin immunohistochemistry.

Results: Blood pressure and blood gases remained stable in all groups. Permanent MCA occlusion resulted in significant increases in ICP over the 24hr monitoring period. Brain

tissue oxygenation dropped to ischaemic levels in both groups but returned to normal levels upon reperfusion in the transient group. On MRI the large MCA stroke was associated with marked midline shift and tonsillar herniation in addition to significant cerebral oedema. TTC staining revealed that permanent MCA occlusion produced large hemispheric infarcts whereas transient MCA occlusion produced discrete cortical infarcts. Such findings were mirrored in the degree of injury seen histologically. Marked ischaemic cell damage was evident within the MCA territory on the H&E, with tissue pallor also observed on the weil stain. Albumin immunohistochemistry revealed a loss of blood-brain barrier integrity within the MCA territory, indicative of vasogenic oedema. Such changes were more pronounced in the permanent group.

Conclusions: The sheep model of MCA occlusion produces many features of clinical stroke including marked cerebral oedema, raised ICP and hallmarks of MCA stroke on MRI. A further advantage of this model is that both permanent stroke and reperfusion can be studied. This ovine MCA occlusion model has already proven beneficial in the validation of novel pharmacological agents already at pre-clinical development stage for the treatment of stroke.

RETROTRANSPOSON RESPONSE TO GLOBAL CEREBRAL ISCHEMIA AND NEUROINFLAMMATION

S. Wang, J. Chien, S. Kelly

New Jersey Neuroscience Institute, JFK Medical Center, Edison, NJ, USA

Objectives: Retrotransposons constitute ~40% vertebrate genome and can affect genomic stability and gene expression leading to deleterious outcomes. The expression of autonomous retrotransposon L1 has been shown to create double strand breaks (DSBs) in genomic DNA and can lead to apoptosis. Moreover, the expression of the non-autonomous LTR retrotransposon VL30 can induce cell death via mitochondrial and lysosomal damage. We investigated whether global cerebral ischemia (GCI) and neuroinflammation altered the expression of retrotransposons with a view to investigating their potentially damaging role in these conditions.

Methods: GCI was induced in adult, male C57BL/6 mice by 20-minute bilateral common carotid artery occlusion. Neuroinflammation was induced by lipopolysaccharides (LPS, 5mg/kg) injection. The animals were euthanized and tissues of hippocampi and striatum were dissected. qRT-PCR was used to study the gene expression of 9 families of retrotransposons and three piwi-like genes. Bisulfate sequencing was performed to study the DNA methylation status of IAP and L1. DNA methylation status was analyzed using BIQ Analyzer software.

Results: The transcription of 7 of the 9 main families of retrotransposons investigated were significantly upregulated by GCI including SINE B1, SINE B2, L1, MT, ORR1, IAP and VL30. Among them, SINE B2, IAP and VL30 were increased dramatically in transcriptional level. We found that the expression of these retrotransposons was already upregulated at 1 and 6-hours, but the expression remained low compared with 24-hours (Figure 1). ORR1, IAP and VL30 were also upregulated by LPS-induced neruoinflammation. DNA methylation status of IAP but not L1 was reduced by GCI. Interestingly, Miwi that encodes a protein that can directly degrade L1 RNA, was significantly decreased by GCI and correlated with L1 upregulation.

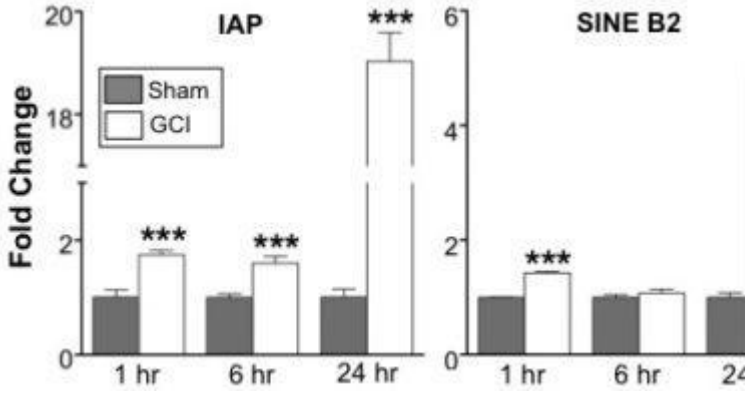

[fig1]

Figure 1: IAP, SINE B2 and VL30 were significantly increased soon after GCI (1 and 6-hours) but there was a dramatic increase in expression between 6 and 24-hours. qRT-PCR was performed in triplicate and data are expressed as mean fold change plus or minus standard deviation, unpaired Student's *t*-test was used to compare means. (****p< 0.0001*, ***p< 0.001*, **p< 0.05*).

Conclusions: We found GCI upregulated 7 of 9 families of retrotransposons while LPS induced neuroinflammation upregulated 3 of 9 retrotransposons, indicating that the retrotransposons were differentially regulated by each insult. We hypothesize that L1 upregulation by GCI is due to the downregulation of the Miwi gene and that upregulation of IAP resulted from DNA demethylation. Current experiments are exploring the degree of retrotransposition following each insult and the direct effects of increased retrotransposition of IAP and VL30 upon neuronal cell death and glial activation.

References:

Noutsopoulos et al., VL30 retrotransposition signals activation of a caspase-independent and p53-dependent death pathway associated with mitochondrial and lysosomal damage. Cell Research. (2010) 20, 553-562.

Reuter et al., Miwi catalysis is required for piRNA amplification-independent LINE1 transposon silencing. Nature. (2011) 480, 264-267.

Gasior et al., The human LINE-1 retrotransposon creates DNA double-strand breaks. J. Mol. Bio. (2006) 357, 1383-1393

THE NEUROPROTECTIVE EFFECT OF PBEF IN ISCHEMIA IS ASSOCIATED WITH ENHANCED MITOCHONDRIAL FUNCTION AND BIOGENESIS, AND REDUCED ENERGY DEPLETION

X. Wang[1], H. Li[2], S. Ding[2]

[1]Dalton Cardiovascular Research Center, Biological Engineeering, [2]University of Missouri, Columbia, MO, USA

Objectives: To study the effect of Pre-B-Cell Colony-Enhancing Factor (PBEF), a rate-limiting enzyme that converts nicotinamide (NAM) to NMN in the salvage pathway of mammalian NAD^+ biosynthesis, on brain and neuronal protection, and mitochondrial function and biogenesis in ischemia.

Methods: For in vivo study, we used photothrombosis model to induce focal ischemia. For in vitro study, we used oxygen-glucose deprivation (OGD) and glutamate excitotoxicity models of primary cultured neurons. We used FRET-based fluorescent sensor AMPKR to image energy depletion during glutamate excitotoxicity in cultured neurons. We used Western blot and immunostaining to detect protein expression in brain and cultured neurons.

Results: PBEF knockout mice had significantly larger infarct volume than WT mice after photothrombosis. From in vitro study, we demonstrated that neuroprotective effect of PBEF is dependent on its enzymatic activity. Wild type (WT), but not PBEF mutants (H247A and H247E) that lack enzymatic activity, can reduce neuronal death and mitochondrial membrane potential depolarization. Furthermore, overexpression of WT PBEF in neurons can suppress AIF translocation from mitochondria to nuclei, and mitochondrial defragmentation. WT PBEF can ameliorate energy depletion during excitotoxic glutamate stimulation. Further more, treatments of neurons with NAM and NAD^+ (a substrate and a downstream product of PBEF respectively) increased mtDNA content, and the protein levels of key molecules for mitochondrial biogenesis including PGC-1a and NRF-1 after ischemia.

Conclusions: Our results demonstrate that PBEF exerts a brain and neuronal protective effect ischemia, such a beneficial effect is associated with enhanced mitochondrial function and biogenesis, reduced energy depletion, and is enzymatic activity dependent.

HSP27 PROTECTS THE BLOOD-BRAIN BARRIER AGAINST ISCHEMIA-INDUCED LOSS OF INTEGRITY

Z. Weng[1,2], L. Zhang[1,2], R.A. Stetler[1,2], R.K. Leak[3], P. Li[1,2], G.B. Atkins[4], Y. Gao[1], J. Chen[1,2,5]

[1]State Key Laboratory of Medical Neurobiology and Institute of Brain Sciences, Fudan University, Shanghai, China, [2]Center for Cerebrovascular Disease Research, University of Pittsburgh School of Medicine Pittsburgh, [3]Division of Pharmaceutical Sciences, Duquesne University, Pittsburgh, PA, [4]Case Cardiovascular Research Institute, Department of Medicine, Case Western Reserve University School of Medicine, Cleveland, OH, [5]Geriatric Research, Educational and Clinical Center, Veterans Affairs Pittsburgh Health Care System, Pittsburgh, PA, USA

Objectives: The integrity of the blood-brain barrier (BBB) is essential for normal neuronal and glial function. Loss of integrity of the BBB in stroke victims initiates a devastating cascade of events including extravasation of blood-borne molecules, water, and inflammatory cells deep into brain parenchyma. Thus, it is important to identify mechanisms by which BBB integrity can be maintained in the face of ischemic injury in experimental stroke. We previously demonstrated that the phylogenetically conserved small heat shock protein 27 (HSP27) protects against transient middle cerebral artery occlusion (tMCAO).[1,2] Despite recent advances in the study of heat shock proteins, the impact of HSP27 on BBB permeability remains to be determined. Thus, the present study tested the hypothesis that the BBB is protected by transgenic HSP27 overexpression in an experimental stroke model.

Methods: Wild-type or HSP27 overexpressing mice were subjected to tMCAO. Neurological scores, infarct volume, and brain edema were assessed. Extravasation of endogenous IgG molecules and FITC-albumin into brain parenchyma was measured. Microvessels were isolated for immunoblotting. TUNEL staining along the endothelial lining was performed. Cytokine expression and neutrophil invasion of the brain were also assessed. Primary endothelial cultures were transfected with lenti-HSP27 constructs and subjected to oxygen-glucose deprivation (OGD). Four viability measurements were performed on these cultures: assays for mitochondrial membrane potential, caspase-3 activity, MTT reduction, and lactate dehydrogenase release.

Results: HSP27 transgenic overexpression protected neurological function, reduced infarct volume, and maintained the integrity of the BBB in mice subjected to tMCAO. Extravasation of IgG and FITC-albumin into the brain was reduced, as was total brain water content. Notably, HSP27 overexpression abolished the appearance of $TUNEL^+$ profiles in microvessel walls. Transgenics also experienced less loss of microvessel proteins occludin, ZO-1, and VE-cadherin. Primary endothelial cells were rescued from OGD by lentiviral HSP27 overexpression according to four viability assays, supporting a direct effect on this cell type. Finally, HSP27 overexpression reduced the appearance of neutrophils in the brain and inhibited the secretion of the five pro-inflammatory cytokines, including interleukin-6.

Conclusions: The present study is the first demonstration that HSP27 reduces extravasation of blood-borne molecules, inflammatory cells, and water into brain parenchyma. Endogenous upregulation of HSP27 after ischemia in wild-type animals may exert similar protective functions. Because loss of BBB integrity after stroke is so debilitating, rational drug design of pharmacological inducers or activators of this small heat shock protein is warranted. Such enhancement of HSP27 may lead to future therapies against a host of injuries, including but not limited to a harmful breach in brain vasculature.

References:

1. Stetler, R.A. *et al.* Hsp27 protects against ischemic brain injury via attenuation of a novel stress-response cascade upstream of mitochondrial cell death signaling. *The Journal of neuroscience,* **28**, 13038-55 (2008).

2. Stetler, R.A. *et al.* Phosphorylation of HSP27 by protein kinase D is essential for mediating neuroprotection against ischemic neuronal injury. *The Journal of neuroscience,* **32**, 2667-82 (2012).

PLASMA KALLIKREIN INDUCES ISCHEMIC BRAIN DAMAGE THROUGH CLEAVAGE-DEPENDENT ACTIVATION OF NMDA RECEPTORS

G. Wu[1], L. Wu[2], D.E. Clapham[2], E.P. Feener[1]

[1]Vascular Cell Biology, Joslin Diabetes Center of Harvard Medical School, [2]Neurobiology, Children's Hospital Boston, Boston, MA, USA

Plasma kallikrein (PK) contributes to vascular hemostasis and edema following brain injury, however, its direct effects on neurons are not fully understood. We report that cerebral PK levels are elevated in murine models of ischemic stroke, Alzheimer's disease, and VEGF-induced blood brain barrier disruption. We show that PK mediates cleavage-dependent activation of NDMA receptors (NMDAR) on cortical neurons and thereby enhances NMDA-induced apoptosis. PK-induced cleavage of NMDAR and neuron apoptosis is prevented by site-directed mutation of the cleavage site in the N-terminal ectodomain of the NR1 receptor subunit. Mutant NR1 that is truncation at the PK cleavage site displays enhanced NMDAR

channel activity and calcium influx. This N-terminal truncation of NR1 also increased glycine and NMDA binding to NR1/NR2A heterodimers by 2-fold compared to the full-length receptor. Middle cerebral artery occlusion-induced NR1 cleavage and ischemic injury was reduced in rodents with PK deficiency caused by Klkb1 gene knockout. Our findings suggest that PK is a potential therapeutic target for reducing neuron injury caused by blood brain barrier disruption.

EFFECTS OF PERFUSION-WEIGHTED MRI ANALYSIS AND ACQUISITION TECHNIQUES ON THE ACCURACY OF PREDICTION OF TISSUE OUTCOME AFTER ISCHEMIC STROKE

O. Wu[1], E. McIntosh[1], R. Bezerra[1], I. Diwan[1], S. Mocking[1], P. Garg[1], W.T. Kimberly[2], E.M. Arsava[1], W.A. Copen[3], P.W. Schaefer[3], H. Ay[1], A.B. Singhal[2], B.R. Rosen[1]

[1]Athinoula A. Martinos Center, Dept Radiology, Massachusetts General Hospital, Charlestown, [2]Dept of Neurology, [3]Dept of Radiology, Massachusetts General Hospital, Boston, MA, USA

Objectives: Algorithms that combine multiple MRI data voxel-wise more accurately predict risk of tissue infarction in acute stroke patients than individual imaging sequences. We speculate that the performances of predictive algorithms are critically linked to the quality of perfusion-weighted MRI (PWI) data. We investigated the effects of different deconvolution methods, PWI parameters and acquisition techniques on algorithm performance for predicting tissue outcome.

Methods: MRI from 111 stroke patients whom received DWI and PWI within 12h from last known well and who had follow-up imaging ≥ 4 days with lesions ≥ 1 cm^3 were analyzed. Subjects were divided according to whether data was acquired with GRE (N=78) or SE (N=33). Maps of apparent diffusion coefficient (ADC), T2-weighted images (T2WI), isotropic DWI (iDWI), CBF, CBV, mean transit time (MTT) and Tmax (time of peak of residue function) were used as covariates in generalized linear models that produced infarction risk maps. PWI parameters were calculated using either standard singular value decomposition (sSVD) or oscillation index regularization (oSVD). Four models were developed per group (oSVD/sSVD with and without Tmax as a covariate) using follow-up lesion outlines. Homogeneous models were trained and applied for each group (GRE or SE) using jack-knifing. Performances of applying models across groups or applying "hybrid models" combining GRE and SE data were evaluated by comparing areas under receiver operating characteristic curves (AUC) using repeated measures one-way ANOVA with post-hoc SNK test.

Results: Follow-up median [IQR] lesion volumes (37.2 [13.5-83.4] vs. 16.3 [5.2 -54.0] cm^3; P=0.04) and admission NIHSS (12 [6-17] vs. 5 [3-12]; P=0.04) for the SE group were significantly larger than the GRE group; no significant differences were found for mean±SD age (64.6±17.0 years-old), time-to-MRI (6.2 [3.7-7.7] h) or time-to-follow-up (10.9 [6.1-46]). Algorithms combining T2WI, ADC, iDWI, and CBF, CBV, MTT and Tmax calculated using oSVD (oTmax+ model) outperformed the other 3 models in terms of AUC (0.88 [0.82-0.93]; P≤0.02). Subsequent analyses were therefore limited to the oTmax+ model. There was no significant difference in AUC between GRE and SE groups (0.88 [0.82-0.93] vs 0.89 [0.79-0.93]; P=0.58). Significant differences were found between model coefficients (Table 1, *P< 0.05 vs. hybrid model). For GRE data, the homogenous oTmax+ model outperformed the SE model (P=0.02) but not the hybrid model (P=0.41).

Conclusion: Our results show that choice of deconvolution techniques and imaging parameters (e.g. inclusion of Tmax) affects the performance of multiparametric predictive algorithms. Separating tracer-arrival timing effects from flow estimates improved model performance. The models tended to perform equivalently regardless of whether GRE or SE PWI data was acquired, likely due to the different model coefficients. Differences in model coefficients may have also been influenced by imbalance in stroke severity between the two groups.

Model	Offset	T2WI	ADC	iDWI	CBF	MTT	CBV	Tmax
GRE	-5.9±0.2	0.1±0.2*	0.1±0.2*	3.9±0.2*	-0.1±0.04	0.9±0.05*	-0.05±0.03	0.06±*
SE	-3.3±0.2*	1.2±0.2	-1.3±0.2*	2.3±0.2*	-0.3±0.04*	0.4±0.05*	0.3±0.04*	0.09±0

Hybrid	-4.5 ±0.2	0.8 ±0.2	-0.7 ±0.2	2.9 ±0.2	-0.2± 0.04	0.7± 0.05	0.03 ±0.03	0.08±0

[Table 1: Model coefficients]

PROTECTION FROM CEREBRAL ISCHEMIA BY INHIBITION OF NEUROINFLAMMATION WITH ADJUDIN IN MICE

T. Liu[1], J. Shao[1], H. Yu[1], **W. Xia**[1,2]

[1]School of Biomedical Engineering and Med-X Research Institute, Shanghai Jiao Tong University, [2]Clinical Stem Cell Center, Renji Hospital, Shanghai Jiao Tong University School of Medicine, Shanghai, China

Objectives: Neuroinflammation caused by microglial activation plays a key role in cerebral ischemia. We previously found Adjudin, a potential non-hormonal male contraceptive, exhibits additional function to inhibit microglial activation in vitro[1]. In this study we investigated whether Adjudin plays a neuroprotective role in experimental ischemia stroke.

Methods: 28 and 16 adult male ICR mice were subjected to pMCAO and tMCAO[2] respectively. In pMCAO group mice were intraperitoneally administrated with 50 mg/kg Adjudin 2 h before surgery. Cresyl violet staining, brain water content measurement, behavioral assessment and CD11b immunohistological staining were performed at 24 h or 72 h after ischemia. In tMCAO group mice were intraperitoneally administrated with 50 mg/kg Adjudin immediately after reperfusion followed by another dose 5 h later. Cresyl violet staining was performed at 24 h after reperfusion.

Results: Adjudin reduced brain edema and improved neurological deficits at 24 h or 72 h after pMCAO. Immunostaining for CD11b showed that Adjudin attenuated ischemia-induced microglial activation. In addition, Adjudin significantly decreased infarct area at 24 h after tMCAO.

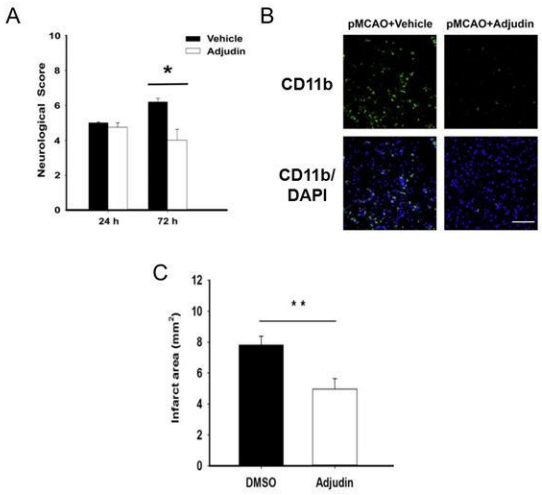

Figure 1

A. Neurological deficits were assessed at 24 h and 72 h after pMCAO. N=4-5, *p< 0.05

B. Immunohistological staining for CD11b in the ischemic cerebral at 24 h after pMCAO

C. Infarct area was examined at 24 h after tMCAO reperfusion. N=9-10, **p< 0.01

Conclusion: We demonstrated that Adjudin had benefits for neuroprotection after cerebral ischemia partially by inhibiting microglial activation, suggesting that Adjudin might be a potential therapeutic candidate for stroke.

References:

1. Shao J, Liu T, Xie QR, Zhang T, Yu H, Wang B, Ying W, Mruk DD, Silvestrini B, Yan Cheng C, Xia W. Adjudin attenuates lipopolysaccharide (LPS)- and ischemia-induced microglial activation. Journal of Neuroimmunology 2012

2. Yang, G., Chan, P.H., Chen, J., Carlson, E., Chen, S.F., Weinstein, P., Epstein, C.J., Kamii, H. Human copper -zinc superoxide dismutase transgenic mice are highly resistant to reperfusion injury after focal cerebral ischemia. *Stroke* 1994; 25, 165- 170

ISCHEMIC POSTCONDITIONING DID NOT INHIBIT ACUTE INFARCTION BUT PROVIDED LONG-TERM PROTECTION BY ENHANCING MTOR ACTIVITY IN NUDE RATS

R. Xie[1], P. Wang[2,3], X. Ji[2], H. Zhao[4]

[1]Neurosurgery, Huashan Hospital, Fudan University, Shanghai, [2]Neurosurgery, Xuanwu Hospital, Capital University, Beijing, [3]Neurosurgery, Huashan Hospital (Jingan Branch), Fudan University, Shanghai, China, [4]Neurosurgery, Stanford University, Stanford, CA, USA

Introduction: Ischemic postconditioning provides protective effects against focal ischemia and improves neurological deficits. Recent studies have shown that T cells play important roles in stroke injury. In this study, we investigated whether postconditioning protects against stroke in nude rats with T-cell deficiency, and examined the potential role of Akt and mammalian target of rapamycin (mTOR) pathway in the protective effects of ischemic postconditioning.

Methods: Focal ischemia was induced by 30 min of transient bilateral CCA occlusion and permanent distal MCA occlusion in nude rats with T-cell deficiency (RNU rats, Charles River). Ischemic postconditioning was conducted immediately after reperfusion by 3 cycles of 30 sec reperfusion and 10 sec occlusion of the bilateral CCAs. Rapamycin, an mTOR inhibitor, was injected into the left lateral ventricle 1 h before stroke onset. For the behavior test, home cage, vibrissa-elicited limb use and postural reflex tests were performed until 30 d after stroke. Peri-infarct and ischemic core tissues were collected 1, 5, 9 and 24 h after stroke for Western blotting and immunostaining. Protein levels of phosphorylated mTOR (p-MTOR), S6K and 4EBP-1 in the mTOR pathway, and the upstream molecule, Akt and its isoforms (Akt1, Akt2, Akt3) were also measured.

Results: Different from wild type rats, the cortical infarction induced by stroke was not significantly reduced by ischemic postconditioning in nude rats when measured 2 d post-stroke (27.1±4.3% in control ischemia vs 23.7±4.2% in postconditioning, n=6). Despite the unaltered infarct size, Western blot showed that postconditioning significantly increased the protein levels of p-Akt (phosphorylated Akt) and Akt isoforms (Akt1, Akt2, Akt3) in the Akt pathway, and p-mTOR, p-S6K, p-4EBP1 in the mTOR pathway, both in the peri-infarct area and core 24 h after stroke ($p< 0.05$). In addition, ischemic postconditioning improved neurological function in nude rats when measured 30 d after stroke (n=6, $p< 0.05$), and reduced brain damage size from 10.2±1.4% to 4.9±1.6% (n=6, $p< 0.05$). The mTOR inhibitor, rapamycin, significantly attenuated p-mTOR and p-S6K levels both in the peri-infart area and core at 1, 5, 9 and 24 h after stroke ($p< 0.05$), and abolished the long-term protective effects of postconditioning.

Conclusions: Ischemic postconditioning did not inhibit acute infarction but provided long-term protection by enhancing Akt and mTOR activity in the acute phase after stroke in nude rats.

NEURONAL PRODUCTION AND FUNCTION OF LIPOCALIN-2 IN ISCHEMIC STROKE

C. Xing, X. Wang, X. Wang, E.H. Lo

Massachusetts General Hospital, Harvard Medical School, Charlestown, MA, USA

Objective: Microglial reactions comprise a key part of stroke evolution. But what signals damaged neurons release to activate microglia remains unknown. In this study, we explored the effects of lipocalin-2 (LCN2) on the activation and function of microglia after ischemic stroke.

Methods: Transient focal cerebral ischemia was induced by 90 min occlusion of the middle cerebral artery in rats, and ELISA, western blotting and immunostaining were used to profile the LCN2 response in vivo. To investigate the mechanisms of LCN2 signaling, cell culture studies were conducted in primary rat neurons and microglia. Cellular levels of LCN2, cytokines and growth factors were quantified with ELISA. Gene expression was detected with real-time PCR. Proteins in cell lysates were analyzed by Western blot. Microglial function was assessed with phagocytic and migration assays. Neuronal viability was measured by MTT assay.

Results: In rat focal cerebral ischemia, LCN2 levels significantly increased in ipsilateral compared to contralateral hemisphere. LCN2-positive cells co-localized with neurons, and not in astrocytes or microglia. After LCN2

treatment, ramified microglia converted into a long-rod morphology with reduced branches. LCN2 treatment significantly increased IL-10 release from microglia, but didn't change IL-1b levels. LCN2-treated microglia showed enhanced phagocytic capacity, but there were no detectable effects on microglia migration. Conditioned media from LCN2-activated microglia significantly reduced OGD-induced neuronal death.

Conclusions: LCN2 is released by injured neurons during ischemic stroke as an inter-cellular signal that modifies microglial activation and function.

THE PROTECTIVE EFFECTS OF T CELL DEFICIENCY AGAINST BRAIN INJURY ARE ISCHEMIC MODEL-DEPENDENT IN RATS

X. Xiong[1], L. Gu[2], H. Zhang[1], B. Xu[1], S. Zhu[3], H. Zhao[1]

[1]Stanford University, Stanford, CA, USA, [2]Hangzhou Normal University, [3]Zhejiang University, Hangzhou, China

Previous studies have reported that T cell deficiency reduced infarct sizes after transient middle cerebral artery (MCA) suture occlusion in mice. However, how reperfusion and different models affect the detrimental effects of T cells have not been studied. We investigated the effects of T cell deficiency in nude rats using two stroke models and compared their infarct sizes with those in WT rats. In the distal MCA occlusion (MCAo) model, the distal MCA was permanently occluded and the bilateral common carotid arteries (CCAs) were transiently occluded for 60 min. In the suture MCAo model, the MCA was transiently occluded for 100 min by the insertion of a monofilament suture. Our results showed that T cell deficiency resulted in about a 50% reduction in infarct size in the suture MCAo model, whereas it had no effect in the distal MCAo model, suggesting the protective effects of T cell deficiency are dependent on the ischemic model used. We further found more total T cells, CD4 T cells and CD8 T cells in the ischemic brains of WT rats in the suture MCAo model than in the distal MCAo model. In addition, we detected more CD68-expressing macrophages in the ischemic brains of WT rats than in nude rats in the suture MCAo but not the distal MCAo model. Lymphocyte reconstitution in nude rats resulted in larger infarct sizes in the suture MCAo, but not in the distal MCAo stroke model. The results of regional CBF measurement indicated a total reperfusion in the MCAo model but only a partial reperfusion in the distal MCAo model. In conclusion, the protective effects of T cell deficiency on brain injury are dependent on the ischemic model used; likely associated with different degrees of reperfusion.

THE EXPRESSION OF FIBULIN-5 IN RATS AFTER CEREBRAL ISCHEMIA REPERFUSION

G. Xu, X. Qin, T. Tao

Department of Neurology, The First Affiliated Hospital of Chongqing Medical University, Chongqing, China

Background and objective: Cerebral ischemic disease is one of the most common disease harmful to human health with the characterristic of high morbidity and mortality. In the early stage of cerebral ischemia, vascular obstruction results in endothelial cells necrosis and apoptosis, destroy intracellular connection, and then induces blood brain barrier disruption and a subsequent cascade reaction. In addition, the destroy of vascular endothelial cells structure and function are the main reason for postischemic hemorrhage. Therefore, the protection of vascular endothelia cells or vascular stability is a prospective way in cerebrovascular disease. Fibulin-5 (FBLN5) is a widely expressed ECM glycoprotein that colocalizes with elastic fibers and is essential for proper elastic fiber assembly and vasculogenesis. Recently, FBLN5 becomes the research hotspot in vascular stability for its function in increasing adhesion between endothelia cells and basement membrane and restraining migration of endothelia cells. The role of FBLN5 in the process of cerebral ischemia is still uncertain and worth to discussion. This study aimed to observe the expression of FBLN5 in the early stage of cerebral ischemia/reperfusion model of Sprageue-Dawley rats, and to explore a new way in therapeutic of cerebrovascular disease.

Materials and methods: Ninety-six male Sprageue-Dawley rats were randomly divided into 6 groups: the control group, sham-operation group, 6 h, 24 h, 48 h and 72 h groups after ischemia reperfusion. The middle cerebral artery occlusion/reperfusion model was induced by ligation with nylon monofilament. The neurological function score

was obtained after rats postoperative awake. Real-time quantitative PCR (RT-qPCR) was used to detect the level of FBLN5 mRNA expression, and Western blot was performed to evaluate the level of FBLN5 protein expression. The location of FBLN5 within brain tissue was observed with laser confocal microscope.

Results:

①The protein expression of FBLN5 was significantly increased at 6 h after ischemia reperfusion (1.26±0.46, P< 0.05), and reached to the summit at 24 h (1.78±0.48) after reperfusion. The expression of fibulin-5 was lower than 24 h group at 72 h (0.89±0.27) after injury, but still higher than the sham-operation group (0.30±0.14, P< 0.05). The expression of FBLN5 mRNA had the similar expression trendency as the protein expression. FBLN5 became to increase at 6 h after reperfusion, reached to the peak at 24 h and then began to reduce. But its was still higher than the sham

-operation group at 72 h (P< 0.05).

② FBLN5 was mainly expressed in the endothelial cells, and occasionally expressed in the parenchymal cells or endothelial cell cytoplasm.

Conclusions: The expression of FBLN5 was significantly increaseded in the brain of rats after ischemia reperfusion.

This study is supported by the National Science Foundation of China（NO:81271307）.

POST-TREATMENT WITH MIR-181 ANTAGOMIR BY INTRACEREBROVENTRICULAR INFUSION REDUCES INJURY AFTER FOCAL CEREBRAL ISCHEMIA

L. Xu, Y.-B. Ouyang, R. Giffard

Anesthesia, Stanford University, Stanford, CA, USA

Objectives: Our previous study reported increased injury with increased levels of miR-181 and a protective effect of miR-181a antagomir to reduce miR-181a levels when administered the day prior to middle cerebral artery occlusion (MCAO) in male mice(1). miR-181a is a promising target because it reduces levels of both the ER stress protein GRP78 as well as two antiapoptotic proteins, so reducing levels of miR-181 provides protection via several mechanisms. Prior work showed that reducing miR-181 was associated with reduced oxidative stress(1). While treatment before stroke provides proof of principal evidence that anti-miR-181 can protect in acute stroke, treatment after stroke onset will be needed in most cases, and in many cases patients do not present until many hours after stroke onset. Thus to have greater translational relevance we tested the effect of post-ischemia treatment with miR-181a antagomir administered by intracerebroventricular (ICV) injection in a transient focal cerebral ischemia model using mice. Reducing levels of miR-181a should provide protection by increasing levels of protective proteins including GRP78 and antiapoptotic proteins.

Methods: Adult male C57B6 mice were anesthetized and focal cerebral ischemia was produced by 1 hour of MCAO with a silicone-coated 6-0 monofilament followed by reperfusion. Two hours after MCAO the mice were infused ICV with miR-181a antagomir (n=9) or a control (mismatch, MM) ipsilateral to the focal ischemia. The antagomir or the control was mixed with the cationic lipid DOTAP as previously described(1). Two days later, the mice were assessed for neurological deficits using a deficit score, then mouse brains were removed after overdose anesthesia and were stained by TTC to assess infarction volume.

Results: TTC staining and evaluation of the neuroscore showed significantly reduced infarction size and significantly improved neurological deficits in miR-181a antagomir treated mice. The infarction size after miR-181a antagomir treatment (31.9±3.8.6%) compared to control group (49.4±2.3%) was markedly smaller.

Conclusion: These findings indicate that post-treatment with miR-181a antagomir after ischemia has neuroprotective effects against acute ischemic neuronal damage and neurological impairment in mice. The ability to alter levels of several proteins at once makes this a promising future therapeutic target. Targets affected by miR-181a antagomir administered after stroke onset remain to be assessed. miR-181a may be an innovative and effective new target for stroke therapy.

Reference: Ouyang YB, Lu Y, Yue S, Xu L, Xiong X, White RE, Sun X, Giffard RG. miR-

181 regulates GRP78 and influences outcome from cerebral ischemia in vitro and in vivo. *Neurobiology of Disease* **45:** 555-563, 2012.

HOW 24-HOUR BLOOD PRESSURE AND HEART RATE ARE ASSOCIATED WITH PROGRESSIVE MOTOR DEFICITS IN ACUTE PENETRATING ARTERY INFARCTS PATIENTS

Y. Yamamoto, Y. Nagakane, M. Makino

Department of Neurology, Kyoto Second Red Cross Hospital, Kyoto, Japan

Objectives: Penetrating artery infarcts (PAI) often show progressive motor deficits (PMD) in acute stage leading to poor functional outcome. The relationship between acute blood pressure and PMD has yet to be clarified. Compared with casually recorded BP, 24-hour ambulatory BP monitoring (ABPM) has been established to be more accurately correlated with cerebrovascular disease status. We performed ABPM for 101 patients with acute PAI and investigated the relationships between acute ABPM values, and PMD and poor functional outcome represented by modified Rankin scale 3 or more at 3 months after ictus.

Methods: We selected PAI patients who entered our hospital within 24-hour after onset of stroke. Twenty-four-hour ABPM (TM-2431; A&D Company, Ltd) was attached within 24-hours after admission. Systolic/diastolic BP (SBP/DBP) and HR were automatically measured every 30 minutes for 24 hours. We categorized high SBP for 24-hour-SBP average> 150 mmHg, high DBP for 24-hour-DBP average> 85 mmHg and high HR for 24-hour-HR average> 70. Patients with LPAI that are predominantly caused by occlusion of the vessel orifices of lager caliber penetrating artery due to atheromatous plaque are categorized as branch atheromatous disease (BAD).

Results: There were 26 patients who showed PMD (25.7%) and16 patients who showed PF (15.8%). PMD (+) : PMD (-) are as follows; 156.9 : 147.5 mmHg, for 24h-SBP （p=0.036）、89.7 : 85.8 mmHg for 24h-DBP （p=0.13）、74.6 : 68.0 for 24h-PR （p=0.014）and 72.6: 65.1 for night HR (p=0.0072). Logistic regression analysis was performed to calculate OR of each ABPM values for PMD and PF. For PMD, age- and sex- adjusted OR of high SBP was 2.8 (p=0.031), that of high HR was 4.2 (p=0.0049) and that of BAD (vs non-BAD) was 5.4 (p=0.0008). After multivariate analysis, high HR and BAD persist significantly (OR 3.6, p=0.0016, and 4.8, p=0.0026, respectively). For PF, age- and sex- adjusted OR of BAD (vs non-BAD) and PMD (vs non-PMD) were 10.4 (p=0.0005) and 9.5 (p=0.0009).

Conclusions: For PMD, high HR and BAD (vs non-BAD) were independently associated. Especially high night HR was higher in PMD. That may suggest nighttime sympathetic acceleration may be correlated with PMD. Only BAD (vs non-BAD) and PMD (vs non-PMD) were correlated with PF.

GENERATION OF SMALL UBIQUITIN-LIKE MODIFIER (SUMO) TRANSGENIC MICE TO IDENTIFY SUMOYLATED PROTEINS IN POST-ISCHEMIC BRAINS BY QUANTITATIVE PROTEOMIC ANALYSIS

W. Yang, H. Sheng, S. Zhao, L. Wang, W. Paschen

Anesthesiology, Duke University Medical Center, Durham, NC, USA

Objectives: SUMO conjugation is a post-translational protein modification that modulates activity, stability and subcellular localization of proteins. Most of the SUMOylation targets are nuclear proteins involved in gene expression, genome stability, DNA damage repair and degradation of proteins. SUMOylation is dramatically activated after cerebral ischemia and this is believed to be a neuroprotective stress response.[1-3] To identify SUMOylated proteins in post-ischemic brains, we have generated a new SUMO transgenic mouse model with neuron-specific expression of tagged SUMO paralogues.

Methods: Animals (wild-type and transgenic) were subjected to 10 minutes global cerebral ischemia and 1-3 hours of reperfusion. Samples were excised from cortices of wild-type and transgenic mice. Tagged SUMO2 and SUMO3 conjugated proteins were pulled down using anti-HA agarose and anti-Flag M2 agarose beads. For proteomic analysis, eluted SUMO3 conjugated proteins were digested with trypsin and peptides evaluated by Duke Proteomics Facility using MS/MS-based label-free quantitative proteomic analysis.

Results: To establish a transgenic mouse line

in which tagged SUMOs are expressed from a single multicistronic transgene in a conditional manner, we constructed a vector based on Cre/loxP recombination and 2A-mediated co-translational cleavage. In this transgene vector, a loxp-flanked STOP cassette containing multiple transcription termination signals was placed between the CMV early enhancer/chicken β actin (CAG) promoter and SUMO coding sequences. GFP and mCherry fluorescence proteins were incorporated in the vector as indicators of transgene expression in the absence or presence of Cre expression, respectively. Several founders showing strong GFP expression in all organs investigated were obtained and line 10 was further characterized and used in this study. To generate a neuron-specific SUMO transgenic mouse line, we crossbred the line 10 transgenic mice with Emx1-Cre mice. SUMO/Emx1-Cre double transgenic mice exhibited strong mCherry expression in neurons of the entire forebrain. Western blot analysis illustrated a dramatic post-ischemic increase in levels of endogenous and transgenic SUMO2/3-conjugated proteins. Fractionation of brain samples illustrated identical subcellular distribution of endogenous and exogenous SUMO2 and SUMO3, with free and conjugated SUMO being highly concentrated in cytosolic and nuclear fractions respectively. HA-SUMO2 and Flag-SUMO3 were efficiently immunoprecipitated from sham and post-ischemic samples. A pilot proteomic analysis identified several potential SUMO target proteins, including TIF-1β and SAE2, only in samples from transgenic but not wild-type animals, thus illustrating high specificity of the approach. Currently a large-scale proteomic analysis is in progress to identify SUMOylated proteins regulated by ischemia.

Conclusions: Our new SUMO transgenic mouse model will allow performing SUMO proteomic analysis from tissue samples. Identifying SUMO target proteins in post-ischemic neurons will help better understand the impact of the SUMOylation pathway on ischemic outcome and will foster breakthroughs in therapeutic treatment that will harness this potentially fundamental pro-survival response of neurons to metabolic stress.

References:

1. Yang W et al., J Cereb Blood Flow Metabol 2008; 28:269-279;

2. Yang W et al., J Cereb Blood Flow Metabol 2008; 28:892-896;

3. Datwyler AL et al., J Cereb Blood Flow Metabol 2011; 31:2152-2159

NEUROVASCULAR REMODELING IS PROMOTED BY MINOCYCLINE AFTER ACUTE STROKE: IMPROVEMENT MONITORED WITH MRI AND CONFIRMED WITH HISTOLOGY AND BIOCHEMISTRY

Y. Yang[1], Y.R. Yang[2], V.M. Salayandia[1], E.Y. Estrada[1], J.F. Thompson[1], G.A. Rosenberg[1]

[1]Neurology, University of New Mexico School of Medicine, [2]College of Pharmacy, University of New Mexico, Albuquerque, NM, USA

Objectives: Neurovascular remodeling after stroke has been recognized as a promising target for neurologic therapies, but the mechanisms underlying angiogenesis and blood-brain barrier (BBB) restoration are uncertain. We previously reported that matrix metalloproteinases (MMPs) are detrimental in the early stages of ischemic injury by opening BBB and by impairing DNA repair with acceleration of neuronal apoptosis. Hence, we hypothesized that therapies targeting the early detrimental roles of MMP action may improve recovery by limiting cerebral injury after stroke. Minocycline has been shown to reduce reperfusion injury in animal stroke models and human stroke. The neuroprotective effect of minocycline is associated with its ability to interfere with MMP activity and neuroinflammation. This study used MRI to monitor the time course of neurovascular remodeling in response to spontaneous and therapy-induced stroke recovery.

Methods: Adult spontaneously hypertensive rats had a 90 min transient middle cerebral artery occlusion with reperfusion. At the onset of reperfusion they received a single dose of minocycline (3 mg/kg, i.v.). They were studied at multiple times up to 4 weeks with MRI, immunohistochemistry, and biochemistry.

Results: Anatomical T2 MR imaging illustrated that early post-stroke treatment with a single dose minocycline significantly reduced the infarct size in ischemic hemispheres from week 2 to week 4 compared with vehicle-treated animals. Increase in the apparent diffusion coefficient (ADC) value was detected in the ischemic hemispheres from week 2 to

week 4 compared with that at 48 h and 7 days of reperfusion, suggesting increased diffusivity in the regions of tissue loss. Significantly lower ADC values in the minocycline-treated ischemic hemisphere were observed compared with the vehicle-treated brains, while improved white matter recovery was revealed by fractional anisotropy at 4 weeks of reperfusion. Arterial spin labeling showed that improvement of cerebral blood flow within peri-infarct regions with minocycline occurred as early as 7 days after reperfusion.

We previously showed that BBB tight junction proteins (TJPs), which disappeared after reperfusion injury, reappeared in newly formed vessels in peri-infarct regions at 3 weeks, and MMPs are involved in BBB restoration during recovery. At 4 weeks, Western blot showed that post-stroke treatment of minocycline significantly increased levels of TJPs, occludin, ZO-1, and claudin-5 in ischemic hemispheres compared with vehicle-treated animals. Increased MMP-2 and -3 levels were detected in the ischemic hemispheres treated with minocycline. Histological staining demonstrated lower tissue loss in ischemic hemispheres and higher number of microvessels within the peri-infarct regions treated with minocycline. With double-immunofluorescent staining, we also found that active microglia/macrophages, surrounding and within the peri-infarct regions, expressed both pro-inflammatory factors (TNF-a and IL-1b) and anti-inflammatory factors (TGF-b and IL-10) at 4 weeks. Western blot analysis showed that treatment with minocycline significantly reduced levels of TNF-a and IL-1b, and increased levels of TGF-b and IL-10.

Conclusion: Our results suggest that early neuroprotective effect of minocycline significantly promotes neurovascular remodeling during stroke recovery by: 1) reducing brain tissue loss; 2) enhancing newly formed vessels and TJP formation; and 3) accelerating functional transition of microglia activation from pro-inflammatory stage to anti-inflammatory stage.

GLUCOSE METABOLISM AT THE PERI-INFARCT ZONE IN ACUTE ISCHEMIC ANIMAL MODEL

H. Yuan[1], J. Frank[2], Y. Hong[2], H. An[1], C. Eldeniz[3], A. Bunevicius[4], J. Nie[1], W. Lin[1]

[1]Radiology, [2]Biomedical Research Imaging Center, [3]Biomedical Enginnering, [4]Neurology, University of North Carolina at Chapel Hill, Chapel Hill, NC, USA

Hyper-uptake of glucose has been observed in the peri-infarct region in ischemic stroke brain, however insights into its temporal and spatial distribution and its relation with the later tissue outcome remains largely unclear. This study was aimed to delineate temporal and spatial distribution of glucose metabolism at the peri-infarct zone using [^{18}F]-2-fluoro-2-deoxy-D-glucose (FDG) PET imaging in conjunction with MRI in acute ischemia stroke model.

Methods: Intraluminal suture model was used to induce middle cerebral artery occlusion (MCAO) in rats. Animals were divided into non-reperfusion and reperfusion with 24hr survival groups. Non-reperfusion group was used for autoradiography study after PET imaging; and the reperfusion with 24hr survival group was used to study any relationship between early FDG PET results and final lesion. All animals underwent sequential MRI and [18]F-FDG PET imaging after MCAO procedure. FDG was injected at various time after MCAO (ranging from 30 -150min after MCAO) to investigate glucose metabolism at different MCAO duration. MR and PET images from the same animal were registered and FDG uptake in the peri-infarct zone was assessed in relation with parameters derived from MR images including cerebral blood flow (CBF), apparent diffusion coefficient (ADC), and final T2 lesion at 24hrs after MCAO.

Results: Elevated FDG uptake was observed from PET images at the peri-infarct zone, consistent with that observed by autoradiolograpy. Dynamic uptake curves indicated that peri-infarct region had low uptake initially and appeared to surpass the contralateral brain tissue at about 15min after FDG injection independence of the time intervals between MCAO onset and animals receiving FDG. The volume and SUV of the observed elevated FDG uptake regions inversely correlate with the duration of MCAO, suggesting that the spatial extent of the

observed elevated FDG uptake may be modulated by the severity of ischemic injury. Registration with the MRI CBF and ADC maps acquired prior to the PET images also demonstrated a mild reduction of CBF (70.5% ± 4.7%) and ADC (96.1% ±1.6%) in hyper-uptake region when compared to the contralateral hemisphere. When FDG PET images and final T2 images in reperfusion group was compared, overlap ratio between FDG hyper-uptake volume and final T2 lesion was only 12.3% ± 1.8% (n=19), and majority of hyper-uptake tissue was not recruited into final infarct volume.

Conclusion: The study depicted temporal and spatial distribution of FDG uptake in peri-infarct zone in acute ischemic stroke model, and our results strongly suggested that the presence of elevated FDG uptake in the peri-ischemic region during acute ischemic stroke may be indicative of viable tissues.

THE ROLE OF DIFFUSING POTASSIUM IN SPREADING DEPOLARIZATION

B.-J. Zandt[1,2], D. Feuerstein[3], **H. Backes**[4], M. Takagaki[5], H. Ima[5], B. ten Haken[1], M.J.A.M. van Putten[2,6], R. Graf[3]

[1]Neuroimaging, [2]Clinical Neurophysiology, MIRA Institute, University of Twente, Enschede, The Netherlands, [3]Multi-Modal Imaging, [4]Medical Physics, [5]Max Planck Institute for Neurological Research, Cologne, Germany, [6]Department of Clinical Neurophysiology, Medisch Spectrum Twente, Enschede, The Netherlands

Introduction: Spreading depolarization (SD) is a phenomenon that manifests as a slowly travelling (mm/min) wave of depolarization of neuronal membranes, combined with large shifts in ionic concentrations and release of glutamate. SD can be triggered by various stimuli, such as hypoxia/ischemia, tissue damage, electrical stimulation and application of KCl or glutamate [1].

When blood flow and energy supply are sufficient, cells recover from the depolarization within minutes. However, after ischemic insults, depolarization waves can cause damage: SD may play a role in the growth of the core and penumbra, the areas with respectively dead and dysfunctioning cells [2]. Therefore, SD is a potential target for therapy in stroke [3].

Despite fifty years of research, the propagation mechanisms of SD are still not fully described. One contributing mechanism is the release of excitatory substances, potassium and glutamate, into the extracellular space. Passive diffusion or active transport of these substances, for example by glia cells [1], drive the propagation of the SD wave.

Objectives: We assess the role of extracellular transport and diffusion of potassium in the propagation of SD.

Methods: By constructing a reaction-diffusion equation, we derived analytical expressions that describe the time course of the potassium concentration at the front of an SD wave (see figure 1). This curve is characterized by a release rate and a concentration threshold. Together with the diffusion (or transport) coefficient, these parameters determine the velocity of the SD wave.

Experiments were performed to measure concentration time courses of potassium during SD in in vivo rat brain. We obtain from these time courses the release rate, the concentration threshold and the diffusion coefficient. With these parameters we determine which pathways may be used for the movement of potassium, as well as assess the relative contribution of extracellular potassium to the propagation of SD.

Conclusions: The contribution of potassium to SD propagation is assessed. We discuss the implications for preventing SD in patients with ischemic damage.

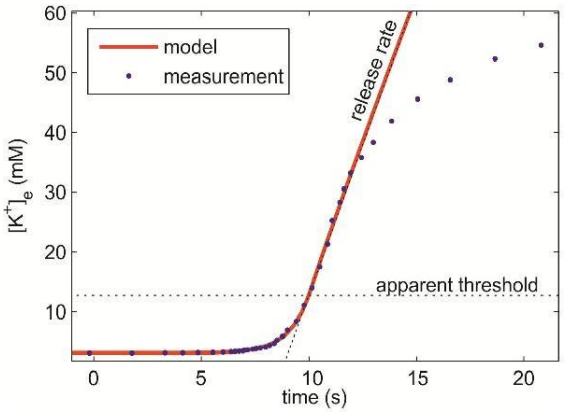

[Figure 1]

Determination of the apparent threshold of potassium during an SD wave. Measurement data from [4].

References:

[1] Somjen GG, Mechanisms of spreading depression and hypoxic spreading depression-like depolarization. Physiol Rev 2001; 81:1065-1096.

[2] Nakamura et al. Spreading depolarizations cycle around and enlarge focal ischaemic brain lesions. Brain 2010: 133

[3] Dreier JP, The role of spreading depression, spreading depolarization and spreading ischemia in neurological disease. 2011; doi:10.1038/nm.2333

[4] Adamek S, Vyskocil F Potassium-selective microelectrode revealed difference in threshold potassium concentration for cortical spreading depression in female and male rat brain. 2011 Brain Res 1370:215-219

NUCLEAR FACTOR E2-RELATED FACTOR 2 (NRF2) ACTIVATION MEDIATES THE NEUROPROTECTIVE EFFECTS OF OMEGA-3 POLYUNSATURATED FATTY ACIDS AGAINST ISCHEMIC STROKE

F. Zhang[1,2], M. Zhang[1,2], S. Wang[1,2], W. Zhang[1], R.K. Leak[3], Y. Gao[1], J. Chen[1,2,4]

[1]State Key Laboratory of Medical Neurobiology, Fudan University, Shanghai, China, [2]Neurology, University of Pittsburgh School of Medicine, [3]Division of Pharmaceutical Sciences, Mylan School of Pharmacy, Duquesne University, [4]Geriatric Research, Educational and Clinical Center, Veterans Affairs Pittsburgh Health Care System, Pittsburgh, PA, USA

Objectives: Omega-3 polyunsaturated fatty acids (n-3 PUFAs) are readily available in fish oil capsules and appear to be a safe and economical prophylaxis against brain disorders and neuroinflammation. For example, n-3 PUFAs are neuroprotective against ischemic stroke, a devastating disease that affects millions of people but lacks effective treatments. However, the protective mechanisms of n-3 PUFAs are not fully understood. We previously showed that n-3 PUFAs upregulate heme oxygenase-1 (HO-1) following ischemia. HO-1 is an Nrf2 target gene. Therefore, this follow-up study was designed to test our hypothesis that n-3 PUFAs activate Nrf2 via an oxidative signaling pathway, mediated by 4-hydroxy-2E-hexenal (4-HHE), a specific end-product of n-3 PUFAs peroxidation.

Methods: Focal brain ischemia was induced by middle cerebral artery occlusion (MCAO; 60 min) in two sets of mice:

1) C57BL/6 mice treated with a regular diet or fish oil-enhanced diet and

2) transgenic mice overexpressing the fatty acid metabolism-1 gene *fat-1*, an enzyme that converts n-6 PUFAs to n-3 PUFAs.

Infarct volumes and neurological dysfunction were evaluated after MCAO. In addition, rat primary neuronal cultures were treated with various n-3 PUFAs, including docosahexaenoic acid (DHA) or eicosapentaenoic acid (EPA) and with alpha, beta-unsaturated carbonyls, including 4-HHE from n-3 PUFAs and 4-hydroxy-2E-nonenal (4-HNE) from n-6 PUFAs. Ischemia was modeled *in vitro* with oxygen-glucose deprivation (OGD; 60 min). Nrf2 activation was detected by its nuclear translocation, NDA binding assay (electrophoretic mobility shift assay, EMSA) and the upregulation of its target phase 2 enzymes.

Results: Infarct volumes were significantly smaller in *fat-1* mice than in their wild-type littermates; fish oil-fed mice were also more resistant to MCAO than mice on a regular diet in both short-term (48 hr) and long-term (21 day) studies. In cultured neurons, DHA or EPA pretreatment (10-100 μM) significantly reduced neuronal death induced by OGD. The protection was associated with increased nuclear translocation and DNA binding activity of Nrf2 as well as HO-1 upregulation. As hypothesized, knockdown of Nrf2 with a specific shRNA significantly attenuated the protective effects of DHA in cultured neurons. Interestingly, low doses of 4-HHE (5-20 μM) also activated Nrf2 and upregulated HO-1 in neuronal cultures; 4-HHE was more effective in activating Nrf2 than 4-HNE, an n-6 PUFA specific carbonyl, as indicated by faster and more potent induction of HO-1 expression. Furthermore, 4-HHE pretreatment increased neuronal resistance to ischemic injury induced by OGD.

Conclusions: Our results demonstrate that n-3 PUFAs robustly protect neurons against ischemic injury *in vitro* and for the long term *in vivo*. The underlying neuroprotective mechanisms involve the activation of Nrf2 by 4-HHE, a specific lipid peroxidation product of

n-3 PUFAs, which can serve as an oxidative signaling molecule. Further studies of the neuroprotective mechanism of n-3 PUFAs and 4-HHE may help develop novel strategies against stroke pathology.

Supported by: NIH grants NS036736, NS43802, NS45048, NS056118, VA Merit Review grant, and AHA grant 10SDG2560122.

DYNAMIC CELLULAR RESPONSE FOLLOWING PHOTOTHROMBOSIS-INDUCED ISCHEMIA

N. Zhang, L. Hailong, S. Ding

Dalton Cardiovascular Research Center, University of Missouri, Columbia, MO, USA

Following ischemic stroke, cells die in ischemic core shortly and the brain experiences a series of alterations including molecular, structural, and functional in the penumbra in ipsilateral hemisphere as well as in contralateral hemisphere. One of the important changes is the scar formation surrounding the infarction region, which is related to cellular proliferation and reactivation, and gene regulation. However, how cellular proliferation and reactivation is dynamically changed over time after focal ischemic stroke is not well understood.

Objectives: To investigate dynamic changes of reactive astrocytes and microglia, and cell proliferation in the penumbra in the cortex after ischemia.

Methods: We used photothrombosis model to induce focal ischemia in the mouse cortex. We used Brdu injection to label proliferating cells in the cortex after ischemia. We injected Brdu in mice in every 2 day up to 12 days in 7 groups of mice following photothrombosis and mice of each group were scarified two days after Brdu injection. We used immunostaining to evaluate the percentage of Brdu+ cells are astrocyte, microglia, and neuron. We used two-photon in vivo microscopy to repeatedly image the same astrocytes in GFAP-GFP mice to monitor astrocyte reactivation in the penumbra over time following ischemia.

Results: Based on GFAP levels from immunostaining and Western Blot analysis, astrocytes became wildly reactivated in the penumbra and in the regions distant from the penumbra in the ipisilateral hemisphere at 2 days after PT, and astrocyte activation reached its peak at 8 days after PT. Eight days later, dense GFAP+ astrocytes were observed in the penumbra and remained thereafter. The morphology of GFAP+ astrocytes in the penumbra experienced significant changes. At 6 days after ischemia, astrocytes in the penumbra were densely packed and formed a stream with their (straight) processes pointing towards the ischemic core. Based on Brdu staining, cellular proliferation was observed mainly from 2 to 6 days after PT, and the number of Brdu+ cells decreased after 8 days following PT. Double immunostaining indicates that the percentage of double positive cells of GFAP and Brdu+ to the total Brdu+ cell is much smaller than double positive cells of Iba1 and Brdu+. Few NeuN+ neurons are Brdu+ positive. In vivo imaging using two-photon fluorescent microscopy revealed that astrocytes experienced morphological changes and new GFP+ astrocytes in the penumbra.

Conclusions: Our results demonstrated that reactive gliosis in the penumbra is highly dependent on the time after ischemia, and proliferating astrocytes only have small contribution to reactive gliosis and the pool of proliferating cells. Microglia proliferation account for a higher percentage of proliferating cells than astrocytes. Results suggest that astrocyte gene regulation, but not proliferation, contributes to glial scar formation.

CASPASE-3 REGULATES ENDOGENOUS NEUROGENESIS AFTER CEREBRAL ISCHEMIA

W. Fan, **B.-Q. Zhao**, Y. Dai, H. Xu, X. Zhu

State Key Laboratory of Medical Neurobiology, Institutes of Brain Science, Fudan University, Shanghai, China

Introduction: The brain has the capacity to regenerate neurons after stroke. Although this neurogenic response may be important for brain repair after injury, the mechanisms underlying stroke-induced neurogenesis are not known. Caspase-3 is a major executioner and has been viewed as a terminal step in the process of programmed cell death. The important role for caspase-3 in neuronal cell death has been demonstrated in a wide range of central nervous system diseases, and acute inhibition of caspase-3 was shown to offer protection of neurons against ischemic and traumatic brain injury. Recently, accumulating data indicate that caspase-3 also participate in

various biological processes that do not cause cell death, such as dendritic pruning, synaptic depression, cell differentiation and proliferation. However, the role of caspase-3 in neurogenesis after stroke is largely unknown.

Methods: We used a permanent focal cerebral ischemia model produced by middle cerebral artery occlusion. Intraperitoneal injections of BrdU (50 mg/kg) were given twice daily during days 5 to 13 after stroke, and animals were killed at 14 or 42 days. Intraventricular injections of the casepase-3 inhibitor Z-DEVD-fmk or vehicle was given twice a week for 2 weeks after stroke. Immunohistochemistry, Western blot analysis and TUNEL staining were performed.

Results: We observed a marked increase in activated caspase-3 in the neurogenic niches at 7-14 days after stroke compared to sham controls. Quantitative analysis showed that the activated caspase-3 enhanced roughly in parallel with the stroke-induced increase in proliferating neuronal precursor cells (NPCs), but not related to an increase in cell death. Furthermore, we found that the proliferating NPCs activate caspase-3 without undergoing apoptosis. At 14 days after stroke, inhibition of caspase-3 activity with Z-DEVD-fmk significantly increased BrdU-positive cells and BrdU and DCX double-positive NPCs in the SVZ and the DG. At 42 days after stroke, Z-DEVD-fmk significantly increased the number of BrdU-positive cells and BrdU-positive neuron in the lesioned cortex and the granular zone of the DG. Finally, we demonstrated that caspase-3 regulated endogenous neurogenesis through a phospho-Akt-dependent pathway.

Conclusion: In the present study, we uncovered a previously unknown caspase-3-dependent mechanism that limits stroke-induced neurogenesis. Considering that caspase-3 also mediates neuronal death during acute stroke, our data should revitalize interest in targeting caspase-3 for treatment of stroke.

THE ROLE OF ZINC IONS IN BRAIN INJURY FOLLOWING TRANSIENT FOCAL CEREBRAL ISCHEMIA IN RATS

Y. Zhao[1], S. Li[1], R. Pan[2], Y. Luo[1], F. Yan[1], X. Ji[1], K. Liu[1,2]

[1]Xuanwu Hospital, Capital Medical University, Beijing, China, [2]Department of Pharmaceutical Sciences, University of New Mexico, Albuquerque, NM, USA

Objectives: Emerging evidence has implicated zinc ion in the pathophysiology of ischemic brain injury. This study investigated the role of zinc in the molecular mechanism of brain injury using a transient focal cerebral ischemia rat model and a membrane-permeable zinc chelator (TPEN) to remove intracellular zinc in the brain.

Methods: Male Sprague-Dawley rats underwent right middle cerebral artery occlusion (MCAO) for 90 min and then reperfusion for 0, 3, 12, 24 and 72 h. TPEN (15 mg/kg) or vehicle was injected intraperitoneally at 30 min prior to MCAO. Neurological deficit score, forelimb foot-fault-placing test, and open-field tests were performed to assess the neurological and motor function of rats. Cerebral infarct volume was measured by TTC-staining. The cytosolic labile zinc level in brain tissue was detected with the zinc-specific fluorescent dyes NG and TSQ. TUNEL staining was performed to elucidate the effect of zinc on apoptosis. The relationship between cytosolic labile zinc and apoptotic cell death in ischemia/reperfusion rats was investigated through the colocalization between TSQ and TUNEL fluorescence. PARP-1 activity was determined using immunohistochemistry with PAR antibody. The cleaved PARP-1 (89 kDa) fragment level were measured by western blot to investigate the effect of zinc on apoptosis.

Results:

1). TPEN treatment dramatically decreased MCAO-induced cerebral infarct volume, indicating that zinc was involved in ischemic cerebral infarction.

2). All three behavioral functional tests showed that compared with vehicle, TPEN administration markedly improved neurological assessment and motor function of ischemic rats.

3). NG and TSQ staining showed that cytosolic labile zinc accumulated in the brain following ischemia and TPEN administration reduced the cytosolic labile zinc.

4). Intraperitoneal injection of TPEN blunted ischemia-induced apoptotic programmed cell death. Co-staining of TSQ and TUNEL fluorescence demonstrated that the majority of TSQ fluorescent cortical neurons displayed TUNEL positive after 24 h reperfusion. Rats pretreated with TPEN displayed fewer TSQ and TUNEL co-located cells in the ischemic region as compared to vehicle, suggesting that cytosolic labile zinc accumulation is associated with apoptotic neuronal death.

5). Treatment with TPEN reduced cleaved PARP-1 level and PAR-positive cells in the ischemic cortex after MCAO, suggesting that zinc contributed to ischemic brain damage through regulating PARP-1 cleavage and PAR accumulation.

Conclusions: Cerebral ischemia results in cytosolic labile zinc accumulation, which is as an important causal factor for the development of neuronal death following ischemic stroke. Zinc-promoted neural apoptosis through PARP-1 activation is a novel mechanism of ischemic brain damage. Chelating zinc could be considered as a potential neuroprotective approach.

References:

1. Bossy-Wetzel E, et al. Neuron, 2004, 41: 351-65.

2. Kitamura Y, et al. J. Pharmacol. Sci., 2006, 100: 142-8.

3. Medvedeva YV, et al. J. Neurosci., 2009, 29: 1105-14.

4. Won SJ, et al. J. Neurosci., 2010, 30: 15409-18.

RHO-ASSOCIATED KINASE INHIBITION AUGMENTS STROKE RECOVERY VIA NEURITE PLASTICITY

Y. Zheng[1], A. Daneshmand[1], F. Blasi[1], N. Yalcin[1], F. Herisson[1], T. Qin[1], M. Balkaya[1], J.N. Camacho[2], J.B. Mandeville[1,3], C. Ayata[1,4]

[1]Radiology, [2]Center for Comparative Medicine, [3]MGH/MIT/HMS Athinoula A. Martinos Center for Biomedical Imaging, [4]Neurology, Massachusetts General Hospital/ Harvard Medical School, Charlestown, MA, USA

Objectives: Stroke is a leading cause of morbidity and mortality worldwide. At least 70% of survivors have residual disability after 3 months. There is no proven pharmacological therapy to enhance neurological recovery and rehabilitation after stroke. Compared to acute therapy, stroke recovery targets a wider therapeutic window and patient population with greater anticipated impact. We investigated the Rho-associated protein kinase as a novel therapeutic target in neurological repair and recovery. Rho-kinase regulates cell polarity, migration, and proliferation in most cell types relevant for stroke, including neurons, astrocytes, oligodendrocytes, vascular endothelium and smooth muscle, and circulating blood cells. Although vascular regulation has been a major focus, Rho-kinase inhibition also has direct effects on neurons to promote axon regeneration, synaptic plasticity and neurogenesis, and has demonstrated promising efficacy on regeneration and repair in CNS disease models such as spinal cord injury.

Methods: C57/BL6 male mice were subjected to 1h filament MCAO. Rho-kinase inhibitor hydroxyfasudil or vehicle was administrated starting 12h after stroke (10 mg/kg, IP, twice per day in first week then once per day in second week). Animals were housed in regular "shoebox" cages, or in an enriched environment allowing physical exercise and social interaction. Acute infarct volumes were quantified using T2/Diffusion Weighted MRI (DWI) at 48h, and subsequent remodeling longitudinally studied using T2/Diffusion Tensor MRI (DTI) at 2, 4, and 8 weeks. Neurological function were examined weekly (adhesive removal, grid walk, corner test, cylinder test) for up to 6 weeks. In addition, a primary neuronal culture model of sublethal 1h oxygen-glucose deprivation (OGD) was developed to study neurite regrowth.

Results: Delayed (12h) administration of hydroxyfasudil after 1h fMCAO did not affect the lesion volume (89±28 vs. 93±35 mm^3, respectively, T2/DWI MRI at 48h) or mortality in mice. All four neurological exams showed improvement in hydroxyfasudil treated groups compared to vehicle, most prominently in grid walk and corner tests. Mice housed in enriched environment displayed a trend of further functional improvement on top of the hydroxyfasudil efficacy. DTI showed white matter remodeling at 2 weeks, which became more conspicuous at 4 weeks and persisted at 8 weeks. Fractional anisotropy was markedly increased in ipsilateral subcortical white matter anterior to the infarct and decreased in ipsilateral internal capsule. Sublethal OGD triggered reversible neurite retraction in primary cultures without causing cell death (LDH and PI/calcein AM). Hydroxyfasudil (10 mM) reduced the number of retracted neurites and promoted reextension when applied after reoxygenation.

Conclusions: These data show that delayed and prolonged treatment with Rho-kinase inhibitor hydroxyfasudil improves neurological outcome in mice after ischemic injury, possibly via axon/neurite regrowth and white matter remodeling. Data suggest that Rho-kinase is a promising therapeutic target to promote stroke recovery and rehabilitation.

INFLUENCE OF PIGMENT EPITHELIUM-DERIVED FACTOR ON NEUROGENESIS AND ANGIOGENESIS AFTER CEREBRAL ISCHEMIA IN THE MOUSE

M. Zille[1], A. Riabinska[2], M. Balkaya[1], M.Y. Terzi[2], V. Prinz[1], B. Schmerl[2], M. Niemminen[2], M. Endres[1], P. Vajkoczy[2], U. Dirnagl[1], A.L. Pina[2]

[1]Department of Experimental Neurology, Center for Stroke Research Berlin, Charite - University Medicine Berlin, [2]Department of Neurosurgery, Charite - University Medicine Berlin, Berlin, Germany

Objectives: Stroke is one of the leading causes of death and disability in the Western societies. Despite the increasing need, the only effective therapy is thrombolysis with recombinant tissue plasminogen activator from which only 7% of the patients can benefit in a time window of up to 4.5 hours [1].

Neurotrophic factors, among others pigment epithelium-derived factor (PEDF), are of increasing interest for therapy because they prevent initialization of cell death while promoting differentiation of neuronal progenitor cells. The endogenous role of PEDF in the CNS has not yet been completely determined, however, its known effects include neurotrophism, neuroprotection [2-3], antitumorigenesis [4], and antiangiogenesis [2-3] and it was shown to be expressed in many areas of the brain.

In this study, we wanted to investigate the effect of PEDF on stroke outcome, neurogenesis and angiogenesis after cerebral ischemia.

Methods: C57Bl6/N mice were implanted with PEDF or CSF (control) osmotic pumps and subjected to transient middle cerebral artery occlusion (MCAO, 60 minutes) 48 hours after pump implantation. Animals received daily BrdU injections (50 mg/kg body weight) for 7 days after MCAO. 24 hours as well as 5 days after reperfusion, T2-weighted magnetic resonance imaging was performed to determine infarct sizes. Pumps were removed on day 5. Behavioral testing (Rotarod, Open Field, Corner Test, Pole Test) was performed between day 8 and 16 after MCAO. After the final behavioral experiment, animals were sacrificed and brains cut and subjected to immunohistochemistry. Brains were analyzed using anti-BrdU (for neurogenesis), TUNEL (for cell death/damage), anti-CD31 (for angiogenesis) as well as cell type-specfic markers (NeuN, GFAP, Iba1).

Results: Preliminary results suggest that mice subjected to MCAO receiving PEDF show decreased infarct sizes and better behavioral outcome compared to controls. They also show increased neurogenesis as revealed by BrdU immunoreactivity. Angiogenesis is modified in animals receiving PEDF compared to CSF only.

Conclusions: Our results support that PEDF can successfully reduce infarct size and improve neurological outcome after cerebral ischemia by modifying angiogenesis and inducing neurogenesis in the brain. Further studies have to be performed to elucidate the molecular mechanisms by which PEDF exerts its effects. Our results give hope to find a therapy for stroke in the future.

References:

1. Wardlaw JM, Murray V, Berge E, del Zoppo

G, Sandercock P, Lindley RL, et al. Recombinant tissue plasminogen activator for acute ischaemic stroke: an updated systematic review and meta-analysis. Lancet. 2012;379:2364-72. doi:S0140-6736(12)60738-7 [pii]

2. Tombran-Tink J. The neuroprotective and angiogenesis inhibitory serpin, PEDF: new insights into phylogeny, function, and signaling. Front Biosci. 2005;10:2131-49. doi:1686 [pii]

3. Tombran-Tink J, Barnstable CJ. PEDF: a multifaceted neurotrophic factor. Nat Rev Neurosci. 2003;4:628-36. doi:10.1038/nrn1176 [pii]

4. Ek ET, Dass CR, Choong PF. Pigment epithelium-derived factor: a multimodal tumor inhibitor. Mol Cancer Ther. 2006;5:1641-6. doi:5/7/1641 [pii]

REAL-TIME MEASUREMENT OF MICRO-VASCULAR CBF AND BLOOD OXYGENATION AFTER THROMBOLYSIS IN PATIENTS WITH ACUTE ISCHEMIC STROKE

P. Zirak[1], R. Delgado-Mederos[2], L. Dinia[2], D. Carrera[2], I. Blanco[1], E. Granell[3], J. Marti-Fabregas[2], T. Durduran[1]

[1]ICFO, Institut de Ciències Fotòniques, Mediterranean Technology Park, Castelldefels, [2]Department of Neurology, Hospital de la Santa Creu i Sant Pau, [3]Department of Radiology, Hospital de la Santa Creu i Sant Pau, Barcelona, Spain

Objectives: To assess potential of hybrid-diffuse-optics[1] for measuring the micro-vascular oxygenation and micro-vascular CBF in the frontal lobes of patients with ischemic stroke due to acute occlusion of the middle-cerebral-artery(MCA) during and after recombinant-tissue-plasminogen-activator(rtPA) therapy.

Methods: Patients with ischemic stroke due to acute MCA occlusion with clinical evidence of involvement of frontal lobe who were selected for treatment with intravenous rtPA(0.9mg/kg) were recruited. Occlusion or recanalization was assessed using a transcranial-Doppler-ultrasound(TCD) with the TIBI flow grade criteria[2].

The hybrid instrument consisted of near-infrared-spectroscopy(CW-NIRS) to measure micro-vascular changes of oxy-hemoglobin(HbO2) and deoxy-hemoglobin(Hb) concentrations and diffuse-correlation-spectroscopy(DCS) for relative-micro-vascular-cerebral-blood-flow(rCBF)[1].

Case1: 91 year old male with right MCA ischemic stroke. A hyperdense right MCA sign was observed at CT. The measurement started 45 minutes after the rtPA infusion at which point TCD showed continued partial occlusion of the right MCA. Admission NIH-stroke-scale(NIHSS) was 16 which increased to 18 at six hours and stayed as such at forty-eight hours. Follow-up TCD confirmed a partial recanalization.Modified-Rankin-scale(mRS) at three months was five. A complete MCA stroke was observed at control CT.

Case2: 92 year old female with left MCA ischemic stroke. A hyper dense left MCA sign was observed by CT. The measurement started 15 minutes after rtPA infusion start. Admission NIHSS was 22 and decreased to 6 at six hours and 1 at forty-eight hours. TCD confirmed a complete recanalization at six hours. mRS at three months was three. Ischemic lesions on the frontal lobe were observed at control CT.

	6 hours after rtPA		
	ΔHbO_2(μM)	**ΔHb(μM)**	**rCBF(%)**
case1			
ischemic side	-0.5±0.5	-3±0.4*	8±13**
healthy side	-0.8±0.7	-0.2±0.9	1±11
case2			
ischemic side	9.7±1.2*	3.2±0.6*	36.6±11*
healthy side	2.9±1.7*	0.9±1.3*	8±7*
Mean±(standard-deviation);* : significant change (U-test, 95% CI);**: marginally significant change.			

[Table 1]

Conclusions: CBF and oxygenation of the both hemispheres increased during the measurement significantly for responsive subject. The non-responsive subject, showed a marginal change for CBF of the ischemic side and significant change for deoxy-

hemoglobin concentration. These measures also correlated with baseline and follow-up NIHSS measures and with patient long term outcome(mRS).

The findings are in agreement with others who measured cerebral tissue oxygenation after recanalization[3] and reperfusion of hypo-perfused tissue upon thrombolysis[4].

The two case studies are promising that the hybrid optical technique may be sensitive to micro-vascular effects of the treatment. More patients are being recruited to evaluate the effects of the intensity and the position of the MCA occlusion as well as the degree and the speed of MCA recanalization on micro-vascular hemodynamics and patient outcome.

Funded by Fundació Cellex Barcelona, Marie Curie(IRG), ISCIII, MICINN, Institució CERCA, Generalitat de Catalunya, FEDER, LASERLAB (FP7).

References:

1. T. Durduran, et al.Rep.Prog.Phys.,73(7):076701,2010.

2. A.M. Demchuk, et al.Stroke,32(1):89-93,2001.

3. H. Nagashima, et al.Surg.neurol.,49(4):420-424,1998.

4. T. Dalkara, et al.JCBFM,32(12):2091-2099,2012.

INHALED NITRIC OXIDE (INO) REDUCES BRAIN DAMAGE AFTER EXPERIMENTAL TRAUMATIC BRAIN INJURY

N.A. Terpolilli[1,2], S.W. Kim[2], S.C. Thal[2,3], W.M. Kuebler[4], N. Plesnila[5]

[1]Neurosurgery, Munich University, [2]Walter Brendel Center for Experimental Medicine, University of Munich, Munich, [3]Anesthesiology, University of Mainz, Mainz, Germany, [4]The Keenan Research Centre, Li Ka Shing Knowledge Institute of St. Michael´s, Toronto, ON, Canada, [5]Institute for Stroke and Dementia Research, University of Munich, Munich, Germany

Objective: We recently demonstrated that inhaled nitric oxide (iNO) reaches the cerebral circulation and leads to selective vasodilation in hypoxic brain regions thus reducing brain damage and improving neurological outcome after experimental ischemic stroke (Terpolilli et al., 2012). Since ischemia, especially regional ischemia in the traumatic penumbra, is a key mechanism determining secondary posttraumatic brain damage we hypothesized that NO inhalation is neuroprotective in a model of experimental traumatic brain injury (TBI) by reducing pericontusional ischemia. The aim of the current study was to evaluate the effect of iNO after experimental Controlled Cortical Impact trauma in mice.

Methods: First we studied possible iNO side effects that might preclude the use of iNO in TBI. Tail bleeding time, systemic mean arterial blood pressure (MAP, A. femoralis catheterization), oxidative damage (immunohistochemistry), intracranial pressure (ICP, intraparenchymal probe), NO - synthase expression in brain tissue (quantitative rt-PCR), and cerebral autoregulation (continuous MAP/ CBF measurements during pharmacological manipulation of MAP) were determined in healthy male C57 bl/6 mice with and without inhalation of 50 ppm iNO. In the second part of the study we studied iNO effects in the early (10-90 minutes after trauma) and longer term (24h - 7d) posttraumatic phase in mice that were subjected to Controlled Cortical Impact (CCI) trauma. iNO was started at different time points after trauma in order to determine a therapeutic window. ICP, cerebral perfusion (Laser Doppler Flowmetry), brain edema formation (wet weight-dry weight method), blood brain barrier disruption (Evans Blue extravasation), lesion volume (histomorphometry in Nissl stained sequential Kryo sections), and neurological outcome (Neurological Severity Score, NSS) were recorded.

Results: NO inhalation significantly improved cerebral blood flow and reduced intracranial pressure after TBI after CCI trauma. Longer-term iNO application over a 24h period caused a reduction of lesion volume, brain edema formation, and blood brain barrier disruption. Neurological outcome as assessed by a muliti-task test was significantly improved up to 7 days. There was no tachyphylaxy; on the contrary, the iNO effect was most pronounced when iNO was initiated within 1 hour after trauma and continued without disruption for 24h. Prolonged exposure to iNO did not influence cerebral auto-regulation, systemic blood pressure, primary homeostasis, endogenous NOS - expression, or oxidative damage.

Conclusion: In the current study NO inhalation effectively reduces brain damage and improves neurological function following TBI without severe systemic side effects. The underlying neuroprotective mechanism most probably consists in a selective dilation of resistance vessels with subsequent increase of cerebral blood flow in the traumatic penumbra, as already demonstrated for cerebral ischemia. NO inhalation has been clinically approved and used for lung diseases for more than 10 years and may therefore represent a promising and safe novel treatment strategy for traumatic brain injury.

References:

Terpolilli,N.A., Kim,S.W., Thal,S.C., Kataoka,H., Zeisig,V., Nitzsche,B., Klaesner,B., Zhu,C., Schwarzmaier,S., Meissner,L., Mamrak,U., Engel,D.C., Drzezga,A., Patel,R.P., Blomgren,K., Barthel,H., Boltze,J., Kuebler,W.M., and Plesnila,N. (2012). Inhalation of nitric oxide prevents ischemic brain damage in experimental stroke by selective dilatation of collateral arterioles. Circ. Res. *110*, 727-738.

OPPOSITE EFFECT OF OXYSTEROLS ON MYELINATION PROCESS IN THE CENTRAL AND PERIPHERAL NERVOUS SYSTEMS AND INTERPLAY WITH WNT PATHWAY

C. Massaad, D. Meffre, J. Grenier, J. Makoukji, G. Shackleford

CNRS, University Paris Descartes, Paris, France

Oxysterols are reactive molecules generated from the oxidation of cholesterol. Few data are available about their functions in myelination of nervous system. Our aim was to study the influence of oxysterols on myelin gene expression and myelin sheath formation by oligodendrocytes (central nervous system), and by Schwann cells (peripheral nervous system). We show by gas chromatography/mass spectrometry that oligodendrocytes and Schwann cells contain 24(S)-hydroxycholesterol, 25-hydroxycholesterol and 27-hydroxycholesterol, and that they express their biosynthetic enzymes and receptors (Liver X Receptors: LXRα and LXRβ). We demonstrate that oxysterols activate the expression of central myelin genes (PLP and MBP) in oligodendrocytes, but inhibit peripheral myelin genes expression (MPZ, PMP22) in a Schwann cells.

In the CNS, we showed that the activating effects of oxysterols were restricted to the cerebellum and dependant of LXR presence as myelin gene expression was drastically reduced in this structure in LXR-KO mice. By, using organotypic cultures of cerebellum slices, we showed that oxysterols were able to stimulate myelin gene expression after lysolecithin-induced demyelination and enhance remyelination process.

In the nerve, the down-regulation of myelin genes is mediated either by LXRα or LXRβ, depending on the promoter context. Importantly, the knockout of LXR in mice results in thinner myelin sheaths surrounding the axons of the nerves (Makoukji et al, J Neuroci 2011). Oxysterols repress peripheral myelin genes via two mechanisms: by binding of LXRs to myelin gene promoters and by inhibiting the Wnt/beta-catenin pathway that is crucial for the expression of myelin genes (Tawk et al, J Neurosci 2011, Makoukji et al, PNAS 2012). Interestingly, oxysterols activate Wnt pathway in the brain.

Altogether our results reveal new mechanisms of action of oxysterols and open new perspectives for the treatment of demyelinating diseases by targeting LXR.

CILOSTAZOL IMPROVES AUTOREGULATORY DYSFUNCTION THROUGH ENOS UPREGULATION IN DIABETIC RATS

S. Takizawa[1], Y. Tsukamoto[1], E. Nagata[1], N. Fukuyama[2]

[1]Division of Neurology, Department of Internal Medicine, [2]Department of Physiology, Tokai University School of Medicine, Isehara, Japan

Objectives: Diabetes leads to autoregulatory dysfunction in smaller arteries, such as cortical branches (CB) of middle cerebral artery, as a result of endothelial damage. Recently, cilostazol, a phosphodiesterase-3 inhibitor, has been clinically used for secondary prevention of ischemic stroke, especially in patients with diabetes[1)]. The aim of the present study is to investigate the effect of cilostazol on autoregulatory responses and endothelial nitric oxide synthase (eNOS) phosphorylation in cerebral small arteries of Otsuka Long-Evans Tokushima Fatty (OLETF) rats as a

model of diabetes, and to compare the results with those in control (LETO) rats.

Methods: Animals were divided into 3 groups: OLETF rats orally given either cilostazol (20-30 g/day for 6 months; n=29) or vehicle (n=22), and LETO rats (n=21). We performed cerebral microangiography in rats anesthetized with pentobarbital under mechanical ventilation using monochromatic synchrotron radiation at SPring-8 and radiographically visualized vasodilation in cortical arteries in response to intravenous administration of acetylcholine (30 pmol/kg/min). The levels of total and phosphorylated eNOS protein in cortex were evaluated by Western blotting.

Results: Arterial diameters in CB were 166±21, 181±38, 186±32 mm in cilostazol-treated OLETF, vehicle-treated OLETF and LETO rats, respectively. In response to acetylcholine, arteries in CB were significantly dilated in cilostazol-treated OLETF (180±35 mm) and LETO rats (215±37 mm), but not in vehicle-treated OLETF rats (147±15 mm). Cilostazol-treated OLETF rats had a significantly higher ratio of phospho-eNOS/total eNOS protein than LETO rats. Cilostazol also increased VEGF protein in striatum of OLETF rats.

Conclusions: It has been reported that cilostazol attenuates ischemic brain injury via activation of eNOS[2)], but it is not clear whether cilostazol affects autoregulatory response in small cerebral arteries. The in-vivo microangiographical procedure we employed can sensitively visualize the autoregulatory response in small cerebral arteries[3)]. Our results indicate that cilostazol has the potential to improve autoregulatory response in cortical cerebral arteries by increasing eNOS phosphorylation in patients with diabetes, and may act as a neurovascular protectant.

References:

1) Shinohara et al., Antiplatelet cilostazol is beneficial in diabetic and/or hypertensive ischemic stroke patients. Subgroup analysis of the cilostazol stroke prevention study. *Cerebrovasc Dis* 26: 63-70, 2008.

2) Oyama et al., Cilostazol, not aspirin, reduces ischemic brain injury via endothelial protection in spontaneously hypertensive rats. *Stroke* 42: 2571-2577, 2011.

3) Yoshino et al., Dilatation of perforating arteries in rat brain in response to systemic hypotension is more sensitive and pronounced than that of pial arterioles. Simultaneous visualization of perforating and cortical vessels by in-vivo microangiography. *Micovasc Res* 77: 230-233, 2009.

EXPOSURE OF DIABETIC RATS TO RECURRENT HYPOGLYCEMIA INCREASES CEREBRAL ISCHEMIC DAMAGE VIA ENHANCED POST-ISCHEMIC MITOCHONDRIAL DYSFUNCTION

K.R. Dave[1], S. Dasani[1], A. Pileggi[2]

[1]Neurology, [2]Diabetes Research Institute, University of Miami, Miami, FL, USA

Objectives: Stroke and heart disease are the most serious complications of diabetes, accounting for more than 84% of the mortality among diabetics (1). Intensive therapy to control blood glucose levels delays the onset and retards the progression of secondary complications of diabetes. The major side effect of intensive therapy in both type 1 and type 2 diabetics is recurrent hypoglycemic (RH) episodes. Earlier we observed that RH exacerbates cerebral ischemic damage in insulin-treated streptozotocin-diabetic rats (2). Because post-ischemic mitochondrial dysfunction plays an important role in cerebral ischemic damage, we tested the hypothesis that post-ischemic mitochondrial dysfunction is severe in RH-exposed diabetic rats.

Methods: Streptozotocin-induced diabetic rats were used as an animal model. Four experimental groups were examined:

1) naïve (non-diabetics, n=6),

2) insulin-treated diabetics (ITD) (n=6),

3) ITD + RH (diabetics on insulin therapy experiencing RH; n=7), and

4) ITD + RH + Glucose (control for additional insulin injected to induce hypoglycemia; n=6).

RH was induced once a day for five days. Global cerebral ischemia was induced the day after the last hypoglycemia treatment by tightening carotid ligatures bilaterally following hypotension (50 mmHg) for eight minutes. Hippocampal mitochondrial function was assessed on the day after induction of global cerebral ischemia by measuring the rate of mitochondrial oxygen consumption in the

presence of different substrates of the mitochondrial electron transport chain.

Results: We observed that the rate of oxygen consumption in the presence of pyruvate and malate was lower in the ITD + RH group by 25% (P< 0.05), 46% (P< 0.001), and 33% (P< 0.001) compared to naïve, ITD, and ITD + RH + Glucose groups, respectively. No statistically significant differences were observed between ITD + RH and the other three control groups when oxygen consumption was measured in the presence of succinate + glycerol-3-phosphate and ascorbate + TMPD as substrates. To confirm results from oxygen consumption studies, we also determined complex I activity enzymatically. Complex I activity was lower in the ITD+RH group by 36% (P< 0.001), 38% (P< 0.001), and 33% (P< 0.01) compared to naïve, ITD, and ITD + RH + Glucose groups, respectively. We are in the process of further characterizing mitochondrial function under these conditions.

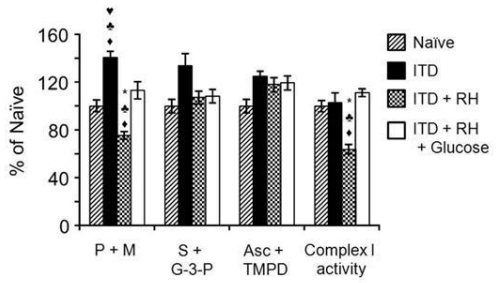

Rate of respiration in presence of pyruvate + Malate (P + M), succinate + glycerol-3-phosphate (S + G-3-P) and ascorbate + TMPD (Asc + TMPD) as substrates and mitochondrial Complex I activity. *, p < 0.05 vs. naïve group. ♥, p < 0.05 vs. naïve group. ♣, p < 0.05 vs. ITD group. ♦, p < 0.05 vs. ITD + RH + Glucose group.

[Figure]

Conclusion: These results demonstrate that RH-induced exacerbation of cerebral ischemic damage in diabetic rats is associated with a lowered rate of respiration in the presence of substrates of complex I of the mitochondrial electron transport chain. These results suggest that enhanced post-ischemic mitochondrial dysfunction may be responsible for exacerbated cerebral ischemic damage in in RH- exposed diabetic rats. Understanding the mechanism by which RH exposure increases cerebral ischemic damage may help lower the severity of ischemic damage in diabetic patients.

References:

1) http://www.diabetes.org/diabetes-basics/diabetes-statistics/ (retrieved on 12/04/2012)

2) Dave et al. Stroke. 2008; 39:50.

This study was supported by AHA (0735106N) and NIH (NS073779).

QUERCETIN PREVENTS MITOCHONDRIAL DYSFUNCTIONS AND BEHAVIORAL DEFICITS IN RODENT MODEL OF HUNTINGTON´S DISEASE

R. Sandhir, A. Mehrotra

Department of Biochemistry, Panjab University, Chandigarh, India

The study was designed to investigate the beneficial effect of quercetin supplementation in 3-nitropropionic acid (3-NP) induced model of Huntington´s disease (HD). HD was induced in rats by administering sub-chronic dose of 3-NP, intraperitoneally, twice daily for 17days. Quercetin was supplemented at a dose of 25mg/kg body weight by oral gavage for 21days. At the end of treatment, mitochondrial bioenergetics, mitochondrial swelling, oxidative stress, neurobehavioral deficits and histopathological changes were analyzed. Quercetin supplementation was able to reverse 3-NP induced inhibition of respiratory chain complexes, restore ATP levels, attenuate mitochondrial oxidative stress in terms of lipid peroxidation and prevent mitochondrial swelling. Quercetin administration also restored the activities of superoxide dismutase and catalase along with thiol content in 3-NP treated animals. Beneficial effect of quercetin administration was observed on 3-NP induced motor deficits analyzed by narrow beam walk and footprint analysis. Histopathological analysis of 3-NP treated rats revealed pyknotic nuclei and astrogliosis in striatum, which were reduced or absent in quercetin supplemented animals. Altogether, our results show that quercetin supplementation to 3-NP induced HD animals ameliorated mitochondrial dysfunctions, oxidative stress and neurobehavioral deficits in rats showing potential of this flavonoid in maintaining mitochondrial functions, suggesting a putative role of quercetin in HD management.

MITOCHONDRIAL BIOGENESIS CONTRIBUTES TO THE NEUROPROTECTIVE EFFECT OF LPS PRECONDITIONING AGAINST GLOBAL CEREBRAL ISCHEMIA VIA INDUCTION OF NRF1

R. Stetler[1,2], S. Lu[1], S.H. Hassan[2], F. Zhang[1,2], Z. Weng[2], Y. Gao[1], J. Chen[1,2]

[1]State Key Laboratory of Medical Neurobiology and Institute of Brain Science, Fudan University, Shanghai, China, [2]Department of Neurology and Center of Cerebrovascular Disease Research, University of Pittsburgh, Pittsburgh, PA, USA

Objectives: We have recently demonstrated that the exposure of cultured neurons to the sublethal preconditioning stimulus lipopolysacchride (LPS) prior to a subsequent ischemic challenge induces mitochondrial biogenesis, and that this induction contributes to LPS-mediated neuroprotection. However, the role of mitochondrial biogenesis in animal models of cerebral ischemia has not been been demonstrated. Using the four-vessel occlusion model of global cerebral ischemia, we explored the contribution of mitochondrial biogenesis to the neuroprotection afforded by LPS preconditioning.

Methods: Male Sprague-Dawley rats (300-350g) were administered a sublethal LPS challenge by intraventricular injection of LPS (3 µg). Tissue was assessed for evidence of mitochondrial biogenesis 24-72 h following injection using in situ hybridization, RT-PCR and immunohistochemistry. For global ischemic studies, 48 h following LPS administration or saline control, animals were subjected to 12 minutes of global cerebral ischemia by undergoing permanent coagulation of the vertebral arteries followed by transient occlusion of the carotid arteries. Blood pressure, blood gases, and blood glucose concentration were monitored and maintained within normal ranges throughout the procedures. Rectal temperature was kept at 37 to 37.5°C in all animals using a heating pad and lamp. Brain temperature was monitored in randomly selected animals using a 29-ga thermocouple implanted into the left striatum, and was kept at 36.4±0.2°C during ischemia and 37 to 37.5°C afterwards. EEG was performed to ensure isoelectricity within 10 s after carotid artery occlusion. To determine the role of the mitochondrial biogenesis-related transcription factor NRF1 in neuroprotection afforded by LPS preconditioning, an AAV vector encoding siRNA targeting NRF1 or a scrambled control was infused into the CA1 sector in the dorsal hippocampus at the rate of 0.1 ul/min over 50 min via a custom-made convection-enhanced microinfusion system linked to a UMP2 microsyringe pump 14 days before LPS administration.

Results: LPS preconditioning significantly increased CA1 neuron survival at 96 h after transient global ischemia. LPS preconditioning alone significantly induced the expression of the NRF1 and TFAM, critical transcription factors required for mitochondrial biogenesis within 24 h following LPS exposure. Similarly, a delayed increase in mitochondrial DNA (mtDNA) content was observed 48-72 h following LPS administration, as well as increased expression of the mitochondrial outer membrane protein TOM20 in neurons of the CA1. These effects were abolished by the knockdown of NRF1, indicating that LPS induces TFAM expression and mtDNA content via NRF1 upregulation. Ischemic neuroprotection afforded by LPS preconditioning was impaired by the knockdown of NRF1, indicating that mitochondrial biogenesis plays a significant role in LPS tolerance to global ischemic neuronal injury.

Conclusions: Our findings indicate that LPS preconditioning induces markers of mitochondrial biogenesis in a global cerebral ischemic animal model via the upregulation of NRF1. Importantly, NRF1 significantly contributes to LPS-mediated neuroprotection against a subsequent ischemic event *in vivo*. These results support a role for mitochondrial biogenesis in preconditioning-afforded neuroprotective effect against ischemic brain injury.

ROLE OF PARL/HTRA2 PATHWAY IN STRIATAL NEURONAL INJURY AFTER GLOBAL CEREBRAL ISCHEMIA

H. Yoshioka[1,2], T. Yagi[1], T. Wakai[1,2], K. Hashimoto[1], P.H. Chan[2], H. Kinouchi[1]

[1]Department of Neurosurgery, University of Yamanashi, Chuo, Japan, [2]Neurosurgery, Stanford University, Stanford, CA, USA

Background and purpose: Presenilin-associated, rhomboid like (PARL) and high temperature requirement factor A2 (HtrA2) play a pivotal role in mitochondrial dysfunction, a key step in ischemic neuronal injury. Mature form of HtrA2, which is processed with PARL

in mitochondria, maintains mitochondrial integrity in physiological condition. Upon apoptotic stimuli, HtrA2 is released into the cytosol, where it induces cell death via inhibiting X-linked inhibitor of apoptosis protein (XIAP) [1,2]. Although HtrA2 is supposed to play an important role in ischemic neuronal injury[3], the exact role of PARL and HtrA2 in cerebral ischemia has not been elucidated. The purpose of this study is to clarify the role of PARL and HtrA2 in the striatal neuronal injury after transient global cerebral ischemia.

Material and methods: C57BL/6 male mice were subjected to 17 or 22 minutes of bilateral common carotid artery occlusion, and neuronal injury was assessed in the striatum. Expression of PARL and HtrA2 in the striatum after 22 minute-ischemia was studied using Western blot analysis and immunohistochemistry. The interaction between HtrA2 and PARL or XIAP was examined by coimmunoprecipitation. The effects of PARL-siRNA administration on processing of HtrA2 and ischemic neuronal injury were analyzed.

Results: Western blot and coimmunoprecipitation analyses revealed that PARL and processed HtrA2 localized to mitochondria in sham animals, and that PARL was bound to HtrA2. Expression of PARL and processed HtrA2 in mitochondria significantly decreased 6-72 hours after 22 minute-ischemia, and the binding of PARL and HtrA2 was disappeared after ischemia. On the other hand, processed HtrA2 was released into the cytosol, and was bound to XIAP 24 hours after ischemia. Administration of PARL-siRNA inhibited processing of HtrA2, and worsened ischemic neuronal injury. The number of TUNEL-positive cells in the PARL-siRNA group increased 5.2- ($P < 0.05$) and 1.1-fold compared to those of the control-siRNA group in the 17 and 22 minutes group, respectively.

Conclusion: Our results indicate that down-regulation of PARL after ischemia inhibits processing of HtrA2, which increases cell vulnerability. In addition, processed HtrA2 released into the cytosol after ischemia contributes ischemic injury via inhibiting XIAP.

References:

1. Vande Walle L, Lamkanfi M, Vandenabeele P. The mitochondrial serine protease HtrA2/Omi: an overview. *Cell Death Differ*. 2008;15:453-460.

2. Chao J-R, Parganas E, Boyd K, Hong CY, Opferman JT, Ihle JN. Hax1-mediated processing of HtrA2 by Parl allows survival of lymphocytes and neurons. *Nature*. 2008;452:98-102.

3. Saito A, Hayashi T, Okuno S, Nishi T, Chan PH. Modulation of the Omi/HtrA2 signaling pathway after transient focal cerebral ischemia in mouse brains that overexpress SOD1. *Brain Res Mol Brain Res*. 2004;127:89-95.

LONG-TERM EXPOSURE TO NUCLEOSIDE ANALOGUES RESULT IN MITOCHONDRAL DNA LOST IN MOUSE CORTICAL NEURONS

Y. Zhang, F. Song, L. Qiao, **D. Chen**

STD/AIDS Research Center, Beijing You An Hospital, Beijing Institute of Hepatology, Capital Medical University, Beijing, China

Nucleoside analogue reverse transcriptase inhibitors (NRTIs), an integral component of highly active antiretroviral therapy (HAART), were widely used to inhibit HIV replication. Long-term exposure to NRTIs can result in mitochondral toxicity which manifests as lipoatrophy, lactic acidosis, cardiomyopathy and myopathy, as well as polyneuropathy. But the cerebral neurotoxicity of NRTIs which is restricted by blood-brain barrier and microenvironment of the central nervous system is still not wellknown. In this study, the Balb/c mice were administered 50 mg/kg stavudine (D4T), 100 mg/kg zidovudine (AZT), 50 mg/kg lamivudine (3TC) and 50mg/kg didanosine (DDI) per day by intraperitoneal injection, five days per week for one or four months, and primary cultured cortical neurons were exposed to 25mM D4T, 50mM AZT, 25mM 3TC or 25mM DDI for seven days. Then, single neuron was captured from mouse cerebral cortical tissues by laser capture microdissection. Mitochondrial DNA (mtDNA) levels of the primary cultured cortical neurons and captured neurons and the tissues of brains and livers and muscles were analysis by relative quantitative real-time PCR. The data showed that mtDNA did not lost in both NRTIs exposed cultured neurons and one month NRTIs fed mouse brains. In four months NRTIs fed mice, brain mtDNA levels remained unchanged even if the mtDNA levels of liver (except for 3TC) and muscle significantly decreased. However, the captured neurons from mtDNA unchanged brains had

significant mtDNA loss. These results suggest that long-term exposure to NRTIs can result in mtDNA lost in mice cortical neurons.

NEUROPROTECTIVE EFFECTS OF METHOXYPENTADECAN ISOLATED FROM *UNCARIA SINENSIS* IN PRIMARY CULTURED CORTICAL NEURONS AND PHOTOTHROMBOTIC STROKE MODEL

J.Y. Jang, H.N. Kim, Y.R. Kim, H.K. Shin, **B.T. Choi**

School of Korean Medicine, Pusan National University, Yangsan, Republic of Korea

The present study was to investigate the neuroprotective effects of a novel methoxypentadecan from *Uncaria sinensis* against glutamate-induced toxicity in primary cultured cortical cells and in photothrombotic rats. Pretreatment with methoxypentadecan resulted in significantly reduced glutamate-induced cell death in a dose-dependent manner. Moreover, pretreatment with methoxypentadecan resulted in decreased the glutamate-induced neuronal apoptotic death, as assessed by hoechst 33342 staining. To clarify the neuroprotective mechanism of methoxypentadecan, we have explored the downstream signaling pathways of N-methyl-D-aspartate receptor (NMDAR)-mediated calpain activation. We found that glutamate treatment leads to the rapid and transient activation of NMDAR NR2B subunit, which in turn leads to activation of STEP and subsequent activation of p38 MAPK. However, pretreatment with methoxypentadecan resulted in significantly attenuated activation of NMDAR NR2B subunit and a decrease in activation of STEP, leading to subsequent p38 MAPK attenuation. Furthermore, in photothrombotic model, methoxypentadecan also significantly reduced infarct volume, edema size and improved neurological function in a concentration-dependent manner. In addition, we found that methoxypentadecan effectively prevent cerebral ischemic damage by down-regulating calpain activity and results in the degradation of active STEP and relieves p38 MAPK activation. These results suggest that the neuroprotective effects of methoxypentadecan were associated with downregulation of NMDAR NR2B subunit-mediated calpain activation and reduction in both the activity of STEP and p38 MAPK activation.

ELECTROACUPUNCTURE CONFERS NEUROPROTECTIVE EFFECTS BY INHIBITING IONOTROPIC GLUTAMATE RECEPTORS AND APOPTOTIC PATHWAYS IN FOCAL CEREBRAL ISCHEMIA IN RATS

Y.R. Kim, H.N. Kim, J.Y. Jang, J.U. Baek, H.K. Shin, **B.T. Choi**

School of Korean Medicine, Pusan National University, Yangsan, Republic of Korea

We investigated the molecular mechanisms underlying the neuroprotective effects of electroacupuncture (EA) to cerebral ischemia in a rat middle cerebral artery occlusion (MCAO) model. Bilateral 2 Hz EA stimulations (1 mA) at acupoints corresponding to Baihui (GV20) and Qihai (CV6) in men strongly reduced infarct volume and improved neurological outcome after stroke. When we focused on the glutamate-evoked excitotoxic injury with coupled pathways, N-methyl-D-aspartate receptor (NMDAR) NR2A and NR2B and α-amino-3-hydroxy-5-methyl-4-isoxazolepropionic acid receptor (AMPAR) GluR2 subunit phosphorylation were significantly arrested by EA treatment in the parietal cortex of the brain. On the contrary, phosphatidylinositol-3 kinase (PI3K) and Akt phosphorylation markedly increased. Moreover, EA treatment significantly decreased the number of apoptotic cells identified by Hoechst 33342 and TUNEL staining. When we analyzed for proteins involved in neuronal apoptosis, EA treatment significantly reduced the expression of death receptor (DR) 5. But, higher expression of anti-apoptotic Bcl-2 and Bcl-X_L, and cIAP-1 and cIAP-2 were detected in EA-treated cerebral cortex. Activities of caspase-3, -8 and -9 in the ischemic cortex were also strongly inhibited by EA treatment. Treatment of MCAO rats with the selective PI3K/Akt pathway inhibitor LY-294002 revealed abrogated neuroprotective effects induced by EA. These results suggest that the neuroprotective effects of EA were associated with reduction of NMDAR and AMPAR phosphorylation and with inhibition of both death receptor and mitochondrial apoptotic pathway. The PI3K/Akt pathway may mainly contribute to EA-induced neuroprotection after stroke.

LATENT TGF-B-BINDING PROTEIN 1 (LTBP-1), A NOVEL SUBSTRATE FOR THE CARASIL-ASSOCIATED PROTEASE HTRA1

C. Haffner[1], N. Beaufort[1], E. Scharrer[1], M. Ehrmann[2], M. Dichgans[1]

[1]Institute for Stroke and Dementia Research, Medical Centre, Ludwig-Maximilians-University, Munich, [2]Centre for Medical Biotechnology, Faculty of Biology, University Duisburg-Essen, Essen, Germany

Objectives: Cerebral autosomal recessive arteriopathy with subcortical infarcts and leucencephalopathy (CARASIL) is an inherited non-hypertensive small vessel disease leading to early-onset ischemic stroke and progressive dementia. It is caused by loss-of-function mutations in the high temperature requirement A1 (HtrA1) gene encoding a secreted serine protease with a putative role in the transforming growth factor-β (TGF-β) signaling pathway [1]. While HtrA1-mediated cleavage of TGF-β has been proposed to be affected in CARASIL patients [2], other components of this pathway might contribute to disease pathology. We investigated latent TGF-β-binding protein 1 (LTBP-1), the predominant TGF-β interactor and regulator of TGF-β bioavailability within the extracellular matrix, as potential HtrA1 substrate.

Methods: Purified HtrA1 and supernatants from LTBP-1 expressing cells were used in protease assays and proteolytic products were identified by immunoblotting. Cleavage specificity and cleavage site location were analysed using HtrA1-deficient fibroblasts from knockout mice and LTBP-1 deletion constructs. To study the binding properties of processed LTBP-1, we developed a solid-phase enzyme immunoassay using the extracellular matrix component fibronectin.

Results: LTBP-1 was found to be processed by HtrA1 at a distinct cleavage site under physiological protease concentrations. Cleavage occurs within the N-terminal fibronectin binding domain of LTBP-1 and is abolished when CARASIL-mutated HtrA1 or HtrA1-deficient cells are used. The LTBP-1 - fibronectin interaction is strongly reduced after HtrA1 treatment when analysed in the *in vitro* binding assay. The effects of LTBP-1 proteolysis on TGF-β activity will be discussed.

Conclusions: LTBP-1 is a novel HtrA1 substrate cleaved at physiological conditions. Conceivably, this might affect structure and function of the extracellular matrix and TGF-β bioavailability within vessels. We propose that loss of LTBP-1 processing in CARASIL patients could be a key event in the development of disease pathology.

References:

1. Hara, K. et al. Association of HtrA1 mutations and familial ischemic cerebral small-vessel disease (2009). *N. Engl. J. Med.*, 360: 1729-39.

2. Shiga, A. et al. Cerebral small-vessel disease protein HtrA1 controls the amount of TGFβ1 via cleavage of pro TGFβ1 (2011). *Hum. Mol. Genet.* 20: 1800-10.

MKP-1 IS INDUCED RAPIDLY AFTER ISCHEMIC STRESS IN NEURON AT PERI-INFARCT AREA AND SHOW NEUROPROTECTION AGAINST OXIDATIVE STRESS *IN VITRO*

H. Horikawa[1], H. Imai[1], C. Murata[2], H. Ono[1], S. Miyawaki[1], T. Ochi[1], A. Ito[1], S. Torii[2], N. Saito[1]

[1]Department of Neurosurgery, The University of Tokyo Graduate School of Medicine, Tokyo, [2]Department of Molecular Medicine, Institute for Molecular and Cellular Regulation, Gunma University, Maebashi, Japan

Objectives: Central nervous system is especially vulnerable to ischemia. Multiple pathways were identified the process of ischemic injury. To analyze the mechanism of ischemic damage or recovery process from ischemia, we performed a microarray analysis of a CA1 region gene expression with rat global ischemia model. We previously showed that Mitogen Activated Protein Kinase Phosphatase-1 (MKP-1) was the most up-regulated gene in much gene expression changes observed under ischemic stress [1]. (Q-PCR revealed a 10-fold increase in MKP-1 mRNA after ischemic insult) MKP-1, a member of the dual specific MKP family phosphatases, negatively regulates Mitogen Activated Protein Kinases (MAPKs) activities through dephospholylation of either Thr or Thy residue. The purpose of this study is to investigate expression and function of MKP-1 and MAPKs in ischemia using both rat permanent MCA occlusion model and HT22 cell model.

Methods: Rat permanent MCA occlusion model was used for evaluating the expression pattern of MKP-1 and MAPKs. MCA occlusion was induced as previously described with modification. Rats were sacrificed at several time points (30min-7day, control, sham, n=3 in each group). Spatiotemporal expression pattern was examined by *in situ* hybridization, qRT-PCR, and immunohistochemistry. HT22 cells originally derived from mouse hippocampus were used as an *in vitro* model for studying the mechanism of neuron under oxidative stress. After glutamate treatment, HT22 cells were extracted to assess the expression pattern of MKP-1 protein and its mRNA by immunoblotting and qRT-PCR, respectively. To verify the effect of MKP-1 for HT22 cell death, MKP-1 was exogenously overexpressed by an adenovirus. Cell viability was assessed by both LDH assay and trypan blue dye exclusion test.

Results: MKP-1 mRNA was induced specifically at peri-infarct area after MCA occlusion immediately and reached it to 8-fold at 3h point. Subsequently, the expression level decreased to a basal level. Similarly, MKP-1 protein induced was observed at peri-infarct area, and MKP-1 positive cells mostly co-localized with neuronal marker NeuN (at 1h point), showing that MKP-1 expresses in neuron at peri-infarct area. We also investigated the expression pattern of total and phosphorylated MAPKs. As the result, strong expression of phosphorylated ERK was detected at peri-infarct area ahead of MKP-1. In addition, rapid activation of ERK, phospho-ERK (pERK), was observed in response to oxidative stress in HT22 cells. Following the activation, the expression of MKP-1 mRNA and protein increased subsequently. These results suggest spatiotemporal correlation between the expressions of MKP-1 and pERK under oxidative stress. At the *in vitro* assay, adenovirus-mediated overexpression of MKP-1 significantly reduced glutamate-induced cell death.

Conclusions: This study revealed that ischemic stress immediately activates ERK specifically at peri-infarct area and that subsequently induce MKP-1 expression in neuron. MKP-1 plays a role in negatively regulating the activation of MAPKs especially ERK under ischemia, resulting in the neuroprotection under oxidative stress.

References: Kawahara, N., et al., *Genome-wide gene expression analysis for induced ischemic tolerance and delayed neuronal death following transient global ischemia in rats.* J Cereb Blood Flow Metab, 2004. **24**(2): p. 212-23.

PHOSPHORYLATION AND ASSEMBLY OF GLUTAMATE RECEPTORS AFTER BRAIN ISCHEMIA

T. Luo[1], F. Zhang[1], A. Guo[2], C. Liu[1], B. Hu[1]

[1]Center for Shock, Trauma and Anesthesiology Research, Baltimore, MD, [2]Cell Signaling Tech, Danvers, MA, USA

Objectives: Synaptic assembly of glutamate receptors plays a key role in neuronal plasticity, but over-assembly of synaptic glutamate receptors leads to excitotoxicity. The goal of this study is to investigate phosphorylation and assembly of AMPA and NMDA receptors after brain ischemia with reperfusion (I/R).

Methods: Rats were subjected to 15 min of global ischemia followed by 0.5, 4, and 24 h of reperfusion. Phosphotyrosine (Ptyr) peptides of glutamate receptors in synaptosomal fraction after I/R were identified and quantified by state-of-the-art immuno-affinity purification of Ptyr peptides followed by LC-MS/MS analysis (IAP-LC/MS/MS). Glutamate receptor phosphorylation and synaptic assembly after I/R were studied by biochemical methods.

Results: Numerous Ptyr sites of AMPA and NMDA were upregulated by about 2- to 37-fold after I/R. A core glutamate receptor kinase, Src kinase, was significantly activated. GluR2/3 and NR2A/B were rapidly clustered from extrasynaptic to synaptic membrane fractions after I/R. GluR2/3 was then translocated into the intracellular pool, whereas NR2A/B remained in the synaptic fraction for as long as 24 h. Consistently, trafficking-related phosphorylation of GluR2/3-S880 was significantly but transiently upregulated, whereas NR2A/B-Y1246 and -Y1472 were significantly and persistently upregulated after I/R.

Conclusions: Phosphorylation of glutamate receptors at synapses may lead to over-assembly of glutamate receptors, probably via activation of Src family kinases, after I/R.

This study is supported by NS040407 and NS03136 (BRH).

MECHANISM OF MORPHINE ON THE EXCITABILITY OF DOPAMINE NEURONS IN THE RAT VENTRAL TEGMENTAL AREA

C. Ming, Z. Ping

State Key Laboratory of Medical Neurobiology and Institutes of Brain Science, Fudan University, Shanghai, China

The dopamine neurons within the ventral tegmental area (VTA) have been known to play a central role in the development of drug addiction. The main model for the acute morphine action on the dopamine neurons of the VTA is the disinhibition model, which proposes that morphine excites the VTA-dopamine neurons by a disinhibitory mechanism involving a decrease in the inhibitory GABAergic inputs[1]. In addition, in recent studies by Jalabert et al[2], an important finding is that blocking glutamatergic signaling in the VTA suppresses the morphine-induced dopamine neuron excitation. However, how acute morphine increases the glutamatergic inputs to the dopamine neurons in the VTA remains unknown. In the present study, we explored the mechanism underlying the excitatory effect of acute morphine on the glutamatergic inputs to the dopamine neurons in the VTA using the whole-cell patch clamp method combined with pharmacological approaches.

Preparation of VTA slices and whole-cell recording. Rats were anesthetized with chloral hydrate (400mg/kg, i.p.). Briefly, following decapitation, the brain was quickly removed and submerged in ice-cold artificial CSF (ACSF) containing the following (in mM): 126 NaCl, 5 KCl, 2 $CaCl_2$, 2 $MgSO_4$, 1.25 NaH_2PO_4, 26 $NaHCO_3$, 10 glucose, 10 sucrose and saturated with 95%O_2/5%CO_2. A block of tissue containing VTA was cut and placed on a layer of moistened filter paper glued to the cutting stage of a vibratome (VT1000M/E; Leica). Serial coronal slices (250 μm) were cut and transferred to an incubating chamber (30-32°C), where they stayed for at least 1 h before recordings were begun. Whole-cell voltage-clamp recordings were made using patch electrodes (2-3MΩ) containing the following (in mM): 140 K-gluconate, 0.1 $CaCl_2$, 2 $MgCl_2$, 1 EGTA, 2 ATP·K_2, 0.1 GTP·Na_3, 2 Lucifer yellow, and 10 HEPES, pH 7.4. Voltage and current signals were recorded with an EPC10 amplifier (HEKA). The data were digitized and stored on disks using PatchMaster (HEKA). sEPSCs were recorded in the holding potential of -70 mV under a voltage clamp mode in the presence of picrotoxin (100μM), which was included in electrode solution to block $GABA_A$ receptors. Fire were recorded in the holding current of 0 pA under a current clamp mode.

The results showed that the enhancement of spontaneous firing in dopamine neurons by morphine was dependent on the excitatory transmission. Morphine increased the glutamatergic transmission through the disinhibition of $GABA_B$ receptor which expressed on the glutamate terminals and tonic inhibited the glutamatergic transmission in normal condition. On the other hand, Morphine inhibited the glutamatergic transmission through activation of MOR. The combined effect of excitation and inhibition showed enhancement of the glutamatergic transmission. These results show the anatomical organization and functional role of local neuronal circuit for acute morphine action on dopamine neurons.

[1] Johnson, S.W. and R.A. North. Opioids excite dopamine neurons by hyperpolarization of local interneurons. J Neurosci. 1992, 12(2): 483-88

[2] Jalabert, M., R. Bourdy, J. Courtin, et al. Neuronal circuits underlying acute morphine action on dopamine neurons. Proc Natl Acad Sci U S A. 2011, 108(39): 16446-50

VEGF UPREGULATES HOMER1A GENE EXPRESSION VIA THE MITOGEN-ACTIVATED PROTEIN KINASE CASCADE IN CULTURED CORTEX NEURONS

Y. Wang, Z. Fei

Xijing Hospital, The Fourth Military Medical University, Xi'an, China

In alternative splice variants of Homer 1 transcripts, Homer 1a messenger RNA (mRNA) has been shown to be upregulated selectively and rapidly by neural stimulation and represents a member of the immediate early gene (IEG) family. In our study, Homer 1 variants were expressed in cultured neurons as investigated by RT-PCR and Western blot analysis. After stimulation of VEGF, neurons selectively upregulated Homer 1a mRNA via Flk-1.The induction of Homer 1a mRNA peaked at 2hr and sustained to 8 hr, while no significant change was observed of Homer 1b/c mRNA levels. Inhibitor analysis as well as

Western blot analysis has indicated that the mitogen-activated protein kinase (MAPK)/extracellular signal-regulated kinase (ERK) cascade plays an important role in VEGF-stimulated induction of Homer 1a mRNA. These results demonstrate that MAPK is a key mediator that links distinct extracellular VEGF stimuli to the transcriptional activation of Homer 1a mRNA.

DALESCONOLS B ACTIVATES NRF2/HO-1 SIGNALLING AND MEDIATES THE ANTI-INFLAMMATORY EFFECTS IN LPS-INDUCED BV2 MICROGLIAV

L. Han[1], K. Yin[1], Z. Wu[1], **Y. Xu**[1,2]

[1]Department of Neurology, Affiliated Drum Tower Hospital of Nanjing University Medical School, [2]Institute of Functional Biomolecules, State Key Laboratory of Pharmaceutical Biotechnology, Nanjing University, Nanjing, China

Objectives: Therapeutic strategies designed to inhibit the activation of microglia may lead to significant advancement in the treatment of most neurodegenerative diseases. Dalesconols B, also termed as TL2, is a newly found polyketide from a mantis-associated fungus and has been reported to exert potent anti-oxidant and immunosuppressive effects. The transcription factor Nrf2 has been reported to play key roles in modulating neuroinflammation in brain via induction of cellular antioxidant enzymes such as heme oxygenase-1 (HO-1). Therefore, the present study was designed to investigate:

1) the anti-inflammatory effects of TL2 in LPS-induced BV2 microglia, and

2) whether this effect was associated with Nrf2/HO-1 activation.

Methods: BV2 microglia was stimulated with LPS (100 ng/ml) with or without 1h pretreatment of TL2. Production of NO was measured by Griess reaction. The mRNA and protein levels of pro-inflammatory mediators were tested by real-time PCR and western blotting, respectively. Nuclear translocation of NF-κB was assayed by immunofluorescence, and the activity of MAPKs and Akt was investigated by western blotting. For the analysis of Nrf2/HO-1 signaling, BV2 microglia was treated with TL2 for indicated time periods. Nuclear translocation of Nrf2 was determined by immunofluorescence. The expression of HO-1 was measured by western blotting. Reporter gene analysis was used to determine the activity of ARE signaling. Also, Nrf2 expression in BV2 microglia was knockdown by Nrf2 siRNA. Significant difference was evaluated by ANOVA test followed by Bonferroni post hoc multiple comparison test. P-values < 0.05 were considered as statistically significant.

Results: Pretreatment with TL2 significantly inhibited the production of NO and suppressed the expression of pro-inflammatory mediators including TNF-α, IL-1β, iNOS, IL-6 in LPS-stimulated BV2 microglia. The nuclear translocation of NF-κB and the phosphorylation level of Akt, p38 and JNK MAP kinase pathways were also inhibited by TL2. Moreover, TL2 protected primary cortical neurons against microglia-mediated neurotoxicity. Additionally, TL2 induced the nuclear translocation of Nrf2 and further up-regulated the expression of HO-l at both mRNA and protein levels. TL2 also significantly increased ARE-luciferase activity in BV2 microglia. However, the anti-inflammatory effects of TL2 in LPS-induced BV2 microglia were significantly suppressed by Nrf2 siRNA.

Conclusion: TL2 decreased the LPS-stimulated production of cytotoxic and pro-inflammatory mediators, which was probably associated with the inactivation of NF-κB, Akt, p38 MAP kinase and JNK in BV2 microglia. TL2-induced activation of Nrf2/HO-1 probably mediates the anti-inflammatory effects of TL2 in BV2 microglia. Overall, our findings indicated that TL2 could be considered as a potential therapeutic agent for neurodegenerative diseases associated with microglia activation.

EFFECT OF MIR-29A ON CELL GROWTH AND APOPTOSIS IN PC12 CELLS UNDER OXIDATIVE STRESS

P. Duan[1,2], Y. Liu[3], B. Li[1,2], X. Han[2], Y. Xu[2], **W. Yan**[2,3], Y. Xing[2,4]

[1]Physiology, [2]Stem Cell Research Center, [3]Pathophysiology, Zhengzhou University, [4]Physiology, Xinxiang Medical University, Zhengzhou, China

Introduction: Oxidative stress contributes to the pathogenesis of neurodegenerative disorders tissue injury and cell death during the development of various diseases. The role

of microRNAs in oxidative stress induced neural damage was still unclear.

Objective: The present study aims at investigating whether oxidative stress triggered by the exposure to hydrogen peroxide (H_2O_2) can regulate cell growth and apoptosis of pheochromocytoma cells (PC12) in a mechanism mediated by miR-29a.

Methods: PC12 cells were treated with 300 μmol/L H_2O_2 for 6 h, and the cells were harvested for further study. In control group, no H_2O_2 was added into the culture medium. miR-29a was determined by RT-PCR. Cell growth and apoptosis were detected by flow cytometry. Then PC12 cells was transfected with lentivirus containing miR-29a precursor or scramble, and G418 and puromycin selection was carried to obtain stable cell line. The predicted genes of miR-29a were determined by RT-PCR and western blot. siRNA virus transfection was use to knockdown genes in PC12 cells.

Result: Extracellular application of H_2O_2 inhibited cell growth, induced apoptosis, and increased miR-29a expression in PC12 cells. The PC12 cells stably expressing miR-29a precursor (miR-29a-PC12 cells) or scramble (scramble control) were obtained after two weeks antibody selection. Exogenous miR-29a expression inhibited cell growth and induced apoptosis in miR-29a-PC12 cells, comparing with scramble control. miR-29a-PC12 cells were more sensitive to apoptosis induced by H_2O_2 than scramble control. The predicted genes of miR-29a, including Mycn, Csda, Hmgn3, and Nfia, decrease in miR-29a-PC12 cells compared with scramble control detected by RT-PCR and western blot. Knockdown of Csda or Hmgn3 gene by siRNA transfection inhibited cell growth and induced apoptosis in PC12 cells.

Conclusion: miR-29a plays an important role in H_2O_2-induced apoptosis in PC12 cells, which might be achieved by targeting multiple genes.

PEROXIREDOXIN 2 BATTLES PARP1- AND P53-DEPENDENT PRO-DEATH PATHWAYS FOLLOWING ISCHEMIC INJURY

L. Zhang[1,2], Y. Luo[2], R.K. Leak[1], P. Li[2], H. Zhao[2], X. Liu[2], F. Ling[2], J. Jia[2], J. Chen[1,2], X. Ji[2]

[1]Neurology, University of Pittsburgh, Pittsburgh, PA, USA, [2]Cerebrovascular Diseases Research Institute and Department of Neurosurgery, Xuan Wu Hospital, Capital Medical University, Beijing, China

Objectives: Ischemic/reperfusion neuronal injury is characterized by accumulation of reactive oxygen species (ROS) and oxidative DNA damage, which can trigger cell death by various signaling pathways. Two of these modes of death include poly(ADP-ribose) polymerase 1 (PARP1)-mediated death or p53- and Bax-mediated apoptosis. The present study tested the hypothesis that the thiol-dependent peroxide scavenger peroxiredoxin2 (PRX2) attenuates DNA damage-mediated pro-death signaling using cellular and animal models of ischemic injury. Our previous studies demonstrated that PRX2 attenuated ASK1/JNK pro-death cascades.[1,2] The second hypothesis was that p53-, PARP1-, and JNK-dependent pathways operate in parallel but interacting manners. The impact of PRX2 on p53- and PARP1-mediated ischemic death was unknown heretofore.

Methods: DCF fluorescence, AP sites, single-strand breaks, Comet tail-length, NAD^+ depletion, and viability were assessed in response to oxygen-glucose deprivation (OGD) in cultures or transient focal cerebral ischemia (tFCI) in mice. Neuronal PRX2 overexpression or knockdown was combined with the PARP1 inhibitor AG14361. AG14361 was also applied to p53 and Bax knockout cultures and mice and combined with the JNK inhibitor SP600125. Additionally, SP600125 was combined with p53 knockout. JNK, ATM, ASK1, p53, PARP1, Bax, H2AX, and caspase activation were measured directly or indirectly in order to assess potential crosstalk between pathways.

Results: PRX2 attenuated ROS, DNA damage, NAD^+ depletion, and cell death after 90 min OGD. PRX2, but not PRX1 knockdown exacerbated these measures following 60 min OGD. PRX2 was protective and ameliorated PARP1, p53, Bax, and caspase activation

following 90 min tFCI. AG14361 reduced ischemic cell death in wild-type and p53 or Bax knockout cultures and animals but had no additional effect in PRX2-overexpressing mice. However, AG14361 elicited additive effects on viability when combined with SP600125 after 90, but not 60 min OGD. SP600125 and p53 knockout also elicited cumulative effects after 90, but not 60 min OGD and after 90 min tFCI. JNK inhibition reduced PARP1 and Bax activation and attenuated NAD^+ depletion. Conversely, p53 knockout reduced JNK activation. Our findings support the existence of multiple parallel pro-death pathways with some crosstalk.

Conclusions: PRX2 scavenges ROS and thereby limits oxidative DNA damage. After mild injury (60 min ischemia), ASK1/JNK pathways predominate, whereas after severe injury (90 min ischemia), PARP1 pathways take over. Both pathways, as well as p53-mediated signaling, are attenuated by PRX2. Additive effects of JNK inhibition with PARP1 inhibition or with p53 knockout after severe injury support the existence of parallel cascades. However, there is crosstalk between the three pathways. For example, JNK activates PARP1 and Bax after mild injury. Conversely, p53 inhibits JNK activity. In summary, the promising therapeutic candidate PRX2 can clamp upstream DNA damage and efficiently inhibit multiple pro-death cascades operating in both parallel and interactive fashions.

References:

1. Gan, Y. *et al.* Transgenic overexpression of peroxiredoxin-2 attenuates ischemic neuronal injury via suppression of a redox-sensitive pro-death signaling pathway. *Antioxidants & redox signaling* **17**, 719-32 (2012).

2. Hu, X. *et al.* Peroxiredoxin-2 protects against 6-hydroxydopamine-induced dopaminergic neurodegeneration via attenuation of the apoptosis signal-regulating kinase (ASK1) signaling cascade. *Journal of neuroscience* **31**, 247-61 (2011).

A PEPTIDE FROM THE RAP1 BINDING DOMAIN OF RALGDS IS A SELECTIVE BLOCKER OF RAP1

Z.-Y. Zhang, M.-F. Yang, D.-W. Li, H.-L. Gao, B.-L. Sun

Key Lab of Cerebral Microcirculation in Universities of Shandong, Department of Neurology, Affiliated Hospital of Taishan Medical University, Taian, China

Objectives: Rap1, a member of the Ras family of small GTPases, regulates many cellular functions such as cell adhesion, polarity, differentiation and growth. The aim of this study was to identify a peptide with the ability to interfere with Rap1-GTP. Therefore, several peptide constructs were developed from the Rap1 binding domain (RBD) of guanine nucleotide dissociation stimulator (RalGDS).

Methods: PC12 cells, HeLa cells and NIH3T3 cells were used in these experiments. Rap1, Ras, and Rac1 activation were measured using the GST pull-down assay and Western Blot analysis.The effect of synthesized peptides on integrin-mediated cell adhesion was measured usinga cell adhesion assay and viability was measured by the MTT assay. A small interfering RNA (siRNA) duplex was used to knock down Rap1 expression. Finally, $ERK_{1/2}$ phosphorylation was measured using Western Blot analysis.

Results: The GST pull-down experiments showed that mutants of GST-RalGDS-RBD (R803A, Y814A, K815A, and S816A of the RBD domain) lose the ability to interact with Rap1-GTP. Based on details of the interaction between RBD with Rap1-GTP, we designed and synthesized peptides and peptide analogs derived from the amino acid sequence 801-818 of the RBD domain:Pep1 (AA801-818), Pep2 (R803A, Y814A, K815A, and S816A), Pep3 (TAT cell-permeable peptide conjugated with Pep1), and Pep4 (Pep1 labeled FAM conjugated with TAT). Rap1-GTP was blocked in HeLa cells after treatment with the peptides Pep1, Pep3 or Pep4, but not Pep2.The peptides Pep1-4 did not affect endogenous Ras-GTP. Unlike Pep2, either Pep1, Pep3 or Pep4 inhibited integrin-mediated cell adhesion without altering cell proliferation. Forskolin-induced $ERK_{1/2}$ phosphorylation was decreased in PC12 cells and PDGF-induced Rac1 activation was inhibited in NIH3T3 cells

after treatment with the peptide Pep1, Pep3 or Pep4, but not Pep2.

Conclusions: Synthetic peptide Pep1, Pep3 or Pep4, but not Pep2, has the ability to interfere with Rap1-GTP. Compared with other methods of interfering with Rap1 signaling, these novel peptide constructs show promise as effective inhibitors of tumor cell adhesion. Furthermore, Pep4 labeled with FAM may be useful as a probe for detecting Rap1-GTP *in vivo*.

METABOTROPIC GLUTAMATE RECEPTOR 5 (MGLUR5) REGULATES NEURITE EXTENSION THROUGH THE SMALL GTPASE RAP1

Z.-Y. Zhang, M.-F. Yang, D.-W. Li, H.-L. Gao, S.-L. Huang, B.-L. Sun

Key Lab of Cerebral Microcirculation in Universities of Shandong, Department of Neurology, Affiliated Hospital of Taishan Medical University, Taian, China

Objectives: Previous studies have shown that group I metabotropic glutamate receptor (mGluR) agonist (*S*)-3,5-Dihydroxyphenylglycine (DHPG) induces the elongation of dendritic spines and protrusions in cultured neurons. However, the signaling pathways contributing to DHPG-induced neurite extension are not well understood. The small GTPase Rap1 directs axon specificationand is transiently activated at the tips of immature,developing neurites. Rap1 signaling has also been implicated in the regulation of neuronal migration in the neocortex. In present study, we investigated the role of the Rap1 signaling pathway in mGluR5-induced neurite extension.

Methods: NG108-15 neuroblastoma ×glioma hybrid cells and E18 rat cortical neurons were used in these experiments. Intracellular calcium release in response to DHPG was measured with the fluorescence microplate reader Flexstation. mGluR5-mediated Rap1 activation was measured using a GST pull-down assay and Western Blot analysis. A small interfering RNA (siRNA) duplex was used to knock down Rap1 expression. Quantitative analysis of neurite outgrowth was performed withthe Zeiss LSM Image Browser software.

Result: Group I mGluR agonist DHPG led to intracellular calcium mobilization and induced neurite extension. Compared with control siRNA-treated cells, cells transfected with Rap1 siRNA displayed significantly shorter neurite lengths in the presence of DHPG (10 μM; 24 h). Rap1 siRNA also decreased the average length of the neurites for each cell in the presence of DHPG (57± 2 μm) relative to control siRNA (85 ± 4 μmn = 7, $P< 0.01$). As expected, DHPG increased levels of the active GTP-bound form of Rap1. Furthermore, 2-Methyl-6-(phenylethynyl)pyridine (MPEP), a selective antagonist of mGluR5, inhibited DHPG-induced Rap1 activation. Finally, we found that chelation of intracellular calcium with 1,2-bis-(2-amino-phenoxy)ethane-N,N,N´,N´-tetraacetic acid (BAPTA) blocked mGluR5-induced Rap1 activation.

Conclusions: Our results suggest that activation of mGluR5 induces neurite extension through the small GTPase Rap1 in a Ca^{2+}-dependent manner.

NOVEL MAGNESIUM-DEPENDENT MODULATION OF JUNCTIONAL CONDUCTANCE AND GATING PROPERTIES OF CONNEXIN36 GAP JUNCTION CHANNELS IN NEURAL CELLS

N. Palacios-Prado[1], A. Marandykina[1,2], L. Rimkute[1,2], S. Chapuis[1], N. Paulauskas[1,2], V.A. Skeberdis[2], J. O'Brien[3], **M.V.L. Bennett**[1], F.F. Bukauskas[1]

[1]Department of Neuroscience, Albert Einstein College of Medicine, Bronx, NY, USA, [2]Institute of Cardiology, Lithuanian University of Health Sciences, Kaunas, Lithuania, [3]Department of Ophthalmology and Visual Science, University of Texas Houston Medical School, Houston, TX, USA

Objectives: Gap junction (GJ) channels formed by connexin36 (Cx36) play an important role in neuronal synchronization, and calcium oscillations in insulin-secreting beta cells. In this study, we characterized a new form of plasticity of Cx36 GJ channels dependent on intracellular free magnesium ($[Mg^{2+}]_i$).

Methods: We examined junctional conductance (g_j) and its dependence on transjunctional voltage (V_j) in HeLa and neuroblastoma N2A cells expressing Cx36 at different $[Mg^{2+}]_i$.

Results: A remarkable ~3.5-fold increase in g_j was observed when $[Mg^{2+}]_i$ was reduced to 0.01 mM, and a reduction to ~1/5th of initial values when $[Mg^{2+}]_i$ was augmented to 5 mM; for $[Mg^{2+}]_i$ action EC_{50}= ~0.45 mM. By using a stochastic 16-state model of voltage gating, we demonstrate that lowered $[Mg^{2+}]_i$ increases open channel probability while enhanced $[Mg^{2+}]_i$ reduces it. Similar changes in conductance and V_j-gating are observed with MgATP or K_2ATP, which increases or decreases $[Mg^{2+}]_i$, respectively. Changes in phosphorylation of Cx36 or $[Ca^{2+}]_i$ are not involved in the observed Mg-dependent modulation of g_j. Magnesium ions permeate the channel and transjunctional asymmetry in $[Mg^{2+}]_i$ results in asymmetric V_j-gating. We propose that the lumen of Cx36 GJ channels contains binding site(s) for Mg^{2+}, and that Mg^{2+} stabilizes a closed channel conformation. Conductance of GJs formed by Cx26, 32, 43, 45 and 47 expressed in HeLa cells are also reduced by increasing $[Mg^{2+}]_i$ above resting levels. However, none of these Cxs show increase in g_j upon reduction in $[Mg^{2+}]_i$; thus, Cx36 is the only tested Cx sensitive to lowering of physiological levels of free Mg^{2+}.

Conclusion: We have identified a new form of plasticity of Cx36 GJ channels regulated by intracellular free Mg^{2+}**.** This novel Mg^{2+}-dependent modulation of Cx36 GJ channels can be important for changes in neuronal synchronization and insulin secretion under physiological and pathological conditions when ATP levels, and consequently $[Mg^{2+}]_i$, are modified.

(This work was supported by National Institutes of Health Grant RO1 NS 55363 and the Sylvia and Robert S. Olnick Professorship of Neuroscience to M.V.L.B.)

CANNABINOID TYPE 2 RECEPTOR ACTIVATION PROMOTES NEUROBLAST MIGRATION AFTER STROKE

G. Camarero[1], J.G. Zarruk[2], M.I. Cuartero[1], V. Gonzalez[1], J. de la Parra[1], T. Atanes[1], **I. Lizasoain**[1], M.A. Moro[1]

[1]Farmacologia, Facultad de Medicina, Universidad Complutense de Madrid, Madrid, Spain, [2]Center for Research in Neuroscience, University Health Center, Montreal, QC, Canada

Introduction: Stroke is a leading cause of death worldwide and the major cause of disability. The cannabinoid type 2 receptor CB2R has been shown to have neuroprotective effects in experimental stroke by downregulating the activation of different subpopulations of microglia/macrophages (Zarruk JG et al., Stroke 2012). Now, the aim of this study is to determine if CB2R might regulate neuroblasts migration as part of the neurorepair processes after experimental ischemia.

Methods: Middle cerebral artery (MCA) was occluded permanently by ligation in mice (MCAO). To label proliferating stem/progenitors and follow their migration towards the damaged area after stroke we used 5-bromo-2´-deoxyuridine (BrdU; 50 mg/Kg i.p for 5 days beginning on day 2 after ischemia). At the same time, mice were treated with either a CB2R agonist (JWH-133, 1.5 mg/Kg), a CB2R antagonist (SR144528, 5 mg/Kg) or vehicle for 14 days. The analysis of neuroblast migration was performed at day 14 by analyzing the integrated density and the total area occupied by doublecortin (DCX) staining, a neuroblast marker, using the Image J1.45 software.

Results: The quantification of the area and intensity of DCX immunoreactivity showed a significant increase in the expression of DCX label in the corpus callosum in the MCAO+vehicle group compared with SHAM+vehicle animals. Administration of JWH-133 increased the values of both parameters in the corpus callosum and in the cortical zone. Treatment with SR144528 (CB2R antagonist) blocked the effect caused by the agonist.

Conclusions: These results support that activation of CB2R increases the neuroblast migration from the subventricular zone (SVZ) to the damage cortex, an effect that might contribute to increase neurogenesis after stroke.

ROLE OF GHRELIN IN DIETARY RESTRICTION-INDUCED HIPPOCAMPAL NEUROGENESIS IN ADULT MICE

Y. Kim, E. Li, S. Kim, S. Park

Pharmacology, Kyunghee University, Seoul, Republic of Korea

Dietary restriction (DR), which is paralleled by elevated circulating ghrelin levels, is known to be associated with increased adult hippocampal neurogenesis in young adult rats and enhanced performance of animals in a variety of behavioral tests that are dependent on the hippocampus. To determine the role of ghrelin in the enhancement of hippocampal neurogenesis resulting from DR, ghrelin knockout (GKO) mice and wild-type mice were maintained for 3 months on DR or ad libitum (AL) diets. Animals were then injected with bromodeoxyuridine (Brdu) and sacrificed either 1 day or 4 weeks later. One day after BrdU injection, the number of BrdU-labeled cells in the dentate gyrus (DG) of the hippocampus was significantly decreased in GKO mice maintained on the AL diet, suggesting the involvement of ghrelin in proliferation of neural progenitor cells. DR had no effect on the proliferation of neural progenitor cells in wile-type or GKO mice. Four weeks after BrdU injection, the number of surviving BrdU-labeled cells remained significantly lower in GKO mice maintained on AL diet. DR significantly improved survival of newly generated cells in wild-type mice, whereas DR had no significant effect on their survival in GKO mice. We also examined the hippocampus-dependent spatial learning and memory of these animals using the Morris water maze tasks. The mean swimming time within the target quadrant and probe crossing number were significantly higher in wild-type mice maintained on DR diet. In contrast, there were no significant differences in these parameters between GKO mice maintained on AL and DR diets. These findings suggest that ghrelin plays an important role in the regulation of basal level of neurogenesis in DG of adult mice, and contribute to the enhancement of neurogenesis and spatial learning and memory induced by DR.

MOLECULAR MECHANISM OF ADULT NEUROGENESIS IN ENRICHED ENVIRONMENT

Y. Komleva[1], A. Salmina[1], A. Morgun[2], N. Kuvacheva[1], N. Malinovskaya[1], A. Chernyh[3], S. Cherepanov[4], N. Yauzina[5]

[1]Biochemistry, [2]Pediatrics, Krasnoyarsk State Medical University, [3]Surgery, City Hospital No 20, [4]Research Institute of Molecular Medicine and Pathobiochemistry, [5]Clinic Medicine, Krasnoyarsk State Medical University, Krasnoyarsk, Russia

Alzheimer's disease (AD) is a neurodegenerative disorder characterized by a progressive deterioration of cognitive function and behavioral alteration in social and non-social spheres. However cognitive and physical stimulation in form of enriched environment (EE) reduced cerebral amyloid deposition in transgenic mouse models of AD. EE is capable to produce significant cellular, molecular and behavioral modification in the brain, and to induce neural plasticity [3]. All these processes may be partly regulated by neuronal and/or astrocytic CD38. Our own data suggest that CD38 expressed in neuronal and glial cells is up-regulated upon neuron-glia interactions and brain injury [2]. Also, the role of CD38 in regulation of neuropeptides release and social behavior has been suggested [1].

Objectives: The objective is to study cellular and molecular processes of structural and functional plasticity of the brain in normal and pathological development which associated with impairment in social and non-social behavior.

Methods: Enriched environment was organized as in [4]. The animal model of neurodegeneration induced by intracerebral injections of ß-amyloid. Alterations in social and non-social behavior were tested in the neuropsychological tests. At two week postinjection brains were removed. Paraffin-embedded 5-µm sections were processed for immunohistochemistry with primary antibodies to markers of neurogenesis (NeuN, Pax-6) and CD38. Apoptosis of brain cells will be detected with TUNEL method.

Results: We have found increased anxiety, reduced cognitive function, social interest and social memory in rats with experimental model of AD. Decreased expression of Pax6 in the cortex, hippocampus and amygdala and NeuN in the hippocampus was detected in brain from amyloid model. These data are based on our results obtained using isolated neurospheres (reduced neurospheres proliferation in vitro), that indicating a reduction in the number of progenitor cells and the intensity of neurogenesis in AD. EE leads to an increase in the number of progenitor cells in the aging brain. Apoptotic index (AI) increased in the hippocampus and cortex of animals with AD and old rats, but AI reduced in the amygdala in amyloid model. Contrary situation were observed in the amygdala of old animals (increasing of AI). Rats with experimental AD have shown reduced expression of CD38 in

hippocampus and cortex, but not the amygdala.

Conclusions: We first show that the intensity of apoptosis and expression of CD38 in the amygdala (but not the hippocampus or cortex) may be a marker that allows differentiating of age-related and amyloid-induced changes in the limbic system of the brain.

References:

1. Higashida H., et al. Oxytocin signal and social behaviour: comparison among adult and infant oxytocin, oxytocin receptor and CD38 gene knockout mice, J. Neuroendocr., 22 (2010), 373-379

2. Higashida H., Salmina A.B., et al., Cyclic ADP-ribose as a universal calcium signal molecule in the nervous system, Neurochem Intl, 51 (2007), 192-199

3. Lazarov O., et al., Environmental enrichment reduced Aβ levels and amyloid deposition in transgenic mice, Cell, 120 (2005), 701-713

4. Yankowsky J.L. et al., Environmental enrichment exacerbates amyloid plaque formation in a transgenic mouse model of Alzheimer Disease, J. Neuropathol. Exp. Neurol., 62 (2003), 1220-1227

GHRELIN STIMULATES ADULT HIPPOCAMPAL NEUROGENESIS IN GROWTH HORMONE/INSULIN-LIKE GROWTH FACTOR-1-DEFICIENT SPONTANEOUS DWARF RATS

E. Li, Y. Kim, S. Kim, S. Park

Pharmacology, Kyunghee University, Seoul, Republic of Korea

Previous studies have demonstrated that ghrelin enhances adult neurogenesis. We previously reported that systemic administration of ghrelin stimulated proliferation of newly generating cells in the hippocampus of adult mice. Furthermore, immunoneutralization of ghrelin by using anti-ghrelin antiserum in adult mice reduces proliferation of hippocampal progenitor cells in the SGZ, suggesting endogenous ghrelin plays an important role in neurogenesis. However, there is a possibility that the action of ghrelin on hippocampal neurogenesis could be, in part, due to the ability of ghrelin to stimulate the growth hormone (GH)/insulin-like growth factor (IGF)-1 axis, where both GH and IGF-1 infusions have been shown to increase hippocampal neurogenesis. Therefore, in this study, to explore the possibility that the effect of ghrelin on neurogenesis might be mediated via indirect action of ghrelin on the GH/IGF-1 axis, we assessed the impact of ghrelin on progenitor cell proliferation and differentiation in the DG of spontaneous dwarf rats (SDRs), a dwarf strain with a mutation of the GH gene resulting in total loss of GH and decreased IGF-1 levels. We found that ghrelin treatment in the SDRs significantly increased the number of BrdU-labeled cells in the DG. proliferating cell nuclear antigen-labeled cells in the DG were also increased by ghrelin treatment in these animals. We also measured the number of doublecortin, a marker of early neuronal differentiation. The number of doublecortin-labeled cells in the DG of ghrelin-treated SDRs was significantly higher than in the vehicle-treated SDRs. To test whether ghrelin has a direct effect on cognitive performance independent of somatotropic axis, hippocampus-dependent learning and memory were assessed using the Y-maze and novel object recognition (NOR) test in the SDRs. Ghrelin treatment for 4 weeks by subcutaneous osmotic pump significantly increased alternation rates in the Y-maze and exploration time for novel object in the NOR test compared to vehicle-treated controls. Our results indicate that ghrelin-induced adult hippocampal neurogenesis and enhancement of cognitive function are mediated independently of somatotropic axis.

HYPOXIA-INDUCIBLE FACTOR-1A (HIF-1A) IS CRITICAL FOR THE MAINTENANCE OF NEURAL STEM/PROGENITOR CELL (NSPC) CELLS WITHIN THE ADULT SUBVENTRICULAR ZONE (SVZ)

L. Li[1], K.M. Candelario[2], K. Wright[1], R. Wang[1], L.A. Cunningham[1]

[1]University of New Mexico School of Medicine, Albuquerque, NM, [2]University of Florida, Gainesville, FL, USA

HIF-1α plays a key role in mediating adaptive responses to hypoxia. We have previously demonstrated that stabilized HIF-1α protein is constitutively expressed within NSPCs of both the adult subventricular zone (SVZ) and subgranular zone (SGZ) under non-hypoxic conditions, and that HIF-1α-mediated VEGF release from NSPCs supports endothelial cell

survival in culture. To determine whether HIF-1a expression is critical for the maintenance of adult NSPCs, we generated inducible Hif1α knockout(Hif1α iKO) mice in which tamoxifen administration results in concomitant expression of yellow fluorescent protein (YFP) and bi-allelic Hif1α exon 2 gene deletion in nestin^{+} NSPCs and their progeny (nestin-CreER^{T2}:R26R-Yfp:Hif1α$^{fl/fl}$). Induced Hif1α gene deletion in neural stem cells resulted in a delayed loss of approximately 50% of YFP+ cells within the SVZ at 45 and 90 days following tamoxifen-induced recombination with no change in YFP+ cell number at two weeks. This did not appear to be due to cell death, because Hif1α iKO mice did not display increased numbers of TUNEL^{+} cells at any time point. This loss in YFP+ cells appeared to be due to a depletion of primitive type B astrocyte stem cells and transit amplifying cells with no change in the number of neuroblasts, as assessed by phenotypic analysis using cell-type specific markers. A BrdU labeling-retaining assay further confirmed depletion of type B cells in Hif1α iKO mice. Importantly, Hif1α iKO mice also displayed early regression of the SVZ vasculature that was apparent at both 14 day and 45 days following tamoxifen administration. Preliminary data also indicate an attenuated neurogenic response in Hif1a iKO mice following transient middle cerebral artery occlusion (MCAO).These studies suggest that HIF-1α plays a critical role in maintenance of the NSPC pool under non-pathologic conditions and following cerebral ischemia.

Support: American Heart Association (09GRNT2290178).

TLR4 DECREASES BRAIN CELL PROLIFERATION AFTER FOCAL CEREBRAL ISCHEMIA IN YOUNG BUT NOT IN AGED MICE

A. Moraga[1], J.M. Pradillo[2], M. Oses[1], A. Perez[1], R. Cañadas[1], M.A. Moro[1], **I. Lizasoain**[1]

[1]Farmacologia. Facultad de Medicina, Universidad Complutense de Madrid, Madrid, Spain, [2]Faculty of Life Sciences, University of Manchester, Manchester, UK

Background: TLR4 has been described to play major roles in the CNS including its participation in brain damage caused by stroke but also its involvement in adult hippocampal neurogenesis under normal conditions. However, the role that TLR4 plays on proliferation after stroke is unknown. The objective of this study is to determine the role of TLR4 in proliferation after stroke and to study how age can modify this process.

Methods: Focal cerebral ischemia was induced by permanent occlusion of the middle cerebral artery (MCA) in young mice (2-3 months) and aged mice (13-14 months). Experiments were performed on TLR4-deficient mice (C57BL/10ScNJ) and animals that express TLR4 normally (C57BL/10ScSn). 5-bromo-2´-deoxyuridine (BrdU, 50 mg/kg) was injected ip twice daily from days 5 to 6 after ischemia. Cerebral infarct size was measured by magnetic resonance imaging (MRI) at 48h and by Nissl staining at 7 and 14 days. Cell proliferation was quantified 7 and 14 days after ischemia by immunofluorescence studies. Cytometric analysis of the peri-infarct area and SVZ was also performed.

Results: TLR4-deficient young but not aged mice had lesser infarct volumes when compared with control mice. In order to study the role of TLR4 on cell proliferation but avoiding differences in infarct volume, we included an additional group in which only a branch of the MCA was occluded in control mice. Thus, infarct volume after stroke was the same in both groups. In the group of young animals, our findings reveal that after stroke, deficiency of TLR4 promotes cell proliferation, increasing the number of Prominin-1+ and BrdU+ cells in the ipsilateral SVZ at 2 and 7 days respectively after ischemic insult. Interestingly, this effect is lost in the group of aged animals. In addition, we did not find any differences in the number of BrdU+ and BrdU/Iba+ in the ipsilateral parietal cortex after ischemic insult between the groups studied. However, aged animals had a higher expression of BrdU+ and BrdU/Iba+ in the ischemic boundary when compared with the young group.

Conclusions: Our data indicate that TLR4 not only mediates brain damage in the acute phase but also might decrease neurorepair mechanisms (inhibiting cell proliferation) during the chronic phase of stroke in young but not aged mice, thus highlighting the importance of using aged animals for translation to clinical studies.

EXERCISE PROMOTE REGENERATION OF NEWBORN STRIATO- AND CORTICONIGRAL PROJECTION NEURONS AND IMPROVE MOTOR RECOVERY IN RATS AFTER STROKE

Q.-W. Zhang[1], X. Sun[1], **F.-Y. Sun**[2]

[1]Dept of Neurobiology and State Key Lab of Medical Neurobiology, [2]Dept of Neurobiology and Institute for Stem Cell and Regeneration, State Key Lab of Medical Neurobiology, Fudan University, Shanghai, China

Background and aims: Rehabilitative training improved motor recovery after ischemic stroke in experimental animals and clinic patients. The aim of this study is to investigate effects of exercise on regeneration of newborn projection neurons in adult rat brains following ischemic stroke.

Methods: Each rats were subjected to a transient middle cerebral artery occlusion (MCAO) to induce ischemic stroke and then randomly divided into MCAO (n=12) and MCAO+Exercise (MCAO+EX) groups (n=13). Rats in the MCAO+EX group were given a 10-minute treadmill pre-training twice daily for 3 days at a speed of 5.5m/min with an electric motor-driven treadmill machine prior to MCAO and subjected to a 30-minute training daily at a speed of 12m/min from 5 to 28 days after MCAO. Rats in the MCAO group were not exposed to the treadmill. Rota-rod test was used to test motor function of rats pre-MCAO and at 3, 7, 14, 21, 28, 35, 42, 49, 56 and 63 days post-MCAO with an accelerating rotarod. We used fluorogold (FG) nigral injection to trace striatonigral and corticonigral projection neurons and to apply GFP-targeting retroviral vectors combined with confocal technique to detect newborn projection neurons. Western blot analysis was used to detect the levels of BDNF, VEGF and Nogo-1 expresion in the stritaum and cortex. Immunostaining was used to detect mature and projection neurons in the striatum, and dopaminergic neurons in the subtantia nigra.

Results: Exercise improved recovery of motor deficits of rats after MCAO. With these rats, we detected triple-staining cells of GFP^+-FG^+-$NeuN^+$ cells in ipsilateral striatum and cerebral cortex of rat brains at 13 weeks after MCAO. Then, double staining cells of GFP^+-FG^+ was quantified as new projection neurons. The results showed that the number of GFP^+-FG^+ cells in MCAO+EX rats increased to 2.52-fold and 1.78-fold of MCAO rats in the cortex and striatum, respectively, suggesting increase of newborn striatonigral and corticonigral neurons by exercise poststroke. Meanwhile, exercise also increase single staining cells of NeuN or FG in the straitum and cortex, ischemic territory, and tyrosine hydroxylase (TH) staining cells in the substantia nigra, a remote region of ischemic territory. Besides, we found that exercise increased BDNF and VEGF while reduced Nogo-A in ischemic brain.

Conclusions: Our results suggest that stroke-induced newly generated neurons could form long projection (striatonigral and coticonigral projection neurons) and establish new neural networks between nuclei, which should be very important for the recovery of motor function deficits. Passive exercise poststroke could effectively enhance the capacity for regeneration of newborn projection neurons in ischemic injured mammalian brains. Our results provided morphological evidence to support the effectiveness of rehabilitative treatment poststroke in the clinic.

PROTEOMIC ANALYSIS OF ISCHEMIC BRAIN IN PSD-93 KNOCKOUT MICE

Q. Zhang, S. Zhang, M. Zhang, **Y. Xu**

Department of Neurology, Affiliated Drum Tower Hospital of Nanjing University Medical School, Nan Jing, China

Objectives: PSD-93, enriched in the postsynaptic density, is involved in N-methyl-D-aspartate receptor (NMDAR)-triggered neurotoxicity through PSD-93/ NMDAR/nNOS signal module. Furthermore, we also find that the targeted disruption of the PSD-93 gene not only attenuate the NMDAR/Ca2+/NO-mediated neurotoxicity but also affect the subcellular distribution of NR2A and NR2B in cultured mouse cortical neurons. However, the exact molecular mechanisms of PSD-93 in reperfusion following transient middle cerebral artery occlusion (tMCAO) in vivo remain largely unknown. To elucidate the underlying molecular mechanism, Proteomic Analysis was used.

Methods: We applied isobaric tag for relative and absolute quantitation (iTRAQ) labeling coupled with on-line two-dimensional LC/MS/MS technology to identify proteins expressed in brain tissues: wild type control, wild type ischemia/reperfusion 12h group, PSD-93 knockout group and PSD-93 knockout ischemia/reperfusion 12h group.

Results: A total of 1892 proteins were identified. Comparing with wild type mice, 9 proteins were up-regulated and 5 were down-regulated significantly in ischemia/reperfusion. Deficiency of PSD-93 increased 32 proteins and decreased 31 proteins. Furthermore, some other proteins from ischemia/reperfusion groups in both wild type and PSD-93 knockout groups were identified their alterations without affecting the protein expression by PSD-93 deficiency. To further explicit the mechanism of PSD-93 in vivo, we selected these proteins to further research. And among them, 13 up-regulated proteins were identified as syntaxin-1A, synaptotagmin-1, complexin-3, ras GTPase-activating protein SynGAP, keratin, isoform beta-I of protein kinase C beta type, isoform 2 of voltage-dependent L-type calcium channel subunit beta-4, isoform 2 of Sodium-driven chloride bicarbonate exchanger, Voltage-dependent anion-selective channel protein 3, isoform Mt-VDAC1 of voltage-dependent anion-selective channel protein 1, n1-specific diacylglycerol lipase alpha, sphingomyelin phosphodiesterase 3 and brain protein 44 and 4 down-regulated proteins were identified as brain fatty acid-binding protein, pyridoxine-5´-phosphate oxidase, ATP-binding cassette sub-family F member 1 and Down syndrome cell adhesion molecule homolog.

Conclusions: The results provide valuable clues for us to study the underlying mechanisms of PSD-93 in neurotoxicity induced by ischemia-reperfusion.

FOCAL BRAIN IRRADIATION AND CXCR4 ANTAGONIST AMD3100 ABOLISH THE ENHANCED FUNCTIONAL RECOVERY INDUCED BY CONSTRAINT-INDUCED MOVEMENT THERAPY AFTER STROKE

S. Zhao, C. Zhao, S. Wang, H. Qu, C. Song

Neurology, The First Hospital of China Medical University, Shenyang, China

Objectives: To explore the effects of constraint-induced movement therapy (CIMT) on the functional recovery in adult rats after stroke and whether these effects were induced by enhancing neurogenesis and through SDF-1/CXCR4 system.

Methods: Male Wistar rats (200-250g) were randomly assigned to five groups (n=8 per group): Sham, ischemia, ischemia treated with CIMT, irradiation followed by ischemia and then treated with CIMT(irradiation group) and ischemia treated with CIMT and AMD3100 (AMD3100 group). Focal brain X-irradiation was used 8 weeks before ischemia to ablate the neurogenic cells of the SVZ and hippocampus. Focal cerebral ischemia was induced by injection of endothelin-1 [1]. Three weeks of CIMT beginning at post-stroke day 7 was performed by fitting a plaster cast around the unimpaired upper limb of rats [2]. A CXCR4 antagonist (AMD3100) was delivered via an osmotic pump 1 week after ischemia induction and lasted for 2 weeks. Functional recovery was analyzed by the beam walking test and the Morris water maze test 4 weeks after ischemia. The proliferation, migration and dendrite growth of neural stem cells in the SVZ and dentate gyrus (DG) of the hippocampus were detected by immunofluorescence staining and captured by confocal microscope. The pixels of DCX-positive signals area in the SVZ and the numbers of DCX-positive cells in the DG were measured by NIH Image J software.

Results: We found that the production of neuroblasts in both the SVZ and DG as well as the dendrite growth of neural stem cells in the DG were significantly increased after stroke. CIMT after stroke not only enhanced the proliferation and dendrite growth of newborn neurons in both the SVZ and DG but also attracted more neuroblasts towards the infarct area. The enhanced neurogenesis induced by CIMT was significantly suppressed by focal brain irradiation and AMD3100. Behavioral assessments showed that the decreases in the number of neuroblasts and their migration to the infarct as well as their dendrite growth correlated with the impaired beam-walking and spatial learning performances.

Conclusions: Reducing neurogenesis by using focal brain irradiation and AMD3100 abolished the enhanced functional recovery induced by CIMT in rats following stroke. CIMT might improve functional recovery by enhancing neurogenesis and through SDF-1/CXCR4 system.

References:

1. Windle V, Szymanska A, Granter-Button S, et al. An analysis of four different methods of producing focal cerebral ischemia with endothelin-1 in the rat. Exp Neurol 2006;201:324-34.

2. Muller HD, Hanumanthiah KM, Diederich K, Schwab S, Schabitz W-R, Sommer C. Brain-

derived neurotrophic factor but not forced arm use improves long-term outcome after photothrombotic stroke and transiently upregulates binding densities of excitatory glutamate receptors in the rat brain. Stroke 2008;39:1012-21.

ISOFLURANE ALONE AND ISOFLURANE PLUS SURGERY INDUCE HIPPOCAMPAL INFLAMMATION AND COGNITIVE DEFICITS

J.K. Callaway[1], C.M. Wood[2], T.A. Jenkins[3], C.F. Royse[1]

[1]Surgery, Royal Melbourne Hospital, The University of Melbourne, [2]Pharmacology, The University of Melbourne, Parkville, [3]Pharmacuetical Sciences, Royal Melbourne Institute of Technology, Bundoora, VIC, Australia

Introduction: Post-operative cognitive dysfunction (POCD) is an impairment of cognitive function that develops after anaesthesia and surgery. POCD occurs in 10% of all surgical patients and presents as a deterioration of mental function with impaired memory and concentration. While it occurs more frequently in the elderly, it also presents in young, previously healthy patients. The duration ranges from weeks to months but may be permanent. POCD is a significant concern as half of all individuals over 65 will have at least one surgery in the remainder of their lifetime. The pathogenesis of POCD remains unclear, however, studies in young and aged animals suggest that anaesthesia and/or inflammation induced by surgical trauma can affect cognitive outcome.

Aim: Using a rat model, this study aims to investigate the role of isoflurane anaesthesia alone, or with added surgery-induced inflammation on cognitive outcome.

Methods: Male Sprague Dawley rats were subjected to isoflurane (n=9, 4h, 1.8% in 100% O_2). Controls were subjected to 10 min of 100% O_2 (n=14). Laparotomy was performed in a sub-group of isoflurane-treated animals (n=9), and the wound left open for 10min then sutured. Eight days after treatments, cognition was tested using a fear-conditioning paradigm. Rats were placed in a chamber in which they received a foot shock (1mA, 1s duration). When returned to the chamber the percentage of time spent in freezing behaviour was recorded as a measure of memory for the shock previously experienced in that chamber. One day after fear conditioning, rats were deeply anaesthetised and transcardially perfused. Hippocampal tissue was collected and processed for cytokine analysis (Bio-Plex™). Separate groups of rats (n=3-6) were treated as described but not subjected to cognitive testing. These rats were sacrificed at 6 and 48h for determination of early cytokine changes only.

Results: Rats exposed to isoflurane or isoflurane plus surgery showed significantly decreased freezing behaviour compared to no-anaesthesia controls, indicating memory impairment (isoflurane: 25.4 ± 9.4% versus 66.21 ± 8.9%, $P< 0.01$, isoflurane plus surgery: 35.3 ± 7.5% versus 66.21 ± 8.9%, $P< 0.05$, respectively). Isoflurane exposure alone was associated with a significant increase in serum IL-1β compared to control, one day after cognitive assessment ($P< 0.05$), while isoflurane plus surgery was not associated with additive effects on serum cytokine levels. When comparing the effects of treatment at 6h, isoflurane and isoflurane plus surgery treatments were associated with a 3-fold decrease in IL-1β, IL-6 and TNF-α in serum compared to control ($P< 0.05$). This was followed by a trend for increases 48h after exposure to treatments. Analysis of hippocampal tissue showed significant increases in pro-inflammatory cytokines IL-6 and TNF-α after isoflurane and after isoflurane plus surgery treatments one day after cognitive testing.

Conclusions: These findings suggest a 4h exposure to isoflurane alone can impair memory and cause fluctuations in cytokines, beginning at early time points and persisting until day 9 after exposure. These fluctuations were closely associated in time with cognitive impairment. Inflammation caused by anaesthesia and by surgical trauma may contribute to post-operative cognitive dysfunction.

P2X7R/CRYOPYRIN INFLAMMASOME AXIS INHIBITION REDUCES NEUROINFLAMMATION AFTER SAH

S. Chen[1,2], Q. Ma[1], P. Krafft[1], Q. Hu[1], W. Rolland[1], P. Sherchan[1], J. Zhang[2], J. Tang[1], J. Zhang[1]

[1]Loma Linda University School of Medicine, Loma Linda, CA, USA, [2]Zhejiang University, Hangzhou, China

Objective: Neuroinflammation contributes to the pathogenesis of early brain injury (EBI) after subarachnoid hemorrhage (SAH). Cytotoxic events following SAH, such as extracellular accumulation of adenosine triphosphate (ATP), may activate the P2X purinoceptor 7 (P2X7R)/cryopyrin inflammasome axis, thus inducing microglial secretion of the proinflammatory cytokines IL-1β/IL-18. We therefore hypothesized that inhibition of P2X7R/cryopyrin inflammasome axis would ameliorate neuroinflammation after SAH.

Methods: SAH was induced by the endovascular perforation in rats. Small interfering RNAs (siRNAs) of P2X7R or cryopyrin were administered intracerebroventricularly 24 hours before SAH. Brilliant Blue G (BBG), a non-competitive antagonist of P2X7R, was administered intraperitoneally 30 minutes following SAH. To investigate the link between P2X7R and cryopyrin inflammasome *in vivo*, Benzoylbenzoyl-ATP (BzATP), a P2X7R agonist was given to lipopolysaccharide (LPS) primed naive rats with scramble or cryopyrin siRNAs. Post-assessments including neurobehavioral test, brain edema, Western blot and immunohistology, were performed.

Results: The P2X7R/cryopyrin inflammasome axis was active in microglia after SAH. Administration of P2X7R and cryopyrin siRNA as well as pharmacologic blockade of P2X7R by BBG ameliorated neurological deficits and brain edema at 24 hours following SAH. Inhibition of P2X7R/cryopyrin inflammasome axis suppressed caspase-1 activation, which subsequently decreased maturation of IL-1β/IL-18. In LPS-primed naïve rats, BzATP induced caspase-1 activation and mature IL-1β release was neutralized by cryopyrin siRNA.

Interpretation: The P2X7R/cryopyrin inflammasome axis may contribute to neuroinflammation via activation of caspase-1 and thereafter mature IL-1β/IL-18 production following SAH. Therapeutic interventions targeting this pathway may be a novel approach to ameliorate EBI following SAH.

References:

Provencio JJ, Vora N. Subarachnoid hemorrhage and inflammation: bench to bedside and back. Semin Neurol 2005;25:435-444.

Lamkanfi M, Dixit VM. Modulation of inflammasome pathways by bacterial and viral pathogens. J Immunol 2011;187:597-602.

Felderhoff-Mueser U, Schmidt OI, Oberholzer A, et al. IL-18: a key player in neuroinflammation and neurodegeneration? Trends Neurosci 2005;28:487-493.

Hafner-Bratkovic I, Bencina M, Fitzgerald KA, et al. NLRP3 inflammasome activation in macrophage cell lines by prion protein fibrils as the source of IL-1beta and neuronal toxicity. Cell Mol Life Sci 2012.

SPLEEN-DERIVED CCR2+ MONOCYTES ARE NOT NECESSARY IN STROKE-INDUCED BRAIN INJURY

E. Kim, C. Beltran, **S. Cho**

Neurology/Neuroscience, Weill Cornell Medical College at Burke Med Res Inst, White Plains, NY, USA

Objectives: The persistent presence of monocytes/macrophages (MMs) in the post-ischemic brain suggests the involvement of mononuclear phagocytes in stroke-induced inflammation and injury. Spleen, the largest organ in the lymphatic system, has been identified as an immediate reservoir for monocyte deployment upon injury. Although studies showed that mouse monocytes display heterogeneity with distinct subsets: a pro-inflammatory CCR2+ ($Ly6C^{hi}$) and anti-inflammatory CCR2- ($Ly6C^{low}$) subsets, the role of monocyte subsets relevant to the spleen in ischemic brain injury has not been investigated. The current study addresses whether the spleen-derived monocytes are required for stroke-induced monocyte trafficking and injury.

Methods: Splenectomy (Spx) or sham surgery (shSpx) was performed in eleven week-old C57BL mice, followed immediately by transient middle cerebral artery occlusion. Leukocytes from the spleen and single cell suspension from the brain were obtained before ischemia as well as at 1d and 3d after stroke. Monocyte subsets were analyzed using flow cytometer after incubation of the cells with combinations of lineage marker (T, B, NK cells, granulocytes), CD45, or CD11b (monocyte/macrophages), and Ly6C (for monocyte subsets).

Results: Stroke caused around 40% reduction in spleen size at 1d and 3d post-ischemia compared to pre-ischemic animals. This was accompanied by a reduction in MM numbers in the spleen without altering the ratio between CCR2+ and CCR2- subsets. In contrast, MM number was increased in the post-ischemic brain. The increase was particularly pronounced in pro-inflammatory CCR2+ ($Ly6C^{hi}$) subset at 1d and 3d post-ischemia. Changes in CCR2- ($Ly6C^{low}$) subset was relatively minor at these time points, suggesting a contributing role of the CCR2+ monocyte subset in acute ischemic injury. Ablation of spleen initially delayed the accumulation of CCR2+ ($Ly6C^{hi}$) MMs at 1d, but did not prevent the accumulation of MMs at 3d in the brain (Figure). Infarct volume determined at 3d was similar between the groups (Spx vs shSpx, 36.3±3.2 mm^3 vs 34.1±5.9 mm^3, n=11-15, ns). Gene expression of MCP-1 and CCR2, a major chemokine/receptor axis for monocyte trafficking, also showed similar levels in the brain between the groups (Spx vs shSpx, CCR2, $5.1\pm0.8x10^{-4}$ vs $4.5\pm0.5x10^{-4}$; MCP-1; $5.0\pm 0.5x10^{-3}$ vs $5.7\pm0.8x10^{-3}$, ns).

Conclusions: Despite its contributing role of pro-inflammatory CCR2+ monocytes in ischemic brain injury, the spleen ablation study clearly demonstrated that the spleen-derived CCR2+ ($Ly6C^{hi}$) monocytes are not required for stroke-induced brain injury. The results suggest the recruitment of monocytes from other sources, probably bone marrow and peritoneum among others, in the absence of spleen. Thus, the ablation of the spleen may not be a useful strategy to attenuate ischemic inflammation and injury.

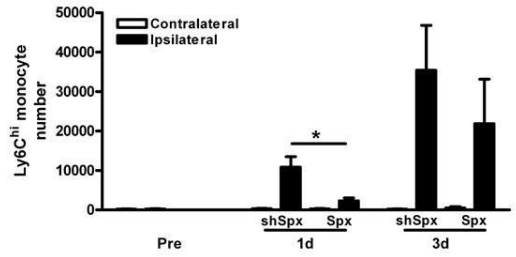

[Brain CCR2+ monocyte number]

NORMALIZATION FOR THE EFFECT OF A GENETIC POLYMORPHISM ON THE TRANSLOCATOR PROTEIN IMPROVES MEASUREMENT OF NEUROINFLAMMATION WITH [^{11}C]DPA-713

J. Coughlin[1], Y. Wang[2], S. Ma[3], C. Yue[4], B. Caffo[4], C. Endres[2], **M. Pomper**[5]

[1]Dept of Psychiatry and Behavioral Sciences, Johns Hopkins University, [2]Radiology, Johns Hopkins Medical Institutions, [3]Health Sciences Informatics, [4]Biostatistics, Johns Hopkins University, [5]Neuroradiology, Johns Hopkins Medical Institutions, Baltimore, MD, USA

Objectives: Accumulating evidence suggests that neuroinflammation may underlie onset of cognitive deficits associated with several brain diseases, including HIV-dementia[1]. Positron emission tomography (PET) with [^{11}C]DPA-713, which binds to the translocator protein (TSPO), can be used to measure neuroinflammation in humans *in vivo*. However, a common single nucleotide polymorphism in the *TSPO* gene causes differential binding patterns when using [^{11}C]DPA-713 as well as several other TSPO-targeting radiotracers[2]. We sought to determine if correcting for this biological confound could improve the sensitivity to detect increased expression of TSPO in the brains of individuals with HIV-associated dementia and in those with repetitive, sports-related mild traumatic brain injury (mTBI).

Methods: Total [^{11}C]DPA-713 binding was measured in young, healthy controls (n = 12), HIV patients (n=5), former NFL players (n=4), and elderly healthy controls (n=5). All subjects were genotyped for the rs6971 TSPO polymorphism. Regional total distribution volume (V_T) measurements were calculated using the Logan method for several cortical and subcortical regions from each subject's 90-min dynamic PET data and their metabolite-corrected plasma input function. Characteristics of tracer uptake, inter-subject variation, and intra-subject reproducibility of regional V_T estimates were assessed before and after the normalization for genotype effect. Population mean and standard deviation measurements were then calculated from the young healthy control data after normalization for genotype effect. Personalized, regional z-scores were then calculated from the regional, normalized V_T data from each HIV and mTBI subject. Results from patient neurocognitive

measures were also correlated with normalized [^{11}C]DPA-713 binding in regions of interest.

Results: Subjects of all three rs6971 genotypes were identified with similar frequencies in healthy control, HIV and former NFL player cohorts. Correction for the binding of effect of genotype on total V_T was achieved through normalization of the regional V_T estimates and resulted in increased reproducibility and improved sensitivity to detect increased expression of TSPO in disease. All five HIV patients had greater binding than controls in the anterior cingulate after genotype correction, with individual z scores ranging from 2.1 to 3.84. Those former NFL players with pronounced neurocognitive deficits had increased binding of [^{11}C]DPA-713 in the supramarginal gyrus, with z scores of 2.8 to 3.8.

Conclusions: The rs6971 TSPO polymorphism results in three different levels of [^{11}C]DPA-713 binding in the brains of young and aged healthy controls, patients with HIV, and individuals with history of sports-related mTBI. Correcting for the effect of rs6971 genotype on [^{11}C]DPA-713 binding improves the reproducibility of the quantified PET binding data. Furthermore, this normalization increases the statistical power of clinical studies to detect areas of increased neuroinflammation in patients with HIV and sports-related mTBI.

References:

1. Hammoud DA, et al. Imaging glial cell activation with [11C]-R-PK11195 in patients with AIDS. *J Neurovirol*. 2005. 346-355.

2. Kreisl WC, et al. A genetic polymorphism for translocator protein 18 kDa affects both in vitro and in vivo radioligand binding in human brain to this putative biomarker of neuroinflammation. *J Cereb Blood Flow Metab*. 2012. 1-6.

DIFFERENTIAL MODULATION OF THE CELLULAR IMMUNE SYSTEM IN SPONTANEOUS INTRACEREBRAL HEMORRHAGE

S. Illanes[1,2], F. Vial[1], V. Simon[2], J. Gajardo[3], V. Diaz[4], P. Conget[2]

[1]Neurology, [2]Instituto de Ciencias, Universidad del Desarrollo-Clínica Alemana, [3]Neurology, Clínica Dávila, [4]Neurology, Hospital Clínico Universidad de Chile, Santiago, Chile

Background and purpose: A stroke-induced immunodeficiency syndrome encompassing innate and adaptive immune cells develops in murine large ischemic stroke models and extensive damage in stroke patients. Intracerebral hemorrhage (ICH) accounts for 15-25% of acute stroke, and is associated with high mortality and morbidity rates. Experimental studies have identified a number of immunological factors that are involved in the pathophysiology of ICH, including leukocyte brain infiltration, initiation of the complement cascade and microglial activation[1]. However, we were able to find only one study[2] characterizing the systemic immune response after an experimental ICH and this has been never replied in humans. Our objective was to analyze peripheral immune cell response and lymphocytes subpopulation in blood in a prospective cohort of ICH patients.

Methods: Adult patient with supratentorial ICH and no previous story of oral anticoagulant treatment, acute infection, chronic inflammatory disease or previous stroke were included. Brain image (CT or MR) was obtained in the emergency room and the day following the ICH in every patient in order to detect hematoma enlargement. Differential blood leukocyte counting was performed and lymphocyte subpopulations were further characterized by flow cytometry in blood 24h, 3d and 7d after the ICH presentation. We compared absolute numbers of helper T cells (CD3+CD4+), cytotoxic T cells (CD3+CD8+), B cells (CD19+), regulatory T cells (CD4+CD25+Foxp3+), Natural Killer cells (CD3+CD16+CD56+) and the percentage of regulatory T cells within the CD4+ population in blood in patients with large hematoma volume (>25ml) versus small hemorrhage size (< 25ml) and presence of intraventricular bleeding versus patients without blood in cerebral ventricles.

Results: 16 patients completed the study. Patients with large hematoma volume had a bigger leucocytes number 24h, 3d and 7d after ICH presentation compared with small hematoma volume patients (ANOVA p< 0.04) with a significant increase regulatory T cells number (ANOVA p=0.03) and a bigger proportion of infections during the first seven days of follow up (X^2 p< 0.01).

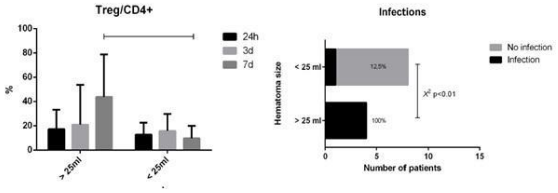

[Size effect over immune response]

Patient with ICH + intraventricular bleeding had a smaller leucocyte number count 24h, 3d and 7d after ICH presentation compared with patients without blood in the cerebral ventricles (ANOVA p< 0.001) and a significant increase regulatory T cells number (ANOVA p=0.03)

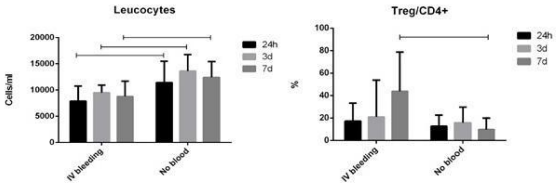

[Intraventricular bleeding effect]

Conclusion: Hemorrhage size is a major determinant of post-stroke systemic immune modulation while the presence of intracerebral bleeding determines a profound immunosuppresion. Large hematoma volume associates with more infections.

References:

1. Chamorro et al. Nat Rev Neurol. 2012 Jun 5;8(7):401-10

2. Illanes S et al. Neuroscience Letters 490 (2011) 170-174

NEUROMODULATORY EFFECTS OF *GINKGO BILOBA* EXTRACT AGAINST TOXICANT-INDUCED HIPPOCAMPAL INJURY BY SUPPRESSION OF MICROGLIAL ACTIVATION AND PRO-INFLAMMATORY CYTOKINES

S. Kaur, B. Nehru

Panjab University, Chandigarh, India

Objective: The present study was an attempt to investigate the efficacy of Ginkgo biloba extract (GBE) against hippocampal microglial activation and pro-inflammatory cytokines by neurotoxicant Trimethyltin (TMT).

Material and methods: Male Sprague-Dawley (SD) rats were administered with Ginkgo biloba extract for 21 days at a dose of 100 mg/kg b.w (i.p) post TMT administration, rats were administered with a single dose of TMT (8.5 mg/kg b.w. i.p). Rats were sacrificed at 21 day post TMT and then Histological and molecular examination were performed.

Results: The co-administered of TMT with GBE showed marked improvement in spatial memory and aggressive behavior as assessed by water maze, active and passive avoidance test and aggression scores. Ginkgo biloba extract suppressed the TMT induced decrease in the number of hippocampal pyramidal neurons in the CA1 region. The TMT-induced up-regulation of the gene and protein expression levels of reactive microglia (Iba-1), astroglia (GFAP) and pro-inflammatory cytokines (IL-1β, IL-6 and TNF-α) were reversed by Ginkgo biloba administration.

Conclusion: These results suggested that the neuroprotective effect of Ginkgo biloba extract on TMT-induced spatial memory impairment could be attributable to its inhibitory effect against microglial activation and its role in synapse formation via neurotrophic factors in the hippocampus.

CO-CULTURE WITH MICROGLIA DRIVES DIFFERENTIATION OF NEURAL PROGENITOR CELLS *IN VITRO*

J.E. Lee[1], J.Y. Choi[1], J.H. Song[2], K.K. Bokara[2], J.H. Choi[2]

[1]Anatomy, Brain Korea 21 Project for Medical Science, Yonsei University, College of Medicine, [2]Anatomy, Yonsei University, College of Medicine, Seoul, Republic of Korea

Objectives: Neural progenitor cells (NPCs) proliferate and differentiate depending on their intrinsic properties and local environment. Recent studies have demonstrated that microglia, one type of glia cells, play an important role in neurogenesis. However, little is known about how activated microglia controls the proliferation and differentiation of NPCs. To evaluate better the contributions of microglia to modulate the NPCs characteristics we investigated the possibility that microglia-derived cytokine factors regulate the behavior of NPCs *in vitro* in a co-culture system.

Methods: In this model, NPCs were cultured under different conditions:

1) NPCs cultured in stem cell supporting medium.

2) NPCs cultured in microglia conditioned medium.

3) NPCs cultured in microglia conditioned medium treated with LPS.

4) NPCs co-cultured along with microglia.

5) NPCs co-cultured along with microglia treated with LPS.

The cellular characteristics of NPCs in all the experimental groups were determined by checking the cell fate markers MAP2, GFAP and Olig-2 expressions. Doublecortin (DCX) immunostaining was performed to check the immature NPCs. Fluorescent staining and western blotting were employed to determine the effect of microglia on NPCs differentiation. Pro inflammatory cytokine release from the LPS activated microglia was detected using Elisa analysis.

Results: Our results showed that, microglia modulated the effects on NPCs cell characteristics and directed the NPCs differentiation. The proliferation rate of NPCs was modulated in the NPCs co-cultured with microglia /microglia conditioned medium. Elisa analysis data showed paracrine factors secreted in the NPCs/microglia co-culture condition might contribute for the cell survival. The neuron specific marker MAP2, the astrocyte specific marker GFAP and oligodendrocyte specific marker olig-2 expressions were modulated in all the experimental groups directing the cell fate. DCX immunostaining showed increase in immature NPCs. Neural cell differentiation in NPCs is activated by co-culture with microglia or microglia-conditioned medium, indicating that microglia activates and secretes cytokines essential for neurogenesis evident through our Elisa analysis.

Conclusion: Neurogenesis in highly expanded NPCs can be induced by co-culture with LPS activated microglia or microglia-conditioned medium, indicating that microglia provide secreted factor (s) essential for neurogenesis, NPCs maintenance, selfrenewal, or propagation. Our findings suggest an instructive role for microglia cells in contributing to neurogenesis in the largest neurogenic niche of the brain.

Acknowledgement: This work was supported by the National Research Foundation of Korea (NRF) grant funded by the Korea government (MEST) (2012-0005440)

EFFECTS OF CURCUMIN ON INFLAMMATORY FACTORS IN SERUM FROM TRANSGENIC MOUSE MODELS OF ALZHEIMER'S DISEASE BY ANTIBODY CHIPS

X. Zhang[1], **Y. Li**[2]

[1]Institute of Neuroscience, Chongqing Medical University, [2]Department of Pathology, Institute of Neuroscience, Chongqing Medical University, Chongqing, China

Purpose: To investigate the effects of Curcumin on inflammatory factors in serum from APP/PS1 double transgenic mouse models of Alzheimer's disease (AD) by antibody chips.

Methods: 10 APP/PS1(-/-) and 30 APP/PS1 double transgenic mouse models of AD aged 2 months were involved into the study and were randomly into the control (untreated) group and Curcumin groups, the latter was divided into low dose (100ppm) group and high dose (1000ppm) group. After half of year, the blood was drawn and centrifuged. The inflammatory factors in serum were detected by QAM-INF-1 kit and the data were analyzed.

Results: Compared to the control, the expression of many inflammatory factors(BLC、CD30、Eotaxin、 Eotaxin2, et al) were higher in the untreated group, while, Curcumin could significantly decrease the expression of them in serum of APP/PS1 double transgenic mouse models of AD;

furthermore, the effect was in a dose-dependent manner (P< 0.05).

Conclusion: Excessive inflammatory response is tightly associated with AD, and Curcumin can inhibit the secretion of a variety of inflammatory factors, which will provide more substantial theoretical basis for the prevention and treatment of AD by Curcumin.

This work was supported by the National Natural Science Foundation of China (NSFC: 81271426, 30973154, 81100948). Corresponding author: Yu Li, M. D., Professor. Email: liyu100@163.com

THE EFFECTS OF SYSTEMIC INFLAMMATION ON FUNCTIONAL HYPEREMIA AND NEUROVASCULAR COUPLING

M. Maczka[1], Y. Couch[2], D. Anthony[2], N.R. Sibson[3], C. Martin[4], **A. Spain**[5]

[1]Department of Statistics, [2]Department of Pharmacology, [3]Department of Oncology, Oxford University, Oxford, [4]Department of Psychology, [5]University of Sheffield, Sheffield, UK

Objectives: Accurate interpretation of functional magnetic resonance imaging (fMRI) signals as evidence for stimulus or task-evoked changes in neuronal activity depends upon neurovascular coupling, whereby alterations in the activity of neurons drive local changes in cerebral hemodynamics. Inflammation, both systemic and within the central nervous system, is increasingly recognised as an important feature of a wide range of neurological diseases and there is experimental evidence for inflammatory effects upon molecular processes that are known to play key roles in neurovascular coupling (e.g. prostaglandins, endothelin-1). We therefore hypothesised that experimentally induced systemic inflammation will modulate the relationship between stimulus-evoked neuronal and hemodynamic response measures.

Methods: Male Sprague-Dawley rats were pre-treated with either lipopolysaccharide (0.5mg/kg, n=3) to induce systemic inflammation or saline (control, n=4) before data collection. Animals were subsequently anesthetised, tracheotomised and the femoral vessels cannulated for monitoring and maintenance of physiological parameters. The skull overlying left sensorimotor cortex was thinned to translucency for laser speckle imaging of cortical blood flow changes and insertion of a recording electrode. Cerebral blood flow and local field potential changes were measured in response to (a) electrical stimulation of the contralateral cortex (1mA, 5-40Hz, 2s duration) and (b) hypercapnia, consisting of a 30s epoch of 10% carbon dioxide added to the animal´s air supply.

Results: We find evidence for inflammation induced alterations in the magnitude and latency of stimulus evoked changes in cortical cerebral blood flow. Specifically, across a range of stimulation frequencies, response magnitudes are not only reduced by LPS administration (Figure 1 and Figure 2A, B, showing CBF responses and magnitude statistics), but their temporal profile is also affected with LPS treated animals displaying a more sluggish hemodynamic response (Figure 2C, showing response full-width-half-maximum). Furthermore, the apparent stimulation-frequency dependent nature of the changes in response magnitude suggest alterations in neurovascular coupling by LPS, although further analysis of our local field potential data is required to verify this.

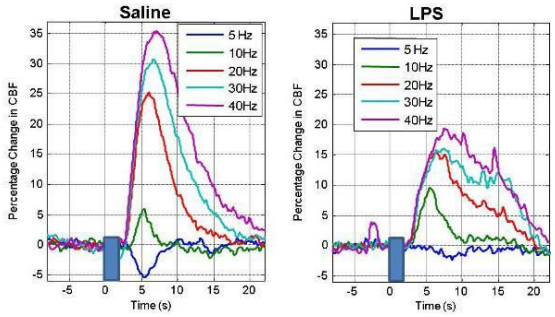

[Figure 1]

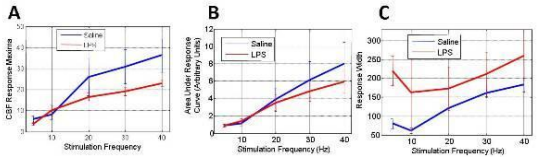

[Figure 2]

Conclusions: Alterations in neurovascular coupling by systemic inflammation may have two important implications. Firstly, these data suggest that the interpretation of neuroimaging data such as that based on the blood oxygen

level dependent signal must take account of possible effects of inflammatory processes on the relationship between hemodynamic and neuronal events, especially where one wishes to compare between patient groups or between patient groups and control subjects. Secondly, these data suggest that alterations in neurovascular coupling, as could be assessed in humans using combined EEG-fMRI, could serve as a useful biomarker for the identification of neuroinflammation in early stage disease.

DIFFERENTIAL ROLE OF CD8+ T LYMPHOCYTES AND NATURAL KILLER CELLS IN ISCHEMIC STROKE: ANTIGEN DEPENDENCY AND PERFORIN-MEDIATED NEUROTOXICITY

E. Mracsko[1], A. Liesz[1], A. Stojanovic[2], M. Oswald[3], W. Zhou[1], S. Karcher[1], F. Winkler[3], A. Cerwenka[2], R. Veltkamp[1]

[1]Department of Neurology, University Heidelberg, [2]Division of Innate Immunity, German Cancer Research Center, [3]Department of Neurooncology, University Heidelberg, Heidelberg, Germany

Objectives: Post-ischemic neuroinflammation plays a crucial role in the pathophysiology of acute brain ischemia. Previous research has focused on the role of pro-inflammatory cytokines such as interferon-γ (IFN-γ) which were identified as key mediators of postischemic neuronal death. In contrast, molecules involved in cell-cell contact-mediated direct cytotoxicity such as perforin have barely been examined. Cytotoxic T lymphocytes (CTL) and natural killer (NK) cells share these neurotoxic effector mechanisms. However, the mechanism of their activation and their contribution to ischemic brain damage is not known. We aimed to characterize the impact of CTL and NK cells on neurological outcome in different experimental murine stroke models, and to elucidate the underlying mechanisms.

Methods: Permanent focal cerebral ischemia was induced by transtemporal middle cerebral artery occlusion (pMCAO) distal from the lenticulostriatal arteries. Transient focal ischemia was induced by introduction of a filament occluding the left MCA for 30 min (tMCAO). We investigated the effect of CTL and NK cells on neurological outcome after focal brain ischemia in mice by *in vivo* depletion of the respective cell populations using monoclonal antibodies against CD8a or NK1.1. The number and the activation state of brain-infiltrating CTL and NK cells was analysed by flow cytometry (FACS). We also characterized the effect of CTL and NK cells on humoral neuroinflammation by measuring the expression of proinflammatory cytokines using real time PCR. To elucidate the activation mechanism of CTL and the role of perforin in their neurotoxic effect, we transferred CD8+ T cells from ovalbumin-specific T cell receptor I (OT-I) transgenic or perforin knockout (*Prf1*$^{-/-}$) mice into lymphocyte-deficient Rag1 knockout (*Rag1*$^{-/-}$) animals. Immunofluorescent histology and 2 photon microscopy was used to visualize the interaction between degenerating neurons and CTL.

Results: CTL depletion significantly reduced infarct volumes in the pMCAO as well as in the tMCAO model and improved behavioural outcome (corner test) 7 days after pMCAO. In contrast, NK cell-depletion did not influence infarct volume and sensorimotor dysfunction. Despite a 3-fold higher number of brain-invading NK cells compared to CTL, only CTL were activated in the ischemic brain. CTL expressing the ovalbumin-specific T cell receptor were not activated and did not increase the infarct volume after cerebral ischemia indicating that the cytotoxic effect of CTL requires antigen-dependent activation. Neither depletion of CTL nor CTL transfer into *Rag1*$^{-/-}$ mice affected cerebral pro-inflammatory cytokine levels including IFN-γ suggesting a more important role of direct cytotoxicity of CTL in ischemia. Accordingly, adoptively trasferred *Prf1*$^{-/-}$ CTL were activated and infiltrated the ischemic brain, but they failed to increase infarct volume. Immunfluorescent histology and 2 photon microscopy confirmed the cell-cell-contact dependent manner of the neurotoxic effect of CTL.

Conclusions: CTL have delayed deleterious effects after acute cerebral ischemia, they require antigen-dependent activation, and perforin secretion is their main effector mechanism. Despite the similar effector repertoire of NK cells, their depletion did not affect outcome after murine stroke.

SYSTEMIC INFLAMMATION IMPAIRS CEREBRAL BLOOD FLOW AFTER FOCAL CEREBRAL ISCHAEMIA

K. Murray[1], W. Holmes[2], K. Davies[3], S. Williams[3], A. Parry-Jones[4], S. Allan[1]

[1]Faculty of Life Sciences, University of Manchester, Manchester, [2]University of Glasgow, Glasgow, [3]Faculty of Medical and Human Sciences, [4]Manchester Academic Health Sciences Centre, University of Manchester, Manchester, UK

Introduction: Stroke is characterised by an interruption in cerebral blood flow (CBF) and the degree of brain damage correlates with the time it takes to re-establish CBF. Inflammation is a key dimension to cerebral ischaemia with experimental studies showing systemic inflammation exacerbates ischaemic damage via interleukin-1 (IL-1) dependent pathways [1]. The mechanism through which systemic inflammation worsens stroke has yet to be elucidated, therefore, this study aimed to investigate effects of systemic IL-1 on CBF during early reperfusion in experimental stroke.

Materials and methods: Transient focal cerebral ischaemia (60min) was induced in male wistar rats by intraluminal filament occlusion. Animals received intraperitoneal recombinant IL-1β (4μg/kg; n=8) or vehicle (0.5% BSA in PBS; n=8). Animals were transferred to a 7-Tesla magnet and remote filament reperfusion performed. Repeated multi-slice diffusion weighted and perfusion (arterial spin labelling) MRI was performed until 4h reperfusion. Diffusion-perfusion mismatch was used to define penumbra and apparent diffusion coefficient (ADC) maps to define ischaemic damage. At 4h reperfusion animals were perfused, organs removed and brains fixed. To further explore actions of IL-1β, quantitative PCR (Q-PCR) was performed on brain homogenates at 15min reperfusion.

Results: IL-1 caused a significant 3-fold increase in the volume and magnitude of tissue hypoperfusion on restoration of MCA patency at 15min, 1 and 2h reperfusion. Q-PCR revealed this was due to IL-1 increasing mRNA levels of the vasoconstrictor, endothelin-1 as well as altering COX-2 gene expression at 15min reperfusion.

Furthermore, IL-1 treated animals had a 2-fold increase in ischaemic volume at 3 and 4h reperfusion compared to vehicle. Immunohistochemistry showed increased numbers of platelets in microvessels and larger platelet aggregates within the vasculature of IL-1 treated animals at 4h reperfusion. This increase in prothrombotic activity was explained by an IL-1 dependent upregulation of P-selectin mRNA in IL-1 treated animals at 15min reperfusion. These results suggest IL-1 causes a reduction in CBF following reperfusion and these compromised flow conditions may favour adhesion of platelets in the vasculature, thus contributing to larger areas of ischaemic damage.

Conclusions: These results show that IL-1 led to a marked increase in the volume and magnitude of tissue hypoperfusion on restoration of MCA patency. This hypoperfused tissue progressed to infarction over 4h due to IL-1 dependent platelet adherence and activation. Poor flow in the microcirculation due to systemic inflammation may lead to an accelerated collapse of salvageable tissue, thus reducing the time window and effectiveness of the only treatment available, thrombolysis. Ultimately, the goal of this research is to intervene acutely to restore CBF and prevent platelet accumulation and subsequent excessive ischaemic damage.

References:

[1] McColl, B.W., N.J. Rothwell, and Allan, S.M., J Neurosci, 2008. **28**(38): p.9451-62.

IMAGING BRAIN METASTASES USING TUMOUR INDUCED GLIOSIS

E. O'Brien[1], V. Kersemans[1], M. Tredwell[2], B. Checa[2], C. Escartin[3], G. Bonvento[3], D. Anthony[4], N. Sibson[1]

[1]Gray Institute of Radiation Oncology Biology, Oxford University, [2]Department of Chemistry, University of Oxford, Oxford, UK, [3]MIRcen, Fontenay-aux-Roses, France, [4]Department of Pharmacology, University of Oxford, Oxford, UK

Introduction: 20-40% of cancer patients develop secondary cancer to the brain, yet the mechanisms underlying disease pathogenesis are still not fully elucidated. An inflammatory tumour microenvironment is established in the brain; microglial cells infiltrate metastases, and

recent studies implicate reactive astrocytes early in disease progression [1-3].

Aim: We aim to quantify astrocyte activation, spatially and temporally, during metastasis pathogenesis in a mouse model of metastatic breast cancer. Secondly, we used a CNTF-expressing lentivirus to induce sustained astrocyte activation in the mouse striatum, in order to determine the effect of astrocyte activation on metastasis seeding and growth in the brain. Thirdly, we used the combined glial response to brain metastasis as a surrogate for imaging tumour growth using the SPECT contrast agent ^{123}I-DPA713, a compound which binds to the translocator protein (TSPO) on activated glia [4].

Methods: Female BALB/c mice were injected with 4T1-GFP cells(intra-cardially or intra-cerebrally). For analysis of the temporal and spatial profile of astrocyte activation, brains were perfusion-fixed at days 10, 14, 21 and 28 post-injection (n=5). Astrocyte and microglial activation was detected immunohistochemically. For the lentiviral study, BALB/c mice were injected intrastriatally with 100ng CNTF-lentivirus (Lenti-CNTF). After 5 weeks, animals were injected intracardially (n=5) or intracerebrally (n=5) with 4T1-GFP cells. At day 10 post-injection, tumour burden was detected immunohistochemically. For the SPECT study, DPA713 [5] was labelled with ^{123}I. Mice were imaged at 13 days post-intra-cerebral injection of 4T1-GFP cells (n=6) or saline (n=3). For the intracardiac model, mice were imaged at 21 days post-injection of 4T1-GFP cells (n=5) or saline (n=5). SPECT/CT was performed 1h after i.v. injection of *ca*. 20MBq ^{123}I.

Results: Brain metastases were found to be surrounded by a ring of activated astrocytes and microglia, from the earliest time point studied. The extent of astrocyte activation correlated positively with tumour size throughout the 28 day time course (r^2 0.6; $P < 0.0001$). Sustained activation of astrocytes following Lenti-CNTF injection appeared to increase metastasis seeding, with a greater proportion of tumours found in the activated hemisphere (63% total tumour number). Using both SPECT and autoradiography, ^{123}I-DPA713 was shown to accumulate at sites of metastases in the brain, with the extent of binding correlating spatially with the extent of gliosis.

Conclusions: We have shown that gliosis is an integral part of the tumour microenvironment. It appears that chronic astrocyte activation increases metastatic seeding to the brain, suggesting a pro-tumorigenic downstream effect of astrocyte activation. In addition, we have shown that gliosis enables early detection of brain metastases through the use of a radiolabelled compound that binds to activated microglia and astrocytes. The ability to image tumour-induced gliosis will not only aid understanding of disease mechanisms, but also has potential for diagnostic imaging.

References:

1. Lorger, M. and B. Felding-Habermann, Am J Pathol, 2010. **176**(6)

2. Fitzgerald, D.P., et al., Clin Exp Metastasis, 2008. **25**(7)

3. Seike, T., et al., Clin Exp Metastasis, 2011. **28**(1)

4. Cosenza-Nashat, M., et al., Neuropathol Appl Neurobiol, 2009. **35**(3)

5. Reynolds, A., et al., Bioorg Med Chem Lett, 2010. **20**(19)

FOCAL CEREBRAL ISCHEMIA IN THE TNFA-TRANSGENIC RAT: COGNITION, FUNCTION AND POST-ISCHEMIC CELL SURVIVAL

L.C. Pettigrew[1,2], R.J. Kryscio[3]

[1]Neurology Service, Department of Veterans Affairs Medical Center, [2]Stroke Program, Sanders-Brown Center on Aging and Department of Neurology, University of Kentucky, [3]Department of Statistics, School of Public Health, University of Kentucky, Lexington, KY, USA

Objectives: Tumor necrosis factor-alpha (TNFα) is an inflammatory mediator that is elevated in ischemic brain. To complement its role as a determinant of cell survival after physiological stress, TNFα is also recognized as an important contributor to neurotransmission and synaptic integrity. Using a transgenic (TNFα-Tg) rat selectively overexpressing the murine TNFα gene in its brain, we tested the following hypothesis: constitutive upregulation of TNFα protein synthesis will affect functional performance by exacerbating hippocampal and ischemic cortical cell loss.

Methods: Construction of the TNFα-Tg rat has been described (Pettigrew et al., 2008). To evaluate the effect of constitutive upregulation of TNFα protein synthesis on cognition and functional outcome, TNFα-Tg rats and wild-type (WT) littermates underwent middle cerebral artery occlusion (MCAO) for 1 hr. Parallel groups of animals (n=6-10 per group) were examined for cognitive performance in a Morris water maze, before and 7 days after MCAO, or in serial Rotarod tasks performed up to 28 days after MCAO. At 28 days, animals were euthanatized for quantitative cell counting in hippocampus and ischemic cortex.

Results: During probe testing of reference memory retention 7 days after MCAO, WT animals selectively targeted one of 4 water maze pool quadrants from which an escape platform had been removed (39.3 ± 14 sec; $p \leq 0.03$ compared to random [25% targeted search]). TNFα-Tg rats did not follow differential search strategy (36.5 ± 13.2 sec; p=NS). In the Rotarod task performed after sham-MCAO, there was no difference between TNFα-Tg and WT rats (p=NS). After MCAO, TNFα-Tg rats performed inferiorly to sham-ischemic animals on 6 of 10 serial test dates up to 28 days ($p \leq 0.05$ per comparison). Ischemic WT rats performed inferiorly on only 3 dates ($p \leq 0.05$). In ischemic hemisphere at 28 days, there was significant between-group variation in CA1 neuronal count among sham-ischemic, TNFα-Tg, and WT rats (ANOVA; $F=2.499$; $p \leq 0.05$); post hoc testing showed no difference between TNFα-Tg and WT animals (p=NS). Between-group variation was also significant in cortical layer 5 neuronal count among all 3 groups ($F=6.331$; $p \leq 0.001$). Among WT animals, the layer 5 neuronal count in ischemic cortex was significantly lower than in unaffected cortex (Tukey's test; $p \leq 0.001$) but was no different from that in TNFα-Tg rats (p=NS).

Conclusions: We found that TNFα-Tg rats displayed weakened retention of reference memory 7 days after MCAO. In the Rotarod task, ischemic TNFα-Tg animals performed inferiorly to sham-ischemic TNFα-Tg rats with two-fold greater frequency than by the same comparison among WT littermates. Despite these discrepancies in cognitive and functional performance, there were no significant differences in CA1 and cortical layer 5 neuronal survival within the ischemic hemisphere among TNFα-Tg and WT rats. We conclude that post-ischemic cognitive and functional impairment in the TNFα-Tg rat may be driven by the chronic effect of increased TNFα on synaptic integrity, rather than post-ischemic hippocampal and cortical neuronal loss.

Reference: Pettigrew LC, Kindy MS, Scheff S, et al. Focal cerebral ischemia in the TNFalpha-transgenic rat. *J Neuroinflammation* 2008:5; 47

Grant support: United States Department of Veteran Affairs Merit Review Award (LCP).

INHIBITION OF NADPH OXIDASE BY APOCYANIN ALTERNATIVELY PREVENTS MICROGLIA INDUCED NEUROINFLAMMATION IN LIPOPOLYSACCHARIDE INDUCED PARKINSONS DISEASE MODEL

N. Sharma, B. Nehru

Biophysics, Panjab University, Chandigarh, India

Recent studies have revealed an essential role for neuroinflammation that is initiated by microglial and infiltrated peripheral immune cells and their toxic products (cytokines. chemokines etc.) in pathogenesis of Parkindon's Disease. Lipopolysaccharide, a bacterial endotoxin is the most extensively utilized glial activator for the induction of inflammatory dnergic neurodegeneration therefore, LPS at a dose of (5ug/5ul PBS) injected stereotaxically into the Substantia Nigra of rat brain was utilised for the establishment of PD model. This in turn leads to microglial activation and hence increased level of pro-inflammtory cytokines and activation of NADPH oxidase complex leading to excessive superoxide anion production which combines with NO to form $OONO^-$ and other ROS/RNS species which further results in neurotransmitter Dopamine loss and behavioural impairment. Apocyanin significantly lowered the production of superoxide anions which was further supported by decreased NADPH oxidase activity and suppressed expression of various NADPH subunits gp91(phox), p47(phox). It significantly decreased microglial activation and suppressed mRNA expression of various proinflammatory cytokines (TNF-α, IL-1α,β, IFN-γ, IL-6), NO/iNOS in mid brain region hence, prevented neurotransmitter dopamine loss and resulted behavioural impairment. Since apocyanin treatment attenuated ROS production which alternatively leads to

decreased cytokine production and iNOS in response to LPS further strengthened the notion that Phox-derived ROS are crucial for proinflammatory gene expression in glial cells. Thus its supplementation can prove to be beneficial for curing PD.

PROBUCOL ATTENUATES HYPERCHOLESTEROLEMIA-INDUCED EXACERBATION IN ISCHEMIC BRAIN INJURY VIA ANTI-NEUROINFLAMMATORY EFFECTS

K.H. Choi, J.H. Kim, Y.J. Jang, B.T. Choi, **H.K. Shin**

Division of Meridian and Structural Medicine, School of Korean Medicine, Pusan National University, Yangsan-si, Republic of Korea

Objectives: Hypercholesterolemia is a major underlying cause for ischemic stroke and therapeutics targeting hypercholesterolemia decrease the risk of stroke in high-risk individuals or in patients with stroke or transient ischemic attack. Probucol, a lipid-lowering agent with anti-oxidant properties, has been implicated in protection against atherosclerosis, whereas its effect on ischemic brain injury with hypercholesterolemia remains to be fully elucidated. In the present study, we investigated the beneficial effects of probucol on focal cerebral ischemia with hypercholesterolemia in mice.

Methods: ApoE knockout (KO) mice were fed a high-fat diet (HFD) with or without 0.3% probucol for 10 weeks. To assess the protective effects of probucol on ischemic injury, the mice received 40 min-middle cerebral artery occlusion (MCAO) and infarct volumes, neurobehavioral deficits and neuroinflammatory cytokines were evaluated 48 h after reperfusion.

Results: Probucol significantly decreased total- and LDL-cholesterol in ApoE KO mice with HFD. 40 min-Middle cerebral artery occlusion resulted in significantly larger infarct volumes in ApoE KO with 10 weeks of HFD compared to ApoE KO fed a regular diet, which was significantly reduced by probucol. Consistent with a smaller infarct size, probucol prominently improved neurological function and motor function. In addition, probucol significantly decreased MCP-1 mRNA levels and MCP-1, CD11b and GFAP immunoreactivity in ischemic cortex. Furthermore, probucol reduced LPS-induced inflammatory cytokine production such as MCP-1, TNF-α, and IL-1β in BV2 microglia cells.

Conclusions: These findings suggest that probucol have protective effect on focal cerebral ischemic injury with hypercholesterolemia and this beneficial effect of probucol might be explained by anti-neuroinflammatory mechanisms. Probucol may be a promising therapeutic drug for reducing the impact of stroke in hypercholesterolemic subjects.

GLIA AND MAST CELLS AS TARGETS FOR PALMITOYLETHANOLAMIDE, AN ANTI-INFLAMMATORY AND NEUROPROTECTIVE LIPID MEDIATOR

S.D. Skaper

Scienze del Farmaco, Universiità degli Studi di Padova, Padova, Italy

Objectives: Glia have emerged as key contributory players in central nervous system disorders ranging from neuropathic pain and epilepsy to neurodegenerative diseases. When over-activated they behave as immunoresponsive cells, releasing glial and neuronal signaling molecules. Glia respond also to pro-inflammatory signals released from cells of immune origin, including the immune-related mast cell (1). Endogenous protective mechanisms/molecules can be activated as a result of tissue damage or stimulation of inflammatory responses, such as N-acylethanolamines, a class of naturally occurring lipid mediators (e.g. N-arachidonoylethanolamine (anandamide) and its congener, N-palmitoylethanolamine (PEA). A key role of PEA may be to maintain cellular homeostasis when faced with external stressors provoking, for example, inflammation (2). PEA is produced/hydrolyzed by microglia, it inhibits mast cell activation, and its levels are elevated in ischemic brain tissue and in spinal cord of experimental allergic encephalomyelitis mice. However, there may be pathological settings where PEA endogenous production is insufficient to control the ensuing inflammatory cascade.

Methods: A number of studies have addressed this question by applying PEA exogenously in experimental animal models of: neuropathic pain (chronic constrictive injury), Parkinson's disease (1-methyl-4-phenyl-1,2,3,6-tetrahydropyridine; MPTP),

Alzheimer's disease (amyloid β-peptide intracerebroventricular injection) ischemia-reperfusion brain injury (middle cerebral artery occlusion), and traumatic brain injury (controlled cortical impact).

Results: In mast-cell/glia mediated preclinical models of acute and neurogenic inflammation PEA displayed anti-allodynic and anti-hyperalgesic effects (3). PEA reduced ischemic brain injury in rats (4), and protected the neurovascular unit and reduced secondary injury after traumatic brain injury in mice (5). PEA is endowed with neuroprotective/anti-neuroinflammatory effects as well, for example in: spinal cord trauma (6); MPTP dopaminergic neuron injury (7); amyloid β-peptide-induced learning and memory impairment in mice (8). These actions appear to be mediated by PEA acting through "receptor pleiotropism" i.e., both direct and indirect interactions of with different receptor targets, e.g. cannabinoid CB1, peroxisome proliferator-activated receptor alpha, and the transient receptor potential cation channel subfamily V member 1 (TrpV1) (2).

Conclusions: Mast cell - glia communication may open new perspectives for designing therapies to target neuroinflammation by differentially modulating the activation of non-neuronal cells normally controlling neuronal sensitization - both peripherally and centrally (9).

References:

(1) Skaper SD, Giusti P, Facci L (2012) FASEB J. 26:3103-3117

(2) Skaper SD, Facci L (2012) Philos Trans R Soc Lond B Biol Sci. 367:3312-3325

(3) Costa B, Comelli F, Bettoni I, Colleoni M, Giagnoni G (2008) Pain 139:541-550

(4) Ahmad A, Genovese T, Impellizzeri D, Crupi R, Velardi E, Marino A, Esposito E, Cuzzocrea S (2012) Brain Res 1477:45-58

(5) Ahmad A, Crupi R, Impellizzeri D, Campolo M, Marino A, Esposito E, Cuzzocrea S (2012) Brain Behav Immun 26:1310-1221

(6) Esposito E, Paterniti I, Mazzon E, Genovese T, Di Paola R, Galuppo M, Cuzzocrea S (2011) Brain Behav Immun 25:1099-1112

(7) Esposito E, Impellizzeri D, Mazzon E, Paterniti I, Cuzzocrea S (2012) PLoS One 7:8 (doi: 10.1371/journal.pone.0041880)

(8) D´Agostino G, Russo R, Avagliano C, Cristiano C, Meli R, Calignano A (2012) Neuropsychopharmacology 37:1784-1792

(9) Petrosino S, Iuvone T, Di Marzo V (2010) Biochimie 92:724-727

IMAGING TRANSLOCATOR PROTEIN EXPRESSION IN GLIOMA PATIENTS: RELATION TO TUMOUR GRADE AND EPILEPTIC SEIZURES

Z. Su[1], K. Herholz[1], R. Hinz[1], D.J. Coope[2], K. Karabatsou[2], F.E. Turkheimer[3], A. Jackson[1], F. Roncaroli[4], A. Gerhard[1]

[1]Wolfson Molecular Imaging Centre, University of Manchester, Manchester, [2]Department of Neurosurgery, Salford Royal NHS Foundation Trust, Salford, [3]Department of Neuroimaging, Institute of Psychiatry, King's College London, [4]'John Fulcher' Neuro-Oncology Laboratory, Imperial College London, London, UK

Background and aims: Translocator protein (TSPO) is a pro-inflammatory molecule over-expressed predominantly in activated microglia under pathological conditions.[1] In glioma samples, TSPO has been found to be up-regulated and correlated with the malignancy of the tumours.[2,3] [^{11}C]-(*R*)PK11195 is a selective radioligand for the TSPO widely applied in PET studies. We aimed to investigate *in vivo* cerebral TSPO expression and microglial activation in glioma patients using [^{11}C]-(*R*)PK11195 PET, and confirm these neuroinflammatory responses in tumour tissue with histopathological examinations.

Methods: 23 glioma patients (14 low-grade and 9 high-grade) and 10 healthy volunteers underwent volumetric MRI and dynamic [^{11}C]-(*R*)PK11195 PET scans. Parametric maps of binding potential (BP_{ND}) were generated using the simplified reference tissue model[4] with a cerebellar input function to calculate both intra- and extra-tumoural [^{11}C]-(*R*)PK11195 binding. Co-registered MRI/PET was used to guide tumour biopsies. Tumour tissue was quantitatively assessed for TSPO expression and microglial infiltration by immunohistochemistry. Patients presenting with epileptic seizures (18 out of 23) were also assessed for the duration of epilepsy history,

severity and type by clinical interview and case notes review.

Results: Low-grade gliomas demonstrated low [^{11}C]-(*R*)PK11195 BP_{ND}, which was even lower than normal-appearing brain regions in the contralateral hemisphere (p=0.0006). High-grade gliomas showed higher BP_{ND} than low-grade tumours (p=0.006). Immunohistochemistry confirmed that TSPO in gliomas was mainly expressed by neoplastic cells, and this expression correlated with [^{11}C]-(*R*)PK11195 BP_{ND} of the tumours (r=0.657, p=0.001). When compared with controls, increased [^{11}C]-(*R*)PK11195 BP_{ND} was found in patients' normal-appearing cerebral structures, being more prominent in the tumour-bearing hemisphere (p=0.0002) than the tumour-free hemisphere (p=0.005). This extra-tumoural [^{11}C]-(*R*)PK11195 binding correlated with the duration of epilepsy history (r=0.5, p=0.037). A predominantly ipsilateral pattern of increased extra-tumoural BP_{ND} was revealed in patients presenting with partial seizures. They demonstrated significantly more asymmetry than patients with generalised seizures, in whom the increase was more bilateral.

Conclusions: Gliomas show differences in [^{11}C]-(*R*)PK11195 binding depending on their grade of malignancy. Within tumours, neoplastic cells are the main cellular sources expressing TSPO and determine the [^{11}C]-(*R*)PK11195 binding. The high extra-tumoural [^{11}C]-(*R*)PK11195 binding indicates widespread microglial activation in normal-appearing cerebral structures of glioma patients, possibly induced by epileptic seizures. It is associated with the duration of epilepsy history and the seizure type, suggesting that modulation of neuroinflammation could be a novel target for seizure control in this patient population.

References:

1. Venneti S, Lopresti BJ, Wiley CA. Molecular imaging of microglia/macrophages in the brain. Glia 2012; **61**:10-23.

2. Vlodavsky E, Soustiel JF. Immunohistochemical expression of peripheral benzodiazepine receptors in human astrocytomas and its correlation with grade of malignancy, proliferation, apoptosis and survival. J Neurooncol 2007; **81**:1-7.

3. Miettinen H, Kononen J, Haapasalo H, et al. Expression of peripheral-type benzodiazepine receptor and diazepam binding inhibitor in human astrocytomas: relationship to cell proliferation. Cancer Res 1995; **55**:2691-5.

4. Lammertsma AA, Hume SP. Simplified reference tissue model for PET receptor studies. NeuroImage 1996; **4**:153-8.

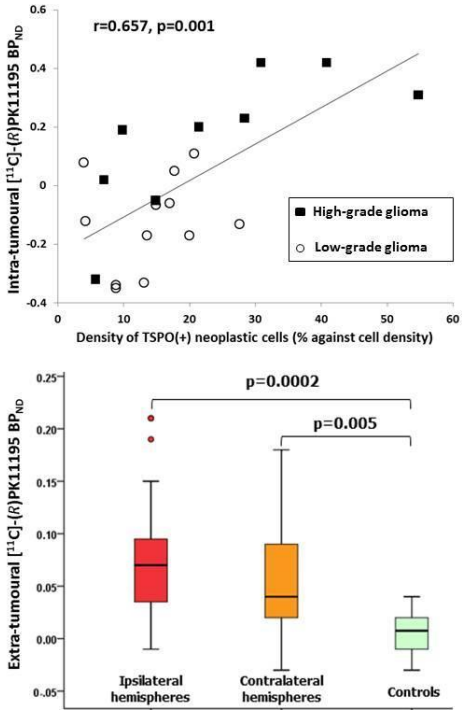

[Intra- and extra-tumoural [11C]-(R)PK11195 binding]

VASCULOPROTECTIVE EFFECTS OF DELAYED LOCAL HYPOTHERMIA AFTER TRANSIENT MIDDLE CEREBRAL ARTERY OCCLUSION IN RATS

J.-H. Kim, M. Seo, H.S. Han, J. Park, **K. Suk**

Kyungpook National University School of Medicine, Daegu, Republic of Korea

Therapeutic hypothermia is one of the robust therapeutic tools in experimental stroke models but has many limitations to be applied in clinics. Optimal conditions for therapeutic hypothermia such as cooling temperature, initiation and duration of cooling time have to be individualized. Here, we evaluated therapeutic effects of delayed (4 hr) and prolonged (44 hr) local hypothermia after transient middle cerebral artery occlusion (tMCAo) using the cooling device that enables improved local hypothermia (31°C) in the

brain. Histological data revealed that the local hypothermia significantly reduced the infarct volume and glial hypertrophic activation. Brain water content, IgG leakage, and Evans Blue extravasation were notably reduced by local hypothermia. The local hypothermia showed strong vasculoprotective effects as determined by immunohistochemistry or Western blot analyses of endothelial barrier antigen (EBA), laminin, aquaporin-4, or tight junction proteins in the brain. Our data indicate that the delayed and prolonged local hypothermia confers neurovascular protection along with reduction of brain edema and inhibition of inflammatory glial activation. Thus, hypothermic conservation of vascular structure and function may account for the therapeutic effects of local hypothermia in the experimental stroke.

THE ROLE OF MICROVESICLES IN GLUTAMINASE REGULATION AND MECHANISMS OF GLUTAMATE GENERATION IN HIV-1-INFECTED MICROGLIA

B. Wu, Y. Huang, L. Zhao, J. Zheng

Department of Pharmacology and Experimental Neuroscience, University of Nebraska Medical Center, Omaha, NE, USA

Objectives: HIV-1-infected and/or activated microglia are pivotal in the pathogenesis of HIV-1-associated neurocognitive disorders (HAND) through production and release of various soluble neurotoxic factors including glutamate. We have previously reported that glutaminase, a glutamate generating enzyme, is upregulated during HIV-1 infection and mediates excess glutamate generation that may contribute to the neurotoxicity in HAND. Recent evidence suggests microvesicles (MVs) contains proteins and nucleic acids, cytokines or chemokines. Microglia shed MVs into the brain microenvironment to transfer crucial information. However, whether MVs is involved in the glutaminase regulation and excess glutamate generation in HIV-1-infected microglia is unknown.

Methods: A human primary microglia culture system and macrophage-tropic HIV-1_{ADA} strain were used to model HIV-1 infection in microglia. Hela cells were used to model MVs release. Glutamate levels in the culture supernatants were determined by reverse phase high-performance liquid chromatography. Differential centrifugation with the *in vitro* culture supernatant was used to obtain MVs. MVs protein contents were analyzed with Western blotting. 6-diazo-5-oxo-L-norleucine and a well-characterized compound 19560 were used to specifically inhibit glutaminase activity in the culture supernatants. A gene over-expression system, delivered via adenovirus vector, was used to overexpress glutaminase. Morphology of MVs was visualized by Confocal Microscopy after immunostaining with Microglia marker, Iba1 and CD11b. Statistical analysis was performed using ANOVA, followed by the Tukey-post-test for paired observations.

Results: To model the upregulation of glutaminase in HIV-1-infected microglia, we used adenovirus vector to overexpress glutaminase in human microglia. After overexpression, we collected the culture supernatants and removed cells through centrifugation. The cell-free supernatants were incubated with or without glutamine and glutaminase inhibitors. The excess glutamate generation was blocked by the removal of glutamine or by addition of glutaminase inhibitors, suggesting that glutaminase was released into extracellular fluid by microglia. We further isolated MVs through differential centrifugation and found that MVs mediated glutamate generation through glutaminase. Consistent with the result, high levels of glutaminase in MVs was detected by Western blotting. Morphology of MVs was visualized in HIV-infected microglia under confocal microscopy after immunostaining with microglia marker, further suggesting that MVs mediate excess glutamate generation through glutaminase.

Conclusions: These findings support MV glutaminase as a potential mechanism of glutaminase regulation and excess glutamate generation in the HAND pathogenic process and identify MV glutaminase as a possible therapeutic target for the treatment of HAND.

Reference:

1. N.Erdmann et al. (2007) Glutamate production by HIV-1-infected human macrophage is blocked by the inhibition of glutaminase. J. neurochem, 102, 539-549.

2. N.Erdmann et al. (2009) In vitro glutaminase regulation and mechanisms of glutamate generation in HIV-1-infected macrophage. J.Neurochem.109, 551-561.

3. Y.Huang et al. (2011) Glutaminase dysregulation in HIV-1-infected human

microglia mediates neurotoxicity: relevant to HIV-1-Associated Neurocognitive Disorders. J. Neurosci, 31(42):15195-15204.

4. B.Li et al. (2012) RhoA triggers a specific signaling pathway that generates transforming microvesicles in cancer cells. Oncogene 1-10.

5.E. Turola. (2012) Microglia microvesicle secretion and intercellular signaling. Frontiers in Physiology, vol.3, Article 149.

MAILUONING PROTECTED AGAINST OXYGEN AND GLUCOSE DEPRIVATION-INDUCED NEURONAL INJURY BY UP-REGULATING PGC-1A

Z. Wang, M. Lu, L. Qian, **Y. Xu**

Department of Neurology, Affiliated Drum Tower Hospital of Nanjing University Medical School, Nan Jing, China

Background and objective: Mailuoning injection (MLN), extracted from traditional Chinese medicine with the main components all being polyphenolic acids, is widely used in China to treat acute ischemic stroke according to its pharmacological effects of anti-platelet aggregation and improvement of hemorrheology. In recent years, antioxidative effect of MLN has been demonstrated, while the potential mechanism remains unknown. In the present study, our objective was to clarify the neuroprotective effect of MLN against ischemic injury and its underlying mechanism.

Methods: Mice primary cortical neurons were subjected to oxygen and glucose deprivation (OGD) to induce ischemic injury in vitro. In MLN administration group, cultures were treated with MLN at different concentrations of 50mg/ml, 100mg/ml, 500mg/ml, 1000mg/ml, 5000mg/ml and 10000mg/ml during OGD and reoxygenation process. Neuronal viability and lactate dehydrogenase (LDH) release were measured after OGD. Flow cytometric analysis was performed to examine cell apoptosis, reactive oxygen species (ROS) production and mitochondrial membrane potential with propidium iodide (PI), 2′,7′-dihydrodichlorofluorescein diacetate (DCFH-DA) and 5,5′,6,6′-tetrachloro-1,1′,3,3′-tetraethyl-benzimidazolyl- carbocyanine iodide (JC-1) employed respectively. In addition, mice treated with MLN/saline were subjected to middle cerebral artery occlusion (MCAO), then the protein and mRNA levels of peroxisome proliferator- activated receptor γ coactivator-1α (PGC-1α) were determined on ischemic cortex by western blotting and qRT-PCR. Furthermore, short hairpin RNAs (shRNAs) targeting PGC-1α were synthesized and transfected into neurons to evaluate whether the neuroprotection of mailuoning was suppressed by RNA interference. Finally, constructed plasmid containing PGC-1α promoter sequence was introduced into HEK293T cells and then the activity of the promoter vectors was determined using luciferase reporter activity assay.

Results: Neurons exposed to OGD presented loss of cell viability, elevation of cell apoptosis and LDH leakage, which were reversed significantly by MLN treatment. MLN also decreased ROS accumulation and improved mitochondrial membrane potential after OGD. It was notable that MLN upregulated PGC-1α protein and mRNA levels which were suppressed by ischemia 12 h, 24 h, 72 h after ischemia/reperfusion. With the interference of shRNA targeting PGC-1α, neuroprotective effect of MLN on OGD neurons was greatly blocked. Interestingly, it was demonstrated that MLN activated PGC-1α promoter to initiate gene transcription at concentrations of 1000 mg/ml, 5000 mg/ml, 10000 mg/ml.

Conclusions: MLN protects against OGD-induced neuronal injury via enhancing PGC-1α expression, which is probably the underlying mechanism contributing to the benefit of MLN in clinic.

HB PROMOTES INTRACEREBRAL HEMORRHAGE INFLAMMATION INJURY THROUGH ASSEMBLY OF A TOLL-LIKE RECEPTOR 2 AND 4 HETERODIMER

Y.-C. Wang[1], S. Lin[2], P.-F. Wang[1], R.-P. Xiong[3], H. Fang[1], M. Song[4], Q.-L. Liang[5], **Q.-W. Yang**[1]

[1]Department of Neurology, [2]Xinqiao Hospital, Third Military Medical University, [3]The Molecular Biology Centre，State Key Laboratory of Trauma, Burn and Combined Injury, Research Institute of Surgery and Daping Hospital, Third Military Medical University, [4]Department of Medical Genetics, Third Military Medical University, Chongqing, [5]School of Pharmacology, Nanjing University of Chinese University, Nanjing, China

Objective: Inflammation is considered to be an important determination of outcome after intracerebral hemorrhage(ICH). However, the

exact mechanism of inflammation injury following ICH has not been elucidated yet. Our recently research indicated that TLR4 may be the key upstream linkage of inflammation injury after ICH. Recent data demonstrated that high expression of TLR2 on peripheral monocytes was positively correlated with neurological functional deficit. Our experiments were designed to understand the mechanisms underlying TLR2 mediated inflammation after ICH, and whether it correlated with TLR4.

Methods: ICH mice models were established by autologous blood infusion of the left caudate putamen. Primary microglia cultures were stimulated with hemoglobin (Hb) which was the main component of hematoma. Expression of TLR2 in perihematoma tissues were assessed by real-time quantitative PCR and western blot. Immunofluoscence and flow cytometry of perihematoma tissues were analyzed to identifying which type of cells expressed TLR2. TLR2 null mice were measured with brain water content, neurological deficit scores, and secretion of inflammation factors, neurons apoptosis and periphery inflammatory cells infiltration. TLR2 and TLR4 heterodimer and their cooperation mechanism were evaluated by immunoprecipitation (IP) and immunolfuorescence assay. In vitro gene transfection experiments suggested that TLR2 and TLR4 heterodimer contributed to poor neurological outcome after ICH. Finally we used SsnB, isolated from a commonly used Chinese herb, to inhibiting TLR2 and TLR4 heterodimer and declining neurologic deficits of ICH.

Results: ICH mice models were established by autologous blood infusion of the left caudate putamen. Primary microglia cultures were stimulated with hemoglobin (Hb) which was the main component of hematoma. Expression of TLR2 in perihematoma tissues were assessed by real-time quantitative PCR and western blot. Immunofluoscence and flow cytometry of perihematoma tissues were analyzed to identifying which type of cells expressed TLR2 (neurons, microglia and astrocytes). TLR2 null mice were measured with brain water content, neurological deficit scores, and secretion of inflammation factors, neurons apoptosis and periphery inflammatory cells infiltration, compared with TLR1 null mice. Primary microglia cultures stimulated with Hb and animal infused with Hb were established to indentifying which hematoma components triggered the TLR2 expression on microglias, and the possible signaling pathway involved in TLR2-mediated inflammatory response. TLR2 and TLR4 heterodimer and their cooperation mechanism were evaluated by immunoprecipitation (IP) and immunolfuorescence in WT, MyD88 and TRIF null mice and primary cell cultures. In vivo and in vitro gene transfection experiments suggested that TLR2 and TLR4 heterodimer contributed to poor neurological outcome after ICH. Finally we used SsnB, isolated from a commonly used Chinese herb, to inhibiting TLR2 and TLR4 heterodimer and declining neurologic deficits of ICH.

Conclusion: To our knowledge, we firstly identify a previously undescribed toll-like receptor heterodimer on microglias that initiates inflammation injury after ICH. Our results suggested that TLR2 and TLR4 heterodimer may be a new target for ICH treatment, and SsnB can be a new candidate for ICH treatment.

SPLENIC IMMUNE CELLS IN EXPERIMENTAL NEONATAL HYPOXIA-ISCHEMIA

N. Fathali, R. Ostrowski, Y. Hasegawa, T. Lekic, J. Tang, **J. Zhang**

Loma Linda University School of Medicine, Loma Linda, CA, USA

Objective: Neuroimmune processes contribute to hypoxic-ischemic damage in the immature brain and may play a role in the progression of particular variants of neonatal encephalopathy. The present study was designed to elucidate molecular mediators of interactions between astrocytes, neurons and infiltrating peripheral immune cells after experimental neonatal hypoxia-ischemia (HI).

Methods: Splenectomy was performed on postnatal day-7 Sprague-Dawley rats 3 days prior to HI surgery; in which the right common carotid artery was permanently ligated followed by 2 hours of hypoxia (8% O_2).

Results: Quantitative analysis showed that natural killer (NK) and T cell expression was reduced in spleen but increased in the brain following HI. Elevations in cyclooxygenase-2 (COX-2) expression after HI by immune cells promoted interleukin-15 expression in astrocytes and infiltration of inflammatory cells to site of injury; additionally, down-regulated the pro-survival protein, phosphoinositide-3-

kinase, resulting in caspase-3 mediated neuronal death. The removal of the largest pool of peripheral immune cells in the body by splenectomy, COX-2 inhibitors, as well as rendering NK cells inactive by CD161 knockdown, significantly ameliorated cerebral infarct volume at 72 hours, diminished body weight loss and brain and systemic organ atrophy, and reduced neurobehavioral deficits at 3 weeks.

Conclusion: Herein we demonstrate with the use of surgical approach (splenectomy), with pharmacological loss-gain function approach using COX-2 inhibitors/agonists, as well as with NK cell-type specific siRNA that after neonatal HI, the infiltrating peripheral immune cells may modulate downstream targets of cell death and neuroinflammation by COX-2 regulated signals.

Reference:

1. Alvarez-Diaz A, Hilario E, de Cerio FG, Valls-i-Soler A, Alvarez-Diaz FJ. Hypoxic-ischemic injury in the immature brain - key vascular and cellular players. Neonatology 2007;92:227-235.
2. Gelderblom M, Leypoldt F, Steinbach K, et al. Temporal and spatial dynamics of cerebral immune cell accumulation in stroke. Stroke 2009;40:1849-1857.
3. Curin Y, Ritz MF, Andriantsitohaina R. Cellular mechanisms of the protective effect of polyphenols on the neurovascular unit in strokes. Cardiovasc Hematol Agents Med Chem 2006;4:277-288.
4. Lo EH. Experimental models, neurovascular mechanisms and translational issues in stroke research. Br J Pharmacol 2008;153:S396-405.

QUANTITATIVE PROTEOMIC ANALYSIS OF POST-TRANSLATIONAL MODIFICATIONS IN ALZHEIMER'S DISEASE BRAIN

S. Zahid[1], M. Oellerich[2], A.R. Asif[2], **N. Ahmed**[1]

[1]Department of Biochemistry, University of Karachi, Karachi, Pakistan, [2]Department of Clinical Chemistry, University Medical Center Goettingen, Goettingen, Germany

Introduction: Post-translational modifications (PTMs) are crucial for the regulation of protein structure and function. It is now widely accepted that protein expression alterations are mainly a consequence of dysregulated PTMs resulting in protein dysfunction. Targeting proteins to specific modifications is a complex process that requires sophisticated proteomics technology. Proteomic analysis represents a new aspect to re-evaluate clinical trials and therapeutics for Alzheimer's disease.

Methods: The present study analyzed the proteome-wide changes in the phosphorylation and S-nitrosylation associated with the activation of signaling pathways and biochemical links. A combinatorial effect of these PTMs on several metabolic and signaling cascades was assessed using computational tools like STRING 8.3 and MINT while the functional enrichment of the altered PTMed proteins was searched through KEGG and REACTOME databases.

Results: A number of proteins involved in several cellular and molecular pathways were identified with aberrant phosphorylation and S-nitrosylation levels in the AD brain regions**.** The identified altered proteins can be helpful for biomarker discovery and can provide a broader understanding of the brain dysfunction. A close interaction pattern was also observed among the identified proteins in AD brain.

Conclusions: The current findings focused on several significant proteins that accounts for biological and morphological alterations in AD that will be helpful to establish a broad database of potential protein targets of aberrant PTMs in AD brain.

PROTECTIVE EFFECT OF ACTEOSIDE ENRICHED FRACTION AGAINST STREPTOZOTOCIN-INDUCED COGNITIVE DYSFUNCTION AND INFLAMMATORY DAMAGE IN RATS

A. Pandey, **S. Bani**

Indian Institute of Integrative Medicine (Council of Scientific & Industrial Research), Jammu, India

Alzheimer´s disease (AD) is an age-associated, irreversible, progressive neurodegenerative disease that is characterized by severe memory loss, unusual behavior, personality changes, and a decline

in cognitive function. The drugs currently available to treat the disease have limited effectiveness. It is believed that therapeutic intervention that could postpone the onset or progression of Alzheimer´s disease would dramatically reduce the number of cases in the coming years.

This study demonstrates the protective effect of Acteoside enriched fraction from the leaves of *Colebrookia oppositifolia* on Intracerebroventricular -streptozotocin (ICV-STZ) induced Alzheimer's in rats.

Chronic treatment with AEF (5,10 and 20 mg/kg) on a daily basis for a period of 21 days, beginning 1 h prior to first ICV-STZ injection, significantly improved cognitive impairment (Fig:1). Oxidative stress and neuroinflammation have been implicated in pathophysiology of sporadic type of dementia. Besides, improving cognitive dysfunction, administration of AEF significantly reduced elevated malondialdehyde, nitrite levels (Fig:2a), and restored reduced glutathione reductase levels in brain tissues.

The ICV STZ injection showed a significant decline in the brain Acetylcholine levels. However, administration of ASF (5, 10 and 20 mg/kg) significantly reversed the elevation in Acetylcholine esterase activity (Fig:2b)

STZ induced Alzheimers altered peripheral T lymphocyte subset distribution and corresponding cytokine secretion patterns in experimental animals. Oral administration of AEF decreased the over expressed cell population of CD4+ and CD8+ T (Fig:3a) cell evident by significant decrease in expression of IFN-γ (Fig:3b).

Figure:1

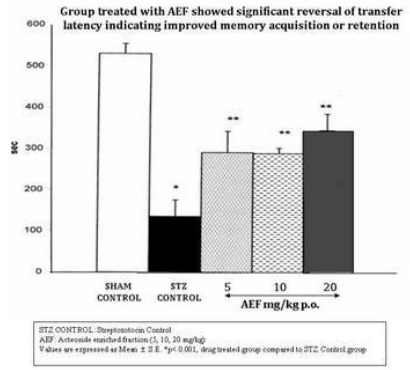

[memory retention]

Figure:2

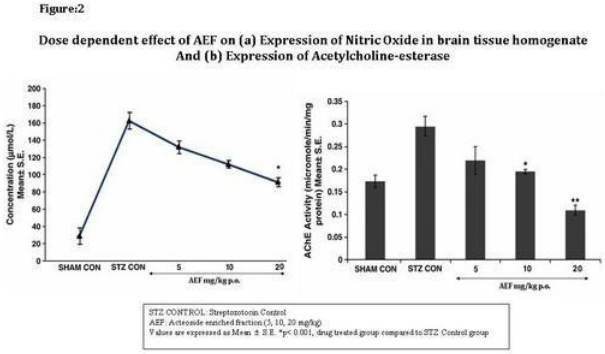

[Estimations]

Figure:3

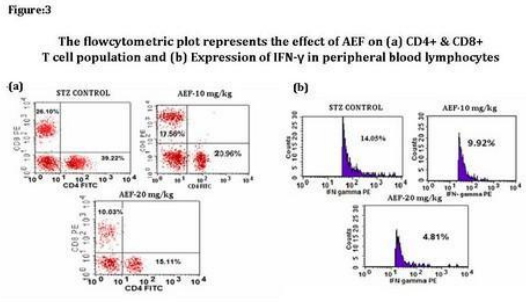

[Flowcytometry]

This preclinical study establishes the unique potential of AEF suggesting its use in AD. Such plant products are sort after to carry out the treatment and prevent the cognitive impairement. There is an urgent need for the implementation of combined and coordinated research endeavors for the development of such herbal moieties for therapeutic interventions and prevention of AD, thus, improving the quality of life of the patients.

HIGH LEVELS OF DIVERGENT HIV-1 QUASISPECIES IN NEUROLOGICAL OPPORTUNISTIC INFECTIONS

D. Chen, Y. Zhang, F. Wei, L. Liu, Z. Liu

STD/AIDS Research Center, Beijing You An Hospital, Beijing Institute of Hepatology, Capital Medical University, Beijing, China

Objectives: Despite survival in people infected with HIV has improved because of an increasingly powerful highly active antiretroviral therapy (HAART), the opportunistic infections (OIs) in the central nervous system (CNS) remain a serious burden worldwide. HIV-1 was confirmed to be capable of entering the CNS by infected peripheral monocytes, but its effect in CNS OIs was still not clear. In this study, we investigated the CNS HIV-1 character in CNS OIs.

Patients and methods: 24 CNS OIs and 16 non-CNS-OIs (control) cases were selected from AIDS patients who infected HIV-1 by paid blood donor in China. HIV-1 loads of plasma and cerebrospinal fluid (CSF) were detected by reverse transcriptase polymerase chain reaction, and C2-V5 area of HIV-1 envelope region was amplified from viral quasispecies isolated from CSF by nest polymerase chain reaction.

Results: CSF HIV-1 load was significantly high in CNS OIs, but no high plasma HIV-1 load were found in these patients. HIV-1 quasispecies isolated from the CSF of CNS OIs patients had a high diversity as the nucleotide sequence analysis of C2-V5 region. Most HIV-1 quasispecies isolated from the CSF of CNS OIs patients were R5 tropism as 11/25 charge rule.

Conclusion: These results suggest that high levels of divergent HIV-1 quasispecies contribute to opportunistic infections in the central nervous system.

DISTRIBUTION OF GLUTAMATE AND VGLUT1 AND THEIR RELATIONSHIP TO CGRP AND CGRP RECEPTOR COMPONENTS IN DURA MATER AND TRIGEMINAL GANGLION

S. Eftekhari[1], L. Edvinsson[1,2]

[1]Department of Clinical Sciences, Division of Experimental Vascular Research, Lund University, Lund, Sweden, [2]Department of Clinical Experimental Research, University of Copenhagen, Glostrup Hospital, Glostrup Reasearch Institute, Glostrup, Denmark

Background and aims: Glutamate is suggested to play a significant role in migraine pathophysiology. The role of glutamate in migraine is implicated by data from animal and human studies. These studies suggest that there is a link between migraine pathology and the glutamate system, putatively in two ways.

(i) The second order neurons in the brainstem contain glutamate as a main signaling molecule.

(ii) Some of the trigeminal neurons contain glutamate as a co-transmitter.

The neuropeptide calcitonin gene related peptide (CGRP) is suggested to play an important role in migraine and CGRP receptor antagonists have antimigraine efficacy.

Methods: Immunofluorescence was used to study the distribution of glutamate and the vesicular glutamate transporter 1 (VGLUT1) in dura mater and trigeminal ganglion (TG). Their relation to CGRP and its receptor components- calcitonin receptor-like receptor (CLR) and receptor activity modifying protein 1 (RAMP1) was studied.

Results: Glutamate immunoreactivity was found in thin fibers, while VGLUT1 was expressed in thicker fibers in dura mater. Double-staining of glutamate or VGLUT1 with CGRP showed no co-expression of the markers. Double-staining of VGLUT1 and CLR showed co-expression in the thick fibers of dura mater. Glutamate and VGLUT1 expression was found in neurons of the TG. In addition, some satellite glial cells in TG displayed glutamate immunoreactivity. Glutamate positive neurons rarely co-expressed CGRP. Double-staining of VGLUT1 and CGRP showed no co-expression. Double-

staining of VLGUT1 and CLR showed that they could be expressed in the same cells, mainly in larger TG neurons. Not all VGLUT1 positive neurons were positive for CLR.

Conclusions: Glutamate expression was found in thin fibers in dura mater and medium-sized trigeminal neurons. VGLUT1 was instead expressed in thicker fibers and larger neurons. In addition, some satellite glial cells displayed glutamate immunoreactivity. Interestingly, we found co-expression of VLUT1 and the CGRP receptor components. These results suggest that there might be an interaction between the glutamatergic system and CGRP receptors.

ASTROCYTIC PARP-1 REGULATES GLUTAMATE TRANSPORTER LEVELS VIA NF-KB IN EXPERIMENTAL WERNICKE´S ENCEPHALOPATHY

S.S. Jhala, D. Wang, **A.S. Hazell**

Medicine, University of Montreal, Montreal, QC, Canada

Introduction: Downregulation of the astrocytic glutamate transporters GLT-1 and GLAST and excitotoxic damage are important features of the pathophysiology of thiamine deficiency (TD), the cause of Wernicke's encephalopathy (Hazell et al., 2001, 2003). Exactly how the levels of these transporters are altered in this disorder, however, is unknown. Poly (ADP) ribose polymerase-1 (PARP-1), an important enzyme of poly (ADP)-ribosylation with a key role in the regulation of transcription and the development of excitotoxicity is associated with the pathogenesis of various disorders of the CNS. In addition, nuclear factor-kappaB (NF-κB) has previously been linked to the regulation of GLT-1, and PARP-1 is required and sufficient for specific transcriptional activation of NF-κB.

Objectives: To understand the relationship between PARP-1 and the regulation of glutamate transporters in TD,

Methods: Primary cultures of astrocytes and adult, male Sprague-Dawley rats (225-250g) rats were treated with pyrithiamine-induced TD. Experiments included the use of immunoblotting, flow cytometry, and immunocytochemistry to study PARP-1 changes in relation to glutamate transporter regulation.

Results: Cells treated with TD displayed a profound increase in the 50 kDa cleaved fragment of PARP-1 and IκB phosphorylation suggestive of NF-kB activation and nuclear translocation. These changes occurred in association with a decrease in levels of the splice-variant GLT-1b and were also apparent in a well-established rat model of TD. Using specific PARP-1 and NF-κB inhibitors (DPQ and PDTC respectively), we demonstrate a strong likelihood that excessive PARP activation due to impaired energy status or oxidative insult as a consequence of TD promotes NF-κB-dependent downregulation of GLT-1b.

Conclusions: Our findings indicate that PARP-1 activation and NF-kB play an important role in the loss of astrocytic glutamate transporters in TD.

References:

Hazell AS, Rao KV, Danbolt NC, Pow DV, Butterworth RF. 2001. Selective down-regulation of the astrocyte glutamate transporters GLT-1 and GLAST within the medial thalamus in experimental Wernicke´s encephalopathy. J Neurochem 78:560-568.

Hazell AS, Pannunzio P, Rama Rao KV, Pow DV, Rambaldi A. 2003. Thiamine deficiency results in downregulation of the GLAST glutamate transporter in cultured astrocytes. Glia 43:175-184.

IMBALANCE OF CA2+ AND K+ FLUXES IN C6 GLIOMA CELLS AFTER PDT MEASURED WITH SCANNING ION-SELECTIVE ELECTRODE TECHNIQUE

S. Hu, H. Feng

Third Military Medical University, Chongqing, China

Objectives: Photodynamic therapy (PDT) possesses the capacity to lead to death of C6 glioma in vitro and in vivo. The purpose of this study was to investigate whether Ca^{2+} and K^{+} homeostasis of C6 glioma cells were affected by PDT.

Methods: We administered α-amino-3-hydroxy-5-methyl-4-isoxazolepropionic acid (AMPA) glutamate receptor antagonist prior to PDT on C6 glioma cells. The changes of glutamate release, expression of AMPAR,

apoptosis of C6 cells, and intracellular free calcium ($[Ca^{2+}]_i$) were examined after PDT. The fluxes of Ca^{2+} and K^+ were studied by using a non-invasive scanning ion-selective electrode technique (SIET).

Results: We found that PDT increased extracellular glutamate and expression of AMPAR subunit GluR1 and GluR2, which might result in Ca^{2+} influx and apoptosis of C6 cells. When AMPAR antagonist was added, intracellular free calcium reduced and apoptosis rate of C6 cells decreased. PDT induced Ca^{2+} influx and K^+ efflux significantly, which resulted in death of C6 cells.

Conclusions: These results indicate that PDT may lead to death of C6 glioma cells partly through glutamate and its receptors AMPAR. Ca^{2+} influx and K^+ efflux may correlate with the treatment effects of PDT on C6 glioma cells.

DUAL MODULATION OF HETEROMERIC ACID-SENSING ION CHANNEL 1A/3 CHANNEL BY ZINC

Q. Jiang, X.-P. Chu

University of Missouri-Kansas City, Kansas City, MO, USA

Acid-sensing ion channels 1a and 3 subunits are all expressed in sensory neurons, where they are though to play critical roles in pain perception associated with tissue acidosis. Previous studies have shown that both homomeric ASIC1a and 3 channels are inhibited by physiological concentrations of zinc. ASIC1a and 3 can form functional channels in heterogonous system, which is believed to be expressed in sensory neurons. Here, we found that heteromeric ASIC1a/3 channels are sensitive to zinc with dual effects. Different from homomeric ASIC1a and ASIC3 in response to zinc, co-application of zinc dose-dependently potentiates the heteromeric ASIC1a/3 channel currents with an EC_{50} of 30 µM, pretreatment with zinc between 3 to 100 µM exert the same potentiation as co-application. However, prolonged pretreatment with zinc induced the significant inhibition of heteromeric ASIC1a/3 channels when concentration of zinc is over 100 µM. The potentiation of heteromeric ASIC1a/3 channels by zinc is pH-dependent, as zinc shifts the pH-dependences of ASIC1a/3 current from a pH_{50} of 6.5 to 6.9; while the inhibition of ASIC1a/3 currents by zinc is pH-independent. The inhibition of ASIC1a/3 currents by pre-applied zinc was independent of pH activation, steady-state desensitization, voltage, or extracellular Ca^{2+}. Further, we showed that the effect of zinc is dependent on the extracellular histidine, but not cysteine residue. Mutating histidine 83, but not other histidine residues (72, 73, 109, and 195), located in the extracellular domain of the ASIC1a/3 subunit abolished the zinc effect. These findings suggest that histidine 83 in the extracellular domain of ASIC1a/3 subunit is critical for zinc-mediated effect and provide the basis for future mechanistic studies addressing the functional importance of heteromeric ASIC1a/3 channels in pain modulation.

BEHAVIOURAL AND HISTOPATHOLOGICAL ASSESSMENT OF THE EFFECTS OF PERIODIC FASTING ON PENTYLENETETRAZOL-INDUCED SEIZURES IN RATS

F. Karimzadeh[1], M. Jafarian[2], M. Gharakhani[3], S. Razeghi[3], A. Gorji[4]

[1]Neuroscience, [2]Tehran University, [3]Shefa Neuroscience Research Center, Tehran, Iran, [4]Muenster University, Muenster, Germany

Objectives: Periodic fasting (PF) was suggested to display antiepileptic and neuroprotective effects, which is in stark contrast to severe fasting or starvation. However, these beneficial effects seem to depend on the type and duration of the used feeding protocol. There are discrepancies concerning both antiepileptic and neuroprotective effects of a PF-diet during repetitive seizures in different epilepsy models. This study was designed to evaluate the effects of different PF protocols on behavioural and histopathological consequences of epilepsy in adult rats.

Methods: Recurrent generalized seizures were caused by repetitive injection of pentylenetetrazol (PTZ) for a period of four weeks every other day. While control animals had free access to food and water, animals on a PF-diet were on intermittent fasting for 24 hours every 48 hours for 4-weeks before (T1), after (T2), or both before and after (T3) the injection of PTZ. Behavioural studies were carried out after PTZ-injections and histological investigations were performed after the experiments were completed.

Results: Seizure assessment showed that the

severity of seizures was significantly decreased in groups T1 and T3 when compared to control rats. Dark neuron densities in hippocampal CA1 and CA3 areas were decreased in PF groups, but never in the temporal cortex. The PF-diet also decreased the number of TUNEL-positive neurons in the hippocampus in both areas and all PF-diet protocols. We observed a correlation between an increase in the density of dark neurons and a decrease in the volume of normal neurons in all PF groups in the CA1 hippocampal area.

Discussion: These results support the idea that a PF-diet has anticonvulsive and neuroprotective effects on epileptic rats but underlines that different PF-diet protocols can have varying effects. Anticonvulsive effects were strongest when the PF-diet started before the onset of excitotoxic injuries, the number of dark neurons was decreased and apoptosis was prevented by all PF-diet protocols investigated in this work. Further evaluation of PF-diet protocols for possible clinical anticonvulsant and neuroprotective effects is suggested.

AUTOPHAGY IS INVOLVED IN NG2 CELL-MEDIATED CLEARANCE OF AMYLOID PEPTIDE

Z. Ke

Key Laboratory of Nutrition and Metabolism, Institute for Nutritional Sciences, Shanghai Institutes for Biological Sciences, Chinese Academy of Sciences, Shanghai, China

Accumulation of β-amyloid peptides is an important pathophysiological hallmark of Alzheimer's disease (AD). Tremendous efforts have been directed to elucidate the mechanisms of β-amyloid peptides degradation and develop strategies to remove β-amyloid accumulation. We showed here that NG2 cells, a subpopulation of oligodendroglial precursor cells, were a new cell type that can clear β-amyloid peptides in vivo and in vitro. NG2 cells were activated around the amyloid plaque, and engulfed β-amyloid peptides through the mechanisms of endocytosis. The presence of β-amyloid peptides stimulated the autophagic pathway in NG2 cells. Once inside the cells, the β-amyloid peptides in NG2 cells were transported to lysosomes and degraded by autophagy/lysosome pathway. The results indicate that NG2 cells are a new cell type that can clear β-amyloid peptides through endocytosis and autophagy. These findings are important as it provides new insight into the mechanisms of β-amyloid degradation and may be helpful in developing a novel strategy to remove β-amyloid accumulation.

AUGMENTATION OF THE SENSORY-EVOKED HEMODYNAMIC RESPONSE IN AN EARLY ALZHEIMER'S DISEASE MOUSE MODEL

J. Kim, Y. Jeong

Bio and Brain Engineering, Korea Advanced Institute of Science and Technology, Daejeon, Republic of Korea

Objectives: We compared hemodynamic response induced by sensory stimulus in an Alzheimer's disease (AD) mouse model, along with amyloid plaque deposition.

Methods: We used 3-7 months old male APP^{SWE}/PS1ΔE9 transgenic mice (Tg) and wild-type littermates (Wt). Mice were anesthetized using ketamine and xylazine (100 and 10 mg/kg, respectively). We utilized intrinsic optical signal imaging, laser Doppler flowmetry, and two-photon microscopy to observe changes in total-, oxy-, and deoxy-hemoglobin concentration, cerebral blood flow, arterial dilation and RBC velocity, respectively. Sensory stimulation was delivered to hindpaw by 0.2 mA, 20 msec, and 2 Hz electric stimulation for 5 sec. To observe amyloid plaque deposition, we injected methoxy-X04 (5 mg/kg) 18 hours before imaging.

Results: APP^{SWE}/PS1ΔE9 transgenic mice (Tg) developed amyloid plaque burden at 5 months of age, and cerebral amyloid angiopathy was observed at 7 months of age. At 7 months of age, but not at earlier ages, sensory stimulation-induced hemodynamic responses were augmented and prolonged in Tg, when observed by changes in total, oxy-, and deoxy-hemoglobin concentration. Vasodilatation of pial arteriole was also augmented and prolonged in 7-month-old Tg. In case of total hemoglobin response and pial arteriole vasodilatation response, both response duration and speed was increased. Cerebral blood flow and RBC velocity response was also augmented, but not prolonged. Baseline cerebral blood flow was significantly lower at 7-month-old Tg compared to Wt.

Conclusions: We observed augmented hemodynamic response in AD model mice at

the stage of cerebral amyloid angiopathy development. The result suggests reduced baseline CBF as an underlying mechanism of this change.

NEUROPROTECTION OF ANXIETY LIKE BEHAVIOUR AND OXIDATIVE DAMAGE IN MICE THROUGH RUTIN

L. Machawal, A. Kumar

Dept of Pharmacology, Panjab University, Chandigarh, India

Introduction: Stress has been in cognitively causing several neurodegnerative problems. Neurobiology of stress and related cascades is also very complex. Besides, has been known to cause anxiety and related complications in human being. However, the exact pathological mechanism as well as suitable adequate treatment is not available so far.

Materials and methods: Male Laca mice were used in the present study. Rutin (20, 40, 80 mg/kg p.o.) and vitamin E (50 mg/kg p.o.) were administered for 5 days before subjecting for immobilisation stress. Animals were immobilised for 6 hour and several behavioural (mirror chamber as well as locomotion performance tasks) and following by biochemical parameters (lipid peroxidation, nitrite concentration, reduced glutathione and catalase) were assessed in the brain and corticosterone level in serum.

Results: 6-hour Immobilisation stress significantly caused anxiety like behavioural both in mirror chamber as well as actophotometer tasks, raised corticosterone level and oxidative damage (as evidenced by raised lipid peroxidation, nitrite concentration, depletion of reduced glutathione and catalase activity) as compared to naïve group. 5-days pre-treatment with rutin (20, 40, 80 mg/kg) significantly attenuated anxiety like behaviuor in the test paradigms, corticosterone level as well as antioxidant like effect and also restored oxidant and antioxidant whole brain.

Conclusion: Results of the present study suggest the neuroprotective potential of rutin against immobilisation stress induced anxiety like behaviour and oxidative damage in mice. Study further provides a hope rutin could be used for effective management of stress induced anxiety like problems.

PROGNOSTIC VALUE OF FREE RADICAL MARKERS AND HYPERGLYCEMIA IN STROKE PATIENTS

A. Orlova[1], E. Silina[1], S. Rumiantseva[2], N. Gomboeva[1], S. Bolevich[1]

[1]I.M. Sechenov First Moscow State Medical University (MSMU), [2]The Russian National Research Medical University named after N.I. Pirogov (RNRMU), Moscow, Russia

Objective: To evaluate the extent and prognostic value of disturbances of free radical processes in patients with DM and hyperglycemia associated with disturbed glucose utilization, developing stroke.

Patients and methods: 395 patients with stroke (mean age 63,3±12,6 years) were included. All patients underwent standard diagnostic procedures for stroke protocol. Free radical formation was assessed additionally in plasma based on oxidative (chemiluminescence intensity index - basal (CIIb) and zymosane-stimulated (CIIs)) and lipid peroxidation markers (anti-peroxide plasma activity (APA), malondialdehyde (MDA).

Results: At admission 41,8% of patients had blood glucose > 6,6 mmol/l; DM, including new-onset, was diagnosed in 19%. Hence, hyperglycemia in acute stroke is 2,2-fold more prevalent than DM ($p< 0,05$). In 22,8% patients hyperglycemia may be attributed to acute phase reactions and insulin resistance, leading to energy deficiency. The highest mortality rate, which correlated with the volume of cerebral lesion, was seen in patients with hyperglycemia (40,5%), including patients without DM (32,2%). In patients with normal blood glucose mortality was significantly lower (22,5%; $p< 0,05$). Presence of DM was associated with mortality rate of 24,3%, which is 1,7-fold lower than in patients with hyperglycemia and no DM ($p< 0,05$). Adverse outcome rate on day 1 was 59% higher, on day 2 - 53% higher, on day 3- 75% higher than in patients with normal blood glucose.

Even on Day 1 there was a marked difference in all free radical formation markers in patients with DM and without DM. There was a tendency to higher levels of CIIs, MDA and decreased APA in patients with DM and stroke ($p< 0,05$), which illustrates the depletion of intracellular antioxidant defenses and energy deficiency. At the same time, the most pronounced free radical imbalance was observed in patients with hyperglycemia, with the most significant decrease in APA ($p< 0,01$)

and increase in cellular destruction marker - MDA.

We postulate that free radical formation markers are early markers of stroke severity, emerging earlier than hyperglycemia and leucocytosis. Unfavorable outcome was associated with MDA >3,5 µmoll and APA< 3 r.u. In a group of patients with high MDA level hyperglycemia was found in 29,7% of discharged and 52,0% of patients with lethal outcome (p< 0,05), in patients with low APA - in 26,8% of survivors and in 50,0% of patients with lethal outcome (p< 0,05).

Blood glucose, leucocyte count, MDA and APA at admission correlate with functional outcome on Rankin scale on discharge. In a group with good functional outcome hyperglycemia was observed in 34,9%, high leucocyte count - in 19,5%, in a group with unfavorable functional outcome - in 52,2% and 52,9%, respectively (p< 0,05). Blood glucose > 15,6 mmol/l, leucocyte count >14,6x10^9/l, MDA >5,3 mmol/l, APA < 1,83 r.u. are associated with poor prognosis and high mortality (accuracy - 86,3%, sensitivity - 81,7%).

Conclusion: High MDA level, decrease of APA, hyperglycemia are associated with unfavorable outcome (lethal outcome, severe disability) in stroke patients. We observed an association of hyperglycemia with poor outcome in stroke.

SCANS WITHOUT EVIDENCE OF DOPAMINERGIC DEFICIT (SWEDD): FROM CLINICAL PRACTICE TO DAT MOLECULAR IMAGING

B. Paghera[1], A. Alkhraisheh[1], I. Delrio[2], E. Premi[2], A. Padovani[2], R. Giubbini[1]

[1]Nuclear Medicine, Spedali Civili Hospital and University of Brescia, [2]Department of Neurology, University of Brescia, Brescia, Italy

Objective: The concept of “scans without evidence of dopaminergic deficit” (SWEDD) has been introduced in the last years, referring to patients with a clinical diagnosis of Parkinson's Disease but with a normal presynaptic nigro-striatal dopaminergic imaging. Firstly recognized in clinical trials setting, it is still partially unknown the effective prevalence of this condition in clinical practice. At this aim, we studied a large group of subjects that underwent (123)I-FP-CIT (DATSCAN) imaging with a clinical diagnosis of degenerative parkinsonism.

Methods: 262 subjects with a clinical diagnosis of degenerative parkinsonism were evaluated at the Department of Neurology, University of Brescia, from March 2003 to March 2012. Every subject underwent a neurological evaluation, a neuropsychological assessment and the DATSCAN study. The result of DAT-imaging and the latest follow-up evaluation were considered to classify the subjects.

Results: 66 (25.2%) subjects presented a normal DAT-imaging. Among them, 21 (8.0%) subjects showed an initial suspect of degenerative parkinsonism, clinically confirmed at follow-up evaluation. This latter group, classified as SWEDD, presented a distinct clinical profile (age of evaluation= 61.3±10.8; disease duration= 3.05±2.33; UPDRS-III at onset=11.9±5.0; UPDRS-III at the latest follow-up=11.2±6.18; MMSE at onset= 27.13±4.12) with no significant decline of motor abilities (UPDRS-III at onset vs. UPDRS-III at follow-up: P=0.8).

Conclusions: Our study suggests that in clinical practice the presence of SWEDD patients could be more pronounced as previously described. The careful clinical description, the normal DAT-imaging and the substantial absence of motor decline represented the key-points to recognize this non-degenerative entity in everyday neurological practice.

CHANGES OF BRAIN TISSUE VOLUMES AND PERFUSION WITH THE NUMBER OF OPTIC NEURITIS ATTACKS IN RELPASING NEUROMYELITIS OPTICA

C. Sánchez-Catasús[1], J. Cabrera-Gomez[1], W. Almaguer Melián[1], J.L. Giroud Benítez[2], R. Rodríguez Rojas[1], J. Bosch Bayard[3], L. Galán[3], R. Galvizu Sánchez[1], N. Pavón Fuentes[1], A. Aguila Ruiz[1], P. Valdes-Sosa[3]

[1]Center for Neurological Restoration (CIREN), [2]'Salvador Allende' Hospital, [3]Cuban Neuroscience Center, Havana, Cuba

Neuromyelitis optica (NMO) is a severely disabling autoimmune inflammatory demyelinating disorder of the central nervous system (CNS) [1]. Recent neuroimaging studies show that brain abnormalities in NMO are more frequent than earlier described. Yet,

more research considering multiple aspects of NMO is necessary to better understand these abnormalities. NMO is characterized by monophasic or recurrent attacks of optic neuritis (ON) and myelitis. A distinctive clinical feature of relapsing NMO (RNMO) is that the incremental disability is attack-related [2]. Therefore, association between the attack-related process and neuroimaging might be expected. On the other hand, the immunopathological analysis of NMO lesions has suggested that CNS microvasculature could be an early disease target [3], which could alter brain perfusion. There are no previous studies confirming brain perfusion abnormalities in NMO. Brain tissue volume changes accompanying perfusion alteration could also be expected.

Objectives: To investigate possible associations between brain tissue volumes and perfusion and the attack-related process in patients with RNMO.

Methods: High resolution T1-weighted MRI and perfusion SPECT imaging, corrected for partial volume effect, were obtained in 15 RNMO patients. Multiple regression analyses in the RNMO group were carried out using statistical parametric mapping. Brain white (WMV) and grey matter volumes (GMV) or perfusion was considered as the dependent variable; while the number of ON attacks, myelitis attacks or total attacks (ON plus myelitis attacks) was considered as the independent variable (covariate of interest). Statistical parametric maps were thresholded at p value < 0.01 (p value < 0.05 corrected for multiple comparisons at the cluster level).

Results: We found significant negative regional correlations of WMV, GMV and perfusion with the number of ON attacks, including important components of the visual system such as the posterior thalamic radiations (WMV), middle/superior temporal gyri (GMV) and the primary visual area (perfusion). This is consistent with clinical findings that blindness was only present in one out of nine patients with less than three ON attacks, while five out of six patients with three or four ON attacks were blind. Unexpectedly, we also found a significant positive regional correlation of perfusion with the number of ON attacks, mostly overlapping the brain area where the WMV showed negative correlation , which could be associated to the complex and not yet fully understood pathophysiology of NMO.

Conclusions: Our study shows for the first time that the increase in ON attack number in patients with RNMO, which is directly related with incremental visual disability, decreases regional brain tissue volumes and perfusion bilaterally, involving important regions of visual pathway . This could be relevant for the comprehension of disease course. Our results also provides evidence that brain microvasculature is an early disease target and suggests that perfusion alteration could be important in the development of brain structural abnormalities in RNMO.

References:

1. Barnett MH, Sutton I. Curr Opin Neurol 25:215-220, 2012.

2. Wingerchuk DM, et al. Neurology 68: 603-605, 2007.

3. Lucchinetti CF, et al. Brain 125: 1450-1461, 2002

GINSENOSIDE-RD ATTENUATES AB-INDUCED TAU PHOSPHORYLATION VIA ALTERING THE FUNCTIONAL BALANCE OF GLYCOGEN SYNTHASE KINASE-3B AND PROTEIN PHOSPHATASE-2A

M. Shi, L. Li, G. Zhao

Xijing Hospital, The Fourth Military Medical University, Xi'an, China

Objectives: Neurofibrillary tangles are aggregates of hyperphosphorylated tau protein that are one of pathological hallmarks of Alzheimer's disease (AD). The phosphorylation level of tau protein is regulated by a balance of kinase and phosphatase activities. Our previous study has demonstrated that ginsenoside Rd, one of the principal active ingredients of *Pana notoginseng*, inhibits okadaic acid-induced phosphorylation of tau protein *in vivo* and *in vitro*, but the underlying mechanism(s) is unknown.

Methods: In this study, using multiple AD models, including Aβ-treated cultured cortical neurons, an AD rat model with Aβ injection into hippocampus CA1 and APP transgenic mice, we explored possible mechanisms of inhibtiory effects of ginsenoside-Rd on tau protein phosphorylation by Western blotting analysis and an *in vitro* biochemical assay.

Results: Ginsenoside Rd pretreatment inhibited tau protein phosphorylation at multiple sites (Ser199/202, Ser396 and Ser404). Ginsenoside Rd not only reduced Aβ-induced increased expression of glycogen synthase kinase 3β (GSK-3β), the most important kinase involving tau phosphorylation, but also inhibited its activity by enhancing and attenuating its phosphorylation at Ser9 and Tyr216, respectively. Moreover, ginsenoside-Rd enhanced the activity of protein phosphatase 2A (PP-2A), a key phosphatase involving tau protein dephosphorylation. Finally, an *in vitro* biochemical assay revealed that ginsenoside Rd could affect GSK-3β and PP-2A activities in a direct way.

Conclusions: Thus, our findings provide the first evidence that ginsenoside Rd attenuates Aβ-induced tau protein phosphorylation by altering the functional balance of GSK-3β and PP-2A, and could be used as a promising pharmacological agent for prevention of AD.

References: Li L, Liu J, Yan X, Qin K, Shi M, Lin T, Zhu Y, Kang T, Zhao G. Protective effects of ginsenoside Rd against okadaic acid-induced neurotoxicity in vivo and in vitro. J Ethnopharmacol. 2011 Oct 31;138(1):135-41.

A NOVEL APPROACH TO ATTENUATE CEREBRAL VASOSPASM: INTRANASAL DELIVERY OF CALCITONIN GENE-RELATED PEPTIDE TO INCREASE NITRIC OXIDE CONTENT

B.-L. Sun, Y. Wang, C.-B. Zheng, Y. Zhao, M.-F. Yang, Z.-Y. Zhang, D.-W. Li, F. Zhang, X.-M. Hu

Key Lab of Cerebral Microcirculation in Universities of Shandong, Department of Neurology, Affiliated Hospital, Taishan Medical University, Taian, China

Objectives: Calcitonin gene-related peptide (CGRP) is a large peptide and one of the most potent endogenous vasodilator. Originated from neural cells, CGRP is quickly consumed from the vessel wall after subarachnoid hemorrhage (SAH), and intranasal or systemic supplement of CGRP attenuates cerebral vasospasm induced by SAH. However, the protective mechanisms of CGRP are not fully understood. Nitric oxide (NO) is another strong vasodilator that mainly originates from endothelial cells. The purpose of this study is to investigate whether intranasal delivery of CGRP stimulates NO generation, leading to synergistic effects of vasodilation in rats after SAH.

Methods: 72 adult Wistar rats were randomly divided into four groups, with 18 rats in each group: sham-operated, SAH only, SAH treated with intranasal saline, and SAH treated with intranasal CGRP. Experimental rat SAH was induced using Suzuki's double-blood injection model with modification. A segment of PE-50 tube was inserted into nasal cavities for drug delivery. Vasospasm was evaluated by measuring the diameter of basal artery (BA). The mRNA levels of endothelial nitric oxide synthetase (eNOS) were determined using RT-PCR, NO contents were measured using nitrate reductase assay, and cyclic guanosine monophosphate (cGMP) contents were measured using radioimmunoassay.

Results: Compared with sham group, SAH group demonstrated a decreased BA diameter and an increased thickness of BA wall, indicating severe vasospasm. Intranasal CGRP treatment significantly attenuated the vasospasm while intranasal saline failed to do so. Nitrate reductase assay demonstrated that rats in SAH and intranasal saline groups showed decreased NO contents, as compared with control group. Intranasal CGRP treatment partially restored NO contents, which was accompanied by an increased content of arterial cGMP, the he second messenger of NO, indicating that CGPR promotes NO product and activity. RT-PCR analysis showed that the levels arterial eNOS mRNA were decreased in both SAH group and intransal saline treated SAH groups, and eNOS mRNA was partially recovered in intranasal CGRP+SAH group.

Conclusions: Impaired NO-cGMP pathway may lead to the cerebral vasospasm after SAH; and intranasal delivery of CGRP protects the brain against cerebral vasospasm via stimulating NO product and activity. Future study will focus on how CGRP treatment increases the production of NO.

GAP-JUNCTION IS A POTENTIAL TARGET FOR EPILEPTIC THERAPY IN HUMAN GELASTIC SEIZURES WITH HYPOTHALAMIC HAMARTOMA

J. Wu[1,2]

[1]Neurology, Barrow Neurological Institute, St. Joseph's Hospital and Medical Center, Phoenix, AZ, USA, [2]Physiology/Pharmacology, Ningbo University Medical College, Ningbo, China

Background and aims: Human hypothalamic hamartoma (HH) is a rare developmental malformation usually characterized by gelastic seizures. Almost all HH patients are refractory to antiepileptic drugs (AEDs). Since the epileptogenic mechanisms of gelastic seizures are unknown, there is no available AEDs that can effectively control seizure activity. Previously, we have found that the neurons within HH tissue are distributed in clusters of variable size, and that most (~90%) of HH neurons are small, GABAergic neurons with pacemaker-like firing. We believe that these neuronal clusters represent the functional unit for seizure initiation within HH tissue, and that hypersynchrony of these small, intrinsically-firing GABAergic neurons is a mechanistic component of ictogenesis.

Methods: Multiple experimental approaches were used for this study, which include electrophysiological recording from HH slices, immunohistochemical staining of HH sections with specific antibodies for gap-junction protein connexin 36 (Cx36) and Cx43, Western-blot to compare Cx36 expression between HH and control tissues, and electron microscopy (EM) to show the gap-junction structures.

Results: Immunostaining and Western-blot experiments show that neuronal type of gap-junction protein connexin 36 (Cx36) is highly expressed in human HH tissues freshly resected from gelastic seizure patients. EM shows a gap-junction-like structure between small HH neuronal pairs. Electrophysiological recordings from HH slices demonstrate that there are spontaneous epileptiform discharges in HH slice in normal artificial cerebrospinal fluid (ACFS) at 33±1 °C. Bath-application of gap-junction blocker (carbenoxolone) significantly eliminates these spontaneous discharges in a concentration-dependent manner.

Conclusion: Our results suggest that the gap-junction is likely an important target for epileptogenesis within HH lesion, and pharmacological block of gap-junction is a novel therapeutic strategy for patients with refractory gelastic seizures and perhaps other forms of intractable epilepsy.

PRENATAL OMEGA-3 POLYUNSATURATED FATTY ACIDS SUPPLEMENT MITIGATES SEVOFLURANE-INDUCED NEUROAPOPTOSIS AND MEMORY IMPAIRMENT IN NEONATAL RATS

L. Xi[1], W. Zhang[2], H. Xiao[1], T. Yuan[3], J. Shao[3], W. Liang[1], W. Xia[3], J. Zhang[1]

[1]Department of Anesthesiology, Huashan Hospital, Fudan University, [2]Medical Neurobiology National Key Laboratory, Shanghai Meical College, Fudan University, [3]School of Biomedical Engineering and Med-X Research Institute, Shanghai, China

Objectives: Animal studies suggest that neonatal exposure to general anesthetics may cause neuronal apoptosis, impairment of neurogenesis and differentiation in the developing brain, which leads to functional deficits. Several restropective human studies also demonstrated exposure to general anesthesia in childhood is associated with impaired neurobehavior in their later life. Sevoflurane, one of commonly used inhalational anesthetics, is especially useful for pediatric anesthesia because of its excellent properties. Omega-3 polyunsaturated fatty acids (n-3 PUFAs) consisting of DHA (docosahexaenoic acid) and EPA (eicosapentaenoic acid)has anti-apoptotic, anti-oxidant, neurogenesis improvement properties. It´s reported prenatal n-3 PUFAs supplement could protect against ischemia cerebral injury in experimental model. We hypothesized that n-3 PUFAs supplement during pregnancy could exert neuroprotective effects against neurotoxicity in their offspring rats receiving sevoflurane anesthesia. In this study, we investigated 1) if sevoflurane has significant neurotoxicity in developing brain; 2) if prenatal n-3 PUFAs supplement can reverse sevoflurane-induced neurotoxicity and cognitive impairment in neonatal rats.

Methods: Female Sprague-dawley rats (n=2 each group) were treated with or without an omega-3 enriched diet from the second day of

pregnancy to 14 days after parturition. Seven-day-old offspring rats (n=15 each group) were treated with six hours sevoflurane administration (one group without sevoflurane/prenatal n-3 PUFAs supplement as control). The 5-bromodeoxyuridine (Brdu) was injected intraperitoneally during and after sevoflurane anesthesia to assess dentate gyrus (DG) progenitor proliferation. Rats were euthanized 18h (n=3) and 3 days (n=3) after anesthesia. Brain tissues were harvested and subjected to Western blot and immunohistochemistry respectively. Morris water maze spatial reference memory, fear conditioning, Morris water maze memory consolidation were tested at 35th day, 63rd day and 70th day after birth(n=9), respectively.

Results: Six hours sevoflurane administration increased the cleaved caspase-3 in the thalamus, parietal cortex and hippocampus of neonatal rat brain, assessed by immunofluorescence microscopy. Sevoflurane anesthesia also decreased the neuronal precursor proliferation of DG in rat hippocampus. However, prenatal n-3 PUFAs supplement could decrease the cleaved caspase-3 in the cerebral cortex of neonatal rats, assessed by immunoblotting, and reverse the decrease in neurogenesis in their hippocampus. In neurobehavioral studies, compared with control and n-3 PUFAs supplement groups, we did not find significant spatial cognitive deficit and early long-term memory impairment in sevoflurane anesthetized neonatal ones in their adulthood. However, sevoflurane administration could damage the immediate fear response and working memory and short-term memory. And n-3 PUFAs could improve neurocognitive function in adulthood period after exposure to sevoflurane in their early life.

Conclusion: Our study demonstrated that neonatal exposure to prolong sevoflurane administration could impair the immediate fear response, working memory and short-term memory of rat in their adulthood, which may through inducing neuronal apoptosis and decreasing neurogenesis. However, these sevoflurane-induced adverse neuronal effects can be mitigated by prenatal n-3 PUFAs supplement.

References:

1. Liu F, et al. Curr Neuropharmacol 9, 256-261 (2011).

2. Stratmann G, et al. Anesthesiology 110, 834-848 (2009).

3. Sun L. Br J Anaesth 105, i61-68 (2010).

4. Tuzun F, et al. Int J Dev Neurosci 30, 315-323 (2012).

5. Beltz BS,et al. Neurosci Lett 415, 154-158 (2007).

ROLE OF SCH79797 IN MAINTAINING VASCULAR INTEGRITY IN RAT MODEL OF SUBARACHNOID HEMORRHAGE

J. Yan[1], A. Manaenko[2], S. Chen[2], N.H. Khatibi[2], Q. Ma[2], K. Duris[2], B. Caner[2], M. Fujii[2], J.H. Zhang[2]

[1]Peking University, Beijing, China, [2]Loma Linda University, Loma Linda, CA, USA

Background and purpose: Plasma thrombin concentration is increased following subarachnoid hemorrhage (SAH). Unfortunately, the role of thrombin receptor (protease activated recptor-1, PAR-1) in endothelial barrier disruption has not been studied. The aim of this study was to investigate the role of PAR-1 in orchestrating vascular permeability and assess the potential therapeutics of a PAR-1 antagonist, SCH79797, through maintaining vascular integrity.

Methods: SCH79797 were injected intraperitoneally to male Sprauge-Dawley rats undergoing SAH by endovascular perforation. Assessment was conducted at 24 hours after SAH for brain water content, Evans blue content and neurobehavioral testing. To explore the role of PAR-1 activation and specific mechanism of SCH79797's effect after SAH, Western blot, immunoprecipitation and immunofluorescence of hippocampus tissue were performed. A p21-activated kinase1 (PAK1) inhibitor, IPA-3, was used to explore the underlying protective mechanism of SCH79797.

Results: At 24 hours after SAH, animals treated with SCH79797 demonstrated a reduction in brain water content, Evans blue content and neurobehavioral deficits. SCH79797 also attenuated PAR-1 expression and maintained the level of Ve-cadherin, an important component of adherens junction. Downstream to PAR-1, c-Src dependent

activation of PAK1 led to an increased serine/threonine phosphorylation of Ve-cadherin; immunoprecipitation results revealed an enhanced binding of phosphorylated Ve-cadherin with endocytosis orchestrator β-arrestin2. These pathological states could be suppressed following SCH79797 treatment.

Conclusions: PAR-1activation following SAH increases microvascular permeability, at least, partly through a PAR-1-c-Src-PAK1-Ve-cadherin phosphorylation pathway. Through suppressing PAR-1 activity, SCH79797 plays a protective role in maintaining microvascular integrity after SAH.

PROTEIN S-NITROSYLATION: IDENTIFICATION OF DIFFERENTIALLY S-NITROSYLATED PROTEINS IN ALZHEIMER'S DISEASE BRAIN

S. Zahid[1,2], R. Khan[1], M. Oellerich[2], N. Ahmed[1], A.R. Asif[2]

[1]Department of Biochemistry, University of Karachi, Karachi, Pakistan, [2]Department of Clinical Chemistry, University Medical Center Goettingen, Goettingen, Germany

Introduction: S-nitrosylation, a reversible post-translational modification resulted by the covalent binding of NO with cysteine residues of target proteins with the formation of nitrosothiols (SNOs), extensively modifies the protein function and plays a key role in the pathology of multiple neurodegenerative diseases. Significant involvement of S-nitrosylation is also suggested in the progression of Alzheimer's disease (AD) pathology specifically in the formation and accumulation of misfolded protein aggregates.

Objective: The identification of S-nitrosylated proteins can be a major step towards the understanding of relatively unknown mechanisms leading to neuronal degeneration.

Methods: Present proteomic analysis identifies S-nitrosylated proteins in AD hippocampus, substantia nigra and cortex in comparison with unaffected controls using classical S-nitrosothiol detection methods combined with ESI QTOF MS/MS identification. Endogenous nitrosocysteines were identified in a total of 45 proteins, mainly involved in metabolism, signaling pathways, apoptosis and redox regulation which was further confirmed by REACTOME and KEGG pathway database analysis.

Results: Superoxide dismutase [Mn], fructose-bisphosphate aldolase C and voltage-dependent anion-selective channel protein 2 showed differential S-nitrosylation signal in AD brain regions. Extensive neuronal atrophy was also observed, which mainly due to increased protein S-nitrosylation. In-silico methods were used to assess the plausible cysteine modification sites via GPS-SNO 1.0 while functional annotations among the modified proteins were generated by STRING 8.3.

Conclusions: The findings will be helpful to characterize the functional aberrations due to S-nitrosylation that may represent a convergent signal pathway contributing to nitric oxide induced protein misfolding and aggregation facilitating a better understanding of AD pathology.

CONVENTIONAL MRI AND DIFFUSION TENSOR IMAGING (DTI) STUDIES IN CHILDREN WITH NOVEL GPR56 MUTATIONS: FURTHER DELINEATION OF A COBBLESTONE-LIKE PHENOTYPE

G. Zanni[1], C.C. Quattrocchi[2], A. Napolitano[3], D. Longo[2], D.M. Cordelli[4], S. Barresi[1], F. Randisi[2], E.M. Valente[5], T. Verdolotti[2], E. Genovese[3], N. Specchio[6], G. Vitiello[5], R. Spiegel[7], E.S. Bertini[1], B. Bernardi[2]

[1]Dept of Neurosciences, Unit of Molecular Medicine, [2]Unit of Neuroradiology, [3]Dept of Occupational Health and Safety, Medical Physics, B. Gesù Children's Hospital IRRCS, Rome, [4]Unit of Child Neuropsychiatry, University o Bologna, Bologna, [5]Unit of Neurogenetics, Mendel Laboratory, IRRCS Casa Sollievo della Sofferenza Institute, San Giovanni Rotondo, [6]Unit of Neurology, B. Gesù Children's Hospital IRRCS, Rome, Italy, [7]Dept of Pediatrics, Ha'Emek Medical Center, Afula and Rappaport School of Medicine, Haifa, Israel

GPR56-related Bilateral FrontoParietal Polymicrogyria (BFPP) is a rare recessively inherited genetic disorder characterized by: global developmental delay, seizures, dysconjugated gaze, pyramidal and cerebellar signs. Neuroradiological features include: symmetrical polymicrogyria (PMG) which extends across the frontal and parietal lobes with a decreasing anterior-to-posterior gradient of severity, irregular gray-whitematter junction,

white matter (WM) abnormalities, small hindbrain and dysmorphic cerebellar cortex with cerebellar cysts. Overall, the appearance of the brain is more similar to that of the so-called cobblestone lissencephaly, generally associated with congenital muscular dystrophies. GPR56 is an orphan G protein-coupled receptor belonging to the adhesion GPCR subfamily of proteins, involved in cell-cell and cell-extracellular matrix interactions. GPR56 mutations have been shown to dysregulate the maintenance of pial basement membrane integrity in the forebrain and the rostral cerebellum, causing ectopic neuronal overmigration in the whitematter and into the leptomeningeal space.To better delineate the neuroradiological spectrum of brain changes in GPR56-related BFPP we analysed six patients from five families carrying 3 novel truncating mutations and a missense mutation, by means of conventional MR and DTI. Six subjects carrying homozygous mutations of GPR56, were prospectively enrolled along with healthy controls matched by age and sex. Four patients underwent an additional MRI scan that included a Diffusion Tensor Imaging (DTI) sequence. The clinical features of all patients included moderate to severe intellectual disability, motor delay, non progressive ataxia, oculomotor disturbances, seizures (4/6) and oromotor dyspraxia (3/6). In all patients, we observed a characteristic morphologic pattern including bilateral frontoparietal-occipital PMG according to an antero-posterior gradient with a relative sparing of the temporal lobes, enlarged perivascular spaces, cerebellar cysts located at the posterior periphery of the hemispheres and patchy subcortical and periventricular white matter abnormalities. Cerebellar vermis was mildly hypoplastic in 5/6 patients, with or without subpial cysts. In all the patients cysts were present in the cerebellar hemispheres without impairments of cortical foliation. Patchy T2 high signal WM abnormalities were also noted in the cerebellum in 3/6 patients. A dysmorphic brainstem was observed in all patients with flattening of the ventral aspectof the pons and a flat to concave aspect of its posterior surface. The exploration of the Fractional Anisotropy colour-coded maps on the axial planes showed a poor representation of the pontine transverse fibers and a size reduction of the ponto-cerebellar fibers of the middle cerebellar peduncle. In the four patients that received DTI sequences during the MRI protocol, fiber tractography showed abnormal connectivity between the two hemispheres with enlarged corpus callosum and abnormal cortico-spinal tract reconstructions. Differential diagnosis of GPR56-related BFPP with Congenital Muscular Distrophies may be challenging, particularly for the Muscle-eye-brain/Walker Warburg syndrome (MEB/WWS) phenotype. The absence of pontine clefts, the distribution of the polymicrogyria and of the cerebellar cysts basically represents the characteristic phenotype of GPR56- related brain dysgenesis that may help in the differential diagnosis with other PMG syndromes. This is the first study documenting DTI changes in the brain and cerebellum of GPR56 mutated patients and adds a layer of complexity to the characterization of malformations of cortical development.

THE NEUROPROTECTIVE EFFECTS OF ANTIDEPRESSANTS IN THE PHARMACOLOGICAL EXPERIMENTS

I.I. Abramets, D.V. Evdokimov, A.N. Talalayenko

Department of Pharmacology, Donetsk National Medical University, Donetsk, Ukraine

Objective: Depression and other mood disorders are characterized by the neuroatrophic alterations in the brain limbic structures such as reduction of hippocampus and prefrontal cortex volume, decreasing of dendrite spine and synaptic contact numbers at the pyramidal projectioning neurons. The antidepressants produce reduction of the psychopathological symptoms and reverse the neuroatrophic alterations.

Rationale: The aim of the study was to reveal the probable neuroprotective activity of the antidepressants in the circumstances of more severe brain injury (excitotoxicity, anoxia/aglycemia).

Methods: The experiments were performed at the slices of hippocampus (Hp) and medial prefrontal cortex (mPFC) of Wistar rats. The dependence between amplitude of the field (f) EPSP of pyramidal neurons of Hp CA1 area and mPFC layer V and intensity of the presynaptic stimulation was estimated. A functional state of Hp and mPFC pyramidal neurons was determined by synaptic reactivity (ratio of fEPSP amplitude to intensity of the presynaptic stimulation). Excitotoxic injury of neurons was induced by application of 50 μM N-methyl-D-aspartate and 10 μM glycine at brain slices during 15 min. Anoxic injury of neurons was induced by exposing of brain slices in chamber where oxygen was replaced

on nitrogen and glucose on mannitol during 5 and 7.5 min. The further experiments were performed 1 h later after the injury cessation. The antidepressants imipramine, fluoxetine and pyrazidol were administrated in rats at dose 20 mg/kg intraperitoneally during 14 days.

Results: We established that the antidepressants reversed a suppression of synaptic reactivity of the Hp and mPFC pyramidal neurons produced by NMDA (from 55.1% (control) to 22.0 - 37.0 % (antidepressants) ($p< 0.05$)). The injury of Hp and mPFC pyramidal neurons induced by anoxia/aglycemia during 5 and 7.5 min has had NMDA-dependent and NMDA-independent components that accompanied by decreasing of synaptic reactivity on 46.7% and 70.0%, respectively. After chronic administration antidepressants decreased the NMDA-dependent and NMDA-independent components of anoxic injury of pyramidal neurons on 20.0% and 36.8%, respectively ($p< 0.05$). The neuroprotective action of chronically administrated antidepressants was increased by sodium orthovanadate (the inhibitor of tyrosine phosphatases) but was decreased by genistein (the inhibitor of receptor tyrosine kinases).

Conclusion: Our results suggest that the neuroprotective action of chronically administrated antidepressants is the result of increasing of tyrosine kinase activity and, as a consequence, enhancement of phosphorylation of neuronal substrates by tyrosine kinases that decreases the functional activity of NMDA receptors and harmful effects of the elevated intraneuronal Ca2+ concentration.

THE NEUROPROTECTIVE EFFECT OF CHOROID PLEXUS EPITHELIAL CELLS CONDITIONED MEDIA AGAINST OXIDATIVE STRESS-INDUCED APOPTOSIS IN PC12 CELLS

A. Aliaghaei, A. Ahmadiani, F. Khodagholi

Shahid Beheshti, Tehran, Iran

Introduction: Choroid plexus epithelial cells are responsible for the secretion of cerebrospinal fluid.These cells can secrete growth factors such as NGF (nerve growth factor), GDNF (glial derived neurotrophic factor), BDNF (brain derived neurotrophic factor). Here we tried to determine whether this media could protect PC12 cells against apoptosis.

Methods: Choroid plexus epithelial cells isolated from rat brain and cultured. Immunocytochemistry and real time PCR was used to identify cells. We studied the anti-apoptotic effects of choroid plexus epithelial cells conditioned media through measurement of Bax, Bcl2 and caspase3 via western blot as well as Hoechst staining. For evaluation of its anti oxidative effects, the levels of MDA and GSH were determined spectrophotometrically. Besides we measured four different parameters of neurite outgrowth.

Results: Choroid plexus cells have polygonal shape and have tight junctions to each other. Immunocytochemistry and real time PCR showed that these cells expressed TTR-1, a marker for choroid plexus cells. We also demonstrated expression of glial derived neurotrophic factor (GDNF) in choroid epithelial cells by real time PCR. Our results determined significant effects of choroid epithelial cells conditioned media on the differentiation and neurite expansion of PC12, through evaluation of the main indicators including neurite length, neurite width, cell body area and bipolar neurons. From the other side Western blot analysis showed a significant reduction in ratio of Bax/Bcl2 and active form of caspase-3 in treated groups compared with H_2O_2-treated cells, showing the anti-apoptotic effect of this media. This result was confirmed by Hoechst staining. The anti-oxidant potential of this media was approved by its ability to decrease MDA and increase of GSH in H_2O_2- exposed PC12 cells.

Conclusion: The results of our study showed that choroid plexus epithelial cells conditioned media can protect PC12 cells against oxidative stress and apoptosis and also cause differentiation and expansion of neurite outgrowth. Our study suggests that growth factors secretion and antioxidative agents produced by choroid epithelial cells have important roles in the health of central nervous system.

NEUROPROTECTIVE EFFECT OF EXTRACTS OF *SPHAERANTHUS INDICUS* ON TRANSIENT CEREBRAL ISCHEMIA REPERFUSION AND LONG-TERM CEREBRAL HYPOPERFUSION IN RATS

D.B. Ambikar[1], G.P. Mohanta[2]

[1]Marathwada Mitra Mandals College of Pharmacy, Pune, [2]Annamalai University, Annamalai Nagar, India

Introduction: Cerebral reperfusion injury results in to free radicals generation and chronic cerebral hypoperfusion in rats is known to produce functional and histopathological disturbances. Chronic cerebral hypoperfusion is considered to be a factor contributing to the memory dysfunction in neurological diseases such as Alzheimer´s disease and vascular dementia

Objective: The present study designed to investigates the effect of petroleum ether (SIP), methanolic (SIM) and aqueous extract (SIA) obtained from *Sphaeranthus indicus* Linn, a claim nervine tonic in Indian system of Medicine, on transient cerebral ischemia and long-term cerebral hypoperfusion in rats.

Methodology: Ischemia reperfusion was induced in wistar rats by occluding bilateral common carotid artery (BCCA) for 30 min followed by 45 min reperfusion. At the end of experiment, rats were sacrificed and subjected to total protein, lipid peroxidation, super oxide dismutase, activity of catalase, activity of reduced glutathione and activity of glutathione peroxidase. Long-term cerebral hypoperfusion induced by permanent occlusion of BCCA for 15 days and drugs were administered for these 15 days. Rats were subjected to exploratory behavior in open-field test and spatial memory testing by Morris water maze. At the end of behavioral testing, the rats were sacrificed by decapitation and brains were taken out for Histopathological examination.

Result and discussion: Ischemia reperfusion resulted in increase in lipid peroxidation and decrease in catalase activity, glutathione level and glutathione peroxides activity. SIM pretreatment (100 mg/kg/day for 10 days) attenuated the ischemia reperfusion induced alteration. Long-term cerebral hypoperfusion demonstrated altered exploratory behavior in open-field testing and memory deficits as tested by Morris water maze. Histopathological examination of hypoperfused animals revealed reactive changes, like cellular edema, gliosis and perivascular inflammatory infiltrate. SIM pretreatment (100 mg/kg/day for 15 days) significantly prevented these hypoperfusion-induced functional and structural disturbances. The results suggest that SIM may be useful in treatment of cerebral ischemia reperfusion injury.

Conclusion: *Sphaeranthus indicus* provided significant neuroprotection via reducing oxidative stress and reactive oxygen species induced by reperfusion and via attenuating behavioral and cognitive deficits induced by hypoprfusion.

Reference:

- Yanpallewar SU, Sunita R, Mohan K, Acharya SB. Evaluation of antioxidant and neuroprotective effect of *Ocimum sanctum* on transient cerebral ischemia and long-term cerebral hypoperfusion. Pharmacol Biochem Behavior, 2004; 79:155-164.
- Yanpallewar SU, Sunita R, Mohan K, Chauhan S, Acharya SB. neuroprotective effect of *Azadirachta indica* on cerebral post-ischemic reperfusion and hypoperfusion in rats. Life Sciences, 2005; 76:1325-1338.

NXY-059 DOES NOT PROTECT STEM CELL-DERIVED HUMAN NEURONS: FIRST USE OF A NOVEL DRUG SCREENING PROTOCOL

A. Antonic[1], M. Dottori[2], J. Leung[2], M. Macleod[3], G.A. Donnan[1], D.W. Howells[1]

[1]Florey Institute of Neuroscience and Mental Health, [2]Centre for Neuroscience Research, Anatomy and Neuroscience, Melbourne University, Melbourne, VIC, Australia, [3]Clinical Neurosciences, Edinburgh University, Edinburgh, UK

Background: NXY-059 proceeded to clinical trial in two cohorts of stroke patients (SAINT I & II) on the basis of reported efficacy in animal models of stroke. While the pre-clinical data set met the prevailing STAIR criteria and the first clinical trial (SAINT I) reported a small but significant improvement in disability scores, the concomitant but larger SAINT II trial was

neutral. Re-evaluation of NXY-059's biochemistry and pharmacodynamics suggested that an active metabolite given in the first trial was not present in the second, or that confinement to the vascular space limited efficacy. Systematic review and meta-analysis of the preclinical data suggested that introduction of bias favoured an overoptimistic interpretation of NXY-059's potential but did not conclude that the drug was without effect [1].

A gap in our understanding of NXY-059, and indeed of most candidate stroke drugs before clinical trial, is whether they in fact have activity in human neurons or other human cells. To fill this gap we have derived neurons from human embryonic stem cells and subjected them to models of ischemia and oxidative stress. Here we report that NXY-059 has no protective activity in this human assay system.

Methods: Human embryonic stem cells were differentiated into neurons in the presence of the bone morphogenic inhibitor protein, Noggin [2]. The mature neurons were maintained for 11 days before induction of injury. Two injury models were used : Oxygen glucose deprivation (OGD) was induced by addition of 2-deoxy-D-glucose to the neuronal cultures in a hypoxic chamber flushed with nitrogen; Oxidative stress was induced by the administration of either 100µM sodium nitroprusside (SNP) or 50µM or 90µM hydrogen peroxide (H_2O_2) to the neuronal cultures. The activity of NXY-059 (1µM - 1mM) was assessed by measuring cell death (lactate dehydrogenase activity and Tunnel Staining) and cell survival (MTT assay).

Results: Following OGD induced injury; NXY-059 had no effect on cell survival at any concentration. Antioxidant cocktail (100µM each of ascorbate, reduced glutathione and dithiothreitol) used as a positive control reduced the cell death by 37±2%. Melatonin, another antioxidant also used as a positive control, provided a dose dependent increase in human neuron survival with maximum protection at 100µM (38.54±1.5%). SNP and H_2O_2 induced cell death was also inhibited by the antioxidant cocktail (24±5% and 24±4% respectively) but not by NXY-059. Tunnel staining indicated that NXY-059 had no effect on apoptosis in these preparations.

Conclusions: This study demonstrates that NXY-059 has no effect on survival of human stem cell-derived neurons in the face of OGD or oxidative stress. This assay system can be used to provide a reproducible and high throughput screen of candidate drugs for human-specific activity in all relevant cell types and insults before progression to clinical trial.

References:

1. Macleod, M.R., et al., *Evidence for the efficacy of NXY-059 in experimental focal cerebral ischaemia is confounded by study quality.* Stroke, 2008. 39(10): p. 2824-9.

2. Dottori, M. and M.F. Pera, *Neuronal differentiation of Human Embryonic Stem Cells.* Methods in Molecular Biology, 2007. 438: p. 19-30.

THERAPEUTIC EFFECT OF CHRONIC AND ACUTE LITHIUM APPLICATION FOLLOWING TRAUMATIC BRAIN INJURY IN MICE

M. Balbi[1,2], S. Schwarzmaier[1,2], N. Plesnila[1,2]

[1]Institute for Stroke and Dementia Research (ISD), LMU, Munich, Germany, [2]Royal College of Surgeons in Ireland (RCSI), Dublin, Ireland

Background: Traumatic Brain Injury (TBI) remains one of the leading causes of death and disability worldwide. Lithium, a drug used in the treatment of bipolar mood disorder, is neuroprotective in various neurodegenerative conditions such as Huntington disease and stroke when it is administered before the injury (1). However, the effect of Lithium given as a therapy for acute brain injury only after the injury has occurred remains unclear. We therefore investigated whether chronic and acute Lithium treatment could be neuroprotective after experimental TBI.

Methods: Male C57Bl6 mice (n= 8 per group) were randomly assigned to the following groups: controlled cortical impact (CCI), CCI + saline i.p., and CCI + Lithium (5 mM) i.p. for 10 days before trauma or impact (CCI), CCI + saline i.c.v., and CCI + Lithium in five different concentrations (0.05 mM; 0.5 mM; 5 mM; 50 m M; 500 mM) i.c.v. 10 min after trauma. Mice were sacrificed 24 h after CCI and brain edema and secondary lesion expansion were assessed by measuring brain water content and contusion volume on Nissl-stained coronal brain sections, respectively.

Results: Mice subjected to sham operation did not show brain damage, whereas mice subjected to CCI had a mean lesion volume of (37 +/- 7 mm^3, mean +/- SD). Mice that received lithium for 10 days prior to injury did not have a significant reduction in secondary lesion growth (37 +/- 11 mm^3). Acute intracerebroventricular injection of Lithium immediately after CCI did not show a significant reduction in secondary brain damage as well.

Conclusion: Long-term intake of Lithium did not show any improvement of contusion volume and brain swelling. Acute treatment following CCI did show a tendency towards smaller contusion volumes but not significantly reduce secondary lesion growth. In contrast to others (2) we could not find neuroprotection of lithium after experimental TBI.

[1] Bian Q,Qian Y. et al. Lithium reduces ischemia-induced hippocampal CA1damage and behavioral deficits in gerbils. Brain Res 2007; 1184: 270-276.

[2] Fengshan Yu De-Maw Chuang et al. Lithium ameliorates neurodegeneration, suppresses neuroinflammation, and improves behavioral performance in a mouse model of traumatic brain injury. Journal of Neurotrauma 2012; 29: 362-374

NEUROPROTECTIVE AND ENDOTELIOTROPICAL FEATURES OF THE NEW MEDICAL DRUG "LISINIY" IN ISCHEMIAL DAMADGE OF THE BRAIN

I.F. Belenichev, L.I. Kutcherenko, I.A. Masur, N.V. Buhtiyarova, S.V. Pavlov

Zaporizhzhya State Medical University, Zaporizhzhya, Ukraine

Actuality: Neurodestructive diseases of the brain are on the 2nd place in causes of the deaths. One of the leading chain of the pathogenesis of the neurodestruction is endothelial dysfunction. Decrease of the speed of the cerebral blood flow initiate pathobiochemical reactions, which leads to the dysballance of the iNOS and eNOS, to the extraproduction of the cytotoxic forms of the NO, depo of the oxide intermediators in the tiol-disulfide system, deprivation of the antioxidant enzymes.

The aim was to study endothelioprotective and neuroprotective activity of the Lisiniy on the modeled brain ischemia.

Materials and methods: In the experiments on the 60 rats with complete oneside occlusion of the cerebral arteries with injected new synthetic compound (S)-2,6-diaminogexane acid 3-methyl-1,2,4-triasolile-5-tyoacetate(named "Lisiniy") in dose 50 mg/kg on the 4th and 21-th day of ischemia was used microscope Axioskop (Ziess, Germany), videocamera COHU - 4922 (USA), system of the digital picture analysis VIDAS -386 (Kontron Elektronic, Germany), BrdU-test (anti-BrdU, clone BU-33).

Results: It was founded that use of the Lisiniy in animals with experimental cerebral ischemia leads to the increase of the endothelium's cells quantity of the capillary net of the cortex, increase of the RNA level and activation of the translate activity of the cells starting from the 4th day of the experiment, complete increase of the endotheliocites quantity on the 21th day due to the increase of the endothelial growth factor (VEGF). Lisiniy decreased death of the neurons of the IV-V layers of the sensomotor cortex, increase of the glutation and protected NO transport in comparison with the control on the 4th and 21th day of ischemia. We suggest that Lisiniy itself can be NO transporter due to the formation of the stabile S-nitrosole complexes. This way it can protect NO from the transforming to the peroxinitrite (decrease of the nitrotirosine supports this theory), but safe NO endotheliotropic activity.

Conclusion: These results show potential positive clinical effect of the Lisiniy in the practical neurology, neurosurgery and neurotrauma.

INFLUENCE ON THE GLUTATIONE SYSTEM OF THE OLD AND YOUNG ANIMALS IN MODELS OF THE CEREBRAL ISCHEMIA

I.F. Belenichev, S.V. Pavlov, N.V. Buhtiyarova

Zaporizhzhya State Medical University, Zaporizhzhya, Ukraine

Modern strategy of the neuroprotection of the cerebral attacks suggests NMD, AMPA-receptors, Ca-channels and β- estrogen receptors as perspective pharmacologic aims. The results of our experiments on the rats with modeled cerebral ischemia showed that

selective modulator of the estrogen receptors **(SERM)** - (Z)-2-[4-(1,2-diphenyl-1-butenyl)phenoxy]-N,N-dimethyletamine citrate in dose 1 mg/kg decreased iNOS expression and nitrosine level in neurons CA_1 of the hippocampus zone and IV-V layers of the sensomotor brain cortex, decreased quantity of the apoptotic and necrotic neuronal cells, increased RNA level in the cytoplasm and nucleus on the 4^{th} day of the experiment. Injection of the SERM leads to the increase of the glutationeperoxidase activity, decrease of the oxide form of the glutation in the mentioned above structures of the central nervous system. SERM stopped mitochondrial dysfunction: normalization of the mitochondrial's membrane potential and decrease of the mitochondrial's nitrotirosinase suspension.

Neuroprotective action of the SERM directed to the decrease of the neurons death, apoptosis, mitochondrial dysfunction most of all was detected in the young animals. Antioxidant component of the neuroprotective action (activity of the glutationperoxidase, level of the defended glutation, nitrotirosine) was detected as in young as in old animals.

VASOACTIVE INTESTINAL PEPTIDE (VIP) REVERSES THE HYPOMYELINATION IN THE AGED RAT BRAIN: ROLE OF BDNF AND IGF-I

L. Cacicedo[1], M. Sanchez-Grande[1], F. Sanchez-Franco[2]

[1]Hospital Ramón y Cajal, [2]Hospital Carlos III, Madrid, Spain

Objective: Vasoactive intestinal peptide (VIP) is a central nervous systemneurotransmitter and neuromodulator with neurotrophic properties. A decrease in the number of VIP-immunoreactive neurons and VIP mRNA, as well as a loss of the white matter in the aged rat brain, have been reported. VIP promotes and accelerates myelination of regenerating axons in the peripheral nervous system. The aim of the present study was first of all to confirm the role of VIP on oligodendrocyte development and myelination during central nervous system development in embryonic rat cerebrocortical cell cultures. Second to investigate whether VIP reverses the age-related hypomyelination in the rat brain.

Methods: Mixed glial and neuronal cells isolated from cerebral hemispheres of 17-day-old rats were cultured in defined medium with bFGF (25 ng/ml) for four days and then exposed to VIP (10^{-7}M to 10^{-13}M) for seven or eight days. Cells were immunostained with specific antibodies for O4, a marker attributed to immature oligodendrocytes (OD), or for myelin basic protein (MBP) to detect mature OD.

Results: VIP increased the expression of O4 and MBP in a dose related manner. In the in vivo experiments, young adult (3 months) and old (29 months) male Wistar rats were used. Old rats were treated with subcutaneous (sc) VIP (20µg/Kg) for 15 days. Both young adult and old control rats received the vehicle. The expression of MBP was analyzed by western immunoblot in brain cortex extracts using a mouse monoclonal antibody against MBP (1:500 dilution, Oncogen). Equal loading of total protein was assessed by simultaneous incubation of membranes with a mouse monoclonal antibody against b-actin.

Results: The densitometric analysis showed a marked decreased in the expression of MBP in the old rats. After VIP treatment, the decreased expression of MBP in the old rats was completely reversed. Moreover, the levels of MBP were higher in the VIP-treated old rats than in the young adult rats.In the present study we confirm that VIP promotes oligodendrocyte development and we also present evidence that VIP stimulates differentiation of oligodendrocytes as demonstrated by the increment observed in the number of cells that express MBP.

Conclusions.- Our findings indicate that VIP treatment reverses the hypomyelination that occurs in the cerebrum of the aged rat.

References:

- ChI Cha, YI Lee, EY Lee, KH Park,SH Baik. Brain Res,753,235,1997

- QL Zhang, J Liu,PX Lin,HF Webster, J Peripher Nerv Syst 7,118,2002

A NOVEL NEUROPROTECTIVE REGIMEN AGAINST ISCHEMIC BRAIN INJURY BY CONCOMITANT INACTIVATION OF THE CASR AND ACTIVATION OF THE GABA-B-R1

J.Y. Kim[1,2], N. Kim[1], H. Ho[2], J. Liu[3], M. Yenari[1], **W. Chang**[2]

[1]Department of Neurology, VA Medical Center, [2]Endocrine Unit, VA Medical Center, [3]Neurological Surgery, VA Medical Center, University of California San Francisco, San Francisco, CA, USA

Objectives: Mechanisms inducing neuronal hyperexcitability and cell death after brain ischemia remain unclear. Concurrent overexpression of the extracellular calcium-sensing receptor (CaSR) and down-regulation of the type B Gamma Aminbutyric Aicd (GABA) receptor 1 (GABA-B-R1) in hippocampal neurons in wild-type (WT) mice subjected to transient global ischemia (TGI) led us to hypothesize that CaSR overactivity may produce neuronal injury and neurobehavioral deficits by stimulating excitatory signaling and by blocking the inhibitory GABA-B-R1 responses in the affected neurons (1).

Methods: We took genetic and pharmacological approaches to test this hypothesis by examining the effects of CaSR and/or GABA-B-R1 gene knockout (KO) and intraperitoneal (IP) or intracerebroventricular (ICV) injections of CaSR antagonists (NPS89636 and NPS 2143), and GABA-B-R1 agonist (Baclofen) on apoptotic responses [assessed by terminal deoxynucleotidyl transferase dUTP nick end labeling (TUNEL) staining] in hippocampal neurons and learning ability (by Morris Water Maize test) in the mice subjected to TGI due to transient (10 min) bilateral occlusion of common carotid arteries, followed by different times of reperfusion.

Results: In ^{Hipp}CaSR-KO mice, knocking out both CaSR gene alleles in their hippocampal neurons significantly ($p< 0.01$) reduced the number of TGI-induced TUNEL-positive neuron by 30, 70, and 80%, respectively, in the CA1, CA3, and dentate gygus (DG) and blocked the ability of TGI to suppress GABA-B-R1 expression in the neurons 72 hrs after TGI. These neuroprotective effects of CaSR KO was blocked by ≈80% by concomitant deletion of one allele of GABA-B-R1 gene in the same population of neurons, suggesting that appropriate restoration of GABA-B-R1 expression is required for the neuroprotective effects of CaSR KO. Daily IP or single ICV injections of NPS89636 or NPS2143 (1 mg/kg b.w.) given 1 hr after TGI also reduced significantly ($p< 0.01$) the number of TGI-induced TUNEL-positive neuron by 30-90% (depending on the regions assessed) and blocked the ability of TGI to suppress GABA-B-R1 expression in the neurons, suggesting that CaSR overactivity decreases GABA-B-R1 expression in the ischemic neurons. Continuous daily IP injections of NPS2143 for 14 days significantly prevented loss of spatial learning ability due to TGI injury. The above data together led us to test a combined therapy with NPS2143 to inhibit CaSR activation and restore GABA-B-R1 expression and baclofen to promote inhibitory signaling by the restored GABA-B-R1. In mice injected with NPS2143, baclofen, and NPS2143+baclofen, the % of TUNEL-positive cell in CA1 were 12.1±2.2, 24.8±3.7, and 5.1±1.1 %, respectively, supporting synergistic neuroprotection by the NPS2143 and baclofen in the mice.

Conclusion: We demonstrated a novel ischemia-induced neuronal injury pathway in which overexpression and overactivity of the CaSR induce neuronal death pathway by suppressing the GABA-B-R1 expression. Concurrent inhibition of CaSR signaling and activation of GABA-B-R1 signaling maximize neuroprotection against the ischemia-induced brain injury.

Reference: (1) J-Y Kim et al, 2011, Transl Stroke Res: 2: 195

OUTLOOK OF PROGESTERONE NEUROPROTECTION: BEYOND THE AGING FEMALE CHIMPANZEES STUDY

W. Chen

Department of Radiology, Tongji Hospital of Tongji University, Shanghai, China

Introduction: Progesterone has a number of physiological effects that are amplified in the presence of estrogen, it is being recognized a “neurosteroid” which affects synaptic function and has demonstrated neuroprotective properties (Kastner, Krust et al., 1990). Also, its neuroprotective property has been demonstrated in traumatic and ischemic brain injury (Gibson 2011, Alejandro 2009). The

current review shed light on rapidly expanding knowledge in brain imaging related to progesterone neuroprotection.

Methods: A search for “progesterone neuroprotection” on Pubmed generated 132 citations, and searching for “progesterone and brain MRI” generated 88 citations. For this review, we selected studies from these lists which were focused primarily progesterone effect on the central nervous system or neurons based on former study of the aging female chimpanzees.

Results and conclusions: In contrast to aging humans, aging female chimpanzees do not develop neurodegenerative diseases like Alzheimer's disease (AD). Progesterone may play a role in myelination. Although the risks and benefits of conventional hormone replacement therapies are very much under debate ((Rossouw, Anderson et al. 2002; Hays, Ockene et al. 2003; Rapp, Espeland et al. 2003; Shumaker, Legault et al. 2003; Wassertheil-Smoller, Hendrix et al. 2003), this study combining with the former findings is to stimulate future communication, cooperation, and collaboration between researchers who use animals and humans to elucidate the exact mechanisms involved in progesterone and aging brain, as well as to open the way for new steroid-based treatments of lesions and diseases of the nervous system.

DANSHENSU PROTECTS AGAINST 6-HYDROXYDOPAMINE-INDUCED DAMAGE OF PC12 CELLS IN VITRO AND DOPAMINERGIC NEURONS IN ZEBRAFISH

C.-M. Chong[1], Z.-Y. Zhou[1], V. Razmovski-Naumovski[2], G.-Z. Cui[1], L.-Q. Zhang[1], F. Sa[1], P.-M. Hoi[1], K. Chan[2], M.-Y.S. Lee[1]

[1]State Key Laboratory of Quality Research in Chinese Medicine, Institute of Chinese Medical Sciences, University of Macau, Macau, Macau, [2]Faculty of Pharmacy, University of Sydney and Centre for Complementary Medicine Research, School of Science & Health, University of Western Sydney, Sydney, NSW, Australia

Objective: The overproduction of reactive oxygen species (ROS) has been implicated in the development of neurodegenerative diseases such as Parkinson's disease (PD) and Alzheimer's disease (AD). Previous studies have indicated that danshensu, a main hydrophilic component of the Chinese materia medica Salviae Miltiorrhizae Radix et Rhizoma (Danshen, Pharmacopoeia of PR China), has ROS scavenging and antioxidant activities, however its mechanism of action was not clear. In this study, we investigated whether the protective effects of danshensu against neurotoxin 6-hydroxydopamine (6-OHDA)-induced oxidative stress involved the Nrf2/HO-1 pathways.

Methods: In cell experiments, PC12 cells were pre-treated with different concentrations of danshensu for 12 h, and then exposed to 250 μM 6-OHDA for 24 h. Cell viability and intracellular ROS level were measured preforming MTT assay and ROS detection assay. The roles of PI3K/Akt pathway and Nrf2/HO-1 pathway in cytoprotective effect of danshensu were evaluated by western blotting. In zebrafish experiment, TH staining was used for detecting dopaminergic neurons.

Results: Pretreatment with danshensu in PC12 cells significantly attenuated 6-OHDA-induced cytotoxicity and the production of ROS. Danshensu regulated intracellular ROS level transiently and activated the nuclear translocation of Nrf2 to increase heme oxygenase-1 (HO-1), conferring protection against ROS. Danshensu induced the phosphorylation of Akt, and its cytoprotective effect was abolished by PI3K, Akt and HO-1 inhibitors. These results confirmed the crucial role of PI3K/Akt and HO-1 signaling pathways as the underlying mechanistic action of danshensu.

Conclusion: Our study suggests that danshensu enhances HO-1 expression to suppress 6-OHDA-induced oxidative damage via PI3K/Akt/Nrf2 signaling pathways. Moreover, 6-OHDA-induced dopaminergic neuronal loss in zebrafish could be reduced by danshensu, further supporting the neuroprotective potential of danshensu.

References:

Alam, J., Stewart, D., Touchard, C., Boinapally, S., Choi, A.M., Cook, J.L., 1999. Nrf2, a Cap´n´Collar transcription factor, regulates induction of the heme oxygenase-1 gene. J Biol Chem **274**, 26071-26078

Cui W, Z.Z., Li WM, Han RW, Mak SH, Zhang H, Hu SQ, Yuan S, Li S, Rong JH, Ma

ED, Lee SM, and Han YF., 2012a. Unexpected Neuronal Protection of SU5416 against 1-Methyl-4-Phenylpyridinium Ion-

Induced Toxicity via Inhibiting Neuronal Nitric Oxide Synthase. Plos One **7**, e46253.

Yu, P.F., Wang, W.Y., Eerdun, G., Wang, T., Zhang, L.M., Li, C., Fu, F.H., 2011. The

Role of P-Glycoprotein in Transport of Danshensu across the Blood-Brain Barrier. Evid Based Complement Alternat Med **2011**, 713523.

MODIFYING NEUROREPAIR AND NEUROREGENERATIVE FACTORS WITH TPA AND EDARAVONE AFTER TRANSIENT MIDDLE CEREBRAL ARTERY OCCLUSION IN RAT BRAIN

K. Deguchi, N. Liu, W. Liu, Y. Omote, T. Yunoki, S. Kono, S. Deguchi, T. Yamashita, K. Abe

Department of Neurology, Okayama University, Okayama, Japan

Background and purpose: Expression changes of neurorepair and neuroregenerative factors were examined after transient cerebral ischemia in relation to the effects of tissue plasminogen activator (tPA) and a free radical scavenger edaravone.

Methods: Physiological saline or edaravone was injected twice during 90 min of transient middle cerebral artery occlusion (tMCAO) in rats, followed by the same saline or tPA at reperfusion. Sizes of the infarct and protein factors relating to neruorepair and neuroregeneration were examined at 4 d after tMCAO on a chondroitin sulfate proteoglycan neurocan, semaphorin type 3A (Sema3A), a myelin-associated glycoprotein receptor (Nogo receptor, Nogo-R), a synaptic regenerative factor (growth associated protein-43, GAP43), and a chemotropic factor netrin receptor (deleted in colorectal cancer, DCC).

Results: Two groups treated by edaravone only or edaravone plus tPA showed a reduction in infarct volume compared to the two groups treated by vehicle only or vehicle plus tPA. Immunohistochemistry and Western blot analyses indicated that protein expressions of neurocan, Sema3A, Nogo-R, GAP43, and DCC were decreased with tPA, but were recovered with edaravone. Additive edaravone prevented such reductions of 5 proteins induced by tPA.

Conclusions: The present study newly demonstrated that exogenous tPA reduced protein factors for inhibiting and promoting axonal growth, but that edaravone ameliorated such damages for acute ischemic brain repair.

PEROXIREDOXIN-2 OVEREXPRESSION SUPPRESSES ISCHEMIC NEURONAL INJURY BY INHIBITING THE REDOX-SENSITIVE ACTIVATION OF THE ASK-1 SIGNALING PATHWAY

S.H. Hassan[1,2], X. Ji[1], Y. Gan[2], X. Hu[2], Y. Luo[1], L. Zhang[2], P. Li[2], X. Liu[1], F. Yan[1], P. Vosler[2], Y. Gao[2], R. Stetler[2], J. Chen[2]

[1]Department of Neurosurgery and Cerebrovascular Disease Research Institute, Xuanwu Hospital, Capital Medical University, Beijing, China, [2]Department of Neurology and Center of Cerebrovascular Disease Research, University of Pittsburgh, Pittsburgh, PA, USA

Objectives: Peroxiredoxin 2 (PRX2) is a neuronal-specific peroxide-scavenging enzyme that has been demonstrated to be neuroprotective under ischemic-like settings. Although it has robust antioxidant capacity, the saturation of oxidized peroxiredoxin can lead to the recruitment of thioredoxin (Trx) as a reducing partner and yielding oxidized Trx. Oxidized Trx is not capable of binding to the apoptosis signal-regulating kinase 1 (ASK1), thus allowing ASK1 to be activated under ischemic settings. Our previous studies have indicated that the apoptosis signal-regulating kinase 1 (ASK1) is a critical regulator of the cell death signal in ischemic neurons. We thus wished to assess the effects of overexpression of PRX2 as a means to maintain the pro-survival interaction between Trx and ASK1 in neural ischemic settings.

Methods: Transgenic PRX2 mice were generated and used for focal cerebral ischemia, and cortical neuronal cultures were prepared using either transgenic PRX2 cultures or wildtype cultures transduced with lentiviral constructs. Adult male mice were subjected to 30 minutes of transient occlusion of the middle cerebral artery (MCAO) and killed at various times following reperfusion. Infarct volume and neurobehavior were assessed. Cortical cultures were subjected to 60 min of oxygen/glucose deprivation (OGD). Cultures were transduced with lentiviral vectors containing PRX2, the catalytic inactive mutant PRX2C/A, or shRNA targeting Trx, ASK1 or scrambled controls. Oxidation states of PRX2 and Trx were assessed by western

blot, and enzymatic activities were assessed using an in vitro activity assays using cell lysates. Association between ASK1 and Trx was determined by immunoprecipitation.

Results: Focal ischemia led to increased oxidation of PRX2 and decreased total PRX cellular activity. Transgenic overexpression of PRX2 exerted robust neuroprotective effects in both the in vivo and in vitro neuronal ischemic models, as well as significantly restored PRX activity. Furthermore, PRX2 overexpression decreased the oxidation of Trx and ASK1 activity compared to wildtype following ischemia. This was associated with a sustained interaction between ASK1 and Trx in PRX2 transgenic neurons. Furthermore, overexpression of PRX2 containing a mutation of its catalytic site yielded no neuroprotective effects or restoration of PRX or Trx activity. Although PRX2 was significantly neuroprotective by itself, no additional neuroprotection was attained by knockdown of ASK1, nor could PRX2 overexpression rescue ischemic neurons with Trx knocked down.

Conclusions: We have identified a novel mechanism by which PRX2 overexpression can confer ischemic neuroprotection by maintaining the interaction between Trx and ASK1, and thus suppressing the activation of downstream cell death signaling. This neuroprotection was dependent on the catalytic site of PRX2, and was associated with increased levels of the PRX oxidation product PRX-SO3 in transgenic animals, indicating that incaresed availability of the enzymatic activity of PRX to scavenge peroxides may be an effective therapeutic target against neural ischemic injury.

CONCURRENT TREATMENT WITH VITAMIN C AND ADENOSINE A1 RECEPTOR ON HIPPOCAMPUS IN GAMMA IRRADIATION

J. Hassanshahi

Physiology, Tehran University of Medical Science, Tehran, Iran

Irradiation is a common therapeutic approach in most cancers but the vulnerability of normal cells can prevent to apply of more effective high doses irradiation and else unwanted irradiation can cause a lot of problems such as the types of irradiation syndromes and even death. Hippocampus is affected by degenerative disease and environmental stresses such as irradiation. Adenosine receptors are belonging to a large family of adrenergic receptors located in the cell membrane. They can increase organs to resistance against stresses and ascorbic acid is known as a potent antioxidant and also is an anti-cancer substance. We have studied the protective role of separate and concurrent treatment of ascorbic acid and Adenosine receptor agonist on hippocampus neurons of mice following irradiation with gamma ray. For this study, 8 groups were designed. In each group, the mice, exposed to 6 Gray radiations in 1 fracture. After a week, the drugs applied daily by intra-peritoneal injection for a week. Y-maze and shuttle box memory tests were applied to scale short term memory and Nissl staining used for cell counting and TUNEL kit utilized to assess apoptotic cell death.

Our finding revealed that after irradiation short-term memory score was improved after treatment with vitamin C and agonist of A1 Adenosine receptor. Cell counting and TUNEL test displayed a significant protective role of both factors.

Concurrent usage of them can be considered as an effective pharmaceutical approach to reduce hippocampus neuron damages after irradiation.

MILD HYPOTHERMIA AFFECT AUTOPHAGY IN RATS AFTER SUBARACHNOID HEMORRHAGE

H. Hui, Z. Fei

Xijing Hospital, The Fourth Military Medical University, Xi'an, China

Objective: To study the effects of mild hypothermia on autophagy in rats after subarachnoid hemorrhage injury.

Methods: Thirty-six SD rats were randomly divided into sham-operation group, mild hypothermia group and normothermia group. SAH model was used to produce subarachnoid hemorrhage injury. Therapeutic hypothermia was achieved 30 minutes after injury by surface cooling and maintained for 4 hours. The expression of brain cathepsin B and Beclin1 was detected by western-blot and real time RT-PCR, electromicroscopy and the flow cytometry were performed to analyze autophagy.

Results: The expression of rat brain cathepsin

B and beclin1 in the mild hypothermia group was much higher than that in the normothermia group at 3 hours, mild hypothermia increased autophagy in acute phase of subarachnoid hemorrhage.

Conclusion: Mild hypothermia can downregulate the expression of cathepsin B and Beclin1 in the acute phase of injury and may play a protective role at the subarachnoid hemorrhage.

PRE-TREADMILL ALLEVIATE THE CEREBRAL CORTEX BLOOD FLOW ON ISCHEMIC STROKE RAT

X. Yang[1], H. Lu[2], **J. Jia**[1]

[1]Department of Rehabilitation, Huashan Hospital, Fudan University, [2]Shanghai Jiao Tong University, Med-X Research Institute, Shanghai, China

The human brain comprises only 2% of the body's mass, but it consumes 20% of the energy that is produced when the body is in a resting state. After a brief period of brain ischemia there is a decrease in blood flow lasting several hours. As an effective prevention approach to improve prognosis in ischemic stroke, pre-treadmill training has been shown ameliorative effect in neurologic deficits, blood-brain barrier (BBB) dysfunction, maintenance of neurovascular integrity, cerebral infarction and edema. Stroke is an sudden disorder disease on cerebral blood circulation. The neurovascular control of cerebral blood flow is also disrupted during ischaemia, with the loss of coupling between neuralactivity and haemodynamic effects, but how does pre-treadmill training effect on cerebral blood flow (CBF) for ischemic stroke is rarely reported.

Objectives: In this study, we described the influence of two-week pre-treadmill training to ischemic stroke on rats to investigate the differences of CBF in arteries, veins, and capillaries between rats with and without pre-ischemic treadmill training. Furthermore, cerebral infarct volume were detected for brain damage estimation.

Methods: Rats were randomly divided into three groups (n=8): sham, ischemic and pre-treadmill group. Rats in the sham and ischemic groups were not exposed to the treadmill before sham or middle cerebral artery occlusion (MCAO) surgery, but in the pre-treadmill group were subjected to two-week pre-treadmill training. All groups were detected CBF before,during and after surgery by using laser speckle imaging (LSI). Cerebral infarct volume was determined by TTC method.

Results: The results demonstrated that pre-treadmill training alleviated the reduction of cerebral blood flow at 1h, 2h and 3h after ischemic injury, compared with the no treadmill training subjects, on the research of artery and vein regions, while capillary CBF is alleviated reduction at 1h, 2h after ischemic injury. And the regions' CBF is going to be similar between groups compared to baseline at 24h after ischemic stroke. Meanwhile, pre-treadmill training reduces cerebral infarct volume after 24 h ischemic injury.

Conclusions: We inferred pre-treadmill training could play a role in neuroprotection through alleviating the changes of very early stage on blood flow after ischemic stroke.

RGD-CONTAINING OTEOPONTIN ICOSAMER PEPTIDE AFFORDS NEUROPROTECTIVE EFFECT IN THE POSTISCHEMIC BRAIN VIA ANTI-INFLAMMATORY FUNCTIONS

Y.-C. Jin[1], I.-D. Kim[1], H.-K. Lee[1], H.-B. Lee[1], L. Luo[1], P.-L. Han[2], J.-K. Lee[1]

[1]Department of Anatomy, Inha University School of Medicine, Inchon, [2]Division of Nano Sciences and Brain Disease Research Institute, Ewha Womans University, Seoul, Republic of Korea

Osteopontin (OPN) is a phosphorylated glycoprotein that is secreted into body fluid after being synthesized in various cells and tissues. OPN contains arginine-glycine-aspartate (RGD)-motif, through which it binds to several cell surface integrins, that mediates a wide range of cellular processes, such as, the adhesion, migration, and survival of a variety of cell types. Delayed, sustained, and differential inductions of OPN in different cell types in the postischemic brain have been reported and the neuroprotective effects of recombinant OPN protein have also been reported in animal models of stroke. In the present study, authors examined the neuroprotective effects of an RGD-containing OPN icosamer peptide (OPNpt20) in a rat model of focal cerebral ischemia, middle cerebral artery occlusion (MCAO), and investigated the molecular mechanisms

underlying the protective effects. The OPNpt20 had a robust neuroprotective effect against ischemic stroke: it reduced mean infarct volume to 29.2% of that in MCAO control animals and markedly ameliorated neurological deficits when administered 1 hr-post-MCAO (30 ng, intraparenchymal). We found that the neuroprotective efficacy of OPNpt20 was greater than that of OPN full protein and the RGD motif is responsible for the neuroprotective effect of OPNpt20, since it was not detected when a mutated OPN peptide (RGD->RAA) was used. Moreover, these protective effects were due to anti-inflammatory effects of the RGD motif, since RGD-containing OPNpt20 significantly suppressed the inductions of iNOS and other cytokines in the postischemic brain and in primary microglial cultures but a mutated OPN peptide (RGD->RAA) did not. Furthermore, we also found that the suppression of iNOS induction by OPNpt20 was mediated by the interaction between OPNpt20 and avb_3 integrin and subsequent induction of ubiquitin-dependent phospho-STAT1 dagradation. Together these results suggest that RGD-containing OPN icosamer affords neuroprotective effect in the postischemic brain via anti-inflammatory functions.

NEUROPROTECTION OF XUESHUANTONG: INHIBITING THE ACTIVATION OF MICROGLIA

H. Jing[1], S. Wang[2], L. Hu[1]

[1]Tianjin State Key Laboratory of Modern Chinese Medicine, Tianjin University of Traditional Chinese Medicine, [2]Tianjin Key Laboratory of Chinese Medicine Pharmacology, Tianjin University of Traditional Chinese Medicine, Tianjin, China

Microglia, as brain macrophages, is widely distributed in the central nervous system. Brain microglia will be a substantial activation and release of inflammatory factors, after brain injure or cerebral ischemia. Xueshuantong is a herbal medicine in treatment of activating blood circulation to dissipate blood stasis. In our study, the mechanisms of neuroprotection by xueshuantong and its major active components (e.g ginsenoside Rd), particularly its anti-inflammatory effects in microglia, were explored. We found that xueshuantong and ginsenoside Rd inhibited lipopolysaccharide (LPS)-induced production of pro-inflammatory mediators such as NO, tumor necrosis factor α (TNF-α), suppressed LPS-stimulated iNOS, TNF-α mRNA expression in microglial cells. Together, the present study reported that xueshuantong can pay neuroprotection by inhibiting the activation of microglia.

ISCHEMIC POSTCONDITIONING PROTECTS AGAINST FOCAL CEREBRAL ISCHEMIA BY INHIBITING BRAIN INFLAMMATION WHILE ATTENUATING PERIPHERAL LYMPHOPENIA IN MICE

S. Joo, W. Xie, X. Xiong, B. Xu, H. Zhao

Stanford University, Stanford, CA, USA

Background: Ischemic postconditioning (IPostC) has been shown to attenuate brain injury in a few rat stroke models. The purpose of this study is to establish an IPostC model in mice, and investigate how IPostC affects infiltration of leukocytes in the ischemic brain and lymphopenia associated with stroke-induced immunodepression.

Material and methods: IPostC was conducted by a series of repetitive, brief occlusion of the middle cerebral artery (MCA) after reperfusion in a focal ischemia model in mice. Infarct sizes, neurological scores, inflammatory cells in the brain, and immune cell populations in the peripheral immune organs were analyzed by FACS.

Results: IPostC performed immediately, 2 min, or 3 hours after reperfusion, significantly reduced infarct sizes and attenuated neurological scores as measured 3 days post-stroke. The spared infarct areas were seen in the ischemic penumbral areas, i.e. the border zones between the cortical territories of the anterior cerebral artery (ACA) and those of the MCA, as well as in the ventromedial and dorsolateral striatum. FACS analyses showed that IPostC blocked increases in the numbers of microglia, macrophages, CD4 and CD8 T lymphocytes, as well as B lymphocytes in the ischemic brain. Nevertheless, reductions in immune cell numbers in the peripheral blood and spleen were attenuated by IPostC, while immune cell populations in the bone marrow were not altered by IPostC.

Conclusions: IPostC reduced brain infarction and improved neurological deficiencies in mice, likely by blocking infiltration of both innate and adaptive immune cells in the ischemic brain. In addition, it robustly attenuated peripheral lymphopenia thus improved systemic immunodepression.

NEUROPROTECTION BY AN AT2 RECEPTOR AGONIST FOLLOWING ISCHEMIC STROKE

S. Lee[1], V.H. Brait[1], T.V. Arumugam[2], M.A. Evans[1], H.A. Kim[1], R.E. Widdop[1], G.R. Drummond[1], E.S. Jones[1], C.G. Sobey[1]

[1]Department of Pharmacology, Monash University, Clayton, VIC, [2]School of Biomedical Sciences, University of Queensland, Brisbane, QLD, Australia

Objectives: Intracerebral administration of the angiotensin II type 2 receptor (AT_2R) agonist, CGP42112, is neuroprotective in a rat model of ischemic stroke. To explore further its possible cellular target(s) and therapeutic utility, we firstly examined whether CGP42112 may exert direct protective effects on primary neurons following glucose deprivation *in vitro*. Secondly, we tested whether CGP42112 is effective when administered systemically in a mouse model of cerebral ischemia.

Methods: Primary cortical neurons were cultured from E17 C57Bl6 mouse embryos for 9 d, exposed to glucose deprivation for 24 h alone or with drug treatments, and percent cell survival assessed using trypan blue exclusion. Ischemic stroke was induced in adult male C57Bl6 mice by middle cerebral artery occlusion for 30 min, followed by reperfusion for 23.5 h. Neurological assessment was performed and then mice were euthanized and infarct and edema volume were analysed.

Results: During glucose deprivation, CGP42112 ($1x10^{-8}$ M and $1x10^{-7}$ M) reduced cell death by ~30%, an effect that was prevented by the AT_2R antagonist, PD123319 ($1x10^{-6}$ M). Neuroprotection by CGP42112 was lost at a higher concentration ($1x10^{-6}$ M) but was unmasked by co-application with the AT_1R antagonist, candesartan ($1x10^{-7}$ M). By contrast, Compound 21 ($1x10^{-8}$ M to $1x10^{-6}$ M), a second AT_2R agonist, had no effect on neuronal survival. Mice treated with CGP42112 (1 mg/kg i.p.) after cerebral ischemia had improved functional outcomes over vehicle-treated mice as well as reduced total and cortical infarct volumes.

Conclusions: These results indicate that CGP42112 can directly protect neurons from ischemia-like injury *in vitro* via activation of AT_2R, an effect opposed by AT_1R activation at high concentrations. Furthermore, systemic administration of CGP42112 can reduce functional deficits and infarct volume following cerebral ischemia *in vivo*.

SEARCH NEUROPROTECTORS WITH ANTIOXIDANT MECHANISM OF ACTION IN A NUMBER DERIVATIVES OF 3-METHYLXANTHINE

K.V. Alexandrova, O.S. Shkoda, D.M. Yurchenko, O.I. Belenicheva, I.F. Belenichev, **S.V. Levich**

Zaporizhzhya State Medical University, Zaporizhzhya, Ukraine

At the present time actively pursued finding new cerebroprotector among compounds affecting the compensatory shunts ATP synthesis at ischemia of the brain, that modulate glutamate and GABA-ergic system, regulate the activity of Ca-channels and nitrogen oxide system, and among antioxidants, neuropeptides, inhibitors expression of proinflammatory cytokines and antagonists of IL-1β-receptors. Thus, it is appropriate to include in the complex therapy of brain stroke drugs that have antioxidantic, anti-ischemic, nootropic actions.

The target of this study was investigation of neuroprotective action of

2-(8-benzylaminotheophyllin-7-yl)-N'-[(1E)-1-phenylethylidene]acetohydrazide (C-4) in a bilateral ligation of common carotid arteries (ischemic stroke) and compared to standard pharmacological neuroprotector-antioxidant - Mexidol.

Researches conducted *in silico* using ShemAxon for compliance with Lipinski-like filters. To evaluate the neuroprotective action of the studied compounds was used model of incomplete global cerebral ischemia, the most adequate clinical manifestations of ischemic stroke. Neurological deficit was determined by scale srtoke - index CP McGrow. Antioxidant system was evaluated *in vitro* by the activity of superoxide dismutase, catalase, glutathione peroxidase, indicators oxidative modification of protein in brain tissue. Statistical data processing was carried out using standard analysis package Microsoft Office Excel 2003, and applications of statistical processing of results «STATISTICA ® for Windows 6.0».

Biochemical studies have shown that bilateral ligation of common carotid arteries leads to typical ischemic disorders. Investigational

compounds led to an increase in ATP synthesis due to activation of aerobic oxidation path, as indicated by a significant increase in malate, reduction of lactate, which is indicative of the reduction of lactic acidosis in nerve tissue and increase pyruvate compared with control. Also found that C-4 has a positive effect on the metabolism of adenine nucleotides, increasing the intensity of utilization of AMP, and thus, in the future, start braking Xanthine reaction of ROS. Mexidol's action is marked by a similar orientation, but less pronounced effect in relation to that of bioenergy.

Important part of antioxidant action of C-4 at CVA - protection of neuron protein molecules at ischemia, due to inhibition of oxidative modification of proteins, which witnessed fairly low APH and KFH in brain tissue of rats, compared with control group. In the brains of animals treated with C-4, observed increased activity of key antioxidant enzymes - SOD, catalase and HPR. Obviously, the studied compound C-4 reduced the degree of oxidative damage not only the protein part of antioxidant enzymes, but also non-protein active site, as shown in our *in vitro* experiments by example of SOD. That is, the mechanism of neuroprotective action of C-4 is a characteristic for the most secondary neuroprotectors with antioxidant mechanism.

Experimental studies have shown significant neuroprotective properties of C-4 in experimental CVA. Found that the leading elements of the mechanism of action are antioxidant activity (inhibition of oxidative modification of proteins of nervous tissue) and anti-ischemic activity (intensification of aerobic reactions of ATP). By virtue of neuroprotective action of C-4 exceeds the referent drug - Mexidol.

SAFETY AND FEASIBILITY OF REMOTE LIMB ISCHEMIC PRECONDITIONING IN PATIENTS WITH UNILATERAL MIDDLE CEREBRAL ARTERY STENOSIS AND IN HEALTHY VOLUNTEERS

S. Li, G. Shao, X. Ji

Xuan Wu Hospital, Capital Medical University, Beijing, China

Objective : The aim of this study is to assess whether upper arm ischemic preconditioning is feasible and safe in healthy volunteers and patients with unilateral middle cerebral artery (MCA) stenosis.

Methods : 10 patients with unilateral middle cerebral artery (MCA) stenosis and 24 healthy volunteers underwent limb ischemic preconditioning consisting of 5 cycles of 5-minute inflations of a blood pressure cuff to 200mm Hg around an upper limb followed by 5 minutes of reperfusion.

Results : Limb ischemia preconditioning has no significant effect on heart rate, oxygenation index, nor mean flow velocity of in patients with unilateral middle cerebral artery (MCA) stenosis or healthy volunteers. However, healthy volunteers showed a reduction in blood pressure 30 minutes following reperfusion.

Conclusions : Limb preconditioning was found to be safe and well tolerated in both patients and healthy volunteers.

NEUROPROTECTIVE EFFECT OF SHEXIANGBAOXIN PILL ON FOCAL CEREBRAL ISCHEMIA IN RATS

X. Liang[1], S. Li[2], L. Jinning[2]

[1]*Qingdao University, School of Medicine,*
[2]*Dept. of Chinese Medicine, Affiliated Yuhuangding Hospital, Qingdao Uni. School of Medicine, Yantai, China*

Objective: Shexiangbaoxin Pill (SXBXP), a traditional Chinese medicine, has been used to treat cardiovascular diseases for many years. In this study, the neuroprotective effect against focal cerebral ischemia in rats be investigated, and the possible mechanism be discussed.

Methods: A rat model of focal cerebral ischemia-reperfusion injury was established by middle cerebral artery occlusion using modified filament method. A total of 60 healthy male SD rats with MCAO were randomly and equally divided into 5 groups: sham control group, model group, SXBXP treated group (5mg and 20mg/kg), positive control edalavone group (6mg/kg). All drugs were administered via tail vein injection within 30 min. after reperfusion. After 2 h ischemia followed 24 h reperfusion the neurological deficits and the size of cerebral infarction were measured. Immunohistochemistry was used to detect the expression of TNF-α, IL-1β and NF-kB proteins.

Results: SXBXP could decrease the neurological deficits and the size of cerebral infarction and also down regulate the expression of TNF-α, IL-1β and NF-kB proteins in a dose-dependent manner. SXBXP low-dose group showed no statistical significance (p>0.05 vs model group), other groups showed significant difference (p< 0.05 or p< 0.01 vs model group).

Conclusion: SXBXP may have the protective effect on focal cerebral ischemia-reperfusion injury through anti-inflammatory effect.

NONSELECTIVE CALCIUM CHANNEL BLOCKER BEPRIDIL DECREASES SECONDARY PATHOLOGY IN HAPP$_{SL}$ MICE AFTER CORTICAL LESION

A. Lipsanen[1], S. Flunkert[2], K. Kuptsova[1], M. Hiltunen[1], M. Windisch[2], B. Hutter-Paier[2], J. Jolkkonen[1]

[1]Institute of Clinical Medicine, University of Eastern Finland, Kuopio, Finland, [2]QPS Austria GmbH, Grambach, Austria

Objectives: Experimental studies have identified a complex link between brain ischemia, β-amyloid (Aβ) and calcium homeostasis. The aim of the present study was to further examine this interaction in transgenic hAPP$_{SL}$ mice subjected to cortical photothrombosis. Our hypothesis was that the vulnerability of hAPP$_{SL}$ transgenic mice to cortical infarct is markedly increased and that treatment with nonselective calcium channel blocker would reverse the secondary pathology in the thalamus.

Materials and methods: Transgenic hAPP$_{SL}$ (n=33) and non-transgenic (n=30) male mice (4-5 months old) were subjected to cortical photothrombosis and treated with nonselective calcium channel blocker, bepridil (50 mg/kg, p.o., once a day) or vehicle for 28 days. After the follow-up, animals were perfused for histological analysis of infarct size and Aβ and calcium accumulation in the thalamus.

Results: Cortical photothrombosis resulted in a small infarct, which was associated with a delayed Aβ and calcium accumulation in the ipsilateral thalamus. Transgenic bepridil treated mice had significantly smaller infarct volumes than non-transgenic littermater (P< 0.05) Ischemia-induced Aβ (*P*< 0.01) and calcium (*P*< 0.01) accumulation in the thalamus was lower in both vehicle and bepridil treated transgenic mice compared to non-transgenic vehicle treated mice. Bepridil decreased both Aβ (*P* < 0.05) and calcium (*P* < 0.01) load in non-transgenic mice.

Conclusions: The present data suggest less pronounced primary and secondary pathology in hAPP$_{SL}$ transgenic mice after cortical injury. Bepridil decreased both Aβ and calcium pathology in the thalamus following ischemia.

THE NEUROPROTECTIVE MECHANISM OF ERYTHROPOIETIN-TAT FUSION PROTEIN AGAINST NEURODEGENERATION FROM ISCHEMIC BRAIN INJURY

P. Liu[1], X. Liu[1], A.K.-F. Liou[2], X. Ji[1], X. Liu[1], H. Zhao[1], F. Yan[1], J. Chen[2], G. Cao[2], Y. Luo[1]

[1]Cerebrovascular Diseases Research Institute, Xuanwu Hospital, Capital Medical University, Beijing, China, [2]University of Pittsburgh, Department of Neurology, Pittsburgh, PA, USA

Aims: Protection conferred by erythropoietin (EPO) against ischemic brain injury has been demonstrated. This study aimed at further examining the effect and mechanism of erythropoietin-TAT fusion protein (EPO-TAT) in rat transient focal cerebral ischemia.

Methods: Transient focal ischemia was induced using the suture method. Rats were divided into 5 groups: sham, saline-treated, 1000 U/kg EPO, 5000 U/kg EPO and 1000 U/kg EPO-TAT-treated group. Neurological deficit scores were assessed at 72 hours after reperfusion. The infarct volume was measured using TTC staining. Apoptosis was detected with terminal deoxynucleotidyl transferase dUTP nick end labeling staining. The expression of phosphorylated AKT (p-AKT) and phosphorylated ERK (p-ERK) were measured with immunohistochemistry and western blot analysis.

Results: 1000 U/kg EPO-TAT conferred comparable protection to 5000 U/kg EPO manifested by a similar decrease in infarct volume, the number of apoptotic cells and neurological deficit in rat model. The p-AKT and p-ERK were both increased, signifying the concurrent activation of the AKT and ERK pathways. The inhibition of either the AKT or ERK pathway abolished the protection

conferred by EPO-TAT, suggesting that these two protective pathways worked in parallel.

Conclusion: our study indicates parallel participation of AKT and ERK pathways in the protective mechanisms of EPO.

LUTEIN ENHANCES SURVIVAL AND REDUCES NEURONAL DAMAGE IN CEREBRAL AND RETINAL ISCHEMIA/REPERFUSION INJURY

A.C.Y. Lo[1,2], S.-Y. Li[1], F.K.C. Fung[1], D. Yang[1], D. Wong[1,2]

[1]Department of Ophthalmology, [2]Research Centre of Heart, Brain, Hormone and Healthy Aging, The University of Hong Kong, Hong Kong, Hong Kong S.A.R.

Purpose: Stroke is one of the leading causes of death worldwide. Protective agents that could diminish the injuries induced by cerebral ischemia/reperfusion (I/R) are crucial to alleviate the detrimental outcome of stroke. Retinal I/R also occurs in many ocular diseases and leads to neuronal death and therefore blindness. Lutein, a safe and potent antioxidant, is known to protect the retina in age-related macular degeneration. The aim of this study is to investigate the protective roles of lutein in cerebral and retinal I/R injury.

Methods: Two-hour cerebral ischemia was induced by unilateral middle cerebral artery occlusion (MCAo) in mice. Either lutein (0.2mg/kg) or vehicle was given to mice intraperitoneally 1hr after MCAo and 1hr after reperfusion. Neurological deficits were evaluated at 22hr after reperfusion while survival rate was assessed daily until 7 days after reperfusion. Flash electroretinogram (flash ERG) was taken to assess retinal function. After sacrifice, mouse brains were cut into 2mm-thick coronal slices and stained with 2% 2,3,5-triphenyltetrazolium chloride to determine the infarct size after MCAo. Eyes were also enucleated. Paraffin-embedded brain and retinal sections were prepared for TUNEL assay and immunohistochemistry. Protein lysate was collected for Western blotting experiments. Lutein's effect on Müller cells was further evaluated using a model of cobalt chloride-induced hypoxia in immortalized rat Müller cells (rMC-1).

Results: Higher survival rate, better neurological scores, smaller infarct area and smaller infarct volume were noted in the lutein-treated group. Immunohistochemistry data showed a decrease of immunoreactivity of nitrotyrosine, poly(ADP-ribose) and NFkB in the lutein-treated brains. Western blotting data showed decreased levels of Cox-2, pERK, and pIkB, but increased levels of Bcl-2, heat shock protein 70 and pAkt in the lutein-treated brains. In the retina, severe cell loss in retinal ganglion cell (RGC) layer was noted after I/R injury. Increased oxidative stress was observed in the injured retina. Lutein treatment protected RGC as well as decreased oxidative stress in I/R retina. Lutein treatment also minimized the deterioration of b-wave/a-wave ratio and oscillatory potentials in flash ERG as well as inhibited the up-regulation of GFAP in retinal I/R injury. In the cultured Müller cells, lutein treatment reduced level of nuclear NF-kB together with decreased levels of IL-1b and Cox-2.

Conclusions: Post-treatment of lutein protected both the brain and retina from I/R injury. The neuroprotective effect of lutein was associated with reduced oxidative stress. Less production of pro-inflammatory factors from Müller cells suggested an anti-inflammatory role of lutein in retinal ischemic/hypoxic injury. Our results suggest that lutein could diminish the deleterious outcomes of cerebral and retinal I/R probably by its anti-apoptotic, anti-oxidative and anti-inflammatory properties. Lutein may have a therapeutic role in protecting the brain in stroke and inner retina in eye diseases with acute ischemia.

REPETITIVE HYPOXIC PRECONDITIONING AMELIORATES COGNITIVE IMPAIRMENT AND WHITE MATTER LESIONS COGNITIVE IMPAIRMENT AND WHITE MATTER LESIONS

G. Li[1], **R. Meng**[1], C. Ren[1], J. Jia[1], X. Wang[2], J. Shi[1], Y. Duan[3], Y. Ding[1], X. Ji[1]

[1]Department of Neurology and Cerebral Vascular Diseases Research Institute (China-America Institute of Neuroscience), Xuanwu Hospital, Capital Medical University, Beijing, China, [2]Massachusetts General Hospital, Harvard Medical School, Boston, MA, [3]Wayne State University School of Medicine, Detroit, MI, USA

Background and purpose: Neuroprotective effects of hypoxic preconditioning have been demonstrated in the transient focal ischemia-reperfusion injury. This study aims to verify the ameliorated effect of repetitive normobaric

hypoxic preconditioning (RNHP) on cognitive impairment and white matter lesions induced by chronic cerebral hypoperfusion.

Methods: To ligate both common carotid arteries in sixteen male Sprague-Dawley rats, eight of them had received 10 days of RNHP before operation and the remaining operated rats (the ambient-air-control) respired ambient air. Another eight rats without both common carotid arteries ligated were as the sham-operated control. Morris water maze tests were used to evaluate cognitive level. White matter lesions were estimated by Klüver-Barrera staining. The immunostain of astroglia, microglia and oligodendrocyte were GFAP, Iba-1 and CNPase antibodies respectively scattered in cerebral white matter.

Results: After common carotid artery occlusion, the spatial reference memory of the rats in both operated groups were declined compared to the sham-operated control, meanwhile, there were persistent axonal loss and myelin disruption with extensive activation of the astroglia and microglia and reduction of oligodendrocyte in the white matter. However, all the phenomena above were slight in the brains of the rats treated with RNHP compared to the control.

Conclusion: Repetitive normobaric hypoxic preconditioning may exert a protective effect on white matter lesions and cognitive impairment induced by chronic cerebral hypoperfusion in rats.

References:

1.Stowe AM, Wacker BK, Cravens PD, Perfater JL, Li MK, Hu R, Freie AB, Stuve O, Gidday JM. Ccl2 upregulation triggers hypoxic preconditioning-induced protection from stroke. *J Neuroinflammation*. 2012;9:33

2.Ran R, Xu H, Lu A, Bernaudin M, Sharp FR. Hypoxia preconditioning in the brain. *Dev Neurosci*. 2005;27:87-92

3.Stowe AM, Altay T, Freie AB, Gidday JM. Repetitive hypoxia extends endogenous neurovascular protection for stroke. *Ann Neurol*. 2011;69:975-985

4.Zhu Y, Zhang Y, Ojwang BA, Brantley MA, Jr., Gidday JM. Long-term tolerance to retinal ischemia by repetitive hypoxic preconditioning: Role of hif-1alpha and heme oxygenase-1. *Invest Ophthalmol Vis Sci*. 2007;48:1735-1743

DHCR24/SELADIN1 PROTECTS THE BRAIN FROM EXPERIMENTAL CEREBRAL ISCHEMIA IN MICE

M. Hernandez[1], O. Hurtado[1], I. Ballesteros[1], I. Garcia-Yebenes[1], C.G. Dotti[2], E. Gabande[2], I. Lizasoain[1], **M.A. Moro**[1]

[1]Farmacologia, Facultad de Medicina, Universidad Complutense de Madrid, [2]Center for Molecular Biology Severo Ochoa, CSIC-UAM, Madrid, Spain

Introduction: DHCR24 (3β-hydroxysteroid-Δ24 reductase), also called Seladin1 (Selective Alzheimer Disease Indicator 1; Greeve et al. J Neurosci 2000) has been implicated in neuroprotection, oxidative stress and inflammation (Kuehnle et al., Mol Cell Biol 2008). However, the possible role of Seladin1 in ischemic stroke remains unexplored. The aim of this study was to characterize the effect of Seladin1 after stroke using an experimental model in mice.

METHODS: Seladin1$^{+/-}$ (SLD$^{+/-}$) and wild type (WT) mice were subjected to permanent focal ischemia by ligature (Middle Cerebral Artery Occlusion, MCAO). In another set of experiments wild-type mice were treated ip either with vehicle or U18666A (Seladin1 inhibitor, 10 mg/kg) 30 min after MCAO. Brains were removed 48 h after pMCAO and stained with 2,3,5-triphenyltetrazolium chloride for infarct volume determination. For Seladin1, iNOS and COX2 protein expression determination, western blot was performed.

Results: SLD$^{+/-}$ mice displayed a larger infarct volume (130 ± 10%, P< 0.01 vs. WT, n=10) after pMCAO than their WT counterparts. In WT mice, treatment with the Seladin1 inhibitor U18666A increased ischemic injury (156 ± 14% of WT-vehicle, P< 0.01 vs. WT-vehicle, n=4). In order to study the effect of Seladin1 in inflammation after ischemia we determined the levels of different molecules that are described to mediate inflammation after stroke. Our results show an increase in the pro-inflammatory mediators iNOS and COX-2 in SLD$^{+/-}$ mice after ischemia.

Conclusions: These results support the idea that DHCR24/Seladin1 plays an important role in neuroprotection against brain ischemia, which may be due to anti-inflammatory effects of this protein.

THE KETOGENIC DIET INHIBITES HIPPOCAMPAL REGENERATIVE MOSSY FIBER SPROUTING BY SUPPRESSING ZNT3 EXPRESSION IN HIPPOCAMPUS FOLLOWING DEVELOPEMTAL SEIZURES

H. Ni, X.-Y. Zhang, T. Tian, B.-L. Sun

Neurology Laboratory, Soochow University, Suzhou, China

For the purpose of investigating the intervention effect and the underlying molecular mechanism of an old anti-epileptic diet therapy (ketogenic diet) on hippocampal regenerative mossy fiber spouting of neonatal rat with prolonged seizures, a seizure was induced by inhalant flurothyl daily in neonatal Sprague-Dawley rats from postnatal day 8 (P8). The authors assigned ten rats each randomly into the non-seizure and normal diet group (NS+ND), the control plus ketogenic diet group (NS+KD), recurrent-seizure and normal diet group (RS+ND)、recurrent-seizure and ketogenic diet group (RS+KD). The NS+KD and RS+KD treated groups received ketogenic diets for three weeks from P21. On P43, mossy fiber sprouting and zinc transporter 3 (ZnT-3) expressions were determined by Timm staining, real-time RT-PCR and Western blot methods, respectively. Ketogenic diet obviously suppressed the aberrant mossy fiber sprouting in the supragranular region of dentate gyrus and CA3 subfield of hippocampus. ZnT-3 expression both in mRNA and protein levels was strongly up-regulated by developmental seizures (RS+ND) compared with that in the NS+ND group. Up-regulation of ZnT-3 was blocked by treatment with ketogenic diet both in mRNA and protein levels. The results of the present study suggests that ketogenic diet, a high-fat content diet which mimics the anticonvulsant effects of fasting, is potentially useful in the inhibition of developmental seizure-induced regenerative aberrant sprouting of mossy fibers in hippocampus through suppressing ZnT-3 expression.

SOME ASPECTS OF THE NEUROPROTECTIVE ACTION OF THE EXOGENOUS HSP70

I.F. Belenichev, S.V. Pavlov, N.V. Buhtiayrova, **E.V. Odnokoz**

Zaporizhzhya State Medical University, Zaporizhzhya, Ukraine

As well as known, HSP70 proteins have neuroprotective action, but it,s mechanism is still unclear.

The aim of our study was to determine the role of the HSP70 in keeping of the optimal antioxidant protection in central nervous system's neurons in rats with cerebral ischemia.

Results: In vivo experiments showed that injection of the deprivator of the glutathione system (1 mM CDNB, chloredinitrobenzole) to the rats leads to the decrease of the citozole and mitochondrial pulls of GSH, big increase of the AFA and decrease of the HSP70 in neuronal cells in rat's brains. Injection of the HSP70 in the neurons, which were incubated with CDNB leads to the increase of the GSH level and decrease of the AFA.

Experiments in vivo showed that in acute cerebral ischemia in rats leads to the quick decrease of the glutathione level, but increase of the HSP70 expression in the central nervous system cells.

Increase of the HSP70 level leads to the normalization of the glutation chain of the tyol-disulfide system and increase of the cells defend to the ischemia. Injection of the exogenous HSP70 increased functional activity of the glutathione system in the cortical neurons in rats with ischemia.

Conclusion: HSP70 is the proteins with clear neuroprotective action, in ischemia mobilize antioxidant sources in neurons, increase citozole and mitochondrial glutathione levels, which prevent oxidative stress.

NEUROPROTECTIVE EFFECT OF A NEW SYNTHETIC ASPIRIN-DECURSINOL ADDUCT IN A RAT MODEL OF ISCHEMIC STROKE

J.H. Park[1], J.-C. Lee[1], S.U. Lee[1], B.C. Yan[1], J.H. Cho[1], Y.L. Lee[2], M.-H. Won[1]

[1]Kangwon National University, [2]Hallym University, Chuncheon, Republic of Korea

Objective: Stroke is a major cause of death. This study investigated the preventative effect of a new synthetic drug on brain function in experimentally induced ischemic stroke.

Methods: Male Sprague-Dawley rats were administered aspirin (ASA), decursinol (DA) or

ASA-DA before and after ischemic insults. Brain and neuronal damage were examined by TTC staining, PEP-CT, NeuN immunohistochemistry and F-J B histofluorescence. Gliosis was also observed by GFAP and iba-1 immunohistochemistry.

Results: Pre-treatment with 20 mg/kg, but not 10 mg/kg, of ASA-DA protected against ischemic neuronal death and damage, and its neuroprotective effect was much more pronounced than that of ASA or DA alone. In addition, treatment with 20 mg/kg ASA-DA reduced the ischemia-induced activation of astrocytes and microglia.

Conclusion: Our findings indicate that ASA-DA, a new synthetic drug, prevents against transient focal cerebral ischemia, which provides a resource for the development of its clinical application for stroke.

LONG TERM PROTECTION AFTER ISCHAEMIC STROKE IN CO-MORBID RATS WITH SUBCUTANEOUS ADMINISTRATION OF IL-1 RECEPTOR ANTAGONIST (IL-1RA)

J.M. Pradillo, K.N. Murray, H. Boutin, N.J. Rothwell, S.M. Allan

Faculty of Life Sciences, University of Manchester, Manchester, UK

Introduction: Stroke is a leading cause of death and disability worldwide. Although several treatments have been successful in experimental stroke, there has been a lack of translation to the clinic(1). This could be due to the absence of experimental studies considering stroke risk factors. Inflammation contributes to poor outcome after stroke, and the proinflammatory cytokine interleukin-1 (IL-1) is a key mediator of experimental ischaemic brain injury(2,3).Recently, we have demonstrated the beneficial effect of the administration of IL-1 receptor antagonist (IL-1Ra) at reperfusion and 3h later in aged and comorbid rats(4). In the present study, we tested whether the IL-1Ra administration at 3 and 6h of reperfusion is also neuroprotective in aged and co-morbid animals when outcome was measured 24h or 7 days after experimental stroke.

Methods: Thirteen months old Corpulent (JCR:LA Cp/Cp, a model of atherosclerosis and obesity) and Lean rats were exposed to 90 min transient experimental stroke was performed (tMCAO). IL-1Ra or placebo was administered subcutaneously (25mg/kg) at 3 and 6h of reperfusion. Infarct volume and stroke outcome were assessed 24h and 7 days after tMCAO by MRI (T_2W images) and functional tests respectively. Seven days after tMCAO, IL-1Ra neuroprotection and blood brain barrier (BBB) disruption were confirmed histologically.

Results: Administration of IL-1ra during reperfusion reduced infarct volume measured by MR at 24h (by approx 40%), and at 7 days (by ≈30%) in lean and Cp rats. Histologically, IL-1Ra also reduced infarct volume and BBB disruption at 7days, and resulted in improved neurological outcome in both lean and Cp rats.

Conclusions: Our results demonstrate for the first time that subcutaneous administration of IL-1Ra during reperfusion is neuroprotective and improves the outcome at 7 days after experimental stroke in aged and co-morbid animals.

References:

(1) Dirgnal U. (2006) J Cereb Blood Flow Metab. 26:1465-78;

(2) McColl B.W. et al. (2009) Neuroscience. 158:1.049-1061;

(3) Allan S.M. et al. (2005) Nat Rev Immunol. 5(8):629-40;

(4) Pradillo JM. et al. (2012) J Cereb Blood Flow Metab. 32(9):1810-19.

This work was supported by Medical Research Council (MRC).

CHOROID PLEXUS SYNTHESIZES TESTOSTERONE FROM ANDROSTENEDIONE: REGULATION OF 17BHSD3 BY THE SEX HORMONE BACKGROUND

T. Quintela[1], F.M. Patriarca[1], I. Gonçalves[1], A.V.M. Canário[2], C.R.A. Santos[1]

[1]CICS-UBI - Health Sciences Research Centre, University of Beira Interior, Covilhã, [2]Centre of Marine Sciences, University of Algarve, Faro, Portugal

Introduction: Neurosteroids have been emerging as important regulators of numerous central nervous system functions, playing essential roles in protecting the brain from

insults such as neurodegeneration or ischemia [1]. The choroid plexus (CP) forming a physical interface between the peripheral blood and the cerebrospinal fluid (CSF), regulate the uptake of nutrients, hormones and several other compounds from the peripheral blood into the CSF, and play pivotal roles in repair processes following trauma [2]. There are evidences that CP is a target of sex steroid hormones, which regulate the expression of some proteins with impact in neuroprotection in this tissue. Unlike other brain regions, there are no current indications that CP may produce sex hormones as well, but a recent cDNA microarray analysis of the CP transcriptome showed that several enzymes involved in steroidogenesis are expressed in this tissue.

Objectives: Therefore, we tested the capacity of CP explants to synthesize testosterone and analyzed the expression of steroidogenic enzymes in response to the hormonal background.

Methods: This study evaluates the presence of steroidogenenic enzymes in rat CP using RT-PCR, immunohistochemistry, Western blot and immunofluorescence. In addition, we assessed the production of neurosteroids by rat CP explants from tritiated androstenedione using thin layer liquid chromatography.

Results: We demonstrate the presence of mRNA transcripts for P450scc (Cyp11A1), P450aro (Cyp19A1), 17βHSD3 (HSD17B3) and 5α-reductase (SRD5A1 and SRD5A2). Protein expression of enzymes required for testosterone synthesis in CP was also confirmed using immunohistochemistry and Western blot. Moreover, we demonstrate that CP explants are capable of converting [^{3}H]-androstenedione to testosterone. Finally, to assess dynamic changes in the expression patterns of 17βHSD3, real-time RT-PCR was performed in CP of female and male rats subjected to gonadectomy. We show that the 17βHSD3 enzyme is up-regulated in female and male rat CP, suggesting that the peripheral hormonal background modulates the synthesis of testosterone in CP.

Conclusions: Collectively these data show that the CP has the potential to synthesize testosterone, thereby being able to regulate the hormonal content of the CSF, counterbalancing changes in peripheral hormone levels.

References:

1. Mellon SH, Griffin LD (2002) Neurosteroids: biochemistry and clinical significance. Trends Endocrinol Metab 13: 35-43.

2. Emerich DF, Borlongan CV (2009) Potential of choroid plexus epithelial cell grafts for neuroprotection in Huntington´s disease: what remains before considering clinical trials. Neurotox Res 15: 205-211.

REPETITIVE HYPOXIA AFTER CHRONIC CEREBRAL HYPOPERFUSION INDUCE VASCULAR REMODELING IN RAT

C. Ren, J. Cao, N. Li, X. Ji

Institute of Hypoxia Medicine, Xuanwu Hospital, Capital Medical University, Beijing, China

Background and purpose: Chronic cerebral hypoperfusion is an important risk factor for dementia states and other brain dysfunctions. Vascular remodeling is an important component that link vascular oxygen supply. Brief systemic hypoxia attenuates the rodent brain damage and memory impairments observed following severe ischemia. However, it is not clear whether systemic hypoxia administered post-ischemia can facilitate vascular remodeling or ameliorate learning and memory. The purpose of the present study was to investigate the effects of repetitive hypoxia intervention following chronic brain ischemia in rats.

Methods: We used permanent occlusion of bilateral common carotid arteries (2-VO) to induce chronic cerebral hypoperfusion in male Sprague-Dawley rats. One week after 2VO surgery, the animals of repetitive hypoxic post-conditioning (RHP) treatment group were exposed in 8% O_2 for one hour each day and continued four weeks. Control groups were handled in the same manner, but exposed only to room air. Spatial learning and memory was determined by Morris water maze task. Immunohistochemical staining for Von Willebrand Factor(vWF) was performed for assessing vascular perimeter and density. Protein expression patterns of MAP-2, VEGF, phosphorylated eNOS were determined by Western blot analysis at five weeks after 2VO. The mRNA expression of angiogenesis 1 and angiogenesis 2 and VEGF were examined by real time PCR at three weeks after 2VO.

Results: RHP treatment significantly

ameliorated spatial learning and memory. RHP treated rats exhibited significantly increased vascular density and vessel perimeter compared with control group. The protein expressions of MAP-2, VEGF, phosphorylated eNOS were significantly upregulated in RHP group compared with control group. RHP treatment significantly attenuated Ang2, but increased Ang1 mRNA expression in the cerebral cortex compared with control group.

Conclusions: RHP following chronic cerebral hypoperfusion ameliorated ischemia-induced spatial learning and memory impairment likely by promote vascular remodeling.

THE OLFACTORY MACHINERY IS EXPRESSED IN RAT CHOROID PLEXUS: CAN IT SMELL THE CEREBROSPINAL FLUID?

C. Santos[1], G. Tavares[1], T. Quintela[1], P. Hubbard[2], I. Gonçalves[1]

[1]CICS-UBI - Health Sciences Research Centre, University of Beira Interior, Covilhã, [2]CCMAR-Centre of Marine Sciences, University of Algarve, Faro, Portugal

Introduction: The choroid plexuses (CPs) are highly vascularized branched structures that protrude into the ventricles of the brain, and form a unique interface between the blood and the cerebrospinal fluid (CSF). The best recognized function of this tissue is cerebrospinal fluid (CSF) production, from which, CP nourish and protect all central nervous system(CNS), providing nutrients and a set of neuropeptides, cytokines and metabolizing enzymes, growth factors and hormones. Therefore CPs plays an important role in monitoring and buffering the brain extracellular fluid, which keeps in balance all CNS (1) . A CP cDNA microarray study was performed to broaden our knowledge about CP transcriptome allowing the identification of several genes associated with olfactory transduction, particularly olfactory receptors.

Objective: As olfactory-like chemosensory signalling has already been identified outside the olfactory epithelium, in tissues where it monitors the composition of body fluids (2, 3), we aimed at confirming that the olfactory machinery is expressed in the CP and forecast its functionality in this tissue.

Material and methods: The expression of key components of the olfactory machinery was analysed by conventional PCR and real-time PCR , DNA sequencing, Western blot, immunohistochemistry and immunofluorescence. In addition, electro-olfactograms (EOGs) were carried out in CP explants stimulated with polyamines, such as spermidine, spermine and cadaverine, which are known ligands of olfactory receptors.

Results: We found that major components of the cAMP olfaction pathway, including olfactory receptors (OR 63, OR 19, OR 600, OR 620/624 e OR 1496), olfactory-related adenylate cyclase (ACIII), olfactory G protein (Gαolf), and cyclic gated nucleotide channel subunit A2 (CNG-2) are expressed in CP. Preliminary data provided by EOGs indicate that polyamines elicit an electrophysiological response in this tissue.

Conclusions: These results suggest that an olfactory-like chemosensory pathway might be active in CP and could function as a detector of soluble chemical molecules in CSF therefore inducing cellular responses according to CNS physiological needs.

References:

1. Redzic, Z. B. and M. B. Segal (2004). "The structure of the choroid plexus and the physiology of the choroid plexus epithelium." Adv Drug Deliv Rev **56**(12): 1695-1716.
2. Itakura, S., K. Ohno, et al. (2006). "Expression of Golf in the rat placenta: Possible implication in olfactory receptor transduction." Placenta **27**(1): 103-108.
3. Pluznick, J. L., D. J. Zou, et al. (2009). "Functional expression of the olfactory signaling system in the kidney." Proc Natl Acad Sci U S A **106** (6): 2059-2064.

THE SEX HORMONE BACKGROUND REGULATES THE RAT CHOROID PLEXUS TRANSCRIPTOME

C. Santos[1], T. Quintela[1], L. Carreto[2], M. Santos[2], H. Marcelino[1], F. Patriarca[1], I. Gonçalves[1]

[1]CICS-UBI - Health Sciences Research Centre, University of Beira Interior, Covilhã,

[2]*RNA Biology Laboratory, Department of Biology and CESAM, University of Aveiro, Aveiro, Portugal*

Introduction: The choroid plexus (CP), consist of numerous villi, in which blood microvessels are enclosed by a single layer of cubical epithelial cells forming the blood-cerebrospinal fluid barrier [1]. Its best known functions are cerebrospinal fluid (CSF) formation, control of brain uptake of nutrients, hormones and other compounds from the peripheral circulation, and the clearance of metabolic products [1]. Recent evidence indicates that these structures are sex-hormone responsive as they express progesterone [2], estrogen alpha and beta [3] and androgen receptors [4] and some peptides synthesized in CP are regulated by them [5,6].

Objective: As sex hormones are considered important neuroprotectants against several brain insults, we aimed at broadening our understanding of the impact of the sex hormone background on the rat CP transcriptome using cDNA microarray technology.

Materials and methods: Rats were handled in compliance with the NIH guidelines and the European Union rules for the use of laboratory animals (Directive 2010/63/EU). Female and male rats were either ovariectomized (OVX) or orchidectomized (OOX), or sham operated. Two weeks after surgery, both lateral ventricular CPs were collected for RNA extraction, which were used for cDNA microarrays (Agilent Technologies).

Results: Microarray analysis of whole CP genome expression in OVX compared to sham female rats identified more than 6,000 (p-value< 0.05) differentially expressed genes (approximately 25%). Differences in the transcriptome of OOX males compared with sham ranged approximately 15% of the rat CP transcriptome. Using a 1.5 - fold change as a cut-off, 1168 genes (4.7%) were up-regulated in CP of female OVX rats, while in CP of male rats only 426 genes (1.7%) were up-regulated comparing to sham animals. Regarding down-regulated genes, 1328 genes (5.3%) were identified in CP of female rats and 123 genes (0.5%) in CP of male rats. Analysis of these genes in the database for Annotation, Visualization and Integrated Discovery (DAVID) v6.7 http://david.abcc.ncifcrf.gov/ [7] showed that the top-five pathways significantly regulated by the sex hormone background are olfactory transduction, taste transduction, metabolism, steroid hormone biosynthesis and circadian rhythm pathways.

Conclusions: These results represent the first overview of global expression changes in CP of female and male rats induced by gonadectomy and emphasize the importance of sex hormones in the regulation of pathways with central roles in CP functions and CSF homeostasis. Moreover, this study provides evidence that CP may be involved in many more functions than previously thought.

References:

1. Redzic ZB, Segal MB (2004) Adv Drug Deliv Rev 56: 1695-1716.

2. Quadros PS, Pfau JL, Wagner CK (2007) J Comp Neurol 504: 42-56.

3. Hong-Goka BC, Chang FL (2004) Neurosci Lett 360: 113-116.

4. Alves CH, Goncalves I, Socorro S, Baltazar G, Quintela T, et al. (2009) J Mol Neurosci 38: 41-49.

5. Quintela T, Alves CH, Goncalves I, Baltazar G, Saraiva MJ, et al. (2008) Brain Res 1229: 18-26.

6. Quintela T, Goncalves I, Baltazar G, Alves CH, Saraiva MJ, et al. (2009) Cell Mol Neurobiol.

7. Huang da W, Sherman BT, Lempicki RA (2009). Nat Protoc 4: 44-57.

CEREBROLYSIN TREATMENT ATTENUATES FUNCTIONALIZED MAGNETIC IRON OXIDE NANOPARTICLES INDUCED CNS INJURY FOLLOWING HYPERTHERMIA

A. Sharma[1], P.K. Menon[1], J.V. Lafuente[2], Z.P. Aguilar[3], A. Wang[3], D.F. Muresanu[4], H. Moessler[5], R. Patnaik[6], H.S. Sharma[1]

[1]Surgical Sciences, Anesthesiology & Intensive Care Medicine, Uppsala University, University Hospital, Uppsala, Sweden, [2]Dept of Neurosciences, University of Basque Countries, Bilbao, Spain, [3]Ocean NanoTech, Springdale, AR, USA, [4]Clinical Neurosciences, University of Medicine & Pharmacy, University Hospital, Cluj-Napoca, Romania, [5]Ever NeuroPharma, Oberburgau, Austria, [6]Biomaterials, School of Biomedical

Engineering, National Institute of Technology, Banaras Hindu University, Varanasi, India

Iron Oxide magnetic nanoparticles (IO) nanoparticles (NPs) or IOMNPs are used for diagnostic purposes in cancer studies. In animal models, IOMNPs showed lower uptake in many organs. However, the effect of these NPs per se on the central nervous system (CNS) is not well known. This study is aimed to find out whether IOMNPs (10 nm in diameter) given in rats (0.25 or 0.50 mg/mL in100 µl, i.v.) could influence the blood-brain barrier (BBB) permeability and neuronal or glial changes within 4 to 24 h after administration. Furthermore, the study was designed to find out whether the IOMNPs given in identical situations after a thermal challenge would affect brain pathophysiology. Finally, whether cerebrolysin, a mixture of several neurotrophic factors and active peptide fragments in a dose of 2. 5 mL/kg, i.v. will influence the IOMNPs induced changes in CNS pathology. Additional thermal challenge was inflicted inflicted in rats by exposing them in a Biological Oxygen Demand Incubator (BOD) maintained at 38° C for 4. The animals were allowed to survive 4 or 24 h after thermal challenge. Cerebrolysin (2.5 ml/kg, i.v.) was given either 30 min before IOMNP injection in the 4 h survival group or 4 h after injury in the 24 h survival groups. In the control group cerebrolysin was administered in identical situation following IOMNPs administration. In all groups, leakage of serum albumin in the CNS as a marker of BBB breakdown and activation of astrocytes using glial fibrillary acidic protein (GFAP) was evaluated by immunohistochemistry. The neuronal injury was examined by Nissl staining. The results indicated that the IOMNPs in low or high doses did not induce albumin or GFAP immunoreactivity or neuronal changes in the CNS following 4 or 24 h after administration. This suggests that IOMNPs were innocuous within the CNS. Thermal challenge and resulting hyperthermia (41.2±0.23° C) significantly induced increased albumin and GFAP immunoreactivity in the cerebral cortex, hippocampus, cerebellum, thalamus and hypothalamus after 4 h and following 24 h after heat exposure. Abnormal neuronal reactions were observed in these brain areas at this time. Interestingly, administration of IOMNPs in heat-exposed group slightly enhanced the pathological changes in the CNS after 24 h but not 4 h after heat exposure. Cerebrolysin treatment alone did not alter neuronal, glial or BBB function but markedly attenuated NPs and/or hyperthermia induced neuronal and glial cell changes and thwarted albumin leakage indicating marked protection of the BBB function. These observations are the first to show that IOMNPs are safe for the CNS and cerebrolysin treatment prevented CNS pathology following a combination of whole body hyperthermia and IOMNPs injection. This indicated that cerebrolysin might be used as adjunct therapy during IOMNPs administration during cancer related therapies, not reported earlier.

NANOPARTICLES AGGRAVATE NEUROPATHIC PAIN SYNDROME AND BLOOD-SPINAL CORD BARRIER BREAKDOWN, ASTROCYTIC ACTIVATION AND NEURAL INJURY: NEUROPROTECTIVE EFFECTS OF CEREBROLYSIN

H.S. Sharma[1], L. Feng[2], D.F. Muresanu[3], H. Moessler[4], A. Sharma[5]

[1]Surgical Sciences, Anesthesiology & Intensive Care Medicine, Uppsala University, Uppsala, Sweden, [2]Dept. of Neurology, Bethune International Peace Hospital, Shijiazhuang, China, [3]Clinical Neurosciences, University of Medicine & Pharmacy, University Hospital, Cluj-Napoca, Romania, [4]Ever NeuroPharma, Obernurgau, Austria, [5]Surgical Sciences, Anesthesiology & Intensive Care Medicine, Uppsala University, University Hospital, Uppsala, Sweden

Neuropathic pain syndrome includes sensitivity to touch and pain perception including phantom pain. Chronic neuropathic pain is either caused by brain or spinal cord injury, nerve lesion, diabetic neuropathy, amputation and neuromuscular disorders. In animal models chronic neuropathic pain simulating some of the clinical symptoms can be introduced by constriction, ligation or transection of sensory and/or motor spinal nerves. Rats develop neuropathic pain slowly and hypersensitivity could be seen up to 2 to 4 weeks after nerve injury. In a rat model of L-4 and L-5 nerve ligation, our laboratory was the first to show that breakdown of the BSCB to albumin and activation of astrocytes occur progressively over 2 to 10 weeks that were most prominent in the ipsilateral side of the cord. Hypersensitivity to pain though lessened after 4 weeks, but neurodegenerative changes progressed over time. This suggests that neuropathic pain could induce remarkable neurodegenerative changes in the spinal cord hindering in development of suitable

therapeutic treatment of neuropathic pain in clinics.

Previous experiments in our laboratory showed that the magnitude and intensity of brain or spinal cord injury are altered by nanoparticles intoxications. However, effects of nanoparticles in modifying neuropathic pain syndrome are still unknown. In present investigation we examined the role of nanoparticles on development of neuropathic pain, BSCB dysfunction, astrocytic reactivity and neural injury after spinal nerve ligation.

Spinal nerve ligation of L-4 & L-5 was performed surgically and rats ware administered Cu, Ag or Al nanoparticles (50 to 60 nm; 50 mg/kg, i.p.) once daily for 10 days. Morphological examination of the cord including albumin immunoreactivity for BSCB dysfunction, GFAP reactivity for astrocytic activation and Nissl staining for neural injuries were examined after 2, 4, 8 and 10 weeks after nerve ligation. Nanoparticles treated rats exhibited prolonged hypersensitivity to external stimulation (fur touching) up to 8 weeks. Leakage of albumin and activation of astrocytes in the spinal cord segments T10, T12 and L5 were exacerbated by 120 % at 4 weeks; 250% at 8 weeks and 300 % at 10 weeks after ligation in nanoparticles treated group. This effect was most marked in Cu and Ag treated animals. Neuronal injury closely corresponded to albumin leakage in the spinal cord. Cerebrolysin in high doses (5 ml/kg) if co-administered with nanoparticles daily was sable to reduce morphological changes in the cord effectively. However, cerebrolysin given after 4 to 6 days of nanoparticles administration failed to induce sufficient neuroprotection. The drug also reduced hyperalgesia if given as pretreatment. These observational are the first to show that

(i) nanoparticles potentiate duration of hyperalgesia of neuropathic pain and exacerbate disturbances in spinal cord microfluid environment and

(ii) Cerebrolysin in high doses is able to thwart these changes indicating a potential role of the drug in pain management.

POSSIBLE INVOLVEMENT OF UBIQUITIN PROTEASOME SYSTEM IN ACUTE AND DELAYED ASPECTS OF ISCHEMIC PRECONDITIONING OF BRAIN IN MICE

T.G. Singh, A.K. Rerhni

Department of Pharmacology, Chitkara College of Pharmacy, Chitkara University, Rajpura, India

Objectives: The present study has been designed to investigate the potential role of ubiquitin proteasome system and other proteases in acute as well as delayed aspects of ischemic preconditioning induced reversal of ischemia-reperfusion injury in mouse brain.

Methods: Bilateral carotid artery occlusion of 17 min followed by reperfusion for 24 h was employed in present study to produce ischemia and reperfusion induced cerebral injury in mice. Cerebral infarct size was measured using triphenyltetrazolium chloride staining. Memory was evaluated using elevated plus-maze test. Rota rod test was employed to assess motor incoordination.

Results: Bilateral carotid artery occlusion followed by reperfusion produced cerebral infarction and impaired memory and motor co-ordination. Three preceding episodes of bilateral carotid artery occlusion for 1 min and reperfusion of 1 min (ischemic preconditioning) both immediately before (for acute preconditioning) and 24 h before (for delayed preconditioning) global cerebral ischemia prevented markedly ischemia-reperfusion-induced cerebral injury as measured in terms of infarct size, loss of memory and motor coordination.

Conclusions: Z-Leu-Leu-Phe-Chinese hamster ovary (CHO) (2 mg/kg, intraperitoneally (i.p.)), an inhibitor of ubiquitin proteasome system and other proteases attenuated the neuroprotective effect of both the acute as well as delayed ischemic preconditioning. It is concluded that the neuroprotective effect of both the acute as well as delayed phases of ischemic preconditioning may be due to the activation of ubiquitin proteasome system and other proteases.

NITROZINE STRESS AND NEUROLOGICAL DISORDERS IN EXPERIMENTAL ALCOHOL INTOXICATION AND THEIR PHARMACOLOGICAL CORRECTION BY NEUROPEPTIDES

E.P. Sokolik

Department of Pharmacology, Zaporozhye State Medical University, Zaporozhye, Ukraine

The article aims to provide a comparative estimation of Cerebrocurin®, Cortexin® and Cerebrolisin® neuroprotective effect on the outcome of experimental chronic alcoholism in rats. 50 Wistar rats were subjected to transient, experimental chronic alcoholism and were randomly assigned to 5 groups (n=10 each):

(1) Intact,

(2) Control,

(3) Cerebricurin®,

(4) Cortexin®,

(5) Cerebrolisin®.

Investigated preparations were administered during 14 days parenteraly after 30-days of violent alcoholization. Functional deficits were quantified by daily neurological examinations (Garcia et al., 1995); rats' behavior was quantified in the test of Passive Avoidance Conditioned Response (PACR). Nitrotirosine values were measured after treatment. Against the background of chronic alcohol intoxication in rats, we have elevated indicators, nitrozile proteins in plasma and brain reflecting the activation processes of nitrozine stress in each groups. We have conducted correlation between the level of nitrotirozine in rat brain and the manifestations of neurological deficit in scores on McGrow in the control group at the end of the experiment. The most active drug was Cerebrocurin®, which demonstrated a significant reduction of nitrotirozine in plasma and especially in the brain of the rats relative vs vehicle-treated controls and normalized neurological status. This is an experimental justification for inclusion of Cerebrocurin® in the traditional model of treatment of chronic alcoholism.

THE IMPACT OF NEUROTROPHIC CEREBROPROTECTION ON THE EXPRESSION OF HSP70 IN THE BRAIN OF RATS WITH PRENATAL CHRONIC ALCOHOLISM

A. Egorov, I. Belenichev, **E.P. Sokolik**

Zaporizhzhya State Medical University, Zaporizhzhya, Ukraine

Epidemiological studies of the last years show that fetal alcohol syndrome (FAS) is found with the frequency of 1-3 per 1,000 births, citing the lack of diagnosis of this syndrome. FAS includes specific morphological cranio-facial changes, pre - and postnatal slower growth, malformations of the internal organs and skeleton, mental disability. The aim of the research is the study of the influence of neurotrophic cerebroprotector (Cerebrocurin) on the expression of heat shock protein HSP70 in the hippocampus and cortex of rats with prenatal chronic alcoholism. The experiments were performed on females white rats weighing 150-180 g. The control rats (n=20) from 5-th to 20-th day of pregnancy received 20% ethanol in a dose of 8 g/kg/day, the intact rats (n=20) received isocaloric sugar solution. Seed of chronic alcoholism rats were introducted Cerebrocurin (0.05 ml/kg) and Piracetam (125 mg/kg) intraperitoneal immediately after the birth for a period of 25 days, the control group received saline solution. In each group were 20 newborns. To identify the expression of HSP70 in the cortex and hippocampus used a method of immunoblotting. Prenatal alcoholism leads to a significant reduction HSP70 in CA-1 area of the hippocampus, sensor and motor area of the cortex of the brain in comparison with the intact group on the first day of life. Depression this indicator remained on the 25 day of observation. The appointment in the period of pregnancy Pyracetam on the backdrop of the admission of alcohol has not exerted any influence on the expression of HSP70 in the brain of the rats. Course introduction of Cerebrocurin in the period of pregnancy had led to a significant increase of HSP70 in the hippocampus and cortex newborns exposed to prenatal action of ethanol, compared with the control group of animals on the 25th day of life.

TREATMENT WITH SELECTIVE GPER1/GPR30 AGONIST G1 REVEALS AGE-STRATIFIED NEUROPROTECTIVE EFFECTS IN MICE AFTER CARDIAC ARREST

K. Shimizu[1], J.L. Exo[2], N. Quillinan[1], R. Vest[1], P.S. Herson[1,3], **R.J. Traystman**[1,3]

[1]Anesthesiology, [2]Pediatrics, [3]Pharmacology, University of Colorado School of Medicine, Anschutz Medical Campus, Aurora, CO, USA

Objectives: Estrogen treatment exerts neuroprotective effects in models of focal and global cerebral ischemia by signaling through several receptors, including the non-classical estrogen receptor GPER1/GPR30[1,2]. Treatment with selective GPER1/GPR30 agonist G1 reduces neuronal injury after global cerebral ischemia[3]. We developed a novel mouse model of pediatric cardiac arrest/cardiopulmonary resuscitation (CA/CPR) to investigate the age-specific response of the developing brain to ischemia. We used our established adult and new juvenile model to investigate the neuroprotective effects of G1 treatment administered at a clinically relevant time point after CA/CPR.

Methods: Adult (12 weeks old, 20-25g) and juvenile (postnatal day 20-25, 10-15g) mice were subjected to CA induced by potassium chloride injection. The duration of arrest was 8 min and 6 min, respectively, and was followed by resuscitation with mechanical ventilation, epinephrine, and chest compressions. 30 min after return of spontaneous circulation, mice were treated with a single intravenous dose of G1 (1 mg/kg) or vehicle. CA1 hippocampal injury was assessed 3 days after CA/CPR. Neuronal ischemic damage was calculated as %ischemic/total neurons. Hippocampal expression of GPER1/GPR30 was compared between sex and age groups using quantitative real-time polymerase chain reaction (RT-PCR).

Results: Adult mice treated with G1 demonstrated significantly less CA1 hippocampal ischemic injury vs. vehicle-treated mice (male mice 20±3% (mean±SEM) (n=9) in G1 vs. 43±7% (n=10, $p< 0.05$) in vehicle; female mice 21±2% (n=12) in G1 vs. 43±5% (n=12, $p< 0.05$) in vehicle treatment). G1 treatment did not reduce CA1 hippocampal ischemic injury in juvenile mice of either sex (male mice 72±3% (n=14) in G1 vs. 74±3% (n=10, $p< 0.05$) in vehicle; female mice 63±7% (n=8) in G1 vs. 68±6% (n=13, $p< 0.05$) in vehicle). GPER1/GPR30 mRNA expression was normalized to adult males, and was similar between adult male (1.00±0.08) and female mice (1.15±0.40) (n=5 per group, $p>0.05$). GPER1/GPR30 expression in juvenile mice was similar to adults, with juvenile male expression levels of 0.75±0.10 and female levels of 0.75±0.11 (n=5 per group, $p>0.05$).

Conclusions: Our data indicate that a single dose of GPER1/GPR30 agonist G1 administered after CA is neuroprotective in adult but not juvenile mice. We also found that hippocampal expression of GPER1/GPR30 did not differ significantly between age groups, suggesting that fundamentally different injury pathways are engaged after CA in juvenile vs. adult mice. Our findings point to the importance of considering developmental stage when evaluating neuroprotective therapies after CA, and underscore the need for robust models of cerebral ischemic injury in this age group.

HYDROGEN SULFIDE ATTENUATES HOMOCYSTEINE INDUCED NEURODEGENERATION IN MICE

N. Tyagi, P.K. Kamat, A. Kalani

University of Louisville, Louisville, KY, USA

Homocysteine (Hcy) is an intermediary amino acid formed during the conversion of methionine to cysteine and its elevated levels, termed as Hyperhomocysteinemia (HHcy), is suggested as a risk factor for most of the neurodegenerative diseases. Brain tissue contains a large number of endogenous hydrogen sulfide (H_2S) which is mainly produced by cystathionine-β-synthase (CBS). The emerging role of H_2S as a new neuromodulator is very promising that could improve physiological and pathological functions of the brain. However, the effect of H_2S has not been explored in Hcy induced neurodegeneration in mice. Therefore, the present study was designed to explore the neuroprotective role of H_2S in neurodegeneration induced with Hcy. To test this hypothesis we employed WT, WT+ Hcy (5µmol) intra-cerebral (i.c., once prior to H_2S treatment), WT+Hcy (5µmol, i.c., once prior to H_2S treatment) +H_2S (30µmol) intra-peritoneally (i.p) 1 injection per-day for one week. Memory was assessed by novel object

recognition test. Oxidative-nitrosative stress, tight junction proteins, neuroinflammation, CBS, cystathionine gamma lyase (CSE, enzyme responsible for conversion of Hcy to H_2S) and neurodegenerative markers were ascertained using Western Blot and RT-PCR methods. Vascular permeability was ascertained along with blood brain vasculature using barium angiogram and in-vital microscopy. Neuronal loss in different groups was measured by Immuno-staining. Hcy administration induced oxidative-nitrosative stress along with neuroinflammation in Hcy treated mice brain. Significant neuronal loss, increased cerebro-vascular permeability, and decreased blood vasculature were determined in Hcy administrated group. Interestingly, administration of H_2S for 7 days significantly improved oxidative-nitrosative stress, neuroinflammation, permeability and angiogenesis in Hcy treated groups. Therefore, the present study concluded that H_2S should be encouraged as a novel therapeutic agent in neurodegenerative diseases such as stroke and Alzheimer's.

This work was supported by NIH grants: HL-107640 to NT

GINSENOSIDE RD ENHANCES AB-IMPAIRED NEUROGENESIS OF SUBVENTRICULAR ZONE THROUGH VEGF INVOLVEMENT

B. Wang

Department of Neurology, Xijing Hospital, Fourth Military Medical University, Xi'an, China

Alzheimer´s disease(AD) is characterized by increased beta-amyloid (Aβ) peptides deposition and aberrant neurogenesis. Vascular endothelial growth factor (VEGF) stimulates the proliferation of neuronal precursors. In this study we examined the protective effects of ginsenoside Rd (Rd) in an Aβ-infusion rat model. Rats administered with Rd or vehicle were subjected to intracerebroventricular injection of Aβ1-40. Aβinjection altered the expression of markers of neurogenesis (Ki67 and doublecortin) and VEGF in the subventricular zone（SVZ）. As compared to control, Aβinjection significantly increased Ki67 and decreased doublecortin immunoreactivity. Compared with the Aβinjection group, Rd pretreatment significantly attenuated the increase in Ki67 and the decreased doublecortin immunoreactivities. Rd significantly increased the level of VEGF in SVZ.We also measured the apoptosis cells by tunnel kit. The number of tunnel positive cells in Rd pretreatment rats is less than that in vehicle pretreatment rats. These results suggested that GSRd may be neuroprotective in Aβ-infusion rat , which involved VEGF up regulation and anti-apoptosis.

NEUROPROTECTIVE EFFECT OF HYPERBARIC OXYGEN PRECONDITIONED AGAINST CEREBRAL ISCHEMIC INJURY IN RAT: INVOLVEMENT OF NOTH1 AND HOMER1A

K. Wang, Z. Fei

Xijing Hospital, The Fourth Military Medical University, Xi'an, China

Objective: To investigate the expressions of notch-1 and holmer1a protein in ischemic penumbra after cerebral ischemia /reperfusion on mice preconditioned with hyperbaric oxygen.

Method: Sixty male LACA mice (20-25g) were randomly divided into hyperbaric oxygen pretreatment group (HBOP-group A group), non-HBOP group (B group) and control group (C group), 20 mice in each group. The mice of group A pretreated with 5 consecutive HBOP (A group: 2.5 absolute atmospheric pressure, 100% O_2, 1h, 1 times / d), The mice of group B were treated with 5 consecutive non-HBOP (hyperbaric oxygen chamber, an absolute atmospheric pressure, air, each time 1 h, 1 times / d,). The mice of group C were normally feed. 24 hours after the last pretreatment, every 15 mice from each group were subjected to ischemia through making MCAO models for 2 hours and then reperfusion. 24 hours after the reperfusion. Every 15 mice were sacrificed and detected with notch-1 and homer-1a proteins by western-blot. The rest of every 5 mice were subjected to Morris water maze test after 5 days of feed detecting its cognitive function.

Results: Compared those mice in the non-HBOP pretreatment group and control group, the expression of notch-1 and holmer1a protein were higher (lower) in the HBO group ($P< 0.05$). The test of Morris water maze in the HBOP group is better than the others. The rest of two groups have no differences in the test of Morris water maze.

Conclusion: The expression of notch-1 and

holmer1a protein were higher (lower) in the HBOP group than the non-HBOP group and control group .The hyperbaric oxygen therapy could promote the ability of mice in the ischemic-reperfusion.

SIMVASTATIN INDUCES NEUROPROTECTION IN 6-OHDA LESIONED PC12 VIA THE PI3K/AKT/CASPASE 3 PATHWAY AND ANTI-INFLAMMATORY RESPONSES

H. Gao, Y. Xu, L. Long, Q. Wang

Neurology Department, The Third Affiliated Hospital of Sun Yat-Sen University, Guangzhou, China

Background: In addition to their original applications for lowering cholesterol, statins display multiple neuroprotective effects. Inflammatory reactions and the PI3K/AKT/caspase 3 pathway are strongly implicated in dopaminergic neuronal death in Parkinson's disease (PD). This study aims to investigate how simvastatin affects 6-hydroxydopamine-lesioned PC12 via regulating PI3K/AKT/caspase 3 and modulating inflammatory mediators.

Methods: 6-hydroxydopamine-treated PC12 **cells** were used to investigate the neuroprotection of simvastatin, its association with the PI3K/AKT/caspase 3 pathway, and anti-inflammatory responses. Dopamine transporters (DAT) and tyrosine hydroxylase (TH) were examined in 6-hydroxydopamine-treated PC12 after simvastatin treatment.

Results: Simvastatin-mediated neuroprotection was associated with a robust reduction in the upregulation induced by 6-OHDA of inflammatory mediators including IL-6, COX2, and **TNF-α**. The downregulated DAT and TH levels in **6-OHDA-lesioned PC12** were restored after simvastatin treatment. Simvastatin reversed 6-OHDA-induced downregulation of PI3K/Akt phosphorylation and attenuated 6-OHDA-induced upregulation of caspase 3 in PC12. Furthermore, the PI3K inhibitor LY294002 pronouncedly abolished the simvastatin-mediated attenuation in caspase 3.

Conclusions and Significance: Our results demonstrate that simvastatin provides robust neuroprotection against dopaminergic neurodegeneration, partially via anti-inflammatory mechanisms and the PI3K/Akt/caspase3 pathway. These findings contribute to a better understanding of the critical roles of simvastatin in treating PD and might elucidate the molecular mechanisms of simvastatin effects in PD.

NEUROGLOBIN INHIBITS OXYGEN-GLUCOSE DEPRIVATION-INDUCED MITOCHONDRIAL PERMEABILITY TRANSITION PORE OPENING IN PRIMARY CULTURED MOUSE CORTICAL NEURONS

Z. Yu, N. Liu, **X. Wang**

Departments of Neurology and Radiology, Massachusetts General Hospital and Harvard Medical School, Charlestown, MA, USA

Background: Accumulating evidences from our laboratory and others have demonstrated that neuroglobin (Ngb) is protective against hypoxic/ischemic brain injury, thus targeting Ngb may be a novel approach for endogenous neuroprotection, but the molecular mechanisms remain undefined. Mitochondrial permeability transition pore (mPTP) opening is a key mitochondrial response to hypoxia/ischemia, followed by release of mitochondrial factors such as Cyt c and activation of Caspase-dependent apoptosis pathways. In this study, we test our hypothesis that Ngb inhibits OGD-induced mPTP opening in primary neurons.

Method: Primary mouse cortical neurons were transduced with AAV-Ngb to achieve Ngb over-expression and Ngb-shRNA to achieve Ngb knockdown. At day 9 of culture, primary neurons were subjected to 4 hr OGD followed by reoxygenation. Neurotoxicity was measured after 20 hr reoxygenation by LDH release assay. mPTP opening was measured at 4 hr after reoxygenation by testing mitochondria swelling, NAD release and Cyt c release. NAD release was also measured using isolated mitochondria treated with OGD after incubation with recombinant Ngb protein.

Results:

(1) Four hour OGD followed by 20 hr reoxygenation caused 40±4.5% neuron death; Ngb overexpression significantly reduced the death rate to 18±5.2% ($n=5$, $p< 0.05$).

(2) Ngb-overexpression significantly reduced OGD-induced mitochondria swelling, and rescued OGD-induced mitochondrial NAD release (mitochondrial NAD content 4±0.56

nmol/mg protein under normoxia, 2.1±0.35 nmol/mg protein after OGD, 3.4±0.46 nmol/mg protein in Ngb-overexpressing group after OGD) (n=4, p< 0.05).

(3) Ngb-overexpression significantly reduced OGD-induced Cyt c release from mitochondria to 0.43±0.08 fold (n=3, p< 0.05).

(4) Incubation with recombinant Ngb protein significantly reduced OGD-induced mitochondria NAD release in isolated mitochondria (mitochondrial NAD content 3.5±0.46 nmol/mg protein under normoxia, 1.8±0.32 nmol/mg protein after OGD, 3.0±0.45 nmol/mg protein in rNgb-incubating group after OGD) (n=4, p< 0.05).

(5) Ngb knockdown significantly increased OGD-induced neuron death from 40±4.5% to 56.4± 7.2%, and worsened OGD-induced mitochondria NAD release, but these changes were rescued by pretreatment of CsA, an mPTP inhibitor (n=3, p< 0.05).

(6) Co-IP detected protein interaction between Ngb and VDAC, an mPTP component, and the interaction was increased after OGD.

Conclusions: Ngb expression level is negatively correlated with OGD-induced mPTP opening, indicating an inhibitory effect of Ngb. The detected interaction between Ngb and mPTP component VDAC, and their increased protein binding in response to OGD, suggest that Ngb-VADC interaction might be the underlying molecular mechanism for the Ngb´s inhibitory effects in OGD-induced mPTP opening.

THE NEUROPROTECTION OF AEROBIC EXERCISE ON THE HSP70 EXPRESSION IN BRAIN OF CUMS RATS EXPOSED TO NOVEL ACUTE STRESS

L. Xin

Department of Medical Psychology, Taishan Medical University, Taian, China

Objective: The chronic, mild and unpredictable stress that human may met daily has got more and more attention on its underlying damage of the brain, especially on the injury of neuron. For coping with daily stress, aerobic exercise may be considered as an easy and useful method for individual to improve one's mood, cognition and self-concept. Though there still exist some controversies on its underlying neurobiological mechanism in central, this research tried to investigate whether aerobic exercise could play a beneficial role in neuroprotection.

Method: Fifty adult male Wistar rats were enrolled and randomly divided into five groups: the control group 1, the control group 2, the exercise model group, the CUMS model group, and the exercise group, with ten rats in each group. The rats of the latter two groups were received 21 days of chronic unpredictable mild stress (CUMS). After the period of CUMS model built, to test the stress resistance of rats, the rats in the latter four groups were given inescapable footshock as the novel acute stress. The behavioral changes were measured by open field test and Morris water maze test. Radioimmunoassay (RIA) was adopted to test the change of serum corticosterone (CORT) and interleukin-1β (IL-1β). The liver and spleen index were also calculated by the weighing method. An important protecting protein in stress, heat shock protein 70 (HSP70), was analyzed by immunohistochemistry in different brain areas such as hippocampus, prefrontal cortex and hypothalamus.

Results : These results demonstrated that aerobic exercise could improve the behavior expressions and cognitive function. These beneficial effects may be correlated with its protection of maintaining the HPA axis function stable, especially when animals exposed to inescapable footshock. And the high HSP70 expressions may play a key role in some critical brain areas of stress as mentioned.

Conclusion: This research showed that the stress resistance of CUMS animals had been improved by aerobic exercise when exposed to novel acute stress. And its underlying mechanism is partly attributed to the neuroprotection of HSP70 in some hippocampus, prefrontal cortex and hypothalamus.

References:

1. Swimming exercise effects on the expression of HSP70 and iNOS in hippocampus and prefrontal cortex in combined stress [J]. Neuroscience Letters. 2010, 476 (2):99-103.

2. Effects of different adrenergic blockades on the stress resistance of Wistar rats [J]. Neuroscience Letters. 2012, 511(2):95-100.

3. K.P. Brooks, T.F. Robles, Recent depressive and anxious symptoms predict cortisol responses to stress in men, Psychoneuroendocrinology 34 (2009)1041-1049.

CEREBROLYSIN, A NEUROPEPTIDE PREPARATION MIMICKING THE ACTION OF NEUROTROPHIC FACTORS, IMPROVES FUNCTIONAL RECOVERY AFTER EXPERIMENTAL TRAUMATIC BRAIN INJURY

Y. Xiong[1], Z.G. Zhang[2], Y. Zhang[1], Y. Meng[1], E. Doppler[3], A. Mahmood[1], M. Chopp[2,4]

[1]Neurosurgery, [2]Neurology, Henry Ford Health System, Detroit, MI, USA, [3]Clinical Research and Pharmacology, EVER Neuro Pharma GmbH, Oberburgau, Austria, [4]Physics, Oakland University, Rochester, MI, USA

Objectives: Traumatic brain injury (TBI) is a leading cause of death and disability worldwide for which there is no effective treatment. Cerebrolysin is a peptide preparation which mimics the action of neurotrophic factors and is widely used in the treatment of stroke, dementia and TBI. In an effort to elicit insight into its mechanism of action, we investigated the effect of Cerebrolysin on neurological function after TBI.

Methods: Adult male Wistar rats (n=60) were subjected to moderate closed head injury (CHI) induced by using the Marmarou impact-acceleration injury model. CHI rats received intraperitoneal (ip) injection of saline (n=30) or Cerebrolysin (2.5 ml/kg, EVER Neuro Pharma, Austria, n=30) starting 1 hour post injury and administered once daily until sacrifice (2 or 14 days after CHI). To evaluate functional outcome, the modified neurological severity score (mNSS), footfault, adhesive removal, and Morris water maze (MWM) tests were performed. Forty of 60 animals were sacrificed at 2 days post injury for evaluating cerebral microvascular patency by fluorescein isothiocyanate (FITC)-dextran perfusion (n=16), or for measuring expression of vascular endothelial growth factor (VEGF), and matrix metalloproteinase-9 (MMP9) by using real-time reverse transcriptase-polymerase chain reaction (RT-PCR, n=8) and by immunohistochemistry (n=16). The remaining rats (n=20) were sacrificed at 14 days after injury and their brains removed and processed for measurement of neuronal cells, axonal damage, apoptosis and neuroblasts.

Results: At 2 days post CHI, the Cerebrolysin group exhibited a significantly higher percentage of phosphorylated neurofilament H (pNF-H)-positive staining area in the striatum ($p< 0.05$), a significant increase in percentage of FITC-dextran- perfused vessels in the brain cortex ($p< 0.05$), a significant increase in VEGF-positive cells ($p< 0.05$) and a significant reduction of MMP9-staining area ($p< 0.05$) compared to the saline-treated group. There is no significant difference in mRNA levels of MMP9 and VEGF in the hippocampus and cortex at 48 hours post injury between Cerebrolysin- and saline-treated CHI rats. At 14 days post CHI, the Cerebrolysin treatment group exhibited significant improvements in functional outcomes (adhesive-removal, mNSS, the footfault, and MWM tests) and significantly more neurons and neuroblasts were present in the dentate gyrus ($p< 0.05$), compared to the saline-treated group ($p< 0.05$).

Conclusions: Acute Cerebrolysin treatment improves functional recovery in rats after CHI. Cerebrolysin is neuroprotective for CHI (increased neurons in the dentate gyrus and the CA3 regions of the hippocampus as well as increased neuroblasts in the dentate gyrus) and may preserve axonal integrity in the striatum (significantly increased % of pNF-H-positive tissue in the striatum). Reduction of MMP9 and elevation of VEGF likely contribute to enhancement of vascular patency and integrity as well as neuronal survival and neuroblast generation induced by Cerebrolysin. These promising results suggest that Cerebrolysin may be a useful treatment to improve the recovery of patients with CHI.

EFFECTS OF ALOGLIPTIN ON THE MTEABOLISM OF NITRIC OXIDE (NO) AND HYDROXY RADICALS IN BRAIN DURING BRAIN ISCHEMIA-REPERFUSION

M. Yamazato[1], Y. Ito[2], R. Nishioka[2], M. Hirayama[2], N. Araki[2]

[1]Department of Neurology, Saitama Medical School, Medical Center, [2]Department of Neurology, Faculty of Medicine, Saitama Medical University, Saitama, Japan

Purpose: The metabolism of nitric oxide (NO) and hydroxy radicals in the brain of C57BL during brain ischemia-reperfusion is

investigated under treatment with Alogliptin, an innovative drug and one of the DPP4 inhibitors for controlling incretin levels in blood sugar metabolism.

Methods: C57BL treated with Alogliptin 45mg/kg/day (n=5) for 4 weeks and and the control group (n=8) were used.

Both NO production and hydroxyl radical metabolism were continuously monitored by *in vivo* microdialysis. Microdialysis probes were inserted into the bilateral striatum. A Laser Doppler probe was placed on the skull surface. Blood pressure, blood gases and temperature were monitored and maintained within normal ranges throughout the procedure. Forebrain cerebral ischemia was produced by occlusion of both common carotid arteries for 10 minutes. Levels of nitric oxide metabolites, nitrite (NO_2^-) and nitrate (NO_3^-), in the dialysate were determined using the Griess reaction. Right side is for 2,3-dihydroxybenzoic acid (2,3-DHBA) and 2,5-dihydroxybenzoic acid (2,5-DHBA). Samples were measured by the salicylic rate trapping method.

Results:

(1) Blood Pressure(Figure1):Alogliptin group (73.2±10.6mmHg; mean±SD) showed significantly lower than those of the control group (88.3±7.35) 20 minutes after the start of reperfusion ($p< 0.05$).

(2) Cerebral Blood Flow (CBF): There were no significant differences between the groups.

(3) Nitric oxide metabolites:

1) NO_2^- ; Alogliptin group (0.86±0.27, 0.73±0.24, 0.73±0.11 mol/L) showed significantly lower level than that of the control group (1.17±0.13, 0.99±0.20, 1.08±0.21) pre-ischemia, ischemia and 50 minutes after the start of reperfusion ($p< 0.05$) (Figure 1).

2) NO_3^- ; There were no significant differences between the groups.

(4) Hydroxyl radical; Alogliptin group (96.3±3.3, 87.6±9.0, 84.8±7.2, 84.3±7.2 %) showed significantly lower level than that of the control group (100±1.1, 98.7±2.6, 98.8±3.4, 98.2±4.6) ischemia and 80- 120 minutes after the start of reperfusion ($p< 0.05$) (Figure 2).

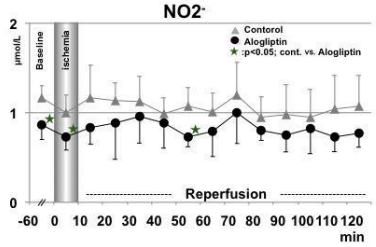

[Figure1]

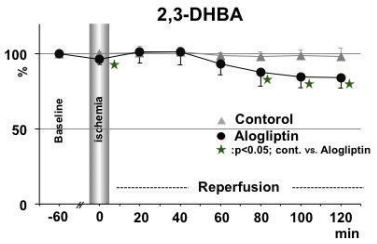

[Figure2]

Conclusion: It has been suggested that Alogliptin can affect the nitric oxide metabolism and hydroxy radical metabolism in the brain after cerebral ischemia-reperfusion in the C57BL mice.

INTRACEREBRAL ADMINISTRATION OF ULTRASOUND-INDUCED DISSOLUTION OF LIPID-COATED GDNF MICROBUBBLES PROVIDES NEUROPRETECTION IN A RAT MODEL OF PARKINSON'S DISEASE

X. Yang[1], G. Cui[1], X. Wang[2], X. Shen[1]

[1]Department of Neurology, [2]Department of Ultrasound, Xuzhou Medical College, Xuzhou, China

Parkinson's disease is a neurodegenerable disease characterized by loss of dopaminerigc neurons in the substantia nigra. Neurotrophic factor such as glial cell derived neurotrophic factor (GDNF) has been shown to provide a neuroprotective effect in PD rats. We have previously reported that ultrosound-induced lipid-coated GDNF microspheres, which release GDNF in a sustained manner after low frequency ultrasound stimulation, can reduce

hypoxic-ischemic injury in neonatal rats. In the present study, we investigated that whether lipid-coated GDNF microspheres can provide a neuroprotective effect in a rat model of PD. After a rat model of PD was produced by 6-hydroxydompamine (6-OHDA) injections. Lipid-coated GDNF microspheres (0.5 mg/kg) were injected into the striatum of PD rats. We found that GDNF levels were increased in the striatum of PD rats after lipid-coated GDNF microspheres administration following low frequency ultrasound stimulation (20 kHz, daily for 4 weeks and each day lasted for 5 min). GDNF microspheres reduced apomorphine-induced rotations. Moreover, GDNF microspheres increased dopamine and TH levels in the striatum of PD rats. Additionally, GDNF microspheres reduced caspase-3, tumor necrosis factor-alpha, MMP-9 and OX-6 levels induced by 6-OHDA injections in PD rats. These data indicated that lipid-coated GDNF microspheres can provide a neuroprotective effect in PD rats.

HSP70 OVEREXPRESSION REDUCES HEMORRHAGE AND IMPROVES BEHAVIOR THROUGH THE REGULATION OF EXPRESSION AND ACTIVATION OF MMPS FOLLOWING TRAUMATIC BRAIN INJURY

J.Y. Kim[1], N. Kim[2], **M.A. Yenari**[2]

[1]Endocirne Research Unit and Neurology, University of California, San Francisco and the San Francisco Veterans Affairs Medical Center, [2]Neurology, University of California and the San Francisco Veterans Affairs Medical Center, San Francisco, CA, USA

Objective: Traumatic brain injury (TBI) causes disruption of the blood brain barrier (BBB) leading to hemorrhage which can complicate an already catastrophic illness. Matrix metalloproteinases (MMPs) have been implicated in the breakdown of the extracellular matrix and BBB leading to brain hemorrhage. Heat shock protein 70 kD (Hsp70) is upregulated by various insults, and whether it inhibit other brain injury model including the expression and activation of MMPs. Whether this function protects against TBI has not yet been demonstrated.

Methods: The left cortex of wildtype (Wt), Hsp70 KO and Tg mice were subjected to TBI using controlled cortical impact (CCI) model (AP: -2.5mm, ML: 2.0mm and depth of 2mm). We evaluated with motor function for 7 d later, and brain hemorrhage and lesion size at 3 and 14 days. Brains were harvested to evaluate the effects of MMPs on immunohistochemistry, western blot and zymography assay at 3 days.

Results: In Hsp70 KO mice, CCI led to larger brain lesions (38.9±5.1%) and hemorrhage (68.5±5.1%) along with increased MMPs expression and activation adjacent to the lesion compared to wildtype mice. CCI also increased right-biased swings and corner turns (n=6, p< 5.01) in the Hsp70 KO mice. Overexpression Hsp70 significantly decreased the expression and activation of MMPs and the size of cortical lesion (24.4±5.1%) and hemorrhage (37.3 ±5.1%) and improved behavioral outcomes indicated by reduced frequency of right-biased swings and corner turns (n=6, p< 0.01) in the Hsp70 Tg mice.

Condclusion: To our knowledge, this is the first direct demonstration of brain protection by Hsp70 expression in a TBI model. Our data establish a novel mechanism that causes TBI-induced neuronal injury and support the development of strategies for the treatment of TBI.

References:

Yenari MA, Fink SL, Sun GH et al. Gene therapy with HSP72 is neuroprotective in rat models of stroke and epilepsy. Ann Neurol. 1998;44:584-591

Lee JE, Yoon YJ, Moseley ME, Yenari MA. Reduction in levels of matrix metalloproteinases and increased expression of tissue inhibitor of metalloproteinase-2 in response to mild hypothermia therapy in experimental stroke. J Neurosurg. 2005;103:289-297

Zheng Z, Kim JY, Ma H et al. Anti-inflammatory effects of the 70 kDa heat shock protein in experimental stroke. J Cereb Blood Flow Metab. 2008;28:53-63

HSP70 INDUCTION BY 17-AAG AS A POTENTIAL THERAPEUTIC FOR TRAUMATIC BRAIN INJURY

N. Kim, J.Y. Kim, E. Kim, **M.A. Yenari**

Neurology, University of California San Francisco (UCSF) and San Francisco VA Medical Center (SF VAMC), San Francisco, CA, USA

Introduction: The 70kDa heat shock protein (Hsp70) is known to protect the brain from injury through multiple mechanisms. Because of its toxicity, Hsp70-inducer geldanamycin lacks translational value. As of this study, no safe pharmacological Hsp70-inducers have been tested in brain injury.

Objective: We explored the efficacy of safe geldanamycin analog 17-AAG as a potential therapy for traumatic brain injury (TBI).

Materials and methods: 3-month-old male C57B6 mice were studied. Naïve animals were given 17-N-allylamino-17-demethoxygeldanamycin (17-AAG) intraperitoneally (IP, 2 mg/kg) or intracerebroventricularly (ICV, 1 ug/kg) to determine whether Hsp70 could be induced in the brain. Immunofluorescent staining and Western blots with anti-Hsp70 were performed from brain tissue to confirm and examine extent of pharmacological induction. Another group of mice were subjected to TBI via cortical controlled impact, and were treated with 17-AAG or vehicle by IP injection according to one of two treatment regimens: (1) 2 mg/kg at the time of injury, (2) a total of three doses (4 mg/kg) at 2 and1d prior to TBI and again at the time of injury. Brains were assessed for hemorrhage volume at 3d and lesion cavity size at 14d post-injury. The swing test and corner test were performed at 3d and 7d to assess motor function recovery.

Results: Both IP and ICV administration of 17-AAG induced HSP70 expression primarily in microglia and in a few neurons by 24h but not in astrocytes. 17-AAG induced Hsp70 in injured brain tissue as early as 6h, peaking at 48h and largely subsiding by 72h after IP injection. Both treatment groups showed decreased hemorrhage volume relative to untreated mice ($p< 0.1$) as well as improved neurobehavioral outcomes in swing test at 3d ($p=0.05$). There was a trend towards reduced lesion size with treatment as well.

Conclusions: 17-AAG-treatment improved neurobehavioral deficits following experimental TBI, and attenuated brain hemorrhage and injury. Further, our research showed that peripheral administration could lead to Hsp70 induction in the brain. These observations indicate that 17-AAG may prove to be a promising, non-invasive treatment for TBI.

References:

Giffard, RG, *et al.* "Regulation of apoptotic and inflammatory cell signaling in cerebral ischemia: the complex roles of heat shock protein 70." *Anesthesiology.* 109 (2008): 339-48.

Kim, N, *et al.* "Anti-inflammatory properties and pharmacological induction of Hsp70 after brain injury." *Inflammopharmacology*. 20 (2012): 177-85.

Wang, G, *et al.* "Protection of murine neural progenitor cells by the Hsp90 inhibitor 17-allylamino-17-demethoxygeldanamycin in the low nanomolar concentration range." *J Neurochem*. 117 (2011): 703-11.

Yenari, MA, *et al*. "Antiapoptotic and anti-inflammatory mechanisms of heat-shock protein protection." *Ann N Y Acad Sci*. 1053 (2005): 74-83. Review.

NEUROPROTECTIVE EFFECTS OF PEROXISOME PROLIFERATOR-ACTIVATED RECEPTOR Γ AGONIST IN TRANSIENT FOREBRAIN ISCHEMIA

H. Yoshioka, T. Wakai, T. Yagi, Y. Fukumoto, K. Hashimoto, T. Horikoshi, H. Kinouchi

Department of Neurosurgery, University of Yamanashi, Chuo, Japan

Background and purpose: Peroxisome proliferator-activated receptor γ (PPARγ) is a nuclear receptor and regulates gene expression in response to ligand binding. Pioglitazone, a PPARγ ligand of the thiazolidinedione class, induces enhancement in insulin-mediated glucose uptake and is used to treat type 2 diabetes. Although pioglitazone exerts pleiotropic effects including neuroprotection [1], its mechanism remains obscure. On the other hand, Akt/glycogen synthase kinase-3β (GSK3β), and signal transducers and activators of transcription 3 (STAT3) are known as surviving factors after cerebral ischemia, and are expected to be regulated by PPARγ[2,3]; however, the effects of pioglitazone on these pathways after cerebral ischemia has not been elucidated. In this study, we investigated neuroprotective efficacy of pioglitazone and its effect on Akt/GSK3β and STAT3 pathways by using a rat model of transient forebrain ischemia.

Material and methods: Male Sprague-Dawley rats were given daily oral administration of vehicle or pioglitazone (0.2, 2, or 20 mg/kg/day) from 5 days before surgery to the

day of decapitation. Transient forebrain ischemia was induced by bilateral common artery occlusion with hypotension. Ischemic neuronal injury was evaluated in the hippocampal CA1 region 5 days after ischemia by Tunnel staining. Samples from the hippocampal CA1 region for western blot analysis and immunohistochemistry were taken 1, 8, 24, 72, or 120 hours after ischemia. Expression of PPARγ after ischemia was investigated by western blot analysis and immunohistochemistry. The effects of pioglitazone on phosphorylation of Akt, GSK3β, and STAT3 were examined by western blot analysis.

Results: Expression of PPARγ in the hippocampal CA1 region was upregulated 1 to 8 hours after ischemia ($n = 4$, $P < 0.05$), which was observed mainly in pyramidal neurons. Administration of pioglitazone reduced TUNEL-positive cells in a dose-dependent manner, with a significant difference in the 20 mg/kg/day group compared with the vehicle group ($n = 6$, $P < 0.05$). Phosphorylation of Akt, GSK3β, and STAT3 was increased after ischemia, and the administration of 20 mg/kg/day dose of pioglitazone significantly increased phosphorylation of these pathways compared to the vehicle ($n = 4$, $P < 0.05$).

Conclusion: Expression of PPARγ is upregurated after transient forebrain ischemia mainly in pyramidal neurons of the hippocampal CA1 region. Administration of PPARγ ligand attenuates neuronal ischemic injury through activation of Akt/GSK3β and STAT3 pathways.

Reference:

1. Dormandy JA, Charbonnel B, Eckland DJA, et al. Secondary prevention of macrovascular events in patients with type 2 diabetes in the PROactive Study (PROspective pioglitAzone Clinical Trial In macroVascular Events): a randomised controlled trial. *Lancet*. 2005;366:1279-1289.

2. Endo H, Nito C, Kamada H, et al. Activation of the Akt/GSK3beta signaling pathway mediates survival of vulnerable hippocampal neurons after transient global cerebral ischemia in rats. *J Cereb Blood Flow Metab*. 2006;26:1479-1489.

3. Yagi T, Yoshioka H, Wakai T, et al. Activation of signal transducers and activators of transcription 3 in the hippocampal CA1 region in a rat model of global cerebral ischemic preconditioning. *Brain Res*. 2011;1422:39-45.

THE EFFECT OF SEVOFLURANE PRECONDITIONING ON PROTEINS WITH CIS-REGULATORY ELEMENT NFKB AGAINST CEREBRAL ISCHEMIA AND REPERFUSION IN RATS

Q. Yu, W. Liang

Department of Anesthesiology, Huashan Hospital, Fudan University, Shanghai, China

Background: In our previous study, we have demonstrated the neuroprotection of sevoflurane preconditioning on blood-brain barrier (BBB) against transient cerebral ischemia and reperfusion (I/R) in rats. This protective effect is achieved partly by suppressing the upregulation of nuclear factor kappa-B (NFkappaB). Cellular adhesion molecules (CAMs) and matrix metalloproteinases (MMPs), proteins with cis-regulatory element NFkappaB, play an important role in secondary post-ischemic neuroinflammation by mediating firm adhesion of leukocytes to inflammatory sites and degrading neurovascular matrix, such as tight-junctions. Therefore, we hypothesize that whether sevoflurane preconditioning provides neuroprotection *via* suppressing the upregulation of CAMs and MMPs against brain I/R.

Methods: Transient focal cerebral I/R was induced by using 60 min of middle cerebral artery occlusion (MCAO) in adult male Sprague-Dawley rats. The animals were exposed for 30min per day on 4 consecutive days to ambient air (sham and vehicle group) or to 1.2% sevoflurane (sevo-pre group), and then subjected to MCAO 24 hours later. Evans blue (EB) extravasation test and biochemical measurements for intracellular adhesion molecule-1 (ICAM-1), vascular cell adhesion molecule-1 (VCAM-1), MMP-2 and MMP-9 were conducted by gelatin zymography, western blot and confocal immunofluorescence 48 hours after I/R. All data was expressed as mean±SEM, and statistic analysis was performed using ANOVA and *post hoc* Fisher's PLSD tests, with $P < 0.05$ considered statistically significant.

Results: Sevoflurane pretreatment markedly improved the integrity of BBB. EB extravasation was lower in sevo-pre group (3.16±0.33 μg/g) than in vehicle group

(7.41±1.19 μg/g, *P*< 0.01, n=6 per group). As determined by western blot analysis (n=4 per group) and immunofluorescence (n=4 per group), ischemia-induced increases of ICAM-1 (582±119% over sham group) and VCAM-1 (758±121% over sham group) were suppressed by sevoflurane pretreatment (ICAM-1, 178±56%, *P*< 0.05; VCAM-1, 98±23%, *P*< 0.01). Upregulated MMP-9 (1589±254% over sham group) and MMP-2 (920±286% over sham group) induced by ischemia were also inhibited in sevo-pre group (MMP-9, 116±31%, *P*< 0.01; MMP-2, 153±50%, *P*< 0.05). The results were confirmed by gelatin zymography (n=4 per group).

Conclusion: Repeated preconditioning with sevoflurane confers beneficial effect on ischemic brain injury. The protective sevoflurane pretreatment may suppress the elevation of proteins with cis-regulatory element NFkappaB, such as ICAM-1, VCAM-1, MMP-2, and MMP-9, *via* blocking NFkappaB mediated inflammatory cascade at the transcriptional level. Therefore, sevoflurane preconditioning is believed to be a potential therapy for ischemic brain injury.

ACUTE AND DELAYED PROTECTIVE EFFECTS OF PHARMACOLOGICALLY INDUCED HYPOTHERMIA IN AN INTRACEREBRAL HEMORRHAGE STROKE MODEL OF MICE

S.P. Yu[1], J. Sun[1,2], J. Li[2], C.L. Hall[3], T.A. Dix[4], L. Wei[1,3]

[1]Department of Anesthesiology, Emory University School of Medicine, Atlanta, GA, USA, [2]Department of Neurology, Beijing Friendship Hospital, Capital University of Medical Sciences, Beijing, China, [3]Department of Neurology, Emory University School of Medicine, [4]Department of Pharmaceutical and Biological Sciences, Medical University of South Carolina, Atlanta, GA, USA

Objectives: Intracerebral hemorrhage (ICH) comprises 10-15% of all strokes. Those suffering from ICH often have abysmal outcomes, with 30-day mortality estimates as high as 44% and survivors typically suffer from lifelong disabilities. Currently, the only FDA approved therapy for acute stroke is tissue plasminogen activators (tPA) which is limited to those with ischemic strokes. To date, there has been no effective drug therapy for the treatment of hemorrhagic stroke.

Mild to moderate hypothermia, or "therapeutic hypothermia" that reduces body temperature by 3-5^{o}C is neuroprotective in both pre-clinical and clinical studies for both ischemic and hemorrhagic stroke subtypes. Clinically, hypothermia has been an approved therapy for patients after cardiac arrest and children with hypoxic-ischemic encephalopathy. A major dilemma that has limited the clinical application of hypothermia stroke patients is the inefficient and often impractical physical cooling methods. We have explored a new concept of "regulated hypothermia" that pharmacologically targets the central thermoreceptors and reduces the set-point in the thermoregulatory center, using our novel neurotensin receptor (NTR) 1 agonists. We refer to this approach as pharmacological hypothermia or pharmacologically induced hypothermia (PIH) and have reported the neuroprotective effect of the novel neurotensin analog ABS-201 against ischemia stroke in mice.

Methods: The present investigation tested the PIH therapy using the second generation of NTR agonist ABS-201 in an adult mouse model of ICH. ICH injury was achieved by the injection of 30 μL of autologous blood into the striatum. Except for the hypothermia group treated at 1 hr after stroke, all animals were kept in an incubator to maintain body temperature at 37±0.5^{o}C for at least 4 hrs after surgery. To avoid postsurgical dehydration, 0.5 mL normal saline was given to each mouse by subcutaneous injection after surgery. Acute and delayed administration of ABS-201 (2 mg/kg bolus injection i.p. followed by 2-3 injections at 1 mg/kg) was initiated at 1 or 24 hrs after ICH, respectively.

Results: ABS-201 effectively induced hypothermia within 30 min and maintained the body and brain temperature at 33.7±0.4°C for at least 6 hrs without causing shivering. With 1 hr delayed treatment, ABS-201-induced hypothermia treatment significantly reduced ICH-induced cell death and brain edema compared to ICH control animals. ABS-201-induced hypothermia initiated 24 hrs after ICH showed significant attenuation of brain edema, cell death and blood brain barrier breakdown. ABS-201 significantly decreased the expression of MMP-9 and caspase-3 and increased the bcl-2 level in the ICH brain. Moreover, mice subjected to ABS-201 treatment showed better functional recovery after ICH.

Conclusion: Our data suggest that the neurotensin analog, ABS-201 is effective in protecting the brain from ICH injury either initiated during the acute phase or with a 1 day delay after the onset of ICH. The neuroprotective effect of PIH is at least in part through the alleviation of apoptosis and neurovascular damage. We suggest that PIH is a promising therapeutic treatment for acute as well as sub-acute ICH.

FOOD RESTRICTION ATTENUATES ISCHEMIC NEURAL INJURY AND FACILITATES FUNCTIONAL RECOVERY IN MICE

J. Zhang[1], S.D. Lu[1], L.L. Mao[1,2], H.J. Pu[1], C.R. An[1], H. Gao[1], W.T. Zhang[1], J. Chen[1,2], Y.Q. Gao[1]

[1]State Key Laboratory of Medical Neurobiology and Institute of Brain Science, Fudan University, Shanghai, China, [2]Center of Cerebrovascular Disease Research, University of Pittsburgh School of Medicine, Pittsburgh, PA, USA

Background: Food restriction and antioxidant supplementation have been proposed as dietary strategies to attenuate age-related diseases. Recent research suggests that food restriction can protect mice against multiple forms of stress, including ischemia-reperfusion injury to the heart. We tested the hypothesis that food restriction attenuates the cerebral ischemic damage resulting from transient middle cerebral artery occlusion (MCAO).

Methods: Adult male C57Bl/6 mice were fed with libitum food (LF) or restricted food (RF; 30% reduction) for 4 weeks prior to 1 hour of MCAO. The concentrations of blood glucose, cholesterol, and triglycerides were tested before, during, or after MCAO. We also examined infarct volume by 2,3,5-triphenyltetrazolium chloride (TTC) staining and assessed cell injury with the Fluoro-Jade C stain. Neurological function was evaluated on days 1, 3, 5, 7, 14, 21 and 28 after ischemia. The expression of sirt3 was assessed using Western blotting.

Results: As expected, food restriction elicited a drop in the concentration of cholesterol and triglycerides (cholesterol: LF, 1.56+0.11 mmol/L; RF, 1.02+0.09 mmol/L; $P < 0.001$; n=10/group; triglycerides: LF, 2.71+0.42mmol/L; RF, 1.84+0.21mmol/L; $P < 0.05$; n=10/group). Blood glucose rose after ischemia in the LF group but failed to increase in the RF group ($P < 0.05$; n≥12/group). RF significantly reduced infarct volume compared with the LF group (RF,16.00+4.02mm3 ; LF, 45.25+7.06mm3; $P < 0.01$; n=8/group). Interestingly, the performance of the RF group in spatial tasks such as the water maze was significantly better than that of ad lib fed mice at 23-27 days after ischemia ($P < 0.05$, n=8/group). These behavioral data were consistent with higher activity levels in the grid-walking test in the RF group ($P < 0.05$, n=11/group). Fluoro-Jade-C staining was reduced in the RF group, suggesting that food restriction prevented ischemic neurodegeneration. Furthermore, ad lib fed mice exhibited marked loss of neurons 28 days after ischemia in the cerebral cortex (n=4/group) and striatum (n=4/group) relative to RF mice. Additionally, food restriction increased the expression of the age-related protein sirt3 after ischemia (LF 1.26+0.11 and RF 1.76+0.26 at 6h after ischemia, $P < 0.05$, n=9; LF 0.88+0.08 and RF 1.17+0.12 at 24h after ischemia, $P < 0.05$, n=10).

Conclusions: These data demonstrate that food restriction can reduce ischemic neurodegeneration and facilitate behavioral recovery. Future mechanistic studies that focus on the role of sirt3 in the neuroprotective effect of restricted food are warranted.

THE EFFECT OF CAFFEINE IN TRAUMATIC BRAIN INJURY INDUCED CEREBRAL BLOOD FLOW CHANGES

S.C.R. Bandaru, S. Kallakuri, Y. Shen, H. Li, E.M. Haacke, **L. Zhang**, J.M. Cavanaugh

Biomedical Engineering, Wayne State University, Detroit, MI, USA

Introduction: Traumatic brain injury (TBI) is a global health problem with significant socio-economic costs. Alteration in cerebral blood flow due to impaired autoregulation is one of the most common consequences of TBI. However, studies to understand the temporal changes in CBF following TBI in experimental models are limited. The few available studies report acute reduction in CBF following TBI; knowledge related to CBF changes at sub-acute periods extending to 7 days after TBI is not known. Reduction in CBF has been associated with unfavorable neurological outcome and can render the brain vulnerable to secondary damage. However, effective

interventions that can restore or have shown the potential to restore neurological outcome are very limited. A few studies have demonstrated that caffeine acts as a neuroprotectant in several neurological disorders, acting through diverse mechanisms. It has been postulated that caffeine may offer neuroprotection by restoring or maintaining adequate CBF following TBI. Thus, studying these CBF changes following TBI and its potential modulation by caffeine pre-treatment forms the central theme of this research.

Methods: The study investigated CBF changes in male Sprague Dawley rats at 4hrs, 24 hrs, 3 days and 7 days following closed head injury, with and without caffeine (chronic and acute) pretreatment. TBI was induced using the Marmarou impact acceleration device (2 m height, 450 g weight). All MRI measurements were performed in a 7T horizontal-bore magnetic resonance spectrometer. Arterial Spin Labeling (ASL) was used to analyze CBF. ASL parameters were repetition time = 3000 ms, echo time = 16 ms, number of slices = 8, slice thickness = 2 mm, inter-slice gap = 0.5 mm and number of acquisitions = 51. Eight coronal slice brain images were obtained for each rat at each time point. Regions of interest (ROI) were analzyed in parietal cortex, striatum, hippocampus, thalamus and brainstem.The mean value of the signal intensity obtained from each ROI served as the arbitrary CBF value for that region.

Results: Rats subjected to TBI showed reduced regional and global CBF at 4hrs and 7 days following TBI. In contrast, rats that underwent chronic caffeine (1.5 g/L) pretreatment for 3 weeks did not show apparent changes in regional and global CBF following TBI, indicating a potential benefit after TBI. Acute caffeine treatment (150 mg/kg, i.p. injection 30 minutes before TBI) showed significant reductions in CBF at 4 hrs post-TBI, further deteriorating the cerebral perfusion. Furthermore, chronic caffeine pretreated rats demonstrated significantly reduced surface righting duration following TBI, compared to acute caffeine treated rats subjected to TBI and rats subjected to TBI without caffeine treatment. Therefore, chronic caffeine treatment may be beneficial in offering a degree of neuroprotection against TBI.

Conclusions: This study was able to support the hypothesis that chronic caffeine can restore or optimize CBF following TBI and this optimization may be related to the ensuring positive outcomes such as reduced surface righting duration. This may form the stepping stone for further studies on beneficial effects of caffeine in TBI.

LOCAL INTRA-ARTERIAL INFUSION OF ERYTHROPOIETIN DELAYED THERAPEUTIC TIME WINDOW OF TPA IN RATS FOLLOWING FOCAL CEREBRAL ISCHEMIA

H. Zhao, X. Liu, R. Wang, J. Gao, X. Liu, F. Yan, L. Ping, X. Ji, Y. Luo

Cerebrovascular Diseases Research Institute, Xuanwu Hospital of Capital Medical University, Beijing, China

Tissue plasminogen activator (tPA) for acute ischemic stroke remains limited primarily because of the narrow time-to-treatment windows. Protection conferred by erythropoietin (EPO) against ischemic brain injury has been demonstrated in some researches. This study aimed to test whether local intra-arterial infusion of erythropoietin delayed therapeutic time window of tPA in rats following focal cerebral ischemia in rats. Adult male Sprague-Dawley rats subject to middle cerebral artery occlusion were randomly divided into 5 groups: sham, tPA+saline-treated (2h or 4h ischemia/24h reperfusion), tPA+800 U/kg EPO-treated (2h or 4h ischemia/24h reperfusion) group. Neurological deficit scores were assessed post 24h reperfusion. The survival rate of rats was observed and infarct volume was measured using TTC staining. Blood routine examination was performed. The levels of phosphorylated AKT (p-AKT) and phosphorylated ERK (p-ERK) were detected by western blot and immunofluorescence. The results showed that local intra-arterial infusion of EPO delayed the therapeutic time window of tPA against transient focal cerebral ischemia in rats manifested by a similar decrease in death rate, infarct volume, and the neurological deficit in rat transient MCAO model. The p-AKT and p-ERK were both increased, signifying the concurrent activation of the AKT and ERK pathways. Our study indicates local intra-arterial infusion of EPO delayed the therapeutic time window of tPA against transient focal cerebral ischemia in rats, which mainly through activation of AKT pathways in the protective mechanisms of EPO.

ACTIVATION OF CEREBRAL PEROXISOME PROLIFERATOR-ACTIVATED RECEPTORS Γ INHIBITS THE MITOCHONDRIAL APOPTOTIC PATHWAY AFTER FOCAL CEREBRAL ISCHAEMIA IN RATS

Y. Zhao[1], U. Lützen[1], M. Zuhayra[1], T. Herdegen[2], J. Culman[2]

[1]Department of Nuclear Medicine, [2]Institute of Experimental and Clinical Pharmacology, University Hospital of Schleswig-Holstein, Campus Kiel, Kiel, Germany

Objectives: Apoptosis plays a crucial role in the progression of neuronal loss and expansion of brain injury after cerebral ischaemia. A number of studies have demonstrated that activation of peroxisome-proliferator-activated receptor(s) γ (PPARγ) in the brain exerts beneficial effects and reduces neuronal cell death after ischaemic stroke. We studied in rats the effects of brain PPARγ activation on the Akt/GSK3β (glycogen synthase kinase-3β) signalling cascade and apoptosis in the frontoparietal cortex ipsilateral to the ischaemic injury after occlusion of the middle cerebral artery (MCAO) followed by reperfusion.

Methods: The PPARγ agonist, pioglitazone, or vehicle was infused intracerebroventricularly (ICV) via osmotic minipumps in male Wistar rats over a 5-day period before, during and 1 or 2 days after MCAO (90 min). The expression of phosphoinositide 3-kinase (PI3K) and its up-stream activator PDK1, Akt3, phospho-Akt (pAkt), phospho-GSK3β (pGSK3β) and the apoptosis markers, apoptotic protease activating factor 1 (Apaf-1), activated caspase 9 and caspase 3, were studied by Western blot in the frontoparietal cortex at the border to the ischaemic core 24 h and 48 h after MCAO.

Results: Activation of cerebral PPARγ by pioglitazone reduced the infarct size at both time points (by 40 % and 38 %, respectively). ICV treatment of rats with pioglitazone tended to induce PDK1, PI3K, Akt3, pAkt (thr 308), pAkt (ser 473), total Akt (tAkt) and pGSK3β already 24 h after MCAO, however significant increases in expression of all parameters were detected 48 h after ischaemic stroke: PDK1 (+103 %, P< 0.01); PI3K (+480 %, P< 0.01); Akt3 (+134 %, P< 0.05); pAkt (thr 308) (+350 %, P< 0.01); pAkt (ser 473) (+ 1000 %, P< 0.001); tAkt (+160 %, P< 0.01) and pGSK3β (+173 %, P< 0.01. Pioglitazone effectively reduced the tissue levels of apoptotic markers at both time points: [24 h after MCAO: Apaf-1 (- 48%, P< 0.001); activated caspase 9 (-45 %, P< 0.001); activated caspase 3 (-25 %, P< 0.01)], [48 h after MCAO: Apaf-1 (- 36 %, P< 0.01); activated caspase 9 (-28 %, P< 0.05); activated caspase 3 (-27 %, P< 0.05)].

Conclusions: Our results show that it is the central effect of pioglitazone which accelerates the phosphorylation of Akt3 and GSK3β. Activation of the Akt/GSK3β signalling cascade mediates the inhibition of the intrinsic apoptotic pathway and supports the survival of neurons in the peri-focal cortical areas. Our data provide evidence that the activation of the Akt/GSK3β signalling pathway is an important mechanism by which pioglitazone effectively suppresses apoptosis in ischaemic brain tissue and limits the progression of ischemic injury.

PROTECTIVE EFFECT OF A NOVEL ROCK INHIBITOR AGAINST MPP^+-INDUCED NEUROTOXICITY THROUGH ENHANCING AKT ACTIVATION AND ROS-SCAVENGING CAPACITY

Z.Y. Zhou[1], C.-M. Chong[1], T.-J. Hou[2], M.-Y. Shen[2], H.-D. Yu[2], Y.-Y. Li[2], P.-C. Pan[2], S.-Y. Zhou[2], L.-L. Zhang[2], **S.M.Y. Lee**[1]

[1]State Key Laboratory of Quality Research in Chinese Medicine, Institute of Chinese Medical Sciences, Macau, [2]Institute of Functional Nano & Soft Materials (FUNSOM) and Jiangsu Key Laboratory for Carbon-Based Functional Materials & Devices, Soochow University, Suzhou, China

Objectives: Rho-associated protein kinase (ROCK) is a member of serine-threonine kinase family and discovered as a first downstream effector of small GTPase Rho. It plays a vital role in different cell phenomena, such as cell migration, cellular construction and cell-substratum contacts, which mainly involve in cytoskeleton dynamic and myosin light chain (MLC) phosphorylation. Recent research reported inhibition of ROCK increases neurite outgrowth and axonal regeneration. Furthermore, some studies suggested that abnormal ROCK activation can be a pathogenesis of neurodegeneration diseases including Parkinson's Disease (PD), Alzheimer Disease (AD) and Huntington Disease (HD). Consequently, inhibition of ROCK may be a promising therapeutic target for neurodegeneration diseases.

Methods: The inhibition activity of the ROCK inhibitor was measured using Kinase activity

assay. In cell experiments, SH-SY5Y cells were pre-treated with different concentrations of this ROCK inhibitor for 1 h, and then exposed to 2 mM 1-methyl-4-phenylpyridinium (MPP^+) for 36 h. Cell viability, cytotoxicity and intracellular ROS level were measured preforming MTT assay, LDH assay and ROS detection assay respectively. The roles of ROCK/Akt signaling, apoptosis proteins and adhesion proteins in neuroprotective effect of this ROCK inhibitor were evaluated by western blotting.

Results: In this study, we identified a novel ROCK inhibitor from chemical database and investigated its pharmacologic effects in PD models in vitro and its action mechanism. The kinase assay showed that this ROCK inhibitor could block ROCK1 activity effectively and had high selectivity between ROCK1 and ROCK2. The pretreatment of this ROCK inhibitor had the potential protective effect against MPP^+-induced SH-SY5Y cells damage and decrease the generation of ROS. This ROCK inhibitor also enhanced Akt signaling and further blocked the MPP^+-induced apoptosis pathways.

Conclusions: All results suggested that this novel ROCK inhibitor was effective in suppressing the neurotoxicity of MPP+ in SH-SY5Y cells via enhancing Akt activation and ROS-scavenging capacity and had the potential therapeutic use in prevention of neurodegeneration process.

References:

Jeon, B. T. et al. (2012). The Rho-Kinase (ROCK) Inhibitor Y-27632 Protects Against Excitotoxicity-Induced Neuronal Death In Vivo and In Vitro. *Neurotoxicity research*.

Lingor, P. et al. (2007). Inhibition of Rho kinase (ROCK) increases neurite outgrowth on chondroitin sulphate proteoglycan in vitro and axonal regeneration in the adult optic nerve in vivo. *Journal of neurochemistry*, 103(1), 181-9.

Raad, M. et al. (2012). Neuroproteomics approach and neurosystems biology analysis: ROCK inhibitors as promising therapeutic targets in neurodegeneration and neurotrauma. *Electrophoresis*, 1-10.

Wu, J. et al. (2012). Rho-kinase inhibitor, fasudil, prevents neuronal apoptosis via the Akt activation and PTEN inactivation in the ischemic penumbra of rat brain. *Cellular and molecular neurobiology*, 32(7), 1187-97.

INVESTIGATING THE NEGATIVE BOLD SIGNAL BY SINGLE IMPULSE NEURAL STIMULATION

L. Boorman, R. Slack, J. Berwick

Psychology, University of Sheffield, Sheffield, UK

Objectives: The neural generators of the negative blood oxygenation level dependant (BOLD) response (NBR) remain incompletely characterised. Previous studies have linked NBR to decreased neural firing occurring in cortical areas associated with localised reductions in blood flow, volume and oxygenation (1, 2). However, the neural processes that trigger and regulate this decreased neural firing are unknown. To investigate stimulus-evoked BOLD responses in rodent models, trains of stimulus pulses are often presented to overcome the low signal to noise ratio of BOLD fMRI, by evoking robust hemodynamic changes. However such stimuli with multiple interacting neural activations make it difficult to uncover any underlying neural mechanisms that drive the subsequent NBR. Thus the aim of the current study was to investigate the neural processes underpinning NBR evoked through single impulse stimulation.

Methods: Single impulses of electrical stimulation were applied to the whisker pad of anaesthetised rats. Neural activity was recorded using multi-channel array electrodes with hemodynamic changes recorded concurrently using two dimensional optical imaging spectroscopy (2D-OIS). One electrode was located in the activated whisker barrel region and another placed in a surrounding cortical region that exhibited stimulus-evoked negative hemodynamic changes. Neural responses were analysed on an individual trial basis, using frequency power analysis similar to that used by Shmuel (1) and analysed for the presence and magnitude of evoked thalamocortical spindles. A general-linear-modelling (GLM) approach was used to detect spindles and rank individual stimulus presentation trials according to spindle magnitude, with the vector of trial rankings applied to the recorded hemodynamic data.

Results: Electrical stimulation of the whisker pad produced neural activation in the whisker barrel cortex with accompanying local positive and surrounding negative hemodynamic responses. The negative hemodynamic has

previously been shown to produce NBR for long duration stimulation (1). It was found that the power of long latency neural activity (0.2 to 2s after stimulation onset, in the 30-130Hz frequency band) in both the whisker and surrounding regions was associated with the magnitude of the negative hemodynamic response. Hemodynamic changes recorded in the activated barrel region showed little difference spatially and in magnitude in trials, when ranked by the magnitude of long latency neural power. In surrounding regions hemodynamic responses were negligible for higher neural power, while large negative hemodynamic responses were observed when neural power was minimal. Spontaneous and stimulus-evoked thalamocortical spindles were observed in many neural recordings and consisted of an oscillation around 12-15Hz with duration of ~800ms. Individual trial analysis of spindles demonstrated little association with the magnitude of negative hemodynamic responses, but that spindles had their own associated hemodynamic response.

Conclusions: The association between decreased neural power and increased negative hemodynamic responses adds further evidence against 'vascular steal' as the primary mechanism generating NBR and demonstrates more of the active neural processes underlying NBR. Single impulse stimulations and individual trial analysis offers the opportunity of deconstructing the hemodynamic response function and by extrapolation the BOLD signal, into its constituent neural generators. References (1) Boorman et. al 2010 J. Neurosci (2) Shmuel et. al 2006 Nat Neurosci

HYDROGEN PROTECTS AGAINST DELAYED NEUROVASCULAR DYSFUNCTION AFTER ASPHYXIA IN PIGLETS

F. Domoki[1], O. Oláh[1], V. Tóth-Szűki[1], P. Temesvári[2], F. Bari[1]

[1]University of Szeged, Szeged, [2]Orosháza Hospital, Orosháza, Hungary

Background and aims: Perinatal asphyxia elicits severe brain injury playing a significant role in perinatal mortality or leading to hypoxic-ischemic encephalopathy (HIE) in the survivors. Although moderate whole body hypothermia provides considerable neuroprotection, clearly further studies on the pathomechanisms of HIE are warranted in order to develop new therapeutic neuroprotective strategies. Previous studies indicated severe, but only transient (1-4h) reactive oxygen species (ROS)-dependent neurovascular dysfunction in newborn pigs after hypoxic/ischemic (H/I) stress contributing to the neuronal injury after birth asphyxia.

We investigated whether neurovascular function is affected 24h after H/I stress, since secondary energy failure (SEF) often occur in this period. We also tested if the hydroxyl radical scavenger H_2 exerted neurovascular protection.

Methods: Anesthetized (Na-thiopenthal ip followed by midazolam+morphine iv), ventilated piglets were assigned to 3 groups: time control, asphyxia/reventilation with air, and asphyxia/reventilation with air+2.1% H_2 for 4h (n=9-9-9). Cerebrovascular reactivity of pial arterioles was determined using closed cranial window/intravital microscopy 24h after 8 min asphyxia induced by suspending artificial ventilation. After euthanasia, the brains were subjected to histopathology examination.

Results: Hemodynamic parameters, blood gases, and core temperature did not differ significantly among the experimental groups. Amplitude-integrated EEG recovered in both asphyxiated groups, albeit with a marked tendency for faster recovery in H_2-treated animals. Cerebrovascular reactivity was severely attenuated both to the endothelium-dependent cerebrovascular stimulus hypercapnia and to the neuronal function-dependent stimulus NMDA by asphyxia/reventilation, however, the vascular responses to norepinephrine and sodium-nitroprusside were unaltered. H_2 fully or partially preserved cerebrovascular reactivity to hypercapnia or NMDA, respectively. Histopathology revealed modest neuroprotection afforded by H_2.

Conclusions: In summary, relatively mild hypoxic/ischemicH/I injury triggers severe delayed dysfunction of the neurovascular unit affecting both cerebrovascular and neurovascular regulatory mechanisms. This delayed functional impairment in cerebrovascular regulation disrupts the relationship between tissue metabolism and cortical blood flow, and thus can contribute to further neuronal damage during the development of HIE. Resuscitation with the antioxidant H_2 in the early reventilation period can alleviate delayed neurovascular damage

indicating a role for ROS in the pathomechanism and may offer an inexpensive and valuable supplementary neuroprotection bridging the gap between resuscitation and the induction of whole body hypothermia.

Support: National Scientific Research Fund of Hungary (OTKA, K81266, K100851) and the EU (HURO/0901/137/2.2.2). Orsolya Oláh was supported through the TÁMOP-4.2.2/B-10/1-2010-0012 grant. Ferenc Domoki was supported by the János Bolyai Research Scholarship of the Hungarian Academy of Sciences.

THE VASCULOME OF MOUSE BRAIN

S. Guo[1], Y. Zhou[2], C. Xing[1], J. Lok[3], A.T. Som[1], M. Ning[4], X. Ji[5], E.H. Lo[1]

[1]Department of Radiology and Neurology, Massachusetts General Hospital, Harvard Medical School, [2]Broad Institute, Massachusetts Institute of Technology and Harvard Medical School, [3]Department of Pediatrics, [4]Department of Neurology, Massachusetts General Hospital, Harvard Medical School, Boston, MA, USA, [5]Xuanwu Hospital, Capital Medical University, Beijing, China

Objectives: As an important part of neurovascular unit, the cerebral endothelium helps to regulate CNS function by actively releasing signals into and receiving signals from the neuronal parenchyma. Here, we propose the concept of a brain vasculome, i.e. a systematic mapping of transcriptome profiles of brain endothelial cells in order to (a) compare with profiles from heart and kidney, (b) define signaling networks, (c) map onto CNS disease genes, and (d) map onto plasma protein databases.

Methods: Brain cortex and hearts were harvested directly from 10-week old male C57BLKS/J mice, and kidney glomerular were purified with inactivated DynaBeads administrated through perfusion. Endothelial cells were purified with anti PECAM-1-coated DynaBeads from digested tissue. Total RNA were extracted and profiled on Affymetrix mouse 430 2.0 micro-arrays for the vasculome of each organ. Three RNA samples for each organ were tested and each sample was pooled from 5 mice. Real-time PCR was used to check cell-specific gene expression markers.

Results: RNA samples with good quality (RIN score larger than 7.0) were used for endothelial cells expression profiles. Analysis of cell type specific markers confirmed that these brain, heart and kidney glomerular preparations were not contaminated by brain cells (astrocytes, oligodendrocytes, or neurons), cardiomyocytes or kidney tubular cells respectively. Comparison of the vasculome between brain, heart and kidney glomeruli showed that endothelial gene expression patterns were highly organ-dependent. Analysis of the brain vasculome demonstrated that many functionally active networks were present, including cell adhesion, transporter activity, plasma membrane, leukocyte transmigration and Wnt signaling pathways, also cytokines expression and angiogenesis system. Analysis of representative genome-wide-association-studies showed that genes linked with Alzheimer's disease, Parkinson's disease and stroke were detected in the brain vasculome. Comparison with established plasma protein databases showed significant overlap with the brain vasculome.

Conclusion: Mapping and dissecting the brain vasculome in health and disease may provide a novel database for investigating disease mechanisms, assessing therapeutic targets and exploring new biomarkers for the CNS.

References:

Gorelick PB, Scuteri A, Black SE, Decarli C, Greenberg SM, et al. (2011) Vascular contributions to cognitive impairment and dementia: a statement for healthcare professionals from the american heart association/american stroke association. Stroke 42: 2672-2713.

Neuwelt EA, Bauer B, Fahlke C, Fricker G, Iadecola C, et al. (2011) Engaging neuroscience to advance translational research in brain barrier biology. Nat Rev Neurosci 12: 169-182.

Daneman R, Zhou L, Agalliu D, Cahoy JD, Kaushal A, et al. (2010) The mouse blood-brain barrier transcriptome: a new resource for understanding the development and function of brain endothelial cells. PLoS One 5: e13741.

Enerson BE, Drewes LR (2006) The rat blood-brain barrier transcriptome. J Cereb Blood Flow Metab 26: 959-973.

Pardridge WM (2007) Blood-brain barrier genomics. Stroke 38: 686-690.

Wallgard E, Larsson E, He L, Hellstrom M, Armulik A, et al. (2008) Identification of a core set of 58 gene transcripts with broad and specific expression in the microvasculature. Arterioscler Thromb Vasc Biol 28: 1469-1476.

DEVELOPMENT OF REMOTE MEDICAL SERVICE SYSTEM AND NEUROVASCULAR TREATMENT PLANNING USING SMARTPHONE

B.T. Kim

Neurosurgery, Soonchunhyang University Bucheon Hospital, Bucheon, Republic of Korea

Background: Telemedicine is the specialty of medicine that uses the evolving telecommunications industry combined with medical information technology to provide remote medical services. The use of smartphone telemedicine is an efficient and effective way for remote specialist consultation and should be considered by the neurovascular surgeon.

Method: The Groupware system has been setup on the hospital computer server. The software engine has been developed for the use of smartphone. Through the remote medical service system, the core information of the patient's database can be displayed for the physician with his ID and password.

Result: Smartphones provide fast and clear access to the patient's laboratory information and to electronically digital images and allows the neurovascular surgeon free mobility, not restricted by the constraints of a desktop personal computer. CT and 3dimensional angiographic images have been showing clearly and the treatment planning can be decided on the remote site with smartphone. Case illustration will be presented.

Conclusion: This allows for improved efficiency of the specialty consultation to the neurovascular treatment and improved care to the stroke patients especially in the emergent situation.

INDUCTION OF NEUROVASCULAR PROTEASES AND PERINATAL CEREBRAL HEMORRHAGE BY VEGF IN THE GERMINAL MATRIX

D. Yang[1], Y.-Y. Sun[1], J. Baumann[2], **A. Kuan**[1]

[1]Emory University, Atlanta, GA, [2]Cincinnati Children's Hospital, Cincinnati, OH, USA

Objectives: Perinatal cerebral hemorrhage, ranging from germinal matrix to intraventricular hemorrhage (GMH-IVH) and ischemic infarction, is a common complication of preterm birth that affects approximately 12,000 infants each year in the USA alone causing death or functional disabilities. Several lines of evidence suggest that vascular endothelium growth factor (VEGF) contributes to GMH-IVH, but whether it is sufficient, and if so, by what means, remain unclear. These questions cannot be answered using current experimental models because they all rely on premature delivery and/or mechanic disruption of cerebral blood vessels, which are better suited for studying the consequences rather than the causes of GMH-IVH. The objective of this study is to invent a transgenic model of GMH-IVH to address the role and mechanisms of VEGF.

Methods:

(a) We used a tetracycline-regulated transgenic system to express murine VEGF in the forebrain germinal matrix by crossing GFAP-tTA (Tet-Off) or Nestin-rtTA (Tet-On) drivers with TetO-VEGF-A164 mice, and examined the resultant phenotypes.

(b) To unravel the downstream mechanisms, gene-profiling analysis was performed in E16 bitransgenic embryos and littermates. The amount and activity of differentially expressed genes were validated in E18-P1 animals.

(c) To assess clinical relevance of the new GMH-IVH model, glucocorticoids (betamethasone) were administered prenatally and the outcome, as well as, the activity of VGEF-induced neurovascular (NV) proteases was examined in bitransgenic embryos/pups and control littermates.

Results:

(a) The expression of VEGF in the forebrain germinal matrix promoted angiogenesis initially, but by near-birth, it transformed into periventricular hemorrhage associated with local activation of NV-proteases, particularly

matrix metalloproteinase-9, cathepsins, and caspases.

(b) Potential concomitant or downstream factors include hypoxia and the ETS1/HIF2a (EPAS1) duo of transcriptional factors.

(c) Antenatal glucocorticoids therapy markedly reduced the incidence and severity of GMH-IVH via inactivation of NV-proteases rather than the expression of VEGF (Figure).

Conclusions: These results not only introduce a transgenic mouse model of GMH-IVH, but also suggest a unique set of NV proteases that are downstream mediators of VEGF (or with hypoxia) during perinatal cerebral hemorrhage, and thus potential targets for therapeutic intervention.

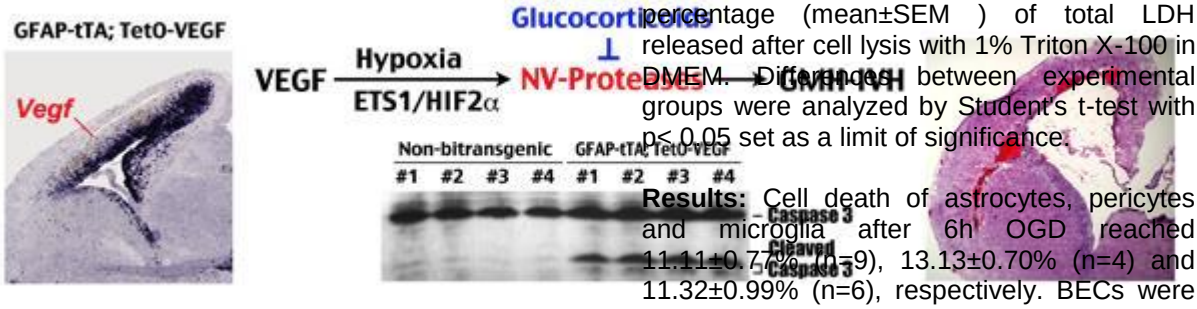

[Hemorrhage]

CELLS OF THE NEUROVASCULAR UNIT DURING OXYGEN GLUCOSE DEPRIVATION: PROTECTIVE AND HARMFUL EFFECTS OF NEUROVASCULAR UNIT-DERIVED SIGNALING MOLECULES

Z.B. Redzic[1,2], T. Rabie[1], B.A. Sutherland[1], A.M. Buchan[1]

[1]Radcliffe Department of Medicine, University of Oxford, Oxford, UK, [2]Department of Physiology, Faculty of Medicine, Kuwait University, Kuwait, Kuwait

Objectives: Cerebral ischemia affects the neurovascular unit (NVU) and could contribute to cerebral vasogenic edema and hemorrhagic transformation. Objectives of this *in vitro* study were to explore cell death in primary cultures of NVU cells including astrocytes, pericytes, brain endothelial cells (BECs) and microglia during oxygen glucose deprivation (OGD) and effects of NVU-derived signaling molecules.

Methods: Cell cultures were produced from SD rats using protocols described earlier [1, 2, 3] and exposed either to OGD (5% CO_2 in N_2 at 37°C in glucose- and pyruvate-free Dulbecco´s Modified Eagle Medium (DMEM)) or to control conditions (5% CO_2 in air at 37°C in DMEM containing 5mM glucose and 1.25 mM pyruvate). Astrocyte-, pericyte- and microglia-conditioned media (ACM, PCM and MCM, respectively) were collected from the corresponding cell culture after 6h OGD, and added to the cell culture media in a 1/3 volume during incubations. In some cases vascular endothelial growth factor (VEGF), angiopoietin 1 (Ang1), transforming growth factor beta 1 (TGFβ1), interleukin 6 (IL-6), VEGF receptor antagonist Cyclo-VEGI or soluble Ang1 receptor Tie 2 were added to OGD or control media. The results were expressed as a percentage (mean±SEM) of total LDH released after cell lysis with 1% Triton X-100 in DMEM. Differences between experimental groups were analyzed by Student's t-test with $p< 0.05$ set as a limit of significance.

Results: Cell death of astrocytes, pericytes and microglia after 6h OGD reached 11.11±0.77% (n=9), 13.13±0.70% (n=4) and 11.32±0.99% (n=6), respectively. BECs were more vulnerable to OGD, with cell death reaching 20.68±2.33% (n=11) after 2h. PCM caused significant increase in cell death of astrocytes during 6h OGD. It exerted protective effects on BECs during 2h OGD, with cell death being reduced to 13.21±1.53 (n=7). Addition of the same amount of Ang1 active protein to OGD medium, as it was present in PCM, had detrimental effects on both astrocytes and BECs during OGD, which were totally abolished by the presence of Tie2. Detrimental effects of Ang1 on BECs during OGD were partially abolished by VEGF. ACM exerted protective effects on pericytes and BECs during OGD ; however, this effect appeared not to be mediated by VEGF, which was abundantly present in ACM. MCM was protective for astrocytes and BECs, with cell death being significantly reduced to 7.76±0.20% (n=4) and 2.79±0.49% (n=4) after 6h and 2h OGD, respectively. Protective effects of ACM and MCM could be mediated by TGFβ1, since addition of this cytokine to OGD medium significantly reduced cell death of astrocytes and BECs to 8.21±0.39% (n=4) and 8.07±1.66% (n=4), respectively. Addition of IL-6 to OGD medium had protective effects only on BECs, with cell death being reduced to 11.15±1.1% (n=4).

Conclusions: NVU-derived signaling molecules exerted complex effects on NVU cells that influenced their ability to survive OGD. Ang1 had detrimental effects on astrocytes and BECs, while ACM and MCM exerted protective effects, which could be, at least partially, mediated by TGFβ1.

References:

1. Methods Mol Biol. 2012; 814:415-30.
2. J Cereb Blood Flow Metab. 2012; 32:919-32.
3. Neurochem Int. 2009; 54:253-63.

DECIPHERING NEURONAL CIRCUITRY CONTROLLING LOCAL BLOOD FLOW IN CEREBRAL CORTEX OF RODENTS WITH OPTOGENETICS AND CHRONIC FUNCTIONAL ULTRASOUND IMAGING

J. Rossier, A. Urban

Centre de Psychiatrie et Neurosciences, INSERM U 894, Paris, France

Although it is know since more than a century that neuronal activity is coupled to blood supply regulation, the underlying neuronal pathways remain to be identified. In the brain, neuronal activation triggers a local increase of cerebral blood flow (CBF) that is controlled by the neurogliovascular unit composed of terminals of neurons, astrocytes and blood vessel muscles. It is generally accepted that the regulation is adjusted to local metabolic demand by local circuits. Today experimental data led us to realize that the regulatory mechanisms are more complex. Indeed, how to explain that a stimulus of the whisker pad in rodents is associated with local increase in the corresponding barrel field but also with decreases in the surrounding deeper area and in the opposite barrel field?

By combining both *in vitro* studies in acute slice and *in vivo* imaging by chronic functional ultrasound imaging in anesthetized rats, we demonstrated that neurovascular coupling is a process through which neuronal activity leads to increases of local CBF in the activated area but also to decreases in other brain regions. In order to explain these observations, we propose that a neuronal system within the brain is devoted to the control of local brain blood flow. Our optogenetic experiments revealed that neurons expressing the calcium binding protein parvalbumin could control local blood flow. We demonstrated that channel rhodopsin-based photostimulation of these cells give rise to an effective contraction of penetrating arterioles. These results therefore support the neurogenic hypothesis of a complex distributed nervous system controlling the CBF.

CEREBRAL VENOUS POTASSIUM EFFLUX DURING SPREADING DEPRESSION

J. Seidel[1], U. Hoffmann[2], C. Ayata[1,3]

[1]Radiology, Stroke and Neurovascular Regulation Lab, Massachusetts General Hospital, Harvard Medical School, Charlestown, MA, USA, [2]Klinik für Anaesthesiologie, TU München, Klinikum rechts der Isar, München, Germany, [3]Neurology, Stroke Service and Neuroscience Intensive Care Unit, Massachusetts General Hospital, Harvard Medical School, Charlestown, MA, USA

Objectives: Cortical spreading depression (CSD) is a wave of depolarization implicated in the pathophysiology of brain injury states and migraine aura. Massive K^+ efflux significantly increases extracellular potassium ($[K^+]_e$) during CSD, often reaching 50 mM or more. Clearance of $[K^+]_e$ is believed to be via astrocytic spatial buffering as well as reuptake by the Na^+/K^+ ATPase. Astrocytes are ideally positioned to siphon $[K^+]_e$ to the vasculature from the extracellular space. However, it is not known whether vascular clearance contributes to the restoration of $[K^+]_e$ after CSD. In order to test this, we measured $[K^+]_e$ in cerebral venous blood during CSD.

Methods: Mice (C57BL/6, male, 25-30 g; n=10) or rats (Sprague Dawley, male, 200-400 g; n=5) were anesthetized (isoflurane 2.5% induction, 1.5% maintenance, in 70% N_2O/30% O_2). Rats were intubated and mechanically ventilated. Arterial blood pressure, pH, pO_2 and pCO_2 were monitored and maintained in both species. Animals were placed in a stereotaxic frame, and two burr holes drilled under saline cooling at (mm from bregma):

(i) anterior 1.5, lateral 2.0 (1 mm diameter for KCl application) and

(ii) posterior 1.5, lateral 2.0 (2-3 mm diameter for DC and K^+ electrodes).

Both cortical $[K^+]_e$ and venous $[K^+]_e$ were measured using double barreled electrodes. Intravenous recordings were made from pial veins of 20 to 50 µm diameter in mice and rats, respectively. Extracellular (DC) potential was recorded using a capillary microelectrode [300 µm deep] adjacent to the K^+ electrode. CSD was induced by topical application of KCl solution (300 mM or 1 M for mice and rats, respectively).

Results: CSD resulted in a large transient increase in cortical $[K^+]_e$ concurrent with the characteristic DC potential shift (Figure 1B). Venous $[K^+]_e$ also increased during CSD. The magnitude of venous $[K^+]_e$ increase was smaller and its duration longer compared to cortical measurements, presumably due at least in part to spatiotemporal averaging created by CSD propagation and dilution in venous watershed. The magnitude of venous $[K^+]_e$ increases were similar in mice and rats, although duration of DC shifts and cortical and venous $[K^+]_e$ elevations were shorter in rats. Anoxic depolarization was associated with a steady increase in venous $[K^+]_e$. The intravenous electrode placement was confirmed at the end of each experiment by direct KCl injections (30mM) into the same vein upstream, as well as by induced systemic $[K^+]_e$ elevations.

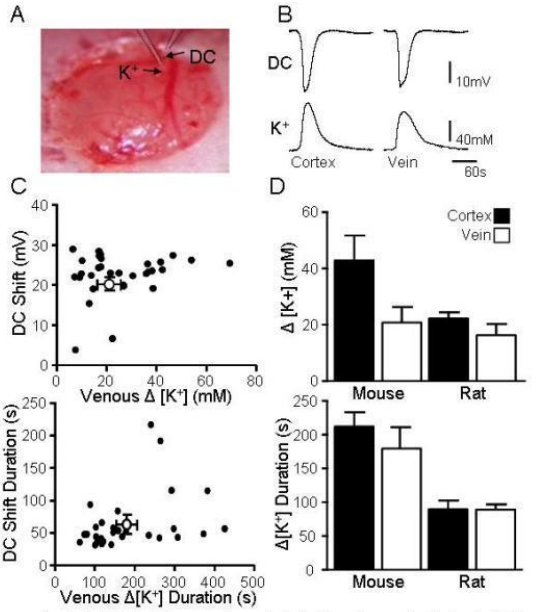

Figure 1: **A** Bright field image of cranial window. Arrows indicate both the venous K^+ electrode and the cortical DC electrode. **B** Representative real-time aligned CSD recordings in mouse. The top panel shows DC shifts recorded from cortical tissue and the bottom panel shows K^+ recordings from both the cortical tissue (left) and pial vein (right). **C** Relationship between cortical DC shift and venous $[K^+]$ changes. The top graph shows the relationship between DC shift amplitude relative to venous increases in $[K^+]$. The bottom graph compares the duration of the DC shift recovery to the duration of venous $[K^+]$ recovery to baseline levels (average: white circle). **D** Average magnitude and duration of $[K^+]$ increases recorded from both the cortex and vein in mouse (n=10) and rat (n=5).

[Figure 1]

Conclusions: These data show that elevated $[K^+]_e$ during CSD is at least in part cleared through venous outflow. Taken together with previous data showing total tissue K^+ depletion in focal ischemic brain (Yushmanov et al., 2011), our findings suggest that $[K^+]_e$ may be cleared directly by the venous network, representing a paradigm shift in our understanding of $[K^+]_e$ regulation during spreading depression and injury depolarizations.

References: Yushmanov VE, Kharlamov A, Ibrahim TS, Zhao T, Boada FE, Jones SC (2011) K dynamics in ischemic rat brain in vivo by Rb MRI at 7 T. NMR Biomed 24:778-783.

THE IMPORTANCE OF MACROSCALE OPTICAL IMAGING SPECTROSCOPY IN A MOUSE MODEL OF NEUROVASCULAR COUPLING

P. Sharp[1,2], A. Kennerley[1], M. Azzouz[2], J. Berwick[1]

[1]Department of Psychology, [2]Department of Neuroscience, University of Sheffield, Sheffield, UK

Introduction: Neural activity in the brain is closely followed by a localised change in cerebral blood flow, a process termed neurovascular coupling. Understanding the temporal and spatial characteristics of the haemodynamic response to neural activity is critical for interpreting functional neuroimaging signals. Furthermore, there is increasing evidence that a disruption to neurovascular coupling may be a key pathogenic factor in several neurological disorders. It is therefore important to develop a stable *in vivo* mouse model for neurovascular coupling studies given the wide availability of transgenic mouse models of these disorders. Currently, the predominant techniques for imaging the haemodynamic response in mice are laser-Doppler flowmetry (LDF) (1) and 2-photon microscopy (2), which are generally limited to blood flow measurements at the level of the capillary bed.

Objective: Here, we aimed to measure haemodynamic responses in mice at the level of the vascular network, by applying optical imaging spectroscopy (OIS) to characterise the global spatiotemporal haemodynamics of surface vessels during neurovascular coupling.

Methods: Anaesthetised mice underwent a thinned cranial window preparation to allow direct illumination of the cortex. For OIS data collection, the cortex was illuminated sequentially with four wavelengths of light (575, 560, 595, 494 nm) and images of the brain were captured at 32 Hz for spectroscopic analysis. The whiskers on the contralateral side were deflected using a piezoelectric stimulator and the recorded light attenuation data across the different wavelengths were used to generate functional maps of changes in deox-, oxy and total haemoglobin (Hbr, HbO and Hbt, respectively), in all compartments of the vascular network.

Results: Under deep anaesthesia, responses to whisker stimulation showed 'inverted' haemodynamics, where levels of Hbr increased and HbO decreased. These results support the findings of the only other report using OIS in mice (3), which also showed this novel type of stimulus evoked response compared to rats and other species. Our analysis of the arterial network, showed failed activation of the middle cerebral artery, which may explain the 'inverted' response. Given the known effects of anaesthesia on vascular reactivity, under a lower anaesthetic depth, we observed a 'normal' haemodynamic response, with a large increase in Hbt/HbO, a decrease in Hbr and arterial recruitment. Interestingly, the capillary blood volume increased in both conditions, albeit greater in the lighter anaesthetised state. Thus, imaging modalities such as LDF and 2-photon microscopy, which primarily focus at the capillary level, may fail to detect important arterial contributions to the evoked haemodynamic response and inaccurately assess neurovascular function.

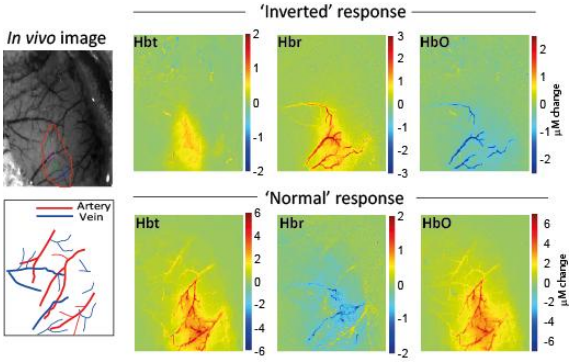

[Functional maps of haemodynamic changes]

Conclusions: Data presented here show the importance of measuring the macroscale haemodynamic response to validate 'normal' physiological regulation of blood flow in anaesthetised mice. These results also indicate a dose-dependent anaesthetic effect on arterial recruitment, which has important methodological implications for *in vivo* neurovascular research using mouse models of disease.

References:

(1) Park et al (2011) PNAS 108, 5063-5068. (2) Prakash et al (2007) Neuroimage 37, S27-36. (3) Shih et al (2012) JCBFM 32, 1277-1309.

INFECTION OF HUMAN PERICYTES BY HIV-1 DISRUPTS THE INTEGRITY OF THE BLOOD-BRAIN BARRIER

S. Nakagawa[1], V. Castro[2], **M. Toborek**[3]

[1]Department of Neurosurgery, University of Kentucky Medical Center, Lexington, KY, [2]Department of Biochemistry and Molecular Biology, [3]Biochemistry and Molecular Biology, University of Miami School of Medicine, Miami, FL, USA

Human immunodeficiency virus type 1 (HIV-1) infection of the central nervous system (CNS) affects cross-talk between the individual cell types of the neurovascular unit, which then contributes to disruption of the blood-brain barrier (BBB) and the development of neurological dysfunctions. While the toxicity of HIV-1 on neurons, astrocytes, and brain endothelial cells has been widely studied, there are no reports addressing the influence of HIV-1 on pericytes. Therefore, the purpose of this study was to evaluate whether pericytes can be infected with HIV-1 and how such an infection affects the barrier function of brain endothelial cells. Our results indicate that human brain pericytes express the major HIV-1 receptor CD4 and coreceptors CXCR4 and CCR5. We also determined that HIV-1 can replicate, though at a low level, in human brain pericytes as detected by HIV-1 p24 ELISA. Pericytes were susceptible to infection with both the X4-tropic NL4-3 and R5-tropic JR-CSF HIV-1 strains. Moreover, HIV-1 infection of pericytes resulted in compromised integrity of an *in vitro* model of the BBB. These findings indicate that human brain pericytes can be infected with HIV-1 and suggest that infected pericytes are involved in the progression of HIV-1-induced CNS damage.

LOWER VITAMIN C LEVELS IN THE BRAIN OF PATIENTS WITH TYPE 2 DIABETES

I.-Y. Choi[1,2,3], M.A. Levine[4], D. Robbins[5], J.A. Drisko[6], D.K. Sullivan[7], Q. Chen[8], J.A. Lierman[1], P. Lee[1,9]

[1]Hoglund Brain Imaging Center, [2]Neurology, University of Kansas Medical Center, [3]Molecular & Integrative Physiology, University of kansas Medical Center, Kansas City, KS, [4]NIDDK, National Institutes of Health, Bethesda, MD, [5]Medicine, [6]Integrative Medicine, [7]Dietetics and Nutrition, [8]Pharmacology, Toxicology and Therapeutics, [9]Molecular & Integrative Physiology, University of Kansas Medical Center, Kansas City, KS, USA

Introduction: Hyperglycemia and insulin resistance or insufficiency during diabetes is known to cause oxidative stress by generation of excessive reactive oxygen species and thereby increase oxidative damage and alter antioxidant status in nerve cells [1].

Objective: The objective of this study was to determine the levels of brain vitamin C (ascorbic acid, ascorbate) *in vivo* in diabetic subjects in comparison with control subjects based on reported increased oxidative stress in diabetes that may lower the levels of vitamin C, a major antioxidant, using a novel magnetic resonance (MR) spectroscopy technique.

Material and methods: Twenty-one patients with type 2 diabetes (age: 47 ± 6 years, mean ± SD) and twenty closely age- and sex-matched healthy controls (age: 45 ± 7 years) were studied. The diabetic patients were selected based on their definite diagnosis of diabetes (type 2 per WHO definition). All experiments were performed on a Siemens Allegra 3 T MR system with a custom-built helmet RF coil and interface [2]. Vitamin C mapping was achieved across the frontal to parietal regions in the axial slices of the human brain using the selective multiple quantum filtered chemical shift imaging (CSI) technique similar to the CSI technique for GSH (8 x 8 phase encoding steps, FOV of 20 cm x 20 cm, and slice thickness of 3 cm) [3].

Results: We found that brain vitamin C was lower by 12% in diabetic subjects compared to controls (p=0.005) while dietary intake of vitamin C in both subject groups was similar: 126 mg vs. 134 mg. Plasma values were lower in diabetic patients (36 µM) compared to controls (60 µM). However, plasma values for both groups were well above Km (6-10 µM) for sodium dependent vitamin C transporter 2 (SVCT2), the dominant vitamin C transporter in the brain.

Discussion and conclusions: Several possibilities may explain why plasma vitamin C values were well above Km for both groups but brain vitamin C values were lower only in diabetic subjects. These include: vitamin C utilization in the brain is increased in diabetes; the mechanism of brain uptake via SVCT2 is aberrant in diabetes; or brain vitamin C uptake *in vivo* may be partially regulated by another mechanism in humans. Using our new MR technique, some of these possibilities can be

tested by studying brain vitamin C values in healthy and diabetic subjects who are given oral and pharmacologic intravenous vitamin C doses.

References:

[1] Baynes & Thorpe, *Diabetes* 48:1 (1999).

[2] Choi et al. *Mag Res Engineering* 31B:71 (2007).

[3] Choi & Lee, *NMR in biomedicine* (2012)

This work is supported partly by NIH, NIDDK (R21 DK081079); the HBIC partly by NIH (C76 HF00201 and P30 HD002528) and the Hoglund Family Foundation.

ROLE OF ENDOGENOUS OPIOIDS AND THEIR INTERACTIONS WITH NITRIC OXIDE (NO) DURING STRESS INDUCED ANXIOGENESIS IN RATS

K. Gulati, R. Anand, J. Joshi, A. Ray

Vallabhbhai Patel Chest Institute, University of Delhi, Delhi, India

Endogenous opioids are important neuromodulators in the brain and their involvement in a variety of neuropsychiatric disorders is known. The present study evaluated the involvement of opioid peptides and their receptors during stress induced anxiogenesis in rats. Male Wistar rats (170-200 g) were used for the study and restraint stress (RS) was used as the experimental stressor. Neurobehavioral activity was studied by the elevated plus maze (EPM) test and levels of NO metabolites (NOx) in brain homogenates was used as the biochemical marker. Interactions of opioidergic agents with NO modulators were also studied. Restraint stress (RS x 1) consistently induced an anxiety-like response in the elevated plus maze (EPM) test, i.e. reduced number of open arm entries and time spent in the open arms, and elevated the plasma corticosterone levels (a reliable indicator of stress), as compared to controls. Pretreatment with the opioid agonists, morphine (mu), SNC-80 (delta), and to a much lesser extent, U-50488 (kappa), attenuated the RS-induced anxiogenic response. Both morphine and SNC-80 treated rats showed more open arm entries and time spent as compared to the vehicle treated RS group, with morphine being markedly more effective. RS induced neurobehavioral suppression was associated with reductions in brain NO metabolite (NOx) levels, which were also reversed with morphine, and to a much lesser extent with SNC-80 or U-50488 treatment. Interaction studies of opioid agonists with NO modulators showed that sub-effective doses of morphine and L-arginine (a NO precursor) had synergistic effects on RS-induced EPM activity, whereas, L-NAME (a NO synthase inhibitor) neutralized the anxiolytic effects of morphine. Repeated RS (x5) induced adaptative changes as evidenced by near normalization of behavioral suppression in the EPM and elevations in brain NOx, as compared to acute RS. Pretreatment with morphine, and to a lesser extent SNC 80 or U 50488H, in combination with repeated RS (x5) showed potentiating effects in the induction of behavioral adaptation in the EPM and elevations in brain NOx, as compared to repeated RS alone. Further, L-NAME, when administered prior to morphine, blocked this effect of morphine on stress adaptation. These results suggest differential opioid receptor involvement during stress induced modulation of anxiety and that opioid-NO interactions may contribute to such effects.

ASCORBATE DEFICIENCY INTERACTS WITH ICV-STZ MODEL OF AD IN MONKEYS

J.-H. Heo[1], K.-M. Lee[2]

[1]Seoul Medical Ceneter, [2]Seoul National University Hospital, Seoul, Republic of Korea

Background: Ascorbate has a major role in neuronal maturation, neurotransmission, neuroprotection, and evidence suggests that it can prevent the pathologic changes in AD. Though the validity of ascorbate in AD has not been exactly identified, it is evident that ascorbate has shown the protective and therapeutic efficacy on oxidative injury as well as AD pathology through numerous basic and clinical research.We have previously demonstrated that intracerebroventricular injection of streptozotocin (icv-STZ) in non-human primates induces changes in glucose metabolism in a manner similar to early states of Alzheimer´s disease. Such models in rodents also showed cellular and behavioral features mimicking the disease.

Methods: Four cynomolgus monkeys (Macaca fascicularis) were deprived of ascorbate for four weeks with the plasma and CSF levels monitored weekly. Then two of the

monkeys received STZ (2 mg/kg), and another two were given normal saline as controls, at the cerebellomedullary cistern (CM) three times (day 1, 7, and 14). FDG-PET, as well as MRI for structural evaluation, was performed immediately before, six weeks after the first icv injection. The results were compared with those obtained previously without ascorbate deprivation.

Results: In the STZ group, FDG uptake decreased significantly in comparison to the pre-injection baseline, at the precuneus, the posterior cingulate, and medial temporal cortices. Increase in sulcal markings suggesting brain atrophy was observed by MRI at six weeks post-injection. The structural changes normalized at 12 weeks, but the reduced FDG uptake persisted at the same loci. The cortical distribution of glucose hypometabolism was similar to that at early stages of AD patients. Furthermore, these changes were worse in ascorbate-deprived monkeys than normal monkeys treated in the same way.

Conclusions: Our findings demonstrate an interaction of ascorbate deficiency and cellular / molecular disruptions induced by icv-STZ. Possible mechanisms of the interaction include 1) exacerbation of oxidative stress prompted by icv-STZ, given that ascorbate is a major anti-oxidant, especially in the nervous system, and 2) worsening of glucose hypometabolism, additively to icv-STZ, by interfering with mitochondrial respiration, given that ascorbate functions as a cofactor for many enzymes in the respiratory chain. Further investigations on these possible mechanisms are under way.

PSYCHO-EMOTIONAL STRESS AND FUNCTIONAL STATUS OF ANTIOXIDANT SYSTEMS IN BRAIN

Z. Kuchukashvili, N. Koshoridze, K. Menabde, G. Burjanadze, M. Chachua

Department of Biology, Faculty of Exact and Natural Sciences, I. Javakhishvili Tbilisi State University, Tbilisi, Georgia

Objectives: The aim of our project was to studying changes in the activity of lipid peroxidation process and antioxidant system taking place parallel to the change in the quantity of NO in laboratory rat brain cells under stress caused by isolation and violation of diurnal cycle.

Methods: The experiment was conducted on 50 adult male Wistar rats divided into 2 groups. Rats in group 1, i.e., socially isolated rats (SI rats), were placed into individual cages in the dark (dark to light ratio, 23.5/0.5 h) during 30 days respectively. The control group contained 25 animals kept in a common cage under natural conditions (dark to light ratio, 14/10 h). Fractionation of brain tissue was performed as per Whittaker. Quantity of NO was defined by the product of the reaction - ($NaNO_2$) between NO and molecular oxygen - O_2. Concentration of active products of thiobarbituric acid, including malondialdehyde and determination of enzymes activity (catalase, superoxide dismutase) was determined by spectrophotometry.

Results: Investigations carried out at the initial stage have revealed that there is a marked increase in the quantity of nitric oxide in mitochondrial and cytosolic fractions of rat brain mitochondria, as a result of 30-day isolation and disruption of circadian rhythms (Table I). For instance, in mitochondria, in comparison with the control data, this value increased by approximately twice, and in cytosol 1.8 times. It becomes obvious that due to the 30 days of stress, the LPO process is activated in mitochondria. This is indicated by the increase in the products of lipid peroxidation. As it becomes evident from the table below, due to 30-day stress to which the animals are subjected, the activity of both enzymes in brain cell mitochondria shows a considerable drop. Namely, the activity of SOD amounts to 63% of the control value, and of catalase equals even less - only 34%. The obtained results point to the accumulation of excess amounts of superoxide radicals in brain mitochondria, and to the activation of oxidative stress as a consequence.

Fraction Type	Enzyme/Product	Control	30-day stress
Mitochondria	Superoxide dismutase (units/mg protein)	14,93±0,25	9,41±1,05
Mitochondria	Catalase (units/mg protein)	12,67±1,04	4,32±2,42
Mitochondria	Malondialdehyde (nM/mg protein)	0.40±0.06	1.45±0.20
Mitochondria	NO (μM)	0.43±0.02	0.95±0.09

Cytosol	Malondialdehyde (nM/mg protein)	1.23±0.01	2.68±0.05
Cytosol	NO (µM)	1.65±0,05	2.99±0.04

[Activities of rat brain antioxidant systems]

Conclusions: It turned out that psycho-emotional stress is a factor causing a number of complex changes in brain cell mitochondria. Such change includes a pathological process consisting in development of oxidative stress, indicated by a dynamics of accumulation of lipid peroxidation products in mitochondria and decreasing enzyme activity in the antioxidant system as a result of 30-day isolation and violation of circadian cycle among animals.

References:

Acta Neurobiol Exp (Wars). 2012;72(1):40-50.

Ukr Biokhim Zh. 2011 May-Jun;83(3):85-90.

Acta Biochim Biophys Sin (Shanghai). 2011 Jun;43(6):480-6. Epub 2011 May 9.

BIOCOMPATIBLE SILVER NANOPARTICLE PRECONDITIONING OF BRAIN: A POSSIBLE ROLE OF FREE RADICAL MEDIATED NUCLEAR FACTOR KAPPA-B ACTIVATION LINKED MECHANISM

A.K. Rehni, T.G. Singh

Pharmacology, Chitkara College of Pharmacy, Chitkara University, Patiala, India

Objectives: The present study has been designed to expound the significance of free radical mediated nuclear factor kappa-B linked mechanism in mediating silver nitrate nanoparticle based preconditioning induced reversal of ischemia and reperfusion induced cerebral injury in mice.

Methods: Bilateral carotid artery occlusion of 17 min followed by reperfusion for 24 hr was employed in present study to produce ischemia and reperfusion induced cerebral injury in mice. Cerebral infarct size was measured using triphenyltetrazolium chloride staining. Memory was evaluated using Morris water-maze test. Rota rod test was employed to assess motor incoordination [1, 2].

Results: Bilateral carotid artery occlusion followed by reperfusion produced cerebral infarction and impaired memory and motor co-ordination. Silver nitrate nanoparticles, prepared using chemical co-precipitation technique [3], were administered by intracerebroventricular injection in the mouse brain 15 minutes prior to the bilateral carotid artery occlusion.

Conclusions: Silver nitrate nanoparticle based preconditioning (Nanopreconditioning) prevented markedly ischemia-reperfusion-induced cerebral injury measured in terms of infarct size, loss of memory and motor coordination. N-acetylcysteine (2 mg/kg, ip), a potent free radical scavenger, and diethyl dithiocarbamate, a selective nuclear factor kappaB, attenuated the neuroprotective effect of nanopreconditioning. It is concluded that neuroprotective effect of nanopreconditioning may be due to the free radical mediated nuclear factor kappaB linked mechanism.

References:

1. Ashish K Rehni; Pradeep Bhateja; Nirmal Singh; Amteshwar S Jaggi. Implication of mast cell degranulation in ischemic preconditioning-induced prevention of cerebral injury. Fundamental and Clinical Pharmacology 22, 179 (2008).

2. Ashish K Rehni; Nirmal Singh; Amteshwar S Jaggi; Manjeet Singh. Amniotic fluid derived stem cells ameliorate focal cerebral ischaemia-reperfusion injury induced behavioural deficits in mice. Behavioural Brain Research 183, 95 (2007).

3. Edelstein, A.S., Cammarata, R. C. (Eds.) Nanomaterials, Synthesis, Properties and applications (1996), Bristol and Philadelphia Publishers, Bristol.

CHARACTERISING EFFECT OF DONEPEZIL ON CEREBRAL ACTIVITY AND METABOLISM BY SIMULTANEOUS IN VIVO EEG AND 2-DEOXYGLUCOSE AUTORADIOGRAPHY

D. Cash[1], C. Simmons[1], D. Duricki[1], A.L. Dixon[1], T. Patel[2], L.A. Dawson[2], D. Lythgoe[1], S.C. Williams[1], M. Mesquita[1]

[1]Neuroimaging, King's College London, London, [2]Biopharmacology & External Drug Discovery, Eisai Limited, HAtfield, UK

Objectives: Donepezil (DNZ), a centrally acting reversible acetylcholinesterase inhibitor, is a cognitive enhancer used for palliative treatment of mild to moderate Alzheimer´s disease. Despite the widespread clinical use and a recognised mechanism, there is a paucity of information about the direct effect of donepezil on the brain as most studies investigate chronic use, or interaction with other compounds. Quantification of temporal and spatial characteristics of acute DNZ would aid drug discovery by enabling comparisons with putative cognitive enhancers or assessment of synergism in combined therapies. To achieve this, we established a method combining *in vivo* cortical electroencephalography (EEG) recording and [^{14}C]2-deoxyglucose metabolic mapping (2DG) in conscious rats.

Methods: One week before recording, stainless steel EEG electrodes were implanted into the skull bone over left cingulate cortex (AP -0.4, MP 0.5) and hippocampus (AP -5.3, MP 5.2) under isoflurane anesthesia. On the day of experiment the animals were anaesthetised, femoral vessels canulated, lower torso immobilized in plaster cast and the anaesthesia withdrawn. EEG recording commenced after 90 min. DNZ (0.1, 1 or 5mg/kg, sc.) or vehicle (saline) was administered 30 min post-EEG start and 2DG administered 20 min post-DNZ/vehicle. Blood sampling, decapitation, brain processing and optical density analysis of brain sections was as previously described[1,2]. Glucose utilization (mmol/min/mg tissue, GU) was calculated[2] for each pixel of digitized brain images. EEG data were separated into five frequency bands (Fig 1) by a customized Matlab function.

Results: Physiology was normal and stable in the vehicle, 0.1 and 1mg/kg DNZ groups, but in the 5mg/kg group blood pressure and blood glucose were significantly elevated. Cerebral GU was significantly increased (>40%) by two lower doses of DNZ in several subcortical (nucleus accumbens, striatum, thalamus) and cortical (cingulate, motor, sensory) regions. GU was unchanged by 5mg/kg. EEG showed dose-dependent changes: most prominent were decreased power in alpha, theta and low beta EEG bands, whereas higher frequencies (high beta and gamma) were unchanged or slightly increased (gamma in cingulate cortex but not hippocampus). Figure 1 shows cingulate cortex EEG recordings; results from hippocampal electrode were similar.

Conclusions: The aim was to develop a combined EEG/2DG *in vivo* technique to characterize the effect of DNZ on brain activity and GU. Widespread GU increases were accompanied by a decreased EEG power in the slow frequency bands, but no significant changes in higher EEG frequencies. The GU effect was not observed in the DNZ (5mg/kg) group which may be due to hyperglycemia, or a depolarization block if there is elevated ACh. These measurements demonstrate that DNZ, at clinically relevant doses[3] increases brain metabolism in regions that are under cholinergic influence and involved with cognition, such as cingulate cortex, hippocampus and thalamus. These data highlight the utility of this methodology for assessing the effects of cognitive enhancing agents.

References:

1. McCulloch, J. (1982).Handbook of Psychopharmacology.Iverson LL. et al.New York, Plenum:321

2. Sokoloff L. et al. (1977).J Neurochem 28(5):897-916

3. Forette, F., R. Anand, et al. (1999).Eur J Neurol 6(4):423-429

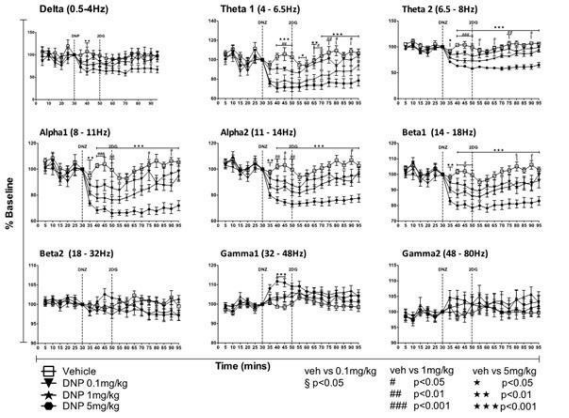

Fig1. EEG power per frequency band in cingulate cortex electrode. 5min time bins normalised to baseline. Each point is mean±sem of 8 rats per group, statistical analysis was 2way repeated measures ANOVA with Bonferroni post hoc test.

[Figure 1]

SCM-198 ATTENUATES LIPOPOLYSACCHARIDE- AND BETA-AMYLOID INDUCED MICROGLIAL INFLAMMATION IN VITRO AND IN VIVO THROUGH TLR4/JNK/NF-ΚB SIGNALING CASCADE

Y.Z. Hong, K. Zhu, R.X. Shi, T.T. Wu, Z.Y. Zhu

School of Pharmacy, Department of Pharmacology, Fudan University, Shanghai, China

Background: Chronic inflammation in central nervous system (CNS) is a conspicuous hallmark in neurodegenerative diseases, including Alzheimer's disease (AD) and microglia activation is now widely accepted as a key factor in neuroinflammatory responses. Leonurine, also called SCM-198, is an alkaloid extracted from *Herba leonuri.* In the present study, we investigated its possible anti-neuroinflammatory therapeutic effects both in vitro and in vivo[1-2].

Methods: Immortalized murine BV-2 microglial cell line and purified rat primary microglia were incubated with 1μg/ml lipopolysaccharide (LPS) or 1μM β-amyloid$_{1-40}$ ($Aβ_{1-40}$) or were preincubated with different concentrations (0.01-10μM) of SCM198 two hours before LPS and $Aβ_{1-40}$ treatments. Cell viability, nitric oxide production, proinflammatory cytokine release were measured by MTT assay, Griess reaction and ELISA, respectively. Real-time PCR and Western Blot were used to analyze gene and protein expressions and immunocytochemistry staining was performed for observing nuclear translocation of NF-κB in microglia. Toll-like receptor 4-small interfering RNA (TLR4-siRNA) and inhibitors of MAPKs were applied to investigate possible mechanisms of SCM-198. Moreover, microglia/neuron co-culture system was applied to investigate whether SCM-198 could protect neuron indirectly via inhibiting the activation of microglia. For in vivo study, Sprague-Dawley (SD) rats with bilateral intrahippocampal $Aβ_{1-40}$ injections were selected as AD model: 60 male SD rats were randomly divided into six groups: sham group, $Aβ_{1-40}$ group, $Aβ_{1-40}$ +SCM198 15, 30, 60 mg/kg groups, Donepezil group (DON, 1.0 mg/kg as a positive control) (n = 10, respectively). Cognitive performance was evaluated by novel object recognition task (NOR) and Morris water maze (MWM), microglia activation was detected by immunohistochemistry staining; gene and protein expressions were analyzed by Real-time PCR, ELISA, Western blot.

Results: We found that SCM-198 could reduce nitric oxide production from LPS-activated microglia and could inhibit iNOS, TNF-α, IL-1β mRNA and protein expressions both in vitro and in vivo. Furthermore, LPS-induced NF-κB translocation in BV-2 cells was effectively mitigated by SCM-198. Consistently, suppression of IκBα degradation, NF-κB p65 activation, phosphorylation of JNK1/2 and tau protein was observed both in vitro and in vivo. Microglia/neuron co-culture assay showed that pretreatment of activated microglia with SCM198 could significantly increase neuronal survival and alleviate excessive tau phosphorylation and synaptophysin degradation in neuron. Animal studies demonstrated that 30mg/kg and 60mg/kg SCM-198 could effectively ameliorate cognitive deficits in $Aβ_{1-40}$ groups and suppress microglial activation in CA1 region of rat hippocampus and cortex. TLR4-siRNA assay revealed that TLR4 might take part in the SCM-198-induced inhibition of microglia.

Conclusions: Our findings are the first to report that SCM-198 has marked neuroprotective effects via its anti-inflammatory effects on inhibiting microglial activation in AD models. Therefore, SCM-198 might be a new potential drug candidate for AD therapy in the future.

Reference:

1 Cameron, B. & Landreth, G. Inflammation, microglia, and Alzheimer´s disease. *Neurobiol Dis* **37**, 503-509, doi:S0969-9961(09)00283-6 [pii]

10.1016/j.nbd.2009.10.006 (2010).

2 Zhang, Y. *et al.* SCM-198 attenuates early atherosclerotic lesions in hypercholesterolemic rabbits via modulation of the inflammatory and oxidative stress pathways. A*therosclerosis* 2**24,** 43-50, doi:10.1016/j.atherosclerosis.2012.06.066 (2012).

DANHONG INJECTION PROTECTS THE BRAIN AGAINST ISCHEMIA-REPERFUSION INJURY

S. Wang, H. Guo, L. Chai, B. Chuluun, X. Wang, H. Yang, **L. Hu**

Tianjin State Key Laboratory of Modern Chinese Medicine, Tianjin University of Trational Chinese Medicine, Tianjin, China

Background: The development of stroke therapeutic agents remains an urgent priority. Danhong injection (DHI), a Chinese Materia Medica standardized product extracted from Radix Salviae miltiorrhizae and Flos Carthami tinctorii, is widely used for treating acute ischemic stroke in China. In the present study, the neuroprotective efficacy of DHI was confirmed in rat temperary MCAO models and the potential mechanisms in this process was evaluated.

Methods: Male Wistar rats pretreated or posttreated with either DHI (0.9, 1.8 and 3.6 ml/kg) were subjected to 1 hours of temporary MCAo. Neurologic status, infarct areas, Blood Brain Barrier (BBB) permeability, malondialdehyde (MDA) and inhibition of microglial activation were determined on days 1 and/or 3d after MCAo.

Results: Pretreatment with DHI (3.6 and 1.8 ml/kg) significantly improved the neurologic score compared with vehicle-treated rats at 24 hours and 72 hours. DHI (1.8 ml/kg) significantly reduced infarct volume compared with vehicle-treated rats. BBB permeability, MDA and microglial activation were also significantly reduced by pretreatment with DHI (1.8 ml/kg) in 24h. Posttreatment with DHI (1.8 ml/kg) also could significantly ameliorate neurologic score and infarct volume compared with vehicle-treated rats.

Conclusions: We conclude that DHI protects the brain against ischemia-reperfusion injury through multimechanism - protection of BBB disruption, antioxidation and inhibition of microglial activation.

THERAPEUTIC EFFECTS OF BRYOSTATIN-1 ADMINISTRATION ON ISCHEMIC STROKE IN AGED RATS

J.D. Huber[1], Z. Tan[2], X. Li[2], R.C. Turner[2], C.L. Rosen[2]

[1]Basic Pharmaceutical Sciences, [2]Neurosurgery, West Virginia University, Morgantown, WV, USA

Background and purpose: Ischemic stroke is the major cause of long-term disability with few therapeutic options. Due to the advanced aging of the population, the problem is only going to get worse and new therapeutics for acute ischemic stroke are needed. Bryostatin-1, a macrolide lactone, is a potent PKC activator that has shown promising therapeutic potential in increasing neuronal outgrowth and improving cognition and memory in models of associative memory, Alzheimer's disease, global ischemia, and traumatic brain injury.. In this study, we tested the hypothesis that administration of bryostatin-1 provides a therapeutic benefit in aged rats following experimental stroke.

Methods: Focal cerebral ischemia was produced by reversible occlusion of the right middle cerebral artery using a fibrin clot in 18-20 month old female Sprague-Dawley rats. After 2 h of ischemia, reperfusion was produced by lysis of the clot using tissue plasminogen activator. At 6 h after MCAO and then at 3, 6, 9, 12, 15, 18, and 21 d, bryostatin-1 or saline was administered. Functional assessment was conducted at 1, 3, 7, 14, and 21 d on the rats after MCAO. After functional assessment at 21 d, rats were euthanized and brains removed. Brains were assayed for infarct volume and immunohistochemistry to determine magnitude of ischemic brain injury.

Results: Bryostatin-1 treated rats showed improved survival following MCAO, especially during the first 4 d. Repeated administration of bryostatin-1 following MCAO resulted in reduced infarct volume and improved neurological function at 21 d after MCAO. Changes in PKC expression in neurons were noted in bryostatin-treated rats at 24 h following MCAO.

Conclusions: Repeated bryostatin-1 administration following MCAO protected the brain from severe neurological injury following

MCAO in aged rats. Bryostatin-1 treatment improved survival rate, reduced infarct volume, salvaged tissue in infarcted hemisphere by reducing necrosis and peri-infarct astrogliosis, and improved functional outcome following MCAO.

EFFECT OF CURCUMIN ON LEARNING AND MEMORY AND THE EXPRESSION OF AB42 IN BRAIN OF TG2576 TRANSGENIC MICE

J. Sun, **Y. Li**

Department of Pathology, Institute of Neuroscience, Chongqing Key Laboratory of Neurobiology, Chongqing Medical University, Chongqing, China

Objective: To observe the effect of curcumin on the ability of learning and memory of APPswe/PS1dE9 double transgenic mice and its influence on the expression of Aβ42 in brain, and to investigate the effect of curcumin in prevention and treatment of Alzheimer's disease.

Methods: 20 six-month-old APPswe/PS1dE9 double transgenic mice were randomly divided into the control group and the curcumin group. The mice in the curcumin group were fed curcumin 500 ppm every day. Morris water maze and fear conditioning test were used to assess the ability of learning and memory of the mice, and the changes of expression of Aβ42 in brain were detected by immunohistochemistry six months later.

Results: Compared with the control group, the ability of learning and memory of mice in the curcumin group was improved significantly ($P < 0.01$), while the expression of Aβ42 in brain was reduced.

Conclusion: Curcumin can reduce the expression of Aβ42 in the brain of APPswe/PS1dE9 double transgenic mice and improve their ability of learning and memory.

This work was supported by the National Natural Science Foundation of China (NSFC: 81271426, 30973154, 81100948). Corresponding author: Yu Li, M. D., Professor . Email: liyu100@163.com

EFFECT OF CURCUMIN ON THE EXPRESSION OF SR-BI AND ABCA1 IN NEURONS OF HIPPOCAMPUS OF APPSWE/PS1DE9 DOUBLE TRANSGENIC MICE

J. Sun, **Y. Li**

Department of Pathology, Institute of Neuroscience, Chongqing Key Laboratory of Neurobiology, Chongqing Medical University, Chongqing, China

Objective: To observe the effect of curcumin on expression of SR-BI and ABCA1 in neurons of hippocampus of APPswe /PS1dE9 double transgenic mice, and to investigate the mechanism of curcumin in prevention and treatment of Alzheimer's disease.

Methods: 20 six-month-old APPswe/PS1dE9 double transgenic mice were randomly divided into the control group and the curcumin group. Each group has 10 mice. The mice in the curcumin group were fed curcumin 500 ppm every day. Six months later the changes of the expression of SR-BI and ABCA1 in neurons of hippicampus were detected by immunohistochemistry.

Results: Compared with the control group, the expression of ABCA1 in neurons of hippocampus of mice in the curcumin group was increased significantly($P=0.007$), while the expression of SR-BI was not detected in both groups.

Conclusion: Curcumin can induce the expression of ABCA1 in neurons of hippocampus of APPswe/PS1dE9 double transgenic mice, while the expression of SR-BI was not detected in neurons.

This work was supported by the National Natural Science Foundation of China (NSFC: 81271426, 30973154, 81100948). Corresponding author: Yu Li, M. D., Professor. Email: liyu100@163.com

LOSARTAN IMPROVES CEREBROVASCULAR FUNCTION IN A MOUSE MODEL OF ALZHEIMER'S DISEASE OVEREXPRESSING AMYLOID-B AND TRANSFORMING GROWTH FACTOR-B1

P. Papadopoulos, X.-K. Tong, E. Hamel

Laboratory of Cerebrovascular Research, Montreal Neurological Institute, McGill University, Montréal, QC, Canada

Objectives: Alterations of the renin-angiotensin system (RAS) are thought to be involved in the pathogenesis of Alzheimer's disease (AD) (1). Here, we tested the efficacy of losartan, a selective angiotensin II type 1 receptor (AT1R) antagonist, in alleviating cerebrovascular and cognitive deficits in A/T mice that overexpress a mutated form of the human amyloid precursor protein $APP_{Swe,Ind}$ and a constitutively active form of the transforming growth factor-β1 (TGF-β1) (2). These mice integrate the comorbidity of cerebrovascular fibrosis and microvascular degeneration (3) to the amyloid-β (Aβ)-induced memory deficits, amyloidosis and cerebrovascular oxidative stress of APP mice (2).

Methods: We tested two doses (10mg/kg/day and 25mg/kg/day in drinking water for 3 months) of losartan in ~6 month-old bitransgenic A/T mice. At endpoint, spatial learning and memory in the hippocampal-based spatial Morris water maze (MWM) were assessed (4). Then, the evoked cerebral blood flow (CBF) response to whisker stimulation was measured by laser Doppler flowmetry. Mice were subsequently sacrificed for functional reactivity of posterior cerebral artery (PCA) segments to dilators and constrictors by online videomicroscopy. Brain tissue and cerebral blood vessels were frozen for subsequent protein studies (Western blot and ELISA). Other mice were perfused for immunohistochemical quantification of astrocytic activation and amyloidosis.

Results: Losartan displayed dose-related rescuing effects on cerebrovascular reactivity, particularly on vasodilatory responses to acetylcholine (ACh) and calcitonin gene-related peptide (CGRP) despite a lack of improvement of the tonic production of nitric oxide. These vasomotor responses occurred without changes in cerebrovascular protein levels of the antioxidant enzyme superoxide dismutase (SOD2). However, losartan failed to normalize the lessened neurovascular coupling response to sensory stimulation and to attenuate the astroglial activation. The impaired learning and memory performances of A/T mice were not rescued by losartan at either dose. Similarly, the increased brain levels of soluble and insoluble $Aβ_{1-40}$ and $Aβ_{1-42}$ in cortex and hippocampus were not normalized by losartan at any dose. Accordingly, Aβ plaque load was not reduced among groups as determined by thioflavin-S staining of dense-core Aβ plaques.

Conclusions: Our results are the first to demonstrate the capacity of losartan to improve cerebrovascular reactivity in a model of combined Aβ- and TGF-β1-induced cerebrovascular dysfunction. Data suggest that losartan and, possibly, other AT1R antagonists, may be a promising therapeutic avenue for restoring cerebrovascular function in patients with vascular diseases at high risk of developing AD, or for AD patients with cardiovascular diseases. Moreover, a combined therapy may be warranted for a complete rescue of both vascular and cognitive deficits.

Supported by: The Canadian Institutes of Health Research (CIHR grant MOP-84275 to EH) and a Jeanne Timmins Costello Fellowship (PP).

References:

1. Wright and Harding, 2010, Exp. Neurol. 233: 326-333

2. Ongali et al., 2010, Am J Pathol. 177: 3071-3080.

3. Wyss-Coray et al., 2000, Am J Pathol. 156: 139-150

4. DeIpolyi et al., 2008, Neurobiol. Aging. 29: 253-266.

COCAINE NEUROTOXICITY AND BEHAVIORAL DYSFUNCTIONS ARE EXACERBATED BY SIZE-DEPENDENT CERIUM OXIDE NANOPARTICLES IN RATS

R. Patnaik[1], A. Sharma[2], D.F. Muresanu[3], H.S. Sharma[2]

[1]Biomaterials, School fo Bioengineering, National Institute of Technology, Banaras Hindu University, Varanasi, India, [2]Surgical Sciences, Anesthesiology & Intesnive Care Medicine, Uppsala University, University Hospital, Uppsala, Sweden, [3]Clinical Neurosciences, University of Medicine & Pharmacy, University Hospital, Cluj-Napoca, Romania

Exposure to Cerium oxide (CeO2) nanoparticles from the environment to humans is quite common now-days. The potential sources of CeO2 nanoparticles are diesel engines exhaust and use of various household products including toothpaste, bacteria free socks or swimsuits. Inhalation or dermal contact of CeO2 is supposed to induce cardiac or pulmonary toxicity over time. However, neurotoxicity of CeO2 is not well known. CeO2 is known to induce oxidative stress in biological material and thus it appears that controlled exposure of this nonmaterial may enhance BBB dysfunction and/or neurotoxicity. The present investigation was carried out to determine whether various particle sizes of CeO2 could be able to enhance cocaine penetration in the brain resulting in exacerbation of neurotoxicity and behavioral dysfunction in a rat model. Rats were intoxicated with CeO2 nanoparticles (20-25 nm or 50 to 60 nm) 25 mg or 50 mg/kg, i.p. once daily for 10 days. This treatment resulted in 12-to 20-fold increase in Ce in the blood plasma (from 5±2 ng/ml to 64±6 ng/ml with 25 mg dose and 96±6 ng/ml with 50 mg dose) in these rats. When cocaine (40 mg/kg) was administered intraperitoneally in CeO2 intoxicated rats, the hyperlocomotor activity and behavioral functions e.g., back side waking on hind legs, jumping and fighting behaviors was exacerbated as compared to saline treated rats that was dose and size related. Thus, small sized CeO2 nanoparticles in high doses induced most aggravated cocaine induced behavioral changes.

Measurement of cocaine levels in the brain in Ce treated rats showed 8 to 18-fold increase (66±5 ng/g with 50 nm Ce nanoparticles 50 mg/kg; and 98±8 ng/g with 25 nm Ce, 50 mg/kg) as compared to saline treated group (8±2 ng/g). This suggests that increase in cocaine concentration in the brain following CeO2 intoxication was related with the dose and size of the nanoparticles. Interestingly, BBB disruption, brain edema formation and brain pathology in terms of neural injuries were much more aggravated by small sized CeO2 nanoparticles in high doses as compared to large size of the nanoparticles in identical doses after cocaine administration. Taken together our results for the first time show that CeO2 nanoparticles are able to induce significant higher brain damage and BBB disruption in a dose and size related manner enabling more penetration of cocaine into the brain causing greater neurotoxicity. The possible mechanism of size related enhanced neurotoxicity by CeO2 nanoparticles appears to be related with their ability to induce oxidative stress in the brain, a feature that is currently being investigated in our laboratory.

ANGIOTENSIN TYPE-1 RECEPTOR BLOCKAGE WAS ASSOCIATED WITH BRAIN PROTECTION BUT NOT IN REPAIR AFTER CEREBRAL INFARCT IN EXPERIMENTAL ANIMAL MODEL

B. Rodríguez-Frutos, M. Gutiérrez-Fernández, J. Ramos-Cejudo, B. Fuentes, E. Díez-Tejedor

La Paz University Hospital, IdiPAZ, UAM, Madrid, Spain

Introduction: After cerebral infarct, the elevated blood pressure is associated with bleeding, worse prognosis and death. The protective properties of angiotensin type 1 receptor blockade (as olmesartan) have been reported by improved cerebral blood flow, the restoration of endothelial nitric oxide synthase, decreased inflammation, or stimulation of the angiotensin type 2 receptor. Olmesartan could be involucrate in brain protection and repair.

Aim: To analyze olmesartan effects (treatment and pre-treatment) on functional recovery associated with brain protection and repair after permanent middle cerebral artery occlusion (pMCAO) in rats.

Methods: Adult male Sprague- Dawley rats distributed into 4 groups (n=4): 1- Sham (surgery without pMCAO); 2-Control (surgery + pMCAO); 3-Olmesartan (surgery + infarct +olmesartan (10 mg/kg per day for 14 days);

4- Olmesartan pre-treatment (olmesartan (10 mg/kg) for 7 days before infarct+surgery+infarct+ olmesartan (10 mg/kg per day for 14 days)). We analyzed: functional recovery (Rogers modified scale and Rota-Rod test) at 3,7 and 14 days, lesion volume by magnetic resonance imaging (MRI) at 3 and 14 days and by hematoxyline-eosin (H&E) at 14 days, cell death by TUNEL at 14 days, anti-inflammatory cytokines (IL-4, IL-10) by ELISA at 7 and 14 days, repair markers implicated in brain plasticity: VEGF (vascular endothelial growth factor), GFAP (glial fibrillar acid protein) and Synaptophysin by western blot and immunofluorescence at 14 days. Rats were sacrificed at day 14.

Results: Olmesartan group showed a significance functional recovery at 14 days ($p = 0,030$) by Rogers' Scale in comparison with Control group. We did not observe a reduction in lesion volume neither at day 3 nor day 14 by MRI ($p>0,05$); however we observed a significance reduction in Olmesartan ($p=0,027$) and Olmesartan pre-treatment ($p=0,006$) groups in comparison with Control group by H&E. Levels of anti-inflammatory cytokines, IL-4 and IL-10, did not showed significant differences between groups ($p>0.05$). Olmesartan ($p=0.011$) and Olmesartan pre-treatment ($p=0,022$) groups showed a decrease in cell death compared to Control group. We did not observe significant differences in VEGF, GFAP and synapthophysin expression between control and treated groups.

Conclusions: Olmesartan treatment, before and after cerebral infarct in experimental animal model, shows benefits effects in respect to brain protection (decrease lesion size and cell death) but not in brain repair markers.

Supported by grants from Pfizer.

THE OPTIMAL DIRECTIONS DEVELOPMENT OF TREATMENT EVOKED BY EXPERIMENTAL CHRONIC INFLAMMATION OF THE ANXIETY-RELATED AND DEPRESSIVE-RELATED BEHAVIORS

Y.V. Sidorova, O.G. Obraztsova, D.V. Evdokimov, I.I. Abramets

Pharmacology, Donetsk National Medical University, Donetsk, Ukraine

Rationale: The inflammation products (interleukines, prostaglandines, leukotrienes et al.) exert influence upon the synaptic transmission and functional state of the brain limbic system neurones. These influences evoke disorders of emotional and motivational processes and require of a pharmacological correction.

Objective: A choise of drugs with optimal activity with regard to remission anxiety- and depression-related behaviors at experimental chronic inflammation.

Methods: The chronic inflammation at white inbred rats evoked by administration of 9 % acetic acid under dorsum skin and in parallel intraperitoneal administration of 200 mg/kg of dextran. A level of depression-related behaviors in the forced swim test estimated by alteration of immobility time. The elevated plus-maze test used up for estimation of anxiety-related behaviors. A level of anxiety estimated by alteration of time spent in open arms of apparatus elevated plus-maze by every rats. We used up the following pharmacological drugs - nimesulide, paracetamol, imipramine, fluoxetine, ketamin, verapamil.

Results: A modeling of chronic inflammation at rats evoked increasing of anxiety-like behavior in the elevated plus-maze and animals showed higher level immobility in the forced swim test. The rats spent less time in the open arms of the elevated plus-maze - $50,6 \pm 3,7$ s against $136,3 \pm 25,2$ s ($p < 0,05$) as compared to control. It was observd increasing a time of immobility - $158,3 \pm 6,3$ s against $125,3 \pm 6,3$ s ($p< 0,05$) as compared to control. Verapamil and imipramine only counteracted to evoked by chronic inflammation increasing anxiety-like behavior - rats spent more time in the open arms of the elevated plus-maze $122,1 \pm 5,4$ s and $73,7 \pm$

4,1 s (p< 0,05) respectively. All the observable drugs counteracted increasing of depressive-like behavior evoked by chronic inflammation by reduction of immobility time to 138,9 ± 3,2 s - 119,4 ± 5,0 s (p< 0,05). We found in early experiments increasing of the 5-hydroxytryptamine neuronal uptake and reduction of serotonergic influences. It were found too up-regulation of neuronal N-methyl-D-aspartate receptors with NR2A subunit. Since the drugs used in our experimrnts influenced differentially on the anxiety-related and depression-related behaviors but anxiety and depression are comorbidity at patients with chronic inflammation treatment these syndromes is difficult.

Conclusion: For simultaneous abatement of the anxiety and depressive syndromes at patients with chronic inflammation accordingly with our experimental data best of all fit the blockers of the voltage-dependent calcium channels including verapamil.

ANGIOTENSIN RECEPTOR BLOCKER CANDESARTAN DIRECTLY BINDS TO MOLECULAR CHAPERONE HSP70 AND STIMULATES ITS PRODUCTION IN THE HIPPOCAMPAL CA1 NEURONS

T. Sugawara[1], K. Kokubun[1], R. Ishida[2], K. Fujiwara[2], S. Yamamoto[2], H. Itoh[2], H. Kinouchi[3], K. Mizoi[1]

[1]Neurosurgery, [2]Material-Process Engineering and Applied Chemistry for Environments, Akita University, Akita, [3]Neurosurgery, University of Yamanashi, Chuo, Japan

Objectives: Angiotensin II type 1 receptor blockers (ARBs) are used worldwide for the treatment of hypertension, and recent clinical trials have revealed protective effects against stroke that are independent of the reduction of blood pressure. Experimental studies also showed ARB ameliorated ischemic neuronal injury. We have previously shown that ARB protected vulnerable hippocampal neurons from apoptotic cell death after ischemia, but the mechanisms of the protection remain obscure. This study is conducted to elucidate the neuroprotective mechanisms of the ARB candesartan.

Methods: Candesartan-specific binding proteins were investigated using candesartan-affinity column and rat hippocampal tissue. Affinities between ARB and binding proteins were further examined by Biacore binding assay. The expression of the proteins in the hippocampus was characterized by immunohistochemistry and Western blot analysis.

Results: The affinity column study identified molecular chaperone heat-shock protein 70 family proteins (HSP70s) as the binding targets of candesartan. Biacore assay proved functional binding of candesartan to inducible and constitutive forms of HSP70s, HSP72 and 73, respectively. Immunohistochemistry showed HSP72 expression was low in the cytosol of the hippocampal CA1 neurons but increased as early as 1 day after candesartan treatment. Western blot analysis confirmed the temporal changes in HSP72 expression.

Conclusions: Modification of HSP70s by candesartan-binding ultimately increases HSP72 expression in the neurons. Since HSP72 induces ischemia tolerance and inhibits apoptosis in vulnerable neurons, increased HSP72 level may explain the mechanism of neuroprotection by ARB.

EDARAVONE SENSITIZES THROMBOLYSIS AND PROPHYLACTICALLY PROTECTS HYPOXIC-ISCHEMIC BRAIN INJURY

Y.-Y. Sun[1], K. Abe[2], D.M. Lindquist[3], C.-Y. Kuan[1]

[1]Department of Pediatrics (Neurology), Emory University School of Medicine, Atlanta, GA, USA, [2]Department of Neurology, Okayama University, Okayama, Japan, [3]Department of Radiology, Cincinnati Children's Hospital Medical Center, Cincinnati, OH, USA

Objectives: The rationale for combined thrombolysis and antioxidant therapy of acute ischemic stroke is sound, despite the negative result of NXY-059 in clinical trials. In the search for more effective antioxidants, edaravone is a promising candidate because it has been used as a stand-alone therapy of acute stroke in Japan and it enhances recanalization by acute tPA-infusion. In animal studies, pre-ischemia administration of edaravone extends the therapeutic window of tPA, but whether post-ischemia edaravone treatment increases the efficacy of thrombolysis is yet to be determined. It is also uncertain if edaravone is an effective prophylactic agent of global hypoxia-ischemia during cardiac surgery. The objective of our study is to answer these two questions.

Methods:

(a) We further modified the adult hypoxia-ischemia (HI) model of thrombotic stroke (Adhami et al., 2006) using transient ligation of carotid artery plus systemic hypoxia (7.5% O2).

(b) Whether such transient HI (tHI) induces thrombosis and responds to post-tHI tPA therapy (10 mg/kg bolus via tail-vein at 0.5, 1, or 4h recovery) was examined.

(c) We tested whether post-tHI edaravone supplement (3 mg/kg, IP, at 0, 1, and 2 h recovery) synergizes with the tPA treatment. (d) The efficacy of edaravone as a stand-alone post-tHI or prophylactic treatment was evaluated.

Results:

(a) The combination of transient common carotid artery occlusion and 30-min hypoxia produced thrombosis and infarction (Fig. A).

(b) Post-tHI treatment with tPA, especially when initiated early as in clinical settings, decreased brain infarct.

(c) Edaravone synergized with acute tPA-injection (Fig. B), and the efficacy of combined tPA/edaravone therapy was evident in the infarct volume, post-tHI cerebral reperfusion, oxidative stress, inflammation, blood-brain barrier damage, and the integrity of white-matter under EM and diffusion tensor imaging (DTI) analysis.

(d) Administration of Edaravone alone also has prophylactic, as well as, acute therapeutic effect.

Conclusions: Using a simple preclinical model of thrombotic stroke, we showed that edaravone synergizes with thrombolysis therapy and has benefits as a stand-alone prophylactic treatment of global HI. Potential clinical benefits of combined tPA/edaravone therapy warrant investigation.

References:

Adhami F et al (2006) Cerebral ischemia-hypoxia induces intravascular coagulation and autophagy. Am J Pathol. 169:566-83.

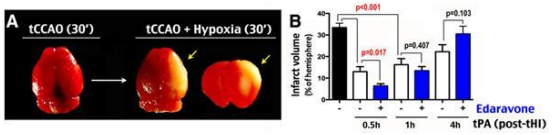

[tPA/Edaravone graph]

SIMVASTATIN RESTORED ENDOTHELIAL AND SMOOTH MUSCLE CELL FUNCTION AND REDUCED STRING VESSEL PATHOLOGY IN TRANSGENIC TRANSFORMING GROWTH FACTOR-B1 MICE

X.-K. Tong, E. Hamel

Laboratory of Cerebrovascular Research, Montreal Neurological Institute, McGill University, Montréal, QC, Canada

Background and objectives: Our previous studies showed that simvastatin, a cholesterol-lowering drug, normalized memory and cerebrovascular deficits, and exerted anti-inflammatory and antioxidative effects in transgenic Alzheimer's disease (AD) mice that recapitulate the amyloid (Aβ) pathology (1, 2). Here, we tested the efficacy of simvastatin in a transgenic mouse model of AD cerebrovascular pathology overexpressing a constitutively active form of transforming growth factor-β1 (TGF mice) (3). TGF mice display thickening of the vascular basement membrane, perivascular astrocytosis, microvascular degeneration (3), and cerebrovascular deficits (4).

Methods: 18 months old TGF mice and wild-type (WT) littermate controls were treated or not with simvastatin (40mg/kg/day in the drinking water, 2 months). Mice were submitted to memory testing (Morris water maze), and subsequently divided in two groups. One group was used for cerebrovascular reactivity measurements of middle (MCA) or posterior (PCA) cerebral artery segments. Proteins extracted from cerebral cortex, hippocampus or from the remaining arteries of the Circle of Willis and attached main branches were used for Western blot analysis. The other group was perfused (4% paraformaldehyde) and brains were sliced in thin (5µm; paraffin) or thick (25µm) sections for immunohistochemical and NADPH diaphorase stainings.

Results: As previously reported (5), TGF mice did not exhibit significant deficits in spatial learning and memory. Simvastatin had no effect on cognitive performance, on brain levels of TGF-β1, and it did not reduce astroglial or microglial cell activation. However, simvastatin improved dilatory function to acetylcholine, completely normalized dilations to calcitonin gene-related peptide (CGRP) and the baseline synthesis of the endothelium-generated dilator nitric oxide (NO). Western blot analysis showed decreased levels of NO synthase protein in TGF brain vessels (-16%, $p< 0.05$) compared to WT, with a slight improvement after simvastatin treatment (+10.6%). The impaired contractions induced by endothelin-1 (ET-1) and dilatations mediated by KATP channels were improved in simvastatin-treated TGF mice. Simvastatin did not rescue cerebrovascular fibrosis since deposition of collagen I and IV in cerebral and intraparenchymal blood vessels was not reduced by treatment. However, simvastatin significantly reduced the number of abnormal large blood vessels in brain cortex and the number of cortical and hippocampal string vessels considered as degenerating capillaries lacking endothelial cells.

Conclusions: Our results indicate that simvastatin has therapeutic benefits in restoring cerebrovascular reactivity mediated by endothelial and smooth muscle cells despite an ongoing cerebrovascular fibrosis. Simvastatin also exerted positive effects on NO synthesis that likely helped reduce the number of degenerating string vessels. However, cerebrovascular fibrosis and glial cell activation were not improved by simvastatin at such an advanced age. We conclude that simvastatin could be a promising drug in the treatment of cerebrovascular dysfunction as seen in AD patients with a cerebrovascular pathology (3).

Supported by: The Canadian Institutes of Health Research (CIHR, grant MOP-84275, EH).

References:

1- Tong XK et al., Neurobiology of Disease, 2009;35:406-14

2- Tong XK et al., J Neuroscience, 2012;32:4705-15

3- Wyss-Coray T et al., Am J Pathology, 2000 156:139-50

4- Tong XK et al., J Neuroscience, 2005;25:11165-74

5- Nicolakakis N et al., J Neuroscience, 2008;28:9287-96

EFFECTS OF RECOMBINANT ANNEXIN A2 COMBINED WITH LOW-DOSE TPA IN LONG-TERM NEUROLOGICAL OUTCOMES OF FOCAL EMBOLIC STROKE IN RATS

X. Wang[1,2], X. Fan[1], Z. Yu[1], Z. Liao[1,2], E. Mandeville[1], N. Liu[1], J. Zhao[1], E.H. Lo[1], **X. Wang**[1]

[1]Departments of Neurology and Radiology, Massachusetts General Hospital and Harvard Medical School, Charlestown, MA, USA, [2]Departments of Neurosurgery, The First Affiliated Hospital, Chongqing Medical University, Chongqing, China

Background and purpose: Clinically given large amount of tPA alone but lacking fibrinolytic assembly of tPA-annexin A2-plasminogen complex formation, which makes tPA converting plasminogen to plasmin insufficiently, in turn it may be partially responsible to the shortcomings of tPA stroke reperfusion therapy, “high dose tPA required, high hemorrhage risk, low reperfusion efficiency, and short therapeutic time window” that have been considerable of a major challenge and priority in our field. We have hypothesized are that tPA combined with recombinant Annexin A2 protein (rA2) will lower the required dose of tPA for reperfusion, while enhancing thrombolytic efficacy, and attenuating intracerebral hemorrhagic transformation. Our previous studies demonstrated that combination of rA2 plus low dose tPA significantly improved reperfusion examined by MRI, and decreased acute brain infarction and intracerebral hemorrhage. In this preclinical study we further tested our hypothesis that mechanisms of improved blood flow and reduced neurovascular side-effects may ultimately translate into smaller infarcts and improved long-term outcomes.

Methods: Male Wistar rats (300-350g) were subjected into a focal embolic stroke model and treated at 3 hours after stroke onset. All animals were randomized assigned to two sets of experiments. In first set, treatment groups were: 10 mg/kg tPA, 5 mg/kg tPA and 5 mg/kg tPA plus 10 mg/kg rA2, respectively. Brain infarction and hemorrhage were examined at

24 hours after stroke. n=20 per group. In second set of experiment for long-term neurological outcomes, treatment groups are: standard ˝rat dose" tPA 10 mg/kg, combination dose of 5 mg/kg tPA plus 10 mg/kg rA2. n=30 per group. Due to unacceptable high mortality, the non-thrombolytic saline control group was not included for long-term study. All treatments were blinded to investigators who made stroke models and measured outcomes. Neurobehavioral tests were assessed with modified neurological severity score (NSS) and foot fault test for motor coordination function, adhesive tap-removal test for sensorimotor neurological deficits on days 1, 3, 7, 14, 21, and 28 after stroke. Mortality and brain infarction were also examined.

Results: In acute brain tissue damage study, there were no significant differences between saline, tPA 5 mg/kg, and tPA 10 mg/kg in 24 hours brain infarction size, while 10 mg/kg tPA significantly increased brain hemorrhage volume. However the combination group significantly reduced both infarction and hemorrhage compared to all other groups. In long-term outcome study, there was no significant difference in the mortality between tPA alone group (13/30) and the combination group (6/30) (two-sided Fisher´s exact test, P=0.095). But the infarction volume in combination group was significantly smaller than tPA alone group with reduction rate of 19.6%. We also found there were significant improvements in combination treatment group at multiple time points including the 28 day after stroke for all the three neurobehavior assessments compared to tPA alone treatment group.

Conclusion: Treated at 3 hours after focal embolic stroke in rats, the combination of 5 mg/kg tPA plus 10 mg/kg rA2 has significant improvements in one month neurological outcomes and smaller brain infarction than the 10 mg/kg tPA alone treatment group.

PROTECTIVE EFFECT OF ORAL LACTULOSE AGAINST CEREBRAL ISCHEMIA-REPERFUSION INJURY IN RATS

X. Zhai[1], X. Chen[1], J.Z. Shi[2], Z.H. Ye[2], Z.M. Kang[3], X.J. Sun[3]

[1]Graduates Management Unit, Changhai Hospital, Second Military Medical University, [2]Graduates Management Unit, Second Military Medical University, [3]Department of Diving Medicine, Faculty of Naval Medicine, Second Military Medical University, Shanghai, China

Objective: To determine the neuroprotective effects of oral lactulose against cerebral ischemia-reperfusion (I/R) injury in rats by inducing endogenous hydrogen.

Methods: The stroke model was created on Sprague-Dawley rats through middle cerebral artery occlusion (MCAO). The rats were randomly divided into four groups: sham operation group (sham group, n = 15); I/R group (MCAO group, n = 20); lactulose group (LAC group, n = 20); lactulose plus antibiotics group (ANTI group, n = 20).The neuroprotective effects of oral lactulose ware verified by behavioral tests, TTC and Nissl staining. Caspase-3 activity, malondialdehyde(MDA) contents, superoxide dismutase(SOD) activity and 8-OHdG counting cells of the affected brain tissue were determined. Exhaled hydrogen concentration was measured.

Results: The biochemical findings were matched with behavioral and histopathological verifications. Brain MDA content, caspase-3 activity and 8-OHdG counting cells in MCAO group and ANTI group significantly increased compared to sham group ($P< 0.05$) and significantly decreased in LAC groupcompared to MCAO group and ANTI group($P< 0.05$). SOD content in MCAO group and ANTI group were significantly decreased compared to sham group($P< 0.05$) and significantly increased in LAC group compared to MCAO group and ANTI group($P< 0.05$). Behaviorally and histopathologically, the changes were in the same direction with biochemical findings.Hydrogen breath concentration was significantly increased in LAC group compared to ANTI group ($P< 0.05$).

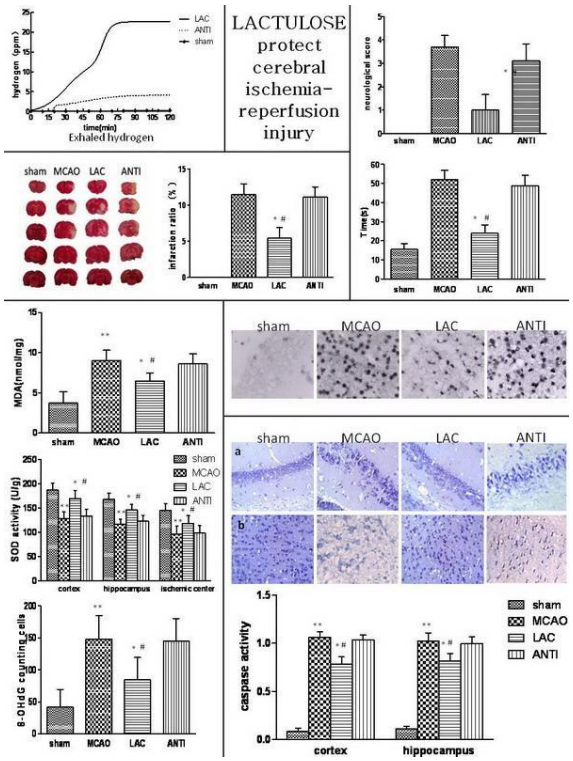

[lactulose results]

Conclusion: This study proved the neuroprotective activity of oral lactulose in experimentally I/R injury rats. The role may be associated with the production hydrogen gas by the fermentation of gut bacteria.

References:

[1] Donnan GA, Fisher M, Macleod M*, et al*. Stroke[J]. Lancet. 2008, 371: 1612-1623.

[2] Chan PH. Oxygen radicals in focal cerebral ischemia[J]. Brain Pathol. 1994, 4: 59-65.

[3] Ozkul A, Akyol A, Yenisey C*, et al*. Oxidative stress in acute ischemic stroke[J]. J Clin Neurosci. 2007, 14: 1062-1066.

[4] Nanetti L, Raffaelli F, Vignini A*, et al*. Oxidative stress in ischaemic stroke[J]. Eur J Clin Invest. 2011, 41: 1318-1322.

[5] Green PS, Simpkins JW. Neuroprotective effects of estrogens: potential mechanisms of action[J]. Int J Dev Neurosci. 2000, 18: 347-358.

[6] Ohsawa I, Ishikawa M, Takahashi K*, et al*. Hydrogen acts as a therapeutic antioxidant by selectively reducing cytotoxic oxygen radicals[J]. Nat Med. 2007, 13: 688-694.

NEUROMODULATORY PROPENSITY OF *WITHANIA SOMNIFERA* EXTRACTS AGAINST ROTENONE-INDUCED NEUROTOXICITY IN *DROSOPHILA MELANOGASTER*: IMPLICATIONS TO PARKINSON'S DISEASE

M.J. Manjunath, D.R. Muralidhara

Department of Biochemistry and Nutrition, CSIR-Central Food Technological Research Institute, Mysore, India

Objective: In recent times, natural product therapy has gained importance in the management of several neurodegenerative diseases such as Alzheimer's and Parkinson's disease (PD). *Withania somnifera* (L.) Dunal. (Solanaceae) root popularly known as the *Indian Ginseng* is widely used in the traditional Indian medicine as a nerve tonic and memory enhancer. We have investigated neuroprotective propensity of WS extracts to mitigate rotenone (ROT)-induced neurotoxicity employing *Drosophila melanogaster*.

Methods: Initially, we determined the ability of WS-enriched diet to modulate the levels of endogenous markers of oxidative status and antioxidant defense in wild *Drosophila (Oregon K).* Further, employing a co-exposure paradigm, we explored the propensity of WS to protect flies against ROT induced lethality, locomotor deficits, oxidative impairments and neurotoxicity. Adult male *Drosophila* maintained on WS-enriched medium (0.01, 0.05% w/v, 5d) were challenged with ROT (500µM). While the incidence of mortality was recorded every 24h, locomotor deficits were assayed by negative geotaxis assay on days 3 and 5. Terminally, flies (cytosol/mitochondria) of both control and treatment groups were subjected to various biochemical determinations (oxidative markers, antioxidant enzymes, cholinergic function and markers of mitochondrial function).

Result: WS offered concentration-dependent protection against ROT-induced lethality (30-95% protection), while the survivor flies performed better in the climbing assay suggesting attenuation of ROT-induced locomotor deficits. Biochemical investigations revealed that WS-enriched diet not only reduced the endogenous levels of various oxidative markers, but also normalized the

ROT-induced oxidative perturbations. Further, ROT exposure significantly diminished the activity levels of antioxidant enzymes which were restored with WS-supplements. In addition, WS markedly attenuated the ROT-induced elevation in the activity levels of acetylcholinesterase. Interestingly, WS restored the activity levels of mitochondrial marker enzymes (Complex I, SDH and MTT reduction assay) and ROT induced depletion in the dopamine levels.

Conclusion: Collectively, based on our previous data in the ROT mice model and current findings in Drosophila system, we suggest that *Withania somnifera* possesses excellent neuromodulatory potency and propose its use as a therapeutic adjuvant in protecting the CNS against oxidative stress mediated neurodegenerative diseases such as PD.

THROMBOPOIETIN REDUCES BRAIN INJURY AND COGNITIVE IMPAIRMENT IN RODENT CEREBROVASCULAR DISEASE MODELS

J. Zhou[1], H. Zhang[2], J. Li[1], J. Zhuang[1], C. Poon[1], D.M. Rosenbaum[1], **F.C. Barone**[1]

[1]SUNY Downstate Medical Center, Brooklyn, NY, USA, [2]Shanghai Institute of Materia Medica, Shanghai, China

Objectives: We recently demonstrated that Thrombopoietin (TPO) reduces brain injury and sensory-motor deficits following suture-focal stroke in the rat. TPO brain protection is mediated (in part) by vascular protection by reducing stroke-induced inflammatory cytokines, matrix metalloproteinase's and blood brain barrier injury. TPO translational information in multiple disease models and species with preservation of cognitive function is required. Embolic stroke is important because it represents closely the clinical stroke condition and allows for the investigation of thrombolysis safety when used with tPA. Mouse stroke is necessary to investigate protective effects following stroke in a second species. Mouse carotid stenosis mimics the forebrain hypoperfusion seen in atherosclerosis. It produces significant white matter injury that results in cognitive impairment. Here we demonstrate TPO increased brain protection and/or reduced vascular cognitive impairment in rat embolic stroke (with and without tissue plasminogen activator; tPA), in mouse suture-focal stroke and in mouse chronic carotid stenosis-induced forebrain hypoperfusion models of cerebrovascular disease.

Methods: Rats (Wistar) underwent embolic middle cerebral artery occlusion (MCAO) using a thrombus. Vehicle, tPA (10 mg/kg, iv), TPO (0.1 mg/kg, iv) or TPO combined with tPA were administered 2 hours post-stroke. Mice (C57Bl/6) underwent suture-MCAO or carotid artery stenosis-induced forebrain hypoperfusion and then received Vehicle or TPO (0.3 or 0.1 mg/kg, iv) at 1 hr or 1 day after surgery. Neurological deficits, complex learning in active place avoidance (APA) and/or hemispheric infarct size were measured for 1-21 days post-surgery.

Results: In rat embolic stroke, tPA or TPO plus tPA improved stroke-induced neurological deficits significantly. Significant post-stroke-induced deficits in APA cognitive performance were improved 87.2±16.4% by TPO or 69.4±9.7% by TPO plus tPA, but not by tPA alone. In mouse suture-focal stroke, brain infarcts were reduced by 64.5±7.7% and neurological deficits were reduced by 90.3±6.4%. In mouse carotid artery stenosis-induced forebrain hypoperfusion a single administration of TPO 1 day after surgery improved APA performance 84.8+3.1% 3 weeks later (all $p< 0.01$).

Conclusions: These data provide valuable information on the use of TPO to preserve/improve neurological and cognitive functions and reduce brain injury in rodent models of cerebrovascular disease. In summary, we have demonstrated TPO long-term protection and safety with and without tPA in rat embolic stroke, TPO acute brain protection in mouse suture-focal stroke and TPO long-term improvement in mouse forebrain hypoperfusion-induced APA learning deficits. The present multiple model and species work provides additional required translational data that further supports the potential multiple use of TPO in the future. Ongoing research is focused on understanding the additional protective mechanisms responsible for TPO efficacy in these cerebrovascular disease models.

SULFORAPHANE-INDUCED NEUROPROTECTION, THE ROLE OF CYSTINE TRANSPORT

J. Xiang[1], N. Zhou[1,2], G. Alesi[1], **R. Keep**[1]

[1]Neurosurgery, University of Michigan, Ann Arbor, MI, USA, [2]Pharmacology, Yunnan University of Traditional Chinese Medicine, Kunming, China

Objectives: Exposure to sulforaphane, a naturally occurring component of cruciferous vegetables, can induce neuroprotection in vitro and in vivo (1,2). Some of these effects involve activation of the transcription factor Nrf2 which regulates many antioxidant proteins, including those regulating glutathione (GSH). However, the acute effects of sulforaphane have received less attention. This study examines a transition from an acute detrimental to a delayed protective effect of sulforaphane in SH-SY5Y cells, that is linked to activation of cystine transport.

Methods: SH-SY5Y cells (a neuroblastoma cell line) were exposed to sulforaphane (1-20 µM) or vehicle for different durations (1-48 hours). Some cells were then exposed to oxidative stress (0.5 mM H_2O_2, 4 hours) or normal medium. The following parameters were examined. Cytotoxicity was assessed by determining lactate dehydrogenase (LDH) release. Effects on total cellular GSH were assessed using a colorimetric assay. The effects of sulforaphane on cystine transport (a determinant of GSH synthesis) were examined by determining the uptake of L-[^{35}S]cystine or L-[^{14}C]cystine.

Results: 24 hours pretreatment with sulforaphane (1-10 µM) protected SH-SY5Y cells from H_2O_2-induced death (e.g. 69±7% reduction in LDH release at 5 µM). However, this protection was time dependent, with an exacerbation of injury with 1 and 4 hrs of pretreatment but protection with 12-48 hrs of sulforaphane treatment (e.g. 36±9% increase in LDH release at 1 hr, and a 37±10% decrease at 48 hrs with 10 µM sulforpahane). The early detrimental effect of sulforaphane was associated with a depletion of cellular GSH (28±5 and 79±5% reduction with 1 and 4 hrs treatment with 5 µM sulforaphane). The transition from an acute detrimental to a chronic protective effect was associated with a marked upregulation in L-cystine transport via system x_c^- (Slc7A11), with 7 and 9-fold increases with 5 and 10 µM sulforaphane. Blocking that transporter with sulfasalazine, prevented the repletion and overshoot in cellular GSH that occurs during prolonged sulforaphane treatment (at 24 hrs, 5 µM sulforaphane caused a 56±6% increase, 5 µM sulforaphane + 250 µM sulfasalazine a 87±1% decrease in cell GSH).

Conclusions: Understanding the acute and long-term effects of sulforaphane on cystine transport and glutathione are important in determining the potential of this naturally occurring neuroprotectant in ischemic and hemorrhagic stroke.

References:

1. Tarozzi A, Morroni F, Merlicco A, Hrelia S, Angeloni C, Cantelli-Forti G, Hrelia P. Sulforaphane as an inducer of glutathione prevents oxidative stress-induced cell death in a dopaminergic-like neuroblastoma cell line. J Neurochem 2009; 111:1161-1171.

2. Zhao J, Kobori N, Aronowski J, Dash PK. Sulforaphane reduces infarct volume following focal cerebral ischemia in rodents. Neurosci Lett 2006; 393:108-112.

ISCHEMIC POST-CONDITIONING MAINTAINS BRAIN MITOCHONDRIAL FUNCTION AND CBF FOLLOWING FOCAL CEREBRAL ISCHEMIA IN RATS

A. Livnat, E. Barbiro-Michaely, **A. Mayevsky**

Faculty of Life Sciences, Bar Ilan University, Ramat Gan, Israel

Objectives: Ischemic post-conditioning is a phenomenon in which interruptions to cerebral blood flow (CBF) during the post ischemic reperfusion phase protect the brain from reperfusion injury and reduced infarct size (1). The present study investigated the effects of transient bilateral carotid occlusion (BCO) prior to reperfusion of focal ischemia on mitochondrial metabolism and CBF.

Methods: Male Wistar rats underwent middle cerebral artery occlusion (MCAO) for 60 minutes, with or without BCO, which was induced 15 minutes before reperfusion. Monitoring in the core and the penumbra of the ischemic brain was performed using a unique Multi-Site - Multi-Parametric (MSMP) system, which measures mitochondrial NADH using surface fluorometry, and CBF using

laser Doppler flowmetry (2). Short anoxia and cortical spreading depression (CSD) waves were induced in order to test the ability of the tissue to cope with oxygen deficiency and metabolic challenges following reperfusion.

Results: MCAO led to a decrease in CBF to 15% (of the control values) in the core and to 40% in the penumbra. Simultaneously, fluorescence increased to 129% in the core and 121% in the penumbra. NADH levels increased to 110% in both core and penumbra, followed by a decrease in the core, due to an artifact caused by an increase in reflectance levels (3). BCO 45 minutes later lead to a further decrease in CBF to 5% in the core and 15% in the penumbra. Reflectance and fluorescence levels further increased in both core and penumbra, leading to levels of 115% in the penumbra. In the core, NADH levels remained low due to the further increase in reflectance. Removal of the occluding filament lead to an increase in CBF in both areas toward levels of 50%, as the rest of the parameters showed no significant change. Restoration of carotid blood perfusion led to an increase in CBF to 180% in both areas, while reflectance, fluorescence and NADH levels decreased toward baseline. CBF levels returned to baseline as well 60 minutes later. Short anoxia and CSD waves, which were induced 60 minutes following carotid reperfusion, showed no significant changes in parameters compared to control.

Conclusions: These results imply that ischemic post-conditioning by BCO assists in maintaining tissue vitality following cerebral focal ischemia and may serve as a protective mechanism to ischemic and reperfusion damage.

References:

1. Pignataro G, Scorziello A, Di Renzo G and Annunziato L. Post-ischemic brain damage: effect of ischemic preconditioning and postconditioning and identification of potential candidates for stroke therapy. FEBS J 276: 46-57, 2009.

2. Livnat A, Barbiro-Michaely E and Mayevsky A. Variability in Mitochondria function and Cerebral Blood Flow following Middle Cerebral Artery Occlusion in Rats. Journal of Neuroscience Methods 188(1): 76-82, 2010.

3. Mayevsky A and Rogatsky G. Mitochondrial function in vivo evaluated by NADH fluorescence: from animal models to human studies. Am J Physiol Cell Physiol 292: C615-C640, 2007.

HYPEREXPRESSION OF ADPONECTIN IMPROVES LONG-TERM STROKE OUTCOME IN AGED MICE

J. Miao[1], L. Shen[1], Y. Zhao[1], Y. Wang[2], G.-Y. Yang[1,3]

[1]Department of Geriatrics, Ruijin Hospital, Shanghai Jiao Tong University School of Medicine, [2]Neuroscience and Neuroengineering Research Center, Med-X Research Institute and School of Biomedical Engineering, [3]Department of Neurology, Ruijin Hospital, School of Medicine, Shanghai Jiao Tong University, Shanghai, China

Objectives: Adiponectin (APN) attenuates ischemic brain injury and promote neuronal repairing.[1] However, aging affects the receptivity of ischemic brain to APN is unknown. The aim of this study is to explore the effect of APN on aged mice after focal cerebral ischemia.

Methods: APN hyper-expression was induced via adeno-associated viral vector carrying APN gene (AAV-APN) transduction. Aged CD-1 mice (n=30, 20-22 months) underwent 90 min transient middle cerebral artery occlusion (tMCAO). Cortical atrophy volume and neurobehavioral tests were quantified up to 28 days after tMCAO. Focal angiogenesis, neurogenesis were determined by immunohistochemistry and phospho-AMPK signaling was assessed via Western blot.

Results: APN was hyperexpressed in aged mice via AAV-APN gene transfer. Aged mice developed larger cortical atrophy compared to young mice after tMCAO ($p< 0.05$). APN attenuated atrophy volume and improved neurobehavioral recovery after tMCAO in both aged and young mice (vs. AAV-GFP group, $p< 0.05$). Additionally, atrophy volume attenuation and neurological outcome recovery in aged mice was better than in young mice after APN treatment (Δinfarct volume, $p< 0.05$). The number of microvessels, small arteries and neuroblasts was increased after APN treatment in aged and young mice, but the angiogenic improvement was similar in both aged groups. Furthermore, the phospho-AMPK and VEGF expression were up-regulated in ischemic perifocal region in young and aged mice.

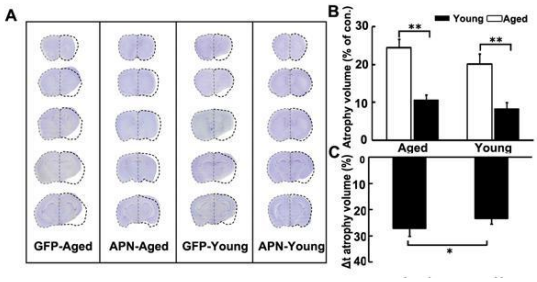

[Figure 1]

Figure 1. A. Photographs represented cresyl violet staining coronal sections from AAV-APN-transduced aged and young mice following 14 days of tMCAO. Dish lines illustrated the atrophy areas compared to the contralateral hemisphere. **B**. Bar graph showed that total atrophy volume in the AAV-APN transduced aged and young mice. Data are mean±SD. N=6 in each group. **: $p< 0.01$, APN vs. GFP groups. **C**. Bar graph showed the extent of atrophy volume attenuation in aged and young stroke mice after APN treatment, data are mean±SD. N=6 in each group. *: $p< 0.05$, aged vs. young groups.

Conclusions: Our results demonstrated that APN hyperexpression reduced cortical atrophy, enhanced angiogenesis and neurogenesis, and improved long term functional recovery in aged mice. We conclude that advanced age does not preclude a beneficial response to APN following experimental ischemia.

Reference:

1. Shen, L., J. Miao, F. Yuan, Y. Zhao, Y. Tang, Y. Wang, *et al*. Overexpression of adiponectin promotes focal angiogenesis in the mouse brain following middle cerebral artery occlusion. *Gene Ther* 2012.

ROLE OF NUCLEAR ERYTHROID 2-RELATED FACTOR 2 IN ISCHEMIC PRECONDITIONING-INDUCED NEUROPROTECTION

S. Narayanan, M. Perez-Pinzon

Neurology, University of Miami Miller School of Medicine, Miami, FL, USA

Objectives: Ischemic preconditioning (IPC) has gained attention as a potential prophylactic treatment for cerebral ischemia resulting from stroke. Evidence from our laboratory suggests that IPC promotes neuroprotection against cerebral ischemia by preventing oxidative damage. We have previously shown protein kinase C ε (PKCε), a serine-threonine kinase, and sirtuins (specifically sirtuin 1, SIRT1), a family of NAD^+-dependent histone deacetylases, to be activated following induction of IPC (1,2). Nuclear factor erythroid-2 related factor (Nrf2), an antioxidant transcription factor, may act downstream of these signaling pathways following IPC to ameliorate oxidative stress. Since Nrf2 activation occurs preferentially in astrocytes (3), our hypothesis was that activation of Nrf2 in astrocytes plays a critical role in mediating IPC-induced neuroprotection against cerebral ischemia.

Methods: Induction of *in vitro* IPC was performed by subjecting rat cortical astrocyte-enriched cultures to 1.5 hours of oxygen glucose deprivation (OGD). 48 hours later, these cultures were then subjected to 6 hours of OGD to simulate lethal ischemia (lethal OGD). Cell death was measured by LDH release assay. *In vivo* IPC was performed on adult male Sprague Dawley (S.D.) rats through 2 vessel-occlusion and hypotension, as previously described (4). Nuclear and cytoplasmic lysates were prepared from astrocyte-enriched cultures and rat cortical tissue following IPC treatment. Nrf2 and NQO-1, a gene under Nrf2 transcriptional control, were probed through immunoblotting.

Results: We tested whether nuclear translocation of Nrf2 was increased in astrocyte-enriched cultures following *in vitro* IPC. Nrf2 nuclear translocation and whole-cell NQO-1 expression were increased 1 hour following IPC compared to sham-treated cultures by 47% and 30%, respectively. To test the effect of PKCε administration on Nrf2 activation, intravenous administration of a PKCε activator peptide (0.2 mg/kg) resulted in increased Nrf2 nuclear translocation 24 hours later in rat cortex compared to Tat peptide-treated animals (vehicle). To test if SIRT1 regulates Nrf2 nuclear translocation, resveratrol, a polyphenol SIRT1 activator (5), was administered intraperitoneally (I.P.) into S.D. rats. I.P. administration of resveratrol (10 mg/kg) increased Nrf2 localization to the cortical nuclear fraction 48 hours later compared to vehicle (DMSO) treated animals. Finally, a 2 hour treatment of cortical astrocyte-enriched cultures with the pharmacologic activator of Nrf2, sulforaphane

(5 µM), reduced cell death 48 hours following lethal OGD by 35% compared to vehicle-treated (0.07% DMSO in saline) cultures.

Conclusions: These results suggest that IPC, PKCε and SIRT1 activation may increase Nrf2 localization to the nucleus and could present an important pathway in IPC-induced astrocyte protection. In addition, pharmacologic preconditioning through activation of Nrf2 may present a novel prophylactic therapy to protect astrocytes against cerebral ischemia. If astrocyte survival is enhanced, this could lead to increased neuroprotection following cerebral ischemia.

References:

1. Raval *et al* 2003, *J Neuroscience* 23: 384-91.

2. Della-Morte *et al* 2009, *J Neuroscience* 159: 993-1002.

3. Bell *et al* 2011, *Proc Natl Acad Sci U S A* 108:E1-2.

4. Perez-Pinzon *et al* 1997, *J Cereb Blood Flow Metab* 17:175-82.

5. Raval *et al* 2006, *J Cereb Blood Flow Metab* 26:1141-7.

Support: This work is supported by PHS grants NS054147, NS45676, NS34773, and F31NS080344-01

EPKC PRECONDITIONING REDUCES EXCITABILITY AND FIRING PROPERTIES OF CA1 HIPPOCAMPAL NEURONS

J.T. Neumann, M.A. Perez-Pinzon

University of Miami Miller School of Medicine, Miami, FL, USA

Cardiopulmonary arrest is a leading cause of death and disability USA, resulting in over 290,000 deaths each year with survival rate around 10%. To date, (with hypothermia being the only exception) all neuroprotective trials against cerebral ischemia have been unsuccessful, suggesting the need for new pharmacological interventions. Previous studies from our laboratory have demonstrated that ischemic preconditioning (IPC, a brief sub-lethal ischemic insult that is protective from lethal ischemia) protected the brain from cardiac arrest. In hippocampus, epsilon protein kinase C (εPKC, novel PKC isoform) played a key role in IPC-induced neuroprotection. One of the mechanisms of εPKC-induced neuroprotection is by enhancing GABAergic activity. A recent study showed that acute εPKC activation modulates voltage-gated Na^+ channels. Therefore, we tested the hypothesis that the direct activation of εPKC (IPC mimetic) alters voltage-gated Na^+ channels and neuronal firing for neuroprotection. To test this hypothesis, we used hippocampal acute slices harvested 48 hours after the administration of ψεRACK (0.2 mg/kg; εPKC activator used to emulate preconditioning pharmacologically) or Tat carrier peptide. Whole cell recordings were made from cornu ammonis 1 (CA1) hippocampal neurons, where under current clamp, action potentials were induced through a series of current injections. Our data showed that CA1 neurons were modified two days after ψεRACK treatment, where εPKC significantly increased the action potential (AP) full width at half max, threshold potential, after hyperpolarization (AHP) amplitude, and AHP location, and decreased the AP amplitude, AP rise to max, and AP frequency (Figure 1). Overall, these data suggest that εPKC activation modulates voltage-gated Na^+/K^+ channel activity to decrease AP frequency and potentially reduce the amount of glutamate released to ameliorate excitotoxicity. This works is supported by R01NS045676-06 and R01NS034773-12.

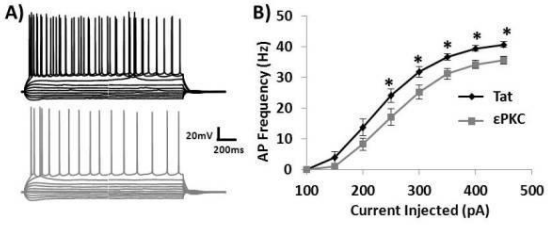

Figure 1. Decreased AP frequency 48hrs after *in vivo* εPKC activation. (A) Example tracing of CA1 firing patterns in acute slices from rats treated with ψεRACK or Tat peptide. Current injection shown are from -250pA to +200pA. (B) Action potential frequency is plotted as a function of current injection ±SEM. Tat n=14; εPKC n=16; *p<0.05.

[Figure 1]

INVOLVEMENT OF SRC-KINASE ACTIVATION IN ISCHEMIC PRECONDITIONING AND POSTCONDITIONING INDUCED PROTECTION OF MOUSE BRAIN

A.K. Rehni[1,2], T.G. Singh[1]

[1]Pharmacology, Chitkara College of Pharmacy, Chitkara University, [2]Department of Pharmaceutical Sciences and Drug Research, Punjabi University, Patiala, India

Aims: To investigate the role of src-kinase in ischemic preconditioning and ischemic postconditioning induced reversal of ischemia and reperfusion induced cerebral injury in mice.

Methods: Bilateral carotid artery occlusion of 17 min followed by reperfusion for 24 hr was employed to produce ischemia and reperfusion induced cerebral injury in mice. Cerebral infarct size was measured using triphenyltetrazolium chloride staining using both by volume and by weight methods differently. Memory was evaluated using elevated plus maze test. Rota rod test was employed to assess motor incoordination [1, 2].

Results: Bilateral carotid artery occlusion followed by reperfusion produced cerebral infarction and impaired memory and motor co-ordination. Three preceding episodes of bilateral carotid artery occlusion for 1 min and reperfusion of 1 min were employed to elicit ischemic preconditioning of brain, while three episodes of bilateral carotid artery occlusion for 10 sec and reperfusion of 10 sec immediately after the completion of ischemia were employed to elicit ischemic postconditioning of brain. SU6656 (2 mg/kg, ip) and PP1 (0.1 mg/kg, ip), highly selective src-kinase inhibitors, attenuated this neuroprotective effect of both prior ischemic preconditioning as well as ischemic postconditioning.

Conclusions: Therefore, neuroprotective effect of ischemic preconditioning and ischemic postconditioning may be due to src-kinase linked mechanism.

References:

1. Ashish K Rehni; Pradeep Bhateja; Nirmal Singh; Amteshwar S Jaggi. Implication of mast cell degranulation in ischemic preconditioning-induced prevention of cerebral injury. Fundamental and Clinical Pharmacology 22, 179 (2008).

2. Ashish K Rehni; Nirmal Singh; Amteshwar S Jaggi; Manjeet Singh. Amniotic fluid derived stem cells ameliorate focal cerebral ischaemia-reperfusion injury induced behavioural deficits in mice. Behavioural Brain Research 183, 95 (2007).

INVOLVEMENT OF CYCLIC ADENOSINE DIPHOSPHORIBOSE RECEPTOR ACTIVATION IN ISCHEMIC PRECONDITIONING INDUCED PROTECTION IN MOUSE BRAIN

A.K. Rehni[1,2], T.G. Singh[3]

[1]Pharmacology, Chitkara College of Pharmacy, Chitkara University, [2]Department of Pharmaceutical Sciences and Drug Research, Punjabi University, [3]Chitkara College of Pharmacy, Chitkara University, Patiala, India

Objectives: The present study has been designed to expound the significance of cyclic adenosine diphosphoribose receptor activation in ischemic preconditioning induced reversal of ischemia and reperfusion induced cerebral injury in mice.

Methods: Bilateral carotid artery occlusion of 17 min followed by reperfusion for 24 hr was employed in present study to produce ischemia and reperfusion induced cerebral injury in mice [1, 2]. Cerebral infarct size was measured using triphenyltetrazolium chloride staining. Memory was evaluated using Morris water-maze test. Rota rod test was employed to assess motor incoordination.

Results: Bilateral carotid artery occlusion followed by reperfusion produced cerebral infarction and impaired memory and motor co-ordination. Three preceding episodes of bilateral carotid artery occlusion for 1 min and reperfusion of 1 min (ischemic preconditioning) prevented markedly ischemia-reperfusion-induced cerebral injury measured in terms of infarct size, loss of memory and motor coordination. 8-bromo-cyclic adenosine diphosphate ribose (2 mg/kg, ip), an antagonist of cyclic ADP-ribose attenuated the neuroprotective effect of ischemic preconditioning.

Conclusions: It is concluded that

neuroprotective effect of ischemic preconditioning may be due to the adenosine diphosphoribose receptor activation.

References:

1. Ashish K Rehni; Pradeep Bhateja; Nirmal Singh; Amteshwar S Jaggi. Implication of mast cell degranulation in ischemic preconditioning-induced prevention of cerebral injury. Fundamental and Clinical Pharmacology 22, 179 (2008).

2. Ashish K Rehni; Nirmal Singh; Amteshwar S Jaggi; Manjeet Singh. Amniotic fluid derived stem cells ameliorate focal cerebral ischaemia-reperfusion injury induced behavioural deficits in mice. Behavioural Brain Research 183, 95 (2007).

POTENTIAL ROLE OF INTERLEUKIN 1 B CONVERTING ENZYME IN ISCHEMIC PRECONDITIONING AND POSTCONDITIONING OF BRAIN IN MICE

T.G. Singh, **A.K. Rehni**

Department of Pharmacology, Chitkara College of Pharmacy, Chitkara University, Rajpura, India

Objectives: The present study has been designed to investigate the potential role of Interleukin 1 β Converting Enzyme in ischemic preconditioning as well as postconditioning induced reversal of ischemia-reperfusion injury in mouse brain.

Methods: Bilateral carotid artery occlusion of 17 min followed by reperfusion for 24 hr was employed in present study to produce ischemia and reperfusion induced cerebral injury in mice. Cerebral infarct size was measured using triphenyltetrazolium chloride staining. Memory was evaluated using elevated plus-maze test and Morris water maze test. Rota rod test was employed to assess motor incoordination.

Results: Bilateral carotid artery occlusion followed by reperfusion produced cerebral infarction, impaired memory and motor co-ordination. Three preceding episodes of bilateral carotid artery occlusion for 1 min and reperfusion of 1 min were employed to elicit ischemic preconditioning of brain, while three episodes of bilateral carotid artery occlusion for 10 sec and reperfusion of 10 sec immediately after the completion of ischemia were employed to elicit ischemic postconditioning of brain. Both prior ischemic preconditioning as well as ischemic postconditioning immediately after global cerebral ischemia prevented markedly ischemia-reperfusion-induced cerebral injury as measured in terms of infarct size, loss of memory and motor coordination.

Conclusions: N-acetyl-Asp-Glu-Val-Asp-al (Ac-DEVD-CHO), a selective interleukin-1β converting enzyme inhibitor, attenuated the neuroprotective effect of both the ischemic preconditioning as well as postconditioning. It is concluded that the neuroprotective effect of both ischemic preconditioning as well as ischemic postconditioning may involve the activation of selective interleukin-1β converting enzyme.

References:

1. Ashish K Rehni; Pradeep Bhateja; Nirmal Singh; Amteshwar S Jaggi. Implication of mast cell degranulation in ischemic preconditioning-induced prevention of cerebral injury. Fundamental and Clinical Pharmacology 22, 179 (2008).

2. Rehni AK, Singh N. Role of phosphoinositide 3-kinase in ischemic postconditioning-induced attenuation of cerebral ischemia-evoked behavioral deficits in mice. Pharmacol Rep 2007;59:192-8.

INVOLVEMENT OF CCR-2 CHEMOKINE RECEPTOR ACTIVATION IN ISCHEMIC PRECONDITIONING AND POSTCONDITIONING OF BRAIN IN MICE

T.G. Singh[1], A.K. Rerhni[2]

[1]Department of Pharmacology, Chitkara University, Patiala, [2]Department of Pharmacology, Chitkara College of Pharmacy, Chitkara University, Rajpura, India

Objectives: The present study has been designed to investigate the potential role of CCR-2 chemokine receptor in ischemic preconditioning as well as postconditioning induced reversal of ischemia-reperfusion injury in mouse brain.

Methods: Bilateral carotid artery occlusion of 17 min followed by reperfusion for 24 h was employed in present study to produce ischemia and reperfusion induced cerebral injury in mice. Cerebral infarct size was

measured using triphenyltetrazolium chloride staining. Memory was evaluated using elevated plus-maze test and Morris water maze test. Rota rod test was employed to assess motor incoordination.

Results: Bilateral carotid artery occlusion followed by reperfusion produced cerebral infarction and impaired memory and motor co-ordination. Three preceding episodes of bilateral carotid artery occlusion for 1 min and reperfusion of 1 min were employed to elicit ischemic preconditioning of brain, while three episodes of bilateral carotid artery occlusion for 10 s and reperfusion of 10 s immediately after the completion of were employed to elicit ischemic postconditioning of brain. Both prior ischemic preconditioning as well as ischemic postconditioning immediately after global cerebral ischemia prevented markedly ischemia-reperfusion-induced cerebral injury as measured in terms of infarct size, loss of memory and motor coordination.

Conclusions: RS 102895, a selective CCR-2 chemokine receptor antagonist, attenuated the neuroprotective effect of both the ischemic preconditioning as well as postconditioning. It is concluded that the neuroprotective effect of both ischemic preconditioning as well as ischemic postconditioning may involve the activation of CCR-2 chemokine receptors.

Reference:

1. Ashish K Rehni; Pradeep Bhateja; Nirmal Singh; Amteshwar S Jaggi. Implication of mast cell degranulation in ischemic preconditioning-induced prevention of cerebral injury. Fundamental and Clinical Pharmacology 22, 179 (2008).

2. Rehni AK, Singh N. Role of phosphoinositide 3-kinase in ischemic postconditioning-induced attenuation of cerebral ischemia-evoked behavioral deficits in mice. Pharmacol Rep 2007;59:192-8.

PRECONDITIONING WITH ENDOPLASMIC RETICULUM STRESS INCREASES RESISTANCE TO CEREBRAL ISCHEMIA/REPERFUSION INJURY

X. Wu[1,2], Y. Luo[1], H. Zhao[1], C. Zhang[2], L. Min[2]

[1]Cerebrovascular Diseases Research Institute, Xuanwu Hospital of Capital Medical University, Beijing, [2]Department of Neurology, First Affiliated Hospital of Liaoning Medical University, Jinzhou, China

Objectives: Preconditioning has been shown protective effects on the following brain injury. In this study, we observe the effects of 2-Deoxyglucose (2-DG) induced endoplasmic reticulum (ER) stress as a preconditioning procedure on the brain ischemic injuries to determine whether preconditioning with ER stress increases resistance to cerebral ischemia reperfusion (I/R).

Methods: A transient cerebral ischemia rat model was used in the study. Rats were pretreated with a sublethal dose of the ER stress inducer 2-DG for 7 d before cerebral I/R was induced. Neurological functional and histopathology of neurons were evaluated, and changes in protein and mRNA levels of the ER stress-inducible chaperones glucose-regulated protein 78 (GRP78) and X-box protein 1 (XBP1) were measured at varying time points following I/R.

Results: Results showed that pre-treatment with 2-DG significantly improved the neurological function and histological damage compared with the untreated I/R group. Both protein and mRNA levels of GRP78 and XBP-1 showed remarkable increase in 2-DG pre-treatment group compared with I/R group.

Conclusion: These results collectively indicate a protective effect of 2-DG induced ER stress preconditioning against cerebral I/R injury, which is likely through activation of XBP-1 mediated unfolded protein response (UPR). These findings suggest the possibility of therapeutic approaches targeting ER stress preconditioning in ischemia stroke.

HYPOXIC PRECONDITIONING ATTENUATES NEURONAL CELL DEATH BY PREVENTING MEK/ERK SIGNALING PATHWAYS ACTIVATION AFTER TRANSIENTGLOBAL CEREBRAL ISCHEMIA IN ADUIL RATS

E. Xu, L. Zhan, H. Yan, H. Zhou, W. Sun, Q. Hou

Institute of Neurosciences and the Second Affiliated Hospital of Guangzhou Medical College, Guangzhou, China

Purpose: Our previous data indicated that hypoxic preconditioning (HPC) ameliorates transient global cerebral ischemia-induced neuronal death in hippocampal CA1 subregion of adult rats. However, the molecular mechanisms for neuroprotection of this kind are not completely known. This study was performed to investigate the role of the mitogen-activated protein kinase/extra-cellular signal-regulated kinase kinase (MEK)/extra-cellular signal-regulated kinase (ERK) pathway in HPC-induced neuroprotection.

Results: Transient global cerebral ischemia (tGCI) was induced by applying the four-vessel occlusion method. Pretreatment with 30 min of hypoxia applied 1 day before 10 min tGCI significantly decreased the level of MEK1/2 and ERK1/2 phosphorylation in ischemic hippocampal CA1 subregion. Also, HPC decreased the expression of phosphorylated ERK1/2 in degenerating neurons and astrocytes. However, the administration of U0126, a MEK kinase inhibitor, partly blocked MEK1/2 and ERK1/2 phosphorylation induced by tGCI. Meanwhile, neuronal survival was improved and glial cell activation was significantly reduced.

Conclusions: Collectively, these data indicated that the MEK/ERK signaling pathway might be involved in hypoxic preconditioning-induced neuroprotection following tGCI. Moreover, hypoxic preconditioning also resulted in a reduction in glial activation.

EFFECT AND SIGNIFICANCE OF MICROGLIA/MACROPHAGE PRE-ACTIVATION ON TLR2/NF-KB ACTIVITY AND INFLAMMATORY RESPONSE FOLLOWING RAT ISCHEMIC BRAIN INJURY

Y. Yang, Z. Chen, H. Feng, G. Zhu

Department of Neurosurgery, Southwest Hospital, Third Military Medical University, Chongqing, China

Objective: To investigate the effect and significance of microglia/macrophage pre-activation on TLR2/NF-κb activity and inflammatory response following rat ischemic brain injury.

Methods: Model of focal cerebral infarct was established by occlusion of middle cerebral artery (MCAO), and modle of cerebral ischemic preconditioning (CIP) was established by transient MCAO. Rats were randomly divided into normal control group、sham surgery group、ischemic group、treatment group. The feature of microglia pre-activation was observed by laser scanning confocal microscope(LSCM), and the mRNA expressions of IκB-α、TNF-α in cerebral cortex were detected by in situ hybridization method. The neurological deficits were evaluated in 0-4 scales. The infarct size was measured by TTC staining. The mortality of each group was also calculated.

Results: The microglia/macrophage activation in cerebral cortex increased after ischemic injury 1 hour and decreased gradually after reaching the highest level at 12h, and was still at a high level after 24h ($P < 0.01$); The mRNA expression of IκB-α increased after ischemic 1 hour, and TNF-α keep at the lower level till 24h ($P < 0.01$) compared with ischemic group($P < 0.05$); CIP could decrease the cerebral infarct, neurological deficits and mortality rate.

Conclusion: CIP could reprogram the activation of microglia/macrophage in ischemic stroke, leading to the inhibition of TLR2/NF-κb activity and inflammatory response following rat ischemic brain injury, which may be involved in this neuroprotection.

DIFFERENT NEUROPROTECTIVE EFFECTS OF SEVOFLURANE POSTCONDITIONING IN THE NORMAL AND HYPERLIPIDEMIC MICE

H. Yu[1,2], Z. Zuo[1]

[1]*Department of Anesthesiology, University of Virginia, Charlottesville, VA, USA,*
[2]*Department of Anesthesiology and Translational Neuroscience Center, West China Hospital, Sichuan University, Chengdu, China*

Background: The postconditioning conferred by volatile anesthetic is known to reduce ischemic heart and brain injury in healthy animals. It has also been shown that hyperlipidemia attenuates the cardioprotective effect of volatile anesthetic postconditioning. However, it remains unclear whether this phenomenon exists in the neuroprotective effect. The aim of the present study was to investigate if hyperlipidemia interferes with the neuroprotective effect of sevoflurane postconditioning and to determine the involvement of LKB1-AMPK in this phenomenon.

Methods: Male wild-type CD1 mice (6 weeks old) were fed with high fat (HFD) or normal diet (ND) for 10 weeks. In the experiment I, hippocampal slices (400 μm) freshly prepared from the mice were subjected to an oxygen-glucose deprivation (OGD; to simulate ischemia in vitro). Sevoflurane postconditioning was performed by exposing hippocampal slices to sevoflurane after a 20-min OGD. For the sevoflurane dose-response study, 2, 4, or 6% sevoflurane was applied for 30 min immediately after the OGD. After a 5-h reperfusion, the hippocampal CA1, CA3 and dentate gyrus (DG) subfields were identified and the optical density of propidium iodide (PI) fluorescence was detected to quantify cell death. In the experiment II, the hippocampal tissues from mice fed with HFD or ND for 5 and 10 weeks were collected to determine the levels of LKB1 and AMPK by western blotting. The hippocampal slices underwent OGD and sevoflurane postconditioning in the experiment I were also used to measure the levels of LKB1 and AMPK. The effects of AMPK inhibitor Compound C on sevoflurane postconditioning were also investigated.

Results: The postconditioning of the hippocampal slices with sevoflurane immediately after OGD reduced cell injury in the mice fed with HFD and ND but with different efficacies in these two types of mice. For the mice fed with ND, 2, 4 and 6% sevoflurane reduced cell injury in the CA1, CA3 and DG subfields. For the mice fed with HFD, 4 and 6% sevoflurane reduced cell injury in the CA3 subfield and only 6% sevoflurane reduced cell injury in the CA1 and DG subfields. Hyperlipidemic animals showed decreased p-LKB1 (Thr189) and p-AMPK (Thr172) levels. Sevoflurane postconditioning had no significant effect on p-LKB1 level in both normal and hyperlipidemic mice. Sevoflurane postconditioning increased p-AMPK level in the ND mice but not in the HFD mice. The AMPK inhibitor Compound C blocked sevoflurane postconditioning-induced the increase in phosphorylated AMPK and increased neuronal damage in the ND mice but not in the HFD mice.

Conclusion: Hyperlipidemia attenuates the neuroprotective effect of sevoflurane postconditioning. Sevoflurane postconditioning has different effects on the LKB1-AMPK signaling pathway in the normal and hyperlipidemic mice.

HYPERLIPIDEMIA ATTENUATES THE NEUROPROTECTIVE EFFECT OF ISOFLURANE POSTCONDITIONING: ROLE OF CTMP-AKT-GSK-3B SIGNALING PATHWAY

H. Yu[1,2], Z. Zuo[1]

[1]*Department of Anesthesiology, University of Virginia, Charlottesville, VA, USA,*
[2]*Department of Anesthesiology and Translational Neuroscience Center, West China Hospital, Sichuan University, Chengdu, China*

Background: The postconditioning conferred by volatile anesthetic is known to reduce ischemic heart and brain injury in healthy animals. It has also been shown that hyperlipidemia attenuates the cardioprotective effect of volatile anesthetic postconditioning. However, it remains unclear whether this phenomenon exists in the neuroprotective effect. The aim of the present study was to investigate if hyperlipidemia interferes with the neuroprotective effect of isoflurane postconditioning and to determine the involvement of Carboxyl-terminal modulator protein (CTMP)-Akt-glycogen synthetase kinase-3 β (GSK-3β) in this phenomenon.

Methods: Male wild-type CD1 mice (6 weeks old) were fed with high fat (HFD) or normal diet (ND) for 10 weeks. In the experiment I,

hippocampal slices (400 μm) freshly prepared from the mice were subjected to an oxygen-glucose deprivation (OGD; to simulate ischemia in vitro). In the time-course experiments, the OGD was maintained for 10, 20, 30 or 60 min. Isoflurane postconditioning was performed by exposing hippocampal slices to isoflurane after a 20-min OGD. For the isoflurane dose-response study, 1, 2, or 3% isoflurane was applied for 30 min immediately after the OGD. After a 5-h reperfusion, the hippocampal CA1, CA3 and dentate gyrus (DG) subfields were identified and the optical density of propidium iodide (PI) fluorescence was detected to quantify cell death. In the experiment II, the hippocampal tissues from mice fed with HFD or ND for 5 and 10 weeks were collected to determine the levels of CTMP, Akt and GSK-3β by western blotting. The hippocampal slices underwent OGD and isoflurane postconditioning in the experiment I were also used to measure the levels of CTMP, Akt and GSK-3β.

Results: The postconditioning of the hippocampal slices with isoflurane immediately after OGD reduced cell injury in the mice fed with HFD and ND but with different efficacies in these two types of mice. For the mice fed with ND, 1, 2 and 3% isoflurane reduced cell injury in the CA1 and CA3 subfields and only 2 and 3% isoflurane reduced cell injury in the DG hippocampal subfield. For the mice fed with HFD, 2 and 3% isoflurane reduced cell injury in the CA1 subfield and only 3% isoflurane reduced cell injury in the CA3 and DG subfields. Hyperlipidemic animals showed an increased CTMP level and decreased p-Akt (Ser473) and p-GSK-3β (Ser9) levels. Isoflurane postconditioning reduced CTMP level and increased p-Akt (Ser473) and p-GSK-3β (Ser9) levels.

Conclusion: Hyperlipidemia attenuates the neuroprotective effect of isoflurane postconditioning via modulating the CTMP-Akt-GSK-3β signaling pathway.

HYPERBARIC OXYGEN PRECONDITIONING ATTENUATES HYPERGLYCEMIA-ENHANCED HEMORRHAGIC TRANSFORMATION BY INHIBITING MATRIX METALLOPROTEINASES IN FOCAL CEREBRAL ISCHEMIA IN RATS

Y. Soejima, Q. Hu, P. Krafft, M. Fujii, J. Tang, **J. Zhang**

Loma Linda University School of Medicine, Loma Linda, CA, USA

Objective: Hyperglycemia dramatically aggravates brain infarct and hemorrhagic transformation (HT) after ischemic stroke. Oxidative stress and matrix metalloproteinases (MMPs) play important role in the pathophysiology of HT. Hyperbaric oxygen preconditioning (HBO-PC) has been proved to decrease oxidative stress and be neuroprotective in experimental stroke models. The present study determined whether HBO-PC would ameliorate HT by a preischemic increase of reactive oxygen species (ROS) generation, and a suppression of MMP-2 and MMP-9 in hyperglycemic middle cerebral artery occlusion (MCAO) rats.

Methods: Rats were pretreated with HBO (100% O_2, 2.5 atmospheres absolute) 1 h daily for 5 days MCAO. Acute hyperglycemia was induced by an injection of 50% dextrose. 24 h after ischemia, neurological deficits, infarction volume and hemorrhagic volume were assessed. Hypoxia-inducible factor-1α (HIF-1α) inhibitor 2-methoxyestradiol (2ME2) and ROS scavenger n-acetyl cysteine (NAC) were administrated for mechanism study. The activity of MMP-2 and MMP-9, and the expression HIF-1α were measured.

Results: HBO-PC improved neurological deficits, and reduced hemorrhagic volume; the expression of HIF-1α was significantly decreased, and the activity of MMP-2 and MMP-9 was reduced by HBO-PC compared with vehicle group.

Conclusion: Our results suggested that HBO-PC attenuated HT via decreasing HIF-1α and its downstream MMP-2 and MMP-9 in hyperglycemic MCAO rats.

Reference:

Kagansky, N., Levy, S., and Knobler, H., 2001. The role of hyperglycemia in acute stroke. Arch Neurol 58, 1209-1212.

Wang, X., and Lo, E. H., 2003. Triggers and mediators of hemorrhagic transformation in cerebral ischemia. Mol Neurobiol 28, 229-244.

Wang, X., Tsuji, K., Lee, S. R., Ning, M., Furie, K. L., Buchan, A. M., and Lo, E. H., 2004. Mechanisms of hemorrhagic transformation after tissue plasminogen activator reperfusion therapy for ischemic stroke. Stroke 35, 2726-2730.

INHIBITION OF AUTOPHAGY CONTRIBUTES TO NEUROPROTECTION IN ISCHEMIC POSTCONDITIONING PROCESS

Y. Zhang, L. Gao

Department of Neurology, Nanjing Hospital of Nanjing Medical University, Nanjing, China

Ischemic postconditioning (IPOC) has now been demonstrated as a novel strategy to harness nature's protection against cerebral ischemia/reperfusion injury. However, the mechanisms underlying are not completely understood. This study aimed to determine the role of autophagy in the neuroprotective effects induced by ischemic postconditioning in rats. A focal cerebral ischemic model with permanent MCA occlusion plus transient CCA occlusion was established and postconditioning was conducted at the onset of reocclusion. As far as the observation revealed, autophagy was activated in the penumbra at various time intervals following ischemia by the expressions of LC3 and Beclin 1 upwnregulation and p62 downregulation. After postconditioning treatment, the infarct size and brain edema was reduced, simultaneously, the autophagosome formation decreased and autophagy induction was attenuated. However, all the aforementioned effects induced by IPOC were partially reversed by the autophagic inducer rapamycin. Conversly, inhibiting autophagy induction with 3-MA attenuated the ischemic insults and upregulated the anti-apoptotic protein Bcl-2, to an extent comparable to IPOC. These results suggest that the inhibition of autophagic activity underlies, at least partly, the mechanism of IPOC-induced tolerance to focal cerebral ischemia.

IS THE HYPERPERFUSION SYNDROME AFTER CAROTID ENDARTERECTOMY ABSCENT OR PREVENTABLE?

S.H. Lee[1], K.H. Kim[2], C.-H. Lee[3], J.H. Ahn[2], Y.-J. Son[1], Y.S. Chung[1]

[1]Neurosurgery, Seoul National University Boramae Hospital, [2]Neurosurgery, Seoul National University, Seoul, [3]Seoul National University Bundang Hospital, Seongnam, Republic of Korea

Objectives: Carotid endarterectomy(CEA) is the principal treatment option of carotid stenosis nowdays. But. the hyperperfusion syndrome after CEA was reported at 0%-18.4%, and it was 0%-6.8% after carotid artery stenting(CAS). The most prevalent peak day hyperperefusion syndrome was 5th-7th day after CEA, the first 24hours after CAS. As these, there are some discrepancies on hyperperfusion syndrome after CEA.

Method: After surgery, we carefully managed the blood pressure not elevating the above level of preoperative status. We investigated retrospectively consecutive cases of the results on postoperative clincal symptoms and signs, transcranial doppler, perfusion brain CT, and SPECT study comparative to each preoperative resulys.

Results: We observed there was no event of hyperperfusion syndrome after CEA. We will discuss about that pathophysioly of hyperperfusion synfrome after CEA and suggest that the hyperperfusion syndrome after CEA can be preventable by way of meticulous post-operative control of blood pressure.

ACUTE AND DELAYED POST-STROKE TREATMENT WITH HUMAN AMNION EPITHELIAL CELLS IMPROVES STROKE OUTCOME

B.R.S. Broughton[1], K.W.E. Taylor[1], V.H. Brait[1], R. Lim[2], E.M. Wallace[2], G.R. Drummond[1], C.G. Sobey[1]

[1]Department of Pharmacology, Monash University, [2]The Ritchie Centre, Monash Institute of Medical Research, Clayton, VIC, Australia

Introduction: Stem cells derived from human tissue, including embryonic, induced pluripotent, neural, and mesenchymal cells, have been reported to rescue injured brain tissue and improve functional recovery in experimental models of stroke. However, ethical issues, concerns regarding tumorigenicity and problems with deriving sufficient cells may hamper their suitability as a widely available cell therapy for stroke patients. In contrast, placental stem cells, particularly human amnion epithelial cells (hAECs) are abundant, non-immunogenic, non-tumorigenic and pose no ethical challenges. Surprisingly, hAECs have received almost no attention as a cell therapy for ischemic stroke. Therefore, the aim of this study was to test whether hAECs were an effective cell therapy for stroke in male C57Bl6

mice subjected to 0.5 h middle cerebral artery occlusion-reperfusion.

Methods: Mice were injected with $1x10^6$ fluorescently-labelled hAECs or saline (vehicle) intravenously at either 1 h (acute treatment) or 72 h (delayed treatment) post-stroke and brains were removed after 3 or 14 d, respectively. Neurological and functional assessment tasks (neurological scoring, hanging wire and adhesive removal tests) were performed and infarct volume as well as neuronal apoptosis were assessed using anatomical approaches.

Results: hAECs injected acutely after stroke were present in the infarct after 3 d, but not in the contralateral hemisphere. This was associated with improved outcomes in infarct damage (hAEC-treated: 11.6±2.9 mm^3 vs vehicle-treated: 34.81±5.6 mm^3; n = 9-12, respectively; $P < 0.05$), hanging wire testing (latency to fall: 38.2±5.4 s vs 16.2±5.0 s; $P < 0.05$) and neurological scoring (median score: 3 vs 1; $P < 0.05$). Immunofluorescence of the key marker of apoptosis, cleaved caspase-3, revealed that ~60% less apoptosis occurred in the ischemic hemisphere of mice treated with hAECs versus vehicle ($P < 0.05$). Moreover, mice that received delayed post-stroke hAEC treatment had markedly increased survival to 14 d compared to vehicle-treated mice (50% vs 0% survival; n = 8-7, respectively) and hanging wire and adhesive removal times were normalized to pre-stroke levels.

Conclusions: Early post-stroke i.v. delivery of hAECs reduces brain injury and functional deficit whereas delayed post-stroke hAEC treatment improves longer term survival and functional performance. Collectively, these findings suggest that hAECs may be an effective clinical therapy for promoting recovery following ischemic stroke.

IPS CELL TRANSPLANTATION INCREASES NEUROGENESIS AND ANGIOGENESIS AFTER NEONATAL ISCHEMIC STROKE

M. Chau, S.P. Yu, L. Wei

Department of Anesthesiology, Emory University, Atlanta, GA, USA

Introduction: Stroke is a leading cause of death and disability worldwide. Neonatal stroke affects 26 of 100,000 live births each year, yet there are limited treatments available. Induced pluripotent stem (iPS) cells from adult somatic cells have provided a new source of stem cells that circumvents the ethical concerns of using embryonic stem cells. The transplantation potential and therapeutic benefits of iPS cells however, is relatively unknown. We hypothesized that iPS cell-derived neural progenitors have a unique potential for stroke therapy by providing cell replacement and beneficial growth factors to the stroke area.

Methods: Pluripotent iPS cells were differentiated into neural progenitors with a retinoic acid protocol and plated for in vitro analysis. Trophic factor expression of these cells was analyzed through Western blot and immunocytochemistry. iPS cell-derived neurons were patch-clamped in vitro to characterize neuronal activity. Cell transplantation (400,000 iPS cell-derived neural progenitors) was performed in an ischemic stroke model of P7 rats 7 days after stroke. The rats received daily BrdU injections and were sacrificed 21d after stroke for immunohistochemistry. Behavioral tests were performed to evaluate functional recovery.

Results: In vitro analysis shows that 87.5% of plated progenitors differentiated into NeuN-positive cells. iPS cell-derived neural progenitors and undifferentiated iPS cells showed the expression of trophic factors including VEGF, EPO, SDF-1, FGF, and GDNF. iPS cell-derived neurons fired action potentials, exhibited inward sodium current and outward potassium currents in vitro. Stroke rats that received iPS cell transplantation showed increased BrdU-positive cells and increased BrdU/NeuN and BrdU/Collagen IV double-positive cells compared to stroke only rats. iPS transplantation animals showed improved sensorimotor function.

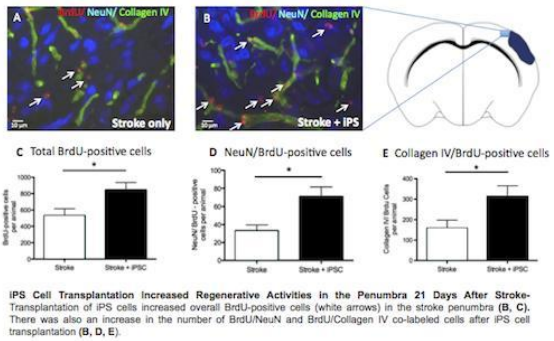

IPS Cell Transplantation Increased Regenerative Activities in the Penumbra 21 Days After Stroke- Transplantation of iPS cells increased overall BrdU-positive cells (white arrows) in the stroke penumbra (**B, C**). There was also an increase in the number of BrdU/NeuN and BrdU/Collagen IV co-labeled cells after iPS cell transplantation (**B, D, E**).

[Regenerative activities after iPSC transplantation]

Conclusion: The increased number of new neurons and vessels in the ischemic brain suggests increased neurogenesis and neurovascular remodeling with iPS cell transplantation. Transplantation of iPS cells may contribute additional trophic support to increase endogenous progenitor migration to the infarct, cell survival, and endogenous neurogenesis. We conclude that iPS cell transplantation shows potential as a therapeutic strategy for ischemic stroke in neonates

References:

Li, W.-lei, Yu, S. P., Ogle, M. E., Ding, X. S., & Wei, L. (2008). Enhanced Neurogenesis and Cell Migration Following Focal Ischemia and Peripheral Stimulation in Mice. *Contract*, (September). doi:10.1002/dneu.20674

Li, Y., Yu, S. P., Mohamad, O., Genetta, T., & Wei, L. (2010). Sublethal Transient Global Ischemia Stimulates Migration of Neuroblasts and Neurogenesis in Mice. *Translational Stroke Research*, *1*(3), 184-196. doi:10.1007/s12975-010-0016-6

Takahashi, K., & Yamanaka, S. (2006). Induction of pluripotent stem cells from mouse embryonic and adult fibroblast cultures by defined factors. *Cell*, *126*, 663-676. .

CXCR7, A NOVEL RECEPTOR OF CXCL12, MEDIATES MIGRATION AND SIGNALING OF NEURAL PROGENITOR CELLS *IN VITRO*

Q. Chen[1], Y. Li[1], A. Song[1,2], D. Xu[2], C. Tian[1], J. Zheng[1,2,3]

[1]Pharmacology and Experimental Neuroscience, University of Nebraska Medical Center, Omaha, NE, USA, [2]Center for Translational Neurodegeneration and Regenerative Therapy, Shanghai Tenth People's Hospital, Tongji University, Shanghai, China, [3]Pathology and Medical Microbiology, University of Nebraska Medical Center, Omaha, NE, USA

Objective: Neural progenitor cell (NPC) migration is a key step in neurogenesis for both proper brain development and neuroregeneration after brain injury. The axis of CXCL12 and its receptor CXCR4 are known to regulate NPC migration. CXCR7, a newly found receptor, has shown higher affinity to CXCL12 than CXCR4; however, the exact role of CXCR7 in CXCL12-mediated NPC migration is unknown.

Methods: To determine the role of CXCR7 in CXCL12-mediated NPC migration, we used *in vitro* NPC cultures derived from CXCR4 knockout, CXCR7 knockout and their corresponding wild type mice for stripe assay and transwell assay to study NPC migration.

Results: Both CXCR4 and CXCR7 were expressed on NPCs in developing mouse brain and adherent cultures *in vitro* by immunostaining. CXCL12 mediated NPC migration in transwell assays and stripe assays, and antagonists for either CXCR4 or CXCR7 blocked the migration. Surprisingly, NPCs from CXCR4 knockout mice migrated to CXCL12, and CXCR7 antagonist completely blocked the migration. To study the signaling for CXCR7-mediated NPC migration, we found Erk1/2 could be activated in CXCR4 knockout NPCs after CXCL12 treatment by western blotting, suggesting that CXCR7 can activate Erk1/2, which is associated with migration. Erk1/2 inhibitor blocked CXCL12-mediated migration of CXCR4 knockout NPCs, indicating that Erk1/2 activation is essential for CXCR7-mediated NPC migration.

Conclusion: Together these results reveal the essential role of CXCR7 for CXCL12-mediated NPC migration that will be important to understand neurogenesis during development and adult neural repair after brain injury, which will provide a novel target for modulating NPC migration.

SYSTEMIC IMMUNE THERAPY OF BONE MARROW DERIVED DC FOR THE BRAIN INJURY

J. Han, X. Wang, Y. Tao, R. El-Kadri, J. Abou-Fadel, **H. Dou**

Biomedical Sciences, Texas Tech University Health Science Center, El Paso, TX, USA

Systemic immune responses play a critical role in neuropathogenesis after brain injuries. The immune system has the ability to modulate multiple brain functions following the brain injury. During the process when pathological changes occur to the brain, activated immune cells along with the local resident microglia act rapidly to initiate an

inflammatory response by secreting cytokines. The recognition of these cytokine signals by both immune system and the central nervous system (CNS) induce a specialized immune activation program. This study is to examine the modified bone marrow derived cells (BMDC) reprogramming systemic immune responses against the brain injury. GM-CSF, MCSF and IL-4 were used to modulate BMDC for treatment of intracerebral hemorrhage (ICH). A mouse model of ICH was developed to explore the correlations of systemic immune response and the neuroprotective efficacy of BMDC. Bone marrow cells were isolated and cultured with seven cytokine combinations. After ICH mice treated with BMDC for 21 days, the bone marrow, spleen, brain and liver were examined by flow cytometry, real-time PCR and histology. RT-PCR analysis of IL1, IL2, IL6, IL10, TNFa, TGFβ and IFNr indicated that immune system respond to the brain injury by regulating cytokine signals. In compared to the control group, BMDC treatment significantly increased the portion of CD34+ cells in bone marrow and anti-inflammatory cytokine IL10 in the brain, liver and blood (12.8% vs 3.5%). Moreover, ICH mice treatment with BMDC increased MAP-2 positive staining in compared with untreated group. The therapeutic application of programming systemic immune system to treat the brain injury is novel and capable to translating into clinic use.

COMPARATION BETWEEN XENOGENIC AND ALLOGENIC ADIPOSSE TISSUE MESENCHYMAL STEM CELLS IN TREATMENT OF ACUTE CEREBRAL INFARCT. CONCEPT PROOF IN RATS

M. Gutiérrez-Fernández, B. Rodríguez-Frutos, J. Ramos-Cejudo, E. Díez-Tejedor

La Paz University Hospital, IdiPAZ, UAM, Madrid, Spain

Introduction: Several studies have suggested that mesenchymal stem cells are appropriate for ischemic stroke treatment, demonstrating safety, feasibility and efficacy. However, more information regarding appropriate cell type is needed from animal model. Therefore, it would be interesting to perform a concept proof: to administer the human Adipose Tissue -derived-Mesenchymal Stem Cells (hAD-MSC) (xenogenic administration) to demonstrate the safety itself in the animal model.

Aims: This study was targeted at analyzing the effects in ischemic stroke of acute intravenous (i.v.) administration of hAD-MSC or rat Adipose Tissue -derived-Mesenchymal Stem Cells (rAD-MSC) (allogenic administration) on functional evaluation results and safety in an experimental model in rat.

Material and methods: Model of permanent Middle Cerebral Artery occlusion (pMCAO) in Sprague Dawley male rats in 4 groups (n=10):

a) Sham: surgery without infarct;

b) Control: surgery + infarct;

c) hAD-MSC: surgery + infarct + i.v injection of hAD-MSC ($2X10^6$ cells);

d) rAD-MSC: surgery + infarct + i.v injection of rAD-MSC ($2X10^6$ cells).

We analyzed: Functional evaluation by the Rogers test; infarct volume by Magnetic Resonance Imaging (MRI) and Hematoxilin-Eosin (H-E); cell migration and implantation were analyzed by Magnetic Resonance Imaging (MRI) and inmmunohistochemistry. All theses parameters were analyzed at 24h and 14 days. Cell death by TUNEL at 14 days and finally, tumor formation at 3 months. Rats were sacrificed at 3 months.

Results: Compared to control group, functional evaluation had significantly improved at 24h and continued at 14d after i.v. administration of either hAD-MSC or rAD-MSC ($p< 0,05$). No reduction in infarct volume or any migration/ implantation of cells into the damaged brain were observed in the treatment groups. Nevertheless, cell death was reduced significantly in both treatment groups with respect to the Control group ($p< 0,05$). Both treatment groups (hAD-MSC and rAD-MSC) we did not observe tumor formation at 3 months.

Conclusion: Both therapies with hAD-MSC or rAD-MSC have demonstrated equal efficacy on functional recovery and decrease ischemic brain damage (reduction cell death). Besides, both treatment groups have demonstrated safety without observe neither side effects nor tumor formation.

Supported by grants from CIDEM (Center for Innovation and Business Development), Health Research Fund (FIS PS09/01606) and by RENEVAS (RD07/0026/2003) (Spanish Neurovascular Network) of the Institute of

Health Carlos III and the Ministry of Health, Economy and Competitively.

FUNCTIONAL CONTRIBUTION OF NEUROGENESIS AFTER FOCAL ISCHEMIA IN MICE

K. Jin[1], X. Mao[2], L. Xie[2], F. Sun[1], D.A. Greenberg[2]

[1]University of North Texas Health Science Center, Fort Worth, TX, [2]Buck Institute for Research on Aging, Novato, CA, USA

Injury stimulates neurogenesis in the adult brain, but the role of injury-induced neurogenesis in brain repair and recovery is uncertain. One strategy for investigating this issue is to ablate neuronal precursors and thereby prevent neurogenesis, but this is difficult to achieve in a specific fashion. We produced transgenic mice that express herpes simplex virus thymidine kinase (TK) under control of the promoter for doublecortin (Dcx), a microtubule-associated protein expressed in newborn and migrating neurons. Treatment for 14 days with the antiviral drug ganciclovir (GCV) depleted Dcx-expressing and BrdU-labeled cells from the rostral subventricular zone and dentate gyrus, and abolished neurogenesis and associated neuromigration induced by focal cerebral ischemia. GCV treatment of Dcx-TK transgenic, but not WT, mice also increased infarct size and exacerbated sensorimotor behavioral deficits measured by rotarod, limb placing, and elevated body swing tests at acute, chronic phases after focal cerebral ischemia in young adult and middle-aged mice at acute. These findings provide evidence that injury-induced neurogenesis contributes to stroke outcome and might therefore be a target for stroke therapy.

THE OVEREXPRESSION OF ADC ENHANCED SURVIVAL RATE OF MSCS, POSSIBLY CONTRIBUTING TO THE IMPROVEMENT OF MOTOR ACTIVITY FOLLOWING SCI

J.E. Lee, S.K. Seo, Y.M. Park, W. Yang

Anatomy, Brain Korea 21 Project for Medical Science, Yonsei University, College of Medicine, Seoul, Republic of Korea

Objectives: Spinal cord injury (SCI) usually results in permanent motor and sensory impairment in patients. Currently, cell transplantation therapy is proposed as an alternative treatment where mesenchymal stem cells (MSCs) are being considered to be the major player. However, there is the obvious challenge that few of MSCs survive following transplantation in injured spinal cord. Arginine decarboxylase (ADC) which can synthesize agmatine reported to confer resistance against oxidative stress both *in vitro* and *in vivo*. This prompted us to address the possibility of arginine decarboxylase (ADC) genes infection to MSCs (ADC-*h*MSCs) could enhance the survival of MSCs against oxidative stress and transplantation of these ADC-*h*MSCs could retrieve the functional impairments following SCI.

Methods: The induced ADC protein expression in ADC-*h*MSCs was confirmed with western blotting. The protective effect of ADC genes was examined by MTT assay and Hoechst/PI staining in *h*MSCs exposed to H_2O_2. To explore the underlying protective mechanism, protein levels of AKT, CREB, and BDNF were checked with western blotting. In the *in vivo* study, mice were injured at thoracic LV9 of spinal cord. One week after SCI, the animals were transplanted with PK26 labeled *h*MSCs injected at both caudal and rostral position of 1mm distant from lesion site of animals. BBB test scores were recorded everyday until 9 weeks for the assessment of behavioral performance in *h*MSCs transplantation and non-transplantation groups. Mice were perfused with saline and the spinal cords were dissected out to examine the effects of ADC-*h*MSCs transplantation at 1^{st}, 3^{rd}, or 9^{th} weeks. Immunohistochemical staining and western blotting were performed with antibodies against Tuj1, GFAP, and Olig2. Simultaneously, the expression patterns of BDNF and VEGF were checked with western blotting.

Results: Induced expression of ADC genes conferred cytoprotection in *h*MSCs against H_2O_2 insult which is evident by MTT assay and Hoechst/PI staining. The survival effects in ADC-hMSCs were related with suppressed caspase-3 activation and increased expression of AKT, CREB, and BDNF thus, suggesting that ADC overexpression contributes to the survival of *h*MSCs against oxidative stress *in vitro*. In the *in vivo* study, mice transplanted with ADC-*h*MSCs recorded better BBB scores, compared to other experimental groups. Immunostaining and western results showed significant increase in

the expression of Tuj-1 and Olig-2 around the lesion site in ADC-*h*MSCs transplantation group. To support these effects, the expression of BDNF and VEGF were elevated in the ADC-*h*MSCs transplantation group suggesting that ADC genes could trigger the neurotrophic factors and stimulate neurogenesis and oligogenesis following SCI.

Conclusions: This study demonstrates that the overexpression of ADC genes improves survival of *h*MSCs against H_2O_2 toxicity *in vitro*. Transplantation of *h*MSCs overexpressing ADC gene improved motor function following SCI. Taken together, our data support the idea that ADC gene can be one of the unique target for improving the survival of *h*MSCs and as a potent transplantable material in various CNS injury models including SCI.

Support: This research was supported by Basic Science Research Program through the National Research Foundation of Korea (NRF) funded by the Ministry of Education, Science and Technology(MEST) (2011-0017276).

DIRECT-CURRENT ELECTRICAL FIELD GUIDES NEURONAL STEM/PROGENITOR CELL MIGRATION

L. Li[1], M. Liao[2], Q. Wan[2]

[1]Research Institute of Surgery, Chongqing, China, [2]School of Medicine, University of Nevada, Reno, NV, USA

Direct-current electrical fields (EFs) promote nerve growth and axon regeneration. We report here that, at physiological strengths, EFs guide the migration of neuronal stem/progenitor cells (NSPCs) towards cathode. EF-directed NSPC migration requires activation of N-methyl-D-aspartate receptors (NMDARs), which leads to an increased physical association of Rho GTPase Rac1-associated signals to the membrane NMDARs and the intracellular actin cytoskeleton. Thus, this study identifies the EF as a directional guidance cue in controlling NSPC migration and reveals a role of the NMDAR/Rac1/actin signal transduction pathway in mediating EF-induced NSPC migration. These results suggest that as a safe physical approach in clinical application, EFs may be developed as a practical therapeutic strategy for brain repair by directing NSPC migration to the injured brain regions to replace cell loss.

EXTERIOR MAGNETIC FORCE ENHANCES THE TREATMENT EFFECT OF SPIO-LABEIED ENDOTHELIAL PROGENITOR CELLS IN MICE WITH TRANSIENT MIDDLE CEREBRAL ARTERY OCCLUSION

Q. Li[1], G. Tang[2], C. Zhang[2], L. Xiong[2], X. He[2], P. Miao[2], Y. Wang[2], G.-Y. Yang[1,2]

[1]Department of Neurology, Ruijin Hospital, School of Medicine, [2]Neuroscience and Neuroengineering Research Center, Med-X Research Institute and School of Biomedical Engineering, Shanghai Jiao Tong University, Shanghai, China

Objectives: Intravenous transplantation of endothelial progenitor cells (EPCs) contributed to reduced ischemic injury,[1] but only a small portion of transplanted cells migrated to damaged sites using this way.[2] In the present study, we transplanted super-paramagnetic iron oxide nanoparticles (SPIO)-labeled EPCs intravenously to cerebral ischemic mouse to explore whether exerting an exterior magnetic field could promote the migration of SPIO-EPCs to cerebral ischemic region and enhanced the treatment effect.

Methods: EPCs were isolated from human umbilical cord blood and labeled with SPIO. Cell proliferation, migration and tube formation were tested to estimate the effect of SPIO and magnetic preconditioning on EPCs. Magnetic devices in the static and flowing conditions were applied to test whether SPIO-EPCs could be captured. Adult male ICR mice underwent transient suture middle cerebral artery occlusion (tMCAO) and SPIO-EPCs transplantation with or without magnetic application. EPCs migration was tested at 24 h after tMCAO. Brain neurological behavior, brain atrophy volume, VEGF release and microvessels quantification were examined at 2 and 4 weeks after tMCAO respectively.

Results: Cell proliferation, migration and tube formation were not affected by SPIO and magnetic preconditioning compared to the control ($p>0.05$). SPIO-EPCs could be captured by exterior magnet in vitro. SPIO-EPCs were greatly increased in ischemic hemisphere at 24 h after tMCAO (3 fold vs. control, $p< 0.05$). Brain atrophy volume was reduced (2W 4.5±1 cm^3 vs. 7.0±1 cm^3; 4W 4.7±1.5 cm^3 vs. 7.3±1 cm^3; $p< 0.05$,) and neurobehavioral outcomes were greatly improved (rotor-rod test: 2W 83±8s vs. 72±7s;

4W 89±8s vs. 75±8s; neurobehavioral score: 2W 3.8±1.0 vs. 5.6±1.0; 4W 3.6±0.8s vs. 5.2±1.1s; $p < 0.05$) in SPIO-EPCs treated mice with magnetic application compared to SPIO-EPCs treated alone. Further study showed that VEGF release ($p < 0.05$) and the number of microvessels in peri-focal region (2W 66±2 vs. 54±3 per field; 4W 68±7 vs. 55±4 per field; $p < 0.05$) were significantly increased in mice with magnetic application compared to mice without magnetic application.

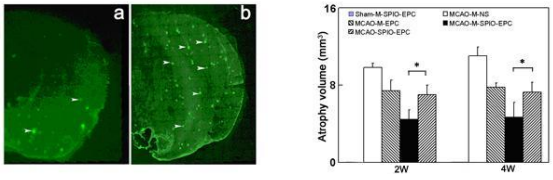

Figure 1. Increased number of SPIO-EPCs (green, arrow points) accumulated in ischemic hemisphere with exterior magnetic application (b) than without exterior magnetic application (a). Brain atrophy volume was reduced in MCAO-Magnetic-SPIO-EPC mice compared with MCAO-SPIO-EPC mice (Bar chart). (*, $p < 0.05$).

Conclusions: SPIO-labeling did not affect EPCs survival and function. Magnetic force greatly promoted EPCs migration and homing; consequently improved neurobehavioral outcomes. Our results suggested that exterior magnetic force enhanced the treatment effect of SPIO-EPCs in mice subjected to tMCAO.

References:

1. Fan Y, Shen F, Frenzel T, Zhu W, Ye J, Liu J, et al. Endothelial progenitor cell transplantation improves long-term stroke outcome in mice. Ann Neurol 2010; 67: 488-497.

2. Politi LS, Bacigaluppi M, Brambilla E, Cadioli M, Falini A, Comi G, et al. Magnetic-resonance-based tracking and quantification of intravenously injected neural stem cell accumulation in the brains of mice with experimental multiple sclerosis. Stem Cells 2007; 25: 2583-2592.

PROGRANULIN EXPRESSION IN NEURAL STEM CELLS AND THEIR DIFFERENTIATED CELL LINEAGES

L. Luo[1,2], L. Lü[1], Y. Lu[2], B. Li[2], K. Guo[2], J. Xu[2]

[1]Institute of Stomatological Research, Guanghua School of Stomatology, Sun Yat-sen University, [2]Department of Anatomy and Neurobiology, Zhongshan School of Medicine, Sun Yat-sen University, Guangzhou, China

Objectives: Progranulin(PGRN) functions as a neurotrophic factor that can regulate neurite outgrowth and enhance neuronal survival. The relationship between PGRN and neural stem cells (NSCs) differentiation may shed light on the underlying pathogenesis and potential treatments for neurodegenerative diseases. To explore the relationship between PGRN and NSCs from the subventricular zone (SVZ) of neonate rats, we prepared primary NSCs from the neonatal brains and PGRN expression profile was investigated in NSCs and its subpopulations.

Methods: NSCs were isolated from the SVZ of the brain from neonatal rats (1d) and cultured in the neural basal medium. After 7 days culture, neural stem cells aggregated into neurospheres, the PGRN expression in the neurospheres were studied by immunocytochemistry. After three passages, when neurospheres were maintained in the differential medium for 7 days, PGRN expression in differentiated NSCs cell lineages (neuron, astrocyte, oligodendrocyte) were evaluated by immunocytochemistry. The PGRN expression and localization were also detected in the neonatal rats (1d, 7d) brains tissue by immunohistochemistry.

Results: PGRN has high expression level in neural stem cells and their differentiated cell lineages in vitro. It is mainly expressed in neuron and microglia but not NSCs, astrocytes and oligodendrocytes in vivo.

Conclusions: The present results suggested that PGRN may have a potential role in the regulation and differentiation of NSCs.

*To whom correspondence should be addressed. E-mail: lvlanhai@mail.sysu.edu.cn or x510y@yahoo.com.cn, Fax: +86 02087332018

References:

Nedachi T, Kawai T, Matsuwaki T, Yamanouchi K, Nishihara M. Progranulin enhances neural progenitor cell proliferation through glycogen synthase kinase 3β phosphorylation. Neuroscience. 185(2011):106-15.

Van Damme P, Van Hoecke A, Lambrechts D, Vanacker P, Bogaert E, van Swieten J, Carmeliet P, Van Den Bosch L, Robberecht W. Progranulin functions as a neurotrophic factor to regulate neurite outgrowth and enhance neuronal survival. J Cell Biol.181(2008):37-41.

PLACENTA DERIVED STEM CELLS AMELIORATE CEREBRAL ISCHAEMIA-REPERFUSION INJURY IN MICE

A.K. Rehni[1,2], T.G. Singh[1]

[1]Pharmacology, Chitkara College of Pharmacy, Chitkara University, [2]Department of Pharmaceutical Sciences and Drug Research, Punjabi University, Patiala, India

Objectives: Administration of stem cells has been shown to exert beneficial effect in neurodegenerative disorders as well neuroprotective action on the ischaemic brain in various models. The present study has been designed to investigate the effect of placenta derived stem cells on cerebral ischaemia-reperfusion injury in mice.

Methods: Bilateral carotid artery occlusion for 17 min followed by reperfusion for 7 days was employed in present study to produce ischaemia and reperfusion induced cerebral injury in mice. The extent of ischaemic neuronal injury in the brain samples was quantitated histopathologically using haematoxylin-eosin staining. Assessment of cognitive behavior was done using elevated plus maze. Inclined beam-walking test was employed to evaluate fore and hind limb motor coordination. Motor coordination was also evaluated by observing the percentage of mice showing resistance to lateral push [1, 2].

Results: Bilateral carotid artery occlusion elicited a marked ischaemic neuronal injury and significantly impaired memory and motor coordination as inferred from the results of elevated plus-maze test, inclined beam-walking test and resistance to lateral push test. Intracerebroventricular administration of placenta derived stem cells/ embryonic neuronal stem cells significantly reversed the cerebral ischaemia-reperfusion induced ischaemic neuronal injury and consequent behavioral deficit measured in terms of loss of short-term memory and motor coordination.

Conclusions: It may be concluded that stem cells derived from mouse placenta exert beneficial effect on the ischaemic brain to an extent comparable to the neuroprotective effect of embryonic neuronal stem cells and therefore, comprise ethically more acceptable form of stem cell therapy.

References:

1. Ashish K Rehni; Pradeep Bhateja; Nirmal Singh; Amteshwar S Jaggi. Implication of mast cell degranulation in ischemic preconditioning-induced prevention of cerebral injury. Fundamental and Clinical Pharmacology 22, 179 (2008).

2. Ashish K Rehni; Nirmal Singh; Amteshwar S Jaggi; Manjeet Singh. Amniotic fluid derived stem cells ameliorate focal cerebral ischaemia-reperfusion injury induced behavioural deficits in mice. Behavioural Brain Research 183, 95 (2007).

HOMING/MIGRATION OF BONE MESENCHYMAL STEM CELL TO RAT WALLERIAN DEGENERATED SCIATIC NERVE

Z. Ren[1,2], Y. Wang[1], J. Peng[1], Q. Zhao[1], S. Lu[1]

[1]Key Laboratory of People's Liberation Army, Institute of Orthopedics, Chinese PLA General Hospital, Beijing, [2]Department of Bone and Soft Tissue Tumor, Tianjin Medical University Cancer Institute and Hospital, Tianjin, China

Background: Stem cell mobilization, homing and repopulation are sequential events with physiological roles, which can be found in nerve system. Stem cell homing is a multistep process resembling leukocyte migration to inflammatory sites and/or their homing into lymph nodes, based on the expression of both the mRNA and protein of the receptors like chemokine recepter 4 (CXCR4), corresponding to the chemokines, as stromal cell derived factor-1 (SDF-1).

Objective: To observe homing and migration of bone mesenchymal stem cell (BMSCs) to Wallerian degenerated peripheral nerve ; To

investigate the characteristic and mechanism of the phenomenon, especially the fate of migrated stem cell.

Methods: RT-PCR, Western blot, Immunofluorescence was used to measure the expression of CXCR4 in BMSCs and the expression of SDF-1 in degenerated rat sciatic nerve.By using Transwell in vitro migration assay system, the effects of SDF-1 and tissular extract from normal and degenerated rat sciatic nerve on BMSCs' migration were observed, the influence of AMD3100 (an antagonist of SDF-1/CXCR4 system) treatment on BMSCs' migration induced by nerve tissular extract were also evaluated. The red fluorescent protein (RFP) gene transfected BMSCs were injected through tail vein into the SD rats with sciatic nerve cut and anastomosised and the migration of BMSCs to the injured nerve 3 days later. The influence of AMD3100 treatment on BMSCs' migration, induced by degenerated nerve, were also evaluated. The RFP transfected BMSCs were injected in or applied around the segmental freeze-treated nerve or chemical extracted acellular nerve allografts (CEANA) bridged to the segmental defect of rat sciatic nerve. 12 weeks later, the fate of transplanted RFP-BMSCs was observed and its effect of promoting nerve regeneration and repair was evaluated through functional assessment and histological observation.

Result: Western blot and Immunofluorescence analysis revealed that BMSCs were CXCR4 positive. The mRNA of CXCR4 in BMSCs and SDF-1 in Wallerian degenerated nerve were successfully reversely transcribed by RT-PCR. Wallerian degenerated nerve tissular extract can induce the migration of BMSCs, and this effect can be suppressed by AMD3100 which is a blocker of CXCR4. Injured and Wallerian degenerated nerve can induce the migration of transplanted BMSCs, and this effect can be suppressed by AMD3100 which is a blocker of CXCR4. The RFP-BMSCs transplanted around the freezed nerve or CEANA had migrated into regenerated nerve fibers, and Nestin, S100, P0 positive, so as the cells directly injected into the freezed nerve or CEANA. Transplanting BMSCs in or around the freezed nerve or CEANA, had equally increased contraction of triceps muscle, recovery rate of muscle, the number of sciatic nerve myelinated fibers and myelin thickness.

Conclusion: Wallerian degenerated nerve can induce the migration of BMSCs, SDF-1/CXCR4 axis play an important role in this process. Compared to directly injected BMSCs into acellular nerve, BMSCs supplied around injured nerve have the similar effect, by differentiated into Schwann cell and promoting myelin formation.

TREATMENT WITH NEURO-PEPTIDE MIXTURE CEREBROLYSIN IMPROVES SURVIVAL OF NEURAL STEM CELL GRAFTS IN APP TRANSGENIC MODEL OF ALZHEIMER DISEASE

E. Rockenstein[1], K. Rockenstein[1], M. Mante[1], C. Inglis[1], A. Adame[1], P. Desplats[1], S. Winter[2], D. Meier[2], H. Moesler[2], E. Masliah[1]

[1]University of California at San Diego, San Diego, CA, USA, [2]EVER Neuro Pharma GmbH, Unterach, Austria

Introduction: Alzheimer's disease (AD) is a progressive neurological disorder characterized neuropathologically by synaptic dysfunction and loss of selected neuronal populations in the neocortex, limbic system and subcortex and clinically by symptoms including memory loss and cognitive alterations. Current treatments for AD are symptomatic but do little to tackle underlying pathology. Stem cell grafts have been investigated as neuro-restorative therapies in neurodegenerative disorders such as Parkinson's disease and AD but their use has been hampered by poor survival of grafted cells. Supply of neurotrophic factors such as brain-derived neurotrophic factor (BDNF) to the graft site has been proposed as a way to augment survival of engrafted cells.

Aim: In this context, we investigated the use of Cerebrolysin (CBL), a peptidergic mixture with neurotrophic-like properties, as an adjunct to stem cell therapy in the APP transgenic (tg) model of AD. CBL has been reported to reduce the accumulation of Aβ-protein, promote synapses and reduce the behavioral deficits in APP tg mice. Additionally, CBL has been shown to enhance the survival of neuronal stem cells (NSC) and to promote endogenous neurogenesis in APP tg mouse models.

Material and methods: Non-tg and APP tg mice were first treated with CBL for 2 weeks and then tagged NSC derived from mouse cortex were grafted into the hippocampus. Groups were assessed at 1 and 3 months

after grafting, both groups were continuously treated with CBL until sacrifice.

Results: Neuropathological analysis with antibodies against active caspase-3, BrDu, GFAP, DCX, NeuN, MAP2 and nestin showed that in vehicle-treated APP tg mice over 50% of the NSC's decayed after 1 month and 90% after 3 months of grafting. In contrast, in CBL-treated APP tg mice over 85% of the grafted NSC survived, a small proportion of them became integrated into the dentate gyrus. Moreover, surviving NSC in combination with CBL rescued the neurodegenerative phenotype in the mice and ameliorated the synaptic loss in the hippocampus and frontal cortex.

Conclusion: These results indicate that CBL treatment increases the survival of transplanted cells and may prove an efficacious adjunct to stem cell therapy based AD treatment options.

CEREBRAL ISCHEMIA AND MATRIX METALLOPROTEINASE-9 MODULATE THE ANGIOGENIC FUNCTION OF ENDOTHELIAL PROGENITOR CELLS

A. Rosell, A. Morancho, M. Hernández-Guillamon, C. Boada, V. Barceló, D. Giralt, J. Montaner

Neurovascular Research Laboratory, Hospital Vall d'Hebron Research Institut, Barcelona, Spain

Objectives: The enhancement of endogenous angiogenesis after stroke will be critical in neurorepair therapies in which endothelial progenitor cells (EPCs) might be key players. Our aim was to determine the influence of cerebral ischemia and the role of matrix metalloproteinase-9 on the angiogenic function of EPCs.

Methods: Permanent cerebral ischemia was induced by MCA occlusion in MMP9 knockout (MMP9/KO) and wild-type (WT) mice. EPCs were obtained for cell counting after ischemia (6, 24 and 72 hours) and in control animals. Matrigel™ assays and time-lapse imaging were conducted to monitor angiogenic function of EPCs.

Results: Cerebral ischemia increased the number of EPCs while MMP9 deficiency decreased their number in non-ischemic mice and delayed their release after ischemia. EPCs from ischemic mice shaped more vessel structures than controls while MMP9 deficiency reduced the angiogenic abilities of EPCs. Treatment with broad-spectrum MMP-inhibitor GM6001 and a specific MMP-9 inhibitor also decreased the number of vessel structures shaped by both human and mouse WT EPCs while exogenous MMP9 could not revert the impaired angiogenic function in MMP9/KO EPCs. Finally live time-lapse imaging showed that the extension of vascular networks was influenced by ischemia and MMP9 deficiency only during the the first steps of the network formation followed by a stable but dynamic vessel remodeling when MMP9 deficient cells could not achieve the extensions shaped by WT cells.

Conclusions: We conclude that ischemia triggers the angiogenic responses of EPCs and, in this context, MMP9 plays a key.

COORDINATED DEVELOPMENT OF VOLTAGE-GATED NA^+ AND K^+ CURRENTS REGULATES FUNCTIONAL MATURATION OF FOREBRAIN NEURONS DERIVED FROM HUMAN IPS CELLS

M. Song, O. Mohamad, D. Chen, L. Wei, S.P. Yu

Emory University School of Medicine, Atlanta, GA, USA

Objectives: Neuronal differentiation of human induced pluripotent stem (hiPS) cells provides a powerful approach to develop new treatment strategies for nervous system diseases. Before practical applications become reality, more effort is needed to thoroughly examine these converted adult cells for safety concerns as well as to better understand their competence in cell replacement therapy. To do so, a practical and reliable approach is to compare the differentiation properties of human iPS with that of embryonic stem (ES) cells. We here characterized the functional development of the pyramidal-like neurons derived from human iPS cells. We deciphered the key relationship between action potential firing patterns and the developmental changes in voltage-gated Na^+ and K^+ currents in human iPS cells, and compared them to neuronal features of cells converted from human ES cells.

Method: Human H1 ES cells (WiCell, Madison, WI) and vector-free hiPS (iPS-DF19-9/7T, WiCell Research Institute, Madison, WI)

were routinely cultured on hES-qualified Matrigel in serum-free and feeder-free mTeSR medium. Cells were passaged every 5to7 days after manual removal of differentiated colonies. For more information on the differentiation of hiPS and ES cells, please refer to the guidelines by Stem Cell Technologies and our publication (Drury-Stewart D et al., 2012). The specific markers of forebrain pyramidal neurons were identified by immunocytochemistry staining. To characterize the functional development of human ES and iPS cell-derived neurons, whole-cell patch clamp recording was performed using an EPC9 amplifier.

Results: This feeder-free differentiation method induces human ES and iPS cell into neural precursors, and then converts them into maturing pyramidal-like neurons over the ensuing 4 weeks. The differentiated neurons express forebrain pyramidal cell markers NeuN, neurofilament (NF), MAP2, PAX6, Tuj1 and FoxG1. The size of developing neurons increased continuously over the 4-week differentiation, and cell resting membrane potentials (RMPs) underwent negative shift from -40 to -70 mV. Expression of the muscarinic receptor-modulated K^+ currents (I_M) participated in the development of cell RMPs and controlled excitability. Immature neurons at week 1 could only fire abortive action potentials (AP) and the frequency of AP firing progressively increased with neuronal maturation. Interestingly, the developmental change of voltage-gated Na^+ current (I_{Na}) did not correlate with the change in AP firing frequency. It is the transient outward K^+ current (I_A) but not the delayed rectifier current (I_K) contributed to the high frequency firing of APs. Synaptic activities were observed throughout the 4-week development. These morphological and electrophysiological features were almost identical between human iPS and ES cell-derived neurons.

Conclusion: The present study provides compelling evidence showing that human iPS cells, like human ES cells, can differentiate into functional forebrain neurons. The morphological features and electrophysiological properties of human iPS cell-derived neurons are similar to human ES cell-derived neurons. These data support that iPS cell-derived neural precursors have the potential for replacing lost neurons in cell-based therapy.

Reference: Drury-Stewart D, Song, M., Mohamad, O., Yu, S.P. and Wei, L. Small Molecule Promoted Feeder Free and Adherent Differentiation of Functional Neurons from Human Embryonic and Induced Pluripotent Stem Cells. Journal of Stem Cells.2012;6:1-8

CO-TRANSPLANTATION OF NEURAL AND VASCULAR PROGENITOR CELLS ENHANCES NEUROVASCULAR UNIT FORMATION AND LONE-TERM RECOVERY AFTER CEREBRAL ISCHEMIA IN RATS

Y. Tang[1], J. Li[1], R. Tang[2], Y. Wang[1], W. Gao[1], G.-Y. Yang[1,2]

[1]Neuroscience and Neuroengineering Research Center, Med-X Research Institute and School of Biomedical Engineering, [2]Shanghai Ruijin Hospital, School of Medicine, Shanghai Jiao Tong University, Shanghai, China

Objectives: Cell-cell signaling between neuronal and vascular elements is important for long term recovery after cerebral ischemia.[1] So far brain ischemia studies emphasize either a “neurocentric” or “vascular-centric” dogma.[2] In this study we investigated if co-transplantation of neural progenitor cells (NPCs) and vascular progenitor cells (VPCs) could promote neurovascular unit remodeling and increase the efficacy of stem cell based therapy after transient middle cerebral artery occlusion (tMCAO).

Methods: 72 adult male Sprague-Dawley rats were subjected to tMCAO. One day after tMCAO, NPCs ($1x10^6$), VPCs ($1x10^6$) or NPCs and VPCs ($5x10^5$ each) were transplanted into the cortical perifocal region. Brain atrophic volume and neurobehavioral tests were performed to evaluate the outcomes of cell transplantation. Cell differentiation, neurovascular repair, angiogenesis and neurogenesis were examined within 14 days following MCAO. Expression of neurotrophic factors VEGF, BDNF, NGF and IGF-1 was also investigated.

Results: MRI analysis and behavioral tests showed that co-transplantation of NPCs and VPCs significantly decreased infarct volume 14 days after ischemia compared to PBS, NPCs and VPCs group (24 $\pm$ 1% vs. 39$\pm$2% in PBS, 30$\pm$2% in NPCs and 38$\pm$2% in VPCs, n=18, $p< 0.05$,) and improved neurobehavioral recovery. Immunostaining showed that angiogenesis and $DCX^+/BrdU^+$ cells were increased in co-transplantation compared to single cell injecting group (195$\pm$14 vs. 80$\pm$17

in NPCs and 85±17 in VPCs, p< 0.05). 14 days after ischemia, NPCs and VPCs were detected in the ipsilateral cortex, which differentiated into neurons, astrocytes and incorporated into host blood vessels as endothelial cells (ECs) and smooth muscle cells (SMCs). Neurons derived from NPCs and ECs and SMCs derived from VPCs were well correlated, suggesting the neurovascular unit was newly-formed. In addition, VEGF, BDNF, NGF and IGF-1 expression was increased in rats treated with NPCs/VPCs (p< 0.05).

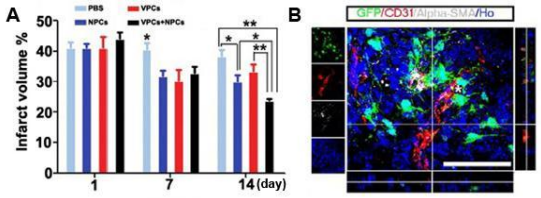

Figure 1.

A. Infarct volume % of ischemic rats calculated from MR images at day 1, 7 and 14 after tMCAO in each group. n=18/group, *, p< 0.05; **, p< 0.01, two-tailed Student's t test.

B. Representative confocal image of CD31+ (red)/α-SMA+ (white) stained blood vessels developed by transplanted Hoechst 33342 labeled VPCs are closely correlated with transplanted GFP positive NPCs (green, * indicates newly formed neurovascular unit). Bar=100 μm.

Conclusions: We demonstrated that co-transplantation of NPCs and VPCs had great benefits for neurovascular unit remodeling and therapeutic efficiency following tMCAO, suggesting that combined transplantation of different types of stem cells may constitute a novel therapeutic strategy for improving the treatment of ischemic diseases.

References:

1. del Zoppo GJ. Stroke and neurovascular protection. N Engl J Med 2006; 354: 553-555.

2. Font MA, Arboix A, and Krupinski J. Angiogenesis, neurogenesis and neuroplasticity in ischemic stroke. Curr Cardiol Rev 2010; 6: 238-244.

NEURORESTORATIVE EFFECT OF URINARY BLADDER MATRIX-MEDIATED NEURAL STEM CELL TRANSPLANTATION FOLLOWING TRAUMATIC BRAIN INJURY IN RATS

J. Wang[1], A. Liou[2], Z. Ren[1], L. Zhang[3], B. Brown[4], X. Cui[3], S. Badylak[4], Y. Cai[1], Y. Guan[1], R.K. Leak[2], J. Chen[1,2], X. Ji[1], L. Chen[1]

[1]Xuanwu Hospital, Capital Medical University, Beijing, China, [2]Center of Cerebrovascular Disease Research, University of Pittsburgh School of Medicine, [3]Department of Bioengineering, University of Pittsburgh, [4]Department of Surgery, University of Pittsburgh School of Medicine, Pittsburgh, PA, USA

Objectives: Traumatic brain injury (TBI) is a leading cause of cell death and disability among young adults without a successful therapeutic strategy. The multiphasic injury prognosis of TBI has limited the success of conventional pharmacological approach. Recent success in stem cell in bioactive scaffold transplantation towards other injury paradigms (*1*) has provided a novel therapeutic strategy for TBI. In this study, we investigated the neurorestorative effect of urinary bladder matrix mediated neural stem cell transplantation after TBI.

Methods: Mouse neural stem cell (NSC, $1x10^5$ cells/ml) used for transplantation were first cultured in a bioactive scaffold derived from porcine urinary bladder called UBM (4 injection sites, 2.5ml each) before injected around the injured sites post-controlled cortical impact (CCI, velocity, 4.0 m/sec; duration, 0.5 sec; depth, 3.2mm) in rats. Recovery of sensory-motor faculties was quantified by fore-limb and hind-limb foot-fault tests whereas memory and cognitive functions was measured by Morris water maze. Tissue loss was determined from integration of area loss in serial coronal sections of CCI rats after cresyl violet staining. The number of viable neurons at CA3 regions of the hippocampus was determined by stereology. Furthermore, white matter injury was measured by the differential intensity of immuno-fluorescent staining for myelin basic protein (MBP) to reflect matured oligodendrocytes and SMI32 to indicate neurofilament integrity.

Results: Before transplantation, the pluripotency of NSC isolated from the

subventricular zone of 2 months old male mouse was ascertained by allowing them to undergo differentiation followed by detecting the emergence of b-tubulin III, GFAP and O4, markers of different linages. Moreover, UBM has emerged to be an ideal scaffold in this study over collagen or matrigel was based on its superior support of NSC proliferation and differentiation, excellent biocompatibility when use *in vivo* since it does not elicit inflammatory response higher than vehicle over the duration of 3-4 weeks. The results indicated that transplantation of UBM alone was sufficient to decrease the loss of motor-sensory skills from TBI (examined 3-28 days post-CCI) as well as cortical tissue loss. The inclusion of NSC did not elicit further motor function improvement or tissue loss. However, UBM containing proliferating neural stem cells were mandatory to recover memory and cognitive impairments (examined 26-28 days post-CCI) and elicit an increase in viable neurons at the CA3 region of the hippocampus. Finally, white matter injury induced by CCI was also attenuated by UBM alone, which was further attenuated from the inclusion of NSC.

Conclusions: In this study, NSC pre-cultured in UBM, when introduced post-CCI, ameliorated neurobehavioral deficits, increase CA3 viable neurons as well as reduce tissue loss and white matter injury. Specifically, UBM alone is able to confer short term protection such as significantly attenuate motor function impairments. However, the presence NSC in the UBM matrix is mandatory for long term protection to ameliorate memory and cognitive deficits.

References:

1. E. Y. Snyder, Y. D. Teng, Stem cells and spinal cord repair. *The New England journal of medicine* **366**, 1940 (May 17, 2012).

GENERATION OF NEURAL PROGENITOR-LIKE CELLS FROM HUMAN DERMAL FIBROBLASTS

Y. Wang[1], C. Tian[1], K. Ma[2], J. Zheng[1,3]

[1]Department of Pharmacology and Experimental Neuroscience, [2]Department of Genetics, Cell Biology and Anatomy, [3]Department of Pathology and Microbiology, University of Nebraska Medical Center, Omaha, NE, USA

Objectives: Human neural progenitor cells (NPCs) provide the promising cell source for the treatment of neurodegenerative disorders, such as Parkinson's and Alzheimer's disease. Recently, mouse somatic cells have been successfully converted into self-renewable and tripotent NPCs. Here, we proposed that the novel combination of transcription factors including BRN2, SOX2, KLF4, and c-MYC could directly reprogram human dermal fibroblasts into induced neural progenitor cells (iNPCs).

Methods: Human dermal fibroblasts, isolated from fetal skin tissues (12-16 weeks post-conception) of elective abortions in full compliance with UNMC and NIH ethical guidelines, were infected with retroviral pool encoding BRN2, SOX2, KLF4, and c-MYC with the ratio of 1:1:1:1. At day three, the medium was changed to NPC culture medium supplemented with 20 ng/ml EGF, 10 ng/ml bFGF, and 2 µg/ml heparin. When observing the iNPC colonies, we picked the colonies into non-adherent bacterial culture dishes. The immunochemistry and Real-time PCR analysis were employed to examine the expression of NPC (SOX2, BRN2, NESTIN, GLAST, BLBP, and GPM6A) and fibroblast (ACTA2 and CTGF) marker genes. Neuron and astrocyte differentiation assay were performed in the medium with 1% B27 and 10% FBS, respectively.

Results: With the ectopic expression of BRN2, SOX2, KLF4, and c-MYC in human dermal fibroblasts, some compact colonies showed up after cultured in NPC medium for around 50 days. These cells shared a bipolar morphology with primary human NPCs, and the expression levels of connective tissue marker CTGF and the skeletal muscle marker ACTA2 were suppressed to levels comparable to those in primary human NPCs. Moreover, the RT-PCR assay revealed that the expression levels of NPC markers including SOX2, BRN2, NESTIN, GLAST, BLBP, and GPM6A were highly up-regulated, and immunostaining also showed that human iNPCs highly expressed NESTIN and SOX2. Upon differentiation, iNPCs produced TUJ^+ neurons and $GFAP^+$ astrocytes exhibiting typical neuronal and astrocytic morphologies.

Conclusions: Human dermal fibroblasts can be directly reprogrammed to iNPCs. These cells share most of similarities with primary human NPCs, including proliferation, self-renewal, and differentiation potentials *in vitro.* Although *in vivo* analysis is still needed, these

human iNPCs offer great promise as the viable candidate for cell replacement therapy of neurodegenerative diseases.

TRANSPLANTATION OF HYPOXIA-PRECONDITIONED IPS/ES CELLS COMBINED WITH PERIPHERAL WHISKER STIMULATION IMPROVED FUNCTIONAL RECOVERY AFTER ISCHEMIC STROKE IN NEONATAL RATS

Z. Wei[1], K. Francis[1], O. Mohamad[1], S.P. Yu[1], L. Wei[1,2]

[1]Department of Anesthesiology, [2]Department of Neurology, Emory University School of Medicine, Atlanta, GA, USA

Objectives: Neonatal ischemic encephalopathy with acute or subacute brain injury causes significant mortality and long-term morbidity. Transplantation therapy using induced pluripotent stem cells (iPSCs) or embryonic stem cells (ESCs) has been identified as a promising treatment for ischemic stroke. We have previously showed that peripheral whisker stimulation promotes cell proliferation and migration in the post-ischemic cortex of mice. The current study is attempting to combine cell-based transplantation and peripheral whisker stimulation to obtain an improvement in tissue repair and functional recovery of stroke neonates.

Methods: Neonatal P7 rats were subjected to middle cerebral artery occlusion (MCAO) that targeted to the right barrel cortex. Neural progenitor cells derived from iPS or ES cells were subjected to sublethal hypoxic treatment and prelabeled with a Hoechst dye and transplanted into the stroke region and penumbra 7 days after stroke. Starting from day 2 after transplantation, the affected whiskers on the left face was mechanically stimulated 3 times (15min) per day. Changes of local cerebral blood flow (LCBF) were measured using a laser Doppler scanner. Whisker stimulation evoked intrinsic optical signals (IOS) were imaged 3-4 weeks post-ischemia. Daily BrdU injections were applied to detect cell proliferation. Immunohistochemical staining was used to measure neuronal, glial, and endothelial cells. Behavioral tests were performed to evaluate functional recoveries after stroke.

Results: In stroke animals, the evoked IOS signaling was absent in the ischemic core while partial recovery could be detected in cell transplantation animals. Better recovery was seen in animals that received cell transplantation plus peripheral stimulation. LCBF was significantly higher in animals that received cell transplantation and transplantation plus stimulation. Immunohistochemical staining demonstrated better cell survival in animals that received hypoxia-preconditioned cells and peripheral stimulation. Many surviving cells were co-stained with Nestin or NeuN, some were double positive to Glut-1 or CD-31 staining, suggesting differentiation into neural lineage and neurovascular cells. Increased proliferating activity was demonstrated with more BrdU-positive cells doubled with NeuN or CD31 in transplantation group compared to non-transplantation group. Moreover, rats that received cell transplantation and peripheral stimulation showed significantly alleviated sensorimotor deficits after stroke.

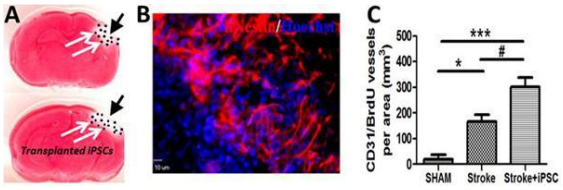

[hiPS Cell Transplantation after Neonatal Stroke]

Figure 1. hiPS Cell Transplantation after Neonatal Stroke

A. TTC staining and immunofluorescence 7 days after ischemia insult showed infarct formation with the cortex.

B. Immunostaining after hiPSC transplant. Nestin (red) indicated neural progenitor cells. Nestin (red)/Hoechst (blue) double staining suggested transplanted iPSC-derived neural progenitors survived and differentiated within the ischemic brain after transplantation.

C. CD31/BrdU-colabeled vessels showed significant increase after stroke and iPSC transplantation. Compared to stroke control group, hiPSC dramatically enhanced generation of new vessels in transplantation area.

Conclusions: Transplantation of hypoxic preconditioned iPSCs/ESCs survived and differentiated into neurons and promoted neurogenesis and angiogenesis in the

ischemic cortex. This combination strategy may help to rebuild neurovascular network and improved functional recovery in neonatal stroke rat.

CXCL12 ACTIVATED INTERACTION OF CXCR4 AND CXCR7 IN STEM CELL SURVIVAL

D. Xu[1], B. Zhu[1], Y. Zhang[1], J. Zheng[2]

[1]Tongji University Affiliated Tenth Hospital, [2]Tongji University, Shanghai, China

Chemokine CXCL12 is widely expressed in the central nervous system (CNS) and essential for the proper functions of human neural progenitor cells (hNPCs). Although CXCL12 is known to function through its receptor CXCR4, recent data has suggested that CXCL12 binds to chemokine receptor CXCR7 with higher affinity than to CXCR4. Using a primary hNPCs culture system, we demonstrated that CXCL12 promotes hNPCs survival in the events of camptothecin-induced apoptosis or growth factor deprivation, and that this effect requires both CXCR7 and CXCR4. Consistent with these findings, significant higher number of apoptotic NPCs were found in the developing brain of CXCR7 knockout mice. Based on FRET imaging , we found that CXCR7 and CXCR4 interaction increased after CXCL12 treatment. Further, we demonstrated increased CXCR7 and CXCR4 interaction is essential for neural stem cell survival in physiology and pathology condition. Since survival of hNPCs is important for neurogenesis, CXCR7 may become a new therapeutic target to properly regulate the critical processes of brain development.

LEVELS OF ENDOTHELIAL PROGENITOR CELLS IN THE HUMAN BRAIN ARTERIOVENOUS MALFORMATIONS OF DIFFERENT AGES AND SYMPTOMS

T. Xu[1], J. Huang[2], G.-Y. Yang[2,3], W. Zhu[1]

[1]Department of Neurosurgery, Huashan Hospital, Fudan University, [2]Neuroscience and Neuroengineering Research Center, Med-X Research Institute and School of Biomedical Engineering, [3]Department of Neurology, Ruijin Hospital, School of Medicine, Shanghai Jiao Tong University, Shanghai, China

Objectives: Brain arteriovenous malformations (BAVMs) are high-flow vascular malformations, which are frequent in newborns, and persist throughout life. They become a significant clinical risk and are characterized by aberrant angiogenesis and vascular remodeling. Endothelial progenitor cells (EPCs) participate in vascular remodeling and were demonstrated to present in the nidus of the BAVMs, which may mediate pathological vascular remodeling. The aim of this study is to investigate the relationship between EPC levels and age, bleeding rate in BAVM patients.

Methods: Forty-two surgical specimens from BAVMs were divided into 6 groups according to the age and symptoms: group 1=ruptured BAVMs patients under 16 years (n=9), group 2=unruptured BAVMs patients under 16 years (n=4), group 3=ruptured BAVMs aged 32 to 39 (n=8), group 4=unruptured BAVMs aged 32 to 39 (n=8), group 5=ruptured BAVMs patients over 50 (n=8) and group 6=unruptured BAVMs patients over 50 (n=5). Brain tissues derived from the temporal lobes of epileptic patient surgery were used as a control. Cells which were double-positive of the endothelial cell marker VEGFR-2 (KDR) and stem cell marker CD34 were identified as EPC. In addition, SDF-1 and VEGF expression in all the samples were identified by immunohistochemistry.

Results: Double labeled CD34 and VEGFR-2, SDF-1 and VEGF-positive staining could be detected in BAVM tissues while these cells could not found in the control group, indicating EPC was greatly increased in BAVM tissues compared to the control ($p< 0.05$). The EPCs are mostly located in the neointima of abnormal blood vessel wall. Further study demonstrated that the number of EPCs was increased in young group (group 1 and 2) compared to the other 4 groups ($p< 0.05$). The number of EPCs was no difference between ruptured and unruptured patients in each age group.

Conclusions: We demonstrated that EPCs were increased in the BAVM patients, especially in teen-age patients, suggesting EPCs plays important role in the process of vascular remodeling. The number of EPCs was similar in both rupture and unruptured BAVMs, suggesting the effect of EPCs in ruptured BAVMs was limited.

DIRECT REPROGRAMMING FROM HUMAN FIBROBLASTS TO HUMAN NEURONAL (HIN) CELLS; A NOVEL METHOD PREPARING CELL RESOURCE FOR STROKE THERAPY

T. Yamashita[1], A. Abeliovich[2], K. Abe[1]

[1]Department of Neurology, Okayama University, Okayama, Japan, [2]Departments of Pathology and Cell Biology, Columbia University, New York, NY, USA

Strokes induce neuronal cell death in the human brain, results in a major cause of death and a reduction in the quality of life. Induced pluripotent stem cells methods supplying neuronal cells, may provide cures for various neurological diseases including stroke, but its high tumorigenesis interferes with clinical applications. Recently we and other laboratory reported novel method supplying neuronal cells, by which neurons are directly reprogrammed from human fibroblasts, without passing pluripotent state (Liang et al, Cell 2011; Pan et al, Nature 2011). We successfully converted human skin fibroblasts to human-induced neuronal (hiN) cells by viral cotransduction of a combination of five transcription factors, Ascl1, Brn2, Myt1l, Olig2, and Zic1. These hiN cells expressed several neuronal markers including Tuj1, MAP2, Tau1, and NeuN with a neuronal morphology. We also confirmed that the hiN cell phenotype can be achieved without expression of the progenitor/stem cell markers Sox2, Pax6, Otx2, or FoxG1 during hiN cell reprogramming. Of note, we demonstrated that GFP-labeled hiN cells, which were transplanted in utero into embryonic day 13.5 mouse brain, could migrate from the ventricles into various brain regions. And the results of voltage-clamp recordings from hiN cells within acutely prepared brain slices, indicating hiN cells can make functional neuronal connection with surrounding neuronal cells in vivo. Taken together, these results suggested that this novel hiN method can supply functional neuronal cells from human skin fibroblasts, without through progenitor/pluripotent state. Here, we propose hiN cells can be promising and safer cell source for cell transplantation therapy to stroke patients.

HUMAN MESENCHYMAL STEM CELLS TRANSPLANTED INTO RATS WITH ISCHEMIC BRAIN INJURY MIGRATE TO NEUROGENIC ZONES WHERE THEY ACTIVATE NEURAL PROGENITORS

K. Yarygin[1,2], V. Burunova[1,3], E. Cherkashova[4], L. Gubski[4], I. Kholodenko[1]

[1]Institute of Biomedical Chemistry, [2]Institute of General Pathology and Pathophysiology, [3]Stemma Company, [4]Russian National Research Medical University, Moscow, Russia

Objectives: Promising preclinical results were obtained using human MSC in animal models of brain ischemia [1-3]. The scope of this study was to explore homing of human placental mesenchymal stem cells (HP-MSC) after transplantation into rats with ischemic brain injury, sham operated animals, and intact rats and to investigate the effects of HP-MSC transplantation upon the recipient's own neural progenitors.

Methods: Rats were subjected to the operation of temporary occlusion of the middle cerebral artery (MCAO), sham operation or left intact. Human placenta mesenchymal stem cells were labeled in vitro with fluorescent magnetic microparticles and infused i.v. or injected into the brain tissue 24 hours after the operation. Labeling did not alter HP-MSC viability, proliferation rate and differentiation. The fate of transplanted cells was monitored by magnetic resonance imaging (MRI) in vivo, on histological slices using fluorescent microscopy and immunohistochemistry, and by PCR revealing human DNA in rat tissues. Rat neural stem cells (NSC) and their derivatives were identified and characterized by immunocytochemistry.

Results: HP-MSC transplantation significantly reduced the volume of the ischemic lesion evaluated by MRI. Both MRI and fluorescent microscopy showed that some transplanted cells concentrated around the infarction area and in brain neurogenic zones - the dentate gyrus (DG) of hippocampus and the subventricular zone (SVZ). Some HP-MSC survived in host brain for over 45 days and expressed glial or neural markers. However, differentiating human cells failed to acquire astrocyte- or neuron-like morphology. Human MSC transplantation further stimulated proliferation of rat cells in SVZ, already enhanced by ischemia, and their migration

towards the lesion site. This effect was more pronounced at the side of lesion.

Conclusions: Transplanted MSC are strongly attracted not just to the loci of injured brain tissue, but also to neurogenic zones and undergo homing at both sites. Favorable effects of HP-MSC transplantation in rat MCAO model are at least partly associated with their targeted migration to brain neurogenic zones and activation of endogenous neural precursors through paracrine mechanisms and cell-to-cell contacts.

References:

1. Kranz A., Wagner DC, Kamprad M et al. Transplantation of placenta-derived mesenchymal stromal cells upon experimental stroke in rats. Brain Res 2010, 1315, 128-136.

2. Shimada IS, Spees JL Stem and progenitor cells for neurological repair: minor issues, major hurdles, and exciting opportunities for paracrine-based therapeutics. J Cell Biochem 2011, 112, 374-380.

3. Yarygin KN, Kholodenko IV, Konieva AA et al. Mechanisms of positive effects of transplantation of human placental mesenchymal stem cells on recovery of rats after experimental ischemic stroke. Bull Exp Biol Med 2009, 148, 862-868.

THERAPEUTIC BENEFIT OF BONE MARROW-DERIVED ENDOTHELIAL PROGENITOR TRANSPLANTATION AFTER EXPERIMENTAL ANEURYSM EMBOLIZATION WITH COIL IN RATS

S. Zhang[1], Q. An[1], X. Chen[1], J. Zhang[2], W. Zhu[1], G.-Y. Yang[3]

[1]Department of Neurosurgery, Huashan Hospital, Fudan University, [2]Department of Radiology, Huashan Hospital, School of Medicine, Fudan University, [3]Neuroscience and Neuroengineering Research Center, Med-X Research Institute and School of Biomedical Engineering, Shanghai Jiao Tong University, Shanghai, China

Objectives: Aneurysm embolization with coil is broadly used clinically. However, the recurrence of aneurysm is still high because the endothelial layer of aneurysm neck lost its integrity after embolization with coil. Bone marrow-derived endothelial progenitor cells (BM-EPCs) could differentiate to mature endothelial cells during vascular repairing processes.[1] The aim of our study is to explore the effects of BM-EPC on aneurysm repairing and remodeling in a rat embolization model of abdominal aortic aneurysm.

Methods: EPCs were isolated from rat bone marrow and labeled with SPIO. Cell proliferation, migration and tube formation were tested to examine the effect of SPIO on EPCs. Aneurysm was developed at the abdominal aortic artery in adult male SD rats (n=15) by end-to-side anastomosis using a donor descending thoracic aorta.[2] Rats were divided randomly into EPC transplant group (EPC group, n=5), HUVEC transplant group (HUVEC group, n=5) and PBS control group (PBS group, n=5). BM-EPCs and HUVECs were labeled with SPIO before injection. $5X10^5$ EPCs or HUVACs were injected via abdominal aortic artery. Tissue appearance assessment and histological examination were performed 6 weeks after cell transplantation to observe whether the labeled cells were in the aneurysm neck and the extent of aneurysm repairing.

Results: EPC proliferation, migration and tube formation were not affected with SPIO labeling compared to the control (p>0.05). The number of SPIO-labeled EPC was greatly increased in the aneurysm neck in EPC transplanted rats compared to the HUVEC and PBS control rats (p< 0.05). The SPIO-labeled EPC mainly located in the aneurysm neck and surrounded by fibrous tissue. HE staining showed that the aneurysm orifice was closed with neointima. The aneurysm was filled with newly formed fibrous tissue while this change did not be detected in the HUVEC and PBS control rats.

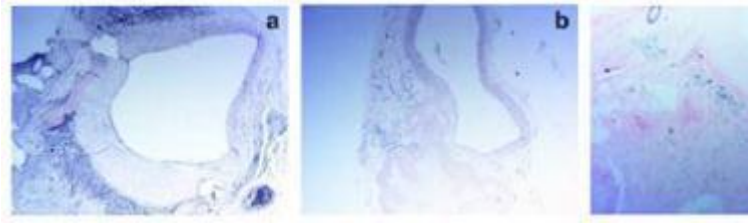

[Figure 1]

Figure 1. Hematoxylin and eosin staining showed that the aneurysm neck tissue repair of the model of EPC transplanted group (a) is better than the control group (b), simultaneously Prussian blue staining showed SPIO-EPC located in the aneurysm neck of

the model of EPC transplanted group (c), in contrast to the control group (d).

Conclusions: The SPIO-EPCs accumulated in the aneurysm neck, which accelerated focal fibrous tissue remodeling, suggesting BM-EPCs play a crucial role in the repairing and remodeling of the aneurysm neck orifice.

References:

1. Fang X, Zhao R, Wang K, Li Z, Yang P, Huang Q, *et al.* Bone marrow-derived endothelial progenitor cells are involved in aneurysm repair in rabbits." *J Clin Neurosci* 2012; 19: 1283-1286.

2. Frosen J, Marjamaa J, Myllarniemi M, Abo-Ramadan U, Tulamo R, Niemela M, *et al.* Contribution of mural and bone marrow-derived neointimal cells to thrombus organization and wall remodeling in a microsurgical murine saccular aneurysm model. *Neurosurgery* 2006; 58: 936-944.

NADPH OXIDASE 1, A NOVEL MOLECULAR SOURCE OF ROS IN HIPPOCAMPAL NEURONAL DEATH OF VASCULAR DEMENTIA

D.-H. Choi[1,2], K.-H. Lee[2], J.-H. Kim[2], J.-H. Seo[2], J. Lee[1,2]

[1]Konkuk University School of Medicine, [2]Center for Neuroscience Research, SMART Institute of Advanced Biomedical Science, Konkuk University, Seoul, Republic of Korea

Objectives: Chronic cerebral hypoperfusion has been demonstrated to be a common pathological factor contributing to neurodegenerative diseases such as vascular dementia (VaD). The main clinical outcomes of chronic cerebral hypoperfusion are cognitive deficits and permanent neural impairment. While oxidative stress has been strongly implicated in the pathogenesis of VaD, the molecular mechanism underlying the selective vulnerability of the hippocampal neurons to oxidative damage remains unknown. Here, we assessed whether the NADPH oxidase complex, a specialized superoxide generation system, plays a role in VaD by permanent ligation of bilateral common carotid arteries in rats. We previously reported that memory impairment becomes exacerbated through the interaction between chronic cerebral hypoperfusion and amyloid toxicity in a rat model (Choi et al., 2011). Moreover, we reported that NADPH oxidase 1(Nox1)-derived reactive oxygen species (ROS) was implicated in dopaminergic neuronal death in a Parkinson's disease animal model (Choi et al., 2012).

Methods: Male Wistar rats submitted to permanent occlusion of bilateral common carotid arteries (2VO) or sham operation (Sham). Rats were used for gene expression studies and protein expression studies at 1, 2, 4, and 10 week after operation. The animals received an i.p. injection of 10 mg/kg/day apocynin or vehicle immediately after the sham or 2VO operation, and received the same dosage every day for 8 weeks. AAV particles containing either Nox1 shRNA/AAV or scrambled shRNA/AAV were stereotaxically injected into hippocampal CA1 subfield 4 weeks prior to the 2VO or sham operation. Behavioral tests and histological evaluation were performed at 10 and 15 weeks post-2VO operation, respectively.

Results: Nox1 expression was gradually increased in hippocampal neurons, starting 1 week post 2VO and sustained until 10 weeks post 2VO. The levels of superoxide and neuronal death in the CA1 subfield of the hippocampus were increased in 2VO rats. Both inhibiton of Nox by apocynin, a putative Nox inhibitor and adeno-associated virus-mediated Nox1 knockdown significantly reduced 2VO-induced ROS generation, oxidative DNA damage and hippocampal neuronal degeneration and cognitive impairment.

Conclusions: These results imply that Nox1-mediated oxidative stress plays an important role in neuronal cell death and cognitive dysfunction in vascular dementia.

References: Choi BR et al., Stroke. 2011;42(9):2595-604; Choi DH et al., Antioxidants & redox signaling. 2012;16(10):1033-45.

PLASTICITY OF THE VISUAL SYSTEM IN HEMIANOPIC PATIENTS

S. Chokron[1], C. Perez[2], C. Peyrin[3], C. Cavezian[4], M. Obadia[5], F. Héran[6], O. Gout[5]

[1]Unité Fonctionnelle Vision et Cognition, CNRS & Fondation Ophtalmologique Rothschild, [2]Unité Fonctionnelle Vision et Cognition, Fondation Ophtalmologique Rothschild, Paris, [3]CNRS, LPNC, Grenoble, [4]CNRS, Université Paris Descartes, [5]Service de Neurologie, [6]Service de Radiologie, Fondation Ophtalmologique Rothschild, Paris, France

Introduction: One way to tackle the question of a hemispheric specialization at the occipital level is to study unilateral occipital damage patients with subsequent homonymous hemianopia, which is a loss of vision in the contralesional visual field. Recent data suggest that vision in the central and the ipsilesional visual field, although previously considered as normal, could be altered as well. The current study aims to investigate visual scene perception and its neuro-anatomical correlates for stimuli presented in the central visual field of patients with homonymous hemianopia, and thereby to assess the effect of a right or a left occipital lesion on brain reorganization.

Aims of the study: The goals of the present study are three-fold. First, visual processing in the central visual field and its underlying neural correlates were assessed in hemianopia. Second, we aimed to test for the effect of the lesion side on the performance pattern as well as cerebral activation, especially in the occipital lobe, when processing information in the central visual field. Finally, we investigated functional neural correlates according to the cognitive demand of the task (low in the detection task or high in the categorization task).

Patients and methods: Fourteen healthy participants, three left brain damaged (LBD) patients with right homonymous hemianopia and five right brain damaged (RBD) patients with left homonymous hemianopia performed a visual detection task (i.e. “Is there an image on the screen?”) and a categorization task (i.e. “Is it an image of a highway or a city?”) during a block-designed functional magnetic resonance imaging (fMRI) recording session.

Results: Cerebral activity analyses of the posterior areas - the occipital lobe in particular - highlighted bi-hemispheric activation during the detection task but more lateralized, left occipital lobe activation during the categorization task in healthy participants. Conversely, in patients, the same network of activity was observed in both tasks. However, LBD patients showed a predominant activation in their right hemisphere (occipital lobe and posterior temporal areas) whereas RBD patients showed a more bilateral activation (in the occipital lobes).

Conclusions: Overall, our preliminary findings suggest a specific pattern of cerebral activation depending on the task instruction in healthy participants and cerebral reorganization of the posterior areas following brain injury in hemianopic patients which could depend upon the side of the occipital lesion.

CHRONIC SUBPRESSIVE ANGIOTENSIN II IS DIRECTLY IMPLICATED IN COGNITIVE DYSFUNCTION, NEURODEGENERATION AND BETA-AMYLOIDES FORMATION

S. Duchemin[1], E. Belanger[2], K. Monteiro-Sylva[3], H. Buck de Sousa[3], G. Ferland[2], H. Girouard[1]

[1]Pharmacology, [2]Nutrition, Université de Montréal, Montréal, QC, Canada, [3]Faculdade de Ciências Médicas da Santa Casa, Sao Paulo, Brazil

Background and objective: Hypertension is a major risk factor for cerebrovascular diseases and neurodegenerative disorders worldwide. It has been involved in beta-amyloids plaque formation found in Alzheimer disease (AD) linking hypertension to AD. An important protein involved in the onset hypertension is the octapeptide, angiotensin II (angII), which had been reported to alter vascular reactivity and raise oxidative stress in the brain. However we do not know how this affects the brain chronically. In this study we aim to determine whether chronic angII administration alters cerebral structure and functions independently of its effect on blood pressure.

Method: Eight weeks old male C57BL6 mice were chronically perfused with hypertensive (1000 ng/kg/min) or subpressive (200 ng/kg/min) concentrations of ang II using osmotic pumps. The Morris water maze

(MWM) was used to determine spatial learning abilities in mice perfused during 14 and 21 days with angII (n=10/group). Afterward brain regions involved in memory were tested for neurodegeneration and amyloid plaque using immunofluorescence with Fluoro-Jade B, 6E10 and thioflavine-S, markers of neurodegeneration, new amyloid plaque, and dense core of amyloid plaque formation, respectively.

Results: The MWM revealed that angII induced a cognitive deficit after 21 days at both concentrations. The cue and probe test of the MWM showed no difference in motor functions or in vision acuity of the perfused mice compared to controls. Therefore we studied brain tissue after 21 days of angII perfusion. In both angII groups we found Fluoro-Jade B positive neurons in the hippocampus. Precursors of amyloid plaque formation identified by 6E10 immunofluorescence was observed in the cortex and the hippocampus whereas no thioflavine-S was observed alone or colocalised with 6E10.

Conclusions: These results suggest that angII can induce the development of amyloid plaques and cause neurodegeneration independently of its effect on blood pressure. Therefore, ang II may be an important factor in neural deterioration as well as a potent precursor in Alzheimer disease and vascular dementia.

THE HISTOPATHOLOGICAL AND ULTRASTRUCTURAL CHANGES IN HIPPOCAMPUS OF RAT MODELS WITH VASCULAR DEMENTIA

J. Sun, **Y. Li**

Department of Pathology, Institute of Neuroscience, Chongqing Key Laboratory of Neurobiology, Chongqing Medical University, Chongqing, China

Objective: To study the histopathological and ultrastructural changes in the hippocampus of rat models with vascular dementia (VD).

Methods: 60 SD rats were randomly divided into the sham-operated and model groups. There were 50 rats in the model group and 10 rats in the sham-operated group. The VD models were constructed by the two-vessel occlusion method and were killed at various time points （1, 7, 14, 21 and 28 d）after operation, while the bilateral common carotid arteries of rats in the sham-operated group were only separated. At each time point 10 VD models were killed, and the histopathological and ultrastructural changes in the hippocampus were observed with microscopy and electron microscopy, respectively.

Results: Compared with the sham-operated group, the number of neurons in CA1 of hippocampus of rats in model groups all decreased significantly（P=0.000）. The rats in model group 14 d after operation has the least neurons in CA1 of hippocampus, and the ultrastructural changes showed that the pyknosis and degeneration of neurons was in hippocampus. However, with the recovery of cerebral blood flow supply, the number of neurons gradually increased, and less neuron degeneration was observed with electron microscopy.

Conclusion: In early course of the chronic cerebral hypoperfusion the degereration of neurons in hippocampus is reversible, which provides theoretic basis for early clinical treatment on patients with chronic cerebral hypoperfusion.

This work was supported by the National Natural Science Foundation of China (NSFC: 81271426, 30973154, 81100948).
Corresponding author: Yu Li, M. D., Professor. Email: liyu100@163.com

CEREBRAL PERFUSION AND COGNITIVE FUNCTION IN POST-STROKE PATIENTS WITH HYPERTENSION

S. Matsumoto, M. Shimodozono, K. Kawahira

Department of Rehabilitation and Physical Medicine, Kagoshima University, Kirishima City, Japan

Background and aim: Hypertension is a major risk factor of stroke, and is the main causes of chronic cerebrovascular insufficiency and cognitive-function decline. Moreover, there is a relationship between hypertension and vascular dementia, the latter of which results in marked neurocognitive dysfunction and social disadaptation of patients. To estimate cerebral perfusion and cognitive function in post-stroke patients with hypertension before and after hypotensive therapy.

Methods: The treatment group comprised 28

post-stroke patients (mean age ± standard deviation [SD], 57.8 ± 8.3 years) with previously untreated or ineffectively treated essential hypertension. All patients underwent brain xenon-enhanced computed tomography (Xe-CT) scanning and comprehensive neuropsychological testing, both before and after 24 weeks of hypotensive therapy using the angiotensin II receptor blocker (ARB) olmesartan medoxomil. The control group comprised 20 age-matched post-stroke patients (mean age ± SD, 56.6 ± 8.5 years) without hypertension, carotid atherosclerosis, coronary artery disease, or psychiatric disorders.

Results: The hypertensive patients had significantly lower levels of cerebral perfusion (4-8%) in all brain regions, a 25% decrease in attention and psychomotor speed, and an 18% decrease in mentation compared with the control subjects. Following 6 months of hypotensive therapy, the hypertensive patients experienced an increase in cerebral perfusion by 8-15% in all brain regions, an 18-36% improvement in attention and psychomotor speed, and an average 19% improvement in abstract mentation.

Conclusions: Hypertensive patients showed marked signs of cerebral hypoperfusion and impaired cognitive function, as indicated by decreased attention, reduced psychomotor speed, and slow mentation; however, these symptoms were improved by 24 weeks of hypotensive treatment with an ARB.

Hypertensive post-stroke patients showed marked signs of cerebral hypoperfusion and impaired cognitive function compared with controls, including decreased attention, reduced psychomotor speed, and slower mentation. Hypotensive treatment with ARB for 24 weeks improved their cerebral perfusion and cognitive function.

A ROLE OF CREB-CRTC SIGNALING IN NICOTINE-INDUCED NEUROPROTECTION

T. Sasaki[1], K. Kitagawa[1], A. Watanabe[1], T. Yukami[1], N. Oyama[1], Y. Yagita[1], H. Takemori[2], H. Mochizuki[1]

[1]Department of Neurology, Osaka University Graduate School of Medicine, Osaka,
[2]Laboratory of Cell Signaling and Metabolism, National Institute of Biomedical Innovation, 7-6-8 Asagi, Saito, Ibaraki, Japan

Background: Neuronal nicotinic acetylcholine receptors (nAChRs) can regulate the activity of many neurotransmitter pathways throughout the central nervous system and are considered to play an important role in neuroprotection. nAChRs consist of five membrane-spanning subunits (α and β isoforms) that can associate in various combinations to form functional nAChR ion channels. We and other groups previously found that nicotine-induced neuroprotection was involved in the activation of CREB-CRE signaling. The discovery of a family of coactivators named transducer of regulated CREB activity (TORC, also known as CREB regulated transcriptional coactivator (CRTC) provided new insights on CREB activation. However, it remains to be clarified whether the intracellular signaling of CRTC coactivator is crucial for CREB-dependent neuronal survival via nAchR.

Methods: Neuronal cultures were prepared from the cortex of embryonic day 16 (E16) rat embryos. Also, microglial cell lines (R2a and C8B4 cell line) were harvested. To directly detect the CREB-CRTC activity, we have transfected adeno-CRE-luciferase reporter, or GAL4-CRTC, and rTK-luciferase (internal control) to cortical neurons and measured these activities using luciferase assays. We have examined both *bdnf* and *IL-10* promoter activities. Western blot analyses were performed to examine phosphorylation of CREB, TORC1, Thr^{202}/Tyr^{204}-phosphorylated p44/42 MAPK (ERK1/2), α7 nAchR, α4 nAchR, β2 nAchR and BDNF after the treatment of nicotine and α7 nAChR allosteric modulator (PNU-120596).

Results: We found that α7 nAChR have activated the CREB-CRTC1 signaling in neurons, but not α4β2 nAchR. Also, the treatment of both nicotine and PNU-120596 has effectively induced the activation CRTC1 transactivation activities and BDNF expression. Also, the treatment enhanced ERK1/2 signaling independently of CREB - CRTC cascade. We found the expression of the α7 nAchR, α4β2 nAchR, and the CRTC family in the microglial cell lines.

Conclusion: The present study demonstrated that both nicotine and PNU-120596 induces neuroprotection, at least in part, mediated by the activation of both CREB-CRTC1 and ERK1/2 signaling. Microglia may contribute to the neuroprotection by nicotine. Further studies are needed to reveal the mechanism of neuroprotective roles of nicotine.

COMBINED HIGH CHOLESTEROL AND CEREBROVASCULAR PATHOLOGY INDUCE MEMORY DEFICITS AND WORSEN CEREBROVASCULAR REACTIVITY IN TRANSGENIC TRANSFORMING GROWTH FACTOR-B1 MICE

X.-K. Tong, E. Hamel

Laboratory of Cerebrovascular Research, Montreal Neurological Institute, McGill University, Montréal, QC, Canada

Introduction: Abnormalities of the brain microvasculature, including degenerating capillaries, is a landmark of Alzheimer's disease (AD), a vascular pathology recapitulated in transgenic mice overexpressing transforming growth factor-β1 (TGF mice) [1, 2]. Interestingly, TGF mice do not display cognitive deficits despite decreased brain perfusion at rest [3] and altered neurovascular coupling [4]. Since cardiovascular diseases and, particularly, hypercholesterolemia enhance the risk of developing AD with increasing age [5], we tested the hypothesis that a high cholesterol diet could trigger learning and memory deficits in TGF mice.

Materials and methods: Two groups of TGF mice and wild-type (WT) littermate controls were fed a high cholesterol diet (HCD, 2% cholesterol and 0.5% cholic acid) for three months, and were tested at 6 (young) and 12 (aged) months of age. Learning and memory were assessed in the Morris water maze [8]. Cerebral blood flow (CBF) responses to whisker stimulation were measured with laser Doppler flowmetry, and cerebrovascular reactivity to dilators (acetylcholine/ACh, calcitonin gene-related peptide/CGRP) or constrictors (endothelin-1/ET-1, inhibition of nitric oxide (NO) production with L-NNA) were measured in isolated and pressurized posterior cerebral artery segments. String vessels, considered as remnants of degenerated capillaries in AD brains, were quantified by collagen IV immunohistochemistry in fixed brain sections.

Results: Body weight gain was comparable between all groups, and total blood cholesterol and LDL were increased in HCD-treated WT and TGF mice at both ages compared to their non-treated controls. HCD impaired learning and memory in young and aged TGF, but not WT mice; aged mice being more severely affected. CBF responses to whisker stimulation were decreased in young and aged TGF mice compared to WT controls, and HCD did not worsen this deficit. Dilatations to ACh and CGRP were selectively reduced in young TGF mice and HCD had no effect on these dilatory deficits. In contrast, HCD exacerbated the already impaired dilatations to ACh and CGRP in aged TGF mice, and strongly reduced baseline NO production. The number of string vessels was markedly increased in the hippocampus, but not cortex, of TGF mice at both ages compared to treated and non-treated WT controls, and HCD further increased (30%, $p < 0.01$) their density in young TGF mice only.

Conclusions: Our results show an age-dependent susceptibility to the deleterious effects of HCD on cognitive and cerebrovascular function in TGF, but not WT mice, suggesting that the comorbidity of hypercholesterolemia is an important contributor to this susceptibility. The greater impact of HCD in aged TGF mice agree with AD pathology developing with increasing age in patients with hypercholesterolemia, and further suggest that early control of this risk factor might prevent AD in susceptible individuals.

Supported by the Canadian Institutes of Health Research (CIHR, grant MOP-84275, EH).

References:

1. Wyss-Coray T et al., J Am Pathol 2000, 156:139-50.

2. Tong X-K, et al., J Neurosci 2005, 25: 11165-74.

3. Gaertner RF et al., Neurobiol Dis 2005, 19: 38-46.

4. Nicolakakis N et al., JCBFM 2011,31: 200-11.

5. Girouard H and Iadecola C, J Appl Physiol 2006, 100: 328-35.

EFFECT OF ANTIHYPERTENSIVE TREATMENT ON CEREBRAL BLOOD FLOW IN A MOUSE MODEL FOR ALZHEIMER'S DISEASE

M. Wiesmann[1,2], C. Capone[1], V. Zerbi[1], L. Mellendijk[1], M.G. Olde Rikkert[2], A. Heerschap[3], A.J. Kiliaan[1], J.A. Claassen[2]

[1]Department of Anatomy, [2]Department of Geriatric Medicine, Radboud University Nijmegen Medical Centre, Donders Institute for Neuroscience, [3]Department of Radiology, Radboud University Nijmegen Medical Centre, Nijmegen, The Netherlands

Objectives: Hypertension is a risk factor for AD, is highly prevalent (60 % > age 60), and is a treatable condition, opening important avenues for prevention of AD. Elevated levels of angiotensin II (AngII) are an important cause of essential hypertension.

Blood pressure lowering treatment may reduce the risk of AD in hypertensive patients, especially agents that block the effects of AngII. However, the mechanistic link between hypertension-AngII and AD remains unknown.

In this study we investigate the interactions between AngII, blood pressure, cerebral perfusion, and cognitive and neuropathological markers of AD, in wild-type and the $APP_{swe}/PS1_{\Delta E9}$ (APP/PS1) mouse model of AD.

To differentiate between effects of AngII and elevated blood pressure per se, we also test intervention with 2 blood pressure lowering agents:

1) the diuretic hydrochlorothiazide and

2) the AngII blocker eprosartan.

Methods: We studied the effect of 2 months of induced hypertension (AngII infusion using osmotic minipumps, vs saline control) and subsequent (after 1 month) treatment with antihypertensives (eprosartan mesylate, 0.35mg/Kg or hydrochlorothiazide, 7.5mg/Kg, vs water) on cerebral blood flow (CBF) in 10 months-old wildtype C57bl/6j (WT) and APP/PS1 mice with MR Flow-sensitive alternating Inversion Recovery (FAIR) at 11.7T magnet (Bruker BioSpec). Blood pressure was monitored daily in the mice via tail cuff plethysmography.

Results: The experiments are ongoing and the final results will be presented. *Preliminary results (Figure 1):* On water treatment, AngII delivered for two months increased blood pressure in WT (n=3; 53.3 mmHg ± 6.4 mmHg) and APP/PS1 mice (n=4; 50.8 mmHg ± 6.8 mmHg). Wild-type mice treated with hydrochlorothiazide had higher cerebral blood flow compared to mice treated with water (14.9 ml(blood)/mg(tissue)/min ± 4.6 ml(blood)/mg(tissue)/min). This effect was not observed in hypertensive APP/PS1 mice.

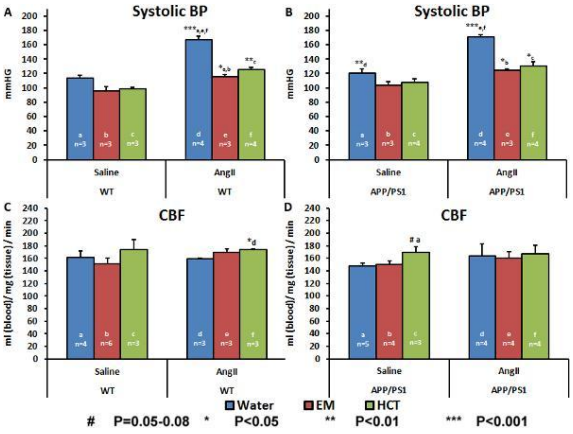

[Figure 1]

Conclusions: AngII infusion induced hypertension, and the 2 antihypertensive agents (angiotensin II receptor blocker and diuretic) successfully counteracted this induced hypertension in WT and APP/PS1 mice. Unexpectedly hydrochlorothiazide and not eprosartan treatment ameliorated CBF, but only in wild-type mice. This is in contrast with observational findings in humans. Cognitive effects and neuropathological findings are underway.

Preliminary conclusions: Only in WT and not in APP/PS1 mice, hydrochlorothiazide is able to increase the CBF indicating an impaired cerebral autoregulation in this AD model. In conclusion, HCT may be able to lower the risk of developing AD in hypertensive patients.

Figure 1 *Preliminary results of CBF and BP measurements in C57bl/6j and APP/PS1 mice*

COGNITIVE DOMAIN DEFICITS IN PATIENTS WITH ANEURYSMAL SUBARACHNOID HEMORRHAGE: PROGNOSTIC SIGNIFICANCE AND SCREENING TOOL

G.K.C. Wong, Cognitive Dysfunction after Aneurysmal Subarachnoid Hemorrhage Investigators

Neurosurgery, The Chinese University of Hong Kong, Hong Kong, Hong Kong S.A.R.

Objective: Cognitive deficits commonly occur after aneurysmal subarachnoid hemorrhage (aSAH) though few studies systemically evaluate its impact. We hypothesized that cognitive deficits in aSAH patients can be screened using the Montreal Cognitive Assessment (MoCA) and correlated with functional outcomes.

Methods: We carried out a prospective observational and diagnostic accuracy study in Hong Kong over a 38-month period, for which patients with aSAH who had been admitted within 96 hours of ictus were recruited, aged 21 to 75 years. The cognitive assessments used were the domain-specific neuropsychological assessment battery, the MoCA, and the Mini-Mental State Examination (MMSE) at 2-4 weeks (n=74) and 1 year (n=80) after ictus. The current study is registered at ClinicalTrials.gov of the U.S. National Institutes of Health (NCT01038193).

Results: The unfavorable outcome (Modified Rankin Scale 3-5) and dependent instrumental activity of daily living (Lawton Instrumental Activity of Daily Living< 15) correlated with significant cognitive impairment and all cognitive domain deficits, with the exception of attention and working memory, at 1 year. At 2-4 weeks, the AUCs between MoCA and MMSE for cognitive domain deficits and significant cognitive impairment were similar; at 1 year, the MoCA had higher AUCs than the MMSE for significant cognitive impairment and all of the cognitive domain deficits, with the exception of visuospatial memory and skill.

Interpretation: Cognitive domain deficits and significant cognitive impairment in patients with aneurysmal subarachnoid hemorrhage can be screened using the MoCA and correlated with functional outcomes in both the subacute and chronic phases.

BRIEF SCREENING FOR MILD COGNITIVE IMPAIRMENT IN SUBCORTICAL ISCHEMIC VASCULAR DISEASE: A COMPARISON STUDY OF MOCA WITH MMSE

Q. Xu, W.-W. Cao, J.-H. Mi, L. Yu, Y. Lin, Y.-S. Li

Department of Neurology, Renji Hospital of Shanghai JiaoTong University School of Medicine, Shanghai, China

Background and purpose: The cognitive syndrome of subcortical ischemic vascular disease (SIVD) is now considered the most frequent subtype of vascular cognitive impairment (VCI). As Montreal Cognitive Assessment (MoCA) incorporate subtests assessing frontal executive functions that are frequently impaired in VCI, it has been proposed as a screening tool for it. MoCA has also demonstrated high sensitivity and specificity for detecting patients with mild cognitive impairment (MCI). However, the most widely used Mini Mental State Examination (MMSE) is relatively insensitive to conditions associated with the subcortical frontal executive, and milder form of cognitive impairment. Therefore, our study was to test the hypothesis that MoCA might be superior to MMSE to detect mild cognitive impairment of vascular origin (VaMCI) in SIVD patients.

Methods: MoCA and MMSE were administrated to 102 SIVD patients along with a set of neuropsychological battery as gold standard. Both cutoff scores of MMSE and MoCA for differentiating VaMCI from NCI or differentiating VaMCI from VaD were determined by the Receiver Operator Characteristic (ROC) analysis. Optimal sensitivity with specificity of cutoff scores for identifying VaMCI from SIVD patients was obtained after the raw scores were adjusted by the education.

Results: Among 102 SIVD patients, 43(42.2%) had VaMCI, 28(27.5%) had vascular dementia (VaD), whereas 31(30.3%) had no cognitive impairment (NCI). The mean ± SD score of MMSE (26.8±3.8) was higher than that of MoCA (21.5±5.6) in SIVD patients. MoCA but not MMSE scores showed statistically significant difference between NCI and VaMCI patients (P< 0.01). After adjusted for education, the MoCA cutoff score for differentiating VaMCI from NCI was at 24/25 and that for differentiating VaMCI from VaD was at 18/19. After applying the adjusted

MoCA scores from 19 to 24 for identifying VaMCI from all SIVD patients, the sensitivity was at 76.7% and specificity at 81.4%. The adjusted cutoff score of MMSE for differentiating VaMCI from NCI was at 28/29 and that for differentiating VaMCI from VaD was at 25/26. The sensitivity/specificity of adjusted MMSE was at 58.1%/83.1% when using the score from 26 to 28 to identifying VaMCI from all SIVD patients.

Conclusions: MoCA showed a better discriminating validity of VaMCI in SIVD patients than MMSE. Further longitudinal studies are needed to determine whether it could be a cognitive surrogate marker of VCI in progression, especially from an early stage.

HYDROXYSAFfIOR YELLOW A INHIBITS INFLAMMATION AND PROTECTS AGAINST AB1-42-INDUCED NEUROTOXICITY

Z. Zhang, L. Qian, **Y. Xu**

Department of Neurology, Affiliated Drum Tower Hospital of Nanjing University Medical School, Nan Jing, China

Objectives: Neuroinflammation is an important contributor to the development of Alzheimer´s disease. Amyloid-β (Aβ) is a major component of the amyloid plaques present in the brains of Alzheimer´s disease patients. Here, we examined whether hydroxysafflor yellow A (HSYA), present in a Chinese medicinal plant, prevents Aβ-induced microglial activation and confers protection against neurotoxicity.

Methods: We used Kunming mice and the murine BV2 microglia cell line to perform in vivo and in vitro assays. The cognitive and learning ability was assessed by the Morris water maze test. BV2-conditioned medium was used to treat primary hippocampal cells in indirect toxicity experiments. Cell viability was assessed using MTT assays. Western Blot was used to determine the protein expression of signal transducers and activators of transcription 3 (STAT3) and phosphorylated signal transducer and activator of transcription 3 p-STAT3. The expression of inflammatory genes was detected by Real-time PCR.

Results: Hydroxysafflor yellow A improved the learning and memory of Aβ-induced AD mice. Aβ increased the mRNA expression of the inflammatory molecules, such as inducible nitric oxide synthase (iNOS), cyclooxygenase-2 (COX-2), interleukin-1β (IL-1β)and tumor necrosis factor-α(TNF-α) in BV2. Hydroxysafflor yellow A significantly reduced the mRNA expression of the inflammatory medium, in addition, it increased anti-inflammatory cytokines, IL-4 and IL-10. Hydroxysafflor yellow A prevented Aβ-induced microglial activation. MTT reduction assay showed that conditioned medium from Aβ-activated BV2 microglia reduces the viability of primary neurons. However, the decrease in cell viability was ameliorated by Hydroxysafflor yellow A. HSYA enhanced the phosphorylation of STAT3. AG490 down-regulated the phosphorylation of STAT3 and attenuated the protection of HSYA.

Conclusions: HSYA could inhibit Aβ-induced inflammation by modulating STAT3, suggesting that HSYA could be a promising medicine in modulating inflammatory conditions of the CNS.

DALESCONOLS B ACTIVATES AKT/GSK-3B/B-CATENIN SIGNALING AND ATTENUATES MEMORY DEFICITS IN AN ALZHEIMER MOUSE MODELV

X. Zhu[1], S. Wang[1,2], H. Yang[2], J. Jin[1], **Y. Xu**[1]

[1]Department of Neurology, Affiliated Drum Tower Hospital of Nanjing University Medical School, [2]Nanjing Drum Tower Hospital Clinical College of Traditional Chinese and Western Medicine, Nanjing University of Chinese Medicine, Nanjing, China

Objectives: Alzheimer's disease (AD) is characterized by cognitive impairment and progressive memory loss due to accumulation of senile plaques, neurofibrillary tangles and loss of synapses and neurons. AKT/GSK-3β/β-catenin signaling exerts an important role in neuronal development and maintenance of the nervous system, and accumulating evidence has indicated that this signaling is involved in neurodegenerative diseases, especially in beta amyloid (Aβ) -mediated neurotoxicity. Dalesconol B is a potential immunosuppressive substance with a novel carbon skeleton isolated from Daldinia eschscholzii in our laboratory. In the present study, the neuroprotective effects of Dalesconol B on Aβ1-42-induced toxicity and potential mechanisms are investigated.

Methods: Ab1-42 was injected to bilateral hippocampus of mice to make the AD models in vivo. Memory impairment was tested by

Morris water maze (MWM), and the induction of synaptic plasticity was assessed electrophysiologically. The expression of AKT/GSK-3β/β-catenin signaling was measured by western blot, and the translocation of β-catenin was also determined by a reporter gene assay and immunostaining. The activities of acetylcholinesterase (AChE) and choline acetyltransferase (ChAT) were measured by the ELISA kits. Statistical analyses were performed using ANOVA followed by Bonferroni's post hoc, with $p < 0.05$ considered statistically significant.

Results: Exposure of primary cortical neurons and SH-SY5Y cells to Aβ1-42 resulted in significant viability loss and cell apoptosis, which were reversed by Dalesconol B treatment. Dalesconol B also increased the activity of ChAT and inhibited AchE activity in the hippocampus of AD mice. In addition, Dalesconol B was able to rescue the long-term potentiation (LTP) induction by protecting synaptic function and attenuate memory deficits in AD mice. Furthermore, Dalesconol B activated AKT/GSK-3β/β-catenin signaling pathway, which induced the translocation and accumulation of β-catenin in the nucleus in vitro and in vivo, and inhibition of this pathway partially blocked the protective effects, suggesting that the neuroprotective effects of Dalesconol B were partially through AKT/GSK-3β/β-catenin signaling pathway.

Conclusion: Using the Aβ1-42-induced AD model in vitro and in vivo, this study for the first time shows:

1) Dalesconol B exerts neuroprotective effects and attenuates the memory deficits;

2) Dalesconol B increases the activity of ChAT and inhibits AchE activity; and

3) Dalesconol B activates AKT/GSK-3β/β-catenin signaling pathway, which might contribute to the neuroprotection of Dalesconol B.

ENRICHED ENVIRONMENT HOUSING PREVENTS THE IMPAIRMENTS OF COGNITIVE FUNCTION AND MOTOR FUNCTION IN A MOUSE MODEL OF CADASIL DISEASE

L.-R. Zhao[1], A. Fagan[2], B. Li[3], X.-Y. Liu[3], M. Gonzalez-Toledo[3], C. Piao[3], S. Zhang[3]

[1]Neurology/Cellular Biology and Anatomy, [2]Cellular Biology and Anatomy, [3]Neurology, Louisiana State University Health Sciences Center, Shreveport, LA, USA

Objective: A large body of evidence has shown that enriched environment housing can repair brain damage and improve motor function and cognitive function in the settings of neurological disorders and neurodegenerative diseases such as stroke and Alzheimer's disease. Cerebral autosomal dominant arteriopathy with subcortical infarcts and leukoencephalopathy (CADASIL) is the most common neurological condition of hereditary stroke and vascular dementia. Currently, there is no treatment available to prevent the progression of this devastating disease. The objective of this study was to determine the therapeutic effects of enriched environment in CADASIL disease.

Methods: Transgenic mice that carry human mutant Notch-3 gene were used as a mouse model of CADASIL disease. CADASIL mice were randomly divided into two groups at age of 5 months: a control environment (CE) housing and an enriched environment (EE) housing. CADASIL mice that in CE group were housed in a standard laboratory cage (3-5 mice per cage), whereas the mice in EE group were housed together (10-15 mice) in a large tank equipped with many toys, which were changed 2-3 times per week. CADASIL mice that were assigned to EE group were transferred into the EE 3 times per week for 18 months. Wild type mice served as normal control. The ability of learning and memory was evaluated with a water maze test, which was performed at 4 and 17 months after first exposure to EE, and motor function was examined with a Rota-Rod test at 18 months after starting EE.

Results: A unique pattern of impaired learning and memory was observed in the CADASIL mice of CE group; however, the impairment of cognitive function was significantly prevented by EE housing. The CADASIL mice in EE

group found the hidden platform in the water maze test much easier than those in CE group, and the improvement of cognitive function was seen at 4 and 17 months after exposure to EE. In addition, the CADASIL mice that were housed in EE for 18 months remained on the Rota-Rod at high speeds much longer than those of CE-housed CADASIL mice.

Conclusions: An enriched environment can improve both the cognitive function and motor function in CADASIL mice. This study would provide insights into the contribution of living environment to preventing brain damage in the gene-mutation-driven diseases such as CADASIL. This study may also help in developing a new therapeutic strategy to inhibit the progress of CADASIL disease.

This study was supported by The American CADASIL Foundation (LRZ)

ASPIRIN PROMOTE THE COGNITIVE FUNCTION RECOVERY IN WML RATS THROUGH ENHANCING NEURAL STEM CELLS TO OLIGODENDROCYTE DIFFERENTIATION

J. Chen

Department of Neurology, FMMU, XiJing Hospital, Xi'an, China

Objectives: To provide evidence for aspirin treatment applying to the white matter lessions.

Material and methods: Thirty mature male Sprague-Dawley rats were choosed and divided into 3 groups randomly,which are Age-matched group, Solvent control group and Aspirin treatment group. All rats were accepted an bilateral common carotid artery ligation surgery except Age-matched group, then Solvent control group given saline and Aspirin treatment group given 25mg/kg, 50mg/kg, 100mg/kg, 200mg/kg aspirin peritoneal injection respectively daily for a month. Morris water maze was used to detect the variation of learning and memory abilities of rats. Then, we interfered neural stem cells cultured in vitro in different concentrations of aspirin and 1% fatal bovine serum,count the number of O4(+) oligodendrocyte precursor cell at Day3 and CNPase(+) mature oligodendrocytes at Day 7 through immunofluorescence staining.

Results: In water maze trail,the escape latency of each group were shortened, the biggest variation in which was 100mg/kg aspirin treatment group, although the shortest of which still longer than Age-matched group. Either learning speed or the shortest escape latency of four different concentration of Aspirin treatment group are better than the Solvent control group. In vitro, we find that aspirin could promote the differentiation of neural stem cells into oligodendrocytes, by reducing the number to the astrocytes.

NETRIN-1 PROMOTES OLIGODENDROGENESIS AFTER EXPERIMENTAL STROKE

X. He[1], Y. Wang[1], Y. Li[1], Y. Lv[1], Y. Tang[1], X. Lin[1], G.-Y. Yang[1,2]

[1]Neuroscience and Neuroengineering Research Center, Med-X Research Institute and School of Biomedical Engineering, [2]Department of Neurology, Ruijin Hospital, School of Medicine, Shanghai Jiao Tong University, Shanghai, China

Objectives: Oligodendrocyte injury after ischemic stroke influences the integrity of white matter and neurological deficits. Netrin-1 (NT-1) promotes oligodendrocyte progenitor cell proliferation during development.[1] In this study, we investigate whether netrin-1 facilitates white matter recovery during focal ischemia and further to explore which specific receptor involves in the white matter reconstruction.

Methods: Ninety adult male ICR mice underwent adeno-associated virus (AAV) mediated AAV-Netrin-1 or AAV-GFPgene transfer and PBS treatment. These mice received one hour transient middle artery occlusion (MCAO).Western blot and immunohischemistry were used to determine exogenous NT-1 expression. Behavior tests and immunohischemistry were tested at 7, 14 and 28 days after MCAO.

Results: NT-1 was highly expressed in the mouse brain after two weeks of AAV-NT-1 gene transfer. Neurobehavioral outcomes were greatly improved at 7, 14 and 28 days after reperfusion in AAV-NT-1 treated mice ($p < 0.05$), The number of proliferated oligodendrocyte progenietor cells, mature oligodendrocytes and MBP positive neurofilaments in the corpus callosum and the

striatum in the ipsilateral hemisphere at 7, 14 and 28 days after reperfusion were increased in the NT-1 treated group compared to GFP and PBS control mice ($p< 0.01$). NT-1 receptor DCC and Unc5H2 are involved in the proliferation of oligodendrocyte progenitor cells, But only Unc5h2 was involved in the re-myelination process.

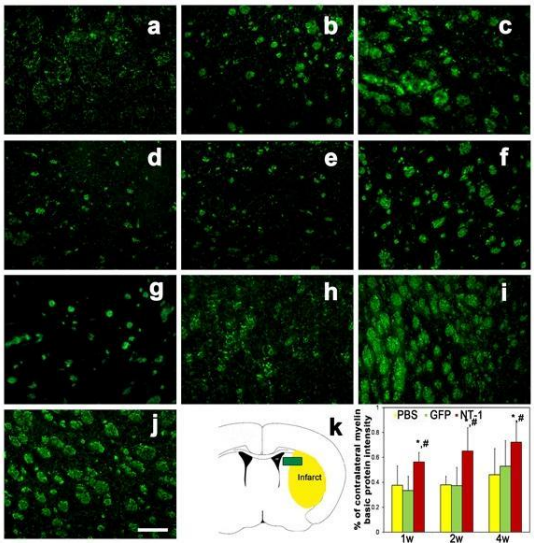

Figure1: MBP staining in striatum area after 7, 14 and 28days reperfusion in PBS, GFP and NT-1 treated mice.

Conclusions: NT-1 overexpression improves neurobehavioral outcomes and promotes

oligodendrocyte progenietor cell proliferation and maturation. Oue results suggest that netrin-1 not only promotes angiogenesis but also enchances remyelination.

Reference:

1.Hui-Hsin Tsai, Wendy B.Macklin, and Robert H.Miller. Netrin-1 Is Required for the Normal Development of Spinal Cord Oligodendrocytes. J Neuroscience 2006; 26: 1913-1922.

COMPREHENSIVE ANALYSIS OF SELECTIVE WHITE MATTER INJURY OF THE RAT MODEL BY USING IMAGING MASS SPECTROMETRY AND CONVENTIONAL HISTOPATHOLOGY

H. Ono[1], H. Imai[1], T. Hayasaka[2], S. Miyawaki[1], H. Horikawa[1], T. Ochi[1], A. Ito[1], H. Nakatomi[1], M. Setou[2], N. Saito[1]

[1]Department of Neurosurgery, Graduate School of Medicine, The University of Tokyo, Tokyo, [2]Department of Cell Biology and Anatomy, Hamamatsu University School of Medicine, Shizuoka, Japan

Background: The importance of the white matter injury (WMI) is increasingly recognized since this is a major cause of functional disability in cerebrovascular disease. White matter is a target of ischemic injury throughout life, which is particularly involved with the stroke in adults and vascular dementia in the aging brain. WMI including axonal disruption may cause disturbance of motor and sensory function, neurobehavioral syndromes, and cognitive impairment. However, in experimental study, grey matter damage induced by cerebral ischemia has historically attracted much more attention than white matter damage. One reason for this imbalance is the lack of an appropriate model as well as methodology for the assessment of white matter damage *in vivo.*

According to the technical innovations in recent years, imaging mass spectrometry (IMS) was introduced, in which mass spectrometry is performed on tissue sections and anatomical information of the living tissue. In this study, we applied IMS to analyze the molecular kinetics of phospholipids of WMI of the rat model. By comparing and contrasting the results of this molecular imaging to conventional histopathological evaluation, we provide the dynamic changes of phospholipids of the lesion from acute to chronic phase after WMI.

Materials and methods: Sprague-Dawley rats (300-350g, total n=30) were anesthetized, endothelin-1 (0.5µg/µl) was stereotactically injected into unilateral internal capsule to induce selective WMI. Animals were euthanized at several time points, from 30 minutes to 3 weeks after the injection. The brain sections were stained with Hematoxylin-Eosin and Kluver-Barrera (KB), and

immunostained for ED1 (activated microglia), APP (axonal injury) and GFAP (gliosis).Also, the adjacent sections ware applied for IMS to analyze PCs comprehensively.

Results: Selective WMI, particularly myelin destruction and axonal injury, was confirmed by KB staining and specific APP immunoreactivity at 3 hours after the operation. The increased immunoreactivitiy for ED1 was observed in the lesion from 3 days to 2 weeks after the operation, showing the activated microglia migrated and occupied the lesion. Notably, IMS revealed that PCs containing arachidonic acid (20:4, AA-PCs), such as PC (16:0/20:4), PC (18:0/20:4) and PC (18:1/20:4), as well as lysophosphatidylchoines (LPCs), especially LPC (16:0), were significantly elevated concomitant with the increased ED1 immunoreactivity in the lesion.

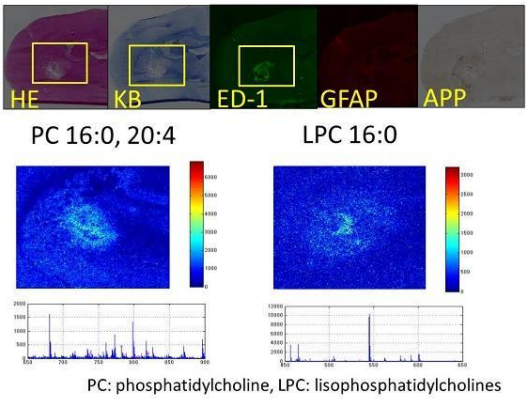

[2 weeks after the operation]

Discussion: In this study, we have analyzed the WMI using both histopathological technique and IMS. On the time-course histopathological investigation, myelin destruction and axonal injury were confirmed, followed by inflammatory reaction and gliosis. Then, IMS revealed the AA-PCs elevation centering the lesion where activated microglia accumulated at 2 weeks after the operation. The increase of AA-PCs, containing a kind of polyunsaturated fatty acid, which is key components of cell membrane to secure more fluidity, may represent the morphological change of microglia. Furthermore, LPCs increased at the same region where AA-PCs elevated, indicating the release of AA and the production of prostaglandins. Although further evaluation is required, IMS has tremendous potentials to provide the new insight comprehensively in terms of the dynamic molecular changes invisible under conventional modality.

BUMETANIDE ATTENUATES WHITE MATTER INJURY AND PROTECTS THE BLOOD-BRAIN-BARRIER IN A MOUSE MODEL OF TRAUMATIC BRAIN INJURY

H. Pu[1], J. Zhang[1], G. Wang[1], X. Jiang[1], W. Zhang[1], D. Sun[2], J. Chen[2], Y. Gao[1]

[1]State Key Laboratory of Medical Neurobiology and Institute of Brain Science, Fudan University, Shanghai, China, [2]Center of Cerebrovascular Disease Research, University of Pittsburgh School of Medicine, Pittsburgh, PA, USA

Objectives: Traumatic Brain Injury (TBI) is a neurological disorder that leads to short and possibly long term motor and cognitive dysfunction. To date, there are no effective therapeutic agents against TBI. Na-K-Cl co-transporter isoform 1 (NKCC1) is expressed in neurons (soma, dendrites, myelinated axon), astrocytes, oligodendrocytes, and blood vessel endothelial cells throughout the brain and plays an important role in regulating neuronal volume and ion homeostasis. Administration of the NKCC1 inhibitor bumetanide significantly attenuates contusion volume, brain edema and neuronal damage after TBI. However, recent research also suggests that bumetanide protects against blood-brain-barrier (BBB) disruption and white matter damage resulting from ischemic injury. In the present study, we investigated the effect of bumetanide on neurobehavioral outcomes, white matter damage, and BBB integrity in a mouse model of controlled cortical impact (CCI).

Methods: TBI was induced in adult male C57BL/6J mice using a CCI model, and the animals were then randomly assigned to sham, vehicle or bumetanide groups. Bumetanide (25 mg/kg) was given intraperitoneally immediately after impact and (maybe we could add the number of treatments here) subsequent treatments were spaced 6 hours apart. For outcome assessments, sensorimotor deficits (hang wire, cylinder and foot fault tests) were determined at 1-35 days after TBI. BBB integrity (Evans blue extravasation and electron microscopy) was determined at 48 hours post-TBI. Brain edema (wet and dry weights) and expression of MMPs and occludin (immunostaining and Western blots)

were examined at 72 hours post-TBI. The integrity of myelin sheaths and axons were assessed by expression of myelin basic protein (MBP; Western blots) and accumulation of amyloid precursor protein (APP, immunohistochemistry).

Results: Our results show that administration of bumetanide attenuated short and long term (up to 35 days post-TBI) sensorimotor deficits. However, bumetanide failed to significantly reduce the cortical lesion size at 35 days post-TBI. In contrast to its ineffectiveness against cortical tissue loss, bumetanide preserved the integrity of myelin sheaths and axons by preventing the loss of MBP and the accumulation of APP, thereby maintaining nerve fiber conductivity. TBI induced short-term brain edema from BBB injury within the lesion and in surrounding brain regions. Bumetanide markedly reduced brain water content after TBI by attenuating BBB injury.

Conclusions: Bumetanide prevents BBB disruption and white matter injury after TBI. These protective effects of bumetanide might be responsible for the improvements in long term neurological outcomes after TBI. Clinical investigations of bumetanide as a potential therapeutic agent for TBI are warranted.

N-METHYL-*D*-ASPARTATE RECEPTOR-MEDIATED AXONAL INJURY IN ADULT CORPUS CALLOSUM

J. Zhang, J. Liu, H.S. Fox, **H. Xiong**

University of Nebraska Medical Center, Omaha, NE, USA

Damage to white matter such as corpus callosum (CC) is a pathological characteristic in many brain disorders. Glutamate (Glut) excitotoxicity through AMPA receptor on oligodendrocyte (OL) was previously considered as a mechanism for white matter damage. Recent studies have shown NMDA receptors (NMDARs) are expressed on myelin sheath of neonatal rat OL processes and activation of these receptors mediated demyelization[1-3]. Whether NMDARs are expressed in the adult CC and involved in excitotoxic axonal injury remain to be determined.

Objectives: To examine the expression of NMDARs in the adult rat CC and their involvement in excitotoxic activity.

Methods: Experiments were carried out on coronal brain slices containing the CC (500 mm in thickness) prepared from Sprague-Dawley rats of either sex (25-40 d old). The slices were divided into different groups to study NR1 subunit of NMDAR (NMDAR1) expression in the CC by immunofluorescent staining and western blotting, and to determine the involvement of NMDAR1 in Glut-induced axonal injury via electrophysiology. Chemical reagents were applied to CC slices via incubation.

Results: Our results showed that NMDARs are expressed in the adult CC. The anti-NMDAR1 immunoreactivity was co-localized with anti-myelin basic protein (MBP) and anti-oligodendrocyte specific protein (OSP). Although the exact relationship between NMDAR1 and MBP, or the ultrastructural localization of NMDAR1 remains to be determined, the distribution pattern of the NMDAR1 positive fibers in adult CC is interesting. These fibers were located predominantly in conjunctional areas between the CC and horizontal corona radiata. Most of these fiber-like structures appeared to extend either from the regions close to the cingulum in front parts of the CC or from the areas around alveus of hippocampus in parietal parts of the CC. We also observed NMDAR1 positive somata in the CC. To examine if the NMDAR1 positive somata are neuronal cells, we perform double immunostaining using each of the two well-established neuronal markers, anti-NeuN [4] and anti-MAP2 [5] together with anti-NMDAR1. However, no double labeled neuronal soma was observed, implying NMDA receptors may not be expressed on neuronal cells in the adult CC. In contrast, anti-OSP, an established OL marker [6] and anti-NMDAR1 double labeled somata were observed. These results suggest the existence of NMDA receptors in the adult OLs, though the number of double labeled soma was relatively low, about 10% of total OSP positive somata. The involvement of NMDARs expressed in the CC in excitotoxicity was demonstrated that incubation the CC slices with Glut or NMDA significantly decreased the amplitude of CC fiber compound action potentials, input-output responses and fast axonal transport which were attenuated NMDAR antagonist MK801.

Conclusions: These results revealed that NMDARs are expressed in the adult CC and they are involved in excitotoxic activity.

References:

1. Salter MG, Nature, 2005. **438**:1167.

2. Karadottir R, et al., Nature, 2005. **438**:1162.

3. Micu I., et al, Nature, 2006. **439**:988.

4. Wolf HK, et al, J Histochem Cytochem, 1996. **44**:1167.

5. Riederer BM, et al Eur J Neurosci, 2004. **19**:2039.

6. Jagessar SA, et al J Neuropathol Exp Neurol, 2008. **67**:326.

MMRI AND MPET ANALYZE REVEAL [^{18}F]-FLT AS A PREDICTIVE MARKER IN DETECTION OF GLIOBLASTOMA RESPONSE TO TEMOZOLOMIDE COMBINED WITH BEVACIZUMAB

A. Corroyer-Dulmont[1,2], E.A. Pérès[1,2], E. Petit[1,2], J.-S. Guillamo[1,3], N. Varoqueaux[4], S. Roussel[1,2], J. Toutain[1,2], D. Divoux[1,2], E.T. MacKenzie[1,2], J. Delmare[1,2], M. Ibazizène[1,2], M. Lecocq[1,2], A.H. Jacobs[5], L. Barré[1,2], M. Bernaudin[1,2], S. Valable[1,2]

[1]CNRS, UMR ISTCT 6301, CERVOxy and LDM-TEP Groups, GIP CYCERON, Université de Caen Basse-Normandie, [2]CEA, DSV/I2BM, UMR ISTCT 6301, CERVOxy and LDM-TEP Groups, GIP CYCERON, [3]CHU de Caen, Service de Radiology, Caen, [4]Roche SAS, Neuilly, France, [5]European Institute for Molecular Imaging (EIMI), Westphalian Wilhelms University (WWU), Münster, Germany

Objectives: The individualized care of glioma patients ought to benefit from imaging biomarkers as precocious predictors of therapeutic efficacy. Contrast-enhanced-MRI (CE-MRI) and [^{18}F]-fluorodeoxyglucose (FDG)-PET are routinely used in clinical settings; their ability to forecast the therapeutic response is controversial. The objectives of our preclinical study were to analyze sensitive µMRI and/or µPET imaging biomarkers to predict the efficacy of anti-angiogenic and/or chemotherapeutic regimens.

Methods: Human U87 and U251 orthotopic glioma cells were implanted in nude rats. Temozolomide and/or bevacizumab were administrated twice a week. The vasculature was characterized by MRI measurement at t1 (i) perfusion after a bolus injection of a contrast agent (P904®), (ii) Cerebral Blood Volume (CBV), (iii) vessel size and (iv) vascular permeability after administration of a second contrast agent (Dotarem®). Glucose metabolism and cell proliferation were studied after injection of [^{18}F]-FDG and [^{18}F]-fluoro-L-thymidine (FLT)-PET. MRI and PET studies were undertaken soon (t1) after the treatment initiation compared to a late anatomical µMRI evaluation of tumor volume (t2) and overall survival.

Results: At t1, anatomical MRI was insensitive to treatments. However, at t2, temozolomide decrease the tumor volume by 86% ($p< 0.001$) and 93% ($p< 0.001$) for the U87 and U251 models. With the anti-angiogenic treatment, at t2, there was a slight limitation in tumor volume (36% and 31% for U87 and U251 models). No synergistic effect was observed in the temozolomide with bevacizumab treatment group. While, at t1, there was no effect of treatments on tumor volume in both models, FDG and FLT uptake were attenuated in response to temozolomide alone or with bevacizumab. The population distribution of FLT values demonstrated a decrease in intratumoral heterogeneity. FDG was less predictive for treatment efficacy than FLT (the latter highly correlated with outcome, $r^2=0.42$, $p=0.001$ and $r^2=0.55$, $p< 0.0001$ for U87 and U251). CBV was significantly decreased by temozolomide with bevacizumab ($p< 0.01$) and was correlated with survival ($r^2=0.28$, $p=0.0016$) for U87 implants. While FLT was highly predictive of treatment efficacy, a combination of biomarkers (FLT+FDG+CBV) was superior than any single imaging technique ($p< 0.0001$ for both tumors with outcome).

Conclusions: Our results indicate that FLT is a sensitive indicator of treatment efficacy and that the predictibility is enhanced by a combination of imaging biomarkers. These data also emphasize the importance to analyze, not just [^{18}F]-FDG, but also novel PET tracers such as [^{18}F]-FLT for the evaluation of cancer treatment efficacy. These findings may translate clinically in that individualized glioma treatments could be decided for given patients after PET/MRI examination. To approximate the clinical vision, we are currently performing these experiments in a model of glioma recurrence considering that, for GBM patients, the association of temozolomide and bevacizumab is not used as a first line of treatment but in a case of recurrence.

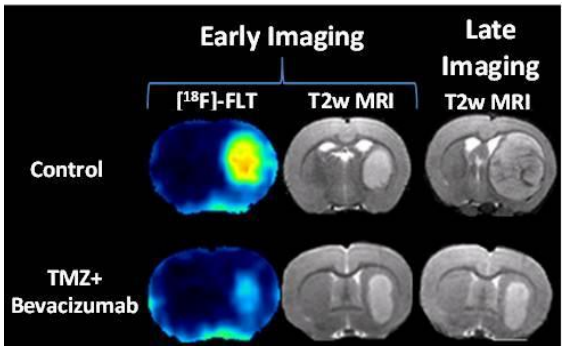

[Predictive value of [18F]-FLT-uptake]

Acknowledgments: INCA, CNRS, Roche, Guerbet, Conseil Regional de Basse-Normandie, European Union (FEDER).

Travel stipend: The primary author is eligible (24 years old) and wishes to be considered for the travel stipend.

COLLAGEN GLYCOSAMINOGLYCAN IMPLANTATION PROVIDES A VASCULAR MICROENVIRONMENT IN PROMOTING NEUROGENESIS IN A SURGICAL BRAIN TRAUMA MODEL OF THE RAT

K.-F. Huang[1], J.-Y. Wang[2], W.-C. Hsu[3]

[1]Division of Neurosurgery, Department of Surgery, Buddhist Tzu Chi General Hospital, Taipei Branch, New Taipei City, [2]Graduate Institute of Medical Sciences, College of Medicine, Taipei Medical University, Taipei, [3]Department of Ophthamology, Buddhist Tzu Chi General Hospital, Taipei Branch, New Taipei City, Taiwan R.O.C.

Objectives: Although most surgical or traumatic brain injury causes loss of cerebral parenchyma, there is still no effective management for neural tissue regeneration. Our previous report shows the implantation of collagen glycosaminoglycan (collagen-GAG, CG) scaffolds following brain damage can be a potential clinical strategy for tissue regeneration and functional recovery. Herein, we investigated the effects of CG scaffold matrix on microenvironment following brain damages.

Methods: A rodent model of SBI was used involving wide resection of a part of the right frontal-parietal cortex area. Sprague-Dawley male rats (weight, 300-350 g) were randomly divided into three groups:

1. Sham,

2. Surgical brain lesion(L),

3. Surgical brain lesion with collagen-GAG matrix implantation (L+CG).

Postoperative all animals were then sacrificed for histological immunohistochemical staining as well as Enzyme-linked immunosorbent assay (ELISA) for measurement of the tissue concentration which was taken from the injured area of the parietal cortex at various time periods (1, 7, 14, 21, 28 days).

Results: Immunohistochemical staining for smooth muscle actin (SMA) and CD31 indicated neovascularization after implantation of CG scaffolds in lesion-boundary zone and intra-matrix zone following implantation of CG scaffolds. The numbers of proliferative (Ki67 positive) and differentiated migratory (DCX positive) cells time-dependently increased after surgery both in lesion-boundary zone and intra-matrix zone following implantation of CG scaffolds. In addition, the tissue concentrations of vascular endothelial growth factor (VEGF), platelet-derived growth factor (PDGF) and basic fibroblast growth factor (bFGF) revealed a sustained increase in both zones up to 28 days following implantation of CG scaffold.

Conclusions: The CG scaffolds provides a microenvironment to facilitate neovascularization and neurogenesis after surgical brain trauma.

ISOFLURANE POST-TREATMENT AMELIORATES GERMINAL MATRIX HEMORRHAGE-INDUCED BRAIN INJURY BY ACTIVATING THE SPHINGOSINE KINASE/AKT PATHWAY IN NEONATAL RATS

A.S. Leitzke[1], W.B. Rolland[2], P.R. Krafft[2], T. Lekic[2], J.J. Flores[2], D. Klebe[2], N.R. Van Allen[2], R.L. Applegate[1], J.H. Zhang[2,3]

[1]Department of Anesthesiology, Loma Linda University Medical Center, [2]Department of Physiology and Pharmacology, [3]Department of Neurosurgery, Loma Linda University, Loma Linda, CA, USA

Objectives: Isoflurane treatment has been shown to confer neuroprotection in rodent

models of adult hemorrhagic stroke [1, 2]. Utilizing a novel rat model of neonatal Germinal Matrix Hemorrhage (GMH) [3], this study intended to determine whether isoflurane ameliorates the neurological sequelae after GMH, through activation of the cytoprotective Sphingosine Kinase/Akt pathway.

Methods: GMH was induced in postnatal day 7 rat pups (P7) by intraparenchymal infusion of bacterial collagenase (0.3U) into the right hemispheric germinal matrix. GMH animals received 2% of isoflurane either once, at 1 hour after surgery, or every 12 hours for a total of 6 sessions. The control group received 30% oxygen and 70% medical air for an equivalent time period (1 hour). Isoflurane treatment was then combined with Sphingosine-1-phoshate (S1P) receptor-1/2 antagonist VPC23019 (VPC) or Sphingosine Kinase 1/2 antagonist N,N-dimethylsphingosine (DMS), given immediately before GMH surgery. Neurofunctional testing was performed at 3 weeks post-GMH using Morris-Water Maze, rotarod and foot-fault assessments. Brain atrophy was studied via histological analysis at 4 weeks post-GMH. Protein expressions of Sphingosine Kinase 1, S1P receptor-1, phosphorylated Akt, and cleaved caspase-3 were determined by Western blotting at 3 days after surgery (n=8 for all groups).

Results: Single and daily isoflurane post-treatment significantly improved balance and coordination ($p < 0.05$ compared to control), but not cognitive functions ($p > 0.05$) in GMH animals at 3 weeks after surgery; however, no improvements were observed after VPC administration ($p > 0.05$). Furthermore, the treatment groups demonstrated significantly less brain atrophy than the control group ($p < 0.05$), which was reversed by VPC. The brain protein levels of Sphingosine Kinase 1 and phosphorylated Akt was significantly increased after isoflurane post-treatment ($p < 0.05$ compared to control); however, VPC and DMS decreased the brain levels of these proteins. Lastly, isoflurane post-treatment resulted in a decreased expression of cleaved capase-3 ($p < 0.05$ compared to control), which was reversed by VPC and DMS at 24 hours after GMH-induction.

Conclusion: The administration of isoflurane after experimental GMH improved the neurofunctional outcome, and decreased brain atrophy in rats. This protective effect may be evoked by isoflurane-induced activation of the Sphingosine Kinase/Akt pathway.

SELENIUM PRESERVES MITOCHONDRIAL FUNCTION, NEACTIVATES MITOCHONDRIAL BIOGENESIS, AND PROTECTS AGAINST GLUTAMATE, HYPOXIA AND ISCHEMIA INDUCED NEURONAL DEATH

P.A. Li[1,2], S.L. Mehta[3], N. Mendelev[1], S. Kumari[1]

[1]Pharmaceutical Sciences, BRITE, North Carolina Central University, Durham, NC, USA, [2]Pathology and Ningxia Key Laboratory for Cerebrocranial Diseases, Ningxia Medical University, Yinchuan, China, [3]Pharmaceutical Sciences, North Carolina Central University, Durham, NC, USA

Objectives: Mitochondrial dysfunction is one of the major events responsible for activation of neuronal cell death pathways during neurodegeneration. Trace element selenium has been shown to protect neurons in various disease conditions. The objectives are

1) to explore whether selenium activates mitochondrial biogenesis and preserves mitochondrial function under normal and pathologic conditions; and

2) to delineate the signaling pathways by which selenium activates mitochondrial biogenesis.

Methods: For cell studies, murine hippocampal neuronal HT22 cells were pretreated (24h) with 100nM selenite and then exposed to glutamate (4 μM) or hypoxia (15 min and 10h). Cells were harvested after 24h for analyses. For animal studies, mice were fed with selenium supplement diet (0.2 mg/kg i.p. once a day for 7 days) and then subjected to 60-min transient MCAO. Brains were harvested after 5 and 24h for analyses. Cell viability was assessed using MTT assay and neuronal death was evaluated by FluoroJade and NeuN immunostaining. ROS was measured with dihydroethidine. Mitochondrial fission and biogenesis related biomarkers were detected using protein blotting. Selenoprotein H (SelH) transfection and knockdown were performed in HT22 cells.

Results:

1) Selenium significantly attenuated both glutamate- and hypoxia-induced cell death and reduced infarct volume after MCAO;

2) The protective effects were associated with reduction of glutamate and hypoxia/ischemia induced ROS production and DNA oxidation;

3) Selenium increased protein levels of peroxisome proliferator-activated receptor (PPAR) gamma-1α (PGC-1α) and nuclear respiratory factor 1 (NRF1), two key nuclear factors that regulate mitochondrial biogenesis;

4) Selenium elevated protein levels of mitochondrial proteins such as cytochrome c and cytochrome *c* oxidase IV (COX IV);

5) Selenium inhibited glutamate-induced expression of mitochondrial fission proteins dynamin-related protein 1 (Drp1) and Fis1 and reduced number of neurons containing fragmented mitochondria;

6) Selenium induced phosphorylation of Akt and cAMP response element-binding protein (CREB), while Akt inhibitor X (AKTX, 5 mM) blocked the activation effects of selenium on CREB and PGC-1α;

7) Selenium enhanced mitochondrial respiration and prevented glutamate- or hypoxia/ischemia-induced suppression on mitochondrial respiration and respiratory complex enzyme activities;

8) Selenium normalized the glutamate- and ischemia-induced activation of Beclin 1 and LC3-II, markers for autophagy;

9) Selenium increased SelH level. Overexpression of SelH activated protein kinase A (PKA)-CREB-PGC-1α, and Akt-CREB-PGC-1α pathways while knockdown of SelH by siRNA suppressed the aforementioned mitochondrial biogenesis pathways.

Conclusion: The neuroprotective effects of selenium against glutamate-, hypoxia-, and ischemia-induced damage are associated with its function to reduce ROS production, to inhibit mitochondrial fission and fragmentation, to stimulate mitochondrial biogenesis, and to restore mitochondrial respiration and respiratory complex enzyme activities after injury.

ACCURATE BRAIN PET/MR QUANTIFICATION USING TIME OF FLIGHT IN COMBINATION WITH MLAA IMAGE RECONSTRUCTION

R. Boellaard, A.A. Lammertsma

Radiology and Nuclear Medicine, VU University Medical Centre, Amsterdam, The Netherlands

Objectives: Quantification of tracer uptake in PET/MR brain studies is hampered by the lack of accuracy of MR based attenuation correction (MR-AC). In general, MR-AC ignores skull resulting in a downward bias in cortical grey matter (cGM) regions of up to 30% (Andersen *et al.*, EJNMMI Suppl 2012 (abstract)). To date, most studies on the effects of MR-AC on tracer uptake have been performed on PET/MR systems without time of flight (TF) capability. New reconstruction methods, such as MLAA (Maximum Likelihood reconstruction of Attenuation and Activity), however, have the potential to improve MR-AC by exploiting TF information in the emission data. So far, MLAA has only been evaluated for overcoming missing information in the MR attenuation map due to, for example, MR coils and truncation. The purpose of the present study was to evaluate the impact of MR-AC on PET image quantification for TF PET/MR systems and to evaluate quantitative PET accuracy when using TF in combination with MLAA reconstructions.

Materials and methods: Based on an FDG PET/CT clinical study, simulations were designed to evaluate

(1) the impact of ignoring skull in MR-AC on PET quantification for different TF windows (ranging from 650 to 250 ps), and

(2) use of TF + MLAA for improving PET quantification. Finally, replicate noisy simulations were performed to determine the impact of both OSEM and MLAA reconstructions on image quality (noise/bias trade-off).

Results: Without TF bias in cGM regions up to -30% was observed, consistent with Andersen *et al.* TF was able to reduce this bias down to -10%, with more accurate results for shorter TF windows, but at the cost of a larger area with a

negative bias. Use of MLAA with a TF of 250 ps (TF-MLAA) was able to reduce cGM biases to within 5% (Figure 1), but at the cost of a ~40% increase in image noise/voxel variance. By including smoothness priors into the MLAA MR-AC method, the increase in PET image noise was reduced to ~20%. MLAA was also able to insert attenuation coefficients for both bone and missing MR coils into the MR-AC image.

Conclusions: Quantitative PET accuracy in cGM regions during PET/MR brain studies improves with the use of TF and with TF performance. Use of TF-MLAA is able to overcome limitations of conventional MR-AC. TF-MLAA was able to reduce quantitative bias to within 5%, although at the cost of somewhat increased image noise levels. TF-MLAA is a promising reconstruction technique to enhance quantitative accuracy of PET/MR studies similar to that seen in conventional PET and PET/CT systems.

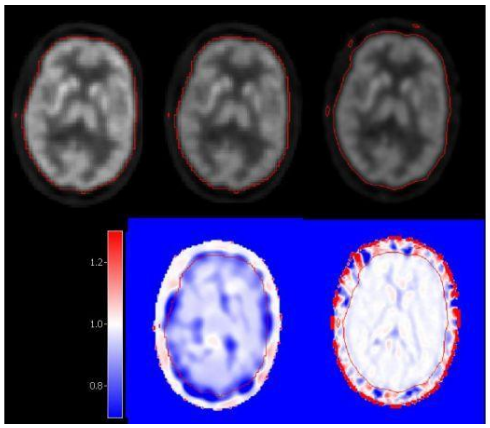

Figure 1: Top row: OSEM using CT based AC (left), OSEM using MR-AC (middle), TF-MLAA using MR-AC (right). Bottom row: Ratio images of OSEM-MRAC divided by OSEM-CTAC (left) and TF-MLAA using MR-AC divided by OSEM-CTAC (right). Blue indicates areas with more than -20% bias, white areas with less than + or - 5% bias and red indicates areas with more than +20% bias

IN VIVO QUANTIFICATION OF TRANSLOCATER PROTEIN (18KDA) BINDING USING [^{123}I] CLINDE SPECT IN HUMANS

L. Feng[1], **C. Svarer**[1], G. Thomsen[1], R. de Nijs[2], V.A. Larsen[3], D. Adamsen[1], A. Dyssegaard[1], G.M. Knudsen[1], L.H. Pinborg[1,4]

[1]Neurobiology Research Unit, [2]Department of Clinical Physiology, Nuclear Medicine and PET, [3]Department of Radiology, [4]Epilepsy Clinic, Department of Neurology, Rigshospitalet, Copenhagen University Hospital, Copenhagen, Denmark

Objective: TSPO is a marker of neuroinflammation associated with microglial activation. [^{125}I]CLINDE has been demonstrated to be suitable for imaging TSPO changes involved in neurodegenerative disorders in rat models [1]. Here we investigate regional [^{123}I]CLINDE binding in a group of patients expected to show microglial activation, and evaluate for the first time the quantification of [^{123}I]CLINDE for in vivo brain imaging in humans.

Methods: Five patients, all male (2 stroke, 2 tumor and 1 multiple sclerosis patient), were included. SPECT (Philips IRIX triple head scanner) images were acquired for 2.5 hours post [^{123}I]CLINDE bolus injection. Arterial blood samples were obtained during scanning, and were corrected for metabolites using HPLC. MR Imaging was conducted in either a 1.5T or a 3T scanner. SPECT and MRI were co-registered using interactive image overlay, and VOIs were manually delineated based on T1 weighted imaging, T1 weighted with gadolinium enhancement, or/and fluid attenuated inversion recovery (FLAIR) sequence. The reference region was defined contralateral of the diseased brain tissue if unaffected; otherwise a region far from the diseased areas was used. Both plasma input models and reference models were investigated, including 1- and 2- and 3-tissue-compartment models (TC), and the simplified reference tissue model (SRTM). Kinetic modeling was done in PMOD (version 3.0). The rs6971 TSPO polymorphism was genotyped from genomic DNA using TaqMan® SNP Genotyping Assay (Applied Biosystems, USA, C_2512465_20).

Results: Increased [^{123}I]CLINDE binding was observed in the border zone of the stroke area

for subject1 and 2. Subject3 and 4 only showed slightly increase of tracer binding in the infarct regions in comparison to the contralateral/reference regions. The tracer binding was clearly present in subject5 remote from the operation cavity. The metabolism among patients was similar, except for subject3, where parent compound was 42% in the blood after 80 min post tracer injection, comparing to only 24% for other subjects. Comparing to the sum of exponential functions, Hill function was favorable in describing the time development of the parent fraction, judged by the Akaike information criterion (AIC). Using plasma as input, the time-activity data were best described by the 2-tissue-compartment model, see Table 1. BP_{ND} estimation by SRTM highly correlates with that of 2-TC (r = 0.979, p = 0.004). However, SRTM underestimated the binding on average by 14% compared to 2-TC, but this was not statistically significant. A time-stability analysis was performed on the truncated datasets corresponding to durations of 150, 130, 110, 90 and 70 min. The trend of reducing the scan time to 90 min was observed. However, due to the limited number of samples, no firm conclusion can be drawn yet.

Conclusions: [^{123}I]CLINDE-SPECT can be reliably estimated with 2-TC, and SRTM estimates kinetic parameters with bias. It may be possible to reduce the total scan time to 90 min.

Table 1: Scan information and modeling parameters

Subj ID	Age	SPECT study	Type	Geno-type		Vt (1-TC) (mL/cm3)	AIC (1-TC)	BP_{ND} (1-TC)	Vt (2-TC) (mL/cm3)	AIC (2-TC)	BP_{ND} (2-TC)	BP_{ND} (SRTM)
1	66	1 month after infarct	MCA Ischemic Stroke	AA	HB	21.99	40.86	1.12	37.07	22.68	1.45	1.04
					Ref	10.38	53.77		15.12	36.81		
2	56	1 month after infarct	PCA Ischemic Stroke	AT	HB	7.26	63.28	1.42	9.92	10.25	1.56	1.32
					Ref	3.00	70.85		3.88	40.34		
3	64	Diagnoised 2 yrs before	Glioblastoma Multiforme	TT	HB	1.56	74.64	0.32	1.93	58.38	0.50	0.41
					Ref	1.18	52.35		1.28	36.48		
4	38		Secondary progressive multiple solerosis	AT	HB	5.76	69.53	0.26	7.41	33.14	0.37	0.39
					Ref	4.58	56.07		5.43	26.70		
5	65	Diagnosed 1yr before, operated 2 months before	Glioblastoma Multiforme	AT	HB	6.94	62.89	1.74	7.88	36.47	1.57	1.39
					Ref	2.53	75.53		3.06	33.57		

Vt: distribution volume; BP_{ND}: Non-displaceable binding potential; HB: high binding region; Ref: reference region; AA: high affinity binder; AT: mixed affinity binder; TT: low affinity binder.

[table1]

References:

1. Arlicot, N., Katsifis, A., et. al, *Eur J Nucl Med Mol Imaging* 35, 2203-2211 (2008)

Acknowledgement: EU FW7 large scale integrating project INMiND (http://www.uni-muenster.de/InMind), Danish Research Council.

SYSTEM DEVELOPMENT AND VALIDATION FOR QUANTITATIVE ASSESSMENT OF CBF AND $CMRO_2$ USING 3-DIMENSIONAL PET

Y. Hori[1], T. Moriguchi[1], K. Koshino[1], S. Iguchi[1], A. Yamamoto[1], J. Enmi[1], H. Kawashima[1], T. Zeniya[1], K. Nakaya[2], A. Shimizu[2], T. Toku[2], N. Morita[2], H. Iida[1]

[1]National Cerebral and Cardiovascular Center Research Institute, [2]National Cerebral and Cardiovascular Center Hospital, Osaka, Japan

Objectives: Despite recent improvement of PET devices, three-dimensional acquisition is still a challenging issue in quantitative ^{15}O-labeled oxygen inhalation PET. This study was intended to develop a novel system which enables accurate assessment of CBF, $CMRO_2$ and OEF using ^{15}O-labeled oxygen and 3-dimensional PET. To validate, systematic experiments were carried out using a realistic 3-dimensional brain phantom [1] with a continuous flow of ^{15}O-gas, and also on healthy young volunteers.

Methods: A dedicated facemask was developed to minimize the radioactivity in the field-of-view (FOV) but outside of the object. Radioactivity gases were supplied to inside the inner mask, while the outer mask was ventilated by room air. PET scanner was Biograph-mCT, in which the single scatter simulation method was utilized to compensate scatter [2]. The process to scale the estimated scatter distribution outside the object was avoided, in order not to exclude the annihilation photons originated from the facemask. Validity was tested on 3-dimensional brain phantom containing ^{18}F-radioactivity,the phantom alone (Case 1), with a continuous flow of ^{15}O-gas through the facemask (Case 2), and with additional activity in the lung region (Case3). Experiments were also performed on 7 healthy volunteers (23.1±1.2 yo, all male), by the $C^{15}O$ and $^{15}O_2$-$C^{15}O_2$-based DARG protocol [3]. Scans were carried out twice on each volunteer. Inter-subject and intra-subject reproducibility of estimated CBF, $CMRO_2$ and OEF values were evaluated.

Results: The two layered facemask was effective to reduce the radioactivity inside FOV, and also contributed to stabilize the

ventilation condition, as confirmed with smaller variation in $EtCO_2$ and respiration rate. The phantom experiment showed that ROI values changed only 3% even for the presence of ^{15}O-gas radioactivity of 0-1500 kBq in the face mask, which is the range in clinical studies (Figure 1).CBF, $CMRO_2$ and OEF values from the volunteers were 39±4.3 mL/min/100g, 3.4±0.30 mL/min/100g and 0.45±0.045 respectively. Reproducibility between 1st and 2nd $^{15}O_2$-$C^{15}O_2$ scans in CBF, $CMRO_2$ and OEF were +5.3±21, -10±18, -16±25% (mean±2SD), respectively (Figure 2).

Conclusions: These results suggested that the use of 3-dimensional PET feasible for ^{15}O-inhalation PET study. Improved scatter compensation procedures, with use of the newly developed facemask system, appeared to be effective to support quantitative assessment of CBF, $CMRO_2$ and OEF using ^{15}O-labeled gases in clinical setting.

References: [1] Iida H et al., Ann Nucl Med 2012 [2] Watson C. C. et al., IEEE Trans Nuc Sci 2000. [3] Kudomi N., et al., J Cereb Blood Flow Metab 2005.

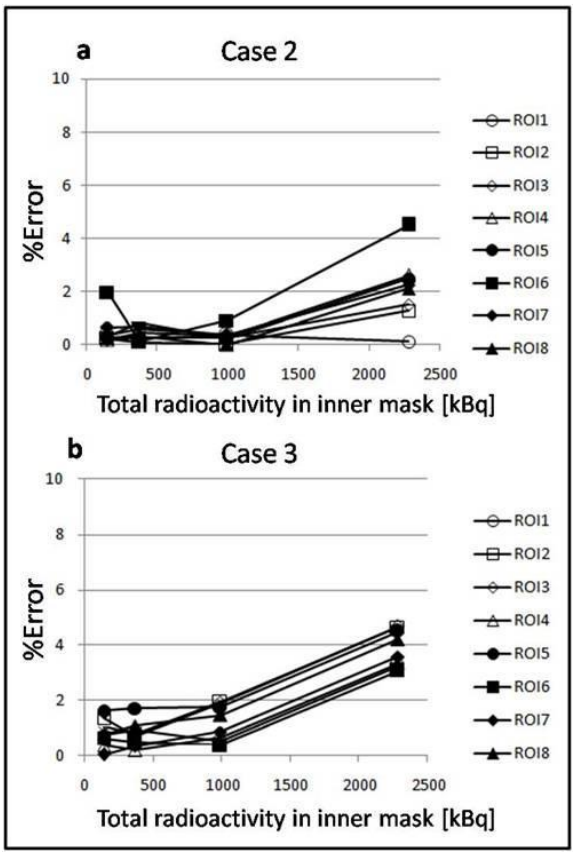

Figure 1: %error plotted against total radioactivity in inner mask in case 2 (a) and case3 (b).

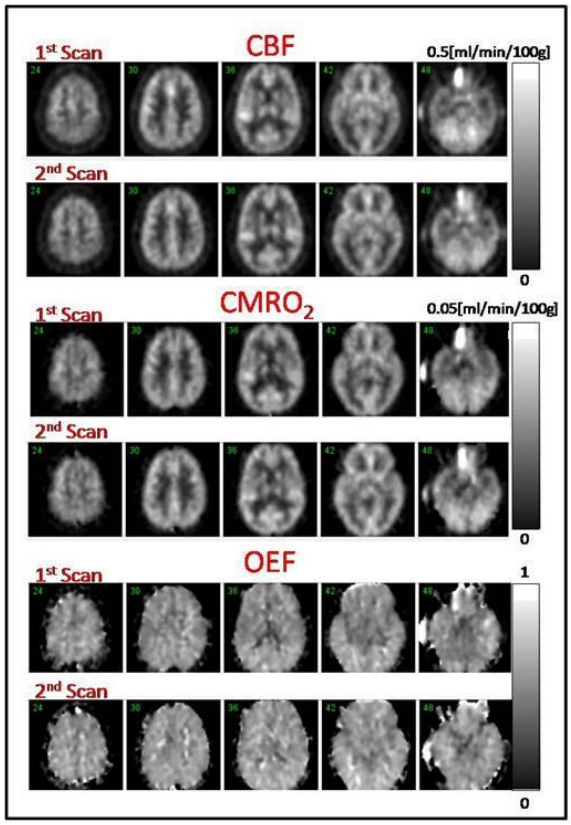

[
Figure 2: Representative images of CBF, $CMRO_2$ and OEF in 1st and 2nd scan.

A SEMI-AUTOMATED CLASSIFICATION OF VASCULAR COMPONENTS IN MOUSE SOMATOSENSORY CORTEX FROM 3D MULTI-PHOTON LASER SCANNING MICROSCOPIC IMAGE

H. Kawaguchi[1], H. Takuwa[1], Y. Tajima[1], J. Taniguchi[1], Y. Ikoma[1], C. Seki[1], K. Masamoto[1,2], I. Kanno[1], H. Ito[1]

[1]Molecular Imaging Center, National Institute of Radiological Sciences, Chiba, [2]Center for Frontier Science and Engineering, University of Electro-Communications, Chofu, Japan

Objectives: In quantitative analyses of positron emission tomography (PET) data, intravascular radioactivity should be diminished considering first-pass extraction fraction of radiotracers for each vascular component including artery, capillary, and vein [1]. The ratio of each vascular component in cerebral blood volume (CBV) are needed for this correction, however, the ratio is assumed to be that in bat wings previously reported [2]. In this study, we developed a semi-automated classification of vascular components in

mouse somatosensory cortex from a 3D multi-photon laser scanning microscopy (MPLSM).

Methods: A glass cranial window was constructed on a mouse head. After the injection of rhodamine dextran 70kDa, the 3D vasculature was acquired on somatosensory cortex of the anesthetized mouse by MPLSM. The lateral FOV was 488 x 488 μm^2 in pixels 0.477 x 0.477 μm^2. The z-stack was acquired with 1mm interval from brain surface to 350 μm deep.

The vessel was extracted from the 3D stack and then classified to vessel components. The vessel region in raw data was blurred in optical axis direction because of the non-focal excitation of fluorescence. In this study, a circuitous approach was employed to solve the problem. This method assumes that the actual vascular shape is locally cylindrical form and the blurred vascular shape has the same centerline with actual shape if the point-spread function is symmetric. The random noise in raw image was reduced by non-local means (NLM) filter. The denoised image was roughly separated to vessel and the others by discriminant analysis method. The centerline of vessels was obtained by a skeletonize algorithm [3]. The minimum distance, L, was calculated from a centerline location, **r**, to pixels that have half pixel intensity of **r**. The vessel was defined as the pixels locating inside of spheres that centers and radius are **r** and L, respectively. Capillary diameter was defined as less than 6 μm. The arteries and veins are manually estimated from the remained vessel region with referencing number of blanches from penetrating or arising vessels.

Results: The figure shows

(a) raw data,

(b) de-noised image by NLM filter,

(c) automatically extracted vessel tree, and

(d) classified vessel components.

The volumetric ratio of vascular component on mouse cortex was 5.5, 7.8 and 86.7% for artery, capillary and vein, respectively, while those on bat wings reported were 15.1, 0.4 and 84.5% [2].

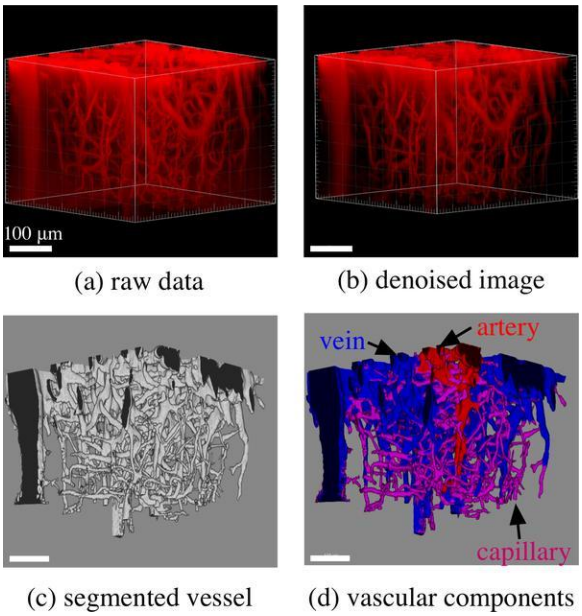

[Classification Procedure of Vascular Components]

Discussion: The vascular component ratio of mouse cortex was different from that of bat wing. However, note that ratios from this study are just from an example, thus further studies are necessary to confirm them. In conclusion, the present technique can estimate the cerebral blood volume with minimal arbitrariness. It can contribute not only quantitative PET analysis but also fundamental researches of microcirculation.

References:

[1] Mintun et al., J Nucl Med 25(2):177-187(1984),

[2] Wiederman, Circ Res 12:375-378(1963).

[3] Reniers, D et al, IEEE TVCG 14(2),355(2008).

Acknowledgements: This work was partially supported by Konica Minolta Science and Technology Foundation and JSPS KAKENHI Grant Number 22700441.

VOI-BASED EVALUATION OF THE SPM5 SPATIAL NORMALIZATION METHOD FOR BRAIN PET STUDIES

H. Kuwabara, H. Jung, D.F. Wong

Department of Radiology, Johns Hopkins University School of Medicine, Baltimore, MD, USA

Objectives: It appears that recent improvements of spatial normalization techniques and voxel-wise statistical analyses have diminished the usefulness of conventional structure-based data analyses for brain PET studies. To apply to PET data, the techniques require post-normalization smoothing of data to overcome expected insufficiencies of spatial normalization. Thus, it was examined whether PET signals were sufficiently recovered for individual brain structures with the widely-used unified segmentation method of the statistical parametric mapping (US-SPM5; Fristone and Ashburner 2003).

Methods: On 395 structural MRIs of young subjects (Age range: 18 - 40 years), 81 brain structures (volumes of interest, VOIs) were defined with Freesurfer software (FS; Fischl et al., 2004). Individual MRIs were spatially normalized to the SPM5-supplied standard brain using US-SPM5. Subsequently FS VOIs were spatially normalized and averaged across subjects to generate tissue probability maps (TPMs) of individual VOIs. A tissue classification map (TCM) was generated by thresholding TPMs at 0.5 to define extents of individual VOIs in the standard space. On individual VOIs, mean probabilities and mean contaminations from white matter (WM) and other gray matter (GM) regions were calculated using TPMs and TCM. These calculations were repeated after smoothing TPMs with a Gaussian kernel of 12 mm full-with at half maximal (FWHM) to simulate native smearing effect of PET (6 mm FWHM; Rousset et al, 2008) and a commonly-used post-normalization smoothing kernel (10 mm FWHM).

Results: Without smoothing, tissue recovery rates (=mean probabilities) were over 80% for subcortical VOIs, between 60 and 75% for cortical VOIs that were close to the anterior commissure point (distances < 5 cm), and less than 60% in the remaining VOIs. After smoothing, tissue recovery rates ranged between 15 and 30% for VOIs less than 5 mL, and between 25 and 40% for the remaining VOIs with a few exceptions. Without smoothing, contaminations from WM ranged between 5 and 30% except for the calcarine gyrus (45%), and were inversely proportional to the mean probability. After smoothing, WM contaminations ranged between 10 to 40%. Subcortical regions which were surrounded by WM appeared to be especially susceptible to WM contaminations. Contaminations from GM structures were less than 14% without smoothing, and between 5 and 40% after smoothing.

Conclusion: This VOI-based evaluation of US-SPM5 showed unacceptably low recovery rates of peripheral cortical regions. It was identified that contaminations from WM were responsible to the low recovery rates. After incorporating PET resolutions and post-normalization smoothing, recovery rates decreased below 40% in most regions and less than 30% for VOIs smaller than 5 mL. Thus, it was concluded that one has to be cautious to apply the method to brain PET studies, and that conventional VOI-based analysis may continue to be useful for data analysis of brain PET studies.

FASTER DISSOCIATION OF CLOZAPINE FROM THE STRIATAL SPECIFIC BINDING SITES THAN HALOPERIDOL: PHARMACOKINETIC PET STUDIES IN HUMANS

H.S. Park, B.S. Moon, N.H. Lim, B.C. Lee, S.E. Kim

Department of Nuclear Medicine, Seoul National University Bundang Hospital, Seoul National University College of Medicine, Seoul, Republic of Korea

Objectives: In an attempt to investigate the atypical antipsychotics' mechanism of action, the pharmacokinetics of clozapine and haloperidol in the human brain were examined using PET and radiolabeled clozapine and haloperidol.

Methods: Healthy human volunteers underwent ^{11}C-clozapine or ^{18}F-haloperidol PET studies. Dynamic PET images were acquired for 120 min after bolus injection of the radiolabeled drugs. Time-activity profiles in the striatal specific binding sites were estimated by the two tissue compartment model and pharmacokinetic parameters were

calculated. We assumed that both radiolabeled drugs bind to single receptor type.

Results: ^{11}C-clozapine attained its peak striatal specific binding of 2.0 ± 0.2 SUV at 43.0 ± 22.0 min after injection with a $T_{1/2}$ of 3.9 ± 0.9 h, while specific binding of ^{18}F-haloperidol in the striatum steadily increased during the scanning time, with 2.9 ± 0.4 SUV at 115 min after injection. Areas under the curves for ^{11}C-clozapine and ^{18}F-haloperidol were 191.5 ± 17.1 and 267.5 ± 49.0 SUV × min, respectively.

Conclusions: These data support the "fast-off-D_2" theory of atypical antipsychotic action. They also demonstrate that PET studies with radiolabeled drug candidates provide valuable information on target pharmacokinetics of drug candidates.

References:

1. Kapur, S., and Seeman, P. (2001). Does fast dissociation from the dopamine d(2) receptor explain the action of atypical antipsychotics?: A new hypothesis. Am J Psychiatry *158*, 360-369.

2. Seeman, P. (2004). Atypical Antipsychotics: Mechanism of Action. FOCUS: The Journal of Lifelong Learning in Psychiatry *2*, 48-58.

QUANTIFICATION OF [^{11}C]ABP688 BINDING IN THE HUMAN BRAIN USING CEREBELLUM AS REFERENCE REGION: INTERPRETATION AND LIMITATIONS

M.S. Milella[1], L. Minuzzi[2], M. Leyton[1], C. Benkelfat[1], J.-P. Soucy[1], A. Kirlow[2], E. Schirrmacher[2], M. Angle[2], J. Verhaeghe[2], G. Massarweh[2], A. Reader[2], A. Alliaga[2], J.E. Peixoto Santos[2], M.-C. Guiot[2], E. Kobayashi[2], **P. Rosa-Neto**[2]

[1]Department of Psychiatry, McGill University, [2]Department of Neurology and Neurosurgery, McGill University, Montreal, QC, Canada

Rationale: *In vitro* data from primates provide conflicting evidence regarding the suitability of the cerebellum as a reference region for quantifying metabotropic glutamate receptor type five (mGLUR5) binding parameters with positron emission tomography (PET).

Aims:

(1) to determine the availability of ABP688 in the human cerebellum using in vitro autoradiography;

(2) to compare binding parameters obtained with cerebellum as a reference region and gold standard methods.

Methods: To address this issue, we first measured mGLUR5 density in postmortem human cerebellum using [^{3}H]ABP688 autoradiography (n=5) and immunohistochemistry (n=6). Second, *in vivo* experiments were conducted in healthy volunteers (n=6) using a high-resolution PET scanner (HRRT) comparing reference tissue methods and two-tissue compartment model with metabolite-corrected arterial input function for determination of [^{11}C]ABP688 binding potentials (BP_{ND}).

Results: Compared to the hippocampus, postmortem data showed 20% less mGLUR5 immunoreactivity in the cerebellum, whereas [^{3}H]ABP688 autoradiography revealed a 15-fold reduction in receptor density. *In vivo* [^{11}C]ABP688 BP_{ND} using the cerebellum as a reference region were highly correlated with BP_{ND} values and distribution volumes derived by arterial input methods. Although immunohistochemistry revealed the presence of cerebellar mGLUR5, autoradiography data showed negligible concentrations of allosteric binding sites in this region.

Discussion and conclusions: Distinct mGLUR5 isoforms or conformational state might explain the absence of cerebellar allosteric binding sites. Altogether, our data support the cerebellum as a reference region for estimation of [^{11}C]ABP688 BP_{ND}.

MOLECULAR IMAGING AND KINETIC ANALYSIS TOOLBOX (MIAKAT)

G. Searle[1], R. Gunn[1,2,3]

[1]Imanova Ltd, [2]Imperial College London, London, [3]Oxford University, Oxford, UK

Objectives: Quantitative analysis of molecular neuroimaging data is typically performed using a combination of different software tools, which perform tasks such as image registration, brain extraction, segmentation, generation of time-activity curves (TACs) and input functions, graphical analysis, kinetic modelling and parametric imaging. These

separate tools are often linked together via manual processes, which can be both labour-intensive and difficult to ensure robustness and reproducibility.

The objective of the work presented here was to develop a set of software tools which provide a flexible system for the analysis of PET imaging data through a pipeline-style implementation of the analysis workflow. The software was designed to enable end-to-end analysis workstreams that are efficient, reproducible and quality-assured without being constrained in terms of the ability to develop and implement novel methodology.

Methods: A suite of software tools was developed in the form of a Matlab[1] toolbox, which we have named Molecular Imaging And Kinetic Analysis Toolbox (MIAKAT). MIAKAT contains many functions for directly performing tasks such as kinetic modelling, as well as some 'wrapper' functions to enable the incorporation of algorithms from packages such as SPM[2] and FSL[3] within the analysis workflow. The MIAKAT analysis pipeline capabilities are delivered through a modular software framework and flexible data structures, together with tools to enable users to perform and review analyses. The source code is managed using the Subversion version control system. This facilitates the inclusion of a detailed audit trail, wherein the exact version of a function used to perform a task is recorded within its output.

Results: The MIAKAT distribution consists of around 60,000 lines of Matlab code. MIAKAT implements a set of default image analysis workflows, as well as providing the ability to easily develop variations or new workflows as required. The standard PET neuroimaging analysis pipeline demonstrated here starts with a subject's dynamic PET data and associated structural MRI in the NIfTI file format, along with associated ancillary data (such as frame times, injected radioactivity data, measure arterial blood, plasma and metabolite activity data) in a well-defined text-based .anc file format. The full analysis pipeline typically takes less than one hour per PET scan to perform all spatial and kinetic analysis processes, and has been used to analyse over 500 clinical PET scans.

Conclusions: MIAKAT enables high quality quantitative analysis of PET neuroimaging studies. The complete analysis of a subject's data (structural MRI and multiple PET scans and associated ancillary data) can be configured and run easily, efficiently and reproducibly through the MIAKAT interface. Key QC steps are performed and recorded through the MIAKAT interface, and a full audit trail is stored in the output data structures. The modular nature of the software design permits easy incorporation of additional algorithms as they become available, and the efficient implementation of alternative workflows.

References:

[1] Matlab R2012b, The MathWorks Inc., Natick, MA, USA (www.mathworks.com)

[2] SPM, Wellcome Trust Centre for Neuroimaging, London, UK (http://www.fil.ion.ucl.ac.uk/spm/)

[3] FSL, FMRIB, Oxford, UK (http://fsl.fmrib.ox.ac.uk)

GENERALIZATION AND OPTIMIZATION OF A POPULATION-BASED INPUT FUNCTION ESTIMATION APPROACH FOR QUANTIFICATION OF SPARSELY SAMPLED DYNAMIC FDG PET DATA

S. Zhang[1,2], J. Zhang[1], R. Wang[1], Y. Zhou[3]

[1]Department of Nuclear Medicine, Peking University First Hospital, Beijing, [2]Department of Nuclear Medicine, Changhai Hospital, Second Military Medical University, Shanghai, China, [3]Department of Radiology, Johns Hopkins University School of Medicine, Baltimore, MD, USA

Introduction: FDG uptake rate constant K_i is a most interested and commonly used parameter for absolute quantification of FDG PET. K_i is usually estimated by fitting a kinetic model with plasma input function (PIF) to the measured dynamic PET data. A graphical analysis using Gjedde-Patlak plot with PIF is suggested for K_i estimation, due to its simplicity and efficiency in computation, and flexibility in data acquisition, where the dynamic PET data can be collected in non-continuously way. However, the need for arterial blood sampling to measure PIF (mPIF) is a main barrier to estimate K_i for clinical FDG PET. Two existing noninvasive PIF estimation methods, image derived PIF and simultaneous fitting method with kinetic model and parametric PIF, require image data to be acquired continuously and immediately post tracer injection. The objective of the study is to validate and optimize a generalized

population-based PIF estimation method for noninvasive quantification of dynamic FDG PET for sparsely sampled PIF.

Methods: Eight 60-min 27-frame monkey dynamic FDG PET studies were collected from a Philips Gemini GXL PET/CT with 3D data acquisition mode. Total 34 arterial blood samples were taken during PET scan as: 22 samples for the first 4 min, and followed by sampling at 5, 6, 8, 10, 12, 15, 20, 25, 30, 40, 50 and 60 min. Time activity curves (TACs) of 7 cerebral regions of interests (ROIs) were generated from each study. A generalized population-based approach to recover full kinetics of the PIF from sparsely sampled blood data is proposed. The estimated PIF from the incomplete PIF sampling data was determined by interpolation and extrapolation using scale-calibrated population mean of normalized PIFs, where the PIF was normalized by $||PIF||_2$ as it is considered as a vector $PIF=[PIF(t_1),...,PIF(t_n)]$, and piecewise scale calibration factor was determined for sparsely sampled PIF. The optimal blood sampling scheme with given sample size m was determined by maximizing coefficient coefficients of K_i estimates between the K_is from measured PIF (mPIF) and estimated PIF (ePIF). To evaluate the generality of the proposed method, leave-two-out cross validation was performed.

Results: The linear correlations between the K_i estimates from the ePIF (with optimal sampling scheme) and those from the mPIF were:

K_i(ePIF; 1 sample at 40 min) = $1.015K_i$(mPIF) -0.000, $R^2 = 0.974$;

K_i(ePIF; 2 samples at 25 and 50 min) = $1.029K_i$(mPIF) - 0.000, $R^2 = 0.985$;

K_i(ePIF; 3 samples at 8, 20, and 50 min) = $1.039K_i$(mPIF) - 0.001, $R^2= 0.993$; and

K_i(ePIF; 4 samples at 8,12, 25, 40, and 55 min) = $1.02K_i$(mPIF)-0.000, $R^2=0.997$.

The correlations of R^2 from leave-2-out validation study were 0.978±0.007, 0.990±0.006, and 0.996±0.003 (mean ±SD) for 1, 2, and 3 samples of optimal sampling scheme, respectively.

Conclusions: The generalized population-based PIF estimation method is a reliable method to estimate PIFs from incomplete blood sampling data for quantification of dynamic FDG PET using the Gjedde-Patlak plot. The method is applicable to noninvasive quantitative multi-bed dynamic FDG PET studies with PIF samples estimated directly from images.

CHARACTERIZATION OF QUANTITATIVE APPROACHES IN [^{18}F]AV-45 PET FOR B-AMYLOID IMAGING IN HIV INFECTION

Y. Zhou[1], D.F. Wong[1], M. Lodge[1], W. Ye[1], J.C. McArthur[2], N. Sacktor[2], M. Mohamed[1]

[1]Department of Radiology, [2]Department of Neurology, Johns Hopkins University School of Medicine, Baltimore, MD, USA

Introduction: [^{18}F]AV-45 PET has been used to measure β-amyloid deposition in the brain in vivo. The kinetic parameters of [^{18}F]AV-45 binding to β-amyloid are usually estimated by fitting a kinetic model to tissue time activity curve (TAC) generated from reconstructed dynamic PET image data. While iterative image reconstruction algorithms such as Ordered Subsets Expectation Maximization (OSEM) are commonly used in clinical static PET, filtered back-projection (FBP) is considered as a standard analytical image reconstruction method in quantitative dynamic PET studies. The objective of the study is to evaluate a Fourier Rebinning-based OSEM (FORE+OSEM) method in [^{18}F]AV-45 human HIV seropositive (HIV+) PET studies.

Methods: Six HIV(+) and two HIV(-) human [^{18}F]AV-45 PET scan data were collected in 3D mode from a GE Advance PET scanner. Four HIV(+) 70-min 33-frame dynamic PET scans with plasma input function were obtained, and the other four 20-min 4-frame dynamic PET scans were acquired from 50 to 70 images post tracer injection. Both OSEM and FBP were used to reconstruct PET images (image volume 128x128x35, voxel size: 2x2x4.25 mm in x-y-z direction). For OSEM, 4 iterations 16 subsets was selected, and 2 mm and 3 mm full width at half maximum (FWHM) Gaussian filters were used during iteration and applied post-reconstruction, respectively. A ramp filter cut off at the Nyquist frequency was used for FBP. The spatial resolution in the OSEM reconstructed images relative to the FBP reconstructed images was estimated by minimizing the sum squares of the intensity differences between the spatially smoothed FBP reconstructed images and the OSEM reconstructed images. Fifteen regions of

interest (ROIs) were manually drawn on MRI images in each subject and applied to dynamic PET images for ROI TACs. A 2-tissue 5-parameter (2T5P) compartment model with plasma input function and a simplified reference tissue model (SRTM) using cerebellum as reference tissue input were used for ROI TAC-based kinetic modeling and parametric imaging. Semi-quantitative standardized uptake value (SUV) in 50 to 70 min post tracer injection and SUV ratio (SUVR) were also calculated for both the OSEM and FBP reconstructed data.

Results: By applying 4 mm FWHM in x, y, and z 3D Gaussian filter to the FBP reconstructed images, the spatially smoothed SUV, parametric R_1, and DVR images were comparable to those obtained by OSEM reconstructed dynamic images (Figure).

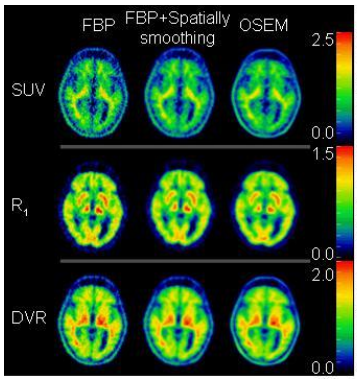

Figure. SUV, parametric R_1 and DVR images from 70min [^{18}F]AV-45 dynamic PET study for a HIV(+) subject (71 years old) of HIV-associated dementia. A SRTM model and linear regression with spatial constraint algorithm (Zhou et al., Neuroimage 2007) was applied to the FBP, FBP with post-reconstruction smoothing (4 mm FWHM 3D Gaussian filter), and OSEM reconstructed dynamic PET images to generate R_1 and DVR images. SUV, R_1, and DVR images at middle are almost same as those generated from OSEM reconstructed dynamic PET images.

[Figure]

For the ROI TAC based kinetic modeling, highly linear correlations between the estimators of K_1, DV, DVR (2T5P), R_1, and DVR (SRTM) from FBP reconstructed images and those from OSEM reconstructed images were obtained:

$K_1(OSEM)=0.95K_1(FBP)+0.00$, $R^2=0.99$

$DV(OSEM)=1.01DV(FBP)-0.15$, $R^2=0.99$

$DVR(OSEM)=1.04DVR(FBP)-0.06$, $R^2=0.99$

for 2T5P; and

$R_1(OSEM)=0.89R_1(FBP)+0.07$, $R^2=0.99$

$DVR(OSEM)=0.99DVR(FBP)-0.00$, $R^2=0.99$

for SRTM; and

$SUV(OSEM)=0.97SUV(FBP)+0.02$, $R^2=1.00$

$SUVR(OSEM)=0.99SUVR(FBP)+0.03$, $R^2=0.99$.

Conclusion: The iterative image reconstruction algorithm FORE+OSEM is as reliable as the FBP to provide dynamic PET images and tissue [^{18}F]AV-45 kinetics for quantitative measurements obtained by kinetic modeling in the scans from HIV+ and HIV- individuals.

Acknowledgment: This study is supported by P30-PilotMH075673 (MAM), P30MH075673 (JM), and R01NS081196 (NCS and MAM).

IS 18F-FDG DYNAMIC PET ABLE TO POINT OUT POTENTIAL CHOROID PLEXUS ALTERATION IN ALZHEIMER'S DISEASE?

B. Chaarani[1,2], J. Daouk[1], M. Rmeily-Haddad[1,2], R. Bouzerar[1], M.-E. Meyer[2], O. Baledent[1]

[1]Image Processing, [2]Nuclear Medicine, University Hospital of Amiens, Amiens, France

Objectives: Recent studies showed that the cerebrospinal fluid (CSF) could be involved in neurodegenerative diseases[1]. However, the physiological activity of the main CSF producer, the choroid plexus (CP), remains unclear. This work investigates the CP activity with ^{18}F-fluorodeoxyglucose (FDG) positron emission tomography (PET) in healthy subjects (HT) compared to neurodegenerative diseases: Alzheimer (AD) and amnesic mild cognitive impairment (MCI).

Methods: A total of 40 elderly patients participated in this study (mean age±SD = 69±7 years). Subjects were divided into 3 groups (17 HT, 13 AD and 10 MCI) after a comprehensive physical and neurological examination performed by an experienced neurologist.

All patients underwent a 45-min, dynamic FDG-PET acquisition performed in 3D mode on a Siemens Biograph 6.13 sinograms were generated starting from roughly 400s to avoid the vascular flow interference, with the following framing: 7×60 sec, 5×300 sec, and the last frame containing the remaining data. After FORE rebinning and scatter correction, each sinogram was reconstructed with 2D attenuation-weighted OSEM with 6 iterations and 16 subsets onto a 256×256×81 matrix. An algorithm was developed to segment the CP in

the cerebral ventricles, based on its distinctive tissue time-activity curves (TTAC) trend in the brain[2]. Regions of interest(ROI) in CP were selected according to the algorithm results(figure1-A). Normalized standardized uptake value means (normSUV) in the CP were calculated at each time point after radioactive decay correction, and then the 3 groups were compared between each other using a multiple analysis of variance.

Results: Segmented CP pixels number in HT, AD and MCI was 870±79, 658±71 and 670±52, respectively. HT subjects had significantly higher normSUV (1.5±0.75) ($p< 0.05$) than AD (0.96±0.23), while normSUV was slightly lower in MCI than in HT (1.33±0.7) (figure1-B). These results showing decreased CP activity in AD are consistent with the literature, stating that the CP epithelium in AD is progressively altered according to the impairment stage and that glucose transport is reduced[3].

MCI often occurs at the very early stages of Alzheimer´s disease or other dementia, which explains the slightly reduced FDG uptake compared to the normal group. CP_{TTACs} trend shows an increase over time in all groups. In fact, once the FDG is transported from the CSF across CP membranes, it became phosphorylated into FDG-6-phosphate. Phosphorylation reduces the glucose concentration in the cell, so less glucose diffuses back out than enters the cell. The enzyme that metabolizes glucose cannot use FDG-6-phosphate as a substrate, and thus, FDG-6-phosphate accumulates.

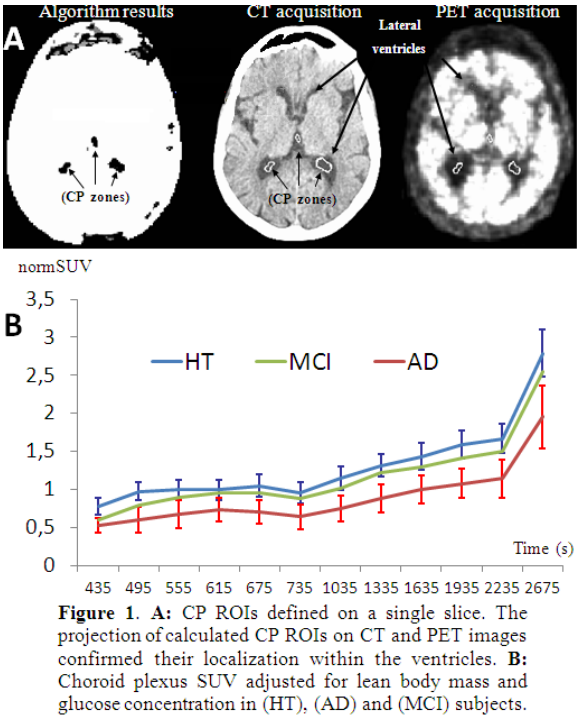

Figure 1. A: CP ROIs defined on a single slice. The projection of calculated CP ROIs on CT and PET images confirmed their localization within the ventricles. **B:** Choroid plexus SUV adjusted for lean body mass and glucose concentration in (HT), (AD) and (MCI) subjects.

[Figure 1]

Conclusions: This in vivo study demonstrated that CP glucose transport in AD is significantly reduced compared to healthy subjects. It may lead to ulterior innovative hypotheses regarding AD early diagnosis and treatment.

References:

[1] El Sankari et al. Cerebrospinal fluid and blood flow in mild cognitive impairment and Alzheimer's disease: a differential diagnosis from idiopathic normal pressure hydrocephalus -2011.

[2] Rmeily-Haddad M et al. The kinetics of 18f-fluorodeoxyglucose uptake in the choroid plexus- 2011.

[3] Serot et al. Choroid plexus, aging of the brain, and Alzheimer's disease-2003.

DIFFERENTIATION OF PARKINSON´S DISEASE SUBTYPES USING MULTI-TRACER POSITRON EMISSION TOMOGRAPHY (PET)

C. Eggers, F. Schwartz, G.R. Fink, L. Timmermann

Neurology, University of Cologne, Cologne, Germany

Introduction: Parkinson´s disease (PD) is a progressive neurodegenerative disorder which is characterized by rigidity, tremor, akinesia, and postural instability. Previous studies have shown clear differences between tremordominant (TD) and akinetic-rigid (AR) subtypes regarding clinical and imaging pattern.

This study compares PD subtypes with respect of clinical and imaging pattern in order to establish a relationship between the clinical subtypes, dopaminergic metabolism (FDOPA- & Raclopride-PET) and glucose metabolism (FDG). We hypothesized that AR and TD patients differ in terms of their disease progress, their binding pattern in the imaging profiles (striatal dopamine uptake and global cortical FDG metabolism), and that both subtypes show a specific FDG pattern (PDRP/PDTP; Parkinson´s Disease Related Pattern / Parkinson's Disease Tremor Pattern).

Methods: In a retrospective analysis, 120 idiopathic PD patients (80 male, 40 female, mean age 57 ± 11.3 years) were divided into the subtypes akinetic-rigid (AR), tremor-dominant (TD) and mixed type (MX) and were compared with respect to clinical and imaging pattern (used tracers: FDOPA, FDG, Raclopride).

Results: The analysis of idiopathic PD patients showed significant differences in the FDOPA uptakes for AR and TD patients, even after matching the subgroups for age, disease duration, Hoehn & Yahr stage, L-dopa dose equivalent dose and gender. There was a significant correlation between PDRP and regional striatal FDOPA uptake for AR patients.

Discussion: The study shows clear differences between the TD and AR subtypes, underscoring the validity of this subdivision of Parkinson´s disease. In accordance with previous FP-CIT-SPECT studies it shows congruent results for the presynaptic dopaminergic system and confirms additionally a relationship between PDRP and F-DOPA uptake for AR PD patients.

As for the FP-CIT SPECT imaging, multitracer PET imaging may support the clinical differentiation into PD subtypes. However, this diagnostic tool is not yet sufficent to differentiate subtypes without considering the clinical features.

ROLE OF [^{18}F]FLUOROETHYL-L-TYROSINE PET AS DIAGNOSTIC TOOL FOR MALIGNANT TRANSFORMATION IN PATIENTS WITH LOW-GRADE GLIOMA

N. Galldiks[1,2], G. Stoffels[2], M.I. Ruge[3], M. Rapp[4], M. Sabel[4], N.J. Shah[2,5], G.R. Fink[1,2], H.H. Coenen[2,5], K.-J. Langen[2,5]

[1]Dept. of Neurology, University of Cologne, Cologne, [2]Institute of Neuroscience and Medicine, Forschungszentrum Jülich, Jülich, [3]Dept. of Functional Neurosurgery and Stereotaxy, University of Cologne, Cologne, [4]Dept. of Neurosurgery, University of Düsseldorf, Düsseldorf, [5]Section JARA-Brain, Jülich-Aachen Research Alliance (JARA), Aachen, Germany

Objectives: In patients with low-grade glioma (LGG) of WHO grade II, the early detection of malignant transformation to WHO grade III or IV is of high clinical importance because the decision to apply a specific treatment depends mainly on the WHO grade. However, in a significant number of patients with LGG, specific information on tumor activity and malignant transformation cannot clearly be obtained on the basis of clinical or MRI findings alone. In this study, we investigated the potential of O-(2-[^{18}F]-fluoroethyl)-L-tyrosine (^{18}F-FET) PET to noninvasively detect malignant transformation in patients with LGG.

Methods: Twenty-eight patients (mean age, 44 ± 15 y) with histologically proven LGG (WHO grade II) were investigated longitudinally using dynamic ^{18}F-FET PET examinations. PET imaging with corresponding biopsy was performed at baseline when a LGG was present and when there were findings suggestive of malignant transformation (WHO grade III or IV) on contrast-enhanced MRI and/or suggestive clinical symptoms. Maximum and mean tumor/brain ratios (20-40 min postinjection) (TBR_{max}, TBR_{mean}) of ^{18}F-FET uptake were

determined. Time-activity curves (TAC) were generated and the time-to-peak (TTP) was calculated. Furthermore, TACs of each lesion were assigned to one of the following curve patterns: (I) constantly increasing ^{18}F-FET uptake; (II) ^{18}F-FET uptake peaking early (TTP ≤ 30 min) followed by a plateau; and (III) ^{18}F-FET uptake peaking early (TTP ≤ 30 min) followed by a constant descent.

Results: In patients with histologically proven malignant transformation (n=20), the TBR_{max} (median increase from 2.2 to 3.6; $P < 0.001$), TBR_{mean} (median increase from 1.7 to 2.3; $P < 0.001$), and the TTP (median decrease from 40 to 23 min; $P < 0.001$) changed significantly. Furthermore, in patients with malignant transformation the TAC curve pattern I changed significantly to curve pattern II or III in 12 of 20 patients ($P < 0.001$). In contrast, in patients without histological confirmation of malignant transformation (n=8), no significant changes of these parameters could be observed.

Conclusions: Both standard and kinetic imaging parameters derived from ^{18}F-FET PET seem to detect noninvasively patients with malignant transformation. Thus, repeated ^{18}F-FET PET provides important additional clinical information and may be helpful for further clinical decision-making, i.e., diagnostic stereotactic biopsy or tumor resection.

References:

Ullrich et al., 2009 *J Nucl Med*

Soffietti et al., 2010 *Eur J Neurol*

Jakola et al., 2012 *JAMA*

CORRELATION OF CSF TOTAL TAU AND AB42 LEVELS WITH FDG PET METABOLISM IN PATIENTS WITH DEMENTIA

V. Garibotto[1], A. Baskin[2], D. Zekry[1], G. Allali[2], H. Zaidi[1], O. Ratib[1], P. Burkhard[1], F. Assal[1]

[1]Geneva University and Geneva University Hospitals, [2]Geneva University Hospitals, Geneva, Switzerland

Background: Alterations in cerebrospinal fluid (CSF) tau and Aβ42 levels and cerebral glucose metabolism on fluorodeoxyglucose positron emission tomography (FDG PET) are validated biomarkers of Alzheimer's disease (AD) pathology. Both measures are considered as markers of amyloid-related neurodegeneration, synaptic dysfunction and neuronal injury, but their relationship remains unclear.

Objective: To determine whether CSF AD markers concentration correlates with regional FDG PET measures, in a population with suspected dementia and reduced β-amyloid peptide 1-42 (Aβ42) CSF levels as a biological indicator of AD.

Design: Retrospective study, based at a University Hospital.

Methods: We included 55 subjects (mean age 70 ± 8, range 51-87) with reduced Aβ42 CSF levels, who underwent FDG PET and CSF tau and Aβ42 measurement for the differential diagnosis of dementia. We analyzed voxelwise (SPM8), correcting for the effect of age, the correlation between relative glucose metabolism and CSF levels of tau and Aβ42.

We also tested the correlation between relative glucose metabolism and quantitative indices, namely tau/Aβ42 ratio and an index of AD CSF profile which combines total tau and Aβ42 values, previously proposed (Hulstaert et al., 1999).

Results: We demonstrated a significant correlation between CSF tau levels, tau/Aβ42 ratio and the AD CSF index with relative glucose metabolism in temporal cortex, parietal cortex and precuneus, bilaterally ($p < 0.05$, FWE corrected at cluster level). The areas correlating with the AD CSF index are shown in Figure 1. Conversely, no correlation was found between glucose metabolism and Aβ42 levels alone.

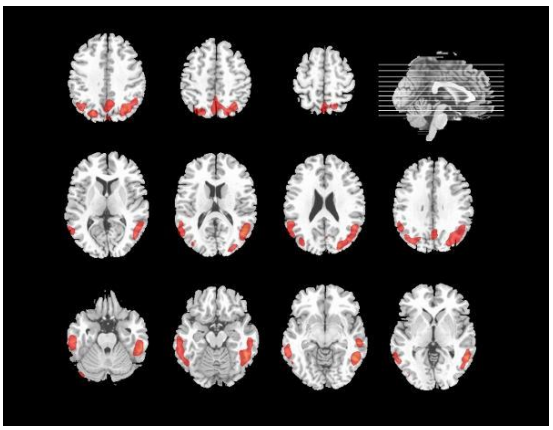

[Figure 1]

Conclusion: We observed an association between reduced relative glucose metabolism and total tau increase or relative total tau increase and Aβ42 reduction in regions typically affected by AD related pathology in patients with biological evidence of amyloid deposition.

This association supports the current view that CSF biomarkers and glucose metabolism provide converging information on neuronal dysfunction in amyloid-related dementia. The analysis of partial volume corrected data, in order to discriminate the effect of atrophy on the metabolic changes we observed, is ongoing.

References: Hulstaert F, Blennow K, Ivanoiu A, et al. Improved discrimination of AD patients using beta-amyloid(1- 42) and tau levels in CSF. Neurology 1999;52:1555-1562.

QUANTITATIVE ANALYSIS OF AMYLOID DEPOSITION IN ALZHEIMER DISEASE USING PET AND [C-11]AZD2184

H. Ito[1], H. Shimada[1], H. Shinotoh[1], H. Takano[1], F. Kodaka[1], H. Fujiwara[1], Y. Kimura[1], Y. Ikoma[1], C. Seki[1], M. Higuchi[1], T. Fukumura[1], É. Lindström Böö[2], L. Farde[2], T. Suhara[1]

[1]Molecular Imaging Center, National Institute of Radiological Sciences, Chiba, Japan, [2]AstraZeneca Translational Sciences Center, Department of Clinical Neuroscience, Karolinska Institutet, Stockholm, Sweden

Objectives: Characteristic neuropathologic changes in Alzheimer disease (AD) are amyloid-β deposits and neurofibrillary tangles. Carbon-11-labeled 5-(6-{[tert-butyl (dimethyl) silyl]oxy}-1,3-benzothiazol-2-yl) pyridin-2-amine ([C-11]AZD2184) is a more recently developed radiotracer for amyloid-β deposits. [C-11]AZD2184 has high affinity in vitro for amyloid fibrils (dissociation constant, KD: 8.4 ± 1.0 nM) [1]. After intravenous injection of [C-11]AZD2184, there was rapid uptake of radioactivity in the brain followed by rapid washout in control subjects as well as in AD patients in an initial human study [2]. In this study, [C-11]AZD2184 binding in control subjects and AD patients was examined in more detail by compartment model analysis using a metabolite-corrected arterial input function. The accuracy of simplified quantitative methods employing a reference brain region was also evaluated.

Methods: After intravenous bolus injection of [C-11]AZD2184, a dynamic PET scan was performed for 90 minutes in 6 control subjects and 8 AD patients. To obtain the arterial input function, arterial blood sampling and HPLC analysis were performed. To interpret the kinetic behaviour of [C-11]AZD2184, the standard two-tissue compartment model with four first-order rate constants (K1, k2, k3 and k4) was employed. The rate constants were estimated by non-linear curve fitting which was performed in a least-squares sense to the regional time-activity curves. Since the cerebellum can be used as a reference brain region, the total distribution volume ratio (DVR) of brain regions to cerebellum. In addition, the standardized uptake value ratio (SUVR) of brain regions to cerebellum obtained from integrated time-activity curves with integration intervals of 20-40 min, 40-60 min, and 60-90 min were calculated as the indicator of amyloid-β deposits.

Results: Time-activity curves in all brain regions could be described using the standard two-tissue compartment model. Binding potentials (BPND, equal to k3/k4) in cerebral cortical regions were higher in AD patients than in control subjects (AD patients: 2.0-2.3, control subjects: 1.0-1.1). Although there was no conspicuous accumulation of radioactivity in white matter as compared with other amyloid radioligands, BPND values were identified by compartment model analysis of the centrum semiovale for both control subjects and AD patients (about 1.7), suggesting binding to myelin. SUVR with each integration interval was in good agreement with DVR (AD patients: 1.8-2.6, control subjects: 1.0-1.2).

Conclusions: It has been estimated that regions-of-interest defined for the cerebral cortex contain about 60% of gray matter and 30% of white matter [3]. This tissue heterogeneity may be one reason for the BPND values of [C-11]AZD2184 in cerebral cortical regions for control subjects. Although the white matter binding of [C-11]AZD2184 may have some effect on cortical uptake, it can be concluded that the kinetic behavior of [C-11]AZD2184 is suitable for quantitative analysis. SUVR can be used as a validated measure of [C-11]AZD2184 binding in clinical investigations without arterial input function.

References:

[1] Johnson AE, et al. J Neurochem 2009; 108: 1177-1186.

[2] Nyberg S, et al. Eur J Nucl Med Mol Imaging 2009; 36: 1859-1863.

[3] Ito H, et al. Neuroimage 2008; 39: 555-565.

BRAIN ACETATE METABOLISM IN PATIENTS WITH LIVER CIRRHOSIS AND HEPATIC ENCEPHALOPATHY

P. Iversen[1], K. Mouridsen[2], M.B. Hansen[2], M. Sørensen[1,3], L.K. Bak[4], H. Waagepetersen[4], A. Schousboe[4], P. Ott[3], H. Vilstrup[3], S. Keiding[1,3], **A. Gjedde**[2,5]

[1]Department of Nuclear Medicine and PET Centre, Aarhus University Hospital, [2]Center of Functionally Integrative Neuroscience (CFIN), Aarhus University, [3]Department of Medicine V (Hepatology), Aarhus University Hospital, Aarhus, [4]Department of Drug Design and Pharmacology, Faculty of Health Sciences, University of Copenhagen, [5]Department of Neuroscience and Pharmacology, University of Copenhagen, Copenhagen, Denmark

Objectives: Patients with impaired liver function and hepatic encephalopathy (HE) have elevated blood ammonia levels, suggesting that ammonia may play a crucial role in the pathogenesis of HE. Recent evidence indicates that low brain blood flow in patients with HE reflects reduced oxidative metabolism,[1-2] but it is unknown whether this reduction reflects glial or neuronal pathology, or both.

Methods: To assess astrocyte metabolism in HE, we used [1-^{11}C]acetate with positron emission tomography (PET). We included 3 groups of subjects: cirrhosis patients with an acute episode of HE (n = 6), cirrhosis patients without HE (n = 7), and healthy subjects (n = 5).

We measured global and regional metabolism of [1-^{11}C]acetate with dynamic PET. Individual PET and magnetic resonance (MR) T1 images were co-registered to align the PET measurements to specific brain regions, comprising cerebellum, frontal lobe, parietal lobe, temporal lobe, occipital lobe, striatum, thalamus, total gray matter, and total white matter. Using a novel mixed model with covariates, the PET data from whole-brain and each of the predefined brain regions in each subject, we obtained estimates of the kinetic parameters K1, k2, k3, k5, and Vp, where k3 represents oxidative metabolism of acetate in mitochondria, and k5 represents efflux of carbon dioxide including the CO_2 in plasma, making k5 less flow dependent.

Results: The whole-brain metabolic clearance of acetate (K=K1*k3/(k2+k3)) averaged 0.0346 mL/(mL tissue)/min in the group of cirrhosis patients with HE, 0.0377 in the group of cirrhosis patients without HE, and 0.0465 in the group of healthy subjects, with a significant difference in K between the group of cirrhosis patients with HE and healthy subjects ($P = 0.002$). No differences in K were found between cirrhosis patients without HE and healthy subjects ($P = 0.466$), or in K between cirrhosis patients with and without HE ($P = 0.234$).

Whole brain estimates of oxidative rates (k3) did not differ among the groups, with a value of 0.0982 ± 0.0140 min^{-1} (mean ± SD) in the group of cirrhosis patients with HE, 0.0941 ± 0.0130 in the group of cirrhosis patients without HE, and 0.1107 ± 0.0154 in the group of healthy subjects. Regional values showed no difference between groups of subjects.

Conclusion: Decline of oxidative metabolism in patients does not appear to be due to glial malfunction and hence implicates neuronal metabolic deficiency in patients with HE.

Interestingly, we found similar K1 values in our previous study[2] in which CBF was measured in the same group of subjects using [^{15}O]-water PET, indicating that [1-^{11}C]acetate may be a potential marker of CBF.

References:

1. Gjedde A et al. Metab Brain Dis 2010 Mar;25(1):57-63.

2. Iversen P et al. Gastroenterology 2009 Mar;136(3):863-871.

A PET STUDY OF STRIATAL DAT BINDING AND PARKINSONISM-RELATED METABOLIC BRAIN NETWORK ACTIVITY IN REM BEHAVIOR DISORDER

S. Peng, Y. Ma, F. Holtbernd, C. Tang, **V. Dhawan**, D. Eidelberg

Center for Neurosciences, The Feinstein Institute for Medical Research, Manhasset, NY, USA

Introduction: Rapid eye movement sleep behavior disorder (RBD) has a high probability of developing motor symptoms of Parkinson's disease (PD) during the clinical course of the disease. In addition to quantifying regional abnormality in dopamine transporter (DAT), PET imaging with [^{18}F]FDG can be used to assess metabolic brain network activity associated with PD, multiple system atrophy (MSA) and progressive supranuclear palsy (PSP) [1]. In our previous longitudinal study we have demonstrated striatal DAT binding loss and elevated PD-related network activity before symptom onset in the presymptomatic hemisphere of 15 hemi-PD patients who were scanned with [^{18}F]FPCIT and [^{18}F]FDG PET at baseline and again 2 and 4 years [2]. Regional abnormalities of striatal DAT binding and brain metabolism may be present in RBD patients as seen in the presymptomatic phase of PD. In this study, we sought to detect imaging features of presymptomatic PD in RBD patients by measuring striatal DAT binding and expressions of parkinsonism-related covariance patterns.

Methods: Using [^{18}F]FPCIT and [^{18}F]FDG PET we investigated a group of nine patients with idiopathic RBD (age 64.2 ± 9.7 yr) who did not have any motor signs of parkinsonism on examination and compared them with nine age-matched healthy control subjects (age 63.9±8.3 yr). [^{18}F]FPCIT binding was calculated in striatal regions at 95 min post-injection. Expressions of PD-, MSA- and PSP-related covariance patterns (i.e., PDRP, MSARP and PSPRP) were also computed using [^{18}F]FDG PET images in individual subjects. Striatal DAT binding values and PDRP expressions in RBD patients were compared to those in the longitudinal hemi-PD study.

Results: In the RBD patients we found mildly decreased [^{18}F]FPCIT binding in bilateral posterior putamen (Fig. 1A; average left/right: 79.2% of the normal mean) which was slightly higher than that (67.4 %) in the preclinical hemisphere [2]. Compared to the controls we also noted increased PDRP scores in the whole-brain (Fig. 1B; $p < 0.05$) that were similar to the significantly ($p < 0.05$) elevated baseline average score of the clinically unaffected hemisphere of our longitudinal patient cohort [2]. In addition, subjects scores of MSARP and PSPRP networks were not elevated in these RBD patients relative to the controls.

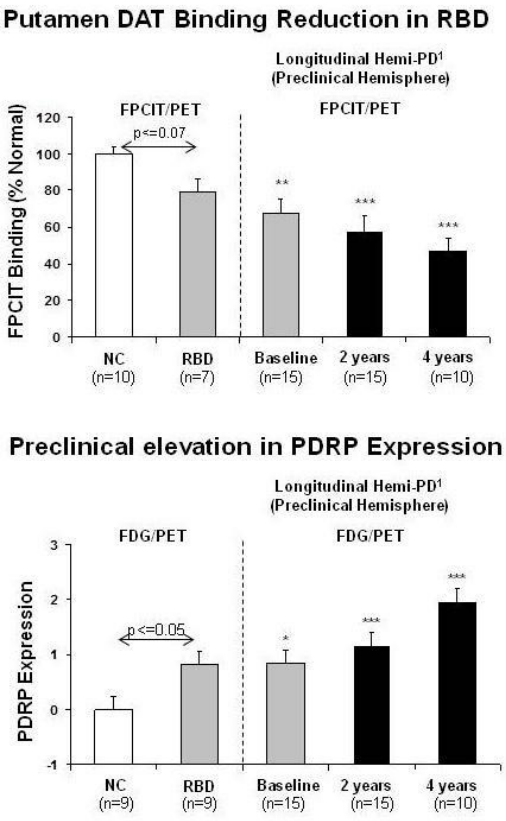

[Fig. 1 DAT Binding and PDRP score in RBD patients.]

Conclusions: PET with [^{18}F]FPCIT and [^{18}F]FDG is capable of identifying patients with RBD destined to develop early signs of PD. Our data suggest a decline in striatal DAT binding in the posterior putamen and elevation of PD-related network activity. This method may offer a useful tool for tracking the phenoconversion of RBD to PD at preclinical stages.

References:

1. Tang, CC et al (2010), 'Differential diagnosis of parkinsonism: a metabolic imaging study

using pattern analysis'. *Lancet Neurol.*, 9:149-58.

2. Tang, CC et al (2010), 'Abnormalities in metabolic network activity precede the onset of motor symptoms in Parkinson´s disease'. *J Neurosci.*, 30:1049-56.

IMPACT OF PARTIAL VOLUME CORRECTION ON THE RELATIONSHIP BETWEEN PIB RETENTION AND POST-MORTEM MEASURES OF AMYLOID LOAD

J.C. Price[1], D.S. Minhas[1], C.M. Laymon[1], E.E. Abrahamson[2], L.A. Weissfeld[3], O.L. Lopez[2], M.L. Debnath[4], L. Shao[4], R.L. Hamilton[2], C.R. Becker[1], C.A. Mathis[1], W.E. Klunk[4], M.D. Ikonomovic[2]

[1]Radiology, [2]Neurology, [3]Biostatistics, [4]Psychiatry, University of Pittsburgh, Pittsburgh, PA, USA

Objectives: Previously we observed that cortical correspondence between [C-11]PiB PET measures of fibrillar amyloid-β (Aβ) plaque deposition and postmortem assessments of Aβ-load generally improved after correction of the PET outcomes for CSF dilution (1). The current work further examines this relationship for different partial volume (PV) averaging correction schemes.

Methods: [C-11]PiB (or PiB) PET imaging was performed over 90 min (n=7) or 60 min (n=1, S1* only), for 8 subjects (S1-S8) who were diagnosed with dementia at autopsy. The longest interval between PET scanning and death for any subject was 42 months. PiB retention was assessed using the simplified SUVR50-70 or SUVR50-60* measure. Post-mortem Aβ plaque load was assessed by applying 6-CN-PiB, the highly fluorescent derivative of PiB, to 12-µm paraffin sections of multiple cortical and sub-cortical regions, that included anterior cingulate (ACG), frontal cortex (FRC) and precuneus (PRC). A region-labeled image of postmortem brain was used to guide region definition on the corresponding ante-mortem MRI and regional sampling of the co-registered PET image. The PiB SUVR was corrected for atrophy-related PV effects using two methods with different segmentation approaches. Method-1 applied a two-compartment (GM+WM, CSF) CSF-dilution correction and Method-2 applied a three-compartment (GM, WM, CSF) least squares fit for extraction of GM+WM concentration. Correlations between PiB SUVR and 6-CN-PiB measures were assessed using Spearman's rho (2-sided, **p< 0.05**).

Results: The uncorrected PiB SUVR values ranged from minimal (1.1 for S3) to high (2.7 for S1*). Method-1 correction yielded PRC SUVR values that ranged from 1.2 (S3) to 3.4 (S1*), while Method-2 yielded SUVR values that ranged from 1.3 (S3) to 3.1 (S5). Correlations for ACG, FRC, and PRC were generally greater after PV-related correction: 0.571, 0.619, **0.905** (Uncorrected); **0.762**, 0.667, **0.952** (Method-1); **0.810**, **0.738**, **0.976** (Method-2). In key cortical areas, linearity between the uncorrected PiB SUVR values and the 6-CN-PiB measures was more apparent at lower fibrillar Aβ load and more asymptotic at higher Aβ load. The relationship was more linear throughout the pathology-load range, after correction for PV-related effects.

Conclusion: Correcting for atrophy-related PV effects can improve the correlation between PiB PET and post-mortem amyloid-load measures. This is consistent with the exclusion of CSF spaces from post-mortem plaque-load analyses. Future studies will characterize the PV corrections and image segmentation approaches for ante-mortem/post-mortem correlations.

(1) NRM12 Abstract: Price JC et al. [^{11}C]PiB PET and post-mortem measures of amyloid load: Regional Correspondence.

Support: NIH (R01AG033042, P50AG005133, P01AG025204), Dana Foundation, Alzheimer's Association, GE Healthcare

EFFECT OF *MANASAMITRA VATAKAM(MMV)* AGAINST AL INDUCED OXIDATIVE STRESSED NEURONAL CELL DEATH

S.V. Thirunavukkarasu, K. Thyalan

Medical Cyclotron Facility, Dr. Kamakshi Memorial Hospital, Chennai, India

Background: *Manasamitra vatakam* (*MMV*) as pivotal role against Aluminium induced neuronal apoptosis. Herbo-mineral formulation of *MMV* prepared by Indian system of Ayurvedic medicine and used to improve cognitive functions against Aluminium induced dysfunction of rats.

Objectives: The study concentrated on *MMV*

as an alternative medicine against cognitive dysfunction as well as neuronal apoptosis induced by Aluminium rats.

Materials and methods: The study consists of five groups, six animals in each. Male healthy Swiss albino rats (200-220 gm) were used and housed in clean polypropylene cages and maintained the room temperature 23°C - 25°C with alternating 12 h light and dark cycles. The animals were treated Aluminium orally and fed with standard pellet diet and clean drinking water. The study was assessed cognitive functions of behavioral parameters like active avoidance and radial arm maze. The whole experimental studies were conducted for 90 days. The biochemical and molecular studies (Western blot, RT-PCR and Immunohistology) were carried out by standard methods.

Results: These results shown that *MMV* treatment is markedly improved neurotransmitters such as 5-HT and AChE as well as cognitive functions of rats and restrain expression of oxidative stress (HSP70) & pro-apoptotic genes like *Bcl-2, Bcl-xL* and *Caspas-3* against Aluminium induced hippocampal region of rat's brain. In aluminium intoxicated animals were observed pro-apoptosis genes like *Bcl-2, Bcl-xL* and *caspas-3* were significantly expressed high in hippocampus and cerebral cortex of brain regions. Whereas *MMV* treated animals were observed normal cognitive function as on control.

Conclusion: The present study reveals that Herbo-mineral formulation of *Manasamitra vatakam* (*MMV)* potentially improved memory function and inhibited oxidative stress, neuronal apoptosis against Aluminium induced neurodegenerative disorder rats.

Acknowledgements: The authors are thankful to ICMR (New Delhi, India) for providing financial assistance to the entire study.

A PRELIMINARY STUDY OF AMYLOID AND FDG-PET IN THE DIFFERENTIAL DIAGNOSIS OF ALZHEIMER´S DISEASE AND FRONTOTEMPORAL LOBAR DEGENERATION

Y. WANG[1], S. GAO[1], L. CAI[1], Z. SHI[2], Y. LI[1], Y. JI[2]

[1]PET/CT Center, General Hospital of Tianjin Medical University, [2]Huanhu Hospital, Tianjin, China

Objective: The aim of this study is to investigate the value of amyloid and FDG-PET in the differential diagnosis of AD and FTLD.

Methods: 14 patients who were difficult to diagnosis for AD and FTLD underwent ^{11}C-PiB and ^{18}F-FDG PET.The statistics parametric mapping(SPM8) software and two sample *t*-test were used for FDG data analysis($P<0.001$) . The 55~60min PiB scans were classified as positive or negative by visual analysis.

Results: After undergoing amyloid and FDG-PET scans, five typical AD images were distinguished, FDG imaging pattern presented as focal cortical hypometabolism in bilateral parietotemporal association cortexes and the posterior cingulated gyrus, the precuneus. The amyloid images were positive in the bilateral frontal lobe, temporal lobe, posterior cingutate and precuneus(image A). Four typical FTLD images were revealed. The significant regional reductions in rCMRglc were in bilateral frontal, the cingualte gyri, insulae and the subcortical structures. Moreover, the amyloid PET was negative(image B). Five patients were difficult to diagnose only after FDG PET. The topographic extent of hypometabolism began to overlap between AD and FTLD. Whereas, three of them were positive in amyloid just like AD(image C), and two of them were negative like FTLD(image D).

Conclusions: Amyloid and FDG-PET could provide dual functional information **i**n the differential diagnosis of AD and FTLD, especially the lower specificity in rCMRglc in some cases, amyloid imaging was helpful.

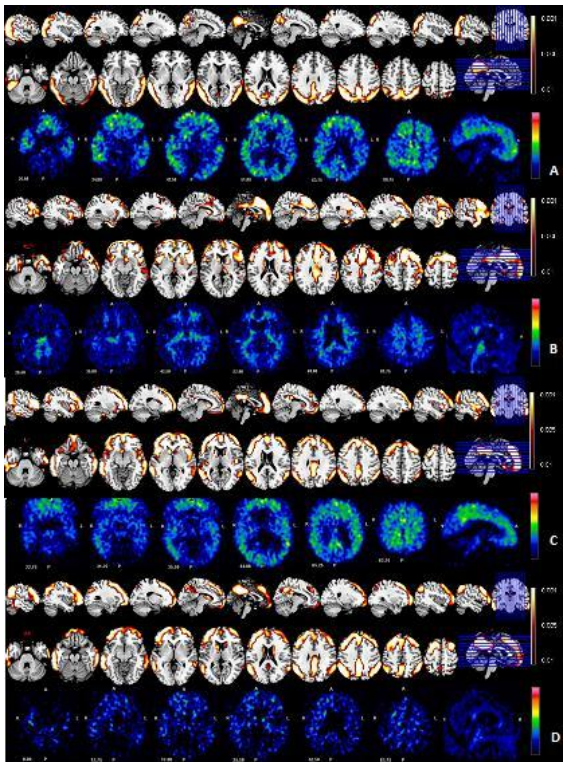

[amyloid and FDG-PET in the differential diagnosis]

For images: The first and second line was 18F-FDG SPM images, *P*< 0.001. The third line was 55~60min11C-PIB images.

References:

[1]Womack KB, Diaz-Arrastia R, Aizenstein HJ, et al. Temporoparietal hypometabolism in frontotemporal lobar degeneration and associated imaging diagnostic errors. Arch Neurol. 2011 Mar;68(3):329-337.

[2]Li ZG, Gao S, Zhang BS, et al. Voxel-based analysis of cerebral glucose metabolism in AD and non-AD degenerative dementia using statistical parametric mapping. Chin J Nucl Med,2008,28(1):13-16.

[3] Klunk WE, Engler H, Nordberg A, et al. Imaging brain amyloid in Alzheimer's disease with Pittsburgh Compound-B, Ann Neurol, 2004, 55(3): 306-319.

[4] Rabinovici GD, Jagust WJ. Amyloid imaging in aging and dementia: testing the amyloid hypothesis in vivo. Behav Neurol, 2009;21(1):117-128.

[5] Ikonomovic MD, Klunk WE, Abrahamson EE, et al. Post-mortem correlates of in vivo PiB-PET amyloid imaging in a typical case of Alzheimer's disease. Brain, 2008, 131(6), 1630-1645.

[6]Rabinovici GD, Rosen HJ, Alkalay A, et al. Amyloid vs FDG-PET in the differential diagnosis of AD and FTLD. Neurology. 2011 Dec 6;77(23):2034-2042.

[7] Herholz K, Salmon E, Perani D, et al. Discrimination between Alzheimer dementia and controls by automated analysis of multicenter FDG PET. NeuroInage,2002,17(1):302-316.

[8] Mielke R, Kessler J, Szelies B, et al. Normal and pathological aging-findings of positron-emission-tomography. J Neural Transm, 1998,105(8-9):821-837.

[9] Savva GM, Wharton SB, Ince PG, et al. Age, neuropathology, and dementia. N Engl J Med, 2009, 360(22):2302-2309.

[10] Engler H, Santillo AF, Wang SX, et al. In vivo amyloid imaging with PET in frontotemporal dementia. Eur J Nucl Med Mol Imaging. 2008 Jan;35(1):100-106.

IN-VIVO SEROTONIN-TRANSPORTER (SERT) AVAILABILITY IN OBESITY

A. Bresch[1], J. Luthardt[1], M. Rullmann[2,3], F. Zientek[2], G. Reissig[2], K. Arelin[3,4], D. Lobsien[5], A. Hilbert[2], P.M. Meyer[1], S. Tiepolt[1], C. Schinke[6], G.A. Becker[1], M. Patt[1], A. Seese[1], M. Blüher[2,7], M. Fasshauer[2,7], O. Sabri[1,2,3], S. Hesse[1,2,3]

[1]Department of Nuclear Medicine, University of Leipzig, [2]IFB Adiposity Diseases, Leipzig University Medical Center, [3]LIFE - Leipzig Research Center for Civilization Diseases, [4]Max-Planck-Institute for Human Cognitive and Brain Sciences, [5]Department of Diagnostic Radiology, [6]Department of Neurology, [7]Department of Medicine, University of Leipzig, Leipzig, Germany

Objectives: SERT plays a key role in the serotonin (5HT) homeostasis by recycling 5HT into the presynaptic neurons. Given the important role in appetite regulation and feeding behaviour, functional differences, especially in the presynaptic SERT system, probably contribute to obesity. However, at present consistent imaging data, in particular in obese subjects with a high body mass index

(BMI) are lacking. The aim of this study is to quantify for the first time the *in-vivo* SERT availability in obese subjects compared to non-obese controls in a cross-over subject study.

Methods: We studied seven obese, non-depressive subjects (BMI 41,8±8,1 kg/m2, age 45±10 years, 2 female) and 13 control subjects (BMI 22,4±2,6 kg/m2, age 36±7 years, 5 female) with C-11-DASB PET (488,0±5,9 MBq iv, 90 min, 3D acquisition mode). From the PET data, parametric image data of the binding potential (BP) have been calculated (MRTM2; Ichise et al JCBFM 2003) and evaluated by VOI analysis (PMOD 3.4) with both standardized brain atlases (AAL and Hammers), based on an individual MR coregistration, and voxel-based analysis (SPM8).

Results: The SPM analysis showed no overall significant group difference. After stratification of the obese population according to the Beck Depression Inventory (BDI) the subgroup of BDI< 10 demonstrates an increased SERT availability (p=0.05) in putamen, pons and in parts of the frontal and temporal cortex. The VOI-analysis confirmed the significantly increased cortical in-vivo SERT availability and also indicated higher BP values for the nucleus accumbens (p< 0.01), which correlated positively with the BMI (p=0.01).

Conclusions: These first results suggest that in obese, non-depressive patients, the *in-vivo* SERT availability is increased in brain regions that are relevant to the reward system and the control of food intake.

Currently, neuropsychological testing, genotyping (5-HTTLPR), adipokines and pharmacological stress response test is being included in our analysis to further sub-characterize the phenotype of obesity.

References:

1. Ichise M, Liow JS, Lu JQ, Takano A, Model K, Toyama H, Suhara T, Suzuki K, Innis RB, Carson RE: Linearized reference tissue parametric imaging methods: application to [^{11}C]DASB positron emission tomography studies of the serotonin transporter in human brain. J Cereb Blood Flow Metab 2003; 23: 1096-1112

REWARD RESPONSIVENESS AND *IN-VIVO* SEROTONIN-TRANSPORTER AVAILABILITY IN OBESITY

S. Hesse[1,2,3], A. Hilbert[2], S. Baldofski[2], **A. Bresch**[1], J. Luthardt[1], M. Rullmann[2,3], F. Zientek[2], G. Reissig[2], K. Arelin[3,4], D. Lobsien[5], C. Schinke[6], A. Rudolph[2], G.A. Becker[1], M. Patt[1], A. Seese[1], P.M. Meyer[1], S. Tiepolt[1], M. Blüher[2,7], M. Fasshauer[2,7], O. Sabri[1,2,3]

[1]Department of Nuclear Medicine, University of Leipzig, [2]IFB Adiposity Diseases, Leipzig University Medical Center, [3]LIFE - Leipzig Research Center for Civilization Diseases, [4]Max-Planck-Institute for Human Cognitive and Brain Sciences, [5]Department of Diagnostic Radiology, [6]Department of Neurology, [7]Department of Medicine, University of Leipzig, Leipzig, Germany

Objectives: The behavioural activation system (BAS) was proposed to regulate the response of appetitive cues via dopaminergic neurotransmission whereas the behavioural inhibition system (BIS) is believed to be controlled by serotonin (5HT) levels. Low 5HT levels may then lead to an overriding intrinsic drive to eat. Such assumptions, however, have not yet been explored by in-vivo 5HT imaging. We used PET and C-11 DASB, a marker of brain 5HT transporter (5HTT) availability, to study 5HT function in obese subjects with body-mass-index (BMI) ≥35 kg/m2, compared to non-obese.

Methods: We studied 8 obese participants (BMI 42±7 kg/m2, age 42±11 years, 2 female) and 14 control subjects (BMI 22±3 kg/m2, age 22±3 years, 5 female) with C-11-DASB PET (487.5±6.0 MBq iv, 90 min. 3D acquisition mode). From the PET data, parametric image data of the binding potential (BP) have been calculated (MRTM2; Ichise et al JCBFM 2003) and evaluated by VOI analysis (PMOD 3.4), based on an individual MR coregistration and with the use of a standardized brain atlas (Hammers). Neuropsychological assessment included BIS/BAS with BAS-drive, BAS-fun, and BAS-reward scores.

Results: Neither BAS-drive, BAS-fun, BAS-reward, nor BIS differed between obese and non-obese. Overall, we found highly significant negative correlations between 5HTT-BP and either BAS-reward or BIS in distinct brain areas (e.g., BAS-reward vs. amygdala r=-.68, p=.001, orbitofrontal r=-.62, p=.003, anterior cingulate cortex r=.68, p=.001, nucleus accumbens r=-.58, p=.006; BIS: amygdala r=-.55, p=.003, anterior cingulate cortex r=-.55, p=.009, precuneus r=.60, p=.004, and others;

Figure). 5HTT-BP did not correlate with BAS-fun or BAS-drive.

Conclusions: These data confirms that sensitivity to reward shows an individual variability, which is driven as suggested here by differences in 5HTT availability in a network of interconnected brain regions, mainly fronto-striatal-limbic. No association between 5HTT and drive or fun seeking have been found. Interestingly, the BIS is also correlated with 5HTT in the same direction with the inclusion of more posterior parts of the brain. Whether these findings contribute to the vulnerability of eating problems (e.g., hyperphagic obesity) and food preferences have to be further investigated in this ongoing study.

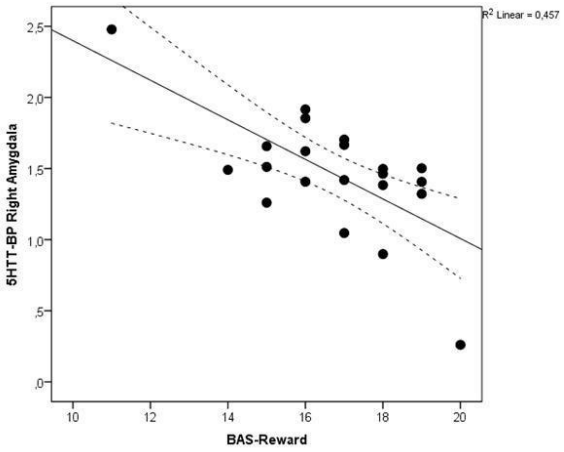

[BAS-reward]

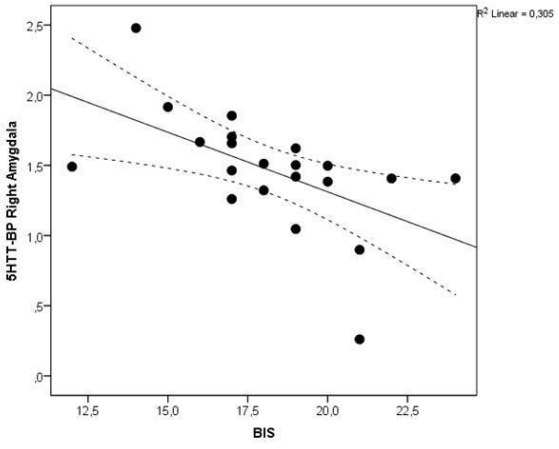

[BIS]

References:

Ichise M, Liow JS, Lu JQ, Takano A, Model K, Toyama H, Suhara T, Suzuki K, Innis RB, Carson RE: Linearized reference tissue parametric imaging methods: application to [^{11}C]DASB positron emission tomography studies of the serotonin transporter in human brain. J Cereb Blood Flow Metab 2003; 23: 1096-1112

DECREASED ALPHA2 ADRENOCEPTOR VOLUME OF DISTRIBUTION AND INCREASED DOPAMINE D1 RECEPTOR BINDING POTENTIAL IN THE FLINDERS SENSITIVE LINE DEPRESSION MODEL

P. Iversen[1], G. Wegener[2], S. Jakobsen[1], J.-A. Phan[1], M. Simonsen[1], D.J. Doudet[1,3], **A.M. Landau**[1,4]

[1]Department of Nuclear Medicine and PET Centre, Aarhus University Hospital, Aarhus, [2]Centre for Psychiatric Research, Aarhus Univeristy Hospital, Risskov, Denmark, [3]Department of Medicine/Neurology, University of British Columbia, Vancouver, BC, Canada, [4]Center of Functionally Integrative Neuroscience (CFIN)/Mindlab, Aarhus University, Aarhus, Denmark

Objective: Depression is a debilitating heterogeneous disorder and the underlying mechanisms remain elusive. Alterations in monoaminergic neurotransmission, including dopaminergic and noradrenergic, have been implicated in the etiology of depression. Although depression is difficult to model in animals, the availability of animal models with face, predictive and construct validity permits in-depth investigations resulting in a greater understanding of the disease. Here we investigated the role of alpha2 adrenoceptors and dopamine D1 receptors in a genetic rat model of depression (1).

Methods: We determined baseline differences in the volume of distribution of alpha2 adrenoceptors in depressed (Flinders Sensitive Line (FSL)) and control (Flinders Resistant Line (FRL) and Sprague-Dawley (SD)) rats using micro-positron emission tomography imaging and the carbon-11 labeled radioligand yohimbine. We studied differences in the binding potential of dopamine D1 receptors in the three groups of rats by receptor autoradiography using tritium labeled SCH23390.

Results: We demonstrate a 63-66% reduction in volume of distribution of yohimbine to alpha2 adrenoceptors in the cortex, striatum

and cerebellum of FSL rats compared to the two control groups. Furthermore, we found increased binding of SCH23390 to dopamine D1 receptors in the ventral striatum and nucleus accumbens (18% and 25%, respectively) in FSL rats compared to controls.

Conclusions: The results indicate that the behavioural deficits expressed in the FSL depression model may correlate with decreased binding of yohimbine to alpha2 adrenoceptors and increased binding of SCH23390 to dopamine D1 receptors in specific brain regions. Data are supported by a previous microdialysis study in which increased levels of dopamine and noradrenaline were found in FSL rats compared to controls (2), together demonstrating specific monoaminergic alterations in a genetic rodent model of anxiety/depression.

References:

1. Overstreet DH, Wegener G. The Flinders Sensitive Line (FSL) Rat Model of Depression: 25 Years and Still Producing. Pharmacol Rev 2013; 65 (1):1-13.

2. Zangen A, Overstreet DH, Yadid G. Increased catecholamine levels in specific brain regions of a rat model of depression: normalization by chronic antidepressant treatment. Brain Res 1999; 824:243-50.

DIFFERENTIAL REGULATION OF LOCOMOTOR ACTIVITYT TO COCAINE IN MICE LACKING ACID-SENSING ION CHANNEL 1A AND 2

Q. Jiang, X. Chu

University of Missouri-Kansas City, Kansas City, MO, USA

Acid-sensing ion channels (ASICs) are densely expressed in the brain with ASIC1a and ASIC2 channels being predominant subtypes. These channels are enriched at synaptic sites and are central for the regulation of normal synaptic transmission. Moreover, increasing evidence links ASICs to the pathogenesis of various neurological and neuropsychiatric disorders. In this study, we explore the putative role of ASIC1a and ASIC2 in the regulation of behavioral sensitivity to the psychostimulant cocaine by utilizing ASIC1a or ASIC2 knockout mice. Acute cocaine injection induced a typical dose-dependent increase in locomotor activities in wild-type (WT) mice. However, in ASIC1a and ASIC2 mutant mice, different motor responses to cocaine were shown. In ASIC1a$^{-/-}$ mice, cocaine induced a significantly less motor response at all doses (5, 10, 20, and 30 mg/kg), while in ASIC2$^{-/-}$ mice, cocaine (5-20 mg/kg) remained to stimulate locomotor activity to an extent comparable to WT mice. Only at 30 mg/kg, the cocaine-stimulated motor activity was reduced in ASIC2$^{-/-}$ mice. In a chronic cocaine administration model (20 mg/kg, once daily for 5 days), a challenge injection of cocaine (10 mg/kg, after 2-week withdrawal) caused an evident behavioral sensitization in cocaine-pretreated WT mice. This behavioral sensitization was augmented in ASIC1a$^{-/-}$ mice and was blocked in ASIC2$^{-/-}$ mice. Our results demonstrate the important role of ASIC1a and ASIC2 channels in the modulation of behavioral sensitivity to cocaine. The two synapse-enriched ASIC subtypes are believed to play distinguishable roles in the regulation of behavioral responses to acute and chronic cocaine administration.

PET IMAGING OF SUGAR ADDICTION IN MINIPIGS: EFFECTS ON THE DOPAMINE D2/3 RECEPTOR

A.M. Landau[1,2], A. Møller[1,2], M. Winterdahl[2], S. Jakobsen[2], A.K.O. Alstrup[2], A.C. Schacht[2], D. Bender[2], J. Scheel-Krüger[1], M.L. Kringelbach[1,3]

[1]Center of Functionally Integrative Neuroscience (CFIN)/Mindlab, Aarhus University, [2]Department of Nuclear Medicine and PET Center, Aarhus University Hospital, Aarhus, Denmark, [3]Department of Psychiatry, Oxford University, Oxford, UK

Objectives: 1.6 billion people worldwide are overweight of which 400 million are clinically obese, resulting in increases in type 2 diabetes, cardiovascular diseases, respiratory problems and clinical depression. Our working hypothesis is that obesity, in addition to being a metabolic disorder, also consists of critical disturbances in the balance of the reward systems in the brain (1), which may override the physiological controls of appetite. Here we investigate the effects of subchronic sugar addiction on the dopamine reward system in healthy Göttingen minipigs of average weight and the potential contribution of social factors.

Methods: Four female minipigs were anesthetized and scanned at baseline with C-

11 labeled raclopride (an antagonist to dopamine D2/3 receptors) in a Siemens PET/CT scanner. Pigs were then given access to sugar water for one hour each morning for 12 consecutive days and were PET scanned again on the 12th day. Two of the minipigs were scanned again 2 weeks later, after cessation of the sugar treatment. PET data were registered to an average minipig MRI atlas and processed using Montreal Neurological Institute software. The binding potential (BP_{ND}) of raclopride was obtained using the Logan graphical analysis and cerebellum activity as input function. Once a general effect was observed, data were further analysed based on the housing conditions of the pigs.

Results: On average in the four pigs, raclopride BP_{ND} was significantly reduced by 25% in the caudate, 13% in the total striatum and 31% in the thalamus after 12 days of sugar access. When comparing the pigs housed individually vs. in pairs, the magnitude of the change in BP_{ND} between baseline and post-sugar scans in the two pigs that were individually housed was larger than the difference observed in the two pigs housed together (caudate: 31% (individual) vs. 19% (together); striatum: 19% vs. 7%; thalamus 38% vs. 23%). Two weeks after the cessation of sugar treatment, the BP_{ND} returned toward baseline values.

Conclusions: After 12 days of sugar access, raclopride binding to dopamine D2/3 receptors decreased in striatal and thalamic brain regions in minipig. This reduced binding is consistent with human studies demonstrating decreased D2/3 BP_{ND} in the brains of obese individuals (2). These observations may indicate increased dopamine release in response to the incentive salience associated with the sugar intake since dopamine is released as part of the wanting of drugs of abuse and other pleasurable activities (reviewed in (3,4)). Alternatively, the decreased D2/3 BP_{ND} may reflect a reduction in the number of receptors. Finally, preliminary data in small groups of minipigs housed individually vs. in pairs may indicate a potential impact of social or environmental conditions on the brain-related changes observed in response to addiction.

References:

1. Kringelbach M.L. et al., Physiology and Behaviour, 2012. 106: p. 307-316.

2. Wang, G-J. et al., Lancet, 2001. 357: p. 354-357.

3. Volkow, N.D., et al. Neuropharmacology, 2009. 56(Suppl 1): p. 3-8.

4. Ahmed, S., et al., Neuroscience in the 21st Century, Springer, 2012.

REGIONAL OCCUPANCY DIFFERENCES OF THE SEROTONIN TRANSPORTER INVESTIGATED BY BRAIN PET

R. Lanzenberger[1], G.S. Kranz[1], P. Baldinger[1], M. Savli[1], D. Haeusler[2], M. Spies[1], A. Hahn[1], W. Wadsak[2], M. Mitterhauser[2], S. Kasper[1]

[1]Department of Psychiatry and Psychotherapy, [2]Department of Nuclear Medicine, Medical University of Vienna, Vienna, Austria

Objectives: Blocking the serotonin transporter (SERT) and thus increasing serotonin concentration in the synaptic cleft is considered to be the initial step of the mechanism of selective serotonin reuptake inhibitors (SSRIs) antidepressant effects. Occupancy levels of approx. 80% in the striatum were proposed as the minimum for adequate treatment response [1]. Compared to the striatum, significantly higher SERT occupancy in the midbrain and lower values in the thalamus were found, indicating that SERT occupancy might be differently distributed throughout the brain [1]. Furthermore, consistent evidence points towards a differentiated regional involvement of brain functions that underlie the recovery of depressive symptoms [2]. The present study therefore aimed at investigating regional SERT occupancies with PET and the radioligand [^{11}C]DASB.

Methods: Nineteen out-patients suffering from major depression (13 females, 42.3±7.8 years (mean±sd)) were included as described previously [3]. Subjects received oral doses of either escitalopram (10mg/day) or citalopram (20mg/day) (Lundbeck A/S, Denmark) and underwent one PET scan before treatment and one 6 hrs. following the first SSRI dose (data taken from a larger longitudinal study, for details see [3]). Quantification of the SERT binding potential (BP_{ND}) [4] was done using the MRTM2 [5]. Cerebellar gray matter was used as reference region [6]. 14 cortical and 8 subcortical regions of interest (ROI) were taken from a standardized ROI atlas [7]. To

assess regional differences of SERT occupancies, mean occupancy values (across subjects) for cortical and subcortical ROIs were tested against an overall occupancy representing the mean of cortical and subcortical regions, respectively, using one-sample T-Tests.

Results: ROI based occupancy values approx. 6 hours following the first SSRI dose ranged between 43.53% and 82.16%, with mean occupancy values of 65.66±10.60% for cortical, and 72.99±6.75% for subcortical regions. Testing the homogeneity of cortical occupancies using one-sample T-test (test value: 65.66) revealed that middle and inferior temporal cortex had significantly lowered occupancies (mean=43.53±18.09 and 47.40±20.67 respectively), whereas the posterior and subgenual cingulate cortex had significantly elevated occupancies (mean=78.49±11.65 and 82.16±7.36, respectively). Likewise, homogeneity of subcortical regions was violated by the putamen and thalamus revealing lowered occupancies (mean=66.71±5.27 and 67.92±6.46, respectively), whereas amygdala, median and dorsal raphe had elevated occupancy values (mean=81.78±6.48, 78.14±6.16 and 81.88±4.52, respectively, test value: 72.99, all $p < 0.05$ Bonferroni corrected).

Conclusions: Our data indicate increased occupancies in regions commonly associated with antidepressant response, such as the subgenual cingulate, amygdala and raphe nuclei. Non-homogeneous SERT occupancies across regions upon SSRI intake is in accordance with animal data showing that SSRI concentration differs between brain regions [8].

References:

[1] Meyer JH, et al. (2004) Am J Psychiatry 161:826-835.

[2] Hoflich A, et al. (2012) Rev Neurosci 23:227-252.

[3] Lanzenberger R, et al. (2012) Neuroimage 63:874-881.

[4] Innis RB, et al. (2007) J Cereb Blood Flow Metab 27:1533-1539.

[5] Ichise M, et al. (2003) J Cereb Blood Flow Metab 23:1096-1112.

[6] Parsey RV, et al. (2006) Journal of Nuclear Medicine 47:1796-1802.

[7] Spindelegger C, et al. (2009) Mol Psychiatry 14:1040-1050.

[8] Kugelberg FC, et al. (2001) Br J Pharmacol 132:1683-1690.

THE COME BACK OF FUNCTIONAL DYNAMIC LESION IN HYSTERIA: FUNCTIONAL NEUROIMAGING NARROWS THE GAP BETWEEN FUNCTIONAL AND ORGANIC AMNESIA

H.J. Markowitsch[1,2,3], A. Staniloiu[4]

[1]Physiological Psychology, University of Bielefeld, [2]CITEC, Bielefeld, [3]Hanse Institute, Delmenhorst, [4]University of Bielefeld, Bielefeld, Germany

Background and introduction: Stress and traumatic experiences could lead to various memory disturbances, including amnesia. Functional amnesia has traditionally been regarded as the opposite of “organic” amnesia. The interchangeable use of the terms psychogenic, dissociative and functional amnesia has implicitly acknowledged that a substantial number of functional amnesias has a psychological basis.

Methods: We analyzed data from over a dozen patients (age range 23 to 54 years) with functional (dissociative) amnesia, whom we investigated with neuropsychological methods, structural brain imaging (computer tomography, magnetic resonance imaging, diffusion tensor imaging [DTI]) and functional neuroimaging (glucose positron emission tomography preponderantly , but also single photon emission computed tomography, functional magnetic resonance imaging). We compared their data with findings from well matched healthy controls.

Results: We evidenced in a substantial sample of patients with functional (dissociative) amnesia with preponderant retrograde memory impairments a hypometabolism on glucose PET during resting state in the right temporo-frontal region, with a decrease in the infero-lateral prefrontal cortex. Standard conventional structural neuroimaging (MRI, CT) yielded no significant abnormalities. In patients with functional (dissociative) anterograde amnesia

we found functional changes (decreased glucose metabolism) in the medial temporal lobe/hippocampal formation. Additional preliminary data from DTI have suggested a decreased integrity of long distance fiber tracts important for conscious mnemonic processing.

Discussion and conclusion: The glucose hypometabolism in the right infero-lateral prefrontal cortex observed in patients with functional (dissociative) amnesia with pronounced retrograde memory impairments in episodic-autobiographical domain suggests that a malfunction of this area (that might be stress hormones mediated) contributes to the retrieval deficit in these patients. Findings from patients with overt brain damage as well as from normal individuals point to the fact that this area might be crucially involved in triggering episodic-autobiographical memory retrieval, by synchronizing emotional and factual components of the personal past linked to the self. The functional changes seen in patients with anterograde functional (dissociative) amnesia are in conformity with data emphasizing the role of hippocampal formation in the acquisition of memories for long term storage. Preliminary data from DTI suggest that the abnormalities of functional connectivity observed in patients with functional amnesia might be underlain by microstructural alterations of fiber tracts involved in mnemonic processing (amnesia as disconnection syndrome).Functional and organic amnesia might therefore be two sides of the same coin and the gap that we still perceive between them might just be the reflection of technological limitations. This gap will likely be reduced by conducting larger scale studies that use combined neuroimaging techniques and increased methodological rigor.

EFFECTS OF THE FRAGILE X MUTATION ON RATES OF CEREBRAL PROTEIN SYNTHESIS IN PATIENTS AND MICE STUDIED UNDER PROPOFOL-SEDATION

M. QIN[1], K.C. Schmidt[1], A. Zametkin[1], S. Bishu[1], L. Horowitz[2], T. Burlin[1], Z. Xia[1], T. Huang[1], Z. Quezado[3], C.B. Smith[1]

[1]Section on Neuroadaptation & Protein Metabolism, [2]Office of the Clinical Director, National Institute of Mental Health, [3]Department of Perioperative Medicine, Clinical Center, National Institutes of Health, Bethesda, MD, USA

Introduction and objectives: Fragile X syndrome (FXS) is the most common inherited form of intellectual disability and recognized monogenic cause of autism. FXS is caused by an expanded CGG repeat sequence in the 5'UTR of *FMR1* that results in gene silencing and the consequent absence of its protein product, FMRP. It is thought that dysregulated protein synthesis is a core phenotype of FXS. In a mouse model (*Fmr1* KO) of FXS, rates of cerebral protein synthesis (rCPS) are increased in selective brain regions[1]. The objective of this study was to investigate the effects of the fragile X mutation on rCPS in human subjects.

Patients and methods: We measured rCPS with the L-[1-^{11}C]leucine PET method[2] in fifteen FXS subjects who, because of their impairments, were studied under deep-sedation. Propofol was used for sedation since we previously found no differences in rCPS between awake and propofol-sedation in controls[3]. We compared results with those of twelve age-matched propofol-sedated controls. We also used the L-[1-^{14}C]leucine autoradiographic method[4] to measure rCPS in wild type (WT) and *Fmr1* KO mice awake and propofol-sedated to see whether effects of propofol on rCPS differ in the presence or absence of FMRP.

Results: Contrary to our hypothesis, FXS subjects under propofol-sedation had *reduced* rCPS in whole brain, cerebellum, and cortex compared with sedated controls (Table). Moreover, propofol decreased rCPS substantially in most regions in *Fmr1* KO mice, but not in WT mice.

Region	Healthy volunteers (12)	Fragile X syndrome (15)
Whole brain	1.67 ± 0.03	1.52 ± 0.03 ***
Cerebellum	1.95 ± 0.04	1.79 ± 0.04 *
Frontal cortex	2.07 ± 0.04	1.86 ± 0.04 ***
Parietal cortex	2.01 ± 0.04	1.82 ± 0.04 **
Values are the means +/- SEM for the number of subjects indicated in parentheses. Statistically significantly different from healthy volunteers, two-tailed t-tests; *, p ≤ 0.05; ** p ≤ 0.01; *** p ≤ 0.005.		

[rCPS (nmol/g/min) in propofol-sedated subjects]

Conclusions: Our results indicate that, in the

absence of FMRP, propofol decreases rCPS in whole brain, cerebellum and cortex. This finding coupled with our original finding that rCPS is increased in the *Fmr1* KO mouse, but decreased in propofol-sedated FXS subjects suggests that propofol may reverse the protein synthesis phenotype in FXS. Propofol is widely used as a hypnotic in clinical medicine and may act through a variety of mechanisms including enhancement of $GABA_A$ receptor activity, increases in endogenous cannabinoids, and blockade of sodium channels. Our future work will address the mechanism through which propofol effects this change in phenotype. The results may yield new therapeutic strategies for treatment of FXS.

References:

1. Qin M**,** Kang J, Burlin T *et al.* (2005) *J Neurosci* 25:5087-5095.
2. Schmidt KC, Cook MP, Qin M *et al.* (2005) *JCBF&M* 25:617-628.
3. Bishu S, Schmidt KC, Burlin T *et al.* (2009) *JCBF&M* 29:1035-1047.
4. Smith CB, Deibler GE, Eng N *et al.* (1988) *Proc Natl Acad Sci USA* 85:9341-9345.

EFFECT OF CHRONIC HALOPERIDOL DOSING ON RAT STRIATAL PHOSPHODIESTERASE 10A LEVELS AS MEASURED BY [^{11}C]MP-10

S.P. Tang[1], S. Natesan[2], S. Ashworth[1], S. Kealey[1,2], C. Salinas[1], R.N. Gunn[1,3], E.A. Rabiner[1,2], S. Kapur[2]

[1]Imanova Limited, [2]Institute of Psychiatry, King's College, [3]Imperial College, London, UK

Objectives: Chronic antipsychotic treatment in rats has been shown to elevate striatal phosphodiesterase 10A (PDE10A) expression[1]. We wanted to estimate the magnitude of any changes in PDE10A following chronic antipsychotic (haloperidol) treatment in the rat, in order to evaluate the feasibility of studying PDE10A alterations in humans using PDE10A selective PET ligands, such as [^{11}C]MP-10.

Methods: The study employed an adaptive design. Eight male Sprague Dawley rats were treated with haloperidol (1mg/kg/day) or vehicle (n=5 haloperidol; n=3 vehicle), and scanned at baseline and at day 21 following the start of treatment. Following interim analysis of these data, another 2 groups of rats treated with an increased dose of haloperidol (2mg/kg/day (n=6)) or vehicle (n=6), were scanned at 21 days following the start of treatment. Haloperidol was administered via subcutaneous implanted osmotic minipumps. Dynamic PET scans (using Siemens INVEON DPET/MM scanner) were acquired under isoflurane anaesthesia following the bolus administration of [^{11}C]MP-10 (9-33MBq, specific activities 50-141GBq/μmol). For each animal, the striatal and cerebellar regions of interest were defined and regional time activity curves (TACs) generated. A simplified reference tissue model with the cerebellum as the reference region was applied to the TACs to generate a striatal BP_{ND} value. Behavioural effects from haloperidol treatment (vacuous chewing movement (VCM) measurement) and haloperidol plasma concentration at the time of the PET scan were analysed to index antipsychotic drug exposure.

Results: High accumulation of [^{11}C]MP-10 radioactivity was seen in the striata, consistent with previous studies[2] and the known distribution of PDE10A[3]. There was no significant increase in striatal BP_{ND} following chronic dosing of haloperidol (1 and 2 mg/kg/day for 3 weeks) compared to baseline or vehicle dosing (p>0.3, one-way ANOVA, see Table). The measured plasma levels of haloperidol confirmed that the rats were correctly exposed to haloperidol. Haloperidol treatment also resulted in significant VCM measurement as compared to vehicle (p< 0.00001).

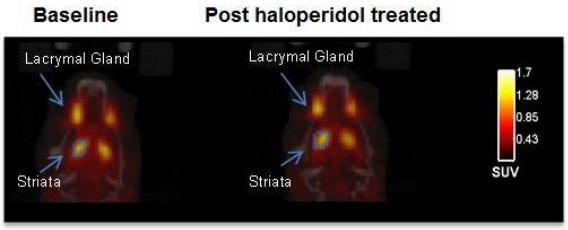

[Figure 1]

Cohort	BPND	Plasma haloperidol concentration (ng/mL)	VCM

Baseline	2.9 ± 0.6	<1	Not determined
Vehicle treated	3.4 ± 0.7	<1	2 ± 1
Haloperidol treated (1mg/kg/day)	3.1 ± 0.5	8.9 ± 2.5	7 ± 3
Haloperidol treated (2mg/kg/day)	2.8 ± 0.7	21.4 ± 5.2	8 ± 2

[Table 1]

Conclusions: Chronic treatment with the antipsychotic haloperidol, does not alter PDE10A levels in rodents as measured by [^{11}C]MP-10 PET imaging, in contrast to a previous study[1] in which PDE10A protein expression in cytosolic fractions of rat striatum were increased by 42% following chronic haloperidol treatment (1mg/kg/day for 3 weeks). As a number of PDE10A inhibitors are entering clinical trials, these findings, if replicated in human studies, have important implications for designing clinical trials of PDE10A inhibitors in patients who have been on chronic antispychotic therapy.

References:

[1] Dlaboga et al., Neuropharmacol, 2008, 745 - 754

[2] Plisson et al., Nucl Med and Biol, 2011, 38, 875 - 884

[3] Seeger et al., Brain Res, 2003, 985, 113 - 126

INTERNET GAME OVERUSE DECREASE STRIATAL DOPAMINE D_2 RECEPTORS

M. Tian[1], Q. Chen[2], Y. Zhang[1], F. Du[1], H. Hou[1], **H. Zhang**[1]

[1]Department of Nuclear Medicine, [2]Department of Psychiatry, The Second Affiliated Hospital of Zhejiang University, Hangzhou, China

Background: Clinical evidence suggests an addiction in some internet users that may resemble compulsive behavior in other addictions. The goal of this study was to compare monoamine receptors distribution between internet game overusers and healthy volunteers, both in rest and game-playing states, to determine if there are similar underlying brain abnormalities.

Methods: Dopamine D_2 receptor availability were acquired in 12 drug naive male internet overusers and 14 matched healthy volunteers using [^{11}C]NMSP PET imaging under both rest and game-playing states.

Results: Lower level of NMSP binding in overusers was found in the right inferior temporal gyrus at rest and in the putamen during games. Both right and left putamen NMSP binding correlated negatively with the severity of internet game use. No significant [^{11}C] NMSP binding changes was found in either healthy or internet game overuse group by comparing internet gaming task and rest state.

Conclusions: Internet game overplayers have decreased striatal dopamine D_2 receptors, a pattern consistent with the decreased executive control and reward sensitivity observed in other addictions.

METABOLIC IMAGING OF DEEP BRAIN STIMULATION IN ANOREXIA NERVOSA: AN ^{18}F-FDG PET/CT STUDY

H.-W. Zhang[1], C.-T. Zuo[1], B.-M. Sun[2], J. Zhao[1], Y.-H. Guan[1]

[1]PET Center, Department of Nuclear Medicine, Huashan Hospital, Fudan University, [2]Department of Neurosurgery, Ruijin Hospital, Shanghai Jiao Tong University of Medicine, Shanghai, China

Objectives: Deep Brain Stimulation (DBS) is a well-established, safe and effective neurosurgical treatment for a variety of movement and psychiatric disorders. Experimental data have suggested that Nucleus Accumbens (NAcc) might be a potential target for DBS in Anorexia Nervosa (AN) patients. But complete clinical trial results are not yet available. In this study we evaluated abnormal metabolic pattern in AN patients by PET imaging to find the possible brain network. Then on the basis of the network, we observed DBS treatment response to establish the hypothesis of DBS mechanism in AN.

Methods: ^{18}F-FDG PET was performed on 6 AN patients and 12 age/sex-matched healthy controls (HC). Statistical parametric mapping (SPM) was used to compare metabolic differences between preoperative images in 6 AN and HCs. Then 4 of the 6 AN took NAcc DBS surgery. Then ^{18}F-FDG PET was performed on the 4 AN post-DBS. We further compared 4 AN patients pre- and post-DBS to detect operative changes and BMI correlations in the patients.

To quantify regionally-specific metabolic changes, we constructed a 4mm radius volume of interest (VOI) within the image space, centered at the peak voxel of clusters that were significant in the unpaired and paired *t*-tests, respectively. We then calculated the relative glucose metabolic rates (i.e. globally normalized) in normal, Pre-Op and Post-Op PET images with the VOI option in *SPM5.*

Results: Compared with healthy volunteers, AN patients showed increases in normalized glucose metabolism in the right putamen and caudate, bilateral NAcc and hippocampus, insula (BA13)and prefrontal gyrus (BA10 and 47) and left subcallosal gyrus (BA25). DBS resulted in decreases of metabolic activity bilaterally in nucleus accumbens (NAcc) and hippocampus, insula (BA13) and prefrontal gyrus. The relative glucose metabolic rates comfirmed the above result. BMI improved individually after the DBS surgery.

Conclusions: This study has revealed increased metabolism in putamen and caudate, bilateral NAcc and hippocampus, insula and prefrontal gyrus, which further confirms the involvement of hedonic mechanisms in the pathophysiology of AN. DBS has regulated the abnormal regional metabolism within the keystones of this system. The present study verifies the potential core role of NAcc in the neurosurgical management of AN patients.

AGE-RELATED CHANGES OF DOPAMINE RECEPTOR-TRANSPORTER RELATIONSHIPS IN HEALTHY ADULTS

K. Chun[1], H. Kuwabara[1], M. McCaul[2], C. Earley[3], R. Allen[3], G. Wand[4], D. Wong[1]

[1]Department of Radiology, [2]Department of Psychiatry and Behavioral Sciences, [3]Department of Neurology, [4]Department of Medicine, Johns Hopkins University School of Medicine, Baltimore, MD, USA

Objectives: Age-related changes in dopaminergic functions have been reported. It appears plausible to postulate that dopamine receptors (DARs) and transporters (DATs) have to have certain relationships to exert optimal dopaminergic functions. We hypothesized that densities of DARs and DATs correlated each other in young subjects, and that the relationships were maintained in older subject in the cognitive and limbic striatum where functions were maintained but not in motor striatum which start show deterioration in later middle age.

Patients and methods: Twenty-four young subjects (Age range: 19 - 30 years; 13 M/11 F) and twenty-one older subjects (Age range: 45 - 77 years; 12 M/9 F) were recruited. Subjects were healthy and free of current and past history of neuropsychiatric disorders and substance addictions. Each subject had one PET scan with [^{11}C]raclopride, an antagonist DAR D_2/D_3 radioligand, and one scan with [^{11}C]methyl-phenidate ([^{11}C]]MP), a DAT radioligand in non-specific baseline conditions. Binding potential (BP_{ND}) of [^{11}C]raclopride and [^{11}C]MP were obtained by the multilinear reference tissue method with 2 parameters (MRTM2; Ichise et al., 2002) in individually defined 5 functional subdivisions of the striatum including anterior putamen(aPU), posterior putamen pPU, anterior caudate nucleus (aCN), posterior caudate nucleus (pCN), and ventral striatum (vS).

Results: The young group showed significantly higher [^{11}C]raclopride and [^{11}C]MP BP_{ND} values than the older group in all striatum subdivisions ($p< 0.001$), while male and female subjects showed similar BP_{ND} values except [^{11}C]MP BP_{ND} at pCN in the young group ($p=0.042$) and aCN in the older group. When all subjects were pooled, all subdivisions showed strong correlation of [^{11}C]raclopride BP_{ND} to [^{11}C]MP BP_{ND} ($p<$

0.0001). When analyzed separately, the young group maintained correlations ($p< 0.0025$) in subdivisions except vS ($R^2=0.020$, $p=0.504$). In contrast, the older group showed conflicting results having no correlations ($p>0.4$) in pPu and aCN, marginal correlations in aPu and pCN ($p>0.038$), and a correlation in vS ($p< 0.003$). In older subjects, it appeared that a wider inter-subject variation of [^{11}C]raclopride BP_{ND} than [^{11}C]MP BP_{ND} in pPu, and a reversed relationship in aCN contributed to the lack of correlations in these subdivisions. In contrast, wider inter-subject variations of both BP_{ND} appeared to have contributed to the correlation in vS.

Conclusion: Consistent with the hypotheses, young subjects showed correlations of [^{11}C]raclopride to [^{11}C]MP BP_{ND} in all functional subdivisions except in vS, and the correlation was not maintained in older subjects in motor striatum (pPu). However, cognitive striatum (aPu, aCN, and pCN) showed mixed results. Further, correlations were confirmed in older subjects alone in limbic striatum (vS). Thus, this preliminary study suggested the need for examining precise relationships of the [^{11}C]raclopride to [^{11}C]MP BP_{ND} relationships in functional subdivisions to results of cognitive and motor function test in individual subjects to better understand whether such optimal DAR-DAT relationships exist.

References: Ishibashi K, Ishii K, Oda K, et al. Regional analysis of age-related decline in dopamine transporters and dopamine D2-like receptors in human striatum. Synapse. 2009;63(4):282-90.

DOSE RESPONSE IN THE BINDING OF 11C-YOHIMBINE TO ALPHA 2 ADRENERGIC RECEPTORS IN RESPONSE TO INCREASING DOSES OF AMPHETAMINE

D. Doudet[1,2], S. Jakobsen[1], A.K.O. Olsen[1], A.M. Landau[1]

[1]Nuclear Medicine/PET, Aarhus University, Aarhus C, Denmark, [2]Medicine/Neurology, University of British Columbia, Vancouver, BC, Canada

Objectives: Noradrenaline plays a crucial role in multiple brain functions and in numerous neurological disorders, including addiction and psychiatric disorders. We previously demonstrated that the binding of 11C yohimbine, a selective antagonist tracer of the alpha 2 receptors in tracer doses, was displaced by a large dose of amphetamine [1]. We hypothesized that this change reflects competition with amphetamine-induced release of NA. To be of clinical utility, the change in tracer binding should reflect change in NA release. We evaluated the sensitivity of the binding of yohimbine to various doses of amphetamine and NA release and the timing of the tracer's response.

Methods: Isofluorane-anesthetized Gottingen minipigs were scanned in a Siemens clinical PET/CT. Three 90 min 11C-Yohimbine (200-300 MBq in 10 mL , injected mass: 1-2 µg per scan) scans were acquired, at baseline and following administration of one of 3 doses of R-amphetamine (1, 2, and 10 mg/kg iv), a potent noradrenaline and dopamine releaser at 20-30 min and 3-4 hrs after challenge. Vital signs were monitored throughout the course of the study. Yohimbine total distribution volume (V_T) was obtained from thalamus, striatum, cerebellum and several cortical and limbic regions as previously described [1] using a standard arterial plasma input function. Modified Lassen plots were constructed from the combined regional data and the non-specific volume of distribution V_{ND} was calculated [2]. The binding potential (BP_{ND}) was obtained from the equation $BP_{ND}= (V_T/V_{ND})-1$ [3]. The percentage change from baseline was evaluated at each dose and each time post challenge and we report the average change for each animal at each time point.

Results: Amphetamine at all 3 doses induced a significant decrease in yohimbine binding, presumably from competition by the endogenous ligand. However, there was a significant variation in the amount of decrease in BP_{ND} at the individual doses. The largest dose of amphetamine, 10mg/kg, induced a 42% decrease in BP_{ND} at 30 min which remained sustained (46%) at 4 hrs post challenge suggesting sustained high NA synaptic concentrations. On the contrary, the lower doses of amphetamine (2 and 1mg/kg) induced smaller decreases in BP_{ND} (26 and 16%, respectively), which tended to be further reduced (19 and 10%, respectively) at 4 hrs post challenge suggesting NA concentrations slowly returning towards baseline.

Conclusions: These data suggest that 11C-Yohimbine may be a potential useful tracer to evaluate acute variations in NA concentrations after acute pharmacological challenges and that the decrease in BP_{ND} may closely reflect changes in extracellular NA.

1. Landau, A, Doudet, D, Jakobsen, S. Amphetamine challenge decreases yohimbine binding to α2 adrenoceptors in Landrace pig brain. Psychopharmacology. 2012:1-9.

2. Cunningham, VJ, Rabiner, EA, Slifstein, M, Laruelle, M, Gunn, RN. Measuring drug occupancy in the absence of a reference region: the Lassen plot re-visited. J Cereb Blood Flow Metab. 2009.

3. Innis, RB, Cunningham, VJ, Delforge, J, Fujita, M, Gjedde, A, Gunn, RN, et al. Consensus nomenclature for in vivo imaging of reversibly binding radioligands. J Cereb Blood Flow Metab. 2007;27:1533-1539.

OCCUPANCY OF DOPAMINE TRANSPORTER AND EFFECT OF DOPAMINE REUPTAKE INHIBITION BY MAZINDOL IN LIVING HUMAN BRAIN

Y. Kimura, H. Ito, J. Maeda, M. Yamada, H. Fujiwara, Y. Eguchi-Suga, C. Seki, F. Kodaka, K. Takahata, Y. Ikoma, H. Takano, T. Minamimoto, M. Higuchi, T. Suhara

Molecular Imaging Center, National Institute of Radiological Sciences, Chiba, Japan

Objectives: Regional alterations in extracellular dopamine levels can be observed in the striatum during performance of neuropsychological tasks using PET[1]. To increase detection of the alteration, dopamine reuptake inhibitor could be useful for producing a greater magnitude of change in ^{11}C-raclopride binding[2]. Mazindol is a non-selective catecholamine reuptake inhibitor, which blocks dopamine reuptake and thus could be used as an enhancer of dopamine release by neuropsyhological tasks[3]. To investigate basic potency of mazindol in human, we measured occupancy of the dopamine transporter and change in ^{11}C-raclopride binding using PET after single oral administration of mazindol.

Methods: Two sets of PET scans were acquired on six healthy volunteers after oral administration of placebo and 1.5 mg of mazindol. ^{11}C-raclopride was injected at 3 hours after the administration of placebo or mazindol, and ^{18}F-FE-PE2I was injected at 5 hours. In the brain, preset volumes of interest were applied on the spatially normalized PET images. Binding potential of sub-regions of striatum was calculated by the simplified reference tissue model using cerebellum as reference region. Dopamine transporter occupancy was calculated by the % change of the binding potential of ^{18}F-FE-PE2I, and change in extracellular dopamine levels was measured by the % change of that of ^{11}C-raclopride.

Results: After oral administration of 1.5 mg of mazindol, the binding potential of ^{18}F-FE-PE2I significantly reduced by 20 - 25 % (*p < 0.01, paired t-test), indicating 20 - 25 % of dopamine transporters in the striatum was occupied by mazindol. Meanwhile, the binding potential of ^{11}C-raclopride reduced by 4 - 6%, but the reduction was not significant, indicating the change in extracellular dopamine levels by mazindol without neuropsyhological tasks was small. The correlation between the occupancy of dopamine transporter and the change in ^{11}C-raclopride binding was not significant, but there seemed a tendency that the occupancy was negatively related to the change in ^{11}C-raclopride binding among subjects in the associative striatum.*

Conclusions: *After oral administration of 1.5 mg of mazindol, dopamine transporters were occupied in a small proportion, and the change in extracellular dopamine levels was minimal. Further studies with a larger sample size would be needed to investigate the relationship between the occupancy of dopamine transporter and the change in extracellular dopamine levels by oral administration of mazindol.*

References:

1. Egerton, A. et al. Neuroscience and Biobehavioral Reviews (2009).

2. Volkow, N. D. et al. Synapse (2002).

3. Javitch, J. A. et al. Mol Pharmacol (1984).

	BP ND		
Regions	**raclopride placebo**	**raclopride mazindol**	**%change**
Associative striatum	2.44 ± 0.34	2.34 ± 0.38	-4.2
Sensorimotor striatum	3.01 ± 0.24	2.83 ± 0.20	-6.0
Limbic	2.22 ±	2.07 ±	-6.8

striatum	0.16	0.33	
	FE-PE2I placebo	**FE-PE2I mazindol**	**Occupancy (%)**
Associative striatum	2.55 ± 0.34	2.06 ± 0.24*	19.1
Sensorimotor striatum	3.14 ± 0.37	2.45 ± 0.21*	21.9
Limbic striatum	2.62 ± 0.29	1.95 ± 0.24*	25.7
*p < 0.01 v.s. placebo			

[Change of binding potential by mazindol]

SEROTONIN TRANSPORTER ASYMMETRY IN FEMALES AND MALES INVESTIGATED BY PET

G.S. Kranz[1]*, A. Hahn*[1]*, D. Haeusler*[2]*, C. Philippe*[2]*, U. Kaufmann*[3]*, W. Wadsak*[2]*, M. Spies*[1]*, M. Mitterhauser*[2]*, S. Kasper*[1]*, R. Lanzenberger*[1]

[1]*Department of Psychiatry and Psychotherapy,* [2]*Department of Nuclear Medicine,* [3]*Department of Obstetrics and Gynecology, University of Vienna, Vienna, Austria*

Objectives: *Several lines of evidence indicate regional brain asymmetries of the serotonergic system, including 5-HT$_{1A}$ receptor distribution, extracellular serotonin concentrations, serotonin turnover or uptake [1-3]. Here, our aim was to investigate a potential asymmetry of the serotonin transporter (SERT) distribution in healthy female and male subjects using PET and the radioligand [^{11}C]DASB in vivo. As brain asymmetries may differ between the sexes [4-5] we further investigated potential differences in SERT asymmetries between both sexes.*

Methods: *22 right-handed healthy subjects (9 females, 13 males), aged 19-54 years were included in this study. SERT binding potential (BP$_{ND}$) was quantified using the multilinear reference tissue model with the cerebellar gray matter (excl. vermis) as reference region in PMOD3.3. Individual summed PET images where spatially normalized to a custom symmetrical PET template in stereotactic MNI space using SPM8. Data were analyzed using repeated measures ANOVA with group as the between subjects factor, SERT asymmetry (right vs. left side) as repeated factor and group*asymmetry as the interaction term.*

Results: *SERT BP$_{ND}$ differences between the left and right hemispheres (main effect of asymmetry) showed leftward, as well as rightward asymmetries in several cortical and subcortical areas (all p< 0.05 corrected cluster). Elevated left compared to right SERT binding, i.e. leftward asymmetry, was found in planum temporale/superior temporal gyrus, middle orbitofrontal cortex, hippocampus, and posterior calcarine cortex among others. A rightward asymmetry was detected e.g., in the middle temporal pole, hippocampus, anterior thalamus, posterior insula, inferior orbitofrontal cortex, anterior calcarine cortex, and caudate. No differences in SERT binding was observed between females and males (main effect of group). There was, however, an interaction in middle cingulate cortex, with post hoc t-tests showing a rightward asymmetry in males (p< 0.05, corrected cluster) but not in females (p>0.7).*

Conclusions: *We observe strong asymmetries of the SERT in a number of cortical and subcortical regions, which may indicate asymmetric serotonergic innervations [6] but may also, at least in some regions, follow known asymmetries in gray matter volume [7]. Most of the observed asymmetries were found in both groups, indicating that they are largely unaffected by organizational effects of sex steroids and assumed differences in adult hormonal levels. Our results in the middle cingulate cortex may relate to a recently observed functional lateralization of this region [8].*

References:

[1] Andersen SL, et al. (1999) Neuroreport 10 (17):3497-3500.

[2] Fink M, et al. (2009) Neuroimage 45 (2):598-605.

[3] Valdes JJ, et al. (1981) Physiol Behav 27 (2):381-383.

[4] Amunts K, et al. (2007) J Neurosci 27 (6):1356-1364.

[5] Amunts VV, (2008) Neurosci Behav Physiol 38 (7):715-720.

[6] Vertes RP, et al. (2010) Brain Struct Funct 215 (1):1-28.

[7] Takao H, et al. (2011) Hum Brain Mapp 32 (10):1762-1773.

[8] Huster RJ, et al. (2011) Brain Struct Funct 215 (3-4):225-235.

Disclosure

G.S. Kranz reports no conflicts of interest with regards to this work.

LINEAR CORRELATION BETWEEN DOPAMINE STORAGE IN DORSAL STRIATUM AND SENSATION-SEEKING

***Y. Kumakura**, A. Moeller, D. Doudet, D. Bender, J. Linnet, A. Gjedde*

Nuclear Medicine and PET Centre, Aarhus University, Aarhus C, Denmark

Dopamine neurotransmission in ventral striatum is thought to be associated with sensation seeking, as revealed by our previous study using the post-synaptic $D_{2/3}$ receptor binding paradigm with Raclopride PET (Gjedde et al. 2010). We hypothesized that PET experiments using FDOPA would help identify involvement of striatal presynaptic dopamine neurons that modulate sensation seeking levels. 18 male normal volunteers (mean age: 27.7) were recruited and their sensation seeking levels were evaluated using 40-point Zuckerman sensation seeking scale, based on the response to questions pertaining to individual proclivity to engage in novel or risky activities. Subjects underwent dynamic three-hour FDOPA PET scanning and arterial blood sampling. Plasma samples were counted for radioactivity, and analyzed by HPLC, in order to subtract the radioactivity contribution of the BBB-penetrating plasma metabolite (Kumakura et al., 2005). We used the reversible "inlet and outlet" model (Kumakura et al., 2006), which enabled measurement of the intrinsic blood-brain clearance (K, ml g^{-1} min^{-1}), a first-order rate constant for the diffusion of [^{18}F]fluorodopamine metabolites from brain (k_{loss}, min^{-1}), and the total tracer distribution volume (V_d, ml g^{-1}), as steady-state dopamine storage capacity. Voxel-based linear regression analysis of correlation between V_d maps and the individual ZSSS scores identified a cluster of voxels with peak t-values in the dorsal part of the left caudate nucleus. The mean kinetic estimates of the three parameters V_d, K, and k_{loss} for the cluster were 4.20 ml g^{-1}, 0.0103 ml g^{-1} min^{-1}, and 0.0034 min^{-1}, respectively. The estimates of V_d were positively correlated with the ZSSS scores (p=0.005), while those of K were not significantly correlated (p=0.6). The estimates of k_{loss} were negatively correlated with the ZSSS scores (p=0.003). We conclude that the dopamine storage capacity/turnover in the left dorsal striatum is linearly associated with sensation seeking in the young male volunteers.

A POSITIVE CORRELATION BETWEEN THE POTENCY OF THE NIGROSTRIATAL DOPAMINERGIC PATHWAY AND RECEPTOR DENSITY MEASURED WITH [^{11}C]PHNO PET

***A.C. Tziortzi**[1,2], D. Erritzoe[3], R. Menke[1], E. Rabiner[2], M. Jenkinson[1], R.N. Gunn[2]*

[1]Clinical Neurosciences, FMRIB Centre, University of Oxford, Oxford, [2]Imanova Centre for Imaging Sciences, [3]School of Medicine, Imperial College London, London, UK

***Objective:** Dopamine is a neurotransmitter that is found to be involved in several neurological conditions. Some of these disorders are due to neurodegenerative processes in the dopaminergic pathways, which, in turn, result in dopamine dysfunction. The aim of this study is to examine whether the potency of the nigrostriatal pathway (NSP), defined by diffusion-weighted MRI (DWI) and image-based probabilistic tractography, is correlated with dopamine PET measurements, which reflect the receptor density (BP_{ND}). The hypothesis under investigation is that the stronger the NSP, the more receptors will be found in the postsynaptic terminal.*

***Methods:** Fourteen healthy male volunteers aged between 27 and 60 were recruited. For each subject, DWI data, a grey-matter nulled (GMN) MRI image[1] and dynamic [^{11}C]PHNO PET at baseline conditions were acquired. The substantia-nigra (SN), caudate (CD) and putamen (PU) ROIs were defined manually[2] for each subject on the GMN image. Probabilistic tractography was run separately for the two hemispheres and the probability of connection between the SN-CD and SN-PU pairs was estimated. For each pair the "connection strength" was estimated as the total number of particles (TNP) that were generated from the SN ROI and reached the respective target region. PET data were analysed with the simplified reference tissue model, using the cerebellum as the reference region. CD and PU ROIs were applied to the data to derive regional estimates of the BP_{ND}.*

Permutation tests were performed to assess the correlation between the TNP and BP_{ND} for each pair and estimate the p-values. Age is one of the subject's intrinsic characteristics that could affect both the NSP and the receptor density. To ensure that this factor is not overlooked or is not responsible for potential significant correlations between the TNP and BP_{ND}, the relationship between age and the parameters of interest was examined.

Results: *No significant correlations were found between age and the BP_{ND} in CD and PU. There was a significant positive correlation between the TNP and [^{11}C]PHNO BP_{ND} estimates in the CD (p = 0.04) and a trend towards significance in the PU (p = 0.11) (see figure). The PU-SN projections were lower compared to the CD-SN projections, which is consistent with the increase in statistical significance in the CD.*

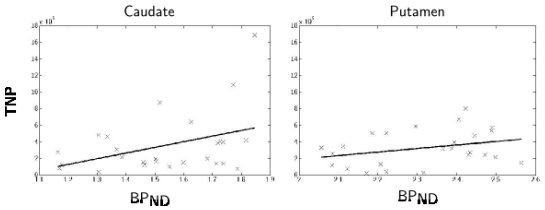

[Figure 1. TNP VS BPND]

Conclusions: *The SN-CD TNP shows a positive correlation with the CD BP_{ND}. In physiological terms, this positive correlation could potentially translate as: The higher the fiber integrity or density, the more receptors are present in the post-synaptic terminal in order to preserve the synaptic equilibrium. The SN-PU projections were weaker than the SN-CD projections. This could be due to a more complex tract geometry for the PU that may simply be more difficult to track with probabilistic tractography. Another possible explanation is that the area of SN that primarily projects to the PU might not be included in the SN ROI.*

Reference:

[1] Turner, JMRI 2012

[2] Tziortzi, Neuroimage 2011

MULTITRACER PET IMAGING REVEALS DISCREPANCY BETWEEN CHANGES IN PRE AND POST-SYNAPTIC MARKERS OF DOPAMINERGIC DEAFFERENTATION IN PARKINSONIAN NON-HUMAN PRIMATES

N. Van Camp[1], *R. Aron Badin*[1], *K. Binley*[2], *M. Guillermier*[1], *Y. Lad*[2], *D. Houitte*[1], *F. Dollé*[3], *C. Lemaire*[4], *B. Kuhnast*[3], *Y. Bramoullé*[1], *M. Kyri*[2], *S. Palfi*[5], *P. Hantraye*[1]

[1]*Life Science Department/I2BM, Molecular Imaging Research Center (MIRCen), Fontenay-aux-Roses, France,* [2]*Oxford BioMedica Ltd./Medawar Centre, Oxford, UK,* [3]*Life Science Department/I2BM, Service Hospitalier Frédéric Joliot (SHFJ), Orsay, France,* [4]*Université de Liège, Centre de Recherches du Cyclotron, Liège, Belgium,* [5]*UF Neurochirurgie Fonctionnelle Assistance Publique-Hôpitaux de Paris (APHP), Groupe Henri-Mondor Albert-Chenevier, Université Paris, Créteil, France*

Objectives: *PD is characterized by uneven striatal dopamine depletion with a preferential deafferentation of the putamen relative to the caudate nucleus and a rostro-caudal gradient of fiber loss within the putamen. The present study aimed at comparing the loco-regional changes in binding (caudate vs putamen and pre vs post-commissural putamen) of a presynaptic AADC marker (6-[^{18}F]fluoro-L-m-tyrosine, FMT) and a post-synaptic D2-receptor marker [^{18}F]Fallypride in a primate model of Parkinson's disease capable of reproducing this rostrocaudal gradient of dopaminergic fiber degeneration.*

Methods: *Five cynomolgus monkeys underwent baseline PET scans before receiving daily intramuscular injections of 0.2mg/kg MPTP (1-methyl-4-phenyl-1,2,3,6-tetrahydropyridine, Sigma-Aldrich, France) for 7 consecutive days. Cycles of MPTP intoxication were repeated until a severe level of parkinsonism was achieved; then PET imaging was performed on stably parkinsonian primates. PET scans were acquired on a dedicated animal PET scanner (FOCUS220, Siemens) under propofol anesthesia with constant monitoring of physiological parameters. For [^{18}F]FMT imaging, animals were pretreated with 2.5mg/kg Benserazide hydrochloride (Sigma-Aldrich, France) 30min before tracer injection. Using the cerebellum as a reference region, parametric BPnd ([^{18}F]Fallypride) or Ki ([18F]-FMT) were*

calculated from dynamic PET images using the graphical methods Logan and Patlak respectively. PET images and parametric maps were coregistered with T2-weighted MRI scans of the same animal, acquired on a 7T Varian scanner. The regions of interest segmented on MRI images included the cerebellum, caudate head and body and pre- and post-commissural putamen.

Results: *As expected, the Ki of [^{18}F]FMT was significantly decreased (p< 0.01) in the MPTP group compared to baseline. Caudate and putamen showed a similar decrease (70%) in the Ki value. Only a small antero-posterior gradient of loss of [^{18}F]FMT uptake was observed in the putamen with a slightly greater decrease of Ki in the post-commisural region. For the post-synaptic marker [^{18}F]Fallypride, the BPnd was significantly increased (p< 0.01) in the striatum of the MPTP group as compared to baseline corresponding to a 60% increase in the caudate and up to 100% increase in the putamen. In contrast to the discrete changes displayed by the presynaptic marker, the post-synaptic marker clearly displayed an antero-posterior gradient change in the BPnd.*

Conclusions: *The lack of an antero-posterior gradient observed by [^{18}F]FMT might be explained by the severe loss of dopaminergic neurons in the primate model and the lack of sensitivity of PET imaging to detect a gradual loss of binding in these conditions. In contrast, BPnd as measured with [^{18}F]Fallypride clearly reflects the rostro-caudal gradient of dopamine loss within the putamen. BPnd measures not only the density of dopaminergic receptors available to bind [^{18}F]Fallypride but depends also on the affinity of the dopaminergic receptors after endogenous dopamine depletion. Our results suggest that a strict relationship may not exist at the sub-regional level between the presynaptic loss in dopamine metabolism visualized with [^{18}F]FMT and the fractional occupancy of D2 receptors by endogenous dopamine visualized by [^{18}F]Fallypride PET. These findings have important implications for the understanding the changes in the PET signal observed after dopamine replenishment therapy in PD patients.*

QUANTIFICATION OF THE HUMAN BRAIN PDE4 OCCUPANCY BY GSK356278: A [^{11}C]-(R)-ROLIPRAM PET STUDY

J. van der Aart[1], *C. Salinas*[1], *R. Dimber*[1], *S. Pampols-Maso*[1], *A.A. Weekes*[1,2], *A. Kamalakaran*[1], *J. Tonkyn*[3], *F.A. Gray*[3], *R.N. Gunn*[1], *E.A. Rabiner*[1]

[1]*Imanova,* [2]*Division of Brain Sciences, Imperial College London, London,* [3]*GlaxoSmithKline, Stevenage, UK*

Objectives: *GSK356278 is a PDE4 inhibitor in development for the treatment of Huntington's disease. This study has characterized the relationship between the plasma concentration of GSK356278 and its occupancy of the PDE4 enzyme in the brain.*

Methods: *[^{11}C]-(R)-rolipram PET scans were acquired before and after a single 14mg oral dose of GSK356278, in 8 healthy male volunteers. GSK356278 plasma concentration was measured at the start of each post-dose scan. Six subjects completed scans at approximately 3 and 8 hours post-dose scans. Two subjects completed a single post-dose scan (one at 8 and one at 3 hours). PET data were motion corrected using frame to frame realignment and regional TACs were generated of the caudate, putamen, thalamus, hippocampus, frontal cortex, parietal lobe, temporal lobe, occipital pole and cerebellum by applying a standard brain atlas. A metabolite corrected arterial input function was used in conjunction with the PET emission data to estimate regional volumes of distribution (V_T) from a two-tissue compartment model [1, 2, 3].*

Results: *The average injected dose was 270±61 MBq with specific activity of 76±56 GBq/μM. The regional V_T values were consistent with the published literature [1]. The administration of GSK356278 produced a consistent reduction in [^{11}C]-(R)-rolipram binding (V_T) at 3 hours post-dose (paired t-test, p< 0.05 in all regions examined), but not at 8 hours post-dose. The quantification of PDE-4 occupancy was hampered by the low specific binding of [^{11}C]-(R)-rolipram, and the limitation of the maximal dose of GSK356278 to 14 mg, so that the non-displaceable volume of distribution (V_{ND}) for each individual could not be estimated reliably. Hence we used a population estimate of the baseline BP^*_{ND} from a previous study (BP^*_{ND}=0.5) [3], and*

estimated V_{ND} for each subject using the formula $V_{ND} = V_T^{baseline} / (1+BP^*_{ND})$, where $V_T^{baseline}$ was the mean V_T value for the regions used to derive BP^*_{ND}. This estimate of V_{ND} was subtracted from V_T to deliver estimates of BP^*_{ND} for each scan. Occupancy was then calculated as the fractional change in calculated BP^*_{ND} between baseline and post-dose scans across all regions. The ΔV_T $(1-V_T^{GSK356278}/V_T^{baseline})$ for subjects 3 and 7 was more than two standard deviations away from the mean ΔV_T of the group, hence they were excluded from the final occupancy analysis. The model Occupancy=[GSK356278] / ([GSK356278] + EC_{50}) was fitted to the data to obtain estimates of EC_{50}.

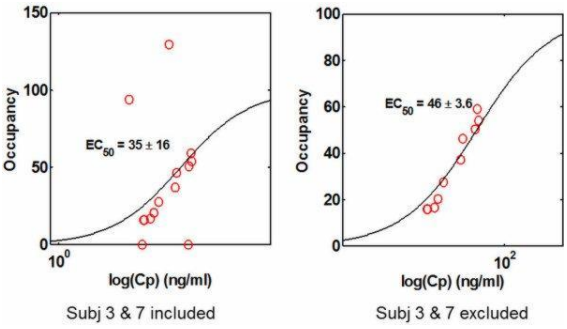

[Plasma-Occupancy Plot]

Conclusions: *The oral administration of 14 mg of GSK356278 led to a significant reduction in the [^{11}C]-(R)-rolipram brain V_T. The in vivo affinity of GSK356278 was estimated as EC_{50}=46 ± 3.6 ng/ml. The average plasma C_{max} was 43.3 ng/ml, leading to an estimated occupancy of PDE4 of 48%. These PET data will be used in conjunction with safety and tolerability data in order to infer the optimal doses to be used in future clinical development.*

References:

1. Zanotti-Fregonara, et al (2011). Neuroimage 54(3): 1903-1909.

2. DaSilva, J. N., et al. (2002). Eur J Nucl Med Mol Imaging 29(12): 1680-1683.

3. Matthews JC, et al. (2003). J Cereb Blood Flow Metab 23:678.

IMPACT OF ACUTE METHYLPHENIDATE CHALLENGE ON PRESYNAPTIC DOPAMINE METABOLISM: AN [18F]FDOPA PET STUDY

I. Schabram[1], S. Prinz[1], K. Henkel[1], C.A. Dietrich[1], M. Felzen[2], O. Winz[3], S. Mohammadkhani Shali[3], G. Gründer[1], F.M. Mottaghy[3], ***I. Vernaleken[1]***

[1]Psychiatry, Psychotherapy and Psychosomatics, [2]Department of Anaesthesiology, [3]Department of Nuclear Medicine, RWTH Aachen University, Aachen, Germany

Introduction: *Methylphenidate (MPH) is a psychostimulant drug mainly used for the treatment of attention deficit hyperactivity disorder. It presynaptically inhibits the reuptake of dopamine and noradrenaline. Studies with positron emission tomography using $D_{2/3}$-receptor ligands indirectly indicated an increase of the striatal dopamine under MPH. Neverthelss, the respective DBP results are of moderate extent may be influenced by several biasing factors. Using [^{18}F]FDOPA PET with the Kumakura 'inlet/outlet-model' proved to be a sensitive tool for detecting changes in the striatal dopamine sythesis capacity and turn-over. The present study was designed to show methylphenidate-related real time changes of striatal dopamine turn-over in healthy subjects.*

Methods: *14 healthy drug-free female subjects (23.3±1.8 years) underwent two [^{18}F]FDOPA-PET scans (124 min.; slow bolus injection; arterial blood sampling; metabolite det.). One scan was performed under unmedicated conditions, the other one after oral intake of methylphenidate (0.5mg/kgBW methylphenidate). The order of scans in respect to placebo and methylphenidate was randomized. Additionally, the subjects underwent a neuropsychological test battery at each session. The images were movement corrected, coregistered to individualized MRI and finally spatially normalized. Time activity curves (TAC) were obtained for ventral and dorsal putamen/caudate and the nucleus accumbens. These TACs were analyzed according to the 'inlet/outlet-model' of Kumakura et al. (2005) to obtain the regional net uptake of [^{18}F]FDOPA (K), the total distribution volume (V_D), and k_{loss} .*

Results: *The subjects showed a substantial*

decrease in the putamen and caudate nucleus k_{loss} when received MPH compared with baseline scan (up to -22% in the caudate nucleus; p=0.021). Correlation analyses showed an association between the baseline syntheses capacity (Vd) and the change of the washout of dopamine (k_{loss}) (MPH -baseline scan) . Furthermore, there is a trend that high dopamine synthesis capacity predicts a greater change in cognition (Trail-Making-Test-B) when received MPH.

Conclusion: *This investigation shows that [^{18}F]FDOPA-PET in combination with the inlet/outlet model of Kumakura et al. (2005) is a suitable tool to observe reasonable and extensive changes in the turn-over and thus in the fate of deaminated metabolites. This observation is in accordance with the proposed mechanism of action of methylphenidate. Methylphenidate inhibits the dopamine reuptake hence increases the dopamine availability. It seems that subjects with a high dopamine synthesis capacity at baseline have a greater change in k_{loss}. Additionally, the analogous relationship with neurocognitive methylphenidate effects (at the moment on trend-level) supports the clinical relevance. Furthermore, the results indicate further support that the 'inlet/outlet-model' is suitable to display in-vivo important parameters of the dopaminergic presynaptic metabolism.*

KINETIC ANALYSIS OF ^{18}F-FDG EXCHANGES ACROSS THE BLOOD-CSF BARRIER

B. Chaarani[1,2]*, R. Bouzerar*[1]*, J. Daouk*[1]*, M.-E. Meyer*[2]*, O. Baledent*[1]

[1]*Image Processing,* [2]*Nuclear Medicine, University Hospital of Amiens, Amiens, France*

Objectives: *Physiological properties like glucose metabolism have been studied using bi-compartmental models approach in brain tissue with ^{18}F-FDG dynamic PET imaging [1] without a particular consideration of the cerebrospinal fluid (CSF) or the blood/CSF barrier. In this work, FDG exchanges in the ventricular CSF across the blood/CSF barrier were investigated with ^{18}F-FDG dynamic PET imaging, and compared with brain tissue kinetics in healthy subjects.*

Methods: *16 healthy subjects participated in this study (mean age±SD = 66±5 years). PET acquisitions were performed in 3D mode on a Siemens Biograph 6. All patients underwent a 45-min, dynamic FDG-PET acquisition (injected 18F-FDG concentration=5MBq/kg). Each acquisition was divided in 34 time frames: 7×5 sec, 7×10 sec, 7×30 sec, 7×60 sec, 5×300 sec, and the last frame containing the remaining data. Each frame was reconstructed with 2D attenuation-weighted OSEM with 6 iterations and 16 subsets onto a 256×256×81 matrix (voxel size= 1.33 x1.33 x 2mm³).*

For each subject, 3 proposed models were studied: blood/brain, blood/parenchyma (following a common model [1]) and blood/CSF (figure 1). For each model, a mask was applied using an intensity threshold: for the blood/brain model, all intracranial voxels were selected. For the blood/parenchyma model, the mask covered the brain matter and arterial voxels (without considering the CSF). And for the blood/CSF model, CSF and arterial voxels were selected. A modified independent component analysis (ICA) [2] was used to extract kinetic parameters (k_1, k_2 and k_3) from the dynamic brain PET images, without the need of serial arterial blood sampling and where anatomic and physiological assumptions were not considered. Means of each parameter were calculated then compared between each model with a Mann-Whitney test. The glucose metabolism rate defined as: $k_i = k_1 * k_3/(k_2+k_3)$ was calculated for the 3 models.

Results: *The glucose metabolism rate of the blood/brain model (k_i=0.083) was consistent with the reference value found in literature (k_i=0.0812 [1]), which indicated that our analysis was reliable. k_i value of blood/parenchyma was found at 0.078 and k_i of blood/CSF at 0.071.*

k_1 (FDG input function) values were not significantly different in the 3 models. k_2 and k_3 were significantly higher in blood/CSF model ($p < 0.05$) than in the other two (Figure1). In blood/CSF model, k_2 represents the CSF to blood FDG transfer and k_3 may combine FDG phosphorylation in blood/CSF barrier cells and another to-be-defined reaction. In this model, k_1 was 4 times greater than k_2, which is consistent with studies done on the animal [3].

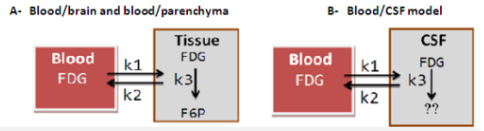

	Blood/Brain	Blood/ parenchyma	Blood/CSF
k1	0.106±0.005	0.1±0.009	0.107±0.012
k2	0.004±0.002	0.004±0.003	0.023±0.005*
k3	0.017±0.006	0.015±0.008	0.044±0.005*
ki	0.083±0.03	0.071±0.009	0.078±0.008

Figure 1: Kinetic parameters of FDG uptake for each model. Values are expressed as mean±SD. * indicates significant differences with the other models. The compartmental models of the FDG uptake for blood/brain and blood/parenchyma follow the common representation as in (A). The blood/CSF model is represented in (B). k3 represents the FDG phosphorylation into FDG-6-Phosphate (A) or the sum of FDG phosphorylation in blood/CSF barrier and another to-be-defined mechanism (B).

[Figure 1]

Conclusions: *FDG transport through the blood/CSF barrier involves different processes than across the blood/parenchyma barrier. This new approach could be applied in neurodegenerative diseases where blood/CSF barrier alterations could play a role.*

References:

[1] Chen et al. Noninvasive Quantification of the Cerebral Metabolic Rate for Glucose Using Positron Emission Tomography-1998.

[2] Naganawa et al. Extraction of a plasma time-activity curve from dynamic brain PET images based on independent component analysis-2005.

[3] Deane et al. The transport of sugars across the perfused choroid plexus of the sheep-1985.

INTRA-VENTRICULAR STRUCTURES SEGMENTATION WITH 18F-FDG DYNAMIC PET IMAGES

B. Chaarani[1,2]*, J. Daouk*[1]*, M. Rmeily-Haddad*[1,2]*, R. Bouzerar*[1]*, M.-E. Meyer*[2]*, O. Baledent*[1]

[1]*Image Processing,* [2]*Nuclear Medicine, University Hospital of Amiens, Amiens, France*

Objectives: *A previous study of the choroid plexus (CP) with* ^{18}*F-fluorodeoxyglucose (FDG) PET images showed that CP had a distinctive behavior in the brain regarding the transport and metabolism of FDG, and as a result, the CP tissue time-activity curve (TTAC) had a different trend than other cerebral structures as white matter (WM) and ventricular cerebrospinal fluid (CSF) [1]. An algorithm was developed to segment CP zones in the cerebral ventricles, based on its particular TTAC trend. It was validated on a numerical phantom and applied in clinical practice.*

Methods: *The proposed algorithm evaluated the curvature of each voxel´s TTAC in the brain by calculating the area under the curve using the trapeze numerical integration method, then subtracting the triangle area defined by the origin and the last time point of the TTAC from the total TTAC area. To assess the validity of the algorithm, a numerical phantom was created with mathematical functions representing different kinds of possible curvatures with easily access to their integration (area under the curve). Afterwards, 34 pseudo-temporal frames were generated to simulate a signal evolution. Normalized mean square error (NMSE) was calculated for the obtained results and theoretical ones calculated analytically.*

For the clinical study, sixteen elderly subjects (Age±SD=66±5 years) with normal neuropsychological behavior and without any brain disorder form, underwent a 45-min dynamic FDG-PET 3D acquisition on a Siemens Biograph 6.13 sinograms were generated starting from roughly 400s to avoid the vascular flow interference, with the following framing: 7×60 sec, 5×300 sec, and the last frame containing the remaining data. Each frame was reconstructed with 2D attenuation-weighted OSEM with 6 iterations and 16 subsets onto a 256×256×81 matrix. Regions of interest (ROI) were manually defined for CSF and WM. CP ROIs, not visible on the PET acquisition, were selected according to the algorithm results (Figure1). Normalized standardized uptake value means (normSUV) for the 3 structures were calculated at each time point then compared between each other using a multiple analysis of variance.

Results: *Acceptable NMSE (0.19) were observed for the algorithm's results.*

The WM had maintained a significantly higher normSUV (mean±SD: 2.28±0.3) than the CP (1.30±0.55) and CSF (1.42±0.3) ($p< 0.05$). CP_{TTAC} was significantly higher than CSF_{TTAC} ($p< 0.05$). CP_{TTAC} were mainly found within the cerebral ventricles, which is consistent with the

hypothesis claiming that this TTAC can be associated to the CP, most likely the only structures within the ventricles capable of maintaining high FDG concentrations due to its particular epithelial cells [2].

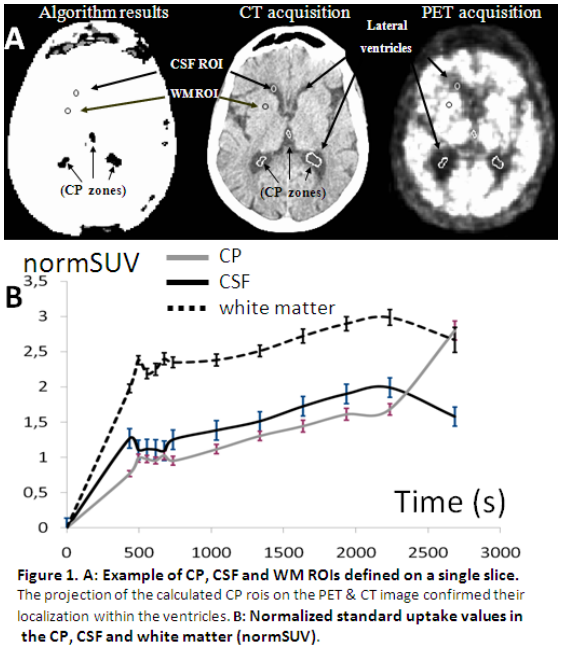

Figure 1. A: Example of CP, CSF and WM ROIs defined on a single slice. The projection of the calculated CP rois on the PET & CT image confirmed their localization within the ventricles. **B: Normalized standard uptake values in the CP, CSF and white matter (normSUV).**

[Figure 1. NormSuv values in CP, CSF and WM.]

Conclusion: *A reliable method was suggested to extract the CP_{TTAC} from dynamic PET images through its distinctive behavior. The characterization and quantification of CP activity using this approach in clinical research on a larger population could help to better understand its role in various brain disorders.*

References:

[1] Rmeily-Haddad et al. The kinetics of 18f-fluorodeoxyglucose uptake in the choroid plexus-2011.

[2] Emerich et al. The Choroid Plexus in the Rise, Fall and Repair of the Brain-2005

MINIMUM CEREBRAL BLOOD TRANSIT TIME MEASUREMENT WITH DYNAMIC ^{18}F-FDG PET: A NOVEL APPROACH FOR ALZEIHMER DISEASE

*J. Daouk[1], **B. Chaarani**[1,2], J. Benathan-Tordjman[3], J. Mallet[3], J. Zmudka[1,4], R. Bouzerar[1,2], M.-E. Meyer[3], O. Balédent[1,2]*

[1]Bio Flow Image, Université de Picardie Jules Verne, [2]Image Processing, [3]Nuclear Medicine, [4]Geriatrics, CHU Amiens, Amiens, France

Objective: *Cerebral blood flow assessment with PET has been studied with non easily available radiotracers such as $H_2{}^{15}0/C^{15}O_2$ coupling (1). However, direct studies of the shortest blood transit time from carotid arteries to major cerebral sinuses due to arterio-veinous shunts have not been performed yet. Several works suggested that Alzheimer disease could be the consequence of a vascular disorder (2). In particular, one study, performed post-mortem, found that the degree of sclerosis of the circle of Willis was a risk factor of the severity of the dementia (3). In this work, we present a method to extract the minimum blood transit time in brain by using ^{18}F-FDG and apply it in Alzheimer patients and cognitively healthy subjects.*

Material and methods: *All acquisitions were performed in 3D-mode on a Biograph 6 (Siemens Medical Solution, Erlangen, Germany). 10 patients presenting an Alzheimer clinical pattern (mean age: 77 y) without vascular component and 6 neurologically healthy subjects (mean age: 68 y) underwent dynamic ^{18}F-FDG PET acquisitions (5MBq/kg).*

The first 10 seconds of the List-Mode data were binned into 23 800ms frames; each of which overlapping half of the previous one to obtain an effective temporal resolution of 400 ms. Each frame was reconstructed with AW-OSEM algorithm (1 iteration, 8 ordered subset, voxel size 1.016x1.016x2 mm³).

For each voxel, we computed the spatio-temporal auto-covariance and we extracted the temporal corresponding profile. Then, we projected the highest auto-covariance of the voxel in a spatial map and the corresponding time in a temporal map. On the spatial map, regions of interest were manually defined on (i) carotid arteries, (ii) straight sinus and (iii) sagital sinus and carried over onto temporal

map to extract the time of arrival of the bolus peek in each region.

Results: *In healthy subjects, the mean transit time from carotids to straight sinus was 1,79 (+/- 0.67) s and 2.26 (+/- 0.61) s from carotids to sagital sinus. For Alzheimer patients, we obtained a mean time of 2.65 (+/- 0.6) s and 3.18 (+/-0.7) s for transit from carotids to straight sinus and sagital sinus respectively. A Mann-Whitney test showed a significant difference of transit time from carotid arteries to straight sinus (p=< 0.017) and from carotids to sagital sinus (p=0.022).*

Conclusion: *Our results are consistent with previous studies (3) and suggest that Alzheimer patients present an increase of the blood transit time from carotid arteries to the straight and sagital sinuses. This may highlight an alteration of the cerebral vascularization.*

References:

1. Nagata K, Maruya H, Yuya H, Terashi H, Mito Y, Kato H, et al. Can PET Data Differentiate Alzheimer's Disease from Vascular Dementia? Annals of the New York Academy of Sciences. 2000;903(1):252-61.

2. Grammas P. A damaged microcirculation contributes to neuronal cell death in Alzheimer's disease ☆. Neurobiology of Aging. mars 2000;21(2):199-205.

3. Roher AE, Esh C, Kokjohn TA, Kalback W, Luehrs DC, Seward JD, et al. Circle of willis atherosclerosis is a risk factor for sporadic Alzheimer's disease. Arterioscler. Thromb. Vasc. Biol. 1 nov 2003;23(11):2055-2062.

CORRECTION OF PARTIAL-VOLUME EFF ECT IN [^{18}F]FDG BRAIN STUDIES USING COREGISTERED MR VOLUMES: VOXEL BASED ANALYSIS OF SUBCORTICAL WHITE MATTER UPTAKE

*C. Coello[1], F. Willoch[1,2], P. Selnes[3,4], **T. Hjørnevik**[1,5], T. Fladby[3,4], A. Skretting[5]*

[1]PET/CT Unit, Dept. of Anatomy, University of Oslo, [2]Aleris, Oslo, [3]Dept. of Neurology, Faculty Division, Akershus University Hospital, University of Oslo, Lørenskog, [4]Dept. of Neurology, Akershus University Hospital, [5]The Interventional Centre, Oslo University Hospital, Oslo, Norway

Introduction: *Link between white matter (WM) dysfunctions and Alzheimer's disease (AD) are known for more than twenty years (Engelund, PMID:3208064). Recent findings suggest that subcortical WM (sbWM) degeneration and GM atrophy could be independent (Selnes, doi:10.1016/j.jalz.2011.07.001) in early stages of AD (SCI/MCI patients). To study metabolism in scWM, one must correct the spill-out activity from high-uptake anatomical structures (e.g. gray matter) into low-uptake anatomical structures (e.g. white matter) in order to quantify only physiological uptake in the sbWM regions*

Methods: *A voxel-based algorithm to correct for partial volume effect (PVE) in [^{18}F]FDG brain volumes is presented. The objective is to correct the spill-out activity from high-uptake anatomical structures (e.g. gray matter) into low-uptake anatomical structures (e.g. white matter) in order to quantify physiological uptake in sbWM regions. For a given voxel, the algorithm models the PVE as a linear mixture of sources adjacent to the voxel. To estimate the contribution of each source, a regularized Regression Analysis is achieved on a Local domain defined around the voxel (thus the name of the method LoReAn). The sources are defined using MRI based segmentation of anatomical regions. No prior knowledge of the average uptake value within a given source is required. Accurate measurements of the effective point spread function (PSF) of the PET imaging process is achieved following a method developed by our group (Skretting, doi:10.1093/rpd/ncq019).*

Materials: *Synthetic and clinical FDG volumes have been used to validate the algorithm against the state of the art region-based geometric transfer matrix (GTM) method. Errors in MRI co-registration and PSF measurement have been introduced in the noisy synthetic PET volumes to measure robustness of proposed method. The robustness criteria calculated are the bias, the standard deviation and the coefficient of variation (Cov). Finally, eighty-nine clinical FDG volumes have been corrected using the proposed algorithm.*

Results: *Both bias (uncorrected: 27%, LoReAn: 1.08%, GTM: 2.45%) and variation across subjects (unc: 11%, LoReAn: 0.6%, GTM: 4%) were improved in the white matter region in the perfect setting with three regions. When the number of sources increased to seven regions including the sbWM, the*

algorithm showed a good precision (unc: 30%, LoReAn: 1.88%) in the estimation of the true uptake in the sbWM. No increase of noise in the estimated true uptake has been measured when increasing the number of sources mainly due to the local approach: only sources contributing to PVE within the local domain are included in the regression analysis. Errors in MR co-registration and PSF measurements don't affect the LoReAn algorithm more than GTM. When tested with clinical data, the variance of sbWM explained by cortical gray matter uptake is reduced when using the proposed algorithm (r^2; unc: 0.86, LoReAn: 0.81). In addition, the CoV is improved when measuring the variability of the voxels within the sbWM (CoV (N=89); unc: 25.8%, LoReAn: 22.1%) and is not modified when measuring inter-subject variation of the average sbWM uptake (CoV (N=89); unc: 7.3%, LoReAn: 7.4%). Further work will focus on studying white matter lesions metabolism using LoReAn algorithm.

QUANTITATIVE RELATIONSHIP BETWEEN CEREBRAL METABOLIC RATE AND NEURAL AND SYNAPTIC ACTIVITIES: APPLICATION TO SYNAPTOGENESIS

J. Karbowski[1,2]

[1]*IBIB Polish Academy of Sciences,* [2]*University of Warsaw, Warszawa, Poland*

Introduction: *Many imaging techniques of brain function rely on glucose utilization rate. This parameter gives us some qualitative estimate of brain electric activity, but does not tell us directly about underlying activities of neurons and synapses. The latter activities, however, are more fundamental for modeling and understanding of brain function. Therefore, there seems to be a need to translate glucose metabolic rate into neural and synaptic dynamics.*

Aim: *The purpose of this study is to provide a link between neural metabolism and neural spiking and synaptic signaling. In particular, a computational model of brain energy use is presented and related to neural physiological parameters that are either known or can be easily measured.*

Results: *The model was tested successfully against available published data on synaptic development, which include 4 mammals (rat, cat, monkey, human) and different regions of the cerebral cortex. A remarkable finding coming from the analysis of the empirical data is that regional metabolic rate per synapse is approximately conserved from birth to adulthood for a given species. The computational model of brain metabolism combined with the data suggests that synaptic efficacy is generally inversely correlated with average firing rate, which resembles the so called synaptic scaling. Additionally, it turns out that synapses consume a bulk of metabolic energy, roughly 50-90 % during most of the developmental process.*

Conclusions:

a) The model is reliable in translating glucose metabolic rate into quantitative neural and synaptic signaling, with analytic formulas related to physiological parameters.

b) The model can be used by others in different contexts, where metabolic data is available.

c) The model combined with the data suggest a tight regulation of brain electric and chemical activities during formation and consolidation of neural connections.

d) Energy is a strong constraint on brain development.

References:

1) Karbowski J (2012). Approximate invariance of metabolic energy per synapse during development in mammalian brains. PLoS ONE 7(3): e33425.

http://dx.doi.org/10.1371/journal.pone.0033425

2) Karbowski J (2009). Thermodynamic constraints on neural dimensions, firing rates, brain temperature, and size. J Comput Neurosci 27: 415-436. http://dx.doi.org/10.1007/s10827-009-0153-7

A NEW METHOD TO ESTIMATE RADIOMETABOLITE PASSING THE BBB USING THE KINETIC COMPARTMENT ANALYSIS

I. Odano[1,2]*, A. Varrone*[1]*, R. Nakao*[1]*, C. Halldin*[1]*, L. Farde*[1]

[1]*Department of Clinical Neuroscience Centre for Psychiatry Research, Karolinska Institutet, Stockholm, Sweden,* [2]*Department of Sensory and Integrative Medicine, Niigata University*

Graduate School of Medicine and Dental Sciences, Niigata, Japan

Introduction: *In quantification for receptor and transporter binding studies, radiometabolites passing the blood-brain barrier (BBB) affect PET measurement. A combined input function consists of unchanged parent input plus radiometabolite provides more accurate binding parameters than only unchanged input function does. However, to identify the radiometabolite that actually passes the BBB is difficult for human subjects. The aim of the present study is to propose a new method to estimate the radiometabolite that passes the BBB using the kinetic compartment analysis.*

Material and methods: *Theory: A radioligand is injected i.v. and sequentially obtained arterial blood samples are analyzed using HPLC. We assume that two radiometabolites (M1 and M2) in arterial plasma are identified by HPLC, and M2 is more lipophilic than M1, thus M2 may pass the BBB. The actual amount of ingredient of M2 for passing the BBB is unknown. The unchanged parent input, C_p^p, and radiometabolite input, C_p^{M2}, are obtained. The ratio of ingredient for M2 actually passing the BBB is defined as ω (0≤ω≤1). Thus radiometabolite input function that passes the BBB is defined as $C_p^{M2*\omega}$, and combined input function consists of C_p^p plus $C_p^{M2*\omega}$ is defined as $C_p^{p+M2*\omega}$.*

A time-activity curve of reference tissue where no specific binding sites exist is analyzed using the two-tissue compartment model (2TCM) and combined input function. As ω is changed from 0 to 1, the goodness of fitting is evaluated by the residual sum of squares (RSS), the Akaike information criterion (AIC) and the Schwarz criterion (SC). When the ω_{best} provides the best fitting, the combined input function, $C_p^{p+M2*\omega best}$, provides accurate binding parameters for the target tissues.

[^{11}C]PE2I, an established radioligand for dopamine trasporter binding, and PET studies were performed on patients with juvenile myoclonic epilepsy (JME) (n = 8). Sequentially obtained arterial blood samples were analyzed using HPLC. Binding potential, k_3/k_4 or BP_{ND} was obtained by the kinetic analysis and reference tissue models, the Reference Tissue Model (SRTM) and the Logan DVR, and compared. To obtain k_3/k_4, the 2TCM with fixed K_1/k_2 for cerebellum was applied.

Results: *The ω gave the best fitting for each JME patient was not uniform and 0.6 ± 0.3 (mean ± s.d). A comparison of binding potential obtained using each input function and the reference tissue model is shown in the Table 1.*

	Kinetic Approaches			Reference Tissue Models	
	Cpp	Cpp+M2	Cpp+M2*ω	SRTM	Logan DVR
	ω=0	ω=1	ω=0.6 ± 0.3		
	k3p/k4p	k3p+M2/k4p+M2	k3p+M2*ω/k4p+M2*ω	BPND	BPND
Putamen	16 ± 4.4	9.8 ± 2.6	11 ± 2.6	7.5 ± 1.3	8.1 ± 1.5
Caudate	14 ± 3.5	8.4 ± 2.1	9.8 ± 2.2	6.2 ± 1.0	6.7 ± 1.1
Midbrain	1.4 ± 0.2	1.1 ± 0.2	1.2 ± 0.2	0.8 ± 0.1	0.8 ± 0.1

[Table 1]

Conclusion: *The present method is useful to estimate radiometabolite that actually passes the BBB and to obtain more accurate binding parameters.*

SIMULTANEOUS FITTING OF METABOLITE DATA ACROSS SUBJECTS

R.T. Ogden[1,2]*, S. Wu*[2]*, J.J. Mann*[2]*, R.V. Parsey*[3]

[1]*Biostatistics, Columbia University,* [2]*Molecular Imaging and Neuropathology, New York State Psychiatric Institute, New York,* [3]*Psychiatry and Behavioral Sciences, Stony Brook University, Stony Brook, NY, USA*

Objectives: *Arterial samples taken during a PET scanning procedure can be used to estimate the concentration of the ligand in plasma over time—an "input function" that is necessary in kinetic modeling to estimate many measures of binding. Total radioactivity counts in the plasma must be corrected for the rate of metabolism of the injected parent compound. This can be accomplished by performing a metabolite analysis on several*

blood samples and fitting a model to estimate the metabolite curve, i.e., the proportion of unmetabolized compound over time. Commonly, very few observations are available for each scan and so accurate estimation of the metabolite curve is difficult. Furthermore, model fits may be greatly impacted if just one or two observations are outliers or unavailable.

Methods: *By modeling plasma data across many subjects at once it is possible to "borrow strength" across subjects in order to make more precise estimates of subject-specific metabolite curves. This can be accomplished by fitting nonlinear mixed effects models that include random effects at the level of individual subjects (or scans). This general approach allows us to fit more complex metabolite models and to consider subject-specific covariates (such as age) that may affect the metabolite curve. Furthermore, estimates will not be as heavily influenced by outliers as when fitting is done separately for each scan.*

Results: *We demonstrate the utility of this approach by fitting metabolite data from 92 subjects scanned using the WAY100635 compound, a serotonin 1A receptor antagonist [1]. Measurements were made at six time points: 2, 6, 12, 20, 40, and 60 minutes. Using the nlme package in R, we applied the Hill model, previously shown to provide good fit for metabolite data with this compound [2], which involves three parameters. We considered models with subject-level random effects for each of these parameters but only one of these (the multiplier) demonstrates significant subject-to-subject variability. We show that fit can be improved by allowing different variances at each time point, and also that age is a significant covariate for the subject-level random effect.*

Conclusions: *Compared to fitting metabolite data separately for each subject, fitting metabolite data from many subjects at once allows us to fit more complex models with greater precision and stability, ultimately resulting in better estimates of binding measures.*

References:

[1] Forster et al. (1995) Eur J Pharmacol 281:81- 88.

[2] Wu et al. (2007) J Nucl Med 48: 926-931.

COMPARISON BETWEEN HYPR-LR-FC AND HYPR-LR-MC ON DETECTION OF SMOKING-INDUCED DOPAMINE RELEASE IN [^{11}C]RACLOPRIDE PET STUDIES OF SMOKING AND CONTROL

S. Wang[1,2], *S.J. Kim*[1], *J.M. Sullivan*[1,2], *J.D. Gallezot*[1,3], *K.P. Cosgrove*[3,4], *E.D. Morris*[1,2,3]

[1]*Yale PET Center,* [2]*Department of Biomedical Engineering,* [3]*Department of Diagnostic Radiology,* [4]*Department of Psychiatry, Yale University, New Haven, CT, USA*

Objectives: *"Highly constrained backprojections to local regions of interest" (HYPR-LR) is a promising image processing method for maximizing signal-to-noise ratio (SNR) of dynamic PET data without sacrificing spatial resolution, particularly for voxel-based analysis (Christian et al., 2010). HYPR-LR used a single composite image formed with all the frames but was found to introduce a positive bias into some regions of the data. An implementation of HYPR-LR that uses multiple temporally summed composite images (HYPR-LR-MC) provided improved tracer kinetic analysis by eliminating the bias introduced by HYPR-LR in high-uptake border regions (Floberg et al., 2012). We decided to apply both HYPR-LR-MC and HYPR-LR-FC to [^{11}C]raclopride prior to using our voxel-by-voxel method for creating movies of smoking-induced dopamine (DA) release and to compare the results.*

Methods: *HYPR filtering was applied to experimental data from 3 healthy human subjects who each received two bolus plus constant infusion (B/I) [^{11}C]raclopride PET scans on the HRRT: a control scan and one including the subject smoking two consecutive cigarettes while inside the PET scanner. Smoking began 45 minutes after the initial tracer bolus. Data were collected for 90 min and subject head motion was recorded. Dynamic data were reconstructed iteratively with MOLAR, including all standard corrections and event-by-event motion correction. The reconstructed data were then processed separately by HYPR-LR-FC (using 0-90 min summed image as the full composite) and HYPR-LR-MC (using 2 composites:0-12 min and 12-90 min) with a 5x5x5 voxel boxcar kernel. Following HYPR processing, voxels with significant DA responses were identified by the F-test ($p < 0.05$) comparing the fit of each voxel-wise TAC with lp-ntPET model*

(Normandin et al., 2012) to its corresponding fit with the standard reference model MRTM, which implicitly considers DA to be time-invariant. The difference in the number of striatal voxels with significant DA responses between smoke and control conditions was defined as the 'contrast'.

Results: *HYPR-LR-FC and HYPR-LR-MC both appeared to smooth the individual voxel-wise TACs comparably. The mean of the contrast between smoke and control was slightly higher in data processed with HYPR-LR-MC as compared with that following processing with HYPR-LR-FC, but the difference was not statistically significant.*

Conclusions: *HYPR-LR-FC and HYPR-LR-MC provided similar contrast in our lpntPET analysis of smoke-vs-control studies for detecting short-lived, smoking-induced DA release imaged during dynamic [^{11}C]raclopride PET. We intend to investigate refinements to our implementation of HYPR-LR-MC to see if better contrast between smoke and control conditions could be achieved by using more than two composite images.*

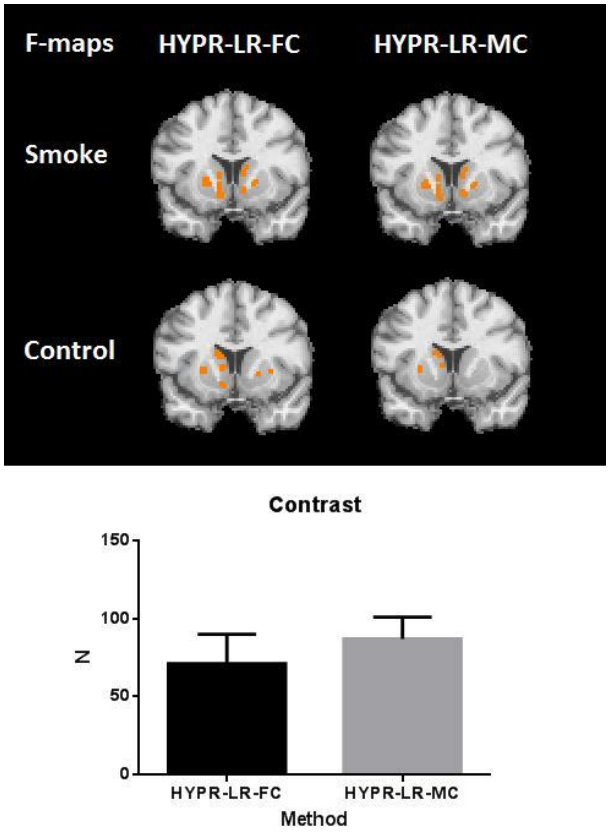

[Figure 1.]

Comparison between HYPR-LR-FC and HYPR-LR-MC on the performance in detection of smoking-induced DA release.

References:

1. Christian et al. Dynamic PET denoising with HYPR processing. J Nucl Med 2010; 51: 1147-1154.

2. Floberg et al. Improved kinetic analysis of dynamic PET data with optimized HYPR-LR. Med Phys 2012; 39: 3319-3331.

3. Normandin et al. A linear model for estimation of neurotransmitter response profiles from dynamic PET data. Neuroimage 2012; 59: 2689-2699.

INVESTIGATING THE DETECTABILITY OF SMALL D2 RECEPTOR DENSITY VARIATIONS ON B'MAX PARAMETRIC MAPPING WITH THE PARTIAL SATURATION APPROACH

C. Wimberley[1]*, A. Reilhac*[2]*, F. Boisson*[2]*, K. Fischer*[3]*, M.C. Gregoire*[2]

[1]*Brain and Mind Research Institute, Faculty of Health Sciences, University of Sydney, Camperdown,* [2]*Life Sciences, Australian Nuclear Science and Technology Organisation, Lucas Heights, NSW, Australia,* [3]*Department of Preclinical Imaging and Radiopharmacy, Laboratory for Preclinical Imaging and Imaging Technology of the Werner Siemens-Foundation, Eberhard-Karls University of Tuebingen, Tuebingen, Germany*

[^{11}C]Raclopride is a commonly used radiotracer for the in vivo quantification of Dopamine D2 receptor binding. The partial saturation approach (PSA) has been proposed to assess the B'max and appKd in a single injection protocol[1]. Previously this method was successfully adapted for a wide range of receptor occupancy levels in healthy animals[2] and for a range of synaptic DA concentrations[4]. This study extends the previous by investigating parametric mapping approaches to distinguish small D2 receptor density variations.

Method: *The PSA uses the general equilibrium equation (B/F = (Bmax-B)/KdVr - dB/dT * (1/koff*F)) which includes a residual term as an indicator of the dynamic equilibrium state(DET). For the dynamic equilibrium assumption to be met, the residual term should be within a certain small value [2,4].*

Data simulations:

1. *Two groups of clean time activity curves (TACs) were generated for a PSA experiment in a healthy mouse with 70% receptor occupancy, (based on experiments by Fischer et al.[3])*
    1. *Control group*
    2. *Group with 10% decrease of B'max in the striatum*
2. *These ideal TACs and a digital mouse phantom were used with the PET SORTEO simulation program[5] to produce the corresponding simulated PET images (9 realisations per group)*

Analysis:

1. *A voxel wise map of B'max and appKd for the striata was created for each simulated experiment using the cerebellum as the reference region. The time window for each voxel estimate was that found for the whole striatum.*
2. *Different variants of the voxel map computation are under investigation: we present here two approaches: i) determining both appKd and B'max at each voxel independently, and ii) determining the appKd for the whole region and computing the B'max estimate at each voxel.*
3. *Voxel wise paired t test was performed between the two groups using the RMINC package[6]. Detectability of the B´max variation between the two groups is computed as the ratio of the voxels found to be statistically different ($p < 0.05$) in the STR with the total number of voxels in the same region.*

Results: *The plot in Figure 1. shows the ratio of the voxels in the striatum that were found to be statistically different between the two B'max maps vs the number of scans included.*

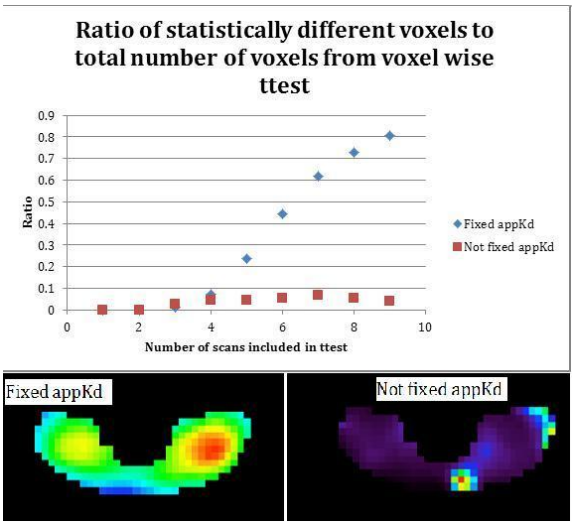

[Figure 1.]

Conclusion: *This study forms a basis to optimise the PSA analysis method for a parametric map. The proposed methodology involving simulated groups of PET scans will help investigate the impact of different approaches onto the detectability of small variations in B'max. Moving from a ROI approach to a voxel wise map brings challenges that need to be addressed, such as the partial volume effect. Further work for this study will include looking at how small changes of B'max within the striatum can be detectable.*

References:

[1] Delforge, et al; J Nulc Med,1996

[2] Wimberley et al; WMIC 2011

[3] Fischer et. Al; Submitted NRM 2012

[4] Wimberley et al; NRM 2012

[5] Boisson et al; IEEE MIC 2012

[6] https://wiki.phenogenomics.ca/display/MICePub/RMINC

INCREASED PDRP EXPRESSION AND DECREASED STRIATAL DAT BINDING IN PATIENTS WITH IDIOPATHIC RAPID-EYE-MOVEMENT SLEEP BEHAVIOR DISORDER

P. Wu[1], *Y. Ma*[2], *C. Zuo*[1], *S. Peng*[2], *H. Yu*[3], *J. Wang*[3]

[1]*PET Center, Huashan Hospital, Fudan University, Shanghai, China,* [2]*Center for Neurosciences, Feinstein Institute for Medical Research, North Shore-Long Island Jewish Health System, Manhasset, NY, USA,* [3]*Department of Neurology, Huashan Hospital, Fudan University, Shanghai, China*

Background and Purpose: *Patients with idiopathic rapid-eye-movement sleep behaviour disorder (iRBD) may develop Parkinson's disease (PD). In patients with PD, reduced dopamine transporter (DAT) binding and elevated expression of PD-related spatial covariance pattern (PDRP) can be detected with PET imaging, which can antecede the appearance of motor signs. In this study, we investigated the abnormalities in PDRP activity and striatal DAT distribution in iRBD patients by using* [18]*F-FDG PET and* [11]*C-CFT PET respectively.*

Materials and methods: *Resting-state brain* [18]*F-FDG PET imaging was performed on a Siemens Biograph 64 PET/CT in a cohort of 12 RBD patients (age: 63.3±5.3 yr, mean±sd) and 12 age-matched healthy controls (age: 63.4±5.9 yr). PDRP expression was computed in each subject based on the PDRP we previously identified in a cohort of 33 PD patients and 33 healthy controls. The same RBD patients and another 12 age-matched healthy controls (age: 61.1±9.8 yr) underwent DAT imaging with* [11]*C-CFT PET. The striatum to occipital cortex binding ratios were calculated for the putamen and caudate nucleus in each hemisphere with asymmetry indices obtained for each striatal region. Comparison between hemispheres was performed using paired t-tests. Differences in PDRP expression and* [11]*C-CFT binding between patients and controls were assessed by use of independent-sample t-tests. All analyses were performed using SPSS software and considered significant for P < 0.05.*

Results: *Computed PDRP scores in the RBD patients were abnormally elevated (P< 0.001) relative to those in the normal subjects. There was no asymmetry in striatal* [11]*C-CFT binding between the two hemispheres in the RBD patients (P≥0.065). Mean* [11]*C-CFT binding in the RBD patients reduced significantly in all striatal regions compared with the controls (caudate nucleus: P=0.010; anterior putamen: P=0.004; posterior putamen: P=0.003).*

Conclusions: *Increased PDRP expression and decreased striatal* [11]*C-CFT binding can be detected in patients with iRBD. These measures from dual-tracer studies might provide useful imaging biomarkers to identify individuals at increased risk for development of PD.*

RESTING STATE METABOLIC CONNECTIVITY AS A MARKER OF HIGHER ORDER COGNITIVE FUNCTIONS: AN 18F-FDG-PET STUDY IN HEALTHY YOUNG ADULTS

I. Yakushev[1], *M. Baydogan*[2], *J. Li*[2], *J. Dukart*[3], *F. Fischer*[4], *M. Schreckenberger*[5], *A. Fellgiebel*[4]

[1]*Nuclear Medicine, Technische Universität München, München, Germany,* [2]*Industrial Engineering, Arizona State University, Tempe, AZ, USA,* [3]*Neurology, Centre Hospitalier Universitaire Vaudois, Lausanne, Switzerland,* [4]*Psychiatry,* [5]*Nuclear Medicine, University Medical Center Mainz, Mainz, Germany*

Introduction: *Higher order cognitive functions rely not on single brain regions but on distributed cerebral networks. Given that regions of the same network have a similar level and variability in baseline glucose metabolism, positron emission tomography with [18F]-fluorodeoxyglucose (FDG-PET) may be helpful in exploring network integrity. Here, we tested the hypothesis that patterns of resting state metabolic connectivity as quantified with FDG-PET may be sensitive to variability in healthy working memory.*

Methods: *FDG-PET and neuropsychological testing was performed in 19 young healthy adults (25.5±4.1 y). According to performance in digit span backward test as index of working memory, subjects were categorized into groups with high and low test performance (median split). The network structure and strength was calculated using a recently proposed technique of sparse inverse covariance estimation (SICE). This method is particularly robust to small sample sizes.*

Results: *The most stable connectivity model as defined with stability approach to regularization selection was based on 18 subjects. Out of 44 pre-defined brain regions 22 appeared to significantly contribute to the model. Connectivity strengths between the regions of the frontal and parietal cortices as well as between the right and left hemisphere were in most instances weaker in the low as compared to the high group (p's< 0.05 FDR corrected).*

Conclusion: *In line with the hypothesis, there was a systematic variability in connectivity of/between regions known to be essential for working memory. Patterns of metabolic connectivity as quantified with FDG-PET and SICE might mirror neuronal networks underlying some higher order cognitive functions. These findings encourage testing metabolic connectivity as a diagnostic marker of cognitive disorders.*

SYNTHESIS OF [^{11}C]CIMBI-772 AND [^{11}C]CIMBI-775, TWO POTENTIAL 5-HT$_7$ PET-LIGANDS

V.L. Andersen[1,2,3]*, M.M. Herth*[1,2,3]*, H.D. Hansen*[1]*, J.L. Kristensen*[2]*, G.M. Knudsen*[1]

[1]*Neurobiology Research Unit, Copenhagen University Hospital,* [2]*Department of Drug Design and Pharmacology, School of Pharmaceutical Sciences, Copenhagen University,* [3]*PET and Cyclotron Unit, Copenhagen University Hospital, Copenhagen, Denmark*

Objectives: *Positron emission tomography (PET) is a valuable tool to investigate the role of the 5-HT$_7$ receptor in various neurological diseases. A well evaluated and successful PET-ligand for this target is yet to be developed [1]. A class of potential PET-ligands for the 5-HT$_7$ receptor is (phenylpiperazinyl-butyl)oxindoles [2]. Previous work on mono-substituted oxindoles in the 3 position have shown rapid racemisation. This is a significant problem for developing an enantiomerically pure compound. The aim of this study is to synthesize a di-substituted oxindole and so block the aforementioned racemisation. Subsequent, ^{11}C-labeling and evaluation should reveal if this blockade has a significant influence on the in vivo PET behaviour.*

Method: *Precursors for [^{11}C]CIMBI-772 and [^{11}C]CIMBI-775 were synthesized through a 2 and 3 step synthesis respectively. [^{11}C]CIMBI-772 was labelled using a previously developed procedure utilizing a Suzuki like reaction [3]. [^{11}C]CIMBI-775 was labeled via an O-methylation using sodium hydroxide in DMF followed by deprotection using TFA in CH_2Cl_2. Both tracers were purified by semi-preparative HPLC and subsequently, analysized by analytical HPLC.*

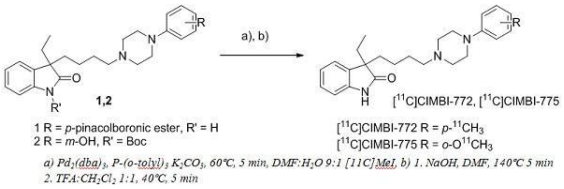

[Labelling of [11C]CIMBI-772 and [11C]CIMBI-775]

Results: *Labeling of both [^{11}C]CIMBI-772 and [^{11}C]CIMBI-775 was successful. Radiochemical yields of both tracers were approx. 30% Average specific activities were between 80 and 180 GBq/µmol.*

Conclusion: *Two compounds have been successfully labelled and purified. As expected, these di-alkylated ligands proved to be resistant against racemisation. Therefore, we decided to evaluate both cmpds regarding their biological in vitro and in vivo behaviour Please, see the poster from Hanne D. Hansen at this conference for further details..*

Acknowledgements: *The SHARE cross faculty PhD initiative, the Intra European Fellowship (MC-IEF-275329), the Faculty of Health and Medical Sciences at the University of Copenhagen and the Lundbeck Foundation are gratefully acknowledged for financial support.*

References:

[1] Herth MM, et al (2012), Bioorg Med Chem, 20, 4574-4581

[2] Herth MM, et al (2012) ACS Chem Neurosci, http://dx.doi.org/10.1021/cn3001137

[3] Andersen VL, et al (2012), Tetrahedron lett, http://dx.doi.org/10.1016/j.tetlet.2012.11.001

HUMAN ESTROGEN SYNTHASE (AROMATASE) AVAILABILITY IS HIGHEST IN THE MALE BRAIN: PET BIODISTRIBUTION STUDIES WITH [11C]VOROZOLE

A. Biegon[1,2], *D. Pareto*[3], *D. Alexoff*[1], *B. Hubbard*[1], *S. Kim*[4], *J. Logan*[1], *G.-J. Wang*[1], *J. Fowler*[1]

[1]*Biosciences, Brookhaven National Lab, Upton,* [2]*Neurology, Stony Brook University, Stony Brook, NY, USA,* [3]*Magnetic Resonance Unit (IDI), University Hospital Vall Hebron, Barcelona, Spain,* [4]*NIAA, Bethesda, MD, USA*

Introduction: *Aromatase is the final enzyme catalyzing estrogen biosynthesis. Vorozole is a potent and selective aromatase inhibitor, and [11C]vorozole was found to be a useful PET tracer for quantification of aromatase availability in the living human brain.*

Aromatase activity, protein and mRNA were also detected in biopsy and postmortem samples from other organs including bone and breast and were found to be increased in some types of cancer.

Objective: *To compare brain levels of aromatase to levels in other body organs in 33 healthy adult men and women.*

Methods: *[11C]vorozole 3-8mCi/subject, was injected iv in subjects (13 men and 20 women, age range 23 to 67) positioned in the PET scanner with the head, torso or pelvis in the center of the camera field of view. PET data were acquired over a 90 minute period. Each subject had 4 scans in total, 2/day separated by 2-6 weeks. Young women were scanned at 2 discrete phases of the menstrual cycle (midcycle and late luteal). Standard uptake values (SUV) were calculated for heart, lungs, liver, kidneys, spleen, muscle, bone and male and female reproductive organs (penis, testes, uterus, ovary) and compared by one way ANOVA followed by Fisher's PLSD posthoc test.*

Results: *The liver SUVs were higher than all other organs, however liver uptake was not blocked by pretreatment with a pharmacological dose of the aromatase inhibitor letrozole (2.5mg p.o 2 hr before tracer injection). Mean brain SUVs in men (e.g. 2.6+/-0.12 in thalamus) were higher than in women, and brain uptake was blocked by letrozole. Male brain SUVs were also higher than all other organs (ranging from 0.48+/-0.05 in lungs to 1.5+/-0.13 in kidneys). In women, mean ovarian SUVs (3.08+/-0.7) were comparable to brain levels and higher than other organs. In young women, ovarian SUVs near the time of ovulation (midcycle) were significantly higher than those measured in the late luteal phase.*

Conclusions: *The human brain has a high capacity for estrogen synthesis, matched only by the ovary in young women at the time of ovulation. Low aromatase levels in all other organs including breast and lung suggest that PET with [11C]vorozole may be used in the future for detecting increased aromatase expression in breast and lung tumors.*

IMAGING OF A7 NICOTINIC ACETYLCHOLINE RECEPTORS: A CHALLENGE FOR PET RADIOTRACER DEVELOPMENT

P. Brust[1], *S. Fischer*[1], *S. Rötering*[1], *M. Scheunemann*[1], *A. Hiller*[1], *B. Wenzel*[1], *C.K. Donat*[1], *D. Peters*[2,3], *J. Steinbach*[1], *W. Deuther-Conrad*[1]

[1]*Institute of Radiopharmacy, Helmholtz-Zentrum Dresden-Rossendorf, Leipzig, Germany,* [2]*DanPET AB, Malmö, Sweden,* [3]*Aniona ApS, Ballerup, Denmark*

Objectives: *Pre- and postsynaptic modulation of different neurotransmitter systems and further non-neuronal mediators connect α7nAChRs to brain development, learning and memory, sleep, pain perception, reward, drug dependency and various neuropsychiatric diseases. Recent approaches to use α7 nAChR as target for neuroimaging interfere with insufficiencies of the available radiotracers connected to a rather low receptor density in brain*[1]*. From a series of highly affine and α7nAChR-specific oxadiazolyl-diazabicyclononanes we have chosen fluoro-phenyl- and N-fluoroethyl-indole-substituted ligands for radiolabelling and comparative preclinical investigation of the respective radiotracers [*[18]*F]NS10743*[2] *and [*[18]*F]NS14490.*

Methods: *[*[18]*F]NS14490 was synthesized by one-step nucleophilic substitution of an unlabelled tosylate precursor (Fig.). Stability against defluorination and partition coefficient (shake-flask method, pH 7.2) and in vitro affinity towards α7nAChR and other nAChR were investigated. [*[18]*F]NS14490 receptor*

autoradiography of mice (Fig.) and pig brain was compared with [^{125}I]bungarotoxin as reference. In female CD-1 mice biodistribution (5´, 15´, 30´, 60´ p.i.) was investigated, and [^{18}F]NS14490 metabolism was studied by radio-HPLC (plasma, brain, urine; 30´, 60´ p.i.). Target specific binding of [^{18}F]NS14490 was demonstrated by pre-administration (10´ before radioligand) of highly specific α7nAChR ligands (SSR180711, NS6740; 10 mg/kg). A preliminary dynamic PET study was performed in female pig (Fig.).

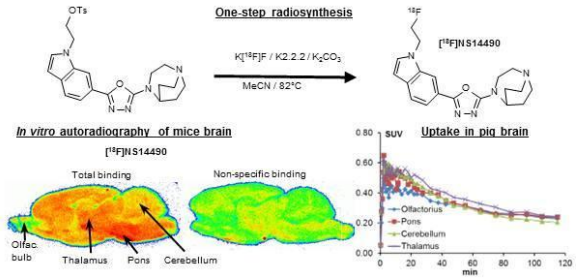

[NS14490_Synthesis_Evaluation]

Results: *[^{18}F]NS14490 was obtained within 2-2.5h with RCY of 36%±3% (n=13), RCP >98%, and A_S ~150 GBq/µmol. It was stable for >2h in TRIS-buffer and PBS. Log$D_{octanol/PBS}$ of 1.11±0.02 (n=12) and log$D_{cyclohexane/PBS}$ of -2.05±0.03 (n=3) were determined. The α7 binding affinity of NS14490 (2.5 nM) is considerably higher than assessed for NS10743 (11.6 nM[2]). [^{18}F]NS14490 binding in mice and pig brain matches the expression of α7nAChR in these species. No receptor-free reference region was identified. Almost similar striatum-to-cerebellum ratios (~1.3) were obtained in pig autoradiography and dynamic PET studies with [^{18}F]NS14490 and [^{18}F]NS10743[2]. However, compared to [^{18}F]NS10743, a much lower fraction of [^{18}F]NS14490 passed the blood-brain barrier (BBB) in mice (SUV 1.2[2] vs. 0.05 at 5´ p.i.). Notably, pre-administration of NS6740 significantly reduced the brain uptake of [^{18}F]NS14490 in mice (30% at 60´ p.i.; p< 0.005) and the maximum SUV of [^{18}F]NS14490 in pig brain (~0.6) was an order of magnitude higher than in mice. [^{18}F]NS14490 is metabolically more stable than [^{18}F]NS10743[2] with 55% vs. 40% of total activity in plasma accounting for parent compound at 60´ p.i. Chromatographic analysis of brain samples revealed that no radiometabolites of [^{18}F]NS14490 crossed the BBB.*

Conclusion: *Radiofluorination of the novel oxadiazolyl-diazabicyclononane analogue NS14490 was achieved and optimized. [^{18}F]NS14490 was obtained with high RCY, RCP and A_S. Although biodistribution data indicate lower brain uptake of [^{18}F]NS14490 in comparison to [^{18}F]NS10743 in mice, the more than ten-fold higher SUV in pig and the target specific binding shown by blocking studies in mice prompt us to continue with the preclinical evaluation of [^{18}F]NS14490.*

Acknowledgements: *Supported by DFG (DE1165/2-1).*

References:

[1]Brust P, Peters D, Deuther-Conrad W (2012) Curr Drug Targets 13, 594-601.

[2]Deuther-Conrad W et al. (2009) Eur J Nucl Med Molec Imaging, 36, 791-800.

THE (R)-(+)- AND (S)-(-)-ENANTIOMERS OF [^{18}F]FLUSPIDINE HAVE DIFFERENT POTENTIAL FOR BRAIN IMAGING OF Σ_1 RECEPTORS

P. Brust[1], *W. Deuther-Conrad*[1], *M. Patt*[2], *C.K. Donat*[1], *G. Becker*[2], *S. Stittsworth*[3], *A. Maisonial*[1], *B. Habermann*[2], *K. Holl*[4], *U. Funke*[1], *S. Fischer*[1], *D. Schepmann*[4], *A. Hiller*[1], *B. Wenzel*[1], *S. Hesse*[2], *S.Z. Lever*[3], *J. Steinbach*[1], *O. Sabri*[2], *B. Wünsch*[4]

[1]Institute of Radiopharmacy, Helmholtz-Zentrum Dresden-Rossendorf, [2]Department of Nuclear Medicine, Universität Leipzig, Leipzig, Germany, [3]Department of Chemistry, University of Missouri, Columbia, MO, USA, [4]Department of Pharmaceutical and Medicinal Chemistry, Westfälische Wilhelms-Universität, Münster, Germany

Objectives: *It is widely accepted that σ_1 receptors represent a novel biological target for the pharmacological treatment of various brain diseases, e.g. depression and neurodegeneration. From our series of σ_1-specific racemic ^{18}F-fluoroalkylated spirocyclic piperidines we have chosen the superior [^{18}F]fluspidine for detailed investigation of the (R)-(+)- and (S)-(-)-enantiomers with the aim to identify their individual potential for disease-related neuroimaging studies.*

Methods: *Racemic fluspidine and tosylate precursor for radiolabelling were*

enantioseparated by semi-preparative chiral HPLC and the latter used in automated radiosynthesis by nucleophilic substitution. Affinities of (R)-(+)- and (S)-(-)-enantiomers were estimated (K_i = 0.52 nM and 2.3 nM, respectively) and biodistribution studies were performed in CD-1 mice (dose: 240-480 kBq). Furthermore brain pharmacokinetics was investigated by dynamic PET studies in pigs (dose: 270-420 MBq).

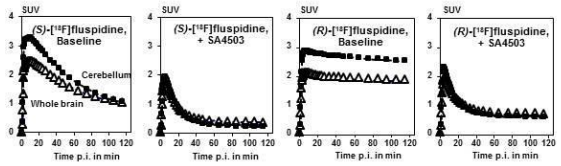

[Fluspidine kinetics in pig brain]

Additionally, the highly selective σ_1 receptor agonist SA4503 (5mg/kg) was used in blocking (bolus plus infusion) studies to assess target specificity. SUV values were calculated for 24 MR-defined brain regions. Using a metabolite-corrected plasma input function compartment modelling was applied to estimate kinetic parameters of both enantiomers.

Results: *Enantiomerically pure (R)-(+)- and (S)-(-)-tosylate precursors were obtained with high enantiomeric excess of >98 % and >96 %. (R)-(+)- and (S)-(-)-[^{18}F]fluspidine were synthesized within ~70 min with RCY of 35-45% (EOS), RCP of >99%, and A_S of >800 GBq/µmol. In mice, both radiotracers readily passed the blood-brain barrier. However, large differences in brain pharmacokinetics of the two enantiomers were found with continuous increase of brain uptake of (R)-(+)-[^{18}F]fluspidine (3.57 %ID/g at 5', 6.01% ID/g at 240' p.i.) in comparison to (S)-(-)-[^{18}F]fluspidine with higher initial brain uptake (4.35 %ID/g at 5' p.i.) and rapid clearance (1.04% ID/g at 240' p.i.). Dynamic PET studies in pigs confirmed these enantiomer-related differences (Fig.). Under baseline conditions, the initial brain uptake of (S)-(-)-[^{18}F]fluspidine was higher than that of (R)-(+)-[^{18}F]fluspidine (e.g. $SUV_{max,\ Cerebellum}$ ~3.4 vs. ~2.9; K_1: 0.72 vs. 0.56 ml/g/min). Clearance of (S)-(-)-[^{18}F]fluspidine from brain was fast ($SUV_{Cerebellum}$ ~1.1 at 95-120' p.i.) whereas the uptake of (R)-(+)-[^{18}F]fluspidine remained close to the initial level ($SUV_{Cerebellum}$ ~2.5 at 95-120' p.i.). Accordingly the binding potential (k_3/k_4) of (S)-(-)-[^{18}F]fluspidine was much lower (1.7) than that of (R)-(+)-[^{18}F]fluspidine (16.3). In comparison to baseline data, application of σ_1 specific SA4503 reduced the uptake of (S)-(-)- and (R)-(+)-[^{18}F]fluspidine in the target region cerebellum by initially 40% and 15% (SUV_{max} ~2.0 and ~2.5, respectively) and later by ~80% (SUV ~0.2 and ~0.6 at 95-120' p.i., respectively). Washout kinetics and SUV values determined under blocking conditions indicate both target specificity of the binding as well as minor nonspecific binding of the two radiotracers.*

Conclusions: *We successfully developed and validated an automated synthesis of the two enantiomers of [^{18}F]fluspidine. The pharmacokinetics of (S)-(+)-[^{18}F]fluspidine, investigated in two different animal models, suggests that this radiotracer is most suitable for upcoming studies of depression-related changes in receptor expression in human brain. The irreversible-like binding behaviour of (R)-(+)-[^{18}F]fluspidine may have advantages for tumor imaging.*

Acknowledgements: *Supported by DFG (STE 601/10-2, WU 176/7-2) and NIH (T32 EB004822).*

INHIBITION OF P-GLYCOPROTEIN WITH TARIQUIDAR INCREASE THE BRAIN UPTAKE OF [^{18}F]MEFWAY

J.Y. Choi[1], *M. Lee*[1], *Y. Seo*[1], *T.J. Jeon*[1], *B.S. Kim*[2], *T.H. Choi*[2], *Y.H. Ryu*[1]

[1]*Department of Nuclear Medicine, Gangnam Severance Hospital, Yonsei University College of Medicine,* [2]*Department of Molecular Imaging, Korea Institute of Radiological & Medical Sciences, Seoul, Republic of Korea*

Introduction: *The activity of the multidrug efflux transporter P-glycoprotein (P-gp) in the blood-brain barrier (BBB) restricts the brain uptake of many tracers for positron emission tomography (PET). Recently, [^{18}F]MEFWAY was developed as a useful radioligand for the imaging serotonin 1A (5-HT_{1A}) receptors*[1,2]*. However, whether [^{18}F]MEFWAY is the substrate of the P-gp has not been reported previously.*

Objectives: *The aim of this research is to determine if the brain uptake of [^{18}F]MEFWAY is influenced by the action of P-gp.*

Method: *Male Sprague-Dawley (SD) rats were used for in vivo imaging of microPET. Each rat was anesthetized with 2.0 % isoflurane in oxygen and placed in the gantry with its head*

centered in the field of view. A catheter was inserted into the tail vein and fluconazole was injected at an infusion rate for 1 h. In the experimental group, a tariquidar (TQD) which is a vivid inhibitor of Pgp[2] was intravenous bolus administrated and then radioactivity (13.1-19.6 MBq) was promptly injected over 1 min to the catheter and dynamic PET scans (Siemens, Inveon PET/CT) were performed for 120 min. In the control group after fluconazole pretreatment, radioactivity was injected over 1 min and we performed the PET experiment. PET data were reconstructed in user-defined time frames in length by 2-dimentional order-subset expectation maximization (OSEM) algorithm. Regions of interests are hippocampus, frontal cortex, and cerebellum. Non-displaceable binding potential (BP_{ND}), commonly used as an indication of receptor density, is the ratio of the peak values of specific binding curve to the non-specific binding curve at the time of the peak. The cerebellum was used as the reference region because it contains very few 5-HT_{1A} receptors in the rats..

Result: *After TQD administration, the hippocampal uptake of radioactivity was four fold than baseline. Moreover, the ratio of specific binding (SUV_{target}-$SUV_{cerebellum}$) to non-specific binding ($SUV_{cerebellum}$) was also two fold than the control group. The increase in the ratio of specific binding to non-specific binding implied that available 5-HT_{1A} receptors in the plasma membrane was augmented since the permeability to the BBB of [^{18}F]MEFWAY was enhanced through the inhibition of Pgp.*

Conclusion: *Our research firstly demonstrated that inhibition of Pgp causes significant incensement of [^{18}F]MEFWAY brain uptake. From these experiment, we conclude that [^{18}F]MEFWAY is the substrate for Pgp.*

References:

1. Saigal N, Pichika R, Easwaramoorthy B, Collins D, Christian BT, Shi B, et al. Synthesis and biologic evaluation of a novel serotonin 5-HT_{1A} receptor radioligand, 18F-labeled mefway, in rodents and imaging by PET in a nonhuman primate. J Nucl Med 2006;47:1697-706.

2. Choi JY, Kim CH, Jeon TJ, et al. Effective MicroPET imaging of brain 5-HT_{1A} receptors in rats with [^{18}F]MeFWAY by suppression of radioligand defluorination. Synapse 2012;66:1015-1023.

3. Fox E, Bates SE. Tariquidar (XR9576): a P-glycoprotein drug efflux pump inhibitor. Expert Rev Anticancer Ther. 2007;7:447-459.

CIS-4-^{18}F-FLUORO-D-PROLINE DETECTS SECONDARY THALAMIC AND HIPPOCAMPAL DEGENERATION INDUCED BY RAT GLIOMA

S. Geisler[1], *A. Willuweit*[1], *M. Schroeter*[2], *K. Zilles*[3,4], *K. Hamacher*[4,5], *N. Galldiks*[2], *N.J. Shah*[1], *H.H. Coenen*[4,5], *K.-J. Langen*[1]

[1]*Institute of Neuroscience and Medicine (INM-4), Forschungszentrum Juelich GmbH, Juelich,* [2]*Department of Neurology, University Hospital Cologne, Cologne,* [3]*Institute of Neuroscience and Medicine (INM-1), Forschungszentrum Juelich GmbH, Juelich,* [4]*C. & O. Vogt-Institute of Brain Research, University of Duesseldorf, Duesseldorf,* [5]*Institute of Neuroscience and Medicine (INM-5), Forschungszentrum Juelich GmbH, Juelich, Germany*

Objectives: *Following cerebral ischemia or trauma, secondary neurodegeneration may occur in brain regions remote from the site of the primary lesion. Little is known about the capacity of cerebral gliomas to induce secondary degeneration in remote brain areas. In a previous study we demonstrated that the PET tracer cis-4-[^{18}F]fluoro-D-proline (D-cis-[^{18}F]FPro) detects secondary reactions of thalamic nuclei after cortical infarction with high sensitivity (1). Here we investigated the potential of D-cis-[^{18}F]FPro uptake to detect secondary neuronal reactions in remote brain areas in the F98 rat glioma model using ex vivo autoradiography.*

Methods: *F98 gliomas were implanted into different brain areas of 10 male Fischer 344 rats (caudate nucleus, motor-, somatosensory-, visual cortex or hippocampus). After 7 to 14 days of tumor growth D-cis-[^{18}F]FPro and [^{3}H]thymidine were injected simultaneously into the tail vein. Within 2 h after injection animals were sacrificed and coronal cryosections of the tumor bearing brains were produced. The brain sections were evaluated by dual tracer autoradiography, histological stainings for myelin, Nissl bodies and cell nuclei and immunostainings for activated astrocytes and microglia. Tracer uptake was determined by regions of interest and quantified by lesion to brain ratios (L/B).*

Results: *Large tumors were present in all animals and showed significant [^{3}H]thymidine accumulation but no D-cis-[^{18}F]FPro uptake in proliferating tumor cells (L/B: 28 ± 9 versus 1.4 ± 0.3, p < 0.001). In 7 out of 10 animals with F98 gliomas strong D-cis-[^{18}F]FPro uptake was noted in nuclei of the ipsilateral thalamus that, however, showed no ^{3}H-thymidine uptake (L/B: 6.5 ± 4.0 versus 1.3 ± 0.5, p < 0.01) or obvious structural changes in the histological stainings. The accumulating thalamic nuclei correlated with the cortical brain areas affected by the tumor according to their specific thalamocortical projections. In addition, pronounced D-cis-[^{18}F]FPro accumulation was observed in hippocampal area CA1 in two animals with ipsilateral F98 gliomas involving hippocampal subarea CA3 rostral to that area. Furthermore, focal D-cis-[^{18}F]FPro uptake was noted in the necrotic center of the tumors (L/B: 9.0 ± 3.0). Immunofluorescent imaging showed that tracer uptake was accompanied by microglial activation in the thalamus, the hippocampus, and in the necrotic center of the tumors but activated microglia in the periphery of F98 gliomas exhibited no D-cis-[^{18}F]FPro uptake.*

Conclusions: *The results of this study suggest that brain tumors induce secondary neuronal reactions in distant brain areas in analogy to the findings with stroke, which may reflect the initial stage of neurodegeneration. D-cis-[^{18}F]FPro appears to be a sensitive PET tracer to detect such effects in different brain areas with high specificity and could be used in various brain injuries or neurodegenerative diseases in humans. In contrast to other amino acid tracers, D-cis-[^{18}F]FPro exhibits a high affinity and specificity for necrotic areas and does not accumulate in neoplastic lesions.*

References:

(1) Langen et al. J Nucl Med. 2007 Sep;48(9):1482-91.

^{124}I-CLR1404 PET/CT IN HIGH GRADE GLIOMAS

L.T. Hall[1,2]*, S.B. Perlman*[1]*, C. Jaskowiak*[1]*, J.S. Kuo*[2,3]*, J. Weichert*[1,4,5]

[1]*Radiology,* [2]*Carbone Cancer Center,*
[3]*Neurosurgery, University of Wisconsin,*
[4]*Novelos Therapeutics, Inc, Madison, WI,*
[5]*Novelos Therapeutics, Inc, Boston, MA, USA*

Introduction: *CLR1404 (aka NM404) is a refined second-generation diapeutic phospholipid ether analogue characterized by preferential tumor uptake and prolonged retention in 50/52 xenograft, spontaneous and transgenic preclinical tumor models, including gliomas. Isosteric iodine substitution in CLR1404 affords either a diagnostic/imaging agent (e.g. using ^{124}I for PET imaging) or a molecular radiotherapeutic agent (e.g. using ^{131}I for cancer-selective cytotoxicity), both of which are in clinical development. CLR1404 and related alkylphospholipids enter malignant cells via membrane lipid rafts which are overexpressed in cancer cells. Our lab is developing radioiodinated CLR1404 as a diagnostic and therapeutic ("diapeutic") agent for the detection and treatment of multiple solid tumors, including brain tumors.*

Objective: *The purpose of this study is to demonstrate the first successful use of ^{124}I CLR1404 PET/CT in humans with high grade gliomas.*

Patients and methods: *Four patients with high grade gliomas (1 untreated and 2 recurrent glioblastoma multiforme, and 1 recurrent gemistocytic astrocytoma) were injected with 74 or 185 MBq ^{124}I-CLR1404 and imaged with brain PET/CT at 6-, 24-, and 48-hours. Quantitative and qualitative analysis of PET images were performed and compared to MRI. Tumor to background ratios (T:B) were calculated by placing regions of interest (ROI's) around tumors and comparing to ROI's in contralateral normal brain.*

Results: *MRI scans demonstrated heterogeneous contrast enhancement in all 3 Grade IV glioblastomas and homogenous enhancement in the Grade III astrocytoma (Images 1-3), with tumor sizes varying from 0.7 x 1.2 cm to 3.1 x 5.4 cm. Three tumors exhibited surrounding edema and T2 white matter changes were observed in 3 patients with previous radiotherapy.*

As early as 6 hours after injection of ^{124}I-CLR1404, all tumors demonstrated initial discrete tumor uptake that significantly intensified at later timepoints. Both areas of concordant and discordant MRI enhancement and PET uptake were present, with areas of CLR1404 uptake present in areas without enhancement on MRI as well as areas of MRI enhancement without CLR1404 uptake. There was no significant background uptake in normal brain or in previously radiated brain

that was tumor-free. Blood pool uptake in major venous sinuses and scalp was present.

Average tumor to brain ratios (T:B) were 8.1 at 6 hours (range 1.8 - 13.7), 11.4 at 24 hours (range 3 - 21), and 15.4 at 48 hours (range 4 - 36.5) were calculated using SUVmax tumor values and SUVavg values for the contralateral normal brain.

Conclusion: *^{124}I-CLR1404 PET/CT successfully images high grade gliomas in humans with highly specific and prolonged tumor uptake verses a very low background in normal brain. These attributes make this novel agent a promising "diapeutic" candidate for brain tumors.*

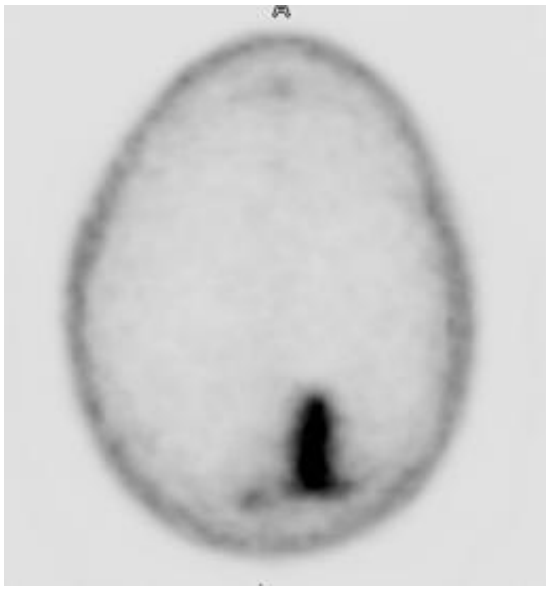

[Axial PET Grade III Astrocytoma]

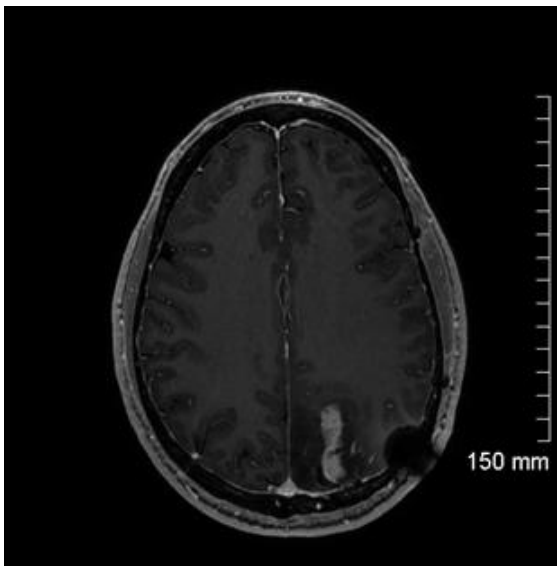

[Axial MRI Grade III Astrocytoma]

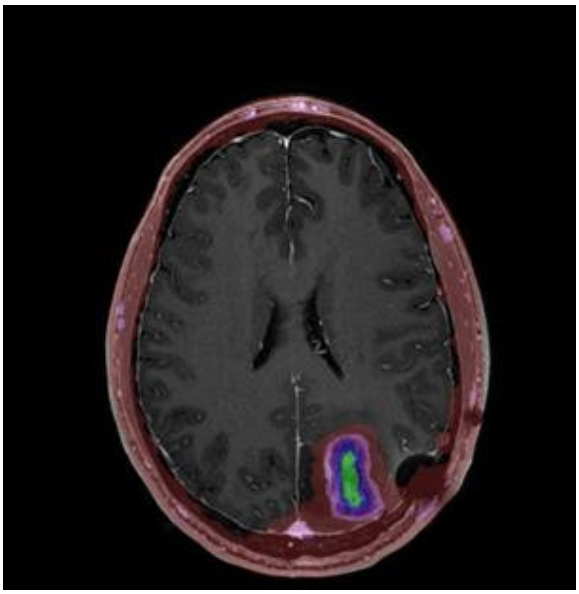

[Axial PET-MRI Grade III Astrocytoma]

Image 1: Axial PET of Grade III gemistocytic astrocytoma

Image 2: Contrast MRI

Image 3: Fused PET-MRI

IMAGING OF CEREBRAL 5-HT$_7$ RECEPTORS WITH [^{11}C]CIMBI-772 AND [^{11}C]CIMBI-775

H.D. Hansen[1], *M.M. Herth*[1,2,3], *V.L. Andersen*[1,2,3], *A. Ettrup*[1], *L. Szabolcs*[2], *A. Dyssegaard*[1], *J.L. Kristensen*[3], *G.M. Knudsen*[1]

[1]*Center for Integrated Molecular Brain Imaging, Rigshospitalet and University of Copenhagen,* [2]*PET and Cyclotron Unit, Rigshospitalet, Copenhagen University Hospital,* [3]*Department of Molecular Drug Research, Faculty of Health and Medical Sciences, University of Copenhagen, Copenhagen, Denmark*

Background: *Because of its possible involvement in brain disorders such as schizophrenia, depression, and circadian rhythm the 5-HT$_7$ receptor is an interesting drug target. We have previously presented results of [^{11}C]Cimbi-717, a promising radiotracer for PET-imaging of the 5-HT$_7$ receptors (1). Here, we evaluated the in vivo behaviour and selectivity of ethyl-derivatives of Cimbi-717: [^{11}C]Cimbi-772 and [^{11}C]Cimbi-775.*

Methods: *We synthesized the two PET radioligands [^{11}C]Cimbi-772 and [^{11}C]Cimbi-775 and studied the in vivo brain distribution of the tracers in female Danish Landrace pigs after intravenous injection of the radiotracers. PET data were acquired over 90 minutes by a HRRT PET scanner. Arterial input measurements including corrections for radiolabeled metabolites were done and regional time-activity curves were retrieved by co-registration to an MRI-based atlas of the pig brain. In every pig, the 5-HT$_7$ receptor selective antagonist SB-269970 (1 mg/kg/h) was given intravenously prior to the second scan to investigate if cerebral [^{11}C]Cimbi-772 and [^{11}C]Cimbi-775 binding was blocked.*

Results: *Time-activity curves (TACs) of [^{11}C]Cimbi-772 and [^{11}C]Cimbi-775 showed reversible tracer kinetics and high brain uptake. For modelling of the data, the one-tissue compartment model was chosen because of the simplicity of the model, and because no reference region was available for reference tissue modelling. The calculated distribution showed a more uniform uptake of the radiotracers across brain regions and also revealed no effects of the pre-treatment of SB-269970, indicating that these radiotracers are not selective for the 5-HT$_7$ receptor. For both radiotracers, the radiometabolite analysis showed two metabolites. [^{11}C]Cimbi-775 metabolized faster than [^{11}C]Cimbi-717, consistent with a previous study comparing the metabolism rate of unsubstituted (analogues of Cimbi-717) versus 3-ethyl substituted oxindole moities (analogues of Cimbi-775)(2).*

Conclusion: *Based on in vivo evaluation in pig, neither [^{11}C]Cimbi-772 nor [^{11}C]Cimbi-775 could be blocked by SB-269970. [^{11}C]Cimbi-717 remains the currently best candidate as a PET-radiotracer for the 5-HT$_7$ receptor.*

References:

(1) Hansen et al, JCBFM 2012 32, P097

(2) Volk B et al., J Med Chem. 2011 Oct 13;54(19):6657-69

A NOVEL RADIOTRACER FOR IN VITRO AND IN VIVO VISUALIZATION OF BACE1 DISTRIBUTION IN THE RODENT AND BABOON BRAIN

M. Honer[1], *L. Gobbi*[2], *A. Polara*[2], *H. Kuwabara*[3], *H. Jacobsen*[4], *T. Hartung*[5], *H. Loetscher*[4], *D. Esterhazy*[6], *M. Stoffel*[6], *R. Dannals*[3], *D.F. Wong*[3], *E. Borroni*[1]

[1]*Neuroscience Biomarkers & Clinical Imaging,* [2]*Discovery Chemistry, F. Hoffmann La Roche Ltd., Basel, Switzerland,* [3]*Johns Hopkins University, Baltimore, MD, USA,* [4]*Neuroscience Discovery,* [5]*Isotope Labeling, F. Hoffmann La Roche Ltd., Basel,* [6]*Institute of Molecular Systems Biology, ETH, Zurich, Switzerland*

Background: *The beta-site amyloid precursor protein cleaving enzyme (BACE1) is responsible for initiating generation of beta-amyloid, the major constituent of amyloid plaques in Alzheimer's disease (AD). Thus, BACE1 is a prime target for the therapeutic inhibition of beta-amyloid production in AD. In the absence of suitable radioligands for BACE1, our aim was to develop a tracer for in vitro and in vivo visualization of BACE1 brain distribution.*

Methods: *A potent BACE1 inhibitor was tritiated and its affinity and specificity for BACE1 was evaluated using rat brain membranes and brain sections from wildtype and BACE1 knockout animals. BACE1 protein distribution was visualized by in vitro autoradiography using brain sections from mouse, rat, monkey and human brain. In vivo uptake and distribution of the radioligand was studied by ex vivo autoradiographical analysis in rats and in vivo PET imaging of baboons after injection of the [^{11}C]-labeled radiotracer.*

Results: *Saturation analysis revealed high-affinity binding (KD = 4 nM) and a low binding site density in rat brain. Specificity of radioligand binding for BACE1 was confirmed by the absence of binding in brain sections of BACE1 knockout animals. A ubiquitous distribution of radioligand binding was found in rodent brain slices with higher binding in the CA1 and CA3 pyramidal cell layers and the granule cell layer of the hippocampus. Autoradiographical experiments in monkey and human hippocampus suggested relatively high BACE1 expression in the cell bodies of the dentate gyrus. The radiotracer revealed*

good penetration in the rat and baboon brain and an in vivo binding pattern comparable with that observed in vitro.

Conclusions: *This study provides the first visualization of the distribution pattern of the BACE1 protein in the rodent and baboon brain. The consistent in vivo binding pattern of this radioligand warrants further development as a PET radiotracer for occupancy studies for BACE1 drug candidates.*

PET IMAGING OF TSPO USING [^{18}F]DPA-714 IN NORMAL AND EXCITOTOXIC-STRIATAL-LESIONED PRIMATE

S. Lavisse[1], *K. Inoue*[1,2], *C. Jan*[1], *M.-A. Peyronneau*[3], *L. Rbah-Vidal*[1,4], *R. Aron Badin*[1], *S. Goutal*[3], *F. Petit*[1], *M. Guillermier*[1], *N. Van Camp*[1], *F. Dollé*[3], *P. Remy*[1,5], *P. Hantraye*[1]

[1]*MIRCen and CNRS URA 2210, Commissariat à Energie Atomique, Fontenay-aux-Roses, France,* [2]*IDAC, Tohoku University, Sendai, Japan,* [3]*SHFJ, Commissariat à Energie Atomique, Orsay,* [4]*Inserm U 990 - Imagerie Moléculaire et Thérapie Vectorisée, Université d'Auvergne, Clermont-Ferrand,* [5]*Neurology, CHU Henri Mondor, AP-HP and UPE-C, Creteil, France*

We aim to investigate TSPO-specific radioligand [^{18}F]-DPA714 binding before and after intrastriatal injection of quinolinic acid in primates, as a model of Huntington disease.

Six cynomolgus monkeys were injected with quinolinic acid into the left putamen.

PET imaging using [^{18}F]DPA-714[1] *was performed on a Focus220 microPET before and 2, 7, 9, 14, 21 and 49 days after lesion. [^{18}F]DPA-714 specificity was further evaluated in blocking and displacement studies with unlabelled PK11195.*

Arterial blood samples were drawn throughout the PET examination to measure arterial plasma radioactivity and quantify the parent radioligand by radio-HPLC and radioactivity counting.

Magnetic resonance images were obtained on a 7-Tesla scanner to delineate brain regions of interest (ROIs) after PET/MRI co-registration. ROIs were bilaterally delineated on putamen, cerebellum and on white and gray matter structures.

The mean radioactivity in each ROI was measured and expressed in time activity curves (TAC).

Kinetic analyses were performed using the modelling PMOD® software. Following 3 models (one and two-tissue compartment models, the graphical analysis Logan plot), the V_T (total distribution volume) was calculated from TACs using a metabolite-corrected arterial input function. Longitudinal trend in [^{18}F]DPA-714 uptake in the lesioned putamen was assessed as a ratio of V_T to those of baseline scans.

After each PET-scan series, animals were euthanized. Sections for immunohistochemical labelling were prepared with following primary antibodies: GFAP, CD68, TSPO, Iba1, NeuN.

In baseline PET scans, the radioactivity distribution in the cranium was widespread. TACs displayed a peak uptake in each ROI occurring within 10 min following [^{18}F]DPA-714 injection.

In displacement experiments, the curve rose to a sharp peak just after injection of unlabelled PK11195 followed by a rapid decline in each ROI. In blocking experiments, the intracranial activity was homogeneously low on the summed PET images. The activity in each ROI was indistinguishable from each other and receptor blockade was evident from the faster washout compared to baseline.

For baseline and lesion studies, the 1-TCM estimated kinetic parameters with good average identifiability but fit deviated from the measured data whereas the 2-TCM fitted the data better but showed poor identifiability. Only the Logan plot provided reliable identified V_T values with negligible overestimation in the putamen.

V_T ratio began to rise around D7, was more than two-fold the baseline value at D21 and started decreasing at D48 but not significantly. It remained around 1 in the unlesioned putamen.

IHC revealed a consistent early microglial and a delayed astrocytic activation induced by the QA injection but TSPO antibody seemed to co-localize rather with CD68-microglia. Further IHC observations and analyses are still on going.

The Quinolinate model induces a univoqual

and long lasting microglial and astrocytic inflammation, enabling evaluation of PET TSPO-radioligands. In this model, the [^{18}F]DPA-714 demonstrated a strong binding as well as specificity to this target. Its uptake could be modelised using the Logan Plot analysis. These observations will be helpful to better understand and analyse [^{18}F]DPA-714 images in current clinical trials involving several neurodegenerative diseases.

1. Damont. J. Label. Compounds Radiopharm. 2008

SYNTHESIS OF [^{18}F]FLUOROMETHYL-PBR28 AND ITS BIOLOGICAL EVALUATION AS A NOVEL RADIOTRACER FOR PET IMAING OF NEUROINFLAMMATION

***B.C. Lee**, B.S. Moon, J.H. Jung, Y.W. Lee, N.H. Lim, H.-Y. Lee, S.E. Kim*

Department of Nuclear Medicine, Seoul National University Bundang Hospital, Seongnam, Republic of Korea

***Objectives:** The translocator protein (TSPO, 18 kDa) which is formerly known as the peripheral benzodiazepine receptor (PBR), are implicated in neuroinflammation including several neurodegenerative disorders. To develop a positron emission tomography (PET) radiotracer for imaging the TSPO in brain and elucidating the relationship between TSPO and brain disease, [^{18}F]fluoromethyl group introduced PBR28 derivative was designed, synthesized and evaluated in neuroinflammation rat models by small animal PET study and also compared with [^{11}C]PBR28.*

***Method:** The novel radiotracer, [^{18}F]fluoromethyl-PBR28 was prepared from nucleophilic aliphatic substitution on triazole triflate salt-PBR28 precursor with fluorine-18 in a single-step radiolabeling procedure. The final pure [^{18}F]fluoromethyl-PBR28 was purified by reverse-phase HPLC system and the collected solution was reformulated with 5% EtOH/saline using tC18 Sep-Pak cartridge. [^{11}C]PBR28 was produced in FXC-pro module using [^{11}C]MeOTf from phenolic PBR28 precursor. Both radiotracers were evaluated in neuroinflammation rat models by small animal PET.*

***Results:** [^{18}F]Fluoromethyl-PBR28 was obtained 25.8 ± 3.2 % (n=11) of radiochemical yield (decay corrected) with over 99% of radiochemical purity. The overall synthesis, labeling, purification and formulation time was about 55 min from end of bombardment (EOB). [^{11}C]PBR28 was produced in 27.1 ± 4.9 % (n=7) of radiochemical yield (decay corrected) based on [^{11}C]CO_2. In small animal PET studies, [^{18}F]fluoromethyl-PBR28 was selectively accumulated in lateral (traumatic brain injury) about 3.7 times compared to contra around 35 min post-injection. However, [^{11}C]PBR28 showed about 2.8 times at same time and reached the highest ratio (about 3.5 times) at 100 min post-injection The in vivo specificity and selectivity of [^{18}F]fluoromethyl-PBR28 exhibited the high specific and selective binding for TSPO in the traumatic brain injury. The stability of [^{18}F]fluoromethyl-PBR28 had about over 99% until 4 h in human serum (37 ^{o}C). Also, the remarkable bone uptake of [^{18}F]fluoromethyl-PBR28 in the rat brain also did not show in small animal PET images.*

***Conclusion:** This study has succeeded in developing a promising PET radiotracer, [^{18}F]fluoromethyl-PBR28, for PET imaging of neuroinflammation with excellent TSPO specific ratio at early time compared with [^{11}C]PBR28.*

CHARACTERIZATION OF THE PDE10A PET RADIOLIGAND, [^{11}C]T-773 IN NONHUMAN PRIMATE, KO MOUSE AND AUTORADIOGAPHY

***A. Takano**[1], V. Stepanov[1], B. Gulyás[1], R. Nakao[1], N. Amini[1], H. Kimura[2], T. Taniguchi[2], S. Miura[1,3], C. Halldin[1]*

[1]Department of Clinical Neuroscience, Center for Psychiatric, Karolinska Institutet, Stockholm, Sweden, [2]Pharmaceutical Research Division, CNS Drug Discovery Unit, [3]Pharmaceutical Research Division, Medicinal Chemistry Research Lab, TAKEDA Pharmaceutical Company, Ltd., Fujisawa, Japan

***Objectives:** Phosphodiesterase 10A (PDE10A) is one of the PDE family of enzymes, that degrades cyclic adenosine monophosphate (cAMP) and cyclic guanosine monophosphate (cGMP). PDE10A is predominantly distributed in the putamen and caudate in the brain. Based on this localization, drug discovery research has focused extensively on using PDE10A inhibitors as a novel therapeutic approach for*

dysfunction in the basal ganglia circuit. PDE10A inhibitors have been shown to have antipsychotic effects in several animal models, spanning positive, cognitive and negative symptoms of schizophrenia. Development of suitable PET radioligands would be helpful to develop and evaluate drugs for this target. T-773 has high affinity for PDE10A (IC50 = 0.36nM) with favorable lipophilicity (LogD=2.13). The aim of this study is to evaluate the newly developed PET radioligand for PDE10A, [^{11}C]T-773 in vivo and in vitro using nonhuman primate (NHP), knock-out mouse and postmortem brains of human and NHP.

Methods: *Horizontal nonhuman and human whole hemisphere brain slices were used to evaluate the distribution of [^{11}C]T-773 and blocking effects by a PDE10A inhibitor, MP-10 for in vitro autoradiographical (ARG) analysis. NHP PET measurements were performed for 120 min at the baseline condition, with displacement (at 40 min) and after administration (at -35 min over 30 min) with 1.8 mg/kg of MP-10, a selective PDE10A inhibitor. In pretreatment conditions, total distribution volume (VT) was calculated with several compartment models using metabolite-corrected plasma input. The binding potential (BP_{ND}) was calculated with distribution volume ratio (DVR) and reference tissue model using the cerebellum as a reference region. Dynamic small-animal PET was performed in wild-type and PDE10A knock-out mice (homozygous and heterozygous) to investigate the change in the brain kinetics of [^{11}C]T-773 in genetic mice model.*

Results: *[^{11}C]T-773 accumulated predominantly in the striatum in ARG study of nonhuman primate and human brain. The high accumulation was highly blocked by MP-10 administration. In NHP PET study, high accumulation was seen in the striatum. Peak accumulation in the putamen was reached at around 10 min. The specific binding (= putamen - cerebellum) peaked at around 50 min. The displacement effect by MP-10 was clearly seen in the putamen. VT decrease after pretreatment with MP-10 was seen in the caudate and putamen but not in the cerebellum. The unchanged fraction of [^{11}C]T-773 was approximately 50% at 90 min. Several metabolites were detected in the HPLC analysis, but they were less lipophilic than [^{11}C]T-773. BP_{ND} was approximately 1.8 in the putamen. Estimated PDE10A occupancy was approximately 70% after pretreatment with 1.8 mg/kg of MP-10. Wild mouse showed high accumulation in the striatum, which peaked at around 20 min. Accumulation of [^{11}C]T-773 in the striatum was highest in wild type and lowest in the homozygous PDE10A KO mice.*

Conclusions: *This study demonstrated that [^{11}C]T-773 is a promising PET radioligand for PDE10A with favorable characteristics for in vivo NHP and mice as well as in vitro evaluation of PDE10A in the brain. Further evaluation would be expected for occupancy study and clinical application.*

PET BRAIN IMAGING OF NEUROPEPTIDE Y2 RECEPTORS USING N-[11C]METHYL-JNJ-31020028 IN PIGS

M. Winterdahl[1]*, H. Audrain*[1]*, A. Landau*[2]*, D. Smith*[3]*, P. Bonaventure*[4]*, J. Shoblock*[4]*, N. Carruthers*[4]*, D. Swanson*[4]*, D. Bender*[1]

[1]*PET Center, Aarhus University Hospital,* [2]*Center of Functionally Integrative Neuroscience (CFIN), Aarhus University, Aarhus,* [3]*Center for Psychiatric Research, Aarhus University Hospital, Risskov, Denmark,* [4]*Janssen Research & Development, LLC, La Jolla, CA, USA*

Objectives: *Neuropeptide Y2 (NPY2) receptors are implicated in diverse brain disorders, but no suitable PET radiotracers are currently available for studying NPY2 receptors in the living brain. The objective of the study was to prepare a positron-emitting radioligand based on a novel NPY2 receptor antagonist, JNJ-31020028(1), and use the compound for PET brain imaging in living pigs.*

Methods: *Yorkshire x Landrace pigs weighing 35-40 kg were used in the study. Autoradiographic studies were carried out to establish the anatomical distribution of NPY2 receptors in pig brain using [^{125}I]polypeptide YY and N-[11C]methyl-JNJ-31020028. Baseline and post-challenge PET recordings of N-[11C]methyl-JNJ-31020028 in pig brain were conducted for 90 min, concurrent with arterial blood sampling, and with unlabelled JNJ-31020028 as pharmacologic challenge. Cyclosporine A was used to enhance levels of the PET radiotracer in the brain. The PET images were manually coregistered to an MR atlas of the pig brain. Maps of the N-[11C]methyl-JNJ-31020028 distribution volume in brain were prepared and regional binding potentials of NPY2 receptors towards*

the radioligand were calculate by the Logan graphical reference region method.

Results: *In autoradiography studies, high densities of N-[^{11}C]methyl-JNJ-31020028 receptor binding sites, inhibited by unlabelled JNJ-31020028, were observed primarily in hippocampus. In vivo N-[^{11}C]-methyl-JNJ-31020028 was metabolized relatively slowly in the bloodstream, in that 25% of [^{11}C]-derived radioactivity at 30 minutes after injection was parent compound. PET imaging showed baseline values of V_e' of 4.50±0.28 in frontal cortex, 5.32±0.43 in caudate nucleus, 5.33±0.68 in cerebellum, and 5.58±0.77 hippocampus. Reference region and graphical analyses showed that the binding of N-[11C]methyl-JNJ-31020028 was reversible; infusion of unlabelled JNJ-31020028 markedly displaced N-[11C]methyl-JNJ-31020028 from binding sites in the hippocampus, thalamus, caudate nucleus, and cerebellum, but not in reference regions (frontal white matter and corpus callosum). A whole-body scan with N-[11C]methyl-JNJ-31020028 furthermore revealed high accumulation of radioactivity in glands, liver, and eyes.*

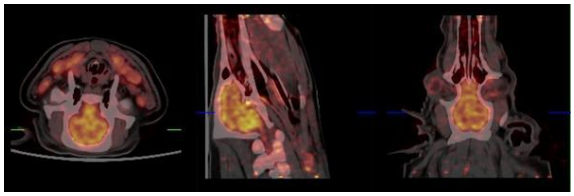

Figure 1. From left to right, PET images of [C11] JNJ-31020028 in pig brain sections in coronal, sagittal, and transaxial views.

Conclusions: *The new radiotracer N-[11C]methyl-JNJ-31020028 seems well-suited for PET investigations of NPY2 receptors in the living brain. This is based on several observations. Firstly, N-[11C]methyl-JNJ-31020028 is metabolized slowly in the bloodstream of pigs. Secondly, using cyclosporine, the target-to-background ratio of N-[11C]methyl-JNJ-31020028 is sufficient for estimating pharmacokinetic parameters. Thirdly, N-[11C]methyl-JNJ-31020028 binds reversibly and competitively to cerebral sites such as the hippocampus, thalamus, caudate nucleus, and cerebellum. Fourthly, white matter, such as corpus callosum, can serve as a reference region for nonspecific binding. To our knowledge, no other radioligand currently exists with these favorable properties and with such specificity for the NPY2 receptor system. Therefore, we view N-[11C]methyl-JNJ-31020028 as a particularly promising radioligand for PET neuroimaging of NPY2 receptors.*

Acknowledgement: *This work was supported by Lundbeck foundation grant (R77-A6608).*

References:

(1) Bonaventure et. al., J. Pharmacol. Exp. Ther. 308, 1130-1137.

PROGRESSIVE LOSS OF STRIATAL DOPAMINE TERMINALS IN MPTP PARKINSONIAN NON-HUMAN PRIMATES USING VESICULAR MONOAMINE TRANSPORTER TYPE 2 PET IMAGING

F. Yue[1], Y. Liu[1], R. Tang[2], L. Zhu[3], ***P. Chan****[1]*

[1]Xuanwu Hospital, Capital Medical University, Beijing, [2]Wincon Theracells Biotechnologies, Inc., Nanning, [3]Beijing Normal University, Beijing, China

The 1-methyl-4-phenyl-1,2,3,4-tetrahydropyridine (MPTP)-induced Parkinson's disease (PD) model, particularly in non-human primate (NHP), remains the gold standard for the study of pathogenesis and assessment of novel therapies. However, whether or not the loss of dopamine neurons in this model is progressive remains controversial. This is mostly due to lacking of in vivo objective assessment of change in the integrity of dopamine neurons in life animals. In the present study, parkinsonism NHPs model was induced by intravenous administration of MPTP (0.2 mg/kg) for up to 15 days and stable parkinsonism was developed for at least 90 days until the symptoms were stable. Noninvasive neuroimaging of vesicular monoamine transporter 2 (VMAT2) with (2R,3R,11bR)-9-(3-[^{18}F-fluoropropoxy) -3-isobutyl-10-methoxy-2,3,4,6,7,11b-hexahydro-1H-pyrido[2,1-a]isoquinolin-2-ol ([^{18}F]AV-133) PET imaging was applied in NHPs before and 15 and 90 days after acute MPTP treatment. The PET imaging results indicated that a longitudinal and progressive loss of striatal uptake of [^{18}F]AV-133 was evident. The dopaminergic denervation severity (DS) showed significant linear correlation with clinical rating scores and subscores of bradykinesia. These findings demonstrated that longitudinal [^{18}F]AV-133 PET imaging could be a useful tool to noninvasively evaluate the evolution of monoaminergic terminals reductions in an

acute MPTP-induced parkinsonism NHPs model.

SUPERVISED CLUSTERING FOR DETERMINING A REFERENCE REGION FOR [^{11}C]PK11195 PET: ADAPTATION TO RAT PET STUDIES

N. Costes[1], *C. Blanc*[1,2], *C. Bouillot*[3], *J. Yankam Njiwa*[2], *R. Bolbos*[3], *F. Chauveau*[4], *D. Le Bars*[1], *F. Turkheimer*[5], *H. Alexander*[2]

[1]*PET Department, CERMEP - Imagerie du Vivant,* [2]*Chair of Neuroimaging, Neurodis Foundation,* [3]*ANIMAGE Department, CERMEP - Imagerie du Vivant,* [4]*BioRan Team, Lyon Neuroscience Research Centre, Lyon, France,* [5]*King's College London, London, UK*

Introduction: *Neuroinflammation is a complex process directly linked to the activation of microglia. The 18 kDa translocator protein (TSPO; previously called PBR for Peripheral-type Benzodiazepine Receptor) is expressed by activated microglia, a hallmark of neuroinflammation. Even if several TSPO radiotracers are now available, [^{11}C]PK11195 remains the most widely used and is the only one not to show intersubject differences in humans. Due to the sparse and discontinuous, but potentially widespread repartition of activated microglia, determining a suitable reference tissue for the quantification of [^{11}C]PK11195 binding is a major challenge. A previous human study detailed a supervised clustering method, called SuperPK, to reliably identify a distributed reference region consisting of voxels with time-activity curves (TACs) similar to those in normal gray matter (Turkheimer et at, 2007). Because of the scanner resolution, SuperPK has to be adapted to rodent brain imaging.*

Material and methods: *PET scans with [^{11}C]PK11195, CT scans, and T2-MRI from four adult rats (Sprague-Dawley) and metabolite-corrected arterial input functions in three, were available. There was one control rat, two rats scanned at day 8 and 33 after status epilepticus, and one after ischemic stroke. SuperPK performs a classification by modelling voxel TACs as a weighted linear combination of three standard kinetic classes. Various standard kinetic classes were tested: 1) the kinetic classes of the original SuperPK derived from human scans, 2) visual selection of inactivated (NORM) and activated (PBR) brain tissue in the experimental PET data, and 3) the metabolite corrected peripheral arterial input curves (BLOOD). SuperPK classification was applied to each voxel TAC. A reference tissue function was constructed by averaging TACs of voxels, weighted by the probability of belonging to a given class. We optimized the choice of the standard kinetics and the parameters for selecting voxels in the absence of a gold standard with a recently described method (Lebenberg et al., 2011). With these optimized parameters, a reference tissue region was obtained for each dataset and used for modelling the relative regional volume of distribution (DVR) with Logan plots. The DVRs were compared to DVs obtained with the Logan method using the individual arterial input function.*

Results: *The best choice for the standard kinetics classes, i.e. closest to the gold standard estimated by bootstrap in the Lebenberg method, was obtained with the mean arterial input function as a template for the BLOOD class, mean tissular TACs selected in our dataset for the NORM class, and mean tissular TAC of activated regions for the PBR class. The best criteria of voxel selection for the reference region were weights of 60% NORM, 0% PBR. An example of the 3-class image classification is shown in Fig.1. There was a tight correlation of regional DVs derived with arterial input function modeling and the adapted SuperPK reference tissue modeling (Fig. 2).*

Conclusion: *These preliminary results suggest that the SuperPK method can be successfully adapted for performing reference tissue modelling with PET tracers that have widespread specific binding sites.*

Fig. 1

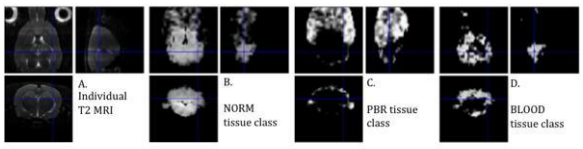

Fig. 2

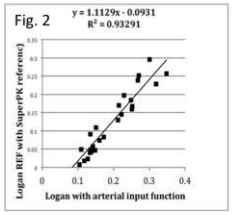

[Fig1-Tissue classification, Fig2 - DV Validation]

CORRECTING FOR ACCURATELY MEASURED GLUCOSE LEVELS IMPROVES THE ROBUSTNESS OF PET RAT BRAIN IMAGE QUANTIFICATION IN LONGITUDINAL EXPERIMENTS

*S. Deleye[1], **J. Verhaeghe**[1], T. Wyckhuys[1], L. Wyffels[1,2], S. Dedeurwaerdere[3], S. Stroobants[1,2], S. Staelens[1]*

[1]Molecular Imaging Center Antwerp, University of Antwerp, [2]Nuclear Medicine, University Hospital Antwerp, [3]Translational Neurosciences, University of Antwerp, Antwerpen, Belgium

Introduction: *Currently the most widely used quantification index in ^{18}F-FDG PET studies is the semi-quantitative $SUV_{(ID/BW)}$ (Standard Uptake Value=%ID*BW) measure. Factors that affect $SUV_{(ID/BW)}$ in rodents such as the effects of various anaesthetics, fasting duration, the route of ^{18}F-FDG administration and the influence of the body temperature have been studied before [1]. Here we investigate whether correction for blood glucose levels can decrease the variability of the $SUV_{(ID/BW)}$ between animals in one group and/or in an animal over time.*

Methods: *Twenty naive male Sprague-Dawley rats were randomly divided into five groups: no fasting, 6h, 12h, 18h and 24h fasting and scanned in a standardized protocol where anesthesia, temperature control and tail vein injection were optimized. Six additional animals were subjected to a longitudinal test - multiple retest paradigm spread over ten days where animals were scanned on days 1, 3, 7, 9 and 10 and every time fasted for 16h. In both experiments, each time before the start of the scan and for all groups whole blood (WBglc) glucose was measured twice manually with a One Touch Ultra strip (LifeScan) and serum glucose (SEglc) was enzymatically determined afterwards on a Vista Dimension (Siemens). These values were then used to normalize the $SUV_{(ID/BW)}$ values to SUV_{WBglc} or SUV_{SEglc}. Intra- and interanimal variability is expressed as percentage coefficient of variation (%COV).*

Results: *A first significant and considerable reduction of glucose levels is shown for the animals of the 12h fasting group as in Fig1A while glucose levels did not decrease further for longer fasting times. The $SUV_{(ID/BW)}$ (Fig. 1B) varied significantly between the various groups and these differences could only be amortized by normalizing to the glucose levels (Fig. 1 C).*

When animals were scanned repeatedly, a clear trend in rising glucose levels (f.i. 46% higher at day 10 for SEglc) is shown by Fig. 1D although fasting times were always 16h before each scan. The $SUV_{(ID/BW)}$ decreased with 23.9 ± 5% by day 10 and correcting for glucose levels normalized this SUV reduction over time to only 5% ± 7% (Fig. 1E) for SUV_{SEglc}. Moreover, the $SUV_{(ID/BW)}$ showed the highest intra-animal and average inter-animal COV: 15.65/17.77% compared to 13.09/13.79% for the SUV_{WBglc} and even further down to only 10.71/9.51% for SUV_{SEglc}.

Conclusion: *SUV brain uptake values are reliable in naive animals when a fasting period of at least 12 hours is considered. For shorter fasting periods in naive animals or when animals are scanned longitudinally, SUV values need to be corrected for the glucose level. We show here that this even largely decreases the intra and inter-animal variability for rat brain imaging. Measuring the serum glucose analytically is preferable and if a manual strip for whole blood is to be used, then blood glucose levels should be measured at least in duplo to reduce variability.*

References:

1. Fueger, 2006. Impact of animal handling on the results of FDG PET studies in mice

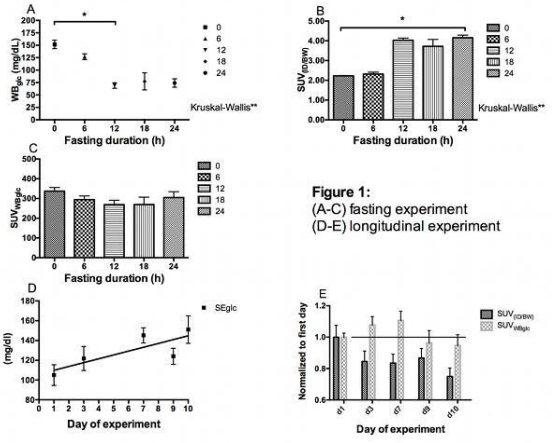

Figure 1:
(A-C) fasting experiment
(D-E) longitudinal experiment

[Figure1]

PET IMAGING OF ORGANIC CATION TRANSPORTERS IN RAT AND PIG BRAIN WITH NOVEL CARBON-11 LABELED BIGUANIDES

S. Jakobsen[1], *N. Jessen*[2,3], *J. Frøkiær*[1]

[1]*Department of Nuclear Medicine and PET Center,* [2]*Department of Clinical Pharmacology,* [3]*The Medical Research Laboratories, Clinical Institute, Aarhus University Hospital, Aarhus, Denmark*

Objectives: *Based on a recent report (Bacq, 2012), that demonstrated organic cation transporter 2 (OCT2) as an important postsynaptic determinant of aminergic tonus and mood-related behaviors in mice, we aim to investigate the possible transport of metformin and related biguanide compounds into the brain. To achieve this, we seek to label metformin, buformin and phenformin with carbon-11 and use brain PET imaging with these novel tracers to monitor the radioactivity concentration in brains of healthy landrace pigs and Sprague-Dawley rats.*

Methods: *Female Landrace pigs (40 kg) are anesthetized and scanned at baseline with either carbon-11 labeled metformin, methyl-metformin, methyl-buformin or methyl-phenformin in a Siemens PET/CT scanner and again after a blocking dose of metformin (40 mg/kg). Male Sprague-Dawley rats are anesthetized and scanned at baseline with carbon-11 labeled metformin, methylmetformin, methylbuformin or methylphenformin in a Concorde R4 microPET scanner, or after a blocking dose of metformin (50 mg/kg).*

Results: *The preliminary results obtained from 2 rats and 1 pig experiments shows clearly that carbon-11 labeled metformin at tracer level does not enter the brain; nor is there any radioactivity accumulated in brain after administration of a blocking dose of metformin. However, liver and in particular kidney show high accumulation of carbon-11 labeled metformin. Experiments with carbon-11 labeled methylbuformin and methylphenformin are underway.*

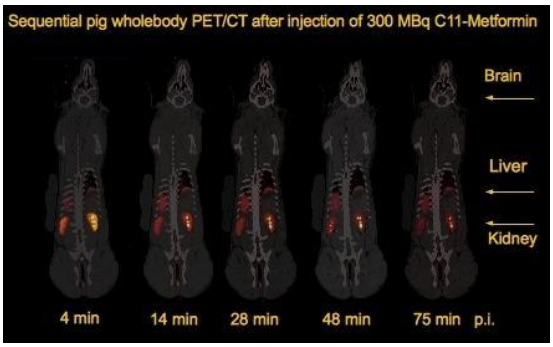

[11C Metformin pig PET/CT]

Conclusions: *At present, the existing data univocally suggest that the known substrate for organic cation transporter 2, metformin, when labeled with carbon-11 does not enter the brain of rodents or pigs. Significant species differences in tissue distribution and function of the OCT1 and OCT2 transporters were observed in tissue from rat kidney, pig and human (Busch 1998), and a similar situation regarding brain OCT1/OCT2 could explain the current findings. Altered OCT2 expression in brain and periphery in immune-compromised or disease-like mice as in the study reported by Bacq offer yet an alternative explanation for the apparent discrepancy. To this end, the carbon-11 labeled metformin may show promise as a candidate to evaluate alterations in OCT1/OCT2 outside the brain.*

References:

Bacq, A., et al., Organic cation transporter 2 controls brain norepinephrine and serotonin clearance and antidepressant response. Molecular Psychiatry, 2012. ***17****: p. 926-39.*

Busch, ., et al., Human Neurons Express the Polyspecific Cation Transporter hOCT2, Which Translocates Monoamine Neurotransmitters, Amantadine, and Memantine.

Molecular Pharmacology, 1998. ***54****(2): p. 342-52.*

THE INDUCTION OF CYCLOLOXYGENASE-2(COX-2) EXPRESSION RESPONDING TO ISCHEMIC NEURONAL INJURY AND PET IMAGING WITH TWO RADIO-LABELED FIRST-GENERATION COX-2 SELECTIVE INHIBITORS

B. Ji[1], *M.-R. Zhang*[2], *H. Onoe*[3], *H. Kaneko*[1], *K. Kumata*[2], *M. Shukuri*[3], *C. Seki*[4], *M. Ono*[1], *M. Tokunaga*[1], *T. Minamihisamatsu*[1], *M. Higuchi*[1], *T. Suhara*[1]

[1]*Molecular Neuroimaging Program,* [2]*Molecular Probe Program, Molecular Imaging Center, National Institute of Radiological Sciences, Chiba,* [3]*Functional Probe Research Laboratory, RIKEN Center for Molecular Imaging Science, Kobe,* [4]*Biophysics Program, Molecular Imaging Center, National Institute of Radiological Sciences, Chiba, Japan*

Objectives: *To clarify whether imaging for cyclooxygenase-2(COX-2) is potential for monitoring pathological advance in ischemic diseases, and labeled COX-2 selective inhibitors are available as positron emission tomography (PET) tracers for COX-2 imaging.*

Methods: *We have investigated the expression of COX-2 in normal and ischemic mouse brain with an original anti-COX-2 antibody with high specificity against murine COX-2 molecule and performed in-vivo living imaging and in-vitro autoradiographic analysis with two radio-synthesized first-generation COX-2 selective inhibitors ([*^{11}*C]celecoxib) and [*^{11}*C]rofecoxib), in normal and ischemic mouse brains.*

Results: *The immunohistochemical analysis showed the expression of COX-2 was exclusively localized in neurons with the most abundant amount in cerebellum and brainstem in normal mouse brain, and such expression was detectable by in-vitro autoradiographic analysis with [*^{11}*C]rofecoxib, not [*^{11}*C]celecoxib. In-vivo imaging with both of these two PET tracers failed to detect COX-2 expression despite their excellent brain permeability. The hypoperfusion-induced ischemia caused overt necrotic neuron death accompanied with gliosis in hippocampus, where significant induction of COX-2 was detected exclusively in injured neuron soma and synapse-like structure. The binding of [*^{11}*C]rofecoxib was also increased in injured hippocampus compared to uninjured corresponding region.*

Conclusions: *COX-2 is suitable biomarker for monitoring progressive ischemic injury and developing PET tracers for COX-2 imaging with COX-2 selective inhibitors is feasible for this purpose, although in-vivo living imaging requires further development of PET tracer with higher affinity than [*^{11}*C]celecoxib and [*^{11}*C]rofecoxib.*

CEREBRAL GLUCOSE METABOLISM WITH THERAPEUTIC HYPOTHERMIA AFTER CARDIAC ARREST

G. Zhen[1], *C. Endres*[2], ***X. Jia***[3,4,5]

[1]*Orthopaedics,* [2]*Radiology,* [3]*Biomedical Engineering,* [4]*Physical Medicine & Rehabilitation,* [5]*Anesthesiology & Critical Care Medicine, Johns Hopkins University, Baltimore, MD, USA*

Induced hypothermia to 32-34°C for 12-24 hours improves survival and functional outcome in cardiac arrest (CA) survivors. Previous clinical PET studies have demonstrated that under normothermia, mean cerebral glucose metabolism after CA was drastically decreased in patients with unfavorable outcome. We investigator with therapeutic hypothermia, whether post-CA brain FDG uptake follows similar pattern in relation to functional outcome. 8 Male Wistar rats underwent 7 min asphyxia CA and were randomized immediately after resuscitation to either normothermia (36.5-37.5 ^{o}*C) or hypothermia (32-34* ^{o}*C) for 2 hours. FDG injection starting 1 h after resuscitation and PET images was acquired on a GE eXplore VISTA (GE Healthcare, Milwaukee, WI, USA) small animal PET system for 1 hour. Previously well-validated neurological deficit scoring (NDS) was used to evaluate functional outcome at 72 hours after CA. Dynamic quantitative FDG activity concentration after CA by standard uptake value (SUV), after normalized for injected dose and body weight, was compared between normothermic and hypothermic animals and correlated with NDS score. Therapeutic hypothermia led to lower mean FDG SUV in hypothermia animals compared to the normothermia animals both in cortex (9.15±1.63 vs. 9.93±1.51, mean±SE) and thalamus (10.14±1.95 vs. 10.48±1.82). NDS demonstrated significant improvement in therapeutic animals than normothermia animals. Unlike under normothermia, with therapeutic hypothermia after CA, the post-resuscitation glucose hypometabolism was not*

correlated with bad neurological outcome. The slowing of cerebral metabolism leading to the reduced glucose consumption may not be the key mechanism underlying hypothermia's protective effects. Further studies may elucidate the detailed mechanisms of hypothermia's effect after CA.

Supported by grants: American Heart Association #09SDG2110140 and NIH #RO1HL071568.

FUNCTION BRAIN IMAGING AFTER ACTIVATION OF CENTRAL VESTIBULAR SYSTEM USING 18F- FDG PET SCAN

M.S. Kim[1]*, R.G. Kim*[2]*, D. Kim*[3]*, H.-I. Kim*[2]

[1]*Physiology, School of Medicine, Wonkwang University, Iksan,* [2]*Medical System and Engineering, Gwangju Institute of Science and Technology, Gwangju,* [3]*School of Information and Communications, Gwangju Institute of Science and Technology, Gwangiu, Republic of Korea*

Objectives: *The central vestibular nuclei with massive neural network in the brain are a key center for regulation of vestibular functions and clinical studies suggest that activation of the vestibular system can affect central pain, post-stroke hemineglect, and phantom limb illusion. However, there is a paucity of informations about functional activation patterns of central vestibular network by the stimulation of the vestibular nucleus in rodent cortex. The purpose of present study is to investigate the effect of stimulation of the medial vestibular nucleus (MVN) to determine the activation patterns in the cortical and subcortical structures*

Methods: *In Sprague-Dalwey rats (n=12), bipolar stimulating electrode was implanted in the unilateral MVN and continuous electrical stimulation was delivered with 200Hz of frequency for 20minutes. The static [F-18]Fluorodeoxyglucose PET images were acquired using micro PET scanner. The statistical analysis was performed to compare the difference between sham-operated and stimulated groups.*

Results: *Unilateral MVN stimulation resulted in a strong activation of the anterior pretectal nucleus (APtN) of the midbrain, subthalamic nuclei and nucleus accumbens. There was also bilateral activation of the somatosenory cortex and retrosplenial cortex with ipsilateral predominance.*

Conclusion: *These results suggest that activation of the central vestibular system may take part in modulation of somatosensory inputs by altering thalamus or APtN activity in rats.*

Reference:

1. Dieterich M, Brandt T. Functional brain imaging of peripheral and central vestibular disorders. Brain. 131:2538-52, 2008

2. Been G, Ngo TT, Miller SM, Fitzgerald PB. The use of tDCS and CVS as methods of non-invasive brain stimulation. Brain Res Rev. 56:346-361, 2007

DOWN-REGULATION OF THE POST-SYNAPTIC SEROTONIN 1A RECEPTORS IN THE HEMI-PARKINSONIAN RAT MODEL

M. Lee[1]*, J.Y. Choi*[1]*, Y. Seo*[1]*, W.G. Cho*[2]*, T.J. Jeon*[1]*, B.S. Kim*[3]*, T.H. Choi*[3]*, Y.H. Ryu*[1]

[1]*Department of Nuclear Medicine, Gangnam Severance Hospital, Yonsei University College of Medicine, Seoul,* [2]*Department of Anatomy, Yonsei University Wonju College of Medicine, Wonju,* [3]*Department of Molecular Imaging, Korea Institute of Radiological & Medical Sciences, Seoul, Republic of Korea*

Introduction: *The pathological characteristic of Parkinson disease (PD) is the degeneration of dopaminergic neuron in substantia nigra pars compacta (SNc) and subsequently the striatum*[1]*. However, PD is not solely a dopaminergic disease but the serotonergic system is also implicated in the PD. Recently, growing evidences suggest that degeneration of the dopaminergic system leads to impair serotonergic system. Until today, there is no report about the integrity of the serotonergic system in the Parkinson´s animal model in vivo.*

Objectives: *The purpose of this research is to investigate the changes the serotonin 1A (5-HT_{1A}) receptor density using [*^{18}*F]MEFWAY which is a highly specific PET radioligand for imaging the 5-HT_{1A} receptors*[2,3]*.*

Method: *The unilaterally 6-OHDA lesioned male Sprague-Dawley rats which are the representative hemi-Parkinsonian model and control male Sprague-Dawley rats were used*

for in vivo imaging of microPET. Each rat was anesthetized with 2.0 % isoflurane in oxygen and placed in the gantry with its head centered in the field of view. A catheter was inserted into the tail vein and fluconazole was injected at an infusion rate for 1 h. Radioactivity (13.1-19.6 MBq) was promptly injected over 1 min to the catheter and dynamic PET scans (Siemens, Inveon PET/CT) were performed for 120 min. PET data were reconstructed in user-defined time frames in length (10 sec x 6 frames, 30 sec x 8 frames, 300 sex x 5 frames, 1800 sec x 5 frames) by a 2-dimentional order-subset expectation maximization (OSEM) algorithm (4 iterations and 16 subsets). Regions of interests are hippocampus and cerebellum. Here, we used a fluconazole as an anti-defluorination drug in vivo. Non-displaceable binding potential (BP_{ND}), commonly used as an indication of receptor density, is the ratio of the peak values of specific binding curve to the non-specific binding curve at the time of the peak. The cerebellum was used as the reference region because it contains very few 5-HT_{1A} receptors in the rats.

Result: *Time activity curves showed that hippocampal uptake in 6-OHDA lesioned rat was 35% lower than in the control group and radioactivity uptake was similar both lesioned hippocampus and intact one. The cerebellar uptake in the 6-OHDA rats were similar to the control rats. The highest specific binding to non-specific binding ratio was obtained at 75 min after PET scan. The BP_{ND} from the 6-OHDA rats was 32% lower than from the control group. This result suggested that 5-HT_{1A} receptors were down-regulated.*

Conclusion: *We conclude that unilateral 6-OHDA lesion induced the down-regulation of post-synaptic 5-HT_{1A} receptors in the rat brain. We suspected that 6-OHDA lesion cause the depression.*

References:

1. Innis RB, Seibyl JP, Scanley BE et al. Single photon emission computed tomographic imaging demonstrates loss of striatal dopamine transporters in Parkinson disease. Proc Natl Acad Sci USA 1993; 90:11965-11969.

2. Saigal N, Pichika R, Easwaramoorthy B et al. Synthesis and biologic evaluation of a novel serotonin 5-HT_{1A} receptor radioligand, 18F-labeled mefway, in rodents and imaging by PET in a nonhuman primate. J Nucl Med 2006;47:1697-706.

SPECT IMAGING OF THE SEROTONERGIC SYSTEM IN WILD TYPE AND MDR1A KNOCKOUT RATS

*N. Dumas[1], M. Moulin-Sallanon[1,2], Y. Charnay[3], **P. Millet**[1]*

[1]Clinical Neurophysiology and Neuroimaging Unit, Department of Psychiatry, University Hospitals of Geneva, Geneva, Switzerland, [2]INSERM Unit 1039, J Fourier University, La Tronche, France, [3]Morphology Unit, Division of Neuropsychiatry, University Hospitals of Geneva, Geneva, Switzerland

Objectives: *Our goal was to evaluate the SB207710[1], p-MPPI[2], ADAM[3] and R91150[4] radioligands, respectively 5HTR4, 5HTR1A, SERT and 5HTR2A ligands, as suitable SPECT tracers for in vivo imaging in rats, and to investigate whether or not efflux proteins of the Mdr1a family had an impact on the kinetics of these tracers.*

Methods: *Radioligands were obtained by iododestannylation. Purification and apparent specific activity measurement were performed by HPLC. Radiotracers were all tested by ex vivo autoradiography to obtain reference images for the in vivo SPECT data. Finally, dynamic SPECT acquisitions were performed on a dedicated small animal SPECT scanner to investigate the potential of each tracer for SPECT imaging in wild type rats as well as in Mdr1a KO rats.*

Results: *Ex vivo autoradiographies: amongst other structures, p-MPPI intensely labelled the hippocampus. SB207710 showed strong binding to the nucleus accumbens and olfactive tubercle. ADAM labelled numerous SERT rich structures like substantia nigra and dorsal raphe nucleus. R91150 labelled the cortex and even more strongly labelled the orbitofrontal cortex.*

Dynamic SPECT experiment in wild type and Mdr1a KO rats: the pharmacokinetics of [^{123}I]-SB207710 and [^{123}I]-p-MPPI did not allow to obtain SPECT data matching the distribution observed ex vivo in either wild type or KO animals. SPECT acquisitions with [^{123}I]-ADAM showed accumulation in the expected structure as compared to ex vivo autoradiograms, and the expression of Mdr1a proteins had little or no impact on this tracer

kinetics. [^{123}I]-R91150 SPECT scans showed little cerebral signal in wild type animals, although the labelling in the expected structures was present. However, the same exam performed in Mdr1a KO animals showed a profoundly modified kinetics with a several folds increased brain uptake.

Conclusions: *Serotonin receptor 4 and serotonin receptor 1A tracers, SB207710 and p-MPPI, are excellent tools for autoradiographic ex vivo or in vitro experiments, but their pharmacokinetic characteristics do not make them suited for SPECT imaging in either wild type or Mdr1a KO rats. The SERT ligand ADAM is readily suitable for in vivo SPECT imaging in wild type rat, and no changes in its pharmacokinetics were observed in the absence of Mdr1a proteins. The brain penetration of R91150 was significantly increased when administered to Mdr1a KO rats in comparison to wild type rats, making the use of this knockout rat line an interesting option to study serotonin receptor 2A by SPECT imaging.*

This work was supported by the Swiss National Science Foundation (grant no. 310030_120369).

References:

1. Pike, V.W., et al. Radioiodinated SB 207710 as a radioligand in vivo: imaging of brain 5-HT4 receptors with SPET. Eur J Nucl Med Mol Imaging 30, 1520-1528 (2003).

2. Kung, H.F., et al. In vivo SPECT imaging of 5-HT1A receptors with [123I]p-MPPI in nonhuman primates. Synapse 24, 273-281 (1996).

3. Oya, S., et al. 2-((2-((dimethylamino)methyl)phenyl)thio)-5-iodophenylamine (ADAM): an improved serotonin transporter ligand. Nucl Med Biol 27, 249-254 (2000).

4. Busatto, G.F., et al. Initial evaluation of 123I-5-I-R91150, a selective 5-HT2A ligand for single-photon emission tomography, in healthy human subjects. European journal of nuclear medicine 24, 119-124 (1997).

THE ACCURACY OF MEASUREMENT OF SMALL RADIOACTIVITY CONCENTRATION BY A WELL COUNTER

T. Morita[1], *T. Watabe*[1], *H. Watabe*[2], *Y. Kanai*[2], *K. Matsunaga*[1], *S. Watanabe*[1], *M. Ishibashi*[1], *K. Isohashi*[1], *H. Kato*[1], *M. Tatsumi*[3], *E. Shimosegawa*[1], *J. Hatazawa*[1]

[1]*Department of Nuclear Medicine and Tracer Kinetics,* [2]*Department of Molecular Imaging in Medicine,* [3]*Department of Radiology, Osaka University Graduate School of Medicine, Suita City, Japan*

Objectives: *Fully quantitative functional imaging using PET requires frequent measurement of radioactivity concentrations in arterial blood. However, a small size of rodents limits an amount of blood sample to a few µl and it makes the quantitative rodent imaging difficult . It is known that the degree of variability of radioactivity count in arterial blood may affect the accuracy of quantitative measurement of cerebral blood flow, metabolism and function using PET in rats(1). This study aimed to evaluate accuracy of blood measurements in small sample by a well counter.*

Methods: *Detector System.*

Our well counter system consisted of a well-type NaI (Tl) scintillator,a 2 inch PMT and a 3 cm lead shield. The NaI (Tl) element measured 5 cm x 5 cm (length x diameter); the well measured 3 cm x 1 cm (diameter x depth).

Measurements: *At first, the radioactivity concentrations and the weight of 10µl,25µl,50µl and 100µl H215O and 18 F-NaF solution were measured by the well counter. We examined the volume dependency of the radioactivity count in the well counter .The radioactivity concentration of each sampled solution (cps: count per second) was corrected for the decay from the sampling time.*

At second, a series of 40 tubes each containing 10µl of 13N-NH3 and 18F-NaF solution were prepared.We prepared 3 dilutions in which each successive dilution is 2-fold, which gave a 2X, 4X, and 8X dulutions. We measured the radioactivity and the weight of the solution by well counter. The radioactivity concentration of each solution

was corrected for the decay from the sampling time.

Results: *The radioactivity concentration(cps/g) was constant for volumes in the range of 25µl to 100µl of H215O and 18 F-NaF solution.We confirmed that the measurement was accurate and reproducibility was feasible in the range of sample volumes from 25µl to 100µl. On the other hand, sample volume of 10µl showed large variability.*

The radioactivity (cps) was constant for volumes in the range of 10µl to 80µl 13N-NH3 and 18F-NaF solution. However, the radioactivity concentration(cps/g) of 10µl 13N-NH3 and 18 F-NaF solution had a larger margin of error compared to radioactivity concentration for volumes in the range of 25µl to 100µl. The degree of variability of weight measurement may affect the accuracy of measurement of small radioactivity concentration.

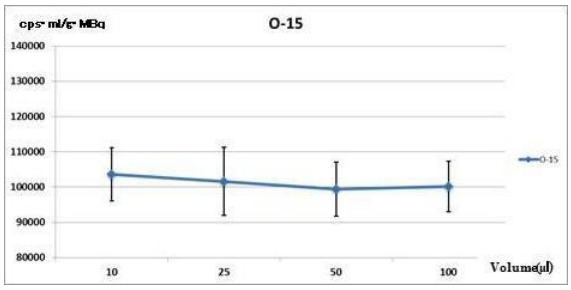

[Relative radioactivity concentration O15-H2O]

Conclusions: *We confirmed that radioactivity concentration in blood can be accurately measured until 25µl by the well counter, and the degree of variability of weight measurement affects the accuracy of measurement of small radioactivity concentration.*

References: *1.Watabe T, et al.Quantitative evaluation of cerebral blood flow and oxygen metabolism in normal anesthetized rats, J Nucl Med 2012 in press.*

EVALUATION OF 2-^{18}F-FLUOROACETATE KINETICS IN MOUSE AND RAT MODELS OF CEREBRAL ISCHEMIA-HYPOXIA

Y. Ouyang[1]*, J.N. Tinianow*[2]*, S.R. Cherry*[1]*, J. Marik*[2]

[1]*Biomedical Engineering, University of California, Davis,* [2]*Biomedical Imaging, Genentech, Inc., South San Francisco, CA, USA*

Specific in vivo imaging markers of glial metabolism are potentially valuable for translational research of stroke and other neurological disorders. Recent work in rodent models of brain injury demonstrated elevated uptake of 2-^{18}F-fluoroacetate (^{18}F-FACE), a positron emission tomography (PET) radiotracer, in lesions compared to normal tissue and suggested its utility for imaging glial metabolism [1]. In this study, we used PET and magnetic resonance imaging (MRI) to evaluate ^{18}F-FACE kinetics in mouse and rat models of cerebral ischemia-hypoxia (I-H).

Methods: *Brain lesions were induced in 7 adult male C57BL/6 mice and 7 young male Sprague-Dawley rats by cerebral ischemia-hypoxia. Animals were imaged at either 3 hours (3 mice, 2 rats) or 24 hours post-hypoxia (4 mice, 5 rats). Parametric maps of T2, and apparent diffusion coefficient (ADC) for mice, were acquired by MRI. Dynamic PET data (30 minutes for mouse, 90 minutes for rat) were acquired with a 1 minute, 100 µL infusion of ^{18}F-FACE (300 µCi for mice, 1 mCi for rat). CT data were acquired to assist in registration. Brain slices were stained with triphenyltetrazolium chloride (TTC). Lesion regions of interest (ROIs) were determined by MRI. Contralateral (non-lesion) ROIs were defined by mirroring the corresponding lesion ROIs about the sagittal plane. Heart blood ROIs were determined by PET and used to estimate whole blood and plasma time activity curves (TACs). ^{18}F-FACE TACs from heart and brain ROIs were fit to several models of fluoroacetate uptake.*

Results: *Lesions observed in MRI and TTC data were consistent. ^{18}F-FACE uptake in lesions was higher than in corresponding area of contralateral hemisphere ($p < .001$, mouse and rat). ^{18}F-FACE cleared slowly from blood (Mean 6.93 ± 0.78 %ID/g in mice, 1.71 ± 0.40 %ID/g in rat at 30 minutes). ^{18}F-FACE lesion and non-lesion time activity curves appeared*

to fit best to a 2 tissue reversible compartment model compared to 1-tissue reversible and 2-tissue irreversible models. In all data, the ratio of influx-to-efflux of free ^{18}F-FACE in brain (K_1/k_2) was higher in lesion than in non-lesion (mouse - lesion: 1.99 ± 0.54, non-lesion: 1.11 ± 0.36; rat - lesion: 2.02 ± 0.28, non-lesion: 1.13 ± 0.039) and driven primarily by lower k_2 in lesions. In addition, the mean values of K_1 and k_2 were consistent in magnitude in all data. The parameters related to ^{18}F-FACE metabolism (k_3, k_4) were not similarly consistent, with orders of magnitude differences within species and imaging time points.

Conclusion: *^{18}F-FACE does not appear to be sufficiently sensitive to the metabolism related parameters k_3 and k_4 due in part to its slow clearance and the relatively low magnitude of these parameters. However, K_1 and k_2 appear to be robust in both animal models. Further work is needed to address the physiological bases of the observed K_1/k_2 differences in ^{18}F-FACE uptake between lesion and non-lesion, which may include changes in monocarboxylate transporter activity in glial cells in response to cerebral ischemia-hypoxia.*

References: *1. Marik, J. et al. JNM, 2009.*

Figure 1

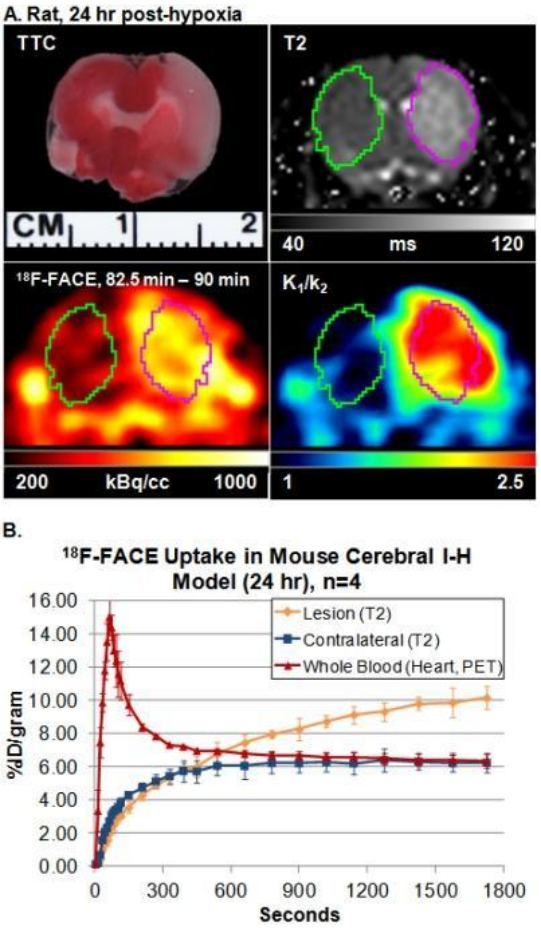

[Figure v2]

DIFFERENTIAL AMPHETAMINE AND LIGAND CONCENTRATION INHIBITION OF ^{11}C-YOHIMBINE BINDING IN BRAIN: EFFECT OF PLASMA PROTEIN BINDING DISPLACEMENT

J.-A. Phan[1], *A.M. Landau*[1], *A. Nahimi*[1,2], *S. Jakobsen*[1], *A. Gjedde*[1,2,3]

[1]*Department of Nuclear Medicine and PET Centre, Aarhus University Hospitals, Aarhus,* [2]*Department of Neuroscience and Pharmacology, University of Copenhagen, Copenhagen, Denmark,* [3]*Department of Radiology and Radiological Science, Division of Nuclear Medicine, Johns Hopkins Medical Institutions, Baltimore, MD, USA*

Objectives: *Central Alpha2 adrenoceptors have gained more attention in recent years as impaired noradrenergic transmission is*

implicated in neurodegenerative diseases such as Alzheimer's and Parkinson's disease, as well as psychiatric disorders. We recently developed a new selective radiotracer, carbon-11 labeled yohimbine, for PET imaging of alpha2 adrenoceptors, which allows in-vivo examination of the physiology and pathophysiology of noradrenergic neuromodulation. Previous porcine studies demonstrate that the estimates of non-displaceable volumes of distribution, V_{ND}, of ^{11}C-yohimbine are consistent, regardless of the use of amphetamine or cold ligand challenge (Jakobsen et al. 2006, Landau et al. 2012, Phan et al. 2012). Based on these findings, we hypothesized that V_{ND} estimates would not differ for the same challenges applied to rat brain.

Methods: *Theory*

Alpha2 adrenoceptors are widely distributed throughout the brain, which entails an absence of a reference region, where non-displaceable binding can be measured. To circumvent this impediment, we implemented the Inhibition plot (Gjedde and Wong, 2000), a version of the Lassen plots (1995), to assess the V_{ND},

$V_{T(i)}=(1-s)\cdot V_{T(0)}+s\cdot V_{ND}$

where $V_{T(0)}$ and $V_{T(i)}$ are volumes of distributions at baseline and at drug challenge, respectively, and 1-s is the fraction of receptors available for ligand binding. Then the binding potentials of ^{11}C-yohimbine are then,

$BP_{ND(0)}=V_{T(0)}/V_{ND}-1$ *and*

$BP_{ND(i)}=V_{T(i)}/V_{ND}-1$

Dynamic PET: *Nine Sprague Dawley rats were included in this study, where six underwent dual PET session at baseline and post-amphetamine and a further three rats underwent the same paradigm with cold challenge. Arterial blood samples were drawn during the scanning to obtain the plasma activity input function. Volumes of distributions were acquired by Logan graphical analysis of acquisition data from 40-90 min.*

Results: *V_{ND} estimates were 0.25 and 0.81 ml/cm^3 when obtained with amphetamine challenge and cold challenge, respectively (figure 1). The binding potentials of ^{11}C-yohimbine were higher in striatum and frontal cortex than in cerebellum (figure 2), which correlated with the estimates of regional saturation.*

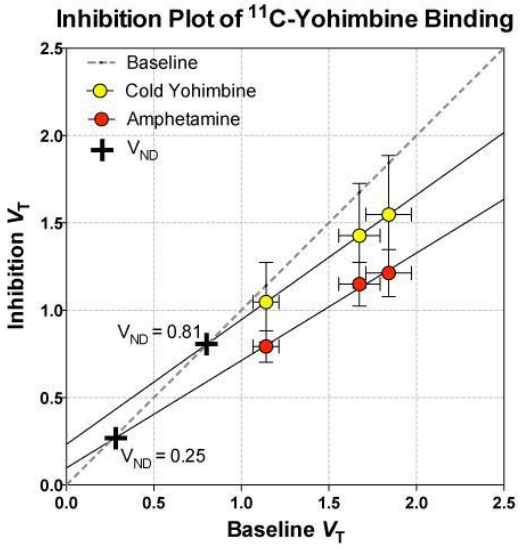

[Figure 1]

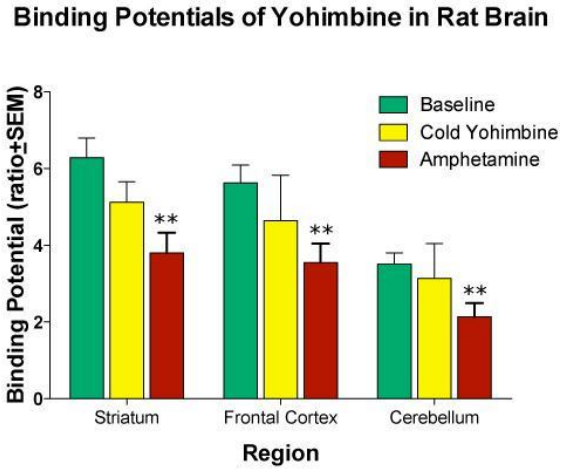

[Figure 2]

Conclusions: *Amphetamine reduced ^{11}C-yohimbine binding significantly; however the cold ligand challenge did not inhibit the binding of ^{11}C-yohimbine with the same non-displaceable volume of distribution as amphetamine. We claim that the cold ligand challenge led to cold ligand displacement of tracer bound non-specifically to plasma proteins, leading to a higher free fraction of radiotracer able to enter the brain.*

In conclusion, these findings indicate that non-specific plasma protein binding importantly influences the estimates of binding potential of ^{11}C-yohimbine in a species-specific manner. We suggest that the amphetamine challenge in rodents yields a more appropriate estimate of V_{ND}, as amphetamine appears to induce competition of tracer binding with endogenous monoamines exclusively in the brain tissue.

References:

Jakobsen et al. (2006) J Nucl Med.47:2008-15.

Gjedde and Wong (2000) NeuroImage. 11:S48

Landau et al. (2012). Psychopharmacology 222:155-63.

Lassen et al. (1995) J Cereb Blood Flow Metab. 15:152-65.

Phan et al. (2012) NRM 2012, J Cereb Blood Flow Metab. 32:S98-99

QUANTITATIVE ANALYSIS OF THE ADENOSINE A_{2A} RECEPTOR LIGAND [^{11}C]SCH442416 IN THE RODENT BRAIN

***L. Wells**, C. Salinas, S.P. Tang, H. Chong, N. Keat, W. Hallett, R.N. Gunn, E.A. Rabiner*

Imanova Ltd, Centre for Imaging Sciences, London, UK

***Objectives:** Adenosine A_{2A} receptors ($A_{2A}R$) are highly expressed in the CNS; their distribution is restricted to areas involved in the control of motivational responses, such as the striatum (Str). $A_{2A}R$ have been implicated in a number of pathological conditions, and both agonist and antagonist treatments are under development for a range of disorders including Parkinsons disease, cerebral ischemia and sleep disorders[1]. [^{11}C]SCH442416, a non-xanthine $A_{2A}R$ antagonist, has been developed as a PET tracer to help elucidate the role of $A_{2A}R$ in pathological conditions and assess occupancy by candidate drugs[2,3]. Here, we performed a rodent biodistribution experiment to measure dosimetry and a PET test-retest experiment to investigate the quantification of [^{11}C]SCH442416 in rat brain.*

***Methods:** Biodistribution - Twelve conscious Sprague-Dawley rats (n=3 per time point) received an i.v. bolus administration of 7.63±1.0 MBq [^{11}C]SCH442416. Activity concentrations at 5, 15, 30, 60mins and the total disintegrations per Bq per ml were obtained for each organ. Human values were estimated using the ratio of rat to human body masses, then multiplied by human organ mass to give total organ disintegrations per Bq. These were entered into OLINDA v1.1 to estimate effective dose in humans.*

Small Animal PET - Two dynamic PET scans (90mins, Siemens Inveon PET-CT) were performed consecutively for each of the three anaesthetised rats following i.v. bolus administrations of 4.9±2.0 MBq of [^{11}C]SCH442416. Blood samples were collected to obtain a plasma curve and metabolite correction was applied to obtain an input function. Regions of interest were drawn on the Str and cerebellum (Cer) of the summed images. Time Activity Curves were fitted with pharmacokinetic models (one-tissue compartment model, 1TC; two-tissue compartment model, 2TC; simplified reference tissue model, SRTM) to estimate the volume of distribution (V_T) and binding potential (BP_{ND}) as appropriate by using Cer as a reference region.

***Results:** The uptake and distribution of activity in tissue was consistent with previous reports[2,3] and the known expression of the $A_{2A}R$. Dosimetry estimates yielded a total effective dose of 4.1uSv/MBq with the ovaries receiving the highest equivalent dose.*

V_T and BP_{ND} estimates derived from 1TC and 2TC models were in good agreement (Table 1) and consistent with the Akaike model selection criteria being split between models. SRTM BP_{ND} estimates in Str showed a consistent, but small underestimation (16%), as compared with 1TC and 2TC models. The mean test-retest variability (VAR: mean of [2|test - retest|/[test +retest]) was lowest for SRTM (VAR = 8.2±5.2%). Metabolism of [^{11}C]SCH442416 was rapid (parent fraction: 71.1±3.2%, 50.1±2.3% and 24.9±2.2% at 5, 20 and 60mins) and a single lipophilic metabolite was identified. The fact that the tissue data was well described by a 1TC model may provide evidence that the lipophilic metabolite does not contribute significantly to the tissue signal.

***Conclusions:** [^{11}C]SCH442416 displays a favourable dosimetry profile for imaging in humans, a heterogeneous distribution*

consistent with $A_{2A}R$ expression and good test-retest variability in rodent brain.

Table 1.[^{11}C] SCH442416 V_T and BP_{ND} in the rodent brain

Model	SRTM	1TC			2TC		
Estimate	BP_{ND} Str	V_T Cer	V_T Str	BP_{ND} Str	V_T Cer	V_T Str	BP_{ND} Str
Rat 1							
Scan 1	1.80	1.37	4.03	1.95	1.48	4.34	1.93
Scan 2	1.81	1.71	5.49	2.21	1.61	6.01	2.74
Rat 2							
Scan 1	1.31	0.94	2.50	1.65	0.99	2.76	1.77
Scan 2	1.23	1.21	2.94	1.42	1.29	3.28	1.55
Rat 3							
Scan 1	1.70	1.20	3.76	2.15	1.26	4.14	2.29
Scan 2	1.42	1.41	4.26	2.01	2.25	4.71	1.09

[Table 1]

References: *[1] Fredholm et al, 2001;[2] Todde et al, 2000;[3] Moresco et al, 2004*

LONG-RANGE PLASTICITY BETWEEN INTACT HEMISPHERES AFTER CONTRALATERAL CERVICAL NERVE TRANSFER IN HUMAN

X.-Y. Hua[1]*, C.-T. Zuo*[2]*, W.-D. Xu*[1]

[1]*Department of Hand Surgery,* [2]*PET Center, Huashan Hospital, Shanghai, China*

Objective: *Peripheral nerve injury in a limb usually causes intrahemispheric functional reorganization of the contralateral motor cortex. Recently, evidence has been emerging for significant interhemispheric cortical plasticity in humans, mostly from studies of direct cortical damage. However, in this study, a long-range interhemispheric plasticity was demonstrated in adults with brachial plexus avulsion injury (BPAI) who had received a contralateral cervical nerve transfer, and this plasticity reversed the BPAI-induced intrahemispheric cortical reorganization.*

Methods: *In this study, 8 adult male patients with BPAI were studied using PET scanning.*

Results: *The results indicated that the right somatomotor cortices, which may contribute to the control of the injured limb before brachial plexus deafferentation, still played an important role when patients with BPAI tried to move their affected limbs, despite the fact that the contralateral C-7 nerve transfer had been performed and the peripheral output had changed dramatically. Such findings are consistent with the results of the authors' previous animal study.*

Conclusions: *The brain may try to restore the control of an injured limb to its original cortex area, and a complicated change of peripheral pathway also can induce long-range interhemispheric cortical reorganization in human motor cortex.*

AGE DECLINE IN THE SUBCORTICAL 5-HT_6 RECEPTOR AS IMAGED IN MALE VOLUNTEERS

D. Matuskey[1]*, E.A. Park*[2]*, B. Planeta*[2]*, N. Nabulsi*[2]*, S.-F. Lin*[2]*, J. Ropchan*[2]*, S. Najafzadeh*[2]*, I. Esterlis*[1]*, W. Williams*[1]*, D.C. D'Souza*[1]*, Y. Huang*[2]*, E.D. Morris*[2]*, R.E. Carson*[2]

[1]*Psychiatry, Yale University School of Medicine,* [2]*Diagnostic Radiology, Yale PET Center, New Haven, CT, USA*

Objective: *Previous imaging studies have suggested an age-related decline in brain serotonin (5-hydroxytryptamine or 5-HT) measures in healthy subjects. This project seeks to investigate via positron emission tomography (PET) imaging whether the availability of 5-HT_6 is also changed with age.*

Methods: *Twenty-nine healthy control subjects (all males; mean age 36±9; range 23-52 years) were scanned with the PET radiotracer [^{11}C]GSK215083 that exhibits high binding affinity for the 5-HT_6 receptor specifically localized in the striatum. Dynamic PET scans were acquired on the Siemens HR+. An early summed PET image was created and registered to the subject's 3T MR anatomical image (6-parameter affine registration) which was then registered to an MR template using a non-linear transform with Bioimagesuite. Automatic regions-of-interest (Anatomical Automatic Labeling (AAL) for SPM2) were then applied to generate time-activity curves (TACs) in the striatum (caudate and putamen). The 90-min TACs were fitted with the MA1 (t*=40) model with a metabolite-corrected arterial input function, and regional binding potential (BP_{ND}) was calculated from the fitted V_T values using the cerebellum as the reference region.*

Results: *Regional [^{11}C]GSK215083 BP_{ND} displayed a negative correlation with age in the caudate ($r = -0.51$, $P = 0.005$) and putamen ($r = -0.46$, $P = 0.01$). 5-HT_6 receptor availability in these two brain regions were found to be 22% (caudate) and 13% (putamen) lower with each decade of life studied.*

Conclusion: *PET imaging studies with [^{11}C]GSK215083 infer an age-related decrease in 5-HT$_6$ receptors in the striatum of healthy males. These findings indicate that age is a relevant factor to take into account when studying potential 5-HT$_6$ receptor alterations in psychiatric disorders.*